



Total Synthesis of Hyperforin

Citation

Sparling, Brian Andrew. 2013. Total Synthesis of Hyperforin. Doctoral dissertation, Harvard University.

Permanent link

<http://nrs.harvard.edu/urn-3:HUL.InstRepos:11181077>

Terms of Use

This article was downloaded from Harvard University's DASH repository, and is made available under the terms and conditions applicable to Other Posted Material, as set forth at <http://nrs.harvard.edu/urn-3:HUL.InstRepos:dash.current.terms-of-use#LAA>

Share Your Story

The Harvard community has made this article openly available.
Please share how this access benefits you. [Submit a story](#).

[Accessibility](#)

Total Synthesis of Hyperforin

A dissertation presented

by

Brian Andrew Sparling

to

The Department of Chemistry and Chemical Biology

in partial fulfillment of the requirements

for the degree of

Doctor of Philosophy

in the subject of

Chemistry

Harvard University

Cambridge, Massachusetts

August, 2013

© 2013 by Brian Andrew Sparling

All rights reserved.

Total Synthesis of Hyperforin

Abstract

Hyperforin (**1**) is the component of the medicinal herb St. John's Wort (*Hypericum perforatum*) responsible for its antidepressant activity. It works by blocking the reuptake of a variety of neurotransmitters through a unique mechanism of action and may be a critical lead for the treatment of depression and possibly other human diseases. However, the therapeutic potential of hyperforin is severely handicapped by its poor water solubility, facile oxidative degradation, and potent activation of pregnane X receptor, leading to increased expression of many genes involved in xenobiotic metabolism. Access to a wide variety of hyperforin analogs is critical for mitigating these shortcomings while maintaining therapeutic activity. While limited semisynthetic manipulation of isolated hyperforin is feasible, total synthesis is the only possible means of obtaining diverse hyperforin analogs.

The goal of the work presented in this thesis was to devise a new enantioselective, versatile approach to hyperforin that would not only incorporate elements of modularity but also exploit latent symmetry within the natural product that would enable facile analog synthesis. Early strategies that we explored included the carbocyclic cyclization of a polyketide and the electrocyclic cascade reaction involving an acylketene. These strategies were inherently flawed, and we subsequently pursued an alternative approach involving a diastereoselective epoxide-opening cascade cyclization.

This approach led to the enantioselective total synthesis of hyperforin. The synthesis is 18 steps in its longest linear sequence and can be deconstructed as the stepwise fusion of six easily obtainable chemicals. The key step in this sequence involved a group-selective, Lewis acid-mediated epoxide-opening cyclization of **381**, in which the strategically placed epoxide functionality relayed stereochemical information to the C1, C5, and C8 carbon centers of hyperforin, allowing 2 quaternary stereocenters and

the bicyclic core of hyperforin to be established in a single transformation in forming **382**. Using this 18-step sequence, we were able to synthesize over 40 mg of the natural product in a single batch.

Further, a small library of analogs has been synthesized using the framework of the hyperforin synthesis. These efforts have resulted in the first total synthesis of the natural product secohyperforin and the first enantioselective synthesis of (–)-nemorosone.

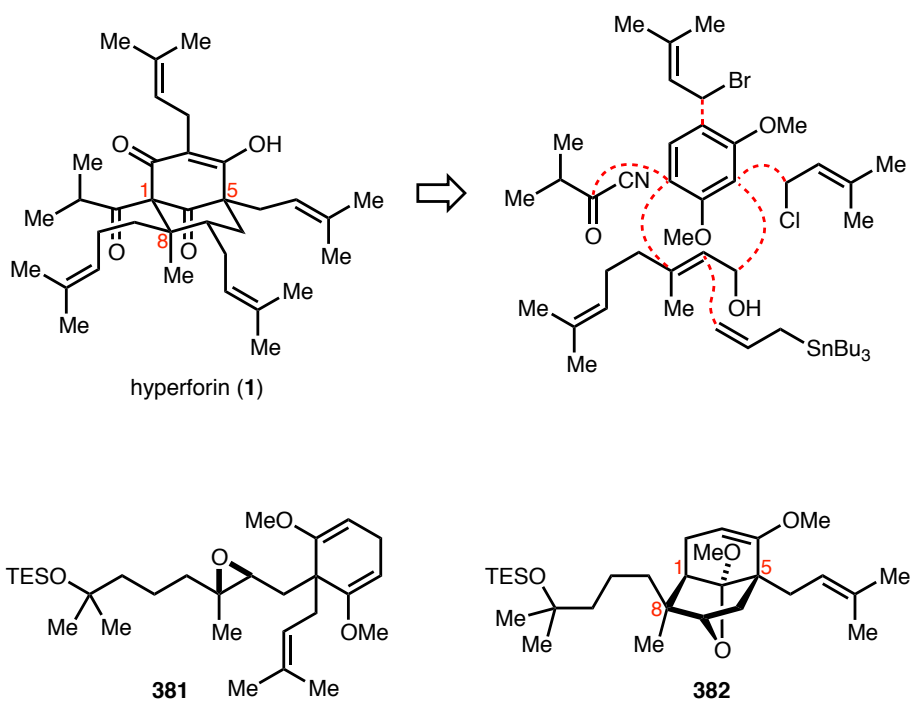


Table of Contents

Abstract.....	iii
Table of Contents	v
Acknowledgements.....	vii
List of Figures, Schemes, and Tables.....	ix
List of Abbreviations.....	xv
 Chapter 1: Polycyclic Polyprenylated Acylphloroglucinols: An Overview	 1
Overview	2
Stereochemistry	4
Distribution	6
Biosynthesis	8
Bioactivity	21
<i>Anti-infective Activity</i>	21
<i>Antioxidant and Anti-inflammatory Activity</i>	37
<i>Chemotherapeutic Activity</i>	52
<i>Activity against Neurological Disorders</i>	72
<i>Other Bioactivity</i>	95
Synthesis Strategies.....	108
 Chapter 2: Strategies Toward Hyperforin Synthesis.....	 130
Synthesis Overview.....	131
Polyketide Cyclization Approach	132
Electrocyclic Cascade Approach.....	138
Experimental Section	151

Chapter 3: Total Synthesis of Hyperforin.....	191
Synthesis Overview	192
Dearomative Allylation Approach	195
Total Synthesis of Hyperforin	221
Experimental Section	232
Appendix A: A Comprehensive Listing of all Polycyclic Polyprenylated Acylphloroglucinols.....	343
Appendix B: Catalog of Spectra	408

Acknowledgments

First and foremost, I thank my advisor, Prof. Matthew Shair. Matt has been a great mentor, teacher, and motivator, and I am truly grateful for the opportunity to work in his lab and to learn from him. One thing I truly appreciate and will try to emulate in my future career is Matt's drive and determination to pursue projects that have profound applications beyond the realm of synthetic organic chemistry. I am truly honored to have helped establish one such research program, and I look forward to seeing further breakthroughs in the hyperforin project after I leave.

Additionally, I thank my graduate advising committee and thesis committee members, Profs. Eric Jacobsen and Andrew Myers. During our annual meetings, they offered me valuable advice not only on my research project but also on chemistry in general. Their implorations for me to not only think about the "how?" but also the much more fundamental "why?" have had a lasting impact on how I approach and evaluate chemical research.

Before starting my graduate studies at Harvard, I was also fortunate to study under Prof. Timothy Jamison at the Massachusetts Institute of Technology. Tim was willing to let an eager, inexperienced freshman start working in his lab, and I would certainly not be who I am today without him doing so. In particular, the freedom and responsibility he gave to me in the last few years in his lab were crucial towards preparing me for graduate research. In addition, Dr. Graham Simpson was my first mentor, and many of my fundamental practical chemistry skills were a direct result of his endless patience.

In the Shair lab, I have had the opportunity to work alongside many talented and amazing colleagues that are too numerous to all be named in this space. Dave Moebius has been my partner in crime for the hyperforin project, and it has been a real joy getting to know him and work with him. I wish him and his family the best as they head west. I also thank my bay mate Ben Milgram for countless hours of entertainment and brainstorming sessions that I hope will continue at our next place of employment. Shota Kikuchi and Brian Liao are pillars of wisdom and have given me valuable advice throughout the

course of my research. Bill Morris was my mentor when I first started my graduate studies, and I thank him for helping me start on a strong foot.

Outside of the lab, I cannot thank my family enough for their support and love throughout my life. My parents have sacrificed so much so that I could have the best education, and I would not be where I am today without their unconditional love. My grandparents have always been an inspiration to me, and I thank all my all my in-laws, cousins, uncles, aunts, and extended family for their love and encouragement.

I do not know what I would do without my loving wife and best friend Jamie, who has stood by my side through thick and thin these last five years. She has been my anchor and my strength, being my neverending source of encouragement and love. Even during my worst days in the lab, I would come home, see that beautiful smile, and be at ease. I love you so much, and I cannot wait for little Abigail Mae to be here!

Finally, I praise the Lord, my God, for giving me the strength, perseverance, and diligence to accomplish all that is in this dissertation. None of this work would be possible without Him, and I thank God for all that I have been able to do. I thank the community of believers, especially at Park Street Church, for their prayers and fellowship during my time in graduate school. I have truly been blessed, and I hope continue to glorify Him as I move on to the next stage in my life.

I can do all things through Christ who strengthens me.

Philippians 4:13

List of Figures, Schemes, and Tables

Figures

Figure 1.1. Structures of hyperforin (1) and isoxanthochymol (2).	2
Figure 1.2. Generic PPAP skeleton and typical substituents.	3
Figure 1.3. Structures of dorstenpictanone (3), spiranthenone A-B (4,5), and xanthochymol (6).	7
Figure 1.4. Structures of garcinol (7) and isogarcinol (8).	8
Figure 1.5. Specific examples of intervening acylphloroglucinols in PPAP biosynthesis.	10
Figure 1.6. Structure of bronianone (42).	18
Figure 1.7. (a) A possible intermediate in Type C PPAP biosynthesis and (b) the only known examples of Type C PPAPs.	19
Figure 1.8. Guttiferone A and semisynthetic analogs.	26
Figure 1.9. Semisynthetic analogs of hyperforin.	31
Figure 1.10. A semisynthetic analog of guttiferone A.	33
Figure 1.11. Semisynthetic hyperforin analogs.	50
Figure 1.12. Semisynthetic PPAP analogs tetrahydrohyperforin (76) and octahydroxanthochymol (77).	63
Figure 1.13. Semisynthetic hyperforin derivatives lacking C4 functionality.	67
Figure 1.14. Structure of hypericin.	74
Figure 1.15. A semisynthetic hyperforin analog evaluated for antidepressant activity.	90
Figure 1.16. (a) Detail of hyperforin bound to the ligand-binding domain of PXR and (b) schematic highlighting the contacts between hyperforin and PXR (solid lines indicate nonpolar contacts, and dotted lines indicate hydrogen bonding).	97
Figure 1.17. Garcinol and several semisynthetic derivatives.	106
Figure 1.18. Various electrophiles utilized in “bottom-up” approaches to PPAPs.	110
Figure 1.19. A Pybox ligand and an olefin metathesis catalyst, both utilized in the total synthesis of <i>ent</i> -hyperforin.	115
Figure 1.20. Various electrophiles utilized in “top-down” annulation strategies.	127

Figure 2.1. Carbethoxyketene 208 and several potential dienylketene precursors.	134
Figure 2.2. Products obtained from the reactions of 246 with 238 .	145
Figure 2.3. Products obtained from the reactions of 266 .	149
Figure 3.1. Various byproducts formed during attempted conversion of 292 to 293 .	197
Figure 3.2. Byproducts from the allylic oxidation of 317 and the structure of peroxyiodoxolone 322 .	205
Figure 3.3. Byproducts obtained from the reaction of 353 with various nucleophiles.	217
Figure 3.4. Structures of 396 and 397 .	228
Figure 3.5. ¹ H NMR spectra comparison of natural and synthetic hyperforin (1).	337

Schemes

Scheme 1.1. The first steps in PPAP biosynthesis.	9
Scheme 1.2. (a) Phenylpyrone synthase activity of Thr135Leu <i>H. androsaemum</i> BPS and (b) benzophenone synthase activity of wild-type <i>H. androsaemum</i> BPS.	11
Scheme 1.3. Melavonate pathway of terpene biosynthesis.	11
Scheme 1.4. Deoxyxylulose phosphate pathway of terpene biosynthesis.	12
Scheme 1.5. Proposed biosynthesis of hyperforin (1) from phlorisobutyrophenone (13).	14
Scheme 1.6. Deoxycohumulone (31) as a biosynthetic precursor to both colupulone (33) and cohumulone (34).	15
Scheme 1.7. The first prenylation step in hyperforin and hop bitter acid biosynthesis.	16
Scheme 1.8. Cyclization modes of grandone (36) after prenylation via intermediate 37 : (a) deprotonation, (b) C1 cyclization, (c) C3 cyclization, and (d) etherification.	17
Scheme 1.9. Formation of PPAPs through an epoxide intermediate of plukenetione D/E (47).	20
Scheme 1.10. Acid- or heat-mediated conversion of xanthochymol (6) to isoxanthochymol (2).	20
Scheme 1.11. (a) The reaction of garcinol (7) with DPPH and (b) a possible mechanism, and (c) the reaction of garcinol (7) with AIBN.	41
Scheme 1.12. Synthesis of aristoforin from hyperforin	66
Scheme 1.13. General PPAP synthesis strategies.	109

Scheme 1.14. Total synthesis of (±)-clusianone by Simpkins (ref. 504).	111
Scheme 1.15. Total synthesis of (±)-nemorosone by Simpkins (ref. 510).	112
Scheme 1.16. Total synthesis of <i>ent</i> -hyperforin by Shibasaki (ref. 512).	114
Scheme 1.17. Intramolecular aldol approaches to PPAPs by (a) Grossman, (b) Mehta, and (c) Chen.	117
Scheme 1.18. Total synthesis of (±)-7- <i>epi</i> -clusianone by Plietker (ref. 520).	118
Scheme 1.19. Young's [3+2] allene-nitrile oxide cycloaddition approach to hyperevolutin A (ref. 526).	119
Scheme 1.20. Total synthesis of (±)-garsubellin A by Danishefsky (ref. 527).	121
Scheme 1.21. Carbocyclization approaches to PPAPs by (a) Jacobsen, (b) Nicolaou, and (c) Couladouros.	123
Scheme 1.22. Other dearomative carbocyclization approaches by (a) Njardarson and (b) Simpkins.	124
Scheme 1.23. Racemic total synthesis of (±)-hyperforin by Nakada (ref. 539).	126
Scheme 1.24. Total synthesis of <i>ent</i> -hyperibone K by Porco (ref. 545).	128
Scheme 2.1. (a) Retrosynthetic analysis of hyperforin and (b) transition-state analysis of key cyclization event.	132
Scheme 2.2. Retrosynthesis of model system 203 via tetraketide 205 .	133
Scheme 2.3. Attempted Synthesis of dioxinone 210 .	135
Scheme 2.4. Synthesis of tetraketides 211 and 212 .	136
Scheme 2.5. Attempted ketene generation from tetraketides 210 and 211 .	136
Scheme 2.6. Synthesis of ketene 206 and coupling with β-ketothioester 218 .	137
Scheme 2.7. (a) Proposed and (b) unsuccessful synthesis of carbocycle 203 from pyrone 222 .	138
Scheme 2.8. (a) Proposed electrocyclic cascade and (b) mechanism for the synthesis of cyclohexadienone 229 .	139
Scheme 2.9. Attempted cycloaddition of alkynyl ether 234 with ketenes 206 and 208 .	140
Scheme 2.10. (a) Thermolytic formation of 238 and 239 , and (b) a possible mechanism for the formation of 239 .	141
Scheme 2.11. The reaction of <i>in situ</i> derived lithium alkynoate 242 with cyclobutenone 238 .	142

Scheme 2.12. (a) Synthesis and (b) possible mechanism for the formation of 248 from the coupling of 246 and 238 .	143
Scheme 2.13. A possible mechanism for the formation of 255 from the reaction of 246 with 238 (Table 2.1, entry 5).	145
Scheme 2.14. Reactivity of alkynyl ether 246 with various ketenes.	146
Scheme 2.15. (a) Synthesis and possible mechanisms for the formation of (b) of 266 and 267 from 265 and 238 .	148
Scheme 2.16. Formation and reactivity of cyclobutenone 276 .	150
Scheme 3.1. Retrosynthetic disconnection of hyperforin at two key positions.	192
Scheme 3.2. (a) Retrosynthesis of hyperforin involving C1–C8 bond cleavage and (b) transition-state analysis of the key cyclization reaction.	194
Scheme 3.3. Synthesis of cyclization precursor 292 .	196
Scheme 3.4. Cascade cyclization of 302 to form 303 .	198
Scheme 3.5. Retrosynthesis of cyclization precursor 309 .	199
Scheme 3.6. Deprotonation of 310 led to isolation of 311 .	200
Scheme 3.7. Nonselective prenylation of cyclohexadiene 308 .	200
Scheme 3.8. Synthesis of 309 from 312 and 289 .	203
Scheme 3.9. Cyclization of 309 to 317 .	203
Scheme 3.10. Reaction of a generic iodosobenzene species 323 with TBHP.	207
Scheme 3.11. A plausible radical-based mechanism for the formation of 318 and other oxidation products from 317 .	208
Scheme 3.12. (a) Retrosynthesis of hyperforin (1) from β -methoxyenone 318 via cyclopropane 330 , and (b) a proposed tandem 1,5-addition-bridgehead acylation of 330 to form <i>O-methyl</i> hyperforin (60).	210
Scheme 3.13. (a) Prenylation and cyclic ketal hydrolysis of 318 , and (b) a possible mechanism for the conversion of 333 to 334 .	212

Scheme 3.14. Byproducts isolated from attempted bridgehead lithiations of 338 and 340 .	213
Scheme 3.15. Synthesis and reactivity of 343 derivatives.	214
Scheme 3.16. Synthesis of cyclopropane 353 .	215
Scheme 3.17. Synthesis of cyclopropane 359 and byproducts 363 and 364 .	219
Scheme 3.18. Synthesis of 359 via benzenesulfonate 366 and unsuccessful formation of 369 from 359 .	220
Scheme 3.19. Reactions of iodide 356 .	221
Scheme 3.20. Synthesis and reactivity of methyl ether 376 .	222
Scheme 3.21. Synthesis of triethylsilyl ether 385 .	224
Scheme 3.22. Installation of the C7 prenyl moiety.	225
Scheme 3.23. Reaction of 393 with MeCu(TMP)CNLi ₂ .	226
Scheme 3.24. Bridgehead acylation of 393 .	227
Scheme 3.25. Desilylation and dehydration of 395 to form 398 , and the structure of double bond isomer 399 .	228
Scheme 3.26. Completion of the total synthesis of hyperforin.	229
Scheme 3.27. A possible mechanism for the formation of 400 and 401 from 1 , and structures of laxifloranone and mahureone A.	230

Tables

Table 1.1. Evaluation of PPAPs against gram-positive bacteria.	22
Table 1.2. Evaluation of PPAPs against gram-negative bacteria.	27
Table 1.3. Antiproteolytic activity of several PPAPs.	30
Table 1.4. Evaluation of PPAPs against <i>Plasmodium falciparum</i> .	31
Table 1.5. Evaluation of PPAPs against chloroquine-resistant <i>P. falciparum</i> .	32
Table 1.6. Evaluation of PPAPs against various <i>Leishmania</i> species.	34
Table 1.7. Evaluation of PPAPs against <i>Trypanosoma brucei</i> and <i>T. cruzi</i> .	36
Table 1.8. Evaluation of PPAPs against various fungi.	37

Table 1.9. <i>In vitro</i> PPAP antioxidant activity.	38
Table 1.10. Evaluation of PPAPs against ROS generation.	43
Table 1.11. Evaluation of PPAPs against several markers of inflammation.	45
Table 1.12. 5-LO inhibition activity of semisynthetic hyperforin analogs. ¹⁹¹	50
Table 1.13. Evaluation of PPAPs against cancer cell proliferation.	52
Table 1.14. Inhibition of synaptosomal [³ H]neurotransmitter uptake by hyperforin.	76
Table 1.15. Inhibition of synaptosomal [³ H]neurotransmitter uptake by adhyperforin.	89
Table 1.16. AChE and BChE inhibition activity of several PPAPs.	91
Table 1.17. Hyperforin pharmacokinetics following oral dosing of SJW extracts.	103
Table 1.18. Inhibition of sirtuins by oblongifolin C, hyperforin, and aristofofin. ⁴⁹⁰	107
Table 2.1. Attempted formation of 249 from 246 and 238 .	144
Table 2.2. Attempted formation of 271 from 266 .	148
Table 3.1. Attempted conversion of cyclohexadienone 292 to bicyclo[3.3.1]nonane 293 .	197
Table 3.2. Prenylation of cyclohexadiene 308 .	202
Table 3.3. Allylic oxidation of enol ether 317 .	204
Table 3.4. Attempted formation of 354 from nucleophilic 1,5-additions to 353 .	217
Table 3.5. NMR data comparison of synthetic 60 with 60 derived from natural hyperforin (ref. 309).	333
Table 3.6. ¹ H NMR data comparison of synthetic and natural hyperforin (1).	340
Table 3.7. ¹³ C NMR data comparison of synthetic and natural hyperforin (1).	341

List of Abbreviations

A	alanine
A2780	human ovarian carcinoma cell line
A2780 _{CP}	cisplatin-resistant A2780 cell line
A2780 _{Dox}	doxorubicin-resistant A2780 cell line
A375	human malignant melanoma cell line
A431	human squamous carcinoma cell line
A549	human lung carcinoma cell line
<i>A.</i>	<i>Actinomyces</i>
ABCG1	ATP-binding cassette subfamily G member 1
ABCG2	ATP-binding cassette subfamily G member 2
ABTS	2,2'-azino-bis(3-ethylbenzothiazoline-6-sulphonic acid)
Ac	acetyl
Ac ₂ O	acetic anhydride
ACF	aberrant crypt foci
AChE	acetylcholinesterase
ACP	acyl carrier protein
AGEs	advanced glycation end-products
AGs	human gastric adenocarcinoma cell line
AIBN	2,2'-azobis(2-methylpropionitrile)
AIDS	acquired immunodeficiency syndrome
Akt	protein kinase B
Aliquat 336	tri- <i>n</i> -octylmethylammonium chloride
aq.	aqueous
Ar	aryl
AR42J	rat pancreas cell line

ARIP	Wistar rat pancreatic tumor cell line
AT-2.1	rat prostatic cancer cell line
ATP	adenosine triphosphate
<i>AUC</i>	area under the curve, integration of concentration-time curve
A β	β -amyloid
B16-LU8	murine melanoma cell line
<i>B.</i>	<i>Bacillus</i>
BAE	bovine aortic endothelial cell line
Bax	Bcl-2–associated X protein
BChE	butyrylcholinesterase
Bcl-2	B-cell lymphoma 2
Bcl-xL	B-cell lymphoma-extra large
BCRP	breast cancer resistance protein
BDX2	rat fibrosarcoma cell line
BEt ₃	triethylborane
BF ₃ ·Et ₂ O	boron trifluoride ethyl etherate
BHT	2,6-di- <i>tert</i> -butyl-4-methylphenol
Bn	benzyl
BnEt ₃ NCI	benzyltriethylammonium chloride
Boc	<i>tert</i> -butoxy carbonyl
BPS	benzophenone synthase
BPX	2-butanone peroxide
BrBMe ₂	bromodimethylborane
BrCH ₂ CO ₂ Et	ethyl bromoacetate
Bs	benzenesulfonyl
BsCl	benzenesulfonyl chloride

BT-549	human breast ductal carcinoma cell line
Bu	<i>n</i> -butyl
Bu ₄ N[Fe(CO) ₃ (NO)]	tetrabutylammonium tricarbonylnitrosylferrate
BUS	isobutyrophenone synthase
BXPC-3	human primary pancreatic adenocarcinoma cell line
Bz	benzoyl
BzCl	benzoyl chloride
BzCN	benzoyl cyanide
BzOO <i>t</i> -Bu	<i>tert</i> -butyl peroxybenzoate
C	Celsius
C6	murine glioblastoma cell line
C8166	human T lymphoblastoid cell line
C-26	murine colon adenocarcinoma cell line
ca.	circa
Caco-2	human epithelial colorectal adenocarcinoma cell line
cAMP	cyclic adenosine monophosphate
CAN	ceric ammonium nitrate
cat.	catalyst
CB	cytochalasin B
CBP	CREB-binding protein
CC ₅₀	half maximal cytotoxic concentration
CCD-18Co	human colon fibroblast cell line
CCD-841 CoN	human colon fibroblast cell line
CD	circular dichroism
CD-1	mouse breed originating from Dr. de Coulon at the Centre Anticancereux Romand, Lausanne, Switzerland

CD4	cluster of differentiation 4 glycoprotein
cDNA	complementary DNA
CDP	cytidyl diphosphate
CEM-SS	human lymphoblastoid cell line susceptible to HIV infection
CEMx174-SEAP	human lymphoblastoid cell line containing SEAP reporter gene
<i>c</i> -Hex	cyclohexane
CHP	cumene hydroperoxide
ClC(S)OPh	<i>O</i> -phenyl chlorothionoformate
CLL	chronic lymphocytic leukemia
<i>cLogP</i>	calculated partition coefficient
cm	centimeter
C_{max}	maximum plasma concentration of a drug after administration
CMP	cytidyl monophosphate
Co-115	human colon carcinoma cell line
CoA	coenzyme A
Colo-320-DM	human colon carcinoma cell line
compound 48/80	a polymer of <i>N</i> -methyl- <i>para</i> -methoxyphenethylamine and formaldehyde
COX-1	cyclooxygenase-1
COX-2	cyclooxygenase-2
CpG	consecutive cytosine and guanine nucleotides
cPLA ₂	cytosolic phospholipase A ₂
CREB	cAMP response element-binding protein
CRL-1623	human tongue squamous cell carcinoma cell line
CRL-1624	human squamous cell carcinoma cell line
CRMM-1	human conjunctival melanoma cell line
CRMM-2	human conjunctival melanoma cell line

CrO ₃ ·DMP	chromium(VI) oxide-3,5-dimethylpyrazole
CSA	10-camphorsulfonic acid
CTP	cytidyl triphosphate
CXCR3	chemokine receptor 3
Cy	cyclohexyl
CYP1A1	cytochrome P450, family 1, subfamily A, polypeptide 1
CYP1A2	cytochrome P450, family 1, subfamily A, polypeptide 2
CYP2C9	cytochrome P450, family 2, subfamily C, polypeptide 9
CYP2C19	cytochrome P450, family 2, subfamily C, polypeptide 19
CYP2D6	cytochrome P450, family 2, subfamily D, polypeptide 6
CYP3A	cytochrome P450, family 3, subfamily A
CYP3A4	cytochrome P450, family 3, subfamily A, polypeptide 4
CYP4F2	cytochrome P450, family 4, subfamily F, polypeptide 2
CYP24A1	mitochondrial 1,25-dihydroxyvitamin D ₃ 24-hydroxylase
CYP27B1	25-hydroxyvitamin D ₃ 1- α -hydroxylase
Cy	cyclohexyl
Cys	cysteine
d	days
D	dextrorotatory
DAOY	human desmoplastic cerebellar medulloblastoma cell line
dba	dibenzylideneacetone
DCE	1,2-dichloroethane
DDQ	2,3-dichloro-5,6-dicyano- <i>para</i> -benzoquinone
DFT	density functional theory
DIBAL	di- <i>iso</i> -butylaluminum hydride
DMAP	4-(dimethylamino)pyridine

DME	1,2-dimethoxyethane
DMF	<i>N,N</i> -dimethylformamide
DMP	Dess–Martin periodinane
DMPU	1,3-dimethyl-3,4,5,6-tetrahydro-2-pyrimidinone
DMSO	dimethyl sulfoxide
DNA	deoxyribonucleic acid
DOHH-2	human non-Hodgkin's B-cell lymphoma cell line
L-dopa	L-3,4-dihydroxyphenylalanine
dppf	1,1'-bis(diphenylphosphino)ferrocene
DPPH	2,2-diphenyl-1-picrylhydrazyl
dr	diastereomeric ratio
DTBMP	2,6-di- <i>tert</i> -butyl-4-methylpyridine
DU145	human prostate cancer cell line
DU145 _{MDR}	multidrug-resistant DU145 cell line
<i>E.</i>	<i>Enterococcus</i> or <i>Escherichia</i>
e.g.	exempli gratia
EC ₅₀	half maximal effective concentration
ECD	electronic circular dichroism
ee	enantiomeric excess
EJ	human endometrioid adenocarcinoma cell line from uterine corpus
<i>ent</i>	enantiomer
<i>epi</i>	epimer
equiv	stoichiometric equivalents
ERK	extracellular signal-regulated kinase
Et	ethyl
Et ₂ AlCl	diethylaluminum chloride

Et ₂ AlI	diethylaluminum iodide
Et ₂ O	diethyl ether
EtAlCl ₂	ethylaluminum dichloride
EtOH	ethanol
EtSH	ethanethiol
f	female
FDA	Federal Drug Administration
fMLP	<i>N</i> -formylmethionine leucyl-phenylalanine
FMO5	flavin containing monooxygenase 5
FRAP	ferric reducing ability of plasma
g	gram
G protein	guanine nucleotide-binding protein
GADD153	growth arrest and DNA damage-inducible gene 153
GI ₅₀	half maximal cell growth inhibition concentration
h	hours
<i>H.</i>	<i>Hypericum</i>
H ₂ DCFDA	6-carboxy-2',7'-dichlorodihydrofluorescein diacetate
H3	histone 3
H4	histone 4
HaCaT	human keratinocyte cell line
HAT	histone acetyltransferase
HC(OMe) ₃	trimethyl orthoformate
HCT-116	human colorectal carcinoma cell line
HCT-116 _{MDR}	multidrug-resistant HCT-116 cell line
HCT-8	human ileocecal colorectal adenocarcinoma cell line
HCT-8 _{Ral}	raltitrexed-resistant HCT-8 cell line

HCT-8 _{SN-38}	7-ethyl-10-hydroxycamptothecin-resistant HCT-8 cell line
HD-MY-Z	human Hodgkin's lymphoma cell line
HDAC	histone deacetylase
HDMEC	human dermal microvascular endothelial cell line
HEK293	human embryonic kidney cell line
HEK293T	human embryonic kidney cell line containing the SV40 large T-antigen
HeLa	human cervical carcinoma cell line
HeLa-C3	cisplatin-resistant human cervical carcinoma cell line
Hep3B	human hepatocellular carcinoma cell line
HEp-2	human larynx carcinoma cell line
HepG2	human hepatocellular carcinoma cell line
HFIP	1,1,1,3,3,3-hexafluoro-2-propanol
Hg(OAc) ₂	mercury(II) acetate
HIV	human immunodeficiency virus
HL-60	human promyelocytic leukemia cell cell line
HL-60 _{Dox}	multidrug-resistant HL-60 cell line
HMPA	hexamethylphosphoramide
HN-5	human tongue carcinoma cell line
HNCy ₂	dicyclohexylamine
HOAc	acetic acid
HPLC	high-performance liquid chromatography
HT1080	human fibrosarcoma cell line
HT144	human malignant melanoma cell line
HT-29	human colorectal adenocarcinoma cell line
HT-29 _{5-FU}	5-fluorouracil-resistant HT-29 cell line
HT-29 _{SN-38}	7-ethyl-10-hydroxycamptothecin-resistant HT-29 cell line

HUVEC	human umbilical vein endothelial cell line
i.e.	id est
<i>i</i> -Pr	isopropyl
<i>i</i> -PrBr	2-bromopropane
<i>i</i> -PrC(O)Cl	isobutyryl chloride
<i>i</i> -PrC(O)CN	isobutyryl cyanide
<i>i</i> -PrCHO	isobutyraldehyde
<i>i</i> -PrMgCl	isopropylmagnesium chloride
<i>i</i> -Pr ₂ NEt	<i>N,N</i> -diisopropylethylamine, Hünig's base
IBX	2-iodoxybenzoic acid
IC ₅₀	half maximal inhibitory concentration
ICAM-1	intercellular adhesion molecule-1
IFN- γ	interferon- γ
IL-8	interleukin-8
imid	imidazole
iNOS	inducible nitric oxide synthase
ITGAM	integrin alpha M
IUPAC	International Union of Pure and Applied Chemistry
JNK	activator protein 1 <i>N</i> -terminal kinase
Jurkat	human leukemic T cell leukemia cell line
Jurkat E6-1	human leukemic T cell leukemia cell line
K	lysine
K_i	dissociation constant
K562	human myelogenous leukemia cell line
K562 _{ADR}	adriamycin-resistant K562 cell line
KB	HeLa contaminated nasopharyngeal carcinoma cell line

KB _{vin}	Vincristine-resistant KB cell line
KE-37	human acute lymphoblastic T cell leukemia cell line
KELLY	human neuroblastoma cell line
kg	kilogram
KG-1	human acute myelogenous leukemia cell line
KHMDS	potassium hexamethyldisilazide
KOt-Bu	potassium <i>tert</i> -butoxide
L	levorotatory
L-(+)-DET	(+)-diethyl L-tartrate
<i>L.</i>	<i>Listeria</i> or <i>Leishmania</i>
L6	rat skeletal muscle cells
LA	Lewis acid (generic)
LAH	lithium aluminum hydride
LAMA-84	human chronic myeloid leukemia cell line
LAN-1	human neuroblastoma cell line
LAN-1 _{5-FU}	5-fluorouracil-resistant LAN-1 cell line
LAN-1 _{ADR}	adriamycin-resistant LAN-1 cell line
LAN-1 _{CP}	cisplatin-resistant LAN-1 cell line
LAN-1 _{ETO}	etoposide-resistant LAN-1 cell line
LD ₅₀	median lethal dose
LDA	lithium di- <i>iso</i> -propylamide
LDL	low-density lipoprotein
Leu	leucine
LHMDS	lithium hexamethyldisilazide
Li(2-Th)CuCN	lithium (2-thienyl)cyanocopper(I)
LiNEt ₂	lithium diethylamide

LiTMP	lithium 2,2,6,6-tetramethylpiperidide
LN-229	human glioblastoma cell line
LNCaP	androgen-sensitive human prostate adenocarcinoma cell line
LNCaP _{ETO}	etoposide-resistant LNCaP cell line
LOE 908	3,4-dihydro-6,7-dimethoxy- α -phenyl- <i>N,N</i> -bis[2-(2,3,4-trimethoxyphenyl)ethyl]-1-isoquinolineacetamide hydrochloride
LPS	lipopolysaccharides
LS180	human intestinal colon adenocarcinoma cell line
LXR	liver X receptor
M	male or molar
M51	human stomach carcinoma cell line
M51 _{CP}	cisplatin-resistant M51 cell line
MAO	monoamine oxidase
MAPK	mitogen-activated protein kinase
MAPKAPK-2	mitogen-activated protein kinase activated protein kinase 2
MAT-Lu	human stomach carcinoma cell line
MBTE	methyl <i>tert</i> -butyl ether
MC ₁₀₀	maximal cytotoxic concentration
MCF 10A	human breast fibrocystic disease cell line
MCF-7	human breast cancer cell line
MCF-7 _{5-FU}	5-fluorouracil-resistant MCF-7 cell line
MCF-7 _{Dox}	doxorubicin-resistant MCF-7 cell line
MCF-7 _{HER2}	MCF-7 cell line overexpressing human epidermal growth factor receptor 2
MDA-MB-231	human breast adenocarcinoma cell line
MDA-MB-468	human breast adenocarcinoma cell line
MDCK	Madin–Darby canine kidney epithelial cells

Me	methyl
Me ₂ S	dimethylsulfide
Me ₂ SO ₄	dimethyl sulfate
Me ₃ Al	trimethylaluminum
MeCN	acetonitrile
MeCu(TMP)CNLi ₂	dilithium (cyano-κC)methyl(2,2,6,6-tetramethyl-1-piperidiny)l)copper
MEF	mouse embryonic fibroblasts
MeI	iodomethane
MeOH	methanol
Mes	2,4,6-trimethylphenyl
MeSO ₂ NH ₂	methanesulfonamide
MFC	minimum fungicidal concentration
MH1C1	rat liver hepatoma cell line
MIA PaCa-2	human pancreas carcinoma cell line
MIHA	human liver cell line
min	minutes
mg	milligram
MIC	minimum inhibitory concentration
mL	milliliters
MLL	myeloid lymphoid leukemia
mm	millimeter
mmol	millimoles
MMP-2	matrix metalloproteinase-2
MMP-9	matrix metalloproteinase-9
Mn(OAc) ₃	manganese(III) acetate
MOM	methoxymethyl

MOMCl	chloromethyl methether ether
mPGES-1	membrane-associated prostaglandin E synthetase-1
MRC-5	human fetal lung fibroblast-like cell line
mRNA	messenger RNA
MS	molecular sieves
Ms	methanesulfonyl
MsCl	methanesulfonyl chloride
MS-G2	human hepatoma cell line
MT-4	CD4+ human lymphocyte cell line
MT-450	rat breast carcinoma cell line
MV3	human melanoma cell line
N9	murine microglial cell line
n.d.	no data
NADPH	nicotinamide adenine dinucleotide phosphate
NaHMDS	sodium bis(trimethylsilyl)amide
NaOEt	sodium ethoxide
NaOMe	sodium methoxide
NB4	human promyelocytic leukemia cell line
NB69	human stage III neuroblastoma cell line
NBT-II	Wistar rat bladder carcinoma cell line
NCI-ADR	human multidrug-resistant breast carcinoma cell line
NCI-H2126	human non-small cell lung adenocarcinoma cell line
NCI-H292	human mucoepidermoid pulmonary carcinoma cell line
NCI-H460	human large cell lung cancer cell line
NEt ₃	triethylamine
Neuro-2a	human neuroblastoma cell line

NF- κ B	nuclear factor kappa-light-chain-enhancer of activated B cells
ng	nanogram
NHA	human astrocyte cell line
NHS	<i>N</i> -hydroxysuccinimide
NIH	National Institutes of Health
NIH-3T3	murine embryonic fibroblast cell line
nM	nanomolar
nm	nanometer
NMDA	<i>N</i> -methyl-D-aspartate
NMO	4-methylmorpholine <i>N</i> -oxide
NQO2	nicotinamide adenine dinucleotide dehydrogenase, quinone 1
Noxa	phorbol-12-myristate-13-acetate-induced protein 1
NTUB1	human bladder carcinoma cell line
OAc	acetate
OP	phosphate
OPP	pyrophosphate or diphosphate
ORAC	oxygen radical absorbance capacity
Tf	trifluoromethanesulfonyl
Tf ₂ O	trifluoromethanesulfonic anhydride
OVCAR 03	human ovarian carcinoma cell line
OZ	opsonized zymosan
<i>p</i>	<i>para</i>
P388	murine leukemia cell line
p53	tumor protein 53
<i>P.</i>	<i>Plasmodium</i>
P-gp	P-glycoprotein 1

<i>p</i> -TsOH	<i>para</i> -toluenesulfonic acid
P(OMe) ₃	trimethyl phosphite
PANC-1	human pancreatic epithelioid carcinoma cell line
Pb(OAc) ₄	lead(IV) acetate
PBCEC	porcine brain capillary endothelial cell line
PBu ₃	tributylphosphine
PC-3	human prostate cancer cell line
PC-3 _{ETO}	etoposide-resistant PC-3 cell line
PC12	rat adrenal medulla pheochromocytoma cell line
PCAF	p300/CBP-associated factor
Pd ₂ (dba) ₃	tris(dibenzylideneacetone)dipalladium(0)
Pd(OAc) ₂	palladium(II) acetate
Pd(OH) ₂ /C	Pearlman's catalyst
PDC	pyridinium dichromate
PdCl ₂ (PPh ₃) ₂	bis(triphenylphosphine)palladium(II) dichloride
PDGFR	platelet-derived growth factor receptor
pentOAc	amyl acetate
Ph	phenyl
PhCl	chlorobenzene
Phe	phenylalanine
PhI	iodobenzene
PhI(OAc) ₂	(diacetoxyiodo)benzene
PhI(TFA) ₂	[bis(trifluoroacetoxy)iodo]benzene
PhIO	iodosobenzene
PhIO ₂	iodylbenzene
PhMe	toluene

PhNCO	phenyl isocyanate
PhNEt ₂	<i>N,N</i> -diethylaniline
PI3K	phosphatidylinositol 3-kinase
Piv	pivaloyl
PivCl	pivaloyl chloride
p <i>K</i> _a	logarithmic acid dissociation constant
PKB	protein kinase B
PKS	polyketide synthase
PMA	phorbol 12-myristate 13-acetate
PMN	human polymorphonuclear leukocyte
pmol	picomole
PPAP	polycyclic polyprenylated acylphloroglucinol
PPh ₃	triphenylphosphine
PPh ₃ CH ₃ Br	methyltriphenylphosphonium bromide
PPTS	pyridinium <i>para</i> -toluenesulfonate
PrCO ₂ Bu	<i>n</i> -butyl butyrate
pUC-19	plasmid cloning vector originating from the University of California
PXR	pregnane X receptor
pyr	pyridine
Pyr3	ethyl-1-(4-(2,3,3-trichloroacrylamide)phenyl)-5-(trifluoromethyl)-1H-pyrazole-4-carboxylate
RAW264.7	murine macrophage cell line
reag.	reagent
ref(s).	reference(s)
RG2	rat glioblastoma cell line
Rh ₂ (cap) ₄	dirhodium(II) caprolactamate

RNA	ribonucleic acid
ROS	reactive oxygen species
rt	room temperature
s	seconds
<i>S.</i>	<i>Staphylococcus</i>
<i>s</i> -Bu	<i>sec</i> -butyl
<i>s</i> -BuLi	<i>sec</i> -butyllithium
Saos-2	human primary osteosarcoma cell line
sat.	saturated
SB1	human melanoma cell line
SB3	human melanoma cell line
SCoA	coenzyme A
Sc(OTf) ₃	scandium(III) trifluoromethanesulfonate
SEAP	secreted alkaline phosphatase
SF-268	human highly anaplastic astrocytoma cell line
SGC-7901	human gastric adenocarcinoma cell line
SIRT1	sirtuin 1
SIRT2	sirtuin 2
SIV	simian immunodeficiency virus
SJW	St. John's wort (<i>Hypericum perforatum</i>)
SK-N-AS	human neuroblastoma cell line
SK-N-BE	human neuroblastoma cell line
SK-OV-3	human ovarian adenocarcinoma cell line
SKF-96365	1-[2-(4-methoxyphenyl)-2-[3-(4-methoxyphenyl)propoxy]ethyl]imidazole, 1-[β-(3-(4-methoxyphenyl)propoxy)-4-methoxyphenethyl]-1H-imidazole hydrochloride

SKW-3	human T cell leukemia cell line
SMMC-7721	human hepatocellular carcinoma cell line
<i>sn</i>	stereospecifically numbered, as in positions of glycerol derivatives
Sn(OTf) ₂	tin(II) trifluoromethanesulfonate
SOCE	store-operated Ca ²⁺ entry
SR12813	tetraethyl 2-(3,5-di- <i>tert</i> -butyl-4-hydroxyphenyl)ethenyl-1,1-bisphosphonate
St.	Saint
STAT-1	signal transducer and activator of transcription-1
STAT-3	signal transducer and activator of transcription-3
<i>Strept.</i>	<i>Streptomyces</i>
SV40	simian vacuolating virus 40
SW480	human colon adenocarcinoma cell line
<i>t</i> _{1/2}	elimination half-life
T24	human bladder carcinoma cell line
T84	human colon carcinoma cell line
<i>T.</i>	<i>Trypanosoma</i>
<i>t</i> -AmOK	potassium <i>tert</i> -pentoxide
T-box	a group of transcription factors involved in limb and heart development
<i>t</i> -Bu	<i>tert</i> -butyl
<i>t</i> -BuLi	<i>tert</i> -butyllithium
<i>t</i> -BuOH	<i>tert</i> -butanol
<i>t</i> -BuOK	potassium <i>tert</i> -butoxide
TBAF	tetrabutylammonium fluoride
TBAI	tetrabutylammonium iodide
TBARS	thiobarbituric acid reactive species
TBHP	<i>tert</i> -butyl hydroperoxide

TBS	<i>tert</i> -butyldimethylsilyl
TBSCl	<i>tert</i> -butyldimethylsilyl chloride
TBSOTf	<i>tert</i> -butyldimethylsilyl trifluoromethanesulfonate
TC ₅₀	half maximal cytotoxicity
TEAC	Trolox equivalent antioxidant capacity
TEMPO	2,2,6,6-tetramethylpiperidine 1-oxyl
TES	triethylsilyl
TESCl	chlorotriethylsilane
TESOTf	triethylsilyl trifluoromethanesulfonate
TFAA	trifluoroacetic anhydride
Th	thienyl
THF	tetrahydrofuran
Thr	threonine
Ti(O <i>i</i> -Pr) ₄	titanium(IV) isopropoxide
TIPSOTf	triisopropylsilyl trifluoromethanesulfonate
<i>t</i> _{max}	time to achieve <i>C</i> _{max}
TMEDA	<i>N,N,N',N'</i> -tetramethylethylenediamine
TMP	2,2,6,6-tetramethylpiperidide
TMS	trimethylsilyl
TMSCl	chlorotrimethylsilane
TMSI	iodotrimethylsilane
TMSOTf	trimethylsilyl trifluoromethanesulfonate
TMSN ₃	trimethylsilyl azide
TNF	tumor necrosis factor
TNF- α	tumor necrosis factor- α
TPAP	tetra- <i>n</i> -propylammonium perruthenate

TPEN	<i>N,N,N',N'</i> -tetrakis(2-pyridylmethyl)ethylenediamine
TPP	thiamine pyrophosphate
TRAIL	TNF-related apoptosis-inducing ligand
TRAMP-C1	murine prostate adenocarcinoma cell line
TrkB	neurotrophic tyrosine kinase receptor, type 2
Trolox	6-hydroxy-2,5,7,8-tetramethylchroman-2-carboxylic acid
TRPC	canonical transient potential protein channel
TRPC3	canonical transient potential protein channel, member 3
TRPC6	canonical transient potential protein channel, member 6
TRPC7	canonical transient potential protein channel, member 7
Ts	<i>para</i> -toluenesulfonyl
U	uniform isotopic labeling
U251	human neuronal glioblastoma cell line
U266	human B cell malignant myeloma cell line
U87	human primary glioblastoma cell line
U937	human histiocytic leukemia cell line
UACC-62	human malignant melanoma cell line
VEGF	vascular endothelial growth factor
VERO	kidney epithelial cell line originating from an African green monkey
VPS	phlorisovalerophenone synthase
W	tryptophan
w/v	weight over volume
WRL-68	human liver carcinoma cell line
wt%	percentage by weight
XO	xanthine oxidase

Z-DEVD-FMK	<i>N</i> -benzyloxycarbonyl-aspartic acid(<i>O</i> -Me)-glutamate(<i>O</i> -Me)-valine-aspartic acid (<i>O</i> -Me)-fluoromethylketone
Z-VAD-FMK	<i>N</i> -benzyloxycarbonyl-valine-alanine-aspartic acid-(<i>O</i> -Me) fluoromethyl ketone
Zn(OTf) ₂	zinc trifluoromethanesulfonate
1F6	human melanoma cell line
3T3-L1	murine preadipocyte cell line
3T3.T4.CCR5	CD4+ human fibroblast cell line
5-LO	5-lipoxygenase
5-HT ₂	serotonin receptor, subfamily 2
5637	human stage II bladder carcinoma cell line
786-0	human renal cell adenocarcinoma cell line
μg	microgram
μL	microliter
μM	micromolar
μm	micrometer
μmol	micromole
μwave	microwave irradiation
(DHQD) ₂ PHAL	hydroquinidine 1,4-phthalazinediyl diether
(PhSe) ₂	diphenyl diselenide
(Sia) ₂ BH	bis(1,2-dimethylpropyl)borane
(<i>S</i>)-tol-BINAP	(<i>S</i>)-(-)-2,2'- <i>para</i> -tolyl-phosphino)-1,1'-binaphthyl
(TMS) ₃ SiH	tris(trimethylsilyl)silane
[O]	oxidation

Chapter 1

Polycyclic Polyprenylated Acylphloroglucinols: An Overview

Overview

In 1971, a group of Soviet scientists studying the antibacterial properties of St. John's wort (*Hypericum perforatum*, SJW) reported the discovery of a natural product hyperforin (**1**, Figure 1.1) from the medicinal herb's alcoholic extract.¹ Using extensive chemical degradation methods, the flat structure of hyperforin was deduced four years later.² Concurrent to these studies was the isolation and X-ray crystallography-guided elucidation of isoxanthochymol (**2**) from the Indian gamboge (*Garcinia xanthochymus*).³ Hyperforin and isoxanthochymol are the founding and prototypical members of a sprawling natural product family known as the polycyclic polyprenylated acylphloroglucinols (PPAPs),⁴ of which there are 260 members to date.

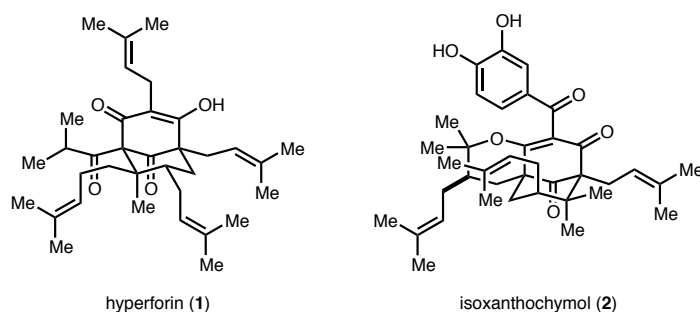


Figure 1.1. Structures of hyperforin (**1**) and isoxanthochymol (**2**).

¹ Gurevic, A. I.; Dobrynin, V. N.; Kolosov, M. N.; Popravko, S. A.; Ryabova, I. D.; Chernov, B. K.; Derbentseva, N. A.; Aizenman, B. E.; Garagulya, A. D. *Antibiotiki* **1971**, *16*, 510-513.

² Bystrov, N. S.; Chernov, B. K.; Dobrynin, V. N.; Kolosov, M. N. *Tetrahedron Lett.* **1975**, *16*, 2791-2794.

³ Karajgoaker, C. G.; Rama Rao, A. V.; Venkataraman, K.; Yemul, S. S.; Palmer, K. J. *Tetrahedron Lett.* **1973**, *14*, 4977-4980.

⁴ For reviews on the structural diversity of PPAP natural products, see: (a) Cuesta-Rubio, O.; Piccinelli, A. L.; Rastrelli, L. *Stud. Nat. Prod. Chem.* **2005**, *32*, 671-720. (b) Baggett, S.; Mazzola, E. P.; Kennelly, E. J. *Stud. Nat. Prod. Chem.* **2005**, *32*, 721-771. (c) Ciochina, R.; Grossman, R. B. *Chem. Rev.* **2006**, *106*, 3963-3986. (d) Singh, I. P.; Bharate, S. B. *Nat. Prod. Rep.* **2006**, *23*, 558-591.

A PPAP natural product may be defined as a bicyclo[3.3.1]nonane (or a larger bridged polycyclic containing a bicyclo[3.3.1]nonane element) bearing a C9 ketone (Figure 1.2).^{5,6} Aside from the C9 position, oxidation is also found at the C2 and C4 positions, and in approximately 80% of PPAPs, these two oxidation sites are conjugated through C3 to form a β -hydroxyenone or β -alkoxyenone functionality array. The periphery of this carbocyclic core is decorated with multiple isoprenoid groups at the C1, C3, C5, C7, and C8 positions. In the great majority of instances, these substituents are derived from the following parent isoprenoids: prenyl in 75% of substituents; lavandulyl in 10% of substituents; and geranyl in 7.5% of substituents. These isoprenoid substituents undergo secondary cyclization to form additional oxacyclic and carbocyclic rings in many PPAPs. Nearly all of these natural products contain a quaternary center at the C8 position, and in 81% of PPAPs, this position is substituted with two methyl groups.

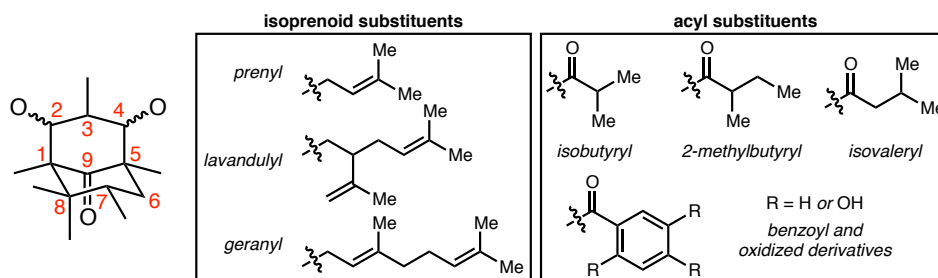


Figure 1.2. Generic PPAP skeleton and typical substituents.

⁵ The general method of PPAP numbering used throughout is in accordance with IUPAC guidelines for bicyclic compounds. For more information, see: Moss, G. P. *Pure Appl. Chem.* **1999**, *71*, 513-529.

⁶ This definition excludes certain polycyclic polyprenylated acylphloroglucinol natural products that do not contain a bicyclo[3.3.1]nonane subunit. For examples of “atypical PPAPs,” see: (a) Winkelmann, K.; Heilmann, J.; Zerbe, O.; Rali, T.; Sticher, O. *J. Nat. Prod.* **2000**, *63*, 104-108 (ialibinone A-E). (b) Wu, J.; Cheng, X.-F.; Harrison, L. J.; Goh, S.-H.; Sim, K.-Y. *Tetrahedron Lett.* **2004**, *45*, 9657-9659 (perforatumone). (c) Thoison, O.; Cuong, D. D.; Gramain, A.; Chiaroni, A.; Van Hung, N.; Sévenet, T. *Tetrahedron* **2005**, *61*, 8529-8525 (garcibracteaton). (d) Tanaka, N.; Kashiwada, Y.; Sekiya, M.; Ikeshiro, Y.; Takaishi, Y. *Tetrahedron Lett.* **2008**, *49*, 2799-2803 (takaneone A-C). (e) Yang, X.-W.; Deng, X.; Liu, X.; Wu, C.-Y.; Li, X.-N.; Wu, B.; Luo, H.-R.; Li, Y.; Xu, H.-X.; Zhao, Q.-S.; Xu, G. *Chem. Commun.* **2012**, *48*, 5998-6000 (hypercohin A).

The placement of an acyl group around the bicyclic ring system is used to classify PPAPs into three different subgroups: (1) “Type A” PPAPs contain a C1 acyl substituent; (2) “Type B” PPAPs contain a C3 acyl substituent; and (3) “Type C” PPAPs contain a C5 acyl substituent. Approximately 52% of PPAPs are Type A, and 46% are Type B. There are only three known Type C PPAPs, and an additional three PPAPs lack acyl substitution all together. When an acyl group is present, it is either an isobutyryl (15%), 2-methylbutyryl (6%), isovaleryl (1.5%), benzoyl (36.5%), or an oxidized benzoyl (41%) group. A comprehensive listing of all published PPAPs with references to chemotaxonomical, geographical, and spectroscopic data is found in Appendix A.

Stereochemistry

The absolute configurations of only a few PPAP natural products have been ascertained. Since the most electron-rich atom found in all PPAPs is oxygen, anomalous scattering is not normally large enough to permit the refinement of the Flack parameter⁷ and thus absolute configuration during X-ray diffraction analysis. To circumvent this issue, the crystal structures of PPAPs that have been appended with various brominated groups have been resolved, which now contain atoms with sufficient electron density to allow determination of the Flack parameter. The absolute configurations of hyperforin,⁸ isogarcinol,⁹ isoxanthochymol,¹⁰ and xanthochymol^{10,11} have been solved using this methodology. Recent advancements using Bijvoet pair analysis and subsequent determination of the Hooft parameter allows for the determination of absolute structure at low temperatures without requiring the presence of heavy atoms.¹² The absolute configuration of 7-*epi*-clusianone has been solved in this manner.¹³

⁷ Flack, H. D. *Acta. Cryst.* **1983**, *A39*, 876-881.

⁸ Brondz, I.; Greibrokk, T.; Groth, P.; Aasen, A. J. *Acta Chem. Scand. A* **1983**, *37*, 263-265.

⁹ Marti, G.; Eparvier, V.; Moretti, C.; Susplugas, S.; Prado, S.; Grellier, P.; Retailleau, P.; Guéritte, F.; Litaudon, M. *Phytochemistry* **2009**, *70*, 75-85.

¹⁰ Venkatswamy, G.; Yemul, S. S.; Rama Rao, A. V.; Palmer, K. J. *Indian J. Chem.* **1975**, *13*, 1355-1355.

¹¹ Blount, J. F.; Williams, T. H. *Tetrahedron Lett.* **1976**, *17*, 2921-2924.

¹² Hooft, R. W. W.; Straver, L. H.; Spek, A. L. *J. Appl. Cryst.* **2008**, *41*, 96-103.

The absolute configurations of several PPAPs have been determined through comparison of spectroscopic data and direct semisynthetic conversion. Isoxanthochymol and isogarcinol have identical spectroscopic properties except for optical rotations of opposite sign. Through the observation of similar Cotton effects in the circular dichroism (CD) spectra of isogarcinol, the absolute configuration of isogarcinol 13-*O*-methyl ether¹⁴ and 13,14-didehydroxyisogarcinol¹⁵ were determined. The absolute configuration of guttiferone E (and thus its enantiomer, garcinol) was determined through acid- and heat-mediated conversion to isoxanthochymol (**2**).¹⁶ Ozonolysis of sinaicone produced the previously characterized (2*R*,4*R*)-2,4-dimethylhexanoic acid.¹⁷ Through comparison of CD spectra with computed electronic circular dichroism (ECD) spectra calculated using density functional theory (DFT), the absolute configurations of 7-*epi*-guttiferone J,¹⁸ oxy-guttiferone K,¹⁹ guttiferone M,¹⁹ 32-hydroxy-*ent*-guttiferone M¹⁸ have been determined.

In addition, several PPAPs have been isolated in both enantiomeric forms. Specifically, these enantiomeric pairs are: chamuangone (cowanone) and guttiferone Q; cycloxanthochymol and *ent*-cycloxanthochymol; garcinialiptone A and *ent*-garcinialiptone A; garcinielliptone I and hyperibone A; garcinol and guttiferone E; guttiferone G (guttiferone I2) and oblongifolin C; guttiferone O2 and oblongifolin F; hyperibone G and propolone D; isogarcinol and isoxanthochymol; and samponione G and *ent*-samponione G.

¹³ Christian, O. E.; Fronczek, F. R.; Ky, K.; Pradham, S.; Manandhar, A.; Richmond, C. *Acta Cryst.* **2012**, E68, o3222-o3223.

¹⁴ Ito, C.; Itoigawa, M.; Miyamoto, Y.; Onoda, S.; Rao, K. S.; Mukainaka, T.; Tokuda, H.; Nishino, H.; Furukawa, H. *J. Nat. Prod.* **2003**, 66, 206-209.

¹⁵ Chen, J.-J.; Ting, C.-W.; Hwang, T.-L.; Chen, I.-C. *J. Nat. Prod.* **2009**, 72, 253-258.

¹⁶ Gustafson, K. R.; Blunt, J. W.; Munro, M. H. G.; Fuller, R. W.; McKee, T. C.; Cardellina, J. H., II; McMahon, J. B.; Cragg, G. M.; Boyd, M. R. *Tetrahedron* **1992**, 48, 10093-10102.

¹⁷ Řezanka, T.; Sigler, K. *Phytochemistry* **2007**, 68, 1272-1276.

¹⁸ Acuña, U. M.; Figueroa, M.; Kavalier, A.; Jancovski, N.; Basile, M. J.; Kennelly, E. J. *J. Nat. Prod.* **2010**, 73, 1775-1779.

¹⁹ Masullo, M.; Bassarello, C.; Bifulco, G.; Piacente, S. *Tetrahedron* **2010**, 66, 139-145.

Distribution

PPAPs have been isolated from 128 different plant species spanning 18 different genii in 6 different families. The great majority (257 out of 260) of PPAPs have been isolated from plants from the Clusiaceae (Guttiferae) and Hypericeae families, members of the Malpighiales order.^{20,21} The genii *Clusia*, *Garcinia*, and *Hypericum* are particularly prolific, having PPAPs isolated from 132 different subordinate species.²² Many PPAPs have been observed in multiple species; hyperforin alone has been detected in 38 distinct species.²³ Only five PPAPs have been isolated outside of the Clusiaceae and Hypericeae families (Figure 1.3): dorstenpictanone (**3**) from *Dorstenia picta* (Moraceae);²⁴ spiranthenones A-B (**4,5**) from *Spiranthera odoratissima* (Rutaceae);²⁵ xanthochymol (**6**) from *Endodesmia calophylloides* (Calophyllaceae);²⁶ and hyperforin (**1**) has been isolated from *Apocynum venetum* (Apocynaceae)²⁷ and from *Scutellaria baicalensis* (Lamiaceae).²⁸

²⁰ Hypericeae has traditionally been regarded as a separate family, but recent phylogenetic analysis based on the chloroplast gene *rbcL* has shown that it can be classified as a tribe (i.e., Hypericoideae) of the Clusiaceae family. For more information, see: Gustafsson, M. H. G.; Bittrich, V.; Stevens, P. F. *Int. J. Plant Sci.* **2002**, *163*, 1045-1054.

²¹ Wurdack, K. J.; Davis, C. C. *Am. J. Bot.* **2009**, *96*, 1551-1570.

²² For reviews of phytochemical and therapeutic aspects of the PPAPs from these genii, see: (a) Cuesta-Rubio, O.; Piccinelli, A. L.; Rastrelli, L. *Stud. Nat. Prod. Chem.* **2005**, *32*, 671-720. (b) Hemshekhar, M.; Sunitha, K.; Santhosh, M. S.; Devaraja, S.; Kemparaju, K.; Vishwanath, B. S.; Niranjana, S. R.; Girish, K. S. *Phytochem. Rev.* **2011**, *10*, 325-351.

²³ For a review of the distribution of hyperforin amongst *Hypericum* species, see: Stojanović, G.; Đorđević, A.; Šmelcerović, A. *Curr. Med. Chem.* **2013**, *20*, 2273-2295.

²⁴ Hussain, H.; Vouffo, B.; Dongo, E.; Riaz, M.; Krohn, K. *J. Asian Nat. Prod. Res.* **2011**, *13*, 547-550.

²⁵ Albernaz, L. C.; Deville, A.; Dubost, L.; de Paula, J. E.; Bodo, B.; Grellier, P.; Espindola, L. S.; Mambu, L. *Planta Med.* **2012**, *78*, 459-464.

²⁶ Talontsi, F. M.; Islam, M. T.; Facey, P.; Douanla-Meli, C.; von Tiedemann, A.; Laatsch, H. *Phytochem. Lett.* **2012**, *5*, 657-664.

²⁷ Zheng, M.; Fan, Y.; Shi, D.; Liu, C. *J. Ethnopharmacol.* **2013**, *147*, 108-113.

²⁸ Murch, S. J.; Rupasinghe, H. P. V.; Goodenowe, D.; Saxena, P. K. *Plant Cell Rep.* **2004**, *23*, 419-425.

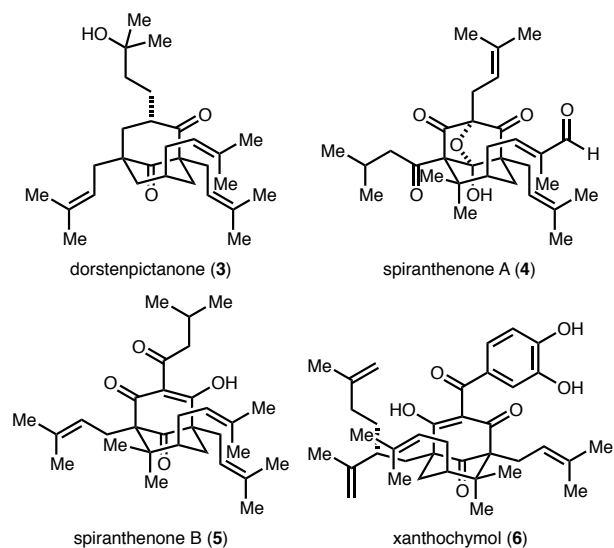


Figure 1.3. Structures of dorstenpictanone (3), spiranthenone A-B (4,5), and xanthochymol (6).

While most species of the Clusiaceae family are found in tropical regions, Hypericeae species are found in temperate climates. Given the fact that most PPAPs exhibit some degree of antibacterial properties, it is unsurprising that these compounds are isolated from the flowers and fruit rinds of these species, protecting vulnerable and sexually important organs from bacterial parasites. Hyperforin may exist in concentrations up to 11% in the flowering parts of *Hypericum perforatum*,²⁹ and its concentration generally decreases as the flowers develop and mature.³⁰ Moreover, PPAPs are also found in the latex of many Clusiaceae species, protecting against the development of infections in injuries to these plants. Garcinol (7) and isogarcinol (8) were initially isolated in “surprisingly in large quantities” from the latex of *Garcinia cambogia*; garcinol comprised 37% of total mass of this material (Figure 1.4).³¹

²⁹ Bergonzi, M. C.; Bilia, A. R.; Gallori, S.; Guerrini, D.; Vincieri, F. F. *Drug Dev. Ind. Pharm.* **2001**, *27*, 491-497.

³⁰ Büter, K. B.; Büter, B. *J. Herbs Spices Med. Plants* **2002**, *9*, 95-100.

³¹ Rao, A. V. R.; Venkatswamy, G.; Pendse, A. D. *Tetrahedron Lett.* **1980**, *21*, 1975-1978.

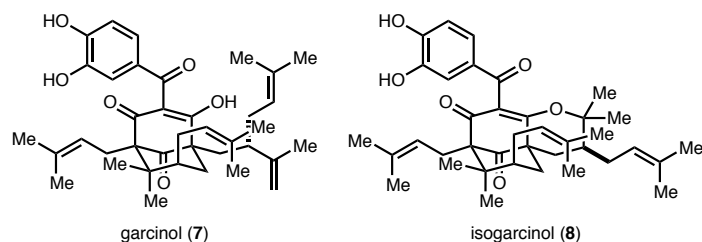


Figure 1.4. Structures of garcinol (7) and isogarcinol (8).

Species of both the Clusiaceae and Hypericeae families are also noted for their high degree of evolutionary plasticity, and this may be a direct result of adaptation to different methods of pollination. Further, while most flowers in general use nectar and pollen as pollinator rewards, a unique adaptation and defining feature of flowering plants from the Clusiaceae family is the additional use of resins as rewards. Certain honeybees will use these resins to create a material known as propolis, which is used to patch holes in their hives as well as to embalm the carcasses of intruders. Propolis is used widely in a variety of folk medicines, and its application traces back to the ancient Egyptians who used this substance in cadaver mummification.³² The contents of propolis vary according to geography and climate, and PPAPs are the dominant chemicals found in the propolis of New World bee colonies from as far north as the Caribbean islands to as far south as central Brazil. It is interesting to note that while the majority of the 25 distinct PPAPs that have been isolated from these propolis have also been found in nearby flora, the plant source of 7 propolis PPAPs have not been identified.

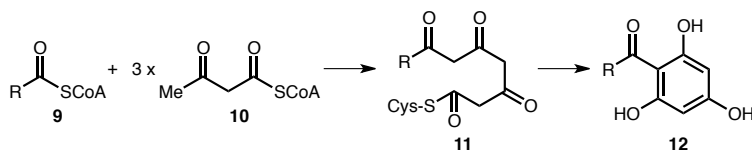
Biosynthesis

Very little evidence beyond conjecture is known specifically about PPAP biosynthesis. The only PPAP that has undergone any biosynthetic experimental scrutiny is hyperforin (1); however, several generalizations about PPAP biosynthesis can be extrapolated from these studies. In general, the biosynthesis of PPAPs can be broken down into three distinct phases: (1) polyketide synthesis of an

³² For reviews on propolis, see: (a) Salatino, A.; Teixeira, É. W.; Negri, G.; Message, D. *Evid. Based Complement. Alternat. Med.* **2005**, 2, 33-38. (b) Miguel, M. G.; Antunes, M. D. *J. Pharm. Bioallied Sci.* **2011**, 3, 479-495. (c) Watanabe, M. A. E.; Amarante, M. K.; Conti, B. J.; Sforcin, J. M. *J. Pharm. Pharmacol.* **2011**, 63, 1378-1386. (d) Salatino, A.; Fernandes-Silva, C. C.; Righi, A. A.; Salatino, M. L. F. *Nat. Prod. Rep.* **2011**, 28, 925-936.

acylphloroglucinol precursor; (2) alkylation of this core with isoprenoid side chains and subsequent cyclization to form the characteristic bicyclo[3.3.1]nonane core of PPAPs; and (3) secondary cyclizations, oxidations, and rearrangements.

The first step in PPAP biosynthesis involves the stepwise, decarboxylative condensation of an alkoyl-SCoA or an aroyl-SCoA group (**9**) with three molecules of malonyl-CoA (**10**, Scheme 1.1). This enzyme-bound linear tetraketide (**11**) then undergoes an intramolecular Claisen cyclization to form an acylphloroglucinol (**12**). The enzymes that catalyze these reactions are members of the type III polyketide synthase (PKS) superfamily. While type I and II PKSs contain acyl carrier proteins (ACPs) that shuttle the growing polyketide across modular functional domains (e.g., ketoreductase and dehydratase), type III PKSs lack ACPs and contain a single active site in which the growing polyketide chain is anchored.³³



Scheme 1.1. The first steps in PPAP biosynthesis.

All known type III PKSs are homodimers and contain a highly conserved cysteine-histidine-asparagine catalytic triad within the active site of each monomer.³⁴ The cysteine acts as the polyketide attachment site, and the histidine and asparagine residues play critical roles in the decarboxylation of malonyl-CoA during chain extension. Additionally, two generally conserved phenylalanine residues near the entrance of the active site facilitate some degree of substrate specificity; however, PKSs in general poorly differentiate starter units *in vitro* and rely upon compartmentalization within plant tissue and cells

³³ For reviews of type III PKS, see: (a) Flores-Sanchez, I. J.; Verpoorte, R. *Plant Physiol. Biochem.* **2009**, *47*, 167-174. (b) Beerhues, L.; Liu, B. *Phytochemistry* **2009**, *70*, 1719-1727.

³⁴ Jez, J. M.; Bowman, M. E.; Noel, J. P. *Proc. Natl. Acad. Sci. USA* **2002**, *99*, 5319-5324.

to engender a high degree of substrate selectivity.^{33a} For PPAPs such as hyperforin (**1**) containing an isopropyl ketone moiety, isobutyrophenone synthase (BUS) is used to synthesize phlorisobutyrophenone (**13**, Figure 1.5). PPAPs containing phenyl and isobutyl ketones utilize benzophenone synthase (BPS) and phlorisovalerophenone synthase (VPS) to synthesize 2,4,6-trihydroxybenzophenone (**14**) and phlorisovalerophenone (**15**), respectively. Only two PKS systems utilized in PPAP biosynthesis have been characterized: the hyperforin and adhyperforin BUS from *Hypericum calycinum*³⁵ and the hyperandrone A BPS from *Hypericum androsaemum*.³⁶ In addition, the gene responsible the PKS involved in hyperforin and adhyperforin biosynthesis in *Hypericum perforatum*, named *HpPKS1*, has also been characterized.³⁷

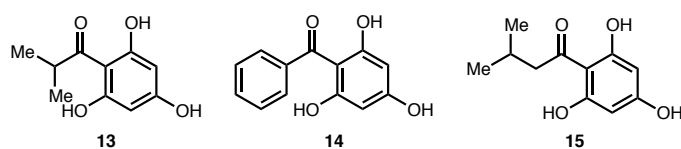


Figure 1.5. Specific examples of intervening acylphloroglucinols in PPAP biosynthesis.

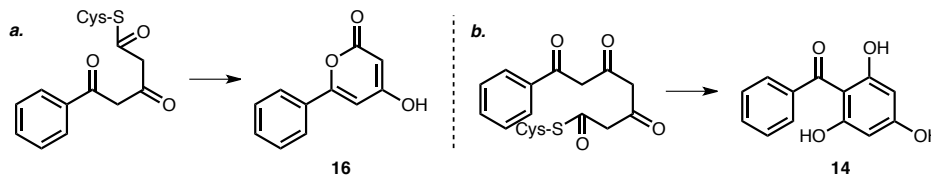
For the biosynthesis of PPAPs, exactly three molecules of malonyl-CoA are condensed with a starter acyl-CoA subunit. For type III PKSs, termination of polyketide chain length is determined by active site volume. For example, if a Thr135Leu point mutation is introduced in the active site of the *Hypericum androsaemum* BPS, the subsequent decrease in active site volume causes this enzyme to become a phenylpyrone synthase without a decrease in catalytic efficiency, in which only two molecules of

³⁵ Klingauf, P.; Beuerle, T.; Mellenthin, A.; El-Moghazy, S. A. M.; Boubakir, Z.; Beerhues, L. *Phytochemistry* **2005**, *66*, 139-145.

³⁶ Liu, B.; Falkenstein-Paul, H.; Schmidt, W.; Beerhues, L. *Plant J.* **2003**, *34*, 847-855.

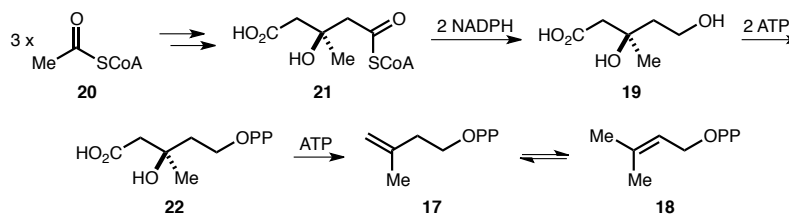
³⁷ Karppinen, K.; Hohtola, A. *J. Plant Physiol.* **2008**, *165*, 1079-1086.

malonyl-CoA are incorporated.³⁸ This triketide then undergoes lactonization to form 6-phenyl-4-hydroxy-2-pyrone (**16**, Scheme 1.2a) instead of 2,4,6-trihydroxybenzophenone (**14**, Scheme 1.2b).



Scheme 1.2. (a) Phenylpyrone synthase activity of Thr135Leu *H. androsaemum* BPS and (b) benzophenone synthase activity of wild-type *H. androsaemum* BPS.

The next step in PPAP biosynthesis involves polyisoprenylation of the acylphloroglucinol nucleus. All isoprenoids are derived from the two C₅ precursors: isopentenyl diphosphate (**17**) and dimethylallyl diphosphate (**18**). Until the early 1990s, it was thought that these precursors were produced from a single pathway involving a melavonate (**19**) intermediate (Scheme 1.3).³⁹ This pathway involves the condensation of three molecules of acetyl-CoA (**20**) to 3-hydroxy-3-methylglutaryl-CoA (**21**), and upon reduction to melavonate (**19**), pyrophosphorylation to **22**, and decarboxylative elimination, **17** is synthesized, which can then be isomerized to **18**. Indeed, this is the pathway by which eukaryotes synthesize sterols and other important metabolites.

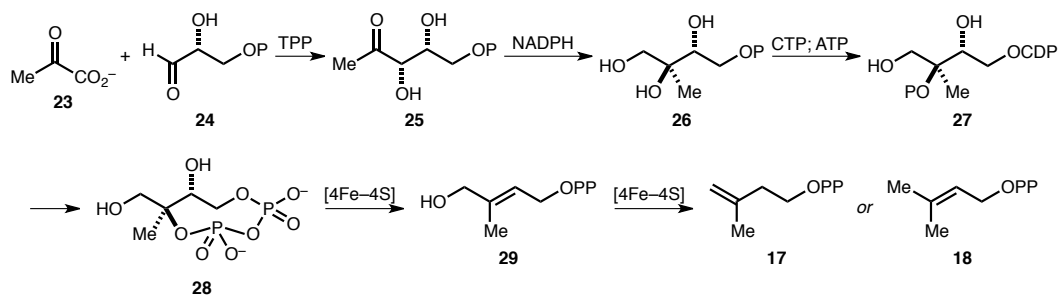


Scheme 1.3. Melavonate pathway of terpene biosynthesis.

³⁸ Klundt, T.; Bocola, M.; Beuerle, T.; Liu, B.; Beerhues, L. *J. Biol. Chem.* **2009**, *284*, 30957-30964.

³⁹ Bach, T. *J. Lipids* **1995**, *30*, 191-202.

However, in the early 1990s, inconsistencies regarding ^{13}C -labelled intermediates led to the independent discoveries of a non-melavonate means of isoprenoid biosynthesis in plants and bacteria by the research groups of Rohmer and Arigoni.⁴⁰ The absence of this pathway in humans has garnered significant attention as a means to develop novel anti-infective pharmaceutical agents.⁴¹ This deoxyxylulose phosphate pathway⁴² commences with the thiamine pyrophosphate (TPP) mediated decarboxylative coupling of pyruvate (**23**) to D-glyceraldehyde-3-phosphate (**24**) to form 1-deoxy-D-xylulose-3-phosphate (**25**, Scheme 1.4). A subsequent rearrangement with concomitant reduction affords 2C-methyl-D-erythritol 4-phosphate (**26**). Sequential cytidyl phosphorylation and phosphorylation yields 4-diphosphocytidyl 2C-methyl-D-erythritol 2-phosphate (**27**). Cytidyl monophosphate (CMP) is then released to form 2C-methyl-D-erythritol-2,4-cyclodiphosphate (**28**). Single-electron transfer from an iron-sulfur cluster cofactor mediates the reductive rearrangement of **28** to *E*-1-hydroxy-2-methyl-2-butenyl diphosphate (**29**) through an unknown mechanism of action. Finally, another iron-sulfur cluster-facilitated single-electron transfer process affords either **17** or **18**, depending on the specific enzyme.



Scheme 1.4. Deoxyxylulose phosphate pathway of terpene biosynthesis.

⁴⁰ (a) Rohmer, M.; Knani, M.; Simonin, P.; Sutter, B.; Sahm, H. *Biochem. J.* **1993**, 295, 517-524. (b) Arigoni, D.; Sagner, S.; Latzel, C.; Eisenreich, W.; Bacher, A.; Zenk, M. H. *Proc. Natl. Acad. Sci. USA* **1997**, 94, 10600-10605.

⁴¹ Gräwert, T.; Groll, M.; Rohdich, F.; Bacher, A.; Eisenreich, W. *Cell. Mol. Life Sci.* **2011**, 68, 3797-3814.

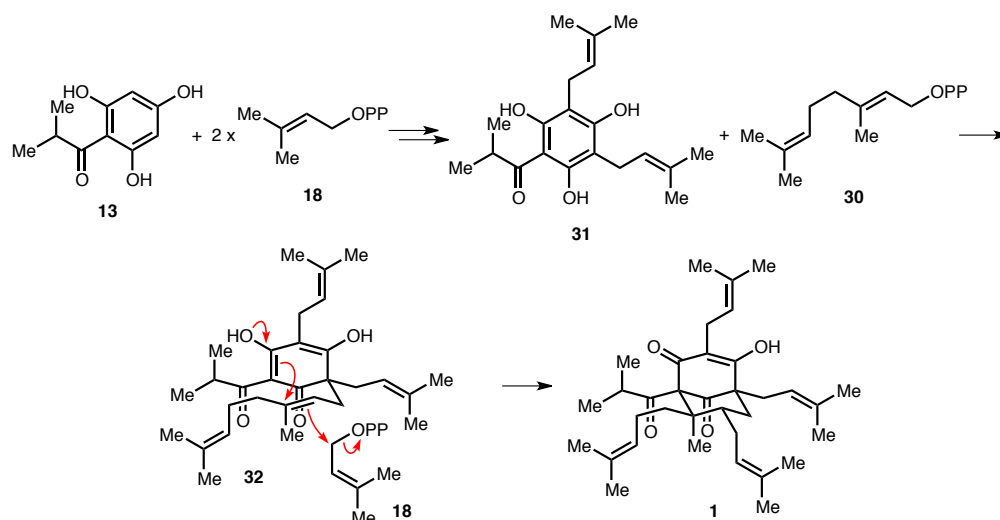
⁴² For reviews of the deoxyxylulose phosphate pathway, see ref. 41 and (a) Rohmer, M. *Nat. Prod. Rep.* **1999**, 16, 565-574. (b) Eisenreich, W.; Rohdich, F.; Bacher, A. *Trends Plant Sci.* **2001**, 6, 78-84. (c) Hunter, W. M. *J. Biol. Chem.* **2007**, 282, 21573-21577.

Higher plants utilize both the mevalonate and deoxyxylulose pathways to synthesize terpenoids, and this is a reason for the relatively belated discovery of the latter. In general, the mevalonate route is used in the cytoplasm and mitochondria, and it is responsible for the synthesis of sesquiterpenoids and ubiquinones. Other metabolites, such as hemiterpenes, monoterpenes, diterpenes, and carotenoids, are formed via the deoxyxylulose pathway localized in the plastids.⁴³ Given the fact that most substituents on PPAPs are hemiterpenoid or monoterpene in origin, it is unsurprising that they are synthesized using the deoxyxylulose phosphate pathway. Due to the presence of a skeletal rearrangement in this pathway (i.e., **25** to **26**), the introduction of isotopically-labeled feedstocks may be used to differentiate between these pathways. A feeding study of *Hypericum perforatum* sprouts performed in the dark utilizing both [1-¹³C]glucose and [U-¹³C₆]glucose provided evidence for the involvement of the deoxyxylulose pathway in hyperforin biosynthesis.⁴⁴

Further, this study demonstrated that hyperforin is synthesized from the alkylation of phlorisobutyrophenone (**13**) with 3 molecules of dimethylallyl diphosphate (**18**) and 1 molecule of geranyl diphosphate (**30**). Although the details concerning the specific order of alkylation remain scant, a reasonable biosynthetic sequence can be deduced for hyperforin (Scheme 1.5). Originally proposed by Bystrov and coworkers in 1975,² conversion of **13** to deoxycoumestrolone (**31**) followed by dearomative alkylation with **30** produces cyclohexadienone **32**. Prenylation of the proximal olefin present in the geranyl side chain of **32** with **18** with either concerted or stepwise cyclization affords hyperforin (**1**).

⁴³ For more information on the biosynthesis of phytochemical terpenoids, see ref. 42b. In some cases, both pathways may be operational in the biosynthesis of a single natural product. For an example, see: Nabeta, K.; Ishikawa, T.; Kawae, T.; Okuyama, H. *J. Chem. Soc., Chem. Commun.* **1995**, 681-682.

⁴⁴ Adam, P.; Arigoni, D.; Bacher, A.; Eisenreich, W. *J. Med. Chem.* **2002**, *45*, 4786-4793.



Scheme 1.5. Proposed biosynthesis of hyperforin (**1**) from phlorisobutyrophenone (**13**).

The intermediates of this hyperforin biosynthesis bear resemblance to other families of natural products. Polyprenylated acylphloroglucinols such as **31**, also known as deoxycohumulone, were first isolated in hops in 1961.⁴⁵ Hops are the female seed cones of *Humulus lupulus* (Cannabaceae) and have been extensively studied by the brewing industry due to the importance of hops in beer flavor and aroma.⁴⁶ Deoxycohumulone (**31**) is a direct precursor of both colupulone (**33**),⁴⁷ a typical hop β -acid, and cohumulone (**34**),⁴⁸ a typical hop α -acid (Scheme 1.6).⁴⁹ In the brewing of beer, hops are boiled with malt and wort in water. Under these conditions, isomerization of cohumulone takes place to give bitter hop iso- α -acids, an important flavoring agent in beer. While hop β -acids like colupulone are thought to

⁴⁵ (a) Hübner, H.; Maier, J.; Riedl, W. *Z. Physiol. Chem.* **1961**, 325, 224-228. (b) Lloyd, R. O. V.; Shannon, P. V. R.; Shaw, S. J. *J. Inst. Brewing* **1969**, 75, 32-36.

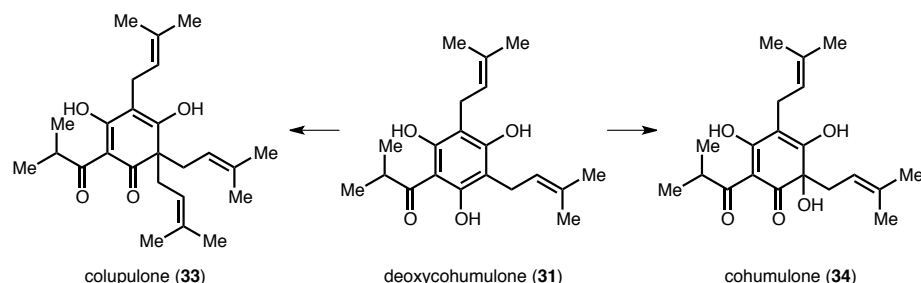
⁴⁶ (a) Stevens, R.; *Chem. Rev.* **1967**, 67, 19-71. (b) Palamand, S. R.; Aldenhoff, J. M. *J. Agric. Food Chem.* **1973**, 21, 535-543.

⁴⁷ Zuurbier, K. W. M.; Fung, S.-Y.; Scheffer, J. J. C.; Verpoorte, R. *Phytochemistry* **1995**, 38, 77-82.

⁴⁸ (a) Fung, S.-Y.; Zuurbier, K. W. M.; Paniego, N. B.; Scheffer, J. J. C.; Verpoorte, R. *Phytochemistry* **1997**, 44, 1047-1053. (b) Goese, M.; Kammhuber, K.; Bacher, A.; Zenk, M. H.; Eisenreich, W. *Eur. J. Biochem.* **1999**, 263, 447-454. (c) Hecht, S.; Kammhuber, K.; Reiner, J.; Bacher, A.; Eisenreich, W. *Phytochemistry* **2004**, 65, 1057-1060.

⁴⁹ Fung, S.-Y.; Brusee, J.; van der Hoeven, R. A. M.; Niessen, W. M. A.; Scheffer, J. J. C.; Verpoorte, R. *J. Nat. Prod.* **1994**, 57, 452-459.

mostly decompose during the wort boiling process, recent studies have shown that they also isomerize to bitter-tasting compounds that may further add to the complex composition of beer flavor.⁵⁰



Scheme 1.6. Deoxycohumulone (31) as a biosynthetic precursor to both colupulone (33) and cohumulone (34).

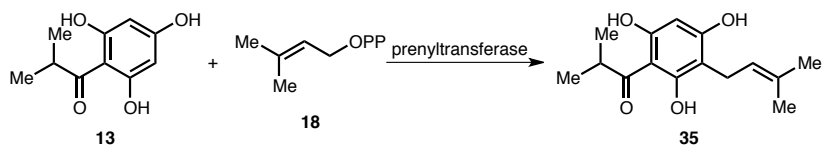
The enzymes responsible for the isoprenylation en route to natural products such as PPAPs and hop acids are collectively known as prenyltransferases.⁵¹ In plants, prenyltransferase activity is mainly located in the plastids, and the alkylating terpenoid is derived from the deoxyxylulose pathway. All known prenyltransferases require a divalent metal cation. The prenyltransferases responsible for the conversion of phlorisobutyrophenone (13) to prenyl phlorisobutyrophenone (35, also known as “compound co-X”), which is the first prenylation step in the biosyntheses of hop bitter acids and hyperforin, has been characterized in both *Humulus lupulus* and *Hypericum calycinum* (Scheme 1.7). The enzyme utilized in *Humulus lupulus* has an unusually wide substrate scope, and there are conflicting reports as to whether this enzyme is membrane-bound or not.⁵² All other plant prenyltransferases are membrane-bound.⁵¹ The analogous prenyltransferase utilized in hyperforin biosynthesis in *Hypericum*

⁵⁰ (a) Haseleu, G.; Intelmann, D.; Hofmann, T. *Food Chem.* **2009**, *116*, 71-81. (b) Haseleu, G.; Intelmann, D.; Hofmann, T. *J. Agric. Food Chem.* **2009**, *57*, 7480-7489.

⁵¹ For a review, see: Yazaki, K.; Sasaki, K.; Tsurumaru, Y. *Phytochemistry* **2009**, *70*, 1739-1745.

⁵² (a) Zuurbier, K. W. M.; Fung, S.-Y.; Scheffer, J. J. C.; Verpoorte, R. (b) Tsurumaru, Y.; Sasaki, K.; Miyawaki, T.; Uto, Y.; Momma, T.; Umemoto, N.; Momose, M.; Yazaki, K. *Biochem. Biophys. Res. Commun.* **2012**, *417*, 393-398.

calycinum has also been characterized as being non-membrane-bound.⁵³ To date, the prenyltransferases involved in the formation of deoxycohumulone or the dearomative prenylation of deoxycohumulone have not been characterized.



Scheme 1.7. The first prenylation step in hyperforin and hop bitter acid biosynthesis.

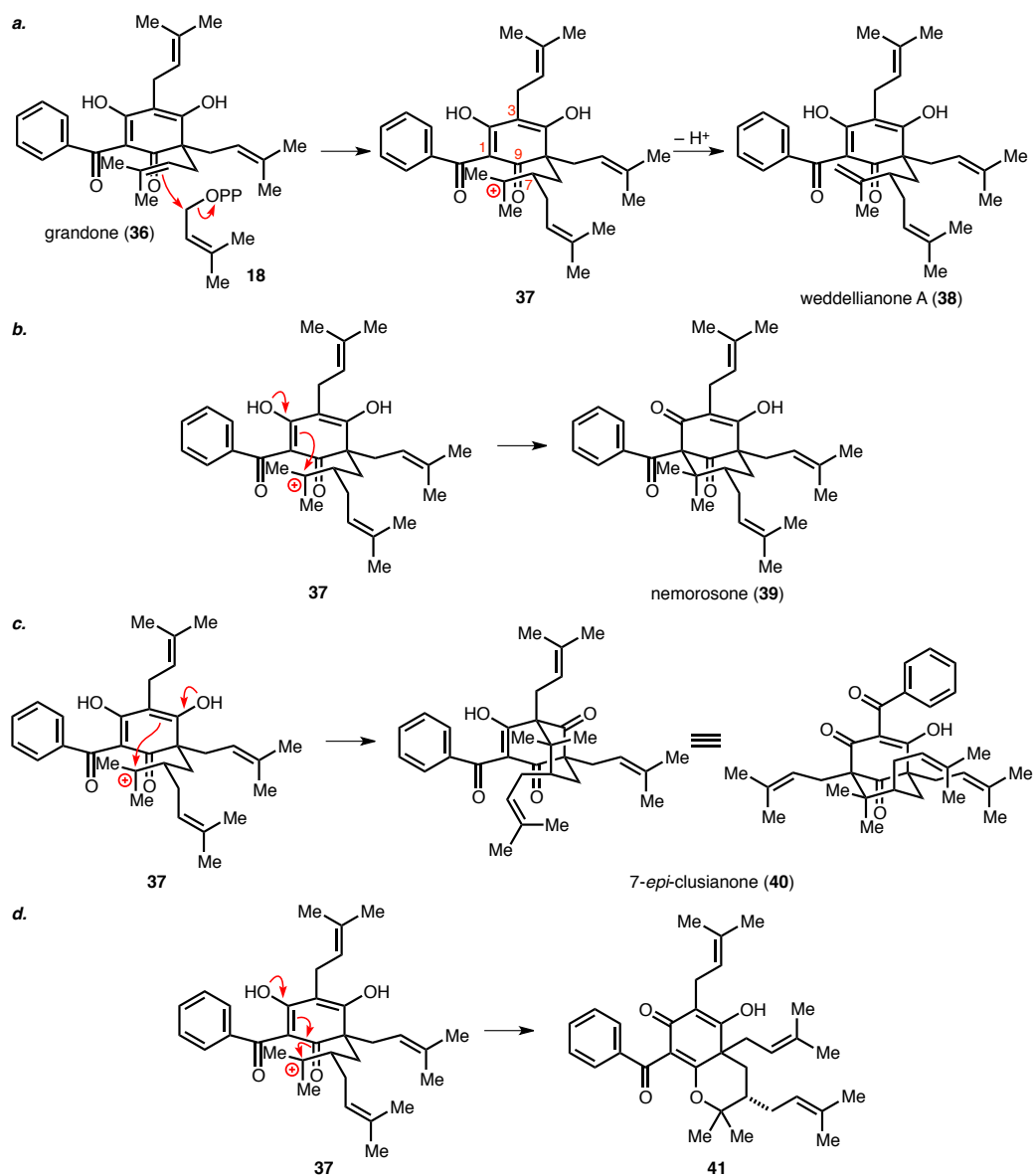
After dearomative poly-isoprenylation of a polyketide acyphloroglucinol, a cascade cyclization takes place to form the characteristic bicyclo[3.3.1]nonane core of PPAP natural products. Hop β -acids, such as colupulone (**33**) are alkylated⁵⁴ to produce a tertiary carbocationic intermediate, which then is trapped through nucleophilic addition of the cyclohexadienone ring (e.g., see Scheme 1.5). Several modes of nucleophilic addition are available to trap this carbocationic intermediate, as illustrated for grandone (**36**)⁵⁵ in Scheme 1.8. Following prenyl transfer and subsequent formation of the carbocation **37**, simple E1-type deprotonation may lead to the formation of weddellianone A (**38**, Scheme 1.8a), a lavandulyl-substituted hop β -acid that has been isolated from *Clusia weddelliana* (Clusiaceae).⁵⁶ In addition, two different nucleophilic carbon centers in the cyclohexadienone ring of **37** may trap this carbocation, either at C1 or at C3, and this divergence leads to either a Type A or Type B PPAP, respectively. If the carbocation is trapped at C1, the Type A PPAP nemorosone^{55b} is generated (**39**,

⁵³ Boubakir, Z.; Beuerle, T.; Liu, B.; Beerhues, L. *Phytochemistry* **2005**, *66*, 51-57.

⁵⁴ Note that two possible diastereomers may be generated at C7 from this alkylation event. Only one diastereomer is depicted throughout Scheme 1.8.

⁵⁵ **36** was first synthesized in 1971 in a study of hop β -acids: Collins, M.; Laws, D. R. J.; McGuinness, J. D.; Elvidge, J. A. *J. Chem. Soc. C* **1971**, 3814-3818. It was later isolated from *Clusia grandiflora*: de Oliveira, C. M. A.; Porto, A. M.; Bittrich, V.; Vencato, I.; Marsaioli, A. J. *Tetrahedron Lett.* **1996**, *37*, 6427-6430.

⁵⁶ Porto, A. L. M.; Machado, S. M. F.; de Oliveira, C. M. A.; Bittrich, V.; Amaral, M. do C. E.; Marsaioli, A. J. *Phytochemistry* **2000**, *55*, 755-768.



Scheme 1.8. Cyclization modes of grandone (36) after prenylation via intermediate 37: (a) deprotonation, (b) C1 cyclization, (c) C3 cyclization, and (d) etherification.

Scheme 1.8b), and if cyclization occurs at C3, the Type B PPAP 7-*epi*-clusianone⁵⁷ is produced (**40**, Scheme 1.8c). An oxygen atom, such as the ketone oxygen attached to C9, may also intercept this carbocation as depicted in Scheme 1.8d to generate benzopyran-type products like **41**. However, only a single analogous natural product that may involve such a cyclization has been isolated to date (bronianone, **42**, Figure 1.6).^{58,59}

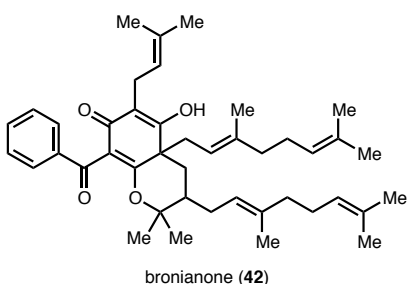


Figure 1.6. Structure of bronianone (**42**).

Unlike Types A and B PPAPs, the relatively rare Type C PPAPs cannot be made via intermediates such as grandone (**36**) but rather an isomeric compound represented as **43** (Figure 1.7a). Only three Type C PPAPs have been isolated to date (Figure 1.7b), garcinielliptone K (**44**), L (**45**), and M (**46**), from *Garcinia subelliptica*.⁶⁰

⁵⁷ (a) Santos, M. H.; Speziali, N. L.; Nagem, T. J.; Oliveira, T. T. *Acta Cryst.* **1998**, C54, 1990-1992. (b) Alves, T. M. de A.; Alves, R. de O.; Romanha, A. J.; dos Santos, M. H.; Nagem, T. J.; Zani, C. L. *J. Nat. Prod.* **1999**, 62, 369-371.

⁵⁸ (a) Ollis, W. D.; Redman, B. T.; Sutherland, I. O.; Jewers, K. *J. Chem. Soc. D, Chem. Commun.* **1969**, 879-880. (b) Rama Rao, A. V.; Venkataraman, K.; Yemul, S. S. *Tetrahedron Lett.* **1973**, 14, 4981-4982.

⁵⁹ The originally proposed structure of xanthochymol (**6**) was similar to **41** and **42** prior to revision. See ref. 3.

⁶⁰ Weng, J.-R.; Tsao, L.-T.; Wang, J.-P.; Wu, R.-R.; Lin, C.-N. *J. Nat. Prod.* **2004**, 67, 1796-1799.

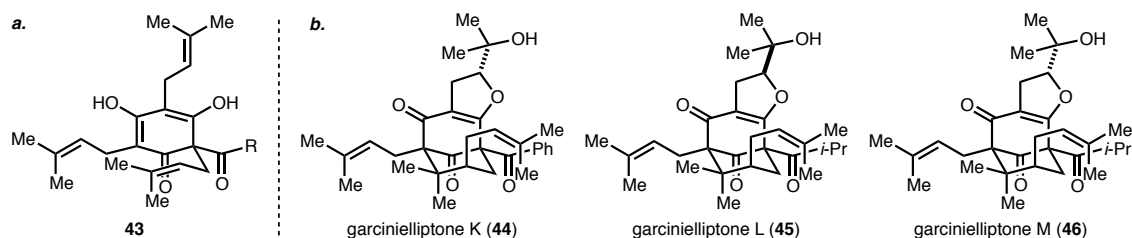
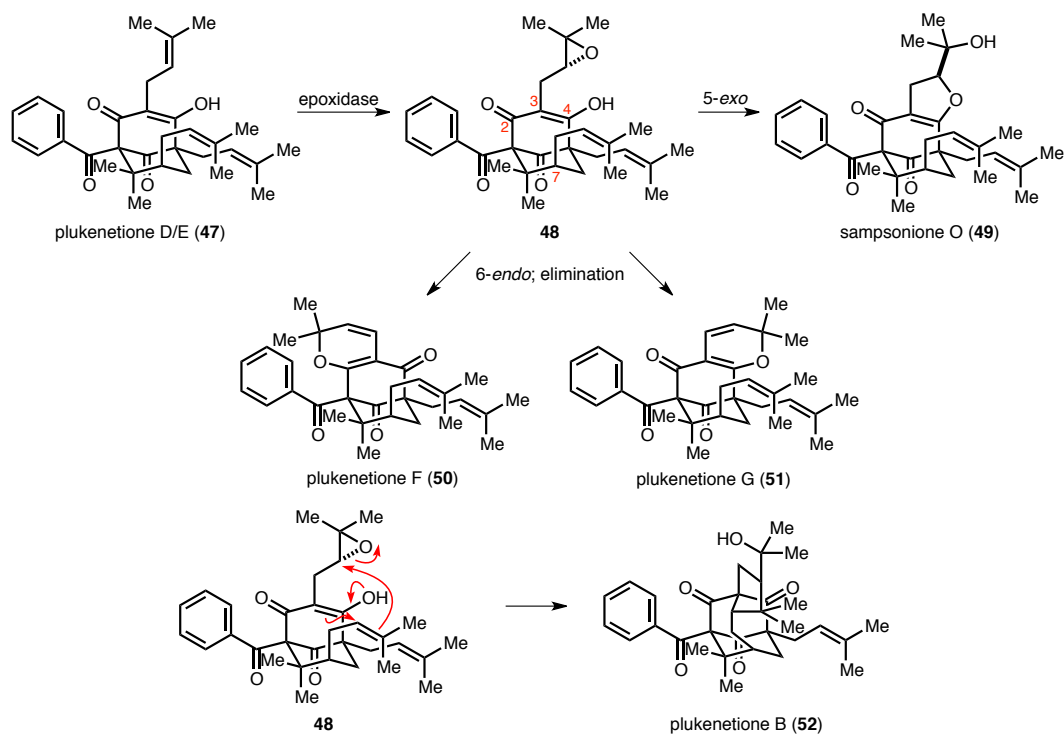


Figure 1.7. (a) A possible intermediate in Type C PPAP biosynthesis and (b) the only known examples of Type C PPAPs.

Following formation of the bicyclo[3.3.1]nonane ring, a variety of oxidations, cyclizations, and isomerizations may occur, further diversifying the family of PPAP natural products. Many of these transformations are potentially facilitated by epoxidation of an isoprenoid side chain. Examples of secondary cyclization are found in Scheme 1.9 involving plukenetione D/E (*7-epi-nemorosone*, **47**)⁶¹ and its epoxidation product **48**. *5-exo* epoxide opening of the epoxide found in **48** by the oxygen attached to C4 leads to a PPAP containing a dihydrofuran ring, sampsonione O (**49**).⁶² A *6-endo* cyclization (followed by elimination of the resulting alcohol) is also possible, illustrated by the natural products plukenetione F (**50**) and G (**51**).⁶¹ Carbocyclization involving the prenyl substituent at C7 is also possible, as evidenced by the formation of plukenetione B (**52**)⁶¹ from **48**, exemplifying the formation of a tetracyclic PPAP bearing a homoadamantyl subunit.

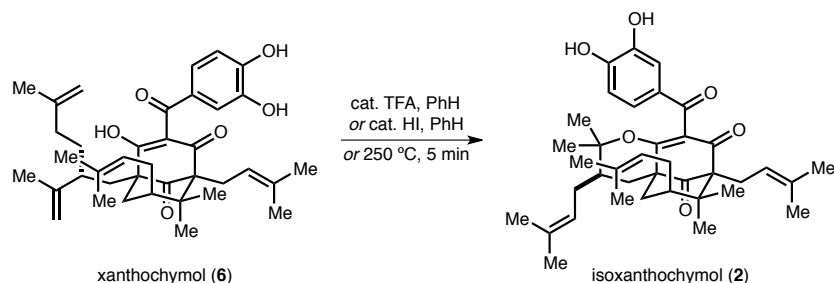
⁶¹ Henry, G. E.; Jacobs, H.; Carrington, C. M. S.; McLean, S.; Reynolds, W. F. *Tetrahedron* **1999**, 55, 1581-1596.

⁶² Xiao, Z. Y.; Mu, Q.; Shiu, W. K. P.; Zeng, Y. H.; Gibbons, S. J. *Nat. Prod.* **2007**, 70, 1779-1782.



Scheme 1.9. Formation of PPAPs through an epoxide intermediate of plukenetione D/E (47).

While some PPAPs containing secondary cyclization may arise through enzymatic processes, some other PPAPs may simply be artifacts of the isolation process. For example, simple treatment of xanthochymol (6) with acid or heat forms isoxanthochymol (2, Scheme 1.10).¹⁰ More in-depth analysis is necessary in order to further elucidate the later stages of PPAP biosynthesis.



Scheme 1.10. Acid- or heat-mediated conversion of xanthochymol (6) to isoxanthochymol (2).

Bioactivity

Widespread interest in the biological activity of PPAPs stems from the prevalence of these compounds in medicinally-relevant herbs used in a variety of traditional and ethnopharmaceutical treatments. Rather than utilizing an organization based upon natural product, this section is organized into distinct disease areas in order to facilitate greater understanding of the relationship between PPAP structure and bioactivity. The structures of PPAPs discussed herein may be found in Appendix A.

Anti-infective Activity

The anti-infective properties of PPAPs were one of the first types of bioactivity to be recognized. As mentioned previously, it has been theorized that plants biosynthesize PPAPs as a defense against infection. A variety of PPAPs are effective antibacterial agents particularly amongst gram-positive bacteria (Table 1.1); however, some are active against gram-negative bacteria as well (Table 1.2). While many of these bacteria are normally harmless and are intestinal commensals or found on normal skin flora (e.g., *B. subtilis*, *E. faecalis*, *S. aureus*, *S. epidermidis*), they may lead to often fatal infections in immunocompromised individuals, particularly in nosocomial environments. Particularly effective, broad-spectrum PPAPs include hyperforin, garcinol, and guttiferone A.

Table 1.1. Evaluation of PPAPs against gram-positive bacteria.

Bacterium	Active PPAPs (MIC in µg/mL)	Inactive PPAPs	References
<i>Actinomyces naeslundii</i>	hyperibone A (1.65-3.3)		63
<i>Bacillus cereus</i>	garcinol (1.5), guttiferone A, ^{a,b} hyperatomarin (1.56), hyperpapuanone (8), isoxanthochymol (9.8), papuaforin A (64), papuaforin C (64), papuaforin D (130), papuaforin E (64)	7- <i>epi</i> -clusianone, guttiferone G	64,65,66, 67,68,69
<i>Bacillus coagulans</i>	garcinol (2.0)		66
<i>Bacillus megaterium</i>	guttiferone G (0.61) ^b	isoxanthochymol	67
<i>Bacillus mesentericus</i>	hyperforin (2)		1
<i>Bacillus mycoides</i>	hyperforin (0.2)		1
<i>Bacillus stearothermophilus</i>	isoxanthochymol (4.88) ^b	guttiferone G	67
<i>Bacillus subtilis</i>	chamuangone (31), enervosanone (0.013), garcinol (0.05), hyperatomarin (3.1), hyperforin (0.2)	methyl clusianone, furohyperforin, furohyperforin A, guttiferone G, isoxanthochymol, pyrohyperforin	1,65,66,67, 70,71,72, 73,74
<i>Caryophanon latum</i>	hyperforin (1)		1
<i>Clavibacter michiganensis</i>	hyperforin (1)		1
<i>Corynebacterium diphtheriae</i>	hyperforin (1)		75

⁶³ Castro, M. L.; do Nascimento, A. M.; Ikegaki, M.; Costa-Neto, C. M.; Alencar, S. M.; Rosalen, P. L. *Bioorg. Med. Chem.* **2009**, *17*, 5332-5335.

⁶⁴ Winkelman, K.; Heilmann, J.; Zerbe, O.; Rali, T.; Sticher, O. *J. Nat. Prod.* **2001**, *64*, 701-706.

⁶⁵ Šavikin-Fodulović, K.; Aljančić, I.; Vajs, V.; Menković, N.; Macura, S.; Gojgić, G.; Milosavljević, S. *J. Nat. Prod.* **2003**, *66*, 1236-1238.

⁶⁶ Negi, P. S.; Jayaprakasha, G. K. *J. Food Sci.* **2004**, *69*, FMS61-FMS65.

⁶⁷ Kuete, V.; Komguem, J.; Beng, V. P.; Meli, A. L.; Tangmouo, J. G.; Etoa, F.-X.; Lontsi, D. *S. Afr. J. Bot.* **2007**, *73*, 347-354.

⁶⁸ Naldoni, F. J.; Claudino, A. L. R.; Cruz, J. W., Jr.; Chavasco, J. K.; e Silva, P. M. F.; Veloso, M. P.; Dos Santos, M. H. *J. Med. Food* **2009**, *12*, 403-407.

⁶⁹ Dias, K. S. T.; Januário, J. P.; D' Deigo, J. L.; Dias, A. L. T.; dos Santos, M. H.; Camps, I.; Coelho, L. F. L.; Viegas, C., Jr. *Bioorg. Med. Chem.* **2012**, *20*, 2713-2720.

⁷⁰ Lokvam, J.; Braddock, J. F.; Reichardt, P. B.; Clausen, T. P. *Phytochemistry* **2000**, *55*, 29-34.

⁷¹ Vajs, V.; Vugdelija, S.; Trifunović, S.; Karadžić, I.; Juranić, N.; Macura, S.; Milosavljević, S. *Fitoterapia* **2003**, *74*, 439-444.

⁷² Taher, M.; Idris, M. S.; Ahmad, F.; Arbain, D. *Phytochemistry* **2005**, *66*, 723-726.

⁷³ Taher, M.; Idris, M. S.; Ahmad, F.; Arbain, D. *Iran. J. Pharm. Th.* **2007**, *6*, 93-98.

⁷⁴ Sakunpak, A.; Panichayupakaranant, P. *Food Chem.* **2012**, *130*, 826-831.

⁷⁵ Schempp, C. M.; Pelz, K.; Wittmer, A.; Schöpf, E.; Simon, J. C. *Lancet* **1999**, *253*, 2129-2129.

Table 1.1 (continued). Evaluation of PPAPs against gram-positive bacteria.

Bacterium	Active PPAPs (MIC in µg/mL)	Inactive PPAPs	References
<i>Enterococcus faecalis</i>	guttiferone G (0.61), ^b isogarcinol (32), xanthochymol (0.78)	hyperforin, isoxanthochymol	1,67,75, 76,77
<i>Enterococcus</i> spp.	chamuangone (31)		74
<i>Listeria monocytogenes</i>	garcinol (25)		66
<i>Micrococcus luteus</i>	furohyperforin, ^c furohyperforin A, ^c hyperatomarin (1.6), hyperpauanone (16), papuaforin C (32)	papuaforin A, papuaforin D, papuaforin E	64,78,79
<i>Mycobacterium</i> B5	hyperforin (1)		1
<i>Rhodococcus equi</i>		methyl clusianone	56
<i>Sarcina lutea</i>	hyperforin (0.1)		1
<i>Staphylococcus aureus</i> (methicillin-sensitive)	chamuangone (2-31), 7- <i>epi</i> -clusianone (0.6-1.2), cycloxanthochymol (25), enervosanone (0.013), furohyperforin A (50), garcinol (0.05-63), ^b guttiferone A (2.4-4.5), guttiferone E, ^d hyperatomarin (1.56), hyperforin (1.0), hyperibone A (0.73-1.4), hyperibone B, ^d hyperibone D, ^d isoxanthochymol (25), makandechamone, ^c nemorosone (8.1), scrobiculatone A (130), scrobiculatone B (130), xanthochymol (3.1) ^b	furohyperforin, guttiferone G, hyperibone C, isogarcinol, isoxanthochymol, propolone A, pyrohyperforin	1,56,63,65, 66,67,68, 71,72,73, 74,75,78, 79,80,81, 82,83,84, 85,86,87, 88,89

⁷⁶ Tandon, R. N.; Srivastava, O. P.; Baslas, R. K.; Kumar, P. *Curr. Sci. India* **1980**, *49*, 472-473.

⁷⁷ Tchakam, P. D.; Lunga, P. K.; Kowa, T. K.; Lonfouo, A. H. N.; Wabo, H. K.; Tapondjou, L. A.; Tane, P.; Kuiate, J.-R. *BMC Complem. Altern. Med.* **2012**, *12*, 136.

⁷⁸ Trifunović, S.; Vajs, V.; Macura, S.; Juranić, N.; Djarmati, Z.; Jankov, R.; Milosavljević, S. *Phytochemistry* **1998**, *49*, 1305-1310.

⁷⁹ Vugdelija, S.; Vajs, V.; Trifunovic, S.; Djokovic, D.; Milosavljevic, S. *Molecules* **2000**, *5*, M158.

⁸⁰ Bakana, P.; Claeys, M.; Totté, J.; Pieters, L. A. C.; van Hoof, L.; Tamba-Vemba; van den Berghe, D. A.; Vlietinck, A. J. *J. Ethnopharmacol.* **1987**, *21*, 75-84.

⁸¹ Iinuma, M.; Tosa, H.; Tanaka, T.; Kanamaru, S.; Asai, F.; Kobayashi, Y.; Miyauchi, K.-i.; Shimano, R. *Biol. Pharm. Bull.* **1996**, *19*, 311-314.

⁸² Cuesta Rubio, O.; Cuellar, A. C.; Rojas, N.; Velez Castro, H.; Rastrelli, L.; Aquino, R. *J. Nat. Prod.* **1999**, *62*, 1013-1015.

⁸³ Lakshmi, C.; Kumar, K. A.; Dennis, T. J. *J. Indian Chem. Soc.* **2002**, *79*, 968-969.

⁸⁴ Trusheva, B.; Popova, M.; Naydenski, H.; Tsvetkova, I.; Rodriguez, J. G.; Bankova, V. *Fitoterapia* **2004**, *75*, 683-689.

⁸⁵ Schiell, M.; Kurz, M.; Haag-Richter, S. (Aventis Pharma Deutschland, GmbH). US Patent 6,956,061, October, 18, 2005.

⁸⁶ Trusheva, B.; Popova, M.; Bankova, V.; Simova, S.; Marcucci, M. C.; Miorin, P. L.; Pasin, F. d. R.; Tsvetkova, I. *Evid. Based Complement. Alternat. Med.* **2006**, *3*, 249-254.

⁸⁷ Xiao, Z. Y.; Zeng, Y. H.; Mu, Q.; Shiu, W. K. P.; Gibbons, S. *Chem. Biodivers.* **2010**, *7*, 953-958.

⁸⁸ Monzote, L.; Cuesta-Rubio, O.; Matheussen, A.; Van Assche, T.; Maes, L.; Cos, P. *Phytother. Res.* **2011**, *25*, 458-462.

Table 1.1 (continued). Evaluation of PPAPs against gram-positive bacteria.

Bacterium	Active PPAPs (MIC in µg/mL)	Inactive PPAPs	References
<i>Staphylococcus aureus</i> (methicillin-resistant)	chamuangone (0.5), ^b 7- <i>epi</i> -clusianone (3.7), cycloxanthochymol (25), garcinol (6.3-16), ^b hyperforin (1.0), hyperibone A, ^d hyperibone B, ^d hyperibone D, ^d isoxanthochymol, (25), peroxyxampson A (62) xanthochymol (25) ^b	hyperibone C, isogarcinol, peroxyxampson B, plukenetione C	62,75,81, 89,90,91, 92
<i>Staphylococcus epidermidis</i>	hyperpapaunone (8), papuaforin E (32), propolone A (100)	guttiferone A, papuaforin A, papuaforin C, papuaforin D	64,69,82
<i>Streptococcus agalactiae</i>	hyperforin (1.0)		75
<i>Streptococcus gordonii</i>	hyperibone A (1.7-3.3)		63
<i>Streptococcus mutans</i>	7- <i>epi</i> -clusianone (1.3-2.5), ^b hyperibone A (3.3-6.6)		63,93,94, 95,96
<i>Streptococcus oralis</i>	hyperibone A (1.7-3.3)		63
<i>Streptococcus pneumoniae</i>	garcinol (125)		80
<i>Streptococcus pyogenes</i>	hyperforin (1.0)		75
<i>Streptococcus sobrinus</i>	hyperibone A (1.7-3.3)		63
<i>Streptococcus viridans</i>	chamuangone (16), garcinol (130)		74,80
<i>Streptomyces aurantigriseus</i>	propolone A (100)		82
<i>Streptomyces chartreusis</i>	propolone A (50)		82

⁸⁹ Trisuwan, K.; Ritthiwigrom, T. *Arch. Pharm. Res.* **2012**, *35*, 1733-1738.

⁹⁰ Matsuhisa, M.; Shikishima, Y.; Takaishi, Y.; Honda, G.; Ito, M.; Takeda, Y.; Shibata, H.; Higuti, T.; Kozhimatov, O. K.; Ashurmetov, O. *J. Nat. Prod.* **2002**, *65*, 290-294.

⁹¹ Hübner, A. T. *Phytomedicine* **2003**, *10*, 206-208.

⁹² Rukachaisirikul, V.; Naklue, W.; Sukpondma, Y.; Phongpaichit, S. *Chem. Pharm. Bull.* **2005**, *53*, 342-343.

⁹³ Murata, R. M.; de Almeida, L. S. B.; Yatsuda, R.; dos Santos, M. H.; Nagem, T. J.; Rosalen, P. L.; Koo, H. *FEMS Microbiol. Lett.* **2008**, *282*, 174-181.

⁹⁴ Almeida, L. S. B.; Murata, R. M.; Yatsuda, R.; Dos Santos, M. H.; Nagem, T. J.; Alencar, S. M.; Koo, H.; Rosalen, P. L. *Phytomedicine* **2008**, *15*, 886-891.

⁹⁵ Murata, R. M.; Branco-de-Almeida, L. S.; Franco, E. M.; Yatsuda, R.; dos Santos, M. H.; de Alencar, S. M.; Koo, H.; Rosalen, P. L. *Biofouling* **2010**, *26* 865-872.

⁹⁶ Branco-de-Almeida, L. S.; Murata, R. M.; Franco, E. M.; dos Santos, M. H.; de Alencar, S. M.; Koo, H.; Rosalen, P. L. *Planta Med.* **2011**, *77*, 40-45.

Table 1.1 (continued). Evaluation of PPAPs against gram-positive bacteria.

Bacterium	Active PPAPs (MIC in µg/mL)	Inactive PPAPs	References
<i>Streptomyces griseus</i>	hyperforin (100)		97
<i>Strept. phaeochromogenes</i>	propolone A (100)		82
<i>Strept. violochromogenes</i>	propolone A (50)		82

^a See text.

^b More active or similar activity as positive control (e.g., vancomycin, chloramphenicol, chlorhexidine).

^c Reported to have activity in a diffusion assay.

^d Reported to have low to moderate activity in an antibiogram assay.

Many PPAPs have been evaluated against bacteria involved in areas beyond nosocomial infections. *B. mesentericus* and *B. stearothersophilus* are responsible for food spoilage (particularly bread),⁹⁸ and hyperforin¹ and isoxanthochymol⁶⁷ show significant activity against these species, respectively. Potato “ring rot” is a particular devastating infection caused by *Clavibacter michiganensis*,⁹⁹ and hyperforin is effective against this bacterium.¹ *B. cereus* is a leading cause of food-borne illness, including “fried rice syndrome.”¹⁰⁰ A variety of PPAPs show activity against this bacterium, including garcinol^{66,73} and hyperatomarin.⁶⁵ Garcinol is effective against *L. monocytogenes*, a cause of listeriosis.⁶⁶

Given that honeybees will utilize *Clusia* plant species resins in propolis, it is unsurprising that both chamone I and nemorosone were active against *Paenibacillus alvei* and *Paenibacillus larvae*, two honeybee pathogens.⁵⁶ Both of these PPAPs have been identified in Caribbean propola.

A variety of PPAPs have also been evaluated against bacteria involved in tooth decay. Typically, bacterial synthesis of extracellular glucans allows for biofilm formation, followed by acidification, plaque

⁹⁷ Derbentseva, N. A.; Aizenman, B. Y.; Harahulya, O. O. *Mikrobiologicheskii Zh.* **1971**, *33*, 569-572.

⁹⁸ Thompson, J. M.; Dodd, C. E. R.; Waites, W. M. *Int. Biodeter. Biodegr.* **1993**, *32*, 55-66.

⁹⁹ van der Wolf, J. M.; van Beckhoven, J. R. C. M.; Hukkanen, A.; Karjalainen, R.; Müller, P. J. *Phytopathol.* **2005**, *153*, 358-365.

¹⁰⁰ Drobniewski, F. C. *Clin. Microbiol. Rev.* **1993**, *6*, 324-338.

development, and the formation of dental caries.¹⁰¹ Hyperibone A is fairly effective against a range of bacteria involved in this process, including *A. naeslundii*, *S. gordonii*, *S. mutans*, *S. oralis*, and *S. sobrinus*. Aside from hyperibone A, 7-*epi*-clusianone also displayed activity against *S. mutans* dental caries.⁹⁴ Analyses of *S. mutans in vitro* have shown that this PPAP inhibits glucosyltransferases B and C, which are involved in glucan synthesis.⁹³ In addition, it inhibited F-ATPase activity, preventing acidification without affecting bacterial viability. Using a rodent model of dental caries, treatment with 7-*epi*-clusianone alone or in combination with fluoride produced significant cariostatic effects by reducing the amount of extracellular glucans and disrupting biofilm development without any observed side effects in the treated rats.⁹⁵ These cariostatic effects were attributed to glucosyltransferase inhibition as well as acidification prevention.⁹⁶

The mechanism of antibacterial activity of PPAPs remains largely unknown. Lipophilicity may play an important role in determining antibacterial activity. PPAPs containing a free β -hydroxyenone functionality at the C2–C4 bridge are more active than similar PPAPs that contain β -alkoxyenone at this site; for instance, garcinol and xanthochymol are more potent antibiotics than isogarcinol and isoxanthochymol, respectively. A series of guttiferone A (**53**) derivatives have been synthesized with functionalization at the phenolic oxygen atoms (Figure 1.8).⁶⁹ The analogs with *cLogP* (octanol/water) lower than guttiferone A (i.e., **54**, **55**, and **56**) had more potent antibacterial activity than the parent compound across a range of bacteria and were more active than chloramphenicol, used as a positive control. Analogs with higher lipophilicity (i.e., **57**, **58**, and **59**) were less active.

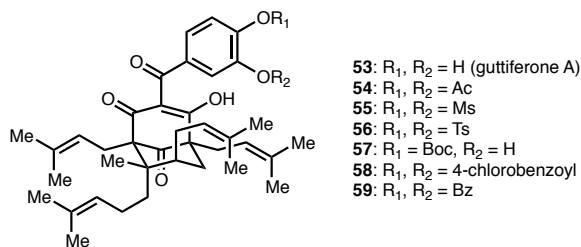


Figure 1.8. Guttiferone A and semisynthetic analogs.

¹⁰¹ Loesche, W. J. *Microbiol. Rev.* **1986**, *50*, 353-380.

Also, it appears that bacterial resistance to PPAPs is orthogonal to that of known antibiotics, which has important implications considering the widespread use of SJW extract to treat depression.⁹² Hyperforin has also been shown to act as an immunomodulatory agent towards bacterial phagocytosis in an *in vitro* model.¹⁰² At concentrations as low as 1 µg/mL, hyperforin activated human polymorphonuclear neutrophils towards either opsonized or non-opsonized *E. coli*.

Table 1.2. Evaluation of PPAPs against gram-negative bacteria.

Bacterium	Active PPAPs (MIC in µg/mL)	Inactive PPAPs	References
<i>Citrobacter freundii</i>	guttiferone G (1.2) ^a	isoxanthochymol	67
<i>Enterobacter aerogenes</i>		guttiferone G, isoxanthochymol	67
<i>Enterobacter cloacae</i>	guttiferone G (1.2) ^a	isoxanthochymol	67
<i>Escherichia coli</i>	cycloxanthochymol (25), enervosanone (0.013), garcinol (25-500), guttiferone E, ^b hyperforin (1), isogarcinol (25), isoxanthochymol (25)	chamuangone, methyl clusianone, 7- <i>epi</i> -clusianone, furohyperforin, furohyperforin A, guttiferone A, guttiferone E, guttiferone G, nemorosone, pyrohyperforin, xanthochymol	1,56,66,67, 68,69,71,72, 73,74,75,79, 80,81,83,86, 88,102
<i>Helicobacter pylori</i>	chamuangone (16), garcinol ^c		74,103
<i>Klebsiella pneumoniae</i>	isogarcinol (16), xanthochymol (1.6)	garcinol, guttiferone G, isoxanthochymol	67,76,77
<i>Morganella morganii</i>		guttiferone G, isoxanthochymol	67
<i>Neisseria gonorrhoeae</i>	garcinol (63)		80
<i>Proteus mirabilis</i>	guttiferone A (170)	guttiferone G, isoxanthochymol	67,69
<i>Proteus vulgaris</i>	guttiferone G (1.2) ^a	hyperforin, isoxanthochymol	1,67
<i>Pseudomonas aeruginosa</i>	enervosanone (0.013), garcinol (0.05-250), isogarcinol (16)	guttiferone A, guttiferone G, hyperforin, isoxanthochymol	1,67,69,72, 73,75,77,80, 97
<i>Salmonella enterica enterica</i>	isogarcinol (5)	guttiferone G, isoxanthochymol	67,77
<i>Salmonella typhimurium</i>	guttiferone A (39) ^a	guttiferone G, isoxanthochymol	67,69
<i>Serratia marcescens</i>		garcinol	80
<i>Shigella dysenteriae</i>		guttiferone G, isoxanthochymol	67
<i>Shigella flexneri</i>	garcinol (31), isogarcinol (16)	guttiferone G, isoxanthochymol	67,77,80
<i>Shigella sonnei</i>		chamuangone	74
<i>Yersinia enterocolitica</i>		garcinol	66

^a More active or similar activity as positive control (e.g., chloramphenicol, gentamycin).

^b Reported to have activity in a diffusion assay.

^c See text.

¹⁰² Brondz, I.; Brondz, A. *J. Biophys. Chem.* **2012**, 3, 304-310.

¹⁰³ Chatterjee, A.; Yasmin, T.; Bagchi, D.; Stohs, S. J. *Mol. Cell. Biol.* **2003**, 243, 29-35.

The antiviral activity of several PPAPs has also been evaluated with limited success. Garcinol was completely ineffective against viral infection of VERO cells with an adenovirus, coxsackievirus, herpes simplex virus type 1, measles, poliomyelitis virus type 1, and the Semliki forest virus.⁸⁰ Garcinol was however active at preventing long-terminal repeat promoter activity of porcine endogenous retrovirus, which increases the likelihood of pig-to-human viral transplantation.¹⁰⁴ Considering that this activity could be replicated using CpG methyltransferase, the antiretroviral activity of garcinol in this case may stem from its ability to act as an epigenetic modulator.

A variety of PPAPs have been evaluated for activity against lentiviruses, particularly human immunodeficiency virus (HIV) strains. HIV infection leads to a progressive failure of the immune system, otherwise known as acquired immunodeficiency syndrome (AIDS), which leaves infected individual susceptible to often fatal opportunistic infections and cancer.¹⁰⁵ Similar to PPAP antibacterial activity, a free C2–C4 β -hydroxyenone moiety generally leads to greater activity against HIV pathophysiology. Clusianone decreased HIV infection of 3T3.T4.CCR5 and Jurkat E6-1 cells in a dose-dependent manner compared to control, while its *O*-methyl ether was inactive at all concentrations tested.¹⁰⁶ Interestingly, *ent*-clusianone was similarly active against both cell lines (its *O*-methyl ether was also inactive). Guttiferones A-E were found to have EC₅₀ values in the range of 1-10 μ g/mL against the cytopathic effects of CEM-SS cells infected HIV, although viral replication was not inhibited.¹⁶ Isoxanthochymol, on the other hand, was inactive in this assay. It should be noted that these compounds were also found to be noncytotoxic to the CEM-SS cells used in this study. Laxifloranone was also found to be active in this CEM-SS HIV assay (EC₅₀ = 0.62 μ g/mL); however, if the free carboxylic acid was blocked, all cytopathic effects were lost.¹⁰⁷ In another assay involving C8166 cells,

¹⁰⁴ Ha, H.-S.; Lee, Y.-C.; Park, S.-J.; Jung, Y.-D.; Ahn, K.; Moon, J.-W.; Han, K.; Oh, K.-B.; Kim, T.-H.; Seong, H.-H.; Kim, H.-S. *Genes Genom.* **2012**, *34*, 217-222.

¹⁰⁵ Douek, D. C.; Roederer, M.; Koup, R. A. *Annu. Rev. Med.* **2009**, *60*, 471-484.

¹⁰⁶ Garnsey, M. R.; Matous, J. A.; Kwiek, J. J.; Coltart, D. M. *Bioorg. Med. Chem. Lett.* **2011**, *21*, 2406-2409.

¹⁰⁷ Bokesch, H. R.; Groweiss, A.; McKee, T. C.; Boyd, M. R. *J. Nat. Prod.* **1999**, *62*, 1197-1199.

aristophenone, clusianone, 7-*epi*-clusianone, nemorosone, and propolone A potently prevented HIV infection.¹⁰⁸ Clusianone was the most effective PPAP screened, with an EC₅₀ of 20 nM, but showed a TC₅₀ value of 0.1 µM in uninfected C8166 cells. The most selective PPAP test was propolone A, with an EC₅₀ of 0.32 µM and a TC₅₀ value of 5.0 µM. Using an MT-4 cell line, guttiferone E, guttiferone O2, and isoxanthochymol did not inhibit HIV replication at subtoxic concentrations.¹⁰⁹

Further, it appears that PPAP anti-HIV activity may occur through several mechanisms of action. Plukenetione A and plukenetione D/E were both evaluated using CEMx174-SEAP cells as well as HEK293T cells infected with a simian immunodeficiency virus vector.¹¹⁰ While both compounds were found to be cytotoxic in the cell lines employed (ca. 4 µM), both were potent below 2 µM against lentiviral infection. The activity of plukenetione A was primarily due to its inhibition of reverse transcriptase (IC₅₀ = 1.75 µM), and the activity of plukenetione D/E was due to its interruption of the Akt/PKB signaling cascade. Guttiferone F and 30-*epi*-isogarcinol were both active in an *in vitro* HIV protease assay, demonstrating that at least some PPAPs might target this enzyme.¹¹¹

The action of several PPAPs against the highly infectious, epidemic-causing influenza and hepatitis B viruses has also been reported. The hepatitis B virus causes liver inflammation and while a vaccine is available in developed countries, a significant portion of the world population remains vulnerable to infection.¹¹² Hypersampsones A-F demonstrated activity against hepatitis B e antigen secretion by infected MS-G2 cells at 10 µg/mL, but viral particle replication was not inhibited.¹¹³

¹⁰⁸ Piccinelli, A. L.; Cuesta-Rubio, O.; Chica, M. B.; Mahmood, N.; Pagano, B.; Pavone, M.; Barone, V.; Rastrelli, L. *Tetrahedron* **2005**, *61*, 8206-8211.

¹⁰⁹ Lannang, A. M.; Louh, G. N.; Biloa, B. M.; Komguem, J.; Mbazoa, C. D.; Sondengam, B. L.; Naesens, L.; Pannecouque, C.; De Clercq, E.; El Ashry, E. S. H. *Planta Med.* **2010**, *76*, 708-712.

¹¹⁰ Diaz-Carballo, D.; Ueberla, K.; Kleff, V.; Ergun, S.; Malak, S.; Freistuehler, M.; Somogyi, S.; Kücherer, C.; Bardenheuer, W.; Strumberg, D. *Int. J. Clin. Pharmacol. Th.* **2010**, *48*, 670-677.

¹¹¹ Magadula, J. J. *J. Pharmaceut. Sci. Innovat.* **2012**, *1*, 31-33.

¹¹² Lok, A. S. F.; McMahon, B. J. *Hepatology* **2007**, *45*, 507-539.

¹¹³ Lin, Y.-L.; Wu, Y.-S. *Helv. Chim. Acta* **2003**, *86*, 2156-2163.

Influenza, otherwise known as the flu, is a highly infectious disease and particularly dangerous owing to the ability of new strains to cross species barriers, incorporating genes from other mammals and birds.¹¹⁴ Guttiferone E, guttiferone O2, and isoxanthochymol have been evaluated against influenza A-infected MDCK cells.¹⁰⁹ All three PPAPs showed minimum cytotoxic concentrations of 4 µg/mL against these infected cells. However, they were inactive at preventing replication of influenza A subtypes H1N1 and H3N2 and influenza B.

Since several retroviruses use proteases during their reproductive cycle, protease inhibitors may be used in antiretroviral therapies. The serine and cysteine protease inhibition ability of several PPAPs have been evaluated (Table 1.3). While both 7-*epi*-clusianone and garciniaphenone modestly inhibited protease activity, guttiferone A moderately inhibited all four proteases screened.

Table 1.3. Antiproteolytic activity of several PPAPs.

PPAP	Protease IC ₅₀ (µM)				References
	Papain	Trypsin	Cathepsin B	Cathepsin G	
7- <i>epi</i> -clusianone	19.5	20.1	73.7-74.1	37.4-37.9	115,116
garciniaphenone	130.8	103.5	102.0-103.5	97.6-98.8	115,116
guttiferone A	1.9	9.4	2.1	2.7	115

The antiparasitic properties of a variety of PPAPs have also been evaluated. Malaria is a highly infectious disease spread by female *Anopheles* mosquitoes and is often caused by the protozoan *Plasmodium falciparum*. There were an estimated 219 million cases of malaria reported in 2010, mostly in sub-Saharan Africa, resulting in 1.2 million deaths.¹¹⁷ A variety of PPAPs and semisynthetic analogs of

¹¹⁴ Hsu, J.; Santesso, N.; Mustafa, R.; Brozek, J.; Chen, Y. L.; Hopkins, J. P.; Cheung, A.; Hovhannisyan, G.; Ivanova, L.; Flottorp, S. A.; Sæterdal, I.; Wong, A. D.; Tian, J.; Uyeki, T. M.; Akl, E. A.; Alonso-Coello, P.; Smaill, F.; Schünemann, H. J. *Ann. Intern. Med.* **2012**, *156*, 512-524.

¹¹⁵ Martins, F. T.; Assis, D. M.; dos Santos, M. H.; Camps, I.; Veloso, M. P.; Juliano, M. A.; Alves, L. C.; Doriguetto, A. C. *Eur. J. Med. Chem.* **2009**, *44*, 1230-1239.

¹¹⁶ Murata, R. M.; Yatsuda, R.; dos Santos, M. H.; Kohn, L. K.; Martins, F. T.; Nagem, T. J.; Alencar, S. M.; de Carvalho, J. E.; Rosalen, P. L. *Phytother. Res.* **2010**, *24*, 379-383.

¹¹⁷ *World Malaria Report 2012*; World Health Organization, WHO Press: Geneva, Switzerland.

hyperforin (Figure 1.9) have been evaluated against *P. falciparum* (Table 1.4) and chloroquine-resistant *P. falciparum* (Table 1.5).

Table 1.4. Evaluation of PPAPs against *Plasmodium falciparum*.

PPAP	IC ₅₀ (μM)	References	PPAP	IC ₅₀ (μM)	References
adhyperforin·HNCy ₂	1.4	118	spiranthenone B	32.1	25
furohyperforin	1.7	118	60	7.8	118
guttiferone A	0.5-3.0	88,119	61	>27	118
hyperforin·HNCy ₂	1.5	118	62	4.8	118
hyperforin, lithium salt	2.1	118	63	>27	118
isoxanthochymol	2.2-4.5	120,121	64	0.6	118
nemorosone	0.4	88	65	6.7	118
oxyhyperforin	2.0	118	66 ·HNCy ₂	1.4	118
spiranthenone A	8.2	25	66 , lithium salt	2.7	118
pyrohyperforin	8.6	118	67	2.1	119

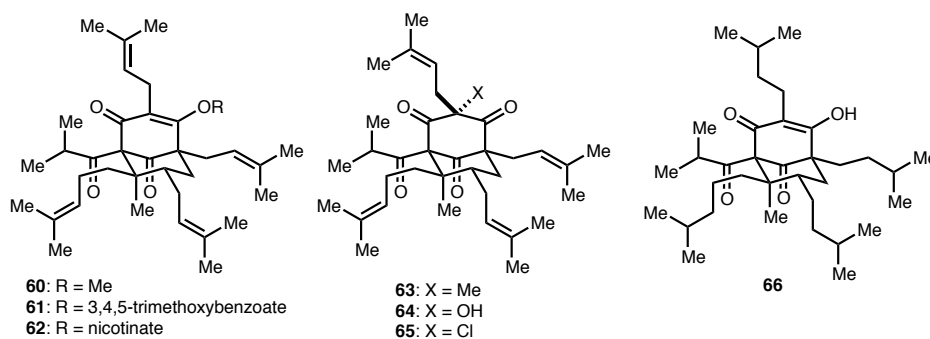


Figure 1.9. Semisynthetic analogs of hyperforin.

¹¹⁸ Verotta, L.; Appendino, G.; Bombardelli, E.; Brun, R. *Bioorg. Med. Chem. Lett.* **2007**, *17*, 1544-1548.

¹¹⁹ Fromentin, Y.; Grellier, P.; Wansi, J. D.; Lallemand, M.-C.; Buisson, D. *Org. Lett.* **2012**, *14*, 5054-5057.

¹²⁰ Lannang, A. M.; Louh, G. N.; Lontsi, D.; Specht, S.; Sarite, S. R.; Flörke, U.; Hussain, H.; Hoerauf, A.; Krohn, K. *J. Antibiot.* **2008**, *61*, 518-523.

¹²¹ Elfita, E.; Muharni, M.; Latief, M.; Darwati, D.; Widiyantor, A.; Supriyatna, S.; Bahti, H. H.; Dachriyanus, D.; Cos, P.; Maes, L.; Foubert, K.; Apers, S.; Pieters, L. *Phytochemistry* **2009**, *70*, 907-912.

Table 1.5. Evaluation of PPAPs against chloroquine-resistant *P. falciparum*.

PPAP	IC ₅₀ (μM)	References	PPAP	IC ₅₀ (μM)	References
coccinone A	4.3	9	guttiferone A	3.17	88,122
coccinone B	5.5	9	isogarcinol	3.5	9,123
7- <i>epi</i> -coccinone B	3.3	124	7- <i>epi</i> -isogarcinol	3.2-5.1	9,124
coccinone C	9.0	9	14-deoxy-7- <i>epi</i> -isogarcinol	2.5	124
coccinone D	7.0	9	symphonone A	2.8	124
coccinone E	4.9	9	symphonone B	3.3	124
coccinone F	17.0	9	symphonone C	2.6	124
coccinone G	19.2	9	symphonone D	2.1	124
coccinone H	16.6	9	symphonone E	2.7	124
cycloxanthochymol	2.1	9	symphonone F	3.2	124
garcinol	12.6	9	symphonone G	2.1	124
7- <i>epi</i> -garcinol	10.1	9,124	symphonone H	3.0	124
14-deoxygarcinol	37.2	9	symphonone I	6.7	124

Nemorosone and oxidized hyperforin analog **64** were most active against chloroquine-sensitive *P. falciparum*, and cycloxanthochymol and symphonones D and G were the most active against chloroquine-resistant *P. falciparum*. Nemorosone was found to be as active as chloroquine against *P. falciparum*.⁸⁸ Amongst the hyperforin derivatives, a limited degree of structural modification of the bicyclo[3.3.1]nonane core does not lead to significant changes in potency; analogs with C4 oxygen atom functionalization, with a quaternary center at C3, or hydrogenation of the pendant olefins had similar activity to that of hyperforin.¹¹⁸ The only inactive derivatives screened were **61** and **63**. A semisynthetic analog of guttiferone A, **67**, was found to be more active than the parent PPAP (Figure 1.10).¹¹⁹ Also noteworthy is the potency trend within the coccinone and symphonone families of PPAPs. Those that contain a free C2–C4 β-hydroxyenone (i.e., coccinones F–H) were significantly less potent than the other members, which bear a tetrahydropyran ring containing the C4 oxygen atom.

¹²² Ngouela, S.; Lenta, B. N.; Nougoué, D. T.; Ngoupayo, J.; Boyom, F. F.; Tsamo, E.; Gut, J.; Rosenthal, P. J.; Connolly, J. D. *Phytochemistry* **2006**, *67*, 302-306.

¹²³ Marti, G.; Eparvier, V.; Litaudon, M.; Grellier, P.; Guéritte, F. *Molecules* **2010**, *15*, 7106-7114.

¹²⁴ Marti, G.; Eparvier, V.; Moretti, C.; Prado, S.; Grellier, P.; Hue, N.; Thoison, O.; Delpech, B.; Guéritte, F.; Litaudon, M. *Phytochemistry* **2010**, *71*, 964-974.

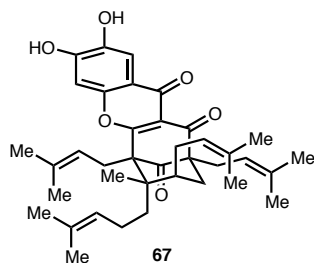


Figure 1.10. A semisynthetic analog of guttiferone A.

Unfortunately, many PPAPs that exhibited antimalarial properties were found to be fairly cytotoxic. Adhyperforin, guttiferone A, hyperforin, isoxanthochymol, octahydrohyperforin (**66**), and **67** had cytotoxicity concentrations comparable to their antimalarial activity, but furohyperforin, and oxyhyperforin, and **62** were marginally less cytotoxic. The only PPAPs screened for cytotoxicity that were significantly more potent than cytotoxic were spiranthenones A and B.

In addition, several PPAPs have been evaluated for possible treatment of leishmaniasis. This disease is caused by a variety of different protozoa belonging to the genus *Leishmania*, and is transmitted through the bite of sand flies from the subfamily Phlebotominae.¹²⁵ During sand fly feeding, *Leishmania* promastigotes enter the body. Upon macrophage phagocytosis, amastigotes are produced and proliferate. Leishmaniasis can take several forms, the most common of which involves skin sores, which appear weeks to months after initial exposure. If the parasite migrates to vital organs, visceral leishmaniasis may occur, which is the second largest fatal parasitic disease in the world, after malaria. Despite its prevalence, especially in developing countries, very few treatment options are available. A summary of PPAPs evaluated for leishmanicidal activity is found in Table 1.6.

¹²⁵ González, U.; Pinart, M.; Rengifo-Pardo, M; Macaya, A.; Alvar, J.; Tweed, J. A. *Cochrane Database Syst. Rev.* **2009**, CD004834.

Table 1.6. Evaluation of PPAPs against various *Leishmania* species.

<i>Leishmania</i> species	Life-cycle phase	Evaluated PPAPs (IC ₅₀ in μ M)	References
<i>L. amazonensis</i>	amastigotes	7- <i>epi</i> -clusianone (3.2), ^a garciniaphenone (inactive), guttiferone A (4.9)	126
	promastigotes	7- <i>epi</i> -clusianone (6.6), ^a garciniaphenone (11.6), garcinielliptone FC (42.8), guttiferone A (15.6-30.1), nemorosone (11.2)	88,126,127
<i>L. donovani</i>	amastigotes	garcinol (0.82), guttiferone A (0.16), ^a guttiferone F (0.20), isogarcinol (0.33) ^a	128
<i>L. infantum</i>	amastigotes	guttiferone A (13.5), isoxanthochymol (2.0), nemorosone (32.9)	88,121
	promastigotes	spiranthenone A (inactive), spiranthenone B (inactive)	25

^a More active or similarly active as a positive control (e.g., amphotericin B or miltefosine).

In general, leishmanicidal activity is inversely related to hydrophobicity. 7-*epi*-Clusianone was one of the most active PPAPs screened, against both the amastigote and promastigote forms of the New World protozoan *L. amazonensis*, and it was found to be more potent than amphotericin B in both cases.¹²⁶ Interestingly, garciniaphenone was active against the promastigote form of this *Leishmania* species but inactive against the amastigote form. While isoxanthochymol was fairly potent against *L. infantum* amastigotes, it was found to be fairly cytotoxic towards MRC-5 cells.¹²¹ Guttiferones A and F and isogarcinol were the most effective leishmanicidal PPAPs screened against the Old World pathogen *L. donovani*.¹²⁸ At 8.0 μ M concentration, both guttiferone A and F inhibited parasite growth by 98%. Since guttiferone A was shown to be relatively noncytotoxic (CC₅₀ = 17.8 μ M in murine peritoneal macrophages),¹²⁶ it may be a lead structure in the development of a treatment for Old World leishmaniasis.

A variety of PPAPs has also been evaluated against trypanosomiasis, another parasitic protozoan disease. There are two major forms of trypanosomiasis: (1) African trypanosomiasis, otherwise known as

¹²⁶ Pereira, I. O.; Marques, M. J.; Pavan, A. L. R.; Codonho, B. S.; Barbiéri, C. L.; Beijo, L. A.; Doriguetto, A. C.; D'Martin, E. C.; dos Santos, M. H. *Phytomedicine* **2010**, *17*, 339-345.

¹²⁷ Júnior, J. S. C.; de Almeida, A. A. C.; Ferraz, A. de B. F.; Rossatto, R. R.; Silva, T. G.; Silva, P. B. N.; Militão, G. C. G.; Citó, A. M. das G. L.; Santana, L. C. L. R.; Carvalho, F. A. de A.; Freitas, R. M. *Nat. Prod. Res.* **2013**, *27*, 470-474.

¹²⁸ Lenta, B. N.; Vonthron-Sénécheau, C.; Weniger, B.; Devkota, K. P.; Ngoupayo, J.; Kaiser, M.; Naz, Q.; Choudhary, M. I.; Tsamo, E.; Sewald, N. *Molecules* **2007**, *12*, 1548-1557.

sleeping sickness, and (2) Chagas disease.¹²⁹ As the name suggests, African trypanosomiasis is most prevalent in sub-Saharan Africa, and it is caused by the protozoa of *Trypanosoma brucei*, transmitted by the tsetse fly. Chagas disease is the most common form of trypanosomiasis in Latin America, in which *Trypanosoma cruzi* is transmitted by a variety of bloodsucking bugs, such as *Rhodnius prolixus* and *Triatoma brasiliensis*.

A summary of the effects of several PPAPs on the viability of trypanosomiasis protozoa is found in Table 1.7. Guttiferone A, isoxanthochymol, and nemorosone were found to be moderately active against both *T. brucei* and *T. cruzi*. As mentioned earlier, isoxanthochymol is cytotoxic against MRC-5 cells at a concentration similar to its concentration for effective trypanocidal outcomes.¹²¹ Guttiferone A and **67** suffer from similar problems. One study established that guttiferone A had MC₁₀₀ values against *T. cruzi* epimastigotes and typanomastigotes of 99.5 μ M and 82.9 μ M, respectively, and these values were well above the 10.7 μ M IC₅₀ value of the PPAP against murine peritoneal macrophages.^{126,130} 7-epi-Clusianone was also evaluated against *T. cruzi*; however, it was found to be ineffective *in vivo* in infected mice.¹³¹ Interestingly, nemorosone was also found to be non-cytotoxic against the predominant insect vector of Chagas disease, *Rhodnius prolixus*, but it displayed dose-dependent anti-molting effects.¹³²

¹²⁹ Coura, J. R.; Borges-Pereira, J. *Acta Trop.* **2010**, *115*, 5-13.

¹³⁰ Abe, F.; Nagafuji, S.; Okabe, H.; Akahane, H.; Estrada-Muñiz, E.; Huerta-Reyes, M.; Reyes-Chilpa, R. *Biol. Pharm. Bull.* **2004**, *27*, 141-143.

¹³¹ Alves, T. M. de A.; Alves, R. de O.; Romanha, A. J.; dos Santos, M. H.; Nagem, T. J.; Zani, C. L. *J. Nat. Prod.* **1999**, *62*, 369-371.

¹³² Kelecom, A.; Reis, G. L.; Fevereiro, P. C. A.; Silva, J. G.; Santos, M. G.; Neto, C. B. M.; Gonzalez, M. S.; Gouvea, R. C. S.; Almeida, G. S. S. *An. Acad. Bras. Cienc.* **2002**, *74*, 171-181.

Table 1.7. Evaluation of PPAPs against *Trypanosoma brucei* and *T. cruzi*.

PPAP	IC ₅₀ (μM)		References
	<i>T. brucei</i>	<i>T. cruzi</i>	
guttiferone A	3.0-13.5	11.8	88,119
isoxanthochymol	1.9	2.7	121
nemorosone	17.5	12.5	88
spiranthenone A	n.d.	inactive	25
spiranthenone B	n.d.	211.3	25
67	2.1	n.d.	119

7-*epi*-Clusianone has also been evaluated for its molluscicidal effects upon *Biomphalaria glabrata*, a Brazilian freshwater snail and known carrier of *Schistosoma mansoni*, one of several parasitic worms responsible for schistosomiasis.¹³¹ However, this PPAP was found to be inactive in the snail toxicity assay.

The antifungal properties of various PPAPs have also been explored, which is summarized in Table 1.8. In general, the PPAPs evaluated were much less effective against fungi than against bacteria, viruses, and parasites, and generalizations about structure-activity relationships cannot be made. Guttiferone A was found to be most active across a wide range of fungi, including several *Candida* species responsible for infections in immunocompromised individuals, the cryptococcosis-causing *Cryptococcus neoformans*, and two *Trichophyton* species involved in tinea-type skin infections.⁶⁹ Two semisynthetic guttiferone A derivatives, **54** and **57**, were generally more active than the parent PPAP, and other semisynthetic analogs, namely **55**, **56**, **58**, and **59**, were less active. Unlike antibacterial activity, *cLogP* values did not correlate with fungicidal activity. Isogarcinol and pyrohyperforin were found to be active against *Candida albicans*, the most common pathogen involved in yeast infections of the genitals and oral cavity.^{71,77} Xanthochymol was found to be active in a dose-dependent manner against *Phomopsis viticola*, a leading cause of grapevine dead arm (grape canker).²⁶ Treatment with xanthochymol in the 1-10 μg/mL range caused motility inhibition and lysis of *Phomopsis viticola* zoospores. Only a few other PPAPs have been evaluated against phytopathogenic fungi (i.e., *Aspergillus flavus*, *Aspergillus niger*,

Cladosporium cucumerinum, and *Fusarium avenaceum*), and while garcinol has some phytopathogenic fungicidal activity,⁸⁰ it would be interesting to see if other PPAPs exhibit activity against these fungi.

Table 1.8. Evaluation of PPAPs against various fungi.

Fungus	Active PPAPs (MIC in µg/mL)	Inactive PPAPs	References
<i>Aspergillus flavus</i>	garcinol (100)		80
<i>Aspergillus fumigatus</i>	garcinol (100)	xanthochymol	76,80
<i>Aspergillus niger</i>	garcinol (100)		80
<i>Candida albicans</i>	guttiferone A (40), ^a isogarcinol (64), pyrohyperforin (25)	7- <i>epi</i> -clusianone, furohyperforin, garcinol, guttiferone A, guttiferone E, guttiferone G, hyperforin, isoxanthochymol, nemorosone, xanthochymol	1,67,68,69,71,75,76,77,80,86,88
<i>Candida glabrata</i>	guttiferone A (5.0) ^a	guttiferone G, isoxanthochymol	67,69
<i>Candida krusei</i>	isogarcinol (64)	guttiferone A, guttiferone G, isoxanthochymol	67,69,77
<i>Candida lusitanae</i>		isogarcinol	77
<i>Candida parapsilosis</i>	guttiferone A (20.0) ^a		69
<i>Candida tropicalis</i>	guttiferone A (20.0) ^a	garcinol	69,80
<i>Cladosporium cucumerinum</i>		hyperevolutin A, hyperevolutin B	133
<i>Cladosporium sphaerospermum</i>		7- <i>epi</i> -clusianone	57
<i>Cryptococcus neoformans</i>	guttiferone A (5.0), ^a isogarcinol (64)		69,77,80
<i>Fusarium avenaceum</i>		hyperforin	1
<i>Microsporium gypseum</i>	guttiferone A (100) ^a		69
<i>Microsporium canis</i>	garcinol (100)		80
<i>Mucor plumbeus</i>		hyperforin	1
<i>Penicillium chrysogenum</i>		hyperforin	1
<i>Phomopsis viticola</i>	xanthochymol ^b		26
<i>Trichophyton ajelloi</i>	isogarcinol (64)		77
<i>Trichophyton interdigitale</i>	garcinol (100), guttiferone A (20.0) ^a	xanthochymol	69,76,80
<i>Trichophyton rubrum</i>	guttiferone A (11.8), ^a isogarcinol (32)	nemorosone	77,88

^a Value reported is IC₅₀ (in µg/mL).

^b See text.

Antioxidant and Anti-inflammatory Activity

The antioxidant properties of PPAPs have also been explored in a variety of contexts, both *in vitro* and *in vivo*. A summary of PPAP performance in various *in vitro* antioxidant assays is found in Table 1.9. Unsurprisingly, PPAPs that bear a 3,4-dihydroxybenzoyl group at the C3 position were found to be the most active at scavenging radical or reactive oxygen species in these assays. If one of the

¹³³ Decosterd, L. A.; Stoeckli-Evans, H.; Chapuis, J.-C.; Msonthi, J. D.; Sordat, B.; Hostettmann, K. *Helv. Chim. Acta* **1989**, 72, 464-471.

phenolic hydroxyl groups is alkylated, as in the 13-*O*-methyl ethers of garcinol and isogarcinol, antioxidant potential is lost.¹⁴ The presence of a C2–C4 β -hydroxyenone was also important but not essential given the strong antioxidant properties of PPAPs such as guttiferone K2, isogarcinol, and isoxanthochymol. A comparison of nemorosone and its *O*-methyl ether illustrates the significance of C2–C4 β -hydroxyenone functionality.¹⁴⁶

Table 1.9. *In vitro* PPAP antioxidant activity.

PPAP	Antioxidant activity ^{a,b}	References
acuminophenone A	DPPH (1.8), ABTS (3.4), TEAC (7.8)	134
aristophenone	DPPH (125)	135
clusianone	DPPH (inactive)	14
7- <i>epi</i> -clusianone	DPPH (inactive), ABTS (inactive)	18,136,137
garcinielliptone A	DPPH (150), ABTS (139.0), XO (53.8)	138
garcinielliptone C	XO (59.9)	139
garcinielliptone F	DPPH (inactive), ABTS (inactive), XO (inactive)	138
garcinielliptone P	XO (48.1)	140
garcinielliptone S	DPPH (inactive), ABTS (inactive), XO (inactive)	138
garcinol	DPPH (10.2), XO (52)	14,66,141
garcinol 13- <i>O</i> -methyl ether	DPPH (inactive)	14
garsubellin A	DPPH (inactive), ABTS (inactive), XO (inactive)	138

¹³⁴ Almanza, G. R.; Quispe, R.; Mollinedo, P.; Rodrigo, G.; Fukushima, O.; Villagomez, R.; Akesson, B.; Sterner, O. *Nat. Prod. Commun.* **2011**, *6*, 1269-1274.

¹³⁵ Baggett, S.; Protiva, P.; Mazzola, E. P.; Yang, H.; Ressler, E. T.; Basile, M. J.; Weinstein, I. B.; Kennelly, E. J. *J. Nat. Prod.* **2005**, *68*, 354-360.

¹³⁶ Carvalho-Silva, L. B.; Oliveira, M. de V.; Gontijo, V. S.; Oliveira, W. F.; Derogis, P. B. M. C.; Stringheta, P. C.; Nagem, T. J.; Brigagão, M. R. P. L.; dos Santos, M. H. *Food Res. Int.* **2012**, *48*, 180-186.

¹³⁷ Santa-Cecília, F. V.; Santos, G. B.; Fuzissaki, C. N.; Derogis, P. B. M. C.; Freitas, L. A. S.; Gontijo, V. S.; Stringheta, P. C.; Nagem, T. J.; Brigagão, M. R. P. L.; dos Santos, M. H. *J. Med. Food* **2012**, *15*, 200-205.

¹³⁸ Lin, K.-W.; Huang, A.-M.; Yang, S.-C.; Weng, J.-R.; Hour, T.-C.; Pu, Y.-S.; Lin, C.-N. *Food Chem.* **2012**, *135*, 851-859.

¹³⁹ Lin, K.-W.; Huang, A.-M.; Tu, H.-Y.; Weng, J.-R.; Hour, T.-C.; Wei, B.-L.; Yang, S.-C.; Wang, J.-P.; Pu, Y.-S.; Lin, C.-N. *J. Agric. Food Chem.* **2009**, *57*, 8782-8787.

¹⁴⁰ Lin, K.-W.; Huang, A.-M.; Tu, H.-Y.; Lee, L.-Y.; Wu, C.-C.; Hour, T.-C.; Yang, C.-H.; Pu, Y.-S.; Lin, C.-N. *J. Agric. Food Chem.* **2011**, *59*, 407-414.

¹⁴¹ Liao, C.-H.; Ho, C.-T.; Lin, J.-K. *Biochem. Biophys. Res. Commun.* **2005**, *329*, 1306-1314.

Table 1.9 (continued). *In vitro* PPAP antioxidant activity.

PPAP	Antioxidant activity ^{a,b}	References
guttiferone A	DPPH (20.8-31.0), ABTS (12.5)	18,122,142,143
guttiferone E	DPPH (68)	86,135
guttiferone F	DPPH (42.8)	144
guttiferone G	DPPH (26.8)	145
guttiferone H	DPPH (64)	135
7- <i>epi</i> -guttiferone J	DPPH (inactive), ABTS (inactive)	18
guttiferone K2	DPPH (3.9), ABTS (18.4), TEAC (2.5)	134
32-hydroxy- <i>ent</i> -guttiferone M	DPPH (38.3), ABTS (45.6)	18
isogarcinol	DPPH (13.3)	14
isogarcinol 13- <i>O</i> -methyl ether	DPPH (inactive)	14
isoxanthochymol	DPPH (4.6-5.8), ABTS (96.3), TEAC (3.7)	134,145
nemorosone	DPPH (44.1)	146
nemorosone <i>O</i> -methyl ether	DPPH (inactive)	146
xanthochymol	DPPH (53)	86,135

^a Assay abbreviations: DPPH, 2,2-diphenyl-1-picrylhydrazyl; ABTS, 2,2'-azino-bis(3-ethylbenzothiazoline-6-sulphonic acid); XO, xanthine oxidase; TEAC, Trolox equivalent antioxidant capacity.

^b Values reported in parentheses refer to IC₅₀ (in µM) for DPPH, ABTS, and XO assays, and Trolox equivalents for TEAC assay.

Other than the results presented in Table 1.9, several other PPAPs have been evaluated for antioxidant properties *in vitro*. Using an HPLC-DPPH assay system, hyperforin and adhyperforin were both identified as very active antioxidant components of alcoholic *Hypericum perforatum* extracts.¹⁴⁷ Similar results were obtained using partially purified HPLC fractions containing hyperforin, adhyperforin, hyperfirin, and adhyperfirin across a variety of tests, including the DPPH assay, FRAP, superoxide anion

¹⁴² Nuñez-Figueroa, Y.; García-Pupo, L.; Ramírez-Sánchez, J.; Alcántara-Isaac, Y.; Cuesta-Rubio, O.; Hernández, R. D.; Naal, Z.; Curti, C.; Padro-Andreu, G. L. *Arzneimittel-Forsch.* **2012**, *62*, 583-589.

¹⁴³ Magadula, J. J. *Int. J. Res. Phytochem. Pharmacol.* **2012**, *2*, 16-20.

¹⁴⁴ Hartati, S.; Triyem; Cahyana, H. *Indo. J. Cancer Chemoprev.* **2010**, *1*, 85-91.

¹⁴⁵ Lannang, A. M.; Komguem, J.; Ngninzeko, F. N.; Tangmouo, J. G.; Lontsi, D.; Ajaz, A.; Choudhary, M. I.; Sondengam, B. L.; Atta-ur-Rahman *Bull. Chem. Soc. Ethiop.* **2006**, *20*, 247-252.

¹⁴⁶ Cuesta-Rubio, O.; Frontana-Urbe, B. A.; Ramírez-Apan, T.; Cárdenas, J. Z. *Naturforsch.* **2002**, *57c*, 372-378.

¹⁴⁷ Gioti, E. M.; Fiamegos, Y. C.; Skalkos, D. C.; Stalikas, C. D. *Food Chem.* **2009**, *117*, 398-404.

test, NO radical inhibition assay, and the lipid peroxidation assay.¹⁴⁸ A mixture of scrobiculatones A and B was found to be active in the DPPH assay.⁸⁴ Guttiferone K and semsinone A were both active in the DPPH, ORAC, and anti-AGEs inhibition assays.¹⁴³

The reactions of garcinol with various radical systems were studied in order to further understand how this PPAP behaves as an antioxidant.¹⁴⁹ Exposure of an acetone solution of garcinol (**7**) to DPPH in the dark afforded two oxidative cyclization products, **68** and **69** (Scheme 1.11a).¹⁵⁰ Coincidentally, these two compounds were later isolated from *Garcinia nuijiangensis* and named nuijiangfolin A and B.¹⁵¹ A possible mechanistic manifold for this transformation is shown in Scheme 1.11b. A resonance-stabilized enoxy radical **70** formed via hydrogen atom abstraction may cyclize onto the electron-rich aromatic ring to form **71**, which after tautomerization provides **68** and **69**. The formation of these two oxidation products from garcinol provides evidence that the antioxidant properties of certain PPAPs may be derived from the 3,4-dihydroxybenzoyl and the C2–C4 β -hydroxyenone functional groups. Similar results were observed when a heated acetone solution of garcinol (**7**) was exposed to AIBN, affording hydroperoxide **72** and isogarcinol (**8**) as well as **68** and **69** (Scheme 1.11c).¹⁵² The formation of **72** likely involves radical 6-*endo*-trig cyclization of the enoxy radical **70** onto the C1 prenyl group, followed by trapping with molecular oxygen. The formation of isogarcinol may not involve radical intermediates, given that its heat-mediated formation from garcinol has been previously reported.^{31,153,154}

¹⁴⁸ Orčić, D. Z.; Mimica-Dukić, N. M.; Francisković, M. M.; Petrović, S. S.; Jovin, E. Đ. *Chem. Cent. J.* **2011**, 5, 34.

¹⁴⁹ For a review of the antioxidant properties of garcinol and its derivatives, see: Padhye, S.; Ahmad, A.; Oswal, N.; Sarkar, F. H. *J. Hematology Oncol.* **2009**, 2, 38.

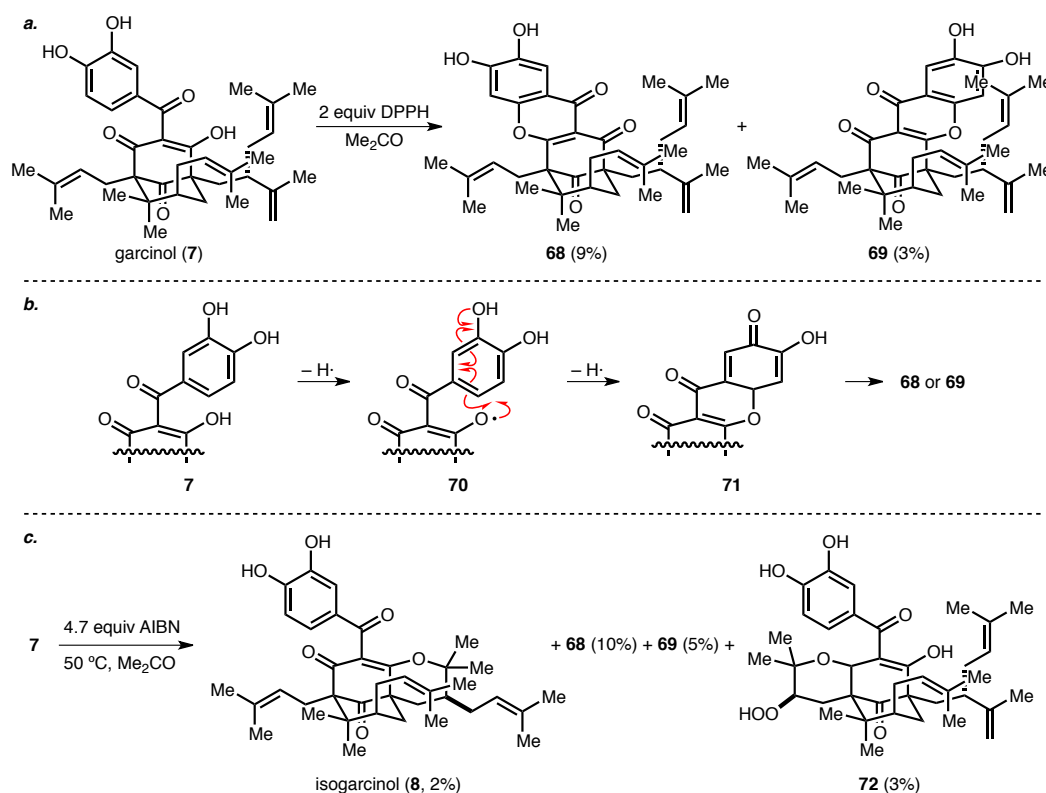
¹⁵⁰ Sang, S.; Pan, M.-H.; Cheng, X.; Bai, N.; Stark, R. E.; Rosen, R. T.; Lin-Shiau, S.-Y.; Lin, J.-K.; Ho, C.-T. *Tetrahedron* **2001**, 57, 9931-9938.

¹⁵¹ Xia, Z.-X.; Zhang, D.-D.; Liang, S.; Lao, Y.-Z.; Zhang, H.; Tan, H.-S.; Chen, S.-L.; Wang, X.-H.; Xu, H.-X. *J. Nat. Prod.* **2012**, 75, 1459-1464.

¹⁵² Sang, S.; Liao, C.-H.; Pan, M.-H.; Rosen, R. T.; Lin-Shiau, S.-Y.; Lin, J.-K.; Ho, C.-T. *Tetrahedron* **2002**, 58, 10095-10102.

¹⁵³ Krishnamurthy, N.; Lewis, Y. S.; Ravindranath, B. *Tetrahedron Lett.* **1981**, 22, 793-796.

¹⁵⁴ Sahu, A.; Das, B.; Chatterjee, A. *Phytochemistry* **1989**, 28, 1233-1235.



Scheme 1.11. (a) The reaction of garcinol (**7**) with DPPH and (b) a possible mechanism, and (c) the reaction of garcinol (**7**) with AIBN.

Several PPAPs have been evaluated in cell-based assays for antioxidant activity. A St. John's wort extract with standardized hyperforin content showed inverse dose-dependent superoxide inhibition in a XO-human placental vein assay.¹⁵⁵ In other words, the most concentrated sample had a pro-oxidant effect, while the most dilute sample had the largest free radical inhibitory effect in this model, showing nearly an 80% decrease compared to control. The radical scavenging ability of hyperforin was further explored in another study involving skin exposed to solar simulated radiation.¹⁵⁶ Hyperforin was found to be more effective than Trolox (and without displaying phototoxicity) in a H₂DCFDA irradiation assay involving HaCaT cells, with an EC₅₀ value of 0.7 μM . A cream containing 1.5% hyperforin was then

¹⁵⁵ Hunt, E. J.; Lester, C. E.; Lester, E. A.; Tackett, R. L. *Life Sci.* **2001**, *69*, 181-190.

¹⁵⁶ Meinke, M. C.; Schanzer, S.; Haag, S. F.; Casetti, F.; Müller, M. L.; Wölflé, U.; Kleeman, A.; Lademann, J.; Schempp, C. M. *Eur. J. Pharm. Biopharm.* **2012**, *81*, 346-350.

formulated and determined to have a radical scavenging ability of $200 \cdot 10^{14}$ radicals/mg, corresponding to a radical protection factor of 39 (comparable to a good sunscreen). After demonstrating that the cream reduced radical formation on irradiated porcine ear skin *ex vivo*, it was applied to 20 volunteers in a randomized, double-blind, vehicle-controlled clinical study. The cream was well tolerated and successfully reduced ultraviolet B-induced erythema. A later study also showed that a hyperforin-rich skin cream provided protection from radical formation in a 9-person study.¹⁵⁷ These results contrast an earlier study, which found that hyperforin was a significant phototoxic component of St. John's wort extracts in an assay involving photosensitized peroxidation of linoleic acid.¹⁵⁸

Several studies of the antioxidant properties of garcinol have been reported. Aside from being almost three times more active by weight than vitamin E in the DPPH assay, it also displayed moderate activity against linoleic acid peroxidation and suppressed protein glycation in an *in vitro* bovine serum albumin/fructose system.¹⁵⁹ Its free radical scavenging ability was also validated in Fenton reaction and H_2O_2 /NaOH/DMSO systems, and *in vivo* by preventing indomethacin-induced acute gastric ulceration in rats through oral administration.¹⁶⁰ Garcinol was also shown to protect DNA and neurons from radical-induced damage.¹⁴¹ With an IC_{50} value of $0.32 \mu M$, garcinol prevented pUC-19 supercoiled DNA from strand breakage under Fenton reaction conditions.

While reactive oxygen species (ROS) are produced normally through metabolism or via immune system oxidative burst, if they accumulate too quickly, cell membrane damage may occur with the concomitant formation of mutagenic or carcinogenic lipid peroxides.¹⁶¹ Table 1.10 summarizes the activity of a variety of PPAPs against ROS formation in polymorphonuclear leukocytes (PMNs), rat

¹⁵⁷ Arndt, S.; Haag, S. F.; Kleemann, A.; Lademann, J.; Meinke, M. C. *Exp. Dermatol.* **2013**, 22, 354-357.

¹⁵⁸ Onoue, S.; Seto, Y.; Ochi, M.; Inoue, R.; Ito, H.; Hatano, T.; Yamada, S. *Phytochemistry* **2011**, 72, 1814-1820.

¹⁵⁹ Yamaguchi, F.; Ariga, T.; Yoshimura, Y.; Nakazawa, H. *J. Agric. Food Chem.* **2000**, 48, 180-185.

¹⁶⁰ Yamaguchi, F.; Saito, M.; Ariga, T.; Yoshimura, Y.; Nakazawa, H. *J. Agric. Food Chem.* **2000**, 48, 2320-2325.

¹⁶¹ Murphy, M. P.; Holmgren, A.; Larsson, N.-G.; Halliwell, B.; Chang, C. J.; Kalyanaraman, B.; Rhee, S. G.; Thornalley, P. J.; Partridge, L.; Gems, D.; Nyström, T.; Belousov, V.; Schumacker, P. T.; Winterbourn, C. C. *Cell Metab.* **2011**, 13, 361-366.

neutrophils, and human neutrophils stimulated with *N*-formylmethionine leucyl-phenylalanine (fMLP) alone or in combination with cytochalasin B (CB), opsonized zymosan (OZ), or phorbol 12-myristate 13-acetate (PMA). The garcimultiflorone family and 13,14-didehydroxyisogarcinol were found to be potent inhibitors of ROS generated from PMNs stimulated with fMLP/CB.¹⁵ 7-*epi*-Clusianone also displayed dose-dependent decrease in ROS in PMNs stimulated with either fMLP or PMA.¹³⁷ Most other PPAPs were either inactive or displayed marginal antioxidant activity, with the only exception being hyperforin, having an IC₅₀ value of 1.8 µM against fMLP-stimulated PMNs.¹⁶⁶ Later studies on hyperforin revealed that its ROS inhibition activity was lost when the PMNs were treated with PMA.¹⁶⁷ This, combined with the observation that hyperforin decreased Ca²⁺ levels in resting PMNs and caused a decreased Ca²⁺ response to fMLP, led the authors to conclude that hyperforin targeted components of G protein signaling cascades involved in both Ca²⁺ homeostasis and inflammatory response. The antioxidant properties garcinielliptone FC have also been investigated.¹⁶² Treatment of male mice with 2 mg/kg garcinielliptone FC caused a statistically significant increase in the activity of superoxide dismutase but not catalase.

Table 1.10. Evaluation of PPAPs against ROS generation.

PPAP	Cell line	Stimulation	IC ₅₀ (µM)	References
garcimultiflorone A	PMN	fMLP/CB	5.6	15
garcimultiflorone B	PMN	fMLP/CB	0.11	15
13-hydroxygarcimultiflorone B	PMN	fMLP/CB	0.40	15
garcimultiflorone C	PMN	fMLP/CB	7.2	15
garcimultiflorone D2	PMN	fMLP/CB	7.2	163
garcinielliptone A	rat neutrophil	fMLP/CB	inactive	164
garcinielliptone A	rat neutrophil	PMA	inactive	164
garcinielliptone B	rat neutrophil	fMLP/CB	inactive	164
garcinielliptone B	rat neutrophil	PMA	inactive	164

¹⁶² Júnior, J. S. da C.; de Almeida, A. A. C.; Costa, J. P.; Citó, A. M. das G. L.; Saffi, J.; de Freitas, R. M. *Pharm. Biol.* **2012**, *50*, 453-457.

¹⁶³ Ting, C.-W.; Hwang, T.-L.; Chen, I.-S.; Yen, M.-H.; Chen, J.-J. *Chem. Biodivers.* **2012**, *9*, 99-105.

¹⁶⁴ Weng, J.-R.; Lin, C.-N.; Tsao, L.-T.; Wang, J.-P. *Chem. Eur. J.* **2003**, *9*, 1958-1963.

Table 1.10 (*continued*). Evaluation of PPAPs against ROS generation.

PPAP	Cell line	Stimulation	IC ₅₀ (μM)	References
garcinielliptone C	rat neutrophil	fMLP/CB	11.5	139
garcinielliptone C	rat neutrophil	PMA	inactive	139
garcinielliptone F	rat neutrophil	fMLP/CB	17.0	165
garcinielliptone F	rat neutrophil	PMA	inactive	165
garcinielliptone H	rat neutrophil	fMLP/CB	inactive	165
garcinielliptone H	rat neutrophil	PMA	inactive	165
garcinielliptone I	rat neutrophil	fMLP/CB	inactive	165
garcinielliptone I	rat neutrophil	PMA	inactive	165
garsubellin A	rat neutrophil	fMLP/CB	inactive	164
garsubellin A	rat neutrophil	PMA	inactive	164
hyperforin	PMN	fMLP	1.8	166
hyperforin	PMN	OZ	inactive	166
hyperforin	PMN	PMA	inactive	167
hyperpapunone	PMN	fMLP	inactive	166
hyperpapunone	PMN	OZ	inactive	166
13,14-didehydroxyisogarcinol	PMN	fMLP/CB	0.88	15
papuaforin A	PMN	fMLP	inactive	166
papuaforin A	PMN	OZ	inactive	166
papuaforin B	PMN	fMLP	inactive	166
papuaforin B	PMN	OZ	inactive	166
papuaforin C	PMN	fMLP	inactive	166
papuaforin C	PMN	OZ	inactive	166
papuaforin D	PMN	fMLP	inactive	166
papuaforin D	PMN	OZ	inactive	166
papuaforin E	PMN	fMLP	8.0	166
papuaforin E	PMN	OZ	inactive	166

Several PPAPs have been evaluated against markers of inflammatory response aside from superoxide burst, such as the release of histamine, elastase, lysozyme, and β-glucuronidase as well as nitrite accumulation (Table 1.11). Given the short half-life of nitric oxide, nitrite accumulation may be used to gauge its release during inflammatory response. The garcimultiflorone family of PPAPs displayed fairly potent activity against elastase release in PMNs.¹⁵ However, to a large degree, the garcinielliptones showed little or no effect on these inflammatory response markers.

¹⁶⁵ Weng, J.-R.; Lin, C.-N.; Tsao, L.-T.; Wang, J.-P. *Chem. Eur. J.* **2003**, *9*, 5520-5527.

¹⁶⁶ Heilmann, J.; Winkelmann, K.; Sticher, O. *Planta Med.* **2003**, *69*, 202-206.

¹⁶⁷ Feißt, C.; Werz, O. *Biochem. Pharmacol.* **2004**, *67*, 1531-1539.

Table 1.11. Evaluation of PPAPs against several markers of inflammation.

PPAP	Cell line	Stimulation	Measured outcome	IC ₅₀ (μM)	Reference
garcimultiflorone A	PMN	fMLP/CB	elastase release	4.7	15
garcimultiflorone B	PMN	fMLP/CB	elastase release	0.14	15
13-hydroxygarcimultiflorone B	PMN	fMLP/CB	elastase release	0.86	15
garcimultiflorone C	PMN	fMLP/CB	elastase release	12.1	15
garcimultiflorone D2	PMN	fMLP/CB	elastase release	6.0	163
garcinielliptone A	rat peritoneal mast cell	compound 48/80	β-glucuronidase release	inactive	164
garcinielliptone A	rat peritoneal mast cell	compound 48/80	histamine release	inactive	164
garcinielliptone B	rat peritoneal mast cell	compound 48/80	β-glucuronidase release	inactive	164
garcinielliptone B	rat peritoneal mast cell	compound 48/80	histamine release	inactive	164
garcinielliptone C	rat neutrophil	fMLP/CB	β-glucuronidase release	30.0	139
garcinielliptone C	rat neutrophil	fMLP/CB	lysozyme release	27.4	139
garcinielliptone C	RAW264.7	LPS	TNF-α formation	inactive	139
garcinielliptone F	rat neutrophil	fMLP/CB	β-glucuronidase release	26.9	165
garcinielliptone F	rat neutrophil	fMLP/CB	lysozyme release	20.0	165
garcinielliptone F	RAW264.7	LPS	nitrite accumulation	inactive	165
garcinielliptone F	N9	LPS/IFN-γ	nitrite accumulation	inactive	165
garcinielliptone H	rat neutrophil	fMLP/CB	β-glucuronidase release	inactive	165
garcinielliptone H	rat neutrophil	fMLP/CB	lysozyme release	inactive	165
garcinielliptone H	RAW264.7	LPS	nitrite accumulation	inactive	165
garcinielliptone H	N9	LPS/IFN-γ	nitrite accumulation	inactive	165
garcinielliptone I	rat neutrophil	fMLP/CB	β-glucuronidase release	inactive	165
garcinielliptone I	rat neutrophil	fMLP/CB	lysozyme release	inactive	165
garcinielliptone I	RAW264.7	LPS	nitrite accumulation	inactive	165
garcinielliptone I	N9	LPS/IFN-γ	nitrite accumulation	7.4	165
garcinielliptone L	rat mast cell	compound 48/80	β-glucuronidase release	22.9	60
garcinielliptone L	rat mast cell	compound 48/80	histamine release	inactive	60
garcinielliptone L	RAW264.7	LPS	nitrite accumulation	22.7	60
garcinielliptone L	N9	LPS/IFN-γ	nitrite accumulation	12.8	60
garcinielliptone M	rat mast cell	compound 48/80	β-glucuronidase release	13.6	60
garcinielliptone M	rat mast cell	compound 48/80	histamine release	19.0	60
garcinielliptone M	RAW264.7	LPS	nitrite accumulation	15.3	60
garcinielliptone M	N9	LPS/IFN-γ	nitrite accumulation	inactive	60
garsubellin A	rat peritoneal mast cell	compound 48/80	β-glucuronidase release	15.6	164
garsubellin A	rat peritoneal mast cell	compound 48/80	histamine release	inactive	164
13,14-didehydroxyisogarcinol	PMN	fMLP/CB	elastase release	1.2	15

The effects of PPAPs on a variety of other markers of inflammation have been explored. Sundaicumones A and B were found to be weak activators of glucocorticoid receptor, which inhibits pro-inflammatory transcription factors.¹⁶⁸ Guttiferones O and P inhibited mitogen-activated protein kinase activated protein kinase 2 (MAPKAPK-2), a serine/threonine kinase involved in inflammation-response

¹⁶⁸ Cao, S.; Low, K.-N.; Glover, R. P.; Crasta, S. C.; Ng, S.; Buss, A. D.; Butler, M. S. *J. Nat. Prod.* **2006**, *69*, 707-709.

transcriptional regulation, both with an IC₅₀ value of 22.0 µM.¹⁶⁹ Hyperforin has also been evaluated in several anti-inflammatory assays. In human primary hepatocytes and intestinal epithelia, hyperforin induced interleukin-8 (IL-8) and intercellular adhesion molecule-1 (ICAM-1) expression.¹⁷⁰ These effects were found to be dependent on extracellular signal-regulated kinase (ERK) 1 and 2 but independent of pregnane X receptor (PXR) and nuclear factor kappa B (NF-κB). The dicyclohexylammonium salt of hyperforin also prevented fMLP-induced PMN chemotaxis and tissue infiltration in a dose-dependent manner (IC₅₀ = 1 µM).¹⁷¹ The authors found that this was caused by decreased expression of the adhesion molecule integrin alpha M (ITGAM) and inhibition of matrix metalloproteinase-9 (MMP-9) activation. Subsequent studies found that hyperforin downregulated other markers in activated T cells (e.g., IFN-γ, T-box, CXCR3) and was successfully evaluated in a murine model of experimental allergic encephalomyelitis, an autoimmune disease of the central nervous system.¹⁷²

Hyperforin, garcinol, garcinielliptone FC, and guttiferone K were all found to potently inhibit lipid oxidation using the thiobarbituric acid reactive species (TBARS) assay. Hyperforin prevented low-density lipoprotein (LDL) oxidation in Cu²⁺- and nonmetal-mediated oxidation at concentrations as low as 2.5 µM.¹⁷³ Garcinol prevented LDL oxidation mediated by both Fe²⁺ (IC₅₀ = 0.42 µM) and AAPH (IC₅₀ = 1.2 µM).¹⁷⁴ This was more potent than vitamin E in both assays. Garcinielliptone FC completely inhibited lipid peroxidation in the TBARS assay at 8.3 µM, and had an IC₅₀ below 2 µM.¹⁷⁵ Garcinol and

¹⁶⁹ Carroll, A. R.; Suraweera, L.; King, G.; Rali, T.; Quinn, R. J. *J. Nat. Prod.* **2009**, *72*, 1699-1701.

¹⁷⁰ Zhou, C.; Tabb, M. M.; Sadatrafiei, A.; Grün, F.; Sun, A.; Blumberg, B. *J. Clin. Immunol.* **2004**, *24*, 623-636.

¹⁷¹ Dell'Aica, I.; Niero, R.; Piazza, F.; Cabrelle, A.; Sartor, L.; Colalto, C.; Brunetta, E.; Lorusso, G.; Benelli, R.; Albini, A.; Calabrese, F.; Agostini, C.; Garbisa, S. *J. Pharmacol. Exp. Ther.* **2007**, *321*, 492-500.

¹⁷² Cabrelle, A.; Dell'Aica, I.; Melchiori, L.; Carraro, S.; Brunetta, E.; Niero, R.; Scquizzato, E.; D'Intino, G.; Calzá, L.; Garbisa, S.; Agostini, C. *J. Leukoc. Biol.* **2008**, *83*, 212-219.

¹⁷³ Laggner, H.; Schrier, S.; Hermann, M.; Exner, M.; Mühl, A.; Gmeiner, B. M. K.; Kapiotis, S. *Free Radical Res.* **2007**, *41*, 234-241.

¹⁷⁴ Hutadilok-Towatana, N.; Kongkachuay, S.; Mahabusarakam, W. *Nat. Prod. Res.* **2007**, *21*, 655-662.

¹⁷⁵ Júnior, J. S. C.; Ferraz, A. B. F.; Filho, B. A. B.; Feitosa, C. M.; Citó, A. M. G. L.; Freitas, R. M.; Saffi, J. J. *Med. Plants Res.* **2011**, *5*, 293-299.

guttiferone K were found to protect human blood platelets from oxidative damage due to peroxynitrite, but these PPAPs did not prevent protein nitration.¹⁷⁶

Several PPAPs have been evaluated for their ability to inhibit general pro-inflammatory response. Garcinol displayed a neuroprotective effect in rat astrocytes exposed to LPS.¹⁴¹ Under normal circumstances, LPS exposure causes an inflammatory response including iNOS and COX-2 induction, which correlates with neurodegenerative processes. It is believed that garcinol not only behaves as an antioxidant but also inhibits this inflammatory response. In rats with carrageenan-induced paw edema and peritonitis, 7-*epi*-clusianone reduced inflammation in a dose-dependent manner, with oral doses of 5, 10, and 15 mg/kg.¹⁷⁷ Topical treatment of the dicyclohexylammonium salt of hyperforin as well as adhyperforin were similarly effective at the reduction of murine croton oil-induced ear edema as indomethacin, with EC₅₀ values of 0.25 and 0.30 $\mu\text{mol}/\text{cm}^2$.¹⁷⁸ In an 8-person clinical trial, the anti-inflammatory effects of hyperforin were found to at least be partly due to the ability of this PPAP to reduce the epidermal cells' ability to recruit alloreactive T cells.¹⁷⁹ These effects were similar to solar-simulated radiation, a known immunosuppressive agent. Hyperforin treatment was also well tolerated and was cosmetically acceptable. When epidermal cells were treated with hyperforin *in vitro*, a dose-dependent reduction of T cell and PMN proliferation was observed. As a result, hyperforin therapy may be a possible treatment option for chronic atopic dermatitis or other skin conditions involving overreactive inflammatory response.

Phagocyte activation of iNOS (inducible nitric oxide synthase) causes the release of nitric oxide; however, excessive NO production may lead to neurodegenerative disease. Garcinielliptone FC was

¹⁷⁶ Kolodziejczyk, J.; Masullo, M.; Olas, B.; Piacente, S.; Wachowicz, B. *Platelets* **2009**, *20*, 487-492.

¹⁷⁷ Santa-Cecília, F. V.; Freitas, L. A. S.; Vilela, F. C.; Veloso, C. de C.; da Rocha, C. Q.; Moreira, M. E. C.; Dias, D. F.; Giusti-Paiva, A.; dos Santos, M. H. *Eur. J. Pharmacol.* **2011**, *670*, 280-285.

¹⁷⁸ Sosa, S.; Pace, R.; Bornancin, A.; Morazzoni, P.; Riva, A.; Tubaro, A.; Loggia, R. D. *J. Pharm. Pharmacol.* **2007**, *59*, 703-709.

¹⁷⁹ Schempp, C. M.; Winghofer, B.; Lüdtkke, R.; Simon-Haarhaus, B.; Schöpf, E.; Simon, J. C. *Br. J. Dermatol.* **2000**, *142*, 979-984.

found to be a potent scavenger of NO in a sodium nitroprusside decomposition assay.¹⁷⁵ Hyperforin inhibited LPS-induced NO release in the 0.25-0.75 μ M range in murine microglia by decreasing iNOS expression.¹⁸⁰ These effects correlated with suppression of the activated states of NF- κ B and cAMP response element-binding protein (CREB). Prior results had suggested hypericin, and not hyperforin, was the component of St. John's wort extracts responsible for inhibition of NF- κ B.¹⁸¹ In rat aorta at concentrations below 10 μ M, 7-*epi*-clusianone induced vasodilation via NO release.¹⁸² Interestingly, at concentrations above 10 μ M, vasoconstriction was observed and was dependent on eicosanoid production.

In addition, several PPAPs have been found to directly inhibit or modulate key proteins involved in the biosynthesis of pro-inflammatory eicosanoids.¹⁸³ 5-Lipoxygenase (5-LO) catalyzes the oxidation of arachidonic acid to arachidonic acid 5-hydroperoxide, an intermediate in the biosynthesis of leukotrienes.¹⁸⁴ Arachidonic acid can also be oxidized by cyclooxygenases 1 and 2 (COX-1 and COX-2) to prostaglandin H₂, the progenitor to prostanoids, prostacyclin, and thromboxanes.¹⁸⁵ While several classes of drugs have been developed to broadly inhibit the action of these enzymes, the discovery and development of specific inhibitors of each of these pro-inflammatory enzymes is still actively pursued.¹⁸⁶

Several PPAPs are reported to be sub-micromolar inhibitors of proteins involved in eicosanoid biosynthesis. Early studies with hyperforin established that it is an uncompetitive inhibitor of both 5-LO

¹⁸⁰ Kraus, B.; Wolff, H.; Elstner, E. F.; Heilmann, J. *Naunyn-Schmied. Arch. Pharmacol.* **2010**, *381*, 541-553.

¹⁸¹ Bork, P. M.; Bacher, S.; Schmitz, M. L.; Kaspers, U.; Heinrich, M. *Planta Med.* **1999**, *65*, 297-300.

¹⁸² Cruz, A. J.; Lemos, V. S.; dos Santos, M. H.; Nagem, T. J.; Cortes, S. F. *Phytomedicine* **2006**, *13*, 442-445.

¹⁸³ For reviews of the biosynthesis and biology of pro-inflammatory eicosanoids, see: (a) Funk, C. D. *Science* **2001**, *294*, 1871-1875. (b) Peters-Golden, M.; Henderson, W. R., Jr. *N. Engl. J. Med.* **2007**, *357*, 1841-1854.

¹⁸⁴ Rådmark, O.; Werz, O.; Steinhilber, D.; Samuelsson, B. *Trends Biochem. Sci.* **2007**, *32*, 332-341.

¹⁸⁵ Ricciotti, E.; FitzGerald, G. A. *Arterioscler. Thromb. Vasc. Biol.* **2011**, *31*, 986-1000.

¹⁸⁶ Werz, O.; Steinhilber, D. *Pharmacol. Therapeut.* **2006**, *112*, 701-718.

and COX-1.¹⁸⁷ Hyperforin inhibited purified 5-LO with an IC₅₀ value of 90 nM and had an IC₅₀ in the range of 1-2 µM in Ca²⁺ ionophore-stimulated (PMNs), which was comparable to the known 5-LO inhibitor zileuton. COX-1 activity was also inhibited in stimulated platelet cells, with IC₅₀ values ranging from 0.3 to 3 µM depending on the method of stimulation. No COX-2 inhibition activity was observed. When RAW264.7 mouse macrophages¹⁸⁸ and LPS-stimulated human blood samples¹⁸⁹ were exposed to hyperforin, prostaglandin E₂ biosynthesis was inhibited. Aside from 5-LO and COX-1, hyperforin acts as an inhibitor of membrane-associated prostaglandin E synthetase-1 (mPGES-1) with an IC₅₀ value of 1 µM.¹⁸⁹ Further, hyperforin may have a unique pharmacological profile compared to other known 5-LO inhibitors. When carrageenan-treated rats were treated with hyperforin (4 mg/kg, intraperitoneal), suppression of leukotriene B₄ was observed; however, when 5-LO point mutations were introduced (W13A-W75A-W102A) or phosphatidylcholine was present, the inhibitory activity of hyperforin was abolished.¹⁹⁰ Other 5-LO inhibitors of different structural classes, ZM230487 and BWA4C, continued to inhibit leukotriene B₄ production in the presence of the modifications.

Given the distinctive nature of hyperforin 5-LO inhibition and moderate potency, a series of semisynthetic hyperforin analogs were evaluated against 5-LO in PMNs.¹⁹¹ Overall, oxidation of hyperforin produced more active 5-LO inhibitors, and alkylation or acylation produced less active 5-LO inhibitors (Table 1.12, Figure 1.11). The most active analog found in the study was oxyhyperforin, which had an IC₅₀ value of 40 nM. Interestingly, analogs featuring a C9 carbinol were similarly active to those

¹⁸⁷ Albert, D.; Zündorf, I.; Dingeramn, T.; Müller, W. E.; Steinhilber, D.; Werz, O. *Biochem. Pharmacol.* **2002**, *64*, 1767-1775.

¹⁸⁸ Hammer, K. D. P.; Hillwig, M. L.; Solco, A. K. S.; Dixon, P. M.; Delate, K.; Murphy, P. A.; Wurtele, E. S.; Birt, D. F. *J. Agric. Food Chem.* **2007**, *55*, 7323-7331.

¹⁸⁹ Koeberle, A.; Rossi, A.; Bauer, J.; Dehm, F.; Verotta, L.; Northoff, H.; Sautebin, L.; Werz, O. *Front. Pharmacol.* **2011**, *2*, 7.

¹⁹⁰ Feißt, C.; Pergola, C.; Rakonjac, M.; Rossi, A.; Koeberle, A.; Dodt, G.; Hoffmann, M.; Hoernig, C.; Fischer, L.; Steinhilber, D.; Franke, L.; Schneider, G.; Rådmark, O.; Sautebin, L.; Werz, O. *Cell. Mol. Life Sci.* **2009**, *66*, 2759-2771.

¹⁹¹ Feißt, C.; Albert, D.; Verotta, L.; Werz, O. *Med. Chem.* **2005**, *1*, 287-291.

containing a C9 ketone functionality. Aside from hyperforin and its derivatives, garcinol also displayed inhibitory activity against various enzymes involved in eicosanoids. Garcinol was found to be most active against 5-LO ($IC_{50} = 0.1 \mu M$), mPGES-1 ($IC_{50} = 0.3 \mu M$), and COX-1 ($IC_{50} = 12 \mu M$) but showed no activity against COX-2.¹⁹²

Table 1.12. 5-LO inhibition activity of semisynthetic hyperforin analogs.¹⁹¹

Hyperforin derivative	IC_{50} (μM)
hyperforin	0.19
furohyperforin	0.90
oxyhyperforin	0.040
hyperforin <i>O</i> -methyl ether (60)	inactive
63	inactive
73	0.17
74	inactive
75	inactive

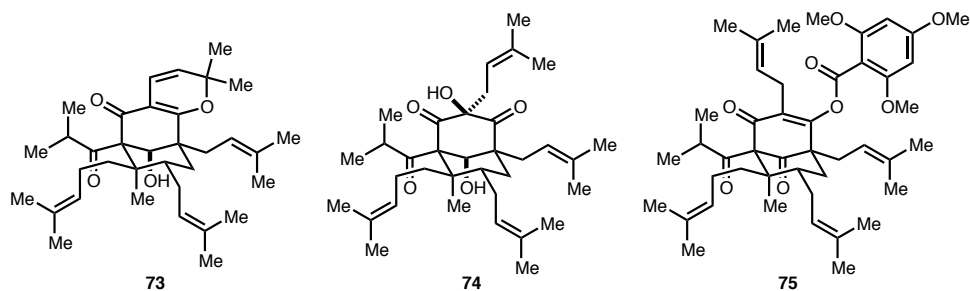


Figure 1.11. Semisynthetic hyperforin analogs.

Aside from being an inhibitor of several enzymes involved in eicosanoid biosynthesis, garcinol also acts as an anti-inflammatory agent by blocking pro-inflammatory protein expression. In a study using LPS-activated RAW264.7 cells, it was found that garcinol (at $1 \mu M$ concentration) inhibited the phosphorylation of cytosolic phospholipase A₂ (cPLA₂).¹⁹³ This phosphorylation activates cPLA₂, which hydrolyzes phospholipids at the *sn*-2 position, releasing arachidonic acid. On the other hand, hyperforin

¹⁹² Koeberle, A.; Northoff, H.; Werz, O. *Biochem. Pharmacol.* **2009**, 77, 1513-1521.

¹⁹³ Hong, J.; Sang, S.; Park, H.-J.; Kwon, S. J.; Suh, N.; Huang, M.-T.; Ho, C.-T.; Yang, C. S. *Carcinogenesis* **2006**, 27, 278-286.

was found to induce phosphorylation of cPLA₂ with its activity more pronounced in cells with depleted intracellular Ca²⁺.¹⁹⁴ The authors proposed that hyperforin inserts itself into lipid membranes and enables cPLA₂ to access phospholipids and thus release arachidonic acid. Along with cPLA₂ inhibition, garcinol reduced iNOS expression and NO release in RAW264.7 cells at 1 µM concentration, presumably through inhibition of signal transducer and activator of transcription-1 (STAT-1) or NF-κB, master transcriptional regulators.¹⁹⁵ Isogarcinol and semisynthetic garcinol derivatives **68** and **69** had similar effects to garcinol across these assays but were not as active. Akin to garcinol, hyperforin has been shown to downregulate both STAT-1 and NF-κB in rat and human pancreatic islets in the 0.5-5 µM range, preventing the cytokine-induced apoptosis of insulin-secreting β-cells, a cause of type 1 diabetes.¹⁹⁶

7-*epi*-Clusianone and guttiferone A have also been evaluated for anti-inflammatory and antioxidant properties in other contexts. 7-*epi*-Clusianone inhibited carbachol- and histamine-induced guinea pig ileum spasms in a dose-dependent manner, with EC₅₀ values in the 2-4 µM range.¹⁹⁷ It also prevented allergen-induced contraction of guinea pig trachea at 10 µM, and these effects were replicated in an *in vivo* mouse model at 25-100 mg/kg oral dosing.¹⁹⁸ The effects of 7-*epi*-clusianone were blocked by the addition of nitric oxide synthase inhibitors as well as cation channel blockers. Guttiferone A dose-dependently reduced the number of ulcerative lesions in a mouse model and was found to be as effective as omeprazole.¹⁹⁹ This indicates that guttiferone A may impart gastroprotective effects.

¹⁹⁴ Hoffmann, M.; Lopez, J. J.; Pergola, C.; Feisst, C.; Pawelczik, S.; Jakobsson, P.-J.; Sorg, B. L.; Glaubitz, C.; Steinhilber, D.; Werz, O. *Biochim. Biophys. Acta* **2010**, *1801*, 462-472.

¹⁹⁵ Liao, C.-H.; Sang, S.; Liang, Y.-C.; Ho, C.-T.; Lin, J.-K. *Molec. Carcinogenesis* **2004**, *41*, 140-149.

¹⁹⁶ Menegazzi, M.; Novelli, M.; Beffy, P.; D'Aleo, V.; Tedeschi, E.; Lupi, R.; Zoratti, E.; Marchetti, P.; Suzuki, H.; Masiello, P. *Int. J. Biochem. Cell Biol.* **2008**, *40*, 1509-1521.

¹⁹⁷ Neves, J. S.; Coelho, L. P.; Cordeiro, R. S. P.; Veloso, M. P.; Rodrigues e Silva, P. M.; dos Santos, M. H.; Martins, M. A. *Planta Med.* **2007**, *73*, 644-649.

¹⁹⁸ Coelho, L. P.; Serra, M. F.; Pires, A. L. de A.; Cordeiro, R. S. B.; Rodrigues e Silva, P. M.; dos Santos, M. H.; Martins, M. A. *J. Pharmacol. Exp. Ther.* **2008**, *327*, 206-214.

¹⁹⁹ Niero, R.; Dal Molin, M. M.; Silva, S.; Damian, N. S.; Maia, L. O.; Delle Monache, F.; Filho, V. C.; de Andrade, S. F. *Naunyn-Schmied. Arch. Pharmacol.* **2012**, *385*, 1103-1109.

Chemotherapeutic Activity

Many PPAPs have been evaluated for their antiproliferative activity against a variety of cancer cell lines. Overall, many PPAPs possess the ability to kill or modify cancer cells to a moderate extent, and a variety of underlying mechanisms have been explored. In many instances, apoptosis activation leads to cell death. A summary of the antiproliferative activity of PPAPs as well as several semisynthetic PPAP derivatives (Figure 1.12) against a variety of cancer cell lines is found in Table 1.13.

Table 1.13. Evaluation of PPAPs against cancer cell proliferation.

PPAP	Cancer cell type	Cell line	IC ₅₀ (μM)	References
aristophenone	human colon adenocarcinoma	SW480	33	135
clusianone	human colorectal carcinoma	HCT-116	3.2	200
clusianone	human cervical carcinoma	HeLa	3-9.6	200,201
clusianone	human breast carcinoma	MCF-7	5.7	201
clusianone	human pancreas carcinoma	MIA PaCa-2	3.8	201
clusianone	human promyelocytic leukemia	NB4	4.4	200
clusianone	human large cell lung carcinoma	NCI-H460	8.3	200
ent-clusianone	human cervical carcinoma	HeLa	5.8	201
ent-clusianone	human breast carcinoma	MCF-7	8.3	201
ent-clusianone	human pancreas carcinoma	MIA PaCa-2	5.2	201
7-epi-clusianone	human renal cell adenocarcinoma	786-0	6.9	116
7-epi-clusianone	human lung carcinoma	A549	27.3	202
7-epi-clusianone	human squamous cell carcinoma	CRL-1623	7.5	116
7-epi-clusianone	human squamous cell carcinoma	CRL-1624	17.8	116
7-epi-clusianone	human Hodgkin's lymphoma	HD-MY-Z	9.8	203
7-epi-clusianone	human myelogenous leukemia	K562	11.8	203
7-epi-clusianone	human T cell leukemia	KE-37	13.6	203
7-epi-clusianone	human breast carcinoma	MCF-7	6.3-19.9	116,202

²⁰⁰ Dal Piaz, F.; Tosco, A.; Eletto, D.; Piccinelli, A. L.; Molto, O.; Franceschelli, S.; Sbardella, G.; Remondelli, P.; Rastrelli, L.; Vesci, L.; Pisano, C.; De Tommasi, N. *ChemBioChem* **2010**, *11*, 818-827.

²⁰¹ Simpkins, N. S.; Holtrup, F.; Rodeschini, V.; Taylor, J. D.; Wolf, R. *Bioorg. Med. Chem. Lett.* **2012**, *22*, 6144-6147.

²⁰² Tanaka, N.; Takaishi, Y.; Shikishima, Y.; Nakanishi, Y.; Bastow, K.; Lee, K.-H.; Honda, G.; Ito, M.; Takeda, Y.; Kodzhimatov, O. K.; Ashurmetov, O. *J. Nat. Prod.* **2004**, *67*, 1870-1875.

²⁰³ Nedialkov, P. T.; Zheleva-Dimitrova, D.; Momekov, G.; Karlov, K.; Girreser, U.; Kitanov, G. M. *Nat. Prod. Res.* **2011**, *25*, 1743-1750.

Table 1.13 (continued). Evaluation of PPAPs against cancer cell proliferation.

PPAP	Cancer cell type	Cell line	IC ₅₀ (μM)	References
7- <i>epi</i> -clusianone	human breast carcinoma	NCI-ADR	9.5	116
7- <i>epi</i> -clusianone	human large cell lung carcinoma	NCI-H460	8.7	116
7- <i>epi</i> -clusianone	human ovarian carcinoma	OVCAR 03	5.9	116
7- <i>epi</i> -clusianone	human prostate carcinoma	PC-3	5.2	116
7- <i>epi</i> -clusianone	human malignant melanoma	UACC-62	5.8	116
cycloxanthochymol	human lung carcinoma	A549	7.5	204
cycloxanthochymol	human prostate carcinoma	DU145	6.1	204
cycloxanthochymol	human nasopharyngeal carcinoma	KB	8.3	204
cycloxanthochymol	human nasopharyngeal carcinoma	KB _{in}	8.1	204
cycloxanthochymol	human colon adenocarcinoma	SW480	16.6	135
<i>ent</i> -cycloxanthochymol	human lung carcinoma	A549	7.5	204
<i>ent</i> -cycloxanthochymol	human prostate carcinoma	DU145	7.8	204
<i>ent</i> -cycloxanthochymol	human nasopharyngeal carcinoma	KB	8.1	204
<i>ent</i> -cycloxanthochymol	human nasopharyngeal carcinoma	KB _{in}	8.6	204
garcicowin A	human colorectal carcinoma	HCT-116	inactive	205
garcicowin B	human colorectal carcinoma	HCT-116	inactive	205
garcicowin C	human colorectal carcinoma	HCT-116	> 5	205
garcicowin C	human cervical carcinoma	HeLa-C3	inactive	206
garcicowin D	human colorectal carcinoma	HCT-116	> 5	205
garcimultiflorone D	human cervical carcinoma	HeLa-C3	17.5	207
18-hydroxygarcimultiflorone D	human cervical carcinoma	HeLa-C3	23.0	207
garcimultiflorone E	human cervical carcinoma	HeLa-C3	14.3	207
garcimultiflorone F	human cervical carcinoma	HeLa-C3	14.9	207
isogarcimultiflorone F	human cervical carcinoma	HeLa-C3	12.4	207
garciniagifolone A	human cervical carcinoma	HeLa	25.3	208
garciniagifolone A	human hepatocellular carcinoma	HepG2	40.0	208
garciniagifolone A	human gastric adenocarcinoma	SGC-7901	9.7	208
garcinialiptone A	human lung carcinoma	A549	7.0	204
garcinialiptone A	human prostate carcinoma	DU145	6.8	204
garcinialiptone A	human nasopharyngeal carcinoma	KB	9.5	204
garcinialiptone A	human nasopharyngeal carcinoma	KB _{in}	9.3	204
<i>ent</i> -garcinialiptone A	human lung carcinoma	A549	7.0	204
<i>ent</i> -garcinialiptone A	human prostate carcinoma	DU145	7.0	204
<i>ent</i> -garcinialiptone A	human cervical carcinoma	HeLa	inactive	209
<i>ent</i> -garcinialiptone A	human nasopharyngeal carcinoma	KB	7.3	204

²⁰⁴ Zhang, L.-J.; Chiou, C.-T.; Cheng, J.-J.; Huang, H.-C.; Kuo, L.-M. Y.; Liao, C.-C.; Bastow, K. F.; Lee, K.-H.; Kuo, Y.-H. *J. Nat. Prod.* **2010**, *73*, 557-562.

²⁰⁵ Xu, G.; Kan, W. L. T.; Zhou, Y.; Song, J.-Z.; Han, Q.-B.; Qiao, C.-F.; Cho, C.-H.; Rudd, J. A.; Lin, G.; Xu, H.-X. *J. Nat. Prod.* **2010**, *73*, 104-108.

²⁰⁶ Gao, X.-M.; Yu, T.; Lai, F. S. F.; Zhou, Y.; Liu, X.; Qiao, C.-F.; Song, J.-Z.; Chen, S.-L.; Luo, K. Q.; Xu, H.-X.; *Bioorg. Med. Chem.* **2010**, *18*, 4957-4964.

²⁰⁷ Liu, X.; Yu, T.; Gao, X.-M.; Zhou, Y.; Qiao, C.-F.; Peng, Y.; Chen, S.-L.; Luo, K. Q.; Xu, H.-X. *J. Nat. Prod.* **2010**, *73*, 1355-1359.

²⁰⁸ Shan, W.-G.; Lin, T.-S.; Yu, H.-N.; Chen, Y.; Zhan, Z.-J. *Helv. Chim. Acta* **2012**, *95*, 1442-1448.

²⁰⁹ Trinh, B. T. D.; Nguyen, N.-T. T.; Ngo, N. T. N.; Tran, P. T.; Nguyen, L.-T. T.; Nguyen, L.-H. D. *Phytochem. Lett.* **2013**, *6*, 224-227.

Table 1.13 (continued). Evaluation of PPAPs against cancer cell proliferation.

PPAP	Cancer cell type	Cell line	IC ₅₀ (μM)	References
ent-garcinaliptone A	human nasopharyngeal carcinoma	KB _{vin}	8.8	204
ent-garcinaliptone A	human breast carcinoma	MCF-7	inactive	209
garcinaliptone C	human nasopharyngeal carcinoma	KB _{in}	7.9	204
garcinaliptone D	human lung carcinoma	A549	7.3	204
garcinaliptone D	human prostate carcinoma	DU145	5.5	204
garcinaliptone D	human nasopharyngeal carcinoma	KB	6.5	204
garcinaliptone D	human nasopharyngeal carcinoma	KB _{in}	7.6	204
garciniaphenone	human renal cell adenocarcinoma	786-0	5.1	116
garciniaphenone	human squamous cell carcinoma	CRL-1623	15.3	116
garciniaphenone	human squamous cell carcinoma	CRL-1624	20.1	116
garciniaphenone	human breast carcinoma	MCF-7	10.3	116
garciniaphenone	human breast carcinoma	NCI-ADR	12.7	116
garciniaphenone	human large cell lung carcinoma	NCI-H460	8.3	116
garciniaphenone	human ovarian carcinoma	OVCAR 03	6.4	116
garciniaphenone	human prostate carcinoma	PC-3	6.6	116
garciniaphenone	human malignant melanoma	UACC-62	6.1	116
garcinielliptone FB	human hepatocellular carcinoma	Hep3B	10.2	210
garcinielliptone FB	human colorectal adenocarcinoma	HT-29	18.1	210
garcinielliptone FB	human breast carcinoma	MCF-7	11.0	210
garcinielliptone FC	human larynx carcinoma	HEp-2	5.0	127
garcinielliptone FC	human promyelocytic leukemia	HL-60	2.3	127
garcinielliptone FC	human pulmonary carcinoma	NCI-H292	5.0	127
garcinielliptone FC	human bladder carcinoma	NTUB1	13.5	138
garcinielliptone I	human colorectal carcinoma	HCT-116	inactive	200
garcinielliptone I	human cervical carcinoma	HeLa	inactive	200
garcinielliptone I	human promyelocytic leukemia	NB4	inactive	200
garcinielliptone I	human large cell lung carcinoma	NCI-H460	inactive	200
garcinol	human pancreatic adenocarcinoma	BXPC-3	^a	211
garcinol	human colorectal carcinoma	HCT-116	10.5-12.0	200,205,212
garcinol	human cervical carcinoma	HeLa	9.8-30.4	200,208
garcinol	human hepatocellular carcinoma	HepG2	inactive	208,213
garcinol	human promyelocytic leukemia	HL-60	9.4-17	150,152,214
garcinol	human colorectal adenocarcinoma	HT-29	11.4-12.0	212
garcinol	human breast carcinoma	MCF-7	^a	215
garcinol	human breast adenocarcinoma	MDA-MB-231	^a	215
garcinol	murine liver hepatoma	MH1C1	< 10	213
garcinol	human promyelocytic leukemia	NB4	9.2	200
garcinol	human large cell lung carcinoma	NCI-H460	8.5	200

²¹⁰ Wu, C.-C.; Weng, J.-R.; Won, S.-J.; Lin, C.-N. *J. Nat. Prod.* **2005**, *68*, 1125-1127.

²¹¹ Parasramka, M. A.; Gupta, S. V. *Nutr. Cancer* **2011**, *63*, 456-465.

²¹² Hong, J.; Kwon, S. J.; Sang, S.; Ju, J.; Zhou, J.-n.; Ho, C.-T.; Huang, M.-T.; Yang, C. S. *Free Radical Bio. Med.* **2007**, *42*, 1211-1221.

²¹³ Ohnishi, H.; Asamoto, M.; Tujimura, K.; Hokaiwado, N.; Takahashi, S.; Ogawa, K.; Kuribayashi, M.; Ogiso, T.; Okuyama, H.; Shirai, T. *Cancer Sci.* **2004**, *95*, 936-942.

²¹⁴ Pan, M.-H.; Chang, W.-L.; Lin-Shaiu, S.-Y.; Ho, C.-T.; Lin, J.-K. *J. Agric. Food Chem.* **2001**, *49*, 1464-1474.

²¹⁵ Ahmad, A.; Wang, Z.; Ali, R.; Maitah, M. Y.; Kong, D.; Banerjee, S.; Padhye, S.; Sarkar, F. H. *J. Cell. Biochem.* **2010**, *109*, 1134-1141.

Table 1.13 (continued). Evaluation of PPAPs against cancer cell proliferation.

PPAP	Cancer cell type	Cell line	IC ₅₀ (μM)	References
garcinol	murine leukemia	P388	8.1	216
garcinol	human gastric adenocarcinoma	SGC-7901	28.6	208
72	human promyelocytic leukemia	HL-60	inactive	152
guttiferone A	human ovarian carcinoma	A2780	8.3-13.3	217,218
guttiferone A	human lung carcinoma	A549	3.3	143
guttiferone A	human prostate carcinoma	DU145	6.4	143
guttiferone A	human colorectal carcinoma	HCT-116	5.0-5.9	200,219
guttiferone A	human cervical carcinoma	HeLa	11.6	200
guttiferone A	human colorectal adenocarcinoma	HT-29	5	219
guttiferone A	human nasopharyngeal carcinoma	KB	7.4	143
guttiferone A	human nasopharyngeal carcinoma	KB _{vin}	6.9	143
guttiferone A	human promyelocytic leukemia	NB4	5.7	200
guttiferone A	human large cell lung carcinoma	NCI-H460	4.2	200
guttiferone A	human colon adenocarcinoma	SW480	21	219
guttiferone B	human colorectal carcinoma	HCT-116	> 5	205
guttiferone E	human colorectal carcinoma	HCT-116	6.4-9	200,220
guttiferone E	human cervical carcinoma	HeLa	11.3	200
guttiferone E	human cervical carcinoma	HeLa-C3	inactive	206
guttiferone E	human colorectal adenocarcinoma	HT-29	14	220
guttiferone E	human promyelocytic leukemia	NB4	10.4	200
guttiferone E	human large cell lung carcinoma	NCI-H460	5.4	200
guttiferone E	human colon adenocarcinoma	SW480	7.5-17	135,220
guttiferone F	human cervical carcinoma	HeLa	20.0	221
guttiferone F	human breast carcinoma	MCF-7	18.4	221
guttiferone F	human large cell lung carcinoma	NCI-H460	19.7	221
guttiferone G	human ovarian carcinoma	A2780	10.1	217
guttiferone G	human cervical carcinoma	HeLa	17.1	209
guttiferone G	human cervical carcinoma	HeLa-C3	inactive	206
guttiferone G	human nasopharyngeal carcinoma	KB	7.0	222
guttiferone G	human breast carcinoma	MCF-7	17.8	209
guttiferone H	human colorectal carcinoma	HCT-116	9	220
guttiferone H	human colorectal adenocarcinoma	HT-29	13	220
guttiferone H	human colon adenocarcinoma	SW480	12-16	135,220
guttiferone I	human ovarian carcinoma	A2780	7.8	218

²¹⁶ Hartari, S.; Wang, H.-B.; Kardono, L. B. S.; Kosela, S.; Qin, G.-W. *Chin. J. Nat. Med.* **2007**, *5*, 272-276.

²¹⁷ Williams, R. B.; Hoch, J.; Glass, T. E.; Evans, R.; Miller, J. S.; Wisse, J. H.; Kingston, D. G. I. *Planta Med.* **2003**, *69*, 864-866.

²¹⁸ Pan, E.; Cao, S.; Brodie, P. J.; Miller, J. S.; Rakotodrajaona, R.; Ratovoson, F.; Birkinshaw, C.; Andriantsiferana, R.; Rasamison, V. E.; Kingston, D. G. I. *Nat. Prod. Commun.* **2010**, *5*, 751-754.

²¹⁹ Yang, H.; Figueroa, M.; To, S.; Baggett, S.; Jiang, B.; Basile, M. J.; Weinstein, I. B.; Kennelly, E. J. *J. Agric. Food Chem.* **2010**, *58*, 4749-4755.

²²⁰ Protiva, P.; Hopkins, M. E.; Baggett, S.; Yang, H.; Lipkin, M.; Holt, P. R.; Kennelly, E. J.; Bernard, W. I. *Int. J. Cancer* **2008**, *123*, 687-694.

²²¹ Nguyen, L.-T. T.; Nguyen, H. T.; Barbič, M.; Brunner, G.; Heilmann, J.; Pham, H. D.; Nguyen, D. M.; Nguyen, L.-H. D. *Tetrahedron Lett.* **2012**, *53*, 4487-4493.

²²² Merza, J.; Mallet, S.; Litaudon, M.; Dumontet, V.; Séraphin, D.; Richomme, P. *Planta Med.* **2006**, *72*, 87-89.

Table 1.13 (continued). Evaluation of PPAPs against cancer cell proliferation.

PPAP	Cancer cell type	Cell line	IC ₅₀ (μM)	References
guttiferone I	human cervical carcinoma	HeLa	28.5	221,223
guttiferone I	human breast carcinoma	MCF-7	31.2	221,223
guttiferone I	human large cell lung carcinoma	NCI-H460	23.9	221,223
guttiferone J	human nasopharyngeal carcinoma	KB	8.5	222
guttiferone K	human ovarian carcinoma	A2780	6.0	224
guttiferone K	human lung carcinoma	A549	4.4	143
guttiferone K	human prostate carcinoma	DU145	4.6	143
guttiferone K	human colorectal carcinoma	HCT-116	10	205,219
guttiferone K	human colorectal adenocarcinoma	HT-29	5.4-25	219,225
guttiferone K	human nasopharyngeal carcinoma	KB	5.2	143
guttiferone K	human nasopharyngeal carcinoma	KB _{vin}	5.3	143
guttiferone K	human colon adenocarcinoma	SW480	23	219
guttiferone K2	human cervical carcinoma	HeLa-C3	inactive	206
guttiferone L	human ovarian carcinoma	A2780	4.8	224
guttiferone Q	human cervical carcinoma	HeLa	6.0	223
guttiferone Q	human breast carcinoma	MCF-7	5.5	223
guttiferone Q	human large cell lung carcinoma	NCI-H460	8.0	223
guttiferone R	human cervical carcinoma	HeLa	inactive	223
guttiferone R	human breast carcinoma	MCF-7	inactive	223
guttiferone R	human large cell lung carcinoma	NCI-H460	inactive	223
guttiferone S	human cervical carcinoma	HeLa	inactive	223
guttiferone S	human breast carcinoma	MCF-7	inactive	223
guttiferone S	human large cell lung carcinoma	NCI-H460	inactive	223
guttiferone T	human cervical carcinoma	HeLa	19.9	209
guttiferone T	human breast carcinoma	MCF-7	14.3	209
hyperatomarin	human stage II bladder carcinoma	5637	1.2	226
hyperatomarin	human endometrioid carcinoma	DOHH-2	0.14	227
hyperatomarin	human endometrioid carcinoma	EJ	8.8	227
hyperatomarin	human Hodgkin's lymphoma	HD-MY-Z	5	227
hyperatomarin	human promyelocytic leukemia	HL-60	2.2	226
hyperatomarin	human promyelocytic leukemia	HL-60 _{Dox}	1.8	226
hyperatomarin	human myelogenous leukemia	K562	15.7	227
hyperatomarin	human acute myelogenous leukemia	KG-1	12.7	226
hyperatomarin	human chronic myeloid leukemia	LAMA-84	12.7	227
hyperatomarin	human breast carcinoma	MCF-7	0.79	227
hyperatomarin	human breast adenocarcinoma	MDA-MB-231	0.86	226
hyperatomarin	human neuroblastoma	Neuro-2a	9.4	227
hyperatomarin	human primary osteosarcoma	Saos-2	1.2	227
hyperatomarin	human T cell leukemia	SKW-3	3	227
hyperatomarin	human B cell malignant myeloma	U266	0.49	227

²²³ Nguyen, H. D.; Trinh, B. T. D.; Nguyen, L.-H. D. *Phytochem. Lett.* **2011**, *4*, 129-133.

²²⁴ Cao, S.; Brodie, P. J.; Miller, J. S.; Ratovoson, F.; Birkinshaw, C.; Randrianasolo, S.; Rakotobe, E.; Rasamison, V. E.; Kingston, D. G. I. *J. Nat. Prod.* **2007**, *70*, 686-688.

²²⁵ Kan, W. L. T.; Yin, C.; Xu, H. X.; Xu, G.; To, K. K. W.; Cho, C. H.; Rudd, J. A.; Lin, G. *Int. J. Cancer* **2013**, *132*, 707-716.

²²⁶ Biljali, S.; Momekov, G.; Nedialkov, P.; Zheleva-Dimitrova, D.; Kitanov, G.; Momekova, D.; Stoyanov, N.; Guenova, M.; Michova, A.; Karaivanova, M. *J. Pharm. Technol. Drug Res.* **2012**, *1*, 6.

²²⁷ Momekov, G.; Ferdinandov, D.; Zheleva-Dimitrova, D.; Nedialkov, P.; Girreser, U.; Kitanov, G. *Phytomedicine* **2008**, *15*, 1010-1015.

Table 1.13 (continued). Evaluation of PPAPs against cancer cell proliferation.

PPAP	Cancer cell type	Cell line	IC ₅₀ (μM)	References
hyperevolutin A	human colon carcinoma	Co-115	1.5	133
hyperevolutin B	human colon carcinoma	Co-115	1.5	133
hyperfoliatin	human lung carcinoma	A549	inactive	202
hyperfoliatin	human breast carcinoma	MCF-7	35.7	202
hyperforin	human melanoma	1F6	8.4	228
hyperforin	human squamous carcinoma	A431	8.4	228
hyperforin	murine pancreatic tumor	ARIP	4.1	228
hyperforin	murine prostatic carcinoma	AT-2.1	3.5	228
hyperforin	murine fibrosarcoma	BDX2	74.5	228
hyperforin	human malignant melanoma	HT144	11.2	228
hyperforin	human T cell leukemia	Jurkat	12.1	228
hyperforin	human myelogenous leukemia	K562	14.9	229
hyperforin	human glioblastoma	LN-229	19.2	229
hyperforin	murine prostatic carcinoma	MAT-Lu	16.8	228
hyperforin	human breast carcinoma	MCF-7	2.8	228
hyperforin	human breast adenocarcinoma	MDA-MB-468	3.7	228
hyperforin	murine breast carcinoma	MT-450	2.8	228
hyperforin	human melanoma	MV3	4.7	228
hyperforin	murine bladder carcinoma	NBT-II	inactive	230
hyperforin	murine glioblastoma	RG2	4.7	228
hyperforin	human melanoma	SB1	8.4	228
hyperforin	human melanoma	SB3	8.4	228
hyperforin	human ovarian adenocarcinoma	SK-OV-3	5.6	228
hyperforin	human bladder carcinoma	T24	inactive	230
hyperforin	human histiocytic leukemia	U937	15.8	229
hyperforin-HNCy ₂	human malignant melanoma	A375	12.4	231
hyperforin-HNCy ₂	human lung carcinoma	A549	3.7	231
hyperforin-HNCy ₂	murine melanoma	B16-LU8	5-8	232
hyperforin-HNCy ₂	murine colon adenocarcinoma	C-26	5-8	232
hyperforin-HNCy ₂	human cervical carcinoma	HeLa	3.1	231
hyperforin-HNCy ₂	human hepatocellular carcinoma	HepG2	2.7	231
hyperforin-HNCy ₂	human fibrosarcoma	HT1080	5-8	232
hyperforin-HNCy ₂	human myelogenous leukemia	K562	8.6-9.9 ^b	231,233
hyperforin-HNCy ₂	human myelogenous leukemia	K562	3.2 ^c	233
hyperforin-HNCy ₂	human myelogenous leukemia	K562 _{ADR}	14.3	231
hyperforin-HNCy ₂	human breast carcinoma	MCF-7	2.8	231

²²⁸ Schempp, C. M.; Kirkin, V.; Simon-Haarhaus, B.; Kersten, A.; Kiss, J.; Termeer, C. C.; Gilb, B.; Kaufmann, T.; Borner, C.; Sleeman, J. P.; Simon, J. C. *Oncogene* **2002**, *21*, 1242-1250.

²²⁹ Hostanska, K.; Reichling, J.; Bommer, S.; Weber, M.; Saller, R. *Eur. J. Pharm. Biopharm.* **2003**, *56*, 121-132.

²³⁰ Skalkos, D.; Stavropoulos, N.; Tsimaris, I.; Gioti, E.; Stalikas, C. D.; Nseyo, U. O.; Ioachim, E.; Agnantis, N. J. *Planta Med.* **2005**, *71*, 1030-1035.

²³¹ Sun, F.; Liu, J.-Y.; He, F.; Liu, Z.; Wang, R.; Wang, D.-M.; Wang, Y.-F.; Yang, D.-P. *J. Asian Nat. Prod. Res.* **2011**, *13*, 688-699.

²³² Donà, M.; Dell'Aica, I.; Pezzato, E.; Sartor, L.; Calabrese, F.; Della Barbera, M.; Donella-Deana, A.; Appendino, G.; Borsarini, A.; Caniato, R.; Garbisa, S. *Cancer Res.* **2004**, *64*, 6225-6232.

²³³ Liu, J.-Y.; Liu, Z.; Wang, D.-M.; Li, M.-M.; Wang, S.-X.; Wang, R.; Chen, J.-P.; Wang, Y.-F.; Yang, D.-P. *Chem.-Biol. Interact.* **2011**, *190*, 91-101.

Table 1.13 (continued). Evaluation of PPAPs against cancer cell proliferation.

PPAP	Cancer cell type	Cell line	IC ₅₀ (μM)	References
hyperforin·HNCy ₂	human breast adenocarcinoma	MDA-MB-231	5	234
hyperforin·HNCy ₂	human neuroblastoma	SK-N-BE	inactive	232
hyperforin·HNCy ₂	murine prostate adenocarcinoma	TRAMP-C1	inactive	232
hyperforin <i>O</i> -acetate	human malignant melanoma	A375	50.6	231
hyperforin <i>O</i> -acetate	human lung carcinoma	A549	41.4	231
hyperforin <i>O</i> -acetate	human cervical carcinoma	HeLa	17.3	231
hyperforin <i>O</i> -acetate	human hepatocellular carcinoma	HepG2	58.9	231
hyperforin <i>O</i> -acetate	human myelogenous leukemia	K562	34.3	231
hyperforin <i>O</i> -acetate	human myelogenous leukemia	K562 _{ADR}	41.6	231
hyperforin <i>O</i> -acetate	human breast carcinoma	MCF-7	21.7	231
octahydrohyperforin (66)	human breast adenocarcinoma	MDA-MB-231	9	234
octahydrohyperforin <i>O</i> -acetate	human malignant melanoma	A375	inactive	231
octahydrohyperforin <i>O</i> -acetate	human lung carcinoma	A549	inactive	231
octahydrohyperforin <i>O</i> -acetate	human cervical carcinoma	HeLa	inactive	231
octahydrohyperforin <i>O</i> -acetate	human hepatocellular carcinoma	HepG2	inactive	231
octahydrohyperforin <i>O</i> -acetate	human myelogenous leukemia	K562	inactive	231
octahydrohyperforin <i>O</i> -acetate	human myelogenous leukemia	K562 _{ADR}	inactive	231
octahydrohyperforin <i>O</i> -acetate	human breast carcinoma	MCF-7	inactive	231
tetrahydrohyperforin (76)	human breast adenocarcinoma	MDA-MB-231	2	234
hyperibone A	human cervical carcinoma	HeLa	0.176	63
hyperibone B	human colorectal carcinoma	HCT-116	inactive	200
hyperibone B	human cervical carcinoma	HeLa	inactive	200
hyperibone B	human promyelocytic leukemia	NB4	inactive	200
hyperibone B	human large cell lung carcinoma	NCI-H460	inactive	200
hyperibone K	human lung carcinoma	A549	27.4	202
hyperibone K	human breast carcinoma	MCF-7	20.0	202
hyperibone L	human lung carcinoma	A549	20.5	202
hyperibone L	human breast carcinoma	MCF-7	33.4	202
hyperpappanone	human nasopharyngeal carcinoma	KB	7.7	64
hypersampson G	human lung carcinoma	A549	inactive	235
hypersampson H	human lung carcinoma	A549	inactive	235
isogarcinol	human colorectal carcinoma	HCT-116	6-8	212
isogarcinol	human cervical carcinoma	HeLa-C3	inactive	206
isogarcinol	human promyelocytic leukemia	HL-60	16-17	152
isogarcinol	human colorectal adenocarcinoma	HT-29	6-8	212
30- <i>epi</i> -isogarcinol	human colorectal carcinoma	HCT-116	5	205
30- <i>epi</i> -isogarcinol	human cervical carcinoma	HeLa-C3	inactive	206
30- <i>epi</i> -isogarcinol	human breast carcinoma	MCF-7	25.9	221
30- <i>epi</i> -isogarcinol	human large cell lung carcinoma	NCI-H460	22.6	221
isoxanthochymol	human lung carcinoma	A549	7.3	204
isoxanthochymol	human colon carcinoma	Colo-320-DM	4.9	236
isoxanthochymol	human prostate carcinoma	DU145	7.0	204
isoxanthochymol	human nasopharyngeal carcinoma	KB	7.5	204
isoxanthochymol	human nasopharyngeal carcinoma	KB _{in}	8.6	204
isoxanthochymol	human breast carcinoma	MCF-7	2.9	236
isoxanthochymol	murine leukemia	P388	2.4	216
isoxanthochymol	human colon adenocarcinoma	SW480	16.6	135
isoxanthochymol	human liver carcinoma	WRL-68	15.5	236

²³⁴ Martínez-Poveda, B.; Verotta, L.; Bombardelli, E.; Quesada, A. R.; Medina, M. Á. *PLoS ONE* **2010**, 5, e9558.

²³⁵ Zheng, Y. H.; Mu, Q.; Xiao, Z. Y.; Xu, Y.; Rahman, M. M.; Gibbons, S. *Chem. Lett.* **2009**, 38, 440-441.

²³⁶ Kumar, S.; Chattopadhyay, S. K.; Darokar, M. P.; Garg, A.; Khanuja, S. P. S. *Planta Med.* **2007**, 73, 1452-1456.

Table 1.13 (continued). Evaluation of PPAPs against cancer cell proliferation.

PPAP	Cancer cell type	Cell line	IC ₅₀ (μM)	References
memorosone	human ovarian carcinoma	A2780	18.3	237
memorosone	human ovarian carcinoma	A2780 _{CP}	12.4	237
memorosone	human ovarian carcinoma	A2780 _{DOX}	13.4	237
memorosone	human conjunctival melanoma	CRMM-1	25.3	238
memorosone	human conjunctival melanoma	CRMM-2	12.9	238
memorosone	human colorectal carcinoma	HCT-116	6.8	200
memorosone	human colorectal adenocarcinoma	HCT-8	8.4	237
memorosone	human colorectal adenocarcinoma	HCT-8 _{Ral}	8.8	237
memorosone	human colorectal adenocarcinoma	HCT-8 _{SN-38}	8.1	237
memorosone	human cervical carcinoma	HeLa	3.3-5.2	146,200,201
memorosone	human larynx carcinoma	HEp-2	3.1	146
memorosone	human colorectal adenocarcinoma	HT-29	10.4	237
memorosone	human colorectal adenocarcinoma	HT-29 _{5-FU}	10.3	237
memorosone	human colorectal adenocarcinoma	HT-29 _{SN-38}	7.0	237
memorosone	human T cell leukemia	Jurkat	92	237
memorosone	human myelogenous leukemia	K562	8.4	237
memorosone	human neuroblastoma	KELLY	5.2	239
memorosone	human neuroblastoma	LAN-1	4.1-16.3	237,239
memorosone	human neuroblastoma	LAN-1 _{5-FU}	4.1-16.4	237,239
memorosone	human neuroblastoma	LAN-1 _{ADR}	4.9-5.0	237,239
memorosone	human neuroblastoma	LAN-1 _{CP}	4.2-16.8	237,239
memorosone	human neuroblastoma	LAN-1 _{ETO}	18.3	237
memorosone	human prostate adenocarcinoma	LNCaP	4.2	237
memorosone	human prostate adenocarcinoma	LNCaP _{ETO}	3.6	237
memorosone	human stomach carcinoma	M51	11.3	237
memorosone	human stomach carcinoma	M51 _{CP}	9.5	237
memorosone	human breast carcinoma	MCF-7	6.5-8.7	201,237
memorosone	human breast carcinoma	MCF-7 _{5-FU}	6.6	237
memorosone	human breast carcinoma	MCF-7 _{DOX}	8.5	237
memorosone	human pancreas carcinoma	MIA PaCa-2	3.4	201
memorosone	human promyelocytic leukemia	NB4	4.8	200
memorosone	human stage III neuroblastoma	NB69	3.1	239
memorosone	human large cell lung carcinoma	NCI-H460	5.0-8.4	200,237
memorosone	human prostate carcinoma	PC-3	4.0-7.2	146,237
memorosone	human neuroblastoma	SK-N-AS	6.3	239
memorosone	human neuronal glioblastoma	U251	3.9	146
ent-memorosone	human cervical carcinoma	HeLa	3.4	201
ent-memorosone	human breast carcinoma	MCF-7	8	201
ent-memorosone	human pancreas carcinoma	MIA PaCa-2	3.5	201
memorosone O-methyl ether	human cervical carcinoma	HeLa	57.1	146
memorosone O-methyl ether	human larynx carcinoma	HEp-2	94.5	146
memorosone O-methyl ether	human prostate carcinoma	PC-3	85.1	146
memorosone O-methyl ether	human neuronal glioblastoma	U251	32.9	146
nujiangefolin A	human malignant melanoma	A375	inactive	151
nujiangefolin A	human lung carcinoma	A549	inactive	151

²³⁷ Díaz-Carballo, D.; Malak, S.; Bardenheuer, W.; Freistuehler, M.; Reusch, H. P. *Bioorg. Med. Chem.* **2008**, *16*, 9635-9643.

²³⁸ Westekemper, H.; Freistuehler, M.; Bornfeld, N.; Steuhl, K.-P.; Scheulen, M.; Hilger, R. A. *Graefes Arch. Clin. Exp. Ophthalmol.* **2013**, *251*, 279-284.

²³⁹ Díaz-Carballo, D.; Malak, S.; Bardenheuer, W.; Freistuehler, M.; Reusch, H. P. *J. Cell. Mol. Med.* **2008**, *12*, 2598-2608.

Table 1.13 (continued). Evaluation of PPAPs against cancer cell proliferation.

PPAP	Cancer cell type	Cell line	IC ₅₀ (μM)	References
nujiangefolin A	human gastric adenocarcinoma	AGs	inactive	151
nujiangefolin A	human pancreatic adenocarcinoma	BXPC-3	inactive	151
nujiangefolin A	human colorectal carcinoma	HCT-116	3.2-5.9	212
nujiangefolin A	human hepatocellular carcinoma	HepG2	inactive	151
nujiangefolin A	human promyelocytic leukemia	HL-60	8.4-17	150,152
nujiangefolin A	human colorectal adenocarcinoma	HT-29	3.2-5.9	212
nujiangefolin A	human breast carcinoma	MCF-7	inactive	151
nujiangefolin A	human breast adenocarcinoma	MDA-MB-231	inactive	151
nujiangefolin A	human lung adenocarcinoma	NCI-H2126	inactive	151
nujiangefolin A	human pancreatic carcinoma	PANC-1	inactive	151
nujiangefolin A	human hepatocellular carcinoma	SMMC-7721	inactive	151
nujiangefolin A	human primary glioblastoma	U87	inactive	151
nujiangefolin B	human malignant melanoma	A375	inactive	151
nujiangefolin B	human lung carcinoma	A549	inactive	151
nujiangefolin B	human gastric adenocarcinoma	AGs	inactive	151
nujiangefolin B	human pancreatic adenocarcinoma	BXPC-3	inactive	151
nujiangefolin B	human colorectal carcinoma	HCT-116	3-7	212
nujiangefolin B	human hepatocellular carcinoma	HepG2	inactive	151
nujiangefolin B	human promyelocytic leukemia	HL-60	8-18	150,152
nujiangefolin B	human colorectal adenocarcinoma	HT-29	3-7	212
nujiangefolin B	human breast carcinoma	MCF-7	inactive	151
nujiangefolin B	human breast adenocarcinoma	MDA-MB-231	inactive	151
nujiangefolin B	human lung adenocarcinoma	NCI-H2126	inactive	151
nujiangefolin B	human pancreatic carcinoma	PANC-1	inactive	151
nujiangefolin B	human hepatocellular carcinoma	SMMC-7721	inactive	151
nujiangefolin B	human primary glioblastoma	U87	inactive	151
nujiangefolin C	human malignant melanoma	A375	inactive	151
nujiangefolin C	human lung carcinoma	A549	inactive	151
nujiangefolin C	human gastric adenocarcinoma	AGs	inactive	151
nujiangefolin C	human pancreatic adenocarcinoma	BXPC-3	inactive	151
nujiangefolin C	human hepatocellular carcinoma	HepG2	inactive	151
nujiangefolin C	human breast carcinoma	MCF-7	inactive	151
nujiangefolin C	human breast adenocarcinoma	MDA-MB-231	inactive	151
nujiangefolin C	human lung adenocarcinoma	NCI-H2126	inactive	151
nujiangefolin C	human pancreatic carcinoma	PANC-1	inactive	151
nujiangefolin C	human hepatocellular carcinoma	SMMC-7721	inactive	151
nujiangefolin C	human primary glioblastoma	U87	inactive	151
oblongifolin B	human colorectal carcinoma	HCT-116	< 5	205
oblongifolin B	human cervical carcinoma	HeLa-C3	inactive	240
oblongifolin C	human colorectal carcinoma	HCT-116	7.3	205,241
oblongifolin C	human colorectal carcinoma	HCT-116 _{MDR}	9.8	241
oblongifolin C	human breast carcinoma	MCF-7	7.7	241
oblongifolin C	human breast carcinoma	MCF-7 _{HER2}	9.7	241
oblongifolin D	human colorectal carcinoma	HCT-116	< 5	205
oblongifolin D	human cervical carcinoma	HeLa-C3	inactive	240

²⁴⁰ Xu, G.; Feng, C.; Zhou, Y.; Han, Q.-B.; Qiao, C.-F.; Huang, S.-X.; Chang, D. C.; Zhao, Q.-S.; Luo, K. Q.; Xu, H.-X. *J. Agric. Food Chem.* **2008**, *56*, 11144-11150.

²⁴¹ Feng, C.; Zhou, L.-Y.; Yu, T.; Xu, G.; Tain, H.-L.; Xu, J.-J.; Xu, H.-X.; Luo, K. Q. *Int. J. Cancer* **2012**, *131*, 1445-1454.

Table 1.13 (continued). Evaluation of PPAPs against cancer cell proliferation.

PPAP	Cancer cell type	Cell line	IC ₅₀ (μM)	References
ochrocarpinone A	human ovarian carcinoma	A2780	12.9	242
ochrocarpinone B	human ovarian carcinoma	A2780	14.3	242
ochrocarpinone C	human ovarian carcinoma	A2780	15.8	242
oxy-thorelione A	human breast carcinoma	MCF-7	17.3	221
oxy-thorelione A	human large cell lung carcinoma	NCI-H460	51.3	221
papuaforin A	human nasopharyngeal carcinoma	KB	18.2	64
papuaforin C	human nasopharyngeal carcinoma	KB	11.5	64
papuaforin D	human nasopharyngeal carcinoma	KB	13.7	64
papuaforin E	human nasopharyngeal carcinoma	KB	11.3	64
paucinone A	human cervical carcinoma	HeLa	10	243
paucinone B	human cervical carcinoma	HeLa	8.2	243
paucinone C	human cervical carcinoma	HeLa	24.3	243
paucinone D	human cervical carcinoma	HeLa	5.8	243
plukenetione A	human ovarian carcinoma	A2780	25.8	237
plukenetione A	human ovarian carcinoma	A2780 _{CP}	31.8	237
plukenetione A	human ovarian carcinoma	A2780 _{Dox}	28.9	237
plukenetione A	human colorectal adenocarcinoma	HCT-8	25.8	237
plukenetione A	human colorectal adenocarcinoma	HCT-8 _{Ral}	24.2	237
plukenetione A	human colorectal adenocarcinoma	HCT-8 _{SN-38}	23.3	237
plukenetione A	human colorectal adenocarcinoma	HT-29	24.0	237
plukenetione A	human colorectal adenocarcinoma	HT-29 _{5-FU}	28.4	237
plukenetione A	human colorectal adenocarcinoma	HT-29 _{SN-38}	26.6	237
plukenetione A	human T cell leukemia	Jurkat	10.5	237
plukenetione A	human prostate adenocarcinoma	LNCaP	4.0	237
plukenetione A	human prostate adenocarcinoma	LNCaP _{ETO}	3.4	237
plukenetione A	human stomach carcinoma	M51	13.0	237
plukenetione A	human stomach carcinoma	M51 _{CP}	15.2	237
plukenetione A	human breast carcinoma	MCF-7	32.5	237
plukenetione A	human breast carcinoma	MCF-7 _{5-FU}	20.0	237
plukenetione A	human breast carcinoma	MCF-7 _{Dox}	30.0	237
plukenetione A	human large cell lung carcinoma	NCI-H460	26.8	237
plukenetione D/E	human prostate carcinoma	DU145	7.3	244
plukenetione D/E	human prostate carcinoma	DU145 _{MDR}	6.8	244
plukenetione D/E	human prostate adenocarcinoma	LNCaP	4.1	244
plukenetione D/E	human prostate adenocarcinoma	LNCaP _{ETO}	4.8	244
plukenetione D/E	human prostate carcinoma	PC-3	5.0	244
plukenetione D/E	human prostate carcinoma	PC-3 _{ETO}	5.1	244
15,16-dihydro-16-hydroperoxy-plukentione F	human ovarian carcinoma	A2780	15.7	242
prolifenone A	human gastric adenocarcinoma	AGs	inactive	245
prolifenone A	human colorectal carcinoma	HCT-116	inactive	245
prolifenone A	human breast carcinoma	MCF-7	inactive	245
prolifenone A	human large cell lung carcinoma	NCI-H460	inactive	245
prolifenone A	human astrocytoma	SF-268	inactive	245

²⁴² Chaturvedula, V. S. P.; Schilling, J. K.; Kingston, D. G. I. *J. Nat. Prod.* **2002**, *65*, 965-972.

²⁴³ Gao, X.-M.; Yu, T.; Lai, F. S. F.; Pu, J.-X.; Qiao, C.-F.; Zhou, Y.; Liu, X.; Song, J.-Z.; Luo, K. Q.; Xu, H.-X. *Tetrahedron Lett.* **2010**, *51*, 2442-2446.

²⁴⁴ Díaz-Carballo, D.; Gustmann, S.; Ackikelli, A. H.; Bardenheuer, W.; Buehler, H.; Jastrow, H.; Ergun, S.; Strumberg, D. *Phytomedicine* **2012**, *19*, 1298-1306.

²⁴⁵ Henry, G. E.; Raithore, S.; Zhang, Y.; Jayaprakasam, B.; Nair, M. G.; Heber, D.; Seeram, N. P. *J. Nat. Prod.* **2006**, *69*, 1645-1648.

Table 1.13 (continued). Evaluation of PPAPs against cancer cell proliferation.

PPAP	Cancer cell type	Cell line	IC ₅₀ (μM)	References
prolifenone B	human gastric adenocarcinoma	AGs	inactive	245
prolifenone B	human colorectal carcinoma	HCT-116	inactive	245
prolifenone B	human breast carcinoma	MCF-7	inactive	245
prolifenone B	human large cell lung carcinoma	NCI-H460	inactive	245
prolifenone B	human astrocytoma	SF-268	inactive	245
propolone A	human colorectal carcinoma	HCT-116	4.4	200
propolone A	human cervical carcinoma	HeLa	10.8	200
propolone A	human promyelocytic leukemia	NB4	6.8	200
propolone A	human large cell lung carcinoma	NCI-H460	6.3	200
propolone B	human colorectal carcinoma	HCT-116	16.4	200
propolone B	human cervical carcinoma	HeLa	inactive	200
propolone B	human promyelocytic leukemia	NB4	inactive	200
propolone B	human large cell lung carcinoma	NCI-H460	23	200
propolone C	human colorectal carcinoma	HCT-116	16.3	200
propolone C	human cervical carcinoma	HeLa	inactive	200
propolone C	human promyelocytic leukemia	NB4	inactive	200
propolone C	human large cell lung carcinoma	NCI-H460	inactive	200
propolone D	human colorectal carcinoma	HCT-116	inactive	200
propolone D	human cervical carcinoma	HeLa	inactive	200
propolone D	human promyelocytic leukemia	NB4	inactive	200
propolone D	human large cell lung carcinoma	NCI-H460	inactive	200
propolone D peroxide	human colorectal carcinoma	HCT-116	inactive	200
propolone D peroxide	human cervical carcinoma	HeLa	inactive	200
propolone D peroxide	human promyelocytic leukemia	NB4	inactive	200
propolone D peroxide	human large cell lung carcinoma	NCI-H460	inactive	200
sampsonione A	murine leukemia	P388	22.2	246
sampsonione I	murine leukemia	P388	11.8	247
sampsonione J	murine leukemia	P388	inactive	247
semsinone A	human lung carcinoma	A549	12.5	143
semsinone A	human prostate carcinoma	DU145	16.4	143
semsinone A	human nasopharyngeal carcinoma	KB	5.9	143
semsinone A	human nasopharyngeal carcinoma	KB _{in}	13.9	143
thorelione A	human cervical carcinoma	HeLa	15.4	221
thorelione A	human breast carcinoma	MCF-7	12.3	221
thorelione A	human large cell lung carcinoma	NCI-H460	17.6	221
uralodin B	human hepatocellular carcinoma	HepG2	171.0	248
uralodin B	human promyelocytic leukemia	HL-60	21.8	248
uralodin B	human myelogenous leukemia	K562	171	248
uralodin B	human gastric adenocarcinoma	SGC-7901	63.7	248
uralodin C	human hepatocellular carcinoma	HepG2	28.5	248
uralodin C	human promyelocytic leukemia	HL-60	14.3	248
uralodin C	human myelogenous leukemia	K562	32.1	248
uralodin C	human gastric adenocarcinoma	SGC-7901	26.1	248

²⁴⁶ Hu, L.-H.; Sim, K.-Y. *Tetrahedron Lett.* **1998**, *39*, 7999-8002.

²⁴⁷ Hu, L. H.; Sim, K. Y. *Org. Lett.* **1999**, *1*, 879-882.

²⁴⁸ Chen, X.-Q.; Li, Y.; Cheng, X.; Wang, K.; He, J.; Pan, Z.-H.; Li, M.-M.; Peng, L.-Y.; Xu, G.; Zhao, Q.-S. *Chem. Biodivers.* **2010**, *7*, 196-204.

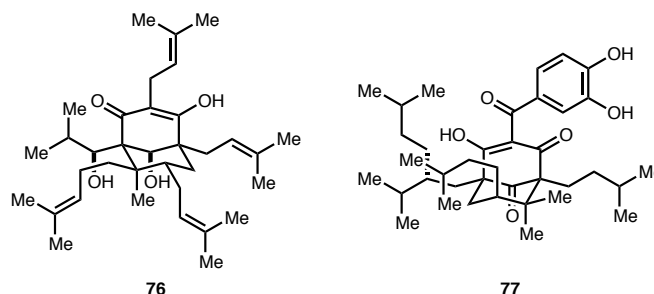
Table 1.13 (*continued*). Evaluation of PPAPs against cancer cell proliferation.

PPAP	Cancer cell type	Cell line	IC ₅₀ (μM)	References
xanthochymol	human lung carcinoma	A549	6.6	204
xanthochymol	human colon carcinoma	Colo-320-DM	0.62	236
xanthochymol	human prostate carcinoma	DU145	6.6	204
xanthochymol	human colorectal carcinoma	HCT-116	10	220
xanthochymol	human colorectal adenocarcinoma	HT-29	15	220
xanthochymol	human nasopharyngeal carcinoma	KB	8.3	204
xanthochymol	human nasopharyngeal carcinoma	KB _{in}	8.1	204
xanthochymol	human breast carcinoma	MCF-7	0.475	236
xanthochymol	human colon adenocarcinoma	SW480	8.3-17	135,220
xanthochymol	human liver carcinoma	WRL-68	2.5	236
octahydroxanthochymol (77)	human nasopharyngeal carcinoma	KB	20	249

^a Antiproliferative activity was observed, but no IC₅₀ value was reported.

^b IC₅₀ value after 48 h of incubation with the compound.

^c IC₅₀ value after 72 h of incubation with the compound.

**Figure 1.12.** Semisynthetic PPAP analogs tetrahydrohyperforin (76) and octahydroxanthochymol (77).

Overall, the presence of a relatively acidic hydroxyl group (either an enolic or phenolic –OH) is imperative for antiproliferative activity. A common feature of inactive PPAPs found in Table 1.13 is the presence of a tetrahydrofuran ring encompassing the C4 (or C2) enolic oxygen atom, such as garcinielliptone I, guttiferone R, hyperibone B, and propolone D. These PPAPs lack any phenolic hydroxyl functionality, as well. Interestingly, while hyperforin *O*-acetate maintains moderate activity across a variety of cell lines, octahydrohyperforin *O*-acetate is inactive.²³¹ A decrease in the activity of nemorosone as its *O*-methyl ether also demonstrates the importance of this free acidic hydroxyl group to antiproliferative activity.¹⁴⁶ In addition to the PPAPs listed in Table 1.13, the tin complex of 7-*epi*-

²⁴⁹ Roux, D.; Hadi, H. A.; Thoret, S.; Guénard, D.; Thoison, O.; Païs, M.; Sévenet, T. *J. Nat. Prod.* **2000**, 63, 1070-1076.

clusianone [SnClPh₃(7-*epi*-clusianone)], has been evaluated against HN-5 cells, however with inconclusive results.²⁵⁰

In some instances, the underlying mechanisms by which PPAPs affect cancer cells have been explored. Several studies have provided evidence that hyperforin influences cancer survival and proliferation through a variety of pathways.²⁵¹ An early study by Schempp and coworkers with MT-450 cells established that hyperforin induces apoptosis through caspase activation.²²⁸ The addition of the nonspecific caspase inhibitor Z-VAD-FMK prevented hyperforin-induced apoptosis. Aside from caspase activation, hyperforin also caused a loss of the mitochondrial transmembrane potential. Given that this latter effect occurred in the presence of Z-VAD-FMK and that hyperforin treatment induced cytochrome *c* release from isolated mitochondria, the authors concluded that hyperforin's ability to increase mitochondrial membrane permeability caused caspase activation and ultimately cell death through apoptosis. Similar results were found in a later study using K562 cells treated with hyperforin·HNCy₂.²³³

In leukemia cells, hyperforin upregulates the pro-apoptotic regulator Noxa in addition to caspase mediated pathways. In cells taken from CLL patients, Noxa upregulation was observed upon treatment with hyperforin, leading to apoptosis.²⁵² siRNA-mediated Noxa silencing partially reduced the effects of hyperforin in these cells. Studies involving various AML cell lines also demonstrated Noxa-induced apoptosis.²⁵³ In U937 cells, Noxa upregulation was accompanied with downregulation of anti-apoptotic Bcl-2, an increase in mitochondrial permeability, and inhibition of the kinase activity of the survival factor PKB.

²⁵⁰ Vieira, F. T.; Maia, J. R. da S.; Vilela, M. J.; Ardisson, J. D.; dos Santos, M. H.; de Oliveira, T. T.; Nagem, T. J. *Main Group Met. Chem.* **2009**, *32*, 235-245.

²⁵¹ For reviews on hyperforin cancer biology, see: (a) Quiney, C.; Billard, C.; Salanoubat, C.; Fourneron, J. D.; Kolb, J. P. *Leukemia* **2006**, *20*, 1519-1525. (b) Billard, C.; Merhi, F.; Bauvois, B. *Curr. Cancer Drug Tar.* **2013**, *13*, 1-10.

²⁵² (a) Zaher, M.; Akrou, I.; Mirshahi, M.; Kolb, J.-P.; Billard, C. *Leukemia* **2009**, *23*, 594-596. (b) Zaher, M.; Tang, R.; Bombarda, I.; Merhi, F.; Bauvois, B.; Billard, C. *Int. J. Oncol.* **2012**, *40*, 269-276.

²⁵³ Merhi, F.; Tang, R.; Piedfer, M.; Mathieu, J.; Bombarda, I.; Zaher, M.; Kolb, J.-P.; Billard, C.; Bauvois, B. *PLoS ONE* **2011**, *6*, e25963.

In addition to acting as a pro-apoptotic, hyperforin also acts as an anti-angiogenic agent and an inhibitor of cancer metastasis. In an *in vitro* assay involving BAE cells, treatment with 1-10 μM hyperforin strongly inhibited proliferation.²⁵⁴ Zymographic analysis revealed that hyperforin significantly inhibited urokinase and MMP-2 production. Similar results were observed in a later study involving a panel of murine and human cancer cell lines,²³² as well as HDMECs and *in vivo* with rats injected with MT-450 cells.²⁵⁵ In cultured B-CLL cells taken from patients, hyperforin inhibited the secretion of MMP-9, with IC_{50} values below 10 μM , and inhibited the formation of microtubules of human bone marrow endothelial cells cultured on Matrigel.²⁵⁶ Along with decreased secretion of urokinase, MMP-2, and MMP-9, hyperforin·HNCy₂ inhibited elastase noncompetitively ($\text{IC}_{50} = 3 \mu\text{M}$). In mouse models involving both B16-LU8 and C-26, sub-cytotoxic administration of hyperforin·HNCy₂ significantly reduced tumor metastasis and infiltration. Capillary-like structure development of HUVECs was also inhibited, and hyperforin treatment prevented the proliferation of the highly angiogenic Kaposi's sarcoma cell line.²⁵⁷ In the latter instance, significant reduction of vascularization and tumor size was observed compared to control. In contrast to these results, sub-micromolar concentrations of hyperforin actually *increased* VEGF expression in DAOY cells.²⁵⁸ No effect was observed in U87 cells, which overexpresses VEGF.

Due to the instability of pure hyperforin, several semisynthetic analogs have been prepared and their antiproliferative properties have been studied. While alkylation of the C4 enolic oxygen atom imparts stability, this may worsen the already marginal water solubility of hyperforin. To address these issues, the semisynthetic derivative aristoforin (**78**) was synthesized in two steps from hyperforin

²⁵⁴ Martínez-Poveda, B.; Quesada, A. R.; Medina, M. Á. *Int. J. Cancer* **2005**, *117*, 775-780.

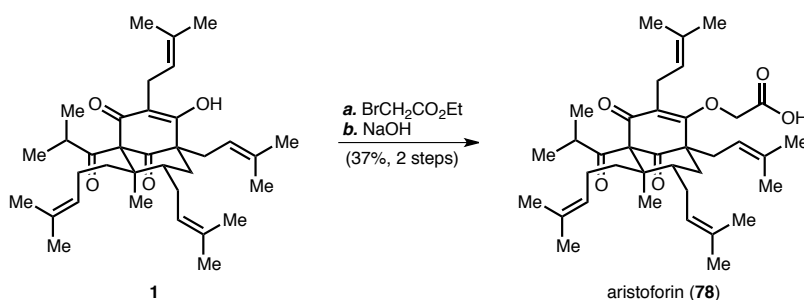
²⁵⁵ Schempp, C. M.; Kiss, J.; Kirkin, V.; Averbeck, M.; Simon-Haarhaus, B.; Kremer, B.; Termeer, C. C.; Sleeman, J.; Simon, J. C. *Planta Med.* **2005**, *71*, 999-1004.

²⁵⁶ Quiney, C.; Billard, C.; Mirshahi, P.; Fourneron, J.-D.; Kolb, J.-P. *Leukemia* **2006**, *20*, 583-589.

²⁵⁷ Lorusso, G.; Vannini, N.; Sogno, I.; Generoso, L.; Garbisa, S.; Noonan, D. M.; Albini, A. *Eur. J. Cancer* **2009**, *45*, 1474-1484.

²⁵⁸ Tassone, E.; Maran, C.; Masola, V.; Bradaschia, A.; Garbisa, S.; Onisto, M. *Pharmacol. Res.* **2011**, *63*, 37-43.

(Scheme 1.12).²⁵⁹ Not only was aristoforin more stable and more water-soluble than hyperforin, it also possessed very similar antiproliferative and pro-apoptotic properties as the parent natural product in MT-450 tumor assays. A loss of activity was observed with octahydroaristoforin, the hydrogenolysis product of aristoforin. Both hyperforin and aristoforin were similarly active at suppressing tumor-induced lymphangiogenesis *in vivo* at concentrations below 10 μM .²⁶⁰ Above 10 μM , both compounds induced apoptosis in lymphatic endothelial cells through increased mitochondrial membrane permeability and induction of caspase 9.



Scheme 1.12. Synthesis of aristoforin from hyperforin.^a

^a Conditions: (a) $\text{BrCH}_2\text{CO}_2\text{Et}$, K_2CO_3 , acetone; (b) NaOH , H_2O , MeOH , 0 $^\circ\text{C}$ to rt, 37% (2 steps).

A variety of oxidized and reduced hyperforin derivatives have also been evaluated, and some of the results are shown in Table 1.13. Both octahydrohyperforin (**66**) tetrahydrohyperforin (**76**) were found to be similarly effective towards MDA-MB-231 cells.²³⁴ Tetrahydrohyperforin displayed antiangiogenic properties comparable to hyperforin·HNCy₂ in a BAE cell growth assay and the Matrigel tubule-like structure formation assay. Several other semisynthetic derivatives, including furohyperforin, oxyhyperforin, **79**, **80**, and **81** (Figure 1.13), were also evaluated but were ineffective at inhibiting angiogenesis. This illustrates the importance of the enolic C4 oxygen atom for anti-angiogenic activity.

²⁵⁹ Gartner, M.; Müller, T.; Simon, J. C.; Giannis, A.; Sleeman, J. P. *ChemBioChem* **2005**, 6, 171-177.

²⁶⁰ Rothley, M.; Schmid, A.; Thiele, W.; Schacht, V.; Plaumann, D.; Gartner, M.; Yektaoglu, A.; Bruyère, F.; Noël, A.; Giannis, A.; Sleeman, J. P. *Int. J. Cancer* **2009**, 125, 34-42.

As mentioned previously, a significant loss of antiproliferative activity was observed with hyperforin *O*-acetate and octahydrohyperforin *O*-acetate across a variety of cancer cell lines.²³¹

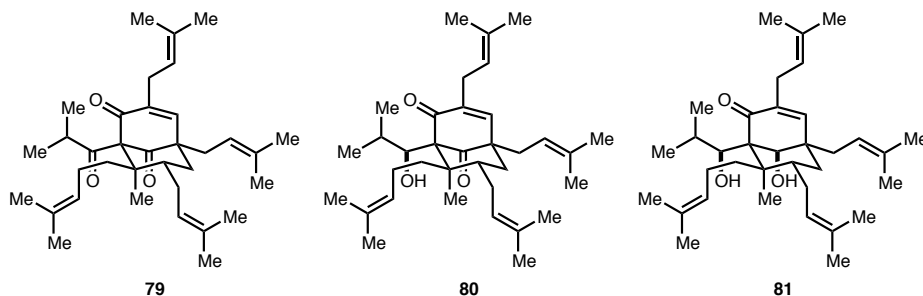


Figure 1.13. Semisynthetic hyperforin derivatives lacking C4 functionality.

Garcinol is another PPAP that has undergone rather extensive mechanistic studies, and it has been found to promote apoptosis and inhibit cancer proliferation, angiogenesis, and metastasis in a variety of ways.²⁶¹ Similar to hyperforin, garcinol activates apoptosis in certain cancer cell lines by increasing mitochondrial membrane permeability. This loss of membrane potential was observed in three different leukemia cell lines and led to activation of caspase 3.²⁶² In this study, similar activity was observed with isogarcinol but not xanthochymol. The addition of the caspase 3 inhibitor Z-DEVD-FMK prevented garcinol-induced apoptotic DNA fragmentation.²¹⁴ Later studies involving pancreatic²¹¹ and breast²¹⁵ cancer cell lines found that garcinol suppressed NF- κ B. In HT-29 cells, 10 μ M garcinol induced apoptosis and prevented migration by inhibiting the phosphorylation of FAK as well as preventing the activation of the MAPK and PI3K/Akt signaling pathways.²⁶³ Downregulation of STAT-3 was observed

²⁶¹ For a review of the chemotherapeutic properties of garcinol, see: Saadat, N.; Gupta, S. V. *J. Oncol.* **2012**, 647206.

²⁶² Matsumoto, K.; Akao, Y.; Kobayashi, E.; Ito, T.; Ohguchi, K.; Tanaka, T.; Iinuma, M.; Nozawa, Y. *Biol. Pharm. Bull.* **2003**, 26, 569-571.

²⁶³ Liao, C.-H.; Sang, S.; Ho, C.-T.; Lin, J.-K. *J. Cell. Biochem.* **2005**, 96, 155-169.

in a variety of cancer cell lines and in an MDA-MD-231 mouse xenograft model.²⁶⁴ In another study involving the MDA-MD-231 and the BT-549 breast carcinoma cell lines, garcinol treatment reversed the epithelial-to-mesenchymal transition and increased phosphorylation of β -catenin.²⁶⁵ These results were also validated in a xenograft mouse model. Breast cancer proliferation may also be inhibited through the ability of garcinol to downregulate the expression of cyclin D3, which is highly upregulated in cancer cells compared to nearby normal tissue.²⁶⁶ Treatment with 1 μ M garcinol in a nicotine-induced MDA-MD-231 cell line prevented cancer proliferation. Garcinol has also been shown to be particularly cytotoxic to cells expressing PDGFRs, kinases implicated in several forms of cancer including medulloblastoma.²⁶⁷ Inhibition of PDGFRs in several cell lines by garcinol led to apoptosis; however, PDGFR-negative MEF cells were not affected by garcinol treatment.

In addition to increased mitochondrial membrane permeability, garcinol may also promote apoptosis through the accumulation of ROS within cancer cells. In garcinol-treated (50 μ M) p53-negative Hep3B cells, this ROS accumulation was observed along with increased expression of endoplasmic reticulum stress modulator GADD153 and loss of mitochondrial membrane potential, leading to cell death.²⁶⁸ Interestingly, an independent study found that while high concentrations of garcinol caused apoptosis in HT-29 and HCT-116 cells, low concentrations (<1 μ M) actually promoted cancer cell proliferation.²¹² This latter effect may be mediated by ROS; in the presence of superoxide dismutase and catalase and with concentrations of garcinol 0.5-1 μ M, cell growth was inhibited.

²⁶⁴ Ahmad, A.; Sarkar, S. H.; Aboukameel, A.; Ali, S.; Biersack, B.; Seibt, S.; Li, Y.; Bao, B.; Kong, D.; Banerjee, S.; Schobert, R.; Padhye, S. B.; Sarkar, F. H. *Carcinogenesis* **2012**, *33*, 2450-2456.

²⁶⁵ Ahmad, A.; Sarkar, S. H.; Bitar, B.; Ali, S.; Aboukameel, A.; Sethi, S.; Li, Y.; Bao, B.; Kong, D.; Banerjee, S.; Padhye, S. B.; Sarkar, F. H. *Mol. Cancer Ther.* **2012**, *11*, 2193-2201.

²⁶⁶ Chen, C.-S.; Lee, C.-H.; Hsieh, C.-D.; Ho, C.-T.; Pan, M.-H.; Huang, C.-S.; Tu, S.-H.; Wang, Y.-J.; Chen, L.-C.; Chang, Y.-J.; Wei, P.-L.; Yang, Y.-Y.; Wu, C.-H.; Ho, Y.-S. *Breast Cancer Res. Treat.* **2011**, *125*, 73-87.

²⁶⁷ Tian, Z.; Shen, J.; Wang, F.; Xiao, P.; Yang, J.; Lei, H.; Kazlauskas, A.; Kohane, I. S.; Wu, E. *PLoS ONE* **2011**, *6*, e21370.

²⁶⁸ Cheng, A.-C.; Tsai, M.-L.; Liu, C.-M.; Lee, M.-F.; Nagabhushanam, K.; Ho, C.-T.; Pan, M.-H. *Food Funct.* **2010**, *1*, 301-307.

Administration of garcinol has been shown to prevent carcinogenesis in several animal models. Dietary feeding of garcinol (0.01-0.05% of diet) caused a significant reduction of the formation of azoxymethane-induced colonic aberrant crypt foci (ACF) in rats compared to control.²⁶⁹ Rats were given a garcinol-laden diet 1 week prior to the induction of ACF and during the next four weeks. Up to 40% reduction of ACF frequency was observed (with the 0.05% dietary garcinol cohort). Dietary feeding of garcinol (0.01-0.05%) also prevented 4-nitroquinoline 1-oxide-induced rat tongue carcinogenesis.²⁷⁰ Rats were given garcinol either for 10 weeks during carcinogen administration or for 22 weeks following exposure, and in both instances, the frequency of tongue lesions were significantly reduced. Topical treatment of garcinol also prevented 7,12-dimethylbenz[*a*]anthracene-induced hamster cheek pouch carcinogenesis.²⁷¹ Both short- and long-term application of garcinol prevented inflammation, lesion formation, and tumor size. In these three studies reported, a possible explanation for the suppression of carcinogenesis by garcinol may be due to its ability to decrease the expression of enzymes involved in inflammation response, such as iNOS, COX-2, and 5-LO.

Nemorosone also displays anti-cancer properties and may operate in a similar manner to hyperforin and garcinol. Nemorosone, in concentrations of 50-500 nM, has been shown to increase membrane permeability in mitochondria isolated from rat livers.²⁷² The authors hypothesized that nemorosone acted as a proton shuttle across the mitochondrial membrane, thus dissipating membrane potential. Indeed, nemorosone was found to be cytotoxic to HepG2 cells in 1-25 μ M concentrations. In various breast cancer cell lines, nemorosone was selectively cytotoxic to cells expressing estrogen receptor 1, and when an estrogen receptor antagonist was used in conjunction with nemorosone, these

²⁶⁹ Tanaka, T.; Kohno, H.; Shimada, R.; Kagami, S.; Yamaguchi, F.; Kataoka, S.; Ariga, T.; Murakami, A.; Koshimizu, K.; Ohigashi, H. *Carcinogenesis* **2000**, *21*, 1183-1189.

²⁷⁰ Yoshida, K.; Tanaka, T.; Hirose, Y.; Yamaguchi, F.; Kohno, H.; Toida, M.; Hara, A.; Sugie, S.; Shibata, T.; Mori, H. *Cancer Lett.* **2005**, *221*, 29-39.

²⁷¹ Chen, X.; Zhang, X.; Lu, Y.; Shim, J.-Y.; Sang, S.; Sun, Z.; Chen, X. *Nutr. Cancer* **2012**, *64*, 1211-1218.

²⁷² Pardo-Andreu, G. L.; Nuñez-Figueroa, Y.; Tudella, V. G.; Cuesta-Rubio, O.; Rodrigues, F. P.; Pestana, C. R.; Uyemura, S. A.; Leopoldino, A. M.; Alberici, L. C.; Curti, C. *Mitochondrion* **2011**, *11*, 255-263.

effects were enhanced.²⁷³ Nemorosone was also found to be cytotoxic toward the neuroblastoma cell line LAN-1.²³⁹ Significant decreases in Akt and ERK activity were observed and may be the cause of apoptosis in this cell line. Aside from facilitating apoptosis in pancreatic cells via mitochondrial membrane potential dissipation and caspase activation, transcription profiling revealed that nemorosone altered the expression of many proteins involved in unfolded protein response.²⁷⁴ This cellular stress response mechanism may be one avenue by which nemorosone facilitates apoptosis in cancer cells.

The mechanisms by which several other PPAPs inhibit cancer cell proliferation have been explored. Unsurprisingly, guttiferone A also increases mitochondrial membrane permeability and caused apoptosis of the pancreatic cancer cell line HepG2.²⁷⁵ Plukenetione A promoted apoptosis in a variety of cancer cell lines, and this may be due to its ability to repress the expression of topoisomerase I and DNA polymerase.²³⁷ In its ability to facilitate LNCaP prostate carcinoma cell apoptosis, 7-*epi*-nemorosone may inhibit MAPK, similar to garcinol.²⁴⁴ The ability of guttiferone K to promote apoptosis may also be due to MAPK inhibition.²²⁵ The addition of a JNK (a type of MAPK) inhibitor partially rescued HT-29 cells from guttiferone K-induced apoptosis. Oblongifolin C promoted apoptosis in HeLa cells via caspase and Bax activation.²⁴¹ In the presence of a pan-caspase inhibitor or the anti-apoptotic protein Bcl-xL, apoptosis was prevented. Caspase activation has also been noted in hyperatomarin-induced cancer cell apoptosis.²²⁶ Cathepsin inhibition has been implicated as a major factor in the antiproliferative properties of 7-*epi*-clusianone and garcinaphenone.¹¹⁶

Further, several other PPAPs have been evaluated specifically for antimutagenic and antimitotic activity. Nemorosone displayed modest inhibitory activity in the Ames mutagenicity assay involving various *Salmonella typhimurium* strains, especially against mitomycin C- and aflatoxin B1-induced

²⁷³ Popolo, A.; Piccinelli, A. L.; Morello, S.; Sorrentino, R.; Cuesta Rubio, O.; Rastrelli, L.; Aldo, P. *Can. J. Physiol. Pharmacol.* **2011**, *89*, 50-57.

²⁷⁴ Holtrup, F.; Bauer, A.; Fellenberg, K.; Hilger, R. A.; Wink, M.; Hoheisel, J. D. *Br. J. Pharmacol.* **2011**, *162*, 1045-1059.

²⁷⁵ Pardo-Andreu, G. L.; Nuñez-Figueredo, Y.; Tudella, V. G.; Cuesta-Rubio, O.; Rodrigues, F. P.; Pestana, C. R.; Uyemura, S. A.; Leopoldino, A. M.; Alberici, L. C.; Curti, C. *Toxicol. Appl. Pharmacol.* **2011**, *253*, 282-289.

mutagenesis.²⁷⁶ Garcinielliptone FC facilitated DNA damage and cleavage in the presence of Cu²⁺, possibly involving the formation of ROS.²⁷⁷ While garcinol, guttiferone B, and oblongifolins A-D were found to be ineffective at microtubule disassembly inhibition, they inhibited tubulin assembly, with IC₅₀ values ranging from 50-100 µM.²⁷⁸ Guttiferones G and J²²² as well as a mixture of cycloxanthochymol and isoxanthochymol²⁴⁹ showed no effect on tubulin assembly.

Several studies have addressed whether certain PPAPs can be used in concert with other therapeutic agents to treat cancer. When hyperforin was combined with hypericin or procyanidin B2, synergistic cytotoxic effects were observed in K562 and U937 cells upon treatment.²²⁹ Thus, the authors of the study purport that the crude St. John's wort extract may be a viable therapeutic option for various leukemias. In another study, an enhancement of activity was observed in hypericin-mediated photodynamic therapy of HT-29 cells when hyperforin or aristoforin was present.²⁷⁹ In leukemia cells, hyperforin has been shown to impair the activity of P-gp and BCRP, ATP-binding cassette transporters responsible for the development of multidrug resistance in several cancer cell lines.²⁸⁰ Hyperforin's ability to inhibit drug efflux from cancer cells may find use in chemotherapies in which drug resistance develops.

Other than hyperforin, garcinol may be useful as a co-therapeutic in cancer treatment. By inhibiting DNA repair via non-homologous end joining, garcinol has been shown to radiosensitize cancer cells.²⁸¹ Garcinol may prevent this DNA damage repair by acting as a histone acetyltransferase inhibitor.

²⁷⁶ Camargo, M. S.; Varela, S. D.; de Oliveira, A. P.; Resende, F. A.; Cuesta-Rubio, O.; Vilegas, W.; Varanda, E. A. *Braz. J. Pharmacogn.* **2011**, *21*, 921-927.

²⁷⁷ Wu, C.-C.; Lu, Y.-H.; Wei, B.-L.; Yang, S.-C.; Won, S.-J.; Lin, C.-N. *J. Nat. Prod.* **2008**, *71*, 246-250.

²⁷⁸ Hamed, W.; Brajeul, S.; Mahuteau-Betzer, F.; Thoison, O.; Mons, S.; Delpech, B.; Hung, N. V.; Sévenet, T.; Marazano, C. *J. Nat. Prod.* **2006**, *69*, 774-777.

²⁷⁹ Šemeláková, M.; Mikeš, J.; Jendželovský, R.; Fedoročko, P. *J. Photochem. Photobiol. B* **2012**, *117*, 115-125.

²⁸⁰ Quiney, C.; Billard, C.; Faussat, A.-M.; Salanoubat, C.; Kolb, J.-P. *Leukemia Lymphoma* **2007**, *48*, 1587-1599.

²⁸¹ Oike, T.; Ogiwara, H.; Torikai, K.; Nakano, T.; Yokota, J.; Kohno, T. *Int. J. Radiation Oncol. Biol. Phys.* **2012**, *84*, 815-821.

Garcinol's ability to change gene expression has also been applied to the sensitization of pancreatic cancer cells to the chemotherapeutic gemcitabine.²⁸² A synergistic effect was noted when garcinol and gemcitabine were co-applied to pancreatic cancer cells. Synergistic antiproliferative and apoptotic effects were also noted between garcinol and curcumin in the pancreatic cancer cell lines BXP-3 and PANC-1.²⁸³ Potency of a combination of the two agents was 2- to 10-fold greater than the individual potency of each agent.

Activity against Neurological Disorders

Diseases and disorders of the central nervous system have also been targeted with PPAP-based therapeutics. The most studied PPAP in this area is hyperforin, a component of the medicinal herb St. John's wort, and much work has been done to elucidate its effects on clinical depression.²⁸⁴ For over 2,000 years, St. John's wort has been used to treat a variety of ailments, and several ancient Greek and Roman historians and doctors have recorded the medicinal use of an herb called *hyperikon* that matches the description of *Hypericum perforatum*.²⁸⁵ Indeed, *hyperikon* is derived from the Latin words *hyper* (meaning "over") and *eikon* (meaning "apparition"), which in the pre-modern medicine era may refer to depression. A traditional English proverb below effectively summarizes the use of St. John's wort prior to the advent of modern medicine:

St. John's wort doth charm all the witches away,

If gathered at midnight on the saint's holy day,

And devils and witches have no power to harm

²⁸² Parasramka, M. A.; Ali, S.; Banerjee, S.; Deryavoush, T.; Sarkar, F. H.; Gupta, S. V. *Mol. Nutr. Food Res.* **2013**, *57*, 235-248.

²⁸³ Parasramka, M. A.; Gupta, S. V. *J. Oncol.* **2012**, 709739.

²⁸⁴ For reviews of hyperforin and SJW antidepressant activity, see: (a) Greeson, J. M.; Sanford, B.; Monti, D. A. *Psychopharmacology* **2001**, *153*, 402-414. (b) Di Carlo, G.; Borrelli, F.; Ernst, E.; Izzo, A. A. *Trends Pharmacol. Sci.* **2001**, *22*, 292-297. (c) Müller, W. E. *Pharmacol. Res.* **2003**, *47*, 101-109. (d) Zanolini, P. *CNS Drug Rev.* **2004**, *10*, 203-218. (e) Hussain, S.; Ansari, Z. H.; Arif, M. *Int. J. Health Res.* **2009**, *2*, 15-22. (f) Solomon, D.; Ford, E.; Adams, J.; Graves, N. *Aust. N.Z. J. Psychiat.* **2011**, *45*, 123-130.

²⁸⁵ For several excerpts of *hyperikon* use in antiquity, see: (a) Aulus Cornelius Celsus *Da Medica* 5.20.6 and 5.23.3. (b) Dioscorides *Materia Medica* 3.173. (c) Pliny the Elder *Naturalis Historiae* XXVI.53.

*Those that do gather the plant for a charm
Rub the lintels and post with that red juicy flower
No thunder nor tempest will then have the power
To hurt or to hinder your houses; and bind
Round your neck a charm of a similar kind.*²⁸⁶

To this day, SJW extract remains a popular therapeutic for depression in European countries; during the period between April 2007 and March 2008, over 9.5 million units of SJW were sold, mostly in Germany, Russia, and Poland.²⁸⁷ In Germany, standardized SJW extracts are one of the most prescribed antidepressants, with sales comparable to synthetic antidepressants. In the United States, sales of SJW peaked in the late 1990's, reaching upwards of an estimated \$310 million.²⁸⁸ However, the discovery of side effects (to be discussed in the next section) has led to a decrease in SJW sales, with 2007 numbers an estimated \$8.1 million, making it the tenth most popular herbal dietary supplement sold in the country that year.²⁸⁹ Dozens of clinical trials involving SJW treatment of depression have appeared in the literature enlisting over 5,000 patients. A Cochrane Collaboration meta-analysis of 29 double-blind, randomized trials involving 5,489 patients found that SJW was indeed effective for treatment of major depression with efficacy comparable to standard antidepressants.²⁹⁰ Importantly, fewer adverse side effects were encountered with SJW extract use than with other antidepressants.

Given the long history of use, efficacy, and safety of SJW extract, identification of the active component has received considerable attention. Chemicals found in the extract fall into three distinct categories: phloroglucinols, flavonoids, and naphthodianthrone.²⁹¹ An early study purported that the

²⁸⁶ Vickery, A. R. *Econ. Bot.* **1981**, 35, 289-295.

²⁸⁷ Linde, K. *Forsch. Komplementmed.* **2009**, 16, 146-155.

²⁸⁸ Golden, F. *TIME* **2001**, 157 (Apr. 30), 60-61.

²⁸⁹ Cavaliere, C.; Rea, P.; Blumenthal, M. *HerbalGram* **2008**, 78, 60-63.

²⁹⁰ Linde, K.; Berner, M. M.; Kriston, L. *Cochrane Database Syst. Rev.* **2008**, CD000448.

²⁹¹ Nahrstedt, A.; Butterweck, V. *Pharmacopsychiatry* **1997**, 30 (Suppl.), 129-134.

active antidepressant component of herb was hypericin (**82**, Figure 1.14), a naphthodianthrone polyketide that had monoamine oxidase (MAO) inhibition activity, with IC₅₀ values of 68 nM and 420 nM for type A and B MAOs, respectively.²⁹² However, there are several reasons to doubt that hypericin, by itself, is the active principle of SJW. Attempts to replicate these original findings have been unsuccessful, using either pure hypericin or crude SJW extracts.²⁹³ In fact, the flavonoid-containing fraction of the extract was the only component to show mild MAO inhibition ability at all. Also, it appears that hypericin does not cross the blood-brain barrier. When rats were orally administered with either SJW extract (1600 mg/kg) or pure hypericin (5 mg/kg), no hypericin was detected in the brain above the detection threshold (16 pmol/g).²⁹⁴

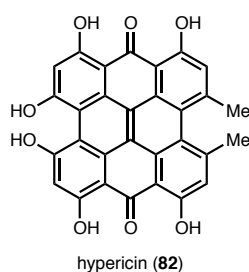


Figure 1.14. Structure of hypericin.

Upon further analysis of the compounds found in SJW extract, multiple sources found that hyperforin was indeed the primary component responsible for its antidepressant activity.²⁹⁵ While it had been known since the 1970's that hyperforin is a significant constituent of the herb,¹ comprising 2-4% of

²⁹² Suzuki, O.; Katsumata, Y.; Oya, M.; Bladt, S.; Wagner, H. *Planta Med.* **1984**, *50*, 272-274.

²⁹³ (a) Thiede, H.-M.; Walper, A. *J. Geriatr. Psychiatry Neurol.* **1994**, *7* (Suppl. 1), 54-56. (b) Bladt, S.; Wagner, H. *J. Geriatr. Psychiatry Neurol.* **1994**, *7* (Suppl. 1), 57-59. (c) Yu, P. H. *Pharmacopsychiatry* **2000**, *33*, 60-65.

²⁹⁴ Paulke, A.; Schubert-Zsilavecz, M.; Wurglics, M. *Monatsh. Chem.* **2008**, *139*, 489-494.

²⁹⁵ For a review of the antidepressant properties of hyperforin, see: (a) Müller, W. E. *Pharmacol. Res.* **2003**, *47*, 101-109. (b) Wurglics, M.; Schubert-Zsilavecz, M. *Clin. Pharmacokinet.* **2006**, *45*, 449-468. (c) Hussain, S.; Ansari, Z. H.; Arif, M. *Int. J. Health Res.* **2009**, *2*, 15-22.

the dry weight of its aerial parts,²⁹⁶ it had been largely disregarded due to its chemical instability. In fact, the inconsistencies of SJW clinical trials may be due to hyperforin instability; prior to the realization of the significance of hyperforin, the PPAP was found in variable amounts in SJW medical preparations.²⁹⁷

Upon exposure to light and air, hyperforin rapidly converts to furohyperforin, among other oxidation products. Furohyperforin is observed when air is bubbled through a methanolic solution of hyperforin for 6.5 h.²⁹⁸ Upon standing neat exposed to air at 40 °C, or dissolved in nonpolar solvents (e.g., hexane, benzene, petroleum ether), furohyperforin, 33-deoxy-33-hydroperoxy-furohyperforin, oxyhyperforin, oxepahyperforin, furohyperforin isomers 1 and 2, and a variety of monocyclic cyclohexanones were observed.²⁹⁹ Similar degradation products are found when hyperforin is photochemically irradiated in acetonitrile³⁰⁰ or exposed to peroxide oxidants.³⁰¹ Despite its apparent instability upon exposure to light, oxidants, and nonpolar solvents, hyperforin may be stabilized in polar protic solvents. In general, the half-life of hyperforin increases with increasing solvent polarity. After 30 days at 20 °C in the dark, over 70% of hyperforin remains in ethanol, methanol, or methanol/water suspensions.³⁰² Storage below -20 °C under nitrogen also prevents degradation of hyperforin; after 8 months, only marginal decomposition of hyperforin occurred.³⁰³ Overall, despite the fact that hyperforin

²⁹⁶ Maisenbacher, P. Thesis, University of Tübingen, Tübingen, Baden-Württemberg, Germany, 1991.

²⁹⁷ (a) Wurglics, M.; Westerhoff, K.; Kauzinger, A.; Wilke, A.; Baumeister, A.; Dressman, J.; Schubert-Zsilavecz, M. *J. Am. Pharm. Assoc.* **2001**, *41*, 560-566. (b) Ang, C. Y. W.; Hu, L.; Heinze, T. M.; Cui, Y.; Freeman, J. P.; Kozak, K.; Luo, W.; Liu, F. F.; Mattia, A.; DiNovi, M. *J. Agric. Food Chem.* **2004**, *52*, 6156-6164. (c) Schulte-Löbbert, S.; Holoubek, G.; Müller, W. E.; Schubert-Zsilavecz, M.; Wurglics, M. *J. Pharm. Pharmacol.* **2004**, *56*, 813-818.

²⁹⁸ Orth, H. C. J.; Hauer, H.; Erdelmeier, C. A. J.; Schmidt, P. C. *Pharmazie* **1999**, *54*, 76-77.

²⁹⁹ (a) Fuzzati, N.; Gabetta, B.; Strepponi, I.; Villa, F. *J. Chromatogr. A* **2001**, *926*, 187-198. (b) Wolfender, J.-L.; Verotta, L.; Belvisi, L.; Fuzzati, N.; Hostettmann, K. *Phytochem. Anal.* **2003**, *14*, 290-297.

³⁰⁰ D'Auria, M.; Emanuele, L.; Racioppi, R. *Lett. Org. Chem.* **2008**, *5*, 583-586.

³⁰¹ Verotta, L.; Lovaglio, E.; Sterner, O.; Appendino, G.; Bombardelli, E. *Eur. J. Org. Chem.* **2004**, 1193-1197.

³⁰² Orth, H. C. J.; Schmidt, P. C. *Pharm. Ind.* **2000**, *62*, 60-63.

³⁰³ Orth, H. C. J.; Rentel, C.; Schmidt, P. C. *J. Pharm. Pharmacol.* **1999**, *51*, 193-200.

may readily decompose upon exposure to light and air, relatively straightforward precautions can be taken in order to preserve hyperforin either as a pure substance or as found in SJW extracts.

The discovery that hyperforin was the principle antidepressant component of SJW came in 1998 with a seminal paper by Müller and coworkers.³⁰⁴ Using two murine models for depression, the behavioral despair test and the learned helplessness test, it was found that the antidepressant potency of SJW extracts correlated with hyperforin content. More importantly, isolated hyperforin inhibited the uptake of tritiated neurotransmitters into isolated murine synaptosomes in a dose-dependent manner. IC₅₀ values for these *in vitro* experiments ranged from 0.011-3.35 µM and have been confirmed in later studies (Table 1.14).³⁰⁵ Unlike synthetic antidepressants, which selectively block the selective reuptake of individual neurotransmitters, hyperforin appeared to block the reuptake of a variety of neurotransmitters, possibly signifying a novel mechanistic paradigm for the treatment of depression.

Table 1.14. Inhibition of synaptosomal [³H]neurotransmitter uptake by hyperforin.

Neurotransmitter	IC ₅₀ (µM)	References
[³ H]serotonin	0.12-3.35	304,306,307,308,309,310
[³ H]noradrenaline	0.033-0.080	304,308
[³ H]dopamine	0.011-0.102	304,308
[³ H]γ-aminobutyric acid	0.184	304,311
[³ H]L-glutamate	0.143-0.829	304,311

³⁰⁴ Chatterjee, S. S.; Bhattacharya, S. K.; Wonnemann, M.; Singer, A.; Müller, W. E. *Life Sci.* **1998**, *63*, 499-510.

³⁰⁵ See also: Müller, W. E.; Singer, A.; Wonnemann, M.; Hafner, U.; Rolli, M.; Schäfer, C. *Pharmacopsychiatry* **1998**, *31* (Suppl.), 16-21.

³⁰⁶ Singer, A.; Wonnemann, M.; Müller, W. E. *J. Pharmacol. Exp. Ther.* **1999**, *290*, 1363-1368.

³⁰⁷ Gobbi, M.; Valle, F. D.; Ciapparelli, C.; Diomedea, L.; Morazzoni, P.; Verotta, L.; Caccia, S.; Cervo, L.; Mennini, T. *Naunyn-Schmied. Arch. Pharmacol.* **1999**, *360*, 262-269.

³⁰⁸ Jensen, A. G.; Hansen, S. H.; Nielsen, E. Ø. *Life Sci.* **2001**, *68*, 1593-1605.

³⁰⁹ Verotta, L.; Appendino, G.; Belloro, E.; Bianchi, F.; Sterner, O.; Lovati, M.; Bombardelli, E. *J. Nat. Prod.* **2002**, *65*, 433-438.

³¹⁰ Leuner, K.; Heiser, J. H.; Derksen, S.; Mladenov, M. I.; Fehske, C. J.; Schubert, R.; Gollasch, M.; Schneider, G.; Harteneck, C.; Chatterjee, S. S.; Müller, W. E. *Molec. Pharmacol.* **2010**, *77*, 368-377.

³¹¹ Wonnemann, M.; Singer, A.; Müller, W. E. *Neuropsychopharmacology* **2000**, *23*, 188-197.

Subsequent to the realization that hyperforin may be responsible for the antidepressant activity of SJW, ensuing preclinical and clinical studies provided more evidence to verify this hypothesis. In the behavioral despair and elevated plus-maze murine models of depression, treatment with pure hyperforin led to more favorable outcomes compared to the ethanolic and supercritical CO₂ SJW extracts, which contained 4.5% and 38.8% hyperforin, respectively.³¹² Hyperforin was significantly effective in the elevated plus-maze test at concentrations as low as 1 mg/kg, and 3-day 20 mg/kg treatment with pure hyperforin in the force swim test caused a 40% reduction of immobilization time compared to vehicle. Using the same ethanolic and CO₂ SJW extracts as above, positive outcomes in a variety of other murine models of depression were shown to correlate with hyperforin content, including rat reserpine syndrome, muricidal rat behavior, 5-hydroxytryptophan-induced mouse head twitches, L-dopa-induced mouse behavior, apomorphine-induced rat stereotypy, and post-swim mouse grooming response.³¹³ In rats that were chronically exposed to unavoidable stress, escape deficit developed along with an anhedonia-type behavior towards palatable food. When these conditioned rats were exposed to SJW extracts or pure hyperforin, this escape deficit behavior diminished and the rats displayed favorable appetitive behavior.³¹⁴ In addition, pure hyperforin was significantly more potent than the SJW extracts used. Hyperforin administration also displayed positive outcome in the murine passive avoidance test.³¹⁵

A variety of clinical trials has also shown that hyperforin is a critical antidepressant component of SJW extracts. In a randomized, 147 out-patient, 42-day, double-blind multicenter study of persons suffering from mild to moderate depression,³¹⁶ the treatment group receiving an extract containing a

³¹² Chatterjee, S. S.; Nöldner, M.; Koch, E.; Erdelmeier, C. *Pharmacopsychiatry* **1998**, *31* (Suppl.), 7-15.

³¹³ Bhattacharya, S. K.; Chakabarti, A.; Chatterjee, S. S. *Pharmacopsychiatry* **1998**, *31* (Suppl.), 22-29.

³¹⁴ Gambanara, C.; Tolu, P. L.; Masi, F.; Rinaldi, M.; Giachetti, D.; Morazzoni, P.; De Montis, M. G. *Pharmacopsychiatry* **2001**, *34* (Suppl. 1), 42-44.

³¹⁵ Misane, I.; Ögren, S. O. *Pharmacopsychiatry* **2001**, *34* (Suppl. 1), 89-97.

³¹⁶ In this particular study, depression severity was determined using the DSM-IV (Diagnostic and Statistical Manual of Mental Disorders-IV), and the HAMD (Hamilton Rating Scale for Depression) 17-item questionnaire was used to assess change in depression severity throughout the study.

standardized 5% amount of hyperforin exhibited significantly larger positive endpoint when compared to treatment groups receiving either placebo or an extract with 0.5% hyperforin.³¹⁷ Patients were given three 300 mg tablets per day. In particular, more severely depressed patients responded particularly well to the 5% treatment. In a Phase I trial, 18 healthy volunteers were given one 900 mg tablet a day for 8 days, containing placebo or SJW extract (0.5% or 5% hyperforin), and monitored via quantitative topographic electroencephalography.³¹⁸ Significant pharmacodynamic effects were seen with both non-placebo treatment groups, peaking 4-8 hours after administration, and the treatment group receiving the higher dose of hyperforin saw more pronounced changes in electrical activity. In a 12-man study involving a SJW extract standardized to hypericin, no significant endpoint was achieved, providing further evidence that hyperforin, and not hypericin, is the active component of SJW.³¹⁹

One important note concerning outpatient clinical trials involving SJW is that results may be exacerbated by the readily available nature of its extracts, leading to patient noncompliance and confounding results. The highly publicized Hypericum Depression Trial Study,³²⁰ which found no difference between SJW and placebo for major depression, was replicated three years later with the addition of monitoring plasma hyperforin levels.³²¹ In this study, involving a total of 340 outpatients, one out of every six taking placebo had significant plasma hyperforin, and one-sixth of patients taking the SJW extract had no detectable hyperforin in their blood.

Interest in the underlying antidepressant mechanism of hyperforin and its biomolecular targets has led to numerous studies. Aside from inhibiting the uptake of neurotransmitters by synaptosomes as previously discussed, intraperitoneal injection of hyperforin (10 mg/kg) also was found to increase the

³¹⁷ (a) Laakmann, G.; Dienel, A.; Kieser, M. *Phytomedicine* **1998**, *5*, 435-442. (b) Laakmann, G.; Schüle, C.; Baghai, T.; Kieser, M. *Pharmacopsychiatry* **1998**, *31* (Suppl.), 54-59.

³¹⁸ Schellenberg, R.; Sauer, S.; Dimpfel, W. *Pharmacopsychiatry* **1998**, *31* (Suppl.), 44-53.

³¹⁹ Franklin, M.; Cowen, P. J. *Pharmacopsychiatry* **2001**, *34* (Suppl. 1), 29-37.

³²⁰ Hypericum Depression Trial Study Group, *J. Am. Med. Assoc.* **2002**, *287*, 1807-1814.

³²¹ Vitiello, B.; Shader, R. I.; Parker, C. B.; Ritz, L.; Harlan, W.; Greenblatt, D. J.; Gadde, K. M.; Krishnan, R. R.; Davidson, J. R. T. *J. Clin. Psychopharmacol.* **2005**, *25*, 243-249.

extracellular concentration of a variety of neurotransmitters in the rat locus coeruleus.³²² Presumably, hyperforin caused the release of synaptic vesicles containing these neurotransmitters into the synaptic cleft and prevented reuptake. This hypothesis was confirmed in a later study in which neurons in rat brain slices were preloaded with radiolabeled serotonin and dopamine.³²³ Hyperforin dose-dependently caused release of these amines. Similar results were obtained with human blood platelets preloaded with [¹⁴C]serotonin; treatment with 300 nM hyperforin caused store depletion of this monoamine.³²⁴

The above results do not support the idea that hyperforin works through direct interaction with reuptake enzymes. Michaelis–Menten kinetic analysis reveals that hyperforin blocks serotonin uptake via noncompetitive inhibition in mouse brain synaptosomes.³⁰⁶ Indeed, rat brain cortical synaptosomes pretreated with hyperforin did not prevent binding of tritiated citalopram, a selective serotonin reuptake inhibitor.³⁰⁷ Further, hyperforin failed to inhibit monoamine binding across a wide variety of neurotransmitter transporters and receptors in *in vitro* binding assays.³²⁵ Hyperforin, while inhibiting the uptake of radiolabeled monoamines in rat forebrain homogenates, did not affect binding of [³H]dihydrotetrabenazine, a known selective vesicular monoamine transporter ligand.³²⁶ Interestingly, SJW extracts do seem to competitively inhibit monoamine receptors in guinea pig hippocampal slices; however, when purified hyperforin was subjected to this *ex vivo* assay, no inhibition was observed.³²⁷

Instead of directly binding to neurotransmitter transports and receptors, numerous studies indicate that hyperforin increases intracellular ion levels, and this mediates not only monoamine uptake inhibition

³²² (a) Kaehler, S. T.; Sinner, C.; Chatterjee, S. S.; Philippu, A. *Neurosci. Lett.* **1999**, 262, 199-202. (b) Philippu, A. *Pharmacopsychiatry* **2001**, 34 (Suppl. 1), 111-115.

³²³ Roz, N.; Rehavi, M. *Life Sci.* **2004**, 75, 2841-2850.

³²⁴ Uebelhack, R.; Franke, L. *Pharmacopsychiatry* **2001**, 34 (Suppl. 1), 146-147.

³²⁵ (a) Gobbi, M.; Moia, M.; Pirona, L.; Morazzoni, P.; Mennini, T. *Pharmacopsychiatry* **2001**, 34 (Suppl. 1), 45-48. (b) Simmen, U.; Higelin, J.; Berger-Büteri, K.; Schaffner, W.; Lundstrom, K. *Pharmacopsychiatry* **2001**, 34 (Suppl. 1), 137-142.

³²⁶ Roz, N.; Mazur, Y.; Hirshfeld, A.; Rehavi, M. *Life Sci.* **2002**, 71, 2227-2237.

³²⁷ Langosch, J. M.; Zhou, X.-Y.; Heinen, M.; Kupferschmid, S.; Chatterjee, S. S.; Nöldner, M.; Walden, J. *Eur. Neuropsychopharmacol.* **2002**, 12, 209-216.

but also vesicular monoamine release. A wide variety of neurotransmitter transports rely on co-transport of sodium cations, and the presence of a sodium ion gradient across the cellular membrane facilitates this process.³²⁸ By diminishing this ion gradient, hyperforin indirectly inhibits monoamine reuptake. Accordingly, treatment of human platelets with 50 μM hyperforin caused an increase in intracellular $[\text{Na}^+]$ over basal levels.³⁰⁶ A similar effect was observed when a known cation transporter monensin was used; however, hyperforin did not elevate $[\text{Na}^+]_i$ to extracellular levels, as in the case of monensin, indicating a different transport mechanism. The addition of benzamil, an amiloride derivative and potent Na^+ ion channel inhibitor, further differentiated hyperforin- and monensin-based pathways.³¹¹ Benzamil attenuated hyperforin-based uptake inhibition but had no effect on monensin's activity. In addition, Ca^{2+} entry or electrical current may facilitate the release of neurotransmitters. In rat cortical synaptosomes, the release of glutamate induced by hyperforin was preceded by an increase of intracellular $[\text{Ca}^{2+}]$, indicating that hyperforin-mediated ion influx appears to be nonselective.³²⁹ Dose-dependent Ca^{2+} influx was also observed when 0.6-18.6 μM hyperforin was added to hamster vas deferens smooth muscle.³³⁰ pH gradient was also dissipated across the membranes of synaptic vesicles isolated from rat striatum and hypothalamus by inhibiting the action of vacuolar H^+ -ATPase with an IC_{50} value of 0.19 μM .³³¹ This facilitated the release of radiolabeled serotonin from preloaded vesicles. In addition, ion influx induces an electrical current across the cell membrane. Using patch clamp techniques, hyperforin caused a dose- and time-dependent inward current in isolated hippocampal pyramidal neurons and cerebellar rat Purkinje

³²⁸ Shi, L.; Quick, M.; Zhao, Y.; Weinstein, H.; Javitch, J. A. *Mol. Cell* **2008**, *30*, 667-677.

³²⁹ Chatterjee, S. S.; Biber, A.; Weibezahn, C. *Pharmacopsychiatry* **2001**, *34* (Suppl. 1), 11-19.

³³⁰ Kock, E.; Chatterjee, S. S. *Pharmacopsychiatry* **2001**, *34* (Suppl. 1), 70-73.

³³¹ Roz, N.; Rehavi, M. *Life Sci.* **2003**, *73*, 461-470.

neurons through ion influx.³³² Low concentrations of hyperforin (100-800 nM) also modulated the activity of P-type calcium channels in Purkinje neurons in a voltage-dependent manner.³³³

To summarize the evidence presented above, the ability of hyperforin to inhibit the reuptake and promote the release of neurotransmitters from neurons may be reliant on nonselective inward ion influx. Taken together, these data suggest that hyperforin may activate an ion channel expressed on neuronal membranes, and elucidation of this ion channel protein may represent a new target for developing antidepressants.³³⁴ Indeed, tetrodotoxin, a potent sodium channel blocker, inhibited hyperforin-mediated monoamine release from mouse cortical neurons.³³⁵ Similar inhibition was observed in human platelets and PC12 cells with both SKF-96365 and LOE 908, two inhibitors of nonselective cation channels.³³⁶ The addition of La^{3+} and Gd^{3+} ions also inhibited the activity of hyperforin in these cells, and these cations are known blockers of the canonical transient receptor potential protein (TRPC) channel family.

TRPC channels are members of the transient receptor potential protein superfamily that can be broadly described as cell-surface ion channels involved in many aspects of sensation and response to physical or chemical stimulation.³³⁷ TRPC channels were the first members of this family discovered, and all contain six transmembrane domains. They assemble into either homo- or hetero-tetramers, and cation selectivity is determined by the size of the pore loop. Several proteins may be anchored onto the cytoplasmic end of the S6 domain, providing control elements to regulate the activity of the cation

³³² Chatterjee, S.; Filippov, V.; Lishko, P.; Maximyuk, O.; Nöldner, M.; Krishtal, O. *Life Sci.* **1999**, *65*, 2395-2405.

³³³ (a) Fisunov, A.; Lozovaya, N.; Tsintsadze, T.; Chatterjee, S.; Nöldner, M.; Krishtal, O. *Pflügers Arch.* **2000**, *440*, 427-434. (b) Fisunov, A. I.; Lozovaya, N. A.; Tsintsadze, T. S.; Yatsenko, N. M.; Chatterjee, S.; Krishtal, O. A. *Neurophysiology* **2001**, *33*, 5-10. (c) Krishtal, O.; Lozovaya, N.; Fisunov, A.; Tsintsadze, T.; Pankratov, Y.; Kopanitsa, M.; Chatterjee, S. S. *Pharmacopsychiatry* **2001**, *34* (Suppl. 1), 74-82.

³³⁴ Müller, W. E.; Singer, A.; Wonnemann, M. *Pharmacopsychiatry* **2001**, *34* (Suppl. 1), 98-102.

³³⁵ Marsh, W. L.; Davies, J. A. *Life Sci.* **2002**, *71*, 2645-2655.

³³⁶ Treiber, K.; Singer, A.; Henke, B.; Müller, W. E. *Br. J. Pharmacol.* **2005**, *145*, 75-83.

³³⁷ For an overview of TRP channels, see: Clapham, D. E. *Nature* **2003**, *426*, 517-524.

channel. There are seven known TRPC proteins, and they may be activated by diacylglycerol, phospholipase C, or tyrosine kinases.³³⁸

Further analysis determined that hyperforin selectively activates TRPC6.³³⁹ Hyperforin (10 μ M) induced nonselective ion entry into PC12 cells expressing TRPC6. Furthermore, the entry of Ca^{2+} ions when TRPC6 was activated by hyperforin (0.1-0.3 μ M) caused neurite outgrowth in these cells, similar to the effects of adding nerve growth factor. Cation influx was suppressed in PC12 cells by expressing a dominant negative mutant of TRPC6. This is noteworthy given that the cell expression of related TRPC proteins remained unaffected, such as TRPC3 and TRPC7, which share approximately 75% sequence homology to TRPC6.³⁴⁰ Given the similarity of TRPC6 to other members of the TRPC family, it seems unlikely that hyperforin interacts directly with TRPC6. When PC12 cells were pre-incubated with various tyrosine kinase and phospholipase C inhibitors, the effects of hyperforin were mitigated, possibly indicating that hyperforin interacts with a protein involved in TRPC6 activation.³⁴¹

Regardless of the nature of hyperforin's interaction with TRPC6, its ability to act as a TRPC6 molecular probe has furthered understanding of this protein in particular and of ion homeostasis in general. When internal stores of Ca^{2+} are depleted from a cell, various ion channels are activated via the store-operated Ca^{2+} entry (SOCE) pathway.³⁴² In murine brain cortical embryonic neurons from which internal Ca^{2+} stores were depleted using thapsigargin, SOCE became activated.³⁴³ Addition of the TRPC3-selective inhibitor Pyr3 potently prevented Ca^{2+} entry; however, the addition of hyperforin facilitated Ca^{2+}

³³⁸ Hofmann, T.; Obukhov, A. G.; Schaefer, M.; Harteneck, C.; Gudermann, T.; Schultz, G. *Nature* **1999**, 397, 259-263.

³³⁹ Leuner, K.; Kazanski, V.; Müller, M.; Essin, K.; Henke, B.; Gollasch, M.; Harteneck, C.; Müller, W. E. *FASEB J.* **2007**, 21, 4101-4111.

³⁴⁰ Dietrich, A.; Mederos y Schnitzler, M.; Emmel, J.; Kalwa, H.; Hofmann, T.; Gudermann, T. *J. Biol. Chem.* **2003**, 278, 47842-47852.

³⁴¹ Treiber, K.; Henke, B.; Müller, W. E. *Pharmacopsychiatry* **2005**, 38, A235.

³⁴² Feske, S. *Pflügers Arch.* **2010**, 460, 417-435.

³⁴³ Gibon, J.; Tu, P.; Bouron, A. *Cell Calcium* **2010**, 47, 538-543.

entry presumably through TRPC6 activation. This indicates that while TRPC3 participates in SOCE, TRPC6 does not.³⁴⁴ Additionally, the activity of hyperforin was attenuated through the Zn^{2+} chelator TPEN, but SOCE-mediated Ca^{2+} entry remained unaffected. Further studies established that hyperforin also promoted the release of Ca^{2+} and Zn^{2+} stores from isolated brain mitochondria.³⁴⁵ The ability of hyperforin to increase the permeability of mitochondrial membrane has been documented.³⁴⁶ Beyond increasing mitochondrial membrane permeability, chronic hyperforin treatment (1 μM treatment for 3 days) has been shown to increase the gene expression of metallothioneins and thus Zn^{2+} storage capacity in cortical neurons.³⁴⁷ Metallothioneins are cysteine-rich proteins and bind to Zn^{2+} among other cationic species. Chronic intraperitoneal injection of rats with hyperforin (4 mg/kg/day) has similar effects, increasing the Zn^{2+} storage capabilities of their brain tissue. Increased intracellular Zn^{2+} stores were also achieved by expressing *TRPC6* in HEK293 cells, but not with *TRPC3* expression.³⁴⁸ These data suggest that TRPC6 is capable of acting as a Zn^{2+} -conducting channel.

Prior studies have suggested that TRPC proteins in general and TRPC6 in particular play crucial roles in neuronal differentiation, plasticity, and outgrowth.³⁴⁹ This may be one avenue by which hyperforin acts as an antidepressant and alters nerve tissue in the brain. Oral dosing (15 mg/kg) of the sodium salt of hyperforin in rats caused changes in the morphology of their brain membranes.³⁵⁰ Another study established that hyperforin treatment of neural stem/progenitor cells promoted the maturation of

³⁴⁴ It should be noted that other hyperforin-activated ion channels mimicking TRPC6 may be present in neurons. For more information, see: Tu, P.; Kunert-Keil, C.; Lucke, S.; Brinkmeier, H.; Bouron, A. *J. Neurochem.* **2009**, *108*, 126-138.

³⁴⁵ Tu, P.; Gibon, J.; Bouron, A. *J. Neurochem.* **2010**, *112*, 204-213.

³⁴⁶ See the discussion in the *Chemotherapeutic Activity* section on page 64.

³⁴⁷ Gibon, J.; Richaud, P.; Bouron, A. *Neuropharmacology* **2011**, *61*, 1321-1326.

³⁴⁸ Gibon, J.; Tu, P.; Bohic, S.; Richaud, P.; Arnaud, J.; Zhu, M.; Boulay, G.; Bouron, A. *Biochim. Biophys. Acta* **2011**, *1808*, 2807-2818.

³⁴⁹ Ramsey, I. S.; Delling, M.; Clapham, D. E. *Annu. Rev. Physiol.* **2006**, *68*, 619-647.

³⁵⁰ Eckert, G. P.; Keller, J.-H.; Jourdan, C.; Karas, M.; Volmer, D. A.; Schubert-Zsilavecz, M.; Müller, W. E. *Neurosci. Lett.* **2004**, *367*, 139-143.

oligodendrocytes without affecting the proliferation of the progenitor cells.³⁵¹ Oligodendrocyte dysfunction may play a role in the pathogenesis of major depressive disorder.³⁵² Hyperforin, via TRPC6 activation, caused changes in dendritic spine morphology in pyramidal neurons in rat hippocampal slices.³⁵³ These effects were blocked by the addition of La^{3+} , indicating the importance of TRPC6 channels on hyperforin-induced morphological effects. Hyperforin has also been shown to generate neuroprotective effects in neurons through the activation of CREB in a tissue-specific manner. Rats treated with daily hyperforin injections (4 mg/kg) for 4 weeks had increased cortical expression of TRPC6 and TrkB, a brain-derived neurotrophic factor receptor.³⁵⁴ Immediately following a middle cerebral artery occlusion in the brains of rats, direct injection of hyperforin into the brain reduced total cell death and increased TRPC6 and CREB activity.³⁵⁵ One day after the ischemic stroke, the rats treated with hyperforin also displayed higher neurologic scores than the control group. Interestingly, expression of TrkB in the hippocampus remained unaffected. Similar effects were observed in a rat model of status epilepticus, a prolonged seizure event that results in significant brain tissue damage.³⁵⁶ In such an event, TRPC6 expression decreases in affected tissue, ultimately leading to neuronal cell death,³⁵⁷ however, prior hyperforin treatment prevented this downregulation and subsequently prevents neurodegeneration. Conversely, hyperforin has also engendered neuroprotective effects by the *downregulation* of TRPC6 and CREB expression in certain situations. As discussed earlier, hyperforin decreased activated CREB levels

³⁵¹ Wang, Y.; Zhang, Y.; He, J.; Zhang, H.; Xiao, L.; Nazarali, A.; Zhang, Z.; Zhang, D.; Tan, Q.; Kong, J.; Li, X.-M. *J. Neurochem.* **2011**, *119*, 555-568.

³⁵² Uranova, N. A.; Vostrikov, V. M.; Orlovskaya, D. D.; Rachmanova, V. I. *Schizophr. Res.* **2004**, *67*, 269-275.

³⁵³ Leuner, K.; Li, W.; Amaral, M. D.; Rudolph, S.; Calfa, G.; Schuwald, A. M.; Harteneck, C.; Inoue, T.; Pozzo-Miller, L. *Hippocampus* **2013**, *23*, 40-52.

³⁵⁴ Gibon, J.; Deloulme, J.-C.; Chevallier, T.; Ladevèze, E.; Abrous, D. N.; Bouron, A. *Int. J. Neuropsychopharmacol.* **2013**, *16*, 189-198.

³⁵⁵ Lin, Y.; Zhang, J.-C.; Fu, J.; Chen, F.; Wang, J.; Wu, Z.-L.; Yuan, S.-Y. *J. Cerebr. Blood Flow Metab.* **2013**, *33*, 253-262.

³⁵⁶ Kim, D.-S.; Ryu, H. J.; Kim, J.-E.; Kang, T.-C. *Cell. Mol. Neurobiol.* **2013**, *33*, 99-109.

³⁵⁷ Du, W.; Huang, J.; Yao, H.; Zhou, K.; Duan, B.; Wang, Y. *J. Clin. Invest.* **2010**, *120*, 3480-3492.

in mouse microglia by decreasing iNOS expression.¹⁸⁰ In PC12 cells that had been previously activated with NGF, hyperforin actually downregulated TRPC6 expression.³⁵⁸ Decreased expression of TRPC6 in this instance may have promoted neuroprotection by regulating the rate of neurite outgrowth.

Due to its expression throughout the human body, TRPC6 may be a unique target for the treatment of a variety of diseases. Many inflammatory skin conditions are characterized by over-proliferating skin cells, and TRPC6 has been associated with Ca^{2+} -induced keratinocyte differentiation.³⁵⁹ Additionally, skin creams formulated with SJW extracts have shown efficacy in several half-side clinical trials involving inflammatory skin diseases,³⁶⁰ including pressure ulcers,³⁶¹ psoriasis,³⁶² and atopic dermatitis.³⁶³ When HaCaT cells were treated with hyperforin (1 μM), an influx of Ca^{2+} was observed and differentiation was triggered, and these effects were mimicked through the addition of a high concentration of extracellular Ca^{2+} .³⁶⁴ When TRPC6 was knocked down, both hyperforin- and Ca^{2+} -induced differentiation was not observed. TRPC6 is also abnormally expressed in several breast cancer cell lines (e.g., MCF-7, MCF 10A, MDA-MB-231), and the antiproliferative effect of hyperforin on these cell lines may be in part due to its interaction with TRPC6 or its effects on TRPC6 expression.³⁶⁵ In

³⁵⁸ Kumar, S.; Chakraborty, S.; Barbosa, C.; Brustovetsky, T. Brustovetsky, N.; Obukhov, A. G. *J. Cell. Physiol.* **2012**, *227*, 1408-1419.

³⁵⁹ (a) Cai, S.; Fatherazi, S.; Presland, R. B.; Belton, C. M.; Izutsu, K. T. *J. Dermatol. Sci.* **2005**, *40*, 21-28. (b) Beck, B.; Lehen'kyi, V.; Roudbaraki, M.; Flourakis, M.; Charveron, M.; Bordat, P.; Polakowska, R.; Prevarskaya, N.; Skryma, R. *Cell Calcium* **2008**, *43*, 492-505. (c) Woelfe, U.; Laszczyk, M. N.; Kraus, M.; Leuner, K.; Kersten, A.; Simon-Haarhaus, B.; Scheffler, A.; Martin, S. F.; Müller, W. E.; Nashan, D.; Schempp, C. M. *J. Invest. Dermatol.* **2010**, *130*, 113-123. (d) Sun, X.-D.; You, Y.; Zhang, L.; Zheng, S.; Hong, Y.; Li, J.; Gao, X.-H. *Med. Hypotheses* **2012**, *78*, 42-44.

³⁶⁰ For a review of the use of SJW extracts in the treatment of treat skin conditions, see: Schempp, C. M.; Müller, K. A.; Winghofer, B.; Schöpf, E.; Simon, J. C. *Hautarzt* **2002**, *53*, 316-321.

³⁶¹ Lomagno, P.; Lomagno, R. C. *Fitoterapia* **1979**, *50*, 201-205.

³⁶² Najafizadeh, P.; Hashemian, F.; Mansouri, P.; Farshi, S.; Surmaghi, M. S.; Chalangari, R. *Australas. J. Dermatol.* **2012**, *53*, 131-135.

³⁶³ (a) Schempp, C. M.; Windeck, T.; Hezel, S.; Simon, J. C. *Phytomedicine* **2003**, *10* (Suppl. 4), 31-37.

³⁶⁴ Müller, M.; Essin, K.; Hill, K.; Beschmann, H.; Rubant, S.; Schempp, C. M.; Gollasch, M.; Boehncke, W. H.; Harteneck, C.; Müller, W. E.; Leuner, K. *J. Biol. Chem.* **2008**, *283*, 33942-33954.

³⁶⁵ Aydar, E.; Yeo, S.; Djamgoz, M.; Palmer, C. *Cancer Cell Int.* **2009**, *9*, 23.

vascular smooth muscle, TRPC6 plays an important role in regulating vascular tone.³⁶⁶ Hyperforin caused dose- and time-dependent smooth muscle constriction in aortic segments taken from mice. In aortic segments taken from TRPC6-knockout mice, no such constriction was observed. In the lung, TRPC6 expression is associated with the induction of platelet-activating factor-induced vascular leakage leading to lung edema.³⁶⁷ Treatment of mouse lungs with hyperforin caused effects similar to platelet-activating factor, including increased intracellular $[Ca^{2+}]$ and weight gain due to fluid entry. TRPC6 malfunction has also been implicated in certain instances of focal segmented glomerulosclerosis, a significant cause of renal disease.³⁶⁸

In addition to TRPC6 and neuronal monoamine receptors, several other potential biomolecular targets of hyperforin have been explored. Both hyperforin and its dicyclohexylamine salt were found to be potent inhibitors of substance P-induced interleukin-6 release in human astrocytoma cells with an IC_{50} value of 1.6 μM .³⁶⁹ Hypersecretion of interleukin-6 and other cytokines may be involved with the pathophysiology of depression. β -Adrenergic receptors may also be involved in depression since downregulation of these proteins correlate with the antidepressant effects of other medicines.³⁷⁰ When rats were treated with methanolic and CO_2 SJW extracts, a significant decrease in β -adrenergic receptor levels was observed in the frontal cortex region of the brain.³⁷¹ In rat C6 glioblastoma cells, treatment with hyperforin led to a decrease in β_2 -adrenergic receptor expression, indicating that hyperforin was one of

³⁶⁶ Ding, Y.; Winters, A.; Ding, M.; Graham, S.; Akopova, I.; Muallem, S.; Wang, Y.; Hong, J. H.; Gryczynski, Z.; Yang, S.-H.; Birnbaumer, L.; Ma, R. *J. Biol. Chem.* **2011**, *286*, 31799-31809.

³⁶⁷ Samapati, R.; Yang, Y.; Yin, J.; Stoerger, C.; Arenz, C.; Dietrich, A.; Gudermann, T.; Adam, D.; Wu, S.; Freichel, M.; Flockerzi, V.; Uhlig, S.; Kuebler, W. M. *Am. J. Respir. Crit. Care Med.* **2012**, *185*, 160-170.

³⁶⁸ Winn, M. P.; Conlon, P. J.; Lynn, K. L.; Farrington, M. K.; Creazzo, T.; Hawkins, A. F.; Daskalakis, N.; Kwan, S. Y.; Ebersviller, S.; Burchette, J. L.; Pericak-Vance, M. A.; Howell, D. N.; Vance, J. M.; Rosenberg, P. B. *Science* **2005**, *308*, 1801-1804.

³⁶⁹ Gobbi, M.; Moia, M.; Funicello, M.; Riva, A.; Morazzoni, P.; Mennini, T. *Planta Med.* **2004**, *70*, 680-682.

³⁷⁰ Racagni, G.; Brunello, N. *Trends Pharmacol. Sci.* **1984**, *5*, 527-531.

³⁷¹ Simbrey, K.; Winterhoff, H.; Butterweck, V. *Life Sci.* **2004**, *74*, 1027-1038.

the primary components of the extracts responsible for this activity.³⁷² Hyperforin treatment was later shown to also decrease β_1 -adrenergic receptor in this cell line.³⁷³

While hyperforin is considered the chief antidepressant component of SJW extracts, it is not exclusively responsible for the herb's antidepressant activity; other chemicals isolated from the extract have shown efficacy in various *in vitro* and *in vivo* models. Hypericin and pseudohypericin³⁷⁴ as well as the biflavonoid amentoflavone³⁷⁵ and various xanthones³⁷⁶ inhibited monoamine receptor binding. Interestingly, SJW extracts devoid of hyperforin displayed antidepressant-like outcomes in a variety of murine behavioral models, including the elevated plus maze,³⁷⁷ tail suspension test, and the forced swim test.³⁷⁸ In other behavioral models, positive outcomes were observed even when no detectable amount of hyperforin was present in the brain.³⁷⁹ Flavonoids,³⁸⁰ such as rutin³⁸¹ and quercetin,³⁸² were found to be active in these behavioral models. Amentoflavone was the most active component of the extract at stopping stress-induced hyperthermia in mice.³⁸³ Quercetin also displayed potent, selective inhibition of

³⁷² Prenner, L.; Sieben, A.; Zeller, K.; Weiser, D. Häberlein, H. *Biochemistry* **2007**, *46*, 5106-5113.

³⁷³ Jakobs, D.; Hage-Hülsmann, A.; Prenner, L.; Kolb, C.; Weiser, D.; Häberlein, H. *J. Pharm. Pharmacol.* **2013**, *65*, 907-915.

³⁷⁴ Simmen, U.; Burkard, W.; Berger, K.; Schaffner, W.; Lundstrom, K. *J. Recept. Signal Transduct. Res.* **1999**, *19*, 59-74.

³⁷⁵ Butterweck, V.; Narhstedt, A.; Evans, J.; Hufeisen, S.; Rauser, L.; Savage, J.; Popadak, B.; Ernsberger, P.; Roth, B. L. *Psychopharmacology* **2002**, *162*, 193-202.

³⁷⁶ Muruganandam, A. V.; Ghosal, S.; Bhattacharya, S. K. *Biogenic Amines* **2000**, *15*, 553-567.

³⁷⁷ Coleta, M.; Campos, M. G.; Cotrim, M. D.; da Cunha, A. P. *Pharmacopsychiatry* **2001**, *34* (Suppl. 1), 20-21.

³⁷⁸ Butterweck, V.; Christoffel, V.; Nahrstedt, A.; Petereit, F.; Spengler, B.; Winterhoff, H. *Life Sci.* **2003**, *73*, 627-639.

³⁷⁹ Cervo, L.; Rozio, M.; Ekalle-Soppo, C. B.; Guiso, G.; Morazzoni, P.; Caccia, S. *Psychopharmacology* **2002**, *164*, 423-428.

³⁸⁰ Butterweck, V.; Jürgenliemk, G.; Nahrstedt, A.; Winterhoff, H. *Planta Med.* **2000**, *66*, 3-6.

³⁸¹ Nöldner, M.; Schötz, K. *Planta Med.* **2002**, *68*, 577-580.

³⁸² Paulke, A.; Nöldner, M.; Schubert-Zsilavecz, M.; Wurglics, M. *Pharmazie* **2008**, *63*, 296-302.

³⁸³ Grundmann, O.; Kelber, O.; Butterweck, V. *Planta Med.* **2006**, *72*, 1366-1371.

monoamine oxidase A, with an IC₅₀ value of 10 nM.³⁸⁴ Modulation of the hypothalamic-pituitary-adrenal axis may be a therapeutic option in the treatment of depression, and while hyperforin did not alter gene expression in brain areas involved with axis control in rats,³⁸⁵ various flavonoids³⁸⁶ and pseudohypericin³⁸⁷ present in SJW extracts modulated axis function. Overall, while hyperforin is the consensus active principle of SJW, various other components display activity across a range of biochemical systems implicated in depression.

Aside from hyperforin, very few PPAPs have been evaluated for antidepressant activity. Adhyperforin is also isolated from SJW, usually in concentrations one-seventh that of hyperforin.³¹² Unsurprisingly, this PPAP also potently inhibits neurotransmitter uptake in the synaptosome uptake assay with IC₅₀ values lower than hyperforin to some extent (Table 1.15). Hyperfoliatin (hyperibone J) has also been evaluated in synaptosomal reuptake assays but was several orders of magnitude less active than hyperforin and adhyperforin (Table 1.15). Like hyperforin, adhyperforin and hyperfoliatin do not bind directly to monoamine receptors.^{308,388} In addition, hyperfoliatin reduced the immobility time of the forced swim test in rats. Hyperatomarin has also been evaluated for uptake inhibition, but was found to be only weakly active against serotonin reuptake (IC₅₀ = 16.8 µM), and was actually one of the least potent

³⁸⁴ Chimenti, F.; Cottiglia, F.; Bonsignore, L.; Casu, L.; Casu, M.; Floris, C.; Secci, D.; Bolasco, A.; Chimenti, P.; Granese, A.; Befani, O.; Turini, P.; Alcaro, S.; Ortuso, F.; Trombetta, G.; Loizzo, A.; Guarino, I. *J. Nat. Prod.* **1999**, *69*, 945-949.

³⁸⁵ Butterweck, V.; Winterhoff, H.; Herkenham, M. *Neuropsychopharmacology* **2003**, *28*, 2160-2168.

³⁸⁶ Butterweck, V.; Hegger, M.; Winterhoff, H. *Planta Med.* **2004**, *70*, 1006-1008.

³⁸⁷ Simmen, U.; Bobirnac, I.; Ullmer, C.; Lübbert, H.; Büter, K. B.; Schaffner, W.; Schoeffter, P. *Eur. J. Pharmacol.* **2003**, *458*, 251-256.

³⁸⁸ do Rego, J.-C.; Benkiki, N.; Chosson, E.; Kabouche, Z.; Seguin, E.; Costentin, J. *Eur. J. Pharmacol.* **2007**, *569*, 197-203.

components of *Hypericum annulatum* evaluated in this study.³⁸⁹ Furohyperforin was reported to have one-tenth the activity of hyperforin against synaptosomal serotonin uptake.³⁹⁰

Table 1.15. Inhibition of synaptosomal [³H]neurotransmitter uptake by adhyperforin.^a

PPAP	[³ H]serotonin	[³ H]noradrenaline	[³ H]dopamine	[³ H]L-glutamate	References
adhyperforin	0.027-0.32	0.014-0.67	0.003	2.40	308,391
hyperfoliatin	3.5	1.8	1.2	n.d.	388

^a All data reported are IC₅₀ values (in μM).

Several semisynthetic hyperforin analogs have been evaluated for antidepressant activity. Crude SJW extracts containing hyperforin and adhyperforin conjugates still retained significant activity in the forced swim test, even though they did not contain detectable hyperforin or adhyperforin.³⁹² In studies involving more resolved hyperforin analogs, hyperforin esters generally show favorable antidepressant activity whereas oxidation products display decreased activity. Across four different animal models of depression (i.e., forced swim test, learned helplessness test, elevated plus maze, and light-dark test), hyperforin *O*-acetate at 3-5 mg/kg dosing showed efficacy.³⁹³ Hyperforin *O*-3,4,5-trimethoxybenzoate (**61**) also shortened immobility time during the forced swim test when injected at 3.1-6.3 mg/kg concentrations.³⁹⁴ At these concentrations, plasma levels of this analog were 30-50 μM and brain levels were found to be 0.3 μM. While both of these analogs were active in animal models of depression, neither possessed the ability to inhibit *in vitro* synaptosomal neurotransmitter uptake.^{309,394} A variety of

³⁸⁹ Tzankova, V.; Nedialkov, P.; Kitanov, G.; Danchev, N. *Pharmacologyonline* **2010**, 2, 142-150.

³⁹⁰ Verotta, L.; Appendino, G.; Belloro, E.; Jakupovic, J.; Bombardelli, E. *J. Nat. Prod.* **1999**, 62, 770-772.

³⁹¹ Wonnemann, M.; Singer, A.; Siebert, B.; Müller, W. E. *Pharmacopsychiatry* **2001**, 34 (Suppl. 1), 148-151.

³⁹² Muruganandam, A. V.; Bhattacharya, S. K.; Ghosal, S. *Indian J. Exp. Biol.* **2001**, 39, 1302-1304.

³⁹³ Zanolli, P.; Rivasi, M.; Baraldi, C.; Baraldi, M. *Behav. Pharmacol.* **2002**, 13, 645-651.

³⁹⁴ Cervo, L.; Mennini, T.; Rozio, M.; Ekalle-Soppo, C. B.; Canetta, A.; Burbassi, S.; Guiso, G.; Pirona, L.; Riva, A.; Morazzoni, P.; Caccia, S.; Gobbi, M. *Eur. Neuropsychopharmacol.* **2005**, 15, 211-218.

other hyperforin analogs were found to be inactive in this uptake assay, including hyperforin *O*-methyl ether (**60**), hyperforin *O*-2,4-dinitrobenzoate, **63**, **64**, oxyhyperforin, pyrohyperforin, and **83** (Figure 1.15).³⁰⁹ It should be noted that various diacylphloroglucinol derivatives have been developed as TRPC6-selective inhibitors, but these compounds bear little resemblance to hyperforin.³⁹⁵

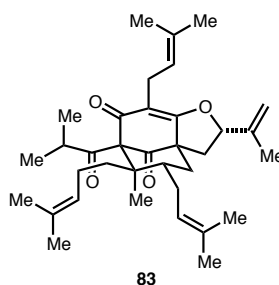


Figure 1.15. A semisynthetic hyperforin analog evaluated for antidepressant activity.

Several PPAPs have been evaluated for their activity against neurological disorders beyond clinical depression.³⁹⁶ Acetylcholinesterase (AChE) and butyrylcholinesterase (BChE) are possible targets for the treatment of various neurological diseases, such as Alzheimer's disease, glaucoma, and myasthenia gravis.³⁹⁷ Various PPAPs exhibit fairly potent inhibition activity against both of these enzymes in an *in vitro* assay (Table 1.16).¹²⁸ At a concentration of 10 μ M, garsubellin A increased choline acetyltransferase activity by 154% in P10 rat septal neurons.³⁹⁸ Mice injected with 1-10 mg/kg hyperforin caused an increase of acetylcholine release, and at the highest concentration tested, a significant decrease in locomotor activity was observed.³⁹⁹ The former results could be explained by the ability of hyperforin

³⁹⁵ Leuner, K.; Heiser, J. H.; Derksen, S.; Mladenov, M. I.; Fehske, C. J.; Schubert, R.; Gollasch, M.; Schneider, G.; Harteneck, C.; Chatterjee, S. S.; Müller, W. E. *Molec Pharmacol.* **2010**, *77*, 368-377.

³⁹⁶ For reviews of therapeutic potential of PPAPs against degenerative diseases, see: (a) Verotta, L. *Phytochem. Rev.* **2002**, *1*, 389-407. (b) Wilson, R. M.; Danishefsky, S. J. *Acc. Chem. Res.* **2006**, *39*, 539-549.

³⁹⁷ Tripathi, A.; Srivastava, U. C. *Ann. Neurosci.* **2008**, *15*, 106-111.

³⁹⁸ Fukuyama, Y.; Kuwayama, A.; Minami, H. *Chem. Pharm. Bull.* **1997**, *45*, 947-949.

³⁹⁹ Buchholzer, M.-L.; Dvorak, C.; Chatterjee, S. S.; Klein, J. *J. Pharmacol. Exp. Ther.* **2002**, *301*, 714-719.

to activate ion channels in neurons, and the latter result may indicate that very high, chronic doses of hyperforin may lead to Parkinson's disease. A subsequent study found that hyperforin-induced acetylcholine release in the rat hippocampus is indeed Ca^{2+} -dependent.⁴⁰⁰

Table 1.16. AChE and BChE inhibition activity of several PPAPs.

PPAP	AChE IC ₅₀ (μM)	BChE IC ₅₀ (μM)
garcinol	0.66	7.39
guttiiferone A	0.88	2.77
guttiiferone F	0.95	3.50
isogarcinol	1.13	8.30

Hyperforin and its reduced derivative tetrahydrohyperforin (**76**) have been evaluated for their ability to affect β -amyloid ($\text{A}\beta$) biochemistry, a poorly understood but important component of the pathophysiology of Alzheimer's disease.⁴⁰¹ In rat PC12 cells, hyperforin treatment accelerated the proteolysis of amyloid precursor protein.⁴⁰² The activity of hyperforin was distinct from other, known activators of amyloid precursor protein proteolytic secretion. Hyperforin also significantly decreased the formation of amyloid deposits in rats injected with amyloid fibrils.⁴⁰³ The rats also displayed more favorable outcomes in the circular water maze test compared to control and decreased $\text{A}\beta$ -related neurotoxicity in hippocampal neurons. Similar *in vivo* effects were observed for tetrahydrohyperforin (**76**).⁴⁰⁴ In amyloid precursor protein-transgenic mice, tetrahydrohyperforin caused a reduction in $\text{A}\beta$

⁴⁰⁰ Kiewert, C.; Buchholzer, M.-L.; Hartmann, J.; Chatterjee, S. S.; Klein, J. *Neurosci. Lett.* **2004**, *364*, 195-198.

⁴⁰¹ For a review of the effects of hyperforin and its derivatives on the pathophysiology of Alzheimer's disease, see: Griffith, T. N.; Varela-Nallar, L.; Dinamarca, M. C.; Inestrosa, N. C. *Curr. Med. Chem.* **2010**, *17*, 391-406.

⁴⁰² Froestl, B.; Steiner, B.; Müller, W. E. *Biochem. Pharmacol.* **2003**, *66*, 2177-2184.

⁴⁰³ Dinamarca, M. C.; Cerpa, W.; Garrido, J.; Hancke, J. L.; Inestrosa, N. C. *Molec. Psychiatry* **2006**, *11*, 1032-1048.

⁴⁰⁴ For a review, see: Carvajal, F. J.; Inestrosa, N. C. *Front. Mol. Neurosci.* **2011**, *4*, 19.

plaque formation, possibly due to the release of AChE from the precursor fibril assemblies⁴⁰⁵ or the prevention of AChE association with amyloid plaques.⁴⁰⁶ Later studies established that this semisynthetic hyperforin derivate dose-dependently prevented cognitive deficit and memory impairment in this transgenic mouse model as well as a decrease in neurotoxicity and an increase in hippocampal neurogenesis.⁴⁰⁷ Part of this activity could be explained by the inhibition of the proteolytic processing of amyloid precursor protein to A β peptide. In addition to affecting A β generation and plaque formation, the ability of hyperforin to upregulate P-gp and thus increase clearance of A β peptide from the brain may also be effective in preventing the onset of Alzheimer's disease.⁴⁰⁸

Deficit of prepulse inhibition is common phenomenon in patients suffering from a variety of neurological disorders including Alzheimer's disease and schizophrenia. Since inhibition of monoamine receptors may be involved in disruption of prepulse inhibition, it is unsurprising that hyperforin caused a significant decrease in rat startle amplitude in the acoustic startle response test.⁴⁰⁹ Given its effects on prepulse inhibition, hyperforin may exacerbate the symptoms of several mental disorders.

Both garcinol and hyperforin have been evaluated for their effects on the acquisition of new memories. Treatment of mice and rats with the sodium salt of hyperforin (1.25 mg/kg/day) for 7 days caused significant increases in learned responses in the conditioned avoidance test.⁴¹⁰ After 9 days

⁴⁰⁵ Dinamarca, M. C.; Arrázola, M.; Toledo, E.; Cerpa, W. F.; Hancke, J.; Inestrosa, N. C. *Chem.-Biol. Interact.* **2008**, *175*, 142-149.

⁴⁰⁶ Carvajal, F. J.; Zolezzi, J. M.; Tapia-Rojas, C.; Godoy, J. A.; Inestrosa, N. C. *J. Alzheimer's Dis.* **2013**, *36*, 99-118.

⁴⁰⁷ (a) Cerpa, W.; Hancke, J. L.; Morazzoni, P.; Bombardelli, E.; Riva, A.; Marin, P. P.; Inestrosa, N. C. *Curr. Alzheimer Res.* **2010**, *7*, 126-133. (b) Inestrosa, N. C.; Tapia-Rojas, C.; Griffith, T. N.; Cavajal, F. J.; Benito, M. J.; Rivera-Dictter, A.; Alvarez, A. R.; Serrano, F. G.; Hancke, J. L.; Burgos, P. V.; Parodi, J.; Varela-Nallar, L. *Transl. Psychiatry* **2011**, *1*, e20. (c) Abbott, A. C.; Toledo, C. C.; Aranguiz, F. C.; Inestrosa, N. C. *J. Alzheimer's Dis.* **2013**, *34*, 873-885.

⁴⁰⁸ Abuznait, A. H.; Cain, C.; Ingram, D.; Burk, D.; Kaddoumi, A. *J. Pharm. Pharmacol.* **2011**, *63*, 1111-1118.

⁴⁰⁹ (a) Tadros, M. G.; Mohamed, M. R.; Youssef, A. M.; Sabry, G. M.; Sabry, N. A.; Khalifa, A. E. *Behav. Brain Res.* **2009**, *199*, 334-339. (b) Tadros, M. G.; Mohamed, M. R.; Youssef, A. M.; Sabry, G. M.; Sabry, N. A.; Khalifa, A. E. *J. Ethnopharmacol.* **2009**, *122*, 561-566.

⁴¹⁰ Klusa, V.; Germane, S.; Nöldner, M.; Chatterjee, S. S. *Pharmacopsychiatry* **2001**, *34* (Suppl. 1), 61-69.

following the last dose of hyperforin, the learned response was retained in the animals. Hyperforin also showed improvement after a single dose in the passive avoidance test and reversed scopolamine-induced amnesia. In another study, direct injection of garcinol into the rat lateral amygdala immediately following fear conditioning reduced the consolidation of the Pavlovian fear memory.⁴¹¹ Similarly, garcinol also prevented the reconsolidation of a fear memory following fear memory retrieval. This property of garcinol may be useful for the treatment of post-traumatic stress disorder.

Hyperforin has also been evaluated for the treatment of other neurological conditions. When rats were injected with hyperforin (10 mg/kg) once a day for 7 days, they showed significantly less aggression across four behavioral models: foot shock-induced aggression, isolation-induced aggression, resident-intruder aggression, and the water competition test.⁴¹² In a study in which rats were given access to alcohol, injection of SJW extracts containing hyperforin caused a reduction of ethanol consumption that was proportional to the amount of hyperforin in the extracts.⁴¹³ Similar dose-dependent results were found using a breed of mice that preferred alcohol.⁴¹⁴ These effects may be due hyperforin-based *N*-methyl-D-aspartate-induced (NMDA) antagonism. NMDA receptors overactivity has been noted in alcohol withdrawal, often causing agitation and seizures in some cases.⁴¹⁵ Hyperforin (at a 10 μ M concentration) inhibited NMDA-induced Ca^{2+} influx in isolated rat cortical neurons and blocked the NMDA receptor-induced release of phospholipid-based choline in rat hippocampal slices.⁴¹⁶ These effects may contribute to apparent reduction alcohol consumption observed with hyperforin treatment.

⁴¹¹ Maddox, S. A.; Watts, C. S.; Doyère, V.; Schafe, G. E. *PLoS ONE* **2013**, 8, e54463.

⁴¹² Kumar, N.; Husain, G. M.; Singh, P. N.; Kumar, V. *Drug Discov. Ther.* **2009**, 3, 162-167.

⁴¹³ Perfumi, M.; Panocka, I.; Ciccocioppo, R.; Vitali, D.; Frolidi, R.; Massi, M. *Alcohol Alcoholism* **2001**, 36, 199-206.

⁴¹⁴ Wright, C. W.; Gotti, M.; Grayson, B.; Hanna, M.; Smith, A. G.; Sunter, A.; Neill, J. C. *J. Psychopharmacol.* **2003**, 17, 403-408.

⁴¹⁵ Grant, K. A.; Valverius, P.; Hudspeth, M.; Tabakoff, B. *Eur. J. Pharmacol.* **1990**, 176, 289-296.

⁴¹⁶ Kumar, V.; Mdzinarischvili A.; Kiewert, C.; Abbruscato, T.; Bickel, U.; van der Schyf, C. J.; Klein, J. J. *Pharmacol. Sci.* **2006**, 102, 47-54.

In addition to hyperforin, garcinol and guttiferone have displayed neuroprotective effects. Garcinol has been shown to promote the development of neurons.⁴¹⁷ Cortical progenitor cells taken from embryonic rats developed into neurospheres upon treatment of garcinol, and this may be facilitated by Ca^{2+} entry through the extracellular signal-regulated kinase pathway, which also promoted neuronal survival. The neuroprotective effects of guttiferone A are most likely derived from its ability to scavenge free radicals. Incubation of PC12 cells with guttiferone A garnered protection from Fe^{3+} auto-oxidation⁴¹⁸ as well as from various reactive oxygen species.¹⁴²

Given its ability to inhibit neurotransmitter reuptake by neurons, hyperforin has also been evaluated for its effects on neuroendocrine response. Injection of 9.3 mg/kg hyperforin into rats increased plasma corticosterone, and lowered haloperidol-induced plasma prolactin levels.⁴¹⁹ Since ketanserin but not WAY-100635 inhibited hyperforin-induced plasma corticosterone effects, 5-HT₂ receptors may be involved in this response. A small-scale, single-blind study involving 12 healthy volunteers found that a hyperforin-enriched SJW extract (at 600, 900, and 1200 mg/kg daily oral dosing over 4 days) stimulated adrenocorticotrophic hormone, while cortisol and prolactin levels remained unaffected.⁴²⁰ Several patients experienced an increase in growth hormone release, but this effect was not statistically significant compared to placebo.

The analgesic properties of several PPAPs have also been evaluated. Through analyzing the components of SJW extracts individually, it was discovered that both hypericin and hyperforin displayed antinociceptive properties in murine models of neuropathic pain.⁴²¹ Hyperforin was particularly effective

⁴¹⁷ Weng, M.-S.; Liao, C.-H.; Yu, S.-Y.; Lin, J.-K. *J. Agric. Food Chem.* **2011**, *59*, 1031-1040.

⁴¹⁸ Figueredo, Y. N.; García-Pupo, L.; Cuesta Rubio, O.; Hernández, R. D.; Naal, Z.; Curti, C.; Andreu, G. L. P. *J. Pharmacol. Sci.* **2011**, *116*, 36-46.

⁴¹⁹ Franklin, M.; Chi, J. D.; Mannel, M.; Cowen, P. J. *J. Psychopharmacol.* **2000**, *14*, 360-363.

⁴²⁰ Schüle, C.; Baghai, T.; Sauer, N.; Laakmann, G. *Neuropsychobiology* **2004**, *49*, 58-63.

⁴²¹ (a) Galeotti, N.; Vivoli, E.; Bilia, A. R.; Vincieri, F. F.; Ghelardini, C. *Biochem. Pharmacol.* **2010**, *79*, 1327-1336. (b) Galeotti, N.; Vivoli, E.; Bilia, A. R.; Bergonzi, M. C.; Bartolini, A.; Ghelardini, C. *J. Pain* **2010**, *11*, 149-159.

at the prevention of thermally induced pain. This pain inhibition was abolished by the addition of naloxone, indicating hyperforin's effects are most likely opioid-dependent. The analgesic effects of 7-*epi*-clusianone were not limited to thermally induced pain in mouse models, imparting antinociceptive effects in tests including acetic acid-induced writhing, hot plate exposure, the formalin subplantar injection.¹⁷⁷ In the acetic acid-induced writhing model, guttiferone A dose-dependently reduced abdominal constrictions with an EC₅₀ value of 4.5 mg/kg.⁴²²

Other Bioactivity

As the popularity of SJW extracts grew in the late 1990's, several instances of alarming side effects were reported.⁴²³ By the end of 1999, more than 8 reported cases suggested that SJW extracts may cause increased hepatic metabolism of prescribed medication.⁴²⁴ In particular, women consuming SJW extracts experienced a significant decrease in co-medicated theophylline, cyclosporin, warfarin, and ethinylestradiol.⁴²⁵ A subsequent study conducted by the NIH in 16 healthy volunteers found that SJW extract caused a decrease in indinavir,⁴²⁶ and two German heart transplant patients suffered acute transplant rejection due to SJW extract-accelerated cyclosporine metabolism.⁴²⁷ These alarming

⁴²² Dal Molin, M. M.; Silva, S.; Alves, D. R.; Quintão, N. L. M.; Delle Monache, F.; Filho, V. C.; Niero, R. *Arch. Pharm. Res.* **2012**, *35*, 623-631.

⁴²³ For reviews of SJW herb-drug interactions, see: (a) Henderson, L.; Yue, Q. Y.; Bergquist, C.; Gerden, B.; Arlett, P. *Br. J. Clin. Pharmacol.* **2002**, *54*, 349-356. Rund, D. *Leukemia Lymphoma* **2007**, *48*, 1470-1471. (c) Borrelli, F.; Izzo, A. A. *AAPS J.* **2009**, *11*, 710-727. (d) Rahimi, R.; Abdollahi, M. *Expert Opin. Drug Metab. Toxicol.* **2012**, *8*, 691-708.

⁴²⁴ Ernst, E. *Lancet* **1999**, *354*, 2014-2016.

⁴²⁵ (a) Rey, J. M. *Med. J. Aust.* **1998**, *169*, 583-586. (b) Stevinson, C.; Ernst, E. *CNS Drugs* **1999**, *11*, 125-132. (c) Nebel, A.; Schneider, B. J.; Baker, R. K.; Kroll, D. J. *Ann. Pharmacother.* **1999**, *33*, 502-506.

⁴²⁶ Piscitelli, S. C.; Burnstein, A. H.; Alfaro, R. M.; Chaïtt, D.; Falloon, J. *Lancet* **2000**, *355*, 547-548.

⁴²⁷ Ruschitzka, F.; Lüscher, T. F.; Noll, G.; Meier, P. J.; Turina, M. *Lancet* **2000**, *355*, 548-549.

observations led the FDA to issue a public healthy advisory⁴²⁸ and the British Medicines Control Agency to issue a reminder to doctors.⁴²⁹

It was soon discovered independently by two different groups that hyperforin is the component of SJW that potently activates pregnane X receptor (PXR, steroid X receptor).⁴³⁰ PXR is a transcription factor that serves as a key regulator of many enzymes involved in xenobiotic metabolism, such as cytochrome P450s and P-gp. It contains a DNA-binding domain and a ligand-binding domain, the latter of which is substantially flexible and allows for the binding of structurally diverse compounds (i.e., xenobiotics). For instance, the compound SR12813 binds to PXR in three distinct orientations.⁴³¹ With an EC₅₀ value of 23 nM, hyperforin is the most potent PXR activator discovered.^{430b} Using tritiated SR12813 in a competition binding assay, it was also discovered that hyperforin binds directly to PXR. A resolved crystal structure of hyperforin bound to PXR provided unambiguous proof of direct interaction (Figure 1.16a).⁴³² Compared to an earlier crystal structure of the ligand-binding domain of PXR in its *apo* form, hyperforin caused a 250 Å³ increase in binding site volume. In addition, most of the contacts hyperforin makes to PXR are through hydrophobic interactions of its prenyl side-chains (Figure 1.16b).

⁴²⁸ (a) Lumpkin, M. M.; Alpert, S. *Public Health Advisory*; U.S. Food and Drug Administration, February 10, 2000. (b) Henney, J. E. *J. Am. Med. Assoc.* **2000**, 283, 1679-1679.

⁴²⁹ Committee on Safety of Medicines, Medicines Control Agency, *Curr. Prob. Pharmacovigilance* **2000**, 26, 6-7.

⁴³⁰ (a) Wentworth, J. M.; Agostini, M.; Love, J.; Schwabe, J. W.; Chatterjee, V. K. K. *J. Endocrinol.* **2000**, 166, R11-R16. (b) Moore, L. B.; Goodwin, B.; Jones, S. A.; Wisely, G. B.; Serabjit-Singh, C. J.; Willson, T. M.; Collins, J. L.; Kliewer, S. A. *Proc. Natl. Acad. Sci. USA* **2000**, 97, 7500-7502.

⁴³¹ Watkins, R. E.; Wisely, G. B.; Moore, L. B.; Collins, J. L.; Lambert, M. H.; Williams, S. P.; Willson, T. M.; Kliewer, S. A.; Rebindo, M. R. *Science* **2001**, 292, 2329-2333.

⁴³² Watkins, R. E.; Maglich, J. M.; Moore, L. B.; Wisely, G. B.; Noble, S. M.; Davis-Searles, P. R.; Lambert, M. H.; Kliewer, S. A.; Rebindo, M. R. *Biochemistry* **2003**, 42, 1430-1438.

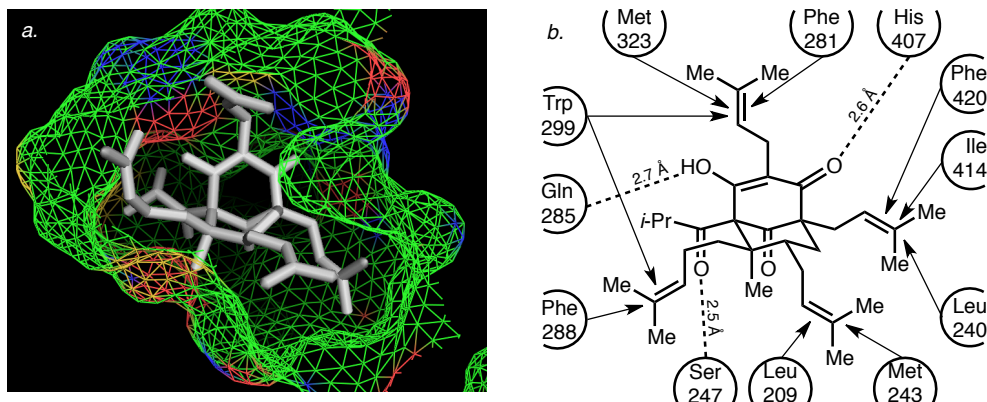


Figure 1.16. (a) Detail of hyperforin bound to the ligand-binding domain of PXR and (b) schematic highlighting the contacts between hyperforin and PXR (solid lines indicate nonpolar contacts, and dotted lines indicate hydrogen bonding).

Further, hyperforin-induced PXR activation directly results in the upregulation of genes involved in xenobiotic metabolism and drug efflux. Treatment of primary human hepatocytes with hyperforin induced increased *CYP3A4* expression.^{430b} *CYP2C9* induction was also noted in the hyperforin treatment of HepG2 cells.⁴³³ The increased expression of these cytochrome P450s is significant since *CYP3A4* and *CYP2C9* are responsible for the metabolism of approximately 50% and 20% of all known drugs, respectively.⁴³⁴ While *CYP3A4* and *CYP2C8* expression did increase upon hyperforin exposure in primary human hepatocytes,⁴³⁵ *CYP24A1* and *CYP27B1* levels remained unchanged.⁴³⁶ In another study, *CYP1A1*, *CYP1A2*, and gene for the monooxygenase *FMO5* were upregulated in HepG2 cells, while *CYP4F2* and *NQO2* were downregulated.⁴³⁷ Hyperforin also caused tissue-specific activation of the ATP-binding cassette transporters, which play important roles in controlling the passage of drugs and xenobiotics

⁴³³ Chen, Y.; Ferguson, S. S.; Negishi, M.; Goldstein, J. A. *J. Pharmacol. Exp. Ther.* **2004**, *308*, 495-501.

⁴³⁴ Zanger, U. M.; Schwab, M. *Pharmacol. Therapeut.* **2013**, *138*, 103-141.

⁴³⁵ Komoroski, B. J.; Parise, R. A.; Egorin, M. J.; Strom, S. C.; Venkataramanan, R. *Clin. Cancer Res.* **2005**, *11*, 6972-6979.

⁴³⁶ Wang, Z.; Lin, Y. S.; Dickmann, L. J.; Poulton, E.-J.; Eaton, D. L.; Lampe, J. W.; Shen, D. D.; Davis, C. L.; Shuhart, M. C.; Thummel, K. E. *J. Bone Miner. Res.* **2013**, *28*, 1101-1116.

⁴³⁷ Krusekopf, S.; Roots, I. *Pharmacogenet. Genom.* **2005**, *15*, 817-829.

across intracellular and extracellular membranes. Using porcine brain capillary endothelial cells (PBCECs) as a model for the blood-brain barrier in humans, hyperforin treatment caused significant increases in mRNA levels for P-gp⁴³⁸ and both ABCG1 and 2.⁴³⁹ P-gp expression also significantly increased in LS180⁴⁴⁰ and T84⁴⁴¹ cells, demonstrating that hyperforin may accelerate the excretion of drugs. Interestingly, while hyperforin caused upregulation of CYP3A4 in Caco-2 cells, P-gp expression actually decreased.⁴⁴² Aside from regulating xenobiotic metabolism, PXR may also play a role in other areas of human health. Hyperforin-induced PXR activation may prevent liver steatosis, given that hyperforin treatment of HepG2 cells overexpressing PXR exacerbated steatogenic effects in these cells.⁴⁴³ PXR may be important in bone homeostasis and thus prevent osteoporosis; treatment of primary osteocytes with vitamin K₂ or hyperforin activated PXR and led to an increase in bone marker expression.⁴⁴⁴ However, chronic activation of PXR may lead to osteomalacia via increased CYP24A1 expression, leading to vitamin D deficiency.⁴⁴⁵

It is also important to note that activation of PXR is species-specific. As mentioned previously, porcine PXR is hyperforin-sensitive.⁴³⁸ It is unclear whether mouse PXR is a hyperforin target. One study found that hyperforin did not induce cytochrome P450 expression in Swiss Webster mice,⁴⁴⁶ but another study found that hyperforin·HNCy₂ increased CYP3A-mediated hepatic erythromycin-*N*-

⁴³⁸ Ott, M.; Fricker, G.; Bauer, B. *J. Pharmacol. Exp. Ther.* **2009**, *329*, 141-149.

⁴³⁹ Lemmen, J.; Tozakidis, I. E. P.; Galla, H.-J. *Brain Res.* **2013**, *1491*, 1-13.

⁴⁴⁰ Tian, R.; Kobayashi, N.; Morimoto, S.; Shoyama, Y.; Ohtani, H.; Sawada, Y. *Drug Metab. Dispos.* **2005**, *33*, 547-554.

⁴⁴¹ Haslam, I. S.; Jones, K.; Coleman, T.; Simmons, N. L. *Biochem. Pharmacol.* **2008**, *76*, 850-861.

⁴⁴² Patel, J.; Buddha, B.; Dey, S.; Pal, D.; Mitra, A. K. *Am. J. Ther.* **2004**, *11*, 262-277.

⁴⁴³ Moya, M.; Gómez-Lechón, M. J.; Castell, J. V.; Jover, R. *Chem.-Biol. Interact.* **2010**, *184*, 376-387.

⁴⁴⁴ Tabb, M. M.; Sun, A.; Zhou, C.; Grün, F.; Errandi, J.; Romero, K.; Pham, H.; Inoue, S.; Mallick, S.; Lin, M.; Forman, B. M.; Blumberg, B. *J. Biol. Chem.* **2003**, *278*, 43919-43927.

⁴⁴⁵ Pascussi, J. M.; Robert, A.; Nguyen, M.; Walrant-Debray, O.; Garabedian, M.; Martin, P.; Pineau, T.; Saric, J.; Navarro, F.; Maurel, P.; Vilarem, M. J. *J. Clin. Invest.* **2005**, *115*, 177-186.

⁴⁴⁶ Bray, B. J.; Brennan, N. J.; Perry, N. B.; Menkes, D. B.; Rosengren, R. J. *Life Sci.* **2002**, *70*, 1325-1335.

demethylase activity in CD-1 mice.⁴⁴⁷ The cynomolgus monkey (i.e., crab-eating macaque) response to hyperforin is very similar to that of humans, making this species an effective animal model for predicting downstream metabolic enzyme induction via PXR activation.⁴⁴⁸ Unlike mouse PXR, rat PXR is unambiguously unaffected by hyperforin exposure.⁴⁴⁹ In order to study which residues in rat PXR confer hyperforin insensitivity, a variety of rat-human PXR cDNA chimeras were prepared.⁴⁵⁰ Rat PXR hyperforin sensitivity was conferred by converting Phe305 to leucine, and human PXR was rendered hyperforin insensitive via mutagenesis of Leu308 to phenylalanine.

Further evidence for hyperforin activation of xenobiotic metabolism was provided through a variety of drug-specific, small-scale clinical trials involving SJW extracts containing variable amounts of the PPAP. In a study involving 10 renal transplant patients, only those that took SJW extracts with significant hyperforin experienced a cyclosporine drug interaction.⁴⁵¹ Similar herb-drug interactions were encountered in studies involving healthy volunteers taking digoxin,^{452,453} theophylline,⁴⁵⁴ alprazolam,⁴⁵³ caffeine,⁴⁵³ tolbutamide,⁴⁵³ midazolam,⁴⁵⁵ ethinylestradiol,⁴⁵⁶ and 3-ketodesogestrel.⁴⁵⁶ SJW extracts with little to no hyperforin content failed to increase cytochrome P450 expression in several studies.⁴⁵⁷

⁴⁴⁷ Cantoni, L.; Rozio, M.; Mangolini, A.; Hauri, L.; Caccia, S. *Toxicol. Sci.* **2003**, *75*, 25-30.

⁴⁴⁸ Kim, S.; Dinchuk, J. E.; Anthony, M. N.; Orcutt, T.; Zoekler, M. E.; Sauer, M. B.; Mosure, K. W.; Vuppugalla, R.; Grace, J. E., Jr.; Simmermacher, J.; Dulac, H. A.; Pizzano, J.; Sinz, M. *Drug Metab. Dispos.* **2010**, *38*, 16-24.

⁴⁴⁹ Nöldner, M.; Chatterjee, S. *Pharmacopsychiatry* **2001**, *34* (Suppl. 1), 108-110.

⁴⁵⁰ Tirona, R. G.; Leake, B. F.; Podust, L. M.; Kim, R. B. *Molec. Pharmacol.* **2004**, *65*, 36-44.

⁴⁵¹ Mai, I.; Bauer, S.; Perloff, E. S.; Johne, A.; Uehleke, B.; Frank, B.; Budde, K.; Roots, I. *Clin. Pharmacol. Ther.* **2004**, *76*, 330-340.

⁴⁵² Mueller, S. C.; Uehleke, B.; Woehling, H.; Petzsch, M.; Majcher-Peszynska, J.; Hehl, E.-M.; Sievers, H.; Frank, B.; Riethling, A.-K.; Drewelow, B. *Clin. Pharmacol. Ther.* **2004**, *75*, 546-557.

⁴⁵³ Arold, G.; Donath, F.; Maurer, A.; Diefenbach, K.; Bauer, S.; Henneicke-von Zepelin, H.-H.; Friede, M.; Roots, I. *Planta Med.* **2005**, *71*, 331-337.

⁴⁵⁴ Morimoto, T.; Kotegawa, T.; Tsutsumi, K.; Ohtani, Y.; Imai, H.; Nakano, S. *J. Clin. Pharmacol.* **2004**, *44*, 95-101.

⁴⁵⁵ Mueller, S. C.; Majcher-Peszynska, J.; Uehleke, B.; Klammt, S.; Mundkowski, R. G.; Miekisch, W.; Sievers, H.; Bauer, S.; Frank, B.; Kundt, G.; Drewelow, B. *Eur. J. Clin. Pharmacol.* **2006**, *62*, 29-36.

Apart from hyperforin, the binding affinity of other PPAPs to PXR has not been explored. The only other PPAP reported to interact with a nuclear receptor is guttiferone G.⁴⁵⁸ Guttiferone G preferentially binds to the liver X receptor α isoform (LXR- α) with an IC_{50} value of 3.4 μ M, having little to no interaction with LXR- β ($IC_{50} > 15 \mu$ M). Since LXRs play important roles in cholesterol homeostasis, guttiferone G may be a lead structure in the development of cholesterol regulation therapy.

Aside from increasing their expression levels via PXR activation, hyperforin appears to inhibit several proteins involved in xenobiotic metabolism. An early study found that hyperforin noncompetitively inhibited CYP2D6 with a K_i of 1.5 μ M and competitively inhibited CYP3A4 ($K_i = 0.48 \mu$ M) and CYP2C9 ($K_i = 1.8 \mu$ M) in *in vitro* binding assays.⁴⁵⁹ Hyperforin also potently inhibited cDNA-expressed CYP1A2, CYP2C9, and CYP2C19 with IC_{50} values of 3.9, 0.01, and 0.02 μ M, respectively.⁴⁶⁰ CYP1A1 was also inhibited by hyperforin ($K_i = 1.1 \mu$ M, $IC_{50} = 1.2 \mu$ M), and this was demonstrated by the prevention of the carcinogen formation from CYP1A1-mediated benzo[*a*]pyrene-7,8-dihydrodiol epoxidation.⁴⁶¹ While hyperforin inhibited CYP3A4 with an IC_{50} value of 0.63 μ M, three of its naturally occurring analogs were found to be more potent inhibitors of the cytochrome P450 isoform (IC_{50} values in parentheses): furoadhyperforin (0.072 μ M), furohyperforin isomer 1 (0.079 μ M), furohyperforin isomer 2 (0.23 μ M).⁴⁶² Furohyperforin was also found to inhibit CYP3A4 with an IC_{50} value of 1.3 μ M. P-gp activity was also moderately inhibited by hyperforin ($IC_{50} = 30 \mu$ M), ascertained by monitoring the active

⁴⁵⁶ Will-Shahab, L.; Bauer, S.; Kunter, U.; Roots, I.; Brattström, A. *Eur. J. Clin. Pharmacol.* **2009**, *65*, 287-294.

⁴⁵⁷ (a) Gödtel-Armbrust, U.; Metzger, A.; Kroll, U.; Kelber, O.; Wojnowski, L. *Naunyn-Schmied. Arch. Pharmacol.* **2007**, *375*, 377-382. (b) Mueller, S. C.; Majcher-Peszynska, J.; Mundkowski, R. G.; Uehleke, B.; Klammt, S.; Sievers, H.; Lehnfeld, R.; Frank, B.; Thurow, K.; Kundt, G.; Drewelow, B. *Eur. J. Clin. Pharmacol.* **2009**, *65*, 81-87.

⁴⁵⁸ Herath, K.; Jayasuriya, H.; Ondeyka, J. G.; Guan, Z.; Borris, R. P.; Stijfhoorn, E.; Stevenson, D.; Wang, J.; Sharma, N.; MacNaul, K.; Menke, J. G.; Ali, A.; Schulman, M. J.; Singh, S. B. *J. Nat. Prod.* **2005**, *68*, 617-619.

⁴⁵⁹ Obach, R. S. *J. Pharmacol. Exp. Ther.* **2000**, *294*, 88-95.

⁴⁶⁰ Zou, L.; Harkey, M. R.; Henderson, G. L. *Life Sci.* **2002**, *71*, 1579-1589.

⁴⁶¹ Schwarz, D.; Kisselev, P.; Roots, I. *Cancer Res.* **2003**, *63*, 8062-8068.

⁴⁶² Lee, J.-y.; Duke, R. K.; Tran, V. H.; Hook, J. M.; Duke, C. C. *Phytochemistry* **2006**, *67*, 2550-2560.

efflux of daunorubicin from NIH-3T3 cells expressing P-gp.⁴⁶³ P-gp and ABCG2 inhibition was also observed in leukemia cell lines.⁴⁶⁴ Using PBCECs and freshly isolated porcine brain capillaries as models for the blood-brain barrier, hyperforin was found to directly inhibit P-gp activity.⁴⁶⁵ Hyperforin also partially inhibited paclitaxel efflux from xenopus oocytes expressing the liver-specific organic anion transporting polypeptide isoform 1B3.⁴⁶⁶

Several preclinical and small-scale clinical trials were performed to determine hyperforin's pharmacokinetic profile in various orally available forms.⁴⁶⁷ This is particularly intriguing considering that hyperforin on one hand activates PXR and on the other inhibits various cytochrome P450s. In rats given a SJW extract containing 5% hyperforin (300 mg/kg) orally, hyperforin plasma levels reached a maximum of 370 ng/mL (approximately 690 nM) after a single dose.⁴⁶⁸ After dosing either an extract containing 4.5% or with pure hyperforin-HNCy₂ once a day for 12 days in mice, plasma concentrations of hyperforin were significantly lower than after a single dose.⁴⁶⁷ These data are unsurprising given the fact that hyperforin may increase xenobiotic metabolism through activation of PXR in mice. When a 5% hyperforin extract was co-medicated with the CYP3A4 inhibitor ritonavir (20 mg/kg) in mice, a significant increase in hyperforin bioavailability was observed.⁴⁶⁷ Co-medication with the P-gp inhibitor valspodar did not have any effect on hyperforin *AUC*. Another study established that hyperforin does indeed cross the blood-brain barrier in mice.^{469,470} While treatment with the purified sodium salt of

⁴⁶³ Wang, E.-j.; Barecki-Roach, M.; Johnson, W. W. *J. Pharm. Pharmacol.* **2004**, *56*, 123-128.

⁴⁶⁴ (a) Weber, C. C.; Kressmann, S.; Fricker, G.; Müller, W. E. *Pharmacopsychiatry* **2004**, *37*, 292-298. (b) Quiney, C.; Billard, C.; Faussat, A.-M.; Salanoubat, C.; Kolb, J.-P. *Leukemia Lymphoma* **2007**, *48*, 1587-1599.

⁴⁶⁵ Ott, M.; Huls, M.; Cornelius, M. G.; Fricker, G. *Pharm. Res.* **2010**, *27*, 811-822.

⁴⁶⁶ Smith, N. F.; Acharya, M. R.; Desai, N.; Figg, W. D.; Sparreboom, A. *Cancer Biol. Ther.* **2005**, *4*, 815-818.

⁴⁶⁷ For an overview of hyperforin pharmacokinetics, see: Caccia, S. *Curr. Drug Metab.* **2005**, *6*, 531-543.

⁴⁶⁸ Biber, A.; Fischer, H.; Römer, A.; Chatterjee, S. S. *Pharmacopsychiatry* **1998**, *31* (Suppl.), 36-43.

⁴⁶⁹ Keller, J.-H.; Karas, M.; Müller, W. E.; Volmer, D. A.; Eckert, G. P.; Tawab, M. A.; Blume, H. H.; Dingeramn, T.; Schubert-Zsilavecz, M. *Anal. Chem.* **2003**, *75*, 6084-6088.

hyperforin (15 mg/kg) produced a 28.8 ng/g brain concentration, treatment with 300 mg/kg SJW extract containing 5% hyperforin only gave a 15.8 ng/g concentration. Hyperforin rat brain concentrations were increased through co-medication with borneol or through electroacupuncture, two techniques that have shown some positive results in increasing blood-brain barrier permeability.⁴⁷¹

Hyperforin pharmacokinetics have been determined in humans through various small-scale studies, and the results of several single- and multiple-dose studies involving various SJW ethanolic extract preparations are shown in Table 1.17. A large degree of pharmacokinetic parameter variation is observed, and this is in part due to the variable nature of the extracts and inherent metabolite ratios as well as inter-individual differences in response to treatment. In general, C_{max} is rapidly attained within 3-4 hours and follows a linear relationship to the amount of hyperforin administered in single-dose studies. Overall, hyperforin plasma concentrations peaked in the range of 0.16-0.81 M. Single-dose AUC also follows a linear relationship up to about 40 mg hyperforin, and at higher concentrations, lower than expected bioavailability is observed. Elimination half-life remained fairly consistent across dosing regimens.

⁴⁷⁰ For an overview of murine brain hyperforin pharmacokinetics, see: Caccia, S.; Gobbi, M. *Curr. Drug Metab.* **2009**, *10*, 1055-1065.

⁴⁷¹ Yu, B.; Ruan, M.; Sun, Y.; Cui, X.; Yu, Y.; Wang, L.; Fang, T. *Neural Regen. Res.* **2011**, *6*, 1876-1882.

Table 1.17. Hyperforin pharmacokinetics following oral dosing of SJW extracts.^a

Extract dose (mg x day)	Participants ^b	Hyperforin per dose (mg)	<i>t</i> _{max} (h)	<i>C</i> _{max} (ng/mL)	<i>AUC</i> (ng/mL·h)	<i>t</i> _{1/2} (h)	References
600 x 1	18 M	13.5	4.4 (1.5)	84 (28)	1009 (203)	19.6 (6.3)	472
600 x 14	18 M	13.5	4.3 (1.0)	97 (30)	826 (176)	4.3 (1.0)	472
300 x 1	6 M	14.8	3.6 (0.6)	153 (21)	1336 (145)	9.5 (1.1)	468
300 x 1	6 M, 6 F	15	3.1 (0.8)	84 (36)	586 (240)	n.d.	473
300 ^c x 1	6 M, 6 F	15	2.5 (0.8)	168 (58)	1483 (897)	n.d.	473
900 x 1	18 M	17.2	4.5 (1.2)	122 (46)	1550 (371)	17.5 (4.5)	474
900 x 14	18 M	17.2	3.9 (1.3)	87 (37)	769 (235)	n.d.	474
600 x 1	6 M	28.6	3.5 (0.3)	302 (47)	2215 (279)	8.5 (0.7)	468
900 x 1	7 M, 2 F	42.8	2.9 (0.3)	300 (23)	3352 (329)	7.2 (0.3)	468
900 x 8	7 M, 2 F	42.8	3.1 (0.4)	246 (22)	2336 (303)	11.2 (1.0)	468
900 x 1	3 M, 9 F ^d	55.1	4.0 (n.d.)	1500 (200)	13600 (2400)	16.6 (1.9)	475
900 x 14 ^e	3 M, 9 F ^d	55.1	3.0 (n.d.)	1300 (200)	10900 (2200)	14.7 (2.2)	475
1200 x 1	6 M	59.2	2.8 (0.3)	437 (101)	3378 (670)	9.7 (0.8)	468

^a Pharmacokinetic data are reported as means (± standard error).

^b Listed are the number of male (M) and female (F) participants. Unless noted, all participants were healthy volunteers.

^c A softgel capsule formulation was used.

^d Patients in these studies were diagnosed with clinical depression prior to treatment. See text below.

^e The SJW extract was co-medicated with the antidepressant amitriptyline (75 mg twice daily).

While most of the data presented in Table 1.17 is derived from studies involving healthy volunteers, one study utilized patients suffering from clinical depression, with initial scores ranging from 10-34 in the Hamilton Rating Scale for Depression.⁴⁷⁵ Intriguingly, hyperforin exposure was significantly higher for these patients than in healthy patients consuming similar amounts of hyperforin. Formulation of the SJW extract also appears to have an effect on oral bioavailability; a softgel capsule formulation led to significant increases in *C*_{max} and *AUC* when directly compared to a traditional two-piece hard gelatin capsule.⁴⁷³

⁴⁷² Schulz, H.-U.; Schürer, M.; Bässler, D.; Weiser, D. *Arzneimittel-Forsch.* **2005**, *55*, 15-22.

⁴⁷³ Agrosí, M.; Mischiatti, S.; Harrasser, P. C.; Savio, D. *Phytomedicine* **2000**, *7*, 455-462.

⁴⁷⁴ Schulz, H.-U.; Schürer, M.; Bässler, D.; Weiser, D. *Arzneimittel-Forsch.* **2005**, *55*, 561-568.

⁴⁷⁵ Johne, A.; Schmider, J.; Brockmöller, J.; Stadelmann, A. M.; Störmer, E.; Bauer, S.; Scholler, G.; Langheinrich, M.; Roots, I. *J. Clin. Psychopharmacol.* **2002**, *22*, 46-54.

Multiple-dose hyperforin pharmacokinetics were also investigated.^{468,472,474} In all three instances, significantly lower *AUC* at the end of the treatment regimen was observed and can be explained by hyperforin's ability to activate PXR and thus upregulate xenobiotic metabolism. Similar results were observed upon co-medication of amitriptyline with hyperforin; aside from decreased amitriptyline plasma concentrations, the concentrations of all hydroxylated metabolites of amitriptyline decreased significantly, indicating increased drug efflux.⁴⁷⁵ A study involving five mothers taking SJW extract daily (containing 22.4 mg hyperforin) demonstrated that hyperforin is present in breast milk, but at low levels.⁴⁷⁶ In two breastfed infants, the plasma concentration of hyperforin was present, albeit at the lowest limit of detection (0.1 ng/mL).

The only other PPAP to have undergone pharmacological studies is xanthochymol.⁷⁶ Doses of 1.0-10.0 mg/kg given to anesthetized cats did not lead to cardiovascular side effects. In mice, the LD₅₀ of xanthochymol was determined to be 1000 mg/kg, and no detrimental nervous system effects were observed at one-fifth the LD₅₀.

The packaging and unpackaging of eukaryotic DNA around histones largely determines the extent to which genes are expressed. Modifications of these histone proteins, such as through acetylation, alter chromatin structure and regulates transcription.⁴⁷⁷ The enzymes responsible for histone acetylation and deacetylation are called histone acetyltransferases (HATs) and histone deacetylases (HDACs), respectively, and alteration of HAT and HDAC activity has been implicated in a variety of diseases, such as cancer and neurodegeneration.⁴⁷⁸ Given the ability of a variety of PPAPs to penetrate cell membranes and perturb a variety of biochemical processes, their ability to modulate HAT/HDAC activity has been

⁴⁷⁶ Klier, C. M.; Schmid-Siegel, B.; Schäfer, M. R.; Lenz, G.; Saria, A.; Lee, A.; Zernig, G. *J. Clin. Psychiatry* **2006**, *67*, 305-309.

⁴⁷⁷ (a) Roth, S. Y.; Denu, J. M.; Allis, C. D. *Annu. Rev. Biochem.* **2001**, *70*, 81-120. (b) Selvi, B. R.; Kundu, T. K. *Biotechnol. J.* **2009**, *4*, 375-390. (c) Huang, J.; Plass, C.; Gerhäuser, C. *Curr. Drug Targets* **2011**, *12*, 1925-1956.

⁴⁷⁸ Lane, A. A.; Chabner, B. A. *J. Clin. Oncol.* **2009**, *27*, 5459-5468.

actively investigated.⁴⁷⁹ Early studies found that hyperforin altered protein expression in hamster smooth muscle cells⁴⁸⁰ and that garcinol altered gene expression in rat livers,⁴⁸¹ implying that these PPAPs may be interacting with epigenetic modulators.

Indeed, garcinol was later found to dose-dependently inhibit two HATs, p300 ($IC_{50} = 7 \mu M$) and PCAF ($IC_{50} = 5 \mu M$) both in *in vitro* assay studies as well as *in vivo* studies involving HeLa cells.⁴⁸² Over a hundred genes were affected in HeLa cells treated with garcinol, and apoptosis was observed. Kinetic analysis revealed that garcinol acted as a competitive inhibitor for both enzymes. However, garcinol also exhibited considerable cytotoxicity. In order to find a HAT inhibition-specific molecular probe, nearly 50 semisynthetic garcinol derivatives were screened for p300 inhibition activity.⁴⁸³ Isogarcinol inhibited p300 activity but was also cytotoxic. Three derivatives of garcinol, **84**, **85**, and **86**, were identified as non-cytotoxic, p300-specific inhibitors with IC_{50} values in the range of 5-7 μM (Figure 1.17). T cells treated with **84** were not only viable but also experienced histone acetylation inhibition after HIV infection, thus preventing viral replication. Subsequent mechanistic studies found that the inhibition of p300 HAT activity by **84** is dissimilar to that of garcinol and isogarcinol.⁴⁸⁴ Using *in silico* docking methods, garcinol and isogarcinol were found to bind p300 in two distinct sites, including the ATP-binding pocket, but **84** bound to a single, allosteric site. These data were supported by experimental isothermal calorimetric data.

⁴⁷⁹ For a review of PPAP HAT chemical biology, see: Dal Piaz, F.; Vassallo, A.; Cuesta Rubio, O.; Castellano, S.; Sbardella, G.; De Tommasi, N. *Mol. Divers.* **2011**, *15*, 401-416.

⁴⁸⁰ Schrattenholz, A.; Schroer, K.; Chatterjee, S. S.; Kock, E. *Planta Med.* **2004**, *70*, 342-346.

⁴⁸¹ Hokaiwado, N.; Asamoto, M.; Tsujimura, K.; Hirota, T.; Ichihara, T.; Satoh, T.; Shirai, T. *Cancer Sci.* **2004**, *95*, 123-130.

⁴⁸² Balasubramanyam, K.; Altaf, M.; Verier, R. A.; Swaminathan, V.; Ravindran, A.; Sadhale, P. P.; Kundu, T. K. *J. Biol. Chem.* **2004**, *279*, 33716-33726.

⁴⁸³ Mantelingu, K.; Reddy, B. A. A.; Swaminathan, V.; Kishore, A. H.; Siddappa, N. B.; Kumar, G. V. P.; Nagashankar, G.; Natesh, N.; Roy, S.; Sadhale, P. P.; Ranga, U.; Narayana, C.; Kundu, T. K. *Chem. Biol.* **2007**, *14*, 645-657.

⁴⁸⁴ Arif, M.; Pradham, S. K.; Thanuja, G. R.; Vedamurthy, B. M.; Agrawal, S.; Dasgupta, D.; Kundu, T. K. *J. Med. Chem.* **2009**, *52*, 267-277.

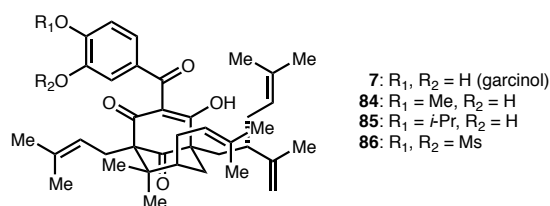


Figure 1.17. Garcinol and several semisynthetic derivatives.

The ability of garcinol to alter gene expression has been applied across several settings relevant to human health. When garcinol was co-administered with the apoptosis-inducing cytokine TRAIL, several cancer cell lines resistant to TRAIL became sensitive.⁴⁸⁵ Garcinol increased expression of death receptors 4 and 5, receptors of TRAIL, and also decreased the expression of various proteins involved in cell survival. In addition, the epigenetic changes mediated by garcinol and **84** in inhibiting MCF-7 cell proliferation were elucidated.⁴⁸⁶ Increased levels of H4K16 acetylation and H4K20 trimethylation accompanied significant reduction in H3K18 acetylation. A major but limited source of hematopoietic stem cells is human cord blood, and when human cord blood cells were treated with either garcinol or isogarcinol in the presence of thrombopoietin, a significant increase in cell proliferation was observed.⁴⁸⁷ This stem cell expansion may be due to the ability of these PPAPs to inhibit HAT activity. In 3T3-L1 preadipocytes, garcinol treatment prevented adipogenesis and lowered expression levels of proteins associated with this differentiation process, including leptin, resistin, and fatty acid synthase.⁴⁸⁸ This epigenetically-induced anti-adipogenic effect of garcinol may be one avenue for the treatment and prevention of obesity.

⁴⁸⁵ Prasad, S.; Ravindran, J.; Sung, B.; Pandey, M. K.; Aggarwal, B. B. *Mol. Cancer Ther.* **2010**, *9*, 856-868.

⁴⁸⁶ Collins, H. M.; Abdelghany, M. K.; Messmer, M.; Yue, B.; Deeves, S. E.; Kindle, K. B.; Mantelingu, K.; Aslam, A.; Winkler, G. S.; Kundu, T. K.; Heery, D. M. *BMC Cancer* **2013**, *13*, 37.

⁴⁸⁷ Nishino, T.; Wang, C.; Mochizuki-Kashio, M.; Osawa, M.; Nakauchi, H.; Iwama, A. *PLoS ONE* **2011**, *6*, e24298.

⁴⁸⁸ Hsu, C.-L.; Lin, Y.-J.; Ho, C.-T.; Yen, G.-C. *Food Funct.* **2012**, *3*, 49-57.

Aside from garcinol and its derivatives, a variety of other PPAPs have been evaluated for HAT and HDAC activity. While garcinielliptone, hyperibone B, propolones A-D, and propolone D peroxide had no significant interaction with p300, guttiferones A and E as well as clusianone inhibited p300 HAT activity with IC₅₀ values in the 5-10 μ M range.⁴⁸⁹ Interestingly, nemorosone was a potent *activator* of p300 HAT activity. Surface plasmon resonance established that guttiferones A and E, clusianone, and nemorosone all interact directly with p300. Aside from modulating HAT activity, oblongifolin C, hyperforin, and the semisynthetic hyperforin derivative aristoforin (**78**) inhibited HDAC activity of sirtuins SIRT1 and SIRT2 (Table 1.18).⁴⁹⁰ Both oblongifolin C and aristoforin were less cytotoxic toward HUVECs than hyperforin.

Table 1.18. Inhibition of sirtuins by oblongifolin C, hyperforin, and aristoforin.⁴⁹⁰

PPAP	SIRT1 IC ₅₀ (μ M)	SIRT2 IC ₅₀ (μ M)
oblongifolin C	9	22
hyperforin	15	28
aristoforin (78)	7	21

Hyperforin has been evaluated for the ability to modulate contractility. Overactive bladder contractions causes a loss of urine control and leads to incontinence. At concentrations as low as 10 μ M, hyperforin inhibited electric field stimulated contractions in isolated rat bladder strips.⁴⁹¹ Naloxone but not neurotransmitter receptor inhibitors and ion channel blockers abrogated the ability of hyperforin to inhibit contractions. This suggests the involvement of opioid receptors. In contrast, at low concentration (10 nM), hyperforin caused a slight increase in carbachol-induced contractions.⁴⁹² Orally dosed hyperforin delayed acetylcholine-induced gastric emptying with an EC₅₀ value of about 1 μ M in a rat

⁴⁸⁹ Dal Piaz, F.; Tosco, A.; Eletto, D.; Piccinelli, A. L.; Moltedo, O.; Franceschelli, S.; Sbardella, G.; Remondelli, P.; Rastrelli, L.; Vesci, L.; Pisano, C.; De Tommasi, N. *ChemBioChem* **2010**, *11*, 818-827.

⁴⁹⁰ Gey, C.; Kyrylenko, S.; Hennig, L.; Nguyen, L.-H. D.; Büttner, A.; Pham, H. D.; Giannis, A. *Angew. Chem. Int. Ed.* **2007**, *46*, 5219-5222.

⁴⁹¹ Capasso, R.; Borrelli, F.; Capasso, F.; Mascolo, N.; Izzo, A. A. *Urology* **2004**, *64*, 168-172.

⁴⁹² Valeri, A.; Capasso, R.; Valoti, M.; Pessina, F. *J. Pharm. Pharmacol.* **2012**, *64*, 1770-1776.

model, which may lead to drug-drug interactions since gastric motility plays an important role in drug uptake.⁴⁹³ Overactive contractions of the vas deferens smooth muscle may lead to premature ejaculation. An early study found that hyperforin, in concentrations as low as 0.6 μ M, inhibited neurotransmitter-induced contractions of hamster vas deferens smooth muscle tissue.³³⁰ Similar inhibition was observed in phenylephrine-induced contractions of both isolated rat and human vas deferens tissue.⁴⁹⁴ A hyperforin-enriched supercritical CO₂ SJW extract was shown to prevent chemically-induced ejaculation acceleration in anesthetized rats, the first instance of hyperforin showing efficacy against premature ejaculation in an animal model.⁴⁹⁵

Synthesis Strategies

Owing to their fascinating biological activity and unique structural features, PPAPs have been popular targets over the past fifteen years, and many strategies have been developed for their synthesis.⁴⁹⁶ Several salient features of PPAP structure apropos to bond construction are summarized in Scheme 1.13. All PPAPs contain a heavily substituted bicyclo[3.3.1]nonane core in which one component carbocycle is highly oxygenated and the other carbocycle contains stereochemically-rich functionalization. In particular, a synthetically challenging C7–C8–C1 stereoarray includes contiguous quaternary centers. All studies toward PPAP total synthesis may be broken down into two general strategic camps: (1) a “bottom-up” approach and (2) a “top-down” approach. Bottom-up tactics rely on the synthesis of a functionalized cyclohexanone followed by attachment of a 1,3-propanedial synthon. Likewise, top-down strategies typically involve the construction of a functionalized phloroglucinol (or cyclohexane-1,3-dione) which

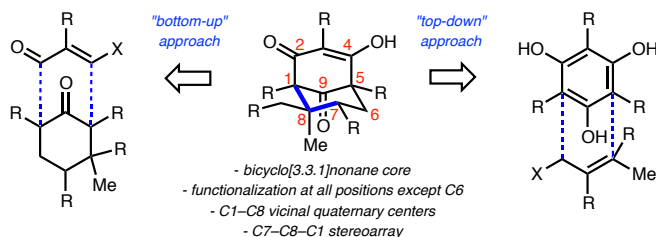
⁴⁹³ Capasso, R.; Borrelli, F.; Aviello, G.; Capasso, F.; Izzo, A. A. *Naunyn-Schmied. Arch. Pharmacol.* **2008**, *376*, 407-414.

⁴⁹⁴ Capasso, R.; Borrelli, F.; Montanaro, V.; Altieri, V.; Capasso, F.; Izzo, A. A. *J. Urology* **2005**, *173*, 2194-2197.

⁴⁹⁵ Thomas, C. A.; Tyagi, S.; Yoshimura, N.; Chancellor, M. B.; Tyagi, P. *Urology* **2007**, *70*, 813-816.

⁴⁹⁶ For reviews of PPAP synthesis methodology, see ref. 4c and: (a) Tsukano, C.; Siegel, D. R.; Danishefsky, S. J. *J. Synth. Org. Chem. Jpn.* **2010**, *68*, 592-600. (b) Njardarson, J. T. *Tetrahedron* **2011**, *67*, 7631-7666. (c) Richard, J.-A.; Pouwer, R. H.; Chen, D. Y.-K. *Angew. Chem. Int. Ed.* **2012**, *51*, 4536-4561. (d) Simpkins, N. S. *Chem. Commun.* **2013**, *49*, 1042-1051.

then undergoes dearomative annulation⁴⁹⁷ or stepwise alkylation-cyclization with a 3-carbon electrophile. An overview of the PPAP synthesis literature is provided below, following this general framework.



Scheme 1.13. General PPAP synthesis strategies.

Several 1,3-dielectrophiles have been utilized in “bottom-up” annulation approaches (Figure 1.18). Malonyl dichloride (**87**) is especially useful for the synthesis of PPAPs considering that annulation would directly afford the correct oxidation state of the C2–C4 bridge. Malonyl dichloride was first used to synthesize bicyclo[3.3.1]nonanes by Effenberger in 1984; however, a fourfold excess of 1-methoxy-1-cyclohexene was required in this initial report.⁴⁹⁸ Stoltz demonstrated that silyl enol ethers may be utilized in addition to alkyl enol ethers and that an excess of malonyl dichloride may be used instead of the enol ether component in this Effenberger annulation.⁴⁹⁹ Nicolaou has utilized methacrylaldehyde (**88**) in acid-mediated annulation reactions to create a series of bicyclic medium-sized rings, including bicyclo[3.3.1]nonanes.⁵⁰⁰ Kraus has explored several strategies toward the construction of PPAP model systems, using the electrophiles vinylsulfone **89**⁵⁰¹ and methyl acrylate **90**.⁵⁰² Simpkins also attempted to utilize diaryl malonate **91** but to no avail.⁵⁰³

⁴⁹⁷ For a review that features dearomative annulation and cyclization approaches to PPAPs, see: Roche, S. P.; Porco, J. A., Jr. *Angew. Chem. Int. Ed.* **2011**, *50*, 4068-4093.

⁴⁹⁸ Schönwälder, K.-H.; Kollat, P.; Stezowski, J. J.; Effenberger, F. *Chem. Ber.* **1984**, *117*, 3280-3296.

⁴⁹⁹ Spessard, S. J.; Stoltz, B. M. *Org. Lett.* **2002**, *4*, 1943-1946.

⁵⁰⁰ Nicolaou, K. C.; Carenzi, G. E. A.; Jeso, V. *Angew. Chem. Int. Ed.* **2005**, *44*, 3895-3899.

⁵⁰¹ Kraus, G. A.; Jeon, I. *Tetrahedron* **2005**, *61*, 2111-2116.

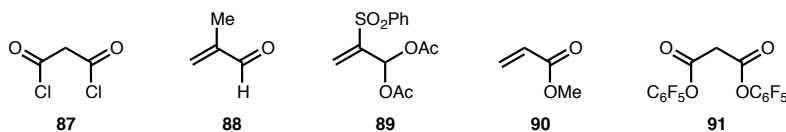


Figure 1.18. Various electrophiles utilized in “bottom-up” approaches to PPAPs.

A total synthesis of (\pm)-clusianone (*rac*-**92**) by Simpkins utilizing an Effenberger annulation strategy is shown in Scheme 1.14.⁵⁰⁴ Starting with 2-methoxycyclohexenone **93**, α -prenylation followed by methyl lithium addition afforded enone **94**. Conjugate addition of methyl cuprate and subsequent methyl enol ether formation afforded **95**.⁵⁰⁵ Exposure of enol ether **95** to malonyl dichloride and subsequent treatment of the product with trimethyl orthoformate afforded vinylogous ester **96** in 24% yield over 2 steps. LDA-mediated bridgehead lithiation and alkylation with prenyl bromide gave **97**, and subsequent benzoylation afforded *rac*-clusianone *O*-methyl ether **98**. Lithium hydroxide-facilitated demethylation revealed *rac*-clusianone. By replacing LDA with a chiral bis-lithium amide in the bridgehead lithiation reaction of **96**, a kinetic resolution allowed **96** to be recovered with 98% ee and facilitated the synthesis of *ent*-clusianone (*ent*-**92**).⁵⁰⁶ Effenberger annulations are also utilized in Delpech and Marazano’s synthesis of *rac*-**92**,⁵⁰⁷ and Coltart has synthesized *ent*-**92** using a chiral auxiliary to

⁵⁰² Kraus, G. A.; Jeon, I. *Tetrahedron Lett.* **2008**, 49, 286-288.

⁵⁰³ Ahmad, N. M.; Rodeschini, V.; Simpkins, N. S.; Ward, S. E.; Blake, A. J. *J. Org. Chem.* **2007**, 72, 4803-4815.

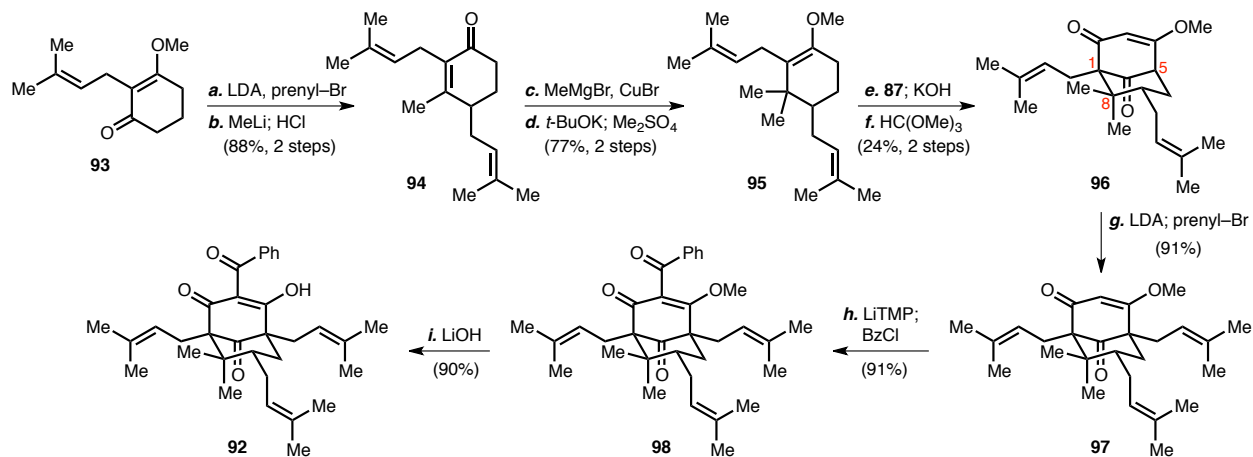
⁵⁰⁴ Rodeschini, V.; Ahmad, N. M.; Simpkins, N. S. *Org. Lett.* **2006**, 8, 5283-5285.

⁵⁰⁵ Prior to 1999, the only synthesis studies directed toward a PPAP are found in a graduate thesis from the University of Arizona: Heidt, J. C. Thesis, University of Arizona, Tucson, Arizona, United States of America, 1988. A compound similar to **95** was the most advanced intermediate synthesized in an approach to hyperforin.

⁵⁰⁶ Rodeschini, V.; Simpkins, N. S.; Wilson, C. *J. Org. Chem.* **2007**, 72, 4265-4267.

⁵⁰⁷ (a) Nuhant, P.; David, M.; Pouplin, T.; Delpech, B.; Marazano, C. *Org. Lett.* **2007**, 9, 287-289. (b) Tolon, B.; Delpech, B.; Marazano, C. *Arkivoc* **2009** (Part xiii), 252-264.

establish absolute stereocontrol.^{106,508} Mehta has utilized an Effenberger annulation in studies directed toward prolifenones A and B.⁵⁰⁹



Scheme 1.14. Total synthesis of (±)-clusianone by Simpkins (ref. 504).^a

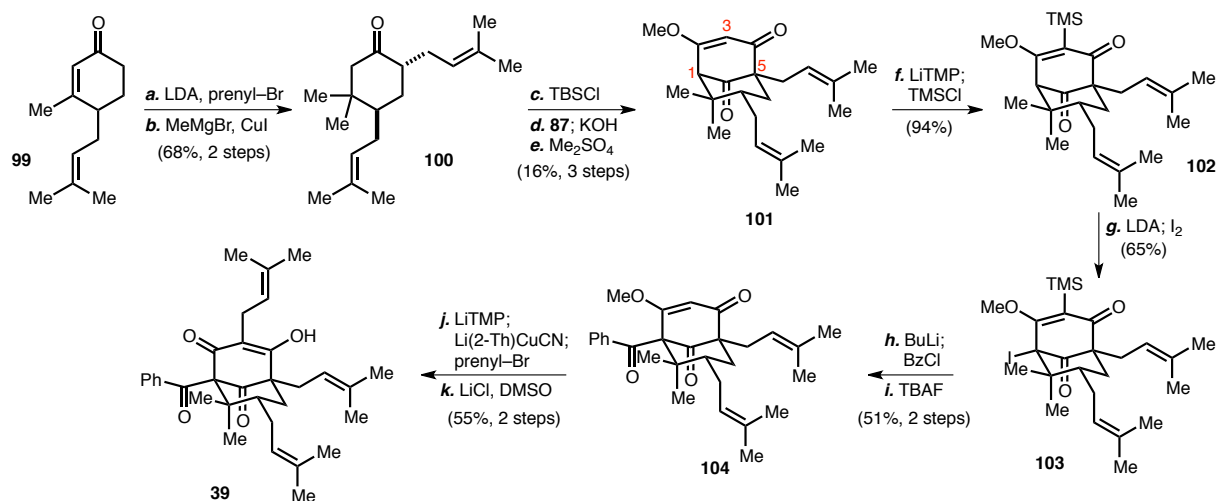
^a Conditions: (a) LDA, prenyl bromide, THF, -78°C ; (b) MeLi, THF, -78°C ; HCl, 88% (2 steps); (c) MeMgBr, CuBr·Me₂S, TMSCl, HMPA, THF, -78 to -30°C , 88%; (d) *t*-BuOK, DMSO; Me₂SO₄, 87% (mixture of enol ethers, dominant enol ether shown); (e) malonyl dichloride (**87**), Et₂O, -20°C ; KOH, BnEt₃NCl, H₂O; (f) HC(OMe)₃, *p*-TsOH, MeOH, 50°C , 24% (2 steps); (g) LDA, THF, -78°C ; prenyl bromide, -78°C , 91% (h) LiTMP, THF, -78°C ; BzCl, 91%; (i) LiOH, H₂O, dioxane, 90°C , 90%.

A prominent feature of Simpkins's total synthesis of clusianone is the bridgehead lithiation and subsequent alkylation of intermediate **96**. The reaction involves the formation of a somewhat unusual pyramidalized carbanionic species from a bridgehead methine whose trajectory limits hyperconjugative delocalization into the neighboring carbonyl π^* molecular orbitals. In the context of PPAP total synthesis, the scope and limitations of bridgehead functionalization has been studied in detail.⁵⁰³ In Scheme 1.14, the bridgehead alkylation occurs at the C5 position of **96**. Bridgehead substitutions at the C1 position, which is proximal to the C8 quaternary center, are understandably more challenging due to its steric environment, and only a limited number of electrophiles have been utilized to functionalize this

⁵⁰⁸ Garnsey, M. R.; Lim, D.; Yost, J. M.; Coltart, D. M. *Org. Lett.* **2010**, *12*, 5234-5237.

⁵⁰⁹ Mehta, G.; Dhanbal, T.; Bera, M. K. *Tetrahedron Lett.* **2010**, *51*, 5302-5305.

position. Simpkins's total synthesis of racemic nemorosone (*rac*-**39**) illustrates the difficulties of direct C1 bridgehead substitution (Scheme 1.15).^{503,510} Starting from enone **99**,⁴⁹⁹ α -prenylation followed by conjugate methyl addition accessed cyclohexanone **100**.⁵⁰³ Sequential silylation, Effenberger annulation with malonyl dichloride (**87**), and methylation revealed **101**, which was silylated at the C3 position to yield **102**.



Scheme 1.15. Total synthesis of (±)-nemorosone by Simpkins (ref. 510).^a

^a Conditions: (a) LDA, prenyl bromide, THF, -78 °C, 77%; (b) MeMgBr, CuI, THF, Me₂S, 0 °C, 88%; (c) TBSCl, NEt₃, NaI, MeCN, reflux, 87%; (d) malonyl dichloride (**87**), Et₂O, -20 °C; BnEt₃NCl, KOH, H₂O; (e) Me₂SO₄, K₂CO₃, acetone, reflux (19%, 2 steps); (f) LiTMP, THF, -78 °C; TMSCl, 94%; (g) LDA, TMSCl, THF, -78 to 0 °C; I₂, 0 °C, 65%; (h) BuLi, THF, -78 °C; BzCl, 63%; (i) TBAF, THF, 81%; (j) LiTMP, THF; Li(2-Th)CuCN; prenyl bromide, 55%; (k) LiCl, DMSO, 120 °C, >99%.

A more direct route to nemorosone would involve C3 prenylation; however, such an intermediate would not undergo bridgehead lithiation owing to an acidic bisallylic methylene subunit.⁵⁰³ A variety of conditions for the bridgehead functionalization of **102**, including the use of several carbogenic electrophiles, did not provide any desired products. This illustrates the difficulty of performing bridgehead substitution chemistry at the C1 position relative to the C5 position when compared to the efficient conversion of **96** to **97** in Scheme 1.14. In the end, metalation of **102** with LDA followed by

⁵¹⁰ Simpkins, N. S.; Taylor, J. D.; Weller, M. D.; Hayes, C. J. *Synlett* **2010**, 639-643.

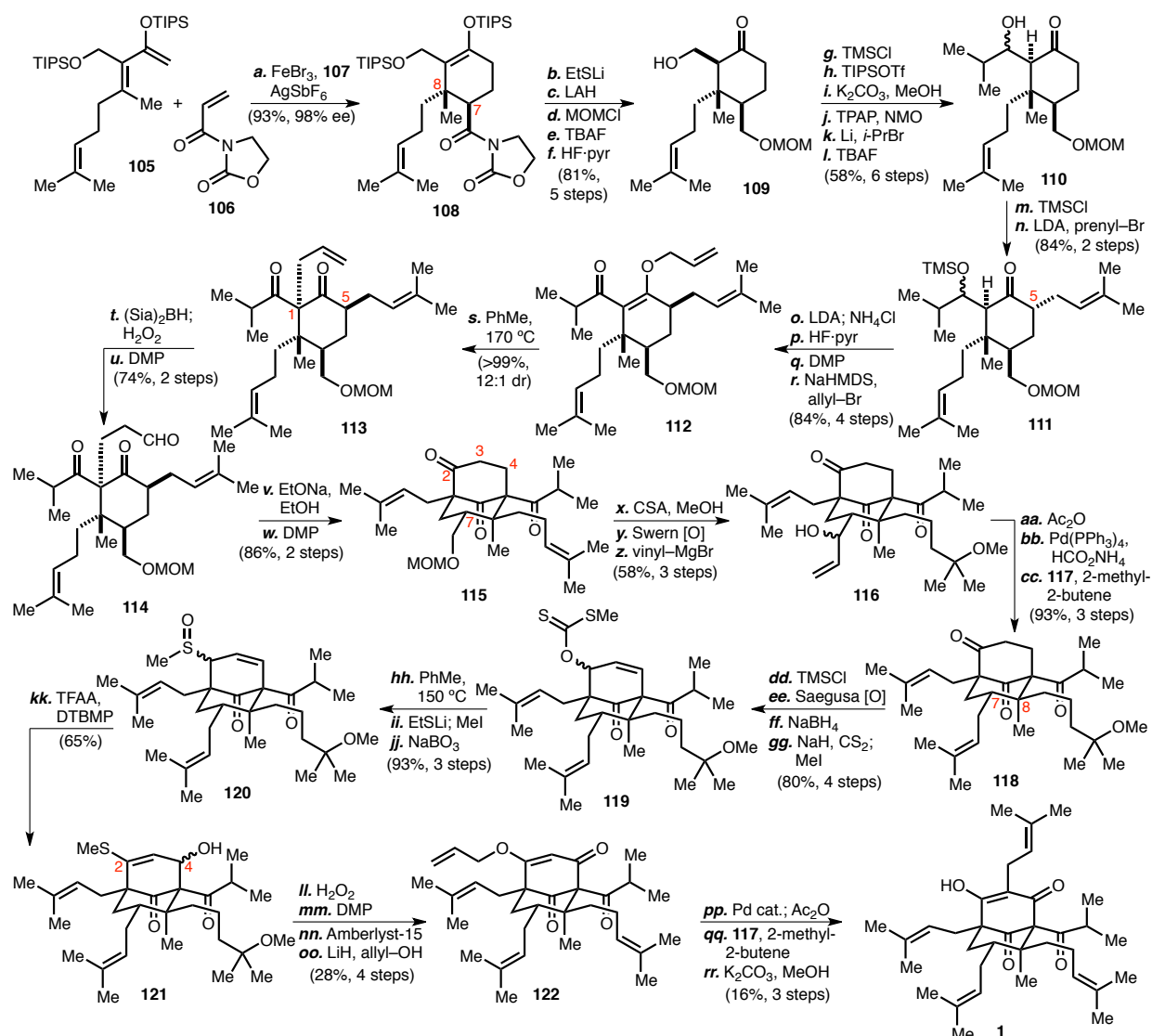
trapping with iodine provided bridgehead iodide **103**. Having installed a functional handle at C1, metalation with butyllithium, trapping with benzoyl chloride, and desilylation provided phenyl ketone **104**. Finally, installation of the C3 prenyl group was facilitated by sequential deprotonation, transmetalation with Lipshutz's cuprate,⁵¹¹ and prenyl bromide alkylation, and demethylation with lithium chloride provided (±)-nemorosone (*rac*-**39**).

Aside from using 1,3-dielectrophiles, several groups have explored the use of an intramolecular aldol reaction to construct the PPAP bicyclo[3.3.1]nonane core. Shibasaki has utilized this reaction in his total synthesis of *ent*-hyperforin (*ent*-**1**), the first enantioselective total synthesis of a PPAP (Scheme 1.16).⁵¹² Starting with diene **105** (available in 7 steps from propargyl bromide)⁵¹³ and oxazolidinone **106**, a catalytic, enantioselective Diels–Alder reaction involving FeBr₃ and pybox ligand **107** (Figure 1.19) afforded siloxycyclohexene **108**. This is a particularly effective transformation for the construction of the cyclohexanone carbocycle of PPAPs, since both the C7 and C8 stereocenters of hyperforin are established in a single step. Removal of the oxazolidinone ring and silyl groups of **108** revealed cyclohexanone **109**, and a subsequent series of reactions including a Barbier reaction produced **110** containing the carbon framework of the isopropyl ketone of hyperforin. α -Prenylation gave **111** as a single epimer at the C5 position. After C5 epimerization and functional group manipulations, *O*-allylation afforded **112**, and heating a toluene solution of **112** quantitatively yielded **113** in a high diastereomeric ratio at the newly formed quaternary C1 stereocenter. The high degree of diastereocontrol in this transformation may be rationalized by assuming the C5 prenyl group of **112** directs the carbon-carbon bond formation to the opposite face of the cyclohexene ring. Hydroboration of the olefin present in **113** followed by DMP-mediated oxidation provided aldehyde **114**. Exposure of this aldehyde to sodium ethoxide in ethanol

⁵¹¹ Lipshutz, B. H.; Koerner, M.; Parker, D. A. *Tetrahedron Lett.* **1987**, 28, 945-948.

⁵¹² (a) Shimizu, Y.; Shi, S.-L.; Usuda, H.; Kanai, M.; Shibasaki, M. *Angew. Chem. Int. Ed.* **2010**, 49, 1103-1106. (b) Shimizu, Y.; Shi, S.-L.; Usuda, H.; Kanai, M.; Shibasaki, M. *Tetrahedron* **2010**, 66, 6569-6584.

⁵¹³ (a) Appar, M.; Barrele, M. *Bull. Soc. Chim. Fr. II* **1983**, 83-86. (b) Usuda, H.; Kuramochi, A.; Kanai, M.; Shibasaki, M. *Org. Lett.* **2004**, 6, 4387-4390.



Scheme 1.16. Total synthesis of *ent*-hyperforin by Shibasaki (ref. 512).^a

^a Conditions: (a) **107**, FeBr₃, AgSbF₆, 5 Å MS, CH₂Cl₂, -70 °C, 93%, 98% ee; (b) EtSLi, THF, 96%; (c) LAH, THF, 99%; (d) MOMCl, TBAI, *i*-Pr₂NEt, CH₂Cl₂, 94%; (e) TBAF, HOAc, THF; (f) HF·pyr, pyr, THF, 91% (2 steps); (g) TMSCl, NEt₃, CH₂Cl₂; (h) TIPSOTf, *i*-Pr₂NEt, CH₂Cl₂; (i) K₂CO₃, MeOH; (j) TPAP, NMO, 4 Å MS, MeCN, CH₂Cl₂; (k) *i*-PrBr, Li, THF; (l) TBAF, HOAc, THF, 58% (6 steps); (m) TMSCl, imid, DMF, 94%; (n) LDA, HMPA, prenyl bromide, THF, 89%; (o) LDA, THF, NH₄Cl, H₂O, 88%; (p) HF·pyr, pyr, THF; (q) DMP, CH₂Cl₂, 96% (2 steps); (r) NaHMDS, allyl bromide, HMPA, THF, >99%; (s) PhMe, *N,N*-diethylaniline, 170 °C, >99%, 12:1 dr; (t) (Sia)₂BH, THF; H₂O₂, NaOH, H₂O, EtOH, 81%; (u) DMP, CH₂Cl₂, 91%; (v) EtONa, EtOH; (w) DMP, CH₂Cl₂, 86% (2 steps); (x) CSA, MeOH, 66% (3 cycles); (y) (COCl)₂, DMSO, CH₂Cl₂; NEt₃, 95%; (z) vinylmagnesium bromide, THF, 92%; (aa) Ac₂O, DMAP, *i*-Pr₂NEt, CH₂Cl₂, 98%; (bb) Pd(PPh₃)₄, HCO₂NH₄, PhMe, 95%; (cc) **117**, 2-methyl-2-butene, CH₂Cl₂, >99%; (dd) TMSCl, NEt₃, DMAP, CH₂Cl₂, 84%; (ee) Pd(OAc)₂, DMSO, O₂, >99%; (ff) NaBH₄, MeOH, 95%; (gg) CS₂, NaH, THF; MeI, >99%; (hh) PhMe, 150 °C; (ii) EtSLi, THF; MeI, NEt₃, 98% (2 steps); (jj) NaBO₃·4H₂O, HOAc, 95%; (kk) TFAA, DTBMP, CH₂Cl₂, -40 °C; H₂O, 65%; (ll) H₂O₂, HFIP, 87%; (mm) DMP, CH₂Cl₂, 86%; (nn) Amberlyst-15DRY, PhMe, 55%; (oo) LiH, allyl alcohol, 67%; (pp) [Pd₂(dba)₃]·CHCl₃, (*S*)-tol-BINAP, THF; Ac₂O, pyr, 50%; (qq) **117**, 2-methyl-2-butene, CH₂Cl₂, 34%; (rr) K₂CO₃, MeOH, 94%.

facilitated the key aldol cyclization reaction,⁵¹⁴ and subsequent DMP-mediated oxidation afforded **115**, which contains the bicyclo[3.3.1]nonane core of hyperforin with all key stereocenters established.

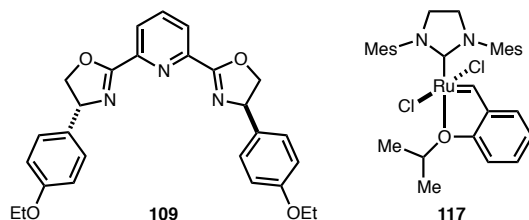


Figure 1.19. A Pybox ligand and an olefin metathesis catalyst, both utilized in the total synthesis of *ent*-hyperforin.

At this point in the synthesis, the only remaining tasks were the installation of the C3 and C7 prenyl groups as well as the 1,3-diketone oxidation state about the C2–C4 bridge. First, the C7 prenyl group was installed via sequential MOM group removal, oxidation, and vinylmagnesium bromide addition of **115** to afford allylic alcohol **116** as a mixture of epimers. Deoxygenation was then accomplished via stepwise acetylation and Pd-catalyzed allylic reduction, and a resulting olefin cross metathesis with 2-methyl-2-butene utilizing Hoveyda–Grubbs second-generation catalyst (**117**, Figure 1.19) afforded **118**. It is noteworthy that the C8 homoprenyl olefin was previously protected as a tertiary methyl ether; if a homoprenyl group was present during this cross metathesis, the authors observed ring-closing metathesis. After considerable experimentation, installation of the C2–C4 1,3-diketone oxidation was accomplished through a vinylogous Pummerer rearrangement. First, a Saegusa oxidation of **118** followed by 1,2-reduction and xanthate formation led to **119**. Thermal [1,3]-rearrangement of the xanthate functionality, thiolysis, *S*-methylation, and *S*-oxidation yielded the rearrangement precursor **120**. Exposure of **120** to trifluoroacetic anhydride and 2,6-di-*tert*-butyl-4-methylpyridine followed by hydrolysis afforded a product, **121**, bearing oxygenation at both the C2 and C4 positions. *S*-Oxidation, DMP-mediated oxidation, elimination of the homoprenyl protecting group, and addition-elimination

⁵¹⁴ This intramolecular aldol strategy for the construction of hyperforin was first revealed in 2007: Shimizu, Y.; Kuramochi, A.; Usuda, H.; Kanai, M.; Shibasaki, M. *Tetrahedron Lett.* **2007**, 48, 4173–4177.

afforded allylic ether **122**. Finally, intramolecular Pd-catalyzed allyl transfer, acetylation, cross metathesis, and deacetylation revealed *ent*-hyperforin (*ent*-**1**).

Other groups have utilized an intramolecular aldol strategy in their studies toward PPAP natural products. Grossman's approach involved a Pb(OAc)₄-mediated α -alkynylation of β -ketoester **123** with stannane **124**, and subsequent hydrosilylation of an insipient Co₂(CO)₆ complex to reveal enal **125**, which upon exposure to aqueous acid afforded allylic alcohol **126** (Scheme 1.17a).⁵¹⁵ Mehta has reported the DIBAL reduction of tetrahydrochromene **127** to bicyclo[3.3.1]nonane **128**, which may proceed through an intermediate hemiacetal **129** that undergoes formal [1,3] rearrangement via aldehyde **130** (Scheme 1.17b).⁵¹⁶ Very similar reductive rearrangements have been reported by Shibasaki⁵¹⁷ and Delpech.⁵¹⁸ In studies toward hyperforin, Chen has reported the synthesis of aldehyde **131** via sequential Pd-catalyzed hydrostannylation of alkyne **132** followed by oxidative cleavage (Scheme 1.17c).⁵¹⁹ Exposure of this aldehyde to NaOEt in EtOH afforded bicyclo[3.3.1]nonane **133**.

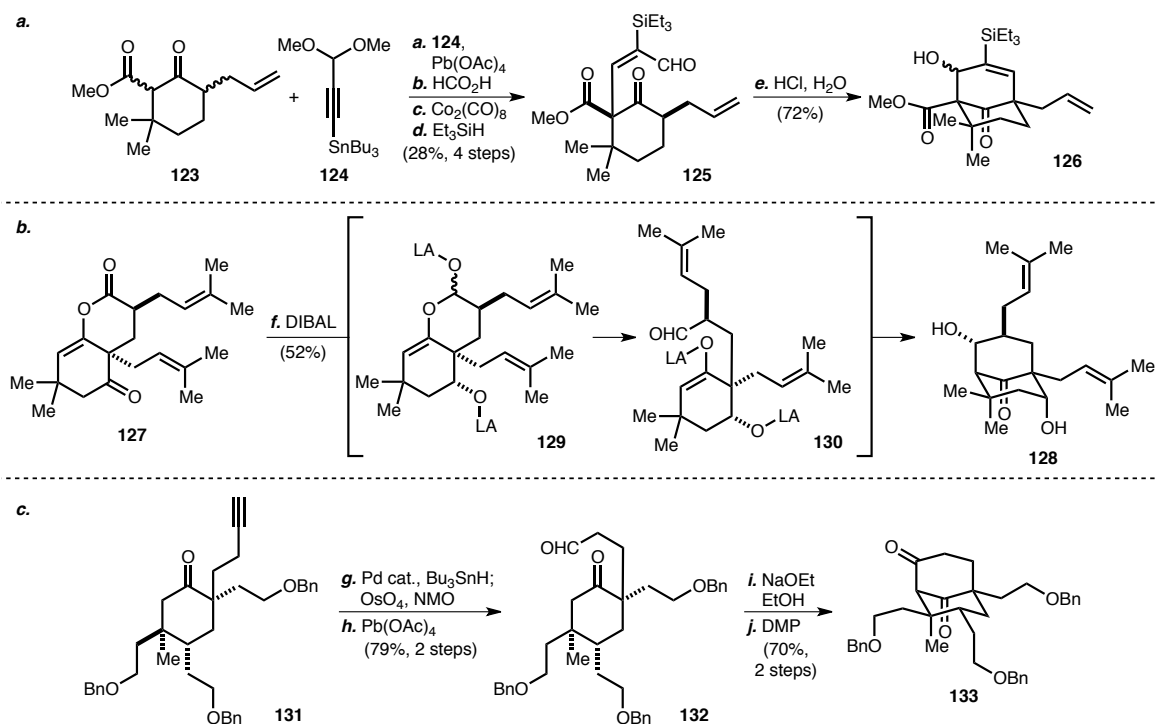
⁵¹⁵ Ciochina, R.; Grossman, R. B. *Org. Lett.* **2003**, *5*, 4619-4621.

⁵¹⁶ (a) Mehta, G.; Bera, M. K. *Tetrahedron Lett.* **2006**, *47*, 689-692. (b) Mehta, G.; Bera, M. K. *Tetrahedron Lett.* **2008**, *49*, 1417-1420. (c) Mehta, G.; Bera, M. K. *Tetrahedron Lett.* **2009**, *50*, 3519-3522. (d) Mehta, G.; Das, M.; Kundu, U. K. *Tetrahedron Lett.* **2012**, *53*, 4538-4542. (e) Mehta, G.; Bera, M. K. *Tetrahedron* **2013**, *69*, 1815-1821.

⁵¹⁷ Usuda, H.; Kanai, M.; Shibasaki, M. *Tetrahedron Lett.* **2002**, *43*, 3621-3624.

⁵¹⁸ Pouplin, T.; Tolon, B.; Nuhant, P.; Delpech, B.; Marazano, C. *Eur. J. Org. Chem.* **2007**, 5117-5125.

⁵¹⁹ Richard, J.-A.; Chen, D. Y.-K. *Eur. J. Org. Chem.* **2012**, 484-487.



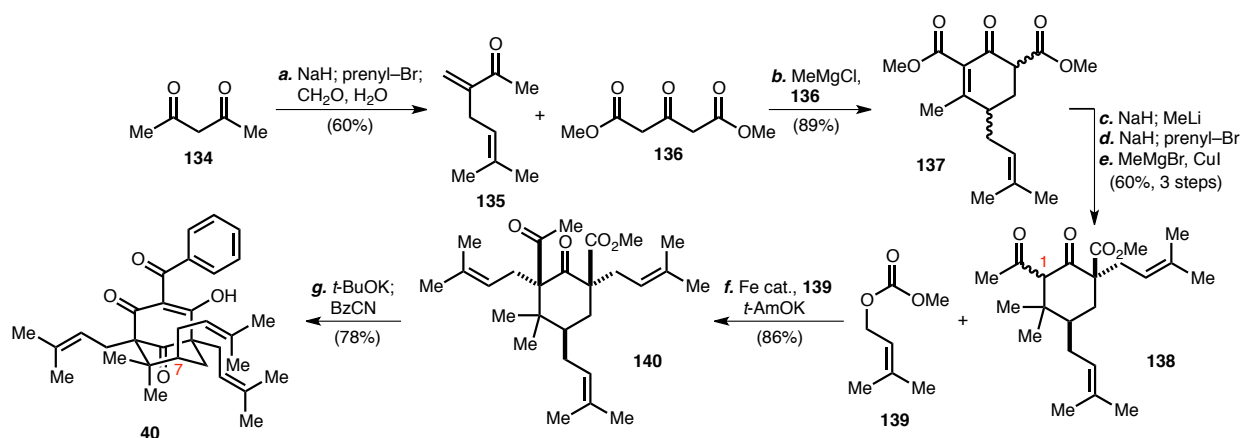
Scheme 1.17. Intramolecular aldol approaches to PPAPs by (a) Grossman, (b) Mehta, and (c) Chen.^a

^a Conditions: (a) **124**, Pb(OAc)₄, THF, −30 °C to rt, 48%; (b) HCO₂H, 71%; (c) Co₂(CO)₈, CH₂Cl₂, 0 °C, 87%; (d) Et₃SiH, bis(trimethylsilyl)acetylene, DCE, 65 °C, 94%; (e) HCl, H₂O, 72%; (f) DIBAL, CH₂Cl₂, 0 °C, 52%; (g) PdCl₂(PPh₃)₂, Bu₃SnH, THF; OsO₄, NMO, H₂O; (h) Pb(OAc)₄, CH₂Cl₂, 79% (2 steps); (i) NaOEt, EtOH, 0 °C to rt; (j) DMP, NaHCO₃, CH₂Cl₂, 70% (2 steps).

In addition to the aldol strategies outlined previously, Plietker has utilized an intramolecular Dieckmann cyclization approach for the synthesis of (±)-7-*epi*-clusianone (*rac*-**40**, Scheme 1.18).⁵²⁰ Starting with acetylacetone (**134**), stepwise prenylation and deacylative aldol methylenation provided enone **135**. Treatment of this enone with dimethyl acetonedicarboxylate (**136**) afforded cyclohexenone **137** as a result of a tandem Michael addition-Knoevenagel condensation. Sequential regioselective methyllithium 1,2-addition, α-prenylation, and conjugate methylation afforded cyclohexanone **138**. In order to facilitate the key Dieckmann cyclization step, stereoselective prenylation at the C1 position of **138** was required in order to position the methyl ketone and methyl ester upon the same face of the

⁵²⁰ Biber, N.; Möws, K.; Plietker, B. *Nature Chem.* **2011**, 3, 938-942.

cyclohexanone ring. After some experimentation, a Fe-catalyzed allylation⁵²¹ using methyl prenyl carbonate (**139**) afforded cyclization precursor **140**. Treatment with KO*t*-Bu followed by BzCN directly afforded (±)-7-*epi*-clusianone (*rac*-**40**). Further, Plietker was able to synthesize racemic hyperpappanone, hyperibone L, and oblongifolin A, highlighting the utility of this methodology to obtain Type B PPAPs bearing an *exo* C7 substituent.



Scheme 1.18. Total synthesis of (±)-7-*epi*-clusianone by Plietker (ref. 520).^a

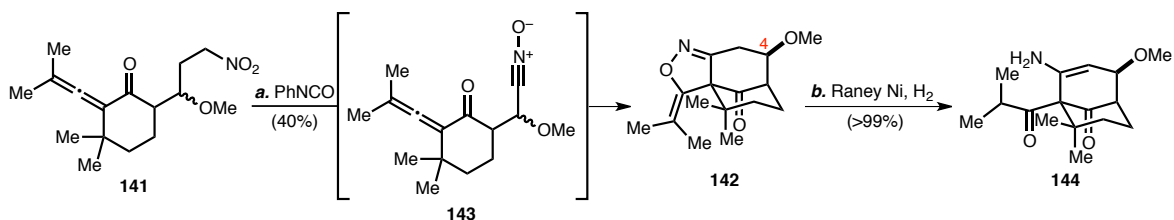
^a Conditions: (a) NaH, EtOH, 0 °C; prenyl bromide, 0 °C to rt; CH₂O, K₂CO₃, H₂O, 60%; (b) MeMgCl, **136**, THF, MeOH, 60 °C, 89%, (c) NaH, THF, 0 °C; MeLi, 0 °C; (d) NaH, 18-crown-6, THF, 0 °C; prenyl bromide, 0 °C to rt, 61% (2 steps); (e) MeMgBr, CuI, TMSCl, LiCl, THF, -78 °C, 96%; (f) *t*-AmOK, 1,3-dimesitylimidazolin-2-ylidene hexafluorophosphate, MTBE, 60 °C; Bu₄N[Fe(CO)₃(NO)], rt to 60 °C; **138**, LiH, THF, 0 °C to rt; (**139**, 100 °C, 86%; (g) *t*-BuOK, THF, 0 °C; BzCN, 0 to 45 °C, 78%.

Other “bottom-up” approaches involve the use of transition metals or cycloaddition chemistry to facilitate the formation of the bicyclo[3.3.1]nonane core of PPAPs. Garsubellin A was the first PPAP to be synthesized, and Shibasaki utilized ring-closing metathesis to establish the C2–C4 bridge.⁵²² Kraus has utilized a Mn(OAc)₃-mediated oxidative free-radical cyclization to facilitate the formation of the PPAP

⁵²¹ Plietker, B. *Angew. Chem. Int. Ed.* **2006**, *45*, 1469-1473.

⁵²² Kuramochi, A.; Usuda, H.; Yamatsugu, K.; Kanai, M.; Shibasaki, M. *J. Am. Chem. Soc.* **2005**, *127*, 14200-14201.

core in several model systems.⁵²³ Mehta has also synthesized a model bicyclo[3.3.1]nonane⁵²⁴ using a Pd-catalyzed Kende cyclization.⁵²⁵ In an approach to hyperevolutin A, Young utilized an allene-nitrile oxide [3+2] cycloaddition reaction (Scheme 1.19).⁵²⁶ Treatment of **141** with PhNCO facilitated the cycloaddition to form isoxazoline **142**, presumably through intermediate nitrile oxide **143**. Only a single C4 epimer of **142** was isolated, indicating that only one diastereomer of **143** underwent cyclization. Reduction of **142** using Raney Ni quantitatively afforded enamine **144** through cleavage of the isoxazoline ring.



Scheme 1.19. Young's [3+2] allene-nitrile oxide cycloaddition approach to hyperevolutin A (ref. 526).^a

^a Conditions: (a) PhNCO, NEt₃, 40%; (b) Raney Ni, H₂, MeOH, >99%.

Contrasting “bottom-up” strategies, “top-down” approaches to PPAP synthesis typically involve dearomatization of an oxidized benzene ring through the attachment of the C6–C8 bridge. Many of these strategies are inspired by the proposed biosynthesis of PPAPs, involving the dearomative alkylation of an acylphloroglucinol (e.g., Scheme 1.5). As previously discussed, a challenge of many “bottom-up” strategies is the oxidation of the C2–C4 subunit; in “top-down” strategies, establishing this oxidation very

⁵²³ (a) Kraus, G. A.; Dneprovskaia, E.; Nguyen, T. H.; Jeon, I. *Tetrahedron* **2003**, *59*, 8975-8978. (b) Kraus, G. A.; Nguyen, T. H.; Jeon, I. *Tetrahedron Lett.* **2003**, *44*, 659-661.

⁵²⁴ Mehta, G.; Bera, M. K. *Tetrahedron Lett.* **2004**, *45*, 1113-1116.

⁵²⁵ (a) Kende, A. S.; Roth, B.; Sanfilippo, P. J. *J. Am. Chem. Soc.* **1982**, *104*, 1784-1785. (b) Kende, A. S.; Roth, B.; Sanfilippo, P. J.; Blacklock, T. J. *J. Am. Chem. Soc.* **1982**, *104*, 5808-5810.

⁵²⁶ Young, D. G. J.; Zeng, D. *J. Org. Chem.* **2002**, *67*, 3134-3137.

early in the synthesis circumvents this problem. Likewise, a difficulty of latter approaches is the installation of stereochemical elements at a late stage.

Many of these principles were incorporated in the total synthesis of (±)-garsubellin A (*rac*-**145**) by Danishefsky (Scheme 1.20).⁵²⁷ Starting with phloroglucinol triether **146**,⁵²⁸ regioselective *ortho* lithiation-prenylation, dihydroxylation, acetonide formation, and desilylation afforded phloroglucinol diether **147**. The reaction of this electron-rich phenol and allyl methyl carbonate under Pd- and Ti-cocatalysis provided divinyllogous carbonate **148** via a dearomative allylation reaction.⁵²⁹ A possible mechanism for this transformation involves Lewis acid-activation of the phenolic hydroxyl group followed by direct *para* C-allylation. Treatment of **148** with perchloric acid facilitated the formation of alcohol **149** as a single diastereomer, bearing the tetrahydrofuran ring of garsubellin A. Cross metathesis with 2-methyl-2-butene facilitated by Grubbs second-generation catalyst (**150**) afforded **151**. Exposure of **151** to iodine not only provided the desired bicyclo[3.3.1]nonane core through a iodocarbocyclization reaction but also promoted iodination at the C1 position, which after treatment with iodine and CAN provided triiodide **152**. Aside from a tandem desired magnesium-iodine exchange with subsequent allylation at the C3 position of **152**, a transannular Wurtz cyclopropanation yielded **153**. Iodide 1,5-addition to the activated cyclopropane in **153** was accomplished by treatment with TMSI, affording **154**. The synthesis of C7 prenylation product **155** was accomplished in two steps: (1) a AIBN-mediated Keck radical allylation⁵³⁰ with allyltributylstannane and (2) cross-metathesis with 2-methyl-2-butene. At this juncture, only C1 acylation was necessary to complete the total synthesis; however, direct bridgehead lithiation-acylation of **155** was not feasible. Accordingly, bridgehead iodination was accomplished using LDA and iodine to afford iodide **156**. Magnesium-iodide exchange, trapping with isobutyraldehyde, DMP-mediated oxidation, and desilylation subsequently afforded (±)-garsubellin A (*rac*-**145**). In

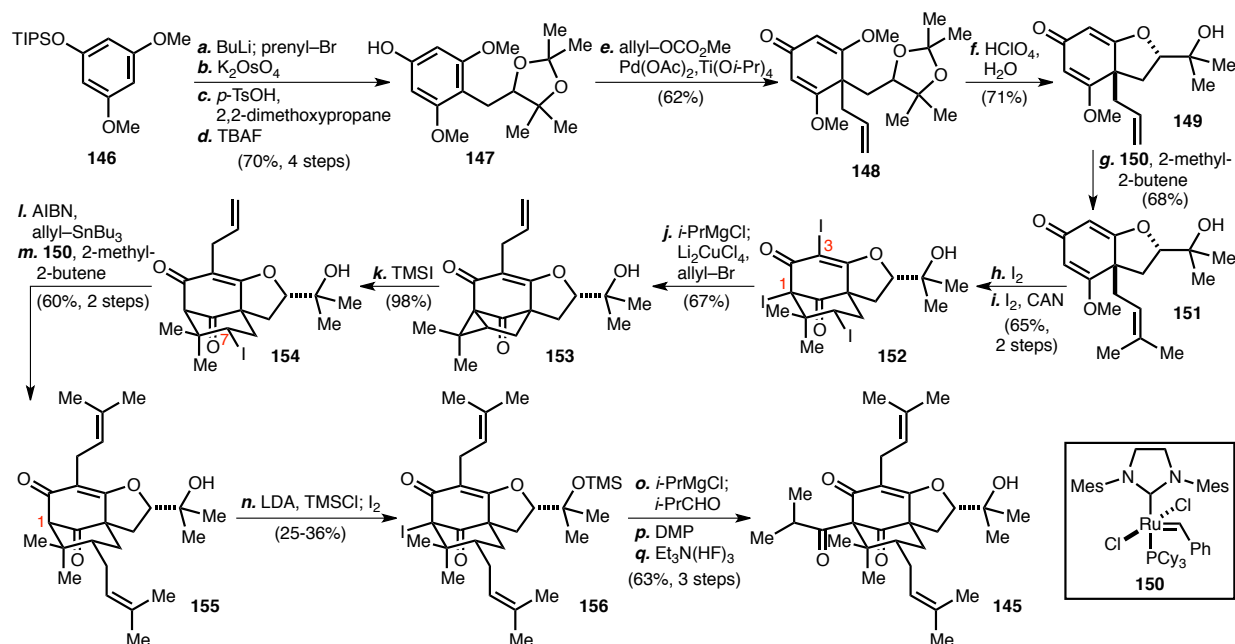
⁵²⁷ Siegel, D. R.; Danishefsky, S. J. *J. Am. Chem. Soc.* **2006**, *128*, 1048-1049.

⁵²⁸ Landi, J. J., Jr.; Ramig, K. *Synth. Commun.* **1991**, *21*, 167-171.

⁵²⁹ Satoh, T.; Ikeda, M.; Miura, M.; Nomura, M. *J. Org. Chem.* **1997**, *62*, 4877-4879.

⁵³⁰ Keck, G. A.; Enholm, E. J.; Yates, J. B.; Wiley, M. R. *Tetrahedron* **1985**, *41*, 4079-4094.

addition, these strategies were later utilized in racemic total syntheses of both nemorosone and clusianone.⁵³¹



Scheme 1.20. Total synthesis of (±)-garsubellin A by Danishefsky (ref. 527).^a

^a Conditions: (a) BuLi, Et₂O, 0 °C; prenyl bromide; (b) K₂OsO₄·2H₂O, K₂CO₃, K₃[Fe(CN)₆], MeSO₂NH₂, *t*-BuOH, H₂O; (c) *p*-TsOH·H₂O, 2,2-dimethoxypropane, acetone; (d) TBAF, THF, 70% (4 steps); (e) Pd(OAc)₂, PPh₃, Ti(O*i*-Pr)₄, allyl methyl carbonate, PhH, 80 °C, 62%; (f) HClO₄, H₂O, dioxane, 60 °C, 71%; (g) **150**, 2-methyl-2-butene, CH₂Cl₂, 40 °C, 68%; (h) I₂, KI, KHCO₃, THF, H₂O, 85%; (i) I₂, CAN, MeCN, 50 °C, 77%; (j) *i*-PrMgCl, THF, −78 °C; Li₂CuCl₄, allyl bromide, −78 to 0 °C, 67%; (k) TMSI, CH₂Cl₂, 0 °C; HCl, H₂O, 0 °C, 98%; (l) AIBN, allyltributylstannane, PhH, 80 °C, 82%; (m) **150**, 2-methyl-2-butene, CH₂Cl₂, 40 °C, 73%; (n) LDA, TMSI, THF, −78 °C; I₂, −78 to 0 °C, 25-36%; (o) *i*-PrMgCl, THF, −78 °C; *i*-PrCHO, −78 to 0 °C, 72%; (p) DMP, CH₂Cl₂; (q) Et₃N(HF)₃, THF, 88% (2 steps).

Other groups have utilized activated-olefin carbocyclization as key steps in their studies toward PPAP natural products. Jacobsen employed a Claisen rearrangement of enol ether **157**, catalyzed by guanidinium catalyst **158**, to yield **159**, in one step garnering the highly congested C1–C8 bond of hyperforin flanked by two stereogenic quaternary centers (Scheme 1.21a).⁵³² Enol ether hydrolysis

⁵³¹ Tsukano, C.; Siegel, D. R.; Danishefsky, S. J. *Angew. Chem. Int. Ed.* **2007**, *46*, 8840-8844.

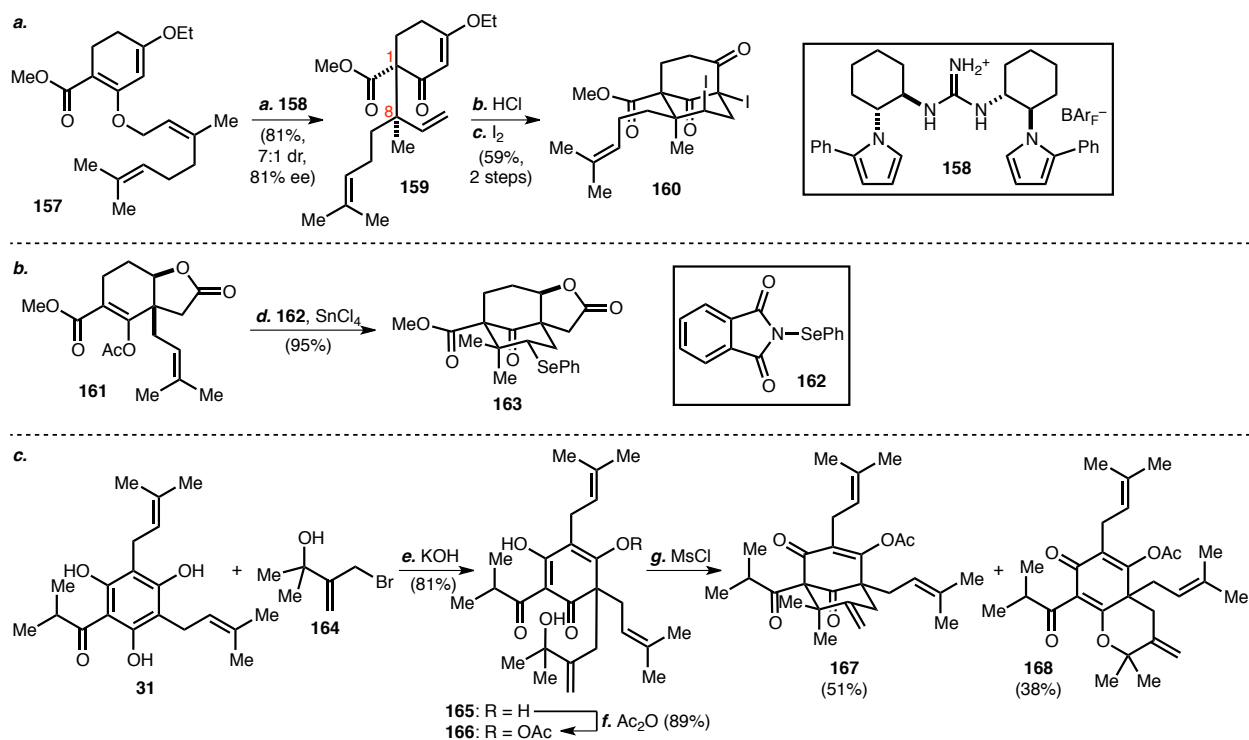
⁵³² Uyeda, C.; Rötheli, A. R.; Jacobsen, E. N. *Angew. Chem. Int. Ed.* **2010**, *49*, 9753-9756.

followed by treatment with iodine yielded bicyclic diiodide **160**. In studies toward garsubellin A, Nicolaou performed a Lewis acid-mediated selenocarbocyclization upon **161** using *N*-(phenylseleno)phthalamide (**162**), yielding bicyclo[3.3.1]nonane **163** (Scheme 1.21b).⁵³³ Couladourous reported a dearomative *C*-alkylation of deoxycohumulone (**31**) with allyl chloride **164** to yield cyclohexadienone **165** (Scheme 1.21c).⁵³⁴ Following monoacetylation to give **166**, exposure to MsCl afforded S_N1-type alkylation product **167**. However, a substantial amount of *O*-alkylation product **168** was produced in addition to the desired *C*-alkylation product. SnCl₄-mediated carbocyclization of a prenylated phloroglucinol derivative has also been reported by Marazano; however, this reaction formed a variety of products.⁵³⁵

⁵³³ (a) Nicolaou, K. C.; Pfefferkorn, J. A.; Kim, S.; Wei, H. X. *J. Am. Chem. Soc.* **1999**, *121*, 4724-4725. (b) Nicolaou, K. C.; Pfefferkorn, J. A.; Cao, G.-Q.; Kim, S.; Kessabi, J. *Org. Lett.* **1999**, *1*, 807-810.

⁵³⁴ Couladourous, E. A.; Dakanali, M.; Demadis, K. D.; Vidali, V. P. *Org. Lett.* **2009**, *11*, 4430-4433.

⁵³⁵ Raikar, S. B.; Nuhant, P.; Delpech, B.; Marazano, C. *Eur. J. Org. Chem.* **2008**, 1358-1369.



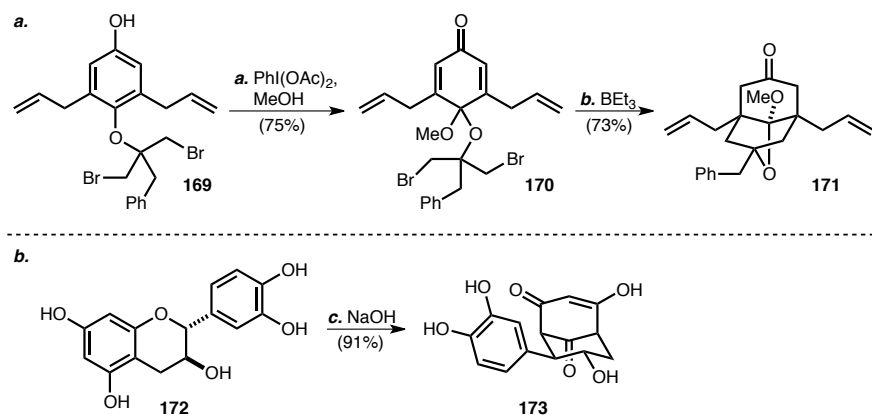
Scheme 1.21. Carbocyclization approaches to PPAPs by (a) Jacobsen, (b) Nicolaou, and (c) Coulaudouros.^a

^a Conditions: (a) **158**, hexane, 30 °C, 81%, 7:1 dr, 81% ee; (b) HCl, THF, 90%; (c) I₂, KI, NHCO₃, THF, H₂O, 65%; (d) **162**, SnCl₄, CH₂Cl₂, -23 °C, 95%. (e) **164**, KOH, Aliquat 336, PhCl, H₂O, 81%; (f) Ac₂O, pyr, acetone, 89%; (g) MsCl, NEt₃, THF, -40 °C, 89% (total yield).

Other unique dearomatization strategies have been explored. Njardarson has pursued an oxidative dearomatization-double radical cyclization strategy for the synthesis of Type B PPAPs (Scheme 1.22a).⁵³⁶ Hypervalent iodine-mediated oxidative deraromatization of **169** afforded cyclohexadienone **170**, and exposure of this compound to BEt₃ gave bicyclo[3.3.1]nonane **171**, the result of two 5-*exo*-trig cyclizations. Simpkins has utilized an unusual rearrangement of the flavonoid catechin (**172**) to catechinic acid (**173**), a reaction previously reported by Sears in 1974 (Scheme 1.22b).⁵³⁷

⁵³⁶ McGrath, N. A.; Binner, J. R.; Markopoulos, G.; Brichacek, M.; Njardarson, J. T. *Chem. Commun.* **2011**, 47, 209-211.

⁵³⁷ (a) Sears, K. D.; Casebier, R. L.; Hergert, H. L.; Stout, G. H.; McCandlish, L. E. *J. Org. Chem.* **1974**, 39, 3244-3247. (b) Ahmad, N. M.; Rodeschini, V.; Simpkins, N. S.; Ward, S. E.; Wilson, C. *Org. Biomol. Chem.* **2007**, 5, 1924-1934.



Scheme 1.22. Other dearomative carbocyclization approaches by (a) Njardarson and (b) Simpkins.^a

^a Conditions: (a) PhI(OAc)₂, MeOH, 75%; (b) BEt₃, (TMS)₃SiH, air, PhMe, 73%; (c) NaOH, H₂O, reflux, 91%.

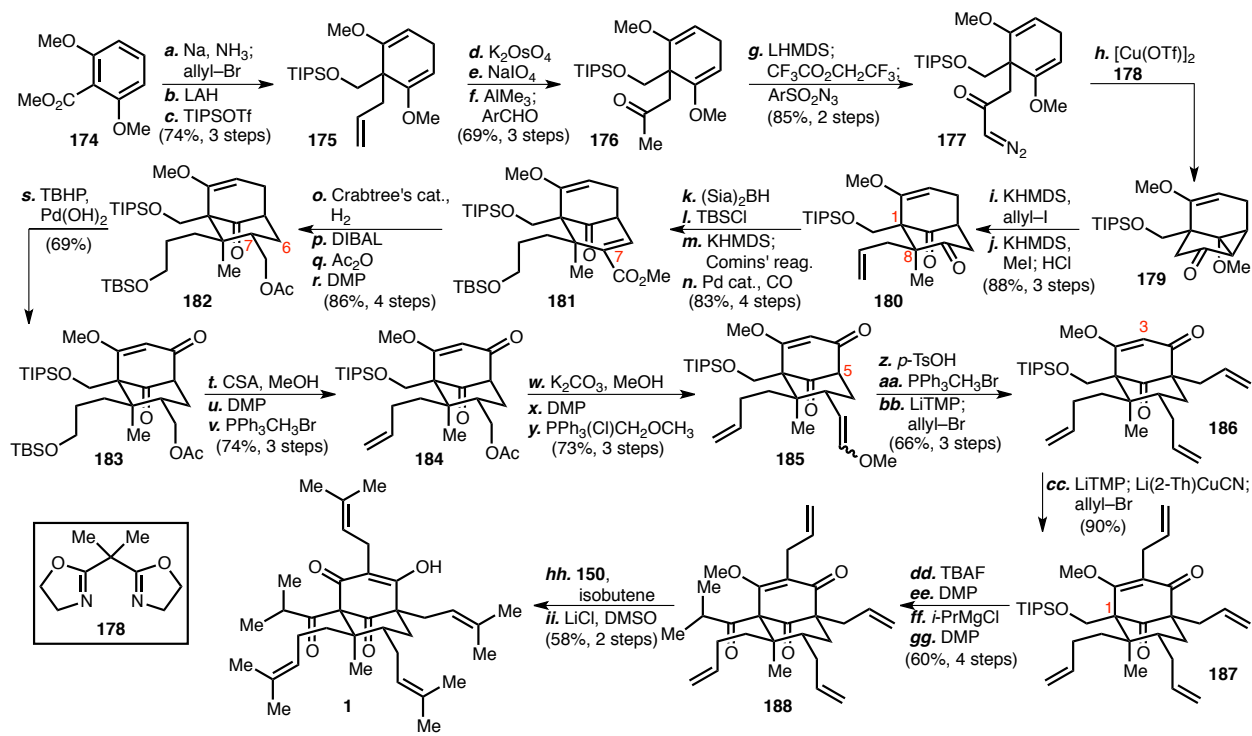
Nakada has explored an alternative approach to PPAPs involving a Birch reduction-cyclopropanation-cyclopropane opening sequence,⁵³⁸ exemplified by the racemic total synthesis of hyperforin (Scheme 1.23).⁵³⁹ Starting with methyl 2,6-dimethoxybenzoate (**174**), Birch reduction with concomitant allylation followed by reduction and silylation produced cyclohexadiene **175**.⁵⁴⁰ The allyl moiety in **175** was converted to a methyl ketone using a three step protocol involving dihydroxylation and oxidative cleavage followed by methyl addition mediated with AlMe₃ with an ensuing Oppenauer oxidation, affording **176**. Subsequent trifluoracetylation of this compound followed by diazo transfer yielded α -diazoketone **177**. Exposure of **177** to [Cu(OTf)]₂ in the presence of achiral bisoxazoline ligand **178** facilitated an intramolecular cyclopropanation reaction, forming **179**. Unfortunately, the use of chiral ligands did not lead to high levels of absolute stereocontrol.^{538c} Stepwise α -alkylation of ketone **179** with allyl iodide and iodomethane followed by acid-mediated cyclopropane opening led to isolation of **180**, a bicyclo[3.3.1]nonane core containing the key C1 and C8 vicinal stereogenic quaternary centers of hyperforin. Formal silanolysis of the allyl group of **180**, formation of an enol triflate at the C7 position,

⁵³⁸ (a) Abe, M.; Nakada, M. *Tetrahedron Lett.* **2006**, 47, 6347-6351. (b) Abe, M.; Nakada, M. *Tetrahedron Lett.* **2007**, 48, 4873-4877. (c) Abe, M.; Saito, A.; Nakada, M. *Tetrahedron Lett.* **2010**, 51, 1298-1302.

⁵³⁹ Uwamori, M.; Nakada, M. *Tetrahedron Lett.* **2013**, 54, 2022-2025.

⁵⁴⁰ Uwamori, M.; Saito, A.; Nakada, M. *J. Org. Chem.* **2012**, 77, 5098-5107.

and subsequent Pd-mediated carbonylation led to ester **181**. Crabtree's catalyst facilitated stereoselective hydrogenation of the C6–C7 olefin, and subsequent functional group manipulations afforded acetate **182**. Allylic oxidation mediated by TBHP and Pearlman's catalyst afforded β -methoxyenone **183**. Mono-desilylation and Wittig homologation produced **184**, and a subsequent aldehyde Wittig homologation yielded enol ether **185**. Hydrolysis of this enol ether, another Wittig homologation, and C5 bridgehead allylation gave **186**. Deprotonation at C3, followed by transmetalation with Lipshutz's cuprate,⁵¹¹ and alkylation with allyl bromide yielded **187**. Conversion of the C1 hydroxymethylene of **187** to an isopropyl ketone afforded **188**, and subsequent global cross metathesis and C2 methyl ether cleavage revealed (\pm)-hyperforin (*rac*-**1**). A similar strategy was utilized in the total synthesis of (\pm)-nemorosone by Nakada.⁵⁴⁰



Scheme 1.23. Racemic total synthesis of (±)-hyperforin by Nakada (ref. 539).^a

^a Conditions: (a) Na, NH₃, *t*-BuOH, Et₂O, −78 °C; allyl bromide; (b) LAH, Et₂O, 0 °C; (c) TIPSOTf, NEt₃, CH₂Cl₂, 0 °C, 74% (3 steps); (d) K₂OsO₄·H₂O, K₃[Fe(CN)₆], K₂CO₃, (DHQD)₂PHAL, *t*-BuOH, H₂O; (e) NaIO₄, MeOH, H₂O, 81% (2 steps); (f) Me₃Al, PhMe, 0 °C; 3-nitrobenzaldehyde, PhMe, 0 °C to rt, 85%; (g) LHMDS, THF, −78 °C; CF₃CO₂CH₂CF₃; 4-nitrobenzenesulfonyl azide, NEt₃, 0 to 40 °C, 85%; (h) [Cu(OTf)]₂·PhMe, **178**, PhMe; (i) KHMDS, HMPA, PhMe, THF, −78 °C; allyl iodide, −78 to 0 °C; (j) KHMDS, HMPA, PhMe, THF, −78 °C; MeI, −78 °C to 0 °C; HCl, H₂O, THF, 88% (3 steps); (k) (Sia)₂BH, THF, −20 °C; NaOH, H₂O₂, H₂O, 78%; (l) TBSCl, NEt₃, DMAP, CH₂Cl₂, 99%; (m) Comins' reagent, KHMDS, PhMe, THF, 78 °C, 90%; (n) CO, Pd(OAc)₂, dppf, MeOH, DMF, 50 °C, 93%; (o) H₂, Crabtree's catalyst, DCE, reflux, 97%; (p) DIBAL, CH₂Cl₂, −78 °C; (q) Ac₂O, DMAP, NEt₃, CH₂Cl₂; (r) DMP, NaHCO₃, CH₂Cl₂, 89% (3 steps); (s) TBHP, Pd(OH)₂/C, K₂CO₃, CH₂Cl₂, 69%; (t) CSA, MeOH, CH₂Cl₂; (u) DMP, NaHCO₃, CH₂Cl₂; (v) PPh₃CH₃Br, *t*-BuOK, THF, 0 °C, 74% (3 steps); (w) K₂CO₃, MeOH; (x) DMP, NaHCO₃, CH₂Cl₂, 93% (2 steps); (y) PPh₃(Cl)CH₂OCH₃, KHMDS, THF, 0 °C, 79%; (z) *p*-TsOH, acetone, H₂O, 40 °C; (aa) PPh₃CH₃Br, *t*-BuOK, THF, 0 °C, 79% (2 steps); (bb) LiTMP, HMPA, THF, −78 °C; allyl bromide, 84%; (cc) LiTMP, THF, −78 °C; Li(2-Th)CuCN; allyl bromide, 90%; (dd) TBAF, THF; (ee) DMP, CH₂Cl₂, 84% (2 steps); (ff) *i*-PrMgCl, CeCl₃·2LiCl, THF, −78 °C; (gg) DMP, NaHCO₃, CH₂Cl₂, 71% (2 steps); (hh) **150**, isobutene, 120 °C, 93%; (ii) LiCl, DMSO, 120 °C, 62%.

While these dearomative alkylation approaches to PPAP natural products are useful and have successfully led to the synthesis of several PPAPs, a more direct strategy would involve *annulation* of a C6–C8 carbon bridge directly onto an aromatic nucleus. However this strategy is not without its

challenges, especially concerning the control of absolute and C7–C8 relative stereochemistry. Both Takagi and Porco have explored such dearomative annulation strategies, utilizing electrophiles such as acrylates **189**,⁵⁴¹ **190**,⁵⁴² and **191**⁵⁴³ as well as enals **192**⁵⁴⁴ and **193**⁵⁴⁵ and vinylsulfone **194**⁵⁴⁴ (Figure 1.20).

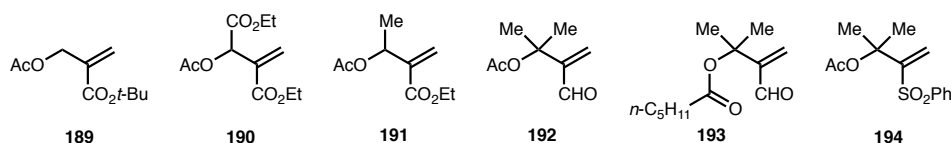


Figure 1.20. Various electrophiles utilized in “top-down” annulation strategies.

The total synthesis of *ent*-hyperibone K (*ent*-**195**) by Porco exemplifies the dearomative annulation strategy for PPAP construction (Scheme 1.24).⁵⁴⁵ bis-Prenylation of 2,4,6-trihydroxybenzophenone (**14**)⁵⁴⁶ using basic, aqueous conditions provided the natural acylphloroglucinol clusiaphenone B (**196**).⁵⁴⁷ Upon exposure of **196** to enal **193** in the presence of *Cinchona* alkaloid-derived phase-transfer catalyst **197**, adamantane **198** was produced enantioselectively. This is a remarkable reaction, considering that two quaternary stereocenters are formed along with the characteristic PPAP bicyclo[3.3.1]nonane core. Initially, this annulation was performed using enal **192**, but shorter reaction times and higher enantioselectivity was garnered using **193**. A mechanistic model for this transformation

⁵⁴¹ Takagi, R.; Nerio, T.; Miwa, Y.; Matsumura, S.; Ohkata, K. *Tetrahedron Lett.* **2004**, 45, 7401-7405.

⁵⁴² Takagi, R.; Miwa, Y.; Nerio, T.; Inoue, Y.; Matsumura, S.; Ohkata, K. *Org. Biomol. Chem.* **2007**, 5, 286-300.

⁵⁴³ (a) Takagi, R.; Inoue, Y.; Ohkata, K. *J. Org. Chem.* **2008**, 73, 9320-9325. (b) Kondo, H.; Inoue, Y.; Fujii, E.; Takagi, R.; Ohkata, K. *Symp. Chem. Nat. Prod.* **2008**, 50, 605-610.

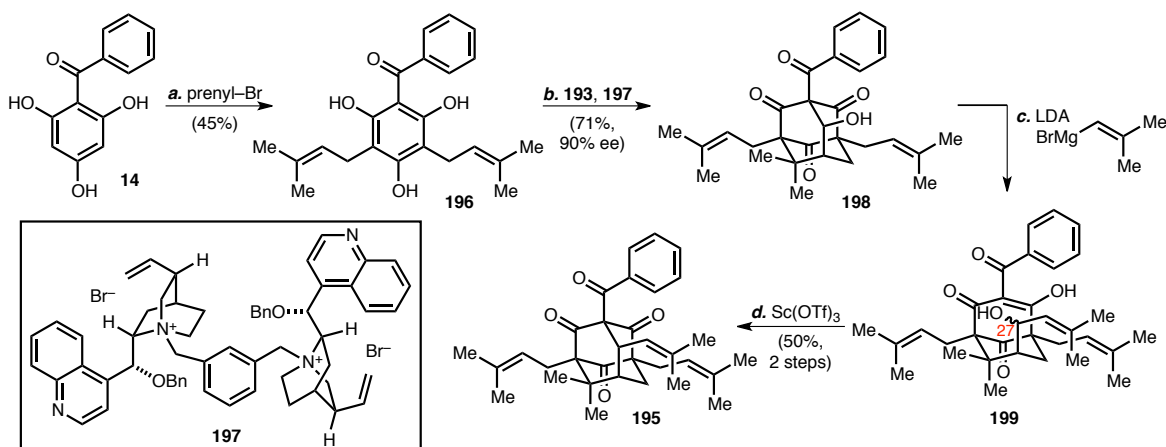
⁵⁴⁴ Qi, J.; Porco, J. A., Jr. *J. Am. Chem. Soc.* **2007**, 129, 12682-12683.

⁵⁴⁵ Qi, J.; Beeler, A. B.; Zhang, Q.; Porco, J. A., Jr. *J. Am. Chem. Soc.* **2010**, 132, 13642-13644.

⁵⁴⁶ **14** is available in 2 steps from 1,3,5-trimethoxybenzene: Mondal, M.; Puranik, V. G.; Argade, N. P. *J. Org. Chem.* **2007**, 72, 2068-2076.

⁵⁴⁷ Delle Monache, F.; Delle Monache, G.; Gacs-Baitz, E. *Phytochemistry* **1991**, 30, 2003-2005.

involves the formation of a tight ion pair between **196** and **197** in which only one face of **196** is available to engage in binding interactions with the enal electrophile. The remaining C–C bond required for the synthesis of hyperibone K from intermediate **198** was installed via deprotonation with LDA, revealing an aldehyde from a retro-aldol reaction, and trapping with 2-methyl-1-propenylmagnesium bromide, forming alcohol **199**. Exposure of this alcohol to $\text{Sc}(\text{OTf})_3$ yielded the enantiomer of hyperibone K (*ent*-**195**). This represents one of the only two total syntheses of adamantyl PPAPs reported to date. Using this synthesis strategy, Porco has successfully prepared (\pm)-clusianone,⁵⁴⁴ (\pm)-plukenetione A,⁵⁴⁸ and (\pm)-plukenetione D/E (7-*epi*-nemorosone).⁵⁴⁹



Scheme 1.24. Total synthesis of *ent*-hyperibone K by Porco (ref. 545).^a

^a Conditions: (a) prenol bromide, KOH, H_2O , 0 °C, 45%; (b) **193**, **197**, $\text{CsOH} \cdot \text{H}_2\text{O}$, 4 Å MS, CH_2Cl_2 , –50 °C, 71%, 90% ee; (c) LDA, 2-methyl-1-propenylmagnesium bromide, THF, –78 to –55 °C; (d) $\text{Sc}(\text{OTf})_3$, CH_3NO_2 , 50% (2 steps).

Aside from the approaches outlined above that were developed specifically for PPAP synthesis, more general strategies toward the construction of bicyclo[3.3.1]nonanes have been developed.⁵⁵⁰ Several

⁵⁴⁸ Zhang, Q.; Mitasev, B.; Qi, J.; Porco, J. A., Jr. *J. Am. Chem. Soc.* **2010**, *132*, 14212–14215.

⁵⁴⁹ Zhang, Q.; Porco, J. A., Jr. *Org. Lett.* **2012**, *14*, 1796–1799.

⁵⁵⁰ For a review of bicyclo[3.3.1]nonane synthesis, see: Butkus, E. *Synlett* **2001**, 1827–1835.

tactics include intramolecular conjugate addition reactions to both enones⁵⁵¹ and ynones.⁵⁵² Intermolecular cascade annulations involving unsaturated carbonyl systems have also been explored.⁵⁵³ Rhenium-,⁵⁵⁴ gold-,⁵⁵⁵ and copper-mediated⁵⁵⁶ additions of cyclohexanones and their enol ether derivatives have yielded bicyclo[3.3.1]nonane systems. Barriault has reported the use of a Prins-pinacol reaction to fashion a variety of bicyclic ring scaffolds.⁵⁵⁷ An S_N2-type cyclization involving primary tosylate displacement has been explored.⁵⁵⁸

Apart from cyclization strategies, Tadano has developed a zinc-mediated Barbier-type allylation reaction utilizing sugar-based aldehydes to construct stereogenic quaternary carbon centers that resemble the C8 center of PPAPs that bear differential substitution at that position (e.g., hyperforin).⁵⁵⁹

⁵⁵¹ Srikrishna, A.; Kumar, P. P.; Reddy, T. J. *Arkivoc* **2003** (Part iii), 55-66.

⁵⁵² Klein, A.; Miesch, M. *Tetrahedron Lett.* **2003**, *44*, 4483-4485.

⁵⁵³ (a) Barboni, L.; Gabrielli, S.; Palmieri, A.; Femoni, C.; Ballini, R. *Chem. Eur. J.* **2009**, *15*, 7867-7870. (b) Zhao, Y.-L.; Chen, L.; Yang, S.-C.; Tian, C.; Liu, Q. *J. Org. Chem.* **2009**, *74*, 5622-5625. (c) Wang, D.; Crowe, W. E. *Org. Lett.* **2010**, *12*, 1232-1235.

⁵⁵⁴ Kuninobu, Y.; Morita, J.; Nishi, M.; Kawata, A.; Takai, K. *Org. Lett.* **2009**, *11*, 2535-2537.

⁵⁵⁵ (a) Barabé, F.; Bétournay, G.; Bellavance, G.; Barriault, L. *Org. Lett.* **2009**, *11*, 4236-4238. (b) Sow, B.; Bellavance, G.; Barabé, F.; Barriault, L. *Beilstein J. Org. Chem.* **2011**, *7*, 1007-1013.

⁵⁵⁶ Zhang, C.; Hu, X.-H.; Wang, Y.-H.; Zheng, Z.; Xu, J.; Hu, X.-P. *J. Am. Chem. Soc.* **2012**, *134*, 9585-9588.

⁵⁵⁷ Lavigne, R. M. A.; Riou, M.; Girardin, M.; Morency, L.; Barriault, L. *Org. Lett.* **2005**, *7*, 5921-5923.

⁵⁵⁸ Majumber, A.; Mandal, A.; Ghosh, P. *J. Atoms Mol.* **2012**, *2*, 176-181.

⁵⁵⁹ Takao, K.-i.; Miyashita, T.; Akiyama, N.; Kurisu, T.; Tsunoda, K.; Tadano, K.-i. *Heterocycles* **2012**, *86*, 147-153.

Chapter 2

Strategies Toward Hyperforin Synthesis

Synthesis Overview

As elaborated above, hyperforin displays a broad spectrum of biological activity.⁵⁶⁰ Moreover, hyperforin is believed to be the component of St. John's wort that is responsible for its antidepressant activity. This is particularly noteworthy given hyperforin's unique mechanism of action and absence of deleterious side effects that often accompany the use of other clinical antidepressants. However, hyperforin's therapeutic potential is handicapped by several factors: (1) its poor water-solubility; (2) its fragility, readily decomposing in the presence of light and air;⁵⁶¹ and (3) its potent activation of PXR, causing increases in gene expression levels of many proteins involved in xenobiotic metabolism.

In order to mitigate these shortcomings while maintaining potential salutary benefits, access to a broad spectrum of hyperforin analogs is necessary. While semisynthetic manipulation of hyperforin has led to a limited number of such derivatives,⁵⁶² total synthesis is the only means by which diverse hyperforin analogs may be obtained. Even though several synthesis endeavors have led to the total synthesis of both racemic and *ent*-hyperforin,⁵⁶³ the considerable length of these routes renders analog synthesis impractical. Therefore, our goal was to devise a short, enantioselective approach to hyperforin that would be amenable to the synthesis of a variety of hyperforin mimetics and enable the first full structure-activity relationship study of hyperforin.

Further, we rationalized that latent symmetry elements in hyperforin may be exploited to expedite total synthesis. Imbedded within the hyperforin bicyclo[3.3.1]nonane core is a 1,3,5-cyclohexanetrione subunit (highlighted in blue in Scheme 2.1a). Retrosynthetic cleavage of the C5–C6 bond in hyperforin (**1**) via intramolecular S_N2-type displacement-cyclization would reveal monocyclic intermediate **200**.

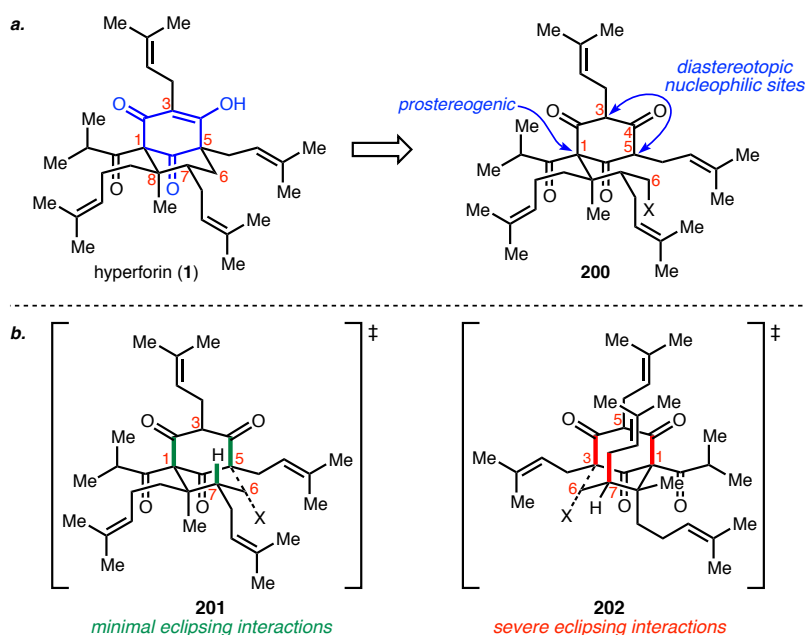
⁵⁶⁰ For reviews of hyperforin biological activity, see: (a) Barnes, J.; Anderson, L. A.; Phillipson, J. D. *J. Pharm. Pharmacol.* **2001**, *53*, 583-600. (b) Zanolì, P. *CNS Drug Rev.* **2004**, *10*, 203-218. (c) Vollmer, J. J.; Rosenson, J. J. *Chem. Ed.* **2004**, *81*, 1450-1456. (d) Medina, M. A.; Martínez-Poveda, B.; Amores-Sánchez, M. I.; Quesada, A. R. *Life Sci.* **2006**, *79*, 105-111. (e) Beerhues, L. *Phytochemistry* **2006**, *67*, 2201-2207.

⁵⁶¹ See discussion on page 75.

⁵⁶² For examples of semisynthetic hyperforin analogs, see refs. 259 and 309, and: Bombardelli, E.; Morazzoni, P.; Riva, A.; Fuzzati, N. US Patent 2005/0222274 A1, October, 6, 2005.

⁵⁶³ See discussion on page 108.

Given the substitution pattern around this cyclohexanetrione ring, the C1 quaternary center of **200** is prostereogenic owing to a plane of symmetry intersecting the C1 and C4 atoms. C1 stereochemistry is introduced during the subsequent alkylation event, in which two possible nucleophilic carbon atoms (i.e., C3 and C5) may engage the electrophilic C6. We rationalized that the C7 prenyl substituent stereochemistry would bias the formation of a C5–C6 bond over C3–C6 bond formation (Scheme 2.1b). The former situation would lead to transition state **201**, bearing a pseudoequatorial C7 prenyl substituent, whereas the latter bond-forming event would lead to transition state **202** containing a pseudoaxial C7 prenyl moiety whose orientation begets two *syn*-pentane-like interactions with the C1–C9 and C3–C4 bonds.

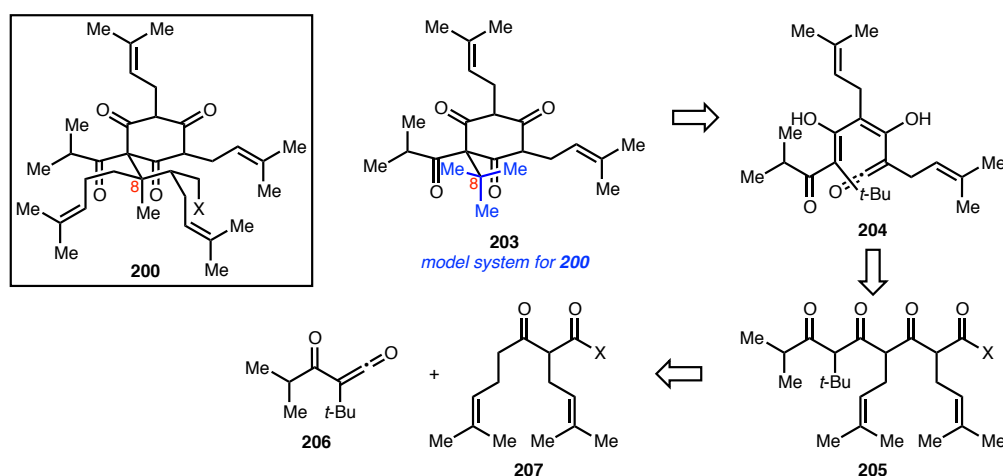


Scheme 2.1. (a) Retrosynthetic analysis of hyperforin and (b) transition-state analysis of key cyclization event.

Polyketide Cyclization Approach

Prior to evaluating the plausibility of using this cyclization to construct hyperforin, synthesis of monocyclic precursor **200** was required. In order to evaluate the feasibility of synthesizing **200**, a model system in which the C8 stereogenic center of hyperforin was replaced with a *tert*-butyl group (**203**) was

established (Scheme 2.2). We hypothesized that **203** would be accessed via dienylketene **204** via either a Dieckmann cyclization or a 6π electrocyclization. Conjugated dienylketenes are known to undergo cyclization under fairly mild conditions,⁵⁶⁴ even to form nonaromatic carbocyclic products.⁵⁶⁵ This dienylketene would be accessed via tetraketide **205**, the product of the coupling reaction between acylketene **206** with β -ketocarbonyl species **207**. This route was particularly appealing owing to the lack of oxidation-state changes and protecting group manipulations.



Scheme 2.2. Retrosynthesis of model system **203** via tetraketide **205**.

Initially, we explored the feasibility of constructing several tetraketide-type species similar to **205** (Figure 2.1). Moreover, we chose to explore the coupling chemistry of the previously characterized and prepared *tert*-butylcarbethoxyketene⁵⁶⁶ (**208**) before exploring the synthesis of the potentially unstable α -ketoketene **206**. Due to both the stabilizing effect of the conjugated ester and the steric nature of the *tert*-

⁵⁶⁴ For reviews, see: (a) Harris, T. M.; Harris, C. M. *Tetrahedron* **1977**, *33*, 2159-2185. (b) Harris, T. M.; Harris, C. M. *Pure Appl. Chem.* **1986**, *58*, 283-294.

⁵⁶⁵ For examples of nonaromatic cyclizations of polyketide-type products, see: (a) Griffiths, J.; Hart, H. *J. Am. Chem. Soc.* **1968**, *90*, 3297-3298. (b) Dannenberg, W.; Perst, H.; Seifert, W. *J. Tetrahedron Lett.* **1975**, *16*, 3481-3484. (c) Fishbein, P. L.; Moore, H. W. *J. Org. Chem.* **1985**, *50*, 3226-3228. (d) Hsung, R. P.; Wulff, W. D. *J. Am. Chem. Soc.* **1994**, *116*, 6449-6450.

⁵⁶⁶ (a) Newman, M. S.; Zuech, E. A. *J. Org. Chem.* **1962**, *27*, 1436-1438. (b) Evans, A. R.; Hafiz, M.; Taylor, G. A. *J. Chem. Soc., Perkin Trans. I* **1984**, 1241-1245.

butyl substituent, **208** can be isolated and distilled in the absence of solvent. Several candidate dienylketene precursors were explored. An α -oxoketene may be generated from the thermolysis of a dioxinone,⁵⁶⁷ such as **209**. α -Oxoketenes may also be generated from the elimination of alcohols and thiols from β -ketoesters and β -ketothioesters, respectively, which also led us to pursue **210** and **211**.⁵⁶⁸

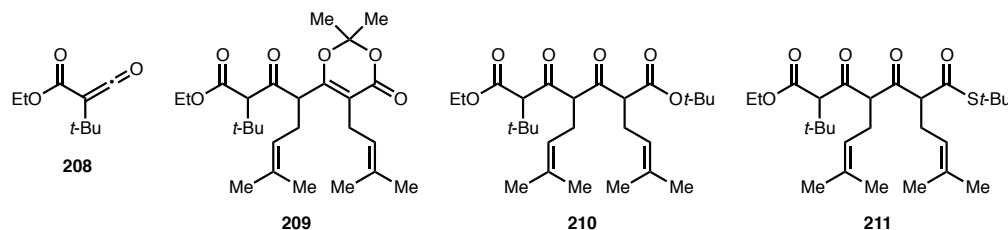


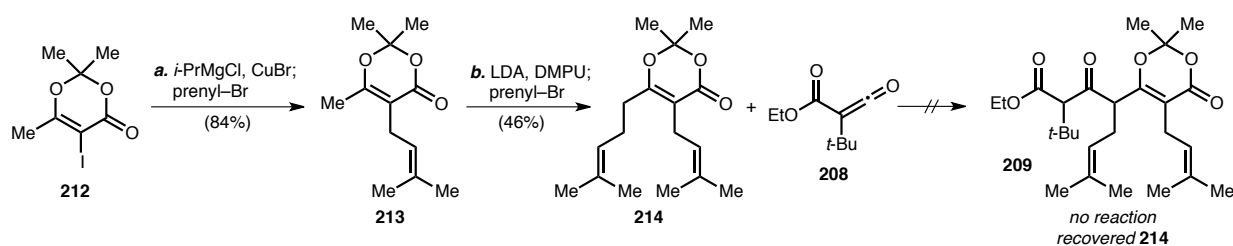
Figure 2.1. Carbethoxyketene **208** and several potential dienylketene precursors.

We first explored the synthesis of dioxinone **209** (Scheme 2.3). Magnesium-iodine exchange of iododioxinone **212**⁵⁶⁹ followed by CuBr-mediated transmetalation and trapping with prenyl bromide afforded intermediate **213**. Deprotonation using LDA and trapping with a second equivalent of prenyl bromide afforded **214**. However, numerous attempts of the coupling of anions derived from **209** as well as its silyl dienyl ether only led to recovery of **214** and hydrolysis of ketene **208**. We concluded that the nucleophilic derivatives of **209** were not reactive enough to engage ketene **208**.

⁵⁶⁷ For a review of dioxinone chemistry, see: Kaneko, C.; Sato, M.; Sakaki, J.-i.; Abe, Y. *J. Heterocyclic Chem.* **1990**, *27*, 25-30.

⁵⁶⁸ For reviews on the synthesis and chemistry of α -oxoketenes, see: (a) Moore, H. W.; Decker, O. H. W. *Chem. Rev.* **1986**, *86*, 821-830. (b) Seikaly, H. R.; Tidwell, T. T. *Tetrahedron* **1986**, *42*, 2587-2613. (c) Tidwell, T. T. *Acc. Chem. Res.* **1990**, *23*, 273-279. (d) Wentrup, C.; Heilmeyer, W.; Kollenz, G. *Synthesis* **1994**, 1219-1248.

⁵⁶⁹ Iwaoka, T.; Murohashi, T.; Katagiri, N.; Sato, M.; Kaneko, C. *J. Chem. Soc., Perkin Trans. 1* **1992**, 1393-1397.



Scheme 2.3. Attempted Synthesis of dioxinone **209**.^a

^a Conditions: (a) *i*-PrMgCl, THF, −30 °C; CuBr, LiCl, −30 °C; prenyl bromide, −30 °C, 84%; (b) LDA, DMPU, THF, 0 °C; **214**, 0 °C; prenyl bromide, −40 °C to rt, 46%.

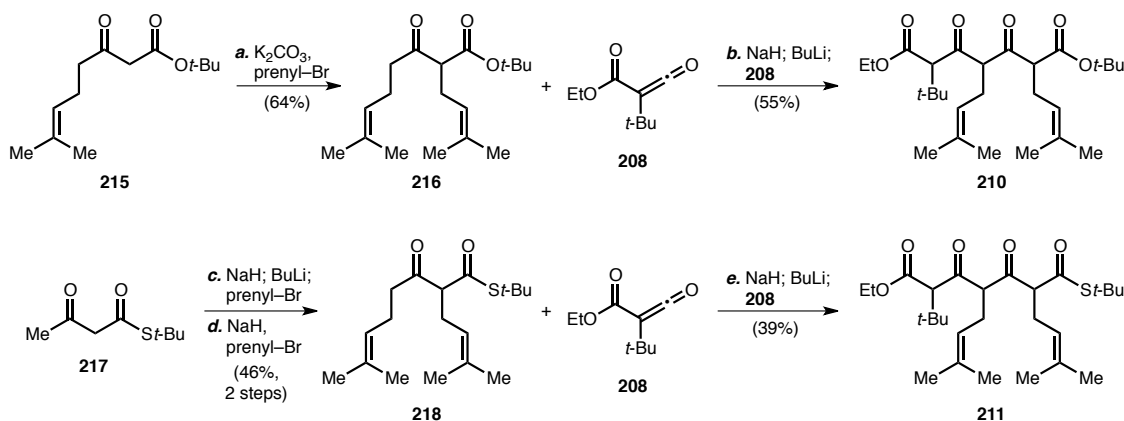
While we failed to observe reactivity using monoanions derived from **214**, we hypothesized that more nucleophilic, Weiler-type dianions generated from β-ketocarbonyl-type systems would react with ketene **208**.⁵⁷⁰ Indeed, both tetraketides **210** and **211** were synthesized (Scheme 2.4). Prenylation of the dianion generated from acetoacetate **215**⁵⁷¹ yielded **216**. The reaction of the dianion generated from this acetoacetate with ketene **208** afforded adduct **210** as a complex mixture of diastereomers and tautomers. Likewise, the synthesis of **211** proceeded in similar fashion. Stepwise prenylation of *tert*-butyl acetothioacetate⁵⁷² (**217**) led to the isolation of **218**. The use of DME as solvent in these alkylations was crucial in preventing the formation of byproducts.⁵⁷³ Coupling with ketene **208** was achieved, affording key tetraketide **211**.

⁵⁷⁰ (a) Hucklin, S. N.; Weiler, L. *J. Am. Chem. Soc.* **1974**, *96*, 1082-1087. (b) Huckin, S. N.; Weiler, L. *Can. J. Chem.* **1974**, *52*, 1343-1351.

⁵⁷¹ Yang, D.; Gao, Q.; Lee, O.-Y. *Org. Lett.* **2002**, *4*, 1239-1241.

⁵⁷² Sakaki, J.-i.; Kobayashi, S.; Sato, M.; Kaneko, C. *Chem. Pharm. Bull.* **1990**, *38*, 2262-2264.

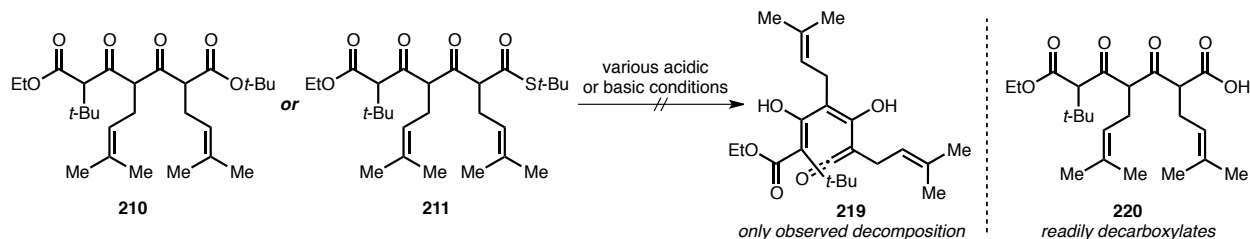
⁵⁷³ (a) Booth, P. M.; Fox, C. M. J.; Ley, S. V. *Tetrahedron Lett.* **1983**, *24*, 5143-5146. (b) Booth, P. M.; Fox, C. M. J.; Ley, S. V. *J. Chem. Soc., Perkin Trans. 1* **1987**, 121-129.



Scheme 2.4. Synthesis of tetraketides **210** and **211**.^a

^a Conditions: (a) K₂CO₃, prenyl bromide, DMF, acetone, reflux, 64%; (b) NaH, THF, 0 °C; BuLi, 0 °C; **208**, 0 °C to rt, 55%; (c) NaH, DME, 0 °C; BuLi, –30 °C; prenyl bromide, –30 °C to rt, 61%; (d) NaH, DME, 0 °C; prenyl bromide, 0 °C to rt, 75%; (e) NaH, DME, 0 °C; BuLi, –30 °C; **208**, –30 °C to rt, 39%.

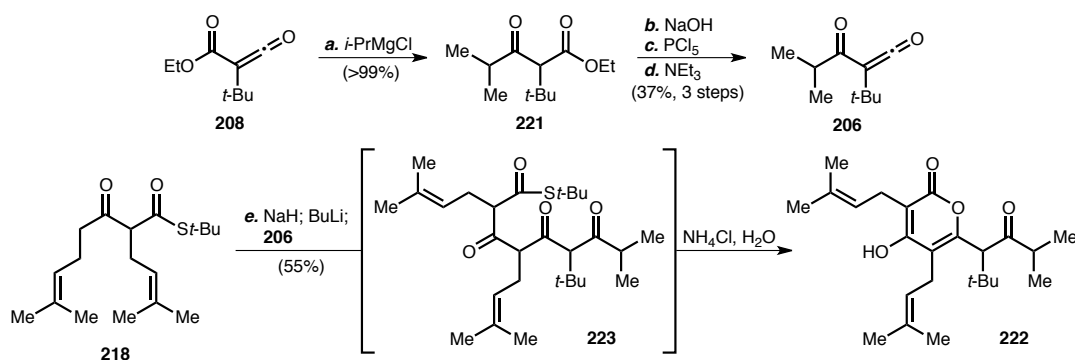
Unfortunately, all attempts at the generation of dienylketene **219** from either **210** or **211** en route to carbocycle **203** were unsuccessful (Scheme 2.5). Treatment of these tetraketides with acid or base in order to directly generate a ketene intermediate led to decomposition. While it was possible to obtain the extremely unstable carboxylic acid **220**, any attempts to activate this intermediate (e.g., formation of an acid chloride) led to facile decarboxylation.



Scheme 2.5. Attempted ketene generation from tetraketides **210** and **211**.

Concurrent to these studies, we also assessed the feasibility of synthesizing and coupling ketoketene **206** (Scheme 2.6). First, *i*-PrMgCl addition to carbethoxyketene **208** gave β-ketoester **221**.

Stepwise saponification, acid chloride formation, and treatment with NEt₃ afforded ketoketene **206** as a volatile liquid that was stable in the absence of solvent. Upon coupling of β -ketothioester **218** with **206**, we were surprised to isolate α -pyrone **222**. Upon careful analysis of the reaction conditions, it was discovered that the direct product of the coupling reaction was linear polyketide **223**, which upon acidic workup afforded pyrone **222**. Performing a basic aqueous workup gave decreased amounts of this product. Similar acid-mediated heterocyclizations of triketothioacids have been reported.⁵⁷⁴ While the formation of pyrone **222** was undesirable, Harris has reported the conversion of 6-acyl-4-hydroxy-2-pyrone, such as product **222**, to acylphloroglucinols through the use of non-nucleophilic bases, such as LDA or LiH, possibly proceeding through a dienylketene intermediate similar to **204**.⁵⁷⁵



Scheme 2.6. Synthesis of ketene **206** and coupling with β -ketothioester **218**.^a

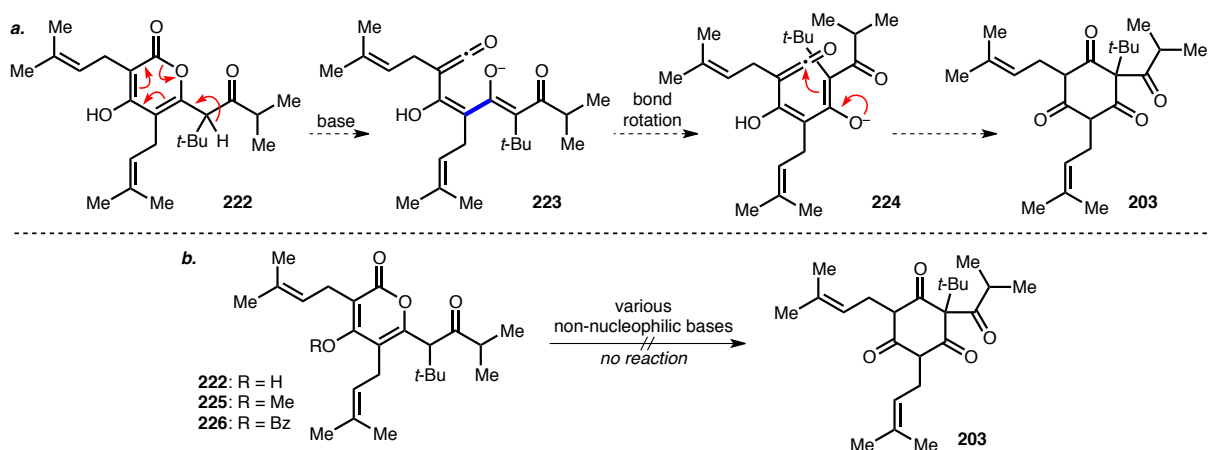
^a Conditions: (a) *i*-PrMgCl, THF, 0 °C to rt, >99%; (b) NaOH, MeOH, H₂O; (c) PCl₅, Et₂O, reflux, 73% (2 steps); (d) NEt₃, PhH, 51%; (e) NaH.

We hypothesized that the conversion of 6-acyl-4-hydroxy-2-pyrone **222** to key intermediate **203** would proceed through deprotonation of the internal, doubly conjugated methine to reveal extended enolate **224** (Scheme 2.7a). Upon bond rotation and carbon-carbon bond formation, cyclohexanetrione **203** would be accessed, an overall internal *O*-to-*C* acyl migration process. Despite screening a variety of

⁵⁷⁴ Harris, T. M.; Harris, C. M. *Tetrahedron* **1969**, 25, 2687-2691.

⁵⁷⁵ Harris, T. M.; Wachter, M. P. *Tetrahedron* **1970**, 26, 5255-5263.

non-nucleophilic bases, we were not able to achieve this transformation (Scheme 2.7b). In most cases, **222** was recovered. Deuterium quench experiments indicated that the isopropyl methine and the pyrone hydroxyl group were the only two positions on **222** being appreciably deprotonated. Use of derivatives of **222** in which the pyrone hydroxyl group was blocked (i.e., **225** and **226**) also did not facilitate desired carbocycle formation. We concluded that not only was deprotonation extremely difficult at the desired site, but the conversion of pyrone **222**, which bears some aromatic character, to the non-aromatic cyclohexanetrione **203** is a thermodynamically unfavorable process.

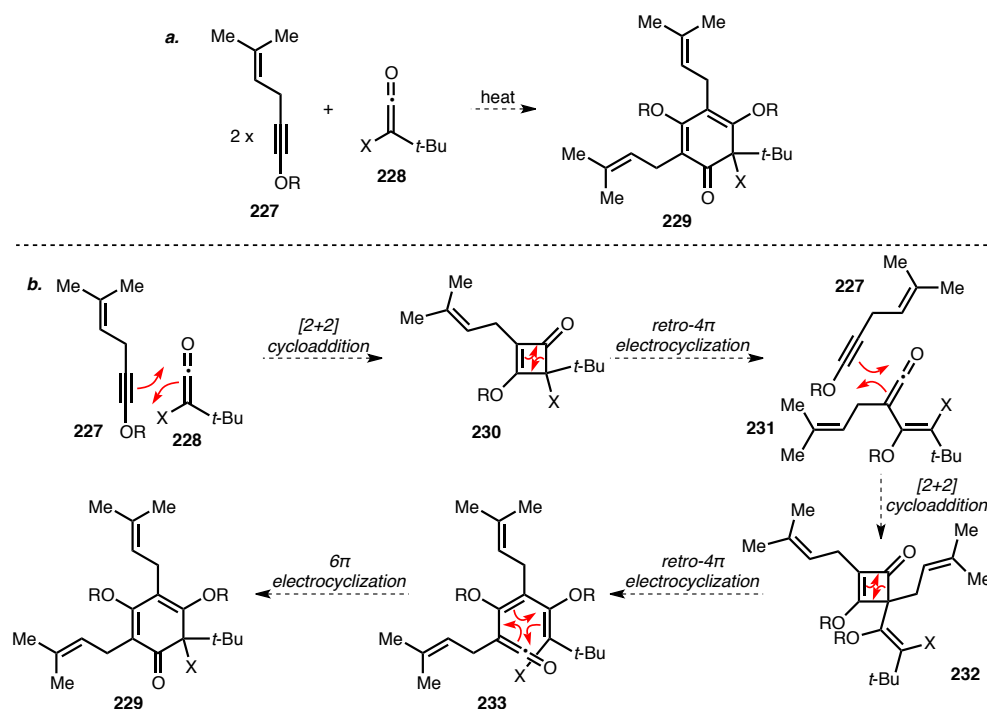


Scheme 2.7. (a) Proposed and (b) unsuccessful synthesis of carbocycle **203** from pyrone **222**.

Electrocyclic Cascade Approach

Due to the propensity of a linear polyketide to undergo *O*-cyclization to form a pyrone, we explored an alternative synthesis strategy that would mitigate heterocycle formation. We surmised that an electrocyclic cascade reaction involving two equivalents of an alkynyl ether (**227**) and a disubstituted ketene (**228**) may be used to construct **229**, which is a diether of carbocycle **203** (Scheme 2.8a). In this reaction, a [2+2] cycloaddition of one equivalent of the alkynyl ether **227** with ketene **228** would produce cyclobutenone **230** (Scheme 2.8b). Subsequent thermolysis would reveal vinylketene **231** via retro-4 π

electrocyclization,⁵⁷⁶ which upon exposure to a second equivalent of alkynyl ether **227** would undergo a second [2+2] cycloaddition to form homologated cyclobutenone **232**. After another retro-4 π electrocyclicization to reveal a dienylketene **233**, a final 6 π electrocyclicization would yield **229**. Analogous electrocyclic cascade reactions have been used to synthesize heavily substituted aryl rings,⁵⁷⁷ and in several instances even non-aromatic cyclohexadienones.⁵⁷⁸



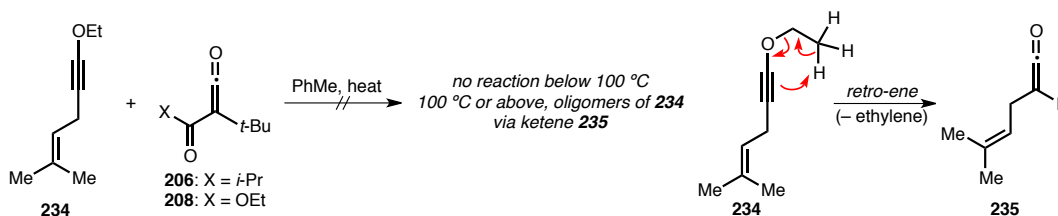
Scheme 2.8. (a) Proposed electrocyclic cascade and (b) mechanism for the synthesis of cyclohexadienone **229**.

⁵⁷⁶ For reviews of electrocyclic opening of cyclobutenones, see: (a) Belluš, D.; Ernst, B. *Angew. Chem. Int. Ed. Engl.* **1988**, *27*, 797-827. (b) Moore, H. W.; Yersa, B. R. *Chemtracts Org. Chem.* **1992**, *5*, 273-313.

⁵⁷⁷ (a) Druey, J.; Jenny, E. F.; Schenker, K.; Woodward, R. B. *Helv. Chim. Acta* **1962**, *45*, 600-610. (b) Swenton, J. S.; Saurborn, E.; Srinivasan, R.; Sonntag, F. I. *J. Am. Chem. Soc.* **1968**, *90*, 2990-2991. (c) Neuse, E. W.; Green, B. R. *Liebigs Ann. Chem.* **1974**, 1534-1535. (d) Mayr, H. *Angew. Chem. Int. Ed. Engl.* **1975**, *14*, 500-501. (e) Danheiser, R. L.; Gee, S. K. *J. Org. Chem.* **1984**, *49*, 1672-1674. (f) Taing, M.; Moore, H. W. *J. Org. Chem.* **1996**, *61*, 329-340. (g) Turnbull, P.; Heileman, M. J.; Moore, H. W. *J. Org. Chem.* **1996**, *61*, 2584-2585. (h) Xiong, Y.; Moore, H. W. *J. Org. Chem.* **1996**, *61*, 9168-9177. (i) Paquette, L. A. *Eur. J. Org. Chem.* **1998**, 1709-1728.

⁵⁷⁸ (a) Fishbein, P. L.; Moore, H. W. *J. Org. Chem.* **1985**, *50*, 3226-3228. (b) Dorsey, D. A.; King, S. M.; Moore, H. W. *J. Org. Chem.* **1986**, *51*, 2814-2816.

We first analyzed the reactivity of ketenes **206** and **208** with the known ethyl alkynyl ether **234**, synthesized from the prenylation of ethoxyacetylene (Scheme 2.9).⁵⁷⁹ At temperatures below 100 °C, no reaction occurred; however, above this threshold, oligomerization of **234** was observed. At such temperatures, a retro-ene reaction may occur with **234**,⁵⁸⁰ producing the very reactive monosubstituted ketene **235**.



Scheme 2.9. Attempted cycloaddition of alkynyl ether **234** with ketenes **206** and **208**.

In order to possibly circumvent this issue, we hypothesized that *tert*-butylcyanoketene⁵⁸¹ (**236**) may react with alkynyl ether **234** at reduced temperatures due to the reduced steric environment surrounding the reactive ketene functionality (Scheme 2.10).⁵⁸² Unlike acylketenes **206** and **208**, cyanoketene **236** cannot be isolated neat; it is generated through the thermolysis of diazidobenzoquinone **237** in toluene solution.^{583,584} After generating a solution of **236**, addition of alkynyl ether **234** afforded not only the [2+2] cycloaddition product, cyclobutenone **238**, but also azabicyclo[4.2.0]octantrienone

⁵⁷⁹ Gao, X.; Hall, D. G. *J. Am. Chem. Soc.* **2005**, *127*, 1628-1629.

⁵⁸⁰ Liang, L.; Ramaseshan, M.; MaGee, D. I. *Tetrahedron* **1993**, *49*, 2159-2168.

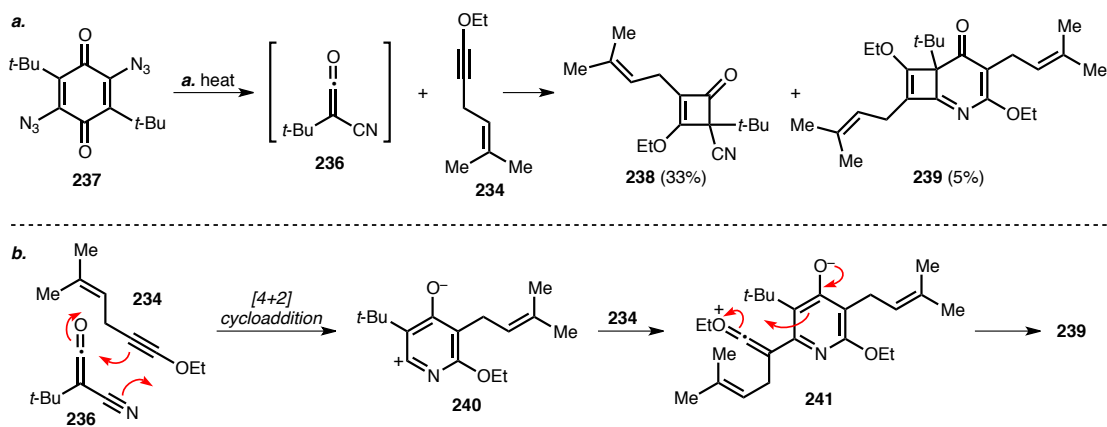
⁵⁸¹ For examples of reactions involving **236**, see: Al-Husaini, A. H.; Moore, H. W. *J. Org. Chem.* **1985**, *50*, 2595-2597.

⁵⁸² For a review of cyanoketene chemistry, see: Moore, H. W.; Gheorghiu, M. D. *Chem. Soc. Rev.* **1981**, *10*, 289-328.

⁵⁸³ Weyler, W., Jr.; Duncan, W. G.; Liewen, M. B.; Moore, H. W. *Org. Synth.* **1976**, *55*, 32-38.

⁵⁸⁴ We attempted to synthesize **236** from a 2-cyanoacetyl chloride (analogous to the synthesis of ketene **206**); however, an allene was cleanly afforded, presumably through NEt₃-promoted hetero-[2+2] cycloaddition of two equivalents of the ketene followed by decarboxylation of the resulting β -lactone.

239. A possible mechanism for the formation of **239** involves the [4+2] cycloaddition of **236** with **234** to form **240**, which may be depicted as a dipole or a diradical. Coupling of this intermediate with a second equivalent of alkynyl ether **234** would afford **239** via **241**. An electrocyclic cascade that may involve an intermediate similar to **240** has been reported.⁵⁸⁵ Further, heating a solution of **238** and **234** did not yield **239**, demonstrating that **238** is not an intermediate in the synthesis of **239**. Subsequent optimization of this reaction for the synthesis of cyclobutenone **238** allowed us to access functional amounts of this intermediate for later electrocyclic cascade cyclization studies.⁵⁸⁶



Scheme 2.10. (a) Thermolytic formation of **238** and **239**, and (b) a possible mechanism for the formation of **239**.^a

^a Conditions: (a) PhMe, reflux; **234**, rt to 120 °C, 33% **238**, 5% **239**.

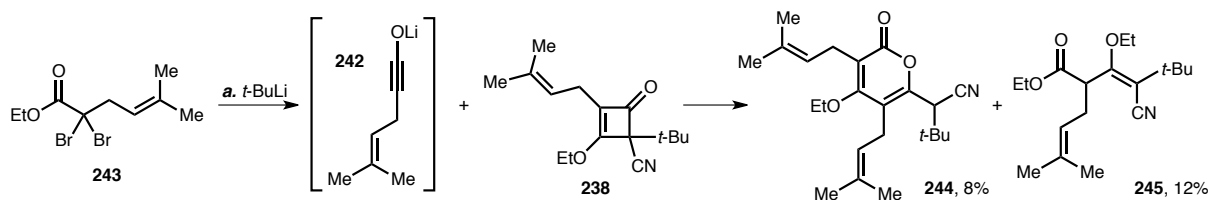
We then explored the use of cyclobutenone **238** as an intermediate toward desired cyclohexadienone **229**. As indicated above, extended heating of **238** with alkynyl ether **234** did not yield further coupling products. Attempted coupling of the more reactive lithium alkynoate **242**, generated from successive lithium-bromine exchanges from α,α -dibromoester **243**,⁵⁸⁷ only gave low yields of α -pyrone **244** and linear ethyl ester **245**, formed through the interception and opening of the cyclobutenone

⁵⁸⁵ Nguyen, N. V.; Chow, K.; Karlsson, J. O.; Doedens, R. J.; Moore, H. W. *J. Org. Chem.* **1986**, *51*, 419-420.

⁵⁸⁶ See the experimental section of this chapter for details.

⁵⁸⁷ (a) Shindo, M.; Sato, Y.; Shishido, K. *Tetrahedron* **1998**, *54*, 2411-2422. (b) Shindo, M.; Sato, Y.; Koretsune, R.; Yoshikawa, T.; Matsumoto, K.; Itoh, K.; Shishido, K. *Chem. Pharm. Bull* **2003**, *51*, 477-478.

by residual ethoxide from the formation of alkynoate **242** (Scheme 2.11). Akin to the polyketide route results, pyrone formation prevails in the absence of oxygen blocking groups. The ethanolysis product **245** along with its double-bond isomer was also generated by heating **238** with ethanol.



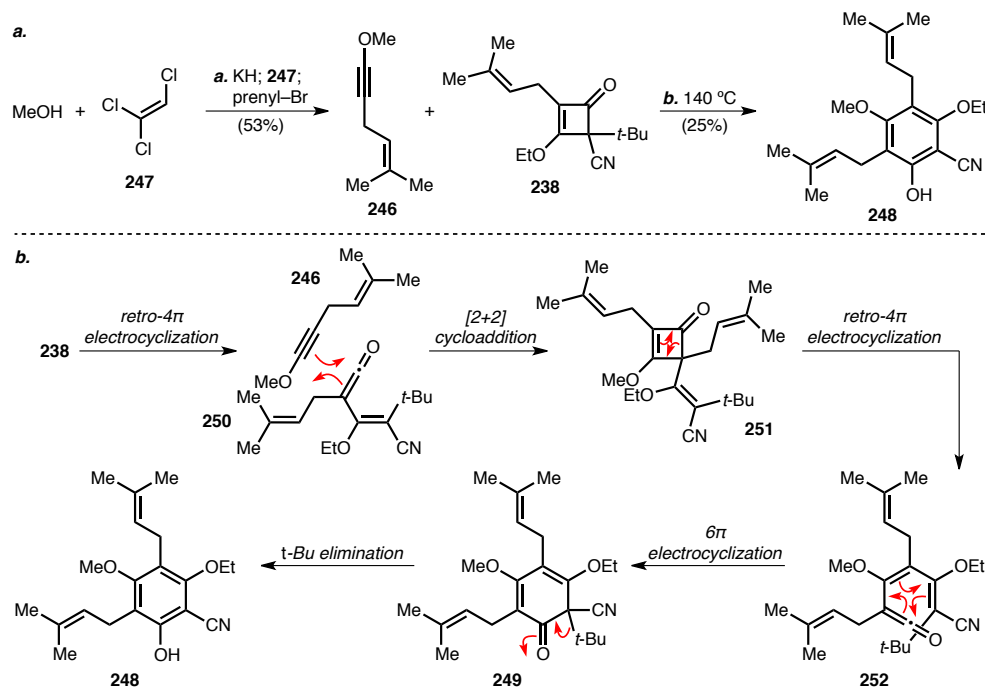
Scheme 2.11. The reaction of *in situ* derived lithium alkynoate **242** with cyclobutenone **238**.^a

^a Conditions: (a) *t*-BuLi, THF, -78 °C to rt; **238**, 8% **244**, 12% **245**.

Owing to pyrone formation from the use of alkynoate **242** and the propensity of ethyl alkynyl ether **234** to undergo retro-ene cyclization, we then investigated the use of methyl alkynyl ether **246**, an alkynyl ether incapable of retro-ene rearrangement. It was synthesized from the base-mediated coupling of dichloroacetylene (generated *in situ* from trichloroethylene, **247**), methanol, and prenyl bromide (Scheme 2.12a).⁵⁸⁸ However, when an excess of **246** was heated to 140 °C with cyclobutenone **238**, the only product isolated was phloroglucinol diether **248**. A plausible mechanism for the formation of this aromatic product is shown in Scheme 2.12b. Coupling of **238** with **246** to afford the desired cyclohexadienone **249** may have occurred via the proposed electrocyclic cascade reaction—[2+2] cycloaddition of ring-opened vinylketene **250** with alkynyl ether **246**, ensuing retro-4 π electrocyclization of cyclobutenone **251** to dienylketene **252**, and subsequent 6 π electrocyclization to give **249**—but under the reaction conditions, rapid loss of the *tert*-butyl group from **249** may have afforded **248**. This dissociation may operate via a concerted retro-ene cyclization process or an ionic retro-S_N1-type reaction.

⁵⁸⁸ (a) Moyano, A.; Charbonnier, F.; Greene, A. E. *J. Org. Chem.* **1987**, 52, 2919-2922. (b) Denmark, S. E.; Dixon, J. A. *J. Org. Chem.* **1998**, 63, 6167-6177.

Miller and others have observed the elimination of sterically demanding alkyl groups from similar “blocked aromatic” cyclohexadienone systems.⁵⁸⁹



Scheme 2.12. (a) Synthesis and (b) possible mechanism for the formation of **248** from the coupling of **246** and **238**.^a

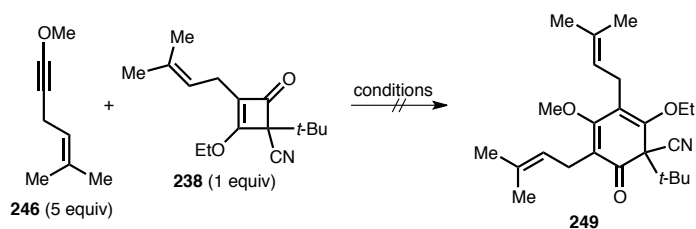
^a Conditions: (a) MeOH, KH, THF; **247**, -60 °C to rt; BuLi, -78 to -10 °C; prenyl bromide, HMPA, -78 °C to rt, 53%; (b) xylenes, 140 °C, 25%.

We then explored potential methods of mitigating this terminal *tert*-butyl elimination step to isolate the desired cyclohexadienone **249** (Table 2.1). As mentioned above, Miller has observed similar *tert*-butyl eliminations from cyclohexadienones, and these processes were mediated by either heat or acid.^{589a-c} We repeated the reaction of alkynyl ether **246** with cyclobutenone **238** in the presence of amine base to determine if trace amounts of acid were promoting this elimination. However, in the presence of

⁵⁸⁹ (a) Miller, B.; Margulies, H. *J. Am. Chem. Soc.* **1965**, *87*, 5106-5111. (b) Miller, B. *J. Am. Chem. Soc.* **1970**, *92*, 6252-6259. (c) Miller, B. *Acc. Chem. Res.* **1975**, *8*, 245-256. (d) Nishinaga, A.; Shimizu, T.; Matsuura, T. *Tetrahedron Lett.* **1981**, *22*, 5293-5296. (e) Tashiro, M.; Itoh, T.; Yoshiya, H.; Fukata, G. *Org. Prep. Proced. Int.* **1984**, *16*, 155-164. (f) Hewgill, F. R.; Stewart, J. M. *J. Chem. Soc., Chem. Commun.* **1984**, 1419-1420. (g) Kende, A. S.; Hebeisen, P. *Tetrahedron Lett.* **1985**, *26*, 3769-3772. (h) Miller, B.; Baghdadchi, J. *J. Chem. Soc., Chem. Commun.* **1986**, 511-512. (i) Miller, B.; Baghdadchi, J. *J. Org. Chem.* **1987**, *52*, 3390-3394.

N,N-diethylaniline (entry 1), not only was a greater proportion of **248** obtained but we also isolated ester **253** (Figure 2.2), the result of opening of cyclobutenone **238** by phenol **248**. Use of the more basic Hünig's base also gave both products with complete mass recovery (entry 2). We did not observe any conversion with the use of microwave irradiation (entry 3). Photolysis (entries 4-6) of a mixture of **238** and **246** in the presence of benzophenone as a triplet sensitizer only gave **254**, the [2+2] cycloaddition product of benzophenone and **246**.⁵⁹⁰ Changing the reaction solvent from xylenes to heptane, with the goal of destabilizing *tert*-butyl cation formation, did not prevent the formation of **248** (entry 7).

Table 2.1. Attempted formation of **249** from **246** and **238**.



Entry	Conditions	Results
1	PhNEt ₂ (0.10 equiv), xylenes, 140 °C	248 (20%), 253 (20%)
2	<i>i</i> -Pr ₂ NEt (0.20 equiv), xylenes, 140 °C	248 (22%), 253 (78%)
3	PhMe, μ wave, 140 °C, 4 h	no reaction
4	<i>h</i> ν , PhH, rt, 1 d	no reaction
5	<i>h</i> ν , acetone, rt, 1 d	decomposition of 246
6	benzophenone, <i>h</i> ν , PhH, rt, 22 h	254 (28%)
7	heptane, 140 °C, 12 h	248 , decomposition
8	BHT (0.20 equiv), 140 °C, PhMe, 12 h	255 (6%)
9	BHT (0.20 equiv), <i>i</i> -Pr ₂ NEt (0.20 equiv), PhMe, 140 °C, 12 h	248 (13%), 255 (5%), 257 (42%)

⁵⁹⁰ For examples of photolytic cyclobutenone ring-opening, see: (a) Baldwin, J. E.; McDaniel, M. C. *J. Am. Chem. Soc.* **1968**, *90*, 6118-6124. (b) Toda, F.; Todo, E. *Chem. Lett.* **1974**, 1279-1280. (c) Toda, F.; Todo, Y.; Todo, E. *Bull. Chem. Soc. Jpn.* **1976**, *49*, 2645-2646. (d) Danheiser, R. L.; Casebier, D. S.; Firooznia, F. *J. Org. Chem.* **1995**, *60*, 8341-8350.

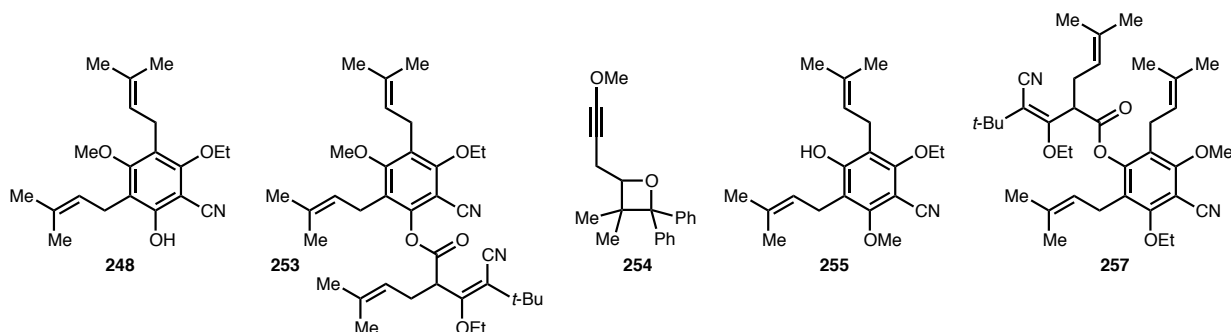
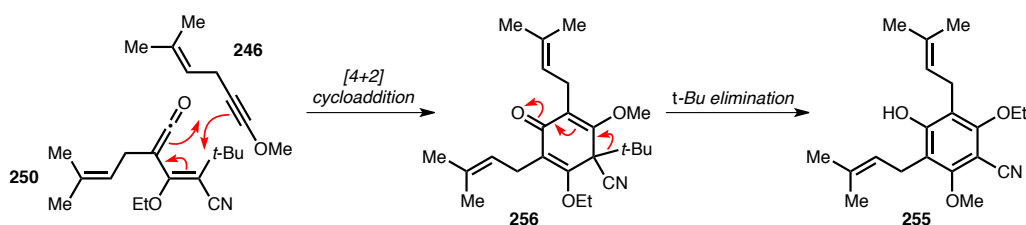


Figure 2.2. Products obtained from the reactions of **246** with **238**.

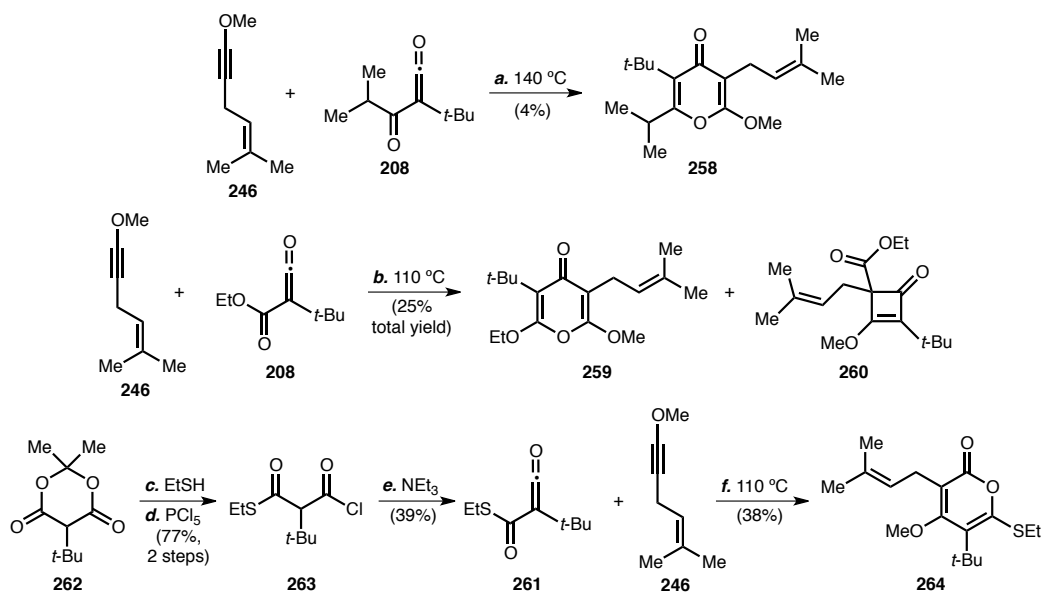
We also repeated the experimental protocol with the addition of BHT to investigate whether radical intermediates were involved (Table 2.1, entry 8); however, the only product isolated was transposed phloroglucinol diether **255**. This product may form via Diels–Alder [4+2] type cycloaddition between ring-opened vinyl ketene **250** to form cyclohexadienone **256** initially, which undergoes *tert*-butyl elimination (Scheme 2.13). The isolation of **255** indicates that a retro-ene cyclization mechanism for this *tert*-butyl elimination is unlikely.⁵⁹¹ Unsurprisingly, the combination of BHT and Hünig’s base additives gave a mixture of products, including **248**, **255**, and the ester adduct **257** (entry 9).



Scheme 2.13. A possible mechanism for the formation of **255** from the reaction of **246** with **238** (Table 2.1, entry 5).

⁵⁹¹ A retro-ene cyclization mechanism cannot be ruled out all together, since a [1,3]-transposition of the *tert*-butyl group may occur, placing the substituent at the α -position of the ketone. Similar alkyl shifts have been observed by Miller. For more information, see ref. 589.

Given the inability to isolate cyclohexadienone **249** from cyclobutenone **238**, we investigated the chemistry of methyl alkynyl ether **246** with other ketenes (Scheme 2.14). Heating a solution of **246** and ketoketene **206** afforded γ -pyrone **258**. A similar product, **259**, was isolated in the reaction of **246** with carbethoxyketene **208** along with cyclobutenone **260**. This cyclobutenone may have formed via initial [2+2] cycloaddition of **246** and **208** followed by [1,3]-acyl shift. We also explored the reactivity of ketenethioate **261**,⁵⁹² which was synthesized⁵⁹³ from Meldrum's acid derivative **262**⁵⁹⁴ via acid chloride **263**. Heating a solution of this ketene with **246** produced α -pyrone **264**.



Scheme 2.14. Reactivity of alkynyl ether **246** with various ketenes.^a

^a Conditions: (a) xylenes, 140 °C, 4%; (b) PhMe, 110 °C, 25% total yield (inseparable mixture of **259** and **260**); (c) *i*-Pr₂NEt, TMSCl, MeCN, 0 °C; EtSH, 43 °C; HCl, H₂O; (d) PCl₅, Et₂O, reflux, 77% (2 steps); (e) NEt₃, PhH, 39%; (f) PhMe, 110 °C, 38%.

⁵⁹² This is the first known (alkanethiol)acylketene to be made and is the first acylketene bearing a non-first row element acyl substituent.

⁵⁹³ Magdziak, D.; Lalic, G.; Lee, H. M.; Fortner, K. C.; Aloise, A. D.; Shair, M. D. *J. Am. Chem. Soc.* **2005**, *127*, 7284-7285.

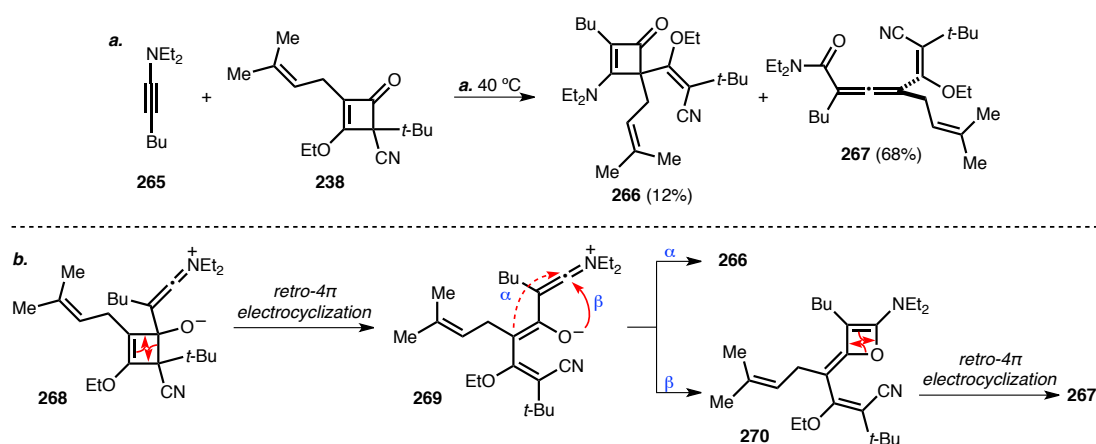
⁵⁹⁴ Huang, X.; Chan, C.-C.; Wu, Q.-L. *Tetrahedron Lett.* **1982**, *23*, 75-76.

Overall, these results indicated that under the conditions necessary to promote the desired electrocyclic cascade reaction, *tert*-butyl elimination to afford an aromatic product was unavoidable. Changes to the nature of the alkynyl ether, ketene coupling partner, solvent, and source of heat did not hinder this deleterious division of the desired product. Another approach we pursued involved the use of an ynamine coupling partner instead of an alkynyl ether.⁵⁹⁵ We hypothesized that a more nucleophilic ynamine may allow the electrocyclic cascade reaction to proceed at a lower temperature and possibly allow for the isolation of our desired product.⁵⁹⁶ Indeed, stirring a solution of diethyl ynamine **265**⁵⁹⁷ and cyclobutenone **238** at 40 °C afforded a mixture of vinylcyclobutenone **266** and allenyl amide **267** (Scheme 2.15a). Both products may originate from 1,2-addition of the ynamine to the cyclobutenone carbonyl to form intermediate ketene-immonium ion **268**, which after retro-4 π electrocyclization may reveal enolate **269** (Scheme 2.15b). C-Alkylation of the immonium ion by the enolate would afford **266** directly, and O-alkylation would provide allenyl amide **267** via retro-4 π electrocyclization of oxetene **270**.

⁵⁹⁵ For reviews on the synthesis and reactivity of ynamines, see: (a) Ficini, J. *Tetrahedron* **1976**, *12*, 1449-1486. (b) Collard-Motte, J.; Janousek, Z. *Top. Curr. Chem.* **1986**, *130*, 89-131. (c) Zifcsak, C. A.; Mulder, J. A.; Hsung, R. P.; Rameshkumar, C.; Wei, L.-L. *Tetrahedron* **2001**, *57*, 7575-7606.

⁵⁹⁶ For an example of a reaction of an ynamine with a cyclobutenone, see: Ficini, J.; Falou, S.; d'Angelo, J. *Tetrahedron Lett.* **1977**, *18*, 1931-1934.

⁵⁹⁷ (a) Ficini, J.; Barbara, C. *Bull. Soc. Chim. Fr.* **1965**, 2787-2793. (b) Sauvêtre, R.; Normant, J. F. *Tetrahedron Lett.* **1982**, *23*, 4325-4328.

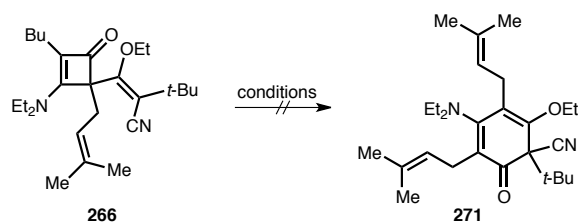


Scheme 2.15. (a) Synthesis and possible mechanisms for the formation of (b) of **266** and **267** from **265** and **238**.^a

^a Conditions: (a) PhMe, rt to 40 °C, 12% **266**, 68% **267**.

We then attempted to convert vinylcyclobutenone **266** to cyclohexadienone **271**. Given the similarity of **266** to intermediate **232** in Scheme 2.8b, we rationalized that a *retro-4 π* electrocycyclization followed by a 6π electrocyclization would afford **271**. However, under a variety of conditions, we were not able to isolate this desired product (Table 2.2). While heating a benzene solution of **266** at 60 °C did not result in any reaction (entry 1), heating at or above 90 °C (entries 2-3) afforded aniline **272** as the sole product (Figure 2.3). The formation of **272** from **266** is analogous to the formation of **255** from the reaction of **246** and **238**, in which *tert*-butyl elimination rapidly occurred in the reaction medium. Further heating, and the addition of BHT and Hünig's base did not inhibit the formation of **272** (entries 4-6). The only product from photolysis of **266** was double-bond isomer **273** (entries 7-8).

Table 2.2. Attempted formation of **271** from **266**.



Entry	Conditions	Results
1	PhH, 60 °C, 19 h	no reaction
2	PhH, 90 °C, 14 h	272 is only product by NMR
3	PhH, 140 °C, 15 min	272 (48%), 266 (27% recovery)
4	BHT, PhH, 90 °C, 14 h	272 is only product by NMR
5	<i>i</i> -Pr ₃ NEt, PhH, 90 °C, 14 h	272 is only product by NMR
6	<i>i</i> -Pr ₃ NEt, BHT, PhH, 90 °C, 14 h	272 is only product by NMR
7	<i>hν</i> , PhH, 4 h	273 (26%), 266 (32% recovery)
8	<i>hν</i> , PhH, 12 h	decomposition

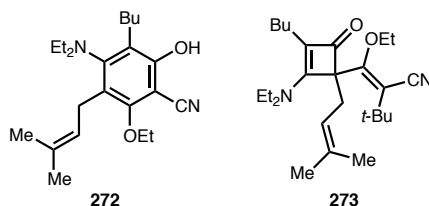
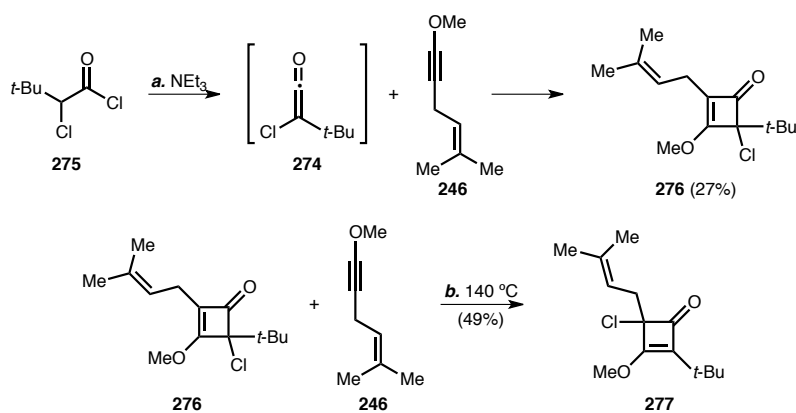


Figure 2.3. Products obtained from the reactions of **266**.

Given the propensity for *tert*-butyl elimination from putative cyclohexadienone intermediates, we also briefly investigated the use of *tert*-butyl(chloro)ketene (**274**) as a coupling partner in this electrocyclic cascade strategy (Scheme 2.16). Replacement of the acyl or cyano group on the ketene with a chlorine atom may prevent undesirable elimination of the bulky alkyl group from a potential cyclohexadienone product. Treating a solution of acyl chloride **275** with base provided *in situ* generation of **274**,⁵⁹⁸ which was trapped with alkynyl ether **246** to form cyclobutenone **276**. However, further heating of this cyclobutenone with alkynyl ether **246** did not afford a desired coupling product; rather, rearranged cyclobutenone **277** was isolated, possibly the product of a [1,3]-chloride shift.

⁵⁹⁸ Brady, W. T.; Scherubel, G. A. *J. Org. Chem.* **1974**, *39*, 3790-3791.



Scheme 2.16. Formation and reactivity of cyclobutenone **276**.^a

^a Conditions: (a) NEt₃, PhH, rt to reflux, 27%; (b) PhMe, 110 °C, 49% (16% recovered **276**).

In summary, a variety of approaches to mitigate *tert*-butyl elimination were explored. Varying the reaction parameters, including ketene coupling partners, heteroatom-functionalized alkynyl coupling partners, use of photolytic conditions, and use of reaction additives, failed to inhibit this process. With the inability to isolate a stable cyclohexadienone bearing a quaternary center functionalized with a *tert*-butyl substituent, we concluded that this electrocyclic cascade approach was inherently flawed, and we therefore sought to explore an alternative strategy for the construction of the bicyclo[3.3.1]nonane core of hyperforin.

Experimental Section

General Procedures. All reactions were performed in oven-dried or flame-dried glassware under a positive pressure of argon unless otherwise noted. Flash column chromatography was performed as described by Still *et al.*⁵⁹⁹ employing silica gel 60 (40-63 μm , Whatman). Both preparatory and analytical thin-layer chromatography (TLC) were performed using 0.25 mm silica gel 60 F₂₅₄ plates.

Materials. Commercial reagents and solvents were used as received with the following exceptions. Tetrahydrofuran, diethyl ether, dichloromethane, toluene, benzene, hexane, acetonitrile, and *N,N*-dimethylformamide were degassed with argon and passed through a solvent purification system (designed by J. C. Meyer of Glass Contour) utilizing alumina columns as described by Grubbs *et al.*⁶⁰⁰ unless otherwise noted. Triethylamine, diisopropylamine, pyridine, and chlorotrimethylsilane were distilled over calcium hydride. Hexamethylphosphoramide was distilled over calcium hydride under reduced pressure. Prenyl bromide was distilled under reduced pressure. Lithium chloride was stored in a vacuum oven for at least 24 h before use. Potassium hydride was washed five times with pentane and dried under reduced pressure directly prior to use. The molarities of butyllithium and *tert*-butyllithium solutions were determined by titration with 1,10-phenanthroline as an indicator (average of three determinations). THF solutions of lithium diisopropylamide were prepared by addition of a hexane solution of butyllithium (1 equiv) to a THF solution of the appropriate amine (1.1 equiv) cooled to $-78\text{ }^{\circ}\text{C}$ and stirring the solution for 30 min at $0\text{ }^{\circ}\text{C}$.

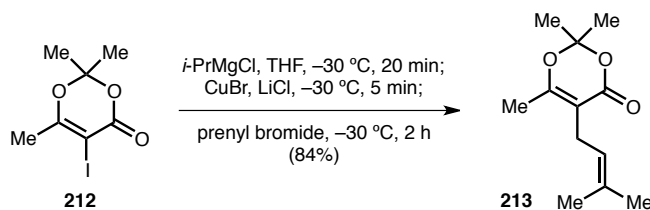
Instrumentation. ^1H NMR spectra were recorded with Varian INOVA-600 and Varian INOVA-500 spectrometers, are reported in parts per million (δ), and are calibrated using residual non-deuterated solvent as an internal reference: CDCl_3 , δ 7.26 (CHCl_3). Data for ^1H NMR spectra are reported as follows: chemical shift (multiplicity, coupling constants, integration). Multiplicities are reported as follows: s = singlet; d = doublet; t = triplet; q = quartet; septet = septet; m = multiplet; br = broad, or

⁵⁹⁹ Still, W. C.; Kahn, M.; Mitra, A. *J. Org. Chem.* **1978**, *43*, 2923-2925.

⁶⁰⁰ Pangborn, A. B.; Giardello, M. A.; Grubbs, R. H.; Rosen, R. K.; Timmers, F. J. *Organometallics* **1996**, *15*, 1518-1520.

combinations thereof. ^{13}C NMR spectra were recorded with a Varian INOVA-500 spectrometer, are reported in parts per million (δ), and are referenced from the central peak of the carbon resonance of the solvent: CDCl_3 , δ 77.23. Infrared (IR) data were recorded on a Varian 1000 FT-IR using NaCl plates or on a Bruker Alpha FT-IR spectrometer outfitted with an Eco-ATR sampling module. High-resolution mass spectra (HRMS) were recorded using electrospray ionization (ESI) mass spectroscopy on an Agilent 6210 TOF LC/MS or a Bruker q-TOF Maxis Impact mass spectrometer. Gas chromatography mass spectra (GCMS) were performed on a Shimadzu GC-2014 equipped with an AOC-20i auto-injector. Microwave irradiation was accomplished using a CEM Discover microwave reactor. Photoirradiation was accomplished using a water-cooled, 5-inch 450-watt Hanovia UV immersion lamp. No filter was used unless specifically indicated.

Note: For clarity, intermediates that have are not explicitly mentioned in this chapter are numbered sequentially in the experimental section beginning with **278**.



2,2,6-Trimethyl-5-(3-methylbut-2-en-1-yl)-4H-1,3-dioxin-4-one (213):

A THF (350 mL) solution of **212**⁵⁶⁹ (18.5 g, 69.0 mmol, 1 equiv) in a 3-neck, 1-L round-bottom flask was cooled to $-30\text{ }^{\circ}\text{C}$ and treated dropwise with a THF solution of isopropylmagnesium chloride (2.0 M, 38 mL, 76 mmol, 1.1 equiv) via equal-pressure dropping funnel. After stirring at $-30\text{ }^{\circ}\text{C}$ for 20 min, copper(I) bromide (990. mg, 6.90 mmol, 0.1 equiv) and lithium chloride (585 mg, 13.8 mmol, 0.2 equiv) were added, and prenyl bromide (12 mL, 100 mmol, 1.5 equiv) was added after 5 min. After stirring at $-30\text{ }^{\circ}\text{C}$ for 2 h, the reaction was quenched with brine and extracted thrice with Et_2O . The organic extracts were combined, washed with brine, dried over MgSO_4 , filtered, and concentrated *in vacuo* to a green oil. Flash column chromatography (500 mL SiO_2 , 95:5 \rightarrow 9:1 hexane:EtOAc) afforded 12.14 g (57.74 mmol, 84% yield) of **213** as a pale yellow oil.

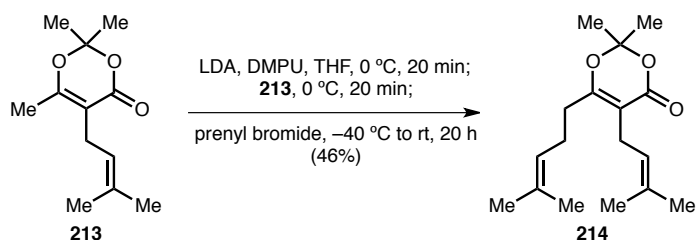
^1H NMR (600 MHz; CDCl_3) δ : 5.05 (t, $J = 6.8\text{ Hz}$, 1H), 2.94 (d, $J = 6.8\text{ Hz}$, 2H), 1.96 (s, 3H), 1.68 (m, 6H), 1.63 (s, 6H).

^{13}C NMR (125 MHz; CDCl_3) δ : 163.5, 162.4, 132.5, 121.8, 105.14, 104.94, 25.8, 25.3, 24.1, 18.0, 17.6.

FTIR (thin film) ν_{max} : 2994, 2916, 2859, 1716, 1643, 1389, 1347, 1268, 1235, 1204, 1148, 1054, 973, 919, 835, 781, 732 cm^{-1} .

HRMS–ESI (m/z): $[\text{M}+\text{Na}]^+$ calculated for $\text{C}_{12}\text{H}_{18}\text{O}_3$, 233.1144; found, 233.1148.

TLC $R_f = 0.43$ (8:2 hexane:EtOAc).



2,2-Dimethyl-5-(3-methylbut-2-en-1-yl)-6-(4-methylpent-3-en-1-yl)-4H-1,3-dioxin-4-one (214):

1,3-Dimethyl-3,4,5,6-tetrahydro-2-pyrimidinone (10.4 mL, 86.3 mmol, 1.5 equiv) was added to a freshly prepared THF solution of lithium diisopropylamide (0.69 M, 82.9 mL, 57.5 mmol, 1 equiv) in a 200-mL recovery flask cooled to 0 °C. After stirring for 20 min, **213** (12.10 g, 57.5 mmol, 1 equiv) was added, and the solution was stirred at 0 °C for 20 min. After cooling to –40 °C, prenyl bromide (8.6 mL, 75 mmol, 1.3 equiv) was added, and the reaction was allowed to slowly warm overnight. After stirring for 20 h at rt, the reaction was quenched by the addition of ice-cold 1 N HCl and extracted thrice with Et₂O. The organic extracts were combined, washed with brine, dried over MgSO₄, filtered, and concentrated *in vacuo* to a brown oil. Flash column chromatography (500 mL SiO₂, 9:1 hexane:EtOAc) afforded 7.30 g (26.2 mmol, 46% yield) of **214** as a pale yellow oil.

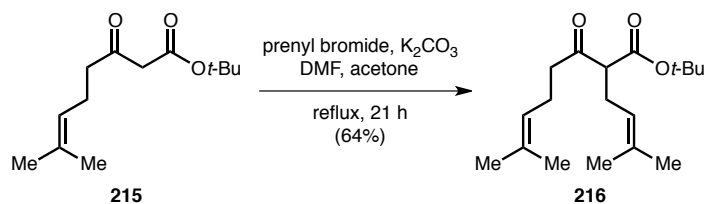
¹H NMR (600 MHz; CDCl₃) δ: 5.07 (t, *J* = 6.9 Hz, 1H), 5.04 (t, *J* = 6.1 Hz, 1H), 2.95 (d, *J* = 6.9 Hz, 2H), 2.29–2.27 (m, 2H), 2.21 (m, 2H), 1.68 (s, 6H), 1.67 (s, 3H), 1.63 (s, 6H), 1.60 (s, 3H).

¹³C NMR (125 MHz; CDCl₃) δ: 166.2, 162.7, 133.4, 132.2, 122.5, 122.3, 105.1, 104.9, 31.2, 25.88, 25.85, 25.3, 25.0, 23.9, 18.04, 17.90.

FTIR (thin film) ν_{max}: 2967, 2915, 2859, 1720, 1637, 1444, 1371, 1268, 1204, 1130, 1047, 979, 845 cm^{–1}.

HRMS–ESI (*m/z*): [M+Na]⁺ calculated for C₁₇H₂₆O₃, 301.1784; found, 301.1774.

TLC R_f = 0.33 (9:1 hexane:EtOAc).



tert-Butyl 7-methyl-2-(3-methylbut-2-en-1-yl)-3-oxooct-6-enoate (216):

An acetone (500 mL) and DMF (30 mL) slurry of **215**⁵⁷¹ (20. g, 88 mmol, 1 equiv), prenyl bromide (11.2 mL, 97.2 mmol, 1.1 equiv), and potassium carbonate (24.4 g, 177 mmol, 2 equiv) in a 3-neck 1-L round-bottom flask outfitted with a reflux condenser was heated to reflux. After refluxing for 21 h, the reaction was cooled to rt and concentrated *in vacuo*. Short-path distillation (6 mmHg, 110-117 °C) afforded 16.71 g (56.8 mmol, 64%) of **216** as a colorless oil.

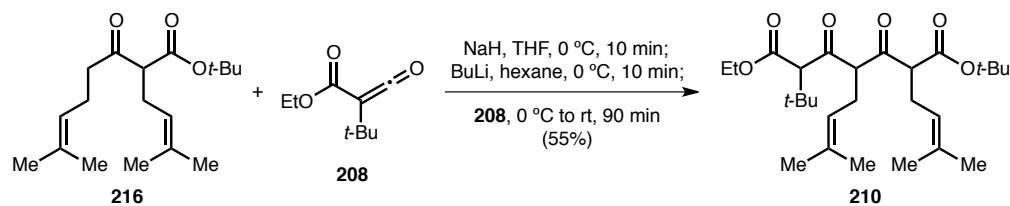
¹H NMR (600 MHz; CDCl₃) δ: 5.04 (t, *J* = 7.2 Hz, 1H), 5.00 (t, *J* = 7.4 Hz, 1H), 3.33 (m, 1H), 2.55 (m, 1H), 2.50-2.43 (m, 3H), 2.26-2.21 (m, 2H), 1.66 (s, 6H), 1.61 (s, 3H), 1.60 (s, 3H), 1.43 (s, 9H).

¹³C NMR (125 MHz; CDCl₃) δ: 205.4, 169.0, 134.4, 132.9, 122.9, 120.4, 81.8, 60.3, 42.3, 28.1, 27.1, 25.95, 25.87, 22.4, 18.00, 17.84.

FTIR (thin film) ν_{max} : 2971, 2916, 2859, 1735, 1712, 1450, 1368, 1249, 1144, 845 cm⁻¹.

HRMS-ESI (*m/z*): [M+H]⁺ calculated for C₁₈H₃₀O₃, 295.2259; found, 295.2268.

TLC *R_f* = 0.39 (9:1 hexane:EtOAc).



1-tert-Butyl 7-ethyl 6-(tert-butyl)-2,4-bis(3-methylbut-2-en-1-yl)-3,5-dioxoheptanedioate (210):

216 (346 mg, 1.18 mmol, 1 equiv) was added to a THF (3 mL) slurry of sodium hydride (60% suspension in mineral oil, 46 mg, 1.23 mmol, 1.05 equiv) cooled to 0 °C in a 10-mL recovery flask. After stirring for 10 min, a hexane solution of butyllithium (2.73 M, 0.65 mL, 1.76 mmol, 1.5 equiv) was added, and the yellow-orange slurry was stirred at 0 °C. After 10 min, **208**⁵⁶⁶ (200 mg, 1.18 mmol, 1 equiv) was added, and the solution was allowed to warm to rt. After 90 min, the reaction was quenched at rt with 2 N HCl, diluted with H₂O, and extracted thrice with Et₂O. The organic extracts were combined, washed with brine, dried over MgSO₄, filtered, and concentrated *in vacuo* to a yellow oil. Flash column chromatography (100 mL SiO₂, 95:5 → 9:1 hexane:EtOAc) afforded 299 mg (0.643 mmol, 55%) of **210** as a yellow oil.

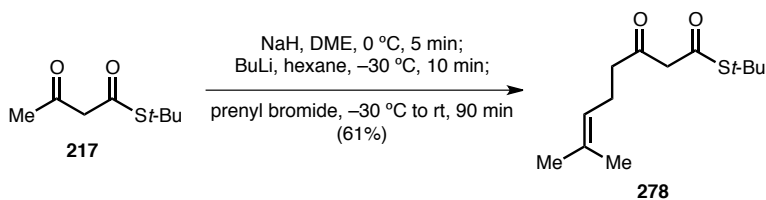
¹H NMR (600 MHz; CDCl₃) δ: 5.86-5.83 (m, ~0.5H), 5.08-4.92 (m, 2H), 4.25-4.09 (m, 2H), 4.00-3.90 (m, ~1H), 3.57-3.44 (m, ~1H), 3.23-3.17 (m, ~1H), 3.11-3.07 (m, ~0.5H), 2.59-2.38 (m, 3H), 1.74-1.56 (m, 12H), 1.46-1.41 (m, 9H), 1.30-1.24 (m, 3H), 1.12-1.04 (m, 9H) (*mixture of tautomers and diastereomers*).

¹³C NMR (125 MHz; CDCl₃) δ: 201.0, 200.1, 199.63, 199.50, 199.02, 198.82, 191.53, 191.51, 187.32, 187.22, 169.4, 169.0, 168.36, 168.34, 168.20, 168.15, 167.96, 167.89, 134.74, 134.60, 134.56, 134.53, 134.40, 134.21, 120.6, 120.41, 120.38, 120.24, 120.19, 120.14, 100.70, 100.69, 82.4, 82.1, 81.7, 67.6, 67.2, 67.0, 66.8, 66.5, 65.7, 63.83, 63.79, 61.5, 61.29, 61.22, 60.9, 60.07, 60.05, 59.5, 56.56, 56.54, 35.2, 35.02, 34.99, 34.82, 34.69, 34.51, 28.35, 28.31, 28.28, 28.25, 28.15, 28.06, 28.01, 27.97, 27.34, 27.23, 27.19, 26.8, 25.87, 25.84, 25.78, 17.92, 17.88, 14.28, 14.25, 14.23 (*mixture of tautomers and diastereomers*).

FTIR (thin film) ν_{max} : 2969, 2933, 2873, 1730, 1598, 1448, 1368, 1246, 1143, 1043, 1025, 845 cm⁻¹.

HRMS–ESI (m / z): $[M+H]^+$ calculated for $C_{27}H_{44}O_6$, 465.3207; found, 465.3211.

TLC R_f = 0.61 (8:2 hexane:EtOAc).



S-tert-Butyl 7-methyl-3-oxooct-6-enethioate (278):

A DME (16 mL) solution of **217**⁵⁷² (5.52 mL, 31.5 mmol, 1 equiv) was added dropwise to a DME (125 mL) slurry of sodium hydride (60% suspension in mineral oil, 1.38 g, 34.6 mmol, 1.1 equiv) cooled to 0 °C in a 500-mL round-bottom flask. After stirring for 5 min, the slurry was cooled to −30 °C, and a hexane solution of butyllithium (2.60 M, 13.3 mL, 34.6 mmol, 1.1 equiv) was added slowly. After stirring the bright orange slurry at −30 °C for 10 min, prenyl bromide (4.0 mL, 34.6 mmol, 1.1 equiv) was added, and the yellow slurry was allowed to slowly warm to rt. After stirring 90 min, the reaction was quenched with sat. aq. NH₄Cl and extracted thrice with EtOAc. The organic extracts were combined, washed with brine, dried over MgSO₄, filtered, and concentrated *in vacuo* to a yellow oil. Short-path distillation (6 mmHg, 100-105 °C) afforded 4.66 g (19.2 mmol, 61% yield) of **278** as a pale yellow oil.

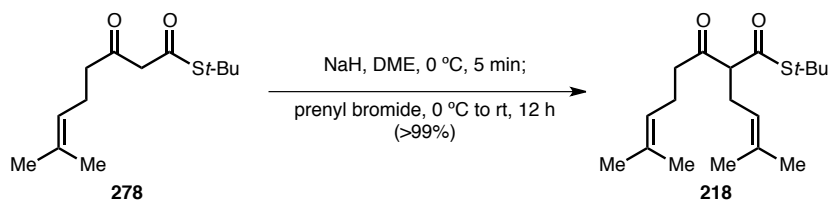
¹H NMR (500 MHz; CDCl₃) δ: 5.32 (s, 1H, *minor tautomer*), 5.09-5.03 (m, 1H, *both tautomers*), 3.55 (s, 2H, *major tautomer*), 2.55 (t, *J* = 7.4 Hz, 2H, *both tautomers*), 2.28-2.22 (m, 3H, *both tautomers*), 2.15-2.12 (m, 1H, *both tautomers*), 1.69 (s, 3H, *minor tautomer*), 1.67 (s, 3H, *major tautomer*), 1.61 (s, 3H, *both tautomers*), 1.51 (s, 9H, *minor tautomer*), 1.47 (s, 9H, *major tautomer*).

¹³C NMR (125 MHz; CDCl₃) δ: 202.3, 196.4, 192.8, 176.1, 133.2, 122.65, 122.51, 99.8, 58.7, 49.2, 48.3, 43.3, 35.3, 30.4, 29.8, 25.9, 25.1, 22.4, 17.91, 17.88 (*mixture of tautomers*).

FTIR (thin film) ν_{max}: 2965, 2924, 2862, 1723, 1674, 1614, 1455, 1364, 1178, 1160, 1080, 978, 863 cm^{−1}.

HRMS–ESI (*m* / *z*): [M+H]⁺ calculated for C₁₃H₂₂O₂S, 243.1421; found, 243.1413.

TLC R_f = 0.43 (9:1 hexane:EtOAc).



S-tert-Butyl 7-methyl-2-(3-methylbut-2-en-1-yl)-3-oxooct-6-enethioate (218):

278 (5.76 g, 23.8 mmol, 1 equiv) was added to a DME (100 mL) slurry of sodium hydride (60% suspension in mineral oil, 950. mg, 30.9 mmol, 1.3 equiv) cooled to 0 °C in a 200-mL recovery flask. After stirring for 5 min, prenyl bromide (3.6 mL, 31 mmol, 1.3 equiv) was added to the yellow solution, and the reaction was allowed to slowly warm to rt overnight. After 12 h, the reaction was quenched with the addition of H₂O and by pouring the resulting mixture onto ice-cold 1 N NaOH. The mixture was then extracted thrice with CHCl₃. The organic extracts were combined, washed with H₂O and brine, dried over MgSO₄, filtered, and concentrated *in vacuo*. The resulting colorless oil was retaken in 98:2 hexane:EtOAc and passed through a short plug of SiO₂, rinsing with 98:2 hexane:EtOAc. Concentration of the filtrate *in vacuo* afforded 7.39 g (23.8 mmol, >99% yield) of **218** as a colorless oil.

¹H NMR (600 MHz; CDCl₃) δ: 5.03 (t, *J* = 7.2 Hz, 1H), 4.98 (t, *J* = 7.3 Hz, 1H), 3.58 (t, *J* = 7.5 Hz, 1H), 2.60-2.46 (m, 4H), 2.24 (q, *J* = 7.2 Hz, 2H), 1.66 (s, 6H), 1.61 (s, 6H), 1.45 (s, 9H).

¹³C NMR (125 MHz; CDCl₃) δ: 204.1, 195.9, 134.8, 133.0, 122.8, 119.9, 68.4, 58.7, 49.0, 42.2, 29.8, 28.0, 25.93, 25.87, 22.5, 17.99, 17.85.

FTIR (thin film) ν_{max} : 2965, 2922, 2859, 1723, 1672, 1454, 1364, 1162, 984, 926, 825 cm⁻¹.

HRMS-ESI (*m/z*): [M+Na]⁺ calculated for C₁₈H₃₀O₂S, 333.1858; found, 333.1859.

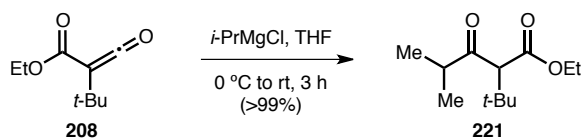
TLC R_f = 0.65 (9:1 hexane:EtOAc).

27.40, 27.14, 26.99, 26.4, 25.74, 25.69, 25.66, 24.6, 17.88, 17.84, 17.78, 17.76, 17.73, 17.67, 14.26, 14.22, 14.18, 14.14 (*mixture of tautomers and diastereomers*).

FTIR (thin film) ν_{max} : 2963, 2914, 2872, 1725, 1671, 1455, 1365, 1302, 1221, 1144, 1043, 935 cm^{-1} .

HRMS–ESI (m/z): $[\text{M}+\text{Na}]^+$ calculated for $\text{C}_{27}\text{H}_{44}\text{O}_5\text{S}$, 503.2802; found, 503.2807.

TLC R_f = 0.51 (8:2 hexane:EtOAc).



Ethyl 2-(tert-butyl)-4-methyl-3-oxopentanoate (221):

A THF (265 mL) solution of **208**⁵⁶⁶ (18.0 g, 106 mmol, 1 equiv) in a 1-L recovery flask was cooled to 0 °C, and a THF solution of isopropylmagnesium chloride (2.0 M, 58 mL, 120 mmol, 1.1 equiv) was added slowly over 10 min. After the addition was complete, the reaction was allowed to slowly warm to rt. After stirring for 3 h, the reaction was quenched via dropwise addition of H₂O followed by sat. aq. NH₄Cl and extracted thrice with EtOAc. The organic extracts were combined, washed with sat. aq. NaHCO₃ and brine, dried over MgSO₄, and filtered through a short plug of SiO₂, rinsing with EtOAc. The filtrate was concentrated *in vacuo* to afford 23 g (110 mmol, >99% yield) of **221** as a colorless oil.

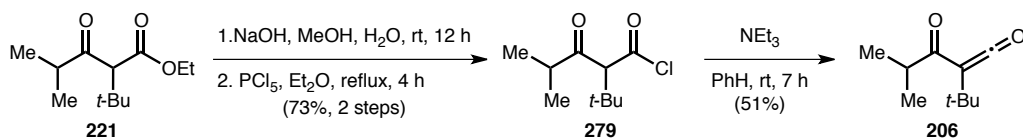
¹H NMR (600 MHz; CDCl₃) δ: 4.15 (q, *J* = 7.1 Hz, 2H), 3.52 (s, 1H), 2.69 (7, *J* = 6.8 Hz, 1H), 1.24 (t, *J* = 7.1 Hz, 3H), 1.09 (d, *J* = 6.8 Hz, 3H), 1.08 (s, 9H), 1.04 (d, *J* = 6.8 Hz, 3H).

¹³C NMR (125 MHz; CDCl₃) δ: 209.1, 168.9, 65.8, 61.0, 42.6, 34.7, 28.4, 18.35, 18.18, 14.4.

FTIR (thin film) ν_{max}: 2964, 2909, 2874, 1736, 1714, 1466, 1366, 1303, 1223, 1206, 1142, 1021 cm⁻¹.

HRMS–ESI (*m/z*): [M+H]⁺ calculated for C₁₂H₂₂O₃, 215.1651; found, 215.1642.

TLC R_f = 0.42 (9:1 hexane:EtOAc).



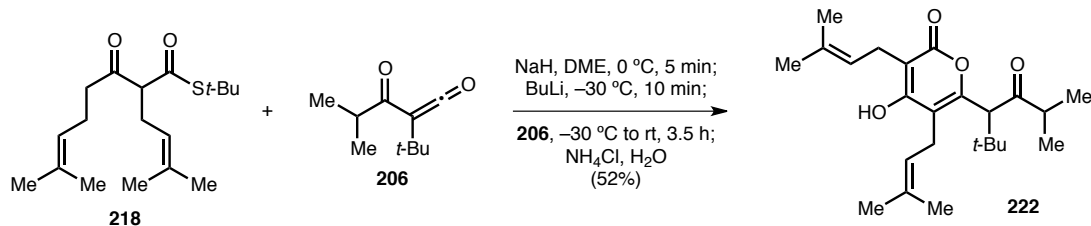
2-(*tert*-Butyl)-4-methylpent-1-ene-1,3-dione (206):

A MeOH (465 mL) solution of **221** (10.0 g, 46.7 mmol, 1 equiv) in a 1-L round-bottom flask was treated with an aqueous solution of sodium hydroxide (50% by weight, 93 mL). The exothermic yellow solution was placed in a rt water bath and stirred for 12 h. The reaction was then concentrated partially *in vacuo*, cooled to 0 °C, and slowly acidified with concentrated HCl. After warming the mixture to rt, it was extracted thrice with EtOAc. The organic extracts were combined, washed with brine, dried over MgSO₄, filtered, and concentrated *in vacuo* to a pale yellow oil. The oil was taken up in Et₂O (210 mL) in a 3-neck 500-mL round-bottom flask outfitted with a reflux condenser. Phosphorous(V) chloride (17.6 g, 84.6 mmol, 2 equiv) was added, and the mixture was heated to reflux. After stirring for 4 h at reflux, the reaction was cooled to rt and transferred via cannula to a Schlenk filter funnel and filtered under positive N₂ pressure. The yellow filtrate was distilled directly (6 mmHg, 62-64 °C) to afford 7.03 g (34.3 mmol, 73% yield over 2 steps) of **279** as a colorless oil. A PhH (48 mL) solution of **279** (6.91 g, 33.8 mmol, 1 equiv) in a 100-mL recovery flask was treated with triethylamine (9.4 mL, 68 mmol, 2 equiv), and the resulting yellow slurry was stored in the dark for 7 h. The slurry was then passed through a Schlenk filter funnel under positive N₂ pressure. The filtrate was distilled directly (6 mmHg, 30-32 °C) to afford 2.89 g (17.2 mmol, 51% yield) of **206** as a colorless oil.

¹H NMR (600 MHz; CDCl₃) δ: 2.54 (septet, *J* = 6.7 Hz, 1H), 1.24 (s, 9H), 1.11 (d, *J* = 6.7 Hz, 5H).

¹³C NMR (125 MHz; CDCl₃) δ: 200.1, 197.1, 59.7, 41.5, 31.7, 29.5, 19.6.

FTIR (thin film) ν_{max}: 2966, 2908, 2874, 2097, 1668, 1459, 1384, 1365, 1248, 1193, 1157, 940 cm⁻¹.



4-Hydroxy-3,5-bis(3-methylbut-2-en-1-yl)-6-(2,2,5-trimethyl-4-oxohexan-3-yl)-2H-pyran-2-one

(222):

A DME (0.6 mL) solution of **218** (336 mg, 1.08 mmol, 1 equiv) was added to a DME (5 mL) slurry of sodium hydride (60% suspension in mineral oil, 48 mg, 1.18 mmol, 1.1 equiv) cooled to 0 °C in a 25-mL round-bottom flask. After stirring the resulting pink solution at 0 °C for 5 min, it was cooled to –30 °C and a hexane solution of butyllithium (1.8 M, 0.65 mL, 1.2 mmol, 1.1 equiv) was added dropwise. After stirring for 10 min at –30 °C, **206** (200. mg, 1.18 mmol, 1.1 equiv) was added and the reaction was allowed to slowly warm to rt. After stirring for 3.5 h, the reaction was quenched with sat. aq. NH₄Cl and extracted thrice with EtOAc. The organic extracts were combined, washed with brine, dried over Na₂SO₄, filtered, and concentrated *in vacuo*. Flash column chromatography (75 mL SiO₂, 95:5 → 9:1 → 1:1 hexane:EtOAc) afforded 218 mg (0.56 mmol, 52% yield) of **222** as a white flocculent solid.

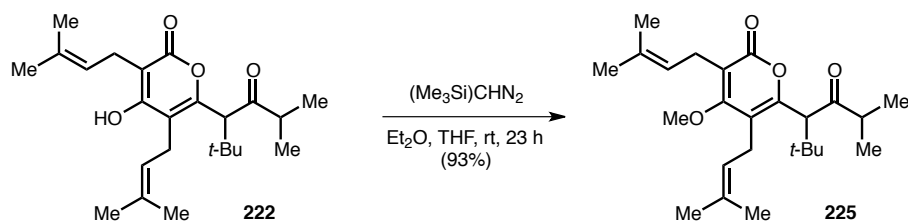
¹H NMR (600 MHz; CDCl₃) δ: 7.95 (br s, 1H), 5.22 (t, *J* = 7.3 Hz, 1H), 5.02 (t, *J* = 6.0 Hz, 1H), 3.57 (s, 1H), 3.21 (d, *J* = 7.3 Hz, 2H), 3.17 (dd, *J* = 16.0, 5.6 Hz, 1H), 3.11 (dd, *J* = 16.0, 7.3 Hz, 1H), 2.68 (septet, *J* = 6.8 Hz, 1H), 1.72 (s, 3H), 1.70 (s, 6H), 1.66 (s, 3H), 1.04 (s, 9H), 0.91 (d, *J* = 6.8 Hz, 3H), 0.90 (d, *J* = 6.8 Hz, 3H).

¹³C NMR (125 MHz; CDCl₃) δ: 209.8, 164.9, 164.5, 156.0, 136.6, 133.3, 121.0, 120.4, 114.6, 103.0, 61.1, 39.9, 35.6, 28.9, 25.92, 25.72, 24.0, 23.3, 19.6, 18.10, 18.08, 18.01.

FTIR (thin film) ν_{max}: 3252 (br), 2967, 2874, 1727, 1666, 1559, 1449, 1217 cm^{–1}.

HRMS–ESI (*m/z*): [M+K]⁺ calculated for C₂₄H₃₆O₄, 427.2245; found, 427.2228.

TLC R_f = 0.41 (7:3 hexane:EtOAc).



4-Methoxy-3,5-bis(3-methylbut-2-en-1-yl)-6-(2,2,5-trimethyl-4-oxohexan-3-yl)-2H-pyran-2-one

(225):

A THF (3 mL) solution of **222** (168 mg, 0.432 mmol, 1 equiv) in a 20-mL scintillation vial was treated with an Et₂O solution of trimethylsilyldiazomethane (2.0 M, 0.43 mL, 0.87 mmol, 2 equiv). After stirring the yellow solution at rt for 23 h, it was quenched with sat. aq. NH₄Cl and extracted thrice with EtOAc. The organic extracts were combined, washed with brine, dried over Na₂SO₄, filtered, and concentrated *in vacuo* to a yellow oil. Flash column chromatography (20 mL SiO₂, 95:5 → 8:2 hexane:EtOAc) afforded 162.3 mg (0.4032 mmol, 93% yield) of **225** as a pale yellow oil.

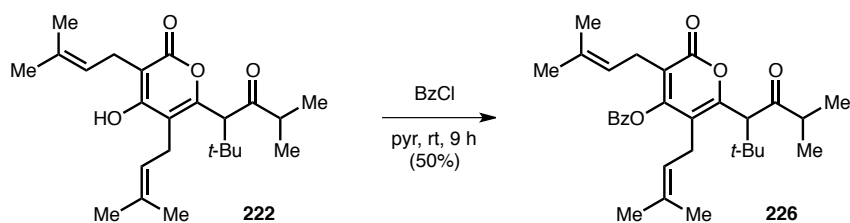
¹H NMR (600 MHz; CDCl₃) δ 5.15 (t, *J* = 7.1 Hz, 1H), 5.10 (t, *J* = 6.8 Hz, 1H), 3.89 (s, 3H), 3.89 (s, 1H), 3.51-3.47 (m, 1H), 3.10-3.06 (m, 2H), 3.02 (dd, *J* = 14.4, 7.1 Hz, 1H), 2.61 (7, *J* = 6.8 Hz, 1H), 1.78 (s, 3H), 1.72 (s, 3H), 1.69 (s, 3H), 1.66 (s, 3H), 1.09 (s, 9H), 1.04 (d, *J* = 6.8 Hz, 3H), 0.94 (d, *J* = 6.8 Hz, 3H).

¹³C NMR (125 MHz; CDCl₃) δ: 210.2, 179.5, 162.5, 154.5, 132.3, 132.1, 126.3, 121.9, 121.6, 104.0, 60.2, 56.1, 41.7, 36.4, 29.0, 25.95, 25.79, 24.2, 21.2, 18.8, 18.28, 18.18, 18.0.

FTIR (thin film) *v*_{max}: 2962, 2913, 2872, 1723, 1652, 1618, 1592, 1462, 1401, 1324, 1266, 1178, 1124, 1021, 974 cm⁻¹.

HRMS–ESI (*m/z*): [M+H]⁺ calculated for C₂₅H₃₈O₄, 403.2846; found, 403.2843.

TLC R_f = 0.55 (8:2 hexane:EtOAc).



3,5-bis(3-Methylbut-2-en-1-yl)-2-oxo-6-(2,2,5-trimethyl-4-oxohexan-3-yl)-2H-pyran-4-yl benzoate

(226):

A pyr (1 mL) solution of **222** (59.8 mg, 0.15 mmol, 1 equiv) in a 5-mL pear-shaped flask was treated with benzoyl chloride (16 μ L, 0.17 mmol, 1.1 equiv). After stirring the reaction for 9 h, it was poured onto sat. aq. NaHCO_3 and extracted thrice with EtOAc. The organic extracts were combined, washed with brine, dried over Na_2SO_4 , filtered, and concentrated *in vacuo* to a brown oil. Flash column chromatography (15 mL SiO_2 , 95:5 hexane:EtOAc) afforded 36.9 mg (74.9 μ mol, 50% yield) of **226** as a pale yellow oil.

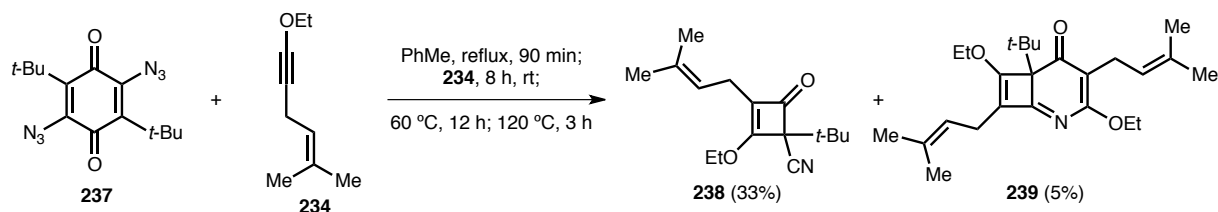
^1H NMR (600 MHz; CDCl_3) δ : 8.13-8.10 (m, 2H), 7.69-7.65 (m, 1H), 7.53 (td, $J = 7.8, 3.8$ Hz, 2H), 5.09 (t, $J = 7.0$ Hz, 1H), 4.96 (t, $J = 5.0$ Hz, 1H), 3.66 (s, 1H), 3.20-2.96 (m, 4H), 2.76 (7, $J = 6.8$ Hz, 1H), 1.56 (s, 3H), 1.55 (s, 3H), 1.47 (s, 3H), 1.42 (s, 3H), 1.12 (s, 9H), 1.02 (d, $J = 6.8$ Hz, 3H), 0.99 (d, $J = 6.8$ Hz, 3H).

^{13}C NMR (125 MHz; CDCl_3) δ : 209.5, 163.12, 163.04, 159.2, 134.5, 133.80, 133.70, 130.5, 128.9, 128.1, 120.9, 119.4, 118.2, 116.0, 61.2, 40.3, 36.0, 32.9, 29.0, 25.81, 25.65, 25.2, 24.6, 19.7, 18.16, 18.02, 17.94.

FTIR (thin film) ν_{max} : 2967, 2931, 2872, 1743, 1723, 1565, 1452, 1375, 1258, 1229, 1176, 1059, 1022, 706 cm^{-1} .

HRMS–ESI (m/z): $[\text{M}+\text{H}]^+$ calculated for $\text{C}_{31}\text{H}_{40}\text{O}_5$, 493.2949; found, 493.2957.

TLC $R_f = 0.66$ (1:1 hexane:EtOAc).



A PhMe (7 mL) solution of **237**⁵⁸² (82 mg, 0.27 mmol, 1 equiv) in a 2-neck 25-mL round-bottom flask outfitted with a reflux condenser was refluxed for 90 min, whereupon the initially orange solution turned yellow. After cooling to rt, **234**⁵⁷⁹ (150. mg, 1.09 mmol, 4 equiv) was added, producing an orange solution. After stirring for 8 h at rt, it was heated at 60 °C for 12 h, and then at 120 °C for 3 h. The bright orange red solution was cooled to rt and concentrated *in vacuo* to an orange red oil. Flash column chromatography (100 mL SiO₂, 95:5 → 9:1 hexane:EtOAc) afforded 46 mg (0.18 mmol, 33% yield) of **238** as an orange oil and 10 mg (0.025 mmol, 5% yield) of **239** as an orange oil.

1-(tert-Butyl)-2-ethoxy-3-(3-methylbut-2-en-1-yl)-4-oxocyclobut-2-enecarbonitrile (238):

¹H NMR (600 MHz; CDCl₃) δ: 5.08 (t, *J* = 7.0 Hz, 1H), 4.43 (q, *J* = 7.1 Hz, 2H), 2.85-2.83 (m, 2H), 1.68 (s, 3H), 1.61 (s, 3H), 1.45 (t, *J* = 7.1 Hz, 3H), 1.09 (s, 9H).

¹³C NMR (125 MHz; CDCl₃) δ: 179.6, 172.9, 134.4, 124.6, 119.3, 117.2, 70.0, 68.3, 34.6, 26.4, 25.7, 22.0, 18.0, 15.2.

FTIR (thin film) ν_{max}: 2972, 2229, 1768, 1654, 1619, 1599, 1381, 1334 cm⁻¹.

HRMS-ESI (*m/z*): [M+Na]⁺ calculated for C₁₆H₂₃NO₂, 284.1621; found, 284.1611.

TLC R_f = 0.39 (8:2 hexane:EtOAc).

6-(tert-Butyl)-3,7-diethoxy-4,8-bis(3-methylbut-2-en-1-yl)-2-azabicyclo[4.2.0]octa-1,3,7-trien-5-one (239):

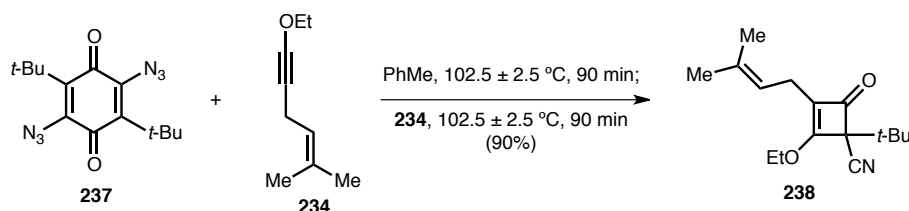
¹H NMR (500 MHz; CDCl₃) δ: 5.23 (t, *J* = 7.1 Hz, 1H), 5.18 (t, *J* = 7.5 Hz, 1H), 4.53 (dq, *J* = 10.0, 7.1 Hz, 1H), 4.46 (dq, *J* = 10.5, 7.1 Hz, 1H), 4.37 (m, 2H), 3.12 (dd, *J* = 14.0, 7.5 Hz, 1H), 3.03 (dd, *J* = 16.2, 7.1 Hz, 1H), 2.94 (dd, *J* = 16.2, 7.0 Hz, 1H), 2.84 (dd, *J* = 14.0, 7.5 Hz, 1H), 1.71 (s, 6H), 1.66 (s, 3H), 1.64 (s, 3H), 1.40 (t, *J* = 7.1 Hz, 3H), 1.34 (t, *J* = 7.1 Hz, 3H), 0.99 (s, 9H).

^{13}C NMR (125 MHz; CDCl_3) δ : 191.9, 180.8, 168.2, 162.7, 133.7, 130.6, 124.8, 123.3, 119.7, 110.6, 69.8, 63.4, 36.8, 29.9, 28.5, 25.98, 25.82, 22.9, 22.5, 18.04, 18.02, 15.53, 15.50.

FTIR (thin film) ν_{max} : 2968, 2942, 1631, 1572, 1370, 1332, 1263 cm^{-1} .

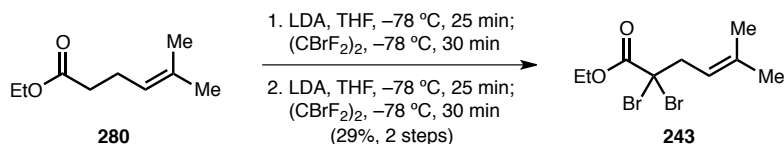
HRMS–ESI (m/z): $[\text{M}+\text{H}]^+$ calculated for $\text{C}_{25}\text{H}_{37}\text{NO}_3$, 400.2846; found, 400.2860.

TLC R_f = 0.30 (8:2 hexane:EtOAc).



*Optimized procedure for the synthesis of **238**:*

An orange PhMe (180 mL) solution of **237**⁵⁸² (5.47 g, 18.1 mmol, 2.5 equiv) in a 3-neck 500-mL round-bottom flask outfitted with a reflux condenser was heated to 102.5 ± 2.5 °C for 90 min. After cooling the reaction to rt, a PhMe (36 mL) solution of **234**⁵⁷⁹ (1.00 g, 7.24 mmol, 1 equiv) was added. The resulting deep red solution was heated to 102.5 ± 2.5 °C for 90 min, cooled to rt, and concentrated *in vacuo* to a dark red oil. Flash column chromatography (500 mL SiO_2 , 95:5 → 9:1 → 8:2 hexane:EtOAc) afforded 1.70 g (6.50 mmol, 90% yield) of **238** as an orange oil.



Ethyl 2,2-dibromo-5-methylhex-4-enoate (243):

A THF (5.5 mL) solution of **280**⁶⁰¹ (3.01 g, 19.3 mmol, 1 equiv) was added dropwise to a freshly prepared THF solution of lithium diisopropylamide (0.30 M, 66 mL, 20. mmol, 1.05 equiv) cooled to $-78\text{ }^{\circ}\text{C}$ in a 200-mL recovery flask. After stirring for 25 min at $-78\text{ }^{\circ}\text{C}$, 1,2-dibromo-1,1,2,2-tetrafluoroethane (3.5 mL, 29 mmol, 1.5 equiv) was added. The resulting black-brown solution was stirred at $-78\text{ }^{\circ}\text{C}$ for 30 min and subsequently quenched by pouring onto sat. aq. NaHCO_3 . The mixture was extracted thrice with hexane. The organic extracts were combined, washed with H_2O and brine, dried over MgSO_4 , filtered, and concentrated *in vacuo* to a yellow oil. Short-path distillation (6 mmHg, $56\text{--}58\text{ }^{\circ}\text{C}$) afforded 2.25 g (9.57 mmol) of a mono-brominated intermediate. A THF (2.8 mL) solution of this intermediate (2.22 g, 9.44 mmol, 1 equiv) was added dropwise to a freshly prepared THF solution of lithium diisopropylamide (0.30 M, 34 mL, 9.9 mmol, 1.05 equiv) cooled to $-78\text{ }^{\circ}\text{C}$ in a 100-mL recovery flask. After stirring for 25 min at $-78\text{ }^{\circ}\text{C}$, 1,2-dibromo-1,1,2,2-tetrafluoroethane (1.7 mL, 14.2 mmol, 1.5 equiv) was added. The pale yellow solution was stirred at $-78\text{ }^{\circ}\text{C}$ for 30 min and subsequently quenched by pouring onto sat. aq. NaHCO_3 . The mixture was extracted thrice with hexane. The organic extracts were combined, washed with H_2O and brine, dried over MgSO_4 , filtered, and concentrated *in vacuo* to a brown oil. Short-path distillation (6 mmHg, $80\text{--}85\text{ }^{\circ}\text{C}$) afforded 1.74 g (5.54 mmol, 29% yield over 2 steps) of **243** as a colorless oil.

^1H NMR (600 MHz; CDCl_3) δ : 5.24 (t, $J = 7.0\text{ Hz}$, 1H), 4.32 (q, $J = 7.1\text{ Hz}$, 2H), 3.31 (d, $J = 7.0\text{ Hz}$, 2H), 1.75 (s, 3H), 1.68 (s, 3H), 1.35 (t, $J = 7.1\text{ Hz}$, 3H).

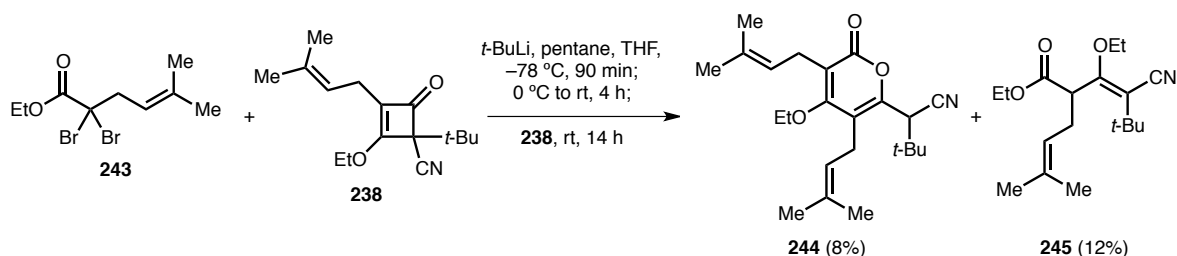
^{13}C NMR (125 MHz; CDCl_3) δ : 166.4, 137.9, 118.7, 64.0, 60.5, 46.0, 26.2, 18.9, 14.0.

FTIR (thin film) ν_{max} : 2980, 2932, 2914, 1733, 1445, 1298, 1222, 1177, 1029, 1014, 859, 793, 628 cm^{-1} .

HRMS–ESI (m/z): $[\text{M}+\text{Na}]^+$ calculated for $\text{C}_9\text{H}_{14}\text{Br}_2\text{O}_2$, 336.9226; found, 336.9233.

⁶⁰¹ Cermak, D. M.; Wiemer, D. F.; Lewis, K.; Hohl, R. J. *Bioorg. Med. Chem.* **2000**, 8, 2729–2737.

TLC $R_f = 0.53$ (9:1 hexane:EtOAc).



A THF (1 mL) solution of **243** (96 mg, 0.31 mmol, 1 equiv) in a 10-mL recovery flask was cooled to $-78\text{ }^{\circ}\text{C}$ and treated with a pentane solution of *tert*-butyllithium (1.70 M, 0.72 mL, 12 mmol, 4 equiv) dropwise over 7 min. The yellow solution was stirred at $-78\text{ }^{\circ}\text{C}$ for 90 min, and then slowly warmed from $0\text{ }^{\circ}\text{C}$ to rt. After 4 hours, **238** (80.0 mg, 0.306 mmol, 1 equiv) was added at rt. After stirring at rt for 14 h, the reaction was quenched by pouring onto sat. aq. NH_4Cl and extracted thrice with Et_2O . The organic extracts were combined, washed with H_2O and brine, dried over Na_2SO_4 , filtered, and concentrated *in vacuo* to a viscous orange-red oil. Flash column chromatography (100 mL SiO_2 , 95:5 \rightarrow 9:1 \rightarrow 8:2 \rightarrow 1:1 hexane:EtOAc) afforded 9 mg (0.02 mmol, 8% yield) of **244** as a pale yellow oil and 10. mg (0.038 mmol, 12% yield) of **245** as a pale yellow oil.

2-(4-Ethoxy-3,5-bis(3-methylbut-2-en-1-yl)-2-oxo-2H-pyran-6-yl)-3,3-dimethylbutanenitrile (244):

^1H NMR (600 MHz; CDCl_3) δ : 5.17 (t, $J = 6.7\text{ Hz}$, 1H), 4.98 (t, $J = 6.5\text{ Hz}$, 1H), 3.96 (dd, $J = 7.0, 1.9\text{ Hz}$, 1H), 3.94 (dd, $J = 7.0, 1.9\text{ Hz}$, 1H), 3.63 (s, 1H), 3.17 (d, $J = 6.7\text{ Hz}$, 2H), 3.13 (dd, $J = 16.3, 6.5\text{ Hz}$, 1H), 2.98 (dd, $J = 16.3, 6.5\text{ Hz}$, 1H), 1.73 (s, 9H), 1.70 (s, 3H), 1.39 (t, $J = 7.0\text{ Hz}$, 3H), 1.17 (s, 9H).

^{13}C NMR (125 MHz; CDCl_3) δ : 165.9, 163.8, 150.9, 134.0, 133.6, 121.1, 120.5, 117.2, 116.9, 116.4, 70.7, 43.5, 36.3, 28.3, 25.91, 25.77, 24.6, 24.0, 18.27, 18.21, 15.8.

FTIR (thin film) ν_{max} : 2969, 2931, 2242, 1720, 1639, 1562, 1445, 1375, 1204, 1063, 1022 cm^{-1} .

HRMS-ESI (m/z): $[\text{M}+\text{H}]^+$ calculated for $\text{C}_{23}\text{H}_{33}\text{NO}_3$, 372.2533; found, 372.2524.

TLC $R_f = 0.24$ (8:2 hexane:EtOAc).

Z-Ethyl 4-cyano-3-ethoxy-5,5-dimethyl-2-(3-methylbut-2-en-1-yl)hex-3-enoate (245):

^1H NMR (600 MHz; CDCl_3) δ : 5.09 (t, $J = 7.5\text{ Hz}$, 1H), 4.23 (dq, $J = 10.8, 7.1\text{ Hz}$, 1H), 4.18 (dq, $J = 10.8, 7.1\text{ Hz}$, 1H), 4.03-3.92 (m, 2H), 3.76 (dq, $J = 8.9, 7.0\text{ Hz}$, 1H), 2.71 (dt, $J = 14.3, 6.7\text{ Hz}$, 1H), 2.44

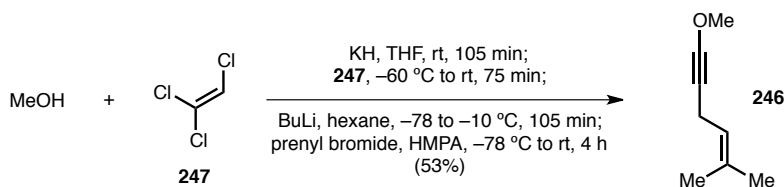
(dt, $J = 14.3, 8.9$ Hz, 1H), 1.70 (s, 3H), 1.64 (s, 3H), 1.31 (t, $J = 7.0$ Hz, 3H), 1.28 (t, $J = 7.1$ Hz, 3H), 1.23 (s, 9H).

^{13}C NMR (125 MHz; CDCl_3) δ : 171.2, 165.8, 134.9, 120.10, 119.99, 108.6, 65.8, 61.7, 49.6, 33.1, 29.9, 27.6, 25.9, 18.0, 15.4, 14.3.

FTIR (thin film) ν_{max} : 2967, 2929, 2872, 2202, 1734, 1600, 1445, 1365, 1296, 1207, 1148, 1030 cm^{-1} .

HRMS–ESI (m/z): $[\text{M}+\text{H}]^+$ calculated for $\text{C}_{18}\text{H}_{29}\text{NO}_3$, 308.2220; found, 308.2218.

TLC $R_f = 0.36$ (8:2 hexane:EtOAc).



1-Methoxy-5-methylhex-4-en-1-yne (246):

A THF (120 mL) solution of methanol (2.5 mL, 61 mmol, 1 equiv) was added via cannula over 15 min to a THF (120 mL) slurry of freshly washed potassium hydride (4.91 g, 122 mmol, 2 equiv) in a 500-mL round-bottom flask. After stirring at rt for 105 min, the reaction was cooled to -60 °C, and a THF (70 mL) solution of trichloroethylene (5.5 mL, 61 mmol, 1 equiv) was added, and the cooling bath was removed. After stirring for 75 min, the reaction was cooled to -78 °C, and a hexane solution of butyllithium (2.73 M, 54 mL, 150 mmol, 2.4 equiv) was added. After slowly warming the reaction to -10 °C over 105 min, the reaction was cooled to -78 °C, and a HMPA (14 mL) solution of prenyl bromide (7.1 mL, 61 mmol, 1 equiv) was added via cannula. The cooling bath was then removed, and the reaction was stirred at rt for 4 h and was subsequently quenched with a small amount of sat. aq. NaHCO₃, diluted with H₂O, and extracted thrice with pentane. The organic extracts were combined, washed with H₂O and brine, dried over Na₂SO₄, filtered, and concentrated *in vacuo* to a dark brown oil. Short-path distillation (6 mmHg, 54-70 °C) afforded 4.04 g (32.5 mmol, 53% yield) of **246** as a pale yellow oil.

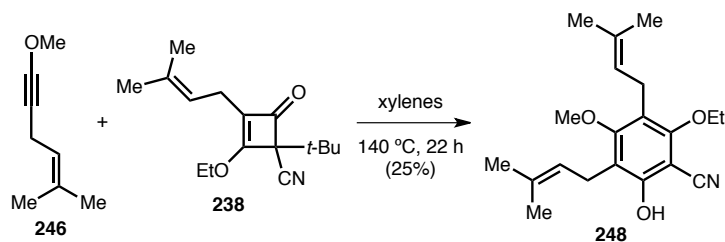
¹H NMR (600 MHz; CDCl₃) δ: 5.16 (t, *J* = 6.9 Hz, 1H), 3.81 (s, 3H), 2.80 (d, *J* = 6.9 Hz, 2H), 1.70 (s, 3H), 1.61 (s, 3H).

¹³C NMR (125 MHz; CDCl₃) δ: 132.9, 121.0, 90.7, 65.5, 35.5, 25.7, 17.8, 16.3.

FTIR (thin film) ν_{max}: 2965, 2927, 2857, 2281, 1449, 1376, 1241, 1172, 961, 841 cm⁻¹.

GCMS (m / z): [M]⁺ 124 (11%), 109 (90%), 69 (25%), 28 (100%).

TLC R_f = 0.32 (99:1 hexane:EtOAc).

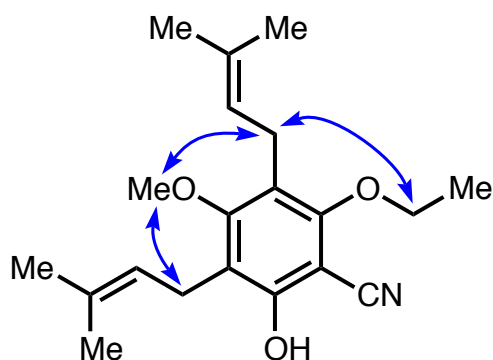


2-Ethoxy-6-hydroxy-4-methoxy-3,5-bis(3-methylbut-2-en-1-yl)benzonitrile (248):

A xylenes (3 mL) solution of **238** (34.3 mg, 0.131 mmol, 1 equiv) and **246** (80. mg, 0.64 mmol, 5 equiv) was heated to 140 °C in a 10-mL sealed tube. After stirring at 140 °C for 22 h, the reaction was cooled to rt and concentrated *in vacuo* to an orange oil. Flash column chromatography (100 mL SiO₂, 95:5 → 9:1 → 8:2 hexane:EtOAc) followed by preparatory thin-layer chromatography (2 × 99:1 hexane:EtOAc) afforded 11 mg (0.033 mmol, 25% yield) of **248** as a white residue.

¹H NMR (600 MHz; CDCl₃) δ: 6.08 (br s, 1H), 5.21 (t, *J* = 7.0 Hz, 1H), 5.10 (t, *J* = 6.7 Hz, 1H), 4.16 (q, *J* = 7.0 Hz, 2H), 3.71 (s, 3H), 3.38 (d, *J* = 7.0 Hz, 2H), 3.27 (d, *J* = 6.7 Hz, 2H), 1.83 (s, 3H), 1.77 (s, 3H), 1.76 (s, 3H), 1.68 (s, 3H), 1.44 (t, *J* = 7.0 Hz, 3H).

¹³C NMR (125 MHz; CDCl₃) δ: 161.9, 159.5, 157.4, 136.7, 132.0, 123.2, 122.0, 121.2, 116.7, 114.9, 92.0, 71.2, 62.0, 26.03, 25.90, 23.61, 23.49, 18.19, 18.13, 15.9.

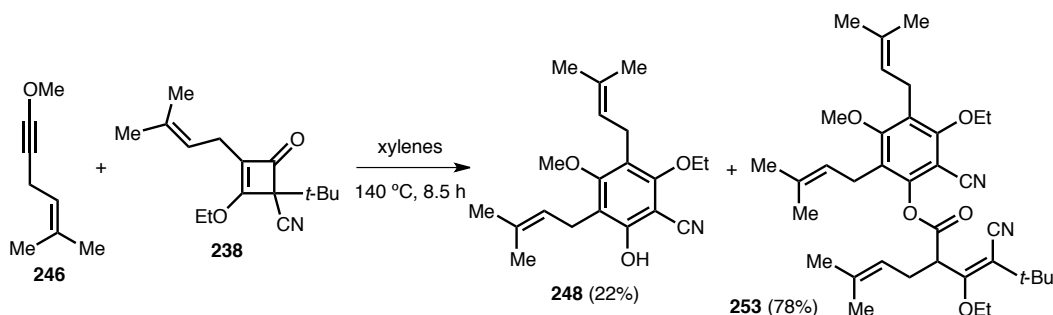


Key 1D nOe correlations.

FTIR (thin film) ν_{max} : 3363 (br), 2978, 2930, 2226, 1597, 1579, 1445, 1385, 1097 cm⁻¹.

HRMS–ESI (*m/z*): [M+H]⁺ calculated for C₂₀H₂₇NO₃, 330.2064; found, 330.2055.

TLC R_f = 0.75 (95:5 hexane:EtOAc).

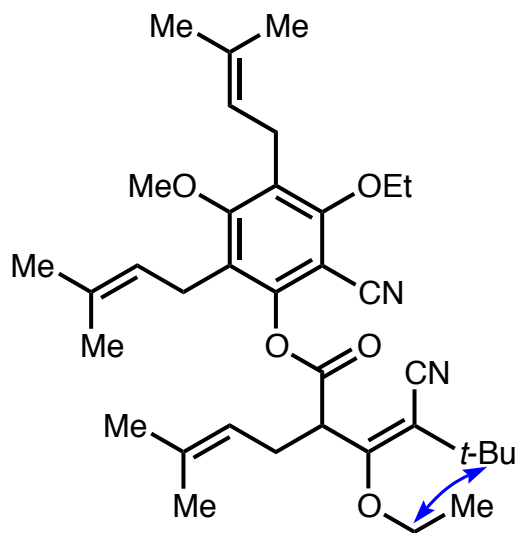


E-2-Cyano-3-ethoxy-5-methoxy-4,6-bis(3-methylbut-2-en-1-yl)phenyl 4-cyano-3-ethoxy-5,5-dimethyl-2-(3-methylbut-2-en-1-yl)hex-3-enoate (253):

A xylenes (1 mL) solution of **238** (12 mg, 0.046 mmol), **246** (28.5 mg, 0.230 mmol, 5 equiv), and Hünig's base (~1 mg, 0.01 mmol, 0.2 equiv) was sparged with N₂ for 5 min in a 10-mL sealed tube and subsequently heated to 140 °C. After stirring for 8.5 h at 140 °C, the reaction was cooled to rt and concentrated *in vacuo*. Flash column chromatography (25 mL SiO₂, 98:2 → 9:1 hexane:EtOAc) afforded 3.4 mg (0.010 mmol, 22% yield) of **248** as a white residue and 10.5 mg (0.018 mmol, 78% yield) of **253** as a colorless residue.

¹H NMR (600 MHz; CDCl₃) δ: 5.14 (t, *J* = 7.3 Hz, 1H), 5.10 (t, *J* = 6.4 Hz, 1H), 5.02 (t, *J* = 5.8 Hz, 1H), 4.27 (dd, *J* = 9.0, 6.0 Hz, 1H), 4.21-4.16 (m, 3H), 4.08-4.05 (m, 1H), 3.73 (s, 3H), 3.33 (d, *J* = 6.4 Hz, 2H), 3.26 (d, *J* = 5.8 Hz, 2H), 2.82 (m, 1H), 2.66 (m, 1H), 1.76 (s, 3H), 1.74 (s, 3H), 1.72 (s, 3H), 1.71-1.69 (s, 9H), 1.44 (t, *J* = 7.0 Hz, 3H), 1.36 (t, *J* = 6.9 Hz, 3H), 1.26 (s, 9H).

¹³C NMR (125 MHz; CDCl₃) δ: 169.0, 164.2, 162.4, 160.0, 150.1, 135.6, 133.5, 132.6, 128.4, 125.5, 122.4, 121.5, 119.7, 119.5, 114.3, 109.8, 79.4, 71.5, 67.1, 62.1, 49.8, 33.4, 29.9, 27.7, 25.95, 25.86, 25.80, 24.1, 23.8, 18.28, 18.17, 18.11, 15.9, 15.3.

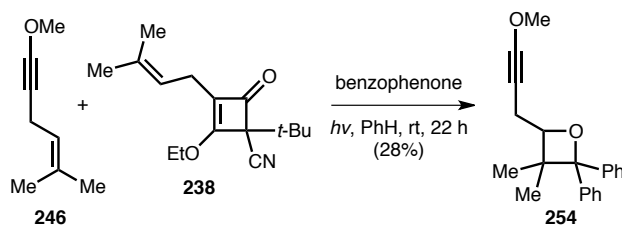


Key 1D nOe correlation.

FTIR (thin film) ν_{max} : 2961, 2923, 2854, 2229, 2203, 1769, 1599, 1440, 1385, 1099 cm^{-1} .

HRMS-ESI (m / z): $[\text{M}+\text{Na}]^+$ calculated for $\text{C}_{36}\text{H}_{50}\text{N}_2\text{O}_5$, 613.3612; found, 613.3611.

TLC R_f = 0.48 (8:2 hexane:EtOAc).



4-(3-Methoxyprop-2-yn-1-yl)-3,3-dimethyl-2,2-diphenyloxetane (254):

A PhH (3 mL) solution of **238** (40. mg, 0.15 mmol, 1 equiv), **246** (95 mg, 0.77 mmol, 5 equiv), and benzophenone (9 mg, 0.05 mmol, 0.3 equiv) in a 10-mL borosilicate test tube placed in a continuous flow H₂O bath was irradiated with quartz-filtered light for 22 h. The reaction was then concentrated *in vacuo* to an orange-yellow oil. Flash column chromatography (30 mL SiO₂, 95:5 hexane:EtOAc) afforded 4.3 mg (0.014 mmol, 28% yield) of **254** as a white flocculent solid.

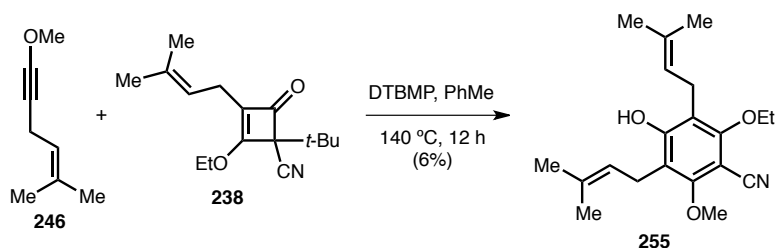
¹H NMR (600 MHz; CDCl₃) δ: 7.58 (dd, *J* = 8.5, 1.2 Hz, 2H), 7.43 (dd, *J* = 8.4, 1.2 Hz, 2H), 7.33-7.27 (m, 4H), 7.20-7.15 (m, 2H), 4.44 (dd, *J* = 9.2, 5.6 Hz, 1H), 3.79 (s, 3H), 2.51 (dd, *J* = 16.1, 5.6 Hz, 1H), 2.40 (dd, *J* = 16.1, 9.2 Hz, 1H), 1.15 (s, 3H), 1.12 (s, 3H).

¹³C NMR (125 MHz; CDCl₃) δ: 145.1, 144.2, 128.2, 127.9, 126.69, 126.54, 125.8, 125.2, 92.2, 91.3, 84.2, 65.5, 46.0, 31.9, 26.6, 20.9, 20.5.

FTIR (thin film) ν_{max} : 3058, 3025, 2972, 2943, 2275, 1449, 1239, 995, 959, 709 cm⁻¹.

HRMS-ESI (*m/z*): [M+H]⁺ calculated for C₂₁H₂₂O₂, 307.1693; found, 307.1697.

TLC R_f = 0.51 (8:2 hexane:EtOAc).



2-Ethoxy-4-hydroxy-6-methoxy-3,5-bis(3-methylbut-2-en-1-yl)benzonitrile (255):

A PhMe (3 mL) solution of **238** (40. mg, 0.15 mmol, 1 equiv), **246** (95 mg, 0.77 mmol, 5 equiv), and 2,6-di-*tert*-butyl-4-methylphenol (7 mg, 0.03 mmol, 0.2 equiv) was heated to 140 °C in a 10-mL sealed tube. After stirring at 140 °C for 12 h, the reaction was cooled to rt and concentrated *in vacuo* to an orange oil. Flash column chromatography (30 mL SiO₂, 95:5 hexane:EtOAc) followed by preparatory thin-layer chromatography (1 × 98:2 CH₂Cl₂:Et₂O) afforded 3 mg (9 μmol, 6% yield) of **255** as a colorless residue.

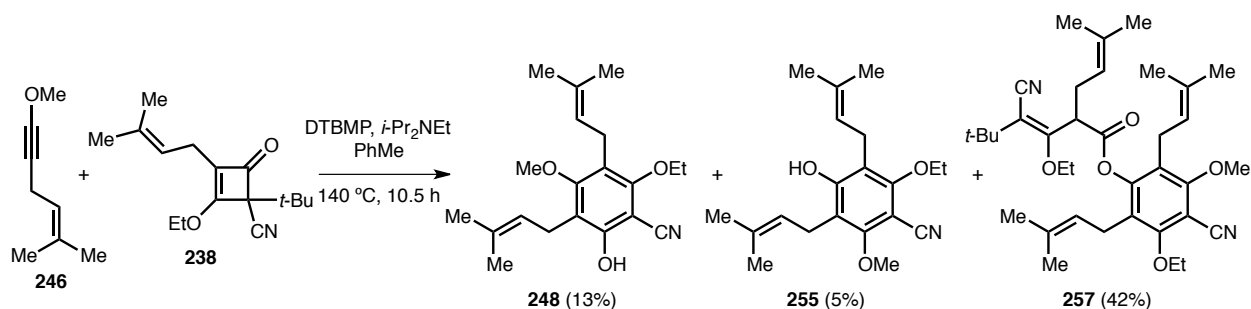
¹H NMR (600 MHz; CDCl₃) δ: 6.11 (s, 1H), 5.17-5.14 (m, 2H), 4.11 (q, *J* = 7.0 Hz, 2H), 3.94-3.92 (m, 3H), 3.37-3.33 (m, 4H), 1.80 (s, 6H), 1.75 (s, 3H), 1.74 (s, 3H), 1.44 (t, *J* = 7.0 Hz, 3H).

¹³C NMR (125 MHz; CDCl₃) δ: 160.2, 159.3, 135.5, 135.1, 121.47, 121.42, 117.73, 117.59, 115.5, 93.4, 71.5, 62.5, 26.0, 23.20, 23.03, 18.18, 18.15, 15.9.

FTIR (thin film) ν_{max} : 3396 (br), 2979, 2928, 2225, 1586, 1438, 1389, 1178, 1097 cm⁻¹.

HRMS–ESI (*m/z*): [M+Na]⁺ calculated for C₂₀H₂₇NO₃, 352.1883; found, 352.1888.

TLC R_f = 0.68 (95:5 CH₂Cl₂:Et₂O).



E-4-cyano-3-ethoxy-5-methoxy-2,6-bis(3-methylbut-2-en-1-yl)phenyl 4-cyano-3-ethoxy-5,5-dimethyl-2-(3-methylbut-2-en-1-yl)hex-3-enoate (257):

A PhMe (3 mL) solution of **238** (40. mg, 0.15 mmol, 1 equiv), **246** (95 mg, 0.77 mmol, 5 equiv), 2,6-di-*tert*-butyl-4-methylphenol (7 mg, 0.03 mmol, 0.2 equiv), and Hünig's base (5 μ L, 0.03 mmol, 0.2 equiv) was heated to 140 °C in a 10-mL sealed tube. After stirring for 10.5 h, the reaction was cooled to rt and concentrated *in vacuo* to a brown-red oil. Flash column chromatography (25 mL SiO₂, 95:5 hexane:EtOAc) afforded 6.3 mg (0.019 mmol, 13% yield) of **248** as a colorless residue, 2.5 mg (7.6 μ mol, 5% yield) of **255** as a colorless residue, and 19.1 mg (0.032 mmol, 42% yield) of **257** as a colorless residue.

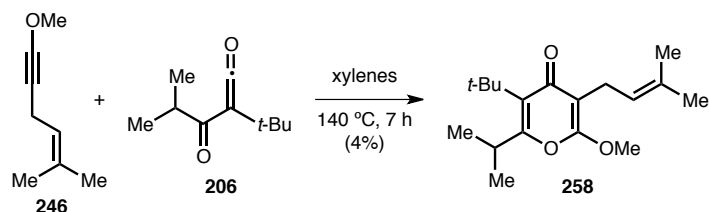
¹H NMR (600 MHz; CDCl₃) δ : 5.24 (t, *J* = 6.4 Hz, 1H), 5.11 (t, *J* = 6.7 Hz, 1H), 5.05 (s, 1H), 5.00 (t, *J* = 6.5 Hz, 1H), 4.27-4.22 (m, 1H), 4.22-4.17 (m, 2H), 4.15-4.11 (m, 1H), 3.74 (s, 3H), 3.33 (d, *J* = 6.6 Hz, 2H), 3.30-3.19 (m, 4H), 1.76 (s, 3H), 1.71 (s, 6H), 1.68 (s, 3H), 1.67 (s, 6H), 1.44 (t, *J* = 5.7 Hz, 3H), 1.42 (t, *J* = 5.8 Hz, 3H), 1.14 (s, 9H).

¹³C NMR (125 MHz; CDCl₃) δ : 166.5, 162.3, 160.1, 150.4, 133.8, 132.9, 132.5, 128.1, 125.2, 122.5, 121.77, 121.63, 118.9, 114.0, 98.4, 72.0, 71.5, 62.1, 43.7, 36.3, 29.9, 28.2, 26.9, 25.88, 25.86, 25.84, 25.80, 24.04, 23.86, 18.26, 18.22, 18.19, 15.95, 15.81.

FTIR (thin film) ν_{max} : 2967, 2930, 2857, 2228, 1729, 1597, 1439, 1387, 1160, 1084, 1041, 1024, 988 cm⁻¹.

HRMS-ESI (*m/z*): [M+Na]⁺ calculated for C₃₆H₅₀N₂O₅, 613.3623; found, 613.3612.

TLC R_f = 0.50 (8:2 hexane:EtOAc).

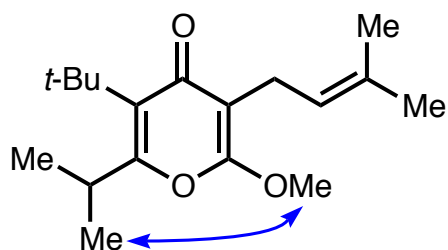


3-(tert-Butyl)-2-isopropyl-6-methoxy-5-(3-methylbut-2-en-1-yl)-4H-pyran-4-one (258):

A xylene (4.8 mL) solution of **206** (41 mg, 0.24 mmol, 1 equiv) and **246** (150 mg, 1.2 mmol, 5 equiv) was heated to 140 °C in a 50-mL sealed tube. After stirring at 140 °C for 7 h, the reaction was cooled to rt and concentrated *in vacuo*. Flash column chromatography (30 mL SiO₂, 95:5 → 9:1 → 8:2 hexane:EtOAc) followed by preparatory thin-layer chromatography (2 × 9:1 hexane:EtOAc) afforded 2.5 mg (8.5 μmol, 4% yield) of **258** as a colorless residue.

¹H NMR (600 MHz; CDCl₃) δ: 5.19 (t, *J* = 6.7 Hz, 1H), 3.93 (s, 3H), 3.67 (septet, *J* = 6.7 Hz, 1H), 3.02 (d, *J* = 6.7 Hz, 2H), 1.72 (s, 3H), 1.67 (s, 3H), 1.44 (s, 9H), 1.25 (d, *J* = 6.8 Hz, 6H).

¹³C NMR (125 MHz; CDCl₃) δ: 181.5, 162.7, 161.0, 131.9, 128.3, 122.4, 103.8, 55.2, 35.1, 31.7, 30.9, 26.0, 21.12, 21.06, 18.0.

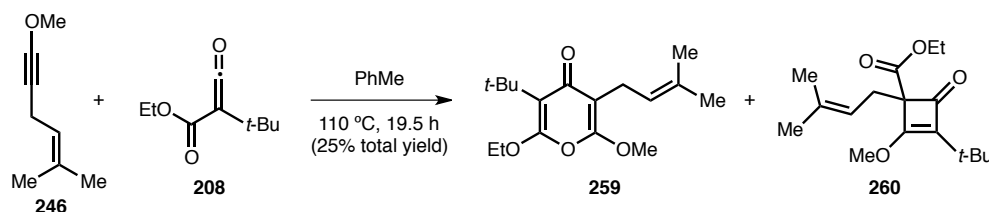


Key 1D nOe correlation.

FTIR (thin film) ν_{max} : 2067, 2921, 1664, 1611, 1462, 1381, 1314, 1262, 1141 cm⁻¹.

HRMS-ESI (*m/z*): [M+Na]⁺ calculated for C₁₈H₂₈O₃, 315.1931; found, 315.1945.

TLC R_f = 0.26 (8:2 hexane:EtOAc).



A PhMe (5.8 mL) solution of **208**⁵⁶⁶ (50. mg, 0.29 mmol, 1 equiv) and **246** (182 mg, 1.47 mmol, 5 equiv) in a 10-mL sealed tube was heated to 110 °C. After stirring for 19.5 h at 110 °C, the reaction was cooled to rt and concentrated *in vacuo* to a yellow oil. Flash column chromatography (30 mL SiO₂, 95:5 hexane:EtOAc) afforded 22.0 mg of an inseparable mixture of **259** and **260** (1.3:1 ratio by ¹H NMR spectroscopy; 0.069 mmol, 25% total yield) as a colorless oil.

FTIR (thin film) ν_{max} : 2967, 2954, 2930, 2916, 1719, 1679, 1624, 1608, 1381, 1350, 1263, 1239 cm⁻¹.

HRMS-ESI (*m/z*): [M+Na]⁺ calculated for C₁₇H₂₆O₄, 317.1723; found, 317.1714.

TLC R_f = 0.43 (8:2 hexane:EtOAc).

3-(tert-Butyl)-2-ethoxy-6-methoxy-5-(3-methylbut-2-en-1-yl)-4H-pyran-4-one (259):⁶⁰²

¹H NMR (600 MHz; CDCl₃) δ : 4.99 (t, *J* = 7.6 Hz, 1H), 4.22 (q, *J* = 7.1 Hz, 2H), 3.89 (s, 3H), 2.90 (dd, *J* = 15.5, 7.6 Hz, 1H), 2.49 (dd, *J* = 15.5, 7.6 Hz, 1H), 1.69 (s, 3H), 1.63 (s, 3H), 1.28 (t, *J* = 7.1 Hz, 3H), 1.15 (s, 9H).

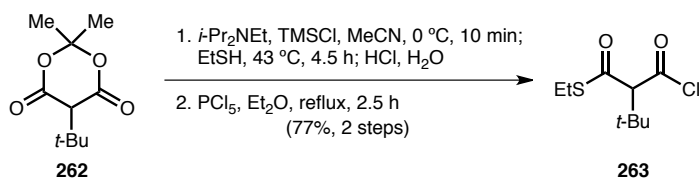
¹³C NMR (125 MHz; CDCl₃) δ : 180.6, 174.4, 171.0, 136.2, 135.2, 117.7, 73.1, 61.7, 59.6, 31.4, 28.4, 27.9, 26.1, 18.04, 14.4.

Ethyl 3-(tert-butyl)-2-methoxy-1-(3-methylbut-2-en-1-yl)-4-oxocyclobut-2-enecarboxylate (260):⁶⁰²

¹H NMR (600 MHz; CDCl₃) δ : 5.15 (t, *J* = 7.0 Hz, 1H), 4.25 (q, *J* = 7.1 Hz, 2H), 3.91 (s, 3H), 3.00 (d, *J* = 7.0 Hz, 2H), 1.69 (s, 3H), 1.65 (s, 3H), 1.41 (t, *J* = 7.1 Hz, 3H), 1.36 (s, 9H).

¹³C NMR (125 MHz; CDCl₃) δ : 182.4, 158.24, 158.17, 131.9, 122.3, 111.1, 104.0, 66.1, 55.9, 33.9, 30.5, 25.9, 21.2, 17.97, 15.0.

⁶⁰² NMR assignments of the mixture were elucidated using heteronuclear 2D-NMR techniques.

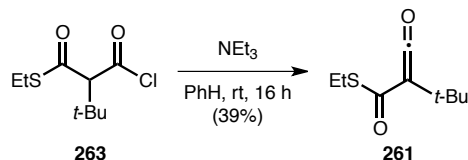


S-Ethyl 2-(chlorocarbonyl)-3,3-dimethylbutanethioate (263):

A MeCN (4 mL) solution of **262**⁵⁹⁴ (813 mg, 4.06 mmol, 1 equiv) in a 20-mL scintillation vial was cooled to 0 °C. Hünig's base (777 μL, 4.47 mmol, 1.1 equiv) followed by chlorotrimethylsilane (567 μL, 4.47 mmol, 1.1 equiv) were added dropwise over 10 min. After stirring an additional 10 min at 0 °C, ethanethiol (316 μL, 4.26 mmol, 1.05 equiv) was added. The resulting white slurry was warmed to 43 °C, whereupon a colorless solution formed. After stirring at 43 °C for 4.5 h, the solution was cooled to rt, quenched with 0.3 M HCl, and extracted thrice with Et₂O. The organic extracts were combined and extracted once with sat. aq. NaHCO₃. This aqueous extract was stirred vigorously while an aqueous 10% HCl solution was added dropwise until the pH of the solution was < 2. This solution was extracted thrice with Et₂O. These organic extracts were combined, washed with brine, dried over MgSO₄, filtered, and concentrated to a colorless oil, which solidified upon cooling. An Et₂O (12 mL) solution of this material and phosphorous(V) chloride (1.46 g, 6.99 mmol, 2 equiv) in a 2-neck 25-mL round-bottom flask outfitted with a reflux condenser was refluxed for 2.5 h. After cooling the solution to rt, it was transferred via cannula to a Schlenk filter funnel and filtered under a positive pressure of N₂ followed by one Et₂O rinse. The filtrate was concentrated under a stream of N₂ and distilled directly. Short-path distillation (6 mmHg, 65-70 °C) afforded 604 mg (2.71 mmol, 77% yield over 2 steps) of **263** as a colorless oil.

¹H NMR (600 MHz; CDCl₃) δ: 3.98 (s, 1H), 2.97 (m, 2H), 1.29 (t, *J* = 7.4 Hz, 3H), 1.15 (s, 9H).

¹³C NMR (125 MHz; CDCl₃) δ: 191.1, 167.1, 80.5, 36.8, 28.3, 24.9, 14.5.



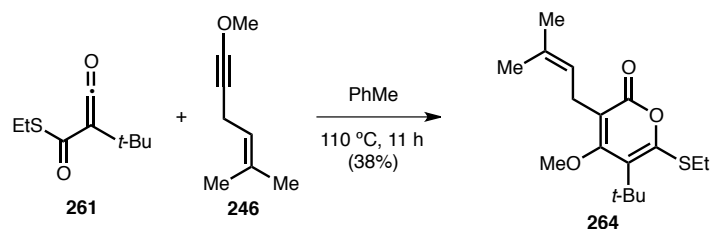
S-Ethyl 3,3-dimethyl-2-oxomethylidenbutanethioate (261):

A PhH (3.8 mL) solution of **263** (593 mg, 2.66 mmol, 1 equiv) in a 10-mL pear-shaped flask was treated with triethylamine (0.74 mL, 5.3 mmol, 2 equiv), immediately causing a white precipitate to form. After allowing the flask to stand for 16 h at rt, the reaction was diluted with PhH and filtered through a Schlenk filter funnel under a positive pressure of N₂. The pale yellow precipitate was washed twice with PhH. The resulting pale yellow filtrate was concentrated *in vacuo*. Short-path distillation (6 mmHg, 45-50 °C) afforded 195 mg (1.05 mmol, 39% yield) of **261** as a colorless oil.

¹H NMR (500 MHz; CDCl₃) δ: 2.96 (q, *J* = 7.4 Hz, 2H), 1.28 (t, *J* = 7.4 Hz, 3H), 1.26 (s, 9H).

¹³C NMR (125 MHz; CDCl₃) δ: 189.5, 110.9, 62.9, 32.8, 29.8, 23.8, 15.4.

FTIR (thin film) ν_{max}: 2965, 2919, 2874, 2108, 1661, 1241, 1158, 864, 773 cm⁻¹.

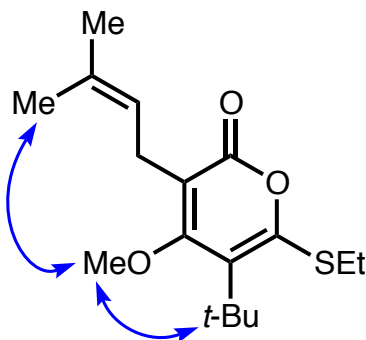


5-(*tert*-Butyl)-6-(ethylthio)-4-methoxy-3-(3-methylbut-2-en-1-yl)-2*H*-pyran-2-one (264):

A PhMe (3.2 mL) solution of **261** (30. mg, 0.16 mmol, 1 equiv) and **246** (100 mg, 0.81 mmol, 5 equiv) was heated to 110 °C in a 10-mL sealed tube. After stirring at 110 °C for 11 h, the reaction was cooled to rt and concentrated *in vacuo*. Flash column chromatography (30 mL SiO₂, 95:5 hexane:EtOAc) afforded 19.0 mg (0.061 mmol, 38% yield) of **264** as a colorless residue.

¹H NMR (600 MHz; CDCl₃) δ: 5.04 (t, *J* = 6.2 Hz, 1H), 3.65 (s, 3H), 3.07 (m, 4H), 1.71 (s, 3H), 1.70 (s, 3H), 1.40 (s, 9H), 1.35 (t, *J* = 7.4 Hz, 3H).

¹³C NMR (125 MHz; CDCl₃) δ: 168.0, 163.9, 155.9, 133.3, 121.6, 120.0, 115.2, 62.3, 35.7, 30.4, 25.8, 25.2, 18.3, 15.5.

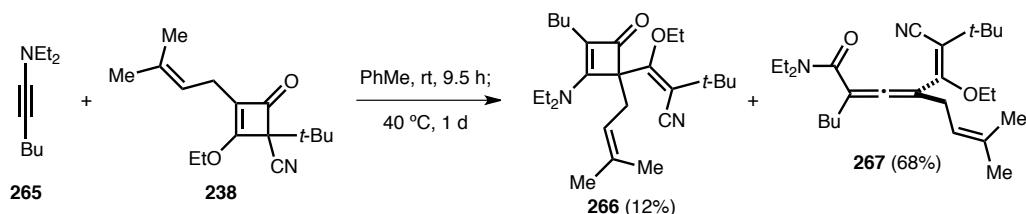


Key 1D nOe correlations.

FTIR (thin film) ν_{max} : 2964, 2930, 1717, 1597, 1509, 1343, 1118, 1008, 942 cm⁻¹.

HRMS-ESI (*m/z*): [M+Na]⁺ calculated for C₁₇H₂₆O₃S, 333.1495; found, 333.1497.

TLC R_f = 0.30 (9:1 hexane:EtOAc).

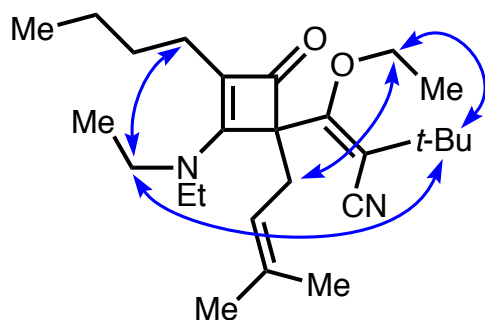


A PhH (2 mL) solution of **238** (171 mg, 0.65 mmol, 1 equiv) and **265**⁵⁹⁷ (100. mg, 0.65 mmol, 1 equiv) was stirred at rt in a sealed tube for 9.5 h. The reaction was then heated to 40 °C for 1 d. The reaction was subsequently cooled to rt and concentrated *in vacuo* to a red oil. Flash column chromatography (100 mL SiO₂, 95:5 → 9:1 → 8:2 hexane:EtOAc) afforded 32 mg (0.077 mmol, 12% yield) of **266** as a pale yellow oil and 183 mg (0.44 mmol, 68% yield) of **267** as a pale yellow oil.

E-2-((3-Butyl-2-(diethylamino)-1-(3-methylbut-2-en-1-yl)-4-oxocyclobut-2-en-1-yl)(ethoxy)methylene)-3,3-dimethylbutanenitrile (266):

¹H NMR (600 MHz; CDCl₃) δ: 4.97 (t, *J* = 7.2 Hz, 1H), 4.58 (dq, *J* = 10.0, 7.1 Hz, 1H), 3.61-3.53 (m, 2H), 3.28-3.21 (m, 3H), 2.64 (dd, *J* = 15.9, 7.2 Hz, 1H), 2.31 (dd, *J* = 15.9, 7.2 Hz, 1H), 2.19-2.10 (m, 2H), 1.66 (s, 3H), 1.62 (s, 3H), 1.57 (m, 2H), 1.36 (m, *J* = 2.9 Hz, 2H), 1.32 (t, *J* = 7.1 Hz, 3H), 1.25 (s, 9H), 1.22 (m, 6H), 0.90 (t, *J* = 7.4 Hz, 3H).

¹³C NMR (125 MHz; CDCl₃) δ: 180.8, 168.9, 165.0, 134.7, 118.64, 118.57, 117.9, 110.3, 72.0, 67.8, 45.9, 42.6, 35.3, 31.1, 30.9, 27.4, 26.2, 23.7, 22.9, 18.4, 14.9, 14.1, 13.8, 12.7.



Key 1D nOe correlations.

HRMS–ESI (*m/z*): [M+Na]⁺ calculated for C₂₆H₄₂N₂O₂, 437.3139; found, 437.3150.

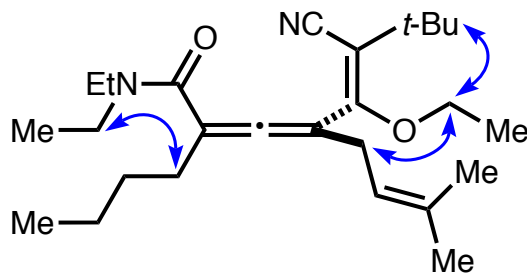
FTIR (thin film) ν_{max}: 2962, 2933, 2873, 2198, 1744, 1586, 1451 cm⁻¹.

TLC R_f = 0.51 (8:2 hexane:EtOAc).

E-2-Butyl-6-cyano-5-ethoxy-N,N-diethyl-7,7-dimethyl-4-(3-methylbut-2-en-1-yl)octa-2,3,5-trienamide (267):

¹H NMR (500 MHz; CDCl₃) δ: 5.14 (t, *J* = 7.3 Hz, 1H), 3.89-3.79 (m, 2H), 3.39-3.28 (m, 4H), 2.90 (dd, *J* = 16.1, 7.3 Hz, 1H), 2.81 (dd, *J* = 16.1, 7.3 Hz, 1H), 2.38-2.30 (m, 2H), 1.66 (s, 3H), 1.58 (s, 3H), 1.43-1.38 (m, 2H), 1.36-1.28 (m, 2H), 1.22 (t, *J* = 7.1 Hz, 3H), 1.15 (s, 9H), 1.07 (t, *J* = 7.1 Hz, 6H), 0.85 (t, *J* = 7.2 Hz, 3H).

¹³C NMR (125 MHz; CDCl₃) δ: 200.4, 166.3, 163.7, 135.0, 119.46, 119.33, 104.7, 103.6, 100.9, 65.8, 42.8 (br), 39.5 (br), 33.0, 30.8, 30.59, 30.47, 29.8, 25.8, 22.4, 17.9, 15.3, 14.6 (br), 13.9, 12.9 (br).

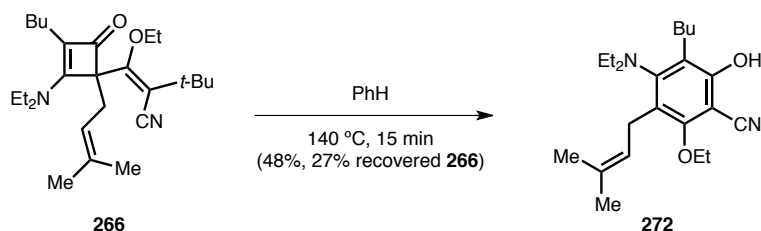


Key 1D nOe correlations.

FTIR (thin film) ν_{max} : 2967, 2934, 2873, 2201, 1959, 1633, 1595, 1458, 1429, 1274, 1220, 739 cm⁻¹.

HRMS-ESI (*m/z*): [M+H]⁺ calculated for C₂₆H₄₂N₂O₂, 415.3319; found, 415.3321.

TLC R_f = 0.31 (8:2 hexane:EtOAc).



3-Butyl-4-(diethylamino)-6-ethoxy-2-hydroxy-5-(3-methylbut-2-en-1-yl)benzonitrile (272):

A PhH (1 mL) solution of **266** (6.0 mg, 14 μmol) was heated to 140 $^\circ\text{C}$ for 15 min in a 10-mL sealed tube. The reaction was subsequently cooled to rt and concentrated *in vacuo* to an orange oil. Preparatory thin-layer chromatography (1 \times 98:2 hexane:EtOAc) afforded 2.4 mg (6.7 μmol , 48% yield) of **272** as a pale yellow oil and 1.6 mg (3.9 μmol , 27% recovery) of **266** as a pale yellow oil.

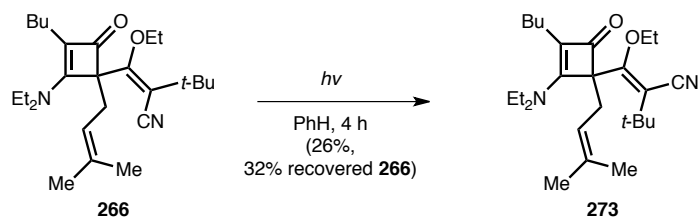
^1H NMR (600 MHz; CDCl_3) δ : 5.39 (br s, 1H), 4.99 (t, $J = 6.1$ Hz, 1H), 4.12 (q, $J = 7.0$ Hz, 2H), 3.30 (d, $J = 6.1$ Hz, 2H), 3.06 (q, $J = 7.1$ Hz, 4H), 2.61-2.58 (m, 2H), 1.73 (s, 3H), 1.67 (s, 3H), 1.52-1.46 (m, 3H), 1.44-1.40 (m, 5H), 1.02 (t, $J = 7.1$ Hz, 6H), 0.96 (t, $J = 7.2$ Hz, 3H).

^{13}C NMR (125 MHz; CDCl_3) δ : 155.8, 155.5, 154.6, 131.0, 128.9, 126.2, 124.3, 115.5, 91.4, 70.8, 48.4, 31.5, 26.7, 25.84, 25.73, 23.8, 18.3, 15.9, 14.8, 14.2.

FTIR (thin film) ν_{max} : 3323 (br), 2965, 2929, 2855, 2228, 1592, 1556, 1447, 1378, 1119 cm^{-1} .

HRMS–ESI (m/z): $[\text{M}+\text{Na}]^+$ calculated for $\text{C}_{22}\text{H}_{34}\text{N}_2\text{O}_2$, 381.2512; found, 381.2505.

TLC $R_f = 0.65$ (95:5 hexane:EtOAc).



Z-2-((3-Butyl-2-(diethylamino)-1-(3-methylbut-2-en-1-yl)-4-oxocyclobut-2-en-1-yl)(ethoxy)methylene)-3,3-dimethylbutanenitrile (273):

A PhH (1 mL) solution of **266** (5.0 mg, 12 μmol) in a 12-mL quartz test tube was irradiated in a continuous flow rt H_2O bath for 4 h. The reaction was then concentrated *in vacuo* to an orange-yellow oil. Preparatory thin-layer chromatography ($1 \times 95:5$ hexane:EtOAc $\rightarrow 1 \times 9:1$ hexane:EtOAc) afforded 1.3 mg (3.1 μmol , 26% yield) of **273** as a pale yellow residue and 1.6 mg (3.9 μmol , 32% recovery) of **266** as a pale yellow residue.

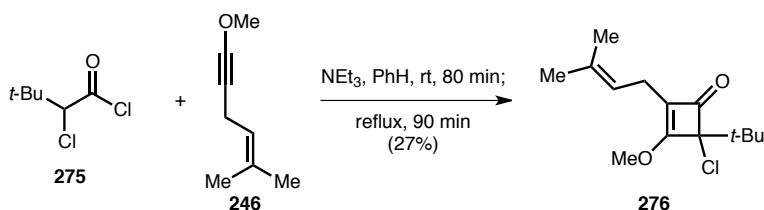
^1H NMR (600 MHz; CDCl_3) δ : 5.01 (t, $J = 7.0$ Hz, 1H), 4.24 (dq, $J = 9.0, 7.0$ Hz, 1H), 3.84 (dq, $J = 9.0, 7.0$ Hz, 1H), 3.38 (m, 2H), 3.23-3.18 (m, 2H), 3.03 (dd, $J = 15.6, 7.0$ Hz, 1H), 2.44 (dd, $J = 15.6, 7.0$ Hz, 1H), 2.16-2.05 (m, 2H), 1.67 (s, 3H), 1.61 (s, 3H), 1.52-1.45 (m, 2H), 1.42 (s, 9H), 1.37-1.32 (m, 2H), 1.30-1.28 (m, 3H), 1.23-1.18 (m, 6H), 0.90 (t, $J = 7.3$ Hz, 3H).

^{13}C NMR (125 MHz; CDCl_3) δ : 179.7, 171.4, 165.9, 134.8, 118.7, 115.9, 114.1, 110.2, 74.6, 73.5, 46.3, 42.0, 33.5, 32.16, 32.12, 31.94, 26.1, 23.5, 22.9, 18.6, 16.0, 14.3, 14.1, 13.5.

FTIR (thin film) ν_{max} : 2959, 2926, 2854, 2207, 1736, 1591, 1459, 1377 cm^{-1} .

HRMS-ESI (m/z): $[\text{M}+\text{H}]^+$ calculated for $\text{C}_{26}\text{H}_{42}\text{N}_2\text{O}_2$, 415.3319; found, 415.3307.

TLC $R_f = 0.37$ (8:2 hexane:EtOAc).



4-(tert-Butyl)-4-chloro-3-methoxy-2-(3-methylbut-2-en-1-yl)cyclobut-2-enone (276):

A PhH (5 mL) solution of **275** (500 mg, 2.96 mmol 1 equiv) was added dropwise via cannula to a PhH (20 mL) solution of triethylamine (412 μ L, 2.96 mmol, 1 equiv) and **246** (771 mg, 6.21 mmol, 2.1 equiv) in a 50-mL recovery flask. The resulting yellow solution was stirred at rt for 80 min. A reflux condenser was then attached to the recovery flask, and the reaction was refluxed for 90 min. The reaction was then cooled to rt and concentrated *in vacuo* to a red-orange oil. This oil was taken up in 9:1 hexane:EtOAc and filtered to remove an off-white solid. The filtrate was concentrated *in vacuo* to a red-orange oil. Flash column chromatography (100 mL SiO₂, 95:5 \rightarrow 9:1 hexane:EtOAc) afforded 209 mg (0.81 mmol, 27% yield) of **276** as a pale yellow oil.

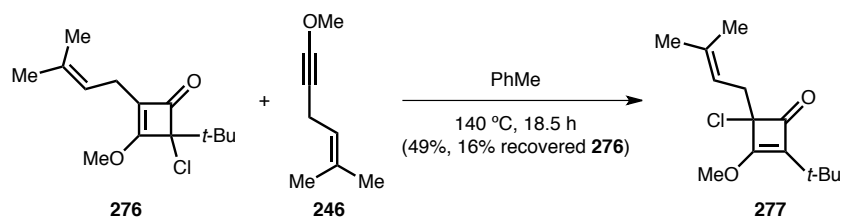
¹H NMR (600 MHz; CDCl₃) δ : 5.04 (t, J = 7.0 Hz, 1H), 4.09 (s, 3H), 2.86-2.78 (m, 2H), 1.61 (s, 3H), 1.56 (s, 3H), 1.02 (s, 9H).

¹³C NMR (125 MHz; CDCl₃) δ : 185.7, 178.7, 133.9, 124.2, 119.4, 89.9, 60.3, 36.6, 26.3, 25.5, 21.4, 17.8.

FTIR (thin film) ν_{max} : 2974, 1771, 1622, 1457, 1356, 1258, 991 cm⁻¹.

HRMS-ESI (m/z): [M+H]⁺ calculated for C₁₄H₂₁ClO₂, 257.1303; found, 257.1314.

TLC R_f = 0.18 (95:5 hexane:EtOAc).



2-(tert-Butyl)-4-chloro-3-methoxy-4-(3-methylbut-2-en-1-yl)cyclobut-2-enone (277):

A PhMe (3 mL) solution of **276** (50. mg, 0.19 mmol, 1 equiv) and **246** (48 mg, 0.39 mmol, 2 equiv) was heated to 140 °C in a 10-mL sealed tube. After stirring at 140 °C for 18.5 h, the reaction was cooled to rt and concentrated *in vacuo* to a yellow-orange oil. Flash column chromatography (30 mL SiO₂, 95:5 → 9:1 hexane:EtOAc) afforded 24 mg (0.094 mmol, 49% yield) of **277** as a pale yellow oil along with 8 mg (0.03 mmol, 16% recovery) of **276** as a pale yellow oil.

¹H NMR (600 MHz; CDCl₃) δ: 4.99 (t, *J* = 7.5 Hz, 1H), 4.15 (s, 3H), 3.02 (dd, *J* = 15.5, 7.5 Hz, 1H), 2.71 (dd, *J* = 15.5, 7.5 Hz, 1H), 1.69 (s, 3H), 1.64 (s, 3H), 1.14 (s, 9H).

¹³C NMR (125 MHz; CDCl₃) δ: 183.2, 176.3, 137.1, 135.3, 117.4, 82.1, 59.2, 35.7, 31.3, 28.1, 26.0, 18.1.

FTIR (thin film) ν_{max} : 2967, 2870, 1769, 1624, 1480, 1459, 1356 cm⁻¹.

HRMS–ESI (*m/z*): [M+H]⁺ calculated for C₁₄H₂₁ClO₂, 257.1303; found, 257.1302.

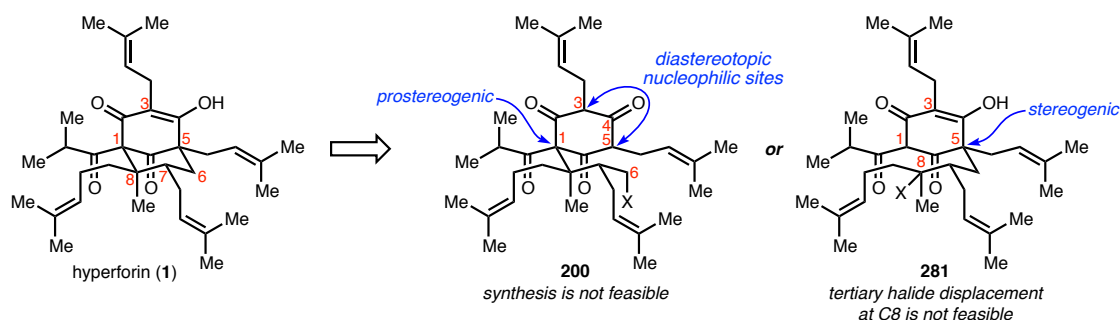
TLC R_f = 0.44 (9:1 hexane:EtOAc).

Chapter 3

Total Synthesis of Hyperforin

Synthesis Overview

Given the inability of prior strategies to construct model systems resembling the core of hyperforin, we pursued an alternative strategy that addressed previously experienced shortcomings. One particular difficulty we encountered was the cyclization to form the phloroglucinol-derived carbocycle component of the bicyclo[3.3.1]nonane core of hyperforin. As previously elaborated, these cyclization strategies often afforded heterocyclic rings, such as pyrones. Further, when such a carbocycle was constructed, a very favorable elimination of a *tert*-butyl group was observed, producing a very stable aromatic product. Given the difficulties with pursuing an intermediate such as alkyl halide **200**, which involves strategic cleavage of the C5–C6 bond of hyperforin (**1**), we elected to pursue an alternative strategy involving cleavage of the extremely hindered C1–C8 bond (Scheme 3.1). At first glance, such an approach would not take advantage of latent symmetry elements that would potentially shorten the synthesis sequence, considering that the C5 position of **281** is stereogenic owing to differential substitution at C1 and at C3. In addition, a nucleophilic displacement strategy would not be feasible, considering the hindered nature of the C8 position.⁶⁰³



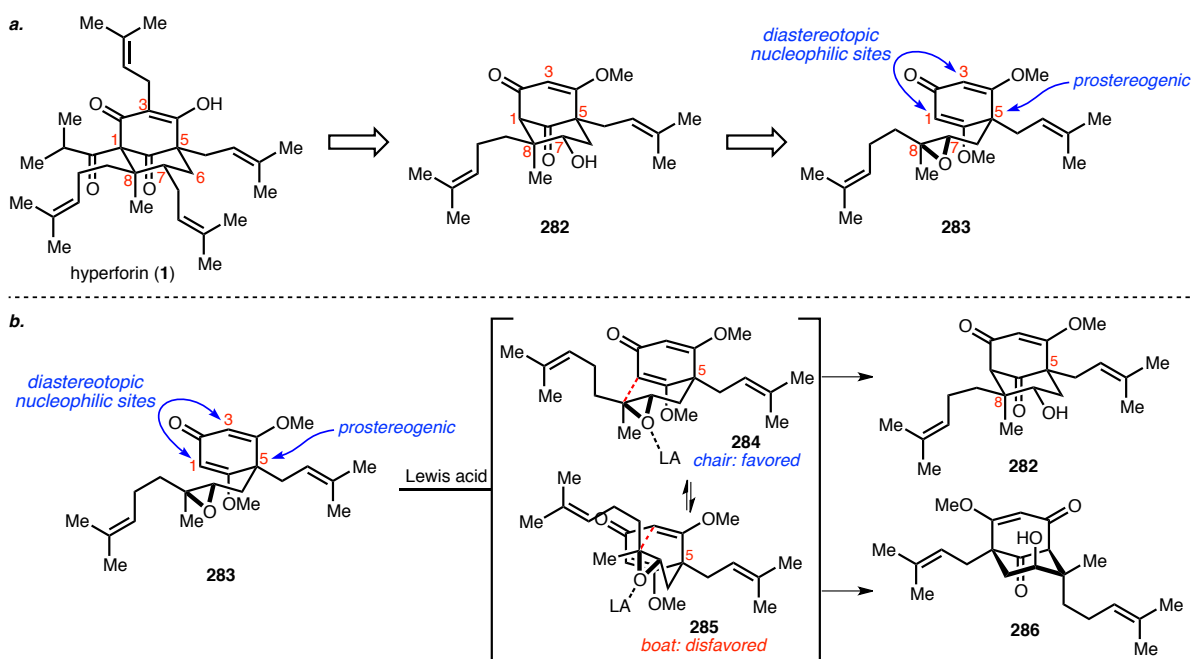
Scheme 3.1. Retrosynthetic disconnection of hyperforin at two key positions.

⁶⁰³ S_N1-type cyclization to form the C1–C8 bond of PPAPs has been explored (see ref. 534). When the C8 position contains differential substitution, as in the case of hyperforin, this cyclization mode produced a 1:1 mixture of diastereomers at the C8 position.

To reconcile these challenges, we developed a new synthesis strategy for hyperforin (Scheme 3.2a). In order to engender prostereogenicity at the key C5 position during a key cyclization event, the C1 isopropyl ketone and the C3 prenyl group were removed to afford intermediate **282**. These substituents may be installed late in the synthesis sequence via precendented bridgehead acylation and metalation-prenylation protocols, respectively.⁶⁰⁴ In addition, the C7 prenyl group was replaced with an alcohol functionality. This functional group exchange in **282** facilitates a mechanistic development of a transform, whereby the C7 alcohol would form an epoxide with the C8 position. The formation of the C1–C8 bond would now be reduced to a 6-*endo*-tet epoxide-opening cyclization reaction of **283**, a reaction that has been utilized previously to form carbon-carbon bonds at hindered positions.⁶⁰⁵

⁶⁰⁴ For examples of PPAP total syntheses that employ these reactions at a late stage, see refs. 510 and 527.

⁶⁰⁵ For examples of 6-*endo*-tet carbocyclization reactions that open epoxides at a tertiary position, see: (a) Armstrong, R. J.; Weiler, L. *Can. J. Chem.* **1986**, *64*, 584-596. (b) Pettersson, L.; Magnusson, G.; Frejd, T. *Acta Chem. Scand.* **1993**, *47*, 196-207. (c) Nakada, M.; Kojima, E.-i.; Iwata, Y. *Tetrahedron Lett.* **1998**, *39*, 313-316. (d) Beszant, S.; Giannini, E.; Zanoni, G.; Vidari, G. *Tetrahedron: Asymmetry* **2002**, *13*, 1245-1255. (e) Tong, R.; Valentine, J. C.; McDonald, F. E.; Cao, R.; Fang, X.; Hardcastle, K. I. *J. Am. Chem. Soc.* **2007**, *129*, 1050-1051. (f) Boone, M. A.; Tong, R.; McDonald, F. E.; Lense, S.; Cao, R.; Hardcastle, K. I. *J. Am. Chem. Soc.* **2010**, *132*, 5300-5308.



Scheme 3.2. (a) Retrosynthesis of hyperforin involving C1–C8 bond cleavage and (b) transition-state analysis of the key cyclization reaction.

An analysis of this key cyclization event is depicted in Scheme 3.2b. Owing to a plane of symmetry in the cyclohexadienone ring, the C5 position of **283** is prostereogenic. During the key epoxide-opening cyclization involving this intermediate, two diastereotopic nucleophilic enol ethers, at C1 and at C3, may engage in bonding interaction with the epoxide when activated with a Lewis acid. Transition state **284** is favored to yield **282** over its diastereomeric transition state **285**, which must adopt a boat-like conformation containing two severe eclipsing interactions in forming **286**. Additionally, due to geometric constraints of orbital overlap, a 6-(*enolendo*)-tet cyclization should be favored over a 5-(*enolendo*)-tet cyclization.⁶⁰⁶ Ultimately, the combinations of these factors culminate in: (1) the construction of the bicyclo[3.3.1]nonane core of hyperforin; (2) the introduction of stereochemistry at the previously prostereogenic C5 position; (3) the creation of a stereogenic quaternary center at C8; and (4) the formation of a conformationally rigid tertiary stereogenic center at C1. Additionally, given our

⁶⁰⁶ Baldwin, J. E.; Lusch, M. J. *Tetrahedron* **1982**, 38, 2939-2947.

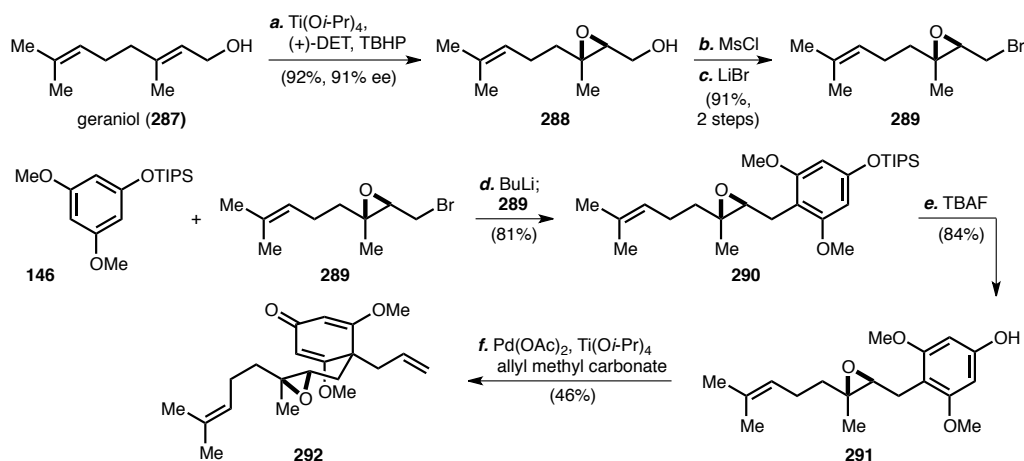
interests in creating a library of hyperforin analogs, alcohol **282** is also an ideal intermediate for diversification, in which a variety of groups may be appended at the C1, C3, and C7 positions.

Dearomative Allylation Approach

Given the difficulties we encountered while attempting to synthesize cyclohexadienones, we chose a well-precedented approach to an intermediate very similar to key cyclization precursor **283**. A Sharpless epoxidation of geraniol⁶⁰⁷ (**287**) afforded (*S,S*)-2,3-epoxygeraniol (**288**) in 91% ee, which upon mesylation and Finkelstein bromination gave epoxygeranyl bromide **289** (Scheme 3.3).⁶⁰⁸ Large quantities of **289** (120-130 g per batch of material) were processed through this three-step protocol, which involved only a single distillation and no silica gel chromatography. Regioselective lithiation of phloroglucinol triether **146**⁵²⁸ followed by coupling with **289** afforded alkylation product **290**. After desilylation to reveal phenol **291**, a Pd- and Ti-catalyzed dearomative allylation reaction, using a protocol developed for the total synthesis of (±)-garsubellin A by Danishefsky,^{527,529} produced cyclohexadienone **292**. This allylation was highly regioselective, and only trace amounts of aromatic allylation products were observed.

⁶⁰⁷ Hanson, R. M.; Sharpless, K. B. *J. Org. Chem.* **1986**, *51*, 1922-1925.

⁶⁰⁸ Gash, R. C.; MacCorquodale, F.; Walton, J. C. *Tetrahedron* **1989**, *45*, 5531-5538.



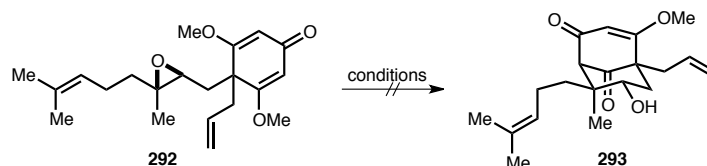
Scheme 3.3. Synthesis of cyclization precursor **292**.^a

^a Conditions: (a) Ti(Oi-Pr)_4 , L-(+)-DET, TBHP, 4Å MS, CH_2Cl_2 , -30 to -10 °C, 92%, 91% ee; (b) MsCl, NEt_3 , CH_2Cl_2 , 0 °C, 97%; (c) LiBr, acetone, reflux, 94%; (d) BuLi, THF, 0 °C to rt; **289**, 0 °C to rt, 81%; (e) TBAF, THF, 84%; (f) Pd(OAc)_2 , Ti(Oi-Pr)_4 , allyl methyl carbonate, PPh_3 , PhH, 50 °C, 46% (48% recovered **291**).

We then screened a variety of acids to promote the conversion of **292** to the desired cyclization product **293** (Table 3.1). Unfortunately, both Lewis (entries 1-12) and Brønsted (entries 13-15) acids failed to produce even trace amounts of our desired product. In many instances (entries 1, 3, 5, 6, 12, and 14), we isolated ketone **294**, the result of acid-mediated epoxide-ketone rearrangement (Figure 3.1). In other cases (entries 2, 10, and 13), acid activation of the epoxide promoted elimination to form allylic alcohols and allylic silyl ethers, such as **295**, **296**, **297**, and **298**.⁶⁰⁹ Byproducts **299** and **300** originated from exogenous nucleophilic opening of the epoxide (entries 5 and 15). The only cyclization product observed was cyclopentanol **301** (entry 7), the result of 5-*exo*-tet opening of the epoxide by the pendant homoprenyl sidechain in **292**.

⁶⁰⁹ These byproducts were not rigorously characterized; we surmised the structure of these compounds via comparison to **292** as well as spectroscopic analysis of reaction mixtures.

Table 3.1. Attempted conversion of cyclohexadienone **292** to bicyclo[3.3.1]nonane **293**.



Entry	Acid	Conditions	Result
1	TMSOTf	CH ₂ Cl ₂ , -78 to 0 °C, 5 h	294 , decomposition
2	TMSOTf	DTBMP, CH ₂ Cl ₂ , -78 to 0 °C, 1 d	295 and 296 are the only observed products
3	BF ₃ ·Et ₂ O	CH ₂ Cl ₂ , -78 °C to rt, 2 h	294 (43%)
4	Et ₃ AlCl	CH ₂ Cl ₂ , -78 °C to rt, 3 d	no reaction
5	EtAlCl ₂	CH ₂ Cl ₂ , -78 °C to rt, 1 d	294 is the only observed product
6	AlCl ₃	CH ₂ Cl ₂ , -78 °C, 75 min	>99% conversion to 294
7	TiCl ₄	CH ₂ Cl ₂ , -78 to 0 °C, 4 h	301 is the only observed product
8	SnCl ₄	CH ₂ Cl ₂ , -78 to -30 °C, 5.5 h	299 is the only observed product
9	MgBr ₂ ·Et ₂ O	CH ₂ Cl ₂ , -78 °C to rt, 1 d	no reaction
10	Sn(OTf) ₂	CH ₂ Cl ₂ , -78 °C to rt, 1 d	297 and 298 are the only observed products
11	Zn(OTf) ₂	CH ₂ Cl ₂ , -78 °C to rt, 3 d	no reaction
12	Sc(OTf) ₃	CH ₂ Cl ₂ , -78 °C to rt, 3.5 h	>99% conversion to 294
13	CSA	CH ₂ Cl ₂ , -78 °C to rt, 1 d	297 and 298 are the only observed products
14	<i>p</i> -TsOH·H ₂ O	CH ₂ Cl ₂ , -78 °C to rt, 1.5 h	294 is the only observed product
15	HCl (pH 2)	H ₂ O, 0 °C to rt, 1 d	300 is the only observed product

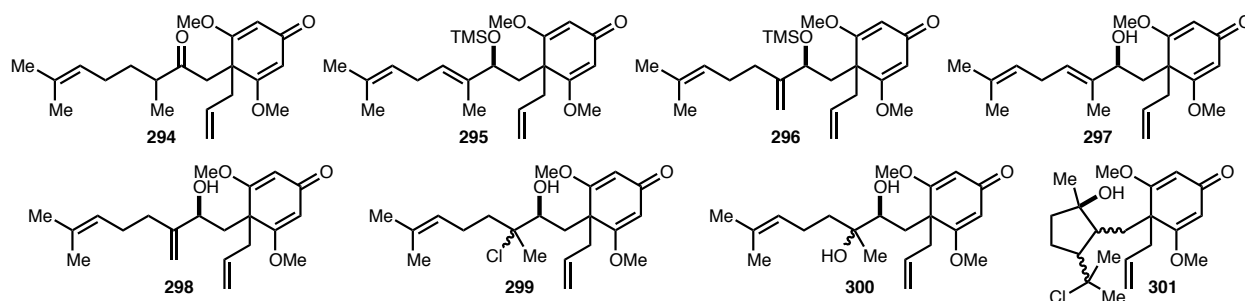
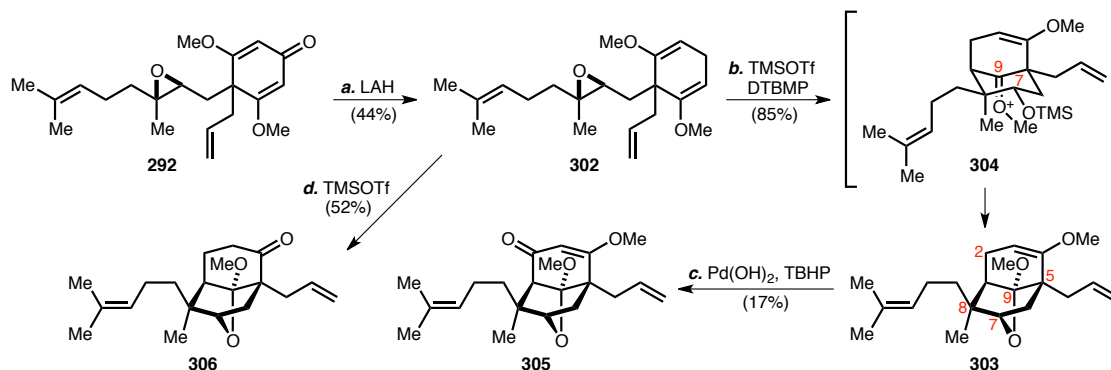


Figure 3.1. Various byproducts formed during attempted conversion of **292** to **293**.

From these studies, we concluded that the cyclohexadienone did not bear sufficient nucleophilic character to engage the activated epoxide. The byproducts obtained involved exogenous nucleophile delivery to the epoxide or even participation of the homoprenyl olefin in the formation of **301**, whereas the cyclohexadienone portion of the molecule remained unchanged. In order to increase the nucleophilic character of the enol ether functionality present in **292**, we attempted to excise the carbonyl group. While several attempts to form a hydrazone failed, hydride reduction of **292** afforded cyclohexadiene **302**

(Scheme 3.4). Gratifyingly, exposure of this compound to TMSOTf in the presence of DTBMP afforded cyclization product **303** as a single diastereomer in 85% yield.



Scheme 3.4. Cascade cyclization of **302** to form **303**.^a

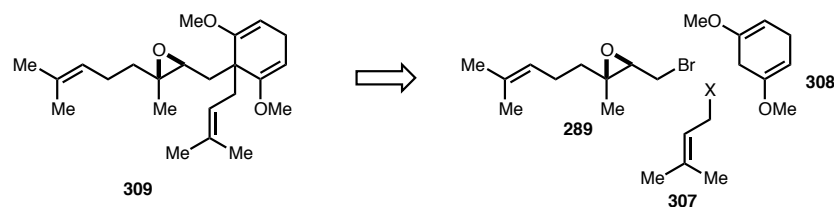
^a Conditions: (a) LAH, CH₂Cl₂, Et₂O, 0 °C, 44%; (b) TMSOTf, DTBMP, CH₂Cl₂, –78 °C, 85%; (c) Pearlman's catalyst, TBHP, Cs₂CO₃, O₂, CH₂Cl₂, 0 to 4 °C, 17%; (e) TMSOTf, CH₂Cl₂, –78 °C, 52%.

In this reaction, the stereochemistry of two key quaternary centers of hyperforin were established: at the previously prostereogenic C5 carbon, and at the C8 position. In addition to the construction of the bicyclo[3.3.1]nonane framework, the formation of a cyclic methyl ketal bridging the C7 and C9 carbons was an unexpected outcome to this reaction, formed from the intramolecular interception of the C9 oxocarbenium ion by the C7 oxygen atom in intermediate **304** (Scheme 3.4). Nevertheless, the establishment of this cyclic ketal was fortuitous, safeguarding the C7 carbinol from oxidation during subsequent allylic oxidation to reestablish carbonyl functionality at the C2 position. This allylic oxidation of **303** was accomplished using Pearlman's catalyst and TBHP⁶¹⁰ to furnish β-methoxyenone **305**. We also briefly screened several other Lewis acids for the conversion of **302** to **303**; however, lower yields of **303** were observed with BF₃·Et₂O and SnCl₄. Omission of DTBMP afforded ketone **306** as the only reaction product.

⁶¹⁰ Yu, J.-Q.; Wu, H.-C.; Corey, E. J. *Org. Lett.* **2005**, 7, 1415-1417.

Double Alkylation Approach

Even though this route allowed us to access β -methoxyenone **305**, we resolved to develop a more straightforward means of accessing advanced intermediates. Over the three-step sequence beginning with cyclohexadienone **292** and ending with **305**, a carbonyl was reduced and subsequently reintroduced. Our solution involved direct, sequential coupling of a prenyl halide (**307**) and epoxygeranyl bromide (**289**) with 1,5-dimethoxy-1,4-cyclohexadiene (**308**)⁶¹¹ to form cyclization precursor **309** (Scheme 3.5). Cyclohexadiene **308** may be synthesized from the Birch reduction of 1,3-dimethoxybenzene,⁶¹² and numerous examples of regioselective alkylations at the methylene proximal to the methoxy groups in **308** have been reported.⁶¹³



Scheme 3.5. Retrosynthesis of cyclization precursor **309**.

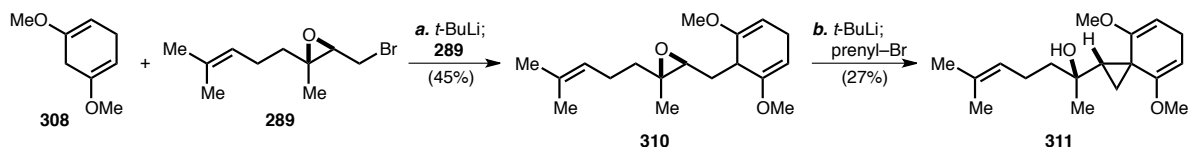
For the synthesis of **309**, we investigated both sequences of additions: (1) coupling of **308** with **289** followed by alkylation with **307** and (2) coupling of **307** with **289** followed by alkylation with **289**. Deprotonation of **308** was accomplished using *t*-BuLi, and subsequent trapping with bromide **289**

⁶¹¹ We also briefly explored a route involving the Birch reduction of 1,3-dimethoxy-2-prenylbenzene; however, the conditions necessary for this reduction (i.e., Na, NH₃, reflux, 12-18 h) also resulted in reduction of the prenyl olefin.

⁶¹² Piers, E.; Grierson, J. R. *J. Org. Chem.* **1977**, *42*, 3755-3757.

⁶¹³ For examples of regioselective alkylation of **308**, see: (a) Nelson, N. A.; Tamura, Y. *Can. J. Chem.* **1965**, *43*, 1323-1328. (b) Harvey, R. G.; Pataki, J.; Lee, H. *J. Org. Chem.* **1986**, *51*, 1407-1412. (c) Pattenden, G.; Teague, S. *J. Tetrahedron* **1987**, *43*, 5637-5652. (d) Toth, J. E.; Hamann, P. R.; Fuchs, P. L. *J. Org. Chem.* **1988**, *53*, 4694-4708. (e) Middleton, D. S.; Simpkins, N. S.; Begley, M. J.; Terrett, N. K. *Tetrahedron* **1990**, *46*, 545-564. (f) Laschat, S.; Narjes, F.; Overman, L. E. *Tetrahedron* **1994**, *50*, 347-358. (g) Mori, K.; Abe, K. *Liebigs Ann.* **1995**, 943-948. (h) Imamura, Y.; Takikawa, H.; Mori, K. *Tetrahedron Lett.* **2002**, *43*, 5743-5746. (i) Studer, A.; Amrein, S.; Schleth, F.; Schulte, T.; Walton, J. C. *J. Am. Chem. Soc.* **2003**, *125*, 5726-5733. (j) Hughes, C. C.; Trauner, D. *Tetrahedron* **2004**, *60*, 9675-9686.

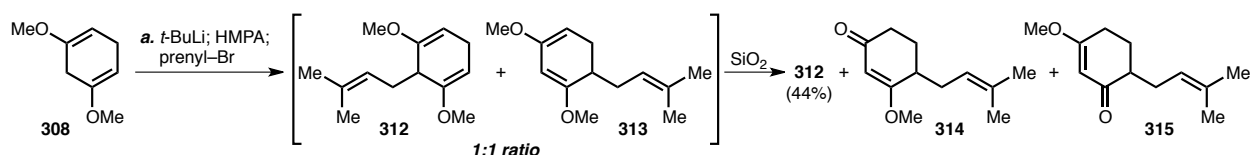
afforded **310** as a single regioisomer (Scheme 3.6). Unfortunately but not unexpectedly, deprotonation of this intermediate afforded bicyclo[5.1.0]octadiene **311**, the product of internal trapping with concomitant opening of the epoxide functionality.



Scheme 3.6. Deprotonation of **310** led to isolation of **311**.^a

^a Conditions: (a) *t*-BuLi, THF, -78 °C; **289**, -78 °C to rt, 45%; (b) *t*-BuLi, THF, -78 to -30 °C; prenyl bromide, -78 °C to rt, 27% (29% recovered **310**).

Prenylation of cyclohexadiene **308** was surprisingly problematic. Initially, alkylation of metalated **308** with prenyl bromide was rather unselective, providing both the desired coupling product **312** as well as its regioisomer **313** in equal amounts (Scheme 3.7). These regioisomers were separated by treatment with SiO₂; exposure of unprocessed reaction mixtures facilitated the selective conversion of **313** to the more-polar β-methoxyenones **314** and **315**, while **312** remained unchanged.



Scheme 3.7. Nonselective prenylation of cyclohexadiene **308**.^a

^a Conditions: (a) *t*-BuLi, THF, -78 °C; HMPA, -78 °C; prenyl bromide, -78 °C to rt; H₂O; SiO₂, 44% **312**.

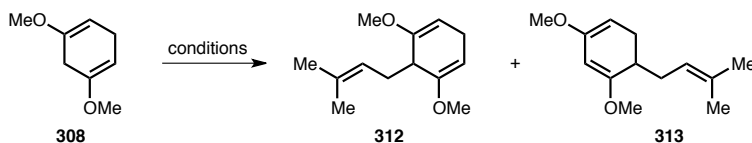
Even though from a practical standpoint, large quantities of **312** were readily available through this selective hydrolysis protocol, we resolved to improve the overall selectivity of this reaction (Table 3.2). In the absence of HMPA, selectivity improved marginally (entry 2). While the addition of MgBr₂

reversed selectivity, the addition of BaI₂ improved selectivity for the formation of **313** (entries 4-5). Substituting *t*-BuLi for *s*-BuLi in the deprotonation step had no effect on regioselectivity (entry 5). When prenyl chloride was used instead of prenyl bromide in otherwise identical conditions to entry 1, regioselectivity improved to 2:1 in favor of the desired regioisomer (entry 6). Several additives were studied in the coupling **308** with prenyl chloride (entries 7-9): ZnCl₂ afforded significant amounts of 3-methoxycyclohex-2-enone, and while both CeCl₃ and BaI₂⁶¹⁴ further improved regioselectivity, the former additive caused a decrease in conversion. The method of preparing anhydrous BaI₂ also had a significant effect on this alkylation. Anhydrous BaI₂ made from drying commercially available BaI₂·2H₂O under vacuum⁶¹⁵ afforded a 3:1 ratio of **312**:**313** with a 61% yield of **313** (entry 9). Preparing BaI₂ *in situ* from the reaction of barium metal with I₂⁶¹⁶ provided complete regiocontrol for the synthesis of **312**, which was isolated in 91% yield (entry 10).

⁶¹⁴ The effects of barium iodide on the regioselectivity of nucleophilic allylation has been studied: (a) Yanagisawa, A.; Yasue, A.; Yamamoto, H. *Synlett* **1993**, 686-688. (b) Yanagisawa, A.; Habaue, S.; Yasue, K.; Yamamoto, H. *J. Am. Chem. Soc.* **1994**, *116*, 6130-6141. (c) Yanagisawa, A.; Yamada, Y.; Yamamoto, H. *Synlett* **1997**, 1090-1092. (d) Van den Bossche, J.; Shin, J.; Thompson, D. H. *J. Org. Chem.* **2007**, *72*, 5005-5007.

⁶¹⁵ Yanagisawa, A.; Yasue, K.; Yamamoto, H. *Org. Synth.* **1997**, *74*, 178-186.

⁶¹⁶ Corey, E. J.; Lin, S.; Luo, G. *Tetrahedron Lett.* **1997**, *38*, 5771-5774. (b) Corey, E. J. Harvard University, Cambridge, MA. Personal communication, 2012.

Table 3.2. Prenylation of cyclohexadiene **308**.

Entry	Metalation conditions	Alkylation conditions	312 : 313 ratio	312 yield
1 ^a	<i>t</i> -BuLi, THF, −78 °C; HMPA	prenyl-Br, −78 °C to rt	1 : 1	44%
2	<i>t</i> -BuLi, THF, −78 °C	prenyl-Br, −78 °C to rt	1.3 : 1	37%
3	<i>t</i> -BuLi, THF, −78 °C; MgBr ₂	prenyl-Br, −78 °C to rt	1 : 2.2	n.d.
4	<i>t</i> -BuLi, THF, −78 °C; BaI ₂	prenyl-Br, −78 °C to rt	2 : 1	n.d.
5	<i>s</i> -BuLi, THF, −78 °C; TMEDA	prenyl-Br, −78 °C to rt	1 : 1	n.d.
6	<i>t</i> -BuLi, THF, −78 °C; HMPA	prenyl-Cl, −78 °C to rt	2 : 1	n.d.
7	<i>t</i> -BuLi, THF, −78 °C; ZnCl ₂	prenyl-Cl, −78 °C to rt	^b	n.d.
8	<i>t</i> -BuLi, THF, −78 °C; CeCl ₃	prenyl-Cl, −78 °C to rt	2.5 : 1	^c
9	<i>t</i> -BuLi, THF, −78 °C; BaI ₂ ^d	prenyl-Cl, −78 °C to rt	3 : 1	61%
10	<i>t</i> -BuLi, THF, −78 °C; BaI ₂ ^e	prenyl-Cl, −78 to −30 °C	>20 : 1	91%

^a The conditions presented in entry 1 are depicted in Scheme 3.7.

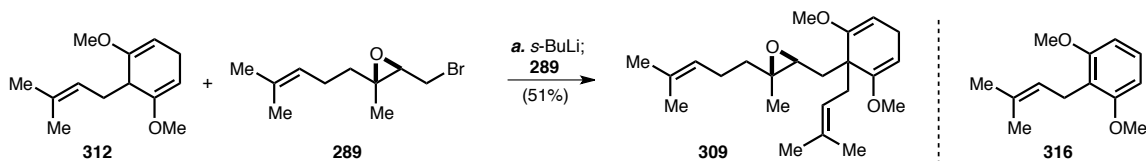
^b Afforded a 2:1 ratio of **312** to 3-methoxycyclohex-2-enone.

^c Low amount of conversion observed.

^d Anhydrous BaI₂ prepared from drying BaI₂·2H₂O at 150 °C at 6 mmHg pressure for 15 h.

^e Anhydrous BaI₂ prepared from the reaction of Ba with I₂. See experimental section for details.

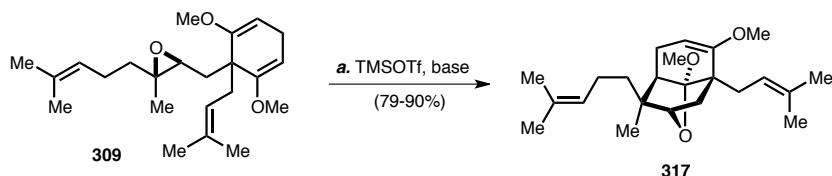
We then explored the alkylation of **312** with epoxygeranyl bromide **289** to form cyclization precursor **309**. Deuterium quench studies revealed that exposure to *tert*-butyllithium at −78 °C did not lead to deprotonation of **312**. We therefore surveyed the use of several bases across a range of temperatures. In general, a major byproduct during this coupling reaction was 1,3-dimethoxy-2-prenylbenzene (**316**), an oxidation product of **312**. Low levels of deprotonation were observed with *t*-BuLi at −45 °C and −30 °C, and increasing the stoichiometry of *t*-BuLi generally favored conversion to **316**. Several additives, including HMPA, TMEDA, MgBr₂, and BaI₂ did not facilitate conversion to **309**. The use of the lithium amide bases LDA and LiTMP did not lead to appreciable deprotonation, even when a solution of LDA and **312** was warmed to rt. Similar results were observed with BuLi when warmed to −30 °C. Eventually, we discovered that optimal yields of **309** could be achieved through deprotonation of **312** with *s*-BuLi at −30 °C followed by addition of **289** (Scheme 3.8). If a solution of **312** and *s*-BuLi was warmed above −30 °C, significant amounts of **316** were produced.



Scheme 3.8. Synthesis of **309** from **312** and **289**.^a

^a Conditions: (a) *s*-BuLi, -78 to -30 °C; **289**, -78 °C to rt, 51%.

The subsequent cyclization of **309** afforded cyclic ketal **317** using conditions identical to the conversion of **302** to **303** (Scheme 3.9). From a practical material throughput standpoint, we chose to replace DTBMP with 2,6-lutidine; no appreciable decline in yield was observed using the latter base, and it was a much easier reagent to obtain, implement, and separate from product with larger scale reactions. Using this new double alkylation strategy, we were able to access large quantities of **317** from 1,3-dimethoxybenzene in 4 steps, a significant improvement from the prior approach involving dearomative allylation of **291**.



Scheme 3.9. Cyclization of **309** to **317**.^a

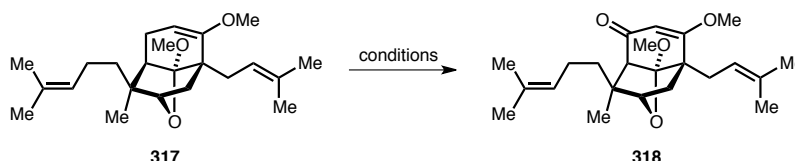
^a Conditions: (a) TMSOTf, DTBMP, CH_2Cl_2 , -78 °C, 90% or TMSOTf, 2,6-lutidine, CH_2Cl_2 , -78 °C, 79%.

The next step in our synthesis sequence involved the allylic oxidation⁶¹⁷ of **317** to β -methoxyenone **318** (Table 3.3). This was an exceptionally challenging transformation given the seven allylic sites present in **303** and the steric environment surrounding the desired oxidation site at the C2 position. Numerous allylic oxidation conditions were screened and can be classified into three distinct categories: (1) the combination of a high-valent metal species and TBHP (entries 1-22); (2) stoichiometric

⁶¹⁷ For a recent review of allylic oxidations in total synthesis, see: Nakamura, A.; Nakada, M. *Synthesis* **2013**, 45, 1421-1451.

metal oxidants (entries 23-32); and (3) the combination of hypervalent iodide species and TBHP (entries 33-65). In many cases, we observed several byproducts, including transposed *tert*-butyl peroxide **319**, enone **320**, and ketone **321** (Figure 3.2).

Table 3.3. Allylic oxidation of enol ether **317**.



Entry	Oxidants (equiv)	Additives (equiv)	Conditions	Results
1	Pd(OH) ₂ /C (0.1), TBHP (5)	K ₂ CO ₃ (5)	CH ₂ Cl ₂ , 4 °C, 12 h	318 (15%)
2	Pd(OH) ₂ /C (0.1), TBHP (5), O ₂	Cs ₂ CO ₃ (5)	CH ₂ Cl ₂ , 4 °C, 4 h	318 (16%), 320 (45%), 317 (37%)
3	Pd(OH) ₂ /C (0.2), TBHP (5)	KOH (1.2)	CH ₂ Cl ₂ , 4 °C, 7 h	318 (24%), 319 (14%)
4	Pd(OH) ₂ /C (0.2), TBHP (5)	K ₃ PO ₄ (1.2)	CH ₂ Cl ₂ , 4 °C, 7 h	low conversion to 319
5	Pd(OH) ₂ /C (0.2), TBHP (5)	K ₂ CO ₃ (5)	CH ₂ Cl ₂ , 4 °C, 20 h	low conversion to 319
6	Pd(OH) ₂ /C (0.2), TBHP (5)	Cs ₂ CO ₃ (5)	CH ₂ Cl ₂ /DMSO, 4 °C, 20 h	no reaction
7	Pd(OH) ₂ /C (1), TBHP (5)	Cs ₂ CO ₃ (5)	CH ₂ Cl ₂ , 4 °C, 3 h	318 (27%), 319 (2%), 320 (26%)
8	Pd(OH) ₂ /C (1), CHP (5)	Cs ₂ CO ₃ (5)	CH ₂ Cl ₂ , 4 °C, 3 h	low conversion to 318 and 319
9	Pd(OAc) ₂ (1), TBHP (5)	K ₂ CO ₃ (1)	CH ₂ Cl ₂ , 4 °C, 3 h	no reaction
10	Pd(OAc) ₂ (1), TBHP (excess)	Cs ₂ CO ₃ (1.2)	MeCN, rt, 12 h	318 (5%)
11	Pd/C (0.2), TBHP (5)	Cs ₂ CO ₃ (5)	CH ₂ Cl ₂ , 4 °C, 17 h	mixture of 318 and 319
12	NaOCl (excess), TBHP (5)	none	EtOAc, rt, 3 h	selectively afforded 319
13	Cr(CO) ₆ (0.05), TBHP (3)	none	PhH, 75 °C, 17 h	selectively afforded 320
14	PDC (2), TBHP (2)	none	PhH, 0 °C to rt, 5 h	318 (14%), 320 (37%)
15	Mn(OAc) ₃ (0.1), TBHP (4)	K ₂ CO ₃ (0.5)	EtOAc, rt, 3.5 h	318 (11%)
16	FeCl ₂ ·4H ₂ O (2), TBHP (3)	none	MeCN, rt, 10 min	selectively afforded 321
17	NiCl ₂ ·6H ₂ O (0.5), TBHP (5)	Cs ₂ CO ₃ (5)	CH ₂ Cl ₂ , 4 °C, 17 h	no reaction
18	CuI (0.1), TBHP (10)	none	MeCN, 55 °C, 16 h	selectively afforded 319
19	SeO ₂ (1), TBHP (4)	none	CH ₂ Cl ₂ , rt, 14 h	decomposition
20	RuCl ₃ (0.1), TBHP (10)	none	<i>c</i> -Hex, rt, 16 h	low conversion to 318 , 319 , and 320
21	Rh ₂ (cap) ₄ (0.1), TBHP (5)	K ₂ CO ₃ (0.5)	CH ₂ Cl ₂ , rt, 12h	decomposition
22	CAN (2), TBHP (5)	none	MeCN, rt, 10 min	321 (29%)
23	DDQ (2)	none	wet acetone, rt, 9 h	selectively afforded 321
24	TEMPO (2.2), <i>s</i> -BuLi (1.1)	none	THF, -78 °C to rt, 12 h	no reaction
25	PDC (20)	none	PhH, rt, 30 h	very low conversion to 320
26	CrO ₃ ·DMP (20)	none	CH ₂ Cl ₂ , 0 °C, 5 h	decomposition
27	(PhSe) ₂ (2), PhIO ₂ (10)	pyr (100), 4Å MS	PhCl, 110 °C, 14 h	decomposition
28	CAN (2)	none	MeCN/H ₂ O, rt, 15 min	mixture of 320 and 321
29	CAN (2)	NEt ₃ (5)	MeCN/DMSO, rt, 3 d	no reaction
30	CAN (2), O ₂	none	MeCN, rt, 10 min	selectively afforded 321
31	CAN (2), TEMPO (4)	none	MeCN, rt, 20 h	decomposition
32	CAN (2), pyridine <i>N</i> -oxide (3)	none	MeCN, rt, 1.5 h	selectively afforded 320
33	PhIO (3), TBHP (4)	K ₂ CO ₃ (0.5)	pentOAc, 4 °C, 20 h	mixture of 318 , 320 , and 321
34	PhIO (3), TBHP (4)	Cs ₂ CO ₃ (4)	EtOAc, 4 °C, 14 h	mixture of 318 , 320 , and 321
35	PhI(OAc) ₂ (3), TBHP (4)	K ₂ CO ₃ (0.5)	EtOAc, 4 °C, 3.5 h	318 (14%)
36	PhI(OAc) ₂ (3), TBHP (4)	K ₂ CO ₃ (0.5)	EtOAc, 4 °C, 12 h	318 (11%)
37	PhI(OAc) ₂ (3), TBHP (4)	K ₂ CO ₃ (0.5)	pentOAc, 4 °C, 10 h	318 (13%), 320 (25%)
38	PhI(OAc) ₂ (3), TBHP (4)	K ₂ CO ₃ (0.5)	PrCO ₂ Bu, 4 °C, 5 h	319 (17%)
39	PhI(OAc) ₂ (3), TBHP (4), O ₂	K ₂ CO ₃ (0.5)	pentOAc, 4 °C, 1 d	mixture of 318 , 320 , and 321

Table 3.3 (continued). Allylic oxidation of enol ether **317**.

Entry	Oxidants (equiv)	Additives (equiv)	Conditions	Results
40	PhI(OAc) ₂ (3), TBHP (4)	Cs ₂ CO ₃ (4)	EtOAc, -78 °C, 4 h	mixture of 318 , 319 , and 321
41	PhI(OAc) ₂ (3), TBHP (4)	none	pentOAc, 4 °C, 12 h	mixture of 318 and 321
42	PhI(TFA) ₂ (2), TBHP (1.5)	Cs ₂ CO ₃ (2)	EtOAc, 4 °C, 75 min	318 (10%), 319 (24%), 320 (28%)
43	PhI(TFA) ₂ (3), TBHP (4)	K ₂ CO ₃ (0.5)	pentOAc, 4 °C, 75 min	318 (23%), 320 (37%)
44	PhI(TFA) ₂ (3), TBHP (4)	K ₂ CO ₃ (0.5), 3Å MS	pentOAc, 4 °C, 2 d	mixture of 318 and 320
45	PhI(TFA) ₂ (3), TBHP (4)	K ₃ PO ₄ (4)	EtOAc, 4 °C, 45 min	mixture of 318 , 320 , and 321
46	PhI(TFA) ₂ (3), TBHP (4)	Cs ₂ CO ₃ (4)	EtOAc, 4 °C, 13 h	318 (21%), 320 (12%)
47	PhI(TFA) ₂ (3), TBHP (4)	Cs ₂ CO ₃ (4)	EtOAc, -30 °C, 90 min	318 (19%), 320 (28%)
48	PhI(TFA) ₂ (3), TBHP (4)	Cs ₂ CO ₃ (4)	EtOAc, -78 °C, 1 h	318 (17%), 319 (4%)
49	PhI(TFA) ₂ (3), TBHP (4)	Cs ₂ CO ₃ (4)	EtOAc, -78 °C, 3.5 h	318 (23%), 319 (10%)
50	PhI(TFA) ₂ (3), TBHP (4)	Cs ₂ CO ₃ (4)	CH ₂ Cl ₂ , -78 °C, 1 h	318 (16%)
51	PhI(TFA) ₂ (3), TBHP (4)	Cs ₂ CO ₃ (4)	MeCN, -40 °C, 2 h	mixture of 318 , 319 , 320 , and 321
52	PhI(TFA) ₂ (3), TBHP (4), O ₂	Cs ₂ CO ₃ (4)	EtOAc, -78 °C, 1 h	318 (30%)
53	PhI(TFA) ₂ (3), TBHP (4)	Cs ₂ CO ₃ (4)	EtOAc, -78 °C, 1 h	318 (16%)
54	PhI(TFA) ₂ (3), TBHP (4)	Cs ₂ CO ₃ (4)	EtOAc, -78 °C, 2 h	318 (17%)
55	PhI(TFA) ₂ (3), CHP (4)	Cs ₂ CO ₃ (4)	EtOAc, -78 °C, 1 h	318 (14%), 319 (5%), 320 (15%)
56	PhI(TFA) ₂ (3), BzOO <i>t</i> -Bu (4)	Cs ₂ CO ₃ (4)	EtOAc, -78 °C to rt, 1 d	no reaction
57	PhI(TFA) ₂ (3), BPX (4)	Cs ₂ CO ₃ (4)	EtOAc, -78 °C, 90 min	decomposition
58	PhI(TFA) ₂ (5), TBHP (excess)	Cs ₂ CO ₃ (10)	EtOAc, -78 °C, 30 min	318 (17%), 320 (11%)
59	322 (2)	K ₂ CO ₃ (4)	PhH, rt, 3 d	319 (26%), 320 (5%)
60	322 (2)	Cs ₂ CO ₃ (4)	PhH, rt, 12 h	mixture of 318 and 319
61	322 (3), TBHP (4)	Cs ₂ CO ₃ (4)	EtOAc, -78 °C to rt, 1 d	mixture of 318 , 320 , and 321
62	322 (2), O ₂	K ₂ CO ₃ (4)	PhH, rt, 1 d	318 (9%)
63	PhIO ₂ (3), TBHP (4)	K ₂ CO ₃ (4)	EtOAc, 4 °C, 12 h	selectively afforded 319
64	IBX (3)	none	DMSO, 110 °C, 14 h	mixture of 318 , 320 , and 321
65	DMP (3)	Cs ₂ CO ₃ (4)	CH ₂ Cl ₂ , rt, 2 d	no reaction

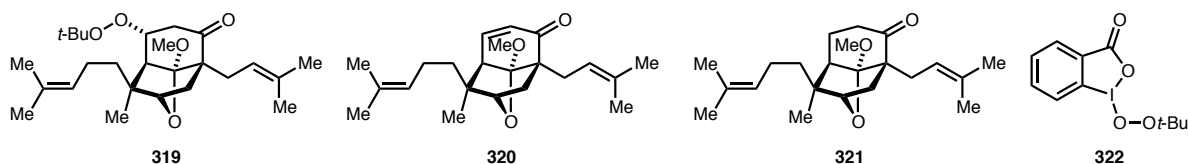


Figure 3.2. Byproducts from the allylic oxidation of **317** and the structure of peroxydioxolone **322**.

Given the early success with the allylic oxidation of **303** to afford **306**, we first focused on the Pearlman's catalyst-TBHP allylic oxidation system (Table 3.3, entries 1-8).⁶¹⁰ Despite increases in catalyst stoichiometry, we typically observed a considerable conversion to enone **320** and variable conversion to peroxide **319**. Additionally, while changing the identity of the base mitigated has enone formation in similar systems,⁶¹⁸ we did not observe significant changes in product distribution through the

⁶¹⁸ (a) Yu, J.-Q.; Corey, E. J. *Org. Lett.* **2002**, *4*, 2727-2730. (b) Yu, J.-Q.; Corey, E. J. *J. Am. Chem. Soc.* **2003**, *125*, 3232-3233.

use of K₂CO₃, KOH, K₃PO₄, or Cs₂CO₃. Using different Pd catalysts had no positive effect on desired yield (entries 9-11). A variety of other known allylic oxidation systems, involving the combination of TBHP and: NaOCl,⁶¹⁹ Cr(CO)₆,⁶²⁰ PDC,⁶²¹ Mn(OAc)₃,⁶²² FeCl₂·4H₂O,⁶²³ NiCl₂·6H₂O,⁶²⁴ CuI,⁶²⁵ SeO₂,⁶²⁶ RuCl₃,⁶²⁷ Rh₂(cap)₄,⁶²⁸ and CAN, also did not afford large proportions of **318** selectively (entries 12-22). When stoichiometric metal oxidants were used (entries 23-32), we did not observe any **318** but rather enone **320** and ketone **321** in cases where significant decomposition was not observed.

In addition to the use of metal-based oxidants, we also investigated the use of hypervalent iodine reagents, both in the presence and in the absence of TBHP (Table 3.3, entries 33-65). Prior studies by the Yeung group illustrated the effectiveness of PhI(OAc)₂-TBHP for the allylic oxidation of a wide range of substrates.⁶²⁹ It is believed that exposure of iodosobenzene species **323** to TBHP generates [bis(*tert*-butylperoxy)iodo]benzene (**324**, Scheme 3.10).⁶³⁰ This is predicted to be a particularly unstable

⁶¹⁹ Kolympadi, M.; Liapis, M.; Ragoussis, V. *Tetrahedron* **2005**, *61*, 2003-2010.

⁶²⁰ (a) Pearson, A. J.; Chen, Y.-S.; Hsu, S.-Y.; Ray, T. *Tetrahedron Lett.* **1984**, *25*, 1235-1238. (b) Pearson, A. J.; Chen, Y.-S.; Han, G. R.; Hsu, S.-Y.; Ray, T. *J. Chem. Soc., Perkins Trans. 1* **1985**, 267-273.

⁶²¹ (a) Chidambaram, N.; Chandrasekaran, S. *J. Org. Chem.* **1987**, *52*, 5048-5051. (b) Schultz, A. G.; Taveras, A. G.; Harrington, R. E. *Tetrahedron Lett.* **1988**, *29*, 3907-3910.

⁶²² Shing, T. K. M.; Yeung, Y.-Y.; Su, P. L. *Org. Lett.* **2006**, *8*, 3149-3151.

⁶²³ (a) Barton, D. H. R.; Le Gloahec, V. N. *Tetrahedron* **1998**, *54*, 15457-15468. (b) Nakanishi, M.; Bolm, C. *Adv. Synth. Catal.* **2007**, *349*, 861-864.

⁶²⁴ Salavati-Niasari, M.; Babazadeh-Arani, H. *J. Mol. Catal. A* **2007**, *274*, 58-64.

⁶²⁵ Salvador, J. A. R.; e Melo, M. L. S.; Campos Neves, A. S. *Tetrahedron Lett.* **1997**, *38*, 119-122.

⁶²⁶ Mateos, A. F.; Barrueco, O. F.; González, R. R. *Tetrahedron Lett.* **1990**, *31*, 4343-4346.

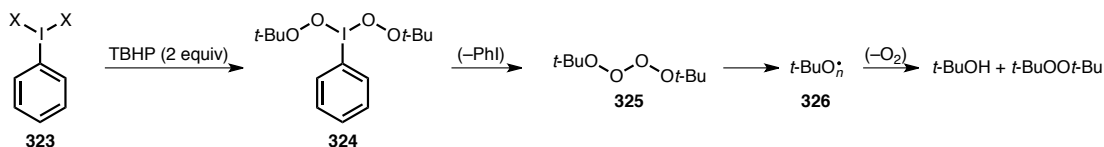
⁶²⁷ Miller, R. A.; Li, W.; Humphrey, G. R. *Tetrahedron Lett.* **1996**, *37*, 3429-3432.

⁶²⁸ (a) Catino, A. J.; Forslund, R. E.; Doyle, M. P. *J. Am. Chem. Soc.* **2004**, *126*, 13622-13623. (b) Catino, A. J.; Nichols, J. M.; Choi, H.; Gottipamula, S.; Doyle, M. P. *Org. Lett.* **2005**, *7*, 5167-5170. (c) McLaughlin, E. C.; Choi, H.; Wang, K.; Chiou, G.; Doyle, M. P. *J. Org. Chem.* **2009**, *74*, 730-738.

⁶²⁹ (a) Zhao, Y.; Yeung, Y.-Y. *Org. Lett.* **2010**, *12*, 2128-2131. (b) Zhao, Y.; Yim, W.-L.; Yan, C. K.; Yeung, Y.-Y. *Org. Lett.* **2011**, *13*, 4308-4311. (c) Zhao, Y.; Chew, X.; Leung, G. Y. C.; Yeung, Y.-Y. *Tetrahedron Lett.* **2012**, *53*, 4766-4769.

⁶³⁰ Milas, N. A.; Plesnicar, B. *J. Am. Chem. Soc.* **1968**, *90*, 4450-4453.

intermediate, which undergoes reductive elimination to afford PhI and di-*tert*-butyl tetroxide (**325**), which decomposes into a variety of *tert*-butyl polyoxide radicals (**326**), eventually leading to oxygen evolution, and to formation of *t*-BuOH and *t*-BuOO*t*-Bu. These processes appear to be solvent dependent.



Scheme 3.10. Reaction of a generic iodosobenzene species **323** with TBHP.

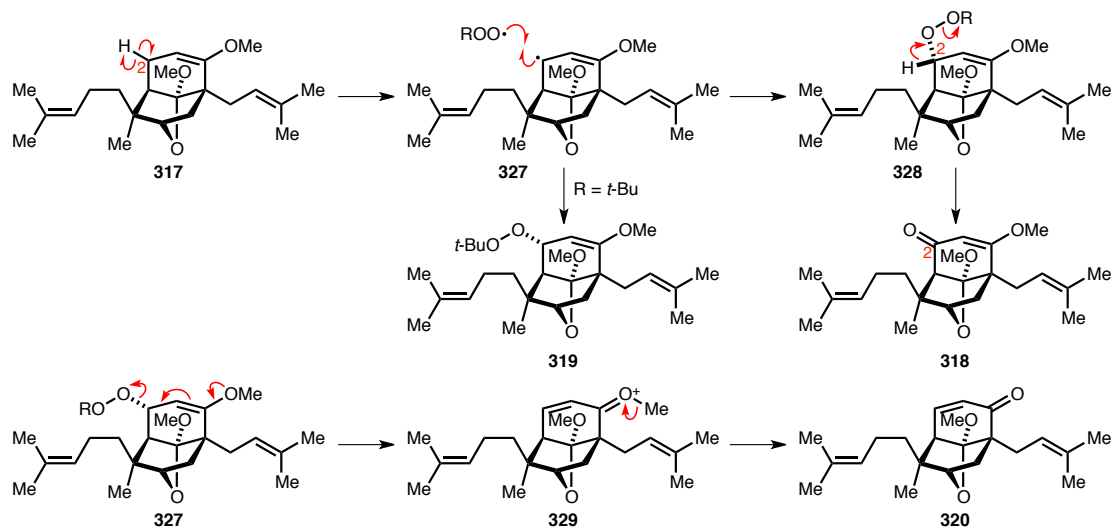
The rate at which **324** forms and decomposes to PhI and **325** is affected by several factors, including solvent and temperature. Exposure of $\text{PhI}(\text{TFA})_2$ to TBHP forms **324** at temperatures as low as $-30\text{ }^\circ\text{C}$ using CH_2Cl_2 ; the use of more Lewis basic solvents EtOAc, acetone, THF, and MeCN led to lower conversion rates in subsequent allylic oxidations at that temperature.⁶³¹ Solvent effects were also observed in the $\text{PhI}(\text{OAc})_2$ -TBHP allylic oxidation system.^{629a} Use of ester solvents containing large alkyl substituents led to higher yields. This may be due to the solvent effects on the conversion of **323** to **324**, with more sterically demanding Lewis basic solvents decreasing the rate of this reaction.

Several mechanisms may be proposed for the allylic oxidation of **317**. One plausible mechanism involves three distinct stages: a radical abstraction; radical combination; and base-promoted elimination (Scheme 3.11). First, the radical abstraction of a hydrogen atom at the C2 position forms allylic radical **327**. This radical may be intercepted to form peroxide **328**, which then may eliminate alkoxide anion via methine deprotonation⁶³² at C2 to afford **318**. This mechanistic proposal may also explain the formation of several byproducts. Interception of allylic radical **327** with a *tert*-buty peroxy radical may form **319**.

⁶³¹ (a) Catir, M.; Kilic, H. *Synlett* **2004**, 2151-2154. (b) Catir, M.; Kilic, H. *Synlett* **2010**, 1319-1322.

⁶³² For an early example of base-mediated cleavage of a dialkyl peroxide, see: Kornblum, N.; DeLaMare, H. E. *J. Am. Chem. Soc.* **1951**, 73, 880-881.

In addition, E1cB-type expulsion of a peroxy anion from **328** may afford enoxonium **329**, which upon demethylation would afford enone **320**.



Scheme 3.11. A plausible radical-based mechanism for the formation of **318** and other oxidation products from **317**.

In many allylic oxidation experiments, we isolated a significant amount of **319**, and we investigated the possible conversion of this peroxide to the desired β -methoxyenone **318**. Exposure of peroxide **319** to a variety of basic, acidic, and reducing conditions did not afford more than trace amounts of **318**. Only upon exposure of **319** to $\text{FeCl}_2 \cdot 4\text{H}_2\text{O}$ ⁶³³ in a Fenton-type reaction,⁶³⁴ appreciable (5-10% yield) amounts of β -methoxyenone **318** were produced. The inability to convert **319** to **318** meant that this peroxide was a detrimental byproduct in this reaction process, and we sought to mitigate its formation to improve the yield of **318**. Since a peroxide would approach from outside the concavity of the bicyclic core of **327** to form the epimer shown in **328**, subsequent C2 deprotonation would be exceedingly

⁶³³ For examples of the reaction of peroxides with Fe(II) salts, see: (a) O'Neill, P. M.; Searle, N. L.; Raynes, K. J.; Maggs, J. L.; Ward, S. A.; Storr, R. C.; Park, B. K.; Posner, G. H. *Tetrahedron Lett.* **1998**, 39, 6065-6068. (b) Singh, C.; Gupta, N.; Tiwari, P. *Tetrahedron Lett.* **2005**, 46, 4551-4554. (c) Opsenica, I.; Terzić, N.; Opsenica, D.; Angelovski, G.; Lehnig, M.; Eilbracht, P.; Tinant, B.; Juranić, Z.; Smith, K. S.; Yang, Y. S.; Diaz, D. S.; Smith, P. L.; Milhous, W. K.; Doković, D.; Šolaja, B. A. *J. Med. Chem.* **2006**, 49, 3790-3799.

⁶³⁴ For a review of the Fenton reaction, see: Koppenol, W. H. *Free Radical Bio. Med.* **1993**, 15, 645-651.

difficult given the steric environment around this position.⁶³⁵ We hypothesized that if oxygen was present, it may intercept **327** and subsequently form a hydroperoxide (**328**, R = H), and this species may undergo more facile C2 deprotonation to form the desired β -methoxyenone **318**.

Taking all these factors into consideration and screening a variety of conditions involving iodine(III) reagents (Table 3.3, entries 33-58), we were obtained **318** in 30% yield (entry 52). While the use of large ester solvents (i.e., amyl acetate and butyl butyrate) decreased the rate at which radical *tert*-butyl polyoxides formed, their relatively high melting points prevented the cooling of the reaction mixtures to further decrease the rate of radical formation. EtOAc was the solvent of choice, allowing reaction mixtures to be cooled to $-78\text{ }^{\circ}\text{C}$ while preventing fast decomposition of TBHP and the hypervalent iodine reagent. In addition, we found that $\text{PhI}(\text{TFA})_2$ was optimal relative to $\text{PhI}(\text{OAc})_2$ and PhIO , and the addition of a vigorous stream of oxygen into the reaction mixture caused a significant increase in product yield. We also assessed the use of several iodine(V) reagents, such as peroxyiodoxolone **322**,⁶³⁶ PhIO_2 , IBX, and DMP (entries 59-65); however, the use of these reagents did not afford the desired allylic oxidation product selectively. Even though yields of the desired β -methoxyenone **318** were not dramatically improved using the optimized $\text{PhI}(\text{TFA})_2$ -TBHP- O_2 system, the use of hypervalent iodine reagents were more conducive for large scale allylic oxidations of **317**, necessary for processing large quantities of material for the total synthesis endeavor.

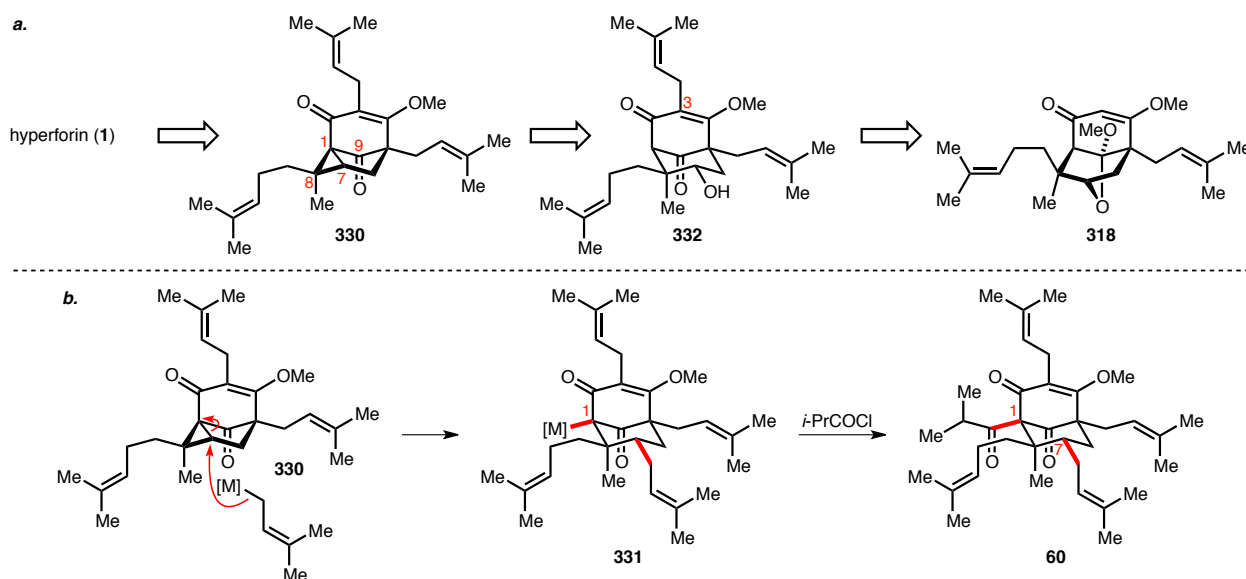
With access to large amounts of β -methoxyenone **318**, we developed a synthesis strategy that would allow us to quickly access hyperforin. We hypothesized that hyperforin (**1**) may be accessed from cyclopropane **330** (Scheme 3.12a). The cyclopropane present in **330** is activated by both the C1 and C9 carbonyl groups,⁶³⁷ and nucleophilic addition of a prenylmetal species may occur selectively at the C7

⁶³⁵ The difficulty with C2 deprotonation of **328** may favor enone **320** formation via enoxonium **329**.

⁶³⁶ Ochiai, M.; Ito, T.; Takahashi, H.; Nakanishi, A.; Toyonari, M.; Sueda, T.; Goto, S.; Shiro, M. *J. Am. Chem. Soc.* **1996**, *118*, 7716-7730.

⁶³⁷ It should be noted that there is very little orbital overlap between the C9-O π^* orbital and the C7-C9 σ orbital.

position and not at the C8 quaternary center.⁶³⁸ This addition would result in an intermediate C1 bridgehead organometallic **331**, which upon exposure to isobutyryl chloride may directly provide the methyl ether of hyperforin (**60**, Scheme 3.12b). In one single operation, two of the three key remaining C–C bonds of hyperforin would be established: prenylation at the C7 position and acylation at the C1 position (highlighted in Scheme 3.12b). The remaining C3 prenyl group would be installed via a precedent tandem deprotonation-transmetalation-alkylation protocol of **318** to afford **332**, the precursor to **330** via sequential bridgehead lithiation and intramolecular cyclization.⁵¹⁰



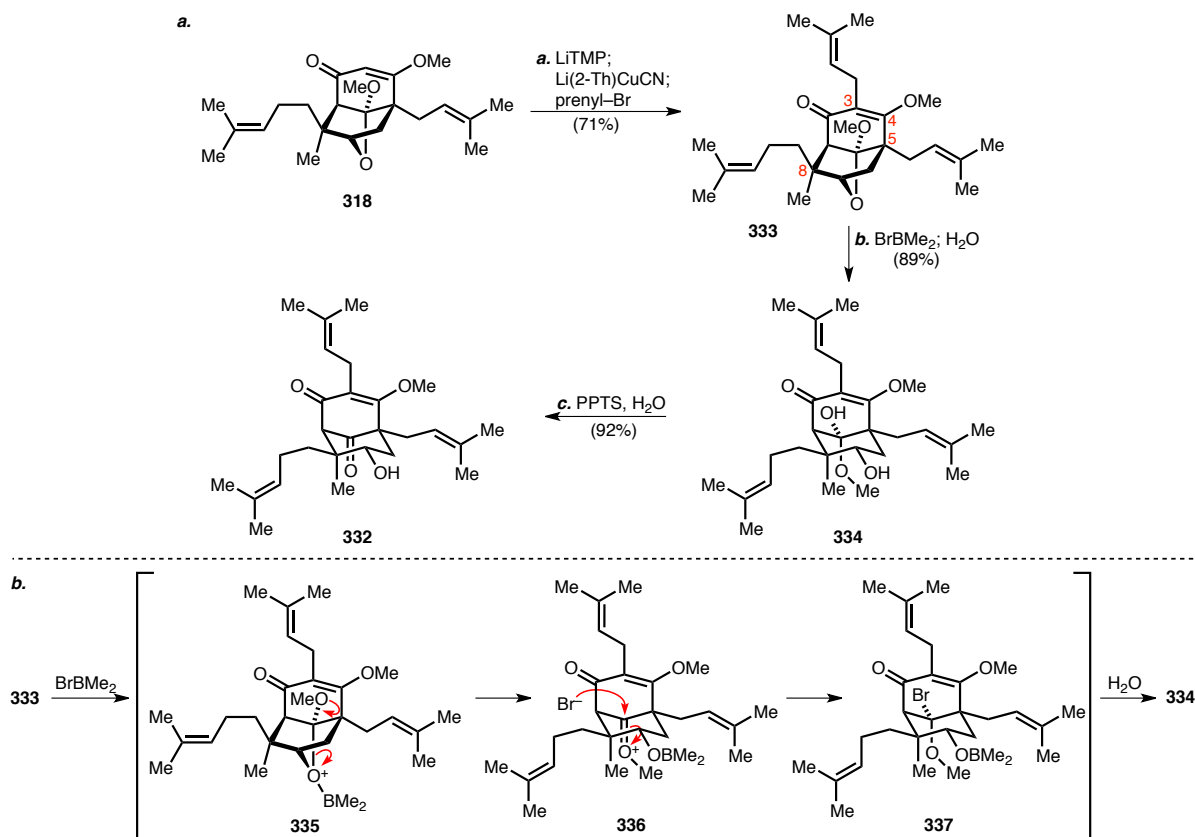
Scheme 3.12. (a) Retrosynthesis of hyperforin (**1**) from β -methoxyenone **318** via cyclopropane **330**, and (b) a proposed tandem 1,5-addition-bridgehead acylation of **330** to form *O*-methyl hyperforin (**60**).

Prenylation at the C3 position of **318** was accomplished through the previously mentioned sequential LiTMP-mediated deprotonation, transmetalation with Li(2-Th)CuCN,⁵¹¹ and trapping with prenyl bromide⁵¹⁰ to afford **333** (Scheme 3.13a). A variety of Lewis and Brønsted acidic conditions were then screened for the hydrolysis of the cyclic ketal present in **333**. No reactivity was observed using

⁶³⁸ For examples of diacylcyclopropane 1,5-addition that is selective for the least hindered position, see: (a) Tanimori, S.; Kainuki, T.; Nakayama, M. *Biosci. Biotech. Biochem.* **1992**, *56*, 1807-1809. (b) Jiang, X.; Covey, D. *F. J. Org. Chem.* **2002**, *67*, 4893-4900.

aqueous HOAc, LiBF₄, Sc(OTf)₃, CuCl₂·2H₂O, or InCl₃, or anhydrous conditions involving Ti(Oi-Pr)₄/MeOH or SmCl₃/TMSCl. Loss of the C3, C5, and C8 olefin functionality was observed when *p*-TsOH·H₂O, TFA, Amberlyst-15 acidic resin, or CAN was employed. While no reactivity was observed with aqueous HCl, PPTS, or BF₃·Et₂O/TBAI at rt, decomposition was observed upon heating. Several reagents led to selective cleavage of the C4 *O*-methyl ether, including HBr, BBr₃, TMSI, and FeCl₃·6H₂O. Selective cyclic ketal hydrolysis was ultimately accomplished using BrBMe₂;⁶³⁹ exposure of **333** to this reagent at -78 °C led to hemiketal **334**. The conversion of **333** to **334** may proceed via coordination of the Lewis acidic reagent to the Lewis basic cyclic ketal oxygen to give intermediate **335**, which may undergo ketal cleavage to form oxocarbenium ion **336** (Scheme 3.13b). The displaced bromide anion may then intercept the oxocarbenium ion to form the unstable geminal bromoether **337**, a species we observed spectroscopically but did not isolate. Upon exposure of **337** to H₂O upon reaction quench, the product hemiketal **334** is formed. The reaction was chemoselective for cyclic ketal cleavage at -78 °C; at higher temperatures, C4 *O*-methyl ether cleavage was also observed. Hydrolysis of **334** was accomplished by refluxing in wet acetone with PPTS to afford **332**.

⁶³⁹ (a) Guidon, Y.; Yoakim, C.; Morton, H. E. *Tetrahedron Lett.* **1983**, 24, 2969-2972. (b) Guidon, Y.; Yoakim, C.; Morton, H. E. *J. Org. Chem.* **1984**, 49, 3912-3920. (c) Guidon, Y.; Girard, Y.; Berthiaume, S.; Gorys, V.; Lemieux, R.; Yoakim, C. *Can. J. Chem.* **1990**, 68, 897-902.



Scheme 3.13. (a) Prenylation and cyclic ketal hydrolysis of **318**, and (b) a possible mechanism for the conversion of **333** to **334**.^a

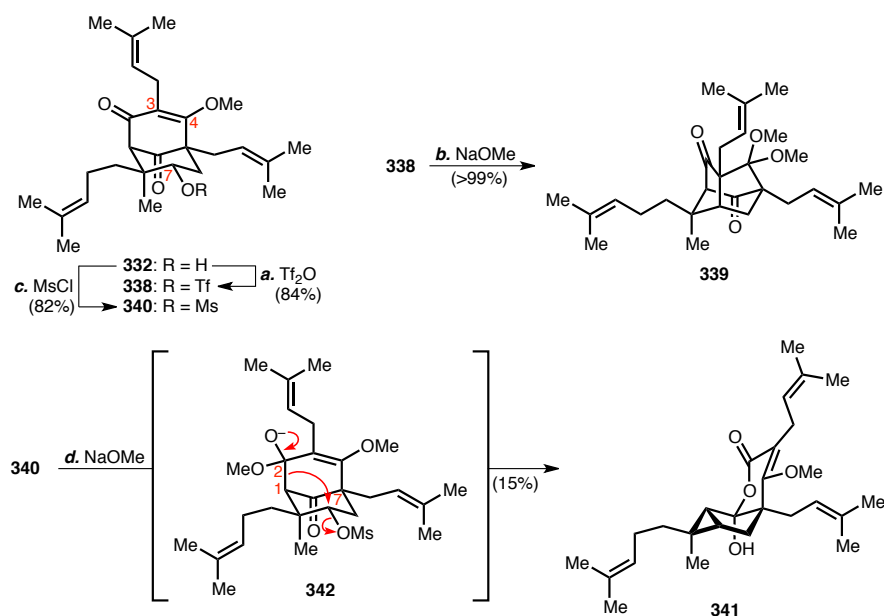
^a Conditions: (a) LiTMP, THF, $-78\text{ }^{\circ}\text{C}$; Li(2-Th)CuCN, THF, -78 to $-40\text{ }^{\circ}\text{C}$; prenyl bromide, -78 to $-40\text{ }^{\circ}\text{C}$, 71%; (b) BrBMe₂, CH₂Cl₂, $-78\text{ }^{\circ}\text{C}$; NEt₃; NaHCO₃, H₂O, 89%; (c) PPTS, acetone/H₂O, reflux, 92%.

We then attempted to synthesize cyclopropane **330** from alcohol **332**; however, we did not obtain this desired product (Scheme 3.14). After conversion to triflate **338**, exposure to LDA led to decomposition, including LDA-mediated hydride transfer to the C9 ketone.⁶⁴⁰ Treatment with NaOMe in MeOH, conditions known to promote bridgehead functionalization,⁶⁴¹ led to quantitative conversion to methanopentalene **339**, the product of methoxide addition to the C4 position followed by cyclization of the resulting C3 enolate to the C7 position. Studies with mesylate **340** were also unsuccessful. While

⁶⁴⁰ The reducing ability of LDA has been reported. For several examples, see ref. 527 and: (a) Kowalski, C.; Creary, X.; Rollin, A. J.; Burke, M. C. *J. Org. Chem.* **1978**, *43*, 2601-2608. (b) Majewski, M. *Tetrahedron Lett.* **1988**, *29*, 4057-4060. For a review of lithium dialkylamide reduction, see: Majewski, M.; Gleave, D. M. *J. Organomet. Chem.* **1994**, *470*, 1-16.

⁶⁴¹ Nickon, A.; Covey, D. F.; Huang, F.-C.; Kuo, Y.-N. *J. Am. Chem. Soc.* **1975**, *97*, 904-905.

treatment with LDA also resulted in decomposition, exposure to NaOMe/MeOH afforded rearranged cyclopropane **341**. This product may have formed via initial cleavage of the C1–C2 bond with concomitant C1–C7 bond formation from C2 hemiketal anion **342**, followed by lactone formation upon aqueous workup.

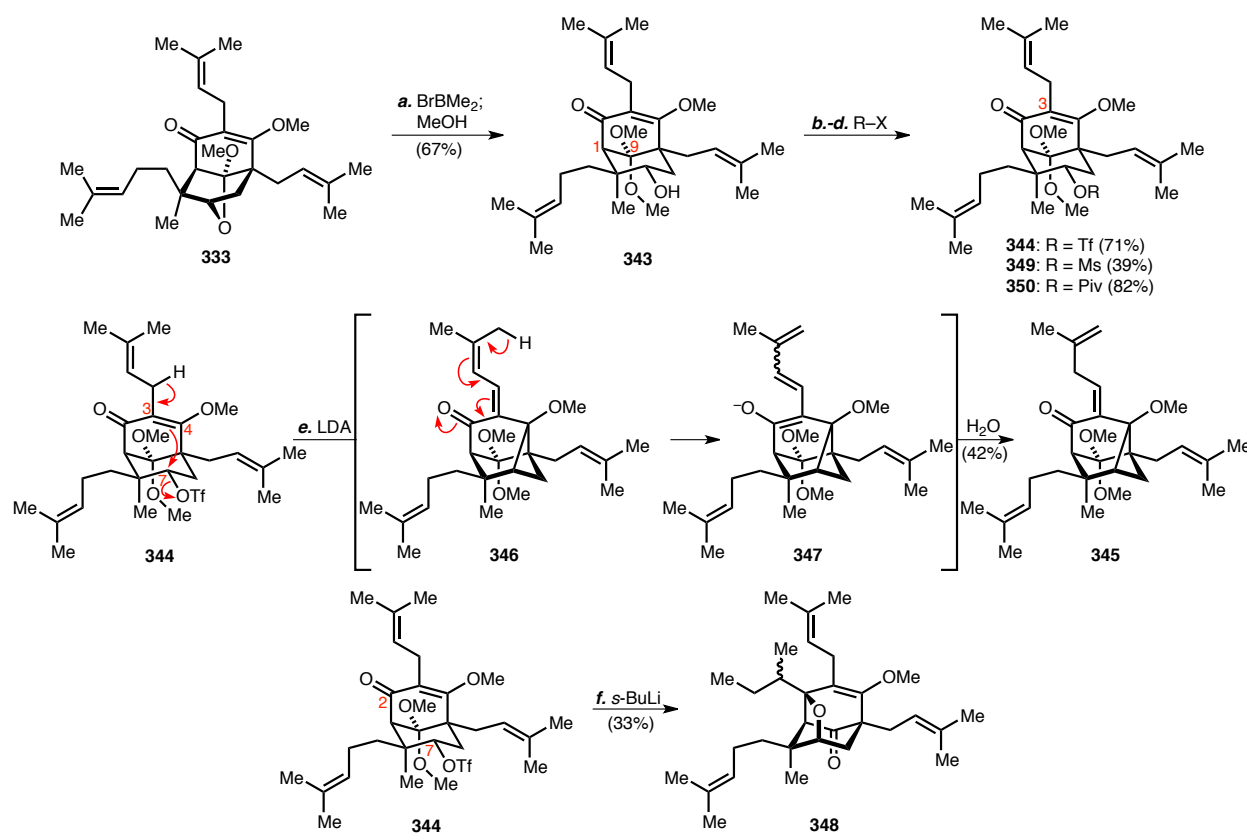


Scheme 3.14. Byproducts isolated from attempted bridgehead lithiations of **338** and **340**.^a

^a Conditions: (a) Tf₂O, pyr, CH₂Cl₂, –43 to 0 °C, 84%; (b) NaOMe, MeOH, 0 °C to rt, >99%; (c) MsCl, NEt₃, CH₂Cl₂, 0 °C, 82%; (d) NaOMe, MeOH, 0 to 70 °C, 15%.

Since there is very poor overlap of the C9 ketone π orbital with the C1–H methine σ^* orbital and that a major source of byproducts was hydride addition to the C9 ketone, we also explored the bridgehead lithiation chemistry of a series of intermediates bearing a C9 dimethyl ketal (Scheme 3.15). By quenching the BrBMe₂-mediated reaction of **333** with MeOH before introduction of H₂O, dimethyl ketal **343** was isolated instead of hemiketal **334**. Reactions of the triflate **344** derived from this intermediate were investigated; however, we did not observe desired cyclopropane formation. Exposure of **344** to LDA afforded tricyclononane **345**, which may have formed via deprotonation of the C3 prenyl methylene with subsequent C4–C7 bond formation, yielding intermediate **346**. After formation of extended enolate

347, quenching with H₂O may afford **345**. Treatment of **344** with *s*-BuLi led to **348**, the result of 1,2-addition of *s*-Bu anion to the C2 ketone followed by displacement of the C7 triflate with the resulting alkoxide. Reactions of mesylate **349** and pivalate **350** were also fruitless; when reactivity was observed, it was typically due to C3 prenyl methylene deprotonation.

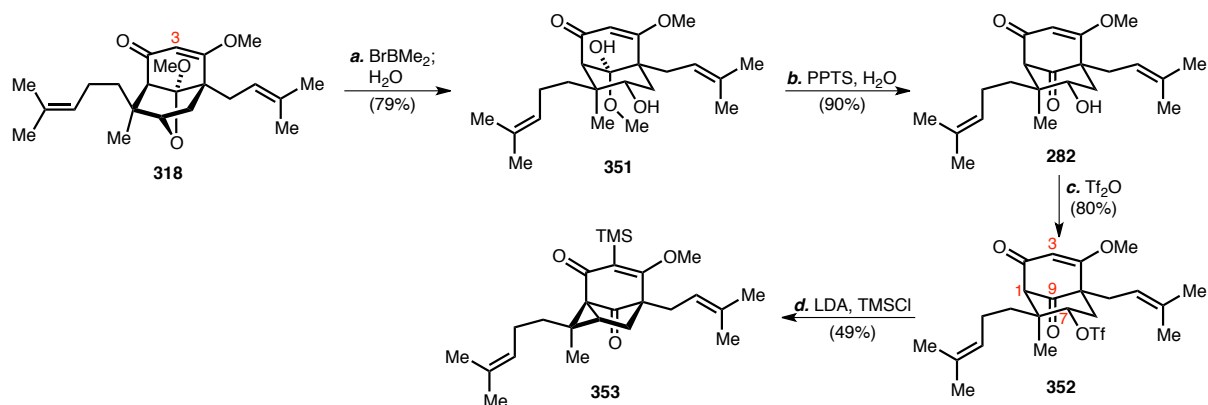


Scheme 3.15. Synthesis and reactivity of **343** derivatives.^a

^a Conditions: (a) BrBMe₂, CH₂Cl₂, -78 °C; MeOH, NEt₃, -78 °C, 67%; (b) Tf₂O, pyr, CH₂Cl₂, -40 to -10 °C, 71%; (c) MsCl, pyr, CH₂Cl₂, 0 °C to rt, 39%; (d) PivCl, pyr, DMAP, 0 °C to rt, 82%; (e) LDA, THF, -78 to -20 °C, 42% (10% recovered **344**); (f) *s*-BuLi, THF, -78 °C, 33%.

Given the enhanced acidity of the bisallylic methylene attached to C3, we elected to pursue a synthesis strategy in which cyclopropanation to form the C1–C7 bond would precede C3 prenylation. BrBMe₂-mediated cyclic ketal hydrolysis of **318** afforded hemiketal **351**, and subsequent hydrolysis afforded alcohol **282** (Scheme 3.16). Triflation of **282** yielded **352**. Gratifyingly, exposure of this triflate

to LDA in the presence of TMSCl produced cyclopropane **353**. In this reaction, silylation of the C3 position accompanied C1 bridgehead lithiation with subsequent C1–C7 bond formation, providing **353**. An observed, unstable byproduct in this reaction was the result of LDA-mediated C9 ketone reduction, which was isolated in variable amounts.



Scheme 3.16. Synthesis of cyclopropane **353**.^a

^a Conditions: (a) BrBMe₂, CH₂Cl₂, –78 °C; NEt₃, –78 °C; NaHCO₃, H₂O, –78 °C to rt, 79%; (b) PPTS, H₂O/acetone, reflux, 90%; (c) Tf₂O, pyr, CH₂Cl₂, –43 to 5 °C, 80%; (d) LDA, TMSCl, THF, –78 °C, 49%.

We then attempted 1,5-addition of a variety of nucleophiles to the activated cyclopropane present in **353**; however, under all conditions screened, we did not isolate any desired products (**354**, Table 3.4). In general, we explored the use of organocuprates⁶⁴² as nucleophiles, given past precedent of the use of these reagents for cyclopropane opening.⁶⁴³ We utilized the Lewis acids TMSCl and BF₃·Et₂O in an attempt to further activate the cyclopropane for nucleophilic attack.^{644,645} The 1,5-addition of

⁶⁴² For reviews of organocuprate chemistry, see: (a) Posner, G. H. *Org. React.* **1975**, 22, 253-400. (b) Lipshutz, B. H. *Synlett* **1990**, 119-128.

⁶⁴³ For examples of allylcuprate additions to activated cyclopropanes, see: (a) Corey, E. J.; Fuchs, P. L. *J. Am. Chem. Soc.* **1972**, 94, 4014-4015. (b) Mioskowski, C.; Manna, S.; Falck, J. R. *Tetrahedron Lett.* **1983**, 24, 5521-5524. (c) Bertz, S. H.; Dabbagh, G.; Cook, J. M.; Honkan, V. *J. Org. Chem.* **1984**, 49, 1739-1743. (d) Taber, D. F.; Kewson, K. R.; Raman, K.; Rheingold, A. L. *Tetrahedron Lett.* **1984**, 25, 5283-5286. (e) He, M.; Tanimori, S.; Nakayama, M. *Biosci. Biotech. Biochem.* **1995**, 59, 900-902.

⁶⁴⁴ Lipshutz, B. H.; Dimock, S. H.; James, B. *J. Am. Chem. Soc.* **1993**, 115, 9283-9284.

alkylcuprates to activated cyclopropanes may also be catalyzed by PBU_3 .⁶⁴⁶ Due to the inability of accessing prenyllithium from lithium insertion into a prenyl halide,⁶⁴⁷ several modes of prenyl cuprate formation were explored. In entry 1, Rieke copper(0) was generated,⁶⁴⁸ but the reagent derived from Cu^* and prenyl chloride did not react with the substrate. The only product we observed in this reaction was **355** (Figure 3.3),⁶⁴⁹ the result of nucleophilic opening of THF solvent. No reactivity was observed with prenylcuprates derived from: (a) prenyl-MgBr and CuI ⁶⁵⁰ (entries 2-3) and (b) prenyl-Li⁶⁵¹ and CuI (entries 4-5). The generation of prenylcuprate⁶⁵² from prenyl-SnBu₃,⁶⁵³ BuLi,⁶⁵⁴ and CuI afforded iodide **356** and proteodesilylation product **357** (entries 6-7).⁶⁵⁵ Iodide **356** was the only product obtained in these

⁶⁴⁵ For a review of the use of Lewis acids in organocopper chemistry, see: Yamamoto, Y. *Angew. Chem. Int. Ed. Engl.* **1986**, 25, 947-959.

⁶⁴⁶ Kauffman, G. B.; Teter, L. A. *Inorg. Synth.* **1963**, 7, 9-12.

⁶⁴⁷ Rapid Wurtz coupling was observed upon attempted halogen-lithium exchange of allyl halides. For more information, see: (a) Seyferth, D.; Weiner, M. A. *J. Org. Chem.* **1959**, 24, 1395-1396. (b) Seyferth, D.; Weiner, M. A. *J. Org. Chem.* **1961**, 26, 4797-4800.

⁶⁴⁸ (a) Ebert, G. W.; Rieke, R. D. *J. Org. Chem.* **1984**, 49, 5282-5283. (b) Wehmeyer, R. M.; Rieke, R. D. *J. Org. Chem.* **1987**, 52, 5057-5059. (c) Rieke, R. D.; Wehmeyer, R. M.; Wu, T.-C.; Ebert, G. W. *Tetrahedron* **1989**, 45, 443-454. (d) Stack, D. E.; Dawson, B. T.; Rieke, R. D. *J. Am. Chem. Soc.* **1991**, 113, 4672-2673. (e) Stack, D. E.; Dawson, B. T.; Rieke, R. D. *J. Am. Chem. Soc.* **1992**, 114, 5110-5116. (f) Stack, D. E.; Klein, W. R.; Rieke, R. D. *Tetrahedron Lett.* **1993**, 34, 3063-3066.

⁶⁴⁹ (a) Sakane, S.; Maruoka, K.; Yamamoto, H. *Tetrahedron* **1986**, 42, 2203-2209. (b) Korthals, K. A.; Wulff, W. D. *J. Am. Chem. Soc.* **2008**, 130, 2898-2899.

⁶⁵⁰ Lipshutz, B. H.; Hackmann, C. *J. Org. Chem.* **1994**, 59, 7437-7444.

⁶⁵¹ Prenyllithium was generated from the reaction of phenyl prenyl ether with Li. For more information, see: Eisch, J. J.; Jacobs, A. M. *J. Org. Chem.* **1963**, 28, 2145-2146.

⁶⁵² (a) Lipshutz, B. H.; Crow, R.; Dimock, S. H.; Ellsworth, E. L.; Smith, R. A. J.; Behling, J. R. *J. Am. Chem. Soc.* **1990**, 112, 4063-4064. (b) Lipshutz, B. H.; Ellsworth, E. L.; Dimock, S. H.; Smith, R. A. J. *J. Am. Chem. Soc.* **1990**, 112, 4404-4410.

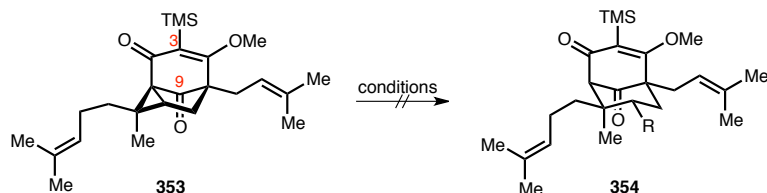
⁶⁵³ For the synthesis of tributylprenylstannane, see: (a) Naruta, Y.; Nishigaichi, Y.; Maruyama, K. *Org. Synth.* **1993**, 71, 118-124. (b) Kiyokawa, K.; Yasuda, M.; Baba, A. *Organometallics* **2011**, 30, 2039-2043.

⁶⁵⁴ For the generation of allyllithium reagents from the reaction of allyltributylstannanes and BuLi, see: Desponds, O.; Schlosser, M. *J. Organomet. Chem.* **1991**, 409, 93-101.

⁶⁵⁵ **357** and **358** were not rigorously characterized; we surmised the structure of these compounds via comparison to **353** as well as spectroscopic analysis of reaction mixtures.

studies in which the cyclopropane ring of **353** was opened. We also briefly explored the TMSOTf-mediated addition of allyltrimethylsilane⁶⁵⁶ (entry 14), but the only product observed was **357**.

Table 3.4. Attempted formation of **354** from nucleophilic 1,5-additions to **353**.



Entry	Reagent (equiv)	Reagent formation	Additives	Solvent	Temperature	Result
1	prenyl-Cu* (10)	LiNap; CuCN, LiBr; prenyl-Cl	TMSCl	THF	-78 to 0 °C	355 is only product
2	prenyl-Cu (2.2)	prenyl-MgBr; CuI, LiCl	TMSCl	THF	-78 to 40 °C	no reaction
3	prenyl-Cu (10)	prenyl-MgBr; CuI	TMSCl	THF	-78 °C to rt	no reaction
4	prenyl-Cu (5)	prenyl-OPh, Li; CuI	BF ₃ ·Et ₂ O, PBu ₃	Et ₂ O/THF	-78 to 10 °C	no reaction
5	prenyl-Cu (25)	prenyl-OPh, Li; CuI	BF ₃ ·Et ₂ O, PBu ₃	Et ₂ O/THF	-78 °C to rt	no reaction
6	prenyl-Cu (5)	prenyl-SnBu ₃ , BuLi; CuI, LiCl	TMSCl	THF	-78 to 0 °C	no reaction
7	prenyl-Cu (30)	prenyl-SnBu ₃ , BuLi; CuI, LiCl	TMSCl	THF	-78 °C to rt	356 (50%), 357 (50%)
8	Bu ₂ CuLi (5)	BuLi, CuI	none	Et ₂ O	-78 to 0 °C	decomposition
9	Bu ₂ CuLi (5)	BuLi, CuI	BF ₃ ·Et ₂ O	Et ₂ O	-78 °C	358 is only product
10	Bu ₂ CuLi (5)	BuLi, CuI	TMSCl	Et ₂ O	-78 °C	358 is only product
11	Bu ₂ Cu(CN)Li ₂ (5)	BuLi, CuCN	BF ₃ ·Et ₂ O	Et ₂ O	-78 °C	358 is only product
12	Bu ₂ Cu(CN)Li ₂ (5)	BuLi, CuCN	TMSCl	Et ₂ O	-78 °C	358 is only product
13	Bu ₂ Cu(CN)Li ₂ (5)	BuLi, CuCN	none	THF	-78 °C to rt	no reaction
14	allyl-TMS	--	TMSOTf	CH ₂ Cl ₂	-78 °C to rt	357 is only product

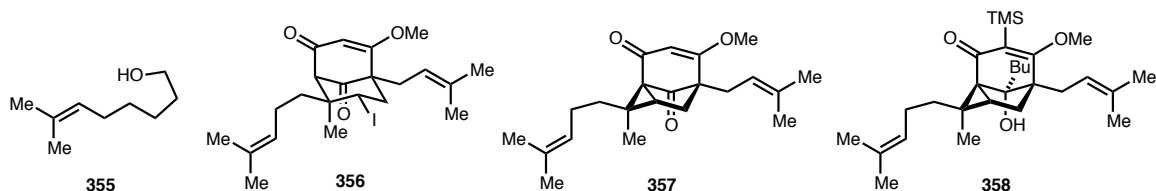


Figure 3.3. Byproducts obtained from the reaction of **353** with various nucleophiles.

Owing to the variability of prenyl-metal formation,⁶⁵⁷ we also assessed the reactivity of butyl-derived cuprate species for this cyclopropane-opening reaction (Table 3.4, entries 8-13). The preparation

⁶⁵⁶ For examples of allyltrimethylsilane addition to activated cyclopropanes, see: (a) Ohno, M.; Matsuoka, S.; Eguchi, S. *J. Org. Chem.* **1986**, *51*, 4553-4558. (b) Bambal, R.; Kemmitt, R. D. W. *J. Chem. Soc., Chem. Commun.* **1988**, 734-735. (c) Monti, H.; Afshari, M.; Léandri, G. *J. Organomet. Chem.* **1995**, *486*, 69-78. (d) Sugita, Y.; Yamadoi, S.; Hosoya, H.; Yokoe, I. *Chem. Pharm. Bull.* **2001**, *49*, 657-658. (e) Gharpure, S. J.; Shukla, M. K.; Vijayasree, U. *Org. Lett.* **2009**, *11*, 5466-5469.

of these reagents was much more straightforward than the preparation of prenylcuprates. Both Gilman⁶⁵⁸ and Lipshutz-type⁶⁵⁹ higher order cuprates were examined. In these cases, the only product we isolated was **358**,⁶⁵⁵ the result of 1,2-addition to the C9 ketone (Figure 3.3).

Given the propensity of nucleophilic 1,2-addition to the C9 ketone, we also synthesized and explored the chemistry of cyclopropane **359**, in which the reactive ketone was masked as a dimethyl ketal. BrBMe₂-mediated cyclic ketal opening of **318** followed by a methanol quench afforded alcohol **360** (Scheme 3.17). A variety of conditions were screened for the synthesis of **359** from the derived triflate **361**.⁶⁶⁰ Exposure of **361** to LDA and TMSCl only afforded vinylsilane **362**.⁶⁶¹ We rationalized that a smaller lithium amide base may promote bridgehead deprotonation, since the presence of the C9 dimethyl ketal significantly increased the steric environment surrounding the C1 methine. Exposure of **362** to excess LiNEt₂ provided the desired cyclopropane **359** along with sulfamate **363**, the product of diethylamide displacement of trifluoromethide from **361**. To the best of our knowledge, this is the only known example of trifluoromethide displacement from an alkyl triflate to form a sulfamate. Such a displacement is thermodynamically tenable, given the relative acidity of fluoroform ($pK_a \sim 25-28$)⁶⁶² versus diethylamine ($pK_a \sim 31$).⁶⁶³ Upon reexposure of **363** to LDA or LiNEt₂, only trace amounts of **359** were produced. Interestingly, upon exposure of **361** to LiNEt₂, *rearranged* cyclopropane **364** was

⁶⁵⁷ For an example of unexpected reactivity involving an allyl cuprate, see: Hutchinson, D. K.; Fuchs, P. L. *Tetrahedron Lett.* **1986**, 27, 1429-1432.

⁶⁵⁸ (a) Gilman, H.; Jones, R. G.; Woods, L. A. *J. Org. Chem.* **1952**, 17, 1630-1634. (b) Whitesides, G. M.; Fischer, W. F., Jr.; Filippo, J. S., Jr.; Bashe, R. W.; House, H. O. *J. Am. Chem. Soc.* **1969**, 91, 4871-4882. (c) Lipshutz, B. H.; Kozlowski, J. A.; Wilhelm, R. S. *J. Org. Chem.* **1983**, 48, 546-550.

⁶⁵⁹ (a) Lipshutz, B. H.; Kozlowski, J.; Wilhelm, R. S. *J. Am. Chem. Soc.* **1982**, 104, 2305-2307. (b) Lipshutz, B. H.; Wilhelm, R. S.; Kozlowski, J. A.; Parker, D. *J. Org. Chem.* **1984**, 49, 3928-3938.

⁶⁶⁰ All intermediates bearing both a C9 dimethyl ketal and a C7 triflate were particularly unstable and were not fully characterized.

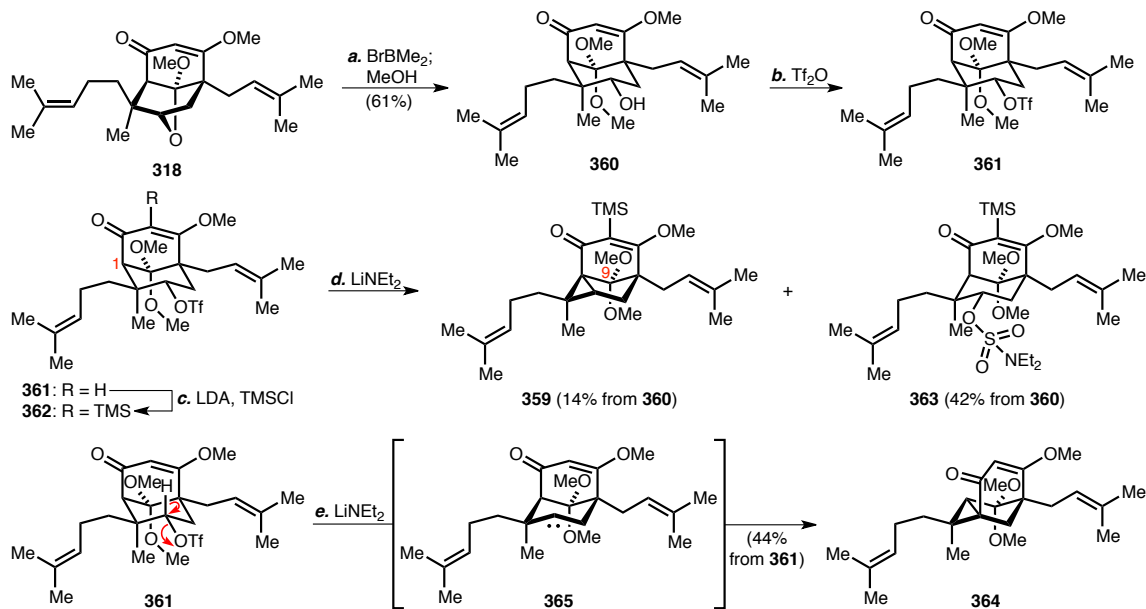
⁶⁶¹ Reexposure of this product to LDA did not afford cyclopropane **359**.

⁶⁶² Klabunde, K. J.; Burton, D. J. *J. Am. Chem. Soc.* **1972**, 94, 5985-5990.

⁶⁶³ Ahlbrecht, H.; Schneider, G. *Tetrahedron* **1986**, 42, 4729-4741.

isolated.⁶⁶⁴ This rearrangement product may arise from 1,2-alkyl shift of carbenoid intermediate **365**.

This reaction is remarkable given the contrasting reactivity of closely related triflate **362**.



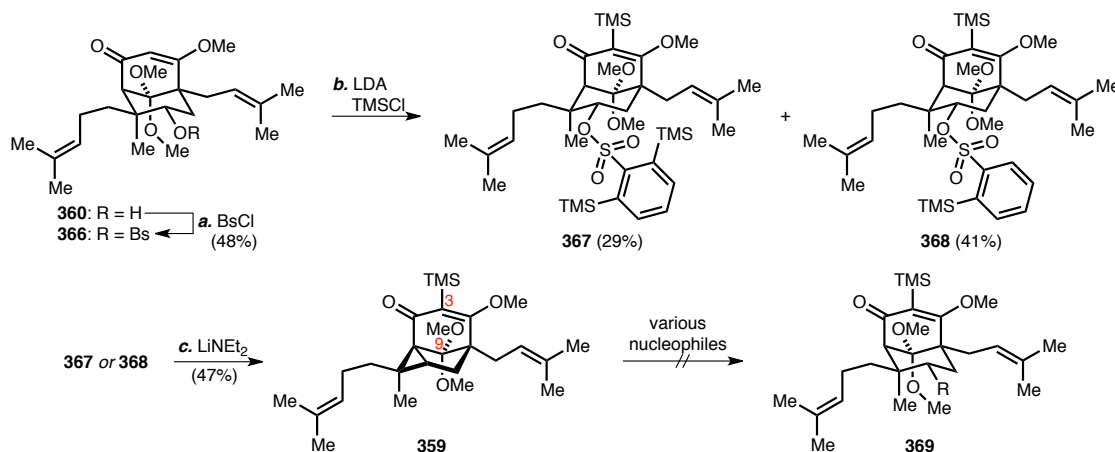
Scheme 3.17. Synthesis of cyclopropane **359** and byproducts **363** and **364**.^a

^a Conditions: (a) BrBMe_2 , NEt_3 , CH_2Cl_2 , $-78\text{ }^\circ\text{C}$; MeOH, NEt_3 ; NaHCO_3 , H_2O , 61%; (b) Tf_2O , CH_2Cl_2 , -40 to $0\text{ }^\circ\text{C}$; (c) LDA, TMSCl, HMPA, THF, -78 to $0\text{ }^\circ\text{C}$; (d) LiNEt_2 , THF, -78 to $-10\text{ }^\circ\text{C}$, 14% **359**, 42% **363** (both yields from **360**); (e) LiNEt_2 , THF, $-78\text{ }^\circ\text{C}$ to rt, 44% (from **360**).

We then sought to improve the yield of **359** through the intermediacy of benzenesulfonate **366**, since displacement of a phenyl anion would be highly unlikely. Treatment of alcohol **360** with BsCl afforded **366** (Scheme 3.18). Exposure of this sulfonate to LDA and TMSCl afforded vinylsilanes **367** and **368**, in which the sulfonate functionality directed lithiation and subsequent silylation upon the attached phenyl ring. Exposure of both of these products to LiNEt_2 afforded **359** in identical yield. Unfortunately, we were unable to successfully convert cyclopropane **359** to a desired ring-opened product

⁶⁶⁴ The structure of **364** was elucidated from the appearance of nOe correlations between the cyclopropyl methine to both ketal methyl groups, circumstances that would be highly unlikely in the desired cyclopropane.

369. A variety of conditions were screened, similar to those found in Table 3.4. Proteodesilylation at the C3 position and hydrolysis of the C9 ketal were the only products we isolated in this endeavor.



Scheme 3.18. Synthesis of **359** via benzenesulfonate **366** and unsuccessful formation of **369** from **359**.^a

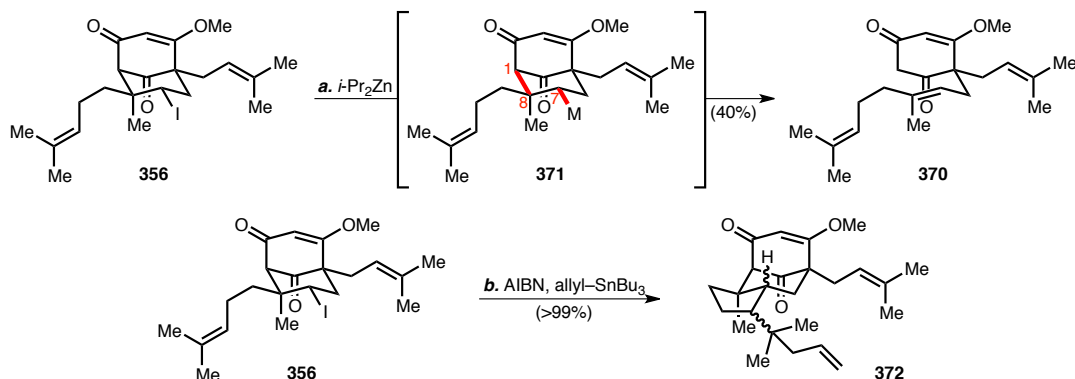
^a Conditions: (a) BsCl, pyr, CH₂Cl₂, -40 °C to rt, 48% yield; (b) LDA, TMSCl, THF, -78 to 0 °C, 29% **367**, 41% **368**; (c) LiNEt₂, THF, -78 °C to rt, 47% (from either **367** or **368**).

In summary, we did not observe desired 1,5-addition to both **353** and **359** despite screening a variety of nucleophiles under a litany of reaction conditions. Iodide **356** was the only product isolated in which 1,5-addition occurred. Given the ability of an iodide to act as a functional handle, we briefly explored the reactivity of this compound (Scheme 3.19).⁶⁶⁵ Attempted metal-iodine exchange of **356** afforded cyclohexenedione **370**.⁶⁶⁶ The formation of this ring-opened product is unsurprising considering the orbital overlap between the σ (C7–M) and the σ^* (C1–C8) bonds of possible intermediate **371**. Keck allylation⁵³⁰ of **356** very cleanly afforded **372**. Upon radical formation at the C7 position, a facile 5-*exo*-

⁶⁶⁵ Due to the paucity of iodide **356**, the products of these reactions were not fully characterized; however, spectroscopic analysis provided sufficient evidence to support the structural assertions made herein.

⁶⁶⁶ Micouin, L.; Knochel, P. *Synlett* **1997**, 327-328.

trig radical cyclization preceded intermolecular allylation. Similar cyclization products were obtained from attempted Ni-catalyzed Fu–Negishi couplings of **356**.⁶⁶⁷



Scheme 3.19. Reactions of iodide **356**.^a

^a Conditions: (a) ZnBr₂, $i\text{-PrMgCl}$, Et₂O, THF, rt; **356**; CuCN, LiCl, –78 °C; prenyl bromide, –78 °C to rt, 40%; (b) AIBN, allyltributylstannane, PhH, 80 °C, >99%.

Total Synthesis of Hyperforin

Even though Keck coupling of **356** provided the undesired cyclization product **372**, we were intrigued by the facility of this radical-based transformation. We resolved to utilize a Keck allylation strategy for the installation of the C7 prenyl group, given the aforementioned result and the successful implementation of a Keck allylation strategy in the total synthesis of (±)-garsubellin A by Danishefsky.⁶⁶⁸ In order to prevent cyclization prior to intermolecular allylation, masking the olefin present in the C8 side chain was required. A similar strategy was utilized in the total synthesis of *ent*-hyperforin by Shibasaki, in which formal methanolysis provided a temporary means of veiling the C8 olefin.⁶⁶⁹ We rationalized

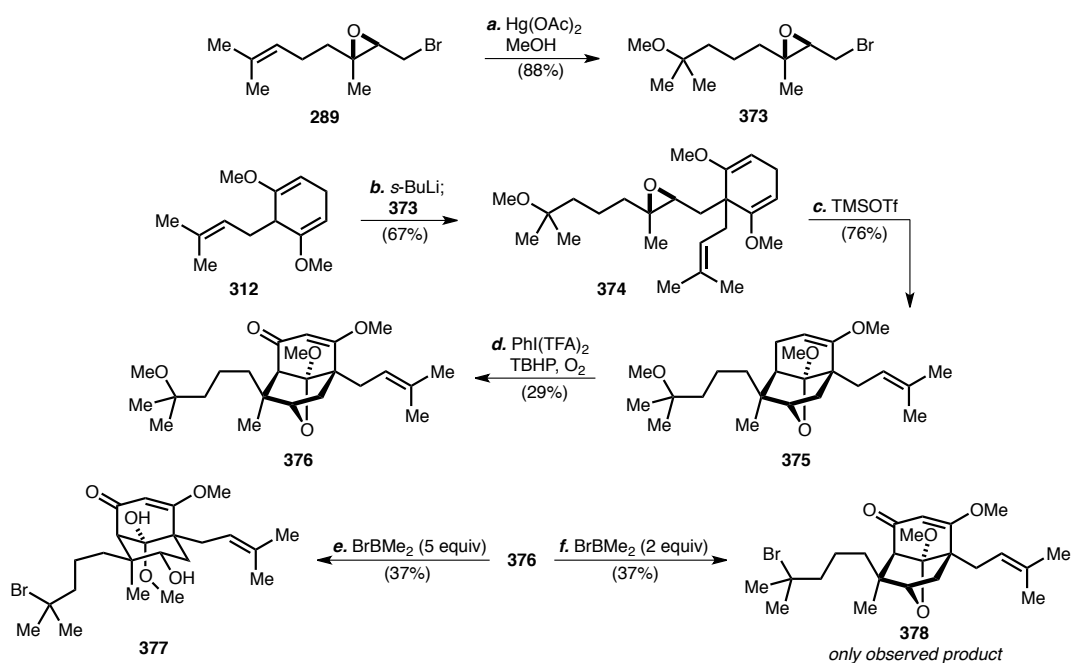
⁶⁶⁷ (a) Zhou, J. (S.); Fu, G. C. *J. Am. Chem. Soc.* **2003**, *125*, 14726–14727. (b) Zhou, J. (S.); Fu, G. C. *J. Am. Chem. Soc.* **2004**, *126*, 1340–1341. (c) Netherton, M. R.; Fu, G. C. *Adv. Synth. Catal.* **2004**, *346*, 1525–1532. (d) Strotman, N. A.; Sommer, S.; Fu, G. C. *Angew. Chem. Int. Ed.* **2007**, *46*, 3556–3558. (e) Saito, B.; Fu, G. C. *J. Am. Chem. Soc.* **2007**, *129*, 9602–9603. (f) Lu, Z.; Fu, G. C. *Angew. Chem. Int. Ed.* **2010**, *49*, 6676–6678.

⁶⁶⁸ See discussion on page 120 and ref. 527.

⁶⁶⁹ Specifically, the strategy was implemented in the sequence starting with intermediate **115** and ending with **122**. See the discussion starting on page 113 and ref. 512.

that a similar protecting group strategy would minimally affect existing methodology while providing a practical and prudent means of achieving a total synthesis of hyperforin.

We began implementing this strategy by synthesizing methyl ether **373** from the methoxymercuration of epoxygeranyl bromide **289** (Scheme 3.20). Coupling of **373** with cyclohexadiene **312** afforded cyclization precursor **374**, and exposure of this intermediate to TMSOTf provided the expected enol ether **375**. Subsequent allylic oxidation using our optimized $\text{PhI}(\text{TFA})_2$ -TBHP- O_2 system provided β -methoxyenone **376**. However, treatment with BrBMe_2 not only hydrolyzed the cyclic ketal of **376** but also displaced the tertiary methyl ether functionality to form bromide **377** as the only isolated product. Decreasing the BrBMe_2 stoichiometry afforded bromide **378**, indicating that methyl ether cleavage preceded cyclic ketal hydrolysis.

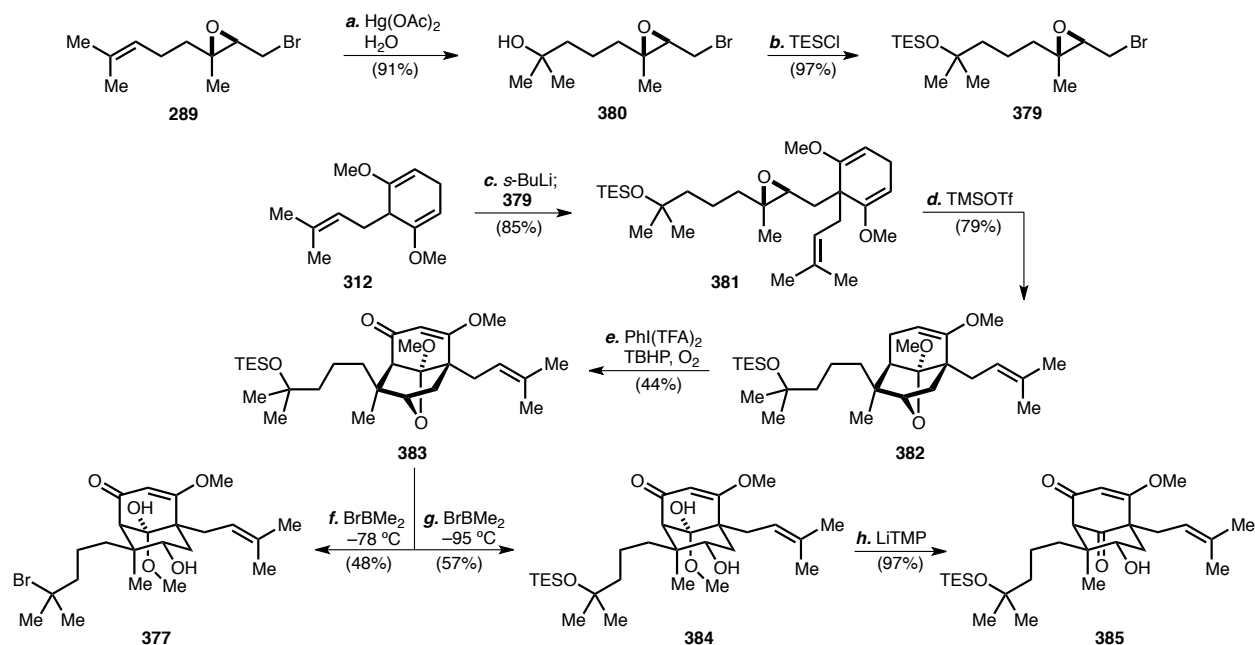


Scheme 3.20. Synthesis and reactivity of methyl ether **376**.^a

^a Conditions: (a) $\text{Hg}(\text{OAc})_2$, MeOH; NaOH, H_2O , 0 °C; NaBH_4 , 0 °C; 88%, 4% recovered **289**; (b) $s\text{-BuLi}$, THF, -78 to -30 °C; **289**, -78 to 0 °C, 67%; (c) TMSOTf, 2,6-lutidine, CH_2Cl_2 , -78 °C, 76%; (d) $\text{PhI}(\text{TFA})_2$, TBHP, Cs_2CO_3 , O_2 , EtOAc, -78 to 0 °C, 29%; (e) BrBMe_2 (5 equiv), NEt_3 , CH_2Cl_2 , -78 °C; NEt_3 , H_2O , NaHCO_3 , 37%; (f) BrBMe_2 (2 equiv), NEt_3 , CH_2Cl_2 , -78 °C; NEt_3 , H_2O , NaHCO_3 , >90% conversion.

Since Lewis acid coordination was a likely cause of this unintended reactivity, we hypothesized that a more sterically encumbered ether would be less prone to cleavage during the ketal hydrolysis step. Accordingly, triethylsilyl ether **379** was synthesized in two steps from epoxygeranyl bromide **289**: (1) oxymercuration of **289**, and (2) silylation of the resulting alcohol **380** (Scheme 3.21). We attempted to append other, more sterically demanding silyl moieties to **380**; however, intramolecular epoxide-opening cyclization preceded silylation. Coupling of **379** with cyclohexadiene **312** yielded **381**, which upon exposure to TMSOTf generated enol ether **382**. Allylic oxidation, using aforementioned conditions with minor modifications, afforded β -methoxyenone **383** in a significantly higher yield than previous, similar allylic oxidations. Unfortunately, exposure of this compound to BrBMe₂ at -78 °C produced the tertiary bromide **377**, previously observed in the reaction of **376**. Nevertheless, we discovered that if the reaction was cooled to below -90 °C, silyl ether cleavage was avoided while negligibly affecting the cyclic ketal hydrolysis, and we obtained the desired hemiketal **384**.⁶⁷⁰ LiTMP-mediated methanol extrusion from **384** yielded **385**.

⁶⁷⁰ Methyl ether cleavage was still observed in the reaction of **376** and BrBMe₂ when performed below -90 °C.



Scheme 3.21. Synthesis of triethylsilyl ether **385**.^a

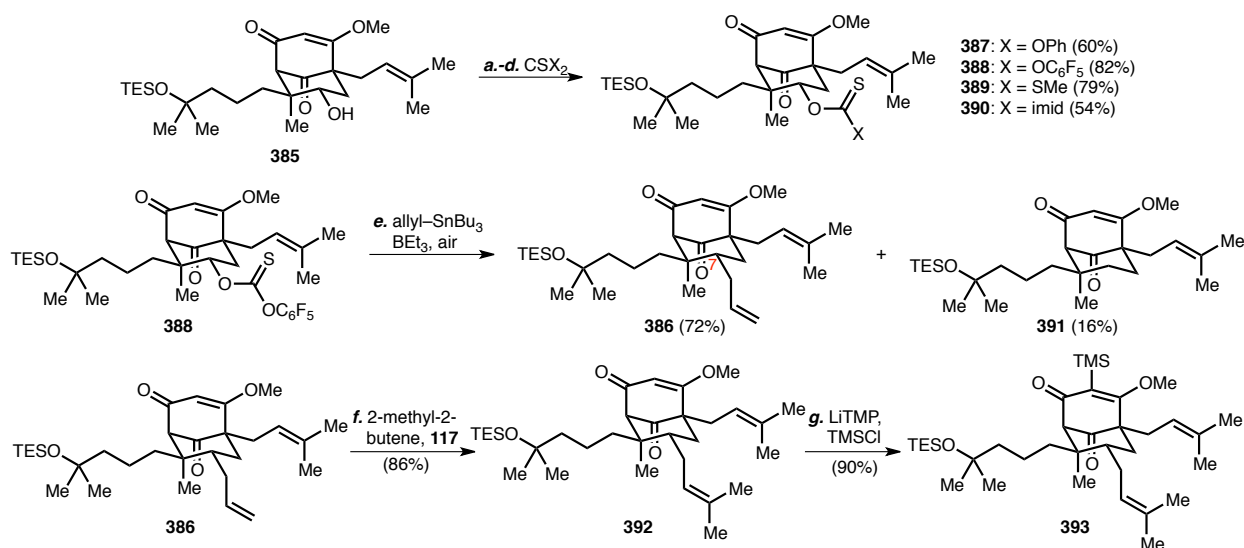
^a Conditions: (a) $\text{Hg}(\text{OAc})_2$, acetone, H_2O ; NaOH , $0\text{ }^\circ\text{C}$; NaBH_4 , $0\text{ }^\circ\text{C}$, 91%; (b) TESCl , imid, DMF, 97%; (c) $s\text{-BuLi}$, THF, -78 to $-30\text{ }^\circ\text{C}$; **379**, -78 to $-40\text{ }^\circ\text{C}$, 85%; (d) TMSOTf , 2,6-lutidine, CH_2Cl_2 , $-78\text{ }^\circ\text{C}$, 79%; (e) $\text{PhI}(\text{TFA})_2$, TBHP, Cs_2CO_3 , 4 \AA MS, EtOAc , O_2 , -78 to $0\text{ }^\circ\text{C}$, 44%; (f) BrBMe_2 , NEt_3 , CH_2Cl_2 , $-78\text{ }^\circ\text{C}$; NEt_3 , NaHCO_3 , H_2O , 48%; (g) BrBMe_2 , NEt_3 , CH_2Cl_2 , $-95\text{ }^\circ\text{C}$; NEt_3 , NaHCO_3 , H_2O , 57%; (h) LiTMP , THF, -78 to $0\text{ }^\circ\text{C}$, 97%.

Installation of the key C7 prenyl group was accomplished in three steps from **385** via a Keck allylation strategy. A variety of radical initiating functional groups were screened in the radical allylation reaction step to afford **386**, including phenyl thiocarbonate **387**,⁶⁷¹ pentafluorophenyl thiocarbonate **388**,⁶⁷² methyl xanthate **389**, and imidazole carbothioate **390** (Scheme 3.22). In addition, we screened several methods of radical generation, including: (1) the use of AIBN, activated both thermally and photochemically; (2) photochemical radical generation (in the absence of a radical promotor); and (3) the combination of BEt_3 and air. A major byproduct in these studies was **391**, the result of reductive deoxygenation. Ultimately, we found that the activation of **388** with BEt_3 and air afforded **386** in

⁶⁷¹ **387** was synthesized in one step from hemiketal **384** rather than from **385**. See experimental section for details.

⁶⁷² *N*-Hydroxysuccinimide (NHS) was utilized in the formation of **388** from **385**. For more information on the use of NHS in the synthesis of thiocarbonates, see: Barton, D. H. R.; Jaszberenyi, J. C. *Tetrahedron Lett.* **1989**, *30*, 2619-2622.

consistently good yield. Past studies have found that the pentafluorophenyl thiocarbonate radical precursor functionality has a relatively long half-life for radical generation;⁶⁷³ this prolonged half-life may prevent the formation of unintended byproducts and favor the selective formation of the intended allylation product. Cross metathesis of **386** with 2-methyl-2-butene catalyzed by Hoveyda–Grubbs second-generation catalyst (**117**) yielded **392**, a product containing the requisite C7 prenyl moiety. Exposure of **392** to LiTMP and TMSCl afforded vinylsilane **393**.



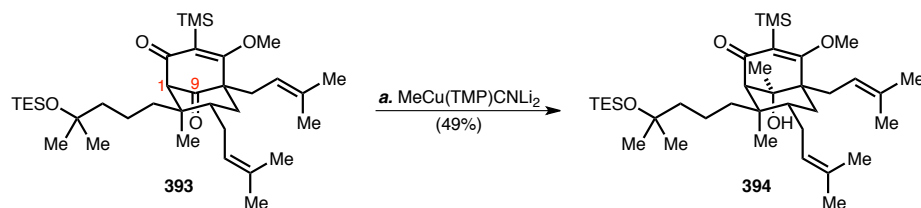
Scheme 3.22. Installation of the C7 prenyl moiety.^a

^a Conditions: (a) BuLi, THF, –78 °C; ClC(S)OPh, –78 °C to rt, 60% (from **384**); (b) ClC(S)OC₆F₅, NHS, pyr, PhMe, 80 °C, 82%; (c) NaH, CS₂, THF, 0 °C; MeI, 0 °C to rt, 79%; (d) 1,1'-thiocarbonyldiimidazole, DMAP, CH₂Cl₂, 40 °C, 54%; (e) allyltributylstannane, BEt₃, air, PhH, 72% **386**, 16% **391**; (f) **117**, 2-methyl-2-butene, CH₂Cl₂, 40 °C, 86%; (g) LiTMP, TMSCl, THF, –78 to 0 °C, 90%.

We then investigated the C1 bridgehead functionalization of **393**. This was an extremely challenging transformation, given the steric environment around the intended reaction center. In addition, considering that we intended to functionalize the C1 position with an isopropyl ketone, this meant that an electrophile bearing an acidic α -proton needed to be employed. In general, we focused our attention on

⁶⁷³ Barton, D. H. R.; Dorchak, J.; Jaszberenyi, J. C. *Tetrahedron* **1992**, *48*, 7435-7446.

several variables in screening this bridgehead functionalization reaction, including: (1) choice of base; (2) deprotonation time and temperature; (3) quenching temperature; (4) choice of electrophile; (5) various additives; and (6) reaction concentration. Specifically, we screened various amide bases, including LDA, LiNEt₂, LiTMP, and various other TMP-derived organometallics (e.g., TMP–MgX, TMP–ZnCl).⁶⁷⁴ In general, reduction of the C9 ketone was observed with LDA and LiNEt₂, and non-lithium TMP organometallics failed to deprotonate the C1 methine. MeCu(TMP)CNLi₂⁶⁷⁵ was the only such base to react with **393**, providing alcohol **394** as the result of methyl addition to the C9 ketone (Scheme 3.23). Appreciable deprotonation using LiTMP was not observed below –20 °C in THF solution; however, prolonged exposure of **393** to LiTMP above –20 °C caused significant decomposition. Eventually, we discovered that optimal deprotonation of **393** with LiTMP was accomplished in 5 min at 0 °C. Likewise, quenching temperature was also an important parameter in LiTMP-mediated reactions owing to the instability of **393** and its coupling products at relatively elevated temperatures. Significant increases in material recovery were observed when reactions were quenched at –20 °C and lower.



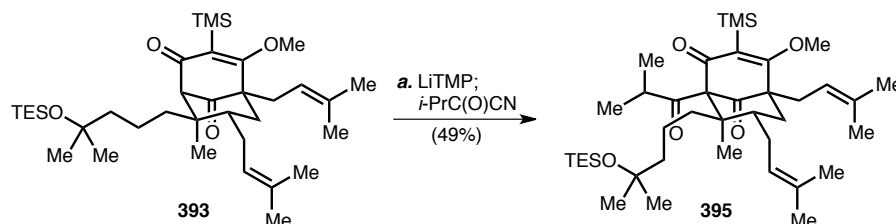
Scheme 3.23. Reaction of **393** with MeCu(TMP)CNLi₂.^a

^a Conditions: (a) MeCu(TMP)CNLi₂, THF, –78 to 0 °C; *i*-PrC(O)Cl, –78 °C to rt, 49%, 15% recovered **393**.

⁶⁷⁴ For examples of the use of TMP-derived organometallics in organic synthesis, see: (a) Krasovskiy, A.; Krasovskaya, V.; Knochel, P. *Angew. Chem. Int. Ed.* **2006**, *45*, 2958–2961. (b) Clososki, G. C.; Rohbogner, C. J.; Knochel, P. *Angew. Chem. Int. Ed.* **2007**, *46*, 7681–7684. (c) Wunderlich, S. H.; Knochel, P. *Angew. Chem. Int. Ed.* **2007**, *46*, 7685–7688. (d) Bresser, T.; Mosrin, M.; Monzon, G.; Knochel, P. *J. Org. Chem.* **2010**, *75*, 4686–4695.

⁶⁷⁵ Usui, S.; Hashimoto, Y.; Morey, J. V.; Wheatley, A. E. H.; Uchiyama, M. *J. Am. Chem. Soc.* **2007**, *129*, 15102–15103.

We also examined the use of several electrophiles. A reaction between the **393** and *i*-PrCHO was observed, but the product obtained in these reactions also contained C9 ketone reduction, possibly through internal hydride transfer. Dimethyl ketene was an ideal coupling partner, having no acidic α -proton, but we were not able to isolate any coupling products from reactions using this electrophile. Coupling reactions with I₂ resulted in decomposition. In the end, we observed our desired product through the use of either isobutyryl chloride or cyanide,⁵²⁰ the latter providing marginally improved yields on a consistent basis. In addition, reaction concentration was an important factor for this reaction. Optimal yields were observed with concentrations above 0.05 M. As a result of these findings, the optimized bridgehead acylation of **393** to afford **395** is depicted in Scheme 3.24. This is a significant improvement over prior PPAP total syntheses involving C1 bridgehead acylation, which required multiple steps involving a bridgehead iodide to synthesize similar intermediates.^{510,527,531}



Scheme 3.24. Bridgehead acylation of **393**.^a

^a Conditions: (a) LiTMP, THF, -78 °C, 10 min; 0 °C, 5 min; *i*-PrC(O)CN, -78 to -30 °C, 49%.

It should be noted that we also briefly explored the bridgehead lithiation chemistry of **396** and **397** (Figure 3.4). Under a variety of conditions, C1 functionalization was not observed in reactions involving **396**. Unsurprisingly, we observed products arising from C3 bisallylic methylene deprotonation upon exposure of **397** to lithium amide bases.

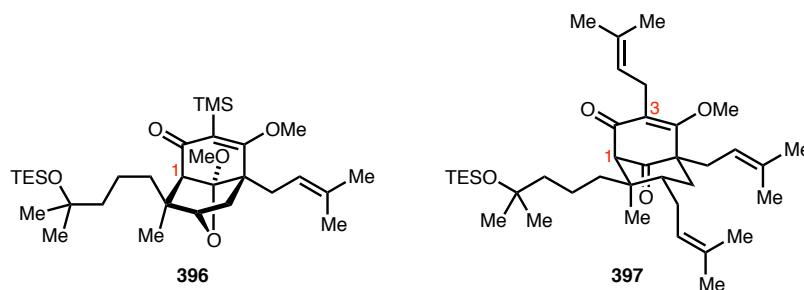
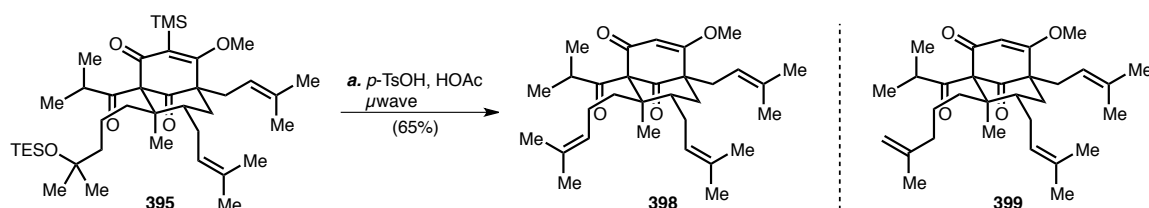


Figure 3.4. Structures of **396** and **397**.

Having achieved bridgehead acylation, we investigated the desilylation and dehydration of **395**. We hypothesized that under certain conditions, both tasks may be accomplished in a single step to afford **398**. Heating **395** in the presence of strong acids, such as CSA and *p*-TsOH, caused slow decomposition of the starting material, and in the presence of weaker acids, desilylation was observed but not elimination of the resulting tertiary carbinol. If microwave irradiation was utilized as the source of heat and using both *p*-TsOH and HOAc, we were able to access our desired product **398** (Scheme 3.25). In addition to **398**, we also isolated variable amounts of double-bond isomer **399**. 2-Methyl-2-butene was used as an additive to this reaction to prevent the isomerization of the other olefins present in **395**.

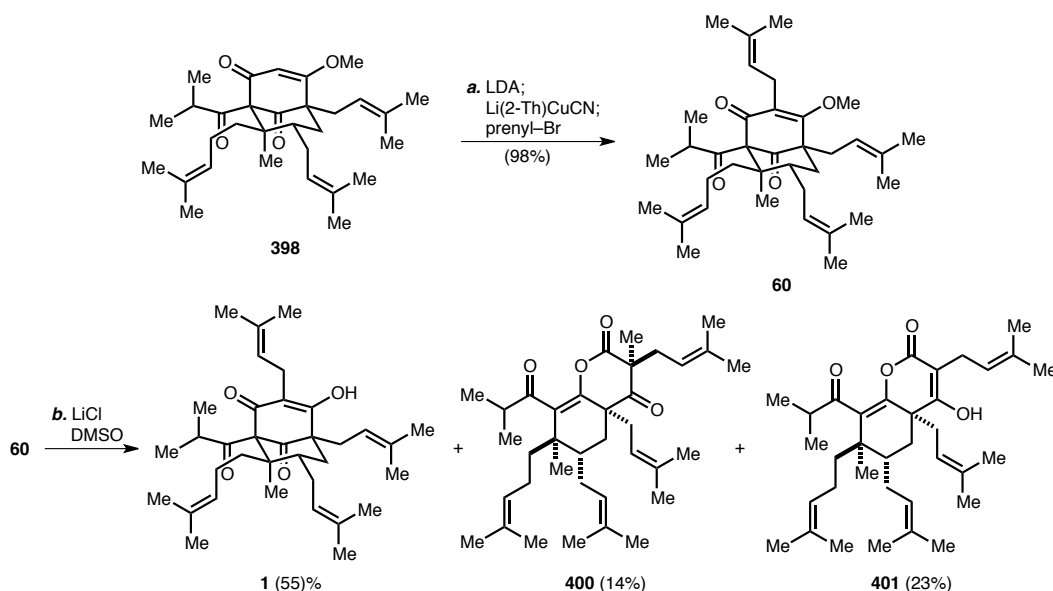


Scheme 3.25. Desilylation and dehydration of **395** to form **398**, and the structure of double bond isomer **399**.^a

^a Conditions: (a) *p*-TsOH·H₂O, HOAc, 2-methyl-2-butene, PhMe, μ wave, 100 °C, 65%.

Total synthesis of hyperforin was accomplished in two steps from **398** (Scheme 3.26). First, C3 prenylation was accomplished using stepwise lithiation, transmetalation with Lipshutz's cuprate,⁵¹¹ and prenyl bromide alkylation to afford hyperforin *O*-methyl ether (**60**). This compound was

spectroscopically identical to **60** semisynthetically derived from hyperforin.^{309,676} Finally, demethylation under Krapcho conditions provided hyperforin (**1**). The hyperforin obtained from this synthesis was spectroscopically indistinguishable from hyperforin that we isolated from SJW as well as published data on the natural product.⁶⁷⁷



Scheme 3.26. Completion of the total synthesis of hyperforin.^a

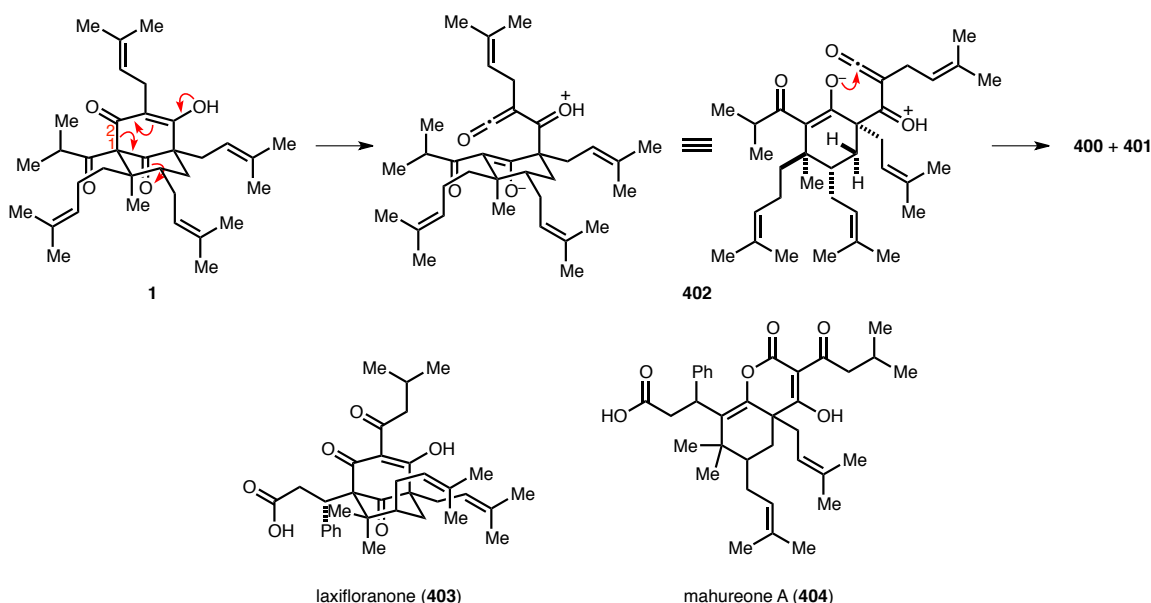
^a Conditions: (a) LDA, THF, -78 °C; Li(2-Th)CuCN, -78 to -40 °C; prenyl bromide, -78 to -30 °C, 98%; (b) LiCl, DMSO, 120 °C, 55% **1**, 14% **400**, 23% **401**.

Two other rearranged products were isolated in this final deprotection step, **400** and **401**. A possible mechanism for the formation of these byproducts involves formal *C*-to-*O* acyl migration of hyperforin, which may be facilitated by cleavage of the C1–C2 bond to form an intermediate ketene **402** (Scheme 3.27). Chloromethane, a byproduct of the demethylation reaction, may react with **400** to form

⁶⁷⁶ See experimental section for more details.

⁶⁷⁷ See experimental section for more details. A detailed procedure for the isolation of hyperforin from St. John's wort extract is also provided.

401. A similar C-to-O migration has been observed previously by Plietker.⁶⁷⁸ Interestingly, the PPAP laxifloranone¹⁰⁷ (**403**) and the chromenone-type acylphoroglucinol mahureone A⁶⁷⁹ (**404**) are analogously related despite being isolated from two disparate plant species.⁶⁸⁰



Scheme 3.27. A possible mechanism for the formation of **400** and **401** from **1**, and structures of laxifloranone and mahureone A.

Overall, these efforts culminated in a total synthesis of the naturally occurring enantiomer of hyperforin. The synthesis is 18 steps at its longest linear sequence, starting from geraniol (**287**). Relative and absolute stereochemistry in the synthesis is established through a Sharpless epoxidation reaction. The route is also considerably scalable; more than 40 mg of synthetic hyperforin were generated in a single batch. By recognizing latent symmetry elements embedded in the hyperforin core, we quickly established

⁶⁷⁸ Möws, K.; Schürmann, M.; Preut, H.; Plietker, B. *Acta Cryst.* **2009**, E65, o1751-o1751.

⁶⁷⁹ Massiot, G.; Long, C.; David, B.; Serrano, M.-J.; Daubié, F.; Alby, F.; Ausseil, F.; Knibiehler, M.; Moretti, C.; Hoffman, J.-S.; Cazaux, C.; Lavaud, C. *J. Nat. Prod.* **2005**, 68, 979-984.

⁶⁸⁰ Mahureone A is a known inhibitor of DNA polymerase β . For more information, see: Boudsocq, F.; Benaim, P.; Canitrot, Y.; Knibiehler, M.; Ausseil, F.; Capp, J. P.; Bieth, A.; Long, C.; David, B.; Shevelev, I.; Frierich-Heinecken, E.; Hübscher, U.; Amalric, F.; Massiot, G.; Hoffmann, J. S.; Cazaux, C. *Mol. Pharmacol.* **2005**, 67, 1485-1492.

the bicyclo[3.3.1]nonane core of hyperforin through a diastereoselective epoxide-opening cascade cyclization reaction. In this key conversion of **381** to **382**, the stereochemical identity of three key carbon centers were established including two quaternary centers. Further, the practicality and modularity of this synthesis may be exploited to quickly access a library of hyperforin analogs.

Experimental Section

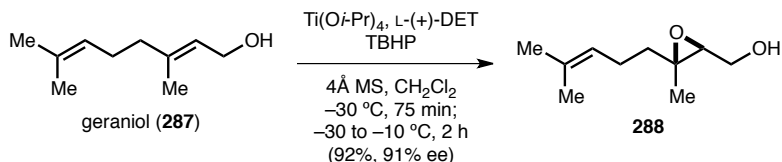
General Procedures. All reactions were performed in oven-dried or flame-dried glassware under a positive pressure of argon unless otherwise noted. Flash column chromatography was performed as described by Still *et al.*⁵⁹⁹ employing silica gel 60 (40-63 μm , Whatman). Both preparatory and analytical thin-layer chromatography (TLC) were performed using 0.25 mm silica gel 60 F₂₅₄ plates.

Materials. Commercial reagents and solvents were used as received with the following exceptions. Tetrahydrofuran, diethyl ether, dichloromethane, toluene, benzene, hexane, acetonitrile, and *N,N*-dimethylformamide were degassed with argon and passed through a solvent purification system (designed by J. C. Meyer of Glass Contour) utilizing alumina columns as described by Grubbs *et al.*⁶⁰⁰ unless otherwise noted. Diethylamine, triethylamine, diisopropylamine, pyridine, 2,2,6,6-tetramethylpiperidine, dimethyl sulfoxide, and chlorotrimethylsilane were distilled over calcium hydride. Hexamethylphosphoramide was distilled over calcium hydride under reduced pressure. Geraniol, titanium(IV) isopropoxide, prenyl chloride, prenyl bromide, allyltributylstannane, and trimethylsilyl trifluoromethanesulfonate were distilled under reduced pressure. *N*-Hydroxysuccinimide was recrystallized using ethanol. [bis(Trifluoroacetoxy)iodo]benzene was crystallized from the reaction of (diacetoxyiodo)benzene with trifluoroacetic acid and subsequently dried under reduced pressure (1 mmHg). Cesium carbonate was dried for at least 12 h at 150 °C under reduced pressure (1 mmHg). Lithium bromide, lithium chloride, and molecular sieves were stored in a vacuum oven for at least 24 h. The molarities of butyllithium, *sec*-butyllithium, and *tert*-butyllithium solutions were determined by titration with 1,10-phenanthroline as an indicator (average of three determinations). THF solutions of lithium diethylamide, lithium diisopropylamide, and lithium 2,2,6,6-tetramethylpiperidide were prepared by addition of a hexane solution of butyllithium (1 equiv) to a THF solution of the appropriate amine (1.1 equiv) cooled to -78 °C and stirring the solution for 30 min at 0 °C. PhH solutions of triethylborane were prepared by addition of neat triethylborane to PhH.

Instrumentation. ¹H NMR spectra were recorded with Varian INOVA-600, Varian INOVA-500, and Varian Mercury 400 spectrometers, are reported in parts per million (δ), and are calibrated using

residual non-deuterated solvent as an internal reference: CDCl_3 , δ 7.26 (CHCl_3); C_6D_6 , δ 7.16 ($\text{C}_6\text{D}_5\text{H}$); CD_3OD , δ 3.31 (CD_2HOD). Data for ^1H NMR spectra are reported as follows: chemical shift (multiplicity, coupling constants, integration). Multiplicities are reported as follows: s = singlet; d = doublet; t = triplet; q = quartet; septet = septet; m = multiplet; br = broad, or combinations thereof. ^{13}C NMR spectra were recorded with a Varian INOVA-500 spectrometer, are reported in parts per million (δ), and are referenced from the central peak of the carbon resonance of the solvent: CDCl_3 , δ 77.23; C_6D_6 , δ 128.06; CD_3OD , δ 49.00. Infrared (IR) data were recorded on a Varian 1000 FT-IR using NaCl plates or on a Bruker Alpha FT-IR spectrometer outfitted with an Eco-ATR sampling module. High-resolution mass spectra (HRMS) were recorded using electrospray ionization (ESI) mass spectroscopy on an Agilent 6210 TOF LC/MS or a Bruker q-TOF Maxis Impact mass spectrometer. Gas chromatography mass spectra (GCMS) were performed on a Shimadzu GC-2014 equipped with an AOC-20i auto-injector. Microwave irradiation was accomplished using a CEM Discover microwave reactor. High-performance liquid chromatography was performed on a Agilent 1100 series HPLC. Chiral high performance liquid chromatography (HPLC) was performed on an Agilent 1200 series HPLC.

Note: For clarity, intermediates that have are not explicitly mentioned in this chapter are numbered sequentially in the experimental section beginning with **405**.



((2*S*,3*S*)-3-Methyl-3-(4-methylpent-3-en-1-yl)oxiran-2-yl)methanol (288):⁶⁸¹

A CH₂Cl₂⁶⁸² solution of *tert*-butyl hydroperoxide⁶⁸³ (4.0 M, 410. mL, 1.64 mol, 1.5 equiv) was added via cannula over 1 h to a CH₂Cl₂ (850 mL) slurry of 4Å molecular sieves (30.43 g, powdered), L-(+)-diethyl tartrate (28.2 mL, 164 mmol, 0.15 equiv), and titanium(IV) isopropoxide (32.5 mL, 110. mmol, 0.1 equiv) in a 3-neck 5-L round-bottom flask cooled to an internal reaction temperature of −25 °C. The resulting yellow slurry was stirred at −25 °C for 30 min and then cooled to an internal reaction temperature of −30 °C. A CH₂Cl₂ (175 mL) solution of geraniol (**287**, 169.08 g, 1.0961 mol, 1 equiv) was added via cannula, followed by a CH₂Cl₂ (50 mL) rinse. Throughout this addition, the internal reaction temperature of the reaction was maintained ≤ −20 °C. After stirring at −30 °C for 75 min, the reaction was warmed to −10 °C over 2 h. The reaction was then quenched at −10 °C with H₂O (500 mL) followed by a 30 wt% H₂O solution of NaOH saturated in NaCl (300 mL). After stirring vigorously at rt for 45 min, the emulsion was diluted with MeOH (1.5 L) and brine (300 mL), and the layers were separated. The aqueous layer was washed thrice with CH₂Cl₂. The organic extracts were combined, washed with brine, dried over MgSO₄, filtered, and concentrated *in vacuo* to an opaque yellow oil. Short-path distillation (6 mmHg, 90–93 °C) afforded 171.05 g (1.0045 mol, 92% yield) of **288** as a pale yellow oil.

¹H NMR (600 MHz; CDCl₃) δ: 5.08 (t, *J* = 7.1 Hz, 1H), 3.82 (ddd, *J* = 11.8, 6.9, 4.7 Hz, 1H), 3.68 (ddd, *J* = 11.7, 6.8, 4.6 Hz, 1H), 2.97 (dd, *J* = 6.6, 4.3 Hz, 1H), 2.12–2.04 (m, 2H), 1.70–1.65 (m, 5H), 1.61 (s, 3H), 1.50–1.45 (m, 1H), 1.30 (s, 3H).

¹³C NMR (125 MHz; CDCl₃) δ: 132.3, 123.5, 63.2, 61.6, 61.4, 38.7, 25.9, 23.9, 17.8, 16.9.

⁶⁸¹ This procedure was adapted from ref. 607.

⁶⁸² The CH₂Cl₂ used in this procedure was dried through storage over 3Å molecular sieves (pelleted) for at least 24 h.

⁶⁸³ See ref. 607 for preparation of a CH₂Cl₂ solution of *tert*-butyl hydroperoxide.

FTIR (thin film) ν_{max} : 3420 (br), 2968, 2928, 2859, 1455, 1385, 1077, 1036, 865 cm^{-1} .

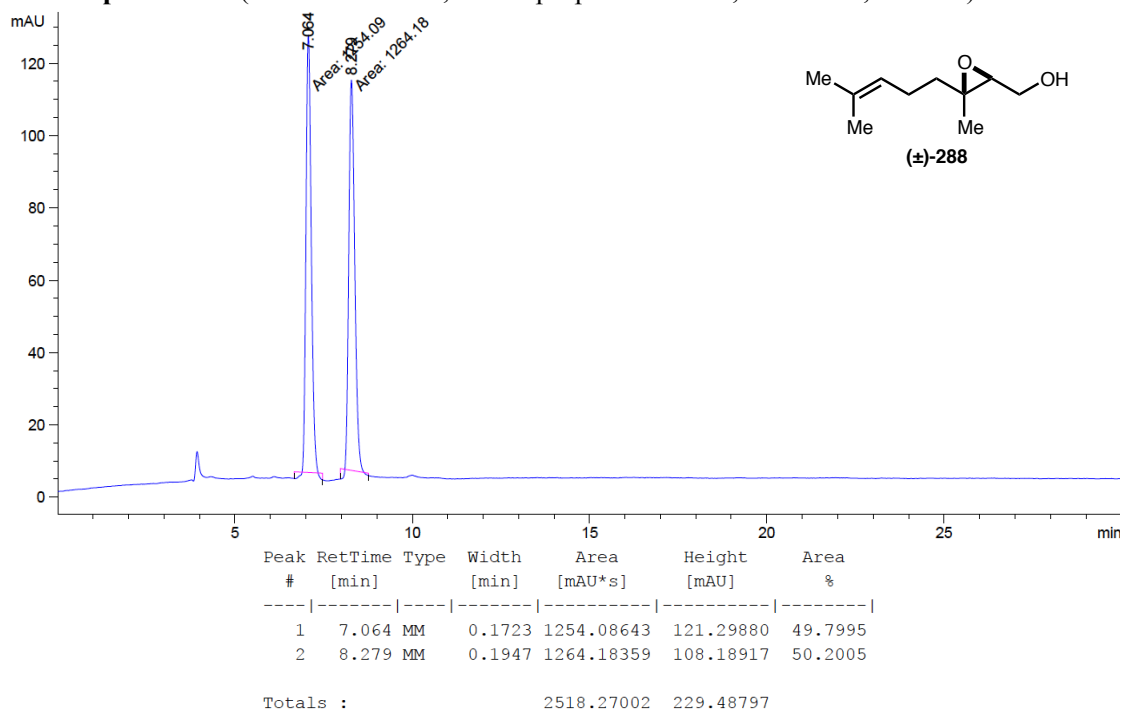
HRMS–ESI (m/z): $[\text{M}+\text{Na}]^+$ calculated for $\text{C}_{10}\text{H}_{18}\text{O}_2$, 193.1199; found, 193.1200.

$[\alpha]_{\text{D}}^{23} = -5.36^\circ$ (c 3.04, CHCl_3); [91% ee sample from literature:⁶⁰⁷ $[\alpha]_{\text{D}}^{25} = -5.3^\circ$ (c 3.0, CHCl_3)].

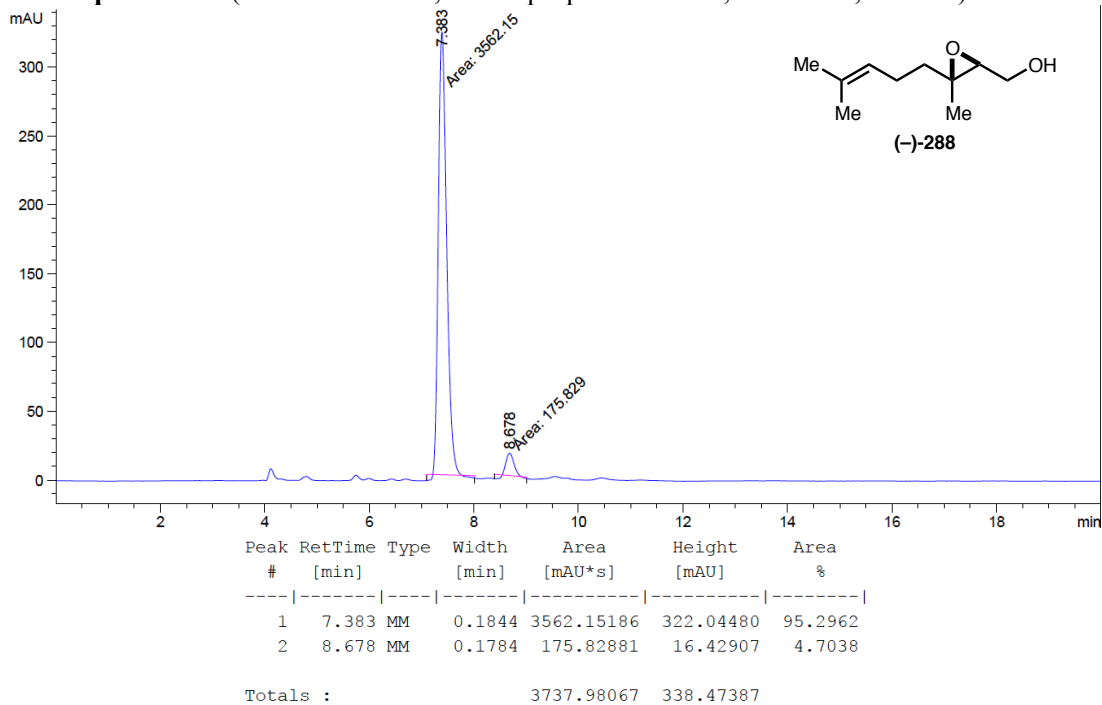
TLC $R_f = 0.45$ (1:1 hexane:EtOAc).

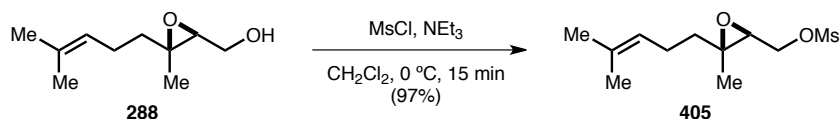
Chiral HPLC Trace of 288

Racemic sample: HPLC (ChiralPak AS-H, 9:1 isopropanol:hexane, 1 mL/min, 210 nm)



Scalemic sample: HPLC (ChiralPak AS-H, 9:1 isopropanol:hexane, 1 mL/min, 210 nm)





((2S,3S)-3-Methyl-3-(4-methylpent-3-en-1-yl)oxiran-2-yl)methyl methanesulfonate (405):⁶⁸⁴

A CH₂Cl₂⁶⁸⁵ (1.2 L) solution of **288** (100.00 g, 587.37 mmol, 1 equiv) and triethylamine (123 mL, 881 mmol, 1.5 equiv) in a 2-neck 2-L round-bottom flask outfitted with an equal pressure dropping funnel was cooled to an internal reaction temperature of −10 °C, and methanesulfonyl chloride (59.5 mL, 763 mmol, 1.3 equiv) was added dropwise via the equal pressure dropping funnel over 30 min, maintaining an internal reaction temperature ≤ 0 °C. After the addition was complete, the yellow slurry was stirred at 0 °C for 15 min, and then quenched at 0 °C with H₂O. The layers were separated, and the aqueous layer was washed thrice with CH₂Cl₂. The organic extracts were combined, washed sequentially with 2 N HCl, brine, and sat. aq. NaHCO₃, dried over Na₂SO₄, filtered, and concentrated *in vacuo*. The resulting yellow oil was dissolved in 95:5 hexane:EtOAc and passed through a plug of SiO₂, rinsing with 95:5 hexane:EtOAc. Concentration of the filtrate *in vacuo* yielded 142.19 g (572.56 mmol, 97% yield) of **405** as a yellow oil that was used without further purification.

¹H NMR (600 MHz; CDCl₃) δ: 5.07 (t, *J* = 7.0 Hz, 1H), 4.42 (dd, *J* = 11.7, 4.1 Hz, 1H), 4.25 (dd, *J* = 11.7, 7.1 Hz, 1H), 3.09-3.07 (m, 4H), 2.12-2.05 (m, 2H), 1.71-1.66 (m, 4H), 1.61 (s, 3H), 1.52-1.47 (m, 1H), 1.33 (s, 3H).

¹³C NMR (125 MHz; CDCl₃) δ: 132.6, 123.1, 68.9, 61.3, 59.3, 38.3, 38.0, 25.8, 23.7, 17.8, 17.0.

FTIR (thin film) ν_{max}: 2969, 2931, 2860, 1456, 1358, 1176, 981, 957, 833 cm^{−1}.

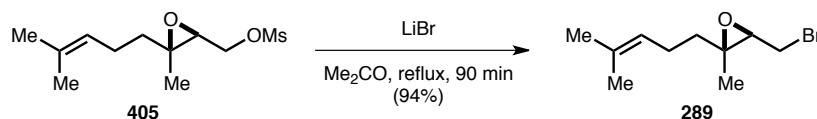
HRMS–ESI (*m/z*): [M+H]⁺ calculated for C₁₁H₂₀O₄S, 249.1155; found, 249.1157.

[α]_D²³ = −13.9° (*c* 4.08, CHCl₃).

TLC R_f = 0.55 (1:1 hexane:EtOAc).

⁶⁸⁴ This procedure was adapted from ref. 608.

⁶⁸⁵ The CH₂Cl₂ used in this procedure was dried through storage over 3Å molecular sieves (pelleted) for at least 24 h.



(2*S*,3*R*)-3-(Bromomethyl)-2-methyl-2-(4-methylpent-3-en-1-yl)oxirane (289):⁶⁸⁶

A Me₂CO (1 L) slurry of **405** (141.96 g, 571.64 mmol, 1 equiv) and lithium bromide (99.29 g, 1.143 mol, 2 equiv) was heated to reflux in a 2-L recovery flask outfitted with a reflux condenser. After refluxing for 90 min, the slurry was cooled to rt and filtered. The yellow filtrate was concentrated *in vacuo*. The resulting yellow oil was diluted with H₂O and extracted thrice with 9:1 hexane:EtOAc. The organic extracts were combined, washed sequentially with H₂O, sat. aq. NaHCO₃, and brine, dried over Na₂SO₄, filtered, and concentrated *in vacuo*. The resulting pale yellow oil was dissolved in 9:1 hexane:EtOAc, and passed through a plug of SiO₂, rinsing with 9:1 hexane:EtOAc. Concentration of the filtrate *in vacuo* yielded 125.35 g (537.64 mmol, 94% yield) of **289** as a pale yellow oil that was used without further purification.

¹H NMR (600 MHz; CDCl₃) δ: 5.10 (t, *J* = 7.1 Hz, 1H), 3.54 (dd, *J* = 10.4, 5.9 Hz, 1H), 3.24 (dd, *J* = 10.4, 7.8 Hz, 1H), 3.08 (dd, *J* = 7.8, 5.9 Hz, 1H), 2.13-2.05 (m, 2H), 1.74-1.70 (m, 4H), 1.61 (s, 3H), 1.45 (ddd, *J* = 13.7, 9.3, 7.1 Hz, 1H), 1.31 (s, 3H).

¹³C NMR (125 MHz; CDCl₃) δ: 132.5, 123.4, 63.2, 61.7, 38.6, 29.9, 25.9, 24.0, 17.9, 16.3.

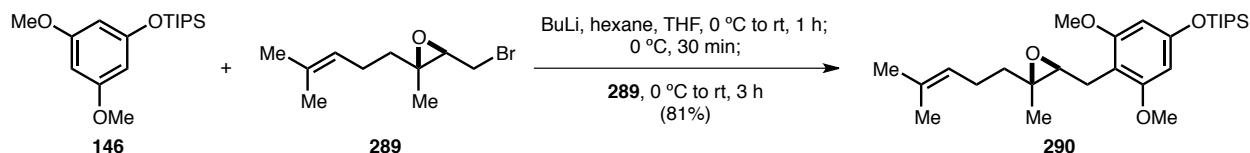
FTIR (thin film) ν_{max}: 2969, 2928, 2859, 1451, 1385, 1217, 1112, 1071, 890, 652 cm⁻¹.

PCI-GC/MS (*m/z*): [M+NH₄]⁺ 250 (100%), 252 (97.7%).

[α]_D²³ = +22.6° (*c* 4.34, CHCl₃).

TLC R_f = 0.72 (1:1 hexane:EtOAc).

⁶⁸⁶ This procedure was adapted from ref. 608.



(3,5-Dimethoxy-4-(((2*S*,3*S*)-3-methyl-3-(4-methylpent-3-en-1-yl)oxiran-2-

yl)methyl)phenoxy)triisopropylsilane (290):

A THF (54 mL) solution of **146** (3.169 g, 10.8 mmol, 1 equiv) in a 200-mL recovery flask was cooled to 0 °C, and a hexane solution of butyllithium (2.60 M, 4.6 mL, 12 mmol, 1.1 equiv) was added dropwise over 5 min. The cooling bath was then removed, and the resulting yellow solution was stirred at rt for 1 h. After cooling the reaction to 0 °C and stirring at that temperature for 30 min, **289** (2.76 g, 11.8 mmol, 1.1 equiv) was added dropwise. The cooling bath was subsequently removed, and the resulting colorless solution was stirred at rt for 3 h. The reaction was then quenched at rt with sat. aq. NH₄Cl, diluted with H₂O, and extracted thrice with EtOAc. The organic extracts were combined, washed with brine, dried over Na₂SO₄, filtered, and concentrated *in vacuo* to a yellow oil. Flash column chromatography (500 mL SiO₂, 95:5 hexane:EtOAc) afforded 4.034 g (8.72 mmol, 81% yield) of **290** as a colorless oil.

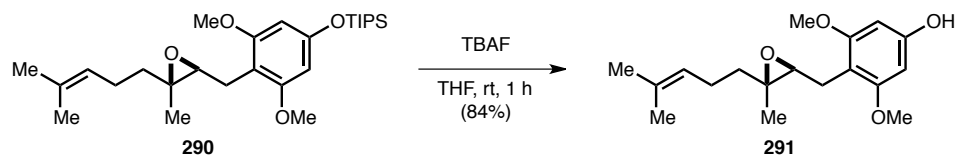
¹H NMR (600 MHz; CDCl₃) δ: 6.10 (s, 2H), 5.29 (s, 1H), 5.00 (t, *J* = 7.1 Hz, 1H), 3.75 (s, 6H), 2.98 (dd, *J* = 13.6, 4.4 Hz, 1H), 2.88 (dd, *J* = 7.6, 4.4 Hz, 1H), 2.68 (dd, *J* = 13.6, 7.6 Hz, 1H), 1.61 (m, 1H), 1.59 (s, 3H), 1.54 (s, 3H), 1.37 (s, 3H), 1.34 (td, *J* = 6.8, 3.2 Hz, 1H), 1.26 (septet, *J* = 7.4 Hz, 3H), 1.12 (d, *J* = 7.4 Hz, 18H).

¹³C NMR (125 MHz; CDCl₃) δ: 159.1, 156.2, 131.7, 124.0, 107.2, 96.4, 63.5, 61.7, 55.7, 39.2, 25.8, 24.1, 22.5, 18.2, 17.7, 16.9, 12.9.

FTIR (thin film) ν_{max}: 2961, 2945, 2868, 1606, 1593, 1496, 1463, 1414, 1200, 1158, 1134, 1021, 883, 686 cm⁻¹.

HRMS–ESI (*m/z*): [M+Na]⁺ calculated for C₂₇H₄₆O₄Si, 485.3058; found, 485.3064.

TLC R_f = 0.55 (8:2 hexane:EtOAc).



3,5-Dimethoxy-4-(((2*S*,3*S*)-3-methyl-3-(4-methylpent-3-en-1-yl)oxiran-2-yl)methyl)phenol (291):

A THF (30 mL) solution of **290** (3.97 g, 8.58 mmol, 1 equiv) in a 100-mL recovery flask was treated with a THF solution of tetrabutylammonium fluoride (1.0 M, 9.0 mL, 9.0 mmol, 1.05 equiv). After stirring at rt for 1 h, the reaction was quenched at rt with sat. aq. NH₄Cl, extracted once with hexane, and extracted twice with EtOAc. The organic extracts were combined, washed with brine, dried over Na₂SO₄, filtered, and concentrated *in vacuo* to a pale yellow oil. Flash column chromatography (400 mL SiO₂, 7:3 → 1:1 hexane:EtOAc) afforded 2.200 g (7.18 mmol, 84% yield) of **291** as a colorless oil.

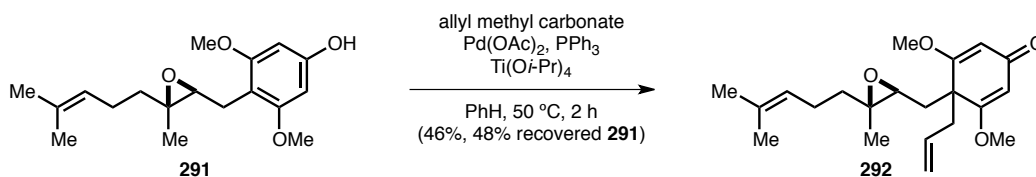
¹H NMR (500 MHz; CDCl₃) δ: 6.06 (s, 2H), 5.11 (s, 1H), 4.99 (t, *J* = 7.1 Hz, 1H), 3.76 (s, 6H), 2.97 (dd, *J* = 13.5, 4.6 Hz, 1H), 2.91 (dd, *J* = 7.3, 4.6 Hz, 1H), 2.69 (dd, *J* = 13.5, 7.3 Hz, 1H), 2.07-1.95 (m, 2H), 1.63 (m, *J* = 5.2 Hz, 1H), 1.59 (s, 3H), 1.54 (s, 3H), 1.38 (s, 3H), 1.37-1.33 (m, 1H).

¹³C NMR (125 MHz; CDCl₃) δ: 159.3, 156.4, 131.9, 123.8, 106.0, 92.1, 64.1, 62.6, 55.7, 39.1, 25.8, 24.1, 22.3, 17.7, 16.9.

FTIR (thin film) ν_{max}: 3368 (br), 2936, 2840, 1618, 1603, 1475, 1431, 1206, 1134, 999 cm⁻¹.

HRMS–ESI (*m/z*): [M+H]⁺ calculated for C₁₈H₂₆O₄, 307.1904; found, 307.1909.

TLC R_f = 0.50 (1:1 hexane:EtOAc).



4-Allyl-3,5-dimethoxy-4-(((2S,3S)-3-methyl-3-(4-methylpent-3-en-1-yl)oxiran-2-yl)methyl)cyclohexa-2,5-dienone (292):

A PhH (36 mL) solution of **291** (2.189 g, 7.14 mmol, 1 equiv), triphenylphosphine (150. mg, 0.572 mmol, 0.08 equiv), and palladium(II) acetate (32 mg, 0.14 mmol, 0.02 equiv) in a 100-mL recovery flask was treated sequentially with allyl methyl carbonate (2.0 mL, 18 mmol, 2.5 equiv) and titanium(IV) isopropoxide (423 μ L, 1.43 mmol, 0.2 equiv). The resulting dark red solution was heated to 50 $^\circ$ C and stirred at that temperature for 2 h. The resulting orange-red solution was subsequently cooled to rt and quenched with sat. aq. NH_4Cl . After stirring at rt for 5 min, 1 N HCl was added, and the mixture was extracted thrice with EtOAc. The organic extracts were combined, washed with brine, dried over Na_2SO_4 , filtered, and concentrated *in vacuo* to a orange slurry. Flash column chromatography (250 mL SiO_2 , 7:3 \rightarrow 6:4 \rightarrow 1:1 hexane:EtOAc) afforded 1.148 g (3.31 mmol, 46% yield) of **292** as a pale yellow oil and 1.060 g (3.46 mmol, 48% recovery) of **291** as a pale yellow oil.

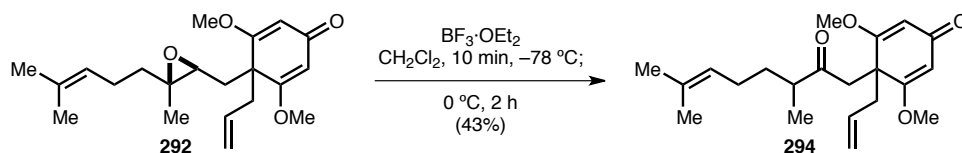
^1H NMR (600 MHz; CDCl_3) δ : 5.59 (s, 1H), 5.58 (s, 1H), 5.39 (ddt, J = 17.1, 10.0, 7.2 Hz, 1H), 5.00-4.92 (m, 3H), 3.73 (s, 3H), 3.70 (s, 3H), 2.61-2.54 (m, 2H), 2.40 (t, J = 5.9 Hz, 1H), 2.14 (dd, J = 13.9, 5.9 Hz, 1H), 2.04 (dd, J = 13.9, 5.9 Hz, 1H), 1.98-1.88 (m, 2H), 1.64 (s, 3H), 1.56 (s, 3H), 1.50 (ddd, J = 13.7, 9.7, 6.3 Hz, 1H), 1.27 (ddd, J = 13.7, 10.0, 6.5 Hz, 1H), 1.17 (s, 3H).

^{13}C NMR (125 MHz; CDCl_3) δ : 188.0, 173.1, 172.6, 132.2, 131.9, 123.6, 118.4, 103.55, 103.45, 60.7, 59.3, 56.2, 56.0, 49.7, 41.7, 38.9, 35.7, 25.8, 23.9, 17.8, 16.7.

FTIR (thin film) ν_{max} : 2928 (br), 1654, 1627, 1592, 1384, 1233, 1206, 1144 cm^{-1} .

HRMS-ESI (m/z): $[\text{M}+\text{Na}]^+$ calculated for $\text{C}_{21}\text{H}_{30}\text{O}_4$, 369.2036; found, 369.2043.

TLC R_f = 0.20 (1:1 hexane:EtOAc).



4-Allyl-4-(3,7-dimethyl-2-oxooct-6-en-1-yl)-3,5-dimethoxycyclohexa-2,5-dienone (294):

A CH₂Cl₂ (1 mL) solution of **292** (3.3 mg, 9.5 μmol, 1 equiv) in a 10-mL pear-shaped flask was cooled to −78 °C, and 1 drop of boron trifluoride ethyl etherate was added. After stirring the reaction for 10 min at −78 °C, it was placed in a 0 °C bath. After stirring the reaction at 0 °C for 2 h, it was quenched at 0 °C with brine, diluted with sat. aq. NH₄Cl, and extracted five times with EtOAc. The organic extracts were combined, dried over Na₂SO₄, filtered, and concentrated *in vacuo* to a yellow residue. Flash column chromatography (4 mL SiO₂, 2:8 hexane:EtOAc) afforded 1.4 mg (4.0 μmol, 43% yield) of **294** as a colorless residue.

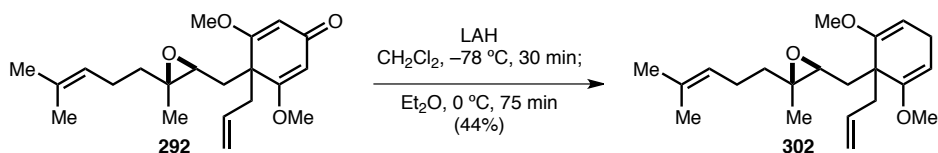
¹H NMR (500 MHz; CDCl₃) δ: 5.55 (s, 2H), 5.48-5.40 (m, 1H), 5.04 (t, *J* = 6.4 Hz, 1H), 4.96 (dd, *J* = 10.3, 1.3 Hz, 1H), 4.94 (dd, *J* = 17.2, 1.3 Hz, 1H), 3.67 (s, 6H), 3.07 (d, *J* = 16.8 Hz, 1H), 3.03 (d, *J* = 16.8 Hz, 1H), 2.45 (d, *J* = 7.5 Hz, 2H), 2.41 (q, *J* = 6.9 Hz, 1H), 1.89 (q, *J* = 7.5 Hz, 2H), 1.68 (s, 3H), 1.66-1.60 (m, 1H), 1.58 (s, 3H), 1.30-1.24 (m, 1H), 1.00 (d, *J* = 6.9 Hz, 3H).

¹³C NMR (125 MHz; CDCl₃) δ: 210.5, 188.4, 172.71, 172.62, 132.5, 131.5, 123.9, 118.8, 102.90, 102.86, 56.08, 56.06, 48.3, 46.3, 45.9, 43.2, 32.9, 25.93, 25.76, 17.9, 16.2.

FTIR (thin film) ν_{max}: 2965, 2922, 2853, 1715, 1654, 1622, 1446, 1388, 1234, 1205, 1147, 851 cm^{−1}.

HRMS–ESI (*m/z*): [M+Na]⁺ calculated for C₂₁H₃₀O₄, 369.2036; found, 369.2036.

TLC R_f = 0.44 (EtOAc).



(2*S*,3*S*)-3-((1-Allyl-2,6-dimethoxycyclohexa-2,5-dien-1-yl)methyl)-2-methyl-2-(4-methylpent-3-en-1-yl)oxirane (302):

A CH₂Cl₂ (0.5 mL) solution of **292** (106 mg, 0.31 mmol, 1 equiv) was transferred via cannula to a CH₂Cl₂ (0.5 mL) slurry of lithium aluminum hydride (23 mg, 0.61 mmol, 2 equiv) in a 10-mL pear-shaped flask cooled to $-78\text{ }^{\circ}\text{C}$, followed by a CH₂Cl₂ (0.5 mL) rinse. After stirring for 30 min at $-78\text{ }^{\circ}\text{C}$, Et₂O (0.5 mL) was added, and the reaction was placed in a $0\text{ }^{\circ}\text{C}$ bath. After stirring at $0\text{ }^{\circ}\text{C}$ for 75 min, the reaction was quenched sequentially at $0\text{ }^{\circ}\text{C}$ with H₂O (23 μL), 15% (w/v) NaOH (23 μL), and H₂O (69 μL). The mixture was warmed to rt, diluted with H₂O, and extracted four times with EtOAc. The organic extracts were combined, washed with H₂O and brine, dried over Na₂SO₄, filtered, and concentrated *in vacuo* to a brown residue. Flash column chromatography (30 mL SiO₂, 95:5 hexane:EtOAc) afforded 45 mg (0.14 mmol, 44% yield) of **302** as a colorless residue.

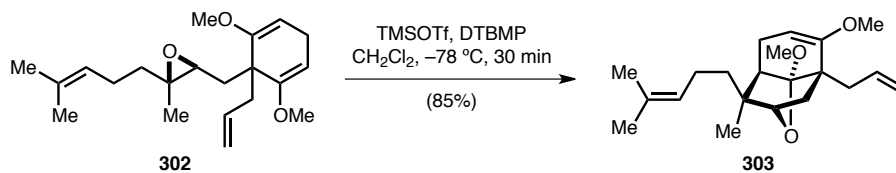
¹H NMR (600 MHz; CDCl₃) δ : 5.57 (ddt, $J = 17.1, 10.1, 7.1\text{ Hz}$, 1H), 5.05 (t, $J = 7.1\text{ Hz}$, 1H), 4.94-4.88 (m, 2H), 4.80 (t, $J = 3.5\text{ Hz}$, 1H), 4.76 (t, $J = 3.5\text{ Hz}$, 1H), 3.54 (s, 3H), 3.49 (s, 3H), 2.78 (q, $J = 3.5\text{ Hz}$, 2H), 2.64 (dd, $J = 8.0, 4.0\text{ Hz}$, 1H), 2.39 (qd, $J = 12.7, 7.2\text{ Hz}$, 2H), 2.03 (dd, $J = 13.7, 4.0\text{ Hz}$, 1H), 1.97 (q, $J = 7.9\text{ Hz}$, 2H), 1.76 (dd, $J = 13.7, 8.0\text{ Hz}$, 1H), 1.67 (s, 3H), 1.58 (s, 3H), 1.57-1.54 (m, 1H), 1.29 (dt, $J = 13.5, 8.4\text{ Hz}$, 1H), 1.18 (s, 3H).

¹³C NMR (125 MHz; CDCl₃) δ : 153.80, 153.73, 135.3, 131.8, 124.2, 116.1, 93.23, 93.17, 61.25, 61.09, 54.6, 54.2, 46.2, 40.2, 39.4, 34.2, 25.8, 24.2, 24.0, 17.8, 16.8.

FTIR (thin film) ν_{max} : 2932, 2831, 1694, 1659, 1451, 1381, 1223, 1206, 1139, 908 cm^{-1} .

HRMS-ESI (m/z): $[\text{M}+\text{H}]^{+}$ calculated for C₂₁H₃₂O₃, 333.2424; found, 333.2425.

TLC $R_f = 0.78$ (1:1 hexane:EtOAc).

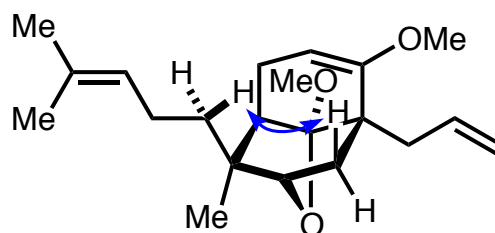


(2*S*,3*S*,3*aR*,7*R*,7*aS*)-7-Allyl-6,7*a*-dimethoxy-3-methyl-3-(4-methylpent-3-en-1-yl)-2,3,3*a*,4,7,7*a*-hexahydro-2,7-methanobenzofuran (303):

A CH₂Cl₂ (6 mL) solution of **302** (100. mg, 0.301 mmol, 1 equiv) and 2,6-di-*tert*-butyl-4-methylpyridine (124 mg, 0.602 mmol, 2 equiv) in a 20-mL scintillation vial was cooled to -78°C , and trimethylsilyl trifluoromethanesulfonate (65 μL , 0.36 mmol, 1.2 equiv) was added dropwise. After stirring the bright yellow solution at -78°C for 30 min, it was quenched at -78°C with sat. aq. NaHCO₃ and extracted four times with EtOAc. The organic extracts were combined, washed with brine, dried over Na₂SO₄, filtered, and concentrated *in vacuo* to a pale yellow oil. Flash column chromatography (50 mL SiO₂, 99:1 hexane:EtOAc) afforded 85 mg (0.26 mmol, 85% yield) of **303** as a colorless oil.

¹H NMR (600 MHz; CDCl₃) δ : 6.02 (ddt, $J = 17.2, 10.1, 7.1$ Hz, 1H), 5.04 (t, $J = 7.1$ Hz, 1H), 5.01-4.95 (m, 2H), 4.54 (dd, $J = 5.7, 2.1$ Hz, 1H), 3.75 (d, $J = 5.3$ Hz, 1H), 3.48 (s, 3H), 3.47 (s, 3H), 2.42 (dd, $J = 14.1, 7.1$ Hz, 1H), 2.29 (dd, $J = 14.1, 7.1$ Hz, 1H), 2.19 (ddd, $J = 18.1, 6.7, 2.2$ Hz, 1H), 2.07-2.02 (m, 2H), 2.01-1.93 (m, 1H), 1.86 (dd, $J = 12.5, 5.3$ Hz, 1H), 1.81 (d, $J = 12.5$ Hz, 1H), 1.72-1.65 (m, 4H), 1.58 (s, 3H), 1.47-1.42 (m, 1H), 1.25-1.20 (m, 1H), 1.14 (s, 3H).

¹³C NMR (125 MHz; CDCl₃) δ : 158.1, 138.3, 131.7, 124.9, 115.8, 112.5, 90.8, 79.1, 54.6, 51.3, 46.3, 44.4, 42.0, 38.88, 38.73, 33.6, 28.1, 25.9, 22.9, 20.1, 17.8.

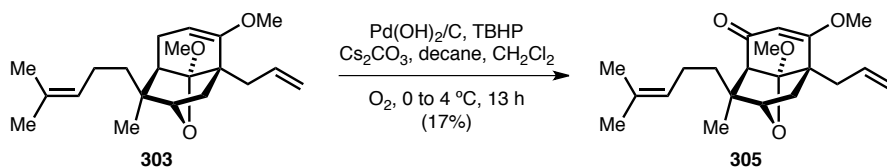


Key 1D nOe correlation.

FTIR (thin film) ν_{max} : 2966, 2930, 1671, 1578, 1460, 1439, 1376, 1304, 1215, 1168, 1136, 1062, 1001, 906 cm⁻¹.

HRMS–ESI (m / z): $[M+Na]^+$ calculated for $C_{21}H_{32}O_3$, 355.2244; found, 355.2245.

TLC R_f = 0.53 (9:1 hexane:EtOAc).



(2*S*,3*S*,3*aS*,7*R*,7*aS*)-7-Allyl-6,7*a*-dimethoxy-3-methyl-3-(4-methylpent-3-en-1-yl)-3,3*a*,7,7*a*-tetrahydro-2,7-methanobenzofuran-4(2*H*)-one (305):

A CH_2Cl_2 (1.7 mL) slurry of **303** (55 mg, 0.17 mmol, 1 equiv) and cesium carbonate (292 mg, 0.83 mmol, 5 equiv) in a 10-mL pear-shaped flask was cooled to 0 °C open to air, and Pearlman's catalyst (4.4 mg, 0.0082 mmol based on Pd, 0.05 equiv) and a decane solution of *tert*-butyl hydroperoxide (5.5 M, 150 μL , 0.83 mmol, 5 equiv) were added in sequence. The flask was sealed, purged with O_2 via O_2 balloon, and stirred at 4 °C for 13 h. The slurry was subsequently diluted with CH_2Cl_2 and filtered through a short plug of SiO_2 , rinsing with CH_2Cl_2 followed by EtOAc. The filtrate was concentrated *in vacuo* to a colorless oil. Flash column chromatography (20 mL SiO_2 , 8:2 hexane:EtOAc) afforded 10.4 mg (0.030 mmol, 17% yield) of **305** as a colorless residue.

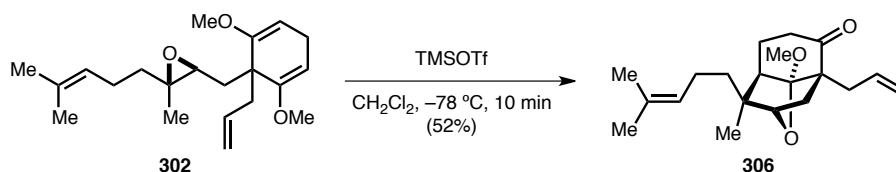
^1H NMR (600 MHz; CDCl_3) δ : 5.98 (m, 1H), 5.35 (s, 1H), 5.06-5.01 (m, 2H), 4.99 (t, J = 7.1 Hz, 1H), 3.91 (d, J = 5.5 Hz, 1H), 3.71 (s, 3H), 3.48 (s, 3H), 2.69 (s, 1H), 2.53 (dd, J = 14.2, 6.7 Hz, 1H), 2.39 (dd, J = 14.2, 7.9 Hz, 1H), 2.06 (d, J = 13.1 Hz, 1H), 2.04-1.98 (m, 2H), 1.73-1.67 (m, 1H), 1.64 (s, 3H), 1.55 (s, 3H), 1.43-1.36 (m, 1H), 1.34-1.28 (m, 1H), 1.25 (s, 3H).

^{13}C NMR (125 MHz; CDCl_3) δ : 197.8, 180.7, 136.8, 132.1, 124.2, 117.3, 115.2, 100.9, 81.0, 56.9, 56.5, 52.1, 48.3, 48.1, 38.3, 38.0, 34.1, 27.9, 25.9, 22.8, 17.8.

FTIR (thin film) ν_{max} : 2964, 2923, 2850, 1652, 1604, 1459, 1373, 1228, 1046, 1001 cm^{-1} .

HRMS-ESI (m/z): $[\text{M}+\text{Na}]^+$ calculated for $\text{C}_{21}\text{H}_{30}\text{O}_4$, 369.2036; found, 369.2034.

TLC R_f = 0.46 (6:4 hexane:EtOAc).

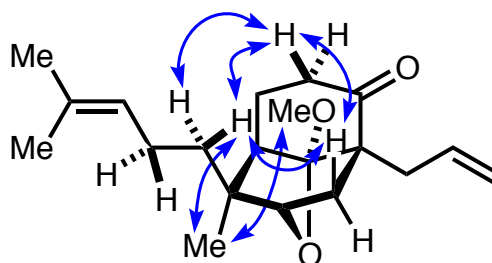


(2*S*,3*aR*,7*R*,7*aS*,8*S*)-3*a*-Allyl-7*a*-methoxy-8-methyl-8-(4-methylpent-3-en-1-yl)hexahydro-2,7-methanobenzofuran-4(2*H*)-one (306):

A CH₂Cl₂ (1 mL) solution of **302** (2.6 mg, 7.8 μmol, 1 equiv) in a 10-mL pear-shaped flask was cooled to −78 °C, and trimethylsilyl trifluoromethanesulfonate (2 μL, 10 μmol, 1.5 equiv) was added. After stirring the resulting yellow solution at −78 °C for 10 min, it was quenched at −78 °C with sat. aq. NaHCO₃, diluted with H₂O, and extracted thrice with EtOAc. The organic extracts were combined, washed with brine, dried over Na₂SO₄, filtered, and concentrated *in vacuo* to a white residue. Flash column chromatography (4 mL SiO₂, 9:1 hexane:EtOAc) afforded 1.3 mg (4.1 μmol, 52% yield) of **306** as a white residue.

¹H NMR (600 MHz; CDCl₃) δ: 5.87 (dddd, *J* = 17.1, 10.2, 8.9, 5.7 Hz, 1H), 5.07 (t, *J* = 7.2 Hz, 1H), 5.05-4.99 (m, 2H), 3.92 (d, *J* = 5.6 Hz, 1H), 3.46 (s, 3H), 2.58 (dd, *J* = 14.0, 5.7 Hz, 1H), 2.52 (ddd, *J* = 15.1, 10.9, 7.6 Hz, 1H), 2.38 (ddd, *J* = 15.1, 7.4, 4.1 Hz, 1H), 2.16-2.10 (m, 2H), 2.10-2.04 (m, 1H), 2.01 (dd, *J* = 13.7, 5.6 Hz, 1H), 1.95 (d, *J* = 13.7 Hz, 1H), 1.92-1.87 (m, 1H), 1.86-1.76 (m, 2H), 1.68 (s, 3H), 1.59 (s, 3H), 1.49 (m, 1H), 1.42 (ddd, *J* = 13.7, 11.9, 4.9 Hz, 1H), 1.20 (s, 3H).

¹³C NMR (125 MHz; CDCl₃) δ: 212.9, 136.4, 132.3, 124.3, 117.7, 116.4, 79.1, 58.4, 52.2, 45.9, 41.6, 36.3, 36.0, 35.1, 33.8, 28.1, 25.9, 23.3, 19.0, 17.9.

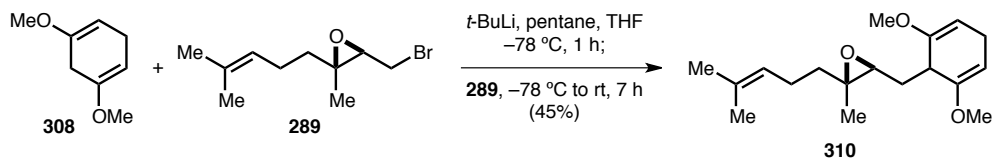


Key 1D nOe correlations.

FTIR (thin film) ν_{max} : 2972, 2924, 1702, 1467, 1439, 1328, 1312, 1219, 1180, 1148, 995, 908 cm^{−1}.

HRMS–ESI (m / z): $[M+H]^+$ calculated for $C_{20}H_{30}O_3$, 319.2268; found, 319.2263.

TLC R_f = 0.47 (8:2 hexane:EtOAc).



(2*S*,3*S*)-3-((2,6-Dimethoxycyclohexa-2,5-dien-1-yl)methyl)-2-methyl-2-(4-methylpent-3-en-1-yl)oxirane (310):

A THF (6 mL) solution of **308** (250. mg, 1.78 mmol, 1 equiv) in a 25-mL recovery flask was cooled to –78 °C, and a pentane solution of *tert*-butyllithium (1.70 M, 2.2 mL, 3.8 mmol, 2.1 equiv) was added dropwise. After stirring the dark yellow solution at –78 °C for 1 h, **289** (873 mg, 3.75 mmol, 2.1 equiv) was added dropwise. The resulting colorless solution was allowed to slowly warm to rt. After stirring for 7 h, the resulting yellow solution was quenched at rt with H₂O and extracted thrice with EtOAc. The organic extracts were combined, washed with brine, dried over Na₂SO₄, filtered, and concentrated *in vacuo* to a yellow oil. Flash column chromatography (150 mL SiO₂, 99:1 → 98:2 → 95:5 → 9:1 → 8:2 hexane:EtOAc) afforded 234 mg (0.80 mmol, 45% yield) of **310** as a colorless oil.

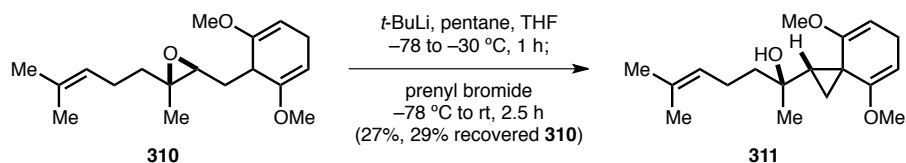
¹H NMR (600 MHz; CDCl₃) δ: 5.07 (t, *J* = 7.4 Hz, 1H), 4.73 (t, *J* = 3.6 Hz, 1H), 4.71 (t, *J* = 3.6 Hz, 1H), 3.56 (s, 3H), 3.54 (s, 3H), 3.01 (quintet, *J* = 5.3 Hz, 1H), 2.87-2.76 (m, 2H), 2.72 (dd, *J* = 8.1, 4.4 Hz, 1H), 2.12 (dt, *J* = 14.0, 4.9 Hz, 1H), 2.01 (q, *J* = 7.4 Hz, 2H), 1.81 (ddd, *J* = 14.0, 8.1, 4.6 Hz, 1H), 1.67 (s, 3H), 1.59 (s, 3H), 1.58-1.53 (m, 1H), 1.39-1.33 (m, 1H), 1.19 (s, 3H).

¹³C NMR (125 MHz; CDCl₃) δ: 154.2, 131.9, 124.2, 91.77, 91.73, 77.2, 61.3, 61.1, 54.6, 54.3, 39.22, 39.14, 29.3, 25.9, 24.7, 23.9, 17.8, 16.7.

FTIR (thin film) ν_{max} : 2963, 2931, 2856, 1693, 1596, 1474, 1383, 1258, 1204, 1146, 1120, 774 cm^{–1}.

HRMS–ESI (*m/z*): [M+Na]⁺ calculated for C₁₈H₂₈O₃, 315.1931; found, 315.1927.

TLC R_f = 0.53 (8:2 hexane:EtOAc).



(S)-2-((S)-4,8-Dimethoxyspiro[2.5]octa-4,7-dien-1-yl)-6-methylhept-5-en-2-ol (311):

A THF (0.8 mL) solution of **310** (50. mg, 0.17 mmol, 1 equiv) in a 10-mL pear-shaped flask was cooled to -78°C , and a pentane solution of *tert*-butyllithium (1.70 M, 111 μL , 0.19 mmol, 1.1 equiv) was added dropwise. The reaction was allowed to slowly warm to -30°C over 1 h. The reaction was subsequently cooled to -78°C , and prenyl bromide (40. μL , 0.34 mmol, 2 equiv) was added. After warming the reaction to rt over 2.5 h, it was quenched at rt with H_2O and extracted thrice with EtOAc. The organic extracts were combined, washed with brine, dried over Na_2SO_4 , filtered, and concentrated *in vacuo* to a pale yellow oil. Flash column chromatography (30 mL SiO_2 , 98:2 \rightarrow 95:5 hexane:EtOAc) afforded 13.6 mg (47 μmol , 27% yield) of **311** as a colorless oil as well as 14.4 mg (49 μmol , 29% recovery) of **310** as a colorless oil.

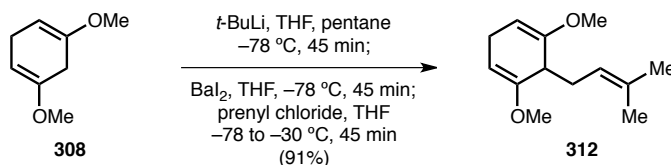
^1H NMR (600 MHz; CDCl_3) δ : 5.14 (t, $J = 7.1$ Hz, 1H), 4.96 (t, $J = 3.8$ Hz, 1H), 4.64 (t, $J = 3.6$ Hz, 1H), 3.98 (s, 1H), 3.58 (s, 3H), 3.47 (s, 3H), 3.00 (dt, $J = 21.2, 2.9$ Hz, 1H), 2.93 (dt, $J = 21.2, 4.6$ Hz, 1H), 2.21-2.11 (m, 2H), 1.68 (s, 3H), 1.62 (s, 3H), 1.55 (t, $J = 8.5$ Hz, 2H), 1.49-1.45 (m, 2H), 1.39-1.35 (m, 1H), 1.17 (s, 3H).

^{13}C NMR (125 MHz; CDCl_3) δ : 154.0, 152.1, 131.3, 125.3, 95.9, 90.2, 69.7, 54.84, 54.69, 45.1, 35.7, 28.4, 25.93, 25.90, 24.0, 22.7, 17.9, 11.4.

FTIR (thin film) ν_{max} : 3506, 2964, 2928, 2833, 1683, 1651, 1595, 1464, 1446, 1394, 1375, 1228, 1206, 1135, 1105, 1042, 979, 770 cm^{-1} .

HRMS-ESI (m/z): $[\text{M}+\text{Na}]^+$ calculated for $\text{C}_{18}\text{H}_{28}\text{O}_3$, 315.1931; found, 315.1920.

FTIR (thin film) ν_{max} : 0.43 (8:2 hexane:EtOAc).



1,5-Dimethoxy-6-(3-methylbut-2-en-1-yl)cyclohexa-1,4-diene (312):

Preparation of barium iodide. Using a hand drill hammer, a chisel,⁶⁸⁷ and a lead brick positioned on the laboratory floor, mineral oil-coated barium rod was portioned into approximately 25 mm segments. Each segment was flattened using the hammer to yield a barium pancake no thicker than 3 mm. A well-sharpened pair of metal cutting snips was used to cut each pancake into 1 mm × 2 mm × 10 mm slivers, which were washed with hexane. A 2-neck 2-L round-bottom flask outfitted with a reflux condenser was charged with barium slivers (63.7 g, 464 mmol, 1.3 equiv) and THF (500 mL). The flask was placed in a rt H₂O bath, and iodine (99.6 g, 392 mmol, 1.1 equiv) was added in four portions over 20 min with vigorous stirring. After subsequently stirring vigorously for 4 d at reflux, a white-gray slurry of barium iodide was produced.

A THF (800 mL) solution of **308** (50.0 g, 357 mmol, 1 equiv) in a 2-neck 3-L round-bottom flask outfitted with an equal pressure dropping funnel was cooled using a −78 °C dry ice/acetone bath. The dropping funnel was charged with a pentane solution of *tert*-butyllithium (1.56 M, 250. mL, 392 mmol, 1.1 equiv), and this solution was added in portions over 1 h, maintaining an internal reaction temperature ≤ −65 °C. The resulting yellow slurry was stirred for an additional 45 min at −78 °C. The THF slurry of barium iodide (preparation described above) was poured into this solution under a heavy stream of Ar, and the resulting yellow-green slurry was stirred at −78 °C for 45 min.⁶⁸⁸ A THF (50 mL) solution of prenyl chloride (44.2 mL, 392 mmol, 1.1 equiv) was added via cannula over 10 min, maintaining an internal reaction temperature ≤ −60 °C, and the yellow-green slurry was allowed to slowly warm to −30 °C over 45 min. The resulting green-gray slurry was then quenched at −30 °C with H₂O. After warming

⁶⁸⁷ If a hand drill hammer and chisel are unavailable, a standard claw hammer and an appropriately-shaped shelving bracket may be employed in this step.

⁶⁸⁸ Directly following the barium iodide addition, the internal reaction temperature rose to −30 °C but returned to −70 °C within 10 min.

to room temperature, the mixture was diluted with hexane and extracted thrice with 9:1 hexane:EtOAc. The organic extracts were combined, sequentially washed twice with H₂O and once with brine, dried over Na₂SO₄, filtered, and concentrated *in vacuo* to a pale yellow oil. Short-path distillation (6 mmHg, 76-82 °C) afforded 67.46 g (323.9 mmol, 91% yield) of **312** as a colorless oil.

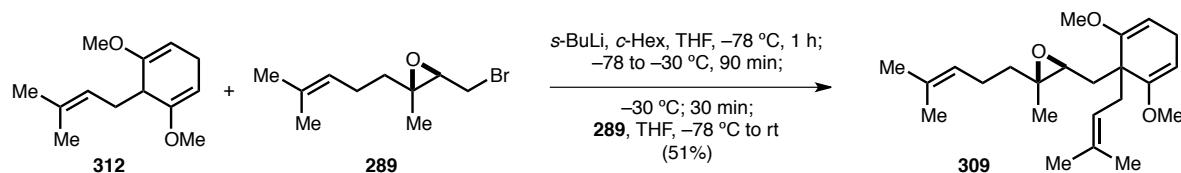
¹H NMR (600 MHz; CDCl₃) δ: 4.99 (t, *J* = 7.4 Hz, 1H), 4.68 (dd, *J* = 4.6, 3.0 Hz, 2H), 3.53 (s, 6H), 2.94–2.91 (m, 1H), 2.78 (ddt, *J* = 20.7, 6.0, 3.0 Hz, 1H), 2.72 (dq, *J* = 20.7, 4.6 Hz, 1H), 2.41 (dd, *J* = 7.4, 4.7 Hz, 2H), 1.64 (s, 3H), 1.55 (s, 3H).

¹³C NMR (125 MHz; CDCl₃) δ: 154.5, 132.8, 120.6, 91.9, 54.4, 41.3, 28.5, 26.1, 24.7, 17.8.

FTIR (thin film) ν_{max} : 2995, 2933, 2910, 2825, 1695, 1663, 1446, 1394, 1230, 1206, 1148, 1048, 965, 775 cm⁻¹.

HRMS–ESI (*m/z*): [M+Na]⁺ calculated for C₁₃H₂₀O₂, 231.1356; found, 231.1350.

TLC *R_f* = 0.77 (9:1 hexane:EtOAc).



(2*S*,3*S*)-3-((2,6-Dimethoxy-1-(3-methylbut-2-en-1-yl)cyclohexa-2,5-dien-1-yl)methyl)-2-methyl-2-(4-methylpent-3-en-1-yl)oxirane (309):

A THF (140 mL) solution of **312** (5.68 g, 27.3 mmol, 1 equiv) in a 500-mL recovery flask was cooled to $-78\text{ }^{\circ}\text{C}$, and a *c*-Hex solution of *sec*-butyllithium (1.43 M, 28.6 mL, 40.9 mmol, 1.5 equiv) was added portionwise over 10 min. After stirring the bright orange solution at $-78\text{ }^{\circ}\text{C}$ for 1 h, it was warmed to $-30\text{ }^{\circ}\text{C}$ over 90 min and maintained at $-30\text{ }^{\circ}\text{C}$ for an additional 30 min. The dark red solution was then cooled to $-78\text{ }^{\circ}\text{C}$, and a THF (25 mL) solution of **289** (9.54 g, 40.9 mmol, 1.5 equiv) was added over 2 min. The resulting bright yellow solution was allowed to slowly warm to rt. After stirring for 3 h, the reaction was quenched at rt with H_2O and extracted thrice with EtOAc. The organic extracts were combined, washed with H_2O and brine, dried over Na_2SO_4 , filtered, and concentrated *in vacuo* to a yellow oil. Flash column chromatography (300 mL SiO_2 , 98:2 \rightarrow 95:5 hexane:EtOAc) afforded 4.97 (13.8 mmol, 51% yield) of **309** as a pale yellow oil.

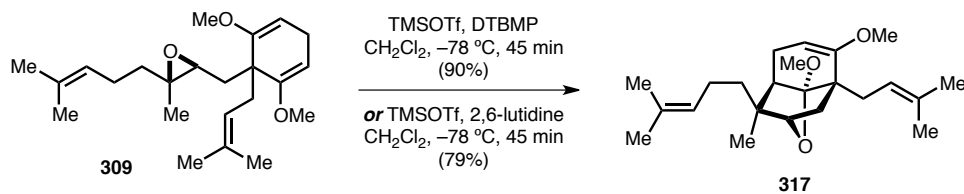
^1H NMR (600 MHz; CDCl_3) δ : 5.05 (t, $J = 6.7\text{ Hz}$, 1H), 4.90 (t, $J = 7.1\text{ Hz}$, 1H), 4.76 (t, $J = 3.5\text{ Hz}$, 1H), 4.72 (t, $J = 3.5\text{ Hz}$, 1H), 3.51 (s, 3H), 3.47 (s, 3H), 2.75 (m, 2H), 2.63 (dd, $J = 8.1, 3.9\text{ Hz}$, 1H), 2.35-2.28 (m, 2H), 2.04 (dd, $J = 13.7, 3.9\text{ Hz}$, 1H), 1.97 (q, $J = 7.9\text{ Hz}$, 2H), 1.76 (dd, $J = 13.7, 8.1\text{ Hz}$, 1H), 1.66 (s, 3H), 1.62 (s, 3H), 1.58-1.56 (m, 4H), 1.54 (s, 3H), 1.27 (dt, $J = 13.6, 8.3\text{ Hz}$, 1H), 1.18 (s, 3H).

^{13}C NMR (125 MHz; CDCl_3) δ : 13-C NMR (126 MHz; CDCl_3): δ 154.11, 154.05, 132.5, 131.8, 124.2, 120.7, 93.02, 92.92, 61.4, 61.1, 54.5, 54.1, 46.2, 39.5, 34.6, 34.1, 26.1, 25.9, 24.3, 24.1, 17.85, 17.79, 16.8.

FTIR (thin film) ν_{max} : 2965, 2924, 2855, 2930, 1693, 1658, 1450, 1380, 1205, 1151, 1122, 1075, 973, 778, 688 cm^{-1} .

HRMS-ESI (m/z): $[\text{M}+\text{Na}]^+$ calculated for $\text{C}_{23}\text{H}_{36}\text{O}_3$, 383.2557; found, 383.2554.

TLC $R_f = 0.54$ (8:2 hexane:EtOAc).



(2*S*,3*S*,3*aR*,7*R*,7*aS*)-6,7*a*-Dimethoxy-3-methyl-7-(3-methylbut-2-en-1-yl)-3-(4-methylpent-3-en-1-yl)-2,3,3*a*,4,7,7*a*-hexahydro-2,7-methanobenzofuran (317):

Method A, using 2,6-di-tert-butyl-4-methylpyridine:

A CH₂Cl₂ (100 mL) solution of **309** (1.88 g, 5.21 mmol, 1 equiv) and 2,6-di-*tert*-butyl-4-methylpyridine (2.14 g, 10.4 mmol, 2 equiv) in a 250-mL round-bottom flask was cooled to –78 °C, and trimethylsilyl trifluoromethanesulfonate (1.13 mL, 6.26 mmol, 1.2 equiv) was added. After stirring the golden yellow solution at –78 °C for 45 min, it was quenched at –78 °C with sat. aq. NaHCO₃. After warming the mixture to rt, it was diluted with H₂O and brine, and extracted thrice with EtOAc. The organic extracts were combined, washed with brine, dried over Na₂SO₄, filtered, and concentrated *in vacuo* to a yellow oil. Flash column chromatography (400 mL SiO₂, 99:1 → 95:5 hexane:EtOAc) afforded 1.70 g (4.72 mmol, 90% yield) of **317** as a colorless oil.

Method B, using 2,6-lutidine:

A CH₂Cl₂ (50 mL) solution of **309** (3.62 g, 10.0 mmol, 1 equiv) and 2,6-lutidine (2.4 mL, 30. mmol, 3 equiv) in a 200-mL round-bottom flask was cooled to –78 °C, and trimethylsilyl trifluoromethanesulfonate (3.6 mL, 20. mmol, 2 equiv) was added. After stirring the golden yellow solution at –78 °C for 45 min, it was quenched at –78 °C with sat. aq. NaHCO₃, warmed to rt, and extracted thrice with EtOAc. The organic extracts were combined, washed sequentially with 2 N HCl, H₂O, and brine, dried over Na₂SO₄, filtered, and concentrated *in vacuo* to a pale orange oil. Flash column chromatography (250 mL SiO₂, 1:1 → 1:3 hexane:CH₂Cl₂) afforded 2.84 g (7.88 mmol, 79% yield) of **317** as a colorless oil.

¹H NMR (600 MHz; CDCl₃) δ: 5.34 (t, *J* = 7.1 Hz, 1H), 5.03 (t, *J* = 7.1 Hz, 1H), 4.52 (dd, *J* = 5.6, 2.2 Hz, 1H), 3.74 (d, *J* = 5.1 Hz, 1H), 3.48 (s, 3H), 3.46 (s, 3H), 2.36 (dd, *J* = 14.8, 6.8 Hz, 1H), 2.22-2.17

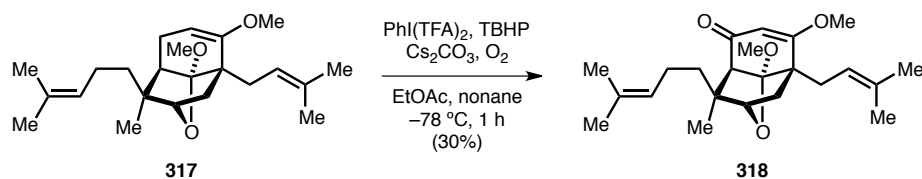
(m, 2H), 2.05-2.01 (m, 2H), 1.98-1.96 (m, 1H), 1.82 (d, $J = 12.4$ Hz, 1H), 1.78 (dd, $J = 12.4, 5.1$ Hz, 1H), 1.70 (s, 3H), 1.69-1.65 (m, 4H), 1.61 (s, 3H), 1.58 (s, 3H), 1.45 (td, $J = 13.1, 4.7$ Hz, 1H), 1.22 (td, $J = 13.1, 4.6$ Hz, 1H), 1.14 (s, 3H).

^{13}C NMR (125 MHz; CDCl_3) δ : 13-C NMR (126 MHz; CDCl_3): δ 158.5, 131.6, 131.1, 124.9, 123.6, 112.7, 90.6, 78.9, 54.6, 51.4, 46.5, 44.4, 42.0, 39.4, 33.6, 32.8, 28.2, 26.4, 25.9, 22.9, 20.1, 17.99, 17.85.

FTIR (thin film) ν_{max} : 2965, 2931, 1670, 1451, 1374, 1214, 1165, 1126, 1079, 1003, 945, 839, 804 cm^{-1} .

HRMS-ESI (m/z): $[\text{M}+\text{H}]^+$ calculated for $\text{C}_{23}\text{H}_{36}\text{O}_3$, 361.2737; found, 361.2730.

TLC $R_f = 0.50$ (9:1 hexane:EtOAc).



(2*S*,3*S*,3*aS*,7*R*,7*aS*)-6,7*a*-Dimethoxy-3-methyl-7-(3-methylbut-2-en-1-yl)-3-(4-methylpent-3-en-1-yl)-3,3*a*,7,7*a*-tetrahydro-2,7-methanobenzofuran-4(2*H*)-one (318):

An EtOAc (30 mL) slurry of **317** (3.30 g, 9.15 mmol, 1 equiv), cesium carbonate (12.9 g, 36.6 mmol, 4 equiv), and a nonane solution of *tert*-butyl hydroperoxide (5.5 M, 6.7 mL, 27 mmol, 4 equiv) in a 3-neck 200-mL round-bottom flask was sparged for 10 min with O₂ and subsequently cooled to −78 °C with vigorous O₂ bubbling. An EtOAc (25 mL) solution of [bis(trifluoroacetoxy)iodo]benzene (11.8 g, 27.5 mmol, 3 equiv) was added dropwise over 8 min, followed by an EtOAc (5 mL) rinse. After stirring the resulting yellow slurry at −78 °C for 1 h, it was quenched at −78 °C with sat. aq. Na₂S₂O₃ and warmed to rt with vigorous stirring over 45 min. The mixture was then extracted thrice with EtOAc. The organic extracts were combined, sequentially washed with H₂O and brine, dried over Na₂SO₄, filtered, and concentrated *in vacuo* to a yellow oil. Flash column chromatography (250 mL SiO₂, 98:2 CH₂Cl₂:Et₂O) afforded 1.01 g (2.69 mmol, 30% yield) of **318** as a pale yellow oil.

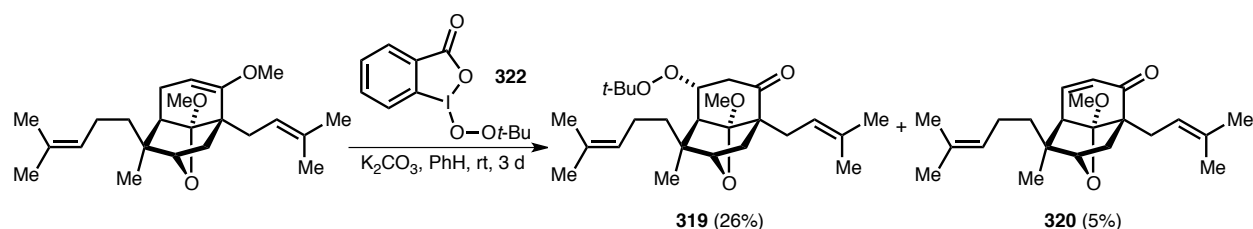
¹H NMR (600 MHz; CDCl₃) δ: 5.34 (s, 1H), 5.29 (t, *J* = 6.4 Hz, 1H), 4.98 (t, *J* = 7.1 Hz, 1H), 3.89 (d, *J* = 5.8 Hz, 1H), 3.70 (s, 3H), 3.47 (s, 3H), 2.68 (s, 1H), 2.42 (dd, *J* = 14.9, 6.3 Hz, 1H), 2.35 (dd, *J* = 14.9, 8.0 Hz, 1H), 2.06 (d, *J* = 13.0 Hz, 1H), 2.03-1.97 (m, 1H), 1.93 (dd, *J* = 13.0, 5.8 Hz, 1H), 1.74-1.67 (m, 1H), 1.70 (s, 3H), 1.64 (s, 3H), 1.62 (s, 3H), 1.55 (s, 3H), 1.38 (ddd, *J* = 14.0, 12.1, 4.8 Hz, 1H), 1.34-1.29 (m, 1H), 1.27 (s, 3H).

¹³C NMR (125 MHz; CDCl₃) δ: 197.9, 181.2, 132.9, 132.0, 124.2, 122.1, 115.4, 100.8, 80.8, 56.8, 56.4, 52.2, 48.6, 48.1, 38.8, 34.2, 32.2, 27.9, 26.3, 25.8, 22.8, 17.97, 17.84.

FTIR (thin film) ν_{max}: 2970, 2927, 1651, 1604, 1452, 1374, 1228, 1071, 1003 cm^{−1}.

HRMS–ESI (*m/z*): [M+H]⁺ calculated for C₂₃H₃₄O₄, 375.2530; found, 375.2528.

TLC R_f = 0.25 (7:3 hexane:EtOAc).

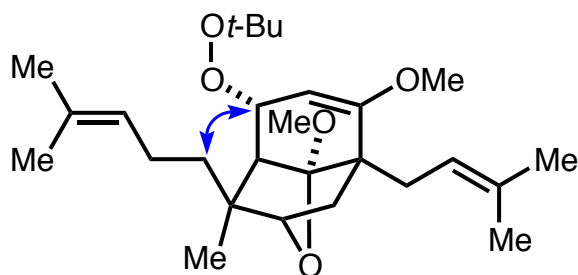


(2*S*,3*aR*,6*R*,7*S*,7*aS*,8*S*)-6-(*tert*-Butylperoxy)-7*a*-methoxy-8-methyl-3*a*-(3-methylbut-2-en-1-yl)-8-(4-methylpent-3-en-1-yl)hexahydro-2,7-methanobenzofuran-4(2*H*)-one (319):

A PhH (2 mL) solution of **317** (21.4 mg, 59 μmol , 1 equiv) in a 2-dram scintillation vial was treated with **322**⁶⁸⁹ (40. mg, 0.12 mmol, 2 equiv) and potassium carbonate (33 mg, 0.24 mmol, 4 equiv). After stirring the reaction at rt for 3 d, it was diluted with 1:1 hexane:EtOAc and filtered through a short plug of SiO₂, rinsing with 1:1 hexane:EtOAc. The filtrate was concentrated *in vacuo* to a white residue. Flash column chromatography (25 mL SiO₂, 992:8 CH₂Cl₂:Et₂O) afforded 7 mg (20 μmol , 26% yield) of **319** as a colorless oil and 1 mg (3 μmol , 5% yield) of **320** as a colorless residue.

¹H NMR (600 MHz; CDCl₃) δ : 5.39 (t, $J = 7.2$ Hz, 1H), 5.02 (t, $J = 6.9$ Hz, 1H), 4.73 (d, $J = 5.3$ Hz, 1H), 4.46 (dd, $J = 5.3, 1.1$ Hz, 1H), 3.75 (d, $J = 5.3$ Hz, 1H), 3.56 (s, 3H), 3.53 (s, 3H), 2.46 (s, 1H), 2.37 (dd, $J = 14.7, 6.9$ Hz, 1H), 2.28 (dd, $J = 14.7, 7.3$ Hz, 1H), 2.04-1.93 (m, 1H), 1.82 (dd, $J = 12.6, 5.3$ Hz, 1H), 1.77 (d, $J = 12.6$ Hz, 1H), 1.69 (s, 3H), 1.68 (m, 1H), 1.67 (s, 3H), 1.60 (s, 3H), 1.57 (s, 3H), 1.36 (td, $J = 12.8, 4.9$ Hz, 1H), 1.29-1.26 (m, 1H), 1.25 (s, 9H), 1.21 (s, 3H).

¹³C NMR (125 MHz; CDCl₃) δ : 164.9, 131.84, 131.68, 124.6, 123.4, 112.3, 89.0, 80.1, 79.1, 77.4, 55.0, 52.2, 47.0, 44.14, 43.95, 38.3, 34.0, 32.1, 27.9, 26.9, 26.4, 25.9, 23.0, 17.99, 17.89.



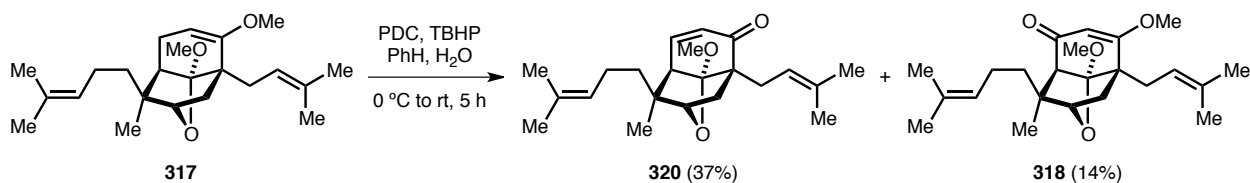
Key 1D nOe correlation.

⁶⁸⁹ **322** was prepared as described in ref. 636.

FTIR (thin film) ν_{max} : 2970, 2925, 2869, 1657, 1450, 1374, 1363, 1225, 1196, 1169, 1069, 1005, 990, 880 cm^{-1} .

HRMS–ESI (m / z): $[\text{M}+\text{H}]^+$ calculated for $\text{C}_{27}\text{H}_{44}\text{O}_5$, 449.3262; found, 449.3248.

TLC R_f = 0.25 (7:3 hexane:EtOAc).



(2*S*,3*aR*,7*R*,7*aS*,8*S*)-7*a*-Methoxy-8-methyl-3*a*-(3-methylbut-2-en-1-yl)-8-(4-methylpent-3-en-1-yl)-

3,3*a*,7,7*a*-tetrahydro-2,7-methanobenzofuran-4(2*H*)-one (320):

A PhH (1 mL) solution of **317** (17.6 mg, 49 μmol , 1 equiv) in a 10-mL pear-shaped flask was cooled to 0 $^{\circ}\text{C}$, and an aqueous solution of *tert*-butyl hydroperoxide (70% by weight, 14 μL , 98 μmol , 2 equiv) and pyridinium dichromate (37 mg, 98 μmol , 2 equiv) were added in sequence. The reaction was allowed to slowly warm to rt over 5 h, whereupon it was passed through a short plug of SiO_2 , rinsing with EtOAc. The filtrate was concentrated *in vacuo* to an orange oil. Flash column chromatography (30 mL SiO_2 , 9:1 \rightarrow 8:2 hexane:EtOAc) afforded 6.2 mg (18 μmol , 37% yield) of **320** as a pale yellow residue and 2.5 mg (6.7 μmol , 14% yield) of **318** as a pale yellow residue.

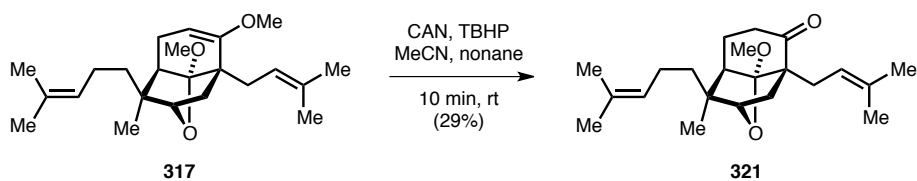
^1H NMR (600 MHz; CDCl_3) δ : 6.74 (dd, $J = 10.2, 7.0$ Hz, 1H), 6.06 (d, $J = 10.2$ Hz, 1H), 5.37 (t, $J = 7.2$ Hz, 1H), 5.01 (t, $J = 7.2$ Hz, 1H), 3.88 (d, $J = 6.0$ Hz, 1H), 3.47 (s, 3H), 2.59 (d, $J = 7.0$ Hz, 1H), 2.46 (dd, $J = 14.7, 6.2$ Hz, 1H), 2.34 (dd, $J = 14.7, 8.2$ Hz, 1H), 1.98 (d, $J = 13.6$ Hz, 1H), 1.95-1.92 (m, 1H), 1.89 (dd, $J = 13.6, 6.0$ Hz, 1H), 1.84-1.77 (m, 1H), 1.71 (s, 3H), 1.66 (s, 3H), 1.63 (s, 3H), 1.57 (s, 3H), 1.44-1.39 (m, 1H), 1.31-1.23 (m, 4H).

^{13}C NMR (125 MHz; CDCl_3) δ : 201.5, 146.4, 132.9, 132.3, 129.2, 124.0, 122.3, 116.2, 80.8, 55.5, 52.5, 48.5, 46.1, 35.6, 34.8, 30.5, 27.0, 26.3, 25.9, 23.4, 18.00, 17.87.

FTIR (thin film) ν_{max} : 2966, 2925, 2870, 1728, 1673, 1449, 1375, 1220, 1005, 833 cm^{-1} .

HRMS-ESI (m/z): $[\text{M}+\text{Na}]^+$ calculated for $\text{C}_{22}\text{H}_{32}\text{O}_3$, 367.2244; found, 367.2238.

TLC $R_f = 0.38$ (8:2 hexane:EtOAc).



(2*S*,3*aR*,7*R*,7*aS*,8*S*)-7*a*-Methoxy-8-methyl-3*a*-(3-methylbut-2-en-1-yl)-8-(4-methylpent-3-en-1-yl)hexahydro-2,7-methanobenzofuran-4(2*H*)-one (321):

A MeCN (0.4 mL) solution of **317** (14.0 mg, 39 μ mol, 1 equiv) and a nonane solution of *tert*-butyl hydroperoxide (5.5 M, 35 μ L, 0.19 mmol, 5 equiv) in a 2-dram scintillation vial was treated with ceric ammonium nitrate (43 mg, 78 μ mol, 2 equiv). After stirring the reaction for 10 min at rt, it was quenched with sat. aq. NaHCO₃, diluted with H₂O, and extracted thrice with EtOAc. The organic extracts were combined, washed with brine, dried over Na₂SO₄, filtered, and concentrated *in vacuo* to a colorless oil. Flash column chromatography (25 mL SiO₂, 95:5 \rightarrow 9:1 hexane:EtOAc) afforded 3.9 mg (11 μ mol, 29% yield) of **321** as a white flocculent solid.

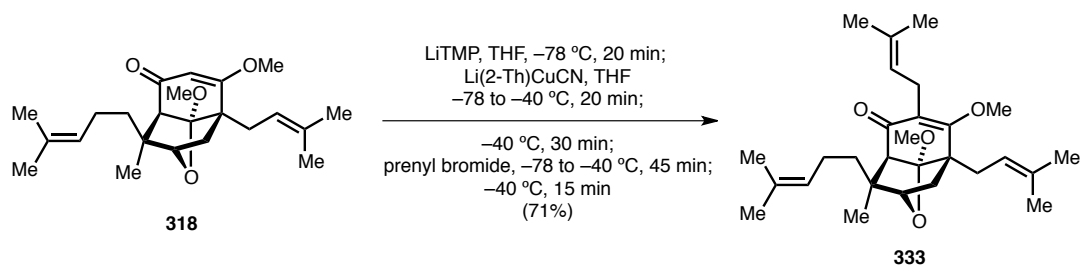
¹H NMR (600 MHz; CDCl₃) δ : 5.16 (t, J = 7.3 Hz, 1H), 5.06 (t, J = 7.1 Hz, 1H), 3.91 (d, J = 5.7 Hz, 1H), 3.46 (s, 3H), 2.52 (ddd, J = 14.8, 11.0, 7.6 Hz, 1H), 2.43-2.35 (m, 2H), 2.20 (dd, J = 14.5, 9.2 Hz, 1H), 2.12-2.04 (m, 2H), 1.97 (d, J = 13.7 Hz, 1H), 1.92-1.86 (m, 2H), 1.85-1.75 (m, 2H), 1.69 (s, 3H), 1.68 (s, 3H), 1.61 (s, 3H), 1.60 (s, 3H), 1.49 (td, J = 12.8, 5.1 Hz, 1H), 1.41 (td, J = 12.8, 4.8 Hz, 1H), 1.20 (s, 3H).

¹³C NMR (125 MHz; CDCl₃) δ : 213.2, 133.8, 132.2, 124.3, 121.5, 116.7, 79.0, 59.1, 52.2, 46.0, 41.5, 36.1, 35.5, 33.8, 29.9, 28.2, 26.3, 25.9, 23.3, 19.1, 18.06, 17.90.

FTIR (thin film) ν_{max} : 2966, 2929, 2859, 1707, 1449, 1375, 1325, 1227, 1150, 1103, 999 cm⁻¹.

HRMS-ESI (m/z): [M+Na]⁺ calculated for C₂₂H₃₄O₃, 369.2400; found, 369.2412.

TLC R_f = 0.65 (7:3 hexane:EtOAc).



(2*S*,3*S*,3*aS*,7*R*,7*aS*)-6,7*a*-Dimethoxy-3-methyl-5,7-bis(3-methylbut-2-en-1-yl)-3-(4-methylpent-3-en-1-yl)-3,3*a*,7,7*a*-tetrahydro-2,7-methanobenzofuran-4(2*H*)-one (333):

A THF (19 mL) solution of **318** (697 mg, 1.86 mmol, 1 equiv) in a 100-mL recovery flask was cooled to $-78\text{ }^{\circ}\text{C}$, and a freshly prepared THF solution of lithium 2,2,6,6-tetramethylpiperidide (0.53 M, 7.0 mL, 3.7 mmol, 2 equiv) was added. After stirring the resulting yellow-orange solution at $-78\text{ }^{\circ}\text{C}$ for 20 min, a THF solution of lithium (2-thienyl)cyanocopper(I) (0.22 M, 17 mL, 3.7 mmol, 2 equiv) was added slowly over 10 min. The resulting brown slurry was allowed to slowly warm to $-40\text{ }^{\circ}\text{C}$ over 20 min. After stirring the brown slurry at $-40\text{ }^{\circ}\text{C}$ for an additional 30 min, it was cooled to $-78\text{ }^{\circ}\text{C}$, and prenyl bromide (1.1 mL, 9.3 mmol, 5 equiv) was added. The reaction was allowed to slowly warm to $-40\text{ }^{\circ}\text{C}$ over 45 min, maintained at that temperature for 15 min, and subsequently quenched at $-40\text{ }^{\circ}\text{C}$ with sat. aq. NH_4Cl . The mixture was warmed to rt and extracted thrice with EtOAc. The organic extracts were combined, sequentially washed with H_2O and brine, dried over Na_2SO_4 , filtered, and concentrated *in vacuo* to a brown oil. Flash column chromatography (200 mL SiO_2 , 95:5 hexane:EtOAc) afforded 586 mg (1.32 mmol, 71% yield) of **333** as a pale yellow oil.

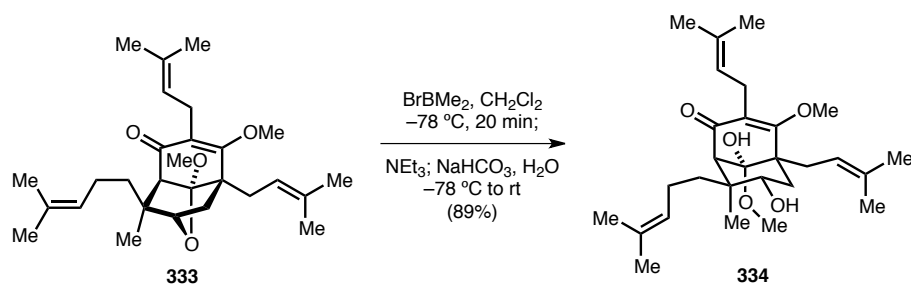
^1H NMR (600 MHz; CDCl_3) δ : 5.30 (t, $J = 6.9\text{ Hz}$, 1H), 4.99 (t, $J = 6.7\text{ Hz}$, 1H), 4.97 (t, $J = 7.1\text{ Hz}$, 1H), 3.87 (d, $J = 5.7\text{ Hz}$, 1H), 3.81 (s, 3H), 3.45 (s, 3H), 3.03-3.01 (m, 2H), 2.72 (s, 1H), 2.47 (dd, $J = 15.2, 6.9\text{ Hz}$, 1H), 2.31 (dd, $J = 15.2, 6.9\text{ Hz}$, 1H), 2.14 (d, $J = 12.7\text{ Hz}$, 1H), 1.99-1.95 (m, 1H), 1.92 (dd, $J = 12.7, 5.7\text{ Hz}$, 1H), 1.74-1.70 (m, 4H), 1.68 (s, 3H), 1.65 (s, 9H), 1.55 (s, 3H), 1.33-1.28 (m, 2H), 1.26 (s, 3H).

^{13}C NMR (125 MHz; CDCl_3) δ : 198.6, 176.3, 132.2, 131.88, 131.80, 124.2, 122.8, 122.34, 122.28, 114.6, 81.0, 61.0, 56.7, 52.1, 49.3, 48.4, 39.3, 34.3, 32.8, 27.9, 26.3, 25.84, 25.81, 22.75, 22.65, 18.10, 18.04, 17.8.

FTIR (thin film) ν_{max} : 2968, 2925, 1655, 1617, 1449, 1375, 1345, 1331, 1233, 1074, 1009, 941, 829 cm^{-1} .

HRMS–ESI (m/z): $[\text{M}+\text{H}]^+$ calculated for $\text{C}_{28}\text{H}_{42}\text{O}_4$, 443.3156; found, 443.3150.

TLC R_f = 0.65 (7:3 hexane:EtOAc).

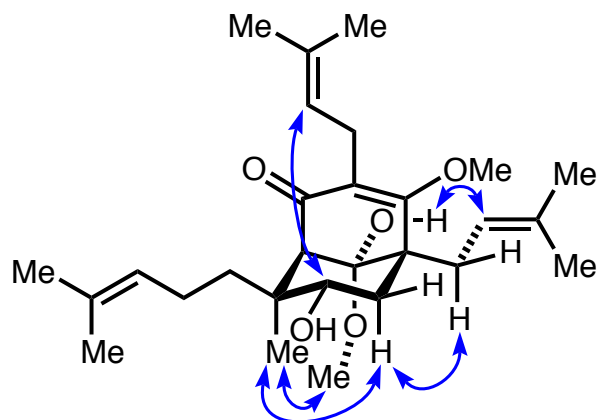


(1*S*,5*R*,7*S*,8*S*,9*S*)-7,9-Dihydroxy-4,9-dimethoxy-8-methyl-3,5-bis(3-methylbut-2-en-1-yl)-8-(4-methylpent-3-en-1-yl)bicyclo[3.3.1]non-3-en-2-one (334):

A CH₂Cl₂ (5 mL) solution of **333** (91 mg, 0.21 mmol, 1 equiv) in a 10-mL recovery flask was cooled to –78 °C, and a CH₂Cl₂ solution of bromodimethylborane (2.65 M, 0.78 mL, 2.1 mmol, 10 equiv) was added dropwise. The resulting yellow solution was stirred at –78 °C for 20 min and sequentially quenched at –78 °C with NEt₃ (2 mL) and sat. aq. NaHCO₃. The mixture was warmed to rt and extracted thrice with EtOAc. The organic extracts were combined, sequentially washed with H₂O, sat. aq. NH₄Cl, and brine, dried over Na₂SO₄, filtered, and concentrated *in vacuo* to a viscous yellow oil. Flash column chromatography (50 mL SiO₂, 9:1 → 8:2 hexane:EtOAc) afforded 85 mg (0.18 mmol, 89% yield) of **334** as a pale yellow oil.

¹H NMR (600 MHz; C₆D₆) δ: 5.56 (d, *J* = 11.5 Hz, 1H), 5.36 (t, *J* = 7.3 Hz, 1H), 5.29 (t, *J* = 6.6 Hz, 1H), 3.72 (s, 1H), 3.68 (dd, *J* = 11.9, 5.3 Hz, 1H), 3.54 (s, 3H), 3.35 (dd, *J* = 15.2, 6.4 Hz, 1H), 3.19-3.15 (m, 2H), 3.07 (s, 3H), 2.93 (dd, *J* = 14.1, 11.5 Hz, 1H), 2.91-2.84 (m, 1H), 2.27 (d, *J* = 14.1 Hz, 1H), 2.11-2.06 (m, 1H), 2.01 (dd, *J* = 12.8, 11.9 Hz, 1H), 1.85 (d, *J* = 0.6 Hz, 3H), 1.73 (s, 3H), 1.73-1.69 (m, 1H), 1.65-1.60 (m, 7H), 1.57 (s, 3H), 1.43 (s, 3H), 1.28 (td, *J* = 12.7, 4.4 Hz, 1H), 1.13 (s, 3H).

¹³C NMR (125 MHz; C₆D₆) δ: 197.4, 171.2, 136.5, 131.9, 131.2, 125.8, 124.5, 123.44, 123.31, 100.3, 73.5, 61.9, 57.6, 52.5, 48.2, 41.0, 39.8, 37.5, 30.9, 26.1, 25.84, 25.80, 23.8, 22.3, 18.08, 17.97, 17.7, 17.4.

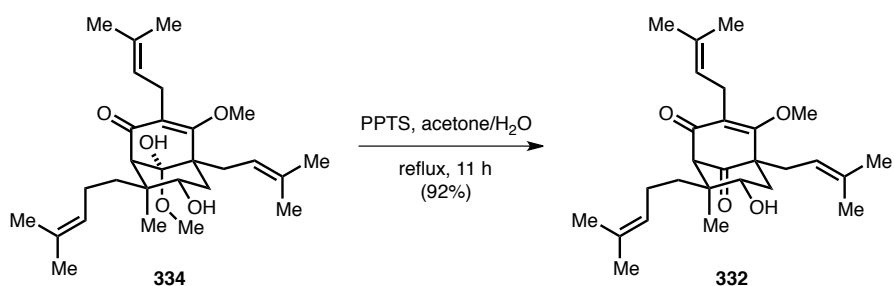


Key 1D nOe correlations.

FTIR (thin film) ν_{max} : 3464 (br), 2969, 2928, 2859, 1665, 1615, 1450, 1376, 1329, 1235, 1087, 1040, 986, 928, 907, 858, 737 cm^{-1} .

HRMS-ESI (m / z): $[\text{M}+\text{H}]^+$ calculated for $\text{C}_{28}\text{H}_{44}\text{O}_5$, 461.3262; found, 461.3254.

TLC R_f = 0.40 (7:3 hexane:EtOAc).



(1*S*,5*R*,7*S*,8*S*)-7-Hydroxy-4-methoxy-8-methyl-3,5-bis(3-methylbut-2-en-1-yl)-8-(4-methylpent-3-en-1-yl)bicyclo[3.3.1]non-3-ene-2,9-dione (332):

A 4:1 acetone:H₂O (10 mL) solution of **334** (84.8 mg, 0.184 mmol, 1 equiv) in a 25-mL recovery flask was treated with pyridinium *para*-toluenesulfonate (231 mg, 0.920 mmol, 5 equiv). The flask was outfitted with a reflux condenser, and the reaction was heated to reflux. After refluxing for 11 h, the reaction was cooled to rt, diluted with H₂O, and extracted thrice with 1:1 hexane:EtOAc. The organic extracts were combined, sequentially washed with sat. aq. NaHCO₃ and brine, dried over Na₂SO₄, filtered, and concentrated *in vacuo* to a colorless oil. Flash column chromatography (35 mL SiO₂, 8:2 hexane:EtOAc) afforded 72.8 mg (0.17 mmol, 92% yield) of **332** as a colorless oil.

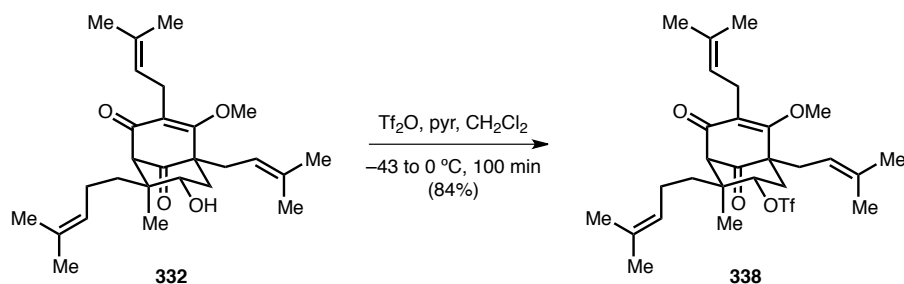
¹H NMR (600 MHz; C₆D₆) δ: 5.37 (t, *J* = 6.9 Hz, 1H), 5.27 (t, *J* = 7.2 Hz, 1H), 5.19 (t, *J* = 6.5 Hz, 1H), 3.63 (dd, *J* = 11.1, 5.1 Hz, 1H), 3.52 (s, 1H), 3.40 (s, 3H), 3.18 (dd, *J* = 15.4, 6.4 Hz, 1H), 3.10 (dd, *J* = 15.4, 6.7 Hz, 1H), 2.67-2.57 (m, 2H), 2.44 (dd, *J* = 14.5, 7.3 Hz, 1H), 1.92-1.87 (m, 2H), 1.75 (s, 3H), 1.69 (s, 3H), 1.66 (s, 3H), 1.64-1.60 (m, 5H), 1.58 (s, 6H), 1.39 (td, *J* = 12.9, 4.8 Hz, 2H), 0.84 (s, 3H), 0.64 (br s, 1H).

¹³C NMR (125 MHz; C₆D₆) δ: 204.5, 193.6, 173.6, 133.5, 132.3, 131.6, 126.1, 125.1, 123.0, 120.6, 72.1, 69.8, 61.7, 57.8, 46.3, 39.8, 38.4, 30.7, 26.00, 25.98, 25.7, 23.7, 22.1, 18.14, 18.01, 17.90, 15.7.

FTIR (thin film) ν_{max} : 3488 (br), 2968, 2922, 2856, 1736, 1656, 1649, 1593, 1447, 1376, 1341, 1236, 1059 cm⁻¹.

HRMS-ESI (*m/z*): [M+Na]⁺ calculated for C₂₇H₄₀O₄, 451.2819; found, 451.2830.

TLC *R_f* = 0.36 (7:3 hexane:EtOAc).



(1*S*,2*S*,3*S*,5*R*)-6-Methoxy-2-methyl-5,7-bis(3-methylbut-2-en-1-yl)-2-(4-methylpent-3-en-1-yl)-8,9-dioxobicyclo[3.3.1]non-6-en-3-yl trifluoromethanesulfonate (338):

A CH₂Cl₂ (3 mL) solution of **332** (33.5 mg, 78.2 μmol, 1 equiv) in a 10-mL test tube was cooled to –43 °C, and pyridine (44 μL, 0.54 mmol, 7 equiv) and trifluoromethanesulfonic anhydride (76 μL, 0.45 mmol, 6 equiv) were added sequentially. The resulting white slurry was allowed to slowly warm to 0 °C over 100 min. The reaction was subsequently quenched at 0 °C with sat. aq. NaHCO₃ and extracted thrice with EtOAc. The organic extracts were combined, washed with H₂O and brine, dried over Na₂SO₄, filtered, and concentrated *in vacuo* to an orange oil. Flash column chromatography (40 mL SiO₂, 9:1 hexane:EtOAc) afforded 36.8 mg (65.6 μmol, 84% yield) of **338** as a colorless oil.

¹H NMR (600 MHz; C₆D₆) δ: 5.22 (t, *J* = 6.9 Hz, 1H), 5.16–5.10 (m, 3H), 3.49 (s, 1H), 3.41 (s, 3H), 3.17 (dd, *J* = 15.3, 7.1 Hz, 1H), 2.97 (dd, *J* = 15.3, 6.5 Hz, 1H), 2.59–2.49 (m, 2H), 2.35 (dd, *J* = 13.1, 5.4 Hz, 1H), 2.29 (dd, *J* = 14.5, 7.5 Hz, 1H), 1.84 (dd, *J* = 13.1, 11.8 Hz, 1H), 1.80–1.73 (m, 1H), 1.72 (s, 3H), 1.64–1.62 (m, 4H), 1.61 (s, 3H), 1.60 (s, 3H), 1.58 (s, 3H), 1.57 (s, 3H), 1.49 (td, *J* = 12.9, 4.6 Hz, 1H), 0.75 (s, 3H).

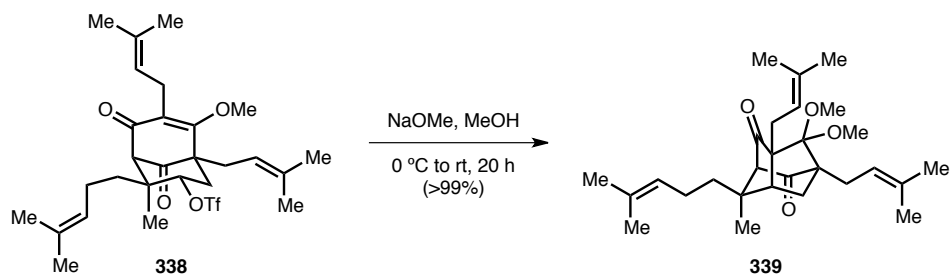
¹³C NMR (125 MHz; C₆D₆) δ: 201.6, 191.8, 172.2, 134.5, 133.7, 132.6, 126.7, 123.7, 121.7, 119.5, 90.9, 69.4, 62.1, 57.4, 45.6, 37.8, 37.0, 30.3, 25.92, 25.86, 25.6, 23.5, 21.6, 18.13, 17.96, 17.87, 16.3.

¹⁹F NMR (470 MHz; C₆D₆) δ: –75.54 (s, 3F).

FTIR (thin film) ν_{max}: 2972, 2916, 2860, 1741, 1661, 1597, 1414, 1244, 1210, 1146, 918 cm^{–1}.

HRMS–ESI (*m/z*): [M+Na]⁺ calculated for C₂₈H₃₉F₃O₆S, 583.2312; found, 583.2293.

TLC R_f = 0.50 (9:1 hexane:EtOAc).

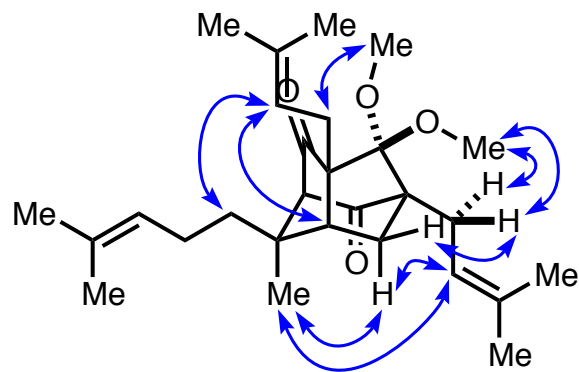


(2*R*,3*R*,3*aR*,5*S*,6*aR*)-6,6-Dimethoxy-3-methyl-5,6*a*-bis(3-methylbut-2-en-1-yl)-3-(4-methylpent-3-en-1-yl)hexahydro-2,5-methanopentalene-1,7(2*H*)-dione (339):

A MeOH (0.25 mL) solution of **338** (12 mg, 21 μ mol) in a 10-mL test tube was cooled to 0 $^{\circ}$ C, and a MeOH solution of sodium methoxide (0.5 M, 1 mL) was slowly added. The reaction was allowed to slowly warm to rt. After stirring for 20 h, the reaction was quenched at rt with sat. aq. NaHCO_3 and extracted thrice with 1:1 hexane:EtOAc. The organic extracts were combined, washed with H_2O and brine, dried over Na_2SO_4 , filtered, and concentrated *in vacuo* to afford 9.1 mg (21 μ mol, >99% yield) of **339** as a white flocculent solid.

^1H NMR (600 MHz; C_6D_6) δ : 5.72 (t, $J = 7.0$ Hz, 1H), 5.45 (t, $J = 7.9$ Hz, 1H), 5.03 (t, $J = 6.9$ Hz, 1H), 3.20 (d, $J = 2.0$ Hz, 1H), 3.12 (s, 3H), 3.04 (s, 3H), 2.81-2.76 (m, 2H), 2.71 (dd, $J = 14.8, 7.7$ Hz, 1H), 2.39 (dd, $J = 14.6, 7.9$ Hz, 1H), 2.17 (dd, $J = 12.4, 5.8$ Hz, 1H), 2.10 (dd, $J = 5.8, 1.9$ Hz, 1H), 1.92 (d, $J = 12.4$ Hz, 1H), 1.87 (dt, $J = 15.7, 7.5$ Hz, 1H), 1.71 (s, 3H), 1.69 (s, 3H), 1.66 (s, 3H), 1.64 (s, 3H), 1.63-1.61 (m, 4H), 1.52 (s, 3H), 1.18 (t, $J = 8.5$ Hz, 2H), 0.77 (s, 3H).

^{13}C NMR (125 MHz; C_6D_6) δ : 203.7, 202.5, 133.6, 132.1, 131.6, 124.5, 122.3, 121.8, 107.7, 75.5, 66.24, 66.07, 51.9, 51.2, 47.0, 44.8, 38.9, 35.0, 27.0, 26.6, 26.07, 26.02, 25.8, 22.2, 19.3, 18.10, 18.01, 17.7.

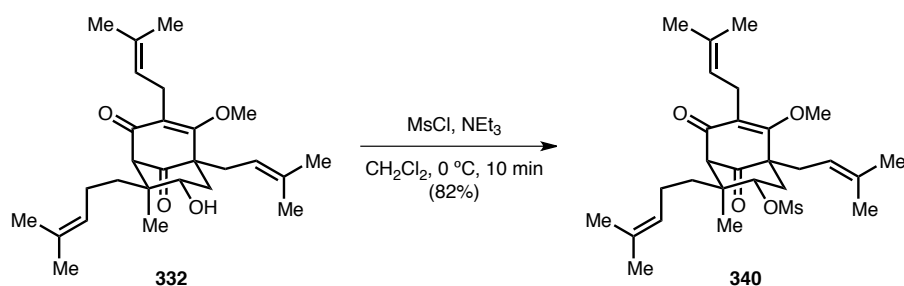


Key 1D nOe correlations.

FTIR (thin film) ν_{max} : 2968, 2926, 2856, 1754, 1706, 1443, 1375, 1308, 1195, 1171, 1141, 1097, 1072, 1046, 858 cm^{-1} .

HRMS-ESI (m / z): $[\text{M}+\text{H}]^+$ calculated for $\text{C}_{28}\text{H}_{42}\text{O}_4$, 443.3156; found, 443.3148.

TLC R_f = 0.41 (9:1 hexane:EtOAc).

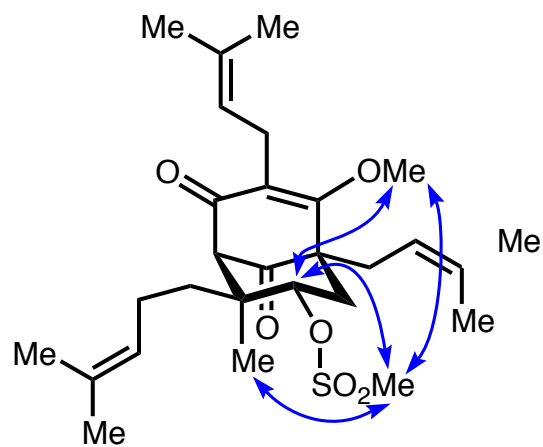


(1*S*,2*S*,3*S*,5*R*)-6-Methoxy-2-methyl-5,7-bis(3-methylbut-2-en-1-yl)-2-(4-methylpent-3-en-1-yl)-8,9-dioxobicyclo[3.3.1]non-6-en-3-yl methanesulfonate (340):

A CH_2Cl_2 (3 mL) solution of **332** (38.7 mg, 90.3 μmol , 1 equiv) in a 10-mL test tube was cooled to 0 $^\circ\text{C}$, and triethylamine (65 μL , 0.47 mmol, 5.2 equiv) and methanesulfonyl chloride (30 μL , 0.39 mmol, 4.3 equiv) were added sequentially. After stirring the reaction at 0 $^\circ\text{C}$ for 10 min, it was quenched with sat. aq. NaHCO_3 and extracted thrice with EtOAc. The organic extracts were combined, washed with H_2O and brine, dried over Na_2SO_4 , filtered, and concentrated *in vacuo* to a colorless residue. Flash column chromatography (40 mL SiO_2 , 9:1 hexane:EtOAc) afforded 37.5 mg (74.0 μmol , 82% yield) of **340** as a colorless oil.

^1H NMR (600 MHz; C_6D_6) δ : 5.31 (t, J = 6.9 Hz, 1H), 5.24-5.19 (m, 2H), 4.92 (dd, J = 11.6, 5.3 Hz, 1H), 3.54 (s, 1H), 3.54 (s, 3H), 3.16 (dd, J = 15.4, 6.9 Hz, 1H), 3.10 (dd, J = 15.4, 6.5 Hz, 1H), 2.64-2.59 (m, 2H), 2.55 (dd, J = 13.3, 5.3 Hz, 1H), 2.38 (dd, J = 14.5, 7.5 Hz, 1H), 2.07 (s, 3H), 1.92 (dd, J = 13.3, 11.6 Hz, 1H), 1.85 (tt, J = 12.6, 6.2 Hz, 1H), 1.75 (s, 3H), 1.66 (s, 3H), 1.63 (s, 3H), 1.62 (s, 3H), 1.59 (s, 3H), 1.59-1.56 (m, 4H), 1.52 (td, J = 12.8, 4.9 Hz, 1H), 0.87 (s, 3H).

^{13}C NMR (125 MHz; C_6D_6) δ : 202.9, 192.6, 173.3, 134.1, 133.2, 132.2, 127.0, 124.4, 122.2, 119.9, 81.5, 69.8, 62.2, 57.6, 45.7, 38.2, 37.73, 37.69, 30.3, 25.99, 25.95, 25.75, 23.6, 21.8, 18.15, 18.00, 17.94, 16.5.

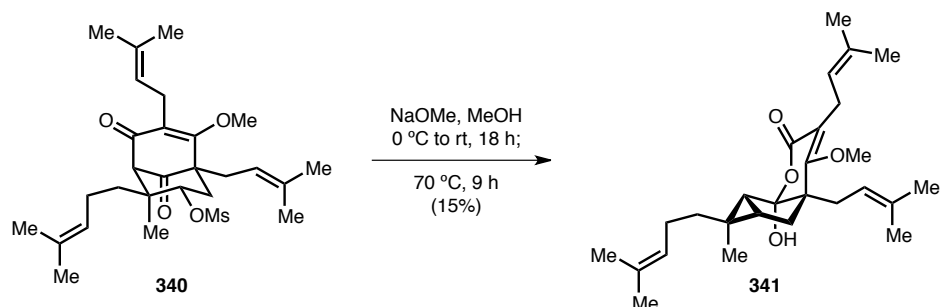


Key 1D nOe correlations.

FTIR (thin film) ν_{max} : 2968, 2918, 2857, 1738, 1658, 1597, 1449, 1360, 1342, 1236, 1178, 1061, 945, 862 cm^{-1} .

HRMS-ESI (m/z): $[\text{M}+\text{H}]^+$ calculated for $\text{C}_{28}\text{H}_{42}\text{O}_6\text{S}$, 507.2775; found, 507.2781.

TLC R_f = 0.50 (7:3 hexane:EtOAc).



(4a*R*,5a*S*,6*S*,6a*R*,6b*R*)-6b-Hydroxy-4-methoxy-6-methyl-3,4a-bis(3-methylbut-2-en-1-yl)-6-(4-methylpent-3-en-1-yl)-4a,5,5a,6,6a,6b-hexahydro-2*H*-cyclopropa[4,5]cyclopenta[1,2-*b*]pyran-2-one (341):

A MeOH solution of sodium methoxide (0.5 M, 1 mL) was slowly added to a 10-mL test tube cooled to 0 °C containing **340** (5.5 mg, 11 μmol). The reaction was allowed to slowly warm to rt. After 18 h, the test tube was sealed and heated to 70 °C. After stirring the reaction at 70 °C for 9 h, it was cooled to rt, quenched with sat. aq. NaHCO₃, and extracted thrice with 1:1 hexane:EtOAc. The organic extracts were combined, sequentially washed with H₂O and brine, dried over Na₂SO₄, filtered, and concentrated *in vacuo* to a pale yellow residue. Preparatory thin-layer chromatography (1 × 8:2 hexane:EtOAc) afforded 0.7 mg (1.6 μmol, 15% yield) of **341** as a colorless residue.

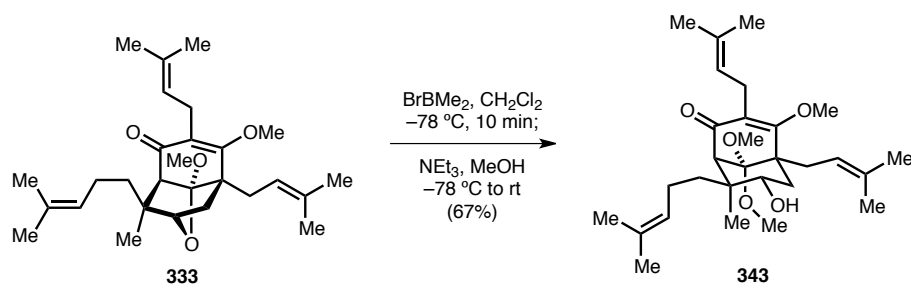
¹H NMR (600 MHz; C₆D₆) δ: 5.46 (t, *J* = 6.4 Hz, 1H), 5.39 (t, *J* = 6.4 Hz, 1H), 5.06 (t, *J* = 7.0 Hz, 1H), 3.47 (s, 3H), 3.37 (dd, *J* = 15.5, 6.5 Hz, 1H), 3.23 (dd, *J* = 15.5, 5.9 Hz, 1H), 3.13-3.13 (br s, 1H), 2.48 (dd, *J* = 14.5, 7.7 Hz, 1H), 2.44 (dd, *J* = 14.7, 5.6 Hz, 1H), 2.29 (dd, *J* = 14.7, 7.7 Hz, 1H), 1.99 (dt, *J* = 11.4, 5.6 Hz, 2H), 1.65 (s, 3H), 1.63 (s, 3H), 1.63 (s, 3H), 1.58 (d, *J* = 8.0 Hz, 1H), 1.54 (s, 3H), 1.52 (s, 3H), 1.49 (dd, *J* = 14.5, 4.7 Hz, 1H), 1.45 (s, 3H), 1.27 (s, 3H), 1.13 (td, *J* = 7.8, 4.8 Hz, 1H), 0.99-0.96 (m, 2H).

¹³C NMR (125 MHz; C₆D₆) δ: 170.3, 165.1, 133.6, 132.2, 131.2, 124.9, 123.2, 120.2, 115.0, 108.0, 65.0, 61.6, 42.7, 41.8, 33.4, 31.9, 30.7, 28.1, 25.84, 25.81, 25.77, 25.6, 25.3, 18.1, 17.88, 17.71, 14.1.

FTIR (thin film) ν_{max} : 3308 (br), 2964, 2920, 2854, 1677, 1631, 1452, 1376, 1342, 1224, 1190, 1093, 1005 cm⁻¹.

HRMS-ESI (*m/z*): [M+H]⁺ calculated for C₂₇H₄₀O₄, 429.2999; found, 429.2991.

TLC $R_f = 0.61$ (8:2 hexane:EtOAc).

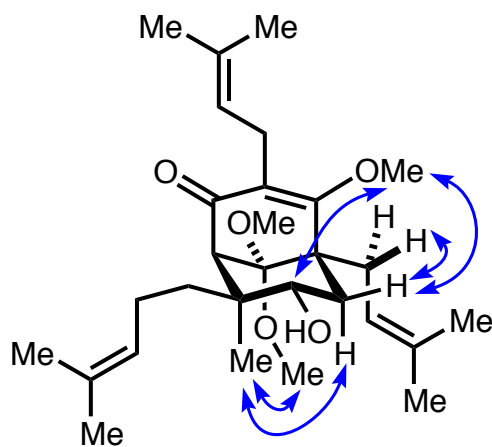


(1*S*,5*R*,7*S*,8*S*)-7-Hydroxy-4,9,9-trimethoxy-8-methyl-3,5-bis(3-methylbut-2-en-1-yl)-8-(4-methylpent-3-en-1-yl)bicyclo[3.3.1]non-3-en-2-one (343):

A CH₂Cl₂ (12 mL) solution of **333** (210 mg, 0.47 mmol, 1 equiv) in a 25-mL recovery flask was cooled to -78°C , and a CH₂Cl₂ solution of bromodimethylborane (2.65 M, 1.8 mL, 4.7 mmol, 10 equiv) was added. The resulting yellow solution was stirred at -78°C for 10 min and sequentially quenched at -78°C with 1:1 NEt₃:MeOH (10 mL) and sat. aq. NaHCO₃. The mixture was warmed to rt and extracted thrice with EtOAc. The organic extracts were combined, washed with H₂O and brine, dried over Na₂SO₄, filtered, and concentrated *in vacuo* to a brown oil. Flash column chromatography (100 mL SiO₂, 9:1 hexane:EtOAc) afforded 149 mg (0.31 mmol, 67% yield) of **343** as a pale yellow oil.

¹H NMR (600 MHz; C₆D₆) δ : 5.27 (t, $J = 7.1$ Hz, 1H), 4.94 (t, $J = 7.2$ Hz, 1H), 4.90 (t, $J = 6.5$ Hz, 1H), 3.76 (s, 3H), 3.47 (ddd, $J = 11.9, 6.5, 5.4$ Hz, 1H), 3.23 (s, 3H), 3.10 (s, 3H), 3.02 (dd, $J = 15.3, 6.5$ Hz, 1H), 2.89 (dd, $J = 15.3, 6.5$ Hz, 1H), 2.82 (s, 1H), 2.57 (dd, $J = 15.4, 7.6$ Hz, 1H), 2.26-2.21 (m, 2H), 1.82-1.74 (m, 2H), 1.68 (dd, $J = 13.2, 5.4$ Hz, 1H), 1.61 (s, 3H), 1.57 (s, 3H), 1.55 (s, 6H), 1.54 (s, 3H), 1.52 (s, 3H), 1.30 (td, $J = 12.8, 4.7$ Hz, 1H), 1.17-1.13 (m, 1H), 1.00 (s, 3H), 0.87 (td, $J = 12.8, 4.6$ Hz, 1H).

¹³C NMR (125 MHz; CDCl₃) δ : 198.7, 174.5, 132.3, 131.8, 131.4, 125.1, 123.6, 122.51, 122.39, 103.1, 74.0, 62.3, 59.2, 53.7, 51.1, 50.5, 40.5, 39.8, 36.1, 30.7, 26.2, 25.93, 25.86, 23.4, 21.8, 18.2, 17.95, 17.89.

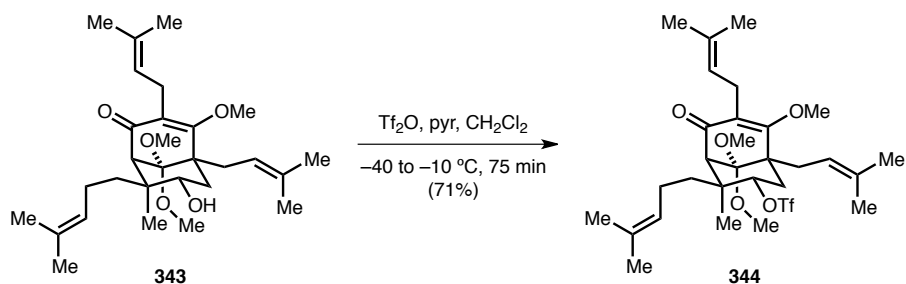


Key 1D nOe correlations.

FTIR (thin film) ν_{max} : 3468 (br), 2965, 2925, 2857, 1683, 1613, 1451, 1376, 1336, 1225, 1153, 1100, 1065 cm^{-1} .

HRMS-ESI (m / z): $[\text{M}+\text{H}]^+$ calculated for $\text{C}_{29}\text{H}_{46}\text{O}_5$, 475.3418; found, 475.3406.

TLC R_f = 0.47 (8:2 hexane:EtOAc).



(1*S*,2*S*,3*S*,5*R*)-6,9,9-Trimethoxy-2-methyl-5,7-bis(3-methylbut-2-en-1-yl)-2-(4-methylpent-3-en-1-yl)-8-oxobicyclo[3.3.1]non-6-en-3-yl trifluoromethanesulfonate (344):

A CH₂Cl₂ (2 mL) solution of **343** (42 mg, 88 μmol, 1 equiv) and pyridine (43 μL, 0.53 mmol, 6 equiv) in a 10-mL recovery flask was cooled to −40 °C, and trifluoromethanesulfonic anhydride (74 μL, 0.44 mmol, 5 equiv) was added. After allowing the reaction to slowly warm from −40 °C to −10 °C over 75 min, it was quenched at −10 °C with sat. aq. NaHCO₃ and extracted thrice with EtOAc. The organic extracts were combined, washed sequentially with H₂O, sat. aq. NH₄Cl, and brine, dried over Na₂SO₄, filtered, and concentrated *in vacuo* to a brown residue. Flash column chromatography (30 mL SiO₂, 95:5 hexane:EtOAc) afforded 37 mg (63 μmol, 71% yield) of **344** as a colorless oil.

¹H NMR (600 MHz; C₆D₆) δ: 5.56 (t, *J* = 6.9 Hz, 1H), 5.27-5.22 (m, 2H), 5.19 (dd, *J* = 12.0, 5.3 Hz, 1H), 3.58 (s, 3H), 3.33 (dd, *J* = 14.9, 7.4 Hz, 1H), 3.09 (s, 1H), 3.02 (dd, *J* = 14.9, 6.4 Hz, 1H), 2.95 (s, 3H), 2.91 (s, 3H), 2.80-2.78 (m, 1H), 2.63 (dd, *J* = 15.7, 7.2 Hz, 1H), 2.37-2.30 (m, 2H), 2.18 (dd, *J* = 12.9, 5.3 Hz, 1H), 1.99 (tt, *J* = 12.5, 6.1 Hz, 1H), 1.80 (s, 3H), 1.70 (s, 3H), 1.68-1.64 (m, 10H), 1.57 (s, 3H), 1.37 (td, *J* = 12.9, 4.3 Hz, 1H), 1.19 (s, 3H).

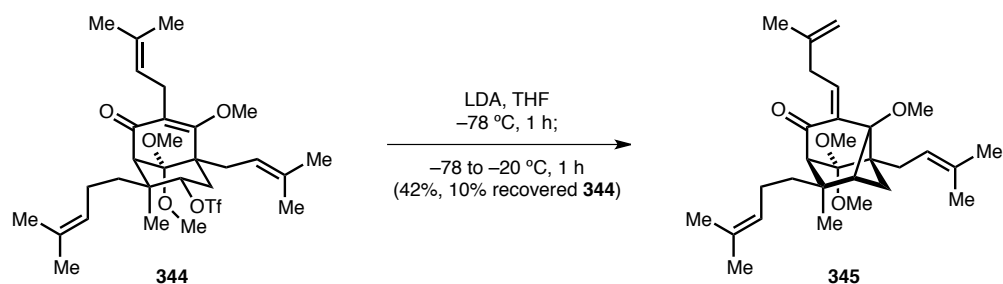
¹³C NMR (125 MHz; C₆D₆) δ: 196.2, 172.5, 133.3, 132.0, 131.6, 128.4, 124.5, 122.37, 122.18, 102.5, 94.7, 62.1, 59.7, 54.3, 50.46, 50.42, 40.3, 39.8, 34.1, 31.3, 25.98, 25.94, 25.7, 23.5, 21.7, 19.3, 18.03, 17.90, 17.82.

¹⁹F NMR (470 MHz; C₆D₆) δ: −75.71 (s, 3F).

FTIR (thin film) ν_{max}: 2973, 2917, 2859, 1739, 1659, 1596, 1413, 1243, 1207, 1145, 915, 881, 626 cm^{−1}.

HRMS–ESI (*m/z*): [M+H]⁺ calculated for C₃₀H₄₅F₃O₇S, 607.2911; found, 607.2892.

TLC R_f = 0.61 (8:2 hexane:EtOAc).

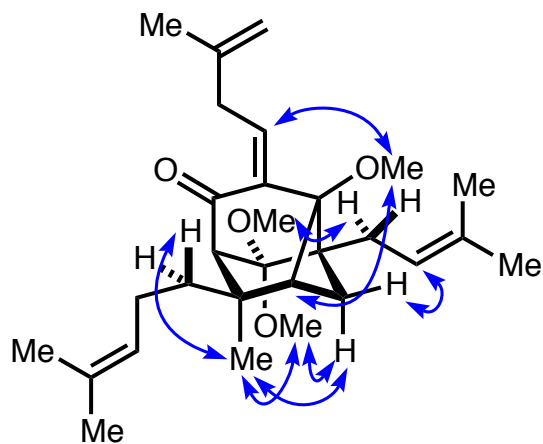


(1R,2S,5S,6R,7R,Z)-2,9,9-Trimethoxy-6-methyl-1-(3-methylbut-2-en-1-yl)-3-(3-methylbut-3-en-1-ylidene)-6-(4-methylpent-3-en-1-yl)tricyclo[3.3.1.0^{2,7}]nonan-4-one (345):

A THF (1.2 mL) solution of **344** (7.0 mg, 12 mmol, 1 equiv) in a 10-mL pear-shaped flask was cooled to $-78\text{ }^\circ\text{C}$, and a freshly prepared THF solution of lithium diisopropylamide (0.088 M, 0.52 mL, 46 μmol , 4 equiv) was added. After stirring the reaction at $-78\text{ }^\circ\text{C}$ for 1 h, it was allowed to slowly warm to $-20\text{ }^\circ\text{C}$ over 1 h. The reaction was quenched at $-20\text{ }^\circ\text{C}$ with sat. aq. NaHCO_3 and extracted thrice with EtOAc. The organic extracts were combined, washed with brine, dried over Na_2SO_4 , filtered, and concentrated *in vacuo* to a yellow residue. Preparatory thin-layer chromatography (2 \times 9:1 hexane:EtOAc) afforded 2.3 mg (5.0 μmol , 42% yield) of **345** as a colorless residue and 0.1 mg (0.2 μmol , 10% recovery) of **345** as a colorless residue.

^1H NMR (600 MHz; C_6D_6) δ : 6.19 (t, $J = 7.9\text{ Hz}$, 1H), 5.59 (t, $J = 7.4\text{ Hz}$, 1H), 5.15 (t, $J = 7.4\text{ Hz}$, 1H), 4.85 (s, 1H), 4.81 (s, 1H), 3.78 (dd, $J = 15.6, 8.2\text{ Hz}$, 1H), 3.69 (dd, $J = 15.6, 7.4\text{ Hz}$, 1H), 3.18 (s, 3H), 3.06 (s, 3H), 3.00 (s, 3H), 2.87 (s, 1H), 2.73 (dd, $J = 16.0, 8.5\text{ Hz}$, 1H), 2.49 (dd, $J = 16.0, 6.4\text{ Hz}$, 1H), 2.38 (dd, $J = 10.1, 7.7\text{ Hz}$, 1H), 2.32 (dtd, $J = 19.2, 6.8, 5.4\text{ Hz}$, 1H), 2.18 (d, $J = 7.7\text{ Hz}$, 1H), 2.01 (tt, $J = 12.8, 6.2\text{ Hz}$, 1H), 1.90 (d, $J = 10.1\text{ Hz}$, 1H), 1.77 (s, 3H), 1.71 (s, 3H), 1.65 (s, 3H), 1.63 (s, 3H), 1.62 (s, 4H), 1.43 (td, $J = 13.1, 4.4\text{ Hz}$, 1H), 1.26 (s, 3H), 1.09 (ddd, $J = 13.1, 12.4, 4.5\text{ Hz}$, 1H).

^{13}C NMR (125 MHz; C_6D_6) δ : 196.9, 144.5, 138.4, 131.9, 131.4, 130.8, 125.1, 123.4, 111.2, 103.9, 87.4, 62.2, 57.6, 52.5, 49.8, 48.1, 44.6, 41.3, 37.1, 36.0, 27.8, 26.3, 25.9, 25.3, 22.8, 22.1, 21.4, 18.0, 17.7.

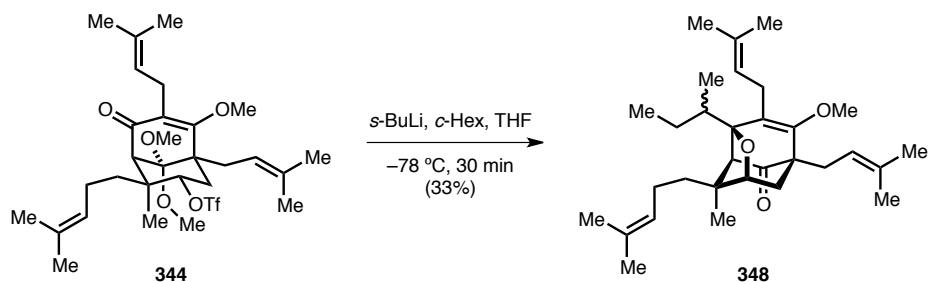


Key 1D nOe correlations.

FTIR (thin film) ν_{max} : 2965, 2933, 2857, 1708, 1625, 1440, 1376, 1354, 1204, 1123, 1079, 1057, 888 cm^{-1} .

HRMS-ESI (m / z): $[\text{M}+\text{Na}]^+$ calculated for $\text{C}_{29}\text{H}_{44}\text{O}_4$, 479.3132; found, 479.3133.

TLC R_f = 0.49 (9:1 hexane:EtOAc).



(2*R*,3*S*,3*aS*,5*R*,7*aR*)-7*a*-(*sec*-Butyl)-6-methoxy-3-methyl-5,7-bis(3-methylbut-2-en-1-yl)-3-(4-methylpent-3-en-1-yl)-3,3*a*,5,7*a*-tetrahydro-2,5-methanobenzofuran-4(2*H*)-one (348):

A THF (1 mL) solution of **344** (15 mg, 25 μ mol, 1 equiv) in a 10-mL pear-shaped flask was cooled to -78 $^{\circ}$ C, and a *c*-Hex solution of *sec*-butyllithium (1.43 M, 69 μ L, 99 μ mol, 4 equiv) was added dropwise. After stirring the resulting yellow-green solution at -78 $^{\circ}$ C for 30 min, it was quenched at -78 $^{\circ}$ C with sat. aq. NaHCO_3 and extracted thrice with EtOAc. The organic extracts were combined, washed with brine, dried over Na_2SO_4 , filtered, and concentrated *in vacuo* to a white residue. Preparatory thin-layer chromatography (1 \times 1:1 CH_2Cl_2 :hexane) afforded 3.9 mg (8.3 μ mol, 33% yield) of **348** as a white residue.

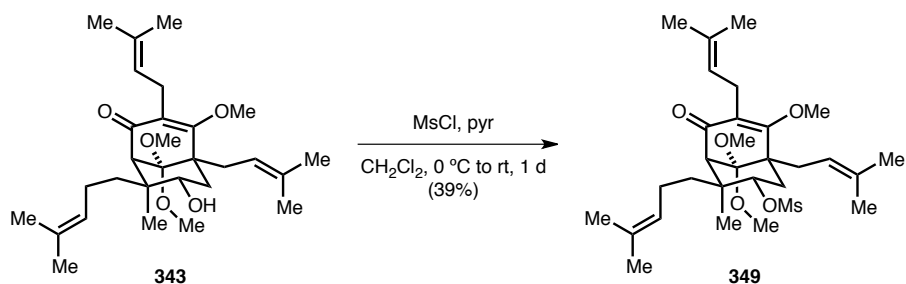
^1H NMR (600 MHz; C_6D_6) δ : 5.73-5.67 (m, 1H), 5.65-5.62 (m, 1H), 5.14 (t, J = 6.5 Hz, 1H), 3.85 (d, J = 16.0 Hz, 1H), 3.38 (s, 3H), 3.32-3.25 (m, 1H), 2.88-2.78 (m, 2H), 2.56-2.43 (m, 1H), 2.02-1.83 (m, 5H), 1.68 (s, 6H), 1.65 (s, 3H), 1.62 (s, 3H), 1.61 (s, 3H), 1.60 (s, 3H), 1.56 (s, 3H), 1.55 (s, 3H), 1.45-1.36 (m, 3H), 1.35 (d, J = 7.3 Hz, 3H, *diastereomer A*), 0.98 (d, J = 7.1 Hz, 1H, *diastereomer B*), 0.92 (t, J = 7.4 Hz, 3H *diastereomer A*), 0.87 (s, 3H), 0.85 (d, J = 7.5 Hz, 3H, *diastereomer B*).

^{13}C NMR (125 MHz; C_6D_6) δ : 206.40, 206.36, 161.2, 161.0, 134.2, 133.4, 133.11, 133.09, 131.6, 131.3, 130.05, 130.02, 125.63, 125.53, 124.6, 121.1, 89.8, 89.36, 89.35, 84.97, 84.81, 61.7, 61.18, 61.14, 54.79, 54.74, 51.78, 51.75, 44.9, 44.6, 38.62, 38.50, 34.99, 34.91, 28.2, 27.39, 27.30, 26.05, 25.89, 25.85, 25.79, 25.75, 25.4, 23.8, 22.96, 22.89, 18.02, 17.99, 17.80, 17.77, 17.44, 17.43, 17.36, 14.9, 14.7, 13.99, 13.98, 13.2 (*mixture of two diastereomers*).

FTIR (thin film) ν_{max} : 2966, 2929, 2874, 1724, 1634, 1451, 1376, 1231, 1124, 1042, 970 cm^{-1} .

HRMS-ESI (m/z): $[\text{M}+\text{H}]^+$ calculated for $\text{C}_{31}\text{H}_{48}\text{O}_3$, 469.3676; found, 469.3677.

TLC $R_f = 0.55$ (1:1 hexane:EtOAc).



(1*S*,2*S*,3*S*,5*R*)-6,9,9-Trimethoxy-2-methyl-5,7-bis(3-methylbut-2-en-1-yl)-2-(4-methylpent-3-en-1-yl)-8-oxobicyclo[3.3.1]non-6-en-3-yl methanesulfonate (349):

A CH₂Cl₂ (2 mL) solution of **343** (30. mg, 63 μmol, 1 equiv) and pyridine (31 μL, 0.38 mmol, 6 equiv) in a 10-mL pear-shaped flask was cooled to 0 °C, and methanesulfonyl chloride (25 μL, 0.32 mmol, 5 equiv) was added. The reaction was allowed to slowly warm to rt. After 1 d, the reaction was quenched at rt with sat. aq. NaHCO₃ and extracted thrice with EtOAc. The organic extracts were combined, washed with brine, dried over Na₂SO₄, filtered, and concentrated *in vacuo* to a pale yellow oil. Flash column chromatography (30 mL SiO₂, 9:1 hexane:EtOAc) afforded 13.7 mg (25 μmol, 39% yield) of **349** as a pale yellow oil.

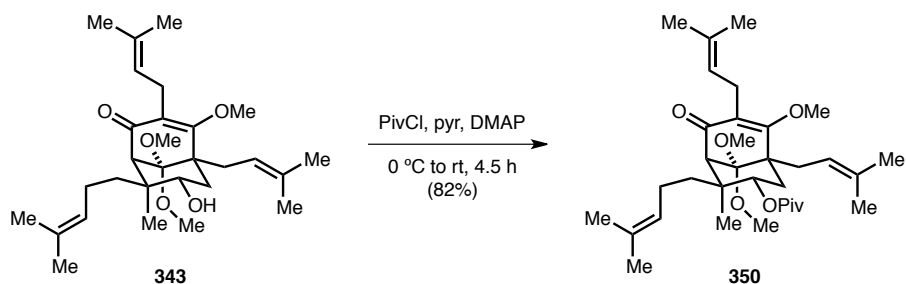
¹H NMR (600 MHz; C₆D₆) δ: 5.65 (t, *J* = 6.8 Hz, 1H), 5.36 (t, *J* = 6.8 Hz, 1H), 5.30 (t, *J* = 7.2 Hz, 1H), 4.93 (dd, *J* = 11.5, 5.8 Hz, 1H), 3.74 (s, 3H), 3.35 (dd, *J* = 15.0, 7.2 Hz, 1H), 3.14-3.11 (m, 2H), 3.03 (s, 3H), 2.97 (s, 3H), 2.91-2.83 (m, 1H), 2.70 (dd, *J* = 15.8, 6.9 Hz, 1H), 2.44 (dd, *J* = 15.8, 6.6 Hz, 1H), 2.37-2.29 (m, 2H), 2.18 (s, 3H), 2.11-2.05 (m, 1H), 1.83 (s, 3H), 1.71 (s, 3H), 1.70 (s, 3H), 1.70-1.63 (m, 7H), 1.59 (s, 3H), 1.40 (td, *J* = 13.0, 4.2 Hz, 1H), 1.29 (s, 3H).

¹³C NMR (125 MHz; C₆D₆) δ: 196.9, 173.5, 132.7, 131.7, 130.9, 125.1, 124.7, 122.85, 122.67, 103.0, 84.5, 62.4, 59.7, 54.1, 50.41, 50.34, 40.8, 39.6, 37.9, 34.7, 31.5, 26.07, 26.03, 25.85, 23.6, 21.9, 19.5, 18.08, 17.98, 17.84.

FTIR (thin film) ν_{max}: 2968, 2925, 2858, 1668, 1615, 1450, 1358, 1336, 1226, 1177, 1065, 933, 862 cm⁻¹.

HRMS-ESI (*m/z*): [M+Na]⁺ calculated for C₃₀H₄₈O₇S, 575.3013; found, 575.3017.

TLC R_f = 0.39 (8:2 hexane:EtOAc).



(1*S*,2*S*,3*S*,5*R*)-6,9,9-Trimethoxy-2-methyl-5,7-bis(3-methylbut-2-en-1-yl)-2-(4-methylpent-3-en-1-yl)-8-oxobicyclo[3.3.1]non-6-en-3-yl pivalate (350):

A CH₂Cl₂ (2 mL) solution of **343** (30. mg, 63 μ mol, 1 equiv), pyridine (31 μ L, 0.38 mmol, 6 equiv), and 4-(dimethylamino)pyridine (46 mg, 0.38 mmol, 6 equiv) in a 10-mL pear-shaped flask was cooled to 0 °C, and pivaloyl chloride (39 μ L, 0.32 mmol, 5 equiv) was added. The resulting colorless solution was allowed to slowly warm to rt. After stirring for 4.5 h, the reaction was quenched at rt with sat. aq. NaHCO₃ and extracted thrice with EtOAc. The organic extracts were combined, washed with brine, dried over Na₂SO₄, filtered, and concentrated *in vacuo* to an oily white residue. Flash column chromatography (25 mL SiO₂, 95:5 hexane:EtOAc) afforded 29 mg (52 μ mol, 82% yield) of **350** as a colorless oil.

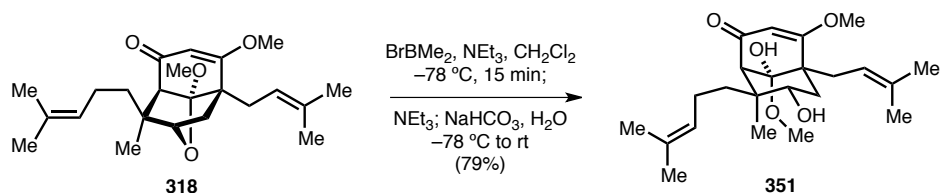
¹H NMR (600 MHz; C₆D₆) δ : 5.70 (t, *J* = 6.7 Hz, 1H), 5.40 (t, *J* = 6.6 Hz, 1H), 5.33 (t, *J* = 7.3 Hz, 1H), 5.18 (dd, *J* = 11.4, 5.5 Hz, 1H), 3.87 (s, 3H), 3.36 (dd, *J* = 15.2, 6.8 Hz, 1H), 3.17 (s, 2H), 3.09 (s, 3H), 3.04 (s, 3H), 2.75 (dd, *J* = 15.9, 6.8 Hz, 1H), 2.52 (dd, *J* = 15.9, 6.6 Hz, 1H), 2.14-2.05 (m, 3H), 1.82 (s, 3H), 1.70 (s, 3H), 1.69 (s, 3H), 1.65 (s, 3H), 1.61 (s, 6H), 1.55 (td, *J* = 13.1, 4.4 Hz, 1H), 1.45-1.36 (m, 4H), 1.11 (s, 9H).

¹³C NMR (125 MHz; C₆D₆) δ : 197.3, 177.6, 174.4, 132.4, 131.5, 130.4, 125.4, 124.6, 123.3, 122.9, 103.5, 76.3, 62.5, 59.9, 53.9, 50.44, 50.35, 41.1, 39.17, 39.05, 32.9, 31.7, 27.2, 26.10, 26.01, 25.8, 23.8, 22.1, 20.2, 18.1, 17.89, 17.84.

FTIR (thin film) ν_{max} : 2971, 2928, 2877, 1726, 1666, 1615, 1460, 1376, 1335, 1283, 1160, 1063 cm⁻¹.

HRMS-ESI (*m/z*): [M+Na]⁺ calculated for C₃₄H₅₄O₆, 581.3813; found, 581.3812.

TLC *R_f* = 0.66 (8:2 hexane:EtOAc).



(1*S*,5*R*,7*S*,8*S*,9*S*)-7,9-Dihydroxy-4,9-dimethoxy-8-methyl-5-(3-methylbut-2-en-1-yl)-8-(4-methylpent-3-en-1-yl)bicyclo[3.3.1]non-3-en-2-one (351):

A CH₂Cl₂ (3 mL) solution of **318** (99 mg, 0.26 mmol, 1 equiv) and triethylamine (22 μ L, 0.16 mmol, 0.6 equiv) in a 25-mL recovery flask was cooled to -78 $^{\circ}$ C, and a CH₂Cl₂ solution of bromodimethylborane (1.54 M, 1.0 mL, 1.6 mmol, 6 equiv)⁶⁹⁰ was added slowly. After stirring the reaction at -78 $^{\circ}$ C for 15 min, it was sequentially quenched at -78 $^{\circ}$ C with NEt₃ (1 mL) and sat. aq. NaHCO₃. After warming the mixture to rt, it was extracted thrice with EtOAc. The organic extracts were combined, washed with H₂O and brine, dried over Na₂SO₄, filtered, and concentrated *in vacuo* to a yellow-orange oil. Flash column chromatography (30 mL SiO₂, 8:2 \rightarrow 7:3 hexane:EtOAc) afforded 81 mg (0.21 mmol, 79% yield) of **351** as a flocculent white solid.

¹H NMR (600 MHz; CDCl₃) δ : 5.48 (s, 1H), 5.26 (d, J = 11.5 Hz, 1H), 5.05 (t, J = 7.2 Hz, 1H), 3.75 (s, 3H), 3.62 (dd, J = 12.1, 5.3 Hz, 1H), 3.57 (s, 1H), 3.26 (s, 3H), 2.88-2.83 (m, 2H), 2.36 (tt, J = 12.7, 6.2 Hz, 1H), 2.25 (d, J = 14.3 Hz, 1H), 1.96 (t, J = 12.1 Hz, 1H), 1.90 (ddd, J = 19.4, 13.1, 6.7 Hz, 1H), 1.73 (s, 3H), 1.71-1.67 (m, 4H), 1.65 (s, 6H), 1.46 (td, J = 12.9, 4.7 Hz, 1H), 1.31-1.22 (br s, 1H), 1.12 (s, 3H), 1.06 (td, J = 12.9, 4.4 Hz, 1H).

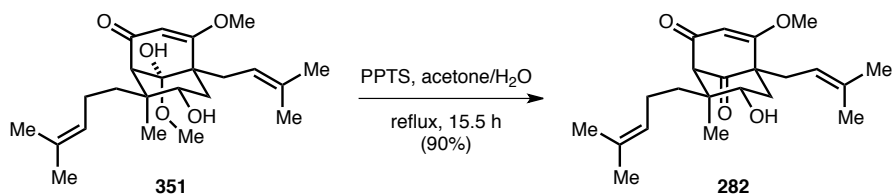
¹³C NMR (125 MHz; CDCl₃) δ : 198.2, 176.1, 137.4, 131.4, 125.0, 122.1, 104.1, 100.6, 73.2, 57.6, 56.6, 51.1, 48.6, 40.5, 39.2, 37.0, 30.0, 26.3, 25.9, 21.9, 18.01, 17.89, 17.0.

FTIR (thin film) ν_{max} : 3460 (br), 2969, 2928, 2859, 1648, 1602, 1451, 1375, 1221, 1084, 908, 731 cm⁻¹.

HRMS-ESI (m/z): [M+H]⁺ calculated for C₂₃H₃₆O₅, 393.2636; found, 393.2632.

TLC R_f = 0.50 (1:1 hexane:EtOAc).

⁶⁹⁰ A CH₂Cl₂ solution of bromodimethylborane was prepared as described in ref. 639b.



(1*S*,5*R*,7*S*,8*S*)-7-Hydroxy-4-methoxy-8-methyl-5-(3-methylbut-2-en-1-yl)-8-(4-methylpent-3-en-1-yl)bicyclo[3.3.1]non-3-ene-2,9-dione (282):

A 4:1 acetone:H₂O (4 mL) solution of **351** and pyridinium *para*-toluenesulfonate (208 mg, 0.83 mmol, 5 equiv) in a 10-mL recovery flask outfitted with a reflux condenser was heated to reflux. After stirring at reflux for 15.5 h, the reaction was cooled to rt, diluted with H₂O, and extracted thrice with 1:1 hexane:EtOAc. The organic extracts were combined, sequentially washed with H₂O and brine, dried over Na₂SO₄, filtered, and concentrated *in vacuo* to a pale yellow oil. Flash column chromatography (20 mL SiO₂, 7:3 hexane:EtOAc) afforded 54 mg (0.15 mmol, 90% yield) of **282** as a white flocculent solid.

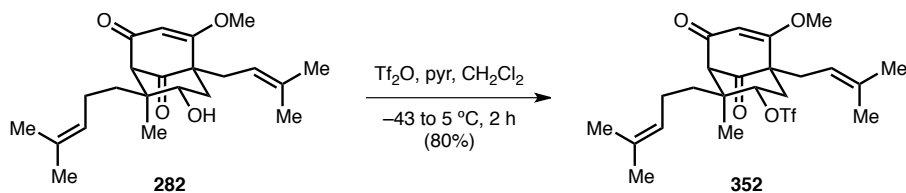
¹H NMR (600 MHz; CDCl₃) δ: 5.68 (s, 1H), 5.09 (t, *J* = 7.2 Hz, 1H), 4.98 (t, *J* = 7.0 Hz, 1H), 3.83–3.81 (m, 1H), 3.75 (s, 3H), 3.19 (s, 1H), 2.50 (dd, *J* = 14.6, 6.4 Hz, 1H), 2.40 (dd, *J* = 14.6, 7.6 Hz, 1H), 2.35 (tt, *J* = 12.6, 6.8 Hz, 1H), 2.12 (dd, *J* = 13.3, 5.4 Hz, 1H), 1.92 (tt, *J* = 12.6, 6.5 Hz, 1H), 1.76 (dd, *J* = 13.3, 11.6 Hz, 1H), 1.67 (s, 3H), 1.66 (s, 3H), 1.65 (s, 3H), 1.65 (s, 3H), 1.56 (td, *J* = 12.9, 4.8 Hz, 1H), 1.32 (td, *J* = 12.8, 4.7 Hz, 1H), 0.91 (s, 3H).

¹³C NMR (125 MHz; CDCl₃) δ: 205.2, 193.1, 177.5, 134.6, 132.2, 124.3, 119.0, 106.1, 72.1, 69.2, 57.1, 56.1, 45.9, 39.4, 38.1, 29.5, 26.1, 25.9, 21.8, 18.1, 17.9, 15.7.

FTIR (thin film) ν_{max} : 3433 (br), 2969, 2915, 2858, 1735, 1649, 1589, 1448, 1352, 1228, 1193, 1052, 1034, 843, 732 cm⁻¹.

HRMS–ESI (*m/z*): [M+H]⁺ calculated for C₂₂H₃₂O₄, 361.2373; found, 361.2378.

TLC R_f = 0.41 (1:1 hexane:EtOAc).



(1*S*,2*S*,3*S*,5*R*)-6-Methoxy-2-methyl-5-(3-methylbut-2-en-1-yl)-2-(4-methylpent-3-en-1-yl)-8,9-dioxobicyclo[3.3.1]non-6-en-3-yl trifluoromethanesulfonate (352):

A CH₂Cl₂ (20 mL) solution of **282** (253 mg, 0.702 mmol, 1 equiv) and pyridine (341 μ L, 4.21 mmol, 6 equiv) in a 50-mL recovery flask was cooled to -43°C , and trifluoromethanesulfonic anhydride (0.59 mL, 3.5 mmol, 5 equiv) was added. The resulting yellow slurry was allowed to slowly warm to 5°C over 2 h, whereupon it was quenched with sat. aq. NaHCO₃ and extracted thrice with EtOAc. The organic extracts were combined, washed with H₂O and brine, dried over Na₂SO₄, filtered, and concentrated *in vacuo* to a yellow oil. The oil was retaken in 8:2 hexane:EtOAc and passed through a plug of SiO₂, rinsing with 8:2 hexane:EtOAc. The filtrate was concentrated *in vacuo* to afford 277 mg (0.562 mmol, 80% yield) of **352** as a yellow-orange oil.

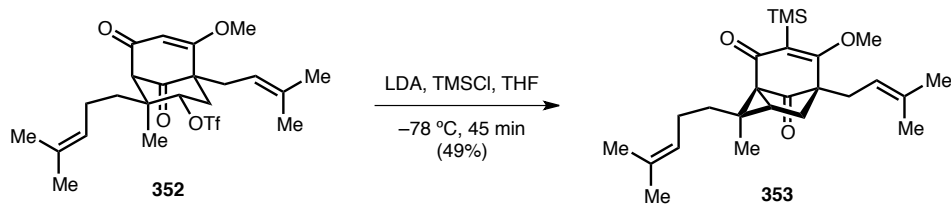
¹H NMR (600 MHz; C₆D₆) δ : 5.32 (s, 1H), 5.19-5.15 (m, 2H), 5.07 (dd, $J = 11.6, 5.5$ Hz, 1H), 3.41 (s, 1H), 2.66 (s, 3H), 2.64-2.57 (m, 1H), 2.45 (dd, $J = 14.4, 6.6$ Hz, 1H), 2.30-2.25 (m, 2H), 1.85 (dd, $J = 12.9, 11.9$ Hz, 1H), 1.81-1.76 (m, 1H), 1.74 (s, 3H), 1.65 (t, $J = 8.4$ Hz, 2H), 1.62 (s, 3H), 1.55 (s, 3H), 1.54 (s, 3H), 0.75 (s, 3H).

¹³C NMR (125 MHz; C₆D₆) δ : 201.6, 189.9, 175.4, 134.9, 132.6, 123.6, 118.8, 106.3, 90.6, 68.8, 56.4, 55.3, 45.3, 37.8, 36.6, 29.5, 25.86, 25.80, 21.7, 17.91, 17.82, 16.3.

¹⁹F NMR (470 MHz; C₆D₆) δ : -75.61 (s, 3F).

FTIR (thin film) ν_{max} : 2969, 2925, 2858, 1738, 1654, 1636, 1592, 1434, 1214, 1138, 922, 820, 602 cm⁻¹.

HRMS–ESI (m/z): $[\text{M}+\text{H}]^{+}$ calculated for C₂₃H₃₁F₃O₆S, 493.1866; found, 493.1865.

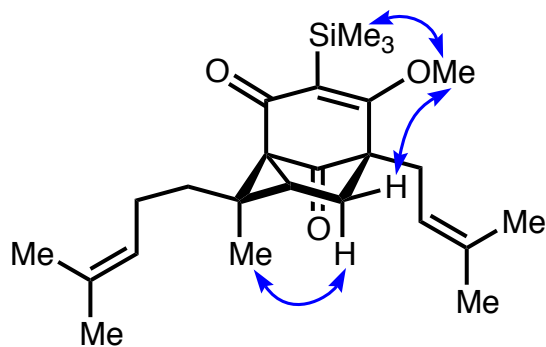


(1*S*,2*S*,3*R*,5*R*)-6-Methoxy-2-methyl-5-(3-methylbut-2-en-1-yl)-2-(4-methylpent-3-en-1-yl)-7-(trimethylsilyl)tricyclo[3.3.1.0^{1,3}]non-6-ene-8,9-dione (353):

A THF (12 mL) solution of **352** (277 mg, 0.562 mmol, 1 equiv) in a 25-mL recovery flask was cooled to $-78\text{ }^{\circ}\text{C}$, and chlorotrimethylsilane (3.6 mL, 28 mmol, 50 equiv) and a THF solution of lithium diisopropylamide (0.50 M, 5.6 mL, 2.8 mmol, 5 equiv) were added sequentially. After stirring the resulting orange solution at $-78\text{ }^{\circ}\text{C}$ for 45 min, it was quenched at $-78\text{ }^{\circ}\text{C}$ with sat. aq. NaHCO_3 . The mixture was warmed to rt and extracted thrice with EtOAc. The organic extracts were combined, sequentially washed with H_2O and brine, dried over Na_2SO_4 , filtered, and concentrated *in vacuo* to a yellow oil. Flash column chromatography (75 mL SiO_2 , 95:5 hexane:EtOAc) afforded 114 mg (0.27 mmol, 49% yield) of **353** as a pale yellow oil.

^1H NMR (600 MHz; C_6D_6) δ : 5.42 (t, $J = 7.4\text{ Hz}$, 1H), 5.29 (t, $J = 7.1\text{ Hz}$, 1H), 3.23 (s, 3H), 2.60 (dd, $J = 15.1, 6.4\text{ Hz}$, 1H), 2.51-2.47 (m, 2H), 2.19 (tt, $J = 12.5, 6.2\text{ Hz}$, 1H), 1.87 (ddd, $J = 13.0, 12.5, 5.2\text{ Hz}$, 1H), 1.80 (ddd, $J = 13.5, 11.2, 6.2\text{ Hz}$, 1H), 1.75 (dd, $J = 14.0, 5.4\text{ Hz}$, 1H), 1.69-1.67 (m, 4H), 1.66 (s, 3H), 1.62 (s, 3H), 1.55 (s, 3H), 1.08 (s, 3H), 0.99 (dd, $J = 7.9, 5.4\text{ Hz}$, 1H), 0.36 (s, 9H).

^{13}C NMR (125 MHz; C_6D_6) δ : 200.3, 194.8, 184.3, 134.5, 131.64, 131.63, 124.7, 119.6, 74.2, 61.9, 56.9, 48.1, 38.8, 37.7, 27.8, 26.29, 26.18, 25.905, 25.898, 18.00, 17.85, 16.4, 0.8.

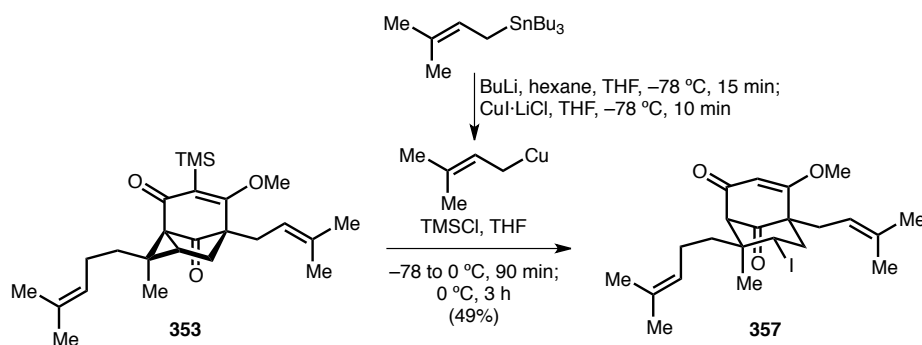


Key 1D nOe correlations.

FTIR (thin film) ν_{max} : 2968, 2918, 2860, 1762, 1664, 1523, 1451, 1438, 1386, 1233, 1201, 1157, 1042, 962, 845, 761, 691 cm^{-1} .

HRMS–ESI (m / z): $[\text{M}+\text{H}]^+$ calculated for $\text{C}_{25}\text{H}_{38}\text{O}_3\text{Si}$, 415.2663; found, 415.2650.

TLC R_f = 0.64 (9:1 hexane:EtOAc).



(1*S*,5*R*,7*S*,8*S*)-7-Iodo-4-methoxy-8-methyl-5-(3-methylbut-2-en-1-yl)-8-(4-methylpent-3-en-1-yl)bicyclo[3.3.1]non-3-ene-2,9-dione (357):

A mixture of copper(I) iodide (20. mg, 0.10 mmol, 30.7 equiv) and lithium chloride (5.3 mg, 0.12 mmol, 36.7 equiv) in a 10-mL recovery flask was subjected to three cycles of heat gun drying under vacuum and purging with Ar. The mixture was subsequently taken up in THF (0.5 mL) and stirred at rt for 3 min. Meanwhile, a THF (1 mL) solution of tributylprenalstannane (37 mg, 0.10 mmol, 30.4 equiv) in a 10-mL pear-shaped flask was cooled to $-78\text{ }^{\circ}\text{C}$, and a hexane solution of butyllithium (1.56 M, 63 μL , 99 μmol , 29.2 equiv) was added. After stirring the resulting bright yellow solution at $-78\text{ }^{\circ}\text{C}$ for 15 min, it was transferred via dry ice-cooled cannula to the copper(I) iodide-lithium chloride solution cooled to $-78\text{ }^{\circ}\text{C}$. After stirring the resulting brown-red solution at $-78\text{ }^{\circ}\text{C}$ for 10 min, chlorotrimethylsilane (22 μL , 0.17 mmol, 51.0 equiv), a THF (0.25 mL) solution of **353** (1.4 mg, 3.4 μmol , 1 equiv), and a THF (0.25 mL) rinse of the flask that contained **353** were added in quick succession. The reaction was then allowed to slowly warm to $0\text{ }^{\circ}\text{C}$ over 90 min and was stirred at $0\text{ }^{\circ}\text{C}$ for 2 h, at which point the reaction turned black. After stirring for an additional 1 h at $0\text{ }^{\circ}\text{C}$, the resulting colorless solution was quenched at $0\text{ }^{\circ}\text{C}$ with sat. aq. NH_4Cl and extracted thrice with EtOAc. The organic extracts were combined, sequentially washed with H_2O and brine, dried over Na_2SO_4 , filtered, and concentrated *in vacuo* to a pale yellow residue. Preparatory thin-layer chromatography (1 \times 8:2 hexane:EtOAc) afforded 0.8 mg (2 μmol , 50% yield) of **357** as a colorless residue.

$^1\text{H NMR}$ (600 MHz; CDCl_3) δ : 5.76 (s, 1H), 5.08 (t, $J = 7.1\text{ Hz}$, 1H), 4.97 (t, $J = 6.9\text{ Hz}$, 1H), 4.35 (dd, $J = 12.8, 5.0\text{ Hz}$, 1H), 3.77 (s, 3H), 3.39 (s, 1H), 2.52-2.46 (m, 2H), 2.44-2.36 (m, 3H), 1.89 (tt, $J = 12.4,$

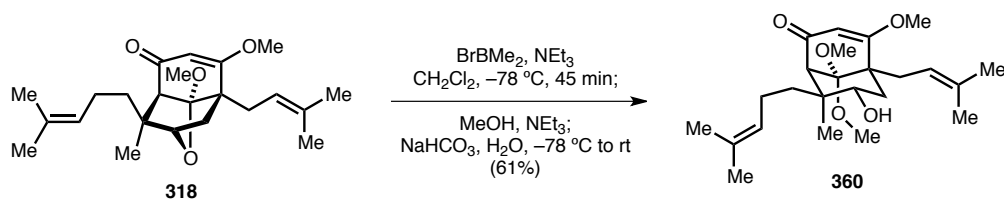
6.0 Hz, 1H), 1.68 (s, 3H), 1.68 (s, 3H), 1.65 (s, 6H), 1.60 (td, $J = 12.9, 4.3$ Hz, 1H), 1.55 (s, 3H), 1.28 (td, $J = 12.9, 4.3$ Hz, 1H), 1.05 (s, 3H).

^{13}C NMR (125 MHz; CDCl_3) δ : 203.7, 192.6, 176.1, 134.9, 132.4, 123.7, 118.7, 106.6, 67.7, 59.5, 57.2, 46.8, 45.1, 41.9, 37.1, 29.2, 26.15, 25.95, 21.9, 21.0, 18.2, 17.9.

FTIR (thin film) ν_{max} : 2962, 2919, 2853, 1736, 1655, 1595, 1453, 1368, 1223, 1191 cm^{-1} .

HRMS–ESI (m/z): $[\text{M}+\text{Na}]^+$ calculated for $\text{C}_{22}\text{H}_{31}\text{IO}_3$, 493.1210; found, 493.1193.

TLC $R_f = 0.41$ (8:2 hexane:EtOAc).



(1*S*,5*R*,7*S*,8*S*)-7-Hydroxy-4,9,9-trimethoxy-8-methyl-5-(3-methylbut-2-en-1-yl)-8-(4-methylpent-3-en-1-yl)bicyclo[3.3.1]non-3-en-2-one (360):

A CH_2Cl_2 (6 mL) solution of **318** (456 mg, 1.22 mmol, 1 equiv) and triethylamine (102 μL , 0.731 mmol, 0.6 equiv) in a 20-mL scintillation vial was cooled to $-78\text{ }^\circ\text{C}$, and a CH_2Cl_2 solution of bromodimethylborane (1.26 M, 5.8 mL, 7.3 mmol, 6 equiv)⁶⁹¹ was added slowly. The resulting orange-red solution was stirred at $-78\text{ }^\circ\text{C}$ for 45 min and subsequently quenched at $-78\text{ }^\circ\text{C}$ through the addition of 1:1 MeOH: NEt_3 (8 mL). The reaction was then poured onto sat. aq. NaHCO_3 and extracted thrice with EtOAc. The organic extracts were combined, sequentially washed with 2 N HCl, sat. aq. NaHCO_3 , and brine, dried over Na_2SO_4 , filtered, and concentrated *in vacuo* to a yellow oil. Flash column chromatography (150 mL SiO_2 , 8:2 hexane:EtOAc) afforded 303 mg (0.745 mmol, 61% yield) of **360** as a flocculent yellow solid.

^1H NMR (600 MHz; CDCl_3) δ : 5.40 (s, 1H), 5.34 (t, $J = 7.2\text{ Hz}$, 1H), 5.04 (t, $J = 7.2\text{ Hz}$, 1H), 3.67 (s, 3H), 3.57-3.54 (m, 1H), 3.35 (s, 3H), 3.23 (s, 3H), 2.89 (s, 1H), 2.68 (dd, $J = 15.3, 8.0\text{ Hz}$, 1H), 2.39-2.33 (m, 2H), 1.92-1.88 (m, 1H), 1.84 (dd, $J = 13.1, 12.1\text{ Hz}$, 1H), 1.72 (dd, $J = 13.1, 5.2\text{ Hz}$, 1H), 1.68 (s, 3H), 1.64 (s, 6H), 1.61 (s, 3H), 1.45 (td, $J = 12.9, 4.8\text{ Hz}$, 1H), 1.37 (m, 1H), 1.11 (s, 3H), 1.04 (td, $J = 12.9, 4.5\text{ Hz}$, 1H).

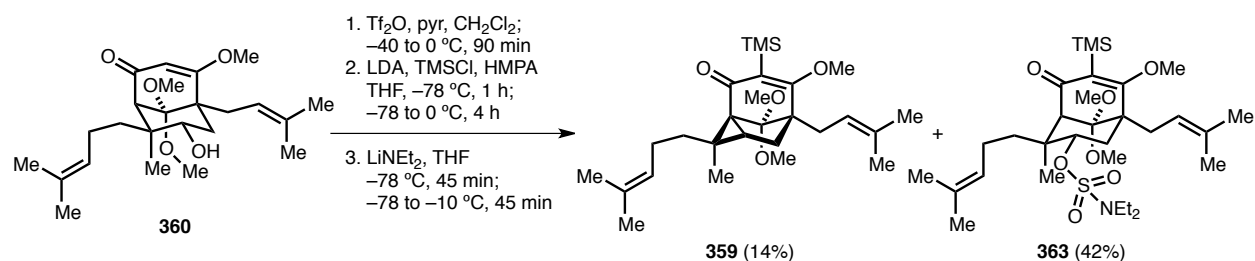
^{13}C NMR (125 MHz; CDCl_3) δ : 198.1, 179.0, 131.9, 131.4, 125.1, 122.1, 103.9, 103.0, 73.5, 59.0, 56.5, 52.4, 51.2, 50.6, 40.6, 39.5, 36.8, 35.9, 30.4, 26.2, 25.9, 21.9, 18.1, 17.9.

FTIR (thin film) ν_{max} : 3455 (br), 2967, 2925, 2859, 1654, 1600, 1454, 1374, 1350, 1224, 1060 cm^{-1} .

HRMS-ESI (m/z): $[\text{M}+\text{Na}]^+$ calculated for $\text{C}_{24}\text{H}_{38}\text{O}_5$, 429.2611; found, 429.2609.

TLC $R_f = 0.49$ (1:1 hexane:EtOAc).

⁶⁹¹ A CH_2Cl_2 solution of bromodimethylborane was prepared as described in ref. 639b.



A CH_2Cl_2 (3 mL) solution of **360** (56.8 mg, 0.140 mmol, 1 equiv) and pyridine (68 μL , 0.84 mmol, 6 equiv) in a 10-mL recovery flask was cooled to -40 $^\circ\text{C}$, and trifluoromethanesulfonic anhydride (118 μL , 0.699 mmol, 5 equiv) was added. The resulting yellow slurry was allowed to slowly warm to 0 $^\circ\text{C}$ over 90 min, whereupon it was quenched at 0 $^\circ\text{C}$ with sat. aq. NaHCO_3 and extracted thrice with 8:2 hexane:EtOAc. The organic extracts were combined, washed with brine, dried over Na_2SO_4 , filtered, and concentrated to an orange-brown oil. A portion of this oil (30. mg, 56 μmol , 1 equiv) was dissolved in THF (1 mL) in a 10-mL test tube, cooled to -78 $^\circ\text{C}$, and treated sequentially with chlorotrimethylsilane (353 μL , 2.7 mmol, 50 equiv), a freshly prepared THF solution of lithium diisopropylamide (0.50 M, 0.56 mL, 0.28 mmol, 5 equiv), and hexamethylphosphoramide (53 μL , 0.31 mmol, 5.5 equiv). The orange slurry was stirred at -78 $^\circ\text{C}$ for 1 h and was then allowed to warm to 0 $^\circ\text{C}$ over 4 h. The reaction was then quenched at 0 $^\circ\text{C}$ with sat. aq. NaHCO_3 and extracted thrice with 8:2 hexane:EtOAc. The organic extracts were combined, sequentially washed five times with H_2O and once with brine, dried over Na_2SO_4 , filtered, and concentrated *in vacuo* to an orange oil. This oil was dissolved in THF (1 mL) in a 10-mL test tube, cooled to -78 $^\circ\text{C}$, and treated with a freshly prepared THF solution of lithium diethylamide (0.50 M, 1.1 mL, 0.56 mmol, 10 equiv). The brown-orange solution was stirred at -78 $^\circ\text{C}$ for 45 min and subsequently allowed to slowly warm to -10 $^\circ\text{C}$ over 45 min. The resulting red solution was then quenched at -10 $^\circ\text{C}$ with sat. aq. NaHCO_3 and extracted thrice with EtOAc. The organic extracts were combined, sequentially washed with H_2O and brine, dried over Na_2SO_4 , filtered, and concentrated *in vacuo* to a brown oil. Preparatory thin-layer chromatography (1 \times 9:1 hexane:EtOAc containing 1% NEt_3) afforded 3.5 mg (7.6 μmol , 14% yield from **360**) of **359** as a colorless oil and 14.5 mg (23.6 μmol , 42% yield from **360**) of **363** as a pale yellow oil.

(1S,2R,3S,5R)-6,9,9-Trimethoxy-2-methyl-5-(3-methylbut-2-en-1-yl)-2-(4-methylpent-3-en-1-yl)-7-(trimethylsilyl)tricyclo[3.3.1.0^{1,3}]non-6-en-8-one (359):

¹H NMR (600 MHz; C₆D₆) δ: 5.54 (t, *J* = 7.1 Hz, 1H), 5.47 (t, *J* = 7.2 Hz, 1H), 3.37 (s, 3H), 2.99 (s, 3H), 2.97 (s, 3H), 2.77-2.71 (m, 2H), 2.42 (dd, *J* = 15.0, 7.0 Hz, 1H), 2.41-2.34 (m, 1H), 2.06 (dd, *J* = 13.3, 6.6 Hz, 1H), 1.84 (td, *J* = 12.3, 5.2 Hz, 1H), 1.74 (s, 3H), 1.73-1.68 (m, 4H), 1.68 (m, 4H), 1.62 (s, 3H), 1.54 (s, 3H), 0.84 (t, *J* = 7.0 Hz, 1H), 0.48 (s, 9H).

¹³C NMR (125 MHz; C₆D₆) δ: 199.0, 184.4, 131.2, 131.0, 129.3, 125.6, 123.2, 110.1, 74.2, 64.1, 53.6, 52.3, 51.1, 50.6, 41.8, 38.1, 31.7, 28.3, 26.7, 26.00, 25.95, 17.89, 17.87, 16.5, 1.0.

FTIR (thin film) ν_{\max} : 2965, 2924, 2854, 1669, 1577, 1453, 1340, 1207, 1145, 1080 cm⁻¹.

HRMS–ESI (*m/z*): [M+Na]⁺ calculated for C₂₇H₄₄O₄Si, 483.2901; found, 483.2908.

TLC R_f = 0.68 (8:2 hexane:EtOAc).

(1S,2S,3S,5R)-6,9,9-Trimethoxy-2-methyl-5-(3-methylbut-2-en-1-yl)-2-(4-methylpent-3-en-1-yl)-8-oxo-7-(trimethylsilyl)bicyclo[3.3.1]non-6-en-3-yl diethylsulfamate (363):

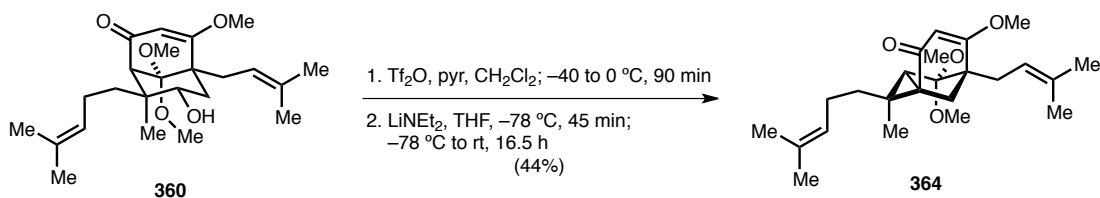
¹H NMR (500 MHz; C₆D₆) δ: 5.66 (t, *J* = 6.8 Hz, 1H), 5.40 (t, *J* = 7.2 Hz, 1H), 4.82 (dd, *J* = 12.0, 5.2 Hz, 1H), 3.79 (s, 3H), 3.08-2.94 (m, 12H), 2.74 (dd, *J* = 15.8, 7.0 Hz, 1H), 2.55-2.51 (m, 2H), 2.42 (t, *J* = 12.6 Hz, 1H), 2.15 (tt, *J* = 12.3, 6.0 Hz, 1H), 1.91 (td, *J* = 13.2, 4.4 Hz, 1H), 1.83 (s, 3H), 1.70 (s, 3H), 1.68 (s, 3H), 1.59-1.51 (m, 4H), 1.34 (s, 3H), 0.85 (t, *J* = 7.1 Hz, 6H), 0.42 (s, 9H).

¹³C NMR (125 MHz; C₆D₆) δ: 201.1, 187.2, 131.6, 131.1, 128.6, 125.2, 122.7, 103.3, 84.3, 65.0, 60.10, 60.07, 55.0, 50.4, 42.7, 41.0, 39.9, 34.0, 31.4, 26.08, 25.99, 22.1, 20.6, 19.7, 17.97, 17.87, 14.2, 13.3, 1.0.

FTIR (thin film) ν_{\max} : 2971, 2937, 1660, 1600, 1458, 1358, 1345, 1222, 1206, 1165, 1102, 1061, 929, 830 cm⁻¹.

HRMS–ESI (*m/z*): [M+Na]⁺ calculated for C₃₁H₅₅NO₇SSi, 636.3361; found, 636.3371.

TLC R_f = 0.55 (8:2 hexane:EtOAc).

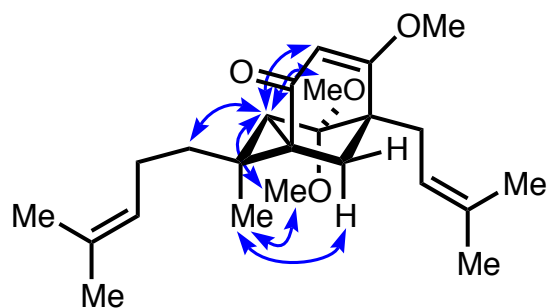


(1*R*,2*S*,3*R*,5*R*)-4,4,6-Trimethoxy-2-methyl-5-(3-methylbut-2-en-1-yl)-2-(4-methylpent-3-en-1-yl)tricyclo[3.3.1.0^{1,3}]non-6-en-8-one (364):

A CH₂Cl₂ (3 mL) solution of **360** (56.8 mg, 0.140 mmol, 1 equiv) and pyridine (68 μ L, 0.84 mmol, 6 equiv) in a 10-mL recovery flask was cooled to -40 $^{\circ}$ C, and trifluoromethanesulfonic anhydride (118 μ L, 0.699 mmol, 5 equiv) was added. The resulting yellow slurry was allowed to slowly warm to 0 $^{\circ}$ C over 90 min whereupon it was quenched at 0 $^{\circ}$ C with sat. aq. NaHCO₃ and extracted thrice with 8:2 hexane:EtOAc. The organic extracts were combined, washed with brine, dried over Na₂SO₄, filtered, and concentrated to an orange-brown oil. A portion of this oil (23 mg, 43 μ mol, 1 equiv) was dissolved in THF (1 mL) in a 10-mL test tube, cooled to -78 $^{\circ}$ C, and treated with a freshly prepared THF solution of lithium diisopropylamide (0.50 M, 0.85 mL, 0.43 mmol, 10 equiv). The resulting brown-orange solution was stirred at -78 $^{\circ}$ C for 45 min and then allowed to slowly warm to rt. After stirring the resulting dark red solution for 16.5 h, it was quenched at rt with sat. aq. NaHCO₃ and extracted thrice with EtOAc. The organic extracts were combined, washed with brine, dried over Na₂SO₄, filtered, and concentrated *in vacuo* to a brown oil. Preparatory thin-layer chromatography (1 \times 8:2 hexane:EtOAc) afforded 7.4 mg (19 μ mol, 44% yield from **360**) of **364** as a pale yellow oil.

¹H NMR (600 MHz; C₆D₆) δ : 5.33 (s, 1H), 5.31 (t, J = 7.2 Hz, 1H), 5.11 (t, J = 7.4 Hz, 1H), 3.24 (s, 3H), 3.05 (s, 3H), 3.03 (s, 3H), 2.84 (dd, J = 14.6, 7.2 Hz, 1H), 2.80 (dd, J = 14.6, 9.0 Hz, 1H), 2.60-2.52 (m, 1H), 2.24-2.18 (m, 1H), 2.00 (d, J = 12.8 Hz, 1H), 1.95-1.86 (m, 2H), 1.78 (d, J = 12.8 Hz, 1H), 1.67 (s, 3H), 1.66 (s, 3H), 1.63 (s, 3H), 1.56 (s, 3H), 1.29 (s, 3H), 1.16 (d, J = 0.9 Hz, 1H).

¹³C NMR (125 MHz; C₆D₆) δ : 13-C NMR (126 MHz; Benzene): δ 195.9, 179.9, 132.5, 131.2, 125.1, 121.8, 111.6, 105.4, 72.2, 55.7, 50.9, 50.0, 48.6, 44.5, 43.8, 39.3, 38.5, 28.6, 26.2, 25.97, 25.91, 18.0, 17.8, 14.7.

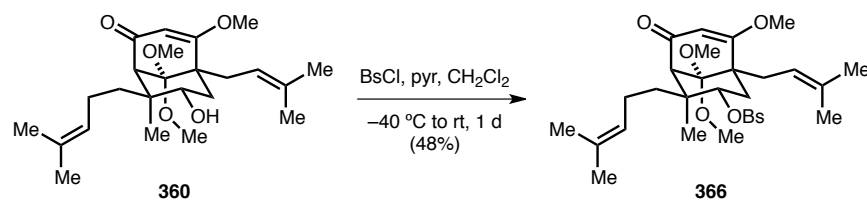


Key 1D nOe correlations.

FTIR (thin film) ν_{max} : 2965, 2926, 2857, 1675, 1575, 1440, 1339, 1225, 1173, 1141, 1063, 997, 834 cm^{-1} .

HRMS–ESI (m / z): $[\text{M}+\text{Na}]^+$ calculated for $\text{C}_{24}\text{H}_{36}\text{O}_4$, 411.2506; found, 411.2512.

TLC R_f = 0.34 (8:2 hexane:EtOAc).



(1*S*,2*S*,3*S*,5*R*)-6,9,9-Trimethoxy-2-methyl-5-(3-methylbut-2-en-1-yl)-2-(4-methylpent-3-en-1-yl)-8-oxobicyclo[3.3.1]non-6-en-3-yl benzenesulfonate (366):

A CH₂Cl₂ (1 mL) solution of **360** (16.1 mg, 39.6 μmol, 1 equiv) and pyridine (19 μL, 0.24 mmol, 6 equiv) in a 10-mL recovery flask was cooled to −40 °C, and benzenesulfonyl chloride (25 μL, 0.20 mmol, 5 equiv) was added. The resulting yellow solution was allowed to slowly warm to rt. After stirring for 1 d, the reaction was quenched at rt with sat. aq. NaHCO₃ and extracted thrice with EtOAc. The organic extracts were combined, sequentially washed with H₂O and brine, dried over Na₂SO₄, filtered, and concentrated *in vacuo* to a pale yellow oil. Flash column chromatography (30 mL SiO₂, 96:4 PhH:EtOAc) afforded 10.5 mg (19.2 μmol, 48% yield) of **366** as a colorless oil.

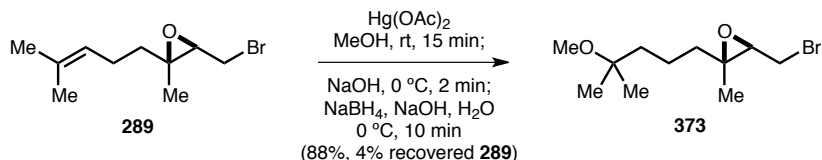
¹H NMR (600 MHz; C₆D₆) δ: 7.79 (d, *J* = 7.9 Hz, 2H), 6.92 (t, *J* = 7.5 Hz, 1H), 6.84 (t, *J* = 7.7 Hz, 2H), 5.44 (t, *J* = 6.9 Hz, 1H), 5.37 (s, 1H), 5.16 (t, *J* = 7.2 Hz, 1H), 4.84 (dd, *J* = 12.0, 5.3 Hz, 1H), 3.05 (s, 1H), 2.97 (s, 3H), 2.96 (s, 3H), 2.92 (s, 3H), 2.87-2.79 (m, 1H), 2.64 (dd, *J* = 15.6, 7.6 Hz, 1H), 2.32 (dd, *J* = 15.6, 6.3 Hz, 1H), 2.19 (dd, *J* = 14.5, 10.6 Hz, 1H), 2.01-1.93 (m, 2H), 1.79 (s, 3H), 1.66 (s, 6H), 1.50-1.46 (m, 4H), 1.32-1.24 (m, 4H).

¹³C NMR (125 MHz; C₆D₆) δ: 195.4, 177.3, 138.3, 133.1, 131.29, 131.14, 129.0, 125.2, 122.5, 103.68, 103.56, 85.7, 59.3, 55.9, 52.6, 50.7, 50.4, 40.8, 39.4, 33.9, 30.8, 26.10, 25.97, 21.9, 19.4, 17.9, 17.7.

FTIR (thin film) ν_{max}: 2965, 2925, 2857, 1655, 1599, 1448, 1363, 1223, 1186, 1097, 1186, 1097, 1050, 940, 853, 723, 689, 590 cm^{−1}.

HRMS–ESI (*m/z*): [M+H]⁺ calculated for C₃₀H₄₂O₇S, 547.2724; found, 547.2718.

TLC R_f = 0.30 (95:5 PhH:EtOAc).



(2S,3R)-3-(Bromomethyl)-2-(4-methoxy-4-methylpentyl)-2-methyloxirane (373):

A MeOH (110 mL) solution of mercury(II) acetate (10.3 g, 32.2 mmol, 1.5 equiv) in a 250-mL round-bottom flask was treated with **289** (5.00 g, 21.4 mmol, 1 equiv). After stirring the resulting white slurry at rt for 15 min, it was cooled to 0 °C and was treated with an aqueous solution of NaOH (3 M, 35 mL). After stirring the resulting bright orange slurry at 0 °C for 2 min, and a basic, aqueous solution of NaBH₄ (0.5 M NaBH₄ in 3 M NaOH aqueous solution, 35 mL) was added. The resulting gray slurry was stirred at 0 °C for 15 min, diluted with H₂O, and extracted thrice with 8:2 hexane:EtOAc. The organic extracts were combined, sequentially washed thrice with H₂O and once with brine, dried over Na₂SO₄, filtered, and concentrated *in vacuo* to a colorless oil. Flash column chromatography (250 mL SiO₂, 9:1 → 8:2 hexane:EtOAc) afforded 4.98 g (18.8 mmol, 88% yield) of **373** as a colorless oil as well as 187 mg (0.802 mmol, 3.7% recovery) of **289** as a colorless oil.

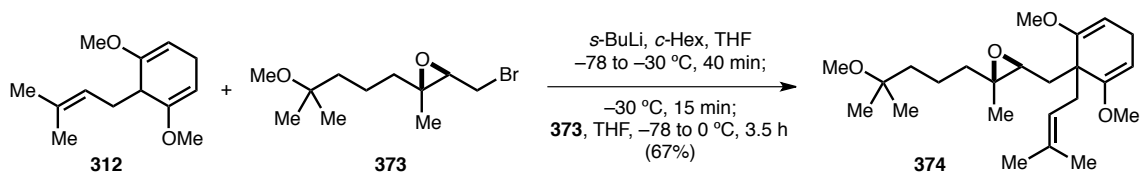
¹H NMR (600 MHz; CDCl₃) δ: 3.53 (dd, *J* = 10.4, 5.9 Hz, 1H), 3.24 (dd, *J* = 10.4, 7.7 Hz, 1H), 3.16 (s, 3H), 3.08 (dd, *J* = 7.7, 5.9 Hz, 1H), 1.67-1.62 (m, 1H), 1.48-1.40 (m, 5H), 1.30 (s, 3H), 1.13 (s, 6H).

¹³C NMR (125 MHz; CDCl₃) δ: 74.6, 63.3, 61.6, 49.4, 39.9, 38.8, 30.0, 25.1, 19.6, 16.3.

FTIR (thin film) ν_{max} : 2971, 2948, 2915, 2826, 1465, 1432, 1382, 1364, 1253, 1221, 1205, 1148, 1083, 891, 652 cm⁻¹.

HRMS–ESI (*m/z*): [M+Na]⁺ calculated for C₁₁H₂₁BrO₂, 287.0617; found, 287.0621.

TLC R_f = 0.18 (9:1 hexane:EtOAc).



(2*S*,3*S*)-3-((2,6-Dimethoxy-1-(3-methylbut-2-en-1-yl)cyclohexa-2,5-dien-1-yl)methyl)-2-(4-methoxy-4-methylpentyl)-2-methyloxirane (374):

A THF (100 mL) solution of **312** (4.35 g, 20.9 mmol, 1 equiv) in a 250-mL round-bottom flask was cooled to $-78\text{ }^{\circ}\text{C}$, and a *c*-Hex solution of *sec*-butyllithium (1.21 M, 21.6 mL, 26.1 mmol, 1.25 equiv) was added slowly over 5 min. The resulting yellow slurry was allowed to slowly warm from $-78\text{ }^{\circ}\text{C}$ to $-30\text{ }^{\circ}\text{C}$ over 40 min and then stirred at $-30\text{ }^{\circ}\text{C}$ for 15 min. The resulting red-orange slurry was cooled to $-78\text{ }^{\circ}\text{C}$, and a THF (20 mL) solution of **373** (4.98 g, 18.8 mmol, 0.9 equiv) was added followed by two THF (10 mL each) rinses. The resulting cream-colored slurry was allowed to slowly warm to $0\text{ }^{\circ}\text{C}$. After stirring for 3.5 h, the reaction was quenched at $0\text{ }^{\circ}\text{C}$ with H_2O and extracted thrice with EtOAc. The organic extracts were combined, sequentially washed with H_2O and brine, dried over Na_2SO_4 , filtered, and concentrated *in vacuo* to a yellow oil. Flash column chromatography (400 mL SiO_2 , 9:1 \rightarrow 8:2 hexane:EtOAc) afforded 4.95 g (12.6 mmol, 67% yield) of **374** as a colorless oil.

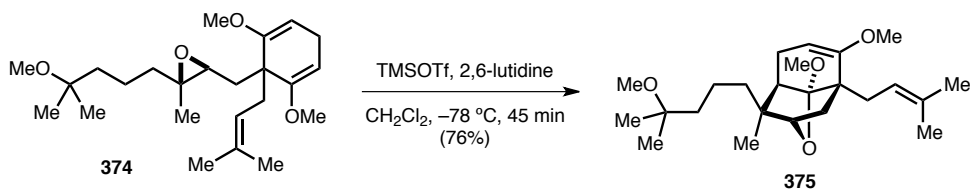
^1H NMR (600 MHz; CDCl_3) δ : 4.89 (t, $J = 7.3\text{ Hz}$, 1H), 4.76 (t, $J = 3.6\text{ Hz}$, 1H), 4.72 (t, $J = 3.6\text{ Hz}$, 1H), 3.51 (s, 3H), 3.46 (s, 3H), 3.15 (s, 3H), 2.75 (t, $J = 3.6\text{ Hz}$, 2H), 2.61 (dd, $J = 8.0, 3.9\text{ Hz}$, 1H), 2.34-2.27 (m, 2H), 2.03 (dd, $J = 13.7, 3.9\text{ Hz}$, 1H), 1.76 (dd, $J = 13.7, 8.0\text{ Hz}$, 1H), 1.62 (s, 3H), 1.54 (s, 3H), 1.54-1.49 (m, 1H), 1.42-1.37 (m, 2H), 1.35-1.30 (m, 2H), 1.27-1.22 (m, 1H), 1.17 (s, 3H), 1.12 (s, 6H).

^{13}C NMR (125 MHz; CDCl_3) δ : 154.09, 154.02, 132.5, 120.7, 93.05, 92.94, 74.7, 61.47, 61.27, 54.5, 54.1, 49.3, 46.2, 40.11, 39.91, 34.6, 34.1, 26.1, 25.23, 25.17, 24.2, 19.8, 17.9, 16.8.

FTIR (thin film) ν_{max} : 2972, 2912, 2828, 1695, 1659, 1453, 1381, 1364, 1223, 1206, 1151, 1124, 1084, 1033, 973, 952, 849, 779, 689 cm^{-1} .

HRMS-ESI (m/z): $[\text{M}+\text{H}]^+$ calculated for $\text{C}_{24}\text{H}_{40}\text{O}_4$, 393.2999; found, 393.3000.

TLC $R_f = 0.37$ (8:2 hexane:EtOAc).

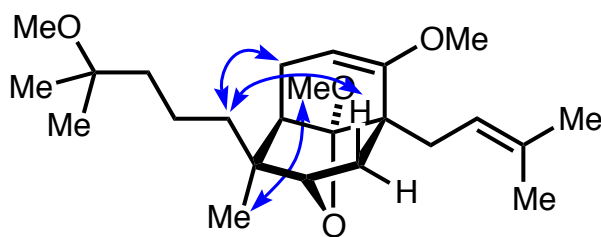


(2*S*,3*S*,3*aR*,7*R*,7*aS*)-6,7*a*-Dimethoxy-3-(4-methoxy-4-methylpentyl)-3-methyl-7-(3-methylbut-2-en-1-yl)-2,3,3*a*,4,7,7*a*-hexahydro-2,7-methanobenzofuran (375):

A THF (63 mL) solution of **374** (4.91 g, 12.5 mmol, 1 equiv) and 2,6-lutidine (3.0 mL, 38 mmol, 3 equiv) in a 200-mL round-bottom flask was cooled to $-78\text{ }^{\circ}\text{C}$, and trimethylsilyl trifluoromethanesulfonate (4.5 mL, 25 mmol, 2 equiv) was added. The resulting golden yellow solution was stirred at $-78\text{ }^{\circ}\text{C}$ for 45 min and subsequently quenched at $-78\text{ }^{\circ}\text{C}$ with sat. aq. NaHCO_3 . The mixture was warmed to rt and extracted thrice with CH_2Cl_2 . The organic extracts were combined, sequentially washed with 1 N HCl, H_2O , and brine, dried over Na_2SO_4 , filtered, and concentrated *in vacuo* to a pale yellow oil. Flash column chromatography (300 mL SiO_2 , 95:5 \rightarrow 9:1 hexane:EtOAc) afforded 3.74 g (9.52 mmol, 76% yield) of **375** as a pale yellow oil.

^1H NMR (600 MHz; CDCl_3) δ : 5.33 (t, $J = 7.1$ Hz, 1H), 4.51 (dd, $J = 5.5, 2.1$ Hz, 1H), 3.74 (d, $J = 4.6$ Hz, 1H), 3.47 (s, 3H), 3.45 (s, 3H), 3.15 (s, 3H), 2.34 (dd, $J = 14.7, 6.8$ Hz, 1H), 2.21 (dd, $J = 6.8, 1.8$ Hz, 1H), 2.18 (dd, $J = 6.7, 2.3$ Hz, 1H), 2.03 (m, 1H), 2.02-1.99 (m, 1H), 1.77 (dd, $J = 12.0, 4.6$ Hz, 1H), 1.75 (d, $J = 12.0$ Hz, 1H), 1.69 (s, 3H), 1.60 (s, 3H), 1.42-1.28 (m, 4H), 1.18 (td, $J = 12.6, 3.0$ Hz, 1H), 1.12 (s, 3H), 1.11 (s, 3H), 1.11 (s, 3H), 1.03-0.95 (m, 1H).

^{13}C NMR (125 MHz; CDCl_3) δ : 158.6, 131.2, 123.6, 112.6, 90.5, 79.0, 74.6, 54.6, 51.4, 49.3, 46.5, 44.5, 41.9, 41.2, 39.3, 34.0, 32.8, 28.2, 26.4, 25.23, 25.15, 20.1, 18.5, 18.0.

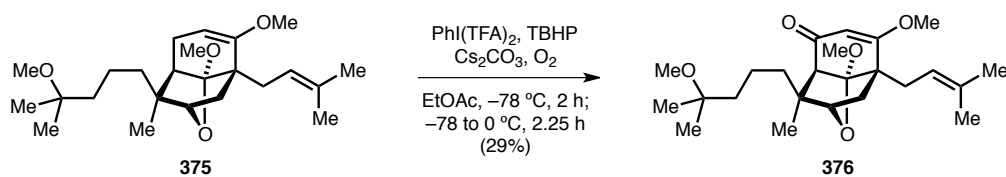


Key 1D nOe correlations.

FTIR (thin film) ν_{max} : 2968, 2839, 1670, 1451, 1374, 1363, 1208, 1166, 1078, 1006, 843, 805, 785 cm^{-1} .

HRMS–ESI (m / z): $[\text{M}+\text{Na}]^+$ calculated for $\text{C}_{24}\text{H}_{40}\text{O}_4$, 415.2819; found, 415.2832.

TLC R_f = 0.49 (8:2 hexane:EtOAc).



(2*S*,3*S*,3*aS*,7*R*,7*aS*)-6,7*a*-Dimethoxy-3-(4-methoxy-4-methylpentyl)-3-methyl-7-(3-methylbut-2-en-1-yl)-3,3*a*,7,7*a*-tetrahydro-2,7-methanobenzofuran-4(2*H*)-one (376):

An EtOAc⁶⁹² (30 mL) slurry of cesium carbonate (12.76 g, 36.2 mmol, 4 equiv), **375** (3.55 g, 9.04 mmol, 1 equiv), and a nonane solution of *tert*-butyl hydroperoxide (5.5 M, 6.6 mL, 36 mmol, 4 equiv) in a 3-neck 300-mL round-bottom flask was cooled to $-78\text{ }^{\circ}\text{C}$ with rapid O₂ bubbling, and an EtOAc (25 mL) solution of [bis(trifluoroacetoxy)iodo]benzene (11.67 g, 27.1 mmol, 3 equiv) was added dropwise over 30 min followed by an EtOAc (5 mL) rinse. After stirring the reaction at $-78\text{ }^{\circ}\text{C}$ for 2 h, it was allowed to slowly warm to $0\text{ }^{\circ}\text{C}$. After stirring the pink slurry for 2.25 h, O₂ bubbling was suspended, and the reaction was quenched at $0\text{ }^{\circ}\text{C}$ with sat. aq. Na₂S₂O₃. The resulting yellow slurry was stirred vigorously at rt for 45 min and then extracted thrice with EtOAc. The organic extracts were combined, sequentially washed with H₂O and brine, dried over Na₂SO₄, filtered, and concentrated *in vacuo* to a yellow oil. Flash column chromatography (300 mL SiO₂, 7:3 hexane:EtOAc) afforded 1.069 g (2.629 mmol, 29% yield) of **376** as a pale yellow oil.

¹H NMR (600 MHz; CDCl₃) δ : 5.33 (s, 1H), 5.29 (t, $J = 7.2\text{ Hz}$, 1H), 3.90 (d, $J = 5.7\text{ Hz}$, 1H), 3.70 (s, 3H), 3.46 (s, 3H), 3.12 (s, 3H), 2.67 (s, 1H), 2.41 (dd, $J = 14.9, 6.1\text{ Hz}$, 1H), 2.34 (dd, $J = 14.9, 8.0\text{ Hz}$, 1H), 2.00 (d, $J = 13.0\text{ Hz}$, 1H), 1.93 (dd, $J = 13.0, 5.7\text{ Hz}$, 1H), 1.69 (s, 3H), 1.62 (s, 3H), 1.39-1.29 (m, 4H), 1.26 (s, 3H), 1.23-1.11 (m, 2H), 1.09 (s, 6H).

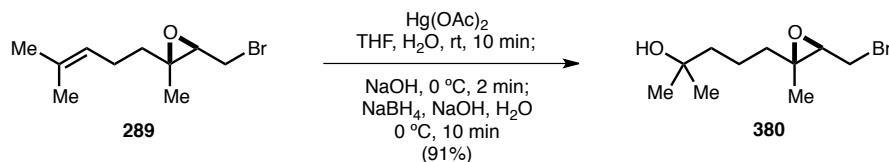
¹³C NMR (125 MHz; CDCl₃) δ : 198.0, 181.3, 133.0, 122.1, 115.4, 100.8, 80.7, 74.5, 56.8, 56.4, 52.2, 49.3, 48.6, 48.1, 40.9, 38.8, 34.6, 32.1, 28.0, 26.3, 25.3, 25.0, 18.2, 17.9.

FTIR (thin film) ν_{max} : 2969, 2943, 2873, 1720, 1649, 1602, 1453, 1372, 1227, 1070, 1003, 681 cm⁻¹.

HRMS-ESI (m/z): [M+Na]⁺ calculated for C₂₄H₃₈O₅, 429.2611; found, 429.2614.

TLC R_f = 0.18 (1:1 hexane:EtOAc).

⁶⁹² The EtOAc used in this procedure was sparged with O₂ for 30 min directly prior to use.



5-((2*S*,3*R*)-3-(Bromomethyl)-2-methyloxiran-2-yl)-2-methylpentan-2-ol (380):

A 1:1 THF/H₂O (1 L) slurry of mercury(II) acetate (255.52 g, 801.82 mmol, 1.5 equiv) in a 2-L recovery flask was treated with **289** (124.63 g, 534.55 mmol, 1 equiv), and the resulting yellow solution was stirred at rt for 10 min. The solution was then cooled using a 0 °C ice bath, and an aqueous solution of NaOH (3 M, 900 mL) was added. The resulting bright yellow-orange slurry was stirred at 0 °C for 2 min, and a basic, aqueous solution of NaBH₄ (0.5 M NaBH₄ in 3 M NaOH aqueous solution, 900 mL) was added, immediately producing a gray slurry. After stirring an additional 10 min at 0 °C, the slurry was extracted thrice with EtOAc. The organic extracts were combined, sequentially washed thrice with H₂O and once with brine, dried over Na₂SO₄, filtered, and concentrated *in vacuo*. The resulting yellow oil was dissolved in 1:1 hexane:EtOAc and passed through a plug of SiO₂, rinsing with 1:1 hexane:EtOAc. Concentration of the filtrate *in vacuo* yielded 122.21 g (486.58 mmol, 91% yield) of **380** as a pale yellow oil that was used without further purification.

¹H NMR (600 MHz; CDCl₃) δ: 3.53 (dd, *J* = 10.4, 5.9 Hz, 1H), 3.24 (dd, *J* = 10.4, 7.8 Hz, 1H), 3.07 (dd, *J* = 7.7, 6.0 Hz, 1H), 1.67-1.63 (m, 1H), 1.51-1.44 (m, 5H), 1.43-1.39 (m, 1H), 1.31-1.29 (s, 3H), 1.20 (s, 6H).

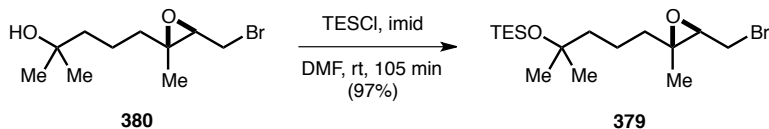
¹³C NMR (125 MHz; CDCl₃) δ: 71.0, 63.3, 61.5, 43.6, 38.7, 29.9, 29.51, 29.42, 20.0, 16.2.

FTIR (thin film) ν_{max} : 3458 (br), 2971, 2947, 2872, 1471, 1386, 1222, 1153, 1073, 891 cm⁻¹.

HRMS–ESI (*m/z*): [M+Na]⁺ calculated for C₁₀H₁₉BrO₂, 273.0461; found, 273.0457.

$[\alpha]_{\text{D}}^{23} = +23.1^\circ$ (*c* 1.83, CHCl₃).

TLC *R_f* = 0.32 (1:1 hexane:EtOAc).



((5-((2*S*,3*R*)-3-(Bromomethyl)-2-methyloxiran-2-yl)-2-methylpentan-2-yl)oxy)triethylsilane (379):

A DMF (1 L) solution of **380** (121.84 g, 485.11 mmol, 1 equiv) and imidazole (132.10 g, 1.940 mol, 4 equiv) in a 2-L recovery flask was placed in a rt H₂O bath and treated with chlorotriethylsilane (163 mL, 0.970 mol, 2 equiv). After stirring the resulting yellow solution at rt for 105 min, the flask was cooled using a 0 °C ice bath and slowly quenched with sat. aq. NaHCO₃. After effervescence ceased, the mixture was extracted thrice with 9:1 hexane:EtOAc. The organic extracts were combined, sequentially washed thrice with H₂O and once with brine, dried over Na₂SO₄, filtered, and concentrated *in vacuo*. The resulting colorless oil was dissolved in 95:5 hexane:EtOAc and passed through a plug of SiO₂, rinsing with 95:5 hexane:EtOAc. Concentration of the filtrate *in vacuo* yielded 171.69 g (469.84 mmol, 97% yield) of **379** as a colorless oil that was used without further purification.

¹H NMR (600 MHz; CDCl₃) δ: 3.55 (dd, *J* = 10.4, 5.9 Hz, 1H), 3.25 (dd, *J* = 10.4, 7.9 Hz, 1H), 3.07 (dd, *J* = 7.8, 5.9 Hz, 1H), 1.66 (ddd, *J* = 13.2, 9.3, 5.3 Hz, 1H), 1.52-1.37 (m, 5H), 1.30 (s, 3H), 1.20 (s, 6H), 0.94 (t, *J* = 7.9 Hz, 9H), 0.56 (q, *J* = 7.9 Hz, 6H).

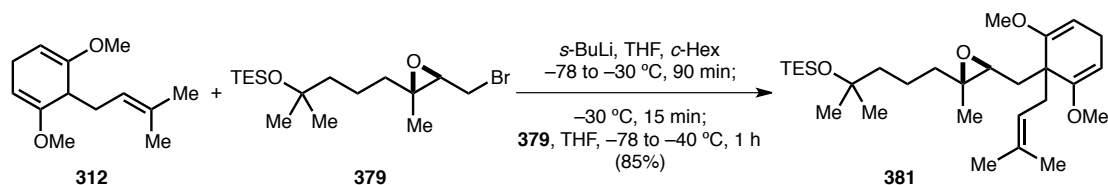
¹³C NMR (125 MHz; CDCl₃) δ: 73.3, 63.4, 61.6, 45.0, 38.9, 30.11, 30.02, 20.2, 16.2, 7.3, 7.0.

FTIR (thin film) ν_{max}: 2953, 2912, 2876, 1462, 1383, 1364, 1233, 1155, 1042, 1017, 743, 724 cm⁻¹.

HRMS–ESI (*m/z*): [M+Na]⁺ calculated for C₁₆H₃₃BrO₂Si, 387.1325; found, 387.1326.

[α]_D²³ = +16.8° (*c* 6.20, CHCl₃).

TLC R_f = 0.83 (1:1 hexane:EtOAc).



((5-((2*S*,3*S*)-3-((2,6-Dimethoxy-1-(3-methylbut-2-en-1-yl)cyclohexa-2,5-dien-1-yl)methyl)-2-methyloxiran-2-yl)-2-methylpentan-2-yl)oxy)triethylsilane (381):

A THF (1 L) solution of **312** (46.52 g, 223.3 mmol, 1 equiv) in a 2-neck 3-L round-bottom flask outfitted with an equal pressure dropping funnel was cooled using a $-78\text{ }^{\circ}\text{C}$ dry ice/acetone bath, and a *c*-Hex solution of *sec*-butyllithium (1.56 M, 170. mL, 235 mmol, 1.05 equiv) was added dropwise over 30 min via the equal pressure dropping funnel, maintaining an internal reaction temperature $\leq -65\text{ }^{\circ}\text{C}$. The resulting yellow-orange slurry was allowed to slowly warm to $-30\text{ }^{\circ}\text{C}$ over 90 min, and the resulting deep red slurry was stirred at $-30\text{ }^{\circ}\text{C}$ for 15 min. The reaction was then cooled using a $-78\text{ }^{\circ}\text{C}$ dry ice/acetone bath, and a THF (200 mL) solution of **379** (73.45 g, 201.0 mmol, 0.9 equiv) was added dropwise via cannula, followed by two THF (50 mL each) rinses, maintaining an internal reaction temperature $\leq -65\text{ }^{\circ}\text{C}$ throughout the addition. The resulting pale yellow solution was allowed to slowly warm to $-40\text{ }^{\circ}\text{C}$ over 1 h and quenched at $-40\text{ }^{\circ}\text{C}$ with sat. aq. NaHCO_3 , which produced a small amount of effervescence. The mixture was warmed to rt and extracted thrice with 1:1 hexane:EtOAc. The organic extracts were combined, sequentially washed sequentially with H_2O and brine, dried over Na_2SO_4 , filtered, and concentrated *in vacuo* to a pale yellow oil. Flash column chromatography (1 L SiO_2 , 98:2 hexane:EtOAc) afforded 83.99 g (170.4 mmol, 85% yield) of **381** as a colorless oil.

^1H NMR (600 MHz; CDCl_3) δ : 4.90 (t, $J = 7.3\text{ Hz}$, 1H), 4.77 (t, $J = 3.5\text{ Hz}$, 1H), 4.72 (t, $J = 3.6\text{ Hz}$, 1H), 3.52 (s, 3H), 3.47 (s, 3H), 2.76 (t, $J = 3.6\text{ Hz}$, 2H), 2.62 (dd, $J = 8.0, 4.0\text{ Hz}$, 1H), 2.31 (qd, $J = 10.8, 7.6\text{ Hz}$, 2H), 2.03 (dd, $J = 13.7, 3.9\text{ Hz}$, 1H), 1.77 (dd, $J = 13.7, 7.9\text{ Hz}$, 1H), 1.63 (s, 3H), 1.55 (s, 3H), 1.53-1.48 (m, 1H), 1.41-1.31 (m, 4H), 1.28-1.21 (m, 1H), 1.18 (s, 3H), 1.17 (s, 6H), 0.94 (t, $J = 7.9\text{ Hz}$, 9H), 0.55 (q, $J = 7.9\text{ Hz}$, 6H).

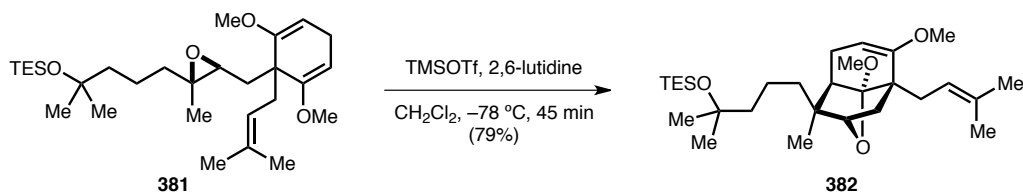
^{13}C NMR (125 MHz; CDCl_3) δ : 154.09, 154.04, 132.5, 120.7, 93.02, 92.90, 73.5, 61.45, 61.32, 54.5, 54.1, 46.2, 45.4, 39.9, 34.6, 34.2, 30.2, 30.0, 26.1, 24.3, 20.2, 17.9, 16.8, 7.3, 7.0.

FTIR (thin film) ν_{max} : 2953, 2913, 2831, 1695, 1660, 1458, 1382, 1224, 1206, 1152, 1124, 1041, 778, 742, 723 cm^{-1} .

HRMS–ESI (m/z): $[\text{M}+\text{H}]^+$ calculated for $\text{C}_{29}\text{H}_{52}\text{O}_4\text{Si}$, 493.3708; found, 493.3708.

$[\alpha]_{\text{D}}^{23} = +22.1^\circ$ (c 0.58, CHCl_3).

TLC $R_f = 0.27$ (95:5 hexane:EtOAc).



((5-((3*S*,3*aR*,7*R*,7*aS*)-6,7*a*-Dimethoxy-3-methyl-7-(3-methylbut-2-en-1-yl)-2,3,3*a*,4,7,7*a*-hexahydro-2,7-methanobenzofuran-3-yl)-2-methylpentan-2-yl)oxy)triethylsilane (382):

A CH₂Cl₂ (30 mL) solution of **381** (2.73 g, 5.54 mmol, 1 equiv) in a 100-mL recovery flask was cooled using a $-78\text{ }^{\circ}\text{C}$ dry ice/acetone bath, and 2,6-lutidine (1.3 mL, 17 mmol, 3 equiv) and trimethylsilyl trifluoromethanesulfonate (2.46 g, 11.1 mmol, 2 equiv) were added sequentially. The resulting yellow solution was stirred at $-78\text{ }^{\circ}\text{C}$ for 45 min and subsequently quenched at $-78\text{ }^{\circ}\text{C}$ with sat. aq. NaHCO₃. After warming the mixture to rt, it was extracted thrice with EtOAc. The organic extracts were combined, sequentially washed with 2 N HCl, H₂O, sat. aq. NaHCO₃, and brine, dried over Na₂SO₄, filtered, and concentrated *in vacuo* to a colorless oil. Flash column chromatography (200 mL SiO₂, 99:1 \rightarrow 98:2 hexane:EtOAc) afforded 2.15 g (4.35 mmol, 79% yield) of **382** as a pale yellow oil.

¹H NMR (600 MHz; CDCl₃) δ : 5.33 (t, $J = 7.1$ Hz, 1H), 4.51 (dd, $J = 5.5, 2.0$ Hz, 1H), 3.72 (t, $J = 2.7$ Hz, 1H), 3.47 (s, 3H), 3.45 (s, 3H), 2.34 (dd, $J = 14.7, 6.8$ Hz, 1H), 2.21-2.16 (m, 1H), 2.21-2.16 (m, 1H), 2.04-2.00 (m, 1H), 2.04-2.00 (m, 1H), 1.76 (d, $J = 2.7$ Hz, 1H), 1.69 (s, 3H), 1.61 (s, 3H), 1.37 (m, 1H), 1.35-1.34 (m, 1H), 1.34-1.31 (m, 1H), 1.31-1.29 (m, 1H), 1.19 (m, 1H), 1.16 (s, 3H), 1.16 (s, 3H), 1.12 (s, 3H), 1.08-1.02 (m, 1H), 0.93 (t, $J = 7.9$ Hz, 9H), 0.54 (q, $J = 7.9$ Hz, 6H).

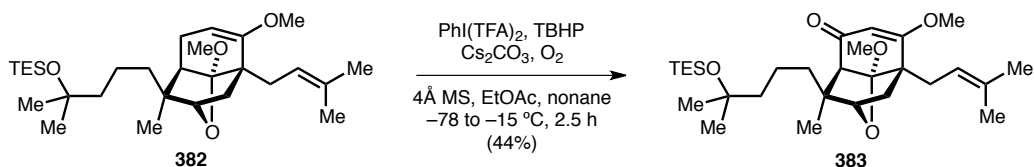
¹³C NMR (125 MHz; CDCl₃) δ : 158.6, 131.1, 123.6, 112.6, 90.5, 79.0, 73.4, 54.5, 51.4, 46.49, 46.34, 44.5, 41.9, 39.3, 34.0, 32.7, 30.2, 30.0, 28.2, 26.3, 20.1, 18.9, 17.9, 7.3, 7.0.

FTIR (thin film) ν_{max} : 2960, 2876, 2839, 1669, 1456, 1375, 1240, 1166, 1007, 853, 803, 743, 722 cm⁻¹.

HRMS-ESI (m/z): [M+H]⁺ calculated for C₂₉H₅₂O₄Si, 493.3708; found, 493.3716.

$[\alpha]_{\text{D}}^{22} = +17.6^{\circ}$ (c 2.76, CHCl₃).

TLC $R_f = 0.50$ (9:1 hexane:EtOAc).



(3*S*,3*aS*,7*R*,7*aS*)-6,7*a*-Dimethoxy-3-methyl-3-(4-methyl-4-((triethylsilyl)oxy)pentyl)-7-(3-methylbut-2-en-1-yl)-3,3*a*,7,7*a*-tetrahydro-2,7-methanobenzofuran-4(2*H*)-one (383):

An EtOAc⁶⁹³ (500 mL) slurry of [bis(trifluoroacetoxy)iodo]benzene (133.9 g, 311.4 mmol, 3 equiv), cesium carbonate (146.5 g, 415.3 mmol, 4 equiv), 4Å molecular sieves (8.0 g, powdered), and **382** (51.16 g, 103.8 mmol, 1 equiv) in an open 2-L recovery flask was cooled using a $-78\text{ }^\circ\text{C}$ dry ice/acetone bath with vigorous O₂ bubbling through the slurry via three foreshortened glass pipettes. An EtOAc (200 mL, sparged for 1 h with O₂ directly prior to the reaction) dilution of a nonane solution of *tert*-butyl hydroperoxide (5.5 M, 38 mmol, 210 mmol, 2 equiv) was added via cannula over 20 min. The resulting yellow slurry was allowed to slowly warm to $-15\text{ }^\circ\text{C}$ over 2.5 h, at which point O₂ bubbling was suspended. The reaction was then quenched at $-15\text{ }^\circ\text{C}$ with sat. aq. Na₂S₂O₃. After warming the slurry to rt, the layers were separated. The aqueous layer was extracted thrice with EtOAc. The organic extracts were combined, sequentially washed twice with H₂O and once with brine, dried over Na₂SO₄, filtered, and concentrated *in vacuo* to a red oil. Flash column chromatography (850 mL SiO₂, 9:1 → 8:2 hexane:EtOAc) afforded 22.92 g (45.23 mmol, 44% yield) of **383** as a viscous yellow syrup.

¹H NMR (500 MHz; CDCl₃) δ : 5.28 (s, 1H), 5.24 (t, $J = 7.1\text{ Hz}$, 1H), 3.82 (d, $J = 5.7\text{ Hz}$, 1H), 3.64 (s, 3H), 3.40 (s, 3H), 2.61 (s, 1H), 2.36 (dd, $J = 14.8, 6.2\text{ Hz}$, 1H), 2.28 (dd, $J = 14.8, 8.1\text{ Hz}$, 1H), 1.95 (d, $J = 13.0\text{ Hz}$, 1H), 1.86 (dd, $J = 13.0, 5.7\text{ Hz}$, 1H), 1.63 (s, 3H), 1.56 (s, 3H), 1.26 (m, 1H), 1.24 (m, 1H), 1.21 (m, 1H), 1.20 (m, 1H), 1.19 (s, 3H), 1.09 (s, 6H), 1.04-0.96 (m, 1H), 0.85 (t, $J = 7.9\text{ Hz}$, 9H), 0.47 (q, $J = 7.9\text{ Hz}$, 6H).

¹³C NMR (125 MHz; CDCl₃) δ : 197.8, 181.1, 132.6, 122.0, 115.2, 100.6, 80.6, 73.1, 56.7, 56.2, 52.0, 48.4, 48.0, 45.7, 38.7, 34.5, 32.0, 30.1, 29.7, 27.8, 26.1, 18.5, 17.8, 7.1, 6.8.

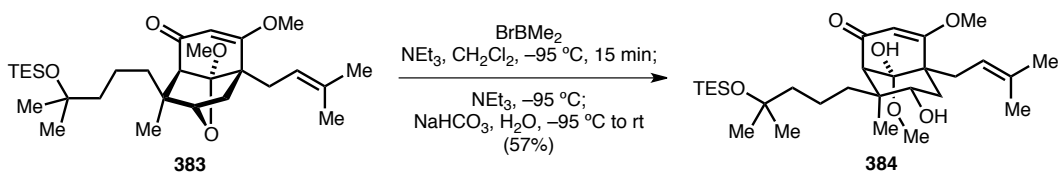
FTIR (thin film) ν_{max} : 2966, 2913, 2875, 1653, 1606, 1457, 1373, 1229, 1172, 1006, 725 cm⁻¹.

⁶⁹³ The EtOAc used in this procedure was sparged with O₂ for 1 h directly prior to use.

HRMS–ESI (m / z): [M+Na]⁺ calculated for C₂₉H₅₀O₅Si, 529.3320; found, 529.3304.

[α]_D²³ = +30.6° (c 3.22, CHCl₃).

TLC R_f = 0.50 (7:3 hexane:EtOAc).



(1*S*,5*R*,7*S*,8*S*,9*S*)-7,9-Dihydroxy-4,9-dimethoxy-8-methyl-8-(4-methyl-4-((triethylsilyl)oxy)pentyl)-5-(3-methylbut-2-en-1-yl)bicyclo[3.3.1]non-3-en-2-one (384):

A CH₂Cl₂ (20 mL) solution of **383** (794 mg, 1.57 mmol, 1 equiv) and triethylamine (131 μ L, 0.940 mmol, 6 equiv) in a 25-mL recovery flask was cooled using a $-95\text{ }^{\circ}\text{C}$ ethanol/liquid nitrogen bath, and a CH₂Cl₂ solution of bromodimethylborane⁶⁹⁴ (1.59 M, 5.9 mL, 0.94 mmol, 6 equiv) was added slowly over 5 min, maintaining a bath temperature below $-90\text{ }^{\circ}\text{C}$. The resulting bright yellow solution was stirred at $-95\text{ }^{\circ}\text{C}$ for an additional 10 min and sequentially quenched at $-95\text{ }^{\circ}\text{C}$ with 6 mL NEt₃ and sat. aq. NaHCO₃. After warming the mixture to rt, it was extracted thrice with EtOAc. The organic extracts were combined, sequentially washed with 2 N HCl, H₂O, sat. aq. NaHCO₃, and brine, dried over Na₂SO₄, filtered, and concentrated *in vacuo* to a yellow-orange oil. Flash column chromatography (150 mL SiO₂, 8:2 \rightarrow 7:3 hexane:EtOAc) afforded 471 mg (0.897 mmol, 57% yield) of **384** as a white flocculent solid.

¹H NMR (600 MHz; CDCl₃) δ : 5.48 (s, 1H), 5.26 (d, $J = 9.0$ Hz, 1H), 5.05 (t, $J = 7.1$ Hz, 1H), 3.74 (s, 3H), 3.63-3.59 (m, 1H), 3.57 (s, 1H), 3.26 (s, 3H), 2.87-2.83 (m, 2H), 2.36 (tt, $J = 12.5, 6.2$ Hz, 1H), 2.25 (d, $J = 14.0$ Hz, 1H), 2.01-1.93 (m, 2H), 1.92-1.86 (m, 1H), 1.73 (s, 3H), 1.68 (s, 3H), 1.65 (s, 6H), 1.46 (td, $J = 13.0, 4.8$ Hz, 1H), 1.32 (d, $J = 5.9$ Hz, 1H), 1.11 (s, 3H), 1.05 (td, $J = 12.9, 4.4$ Hz, 1H).

¹³C NMR (125 MHz; CDCl₃) δ : 198.2, 176.1, 137.4, 131.4, 125.0, 122.1, 104.1, 100.6, 73.2, 57.6, 56.6, 51.1, 48.5, 40.5, 39.2, 36.9, 30.0, 26.2, 25.9, 21.9, 18.00, 17.88, 17.0.

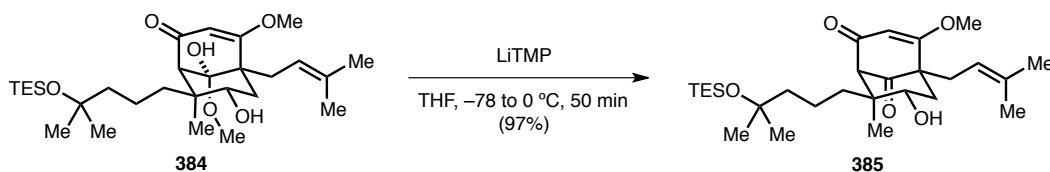
FTIR (thin film) ν_{max} : 3465(br), 2954, 2913, 2876, 1659, 1645, 1606, 1456, 1365, 1225, 1173, 1087, 1044, 1016, 742, 725 cm⁻¹.

HRMS-ESI (m/z): [M+H]⁺ calculated for C₂₃H₃₆O₅, 393.2636; found, 393.2632.

$[\alpha]_{\text{D}}^{23} = -24^{\circ}$ (c 0.70, CHCl₃).

⁶⁹⁴ A CH₂Cl₂ solution of bromodimethylborane was prepared as described in ref. 639b.

TLC $R_f = 0.50$ (1:1 hexane:EtOAc).



(1*S*,5*R*,7*S*,8*S*)-7-Hydroxy-4-methoxy-8-methyl-8-(4-methyl-4-((triethylsilyl)oxy)pentyl)-5-(3-methylbut-2-en-1-yl)bicyclo[3.3.1]non-3-ene-2,9-dione (385):

A THF (8 mL) solution of **384** (419.9 mg, 0.8001 mmol, 1 equiv) in a 50-mL recovery flask was cooled using a $-78\text{ }^{\circ}\text{C}$ dry ice/acetone bath, and a freshly prepared THF solution of lithium 2,2,6,6-tetramethylpiperidide (0.50 M, 4.0 mL, 2.0 mmol, 2.5 equiv) was added. The resulting orange solution was allowed to warm to $0\text{ }^{\circ}\text{C}$ over 50 min. The reaction was then quenched at $0\text{ }^{\circ}\text{C}$ with sat. aq. NaHCO_3 at $0\text{ }^{\circ}\text{C}$. The mixture was warmed to rt and extracted thrice with EtOAc. The organic extracts were combined, sequentially washed with H_2O and brine, dried over Na_2SO_4 , filtered, and concentrated *in vacuo* to an orange oil. Flash column chromatography (100 mL SiO_2 , 7:3 hexane:EtOAc) afforded 381.6 mg (0.7744 mmol, 97% yield) of **385** as a viscous yellow oil.

^1H NMR (600 MHz; CDCl_3) δ : 5.63 (s, 1H), 4.95 (t, $J = 7.0$ Hz, 1H), 3.78 (d, $J = 7.8$ Hz, 1H), 3.73 (s, 3H), 3.15 (s, 1H), 2.47 (dd, $J = 14.5, 6.4$ Hz, 1H), 2.37 (dd, $J = 14.5, 7.6$ Hz, 1H), 2.09 (dd, $J = 13.4, 5.4$ Hz, 1H), 1.88 (s, 1H), 1.73 (dd, $J = 13.3, 11.6$ Hz, 1H), 1.65 (m, 7H), 1.52 (td, $J = 12.6, 3.5$ Hz, 1H), 1.39 (td, $J = 12.5, 4.1$ Hz, 1H), 1.34-1.27 (m, 2H), 1.23 (m, 4H), 1.18 (s, 3H), 0.92 (t, $J = 7.9$ Hz, 9H), 0.86 (s, 3H), 0.54 (q, $J = 7.8$ Hz, 6H).

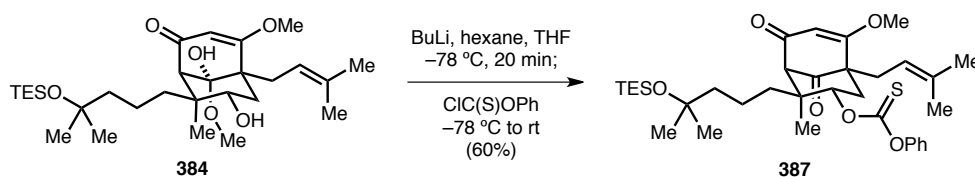
^{13}C NMR (125 MHz; CDCl_3) δ : 205.4, 193.1, 177.4, 134.4, 119.0, 105.9, 73.6, 72.0, 69.2, 57.0, 56.0, 46.2, 45.6, 39.4, 38.4, 30.6, 29.50, 29.48, 26.1, 18.1, 17.9, 15.7, 7.3, 6.9.

FTIR (thin film) ν_{max} : 3458(br), 2953, 2876, 1740, 1733, 1661, 1594, 1454, 1364, 1231, 1038, 842, 743, 724 cm^{-1} .

HRMS-ESI (m/z): $[\text{M}+\text{Na}]^+$ calculated for $\text{C}_{28}\text{H}_{48}\text{O}_5\text{Si}$, 515.3163; found, 515.3170.

$[\alpha]_{\text{D}}^{23} = +32.1^{\circ}$ (c 2.30, CHCl_3).

TLC $R_f = 0.56$ (1:1 hexane:EtOAc).



O-((1*S*,2*S*,3*S*,5*R*)-6-Methoxy-2-methyl-2-(4-methyl-4-((triethylsilyl)oxy)pentyl)-5-(3-methylbut-2-en-1-yl)-8,9-dioxobicyclo[3.3.1]non-6-en-3-yl) O-phenyl carbonothioate (387):

A THF solution of **384** (71 mg, 0.14 mmol, 1 equiv) in a 10-mL recovery flask was cooled to $-78\text{ }^{\circ}\text{C}$, and a hexane solution of butyllithium (2.02 M, 141 μL , 0.28 mmol, 2.1 equiv) was added dropwise over 5 min. After stirring the reaction at $-78\text{ }^{\circ}\text{C}$ for 20 min, *O*-phenyl chlorothionoformate (39 μL , 0.28 mmol, 2.1 equiv) was added in one portion. The resulting yellow solution was allowed to slowly warm to rt. After stirring for 90 min, the reaction was quenched at rt with sat. aq. NaHCO_3 and extracted thrice with EtOAc. The organic extracts were combined, sequentially washed with H_2O and brine, dried over Na_2SO_4 , filtered, and concentrated *in vacuo* to an orange oil. Flash column chromatography (50 mL SiO_2 , 95:5 hexane:EtOAc) afforded 51 mg (81 μmol , 60% yield) of **387** as a yellow oil.

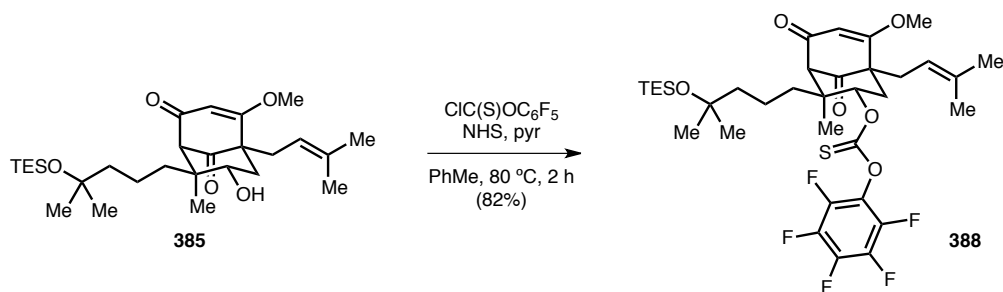
^1H NMR (600 MHz; CDCl_3) δ : 7.41 (dd, $J = 8.4, 7.5\text{ Hz}$, 2H), 7.30 (t, $J = 7.5\text{ Hz}$, 1H), 7.08-7.06 (m, 2H), 5.74 (s, 1H), 5.53 (dd, $J = 11.5, 5.4\text{ Hz}$, 1H), 4.99 (t, $J = 7.0\text{ Hz}$, 1H), 3.80 (s, 3H), 3.25 (s, 1H), 2.56-2.53 (m, 2H), 2.44 (dd, $J = 14.6, 7.4\text{ Hz}$, 1H), 1.86 (dd, $J = 12.9, 11.7\text{ Hz}$, 1H), 1.69-1.65 (m, 7H), 1.58-1.56 (m, 1H), 1.47-1.41 (m, 2H), 1.37 (m, 2H), 1.23 (s, 3H), 1.23 (s, 3H), 1.03 (s, 3H), 0.95 (t, $J = 7.9\text{ Hz}$, 9H), 0.58 (q, $J = 7.9\text{ Hz}$, 6H).

^{13}C NMR (125 MHz; CDCl_3) δ : 204.2, 194.6, 192.2, 177.0, 153.4, 134.9, 129.8, 126.9, 122.0, 118.7, 106.3, 84.6, 73.6, 69.8, 57.4, 55.7, 45.66, 45.60, 38.1, 34.3, 30.5, 29.7, 29.4, 26.2, 18.2, 17.8, 17.5, 7.4, 7.0.

FTIR (thin film) ν_{max} : 2958, 2911, 2874, 1739, 1659, 1594, 1490, 1275, 1206, 1034, 1017, 743 cm^{-1} .

HRMS-ESI (m/z): $[\text{M}+\text{Na}]^+$ calculated for $\text{C}_{35}\text{H}_{52}\text{O}_7\text{SSi}$, 651.3152; found, 651.3130.

TLC R_f = 0.57 (7:3 hexane:EtOAc).



***O*-((1*S*,2*S*,3*S*,5*R*)-6-Methoxy-2-methyl-2-(4-methyl-4-((triethylsilyl)oxy)pentyl)-5-(3-methylbut-2-en-1-yl)-8,9-dioxobicyclo[3.3.1]non-6-en-3-yl) *O*-(perfluorophenyl) carbonothioate (388):**

A PhMe (100 mL) solution of **385** (5.40 g, 11.0 mmol, 1 equiv), *N*-hydroxysuccinimide (1.26 g, 11.0 mmol, 1 equiv), and pyridine (4.4 mL, 55 mmol, 5 equiv) in a 200-mL recovery flask was treated with pentafluorophenyl chlorothionoformate (8.8 mL, 55 mmol, 5 equiv), and the resulting yellow-orange slurry was stirred at 80 °C for 2 h. After cooling the resulting orange slurry to rt, it was diluted with EtOAc and sequentially washed twice with H₂O and once with brine, dried over Na₂SO₄, filtered, and concentrated *in vacuo* to a black oil. Flash column chromatography (700 mL SiO₂, 98:2 → 9:1 hexane:EtOAc) afforded 6.47 g (9.00 mmol, 82% yield) of **388** as viscous brown-orange syrup.

¹H NMR (600 MHz; CDCl₃) δ: 5.74 (s, 1H), 5.45 (dd, *J* = 11.6, 5.4 Hz, 1H), 4.98 (t, *J* = 6.9 Hz, 1H), 3.80 (s, 3H), 3.27 (s, 1H), 2.55 (dd, *J* = 14.5, 6.3 Hz, 1H), 2.50 (dd, *J* = 13.0, 5.4 Hz, 1H), 2.45 (dd, *J* = 14.5, 7.5 Hz, 1H), 1.92 (t, *J* = 12.3 Hz, 1H), 1.69-1.68 (m, 7H), 1.42-1.29 (m, 5H), 1.21 (s, 6H), 1.07 (s, 3H), 0.94 (t, *J* = 7.9 Hz, 9H), 0.57 (q, *J* = 8.0 Hz, 6H).

¹³C NMR (125 MHz; CDCl₃) δ: 203.7, 191.8, 176.8, 135.1, 118.4, 106.3, 87.2, 73.5, 69.6, 57.4, 55.6, 45.64, 45.45, 38.0, 34.0, 30.4, 29.7, 29.3, 26.1, 18.2, 17.7, 17.4, 7.3, 7.0.

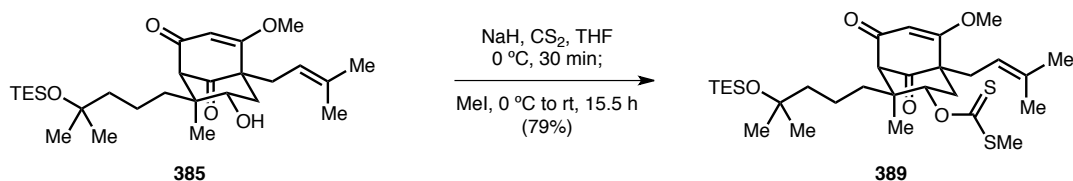
¹⁹F NMR (282 MHz; CDCl₃) δ: −152.71 (d, *J* = 18.1 Hz, 2F), −156.71 (t, *J* = 21.9 Hz, 1F), −162.21 (t, *J* = 19.8 Hz, 2F).

FTIR (thin film) ν_{max} : 2960, 2914, 2876, 1742, 1668, 1599, 1523, 1456, 1380, 1312, 1222, 1158, 1043, 966, 845, 743, 725 cm^{−1}.

HRMS–ESI (*m/z*): [M+Na]⁺ calculated for C₃₄H₄₇F₅O₆SSi, 741.2675; found, 741.2667.

[α]_D²³ = +5.16° (*c* 2.28, CHCl₃).

TLC $R_f = 0.69$ (7:3 hexane:EtOAc).



***O*-((1*S*,2*S*,3*S*,5*R*)-6-Methoxy-2-methyl-2-(4-methyl-4-((triethylsilyl)oxy)pentyl)-5-(3-methylbut-2-en-1-yl)-8,9-dioxobicyclo[3.3.1]non-6-en-3-yl) *S*-methyl carbonodithioate (389):**

A THF (2 mL) solution of **385** (18.0 mg, 36.5 μmol , 1 equiv) and carbon disulfide (22 μL , 0.37 mmol, 10 equiv) in a 10-mL recovery flask was cooled to 0 $^{\circ}\text{C}$, and sodium hydride (60% suspension in mineral oil, 15 mg, 0.37 mmol, 10 equiv) was added. After stirring the resulting white slurry at 0 $^{\circ}\text{C}$ for 30 min, iodomethane (23 μL , 0.37 mmol, 10 equiv) was added. The resulting yellow slurry was allowed to slowly warm to rt. After stirring for 15.5 h, the reaction was quenched at rt with sat. aq. NaHCO_3 and extracted thrice with EtOAc. The organic extracts were combined, sequentially washed with H_2O and brine, dried over Na_2SO_4 , filtered, and concentrated *in vacuo* to a yellow oil. Flash column chromatography (20 mL SiO_2 , 98:2 \rightarrow 95:5 \rightarrow 9:1 hexane:EtOAc) afforded 16.8 mg (28.8 μmol , 79% yield) of **389** as a colorless oil.

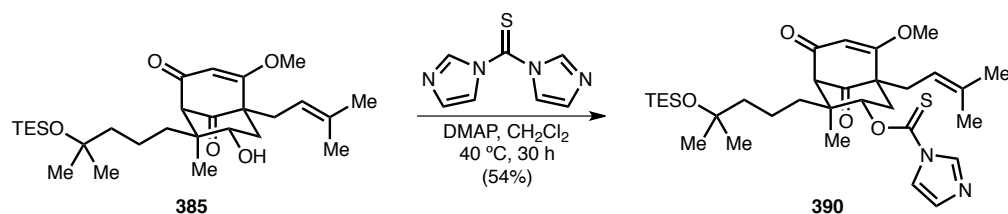
^1H NMR (600 MHz; CDCl_3) δ : 5.88 (dd, $J = 11.6, 5.4$ Hz, 1H), 5.73 (s, 1H), 4.97 (t, $J = 7.0$ Hz, 1H), 3.80 (s, 3H), 3.23 (s, 1H), 2.55-2.50 (m, 4H), 2.48 (dd, $J = 13.0, 5.4$ Hz, 1H), 2.40 (dd, $J = 14.6, 7.3$ Hz, 1H), 1.76 (dd, $J = 13.0, 11.6$ Hz, 1H), 1.62-1.60 (m, 7H), 1.40-1.22 (m, 5H), 1.19 (s, 6H), 1.07 (s, 3H), 0.94 (t, $J = 7.9$ Hz, 9H), 0.56 (q, $J = 7.9$ Hz, 6H).

^{13}C NMR (125 MHz; CDCl_3) δ : 215.8, 204.3, 192.2, 177.1, 134.8, 118.7, 106.2, 83.2, 73.5, 70.1, 57.3, 55.7, 45.8, 45.5, 38.3, 34.5, 30.5, 29.7, 29.3, 26.1, 19.2, 18.2, 17.86, 17.74, 7.4, 7.0

FTIR (thin film) ν_{max} : 2956, 2911, 2874, 1739, 1658, 1595, 1458, 1353, 1231, 1208, 1050, 742, 724 cm^{-1} .

HRMS-ESI (m/z): $[\text{M}+\text{Na}]^+$ calculated for $\text{C}_{30}\text{H}_{50}\text{O}_5\text{S}_2\text{Si}$, 605.2761; found, 605.2737.

TLC R_f = 0.28 (9:1 hexane:EtOAc).



***O*-((1*S*,2*S*,3*S*,5*R*)-6-Methoxy-2-methyl-2-(4-methyl-4-((triethylsilyl)oxy)pentyl)-5-(3-methylbut-2-en-1-yl)-8,9-dioxobicyclo[3.3.1]non-6-en-3-yl) 1*H*-imidazole-1-carbothioate (390):**

A CH₂Cl₂ (1 mL) solution of **385** (19.2 mg, 39.0 μmol, 1 equiv), 1,1'-thiocarbonyldiimidazole (69 mg, 0.390 mmol, 10 equiv), and 4-(dimethylamino)pyridine (5 mg, 40 μmol, 1 equiv) in a 10-mL test tube was sealed and heated to 40 °C. After stirring the brown-orange solution at 40 °C for 30 h, it was cooled to rt, and quenched with a few drops of MeOH. The mixture was diluted with sat. aq. NaHCO₃ and extracted thrice with EtOAc. The organic extracts were combined, sequentially washed with H₂O and brine, dried over Na₂SO₄, filtered, and concentrated *in vacuo* to an orange oil. Flash column chromatography (25 mL SiO₂, 8:2 → 7:3 hexane:EtOAc) afforded 12.8 mg (21.2 μmol, 54% yield) of **390** as a colorless oil.

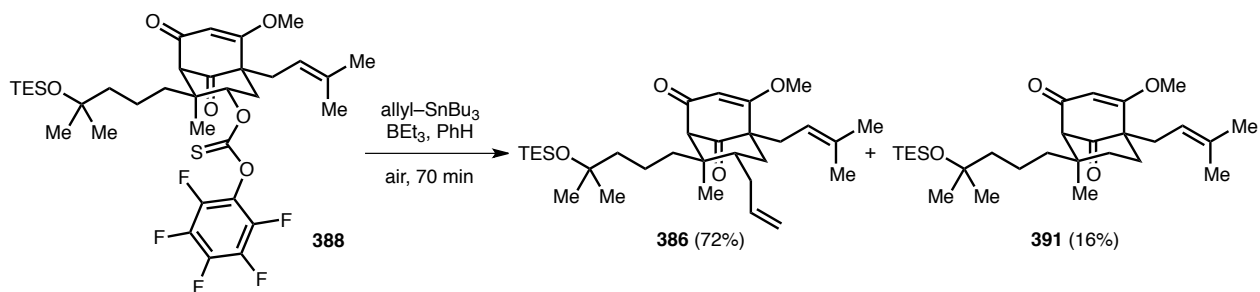
¹H NMR (600 MHz; CDCl₃) δ: 8.28 (s, 1H), 7.55 (s, 1H), 7.05 (s, 1H), 5.80-5.75 (m, 2H), 4.99 (t, *J* = 7.0 Hz, 1H), 3.85 (s, 3H), 3.29 (s, 1H), 2.56-2.51 (m, 2H), 2.44 (dd, *J* = 14.6, 7.5 Hz, 1H), 1.85 (t, *J* = 12.3 Hz, 1H), 1.71-1.64 (m, 7H), 1.40-1.23 (m, 5H), 1.17 (s, 3H), 1.17 (s, 3H), 1.13 (s, 3H), 0.91 (t, *J* = 7.9 Hz, 9H), 0.53 (q, *J* = 7.9 Hz, 6H).

¹³C NMR (125 MHz; CDCl₃) δ: 203.7, 191.8, 183.4, 176.9, 137.0, 135.2, 131.4, 118.4, 117.9, 106.3, 83.8, 73.4, 69.6, 57.5, 55.6, 45.6, 45.4, 38.4, 34.2, 30.5, 29.6, 29.3, 26.2, 18.18, 18.04, 17.8, 7.4, 7.0.

FTIR (thin film) ν_{max}: 2957, 2913, 2874, 1740, 1656, 1595, 1460, 1390, 1332, 1285, 1221, 1108, 1042, 986, 742, 724 cm⁻¹.

HRMS-ESI (*m/z*): [M+Na]⁺ calculated for C₃₂H₅₀N₂O₅SSi, 625.3102; found, 625.3082.

TLC R_f = 0.58 (1:1 hexane:EtOAc).



388 (6.46 g, 8.99 mmol, 1 equiv) was taken up in PhH (10 mL) and allyltributylstannane (30 mL) in a 200-mL recovery flask open to air, and a PhH solution of triethylborane (5.0 M, 0.90 mL, 4.5 mmol, 0.5 equiv) was added. The resulting golden yellow solution was stirred vigorously open to air for 30 min, and a PhH solution of triethylborane (5.0 M, 0.90 mL, 4.5 mmol, 0.5 equiv) was added. After stirring an additional 40 min, the solution was concentrated partially *in vacuo* and purified using flash column chromatography (700 mL SiO₂, 98:2 → 95:5 hexane:EtOAc) to afford 3.35 g (6.48 mmol, 72% yield) of **386** as a colorless oil and 701 mg (1.47 mmol, 16% yield) of **391** as a pale yellow oil.

(1*S*,5*R*,7*S*,8*R*)-7-Allyl-4-methoxy-8-methyl-8-(4-methyl-4-((triethylsilyl)oxy)pentyl)-5-(3-methylbut-2-en-1-yl)bicyclo[3.3.1]non-3-ene-2,9-dione (386):

¹H NMR (600 MHz; CDCl₃) δ: 5.69 (s, 1H), 5.65 (dddd, *J* = 16.8, 10.3, 8.5, 5.5 Hz, 1H), 5.01 (dd, *J* = 4.9, 0.8 Hz, 1H), 4.99 (dd, *J* = 11.7, 0.8 Hz, 1H), 4.96 (t, *J* = 7.0 Hz, 1H), 3.73 (s, 3H), 3.13 (s, 1H), 2.46 (dd, *J* = 14.4, 5.9 Hz, 1H), 2.36 (dd, *J* = 14.7, 7.8 Hz, 1H), 2.34-2.30 (m, 1H), 1.97 (dd, *J* = 13.9, 4.6 Hz, 1H), 1.77-1.69 (m, 2H), 1.67-1.64 (m, 4H), 1.63 (s, 3H), 1.48-1.38 (m, 3H), 1.34-1.32 (m, 1H), 1.27 (m, 1H), 1.24-1.22 (m, 4H), 1.21 (s, 3H), 0.94 (t, *J* = 7.9 Hz, 9H), 0.81 (s, 3H), 0.57 (q, *J* = 7.8 Hz, 6H).

¹³C NMR (125 MHz; CDCl₃) δ: 207.2, 193.9, 177.5, 137.2, 133.9, 119.5, 116.8, 106.5, 73.7, 70.8, 56.98, 56.95, 46.2, 45.7, 39.8, 39.29, 39.16, 33.9, 30.6, 29.8, 29.6, 26.1, 18.13, 18.06, 17.90, 7.4, 7.0.

FTIR (thin film) ν_{max} : 2961, 2917, 2876, 1733, 1657, 1599, 1460, 1365, 1227, 1171, 1042, 1017, 743, 724 cm⁻¹.

HRMS-ESI (*m/z*): [M+Na]⁺ calculated for C₃₁H₅₂O₄Si, 539.3527; found, 539.3521.

[α]_D²³ = +23.5° (*c* 0.54, CHCl₃).

TLC R_f = 0.45 (8:2 hexane:EtOAc).

(1*S*,5*S*,8*R*)-4-Methoxy-8-methyl-8-(4-methyl-4-((triethylsilyl)oxy)pentyl)-5-(3-methylbut-2-en-1-yl)bicyclo[3.3.1]non-3-ene-2,9-dione (391):

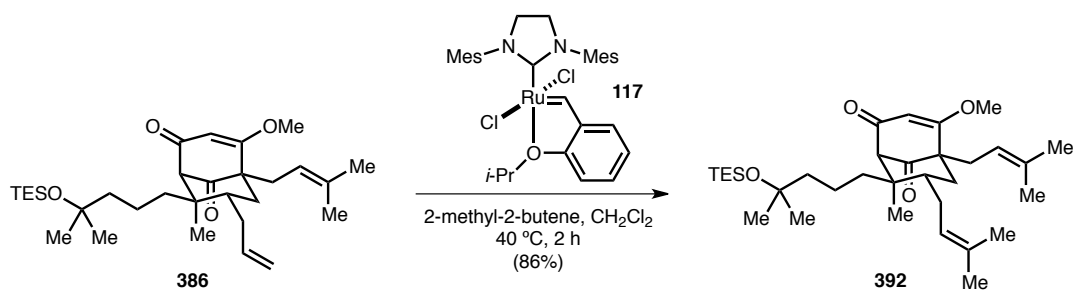
¹H NMR (500 MHz; CDCl₃) δ: 5.72 (s, 1H), 4.96 (t, *J* = 7.0 Hz, 1H), 3.74 (s, 3H), 2.97 (s, 1H), 2.50 (dd, *J* = 14.5, 6.0 Hz, 1H), 2.38 (dd, *J* = 14.5, 7.8 Hz, 1H), 1.84-1.80 (m, 1H), 1.77 (dd, *J* = 13.7, 4.2 Hz, 1H), 1.69-1.67 (m, 1H), 1.65 (s, 3H), 1.63 (s, 3H), 1.52-1.27 (m, 7H), 1.25-1.20 (m, 3H), 1.18 (s, 6H), 0.92 (t, *J* = 7.9 Hz, 9H), 0.54 (q, *J* = 7.9 Hz, 6H).

¹³C NMR (125 MHz; CDCl₃) δ: 207.1, 194.1, 177.1, 133.9, 128.5, 119.5, 106.4, 73.6, 72.3, 56.9, 45.6, 43.5, 42.3, 33.4, 31.8, 30.5, 29.80, 29.76, 26.1, 22.0, 18.16, 18.12, 7.3, 7.0.

FTIR (thin film) ν_{max} : 2954, 2911, 2875, 1733, 1655, 1597, 1458, 1365, 1224, 1044, 1015, 743, 724 cm⁻¹.

HRMS–ESI (*m/z*): [M+Na]⁺ calculated for C₂₈H₄₈O₄Si, 499.3214; found, 499.3204.

TLC *R_f* = 0.38 (8:2 hexane:EtOAc).



(1*S*,5*R*,7*S*,8*R*)-4-Methoxy-8-methyl-8-(4-methyl-4-((triethylsilyl)oxy)pentyl)-5,7-bis(3-methylbut-2-en-1-yl)bicyclo[3.3.1]non-3-ene-2,9-dione (392):

A CH₂Cl₂ (0.5 mL) and 2-methyl-2-butene (0.5 mL) solution of **386** (18.4 mg, 35.6 μmol, 1 equiv) and Hoveyda–Grubbs 2nd generation catalyst **117** (3.3 mg, 5.3 μmol, 0.15 equiv) in a sealed 10-mL test tube was stirred at 40 °C for 2 h. The olive-black solution was subsequently cooled to rt and concentrated *in vacuo*. Flash column chromatography (50 mL SiO₂, 95:5 hexane:EtOAc) afforded 16.7 mg (30.6 μmol, 86% yield) of **392** as a colorless oil.

¹H NMR (600 MHz; CDCl₃) δ: 5.69 (s, 1H), 4.98-4.94 (m, 2H), 3.73 (s, 3H), 3.12 (s, 1H), 2.45 (dd, *J* = 14.2, 6.0 Hz, 1H), 2.36 (dd, *J* = 14.6, 7.7 Hz, 1H), 2.14-2.11 (m, 1H), 1.93 (dd, *J* = 14.0, 4.1 Hz, 1H), 1.69 (s, 3H), 1.67-1.65 (m, 4H), 1.63 (s, 3H), 1.58-1.54 (m, 4H), 1.50-1.45 (m, 2H), 1.44-1.38 (m, 3H), 1.34-1.30 (m, 2H), 1.22 (s, 3H), 1.21 (s, 3H), 0.94 (t, *J* = 7.9 Hz, 9H), 0.82 (s, 3H), 0.57 (q, *J* = 7.8 Hz, 6H).

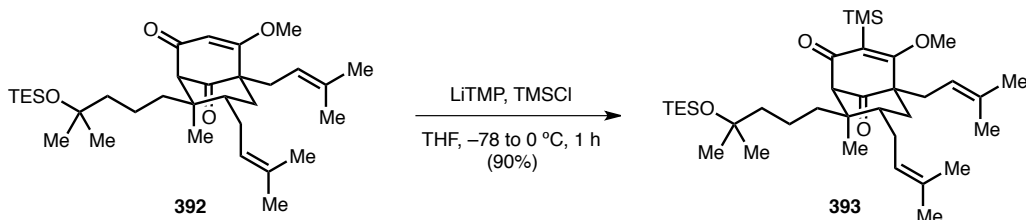
¹³C NMR (125 MHz; CDCl₃) δ: 207.4, 194.0, 177.5, 133.8, 133.3, 122.9, 119.7, 106.5, 73.7, 70.9, 57.1, 56.9, 46.4, 45.7, 40.9, 39.5, 39.2, 30.6, 29.9, 29.6, 27.9, 26.10, 26.05, 18.16, 18.13, 18.06, 17.92, 7.4, 7.0.

FTIR (thin film) ν_{max} : 2964, 2914, 2876, 1733, 1659, 1656, 1600, 1453, 1368, 1227, 1045, 1017, 723 cm⁻¹.

HRMS–ESI (*m/z*): [M+Na]⁺ calculated for C₃₃H₅₆O₄Si, 567.3840; found, 567.3831.

[α]_D²² = +27.2° (*c* 3.61, CHCl₃).

TLC R_f = 0.49 (9:1 hexane:EtOAc).



(1*R*,5*R*,7*S*,8*R*)-4-Methoxy-8-methyl-8-(4-methyl-4-((triethylsilyl)oxy)pentyl)-5,7-bis(3-methylbut-2-en-1-yl)-3-(trimethylsilyl)bicyclo[3.3.1]non-3-ene-2,9-dione (393):

A THF (1 mL) solution of **392** (22.9 mg, 42.0 μ mol, 1 equiv) in a 10-mL test tube was cooled to -78°C , and chlorotrimethylsilane (53 μ L, 420 μ mol, 10 equiv) and a freshly prepared THF solution of lithium 2,2,6,6-tetramethylpiperidide (0.50 M, 420 μ L, 210 μ mol, 5 equiv) were added sequentially. After allowing the resulting golden yellow solution to slowly warm to 0°C over 1 h, it was quenched at 0°C with sat. aq. NaHCO_3 . The mixture was then extracted thrice with EtOAc. The organic extracts were combined, sequentially washed with H_2O and brine, dried over Na_2SO_4 , filtered, and concentrated *in vacuo* to a yellow oil. Flash column chromatography (20 mL SiO_2 , 98:2 hexane:EtOAc) afforded 23.4 mg (37.9 μ mol, 90% yield) of **393** as a viscous yellow syrup.

^1H NMR (600 MHz; CDCl_3) δ : 5.02-4.97 (m, 2H), 3.83 (s, 3H), 3.11 (s, 1H), 2.51 (dd, $J = 14.4, 6.3$ Hz, 1H), 2.37 (dd, $J = 14.5, 7.5$ Hz, 1H), 2.15-2.11 (m, 1H), 1.99 (dd, $J = 14.0, 3.7$ Hz, 1H), 1.69 (s, 3H), 1.68-1.63 (m, 9H), 1.57 (s, 3H), 1.48 (td, $J = 12.7, 3.9$ Hz, 1H), 1.46-1.37 (m, 2H), 1.30 (td, $J = 12.2, 4.1$ Hz, 1H), 1.26-1.24 (m, 1H), 1.21 (s, 3H), 1.21 (s, 3H), 1.14 (td, $J = 12.6, 4.2$ Hz, 1H), 0.94 (t, $J = 7.9$ Hz, 9H), 0.80 (s, 3H), 0.57 (q, $J = 8.1$ Hz, 6H), 0.23 (s, 9H).

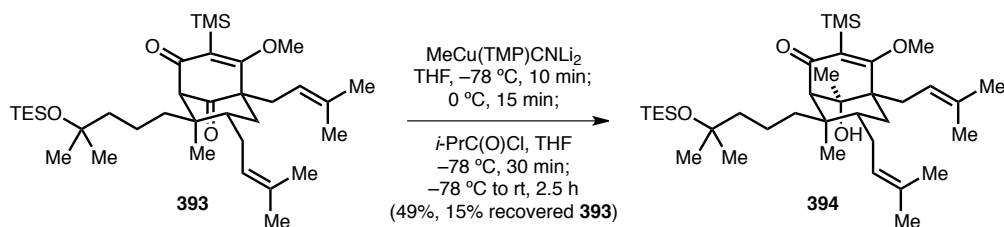
^{13}C NMR (125 MHz; CDCl_3) δ : 207.9, 198.6, 185.7, 133.70, 133.59, 127.7, 122.8, 120.0, 73.7, 72.6, 64.1, 59.7, 46.7, 45.7, 41.8, 39.29, 39.27, 30.6, 30.0, 29.7, 27.6, 26.02, 25.97, 18.21, 18.14, 17.88, 17.83, 7.4, 7.0, 0.8.

FTIR (thin film) ν_{max} : 2962, 2914, 2876, 1729, 1652, 1556, 1461, 1440, 1382, 1247, 1216, 1045, 845, 743, 724 cm^{-1} .

HRMS-ESI (m/z): $[\text{M}+\text{H}]^+$ calculated for $\text{C}_{36}\text{H}_{64}\text{O}_4\text{Si}_2$, 617.4416; found, 617.4395.

$[\alpha]_{\text{D}}^{23} = +29.8^{\circ}$ (c 1.24, CHCl_3).

TLC $R_f = 0.40$ (95:5 hexane:EtOAc).



(1R,5S,7S,8R,9S)-9-Hydroxy-4-methoxy-8,9-dimethyl-8-(4-methyl-4-((triethylsilyl)oxy)pentyl)-5,7-bis(3-methylbut-2-en-1-yl)-3-(trimethylsilyl)bicyclo[3.3.1]non-3-en-2-one (394):

A THF (0.5 mL) solution of **393** (7.4 mg, 12 μmol , 1 equiv) in a 10-mL test tube was cooled to -78°C , and a freshly prepared THF solution of dilithium (cyano- κC)methyl(2,2,6,6-tetramethyl-1-piperidiny)copper⁶⁹⁵ (0.17 M, 353 μL , 60. μmol , 5 equiv) was added dropwise. The resulting pale yellow solution was stirred at -78°C for 10 min and at 0°C for 15 min. The resulting yellow solution was subsequently cooled to -78°C , and a THF solution of isobutyryl chloride (1.0 M, 60. μL , 60. μmol , 5 equiv) was added. The reaction was stirred at -78°C for 30 min and then allowed to slowly warm to rt. After stirring an additional 2.5 h, the reaction was quenched at rt with sat. aq. NH_4Cl and extracted thrice with EtOAc. The organic extracts were combined, sequentially washed with H_2O , sat. aq. NaHCO_3 , and brine, dried over Na_2SO_4 , filtered, and concentrated *in vacuo* to a yellow residue. Preparatory thin-layer chromatography (1 \times 95:5 hexane:EtOAc) afforded 3.7 mg (5.8 μmol , 49% yield) of **394** as a white flocculent solid and 1.1 mg (1.8 μmol , 15% recovery) of **393** as a pale yellow residue.

^1H NMR (600 MHz; CDCl_3) δ : 5.40 (t, $J = 6.8$ Hz, 1H), 5.05 (t, $J = 7.3$ Hz, 1H), 3.73 (s, 3H), 2.43-2.41 (m, 2H), 2.27 (s, 1H), 2.14 (dd, $J = 13.2, 5.4$ Hz, 1H), 2.02 (t, $J = 13.2$ Hz, 1H), 1.80-1.75 (m, 1H), 1.74-1.72 (m, 4H), 1.67-1.63 (m, 7H), 1.61 (s, 3H), 1.50-1.36 (m, 4H), 1.34-1.24 (m, 5H), 1.23 (s, 3H), 1.21 (s, 3H), 1.20 (s, 3H), 1.06 (s, 3H), 0.94 (t, $J = 7.9$ Hz, 9H), 0.56 (q, $J = 7.9$ Hz, 6H), 0.22 (s, 9H).

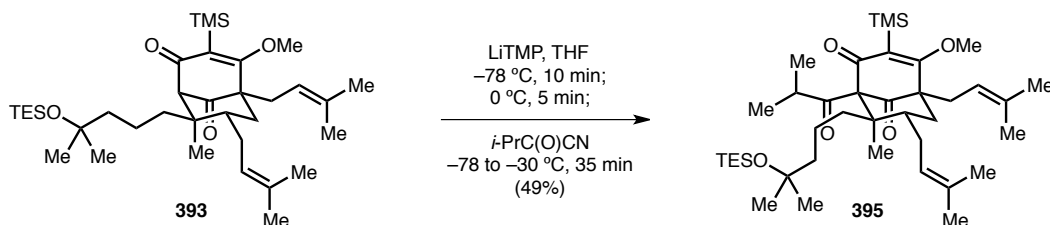
^{13}C NMR (125 MHz; CDCl_3) δ : 205.2, 187.1, 133.3, 132.8, 125.8, 124.1, 122.0, 100.3, 75.9, 74.0, 66.7, 63.7, 52.6, 46.1, 42.9, 41.9, 38.0, 31.02, 30.83, 30.66, 29.4, 28.5, 27.3, 26.4, 26.0, 22.1, 18.2, 17.8, 7.4, 7.0, 0.9.

⁶⁹⁵ For the preparation of a THF solution of dilithium (cyano- κC)methyl(2,2,6,6-tetramethyl-1-piperidiny)copper, see ref. 675.

FTIR (thin film) ν_{max} : 3503 (br), 2957, 2913, 1651, 1564, 1459, 1380, 1244, 1050, 843, 742, 723 cm^{-1} .

HRMS–ESI (m / z): $[\text{M}+\text{H}]^+$ calculated for $\text{C}_{37}\text{H}_{68}\text{O}_4\text{Si}_2$, 633.4729; found, 633.4726.

TLC R_f = 0.18 (95:5 hexane:EtOAc).



(1*S*,5*R*,7*S*,8*R*)-1-Isobutyryl-4-methoxy-8-methyl-8-(4-methyl-4-((triethylsilyl)oxy)pentyl)-5,7-bis(3-methylbut-2-en-1-yl)-3-(trimethylsilyl)bicyclo[3.3.1]non-3-ene-2,9-dione (395):

A THF (200 μ L) solution of **393** (15.9 mg, 25.8 μ mol, 1 equiv) in a 10-mL pear-shaped flask was cooled to -78 $^{\circ}$ C, and a freshly prepared THF solution of lithium 2,2,6,6-tetramethylpiperidide (0.50 M, 155 μ L, 77.3 μ mol, 3 equiv) was added dropwise. The resulting yellow solution was stirred at -78 $^{\circ}$ C for 10 min and at 0 $^{\circ}$ C for 5 min. The resulting orange solution was then cooled to -78 $^{\circ}$ C, and isobutyryl cyanide⁶⁹⁶ (12.5 mg, 129 μ mol, 5 equiv) was added. The resulting yellow solution was slowly warmed to -30 $^{\circ}$ C over 35 min and subsequently quenched with sat. aq. NaHCO_3 . The mixture was warmed to rt and extracted thrice with EtOAc. The organic extracts were combined, sequentially washed with H_2O and brine, dried over Na_2SO_4 , filtered, and concentrated *in vacuo* to a yellow residue. Preparatory thin-layer chromatography (3 \times 98:2 hexane:EtOAc) afforded 8.6 mg (13 μ mol, 49% yield) of **395** as a colorless residue.

^1H NMR (600 MHz; CDCl_3) δ : 4.98 (m, 1H), 4.97 (m, 1H), 3.91-3.88 (s, 3H), 2.55 (dd, $J = 14.5, 6.2$ Hz, 1H), 2.41 (dd, $J = 14.4, 7.6$ Hz, 1H), 2.08 (d, $J = 13.5$ Hz, 1H), 1.97 (septet, $J = 6.5$ Hz, 1H), 1.92-1.89 (m, 1H), 1.89-1.85 (m, 1H), 1.78-1.70 (m, 1H), 1.68 (s, 3H), 1.66 (s, 3H), 1.66 (s, 3H), 1.60-1.59 (m, 1H), 1.57-1.56 (s, 3H), 1.50-1.45 (m, 1H), 1.45-1.42 (m, 1H), 1.38-1.35 (m, 1H), 1.34-1.33 (m, 1H), 1.33-1.30 (m, 1H), 1.29-1.25 (m, 1H), 1.17 (s, 3H), 1.16 (s, 3H), 1.13 (d, $J = 6.5$ Hz, 3H), 1.02 (d, $J = 6.5$ Hz, 3H), 0.98 (s, 3H), 0.92 (t, $J = 7.9$ Hz, 9H), 0.54 (q, $J = 8.0$ Hz, 6H), 0.26 (s, 9H).

^{13}C NMR (125 MHz; CDCl_3) δ : 209.4, 197.6, 187.3, 134.4, 133.7, 128.3, 122.9, 119.4, 85.2, 73.6, 64.8, 59.6, 49.5, 46.1, 44.4, 43.0, 38.4, 37.4, 30.4, 30.0, 27.3, 26.13, 25.96, 21.7, 21.1, 20.7, 18.28, 18.12, 13.8, 7.4, 7.0, 0.7.

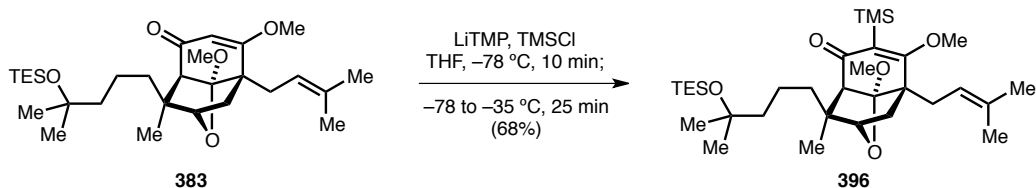
⁶⁹⁶ For the preparation of isobutyryl cyanide, see ref. 520.

FTIR (thin film) ν_{max} : 2965, 2914, 2876, 1730, 1637, 1565, 1561, 1456, 1379, 1315, 1249, 1220, 1156, 1049, 845, 743, 724 cm^{-1} .

HRMS–ESI (m / z): $[\text{M}+\text{Na}]^+$ calculated for $\text{C}_{40}\text{H}_{70}\text{O}_5\text{Si}_2$, 709.4654; found, 709.4626.

$[\alpha]_{\text{D}}^{22} = -42.9^\circ$ (*c* 0.46, CH_2Cl_2).

TLC $R_{\text{f}} = 0.47$ (95:5 hexane:EtOAc).



(2*S*,3*S*,3*aS*,7*R*,7*aS*)-6,7*a*-Dimethoxy-3-methyl-3-(4-methyl-4-((triethylsilyl)oxy)pentyl)-7-(3-methylbut-2-en-1-yl)-5-(trimethylsilyl)-3,3*a*,7,7*a*-tetrahydro-2,7-methanobenzofuran-4(2*H*)-one (396):

A THF (3 mL) solution of **383** (147 mg, 0.290 mmol, 1 equiv) in a 10-mL test tube was cooled to $-78\text{ }^{\circ}\text{C}$, and chlorotrimethylsilane (184 μL , 1.45 mmol, 5 equiv) and a freshly prepared THF solution of lithium 2,2,6,6-tetramethylpiperidide (0.50 M, 1.7 mL, 0.87, 3 equiv) were added sequentially. The resulting bright yellow solution was stirred at $-78\text{ }^{\circ}\text{C}$ for 10 min and then allowed to slowly warm to $-35\text{ }^{\circ}\text{C}$ over 25 min. The reaction was subsequently quenched at $-35\text{ }^{\circ}\text{C}$ with sat. aq. NaHCO_3 and extracted thrice with EtOAc. The organic extracts were combined, sequentially washed with H_2O and brine, dried over Na_2SO_4 , filtered, and concentrated *in vacuo* to a yellow oil. Flash column chromatography (50 mL SiO_2 , 95:5 hexane:EtOAc) afforded 114 mg (0.197 mmol, 68% yield) of **396** as a colorless oil.

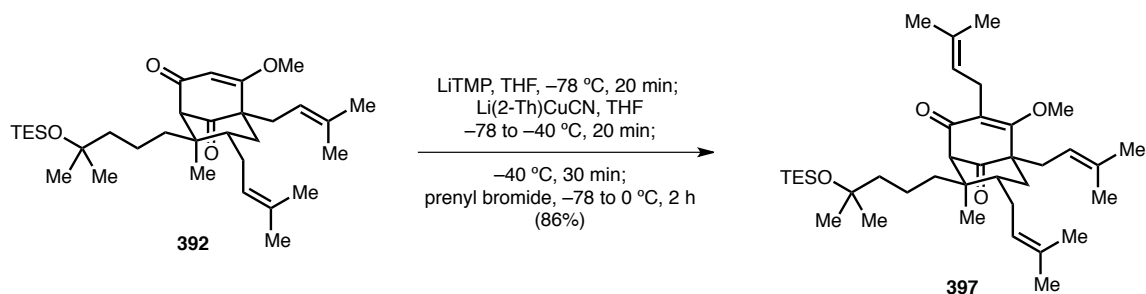
^1H NMR (600 MHz; CDCl_3) δ : 5.27 (t, $J = 6.9\text{ Hz}$, 1H), 3.85 (d, $J = 5.6\text{ Hz}$, 1H), 3.72 (s, 3H), 3.43 (s, 3H), 2.62 (s, 1H), 2.51 (dd, $J = 15.3, 6.9\text{ Hz}$, 1H), 2.28 (dd, $J = 15.3, 6.9\text{ Hz}$, 1H), 2.12 (d, $J = 12.6\text{ Hz}$, 1H), 1.90 (dd, $J = 12.6, 5.6\text{ Hz}$, 1H), 1.69 (s, 3H), 1.62 (s, 3H), 1.40-1.23 (m, 4H), 1.25-1.17 (m, 5H), 1.16 (s, 3H), 1.14 (s, 3H), 0.90 (t, $J = 7.8\text{ Hz}$, 9H), 0.52 (q, $J = 7.8\text{ Hz}$, 6H), 0.19 (s, 9H).

^{13}C NMR (125 MHz; CDCl_3) δ : 202.7, 187.3, 132.1, 122.2, 121.6, 115.2, 80.7, 73.3, 61.2, 57.5, 52.2, 49.1, 48.1, 46.0, 39.4, 35.1, 32.7, 30.6, 29.6, 28.0, 26.2, 18.7, 18.0, 7.3, 7.0, 1.1.

FTIR (thin film) ν_{max} : 2953, 2910, 2875, 1646, 1571, 1458, 1311, 1244, 1224, 1070, 1045, 1011, 843, 723 cm^{-1} .

HRMS-ESI (m/z): $[\text{M}+\text{K}]^+$ calculated for $\text{C}_{32}\text{H}_{58}\text{O}_5\text{Si}_2$, 617.3454; found, 617.3437.

TLC $R_f = 0.67$ (8:2 hexane:EtOAc).



(1*S*,5*R*,7*S*,8*R*)-4-Methoxy-8-methyl-8-(4-methyl-4-((triethylsilyl)oxy)pentyl)-3,5,7-tris(3-methylbut-2-en-1-yl)bicyclo[3.3.1]non-3-ene-2,9-dione (397):

A THF (0.5 mL) solution of **392** (7.2 mg, 13 μmol , 1 equiv) in a 10-mL test tube was cooled to -78°C , and a freshly prepared THF solution of lithium 2,2,6,6-tetramethylpiperidide (0.50 M, 53 μL , 26 μmol , 2 equiv) was added dropwise. After stirring the resulting bright yellow solution at -78°C for 20 min, a THF solution of lithium (2-thienyl)cyanocopper(I)⁵¹¹ (0.10 M, 264 μL , 26.4 mmol, 2 equiv) was added. The resulting brown slurry was allowed to slowly warm to -40°C over 20 min and subsequently stirred at -40°C for 30 min. The resulting pale yellow solution was cooled to -78°C , and prenyl bromide (7.6 μL , 66 μmol , 5 equiv) was added. The reaction was allowed to slowly warm to 0°C over 2 h, and was then quenched at 0°C with sat. aq. NH_4Cl and extracted thrice with EtOAc. The organic extracts were combined, sequentially washed with H_2O , sat. aq. NaHCO_3 , and brine, dried over Na_2SO_4 , filtered, and concentrated *in vacuo* to a brown oil. Flash column chromatography (20 mL SiO_2 , 98:2 hexane:EtOAc) afforded 7.0 mg (11 μmol , 86% yield) of **397** as a colorless oil.

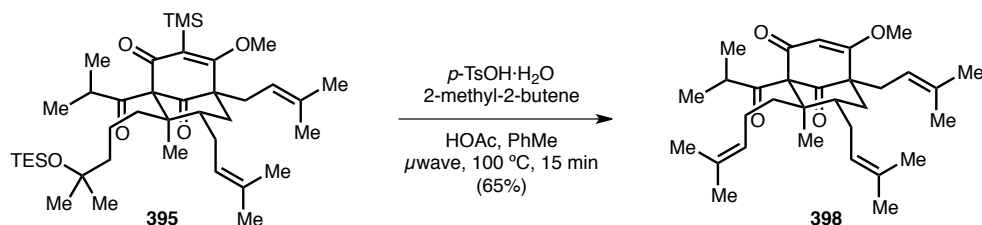
^1H NMR (600 MHz; CDCl_3) δ : 5.03-4.99 (m, 2H), 4.97 (t, $J = 7.4$ Hz, 1H), 3.88 (s, 3H), 3.17 (s, 1H), 3.11 (d, $J = 6.3$ Hz, 2H), 2.47 (dd, $J = 14.7, 6.0$ Hz, 1H), 2.34 (dd, $J = 14.7, 7.1$ Hz, 1H), 2.15-2.10 (m, 1H), 1.98 (dd, $J = 14.0, 3.9$ Hz, 1H), 1.71-1.68 (m, 4H), 1.67 (s, 6H), 1.66-1.65 (m, 4H), 1.65 (s, 3H), 1.57 (s, 3H), 1.47 (td, $J = 12.7, 4.1$ Hz, 1H), 1.43-1.36 (m, 3H), 1.36-1.28 (m, 2H), 1.22 (s, 3H), 1.21 (s, 3H), 1.11 (td, $J = 12.7, 4.0$ Hz, 1H), 0.94 (t, $J = 7.8$ Hz, 9H), 0.80 (s, 3H), 0.57 (q, $J = 7.8$ Hz, 6H).

^{13}C NMR (125 MHz; CDCl_3) δ : 207.5, 195.0, 174.3, 133.51, 133.37, 132.6, 126.9, 122.9, 122.5, 120.2, 73.7, 71.3, 62.3, 58.8, 46.7, 45.8, 41.3, 39.27, 39.07, 30.7, 30.3, 29.5, 27.7, 26.05, 26.00, 25.84, 23.5, 18.23, 18.19, 18.12, 17.99, 17.82, 7.4, 7.0.

FTIR (thin film) ν_{max} : 2963, 2914, 2875, 1732, 1655, 1601, 1452, 1382, 1340, 1233, 1170, 1043, 1016, 743, 723 cm^{-1} .

HRMS–ESI (m/z): $[\text{M}+\text{Na}]^+$ calculated for $\text{C}_{38}\text{H}_{64}\text{O}_4\text{Si}$, 635.4466; found, 635.4449.

TLC R_f = 0.45 (9:1 hexane:EtOAc).



(1*R*,5*R*,7*S*,8*R*)-1-Isobutyryl-4-methoxy-8-methyl-5,7-bis(3-methylbut-2-en-1-yl)-8-(4-methylpent-3-en-1-yl)bicyclo[3.3.1]non-3-ene-2,9-dione (398):

A PhMe (0.5 mL) solution of **395** (2.2 mg, 3.2 μ mol, 1 equiv) in a 7-mL microwave vial was treated with 2-methyl-2-butene (100 μ L), HOAc (50 μ L), and a HOAc solution of *para*-toluenesulfonic acid monohydrate (1.0 M, 6.4 μ L, 6.4 μ mol, 2 equiv). The vial was sealed and irradiated in a microwave reactor (200 watt power) to 100 $^{\circ}$ C and held at that temperature for 15 min. The resulting yellow solution was cooled to rt, quenched with sat. aq. NaHCO₃, and extracted thrice with EtOAc. The organic extracts were combined, sequentially washed with H₂O and brine, dried over Na₂SO₄, filtered, and concentrated *in vacuo* to a yellow residue. Preparatory thin-layer chromatography (3 \times 1:1 hexane:CH₂Cl₂) afforded 1.0 mg (2.1 μ mol, 65% yield) of **398** as a colorless residue.

¹H NMR (600 MHz; CDCl₃) δ : 5.89 (s, 1H), 5.04 (t, *J* = 6.8 Hz, 1H), 4.98 (t, *J* = 6.8 Hz, 1H), 4.93 (t, *J* = 6.3 Hz, 1H), 3.80 (s, 3H), 2.49 (dd, *J* = 14.8, 6.5 Hz, 1H), 2.42 (dd, *J* = 14.7, 7.6 Hz, 1H), 2.15-2.07 (m, 3H), 1.95-1.82 (m, 3H), 1.78-1.73 (m, 1H), 1.69 (s, 3H), 1.72-1.64 (m, 1H), 1.663 (s, 3H), 1.661 (s, 3H), 1.64 (s, 3H), 1.59 (s, 3H), 1.56 (s, 3H), 1.46-1.40 (m, 2H), 1.13 (d, *J* = 6.5 Hz, 3H), 1.05 (d, *J* = 6.5 Hz, 3H), 1.00 (s, 3H).

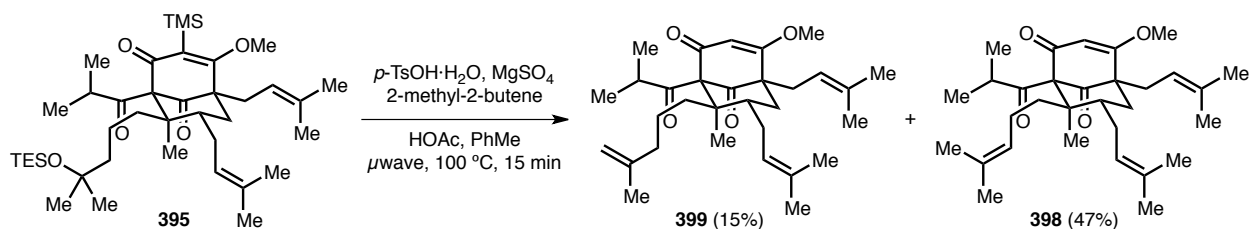
¹³C NMR (125 MHz; CDCl₃) δ : 209.5, 207.1, 193.0, 177.4, 134.4, 133.5, 131.3, 124.9, 122.6, 119.3, 107.0, 84.4, 57.30, 57.12, 49.1, 43.2, 42.7, 39.4, 36.8, 29.7, 27.5, 26.18, 26.08, 25.91, 25.2, 21.7, 20.7, 18.21, 18.19, 17.9, 13.8.

FTIR (thin film) ν_{max} : 2967, 2926, 2855, 1728, 1722, 1645, 1601, 1456, 1376, 1227 cm⁻¹.

HRMS-ESI (*m/z*): [M+H]⁺ calculated for C₃₁H₄₆O₄, 483.3468; found, 483.3469.

[α]_D²² = +37.0° (*c* 0.13, CHCl₃).

TLC R_f = 0.26 (9:1 hexane:EtOAc).



(1*R*,5*R*,7*S*,8*R*)-1-Isobutyryl-4-methoxy-8-methyl-5,7-bis(3-methylbut-2-en-1-yl)-8-(4-methylpent-4-en-1-yl)bicyclo[3.3.1]non-3-ene-2,9-dione (399):

A PhMe (3 mL) solution of **395** (58.0 mg, 84.4 μ mol, 1 equiv) in a 7-mL microwave vial was treated with 2-methyl-2-butene (100 μ L), HOAc (100 μ L), magnesium sulfate (51 mg, 0.42 mmol, 5 equiv), and a HOAc solution of *para*-toluenesulfonic acid monohydrate (1.0 M, 60. μ L, 60. μ mol, 0.7 equiv). The vial was sealed and irradiated in a microwave reactor (200 watt power) to 100 $^{\circ}$ C and held at that temperature for 15 min. The resulting yellow slurry was cooled to rt, quenched with sat. aq. NaHCO₃, and extracted thrice with EtOAc. The organic extracts were combined, sequentially washed with H₂O and brine, dried over Na₂SO₄, filtered, and concentrated *in vacuo* to a yellow oil. The oil was split into two samples and purified using preparatory high-performance liquid chromatography with a 30 mm \times 250 mm Agilent Prep-SIL 10 μ m column (injection volume: 500 μ L each, hexane; detection at 254 nm; 23 $^{\circ}$ C \pm 2 $^{\circ}$ C column temperature; 40 mL/min flow rate; gradient elution from 100:0 \rightarrow 60:40 hexane:CH₂Cl₂ over 45 min). The fractions eluting at 34-37 min were collected and concentrated *in vacuo* to afford 6.2 mg (13 μ mol, 15% yield) of **399** as a colorless oil. The fractions eluting at 28-33 min were collected and concentrated *in vacuo* to afford 19.3 mg (39.8 μ mol, 47% yield) of **398** as a colorless oil.

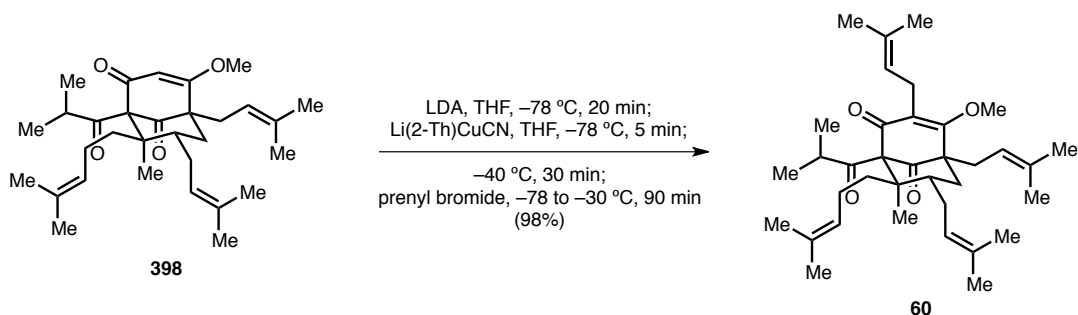
¹H NMR (600 MHz; CDCl₃) δ : 5.89 (s, 1H), 4.98 (t, *J* = 6.9 Hz, 1H), 4.93 (t, *J* = 6.8 Hz, 1H), 4.71-4.59 (m, 2H), 3.80 (s, 3H), 2.48 (dd, *J* = 14.5, 6.0 Hz, 1H), 2.42 (dd, *J* = 14.5, 7.8 Hz, 1H), 2.11 (septet, *J* = 6.5 Hz, 1H), 2.06 (dd, *J* = 13.9, 5.3 Hz, 1H), 1.96-1.83 (m, 4H), 1.76-1.72 (m, 1H), 1.70 (s, 3H), 1.69 (s, 3H), 1.66 (s, 6H), 1.59-1.55 (m, 5H), 1.45-1.34 (m, 3H), 1.12 (d, *J* = 6.5 Hz, 3H), 1.05 (d, *J* = 6.5 Hz, 3H), 0.99 (s, 3H).

^{13}C NMR (125 MHz; CDCl_3) δ : 209.6, 207.1, 193.0, 177.4, 146.3, 134.4, 133.5, 122.7, 119.3, 110.0, 107.0, 84.4, 57.32, 57.12, 49.1, 43.3, 42.7, 39.4, 38.8, 36.8, 29.7, 27.5, 26.19, 26.10, 24.5, 22.7, 21.7, 20.7, 18.22, 18.17, 13.8.

FTIR (thin film) ν_{max} : 2968, 2927, 2872, 1729, 1645, 1601, 1449, 1374, 1231 cm^{-1} .

HRMS–ESI (m/z): $[\text{M}+\text{Na}]^+$ calculated for $\text{C}_{31}\text{H}_{46}\text{O}_4$, 505.3288; found, 505.3278.

TLC R_f = 0.26 (9:1 hexane:EtOAc).



(1*R*,5*R*,7*S*,8*R*)-1-Isobutyryl-4-methoxy-8-methyl-3,5,7-tris(3-methylbut-2-en-1-yl)-8-(4-methylpent-3-en-1-yl)bicyclo[3.3.1]non-3-ene-2,9-dione (60, hyperforin *O*-methyl ether):³⁰⁹

A THF (5 mL) solution of **398** (107.4 mg, 222.5 μ mol, 1 equiv) in a 50-mL pear-shaped flask was cooled using a $-78\text{ }^{\circ}\text{C}$ dry ice/acetone bath, and a freshly prepared THF solution of lithium diisopropylamide (0.50 M, 1.3 mL, 670 μ mol, 3 equiv) was added dropwise. After stirring the resulting yellow solution at $-78\text{ }^{\circ}\text{C}$ for 20 min, a freshly prepared THF solution of 2-thienyl(cyano)copper lithium⁵¹¹ (0.10 M, 6.7 mL, 0.67 mmol, 3 equiv) was added dropwise. The resulting light brown solution was stirred at $-78\text{ }^{\circ}\text{C}$ for 5 min and at $-40\text{ }^{\circ}\text{C}$ for 30 min. The solution was then cooled using a $-78\text{ }^{\circ}\text{C}$ dry ice/acetone bath, and prenyl bromide (437 μ L, 3.34 mmol, 15 equiv) was added dropwise. After slowly warming the golden yellow solution to $-30\text{ }^{\circ}\text{C}$ over 90 min, it was quenched at $-30\text{ }^{\circ}\text{C}$ with sat. aq. NH_4Cl , warmed to rt, and extracted thrice with EtOAc. The organic extracts were combined, sequentially washed with H_2O , sat. aq. NaHCO_3 , and brine, dried over Na_2SO_4 , filtered, and concentrated *in vacuo* to a yellow oil. Flash column chromatography (75 mL SiO_2 , 98:2 hexane:EtOAc) afforded 120.6 mg (219.0 μ mol, 98% yield) of **60** as a colorless oil.

^1H NMR (500 MHz; CDCl_3) δ : 5.07-5.02 (m, 2H), 4.99 (t, $J = 6.7\text{ Hz}$, 1H), 4.95 (t, $J = 7.1\text{ Hz}$, 1H), 3.92 (s, 3H), 3.18 (d, $J = 6.5\text{ Hz}$, 2H), 2.50 (dd, $J = 14.7, 6.0\text{ Hz}$, 1H), 2.41 (dd, $J = 14.7, 7.4\text{ Hz}$, 1H), 2.11-2.06 (m, 2H), 1.99 (septet, $J = 6.5\text{ Hz}$, 1H), 1.92-1.84 (m, 3H), 1.77-1.70 (m, 1H), 1.69-1.66 (m, 15H), 1.64 (s, 3H), 1.63-1.62 (m, 1H), 1.59 (s, 3H), 1.56 (s, 3H), 1.44-1.41 (m, 1H), 1.39-1.37 (m, 1H), 1.11 (d, $J = 6.5\text{ Hz}$, 3H), 1.02 (d, $J = 6.5\text{ Hz}$, 3H), 0.99 (s, 3H).

^{13}C NMR (125 MHz; CDCl_3) δ : 209.3, 207.3, 194.1, 174.1, 134.0, 133.5, 133.2, 131.2, 127.6, 125.0, 122.7, 121.9, 119.9, 84.3, 62.6, 58.9, 49.4, 43.4, 42.8, 39.1, 36.7, 30.3, 27.3, 26.10, 26.01, 25.88, 25.80, 25.1, 23.6, 21.5, 20.6, 18.27, 18.14, 18.12, 17.9, 13.8.

FTIR (thin film) ν_{max} : 2968, 2927, 2874, 1730, 1725, 1645, 1601, 1447, 1377, 1338, 1236, 1100, 1079, 1060 cm^{-1} .

HRMS–ESI (m/z): $[\text{M}+\text{H}]^+$ calculated for $\text{C}_{36}\text{H}_{54}\text{O}_4$, 551.4095; found, 551.4102.

$[\alpha]_{\text{D}}^{22} = +49.6^\circ$ (c 0.33, CHCl_3).

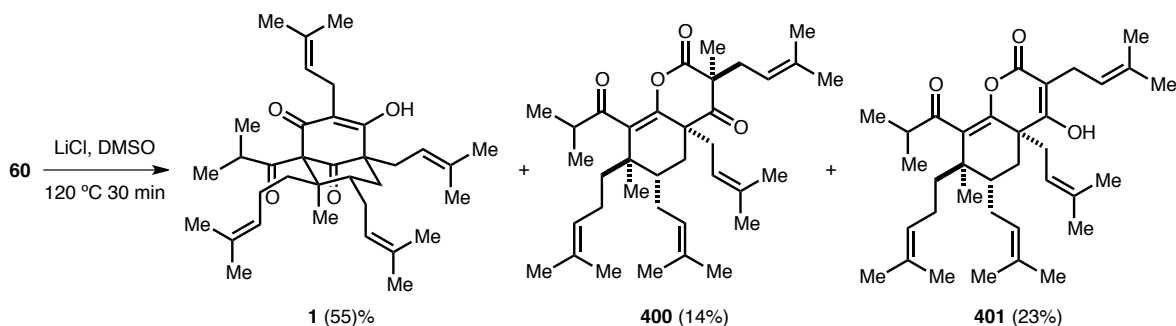
TLC $R_f = 0.52$ (9:1 hexane:EtOAc).

Table 3.5. NMR data comparison of synthetic **60** with **60** derived from natural hyperforin (ref. 309).

¹ H NMR (500 MHz, CDCl ₃)		¹³ C NMR (125 MHz, CDCl ₃)	
Hyperforin-derived	Synthetic	Hyperforin-derived	Synthetic ^b
5.05 (t, <i>J</i> = 7.0, 1H)	5.07-5.02 (m, 2H)	209.1	209.1
5.03 (t, <i>J</i> = 7.0, 1H)		207.1	207.1
4.99 (t, <i>J</i> = 7.0, 1H)	4.99 (t, <i>J</i> = 6.7, 1H)	193.9	193.9
4.94 (t, <i>J</i> = 7.1, 1H)	4.95 (t, <i>J</i> = 7.1, 1H)	173.9	173.9
3.91 (s, 3H)	3.92 (s, 3H)	133.8	133.7
3.17 (d, <i>J</i> = 6.5, 1H) ^a	3.18 (d, <i>J</i> = 6.5, 2H)	133.3	133.3
2.49 (dd, <i>J</i> = 15.0, 6.0, 1H)	2.50 (dd, <i>J</i> = 14.7, 6.0, 1H)	132.9	132.9
2.40 (dd, <i>J</i> = 15.0, 7.5, 1H)	2.41 (dd, <i>J</i> = 14.7, 7.4, 1H)	131.0	131.0
2.10 (m, 1H)	2.11-2.06 (m, 2H)	127.4	127.4
2.07 (m, 1H)		124.7	124.8
^a	1.99 (septet, <i>J</i> = 6.5, 1H)	122.5	122.5
1.87 (m, 1H)	1.92-1.84 (m, 3H)	121.7	121.7
1.85 (m, 1H)		119.7	119.7
1.73 (m, 1H)	1.77-1.70 (m, 1H)	84.1	84.1
1.67 (s, 3H)	1.69-1.66 (m, 15H)	^a	62.3
1.67 (s, 3H)		58.6	58.6
1.67 (s, 3H)		49.2	49.1
1.67 (s, 3H)		43.2	43.2
1.63 (s, 3H)		42.6	42.6
1.63 (s, 3H)		38.8	38.8
^a	1.64 (s, 3H)	36.5	36.5
	1.63-1.62 (m, 1H)	30.1	30.1
1.58 (s, 3H)	1.59 (s, 3H)	27.1	27.1
1.55 (s, 3H)	1.56 (s, 3H)	25.9	25.9
^a	1.44-1.41 (m, 1H)	25.8	25.8
1.39 (m, 1H)	1.39-1.37 (m, 1H)	25.7	25.7
1.10 (d, <i>J</i> = 6.5, 3H)	1.11 (d, <i>J</i> = 6.5, 3H)	25.6	25.6
1.01 (d, <i>J</i> = 6.5, 3H)	1.02 (d, <i>J</i> = 6.5, 3H)	24.9	24.9
0.98 (s, 3H)	0.99 (s, 3H)	23.4	23.4
		21.3	21.3
		20.4	20.4
		18.0	18.0
		17.9	17.91
		17.9	17.89
		17.6	17.6
		13.6	13.6

^a Several NMR signals for **60** are not reported in ref. 309. In particular, there are only 50 protons reported for **60**, which contains 54 protons. Also, the shift of the *O*-methyl group is not reported in the ¹³C NMR data.

^b For the purpose of this analysis, the CDCl₃ signal in the ¹³C NMR of synthetic **60** was re-referenced to 77.00 ppm to match the reported chemical shift reference in ref. 309.



Note: All manipulations for the following procedure were conducted in the dark. Solvents used during the workup procedure were sparged for at least 15 min with N₂ prior to use.

A DMSO (3 mL) slurry of **60** (74.9 mg, 136 μmol , 1 equiv) and lithium chloride (58 mg, 1.4 mmol, 10 equiv) in a 15-mL round-bottom flask was heated to 120 $^{\circ}\text{C}$. After stirring the pale yellow solution for 30 min at 120 $^{\circ}\text{C}$, it was cooled to rt, diluted with H₂O, and extracted thrice with 1:1 hexane:EtOAc. The organic extracts were combined, sequentially washed thrice with H₂O and once with brine, dried over Na₂SO₄, filtered, and concentrated *in vacuo* to afford a yellow oil. Flash column chromatography (30 mL SiO₂, 95:5 hexane:EtOAc) afforded 40.0 mg (74.5 μmol , 55% yield) of **1** as a colorless oil, 10.8 mg (19.6 μmol , 14% yield) of **400** as a colorless oil, and 12.5 mg (23.3 μmol , 23% yield) of **401** as a colorless oil.

Hyperforin (1):

¹H NMR (500 MHz; CD₃OD) δ : 5.12 (t, J = 7.0 Hz, 1H), 5.04-4.95 (m, 3H), 3.12 (dd, J = 14.6, 7.2 Hz, 1H), 3.07 (dd, J = 14.7, 7.1 Hz, 1H), 2.49 (dd, J = 14.4, 6.9 Hz, 1H), 2.40 (dd, J = 14.6, 6.8 Hz, 1H), 2.14 (septet, J = 6.5 Hz, 1H), 2.10-2.02 (m, 1H), 2.02-1.87 (m, 3H), 1.78-1.72 (m, 3H), 1.71 (s, 3H), 1.68 (s, 6H), 1.66 (s, 3H), 1.66-1.63 (m, 1H), 1.64 (s, 3H), 1.63 (s, 3H), 1.59 (s, 3H), 1.58 (s, 3H), 1.37 (dd, J = 13.3, 12.2 Hz, 1H), 1.09 (d, J = 6.5 Hz, 3H), 1.04 (d, J = 6.5 Hz, 3H), 0.97 (s, 3H).

¹³C NMR (125 MHz; CD₃OD) δ : 211.7, 208.8, 134.6, 134.2, 133.5, 131.8, 126.1, 123.8, 122.6, 122.1, 120.9, 82.6, 60.7, 49.5, 43.05, 43.02, 40.8, 37.9, 30.7, 28.6, 26.16, 26.06, 25.99, 25.92, 25.4, 22.5, 22.0, 21.2, 18.27, 18.16, 18.11, 17.86, 15.3.

FTIR (thin film) ν_{max} : 3326 (br), 2969, 2925, 2876, 1725, 1601, 1447, 1377, 1232, 838 cm⁻¹.

HRMS-ESI (m/z): [M+H]⁺ calculated for C₃₅H₅₂O₄, 537.3938; found, 537.3937.

$[\alpha]_{\text{D}}^{23} = +39.5^{\circ}$ (*c* 3.02, EtOH); [natural sample from literature:¹ $[\alpha]_{\text{D}}^{18} = +41^{\circ}$ (*c* 5, EtOH)].

TLC $R_f = 0.26$ (9:1 hexane:EtOAc).

(3*S*,4*aS*,6*S*,7*R*)-8-Isobutyryl-3,7-dimethyl-3,4*a*,6-tris(3-methylbut-2-en-1-yl)-7-(4-methylpent-3-en-1-yl)-4*a*,5,6,7-tetrahydro-2*H*-chromene-2,4(3*H*)-dione (400):

¹H NMR (500 MHz; CDCl₃) δ : 5.09 (t, *J* = 6.1 Hz, 1H), 5.01-4.96 (m, 2H), 4.93 (t, *J* = 6.4 Hz, 1H), 2.71 (septet, *J* = 6.9 Hz, 1H), 2.64 (dd, *J* = 13.7, 8.1 Hz, 1H), 2.57 (dd, *J* = 13.7, 7.1 Hz, 1H), 2.46 (dd, *J* = 13.5, 2.7 Hz, 1H), 2.25 (dd, *J* = 14.5, 7.0 Hz, 1H), 2.06 (dd, *J* = 13.8, 4.9 Hz, 1H), 1.84-1.76 (m, 5H), 1.74-1.69 (m, 4H), 1.69-1.63 (m, 4H), 1.62 (s, 3H), 1.62 (s, 3H), 1.60 (s, 3H), 1.59 (s, 3H), 1.52 (s, 3H), 1.52-1.49 (m, 1H), 1.47 (s, 3H), 1.37 (t, *J* = 13.3 Hz, 1H), 1.31-1.25 (m, 1H), 1.21 (d, *J* = 6.9 Hz, 3H), 1.15 (d, *J* = 6.9 Hz, 3H), 1.14 (s, 3H), 1.11-1.07 (m, 1H).

¹³C NMR (125 MHz; CDCl₃) δ : 209.0, 205.2, 169.8, 144.5, 137.2, 136.25, 136.11, 133.4, 132.0, 124.0, 122.5, 119.3, 117.1, 56.8, 52.3, 42.6, 40.9, 37.51, 37.37, 34.3, 31.5, 27.27, 27.15, 26.24, 26.14, 26.10, 25.9, 25.2, 23.2, 22.8, 18.7, 18.31, 18.28, 18.25, 17.8, 17.5.

FTIR (thin film) ν_{max} : 2971, 2930, 2875, 1778, 1724, 1699, 1665, 1451, 1377, 1255, 1237, 1136, 1094, 1056, 844 cm⁻¹.

HRMS–ESI (*m/z*): [M+H]⁺ calculated for C₃₆H₅₄O₄, 551.4096; found, 551.4095.

TLC $R_f = 0.66$ (9:1 hexane:EtOAc).

(4*aR*,6*S*,7*R*)-4-Hydroxy-8-isobutyryl-7-methyl-3,4*a*,6-tris(3-methylbut-2-en-1-yl)-7-(4-methylpent-3-en-1-yl)-4*a*,5,6,7-tetrahydro-2*H*-chromen-2-one (401):

¹H NMR (500 MHz; CDCl₃) δ : 5.11-4.98 (m, 3H), 4.93 (t, *J* = 6.5 Hz, 1H), 3.35-3.33 (m, ~0.7H), 3.22 (dd, *J* = 8.3, 5.8 Hz, ~0.3H), 2.77-2.56 (m, 3H), 2.52-2.42 (m, 1H), 2.25 (dd, *J* = 14.2, 6.3 Hz, ~0.3H), 2.17-2.02 (m, 2H), 1.91 (dd, *J* = 14.5, 8.2 Hz, ~0.7H), 1.88-1.80 (m, 1H), 1.76 (s, ~1H), 1.75 (s, ~2H), 1.72 (s, 3H), 1.69 (s, 3H), 1.66 (s, 3H), 1.63-1.62 (m, 4H), 1.62-1.61 (m, 4H), 1.60 (s, 3H), 1.60-1.44 (m, 7H), 1.44-1.25 (m, 3H), 1.23 (s, 3H), 1.15-1.11 (m, 3H) (*mixture of tautomers and diastereomers*).

^{13}C NMR (125 MHz; CDCl_3) δ : 208.9, 202.3, 201.7, 167.2, 166.2, 145.3, 144.9, 137.75, 137.65, 137.4, 136.9, 135.3, 133.50, 133.40, 132.00, 131.94, 124.03, 123.93, 122.49, 122.37, 119.7, 118.0, 116.97, 116.88, 55.2, 54.6, 53.1, 52.6, 42.78, 42.64, 41.1, 37.9, 37.63, 37.46, 37.32, 34.1, 32.7, 29.6, 28.1, 27.34, 27.31, 27.27, 26.24, 26.09, 26.07, 26.04, 25.90, 23.41, 23.21, 23.06, 22.97, 22.85, 18.95, 18.76, 18.35, 18.28, 18.24, 18.22, 18.10, 17.86, 17.83, 17.81, 17.63 (*mixture of tautomers and diastereomers*).

FTIR (thin film) ν_{max} : 2969, 2916, 2875, 1781, 1728, 1697, 1665, 1447, 1377, 1254, 1223, 1142, 1102, 1050 cm^{-1} .

HRMS–ESI (m/z): $[\text{M}+\text{Na}]^+$ calculated for $\text{C}_{35}\text{H}_{52}\text{O}_4$, 559.3758; found, 559.3756.

TLC R_f = 0.51 (9:1 hexane:EtOAc).

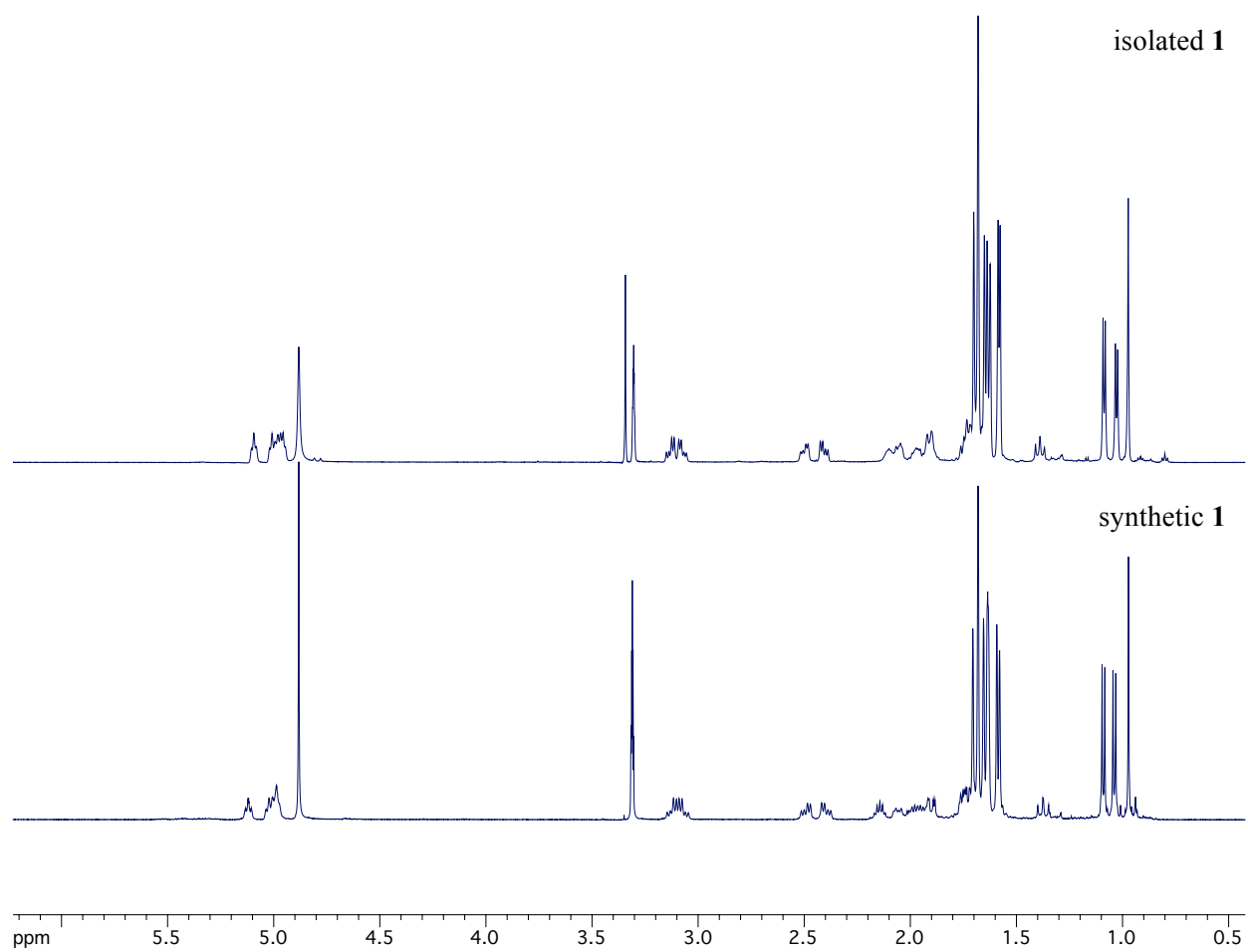


Figure 3.5. ^1H NMR spectra comparison of natural and synthetic hyperforin (**1**).

NMR Data Comparison of Synthetic and Natural Hyperforin (1).

On the following pages, the ^1H and ^{13}C NMR data for synthetic **1** are compared to published data for natural **1** as well as synthetic *ent*-**1**. All NMR data have been acquired using CD_3OD solvent. NMR spectrometer frequencies are noted.

The references from which NMR data for natural **1** are presented include:

Reference A: Erdelmeier, C. A. J. *Pharmacopsychiatry* **1998**, 31 (Supplement 1), 2-6.

Reference B: Adam, P. A.; Arigoni, D.; Bacher, A.; Eisenreich, W. *J. Med. Chem.* **2002**, 45, 4786-4793.

Reference C: Cui, Y.; Ang, C. Y. W.; Beger, R. D.; Heinze, T. M.; Hu, L.; Leakey, J. *Drug Metab. Dispos.* **2004**, 32, 28-34.

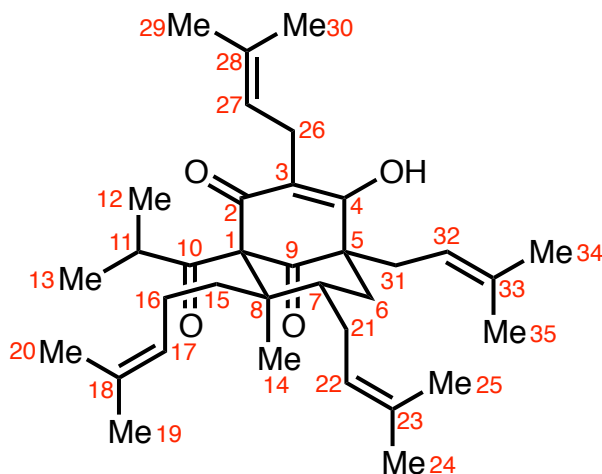
Reference D: Lee, J.-y.; Duke, R. K.; Tran, V. H.; Hook, J. M.; Duke, C. C. *Phytochemistry* **2006**, 67, 2550-2560.

Reference E: Cao, X.; Wang, Q.; Li, Y.; Bai, G.; Ren, H.; Xu, C.; Ito, Y. *J. Chromatogr. B* **2011**, 879, 480-488.

The reference from which NMR data for *ent*-**1** are presented:

Reference F: Shimizu, Y.; Shi, S.-L.; Usuda, H.; Kanai, M.; Shibasaki, M. *Tetrahedron* **2010**, 66, 6569-6584.

The positional numbering scheme used for these tables is shown below.



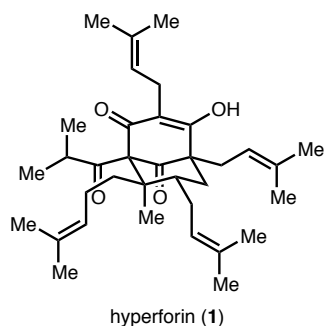
As previously noted,⁴⁶² small deviations in the NMR data from the different references may be attributed to not only different chemical shift references but also to the concentration of **1** and to the water content in the NMR sample, which influence the keto-enol tautomerization at the hyperforin C2–C4 position. In the ¹H NMR analysis of **1**, we observed concentration- and water-dependent changes in the lineshape of the C26 proton signals and in the chemical shifts of the C11, C12, and C13 proton signals. We also observed broadening of the C1 and C5 signals and an absence of the C2 and C4 signals in the ¹³C NMR spectrum of **1**.

Table 3.6. ^1H NMR data comparison of synthetic and natural hyperforin (**1**).

	Ref. A	Ref. B	Ref. C	Ref. D	Ref. E	Ref. F	This work
Position	200 MHz	500 MHz	600 MHz	600 MHz	600 MHz	500 MHz	500 MHz
27		5.00 (m, 1H)	5.04 (t, $J = 5.8$, 1H)	5.10 (t-quint, $J = 7.2$, 1.5, 1H)	5.18 (tt, $J = 7.2$, 1.2, 1H)	5.15-5.11 (m, 1H)	5.12 (t, $J = 7.0$, 1H)
22	5.14-4.92 (m, 4H)	4.92 (m, 1H)	4.93 (m, 1H)	5.01 (t-quint, $J = 7.3$, 1.5, 1H)	5.11 (tt, $J = 7.2$, 1.2, 1H)		
32		4.90 (m, 1H)	4.91 (m, 1H)	4.99 (br t, $J = 7.8$, 1H)	4.76 (tq, $J = 7.2$, 1.2, 1H)	5.07-4.97 (m, 3H)	5.04-4.95 (m, 3H)
17		4.87 (m, 1H)	4.89 (m, 1H)	4.96 (t, $J = 6.5$, 1H)	4.76 (tq, $J = 7.2$, 1.2, 1H)		
26a	3.20-3.00 (m, 2H)	3.05 (dd, 1H)	3.03 (dd, $J = 14.8$, 7.3, 1H)	3.14 (dd, $J = 14.6$, 7.2, 1H)	3.20 (septet, $J = 7.2$, 2H)	3.17 (dd, $J = 14.7$, 7.0, 1H)	3.12 (dd, $J = 14.6$, 7.2, 1H)
26b		2.99 (dd, 1H)	2.99 (dd, $J = 14.8$, 7.1, 1H)	3.09 (br, 1H)		3.11 (dd, $J = 14.7$, 6.7, 1H)	3.07 (dd, $J = 14.7$, 7.1, 1H)
31a	2.57-2.34 (m, 2H)	2.41 (dd, 1H)	2.38 (dd, $J = 14.5$, 7.0, 1H)	2.51 (dd, $J = 14.7$, 6.7, 1H)		2.54 (dd, $J = 14.1$, 6.7, 1H)	2.49 (dd, $J = 14.4$, 6.9, 1H)
31b		2.32 (dd, 1H)	2.29 (dd, $J = 14.5$, 6.5, 1H)	2.41 (dd, $J = 14.6$, 7.0, 1H)	2.49 (dd, $J = 7.2$, 4.8, 2H)	2.44 (dd, $J = 14.1$, 7.0, 1H)	2.40 (dd, $J = 14.6$, 6.8, 1H)
11	2.10 (sept, $J = 6.5$, 1H)	2.02 (m, 1H)	2.07 (m, $J = 6.5$, 1H)	2.10 (br, 1H)	2.11 (m, 1H)		2.14 (septet, $J = 6.5$, 1H)
16a		1.95 (m, 1H)	1.97 (m, 1H)	2.06 (m, 1H)			2.10-2.02 (m, 1H)
6a		1.85 (m, 2H)	1.88 (dd, $J = 13.4$, 4.1, 1H)	1.97 (m, 1H)	2.02 (m, 2H)	2.19-1.90 (m, 5H)	2.02-1.87 (m, 3H)
21a			1.87 (m, 2H)	1.91 (m, 2H)			
21b		1.82 (m, 1H)			1.92 (m, 1H)		
7	2.15-1.20 (m, 9H)	1.65 (m, 1H)	1.70 (m, 1H)	1.91 (m, 1H)	1.80 (m, 2H)		1.78-1.72 (m, 3H)
15a		1.64 (m, 1H)	1.66 (m, 1H)	1.74 (m, 1H)			
16b			1.64 (m, 1H)	1.73 (m, 1H)	1.80 (m, 1H)	1.79-1.66 (m, 4H)	
15b		1.59 (m, 2H)	1.60 (m, 1H)	1.68 (m, 2H)	1.75 (m, 1H)		1.66-1.63 (m, 1H)
6b		1.30 (m, 1H)	1.27 (dd, $J = 13.4$, 13.0, 1H)		1.27 (m, 1H)	1.47-1.38 (m, 1H)	1.37 (dd, $J = 13.3$, 12.2, 1H)
30	1.71-1.69 (m, 3H)	1.61 (s, 3H)	1.60 (s, 3H)	1.71 (s, 3H)	1.70 (s, 3H)	1.74 (s, 3H)	1.71 (s, 3H)
19	1.68 (m, 6H)	1.59 (s, 3H)	1.58 (s, 3H)	1.69 (s, 3H)	1.64 (s, 3H)		1.68 (s, 6H)
34		1.59 (3H)	1.58 (s, 3H)	1.69 (s, 3H)		1.72 (s, 6H)	
35		1.56 (3H)	1.55 (s, 3H)	1.66 (s, 3H)	1.60 (s, 6H)		1.66 (s, 3H)
24	1.66-1.62 (m, 9H)	1.55 (3H)	1.53 (s, 3H)	1.646 (s, 3H)	1.50 (s, 3H)	1.68 (s, 3H)	1.64 (s, 3H)
29		1.53 (3H)	1.53 (s, 3H)	1.63 (s, 3H)	1.50 (s, 3H)	1.66 (s, 3H)	1.63 (s, 3H)
25		1.49 (s, 3H)	1.49 (s, 3H)	1.59 (s, 3H)	1.50 (s, 3H)	1.62 (s, 3H)	1.59 (s, 3H)
20	1.58 (s, 6H)	1.48 (s, 3H)	1.46 (s, 3H)	1.585 (s, 3H)	1.47 (s, 3H)	1.61 (s, 3H)	1.58 (s, 3H)
12	1.09 (d, $J = 6.5$, 3H)	0.99 (d, 3H)	0.99 (d, $J = 6.5$, 3H)	1.09 (d, $J = 6.5$, 3H)	1.15 (dd, 6H)	1.12 (d, $J = 6.4$, 3H)	1.09 (d, $J = 6.5$, 3H)
13	1.03 (d, $J = 6.5$, 3H)	0.94 (d, 3H)	0.95 (d, $J = 6.5$, 3H)	1.03 (br, 3H)		1.06 (d, $J = 6.4$, 3H)	1.04 (d, $J = 6.5$, 3H)
14	0.97 (s, 3H)	0.88 (s, 3H)	0.87 (s, 3H)	0.98 (s, 3H)	0.98 (s, 3H)	1.01 (s, 3H)	0.97 (s, 3H)

Table 3.7. ^{13}C NMR data comparison of synthetic and natural hyperforin (1).

	Ref. A	Ref. B	Ref. C	Ref. D	Ref. E	Ref. F	This work
Position	50 MHz	125 MHz	150 MHz	150 MHz	150 MHz	125 MHz	125 MHz
1	82.6 (br)	82 (br)	82.7	82.74	82.42	--	82.6 (br)
2	185.3 (br)	--	212.9	--	209.64	--	--
3	122.1	122.12	121.3	122.1	120.25	121.90	122.1
4	181.2 (br)	--	182.2	--	181.59	--	--
5	60.8 (br)	60 (br)	61.2	--	58.27	--	60.7 (br)
6	40.8	40.82	40.7	40.8	40.27	41.68	40.8
7	43.0	42.95	43.3	43.1	42.57	43.94	43.02
8	49.5	49.10	49.5	49.54	47.81	--	49.5
9	208.8	208.85	210.0	208.82	208.35	--	208.8
10	211.7	211.78	212.9	211.7	209.64	--	211.7
11	43.0	43.00	42.8	43.0	41.57	43.68	43.05
12	22.0	21.98	21.0	21.99	20.44	22.86	22.0
13	21.2	21.16	19.8	20.85	19.36	22.01	21.2
14	15.3	15.31	15.2	15.3	15.8	16.13	15.3
15	37.9	37.92	38.0	37.88	37.68	38.81	37.9
16	25.4	25.42	28.8	28.62	27.66	26.33	25.4
17	126.1	126.04	123.7	120.85	122.31	122.82	126.0
18	131.8	131.84	133.9	134.69	133.36	--	131.8
19	25.9	25.87	25.9	25.90	24.88	26.74	25.92
20	18.1	18.09	17.9	17.84	17.92	18.94	18.11
21	28.6	28.62	25.6	25.43	24.0	29.52	28.6
22	123.8	123.77	126.3	126.05	126.61	126.98	123.8
23	134.2	134.25	131.6	131.81	131.61	135.04	134.2
24	26.0	25.97	26.0	25.98	24.90	26.83	25.99
25	18.2	18.15	18.1	18.1	18.01	19.01	18.16
26	22.5	22.50	22.8	22.50	22.40	23.43	22.5
27	122.6	122.53	124.1	122.54	122.71	124.73	122.6
28	133.5	133.60	132.5	133.58	133.19	132.63	133.5
29	26.1	26.05	26.1	26.16	24.99	26.90	26.06
30	17.9	17.84	18.2	18.15	18.10	18.70	17.86
31	30.7	30.69	30.8	30.70	30.03	31.59	30.7
32	120.9	120.86	121.5	123.74	121.21	123.66	120.9
33	134.7	134.71	134.1	134.25	132.93	135.44	134.6
34	26.2	26.15	26.0	26.05	25.01	27.02	26.16
35	18.3	18.25	18.2	18.25	18.14	19.10	18.27



Isolation of hyperforin (1) from St. John's Wort extract:⁶⁹⁷

Supercritical CO₂ extract of St. John's wort was obtained from Flavex Naturextrakte GmbH as a generous gift or was purchased from "From Nature with Love." The brown resinous extract (1.468 g) was dissolved in MeOH (150 mL, saturated in heptane) and heptane (50 mL, saturated in MeOH) with the aid of sonication. The layers were separated, and the heptane fraction was extracted twice with MeOH (75 mL each, saturated in heptane). The MeOH extracts were combined, washed twice with heptane (50 mL, saturated in MeOH), and concentrated *in vacuo* to a brown-yellow syrup. Flash column chromatography (500 mL SiO₂, 98:2 → 95:5 → 9:1 hexane:EtOAc) afforded 572 mg (1.07 mmol, 38% yield by weight of initial extract) of **1** as a pale yellow syrup.

⁶⁹⁷ This procedure was adapted from ref. 44.

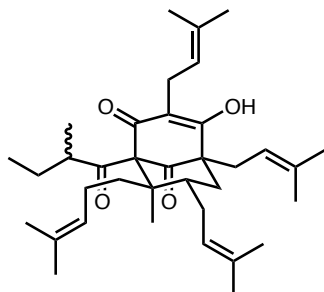
Appendix A

A Comprehensive Listing of all Polycyclic Polyprenylated Acylphloroglucinols

In the table below, all known 260 PPAPs are listed. The PPAPs are presented in alphabetical order, except for certain instances (e.g., epimers, ethers). Along with the name and structure of each PPAP, the plant species and geographical location from which that PPAP has been isolated is listed. In cases where a PPAP has been isolated from multiple species, the species from which the PPAP was initially isolated is listed in boldface text. In addition, references to spectroscopic data (i.e., NMR, UV, IR) and relevant crystal structure refinements are provided. Optical rotation data is also listed. Unless indicated by an explicit reference to an absolute configuration determination, an arbitrary enantiomer is depicted for each PPAP. For certain PPAPs, multiple names have been given, mostly due to simultaneous discovery of the PPAP by several groups. All alternative names are provided in italicized text below name that was provided by the initial published report. If a PPAP has been isolated in both enantiomeric forms, the name of its corresponding enantiomeric PPAP is also found below its name. All references herein are found at the end of this appendix.

acuminophenone A (1)		<i>Rheedia acuminata</i> (La Paz, Bolivia) ¹ (NMR, UV, IR) ¹ [α] _D = +208° (CHCl ₃) ¹
adhyperfirin (2)		<i>Hypericum empetrifolium</i> (northern Jordan) ² <i>H. perforatum</i> Germany ³ Epirus, Greece ⁴ Cemernik Mountain, southern Serbia ⁵ <i>H. reflexum</i> (Halle-Wittenberg, Germany) ³ <i>H. triquetrifolium</i> (Al-Mafraq, Jordan) ⁶ ¹ H NMR ⁴

adhyperforin
(3)



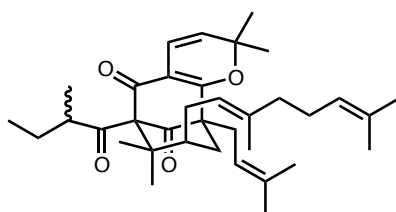
Hypericum calycinum (Bonn, Germany)⁷
H. elodes (Umbrian-Marchean Apennines, Italy)⁸
H. maculatum (Prakovce, Slovakia)⁹
H. perforatum (El Feidja, northwestern Tunisia)¹⁰

H. perforatum

Mt. Taylor, Canberra, Australia¹¹
Alpirsbach, Black Forest, Germany¹²
 Epirus, Greece⁴
 Italy¹³
 Cemernik Mountain, southern Serbia⁵
 Nová Ľubovňa, Slovakia¹⁴
 El Feidja, northwestern Tunisia¹⁰
H. ericoides (El Feidja, northwestern Tunisia)¹⁰

¹H NMR^{4,12} (¹³C NMR, UV, IR)¹²

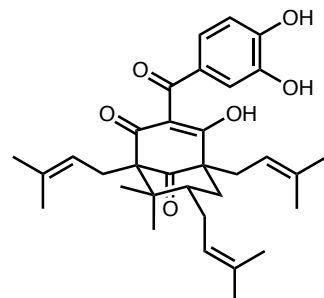
androforin A
(4)



Hypericum androsaemum (Yunnan, China)¹⁵

(NMR, UV, IR)¹⁵ [α]_D = -59.3° (MeOH)¹⁵

aristophenone
18,19-dihydroxy-
clusianone
(5)



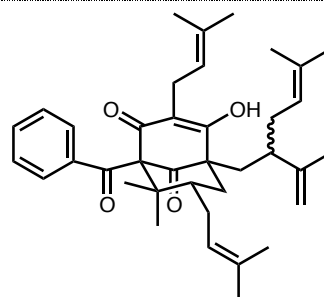
Clusia torresii (Turrialba, Cartago, Costa Rica)¹⁶

***Garcinia aristata* (Havana, Cuba)**¹⁷

G. multiflora (Diaoluo Mountain, Hainan, China)¹⁸
G. xanthochymus (Homestead, Florida, USA)¹⁹
 propolis (Manaus, Brazil)²⁰

(NMR, UV, IR)¹⁷ [α]_D = +58° (CHCl₃)¹⁷

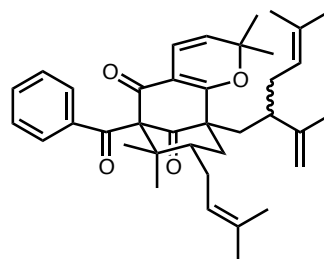
chamone I
(6)



Clusia grandiflora (Canaima, Venezuela)²¹

O-Me ether (NMR, IR)²¹

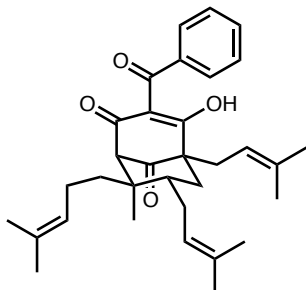
chamone II
(7)



Clusia grandiflora (Canaima, Venezuela)²¹

(NMR, IR)²¹

chamuangone
cowanone
ent-guttiferone Q
(8)

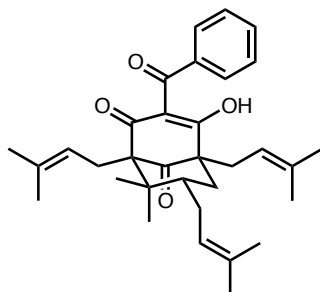


Garcinia cowa

Hat-Yai, Songkhla, Thailand²²
Nong Khai, Thailand²³

(NMR, UV, IR)^{22,23} $[\alpha]_D = +5.3^\circ$ (CHCl₃)²³

clusianone
(9)



Clusia burchellii (Campinas, São Paulo, Brazil)²⁴

C. congestiflora (Fresno, Colombia)²⁵

C. fluminensis

Campinas, São Paulo, Brazil²⁴

Viçosa, São Paulo, Brazil²⁶

C. lanceolata (Campinas, São Paulo, Brazil)²⁴

C. pana-panari (Campinas, São Paulo, Brazil)²⁴

C. paralicola (Campinas, São Paulo, Brazil)²⁴

C. pernambucensis (Campinas, São Paulo, Brazil)²⁴

C. sandiensis (Machu Pichu, Peru)²⁷

C. spiritu-sanctensis (Campinas, São Paulo, Brazil)^{24,28}

C. weddelliana (Campinas, São Paulo, Brazil)²⁴

C. torresii (Turrialba, Cartago, Costa Rica)¹⁶

Garcinia assigu (Central Province, Papua New Guinea)²⁹

G. brevipedicellata (Cameroon)³⁰

G. preussii (Cameroon)³⁰

Hypericum hypericoides (St. Andrew, Jamaica)³¹

H. sampsonii (Jinhua, Zhejiang, China)³²

propolis (Campinas, São Paulo, Brazil)²⁴

NMR^{26,27,16} (UV, IR)^{27,16} $[\alpha]_D = +60^\circ$, ²⁷ $+58.3^\circ$ ¹⁶ (CHCl₃)

O-Me ether (NMR, IR, UV)²⁸ $[\alpha]_D = +60.7^\circ$ (CHCl₃)²⁸

structural revision;¹⁶ crystal structure;²⁵

O-Me ether crystal structure²⁸

Calophyllum thorelii (central Vietnam)³³

Clusia torresii (Turrialba, Cartago, Costa Rica)¹⁶

Garcinia brasiliensis (Viçosa, Minas Gerais, Brazil)^{34,35,36}

G. brevipedicellata (Cameroon)³⁰

G. preussii (Cameroon)³⁰

Hypericum hypericoides (St. Andrew, Jamaica)³¹

H. sampsonii (Hunan, China)³⁷

H. scabrum (Chimgan, Uzbekistan)³⁸

H. elegans (Balgarevo, Kavarna, Bulgaria)³⁹

Rheedia brasiliensis (Viçosa, Minas Gerais, Brazil)⁴⁰

R. edulis (Broward County, Florida, USA)⁴¹

R. gardneriana (Viçosa, Minas Gerais, Brazil)^{42,43}
propolis (Manaus, Brazil)²⁰

NMR^{16,34,44} IR^{16,44} UV^{16,41,44}

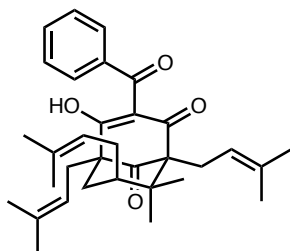
$[\alpha]_D = +60^\circ$, ^{34,44} $+62.3^\circ$, ¹⁶ $+66^\circ$ (CHCl₃)⁴⁵

$+15.6^\circ$ (MeOH)⁴¹

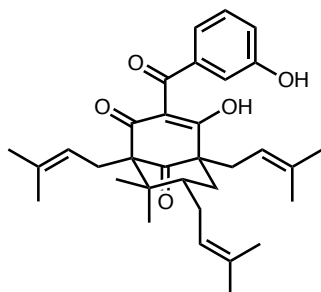
structural revision;¹⁶ crystal structure;^{37,42,45}

absolute configuration⁴⁵

7-*epi*-clusianone
(10)

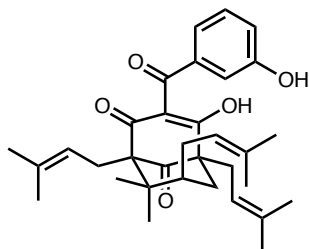


**18-hydroxycusianone
(11)**



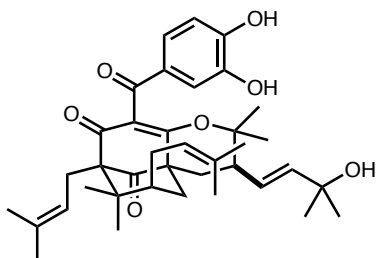
Hypericum hypericoides (St. Andrew, Jamaica)³¹
(NMR, UV, IR)³¹

**18-hydroxy-7-*epi*-
cusianone
(12)**



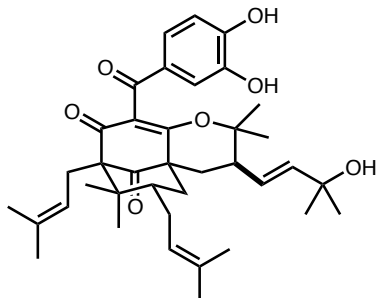
Hypericum hypericoides (St. Andrew, Jamaica)³¹
(NMR, UV, IR)³¹ $[\alpha]_D = +64^\circ$ (CHCl₃)³¹

**coccinone B
(13)**



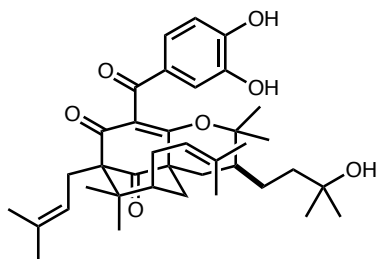
Moronobea coccinea (dense rain forest, French
Guyana)⁴⁶
(NMR, UV, IR)⁴⁶ $[\alpha]_D = -55^\circ$ (CHCl₃)⁴⁶

**7-*epi*-coccinone B
(14)**



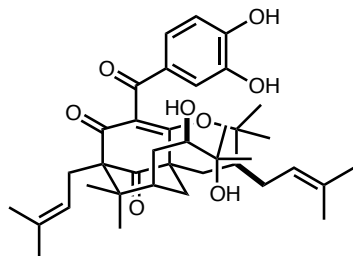
Symphonia globulifera (dense rain forest, French
Guyana)⁴⁷
(NMR, UV, IR)⁴⁷ $[\alpha]_D = -50^\circ$ (CHCl₃)⁴⁷

**coccinone C
(15)**



Moronobea coccinea (dense rain forest, French
Guyana)⁴⁶
(NMR, UV, IR)⁴⁶ $[\alpha]_D = -60^\circ$ (CHCl₃)⁴⁶

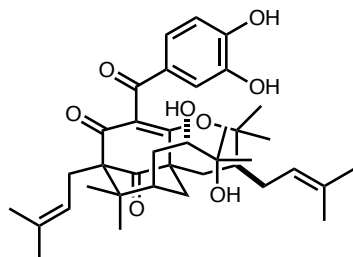
**coccinone D
(16)**



Moronobea coccinea (dense rain forest, French Guyana)⁴⁶

(NMR, UV, IR)⁴⁶ $[\alpha]_D = -76^\circ$ (CHCl₃)⁴⁶

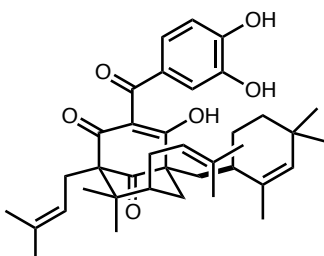
**coccinone E
(17)**



Moronobea coccinea (dense rain forest, French Guyana)⁴⁶

(NMR, UV, IR)⁴⁶ $[\alpha]_D = -70^\circ$ (CHCl₃)⁴⁶

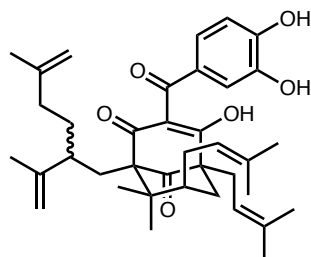
**coccinone F
(18)**



Moronobea coccinea (dense rain forest, French Guyana)⁴⁶

(NMR, UV, IR)⁴⁶ $[\alpha]_D = -32^\circ$ (CHCl₃)⁴⁶

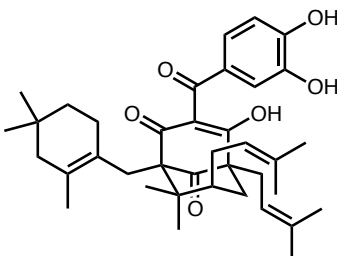
**coccinone G
(19)**



Moronobea coccinea (dense rain forest, French Guyana)⁴⁶

(NMR, UV, IR)⁴⁶ $[\alpha]_D = -16^\circ$ (CHCl₃)⁴⁶

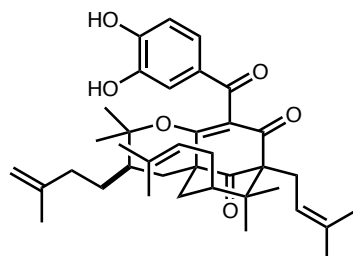
**coccinone H
(20)**



Moronobea coccinea (dense rain forest, French Guyana)⁴⁶

(NMR, UV, IR)⁴⁶ $[\alpha]_D = +2^\circ$ (CHCl₃)⁴⁶
crystal structure⁴⁶

**cycloxanthochymol
(21)**



Garcinia livingstonei (Homestead, Florida, USA)⁴⁸

G. nujiangensis (Nuijiang, Yunnan, China)⁴⁹

G. pyrifera (Sungai Petani, Kedah, Malaysia)⁵⁰

G. subelliptica (Okinawa, Japan)⁵¹

G. xanthochymus (Homestead, Florida, USA)¹⁹

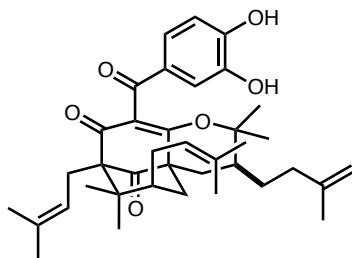
Moronobea coccinea (dense rain forest, French Guyana)⁴⁶

(UV, IR)⁴⁶ $[\alpha]_D = +112^\circ$ (CHCl₃)⁴⁶

characterized as mixture with **153** (NMR, UV, IR)^{50,51}

$[\alpha]_D = +142^\circ$ (CHCl₃)⁵⁰ $[\alpha]_D = +158^\circ$ (MeOH)⁵¹

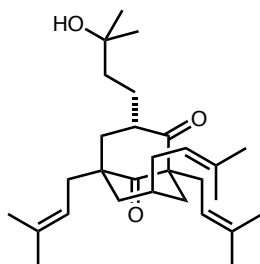
ent-cycloxanthchymol
(22)



Garcinia nuijiangensis (Nuijiang, Yunnan, China)⁴⁹
G. subelliptica (northern mountains, Taiwan)⁵²

(NMR, UV, IR)⁵² $[\alpha]_D = -80.9^\circ$ (MeOH)⁵²

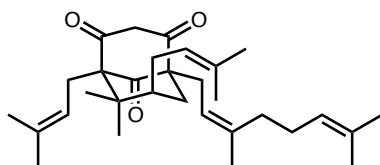
dorstenpictanone
(23)



Dorstenia picta (Moraceae; Nkolbibanda, Cameroon)⁵³

(NMR, IR)⁵³

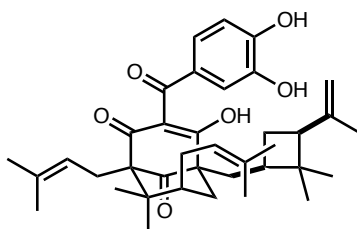
enervosanone
(24)



Calophyllum enervosum (Bukitinggi, West Sumatra, Indonesia)^{54,55}

(NMR, UV, IR)⁵⁴ $[\alpha]_D = +10^\circ$ (MeOH)⁵⁴

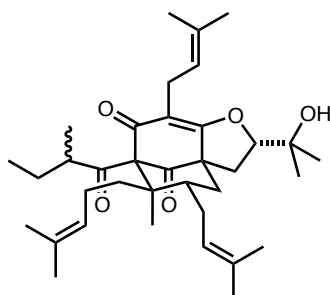
eugeniaphenone
(25)



Garcinia eugeniaefolia (Riau Islands, Indonesia)⁵⁶

(NMR, IR);⁵⁶ crystal structure⁵⁶

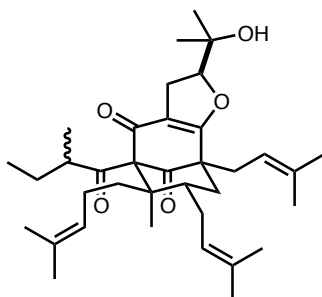
furoadhyperforin
(26)



Hypericum perforatum
Mt. Taylor, Canberra, Australia¹¹
Mt. Orzen, southeast Serbia^{57,58}

¹H NMR^{11,57} ¹³C NMR¹¹

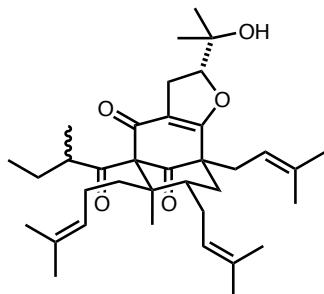
furoadhyperforin isomer A
(27)



Hypericum perforatum (Tokushima, Japan)⁵⁹

(NMR, IR)⁵⁹ $[\alpha]_D = +33.8$ (CHCl₃)⁵⁹

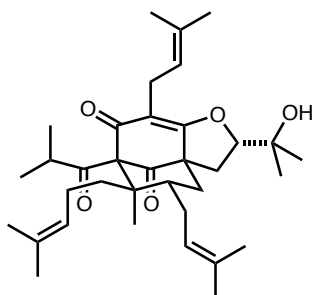
**furoadhyperforin
isomer B
(28)**



Hypericum perforatum (Tokushima, Japan)⁵⁹

(NMR, IR)⁵⁹ $[\alpha]_D = +13.8$ (CHCl₃)⁵⁹

**furohyperforin
(29)**



Hypericum henryi (Lünnchun, Yunnan, China)⁶⁰

Hypericum perforatum

Mt. Taylor, Canberra, Australia¹¹

Chile⁶¹

China⁶²

Italy¹³

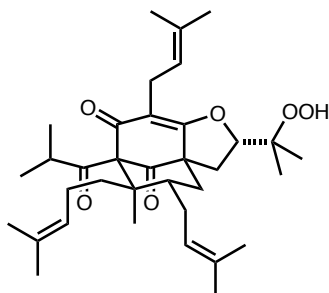
Tokushima, Japan⁵⁹

Mt. Orzen, southeast Serbia^{57,58,63}

NMR^{11,58,61,62} (UV, IR)^{58,61}

$[\alpha]_D = +68^\circ$,⁵⁸ $+62.4^\circ$ ⁶¹ (CHCl₃) $[\alpha]_D = +81.9^\circ$ (MeOH)⁶¹

**33-deoxy-33-
hydroperoxy-
furohyperforin
(30)**



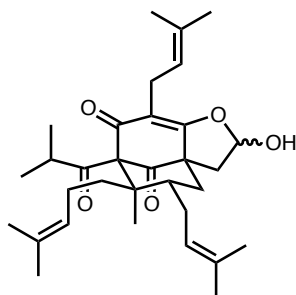
Hypericum perforatum

Chile⁶⁴

Tokushima, Japan⁵⁹

(NMR, UV, CD)⁶⁴ $[\alpha]_D = +75.0^\circ$ (CHCl₃)⁶⁴

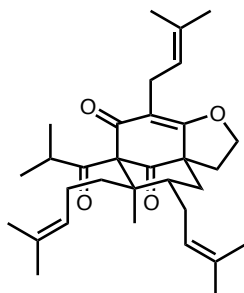
**furohyperforin A
(31)**



Hypericum perforatum (Mt. Orzen, southeast Serbia)^{58,63}

(NMR, UV, IR)⁶³

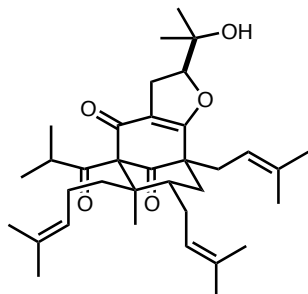
**deoxyfurohyperforin
A
(32)**



Hypericum perforatum (Mt. Orzen, southeast Serbia)⁵⁸

(NMR, UV, IR)⁵⁸ $[\alpha]_D = +42$ (CH₂Cl₂)⁵⁸

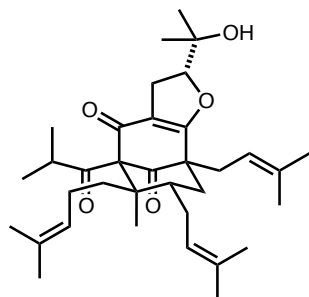
**furohyperforin
isomer 1
(33)**



Hypericum perforatum
Mt. Taylor, Canberra, Australia¹¹
Tokushima, Japan⁵⁹

NMR^{11,59} $[\alpha]_D = +49.7$ (CHCl₃)⁵⁹

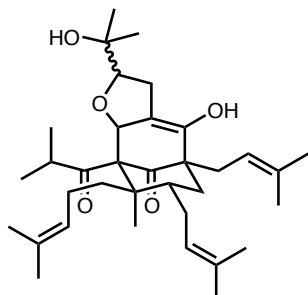
**27-*epi*-furohyperforin
isomer 1
(34)**



Hypericum perforatum (Tokushima, Japan)⁵⁹

NMR⁵⁹ $[\alpha]_D = +14.5$ (CHCl₃)⁵⁹

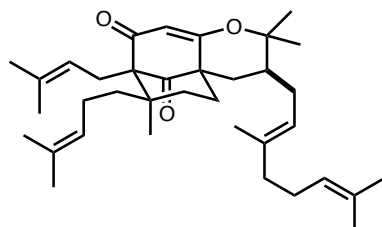
**furohyperforin
isomer 2
(35)**



Hypericum perforatum
Mt. Taylor, Canberra, Australia¹¹
Tokushima, Japan⁵⁹

NMR¹¹

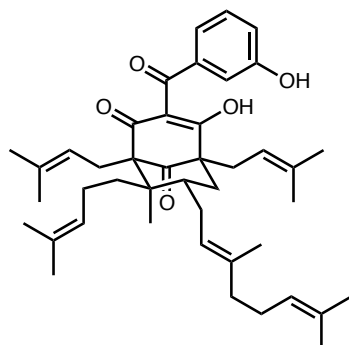
**garcicowin A
(36)**



Garcinia cowa (Yunnan, China)⁶⁵

(NMR, UV, IR)⁶⁵ $[\alpha]_D = -219.0^\circ$ (CHCl₃)⁶⁵

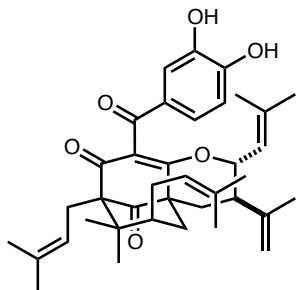
**garcicowin B
(37)**



***Garcinia cowa* (Yunnan, China)**^{65,66}
G. lancilimba (Xishuangbanna, Yunnan, China)⁶⁶
G. yunnanensis (Dehong, Yunnan, China)⁶⁶

(NMR, UV, IR)⁶⁵ $[\alpha]_D = -16.0^\circ$ (CHCl₃)⁶⁵

garcicowin C
(38)



***Garcinia cowa* (Yunnan, China)^{65,66}**

G. lancilimba (Xishuangbanna, Yunnan, China)⁶⁶

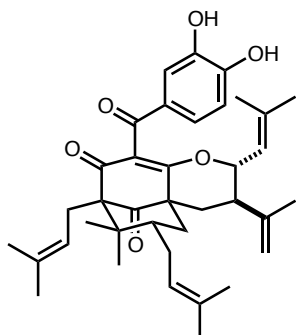
G. oblongifolia (Bobai, Guangxi, China)⁶⁶

G. paucinervis (Xishuangbanna, Yunnan, China)⁶⁷

G. xanthochymus (Xishuangbanna, Yunnan, China)⁶⁶

(NMR, UV, IR)⁶⁵ [α]_D = -72.1° (CHCl₃)⁶⁵

garcicowin D
(39)



***Garcinia cowa* (Yunnan, China)^{65,66}**

G. lancilimba (Xishuangbanna, Yunnan, China)⁶⁶

G. multiflora (Wanning, China)⁶⁶

G. oblongifolia (Bobai, Guangxi, China)⁶⁶

G. paucinervis (Xishuangbanna, Yunnan, China)⁶⁶

G. subelliptica (Shenzhen, Guangdong, China)⁶⁶

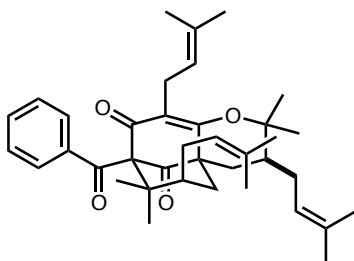
G. xanthochymus (Xishuangbanna, Yunnan, China)⁶⁶

G. xipshuangbannaensis (Xishuangbanna, Yunnan, China)⁶⁶

G. yunnanensis (Dehong, Yunnan, China)⁶⁶

(NMR, UV, IR)⁶⁵ [α]_D = +336.0° (CHCl₃)⁶⁵

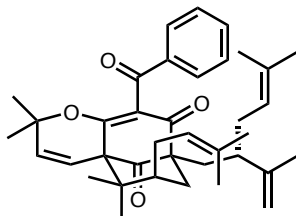
garcimultiflorone A
(40)



Garcinia multiflora (Mudan, Taiwan)⁶⁸

(NMR, UV, IR, CD)⁶⁸ [α]_D = -173° (CHCl₃)⁶⁸

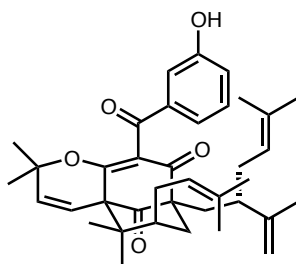
garcimultiflorone B
(41)



Garcinia multiflora (Mudan, Taiwan)⁶⁸

(NMR, UV, IR, CD)⁶⁸ [α]_D = -132° (CHCl₃)⁶⁸

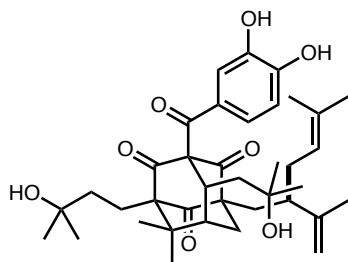
13-hydroxy-
garcimultiflorone B
(42)



Garcinia multiflora (Mudan, Taiwan)⁶⁸

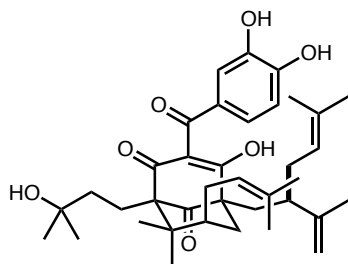
(NMR, UV, IR, CD)⁶⁸ [α]_D = -115° (CHCl₃)⁶⁸

garcimultiflorone C
(43)



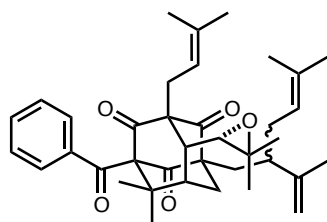
Garcinia multiflora (Mudan, Taiwan)⁶⁸
(NMR, UV, IR, CD)⁶⁸ $[\alpha]_D = -25.3^\circ$ (CHCl₃)⁶⁸

garcimultiflorone D
(44)



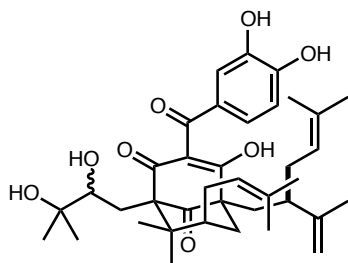
Garcinia multiflora (Diaoluo Mountain, Hainan, China)¹⁸
(NMR, UV, IR)¹⁸ $[\alpha]_D = -53.6^\circ$ (MeOH)¹⁸

garcimultiflorone D2
(45)



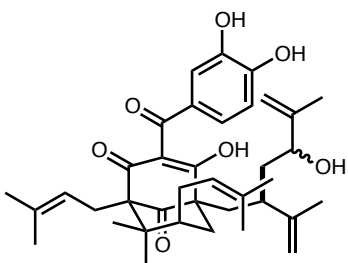
Garcinia multiflora (Mudan, Pingtung, Taiwan)⁶⁹
(NMR, UV, IR)⁶⁹ $[\alpha]_D = +5.6^\circ$ (CHCl₃)

**18-hydroxy-
garcimultiflorone D**
(46)



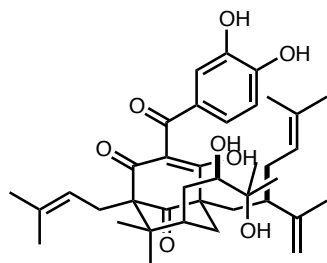
Garcinia multiflora (Diaoluo Mountain, Hainan, China)¹⁸
(NMR, UV, IR)¹⁸ $[\alpha]_D = -33.3^\circ$ (MeOH)¹⁸

garcimultiflorone E
(47)



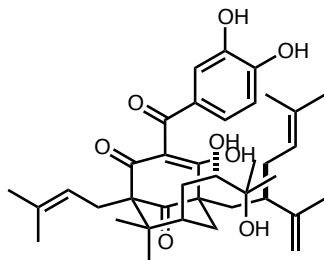
Garcinia multiflora (Diaoluo Mountain, Hainan, China)¹⁸
(NMR, UV, IR)¹⁸ $[\alpha]_D = -43.6^\circ$ (MeOH)¹⁸

garcimultiflorone F
(48)



Garcinia multiflora (Diaoluo Mountain, Hainan, China)¹⁸
(NMR, UV, IR)¹⁸ $[\alpha]_D = -48.7^\circ$ (MeOH)¹⁸

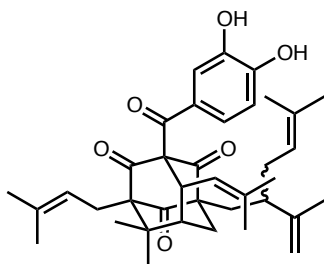
isogarcimultiflorone F
(49)



Garcinia multiflora (Diaoluo Mountain, Hainan, China)¹⁸

(NMR, UV, IR)¹⁸ $[\alpha]_D = -46.0^\circ$ (MeOH)¹⁸

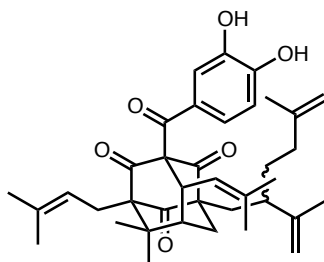
garciniagifolone A
(50)



Garcinia oblongifolia (Hainan, China)⁷⁰

(NMR, UV, IR)⁷⁰ $[\alpha]_D = +7.0^\circ$ (MeOH)⁷⁰

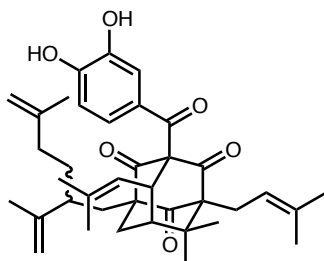
garcinialiptone A
(51)



Garcinia subelliptica (northern mountains, Taiwan)⁵²

(NMR, UV, IR)⁵² $[\alpha]_D = +12.1^\circ$ (MeOH)⁵²

ent-garcinialiptone A
(52)



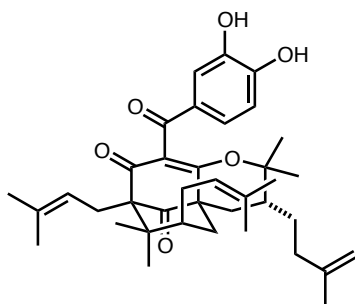
Garcinia cochinchinensis (southern Vietnam)⁷¹

G. nuijiangensis (Nuijiang, Yunnan, China)⁴⁹

***G. subelliptica* (northern mountains, Taiwan)⁵²**

(NMR, UV, IR)⁵² $[\alpha]_D = -17.3^\circ$ (MeOH)⁵²

garcinialiptone B
(53)

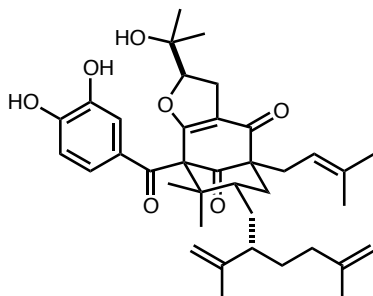


Garcinia nuijiangensis (Nuijiang, Yunnan, China)⁴⁹

***G. subelliptica* (northern mountains, Taiwan)⁵²**

(NMR, UV, IR)⁵² $[\alpha]_D = +84.8^\circ$ (MeOH)⁵²

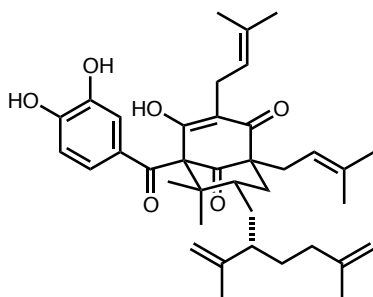
**garcinialiptone C
(54)**



Garcinia subelliptica (northern mountains, Taiwan)⁵²

(NMR, UV, IR)⁵² $[\alpha]_D = -94.0^\circ$ (MeOH)⁵²

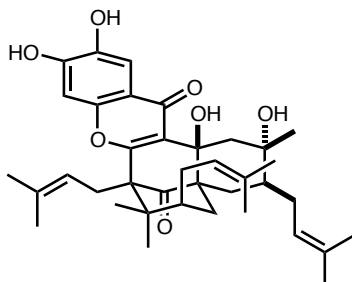
**garcinialiptone D
(55)**



Garcinia subelliptica (northern mountains, Taiwan)⁵²

(NMR, UV, IR)⁵² $[\alpha]_D = -79.1^\circ$ (MeOH)⁵²

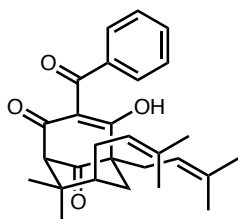
**garcinialone
(56)**



Garcinia multiflora (Taiwan)⁷²

(NMR, UV, IR)⁷² $[\alpha]_D = -2.0^\circ$ (MeOH)⁷²

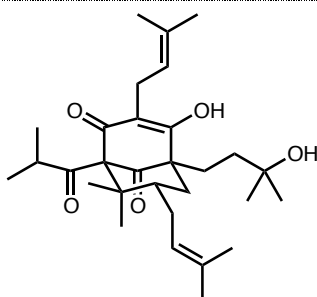
**garciniaphenone
(57)**



Garcinia brasiliensis (Viçosa, Minas Gerais, Brazil)^{34,35}

(NMR, UV, IR)³⁴ $[\alpha]_D = -52.8$ (CHCl₃)³⁴
crystal structure³⁵

**garcinielliptone A
(58)**

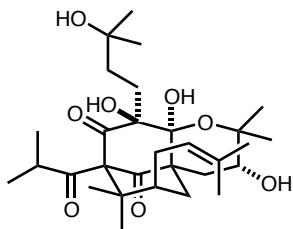


Garcinia subelliptica (Kaohsiung, Taiwan)^{73,74}

(NMR, UV, IR)⁷³ $[\alpha]_D = -33^\circ$ (CHCl₃)⁷³

garcinielliptone B (59)		<i>Garcinia subelliptica</i> (Kaohsiung, Taiwan) ⁷³ (NMR, UV, IR) ⁷³ [α] _D = -23° (CHCl ₃) ⁷³
garcinielliptone C (60)		<i>Garcinia subelliptica</i> (Kaohsiung, Taiwan) ⁷³ (NMR, UV, IR) ⁷³ [α] _D = -40° (CHCl ₃) ⁷³
garcinielliptone D (61)		<i>Garcinia subelliptica</i> (Kaohsiung, Taiwan) ⁷³ (NMR, UV, IR) ⁷³ [α] _D = -22° (CHCl ₃) ⁷³
garcinielliptone F (62)		<i>Garcinia subelliptica</i> (Kaohsiung, Taiwan) ^{74,75} (NMR, UV, IR) ⁷³ [α] _D = -23° (CHCl ₃) ⁷³
garcinielliptone FB (63)		<i>Garcinia subelliptica</i> (Kaohsiung, Taiwan) ⁷⁶ (NMR, UV, IR) ⁷⁶ [α] _D = -66° (CHCl ₃) ⁷⁶
garcinielliptone FC (64)		<i>Garcinia subelliptica</i> Kaohsiung, Taiwan ⁷⁴ Ping-Tung Hsien, Taiwan ⁷⁷ <i>Platonia insignis</i> (Barras, Piauí, Brazil) ⁷⁸ NMR ^{77,78} (UV, IR) ⁷⁷ [α] _D = +12.6° (CHCl ₃) ⁷⁷

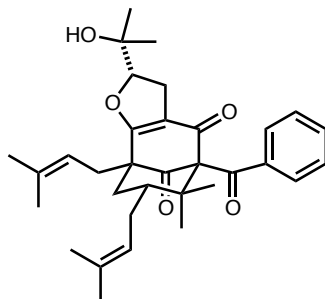
garcinielliptone H
(65)



Garcinia subelliptica (Kaohsiung, Taiwan)⁷⁵

(NMR, UV, IR)⁷⁵ $[\alpha]_D = -143^\circ$ (CHCl_3)⁷⁵

garcinielliptone I
ent-hyperibone A
(66)

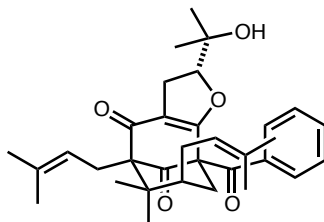


Clusia minor (Havana, Cuba)⁷⁹

Garcinia subelliptica (Kaohsiung, Taiwan)⁷⁵
propolis (Guantanamo, Cuba)⁸⁰

NMR^{75,79} (UV, IR)⁷⁵ $[\alpha]_D = +57^\circ$, ⁷⁵ $+63.7^\circ$ ^{79,80} (CHCl_3)

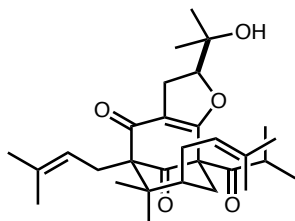
garcinielliptone K
(67)



Garcinia subelliptica (Kaohsiung, Taiwan)⁸¹

(NMR, UV, IR)⁸¹ $[\alpha]_D = +27^\circ$ (CHCl_3)⁸¹

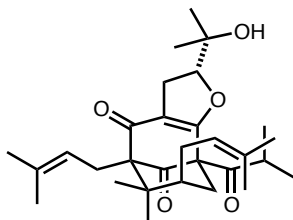
garcinielliptone L
(68)



Garcinia subelliptica (Kaohsiung, Taiwan)⁸¹

(NMR, UV, IR)⁸¹ $[\alpha]_D = -41^\circ$ (CHCl_3)⁸¹

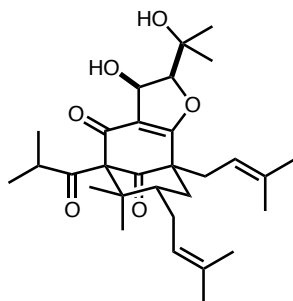
garcinielliptone M
(69)



Garcinia subelliptica (Kaohsiung, Taiwan)⁸¹

(NMR, UV, IR)⁸¹ $[\alpha]_D = +73^\circ$ (CHCl_3)⁸¹

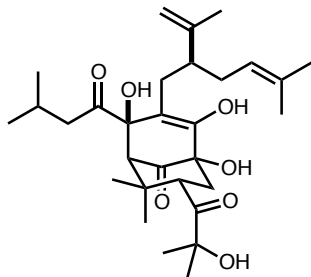
garcinielliptone P
(70)



Garcinia subelliptica (Ping-Tung Hsien, Taiwan)⁸²

(NMR, UV, IR)⁸² $[\alpha]_D = -2^\circ$ (CHCl_3)⁸²

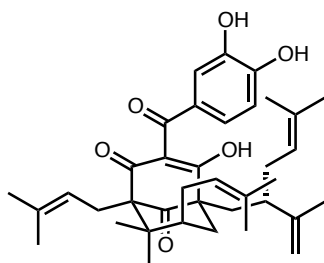
**garcinielliptone R
(71)**



Garcinia subelliptica (Kaohsiung, Taiwan)⁷⁴

(NMR, UV, IR)⁷⁴ [α]_D = -38° (CHCl₃)⁷⁴

**garcinol
camboginol
ent-guttiferone E
(72)**



Allanblackia monticola (West Province, Cameroon)⁸³

Garcinia assigu (Central Province, Papua New Guinea)²⁹

G. bancana (Naratiwath, Thailand)⁸⁴

G. brevipedicellata (Cameroon)³⁰

G. cambogia

Dapoli,⁸⁵ Maharastra, **India**^{86,87}

Sri Lanka^{88,89}

G. cowa (Yunnan, China)^{65,90}

G. dulcis (Songkhla, Thailand)⁹¹

G. huillensis (western Democratic Republic of the Congo)⁹²

G. indica (Kerela,⁸⁵ India^{93,94})

G. maingayii (Riau Islands, Indonesia)⁹⁵

G. oblongifolia

Hainan, China⁷⁰

Nhu Xuan, Vietnam⁹⁶

G. paucinervis (Xishuangbanna, Yunnan, China)⁶⁷

G. pedunculata (Jorhat, Assam, India)⁹⁷

G. preussii (Cameroon)³⁰

G. purpurea (Japan)⁵¹

G. tetrandra (West Kalimantan, Indonesia)⁹⁸

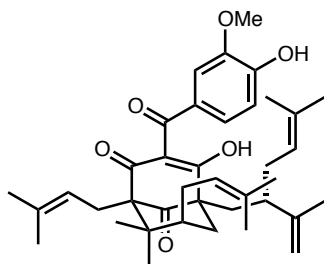
Moronobea coccinea (dense rain forest, French Guyana)⁴⁶

¹H NMR^{86,90,92,95,97,98,99} ¹³C NMR^{86,90,92,95,98,99}

(UV, IR)^{46,51,86,90,92,93,97} CD^{29,90}

[α]_D = -135°, ⁴⁶ -138°, ⁵¹ -132.9°, ⁸⁶ -143°, ⁹³ -125.3°, ⁹² -142.0°⁹⁷ (CHCl₃) -192.0°, ⁹⁰ -128.5°, ⁹¹ -149.2°⁹⁴ (MeOH) -125.3° (EtOH)⁹²

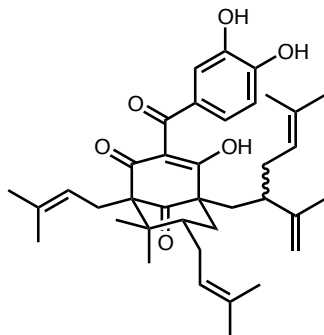
**garcinol
13-O-methyl ether
(73)**



Garcinia assigu (Central Province, Papua New Guinea)²⁹

(NMR, UV, IR, CD)²⁹ [α]_D = -117° (CHCl₃)²⁹

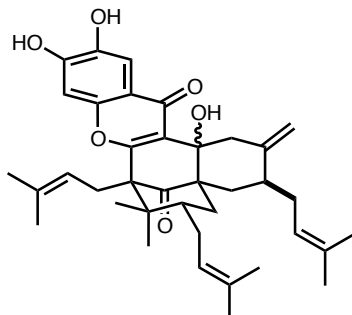
**7-*epi*-garcinol
(74)**



Garcinia brevipedicellata (Cameroon)³⁰
G. nujiangensis (Nujiang, Yunnan, China)⁴⁹
G. preussii (Cameroon)³⁰
***Moronobea coccinea* (dense rain forest, French Guyana)⁴⁶**
Symphonia globulifera (dense rain forest, French Guyana)⁴⁷

NMR⁴⁶ (UV, IR)^{46,47} [α]_D = -86° (CHCl₃)^{46,47}

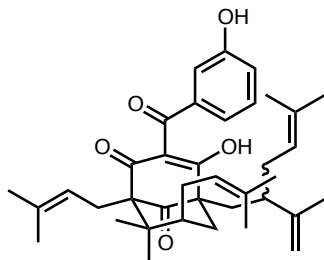
**no name
cyclogarcinol
(75)**



Garcinia indica (Bengaluru, India)⁹⁴

(NMR, UV, IR)⁹⁴ [α]_D = +18.9 (MeOH)⁹⁴

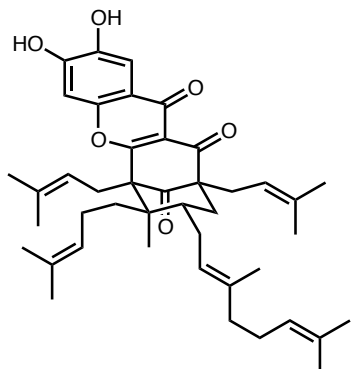
**14-deoxygarcinol
(76)**



Moronobea coccinea (dense rain forest, French Guyana)⁴⁶

(NMR, UV, IR)⁴⁶ [α]_D = -42° (CHCl₃)⁴⁶

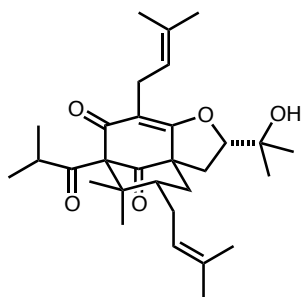
**garciyunnanin B
(77)**



Garcinia lancilimba (Xishuangbanna, Yunnan, China)⁶⁶
G. multiflora (Wanning, China)⁶⁶
G. xanthochymus (Xishuangbanna, Yunnan, China)⁶⁶
***G. yunnanensis* (Dehong, Yunnan, China)^{66,100}**

(NMR, UV, IR)¹⁰⁰ [α]_D = +18.1° (CHCl₃)¹⁰⁰

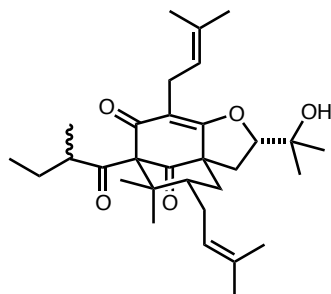
**garsubellin A
(78)**



Garcinia subelliptica
Ishigaki Island, Japan^{101,102}
 Kaohsiung, Taiwan^{73,74}

NMR^{101,102} (UV, IR)¹⁰¹ [α]_D = -21.3° (EtOH)¹⁰¹

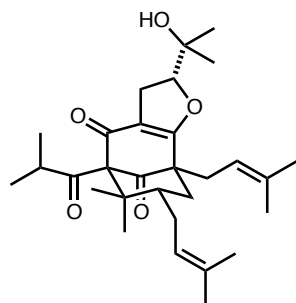
**garsubellin B
(79)**



Garcinia subelliptica (Ishigaki Island, Japan)¹⁰²

(NMR, UV, IR)¹⁰² [α]_D = -36° (EtOH)¹⁰²

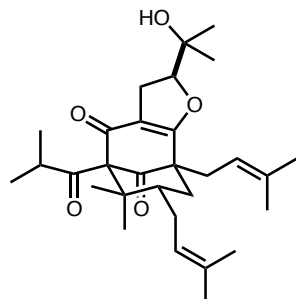
**garsubellin C
(80)**



Garcinia subelliptica (Ishigaki Island, Japan)¹⁰²

(NMR, UV, IR)¹⁰² [α]_D = +39° (EtOH)¹⁰²

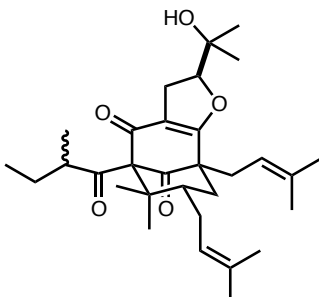
**garsubellin D
(81)**



Garcinia subelliptica
Ishigaki Island, Japan¹⁰²
Kaohsiung, Taiwan⁷³

(NMR, UV, IR)¹⁰² [α]_D = -12° (EtOH)¹⁰²

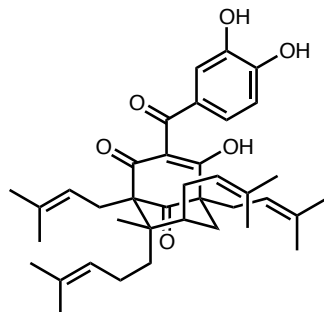
**garsubellin E
(82)**



Garcinia subelliptica (Ishigaki Island, Japan)¹⁰²

(NMR, UV, IR)¹⁰² [α]_D = -7° (EtOH)¹⁰²

**guttiferone A
(83)**



Clusia rosea (Havana, Cuba)¹⁰³

Garcinia achachairu (Camboriú, Santa Catarina, Brazil)¹⁰⁴

G. aristata (Homestead, Florida, USA)¹⁰⁵

G. brasiliensis (Viçosa, Minas Gerais, Brazil)^{36,35}

G. cowa (Xishuangbanna, Yunnan, China)⁶⁵

G. intermedia (Ejido Benigno Mendoza, Veracruz, Mexico)^{105,106}

G. livingstonei

Iringa, Mufindi, Tanzania¹⁰⁷

Southeastern Florida, USA^{48,105}

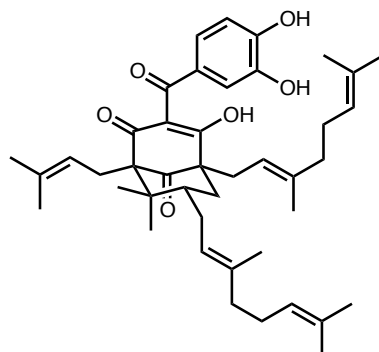
G. macrophylla (Supaliwini, Suriname)¹⁰⁸

G. semsei (Morogoro, Tanzania)¹⁰⁹

G. spicata (Homestead, Florida, USA)¹⁰⁵

Rheedia edulis (Broward County, Florida, USA)⁴¹

**guttiferone B
(84)**



Symphonia globulifera

Fundong, Northwest Province, Cameroon^{110,111}
West Province, Cameroon⁸³

Ndakan Gorilla Study Area, Central African Republic¹⁰⁷

S. pauciflora (Zahamena National Park, Madagascar)¹¹²

NMR^{107,113,114} IR^{107,113} UV^{41,107,113} $[\alpha]_D = +34^\circ$,¹⁰⁷
 $+32^\circ$,¹⁰⁸ $+47.6^\circ$ ¹¹³ (CHCl₃) $+31.4^\circ$ (MeOH)⁴¹
crystal structure^{113,115}

Garcinia cowa (Yunnan, China)^{65,66}

G. lancilimba (Xishuangbanna, Yunnan, China)⁶⁶

G. multiflora (Wanning, China)⁶⁶

G. oblongifolia

Bobai, Guangxi, China^{66,116}

Nhu Xuan, Vietnam⁹⁶

G. subelliptica (Shenzhen, Guangdong, China)⁶⁶

G. xanthochymus (Xishuangbanna, Yunnan, China)⁶⁶

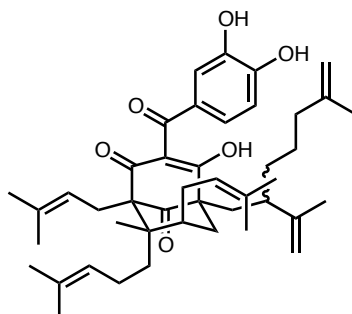
G. xipshuangbannaensis (Xishuangbanna, Yunnan, China)⁶⁶

G. yunnanensis (Dehong, Yunnan, China)⁶⁶

***Symphonia globulifera* (Ndakan Gorilla Study Area, Central African Republic)**¹⁰⁷

(NMR, UV, IR)¹⁰⁷ $[\alpha]_D = -44^\circ$ (CHCl₃)¹⁰⁷

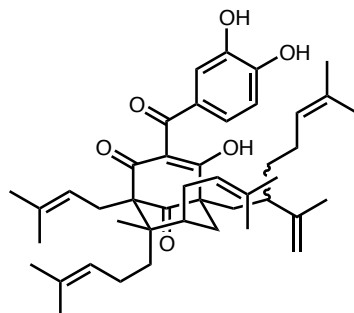
**guttiferone C
(85)**



Symphonia globulifera (Ndakan Gorilla Study Area, Central African Republic)¹⁰⁷

characterized as mixture with **86** (NMR, UV, IR)¹⁰⁷
 $[\alpha]_D = +92^\circ$ (CHCl₃)¹⁰⁷

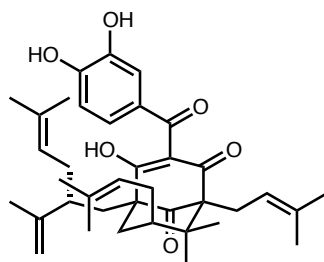
**guttiferone D
(86)**



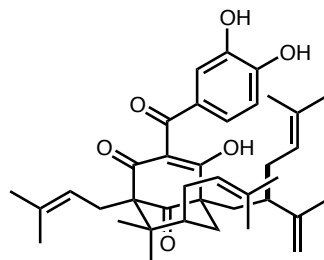
Symphonia globulifera (Ndakan Gorilla Study Area, Central African Republic)¹⁰⁷

characterized as mixture with **85** (NMR, UV, IR)¹⁰⁷
 $[\alpha]_D = +92^\circ$ (CHCl₃)¹⁰⁷

guttiferone E
ent-garcinol
(87)



guttiferone F
(88)



***Clusia rosea* (Dominican Republic)¹⁰⁷**

Garcinia afzelii (Mt. Eloumdem, Centre Province, Cameroon)¹¹⁷

G. intermedia (Homestead, Florida, USA)¹⁰⁵

G. livingstonei (Homestead, Florida, USA)⁴⁸

G. multiflora (Diaoluo Mountain, Hainan, China)¹⁸

***G. ovalifolia* (Ndakan Gorilla Study Area, Central African Republic)¹⁰⁷**

G. paucinervis (Xishuangbanna, Yunnan, China)⁶⁷

G. pyrifera (Sungai Petani, Kedah, Malaysia)⁵⁰

G. spicata (Homestead, Florida, USA)¹⁰⁵

G. xanthochymus (Homestead, Florida, USA)^{19,105}

G. xipshuangbannaensis (Xishuangbanna, Yunnan, China)¹¹⁸

G. virgata (Aoupinié, New Caledonia)¹¹⁹

Rheedia edulis (Broward County, Florida, USA)⁴¹

propolis (throughout Cuba)¹²⁰

red propolis (Maceio City, Alagoas, Brazil)¹²¹

NMR^{50,107} UV^{41,107} IR¹⁰⁷ [α]_D = +106°, ¹⁹ +104°, ⁵⁰ +101°¹⁰⁷ (CHCl₃) +120° (EtOH)¹⁹
absolute configuration¹⁰⁷

Allanblackia monticola (West Province, Cameroon)⁸³

A. gabonensis (Mbankomo, Centre Province, Cameroon)¹²²

***A. stuhlmannii* (Mufundi, Tanzania)¹²³**

A. ulugurensis (Morningside, Morogoro, Tanzania)¹²⁴

Calophyllum thorelii (central Vietnam)³³

Garcinia bancana (West Kalimantan, Indonesia)¹²⁵

G. cowa (Yunnan, China)^{65,66}

G. esculenta (Dehong, Yunnan, China)⁶⁶

G. multiflora

Diaoluo Mountain, Hainan, China¹⁸

Wanning, China⁶⁶

G. lancilimba (Xishuangbanna, Yunnan, China)⁶⁶

G. oblongifolia

Bobai, Guangxi, China⁶⁶

Vietnam¹²⁶

G. paucinervis (Xishuangbanna, Yunnan, China)⁶⁶

G. subelliptica (Shenzhen, Guangdong, China)⁶⁶

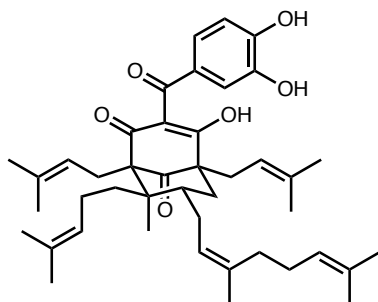
G. xanthochymus (Xishuangbanna, Yunnan, China)⁶⁶

G. xipshuangbannaensis (Xishuangbanna, Yunnan, China)⁶⁶

G. yunnanensis (Dehong, Yunnan, China)⁶⁶

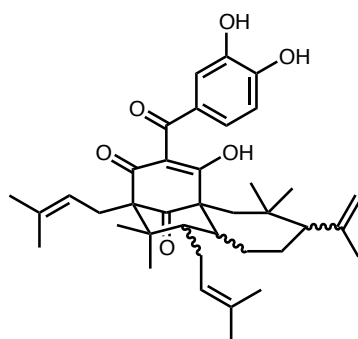
(NMR, IR)^{123,125} UV¹²³ [α]_D = -293° (CHCl₃)¹²³

guttiferone G
guttiferone I2
ent-oblongifolin C
(89)



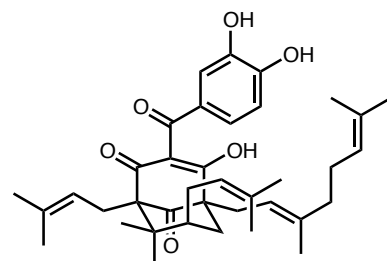
Calophyllum thorelii (central Vietnam)³³
Garcinia cambogia (Sri Lanka)⁸⁸
G. cochinchinensis (southern Vietnam)^{71,127}
G. griffithii (Lembah Arau, West Sumatra, Indonesia)¹²⁸
G. humilis (Dominica)¹²⁹
***G. macrophylla* (Supaliwini, Suriname)¹⁰⁸**
G. paucinervis (Xishuangbanna, Yunnan, China)⁶⁷
G. smeathmannii (Cheffou-Baham, West Province, Cameroon)^{130,131}
G. virgata (Aoupinié, New Caledonia)¹¹⁹
(NMR, UV, IR)^{108,119,129} $[\alpha]_D = -25^\circ$, -14.3° ¹¹⁹
(CHCl₃)
+8.7 (MeOH)¹²⁹
structural revision¹³²

guttiferone H
(90)



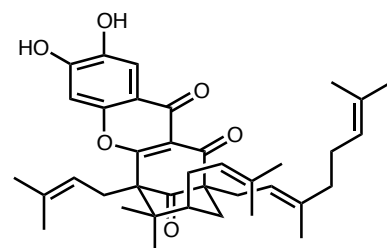
Garcinia xanthochymus (Homestead, Florida, USA)¹⁹
(NMR, UV)¹⁹ $[\alpha]_D = +94^\circ$ (CHCl₃)¹⁹ +57° (MeOH)¹⁹

guttiferone I
(91)



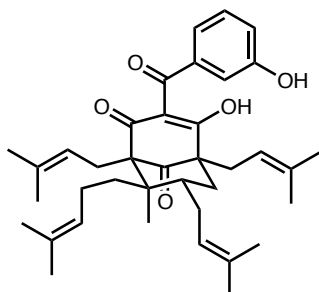
Garcinia cochinchinensis (Dong Nai, Vietnam)¹³³
***G. giffithii* (Singapore)¹³⁴**
Symphonia pauciflora (Zahamena National Park, Madagascar)¹¹²
(NMR, UV, IR)¹³⁴ $[\alpha]_D = -68^\circ$ (CHCl₃)¹³⁴

oxy-guttiferone I
(92)



Garcinia cambogia (Sri Lanka)¹³⁵
(NMR, UV, IR)¹³⁵ $[\alpha]_D = +23.8^\circ$ (MeOH)¹³⁴

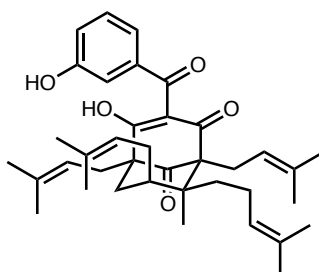
guttiferone J
garciyunnanin A
(93)



Garcinia cambogia (Sri Lanka)⁸⁸
Garcinia cowa (Xishuangbanna, Yunnan, China)⁶⁶
G. lancilimba (Xishuangbanna, Yunnan, China)⁶⁶
G. multiflora (Wanning, China)⁶⁶
G. oblongifolia (Bobai, Guangxi, China)⁶⁶
G. paucinervis (Xishuangbanna, Yunnan, China)⁶⁶
G. subelliptica (Shenzhen, Guangdong, China)⁶⁶
G. xanthochymus (Xishuangbanna, Yunnan, China)⁶⁶
G. xipshuangbannaensis (Xishuangbanna, Yunnan, China)⁶⁶
***G. virgata* (Aoupinié, New Caledonia)¹¹⁹**
G. yunnanensis (Yunnan, China)^{66,100}

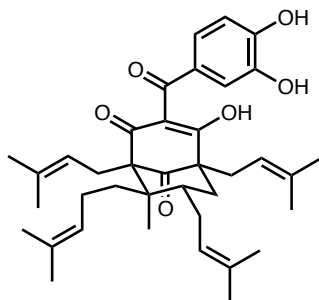
(NMR, UV, IR)^{100,119}
 $[\alpha]_D = -3^\circ$ (CHCl₃)¹⁰⁰ -34.3° (MeOH)¹¹⁹

7-*epi*-guttiferone J
(94)



Rheedia edulis (Broward County, Florida, USA)⁴¹
 (NMR, UV, IR, CD)⁴¹ $[\alpha]_D = +10.8^\circ$ (MeOH)⁴¹
 absolute configuration⁴¹

guttiferone K
(95)

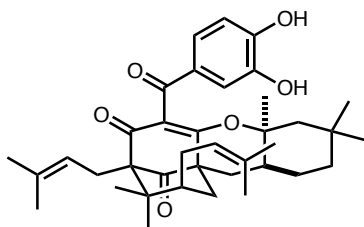


Garcinia cambogia (Sri Lanka)^{88,89,135}
G. cowa (Yunnan, China)^{65,66}
G. lancilimba (Xishuangbanna, Yunnan, China)⁶⁶
G. livingstonei (Homestead, Florida, USA)⁴⁸
G. multiflora (Wanning, China)⁶⁶
G. oblongifolia (Bobai, Guangxi, China)⁶⁶
G. paucinervis (Xishuangbanna, Yunnan, China)^{66,67}
G. semseii (Morogoro, Tanzania)¹⁰⁹
G. subelliptica (Shenzhen, Guangdong, China)⁶⁶
G. xanthochymus (Xishuangbanna, Yunnan, China)⁶⁶
G. xipshuangbannaensis (Xishuangbanna, Yunnan, China)⁶⁶
G. yunnanensis
 Dehong, Yunnan, China⁶⁶
 Luxi, Yunnan, China¹⁰⁰

***Rheedia calcicola* (Antsiranana, Madagascar)¹³⁶**

(NMR, UV, IR)¹³⁶ $[\alpha]_D = -2^\circ$ (CHCl₃)¹³⁶

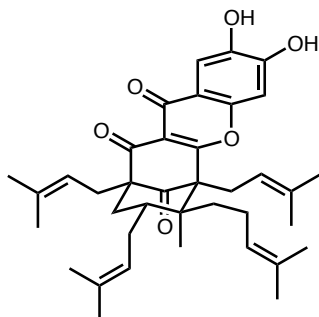
guttiferone K2
coccinone A
(96)



***Garcinia cowa* (Yunnan, China)⁹⁰**
Moronobea coccinea (dense rain forest, French Guyana)⁴⁶
Rheedia acuminata (La Paz, Bolivia)¹

NMR^{1,46,90} (UV, IR)^{46,90} CD⁹⁰
 $[\alpha]_D = +28^\circ$ (CHCl₃)⁴⁶ $+106.45$ (MeOH)⁹⁰

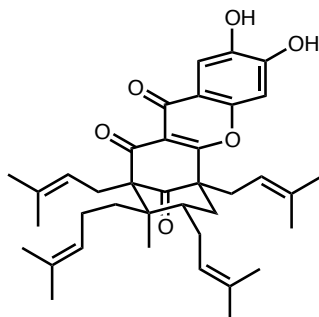
**oxy-guttiferone K
(97)**



Garcinia cambogia (Sri Lanka)^{88,135}

(NMR, UV, IR)⁸⁸ $[\alpha]_D = +20.9^\circ$ (CHCl₃)⁸⁸
absolute configuration¹³⁵

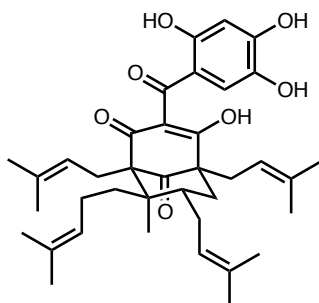
**oxy-guttiferone K2
(98)**



Garcinia cambogia (Sri Lanka)¹³⁵

(NMR, UV, IR)¹³⁵ $[\alpha]_D = +12.2^\circ$ (MeOH)¹³⁵

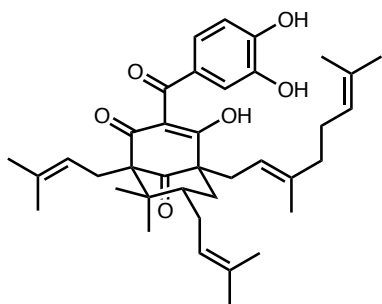
**guttiferone L
(99)**



Rheedia calcicola (Antsiranana, Madagascar)¹³⁶

(NMR, UV, IR)¹³⁶ $[\alpha]_D = -8^\circ$ (CHCl₃)¹³⁶

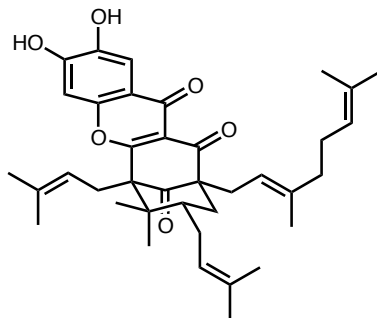
**guttiferone M
(100)**



Garcinia cambogia (Sri Lanka)^{88,135}

(NMR, UV, IR)⁸⁸ $[\alpha]_D = -29.8^\circ$ (MeOH)⁸⁸
absolute configuration¹³⁵

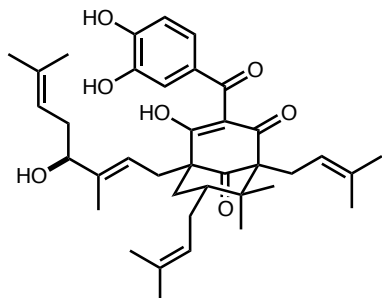
**oxy-guttiferone M
(101)**



Garcinia cambogia (Sri Lanka)¹³⁵

(NMR, UV, IR)¹³⁵ $[\alpha]_D = -96.2^\circ$ (MeOH)¹³⁵

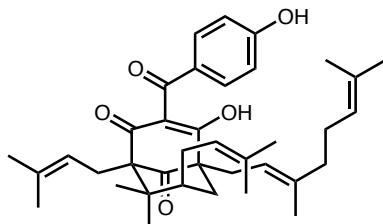
**32-hydroxy-*ent*-
guttiferone M
(102)**



Rheedia edulis (Broward County, Florida, USA)⁴¹

(NMR, UV, IR, CD)⁴¹ $[\alpha]_D = +9.6^\circ$ (MeOH)⁴¹
absolute configuration⁴¹

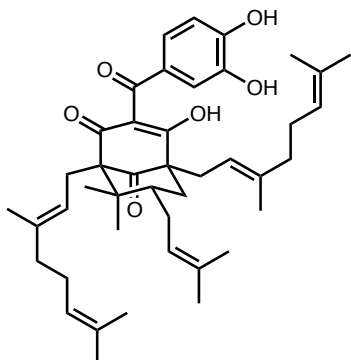
**guttiferone N
(103)**



Garcinia cambogia (Sri Lanka)⁸⁸

(NMR, UV, IR)⁸⁸ $[\alpha]_D = -34.5^\circ$ (MeOH)⁸⁸

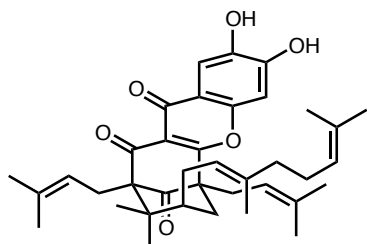
**guttiferone O
(104)**



Garcinia solomonensis (Central Province, Papua New Guinea)¹³⁷

(NMR, UV, IR)¹³⁷ $[\alpha]_D = +30.7^\circ$ (CHCl₃)¹³⁷

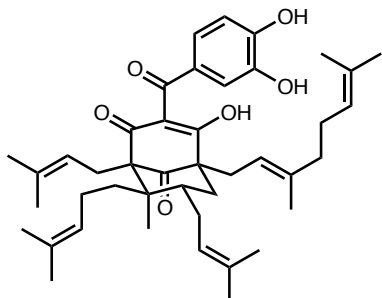
**guttiferone O2
ent-oblongifolin F
(105)**



Garcinia afzelii (Mt. Eloumdem, Centre Province, Cameroon)¹¹⁷

(NMR, UV, IR)¹¹⁷ $[\alpha]_D = +45^\circ$ (acetone)¹¹⁷

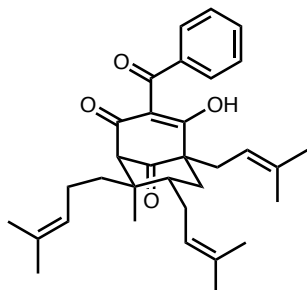
**guttiferone P
(106)**



Garcinia solomonensis (Central Province, Papua New Guinea)¹³⁷

(NMR, UV, IR)¹³⁷ $[\alpha]_D = +18.2^\circ$ (CHCl₃)¹³⁷

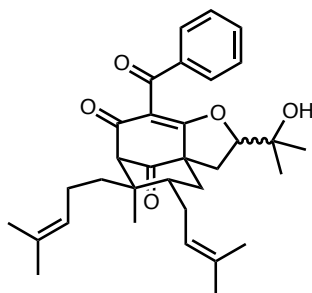
guttiferone Q
ent-chamuangone
ent-cowanone
(107)



Garcinia cochinchinensis (Dong Nai, Vietnam)¹³³

(NMR, UV, IR)¹³³ $[\alpha]_D = -50.0^\circ$ (MeOH)¹³³

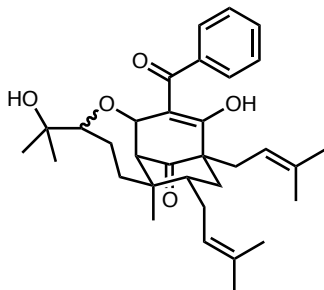
guttiferone R
(108)



Garcinia cochinchinensis (Dong Nai, Vietnam)¹³³

(NMR, UV, IR)¹³³ $[\alpha]_D = -57.5^\circ$ (MeOH)¹³³

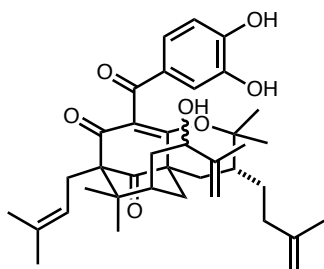
guttiferone S
(109)



Garcinia cochinchinensis (Dong Nai, Vietnam)¹³³

(NMR, UV, IR)¹³³ $[\alpha]_D = -10.0^\circ$ (MeOH)¹³³

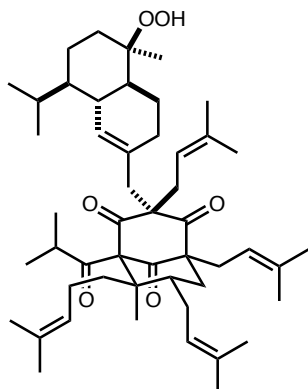
guttiferone T
(110)



Garcinia cochinchinensis (southern Vietnam)⁷¹

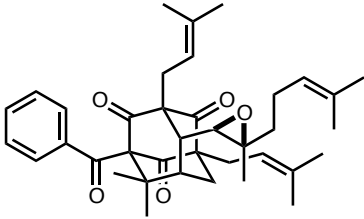
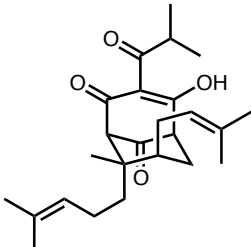
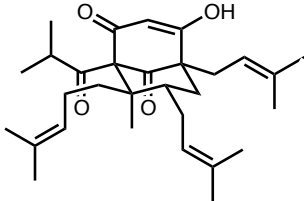
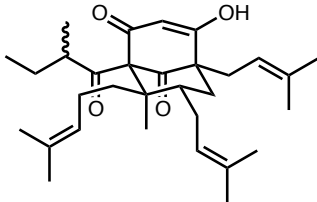
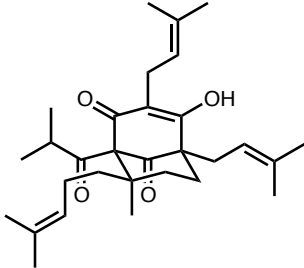
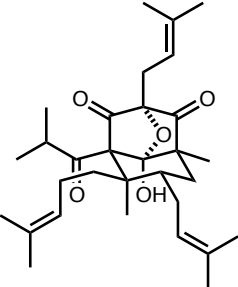
(NMR, UV, IR)⁷¹ $[\alpha]_D = -14.0^\circ$ (CHCl₃)⁷¹

hydroperoxycadiforin
(111)

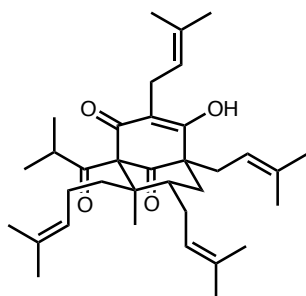


Hypericum perforatum (Bonn-Beuel, Germany)¹³⁸

(NMR, UV, IR)¹³⁸ $[\alpha]_D = +26.5^\circ$ (hexane)¹³⁸

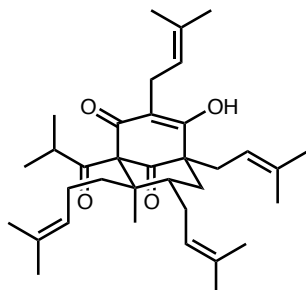
hyperandrone A (112)		<i>Hypericum androsaemum</i> (Yunnan, China) ¹⁵ (NMR, UV, IR) ¹⁵ $[\alpha]_D = +20.9^\circ$ (MeOH) ¹⁵
hyperatomarin (113)		<i>Hypericum annulatum</i> (Rhodope Mountains, Bulgaria) ^{139,140} <i>H. atomarium</i> (Nišava District, Serbia) ¹⁴¹ (NMR, UV, IR) ¹⁴¹ $[\alpha]_D = +19.4^\circ$ (CH ₂ Cl ₂) ¹⁴¹
hyperrevolutin A (114)		<i>Hypericum revolutum</i> (Zomba, Malawi) ¹⁴² (NMR, UV, IR) ¹⁴² $[\alpha]_D = +84.4^\circ$ (MeOH) ¹⁴² crystal structure ¹⁴²
hyperrevolutin B (115)		<i>Hypericum revolutum</i> (Zomba, Malawi) ¹⁴² (NMR, UV) ¹⁴²
hyperfirin (116)		<i>Hypericum perforatum</i> Germany ³ Epirus, Greece ⁴ Cemernik Mountain, southern Serbia ⁵ <i>H. reflexum</i> (Halle-Wittenberg, Germany) ³ <i>H. triquetrifolium</i> (Al-Mafraq, Jordan) ⁶ ¹ H NMR ⁴
hyperfoliatin hyperibone J (117)		<i>Hypericum perfoliatum</i> (Jijel, Algeria) ¹⁴³ <i>H. perforatum</i> (Tokushima, Japan) ⁵⁹ <i>H. scabrum</i> (Chimgan, Uzbekistan) ³⁸ <i>H. tomentosum</i> (Bekira-Constantine, eastern Algeria) ¹⁴⁴ (NMR, IR) ^{143,38} UV ¹⁴³ $[\alpha]_D = +17$ (MeOH) ¹⁴³ $+16.9$ (CHCl ₃) ³⁸

hyperforin
(118)



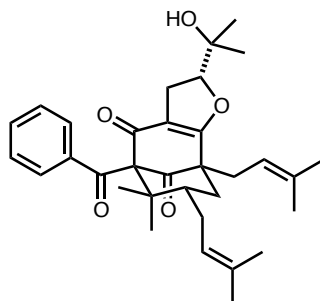
- Hypericum androsaemum* (northern Turkey)¹⁴⁵
H. aviculariifolium (northern Turkey)¹⁴⁵
H. barbatum (throughout Macedonia and Serbia)^{146,147}
H. bithynicum (northern Turkey)¹⁴⁵
H. bupleuroides (Maçka district, Trabzon, Turkey)¹⁴⁸
H. calabricum (Calabria, Italy)¹⁴⁹
H. calycinum (Bonn, Germany)⁷
H. confertum (Uludağ Mountain, Bursa, Turkey)¹⁵⁰
H. elodes (Umbrian-Marchean Apennines, Italy)^{8,151}
H. empetrifolium (Irbid, northern Jordan)¹⁵²
H. ericoides (El Feidja, northwestern Tunisia)¹⁰
H. grandifolium (Pedro Álvarez, Tenerife, Canary Islands)¹⁵³
H. heterophyllum (northern Turkey)¹⁴⁵
H. hircinum (Umbrian-Marchean Apennines, Italy)¹⁵⁴
H. hirsutum
 Umbrian-Marchean Apennines, Italy¹⁵⁴
 Throughout Macedonia and Serbia^{146,147}
 Spiška Tomašovca, Slovakia¹⁵⁵
 Northern Turkey¹⁴⁵
H. hyssopifolium
 Umbrian-Marchean Apennines, Italy^{151,154}
 Northern Turkey¹⁴⁵
H. leschenaultii (Indonesia)¹⁵⁶
H. leptophyllum (Yozgat, Turkey)¹⁵⁷
H. linarioides (throughout Macedonia and Serbia)^{146,147}
H. maculatum
 Prakovce, Slovakia⁹
 Spiška Tomašovca, Slovakia¹⁵⁵
 Throughout Macedonia and Serbia^{146,147}
H. microsepalum (southeastern USA)¹⁵⁶
H. montanum (Umbrian-Marchean Apennines, Italy)^{151,154}
H. montbretii (Cakalli,¹⁵⁸ Samsun, Turkey¹⁴⁵)
H. nummularioides (northern Turkey)¹⁴⁵
H. olympicum (throughout Macedonia and Serbia)¹⁴⁶
H. orientale (northern Turkey)^{145,159}
H. perfoliatum
 Northern Turkey¹⁴⁵
 El Feidja, northwestern Tunisia¹⁰
H. perforatum
 Yerevan,¹⁶⁰ Armenia¹⁶¹
 Mt. Taylor, Canberra, Australia¹¹
 Ontario, Canada¹⁶¹
 Longxi, Gansu, China¹⁶²
 Throughout Estonia¹⁶³
 Alpirsbach, Black Forest,¹² Germany³
 Epirus, Greece⁴
 Throughout India^{155,164}
 Throughout Italy^{13,151,154,165,166}
 Throughout Macedonia and Serbia¹⁴⁶
Russia¹⁶⁷
 Cemernik Mountain, southern Serbia⁵
 Nová Ľubovňa, Slovakia¹⁴
 Slovenia¹⁶⁸
 Throughout Switzerland¹⁶⁹
 Throughout northern Turkey^{145,170}
 El Feidja, northwestern Tunisia¹⁰
 Western Montana, USA¹⁶¹
 Ithaca, New York, USA¹⁶¹
 Southeastern USA¹⁵⁶

hyperforin
(continued)
(118)



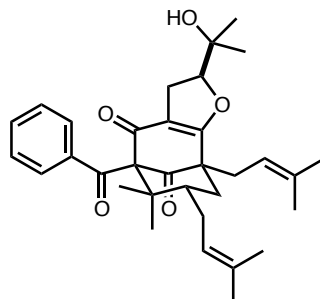
H. pruinatum (northern Turkey)¹⁴⁵
H. reflexum (Halle-Wittenberg, Germany)³
H. richeri
 Umbrian-Marchean Apennines, Italy¹⁵¹
 Throughout Macedonia and Serbia¹⁴⁶
H. rumeliacum (throughout Macedonia and Serbia)^{146,147}
H. scabrum (northern Turkey)¹⁴⁵
H. sinaicum (northern Jordan)^{2,152}
H. tetrapterum
 Umbrian-Marchean Apennines, Italy^{151,154}
 Throughout Macedonia and Serbia^{146,147}
 Nová Sedlica, Slovakia¹⁵⁵
H. triquetrifolium
 Ajloun Nature Preserve, northern Jordan¹⁵²
 Northern Turkey¹⁴⁵
H. venustum (throughout Turkey)^{145,171}
Apocynum venetum (Apocynaceae)¹⁷²
Scutellaria baicalensis (Lamiaceae)¹⁷³
¹H NMR^{4,9,167,174,175,176,177} ¹³C NMR^{11,174,175,176,177}
 (UV, IR)^{167,174} [α]_D = +41° (EtOH)¹⁶⁷
 structural elucidation,^{178,179} crystal structure^{179,180}
 absolute configuration¹⁸⁰

hyperibone A
ent-garcinielliptone I
(119)



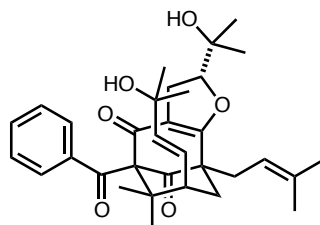
Hypericum scabrum (Chimgan, Uzbekistan)¹⁸¹
 propolis, type 6 (Atlantic forest, Bahia, Brazil)¹⁸²
 (NMR, IR)^{181,182} UV¹⁸¹ [α]_D = -37.7° (CHCl₃)¹⁸¹

hyperibone B
(120)



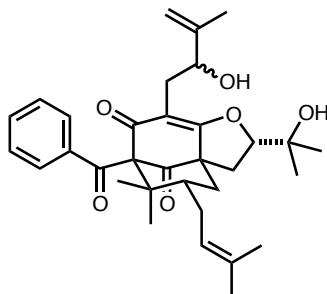
Clusia minor (Havana, Cuba)⁷⁹
Hypericum scabrum (Chimgan, Uzbekistan)¹⁸¹
 propolis (Guantanamo, Cuba)⁸⁰
 NMR^{79,181} (UV, IR)¹⁸¹
 [α]_D = -42.2°^{79,80} -20.8°¹⁸¹ (CHCl₃)

hyperibone C
(121)



Hypericum scabrum (Chimgan, Uzbekistan)¹⁸¹
 (NMR, UV, IR)¹⁸¹ [α]_D = -27.3° (CHCl₃)¹⁸¹
 structural revision¹³²

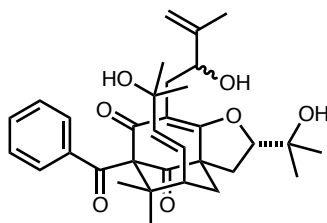
**hyperibone D
(122)**



Hypericum scabrum (Chimgan, Uzbekistan)¹⁸¹

(NMR, UV, IR)¹⁸¹ $[\alpha]_D = -61.9^\circ$ (CHCl₃)¹⁸¹

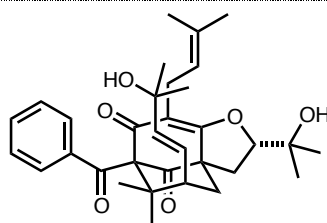
**hyperibone E
(123)**



Hypericum scabrum (Chimgan, Uzbekistan)¹⁸¹

(NMR, UV, IR)¹⁸¹ $[\alpha]_D = -56.0^\circ$ (CHCl₃)¹⁸¹
structural revision¹³²

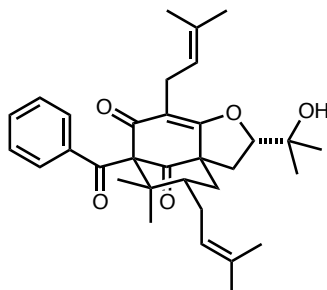
**hyperibone F
(124)**



Hypericum scabrum (Chimgan, Uzbekistan)¹⁸¹

(NMR, UV, IR)¹⁸¹ $[\alpha]_D = -31.0^\circ$ (CHCl₃)¹⁸¹
structural revision¹³²

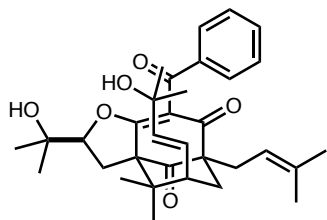
**hyperibone G
(125)**



Hypericum scabrum (Chimgan, Uzbekistan)¹⁸¹

(NMR, UV, IR)¹⁸¹ $[\alpha]_D = -29.3^\circ$ (CHCl₃)¹⁸¹

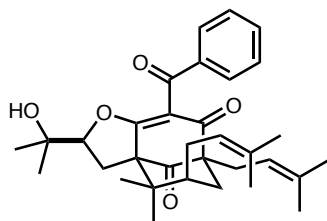
**hyperibone H
(126)**



Hypericum scabrum (Chimgan, Uzbekistan)¹⁸¹

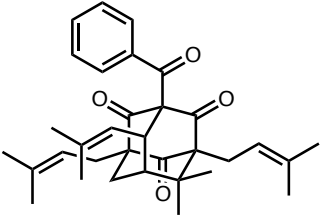
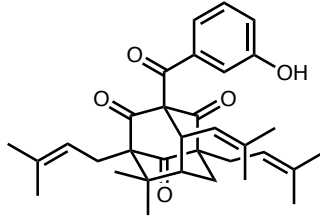
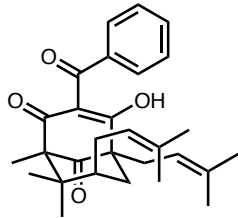
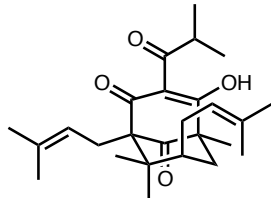
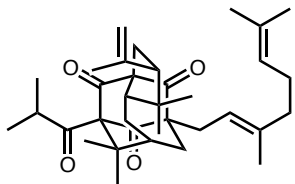
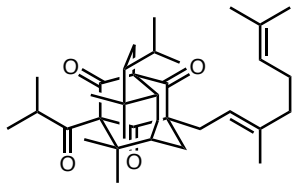
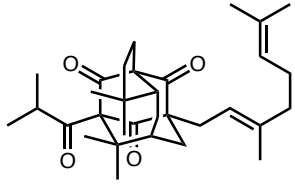
(NMR, UV, IR)¹⁸¹ $[\alpha]_D = +12.4^\circ$ (CHCl₃)¹⁸¹
structural revision¹³²

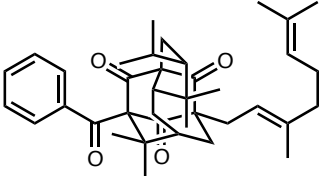
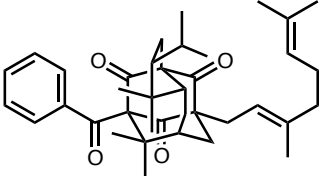
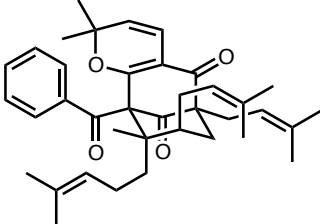
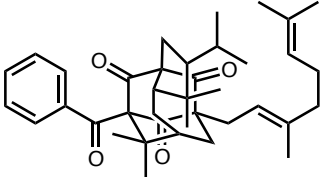
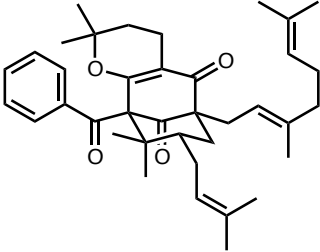
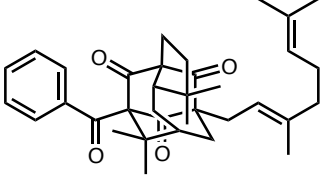
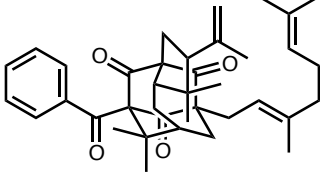
**hyperibone I
(127)**

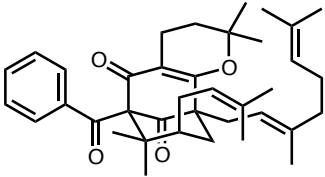
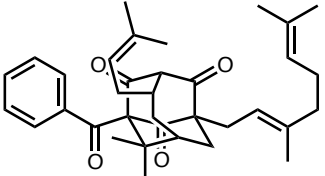
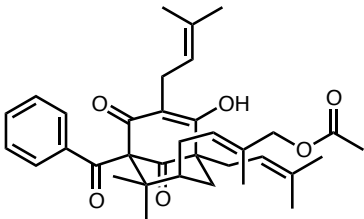
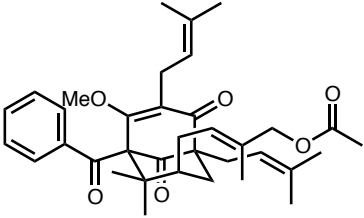


Hypericum scabrum (Chimgan, Uzbekistan)¹⁸¹

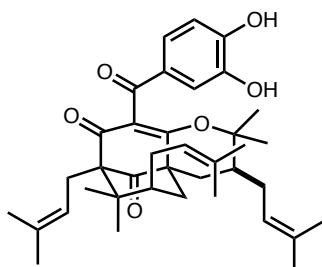
(NMR, UV, IR)¹⁸¹ $[\alpha]_D = +13.3^\circ$ (CHCl₃)¹⁸¹
structural revision¹³²

hyperibone K (128)		<i>Hypericum scabrum</i> (Chimgan, Uzbekistan) ³⁸ (NMR, UV, IR) ³⁸ $[\alpha]_D = +22.3^\circ$ (CHCl ₃) ³⁸ absolute configuration ¹⁸³
18-hydroxyhyperibone K (129)		<i>Hypericum hypericoides</i> (St. Andrew, Jamaica) ³¹ (NMR, IR) ³¹
hyperibone L (130)		<i>Hypericum scabrum</i> (Chimgan, Uzbekistan) ³⁸ (NMR, UV, IR) ³⁸ $[\alpha]_D = +69.5^\circ$ (CHCl ₃) ³⁸
hyperpapuanone (131)		<i>Hypericum papuanum</i> (Ialibu, Papua New Guinea) ¹⁸⁴ (NMR, UV) ¹⁸⁴ $[\alpha]_D = +15^\circ$ (MeOH) ¹⁸⁴
hypersampson A (132)		<i>Hypericum sampsonii</i> (Chia-Yi, Taiwan) ¹⁸⁵ (NMR, IR) ¹⁸⁵ $[\alpha]_D = +21^\circ$ (CHCl ₃) ¹⁸⁵
hypersampson B (133)		<i>Hypericum sampsonii</i> (Chia-Yi, Taiwan) ¹⁸⁵ (NMR, IR) ¹⁸⁵ $[\alpha]_D = +12^\circ$ (CHCl ₃) ¹⁸⁵
hypersampson C (134)		<i>Hypericum sampsonii</i> (Chia-Yi, Taiwan) ¹⁸⁵ (NMR, IR) ¹⁸⁵ $[\alpha]_D = +14.3^\circ$ (CHCl ₃) ¹⁸⁵

hypersampsonone D (135)		<i>Hypericum sampsonii</i> (Chia-Yi, Taiwan) ¹⁸⁵ (NMR, UV, IR) ¹⁸⁵ $[\alpha]_D = -35^\circ$ (CHCl ₃) ¹⁸⁵
hypersampsonone E (136)		<i>Hypericum sampsonii</i> (Chia-Yi, Taiwan) ¹⁸⁵ (NMR, UV, IR) ¹⁸⁵ $[\alpha]_D = +39^\circ$ (CHCl ₃) ¹⁸⁵
hypersampsonone F (137)		<i>Hypericum sampsonii</i> (Chia-Yi, Taiwan) ¹⁸⁵ (NMR, UV, IR) ¹⁸⁵ $[\alpha]_D = +30.0^\circ$ (CHCl ₃) ¹⁸⁵ structural revision ¹³²
hypersampsonone G (138)		<i>Hypericum sampsonii</i> (China) ¹⁸⁶ IR ¹⁸⁶ $[\alpha]_D = +10.25^\circ$ (CHCl ₃) ¹⁸⁶ crystal structure ¹⁸⁶
hypersampsonone H (139)		<i>Hypericum sampsonii</i> (China) ¹⁸⁶ (NMR, IR) ¹⁸⁶ $[\alpha]_D = +44.37^\circ$ (CHCl ₃) ¹⁸⁶
hypersampsonone I (140)		<i>Hypericum sampsonii</i> (Chalin, Hunan, China) ¹⁸⁷ (NMR, UV, IR) ¹⁸⁷ $[\alpha]_D = +18.6^\circ$ (CHCl ₃) ¹⁸⁷ crystal structure ¹⁸⁷
hypersampsonone J (141)		<i>Hypericum sampsonii</i> (Chalin, Hunan, China) ¹⁸⁷ (NMR, UV, IR) ¹⁸⁷ $[\alpha]_D = +11.4^\circ$ (CHCl ₃) ¹⁸⁷ crystal structure ¹⁸⁷

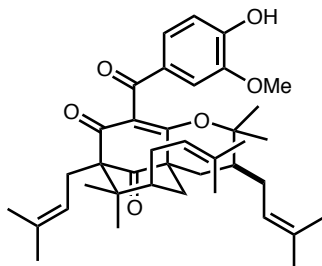
hypersampsonone K (142)		<i>Hypericum sampsonii</i> (Chalin, Hunan, China) ¹⁸⁷ (NMR, UV, IR) ¹⁸⁷ $[\alpha]_D = +31.7^\circ$ (CHCl ₃) ¹⁸⁷
hypersampsonone L (143)		<i>Hypericum sampsonii</i> (Chalin, Hunan, China) ¹⁸⁷ (NMR, UV, IR) ¹⁸⁷ $[\alpha]_D = -67.4^\circ$ (CHCl ₃) ¹⁸⁷
insignone (144)		<i>Clusia insignis</i> (Campinas, São Paulo, Brazil) ²⁴ <i>O</i> -Me ether (¹ H NMR, UV) ²⁴ $[\alpha]_D = +92.7^\circ$ (CHCl ₃) ²⁴
methyl insignone (145)		propolis (Manaus, Brazil) ²⁰ (¹ H NMR, UV) ²⁴ $[\alpha]_D = +92.7^\circ$ (CHCl ₃) ²⁴

isogarcinol
cambogin
ent-isoxanthochymol
(146)



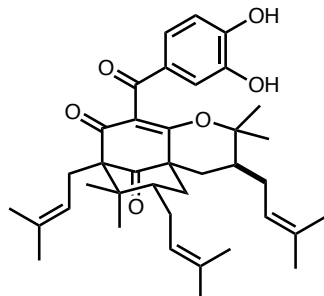
Allanblackia monticola (West Province, Cameroon)⁸³
Calophyllum enervosum (Bukitinggi, West Sumatra, Indonesia)⁵⁴
C. thorelii (central Vietnam)³³
Hypericum lanceolatum (Mt. Bamboutos, West Province, Cameroon)^{188,189}
Garcinia assigu (Central Province, Papua New Guinea)²⁹
G. bancana (Naratiwath, Thailand)⁸⁴
G. brevipedicellata (Cameroon)³⁰
***G. cambogia* (India)**^{86,87}
G. cowa (Yunnan, China)^{65,66}
G. esculenta (Dehong, Yunnan, China)⁶⁶
G. giffithii (Singapore)¹³⁴
G. indica (India)^{93,94}
G. lancilimba (Xishuangbanna, Yunnan, China)⁶⁶
G. latissima (Central Province, Papua New Guinea)¹⁹⁰
G. multiflora
Wanning, China⁶⁶
Mudan, Taiwan⁶⁸
G. nuijiangensis (Nuijiang, Yunnan, China)⁴⁹
G. oblongifolia (Bobai, Guangxi, China)⁶⁶
G. paucinervis (Xishuangbanna, Yunnan, China)⁶⁶
G. pedunculata (Jorhat, Assam, India)⁹⁷
G. preussii (Cameroon)³⁰
G. purpurea (Japan)⁵¹
G. subelliptica (Shenzhen, Guangdong, China)⁶⁶
G. tetrandra (West Kalimantan, Indonesia)⁹⁸
G. xanthochymus (Xishuangbanna, Yunnan, China)⁶⁶
G. xipshuangbannaensis (Xishuangbanna, Yunnan, China)⁶⁶
G. yunnanensis (Dehong, Yunnan, China)⁶⁶
Moronobea coccinea (dense rain forest, French Guyana)⁴⁶
Rheedia acuminata (French Guyana)¹⁹¹
¹H NMR^{46,97,98,191} ¹³C NMR^{46,86,98,191}
(UV, IR)^{46,51,93,94,97,191} CD²⁹
 $[\alpha]_D = -158^\circ$,⁴⁶ -160° ,¹⁹¹ (CHCl₃) -224° ,⁵¹ -209.9° ,⁸⁶
 -269.8° ,⁹⁴ (MeOH) -203° ,⁹³ -211° ,⁹⁷ (EtOH)
structural revision,¹⁹² crystal structure¹⁹²
absolute configuration⁴⁶

isogarcinol
13-O-methyl ether
(147)



Garcinia assigu (Central Province, Papua New Guinea)²⁹
(NMR, UV, IR, CD)²⁹ $[\alpha]_D = -199^\circ$ (EtOH)²⁹
absolute configuration²⁹

**7-*epi*-isogarcinol
(148)**

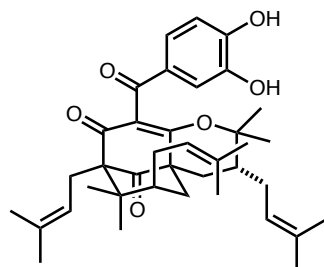


Garcinia nuijiangensis (Nuijiang, Yunnan, China)⁴⁹
Moronobea coccinea (dense rain forest, French
Guyana)⁴⁶

Rheedia acuminata (French Guyana)¹⁹¹
Symphonia globulifera (dense rain forest, French
Guyana)⁴⁷

(NMR, UV, IR)^{46,47,191} $[\alpha]_D = -158^\circ$ (CHCl₃)^{46,47,191}

**30-*epi*-isogarcinol
(149)**



Allanblackia ulugurensis (Morningside, Morogoro,
Tanzania)¹²⁴

Garcinia cochinchinensis (southern Vietnam)⁷¹

G. cowa (Yunnan, China)^{65,66}

G. esculenta (Dehong, Yunnan, China)⁶⁶

G. lancilimba (Xishuangbanna, Yunnan, China)⁶⁶

G. multiflora (Wanning, China)⁶⁶

G. oblongifolia (Vietnam)¹²⁶

G. paucinervis (Xishuangbanna, Yunnan, China)^{66,67}

G. subelliptica (Shenzhen, Guangdong, China)⁶⁶

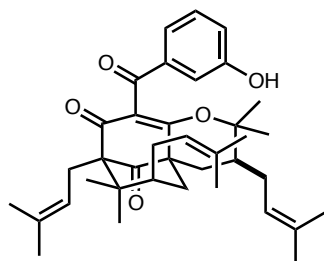
G. xanthochymus (Xishuangbanna, Yunnan, China)⁶⁶

G. xipshuangbannaensis (Xishuangbanna, Yunnan,
China)⁶⁶

G. yunnanensis (Dehong, Yunnan, China)⁶⁶

(NMR, UV)¹²³ $[\alpha]_D = -125^\circ$ (CHCl₃)¹²³

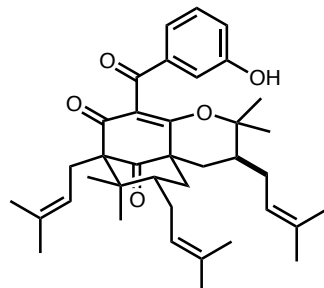
**14-deoxyisogarcinol
(150)**



Garcinia indica (Bengaluru, India)⁹⁴

(NMR, UV, IR)⁹⁴ $[\alpha]_D = -178.0^\circ$ (MeOH)⁹⁴
crystal structure¹⁹³

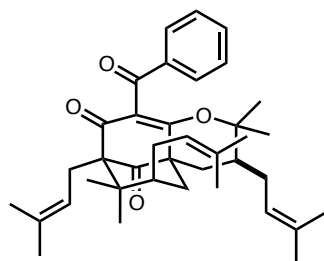
**14-deoxy-7-*epi*-
isogarcinol
(151)**



Symphonia globulifera (dense rain forest, French
Guyana)⁴⁷

(NMR, UV, IR)⁴⁷ $[\alpha]_D = -77^\circ$ (CHCl₃)⁴⁷

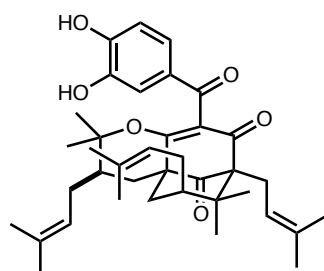
**13,14-didehydroxy-
isogarcinol
(152)**



Garcinia multiflora (Mudan, Taiwan)⁶⁸

(NMR, UV, IR, CD)⁶⁸ $[\alpha]_D = -185^\circ$ (CHCl₃)⁶⁸
absolute configuration⁶⁸

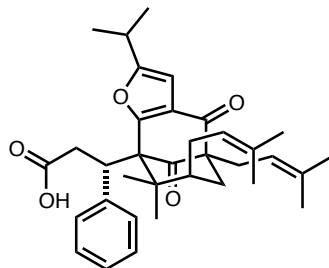
**isoxanthochymol
ent-isogarcinol
(153)**



Garcinia afzelii (Mt. Eloumdem, Centre Province, Cameroon)¹¹⁷
G. cambogia (Kerela, India)⁸⁵
G. griffithii (Lembah Arau, West Sumatra, Indonesia)¹⁹⁴
G. indica (Dapoli,⁸⁵ Maharastra, India¹⁹⁵)
G. livingstonei (Homestead, Florida, USA)⁴⁸
G. maingayii
 Riau Islands, Indonesia⁹⁵
 Pahang, Malaysia¹⁹⁶
G. multiflora
 Diaoluo Mountain, Hainan, China¹⁸
 Taiwan⁷²
G. ovalifolia
 Douala-Edea Reserve, Cameroon^{197,198}
 Ndakan Gorilla Study Area, Central African Republic¹⁰⁷
G. polyantha (Cheffou-Baham, West Province, Cameroon)¹⁹⁹
G. pyrifera (Sungai Petani, Kedah, Malaysia)⁵⁰
G. smeathmannii (Cheffou-Baham, West Province, Cameroon)^{130,131}
G. subelliptica (Okinawa, Japan)⁵¹
G. xanthochymus
 South Canara,²⁰⁰ **India**^{201,202}
 Homestead, Florida, USA¹⁹
G. xipshuangbannaensis (Xishuangbanna, Yunnan, China)²⁰³
Rheedia acuminata (La Paz, Bolivia)¹
R. edulis (Broward County, Florida, USA)⁴¹

(¹H NMR, IR)^{95,107,202,203} ¹³C NMR^{95,107,203}
 IR^{95,203} UV^{41,107,202}
 [α]_D = +181°, ¹⁰⁷+208°, ²⁰⁴(MeOH)
 +208°, ²⁰²+207.6°²⁰⁵ (EtOH)
 characterized as mixture with **21** (NMR, UV, IR)^{50,51}
 [α]_D = +142° (CHCl₃)⁵⁰ [α]_D = +158° (MeOH)⁵¹
 absolute configuration,²⁰⁵ crystal structure⁹⁵
 structural revision²⁰⁴

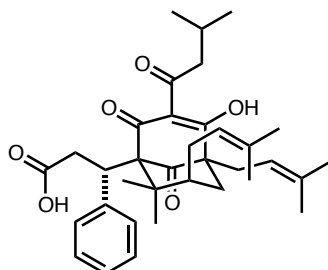
**lathrophytoic acid B
(154)**



Kielmeyera lathrophyton (Chapada Diamantina, Brazil)²⁰⁶

O-Me ether (NMR, IR)²⁰⁶

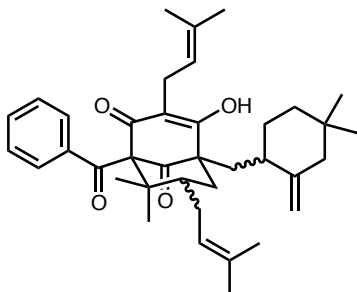
**laxifloranone
(155)**



Marila laxiflora (Guatemala)²⁰⁷

(NMR, UV, IR)²⁰⁷ [α]_D = +23.6° (MeOH)²⁰⁷

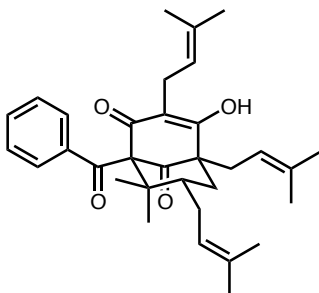
**makandechamone
(156)**



Garcinia punctata (northern Gabon)²⁰⁸

(NMR, UV)²⁰⁸

**nemorosone
(157)**



Clusia rosea

Campinas, São Paulo, Brazil²⁰⁹

Havana, Cuba^{103,210}

C. grandiflora

Campinas, São Paulo, Brazil²⁸

Canaima, Venezuela²¹

C. hilariana

Campinas, São Paulo, Brazil²⁴

Jurubatiba, Brazil²¹¹

C. insignis (Campinas, São Paulo, Brazil)²⁸

C. nemorosa (Campinas, São Paulo, Brazil)²⁸

C. rosea

Campinas, São Paulo, Brazil²⁸

Havana, Cuba¹⁰³

brown propolis (throughout Cuba)^{120,212,213}

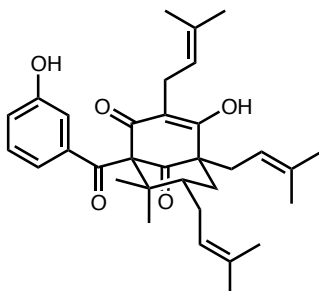
(NMR, UV, IR)^{210,211} UV²¹⁰ $[\alpha]_D = +112.8$ (CHCl₃)²¹⁰

O-Me ether (NMR, IR)^{28,209} UV²⁸

$[\alpha]_D = +150^\circ$ (MeOH)²⁸ +48.6° (CHCl₃)²⁰⁹

structural revision,²¹⁰ crystal structure²¹⁴

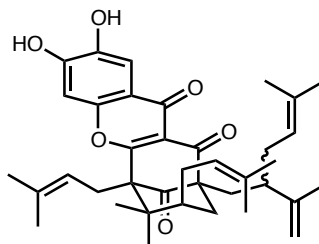
**hydroxynemorosone
(158)**



Clusia nemorosa (Campinas, São Paulo, Brazil)²⁸

O-Me ether (NMR, IR)²⁸ $[\alpha]_D = +142.8^\circ$ (MeOH)²⁸

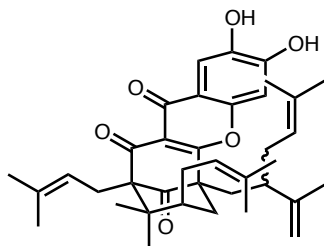
**nujiangefolin A
(159)**



Garcinia nujiangensis (Nujiang, Yunnan, China)⁴⁹

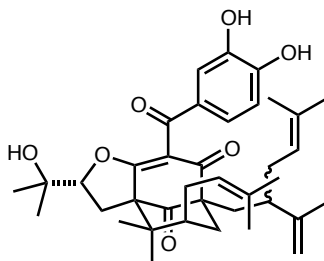
(NMR, UV, IR)⁴⁹ $[\alpha]_D = -2^\circ$ (MeOH)⁴⁹

**nujiangefolin B
(160)**



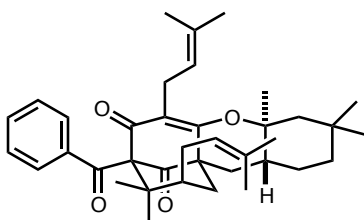
Garcinia nujiangensis (Nujiang, Yunnan, China)⁴⁹
(NMR, UV, IR)⁴⁹ $[\alpha]_D = +5^\circ$ (MeOH)⁴⁹

**nujiangefolin C
(161)**



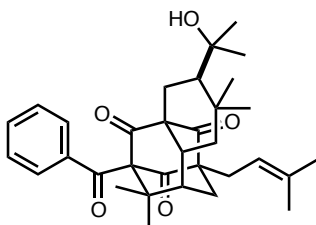
Garcinia nujiangensis (Nujiang, Yunnan, China)⁴⁹
(NMR, UV, IR)⁴⁹ $[\alpha]_D = +20^\circ$ (MeOH)⁴⁹

**no name
obdeltifolin A
(162)**



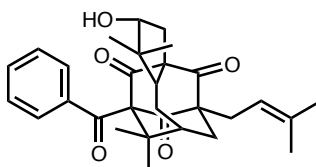
Clusia obdeltifolia (Chapada Diamantina, Brazil)²¹⁵
NMR²¹⁵ $[\alpha]_D = +30.9^\circ$ (CHCl₃)²¹⁵

**no name
obdeltifolin B
(163)**



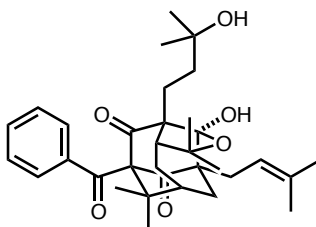
Clusia obdeltifolia (Chapada Diamantina, Brazil)²¹⁵
NMR²¹⁵ $[\alpha]_D = +10.0^\circ$ (CHCl₃)²¹⁵

**no name
obdeltifolin C
(164)**



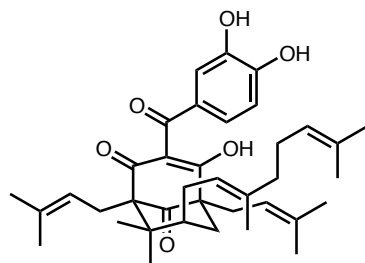
Clusia obdeltifolia (Chapada Diamantina, Brazil)²¹⁶
(NMR, IR)²¹⁶

**no name
obdeltifolin D
(165)**



Clusia obdeltifolia (Chapada Diamantina, Brazil)²¹⁶
(NMR, IR)²¹⁶ $[\alpha]_D = -5.1^\circ$ (CHCl₃)²¹⁶

**oblongifolin A
(166)**



Garcinia cowa (Yunnan, China)^{65,66}
G. lancilimba (Xishuangbanna, Yunnan, China)⁶⁶
G. multiflora (Wanning, China)⁶⁶

G. oblongifolia

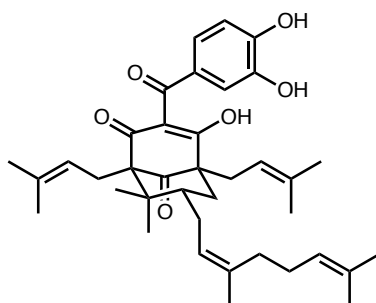
Bobai, Guangxi, China^{66,116}

Nhu Xuan, Vietnam^{96,126}

G. paucinervis (Xishuangbanna, Yunnan, China)⁶⁶
G. xanthochymus (Xishuangbanna, Yunnan, China)⁶⁶
G. xipshuangbannaensis (Xishuangbanna, Yunnan, China)⁶⁶
G. yunnanensis
 Dehong, Yunnan, China⁶⁶
 Luxi, Yunnan, China¹⁰⁰

(NMR, UV, IR)⁹⁶ [α]_D = +23° (CHCl₃)⁹⁶

**oblongifolin B
(167)**



Garcinia cowa (Yunnan, China)^{65,66}
G. lancilimba (Xishuangbanna, Yunnan, China)⁶⁶
G. multiflora (Wanning, China)⁶⁶

G. oblongifolia

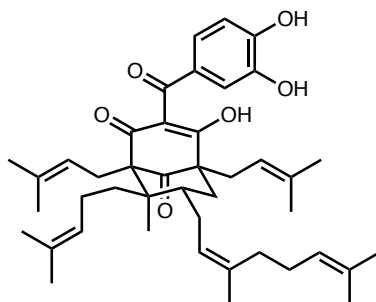
Bobai, Guangxi, China^{66,116}

Nhu Xuan, Vietnam⁹⁶

G. paucinervis (Xishuangbanna, Yunnan, China)⁶⁶
G. subelliptica (Shenzhen, Guangdong, China)⁶⁶
G. xanthochymus (Xishuangbanna, Yunnan, China)⁶⁶
G. xipshuangbannaensis (Xishuangbanna, Yunnan, China)⁶⁶
G. yunnanensis
 Dehong, Yunnan, China⁶⁶
 Luxi, Yunnan, China¹⁰⁰

(NMR, UV, IR)⁹⁶ [α]_D = +17.6° (CHCl₃)⁹⁶

**oblongifolin C
ent-guttiferone G
(168)**



Garcinia cowa (Yunnan, China)^{65,66}
G. lancilimba (Xishuangbanna, Yunnan, China)⁶⁶
G. multiflora (Wanning, China)⁶⁶

G. oblongifolia

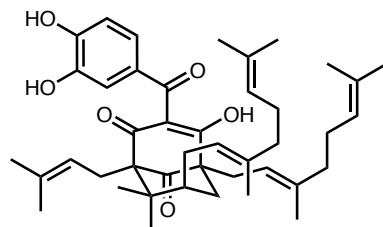
Bobai, Guangxi, China^{66,116}

Nhu Xuan, Vietnam⁹⁶

G. paucinervis (Xishuangbanna, Yunnan, China)⁶⁶
G. subelliptica (Shenzhen, Guangdong, China)⁶⁶
G. xanthochymus (Xishuangbanna, Yunnan, China)⁶⁶
G. xipshuangbannaensis (Xishuangbanna, Yunnan, China)⁶⁶
G. yunnanensis
 Dehong, Yunnan, China⁶⁶
 Luxi, Yunnan, China¹⁰⁰

(NMR, UV, IR)⁹⁶ [α]_D = +14.5° (CHCl₃)⁹⁶

**oblongifolin D
(169)**



Garcinia cowa (Yunnan, China)^{65,66}
G. lancilimba (Xishuangbanna, Yunnan, China)⁶⁶
G. multiflora (Wanning, China)⁶⁶

G. oblongifolia

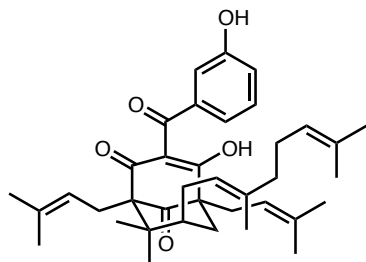
Bobai, Guangxi, China^{66,116}

Nhu Xuan, Vietnam⁹⁶

G. subelliptica (Shenzhen, Guangdong, China)⁶⁶
G. yunnanensis
 Dehong, Yunnan, China⁶⁶
 Luxi, Yunnan, China¹⁰⁰

(NMR, UV, IR)⁹⁶ [α]_D = +44.6° (CHCl₃)⁹⁶

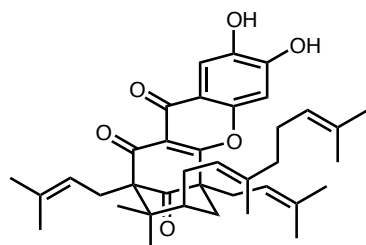
oblongifolin E
(170)



Garcinia oblongifolia (Bobai, Guangxi, China)¹¹⁶

(NMR, UV, IR)¹¹⁶ $[\alpha]_D = +65.1^\circ$ (CHCl₃)¹¹⁶

oblongifolin F
ent-guttiferone O2
(171)



Garcinia multiflora (Wanning, China)⁶⁶

***G. oblongifolia* (Bobai, Guangxi, China)¹¹⁶**

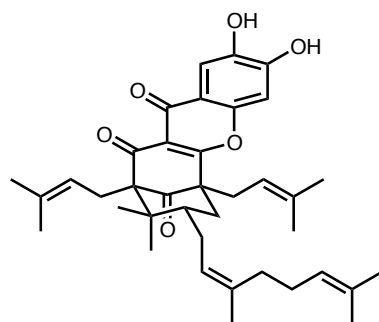
G. subelliptica (Shenzhen, Guangdong, China)⁶⁶

G. xipshuangbannaensis (Xishuangbanna, Yunnan, China)⁶⁶

G. yunnanensis (Dehong, Yunnan, China)⁶⁶

(NMR, UV, IR)¹¹⁶ $[\alpha]_D = -85.6^\circ$ (CHCl₃)¹¹⁶

oblongifolin G
(172)



Garcinia oblongifolia (Bobai, Guangxi, China)⁶⁶

***G. oblongifolia* (Bobai, Guangxi, China)¹¹⁶**

G. paucinervis (Xishuangbanna, Yunnan, China)⁶⁶

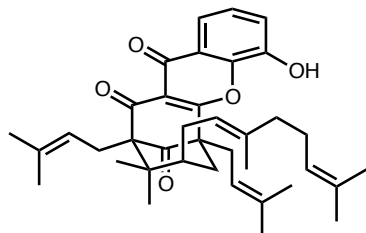
G. subelliptica (Shenzhen, Guangdong, China)⁶⁶

G. xipshuangbannaensis (Xishuangbanna, Yunnan, China)⁶⁶

G. yunnanensis (Dehong, Yunnan, China)⁶⁶

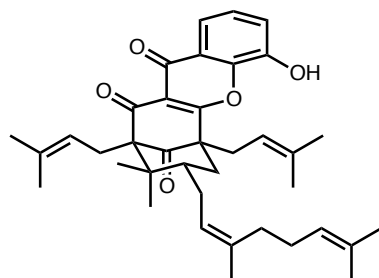
(NMR, UV, IR)¹¹⁶ $[\alpha]_D = +5.9^\circ$ (CHCl₃)¹¹⁶

oblongifolin H
(173)



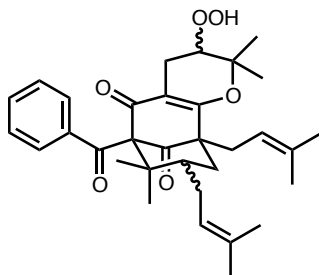
Garcinia oblongifolia (Bobai, Guangxi, China)⁶⁶

oblongifolin I
(174)



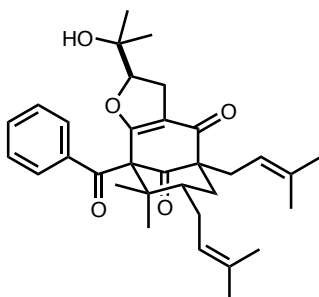
Garcinia oblongifolia (Bobai, Guangxi, China)⁶⁶

**ochrocarpinone A
(175)**



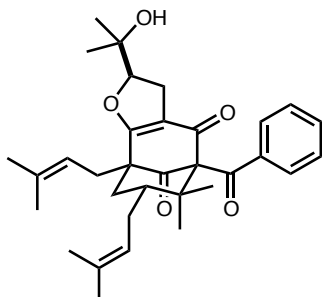
Ochrocarpos punctatus (Mahajanga, Madagascar)²¹⁷
(NMR, UV, IR)²¹⁷ $[\alpha]_D = +8.7^\circ$ (CHCl₃)²¹⁷

**ochrocarpinone B
(176)**



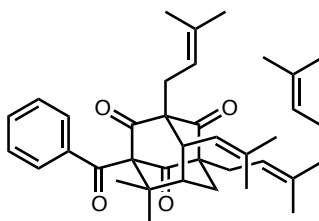
Ochrocarpos punctatus (Mahajanga, Madagascar)²¹⁷
(NMR, UV, IR)²¹⁷ $[\alpha]_D = -3.5^\circ$ (CHCl₃)²¹⁷

**ochrocarpinone C
ent-hyperibone B
(177)**



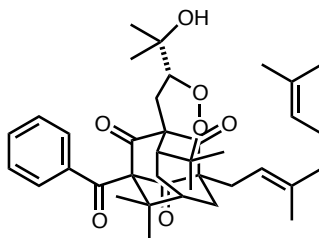
Ochrocarpos punctatus (Mahajanga, Madagascar)²¹⁷
(NMR, UV, IR)²¹⁷ $[\alpha]_D = +10.2^\circ$ (CHCl₃)²¹⁷

**otogirinin A
(178)**



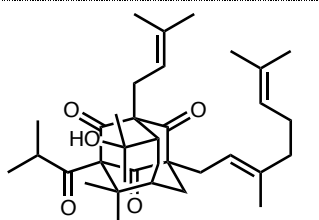
Hypericum erectum (Japan)²¹⁸
(NMR, UV, IR, CD)²¹⁸ $[\alpha]_D = -8.1^\circ$ (MeOH)²¹⁸

**otogirinin B
(179)**



Hypericum erectum (Japan)²¹⁸
(NMR, UV, IR, CD)²¹⁸ $[\alpha]_D = +12.0^\circ$ (MeOH)²¹⁸

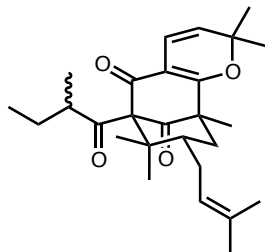
**otogirinin C
(180)**



Hypericum erectum (Japan)²¹⁸
NMR²¹⁸

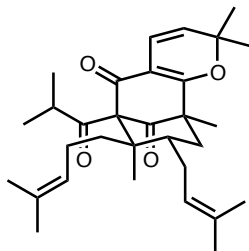
<p>otogirinin D (181)</p>		<p><i>Hypericum erectum</i> (Japan)²¹⁸ (NMR, UV, IR)²¹⁸ $[\alpha]_D = +160.0^\circ$ (MeOH)²¹⁸</p>
<p>otogirinin E (182)</p>		<p><i>Hypericum erectum</i> (Japan)²¹⁸ NMR²¹⁸</p>
<p>oxepahyperforin (183)</p>		<p><i>Hypericum perforatum</i> (Chile)⁶⁴ (NMR, UV, IR, CD)⁶⁴ $[\alpha]_D = -73.7^\circ$ (CHCl₃)</p>
<p>oxyhyperforin 8-hydroxyhyperforin 8,1-hemiacetal (184)</p>		<p><i>Hypericum perforatum</i> Chile⁶⁴ Italy¹³ Tokushima, Japan⁵⁹ (NMR, UV, IR, CD)⁶⁴ $[\alpha]_D = +34.0^\circ$ (CHCl₃)</p>
<p>papuaforin A (185)</p>		<p><i>Hypericum papuanum</i> (Ialibu, Papua New Guinea)¹⁸⁴ (NMR, UV)¹⁸⁴ $[\alpha]_D = +13^\circ$ (MeOH)¹⁸⁴</p>
<p>papuaforin B (186)</p>		<p><i>Hypericum papuanum</i> (Ialibu, Papua New Guinea)¹⁸⁴ NMR¹⁸⁴</p>

**papuaforin C
(187)**



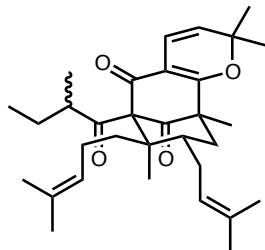
Hypericum papuanum (Ialibu, Papua New Guinea)¹⁸⁴
(NMR, UV)¹⁸⁴ $[\alpha]_D = +23^\circ$ (MeOH)¹⁸⁴

**papuaforin D
(188)**



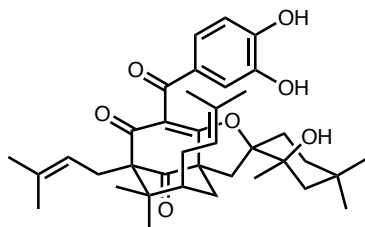
Hypericum papuanum (Ialibu, Papua New Guinea)¹⁸⁴
(NMR, UV)¹⁸⁴ $[\alpha]_D = +64^\circ$ (MeOH)¹⁸⁴

**papuaforin E
(189)**



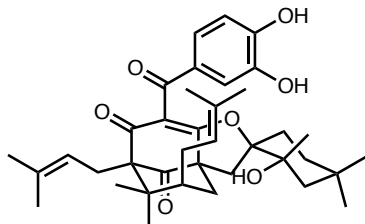
Hypericum papuanum (Ialibu, Papua New Guinea)¹⁸⁴
(NMR, UV)¹⁸⁴ $[\alpha]_D = +41^\circ$ (MeOH)¹⁸⁴

**paucinone A
(190)**



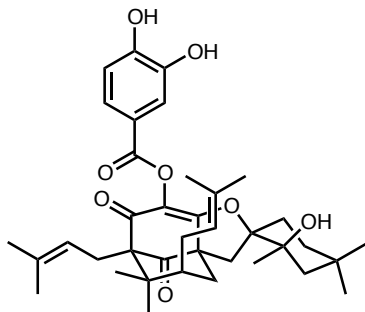
Garcinia paucinervis (Xishuangbanna, Yunnan, China)^{219,220}
(NMR, UV, IR)^{219,220} $[\alpha]_D = -6.2^\circ$ (MeOH)^{219,220}

**paucinone B
(191)**



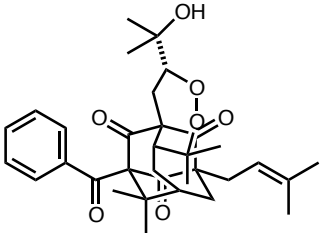
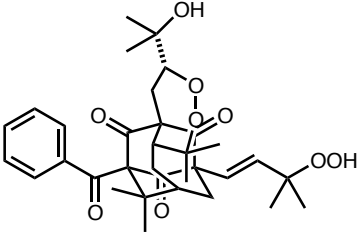
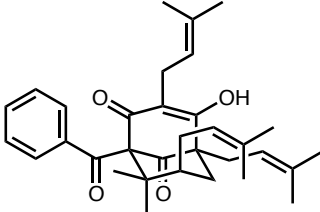
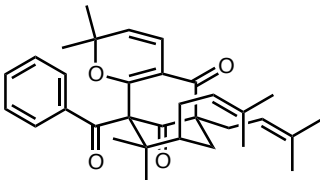
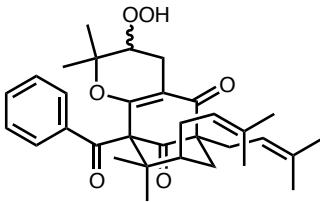
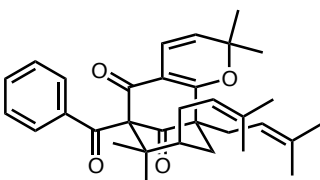
Garcinia paucinervis (Xishuangbanna, Yunnan, China)^{219,220}
(NMR, UV, IR)^{219,220} $[\alpha]_D = +58.7^\circ$ (MeOH)^{219,220}

**paucinone C
(192)**

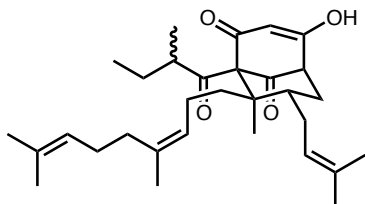


Garcinia paucinervis (Xishuangbanna, Yunnan, China)^{219,220}
(NMR, UV, IR)^{219,220} $[\alpha]_D = +19.2^\circ$ (MeOH)^{219,220}

paucinone D (193)		<i>Garcinia paucinervis</i> (Xishuangbanna, Yunnan, China) ^{219,220} (NMR, UV, IR) ^{219,220} $[\alpha]_D = +41.6^\circ$ (MeOH) ^{219,220}
pedunculol (194)		<i>Garcinia pedunculata</i> (Jorhat, Assam, India) ⁹⁷ (NMR, UV, IR) ⁹⁷ $[\alpha]_D = -159^\circ$ (EtOH) ⁹⁷
peroxysampsonone A (195)		<i>Hypericum sampsonii</i> (Cha Lin, Hunan, China) ²²¹ (NMR, UV, IR) ²²¹ $[\alpha]_D = +17.0^\circ$ (CHCl ₃) ²²¹
peroxysampsonone B (196)		<i>Hypericum sampsonii</i> (Cha Lin, Hunan, China) ²²¹ (NMR, UV, IR) ²²¹ $[\alpha]_D = -41.2^\circ$ (CHCl ₃) ²²¹
plukenetione A (197)		<i>Clusia plukenetii</i> (Barbados) ²²² propolis (throughout Cuba) ²¹² (NMR, UV, IR) ²²² $[\alpha]_D = +1^\circ$ (CHCl ₃) ²²²
28,29- epoxyplukenetione A (198)		<i>Clusia havetiodes</i> (Ecclesdown, Portland, Jamaica) ²²³ <i>C. obdeltifolia</i> (Chapada Diamantina, Brazil) ²¹⁵ (NMR, UV, IR) ²²³ $[\alpha]_D = -4.4^\circ$ (CHCl ₃) ²²³
plukenetione B (199)		<i>Clusia plukenetii</i> (St. Thomas, Barbados) ²²⁴ (NMR, UV, IR) ²²⁴ $[\alpha]_D = +17.2^\circ$ (CHCl ₃) ²²⁴ structural revision ²²⁵

<p>plukenetione C (200)</p>		<p><i>Clusia havetiodes</i> (Ecclesdown, Portland, Jamaica)²²³ <i>C. plukenetii</i> (St. Thomas, Barbados)²²⁴ <i>Hypericum sampsonii</i> (Cha Lin, Hunan, China)²²¹</p> <p>(NMR, UV, IR)^{221,223,224} $[\alpha]_D = +27.5^\circ, ^{221} +15.0^\circ, ^{223} +65.9^\circ$ (CHCl₃)</p>
<p>33-hydroxyperoxyiso-plukenetione C (201)</p>		<p><i>Clusia havetiodes</i> (Ecclesdown, Portland, Jamaica)²²³</p> <p>(NMR, UV, IR)²²³ $[\alpha]_D = -3.9^\circ$ (CHCl₃)²²³</p>
<p>plukenetione D/E 7-<i>epi</i>-nemorosone (202)</p>		<p><i>Clusia hilariana</i> (Campinas, São Paulo, Brazil)²⁴ <i>C. nemorosa</i> (Campinas, São Paulo, Brazil)²⁰⁹ <i>C. plukenetii</i> (St. Thomas, Barbados)²²⁴ <i>C. rosea</i> (Florida, USA)²²⁶ <i>Tovomitopsis saldanhae</i> (southeastern Brazil)²²⁷ Propolis Caribbean²²⁶ Manaus, Brazil²⁰</p> <p>NMR^{20,227} (UV, IR)²⁰ <i>O</i>-Me ether (NMR, IR)²⁰⁹ $[\alpha]_D = +140.7$ (CHCl₃)²⁰⁹ acetate ester (NMR, UV, IR)²²⁴ $[\alpha]_D = +34.5^\circ$ (D), -37.6° (E) (CHCl₃)²²⁴ structural revision^{225,227}</p>
<p>plukenetione F (203)</p>		<p><i>Clusia plukenetii</i> (St. Thomas, Barbados)²²⁴</p> <p>(NMR, UV, IR)²²⁴ $[\alpha]_D = -53.6^\circ$ (CHCl₃)²²⁴ characterized as mixture with 205 (NMR, UV, IR)²²³ structural revision¹³²</p>
<p>15,16-dihydro-16-hydroperoxy-plukenetione F (204)</p>		<p><i>Clusia havetiodes</i> (Ecclesdown, Portland, Jamaica)²²³ <i>Ochrocarpos punctatus</i> (Mahajanga, Madagascar)²¹⁷</p> <p>(NMR, UV, IR)²²³ $[\alpha]_D = +24.7^\circ$ (CHCl₃)²²³ structural revision¹³²</p>
<p>plukenetione G (205)</p>		<p><i>Clusia havetiodes</i> (Ecclesdown, Portland, Jamaica)²²³ <i>C. plukenetii</i> (St. Thomas, Barbados)²²⁴</p> <p>(NMR, UV, IR)²²⁴ characterized as mixture with 203 (NMR, UV, IR)²²³ structural revision¹³²</p>

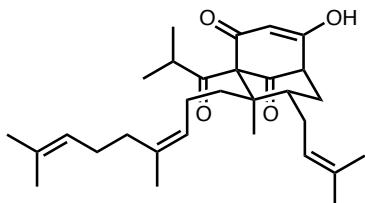
**prolifenone A
(206)**



Hypericum prolificum (Lawrence County, Pennsylvania, USA)²²⁸

(NMR, UV, IR)²²⁸ $[\alpha]_D = +13.3^\circ$ (MeOH)²²⁸

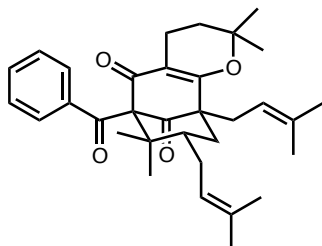
**prolifenone B
(207)**



Hypericum prolificum (Lawrence County, Pennsylvania, USA)²²⁸

(NMR, UV, IR)²²⁸ $[\alpha]_D = -0.58^\circ$ (MeOH)²²⁸

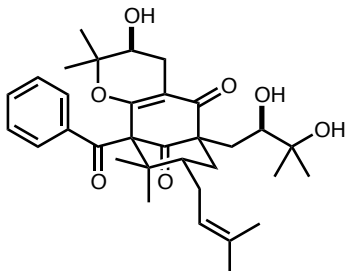
**propolone A
(208)**



propolis (Nuevitas, Cuba)²²⁹

(NMR, UV, IR)²²⁹ $[\alpha]_D = +40^\circ$ (CHCl₃)²²⁹

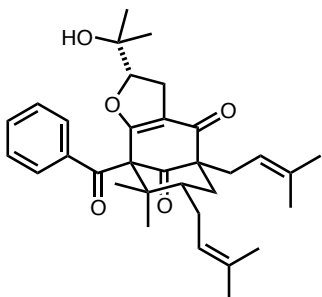
**propolone B
(209)**



propolis (Guantanamo, Cuba)⁸⁰

(NMR, UV, IR)⁸⁰ $[\alpha]_D = +38.2^\circ$ (CHCl₃)⁸⁰

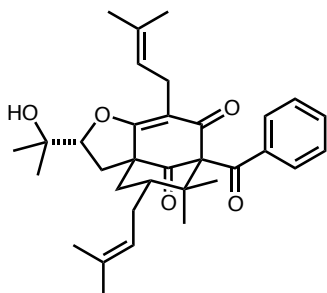
**propolone C
(210)**



propolis (Guantanamo, Cuba)⁸⁰

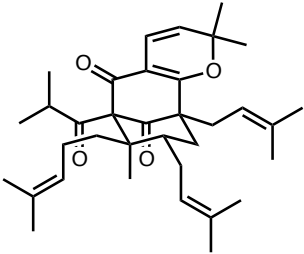
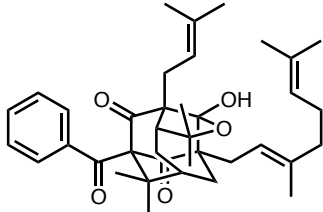
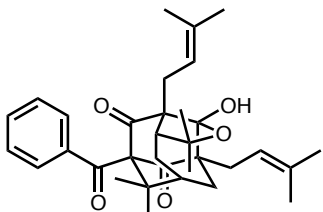
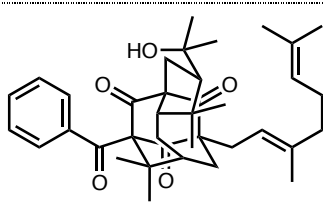
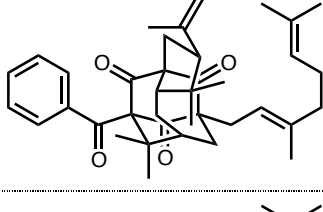
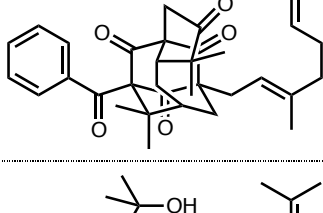
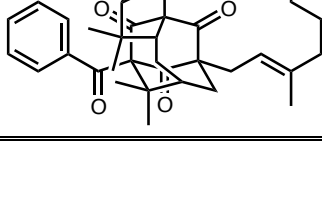
(NMR, UV, IR)⁸⁰ $[\alpha]_D = +35.7^\circ$ (CHCl₃)⁸⁰

**propolone D
ent-hyperibone G
(211)**



Clusia minor (Havana, Cuba)⁷⁹
propolis (Guantanamo, Cuba)⁸⁰

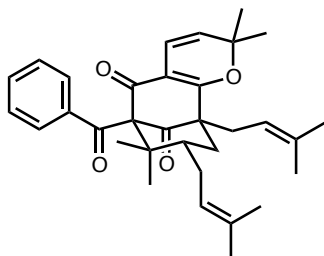
NMR⁷⁹ $[\alpha]_D = +48.5^\circ$ (CHCl₃)^{79,80}

<p>pyrohyperforin <i>pyrano[7,28-b]hyperforin</i> (212)</p>		<p><i>Hypericum perforatum</i> Longxi, Gansu, China^{162,230} Tokushima, Japan⁵⁹ Mt. Orzen, southeast Serbia⁵⁸</p> <p>(NMR, UV, IR)^{162,230} $[\alpha]_D = +83.5$ (CHCl₃)^{162,230}</p>
<p>sampsonione A (213)</p>		<p><i>Hypericum erectum</i> (Japan)²¹⁸ <i>H. sampsonii</i> Jinhua, Zhejiang, China^{32,231} Yunnan, China²³²</p> <p>(NMR, UV, IR)^{231,232} $[\alpha]_D = -49.10^\circ$ (CHCl₃)²³¹</p>
<p>sampsonione B (214)</p>		<p><i>Clusia obdeltifolia</i> (Chapada Diamantina, Brazil)²¹⁶ <i>Hypericum sampsonii</i> Hunan, China³⁷ Jinhua, Zhejiang, China^{32,231}</p> <p>NMR²³¹ IR²¹⁶ $[\alpha]_D = +10.0$ (CHCl₃)²¹⁶</p>
<p>sampsonione C (215)</p>		<p><i>Hypericum sampsonii</i> (Jinhua, Zhejiang, China)^{32,233}</p> <p>(NMR, UV, IR)²³³ $[\alpha]_D = +13.39^\circ$ (CHCl₃)²³³</p>
<p>sampsonione D (216)</p>		<p><i>Hypericum sampsonii</i> Jinhua, Zhejiang, China^{32,233} Chia-Yi, Taiwan¹⁸⁵</p> <p>(NMR, UV, IR)²³³ $[\alpha]_D = +12.27^\circ$ (CHCl₃)²³³</p>
<p>sampsonione E (217)</p>		<p><i>Hypericum sampsonii</i> (Jinhua, Zhejiang, China)^{32,233}</p> <p>(NMR, UV, IR)²³³ $[\alpha]_D = +57.69^\circ$ (CHCl₃)²³³</p>
<p>sampsonione F (218)</p>		<p><i>Hypericum sampsonii</i> Jinhua, Zhejiang, China^{32,233} Yunnan, China²³²</p> <p>(NMR, UV, IR)^{232,233} $[\alpha]_D = +14.52^\circ$ (CHCl₃)²³³</p>

sampsone G (219)		<i>Clusia obdeltifolia</i> (Chapada Diamantina, Brazil) ²¹⁶ <i>Hypericum sampsonii</i> (Jinhua, Zhejiang, China) ^{32,233} (NMR, UV) ²³³ IR ^{216,233} [α] _D = +10.00° (CHCl ₃) ²³³
<i>ent</i> -sampsone G (220)		<i>Clusia havetiodes</i> (Ecclesdown, Portland, Jamaica) ²²³ (NMR, UV, IR) ²²³ [α] _D = -3.5° (CHCl ₃) ²²³
sampsone H (221)		<i>Hypericum sampsonii</i> Jinhua, Zhejiang, China ²³³ Chia-Yi, Taiwan ¹⁸⁵ (NMR, UV, IR) ²³³ [α] _D = +5.15° (CHCl ₃) ²³³
sampsone I (222)		<i>Hypericum sampsonii</i> (Jinhua, Zhejiang, China) ^{32,234} (NMR, UV, IR) ²³⁴ [α] _D = +16.88° (CHCl ₃) ²³⁴
sampsone J (223)		<i>Garcinia multiflora</i> (Mudan, Pingtung, Taiwan) ⁶⁹ <i>Hypericum sampsonii</i> (Jinhua, Zhejiang, China) ^{32,234} (NMR, UV, IR) ²³⁴ [α] _D = +1.48° (CHCl ₃) ²³⁴
sampsone K (224)		<i>Hypericum sampsonii</i> Jinhua, Zhejiang, China ³² Yunnan, China ²³² (NMR, UV, IR) ^{32,232} [α] _D = -5.60° (CHCl ₃) ³²
sampsone L (225)		<i>Hypericum sampsonii</i> Hunan, China ³⁷ Jinhua, Zhejiang, China ³² (NMR, UV, IR) ³² [α] _D = +55.00° (CHCl ₃) ³²

sampsone M (226)		<i>Hypericum sampsonii</i> (Jinhua, Zhejiang, China) ³² (NMR, UV, IR) ³² $[\alpha]_D = +54.77^\circ$ (CHCl ₃) ³²
sampsone N (227)		<i>Hypericum sampsonii</i> (Hunan, China) ³⁷ (NMR, UV, IR) ³⁷ $[\alpha]_D = +22.0^\circ$ (CHCl ₃) ³⁷
sampsone O (228)		<i>Hypericum sampsonii</i> (Hunan, China) ³⁷ (NMR, UV, IR) ³⁷ $[\alpha]_D = +87.9^\circ$ (CHCl ₃) ³⁷
sampsone P (229)		<i>Hypericum sampsonii</i> (Hunan, China) ³⁷ (NMR, UV, IR) ³⁷ $[\alpha]_D = +18.6^\circ$ (CHCl ₃) ³⁷
sampsone Q (230)		<i>Hypericum sampsonii</i> (Hunan, China) ³⁷ (NMR, UV, IR) ³⁷ $[\alpha]_D = -9.65^\circ$ (CHCl ₃) ³⁷ crystal structure ³⁷
no name sampsone R (231)		<i>Clusia obdeltifolia</i> (Chapada Diamantina, Brazil) ²¹⁶ <i>Hypericum sampsonii</i> (Hunan, China) ³⁷ (NMR, IR) ²¹⁶ $[\alpha]_D = +10.8^\circ$ (CHCl ₃) ²¹⁶

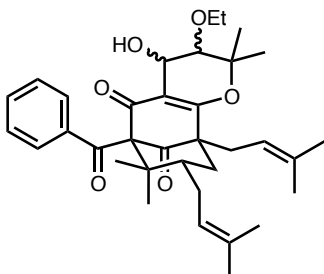
**scrobiculatone A
(232)**



Clusia scrobiculata (Campinas, São Paulo, Brazil)²⁴
propolis (Andes Trujillo, Venezuela)²³⁵
brown propolis (throughout Cuba)²¹²

(¹H NMR, UV, IR)²⁴ [α]_D = +44.7° (CHCl₃)²⁴

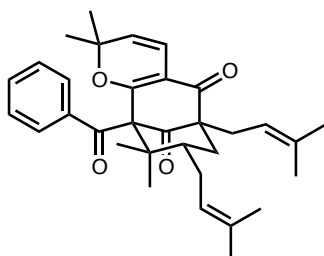
**18-ethyloxy-17-
hydroxy-17,18-
dihydro-
scrobiculatone A
(233)**



propolis (Andes Trujillo, Venezuela)²³⁵

(NMR, UV)²³⁵

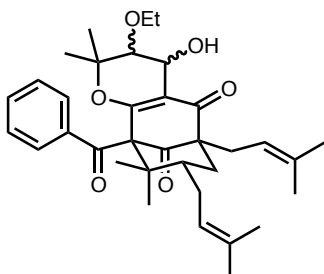
**scrobiculatone B
(234)**



Clusia scrobiculata (Campinas, São Paulo, Brazil)²⁴
propolis (Andes Trujillo, Venezuela)²³⁵
brown propolis (throughout Cuba)²¹²

(¹H NMR, UV, IR)²⁴ [α]_D = +44.7° (CHCl₃)²⁴

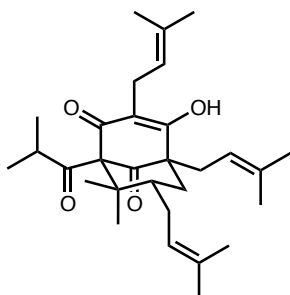
**18-ethyloxy-17-
hydroxy-17,18-
dihydro-
scrobiculatone B
(235)**



Propolis
Manaus, Brazil²⁰
Andes Trujillo, Venezuela²³⁵

(NMR, UV)²³⁵

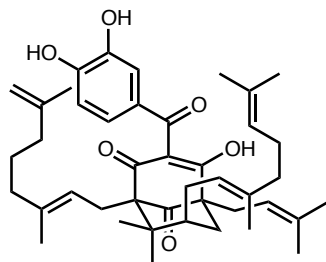
**secohyperforin
(236)**



Hypericum perforatum (Yerevan, Armenia)¹⁶⁰

NMR¹⁶⁰

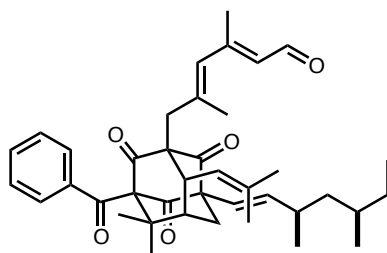
**semsinone A
(237)**



Garcinia semseii (Morogoro, Tanzania)^{109,236}

(NMR, UV, IR)²³⁶ $[\alpha]_D = +52^\circ$ (CHCl₃)²³⁶

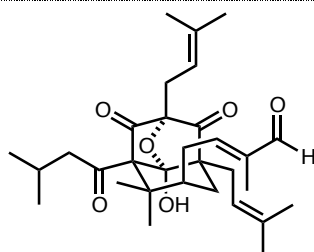
**sinaicinone
(238)**



Hypericum sinaicum (Sinai peninsula, Egypt)²³⁷

(NMR, UV, IR)²³⁷ $[\alpha]_D = +37.5^\circ$ (CH₂Cl₂)²³⁷
absolute configuration²³⁷

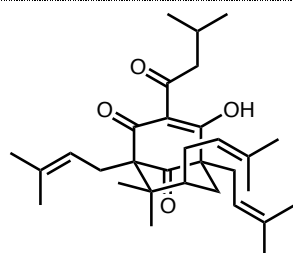
**spiranthenone A
(239)**



Spiranthera odoratissima (Rutaceae; Brasilia, Brazil)²³⁸

(NMR, IR)²³⁸ $[\alpha]_D = +11^\circ$ (CHCl₃)²³⁸

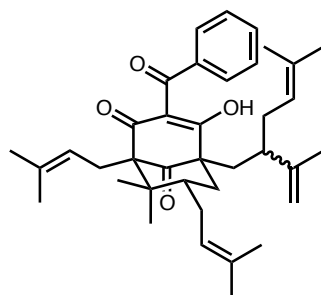
**spiranthenone B
(240)**



Spiranthera odoratissima (Rutaceae; Brasilia, Brazil)²³⁸

(NMR, IR)²³⁸ $[\alpha]_D = +13^\circ$ (CHCl₃)²³⁸

**spiritone
(241)**



Clusia burchellii (Campinas, São Paulo, Brazil)²⁴

C. fluminensis (Campinas, São Paulo, Brazil)²⁴

C. pana-panari (Campinas, São Paulo, Brazil)²⁴

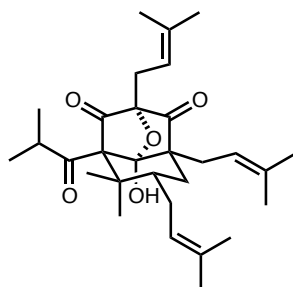
C. pernambucensis (Campinas, São Paulo, Brazil)²⁴

C. spiritu-santensis (Campinas, São Paulo, Brazil)²⁴

C. weddelliana (Campinas, São Paulo, Brazil)²⁴

O-Me ether (¹H NMR, UV, IR)²⁴

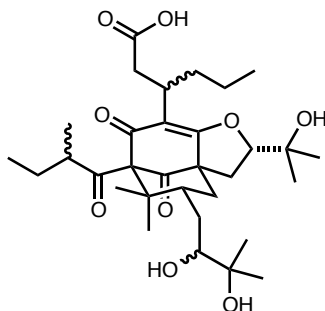
**subellinone
(242)**



Garcinia subelliptica (Ishigaki Island, Japan)²³⁹

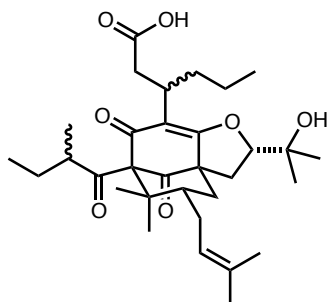
(NMR, IR)²³⁹ $[\alpha]_D = -2.8^\circ$ (EtOH)²³⁹

**sundaicumone A
(243)**



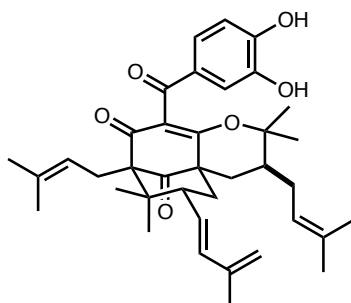
Calophyllum sundaicum (Singapore)²⁴⁰
(NMR, UV, IR)²⁴⁰ $[\alpha]_D = +52^\circ$ (EtOH)²⁴⁰

**sundaicumone B
(244)**



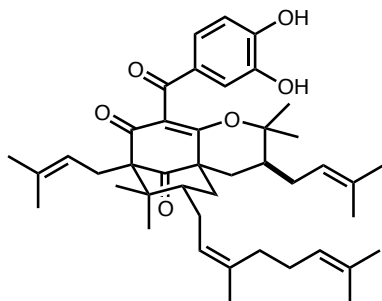
Calophyllum sundaicum (Singapore)²⁴⁰
(NMR, UV, IR)²⁴⁰ $[\alpha]_D = +48^\circ$ (EtOH)²⁴⁰

**symphonone A
(245)**



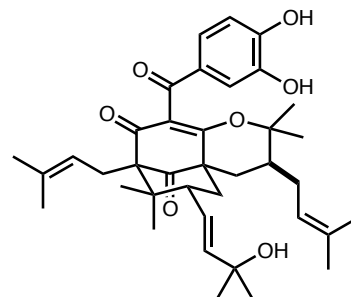
Symphonia globulifera (dense rain forest, French
Guyana)⁴⁷
(NMR, UV, IR)⁴⁷ $[\alpha]_D = -37^\circ$ (CHCl₃)⁴⁷

**symphonone B
(246)**



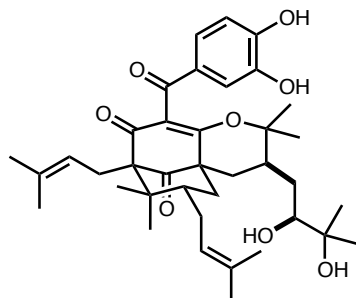
Symphonia globulifera (dense rain forest, French
Guyana)⁴⁷
(NMR, UV, IR)⁴⁷ $[\alpha]_D = -81^\circ$ (CHCl₃)⁴⁷

**symphonone C
(247)**



Symphonia globulifera (dense rain forest, French
Guyana)⁴⁷
(NMR, UV, IR)⁴⁷ $[\alpha]_D = -67^\circ$ (CHCl₃)⁴⁷

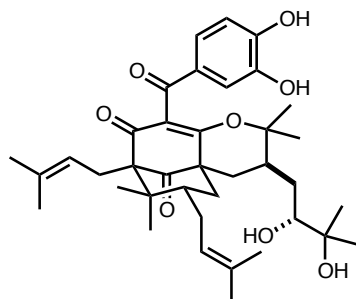
**symphonone D
(248)**



Symphonia globulifera (dense rain forest, French Guyana)⁴⁷

(NMR, UV, IR)⁴⁷ $[\alpha]_D = -41^\circ$ (CHCl₃)⁴⁷

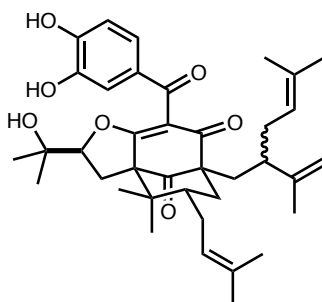
**symphonone E
(249)**



Symphonia globulifera (dense rain forest, French Guyana)⁴⁷

(NMR, UV, IR)⁴⁷ $[\alpha]_D = -50^\circ$ (CHCl₃)⁴⁷

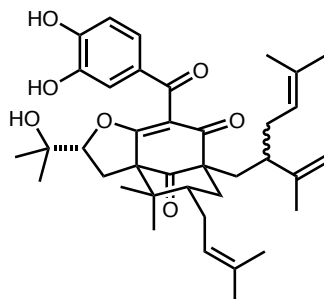
**symphonone F
(250)**



Symphonia globulifera (dense rain forest, French Guyana)⁴⁷

(NMR, UV, IR)⁴⁷ $[\alpha]_D = -9^\circ$ (CHCl₃)⁴⁷

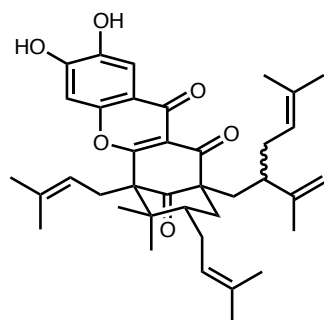
**symphonone G
(251)**



Symphonia globulifera (dense rain forest, French Guyana)⁴⁷

(NMR, UV, IR)⁴⁷ $[\alpha]_D = -4^\circ$ (CHCl₃)⁴⁷

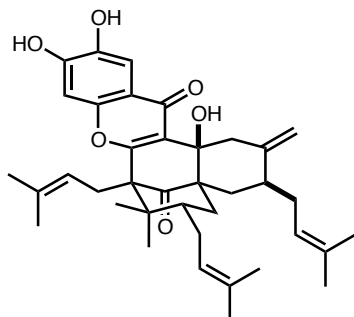
**symphonone H
(252)**



Symphonia globulifera (dense rain forest, French Guyana)⁴⁷

(NMR, UV, IR)⁴⁷ $[\alpha]_D = -37^\circ$ (CHCl₃)⁴⁷

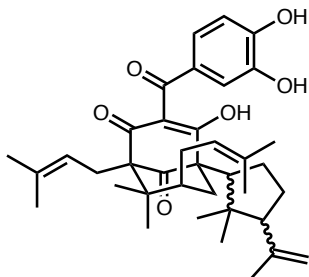
**symphonone I
(253)**



Symphonia globulifera (dense rain forest, French Guyana)⁴⁷

(NMR, UV, IR)⁴⁷ $[\alpha]_D = -22^\circ$ (CHCl₃)⁴⁷

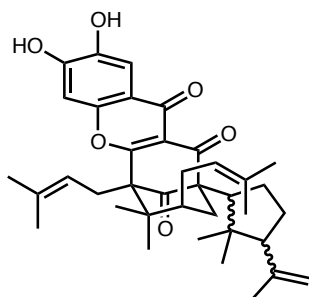
**thorelione A
(254)**



Calophyllum thorelii (central Vietnam)³³

(NMR, UV, IR)³³ $[\alpha]_D = +91.9^\circ$ (MeOH)³³

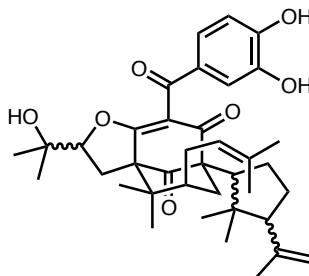
**oxy-thorelione A
(255)**



Calophyllum thorelii (central Vietnam)³³

(NMR, UV, IR)³³ $[\alpha]_D = +323.0^\circ$ (MeOH)³³

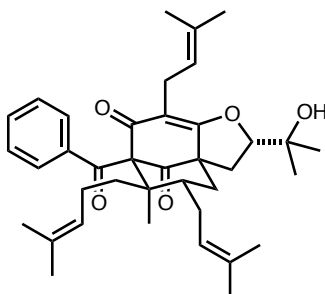
**thorelione B
(256)**



Calophyllum thorelii (central Vietnam)³³

(NMR, UV, IR)³³ $[\alpha]_D = +412.0^\circ$ (MeOH)³³

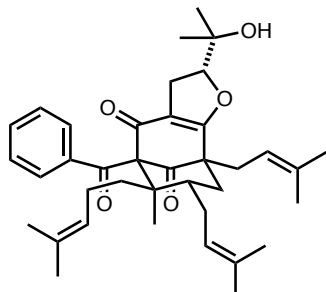
**uralodin A
(257)**



Hypericum henryi
Jinping, Yunnan, China²⁴¹
Lüchun, Yunnan, China⁶⁰

(NMR, UV, IR)²⁴¹ $[\alpha]_D = -55^\circ$ (MeOH)²⁴¹

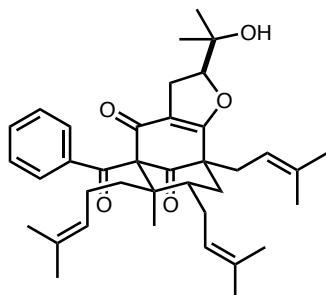
**uralodin B
(258)**



Hypericum henryi (Lünnchun, Yunnan, China)⁶⁰

(NMR, UV, IR)⁶⁰ $[\alpha]_D = -24.6^\circ$ (MeOH)⁶⁰

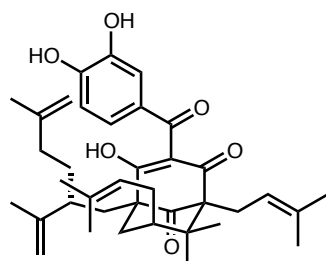
**uralodin C
(259)**



Hypericum henryi (Lünnchun, Yunnan, China)⁶⁰

(NMR, UV, IR)⁶⁰ $[\alpha]_D = -55.0^\circ$ (MeOH)⁶⁰

**xanthochymol
(260)**



Clusia rosea

Dominican Republic¹⁰⁷

Hilo, Hawaii, USA²⁴²

Endodesmia calophylloides (Calophyllaceae; Balmayo, Centre Province, Cameroon)²⁴³

Garcinia densivenia (Douala-Edea Reserve, Cameroon)¹⁹⁸

G. indica (India)¹⁹⁵

G. intermedia (Homestead, Florida, USA)¹⁰⁵

G. livingstonei (Homestead, Florida, USA)⁴⁸

G. mannii (Douala-Edea Reserve, Cameroon)^{198,244}

G. ovalifolia (Douala-Edea Reserve, Cameroon)^{197,198}

G. pyrifera (Sungai Petani, Kedah, Malaysia)⁵⁰

G. spicata (Homestead, Florida, USA)¹⁰⁵

G. staudtii (Douala-Edea Reserve, Cameroon)²⁴⁵

G. subelliptica

northern mountains, Taiwan⁵²

Okinawa, Japan⁵¹

G. xanthochymus

South Canara, ²⁰⁰ **India**^{201,202,246}

Homestead, Florida, USA^{19,105}

G. xipshuangbannaensis (Xishuangbanna, Yunnan, China)^{118,203}

G. virgata (Aoupinié, New Caledonia)¹¹⁹

Rheedia edulis (Broward County, Florida, USA)⁴¹

R. madrunno (Caracas, Venezuela)²⁴⁷

propolis

Manaus, Brazil²⁰

throughout Cuba¹²⁰

red propolis (Maceio City, Alagoas, Brazil)¹²¹

¹H NMR^{20,50,51,201,202,203,242,248} ¹³C NMR^{20,50,51,203,242,248}

UV^{20,41,51,201,202,242} IR^{20,51,201,202,203,242} $[\alpha]_D = +141^\circ$ ⁵⁰

+138⁵¹, +143.5^{202,205} (CHCl₃) +209.9²⁰⁴ (MeOH)²⁰⁴

structural revision,²⁴⁸ crystal structure²⁴⁸

absolute configuration^{205,248}

Appendix A References

- ¹ Almanza, G. R.; Quispe, R.; Mollinedo, P.; Rodrigo, G.; Fukushima, O.; Villagomez, R.; Akesson, B.; Sterner, O. *Nat. Prod. Commun.* **2011**, *6*, 1269-1274.
- ² Alali, F. Q.; Tawaha, K.; Gharaibeh, M. Z. *Naturforsch.* **2009**, *64c*, 476-482.
- ³ Hölscher, D.; Shroff, R.; Knop, K.; Gottschaldt, M.; Crecelius, A.; Schneider, B.; Heckel, D. G.; Schubert, U. S.; Svatoš, A. *Plant J.* **2009**, *60*, 907-918.
- ⁴ Tatsis, E. C.; Boeren, S.; Exarchou, V.; Troganis, A. N.; Vervoot, J.; Gerothanassis, I. P. *Phytochemistry* **2007**, *68*, 383-393.
- ⁵ Orčić, D. Z.; Mimica-Dukić, N. M.; Francisković, M. M.; Petrović, S. S.; Jovin, E. Đ. *Chem. Cent. J.* **2011**, *5*, 34.
- ⁶ Alali, F. Q.; Tawaha, K. *Saudi Pharm. J.* **2009**, *17*, 269-274.
- ⁷ Klingauf, P.; Beuerle, T.; Mellenthin, A.; El-Moghazy, S. A. M.; Boubakir, Z.; Beerhues, L. *Phytochemistry* **2005**, *66*, 139-145.
- ⁸ Piovan, A.; Filippini, R.; Caniato, R.; Borsarini, A.; Maleci, L. B.; Cappelletti, E. M. *Phytochemistry* **2004**, *65*, 411-414.
- ⁹ Mártonfi, P.; Repčák, M.; Mihoková, L. *Folia Geobot. Phytotax.* **1996**, *31*, 245-250.
- ¹⁰ Hosni, K.; Msaâda, K.; Taârit, M. B.; Hammami, M.; Marzouk, B. *Ind. Crop. Prod.* **2010**, *31*, 158-163.
- ¹¹ Lee, J.-y.; Duke, R. K.; Tran, V. H.; Hook, J. M.; Duke, C. C. *Phytochemistry* **2006**, *67*, 2550-2560.
- ¹² Maisenbacher, P.; Kovar, K.-A. *Planta Med.* **1992**, *58*, 291-293.
- ¹³ Bergonzi, M. C.; Bilia, A. R.; Gallori, S.; Guerrini, D.; Vincieri, F. F. *Drug Dev. Ind. Pharm.* **2001**, *27*, 491-497.
- ¹⁴ Repčák, M.; Mártonfi, P. *Biológia* **1997**, *52*, 91-94.
- ¹⁵ Wang, K.; Wang, Y.-Y.; Gao, X.; Chen, X.-Q.; Peng, L.-Y.; Li, Y.; Xu, G.; Zhao, Q.-S. *Chem. Biodivers.* **2012**, *9*, 1213-1220.
- ¹⁶ Piccinelli, A. L.; Cuesta-Rubio, O.; Chica, M. B.; Mahmood, N.; Pagano, B.; Pavone, M.; Barone, V.; Rastrelli, L. *Tetrahedron* **2005**, *61*, 8206-8211.
- ¹⁷ Cuesta-Rubio, O.; Padron, A.; Vastro, H. V.; Pizza, C.; Rastrelli, L. *J. Nat. Prod.* **2001**, *64*, 973-975.
- ¹⁸ Liu, X.; Yu, T.; Gao, X.-M.; Zhou, Y.; Qiao, C.-F.; Peng, Y.; Chen, S.-L.; Luo, K. Q.; Xu, H.-X. *J. Nat. Prod.* **2010**, *73*, 1355-1359.
- ¹⁹ Baggett, S.; Protiva, P.; Mazzola, E. P.; Yang, H.; Ressler, E. T.; Basile, M. J.; Weinstein, I. B.; Kennelly, E. J. *J. Nat. Prod.* **2005**, *68*, 354-360.
- ²⁰ Ishida, V. F. de C.; Negri, G.; Salatino, A.; Bandeira, M. F. C. L. *Food Chem.* **2011**, *125*, 966-972.
- ²¹ Lokvam, J.; Braddock, J. F.; Reichardt, P. B.; Clausen, T. P. *Phytochemistry* **2000**, *55*, 29-34.
- ²² Sakunpak, A.; Panichayupakaranant, P. *Food Chem.* **2012**, *130*, 826-831.

- ²³ Trisuwan, K.; Ritthiwigrom, T. *Arch. Pharm. Res.* **2012**, *35*, 1733-1738.
- ²⁴ Porto, A. L. M.; Machado, S. M. F.; de Oliveira, C. M. A.; Bittrich, V.; Amaral, M. do C. E.; Marsaioli, A. J. *Phytochemistry* **2000**, *55*, 755-768.
- ²⁵ McCandlish, L. E.; Hanson, J. C.; Stout, G. H. *Acta Cryst.* **1976**, *B32*, 1793-1801.
- ²⁶ da Silva, M. C. A.; Heringer, A. P.; Figueiredo, M. R.; de Paiva, S. R. *Liq. Chromatogr. Relat. Technol.* **2012**, *35*, 2313-2321.
- ²⁷ Monache, F. D.; Monache, G. D.; Gacs-Baitz, E. *Phytochemistry* **1991**, *30*, 2003-2005.
- ²⁸ de Oliveira, C. M. A.; Porto, A. M.; Bittrich, V.; Vencato, I.; Marsaioli, A. J. *Tetrahedron Lett.* **1996**, *37*, 6427-6430.
- ²⁹ Ito, C.; Itoigawa, M.; Miyamoto, Y.; Onoda, S.; Rao, K. S.; Mukainaka, T.; Tokuda, H.; Nishino, H.; Furukawa, H. *J. Nat. Prod.* **2003**, *66*, 206-209.
- ³⁰ Biloa Messi, B.; Marti, G.; Ho, R.; Ndjoko Ioset, K.; Meli Lannang, A.; Hostettmann, K.; Wolfender, J.; *Planta Med.* **2010**, *76*, 1334-1334.
- ³¹ Christian, O. E.; McLean, S.; Reynolds, W. F.; Jacobs, H. *Nat. Prod. Commun.* **2008**, *3*, 1781-1786.
- ³² Hu, L.-H.; Sim, K.-Y. *Tetrahedron* **2000**, *56*, 1379-1386.
- ³³ Nguyen, L.-T. T.; Nguyen, H. T.; Barbič, M.; Brunner, G.; Heilmann, J.; Pham, H. D.; Nguyen, D. M.; Nguyen, L.-H. D. *Tetrahedron Lett.* **2012**, *53*, 4487-4493.
- ³⁴ Derogis, P. B. M. C.; Martins, F. T.; de Souza, T. C.; Moreira, M. E. de C.; Filho, J. D. S.; Doriguetto, A. C.; de Souza, K. R. D.; Veloso, M. P.; dos Santos, M. H. *Mag. Reson. Chem.* **2008**, *46*, 278-282.
- ³⁵ Martins, F. T.; Camps, I.; Doriguetto, A. C.; dos Santos, M. H.; Ellena, J.; Barbosa, L. C. A. *Helv. Chim. Acta* **2008**, *91*, 1313-1325.
- ³⁶ Naldoni, F. J.; Claudino, A. L. R.; Cruz, J. W., Jr.; Chavasco, J. K.; Faria e Silva, P. M.; Veloso, M. P.; Dos Santos, M. H. *J. Med. Food* **2009**, *12*, 403-407.
- ³⁷ Xiao, Z. Y.; Mu, Q.; Shiu, W. K. P.; Zeng, Y. H.; Gibbons, S. *J. Nat. Prod.* **2007**, *70*, 1779-1782.
- ³⁸ Tanaka, N.; Takaishi, Y.; Shikishima, Y.; Nakanishi, Y.; Bastow, K.; Lee, K.-H.; Honda, G.; Ito, M.; Takeda, Y.; Kodzhimatov, O. K.; Ashurmetov, O. *J. Nat. Prod.* **2004**, *67*, 1870-1875.
- ³⁹ Nedialkov, P. T.; Zheleva-Dimitrova, D.; Momekov, G.; Karlov, K.; Girreser, U.; Kitanov, G. M. *Nat. Prod. Res.* **2011**, *25*, 1743-1750.
- ⁴⁰ Carvalho-Silva, L. B.; Oliveira, M. de V.; Gontijo, V. S.; Oliveira, W. F.; Derogis, P. B. M. C.; Stringheta, P. C.; Nagem, T. J.; Brigagão, M. R. P. L.; dos Santos, M. H. *Food Res. Int.* **2012**, *48*, 180-186.
- ⁴¹ Acuña, U. M.; Figueroa, M.; Kavalier, A.; Jancovski, N.; Basile, M. J.; Kennelly, E. J. *J. Nat. Prod.* **2010**, *73*, 1775-1779.
- ⁴² Santos, M. H.; Speziali, N. L.; Nagem, T. J.; Oliveira, T. T. *Acta Cryst.* **1998**, *C54*, 1990-1992.
- ⁴³ Alves, T. M. de A.; Alves, R. de O.; Romanha, A. J.; dos Santos, M. H.; Nagem, T. J.; Zani, C. L. *J. Nat. Prod.* **1999**, *62*, 369-371.

-
- ⁴⁴ Derogis, P. B. M. C.; Martins, F. T.; de Souza, T. C.; Moreira, M. E. de C.; Filho, J. D. S.; Doriguetto, A. C.; de Souza, K. R. D.; Veloso, M. P.; Dos Santos, M. H. *Magn. Reson. Chem.* **2008**, *46*, 278-282.
- ⁴⁵ Christian, O. E.; Fronczek, F. R.; Ky, K.; Pradham, S.; Manandhar, A.; Richmond, C. *Acta Cryst.* **2012**, *E68*, o3222-o3223.
- ⁴⁶ Marti, G.; Eparvier, V.; Moretti, C.; Susplugas, S.; Prado, S.; Grellier, P.; Retailleau, P.; Guéritte, F.; Litaudon, M. *Phytochemistry* **2009**, *70*, 75-85.
- ⁴⁷ Marti, G.; Eparvier, V.; Moretti, C.; Prado, S.; Grellier, P.; Hue, N.; Thoison, O.; Delpech, B.; Guéritte, F.; Litaudon, M. *Phytochemistry* **2010**, *71*, 964-974.
- ⁴⁸ Yang, H.; Figueroa, M.; To, S.; Baggett, S.; Jiang, B.; Basile, M. J.; Weinstein, I. B.; Kennelly, E. J. *J. Agric. Food Chem.* **2010**, *58*, 4749-4755.
- ⁴⁹ Xia, Z.-X.; Zhang, D.-D.; Liang, S.; Lao, Y.-Z.; Zhang, H.; Tan, H.-S.; Chen, S.-L.; Wang, X.-H.; Xu, H.-X. *J. Nat. Prod.* **2012**, *75*, 1459-1464.
- ⁵⁰ Roux, D.; Hadi, H. A.; Thoret, S.; Guénard, D.; Thoison, O.; Païs, M.; Sévenet, T. *J. Nat. Prod.* **2000**, *63*, 1070-1076.
- ⁵¹ Iinuma, M.; Tosa, H.; Tanaka, T.; Kanamaru, S.; Asai, F.; Kobayashi, Y.; Miyauchi, K.-i.; Shimano, R. *Biol. Pharm. Bull.* **1996**, *19*, 311-314.
- ⁵² Zhang, L.-J.; Chiou, C.-T.; Cheng, J.-J.; Huang, H.-C.; Kuo, L.-M. Y.; Liao, C.-C.; Bastow, K. F.; Lee, K.-H.; Kuo, Y.-H. *J. Nat. Prod.* **2010**, *73*, 557-562.
- ⁵³ Hussain, H.; Vouffo, B.; Dongo, E.; Riaz, M.; Krohn, K. *J. Asian Nat. Prod. Res.* **2011**, *13*, 547-550.
- ⁵⁴ Taher, M.; Idris, M. S.; Ahmad, F.; Arbain, D. *Phytochemistry* **2005**, *66*, 723-726.
- ⁵⁵ Taher, M.; Idris, M. S.; Ahmad, F.; Arbain, D. *Iran. J. Pharm. Th.* **2007**, *6*, 93-98.
- ⁵⁶ Hartati, S.; Soemiati, A.; Wang, H.-B.; Kardono, L. B. S.; Hanafi, M.; Kosela, S.; Qin, G.-W. *J. Asian Nat. Prod. Res.* **2008**, *10*, 509-513.
- ⁵⁷ Vugdelija, S.; Vajs, V.; Trifunovic, S.; Djokovic, D.; Milosavljevic, S. *Molecules* **2000**, *5*, M158.
- ⁵⁸ Vajs, V.; Vugdelija, S.; Trifunović, S.; Karadžić, I.; Juranić, N.; Macura, S.; Milosavljević, S. *Fitoterapia* **2003**, *74*, 439-444.
- ⁵⁹ Hashida, C.; Tanaka, N.; Kashiwada, Y.; Ogawa, M.; Takaishi, Y. *Chem. Pharm. Bull.* **2008**, *56*, 1164-1167.
- ⁶⁰ Chen, X.-Q.; Li, Y.; Cheng, X.; Wang, K.; He, J.; Pan, Z.-H.; Li, M.-M.; Peng, L.-Y.; Xu, G.; Zhao, Q.-S. *Chem. Biodivers.* **2010**, *7*, 196-204.
- ⁶¹ Verotta, L.; Appendino, G.; Belloro, E.; Jakupovic, J.; Bombardelli, E. *J. Nat. Prod.* **1999**, *62*, 770-772.
- ⁶² Li, Y.; Cao, X. *J. Liq. Chromatogr. Relat. Technol.* **2012**, *35*, 2558-2566.
- ⁶³ Trifunović, S.; Vajs, V.; Macura, S.; Juranić, N.; Djarmati, Z.; Jankov, R.; Milosavljević, S. *Phytochemistry* **1998**, *49*, 1305-1310.
- ⁶⁴ Verotta, L.; Appendino, G.; Jakupovic, J.; Bombardelli, E. *J. Nat. Prod.* **2000**, *63*, 412-415.

-
- ⁶⁵ Xu, G.; Kan, W. L. T.; Zhou, Y.; Song, J.-Z.; Han, Q.-B.; Qiao, C.-F.; Cho, C.-H.; Rudd, J. A.; Lin, G.; Xu, H.-X. *J. Nat. Prod.* **2010**, *73*, 104-108.
- ⁶⁶ Zhou, Y.; Lee, S.; Choi, F. F. K.; Xu, G.; Liu, X.; Song, J.-Z.; Li, S.-L.; Qiao, C.-F.; Xu, H.-X. *Anal. Chim. Acta* **2010**, *678*, 96-107.
- ⁶⁷ Gao, X.-M.; Yu, T.; Lai, F. S. F.; Zhou, Y.; Liu, X.; Qiao, C.-F.; Song, J.-Z.; Chen, S.-L.; Luo, K. Q.; Xu, H.-X.; *Bioorg. Med. Chem.* **2010**, *18*, 4957-4964.
- ⁶⁸ Chen, J.-J.; Ting, C.-W.; Hwang, T.-L.; Chen, I.-C. *J. Nat. Prod.* **2009**, *72*, 253-258.
- ⁶⁹ Ting, C.-W.; Hwang, T.-L.; Chen, I.-S.; Yen, M.-H.; Chen, J.-J. *Chem. Biodivers.* **2012**, *9*, 99-105.
- ⁷⁰ Shan, W.-G.; Lin, T.-S.; Yu, H.-N.; Chen, Y.; Zhan, Z.-J. *Helv. Chim. Acta* **2012**, *95*, 1442-1448.
- ⁷¹ Trinh, B. T. D.; Nguyen, N.-T. T.; Ngo, N. T. N.; Tran, P. T.; Nguyen, L.-T. T.; Nguyen, L.-H. D. *Phytochem. Lett.* **2013**, *6*, 224-227.
- ⁷² Chien, S.-C.; Chyu, C.-F.; Chang, I.-S.; Chiu, H.-L.; Kuo, Y.-H. *Tetrahedron Lett.* **2008**, *49*, 5276-5278.
- ⁷³ Weng, J.-R.; Lin, C.-N.; Tsao, L.-T.; Wang, J.-P. *Chem. Eur. J.* **2003**, *9*, 1958-1963.
- ⁷⁴ Lin, K.-W.; Huang, A.-M.; Yang, S.-C.; Weng, J.-R.; Hour, T.-C.; Pu, Y.-S.; Lin, C.-N. *Food Chem.* **2012**, *135*, 851-859.
- ⁷⁵ Weng, J.-R.; Lin, C.-N.; Tsao, L.-T.; Wang, J.-P. *Chem. Eur. J.* **2003**, *9*, 5520-5527.
- ⁷⁶ Wu, C.-C.; Weng, J.-R.; Won, S.-J.; Lin, C.-N. *J. Nat. Prod.* **2005**, *68*, 1125-1127.
- ⁷⁷ Wu, C.-C.; Lu, Y.-H.; Wei, B.-L.; Yang, S.-C.; Won, S.-J.; Lin, C.-N. *J. Nat. Prod.* **2008**, *71*, 246-250.
- ⁷⁸ Júnior, J. S. C.; Ferraz, A. B. F.; Filho, B. A. B.; Feitosa, C. M.; Citó, A. M. G. L.; Freitas, R. M.; Saffi, J. J. *Med. Plants Res.* **2011**, *5*, 293-299.
- ⁷⁹ Mangas-Marín, R.; Bello-Alarcón, A.; Cuesta-Rubio, O.; Piccinelli, A. L.; Rastrelli, L. *Latin Am. J. Pharm.* **2008**, *27*, 762-765.
- ⁸⁰ Hernández, I. M.; Fernandez, M. C.; Cuesta-Rubio, O.; Piccinelli, A. L.; Rastrelli, L. *J. Nat. Prod.* **2005**, *68*, 931-934.
- ⁸¹ Weng, J.-R.; Tsao, L.-T.; Wang, J.-P.; Wu, R.-R.; Lin, C.-N. *J. Nat. Prod.* **2004**, *67*, 1796-1799.
- ⁸² Lin, K.-W.; Huang, A.-M.; Tu, H.-Y.; Lee, L.-Y.; Wu, C.-C.; Hour, T.-C.; Yang, C.-H.; Pu, Y.-S.; Lin, C.-N. *J. Agric. Food Chem.* **2011**, *59*, 407-414.
- ⁸³ Lenta, B. N.; Vonthron-Sénécheau, C.; Weniger, B.; Devkota, K. P.; Ngoupayo, J.; Kaiser, M.; Naz, Q.; Choudhary, M. I.; Tsamo, E.; Sewald, N. *Molecules* **2007**, *12*, 1548-1557.
- ⁸⁴ Rukachaisirikul, V.; Naklue, W.; Sukpondma, Y.; Phongpaichit, S. *Chem. Pharm. Bull.* **2005**, *53*, 342-343.
- ⁸⁵ Kumar, S.; Sharma, S.; Chattopadhyay, S. K. *Biomed. Chromatogr.* **2009**, *23*, 888-907.
- ⁸⁶ Rao, A. V. R.; Venkatswamy, G.; Pendse, A. D. *Tetrahedron Lett.* **1980**, *21*, 1975-1978.

- ⁸⁷ Iinuma, M.; Ito, T.; Miyake, R.; Tosa, H.; Tanaka, T.; Chelladurai, V. *Phytochemistry* **1998**, *47*, 1169-1170.
- ⁸⁸ Masullo, M.; Bassarello, C.; Suzuki, H.; Pizza, C.; Piacente, S. *J. Agric. Food Chem.* **2008**, *56*, 5205-5210.
- ⁸⁹ Kolodziejczyk, J.; Masullo, M.; Olas, B.; Piacente, S.; Wachowicz, B. *Platelets* **2009**, *20*, 487-492.
- ⁹⁰ Shen, J.; Yang, J.-S. *Acta Chim. Sinica* **2007**, *65*, 1675-1678.
- ⁹¹ Hutadilok-Towatana, N.; Kongkachuay, S.; Mahabusarakam, W. *Nat. Prod. Rep.* **2007**, *21*, 655-662.
- ⁹² Bakana, P.; Claeys, M.; Totté, J.; Pieters, L. A. C.; van Hoof, L.; Tamba-Vemba; van den Berghe, D. A.; Vlietinck, A. J. *J. Ethnopharmacol.* **1987**, *21*, 75-84.
- ⁹³ Krishnamurthy, N.; Lewis, Y. S.; Ravindranath, B. *Tetrahedron Lett.* **1981**, *22*, 793-796.
- ⁹⁴ Kaur, R.; Chattopadhyay, S. K.; Tandon, S.; Sharma, S. *Ind. Crop. Prod.* **2012**, *37*, 420-426.
- ⁹⁵ Hartari, S.; Wang, H.-B.; Kardono, L. B. S.; Kosela, S.; Qin, G.-W. *Chin. J. Nat. Med.* **2007**, *5*, 272-276.
- ⁹⁶ Hamed, W.; Brajeul, S.; Mahuteau-Betzer, F.; Thoison, O.; Mons, S.; Delpech, B.; Hung, N. V.; Sévenet, T.; Marazano, C. *J. Nat. Prod.* **2006**, *69*, 774-777.
- ⁹⁷ Sahu, A.; Das, B.; Chatterjee, A. *Phytochemistry* **1989**, *28*, 1233-1235.
- ⁹⁸ Hartati, S.; Kadono, L. B. S.; Kosela, S.; Harrison, L. J. *J. Biol. Sci.* **2008**, *8*, 137-142.
- ⁹⁹ Negi, P. S.; Jayaprakasha, G. K. *J. Food Sci.* **2004**, *69*, FMS61-FMS65.
- ¹⁰⁰ Xu, G.; Feng, C.; Zhou, Y.; Han, Q.-B.; Qiao, C.-F.; Huang, S.-X.; Chang, D. C.; Zhao, Q.-S.; Luo, K. Q.; Xu, H.-X. *J. Agric. Food Chem.* **2008**, *56*, 11144-11150.
- ¹⁰¹ Fukuyama, Y.; Kuwayama, A.; Minami, H. *Chem. Pharm. Bull.* **1997**, *45*, 947-949.
- ¹⁰² Fukuyama, Y.; Minami, H.; Kuwayama, A. *Phytochemistry* **1998**, *49*, 853-857.
- ¹⁰³ Monzote, L.; Cuesta-Rubio, O.; Matheeußen, A.; Van Assche, T.; Maes, L.; Cos, P. *Phytother. Res.* **2011**, *25*, 458-462.
- ¹⁰⁴ Dal Molin, M. M.; Silva, S.; Alves, D. R.; Quintão, N. L. M.; Delle Monache, F.; Filho, V. C.; Niero, R. *Arch. Pharm. Res.* **2012**, *35*, 623-631.
- ¹⁰⁵ Acuña, U. M.; Dastmalchi, K.; Basile, M. J.; Kennelly, E. J. *J. Food Compos. Anal.* **2012**, *25*, 215-220.
- ¹⁰⁶ Abe, F.; Nagafuji, S.; Okabe, H.; Akahane, H.; Estrada-Muñiz, E.; Huerta-Reyes, M.; Reyes-Chilpa, R. *Biol. Pharm. Bull.* **2004**, *27*, 141-143.
- ¹⁰⁷ Gustafson, K. R.; Blunt, J. W.; Munro, M. H. G.; Fuller, R. W.; McKee, T. C.; Cardellina, J. H., II; McMahon, J. B.; Cragg, G. M.; Boyd, M. R. *Tetrahedron* **1992**, *48*, 10093-10102.
- ¹⁰⁸ Williams, R. B.; Hoch, J.; Glass, T. E.; Evans, R.; Miller, J. S.; Wisse, J. H.; Kingston, D. G. I. *Planta Med.* **2003**, *69*, 864-866.
- ¹⁰⁹ Magadula, J. J. *Int. J. Res. Phytochem. Pharmacol.* **2012**, *2*, 16-20.
- ¹¹⁰ Lenta, B. N.; Ngouela, S.; Nounou, D. T.; Tsamo, E.; Connolly, J. D. *Bull. Chem. Soc. Ethiop.* **2004**, *18*, 175-180.

-
- ¹¹¹ Ngouela, S.; Lenta, B. N.; Nougoué, D. T.; Ngoupayo, J.; Boyom, F. F.; Tsamo, E.; Gut, J.; Rosenthal, P. J.; Connolly, J. D. *Phytochemistry* **2006**, *67*, 302-306.
- ¹¹² Pan, E.; Cao, S.; Brodie, P. J.; Miller, J. S.; Rakotodrajaona, R.; Ratovoson, F.; Birkinshaw, C.; Andriantsiferana, R.; Rasamison, V. E.; Kingston, D. G. I. *Nat. Prod. Commun.* **2010**, *5*, 751-754.
- ¹¹³ Martins, F. T.; Cruz, J. W., Jr.; Derogis, P. B. M. C.; dos Santos, M. H.; Veloso, M. P.; Ellena, J.; Doriguetto, A. C. *J. Braz. Chem. Soc.* **2007**, *18*, 1515-1523.
- ¹¹⁴ Dias, K. S. T.; Januário, J. P.; D' Deogo, J. L.; Dias, A. L. T.; dos Santos, M. H.; Camps, I.; Coelho, L. F. L.; Viegas, C., Jr. *Bioorg. Med. Chem.* **2010**, *18*, 4957-4964.
- ¹¹⁵ Lenta, B. N.; Nougoué, D. T.; Devkota, K. P.; Fokou, P. A.; Ngouela, S.; Tsamo, E.; Sewland, N. *Acta Cryst.* **2007**, *E63*, o1282-o1284.
- ¹¹⁶ Huang, S.-X.; Feng, C.; Zhou, Y.; Xu, G.; Han, Q.-B.; Qiao, C.-F.; Chang, D. C.; Luo, K. Q.; Xu, H.-X. *J. Nat. Prod.* **2009**, *72*, 130-135.
- ¹¹⁷ Lannang, A. M.; Louh, G. N.; Biloa, B. M.; Komguem, J.; Mbazoa, C. D.; Sondengam, B. L.; Naesens, L.; Pannecouque, C.; De Clercq, E.; El Ashry, E. S. H. *Planta Med.* **2010**, *76*, 708-712.
- ¹¹⁸ Han, Q.-B.; Yang, N.-Y.; Tian, H.-L.; Qiao, C.-F.; Song, J.-Z.; Chang, D. C.; Chen, S.-L.; Luo, K. Q.; Xu, H.-X. *Phytochemistry* **2008**, *69*, 2187-2192.
- ¹¹⁹ Merza, J.; Mallet, S.; Litaudon, M.; Dumontet, V.; Séraphin, D.; Richomme, P. *Planta Med.* **2006**, *72*, 87-89.
- ¹²⁰ Cuesta-Rubio, O.; Frontana-Urbe, B. A.; Ramírez-Apan, T.; Cárdenas, J. *Z. Naturforsch.* **2002**, *57c*, 372-378.
- ¹²¹ Trusheva, B.; Popova, M.; Bankova, V.; Simova, S.; Marcucci, M. C.; Miorin, P. L.; Pasin, F. d. R.; Tsvetkova, I. *Evid. Based Complement. Alternat. Med.* **2006**, *3*, 249-254.
- ¹²² Azebaze, A. G. B.; Ouahouo, B. M. W.; Vardamides, J. C.; Valentin, A.; Kuete, V.; Acebey, L.; Beng, V. P.; Nkengfack, A. E.; Meyer, M. *Chem. Nat. Compd.* **2008**, *44*, 582-587.
- ¹²³ Fuller, R. W.; Blunt, J. W.; Boswell, J. L.; Cardellina, J. H., II; Boyd, M. R. *J. Nat. Prod.* **1999**, *62*, 130-132.
- ¹²⁴ Magadula, J. J. *J. Pharm. Sci. Innovat.* **2012**, *1*, 31-33.
- ¹²⁵ Hartati, S.; Triyem; Cahyana, H. *Indo. J. Cancer Chemoprev.* **2010**, *1*, 85-91.
- ¹²⁶ Doan, T. N.; Kim, E. K.; Qui, H. J.; Son, E. M.; Lee, J. E.; Galaaraidii, O.; Lee, B. J.; Youn, H. J.; Koo, K. A. *Planta Med.* **2008**, *74*, 1034.
- ¹²⁷ Gey, C.; Kyrylenko, S.; Hennig, L.; Nguyen, L.-H. D.; Büttner, A.; Pham, H. D.; Giannis, A. *Angew. Chem. Int. Ed.* **2007**, *46*, 5219-5222.
- ¹²⁸ Elfita; Supriyatna; Bahti, H. H.; Dachriyanus *Indo. J. Chem.* **2008**, *8*, 97-100.
- ¹²⁹ Herath, K.; Jayasuriya, H.; Ondeyka, J. G.; Guan, Z.; Borris, R. P.; Stijfhoorn, E.; Stevenson, D.; Wang, J.; Sharma, N.; MacNaul, K.; Menke, J. G.; Ali, A.; Schulman, M. J.; Singh, S. B. *J. Nat. Prod.* **2005**, *68*, 617-619.
- ¹³⁰ Lannang, A. M.; Komguem, J.; Ngninzeko, F. N.; Tangmouo, J. G.; Lontsi, D.; Ajaz, A.; Choudhary, M. I.; Sondengam, B. L.; Atta-ur-Rahman *Bull. Chem. Soc. Ethiop.* **2006**, *20*, 247-252.

-
- ¹³¹ Kuete, V.; Komgwen, J.; Beng, V. P.; Tangmouo, J. G.; Etoa, F.-X.; Lontsi, D. *S. Afr. J. Bot.* **2007**, *73*, 347-354.
- ¹³² Ciochina, R.; Grossman, R. B. *Chem. Rev.* **2006**, *106*, 3963-3986.
- ¹³³ Nguyen, H. D.; Trinh, B. T. D.; Nguyen, L.-H. D. *Phytochem. Lett.* **2011**, *4*, 129-133.
- ¹³⁴ Nilar; Nguyen, L.-H. D.; Venkatraman, G.; Sim, K.-Y.; Harrison, L.-J. *Phytochemistry* **2005**, *66*, 1718-1723.
- ¹³⁵ Masullo, M.; Bassarello, C.; Bifulco, G.; Piacente, S. *Tetrahedron* **2010**, *66*, 139-145.
- ¹³⁶ Cao, S.; Brodie, P. J.; Miller, J. S.; Ratovoson, F.; Birkinshaw, C.; Randrianasolo, S.; Rakotobe, E.; Rasamison, V. E.; Kingston, D. G. I. *J. Nat. Prod.* **2007**, *70*, 686-688.
- ¹³⁷ Carroll, A. R.; Suraweera, L.; King, G.; Rali, T.; Quinn, R. J. *J. Nat. Prod.* **2009**, *72*, 1699-1701.
- ¹³⁸ Rücker, G.; Manns, D.; Hartmann, R.; Bonsels, U. *Arch. Pharm.* **1995**, *328*, 725-730.
- ¹³⁹ Momekov, G.; Ferdinandov, D.; Zheleva-Dimitrova, D.; Nedialkov, P.; Girreser, U.; Kitanov, G. *Phytomedicine* **2008**, *15*, 1010-1015.
- ¹⁴⁰ Biljali, S.; Momekov, G.; Nedialkov, P.; Zheleva-Dimitrova, D.; Kitanov, G.; Momekova, D.; Stoyanov, N.; Guenova, M.; Michova, A.; Karaivanova, M. *J. Pharm. Technol. Drug Res.* **2012**, *1*, 6.
- ¹⁴¹ Šavikin-Fodulović, K.; Aljančić, I.; Vajs, V.; Menković, N.; Macura, S.; Gojčić, G.; Milosavljević, S. *J. Nat. Prod.* **2003**, *66*, 1236-1238.
- ¹⁴² Decosterd, L. A.; Stoeckli-Evans, H.; Chapuis, J.-C.; Msonthi, J. D.; Sordat, B.; Hostettmann, K. *Helv. Chim. Acta* **1989**, *72*, 464-471.
- ¹⁴³ Benkiki, N.; Kabouche, Z.; Tillequin, F.; Vérité, P.; Chosson, E.; Seguin, E. *Z. Naturforsch.* **2003**, *58c*, 655-658.
- ¹⁴⁴ Touafek, O.; Kabouche, Z.; Boustie, J.; Bruneau, C. *Nat. Prod. Commun.* **2012**, *7*, 63-64.
- ¹⁴⁵ Smelcerovic, A.; Zuehlke, S.; Spiteller, M.; Raabe, N.; Özen, T. *Biochem. Syst. Ecol.* **2008**, *36*, 316-319.
- ¹⁴⁶ Smelcerovic, A.; Spiteller, M. *Pharmazie* **2006**, *61*, 251-252.
- ¹⁴⁷ Smelcerovic, A.; Verma, V.; Spiteller, M.; Ahmad, S. M.; Puri, S. C.; Qazi, G. N. *Phytochemistry* **2006**, *67*, 171-177.
- ¹⁴⁸ Ayan, A. K.; Radušienė, J.; Çirak, C.; Ivanauskas, L.; Janulis, V. *Pharm. Biol.* **2008**, *47*, 847-853.
- ¹⁴⁹ Statti, G. A.; Conforti, F.; Menichini, F.; Marrelli, M.; Carmen, G.; Tundis, R.; Loizzo, M. R.; Bonesi, M.; Menichini, F. *Biol. Res.* **2011**, *44*, 213-218.
- ¹⁵⁰ Çirak, C.; Radušienė, J.; Janulis, V.; Ivanauskas, L. *Nat. Prod. Commun.* **2010**, *5*, 897-898.
- ¹⁵¹ Maggi, F.; Ferretti, G.; Pocceschi, N.; Menghini, L.; Ricciutelli, M. *Fitoterapia* **2004**, *75*, 702-711.
- ¹⁵² Tawaha, K.; Gharaibeh, M.; El-Elmat, T.; Alali, F. Q. *Ind. Crop. Prod.* **2010**, *32*, 241-245.
- ¹⁵³ Bonkanka, C. X.; Smelcerovic, A.; Zuehlke, S.; Rabanal, R. M.; Spiteller, M.; Sánchez-Mateo, C. del C. *Planta Med.* **2008**, *74*, 719-725.
- ¹⁵⁴ Sagratini, G.; Ricciutelli, M.; Vittori, S.; Öztürk, N.; Örtürk, Y.; Maggi, F. *Fitoterapia* **2008**, *79*, 210-213.

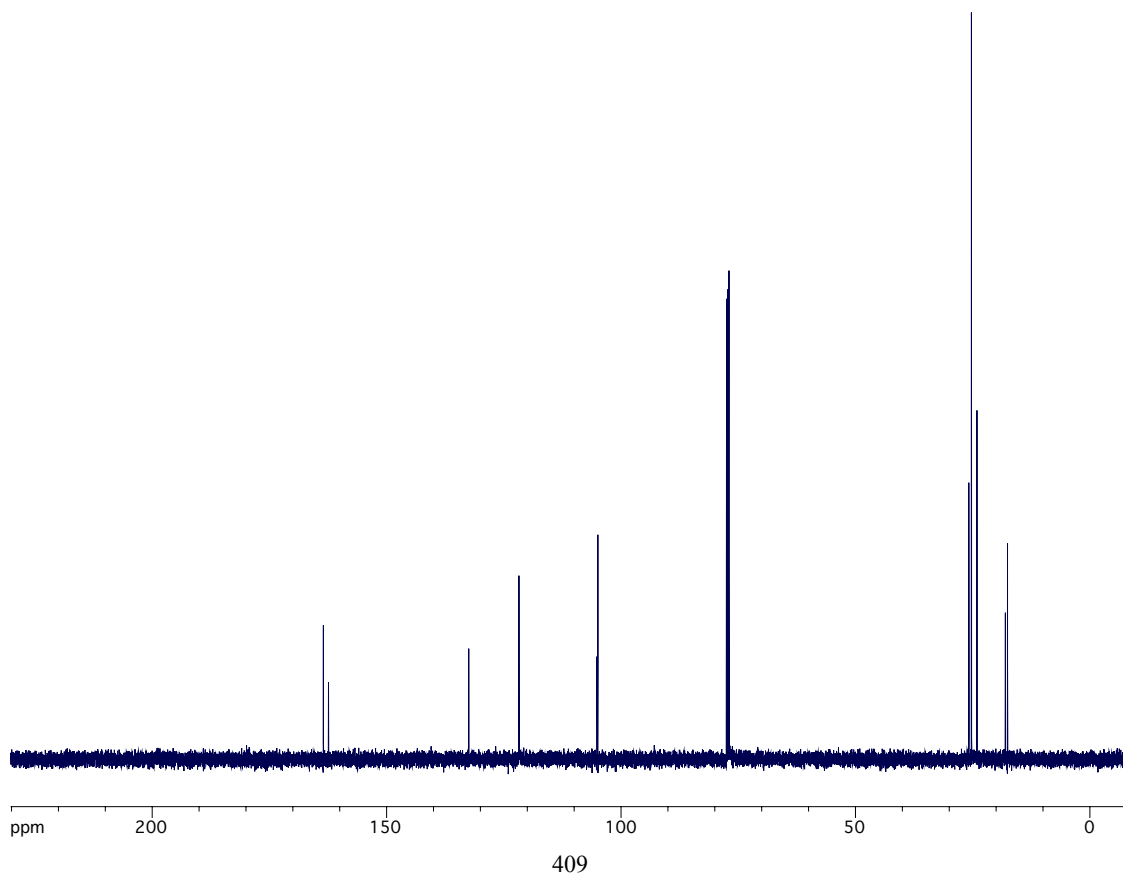
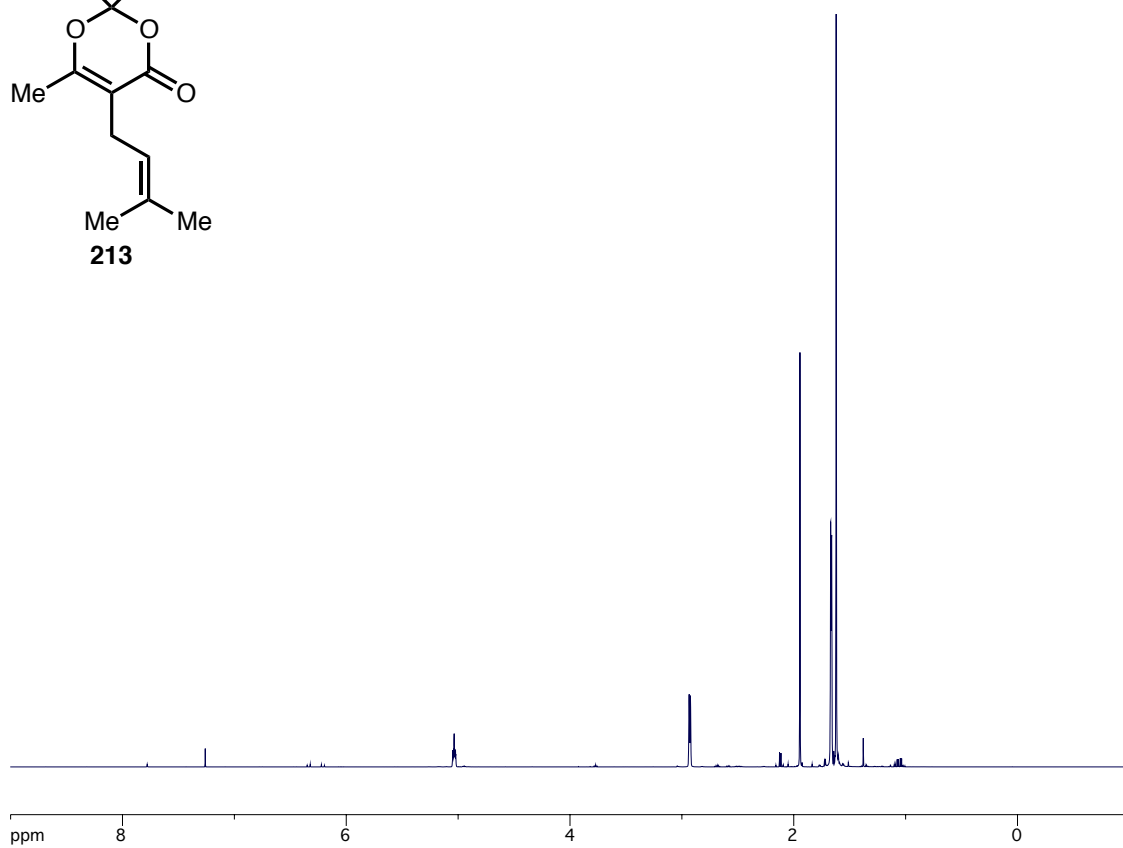
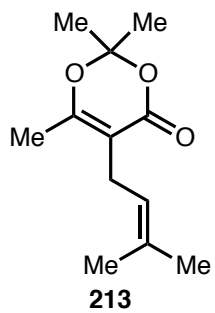
-
- ¹⁵⁵ Kusari, S.; Zühlke, S.; Borsch, T.; Spiteller, M. *Phytochemistry* **2009**, *70*, 1222-1232.
- ¹⁵⁶ Crockett, S. L.; Schaneberg, B.; Khan, I. A. *Phytochem. Anal.* **2005**, *16*, 479-485.
- ¹⁵⁷ Camas, N.; Radusiene, J.; Stanius, Z.; Caliskan, O.; Cirak, C. *Sci. World J.* **2012**, 501027.
- ¹⁵⁸ Çirak, C.; Radušienė, J. *Nat. Prod. Res.* **2007**, *21*, 1151-1156.
- ¹⁵⁹ Cirak, C.; Radusiene, J.; Stanius, Z.; Camas, N.; Caliskan, O.; Odabas, M. S. *Acta Physiol. Plant.* **2012**, *34*, 1313-1320.
- ¹⁶⁰ Charchoglyan, A.; Abrahamyan, A.; Fujii, I.; Boubakir, Z.; Gulder, T. A. M.; Kutchan, T. M.; Vardapetyan, H.; Bringmann, G.; Ebizuka, Y.; Beerhues, L. *Phytochemistry* **2007**, *68*, 2670-2677.
- ¹⁶¹ Kirakosyan, A.; Gibson, D. M.; Sirvent, T. *J. Herbs Spices Med. Plants* **2003**, *10*, 73-88.
- ¹⁶² Shan, M. D.; Hu, L. H.; Chen, Z. L. *J. Nat. Prod.* **2001**, *64*, 127-130.
- ¹⁶³ Helmja, K.; Vaher, M.; Püssa, T.; Orav, A.; Viitak, A.; Levandi, T.; Kaljurand, M. *Nat. Prod. Res.* **2011**, *25*, 496-510.
- ¹⁶⁴ Verma, V.; Smelcerovic, A.; Zuehlke, S.; Hussain, M. A.; Ahmad, S. M.; Ziebach, T.; Qazi, G. N.; Spiteller, M. *Biochem. Syst. Ecol.* **2008**, *36*, 201-206.
- ¹⁶⁵ Pietta, P.; Gardana, C.; Pietta, A. *Il Farmaco* **2001**, *56*, 491-496.
- ¹⁶⁶ Filippini, R.; Piovan, A.; Borsarini, A.; Caniato, R. *Fitoterapia* **2010**, *81*, 115-119.
- ¹⁶⁷ Gurevich, A. I.; Dobrynin, V. N.; Kolosov, M. N.; Popravko, S. A.; Ryabova, I. D.; Chernov, B. K.; Derbentseva, N. A.; Aizenman, B. E.; Garagulya, A. D. *Antibiotiki* **1971**, *16*, 510-513.
- ¹⁶⁸ Umek, A.; Kreft, S.; Kartnig, T.; Heydel, B. *Planta Med.* **1999**, *65*, 388-390.
- ¹⁶⁹ Büter, B.; Orlacchio, C.; Soldati, A.; Berger, K. *Planta Med.* **1998**, *64*, 431-437.
- ¹⁷⁰ Çirak, C.; Radusiene, J.; Janulis, V.; Ivanauskas, L. *J. Integr. Plant Biol.* **2008**, *50*, 575-580.
- ¹⁷¹ Spiteller, M.; Özen, T.; Smelcerovic, A.; Zuehlke, S.; Mimica-Dukić, N. *Fitoterapia* **2008**, *79*, 191-193.
- ¹⁷² Zheng, M.; Fan, Y.; Shi, D.; Liu, C. *J. Ethnopharmacol.* **2013**, *147*, 108-113.
- ¹⁷³ Murch, S. J.; Rupasingh, H. P. V.; Goodenowe, D.; Saxena, P. K. *Plant Cell Rep.* **2004**, *23*, 419-425.
- ¹⁷⁴ Erdelmeier, C. A. J. *Pharmacopsychiatry* **1998**, *31* (Supplement 1), 2-6.
- ¹⁷⁵ Adam, P. A.; Arigoni, D.; Bacher, A.; Eisenreich, W. *J. Med. Chem.* **2002**, *45*, 4786-4793.
- ¹⁷⁶ Cui, Y.; Ang, C. Y. W.; Beger, R. D.; Heinze, T. M.; Hu, L.; Leakey, J. *Drug Metab. Dispos.* **2004**, *32*, 28-34.
- ¹⁷⁷ Cao, X.; Wang, Q.; Li, Y.; Bai, G.; Ren, H.; Xu, C.; Ito, Y. *J. Chromatogr. B* **2011**, *879*, 480-488.
- ¹⁷⁸ Bystrov, N. S.; Chernov, B. K.; Dobrynin, V. N.; Kolosov, M. N. *Tetrahedron Lett.* **1975**, *16*, 2791-2794.

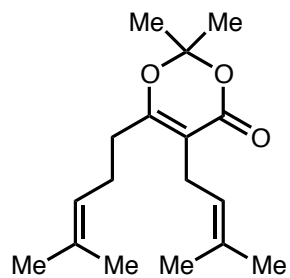
- ¹⁷⁹ Brondz, I.; Greibokk, T.; Groth, P. A.; Aasen, A. J. *Tetrahedron Lett.* **1982**, *23*, 1299-1300.
- ¹⁸⁰ Brondz, I.; Greibokk, T.; Groth, P.; Aasen, A. J. *Acta Chem. Scand. A* **1983**, *37*, 263-265.
- ¹⁸¹ Matsuhisa, M.; Shikishima, Y.; Takaishi, Y.; Honda, G.; Ito, M.; Takeda, Y.; Shibata, H.; Higuti, T.; Kozhimatov, O. K.; Ashurmetov, O. *J. Nat. Prod.* **2002**, *65*, 290-294.
- ¹⁸² Castro, M. L.; do Nascimento, A. M.; Ikegaki, M.; Costa-Neto, C. M.; Alencar, S. M.; Rosalen, P. L. *Bioorg. Med. Chem.* **2009**, *17*, 5332-5335.
- ¹⁸³ Qi, J.; Beeler, A. B.; Zhang, Q.; Porco, J. A., Jr. *J. Am. Chem. Soc.* **2010**, *132*, 13642-13644.
- ¹⁸⁴ Winkelmann, K.; Heilmann, J.; Zerbe, O.; Rali, T.; Sticher, O. *J. Nat. Prod.* **2001**, *64*, 701-706.
- ¹⁸⁵ Lin, Y.-L.; Wu, Y.-S. *Helv. Chim. Acta* **2003**, *86*, 2156-2163.
- ¹⁸⁶ Zheng, Y. H.; Mu, Q.; Xiao, Z. Y.; Xu, Y.; Rahman, M. M.; Gibbons, S. *Chem. Lett.* **2009**, *38*, 440-441.
- ¹⁸⁷ Zeng, Y.-H.; Osman, K.; Xiao, Z.-Y.; Gibbons, S.; Mu, Q. *Phytochem. Lett.* **2012**, *5*, 200-205.
- ¹⁸⁸ Wabo, H. K.; Kowa, T. K.; Lonfouo, A. H. N.; Tchinda, A. T.; Tane, P.; Kikuchi, H.; Frédérick, M.; Oshima, Y. *Rec. Nat. Prod.* **2012**, *6*, 94-100.
- ¹⁸⁹ Tchakam, P. D.; Lunga, P. K.; Kowa, T. K.; Lonfuou, A. H. N.; Wabo, H. K.; Tapondjou, L. A.; Tane, P.; Kuate, J.-R. *BMC Complem. Altern. Med.* **2012**, *12*, 136.
- ¹⁹⁰ Ito, C.; Miyamoto, Y.; Nakayama, M.; Kawai, Y.; Rao, K. S.; Furukawa, H. *Chem. Pharm. Bull.* **1997**, *45*, 1403-1413.
- ¹⁹¹ Marti, G.; Eparvier, V.; Litaudon, M.; Grellier, P.; Guéritte, F. *Molecules* **2010**, *15*, 7106-7114.
- ¹⁹² Krishnamurthy, N.; Ravindranath, B.; Guru Row, T. N.; Venkatesan, K. *Tetrahedron Lett.* **1982**, *23*, 2233-2236.
- ¹⁹³ Kaur, R.; Vasudev, P. G.; Chattopadhyay, S. K. *Acta Cryst.* **2012**, *E68*, o1861-o1862.
- ¹⁹⁴ Elfita, E.; Muharni, M.; Latief, M.; Darwati, D.; Widiyantoro, A.; Supriyatna, S.; Bahti, H. H.; Dachriyanus, D.; Cos, P.; Maes, L.; Foubert, K.; Apers, S.; Pieters, L. *Phytochemistry* **2009**, *70*, 907-912.
- ¹⁹⁵ Kumar, S.; Chattopadhyay, S. K. *Biomed. Chromatogr.* **2007**, *21*, 139-163.
- ¹⁹⁶ Ee, G. C. L.; Cheow, Y. L. *Asian J. Chem.* **2008**, *20*, 343-351.
- ¹⁹⁷ Waterman, P. G.; Crichton, E. G. *Planta Med.* **1980**, *40*, 351-355.
- ¹⁹⁸ Waterman, P. G.; Hussain, R. A. *Biochem. Syst. Ecol.* **1983**, *11*, 21-28.
- ¹⁹⁹ Lannang, A. M.; Louh, G. N.; Lontsi, D.; Specht, S.; Sarite, S. R.; Flörke, U.; Hussain, H.; Hoerauf, A.; Krohn, K. *J. Antibiot.* **2008**, *61*, 518-523.
- ²⁰⁰ Lakshmi, C.; Kumar, K. A.; Dennis, T. J. *J. Indian Chem. Soc.* **2002**, *79*, 968-969.
- ²⁰¹ Karajgoaker, C. G.; Rama Rao, A. V.; Venkataraman, K.; Yemul, S. S.; Palmer, K. J. *Tetrahedron Lett.* **1973**, *14*, 4977.
- ²⁰² Rama Rao, A. V.; Venkatswamy, G.; Yemul, S. S. *Indian J. Chem.* **1980**, *19B*, 627-633.

-
- ²⁰³ Zhong, J.-Y.; Wang, W.-D.; Tao, G.-D.; Li, K.-L. *Acta Bot. Sin.* **1986**, *28*, 533-537.
- ²⁰⁴ Rama Rao, A. V.; Venkatswamy, G.; Yemul, S. S. *Chem. Indust.* **1979**, 92-92.
- ²⁰⁵ Venkatswamy, G.; Yemul, S. S.; Rama Rao, A. V.; Palmer, K. J. *Indian J. Chem.* **1975**, *13*, 1355-1355.
- ²⁰⁶ de Almeida, M. F.; Guedes, M. L. S.; Cruz, F. G. *Tetrahedron Lett.* **2011**, *52*, 7108-7112.
- ²⁰⁷ Bokesch, H. R.; Groweiss, A.; McKee, T. C.; Boyd, M. R. *J. Nat. Prod.* **1999**, *62*, 1197-1199.
- ²⁰⁸ Schiell, M.; Kurz, M.; Haag-Richter, S. (Aventis Pharma Deutschland, GmbH). US Patent 6,956,061, October, 18, 2005.
- ²⁰⁹ de Oliveira, C. M. A.; Porto, A. L. M.; Bittrich, V.; Marsaioli, A. J. *Phytochemistry* **1999**, *50*, 1073-1079.
- ²¹⁰ Cuesta-Rubio, O.; Velez-Castro, H.; Frontana-Urbe, B. A.; Cárdenas, J. *Phytochemistry* **2001**, *57*, 279-283.
- ²¹¹ Kelecom, A.; Reis, G. L.; Fevereiro, P. C. A.; Silva, J. G.; Santos, M. G.; Neto, C. B. M.; Gonzalez, M. S.; Gouvea, R. C. S.; Almeida, G. S. S. *An. Acad. Bras. Cienc.* **2002**, *74*, 171-181.
- ²¹² Cuesta-Rubio, O.; Piccinelli, A. L.; Fernandez, M. C.; Hernández, I. M.; Rosado, A.; Rastrelli, L. *J. Agric. Food Chem.* **2007**, *55*, 7502-7509.
- ²¹³ Díaz-Carballo, D.; Malak, S.; Bardenheuer, W.; Freistuehler, M.; Reusch, H. P. *Bioorg. Med. Chem.* **2008**, *16*, 9635-9643.
- ²¹⁴ Pagano, B.; Pavone, M.; Piccinelli, A. L.; Rastrelli, L.; Cuesta-Rubio, O.; Mattia, C. A.; Barone, V. *Chem. Phys. Lett.* **2008**, *462*, 158-163.
- ²¹⁵ Teixeira, J. S. R.; Cruz, F. G. *Tetrahedron Lett.* **2005**, *46*, 2813-2816.
- ²¹⁶ Cruz, F. G.; Teixeira, J. S. R. *J. Braz. Chem. Soc.* **2004**, *15*, 504-508.
- ²¹⁷ Chaturvedula, V. S. P.; Schilling, J. K.; Kingston, D. G. I. *J. Nat. Prod.* **2002**, *65*, 965-972.
- ²¹⁸ Ishida, Y.; Shiota, O.; Sekita, S.; Someya, K.; Tokita, F.; Nakane, T.; Kuroyanagi, M. *Chem. Pharm. Bull.* **2010**, *58*, 336-343.
- ²¹⁹ Gao, X.-M.; Yu, T.; Lai, F. S. F.; Pu, J.-X.; Qiao, C.-F.; Zhou, Y.; Liu, X.; Song, J.-Z.; Luo, K. Q.; Xu, H.-X. *Tetrahedron Lett.* **2010**, *51*, 2442-2446.
- ²²⁰ Gao, X.-M.; Yu, T.; Luo, K. Q.; Xu, H. X. US Patent Appl. 2011/0301233, December 8, 2011.
- ²²¹ Xiao, Z. Y.; Zeng, Y. H.; Mu, Q.; Shiu, W. K. P.; Gibbons, S. *Chem. Biodivers.* **2010**, *7*, 953-958.
- ²²² Henry, G. E.; Jacobs, H.; Carrington, C. M. S.; McLean, S.; Reynolds, W. F. *Tetrahedron Lett.* **1996**, *37*, 8663-8666.
- ²²³ Christian, O. E.; Henry, G. E.; Jacobs, H.; McLean, S.; Reynolds, W. F. *J. Nat. Prod.* **2001**, *64*, 23-25.
- ²²⁴ Henry, G. E.; Jacobs, H.; Carrington, C. M. S.; McLean, S.; Reynolds, W. F. *Tetrahedron* **1999**, *55*, 1581-1596.
- ²²⁵ Grossman, R. B.; Jacobs, H. *Tetrahedron Lett.* **2000**, *41*, 5165-5169.

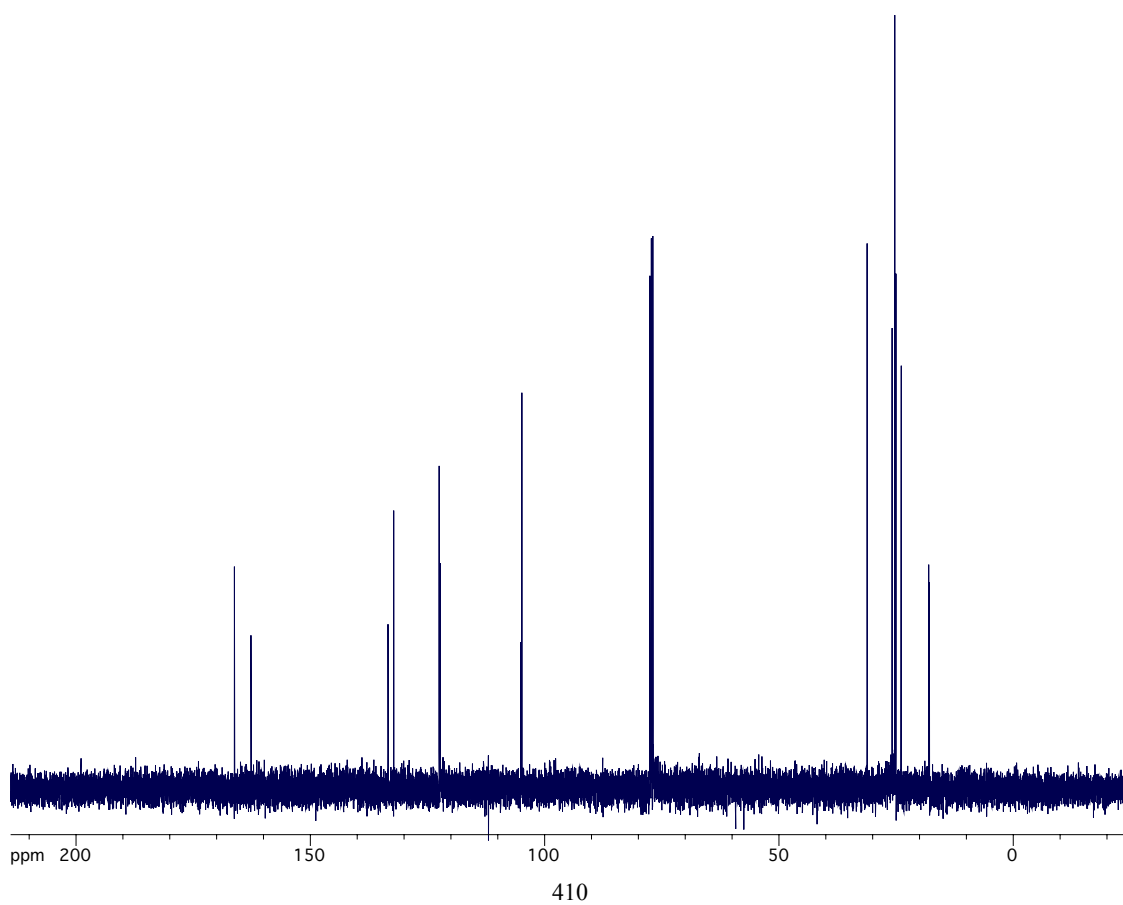
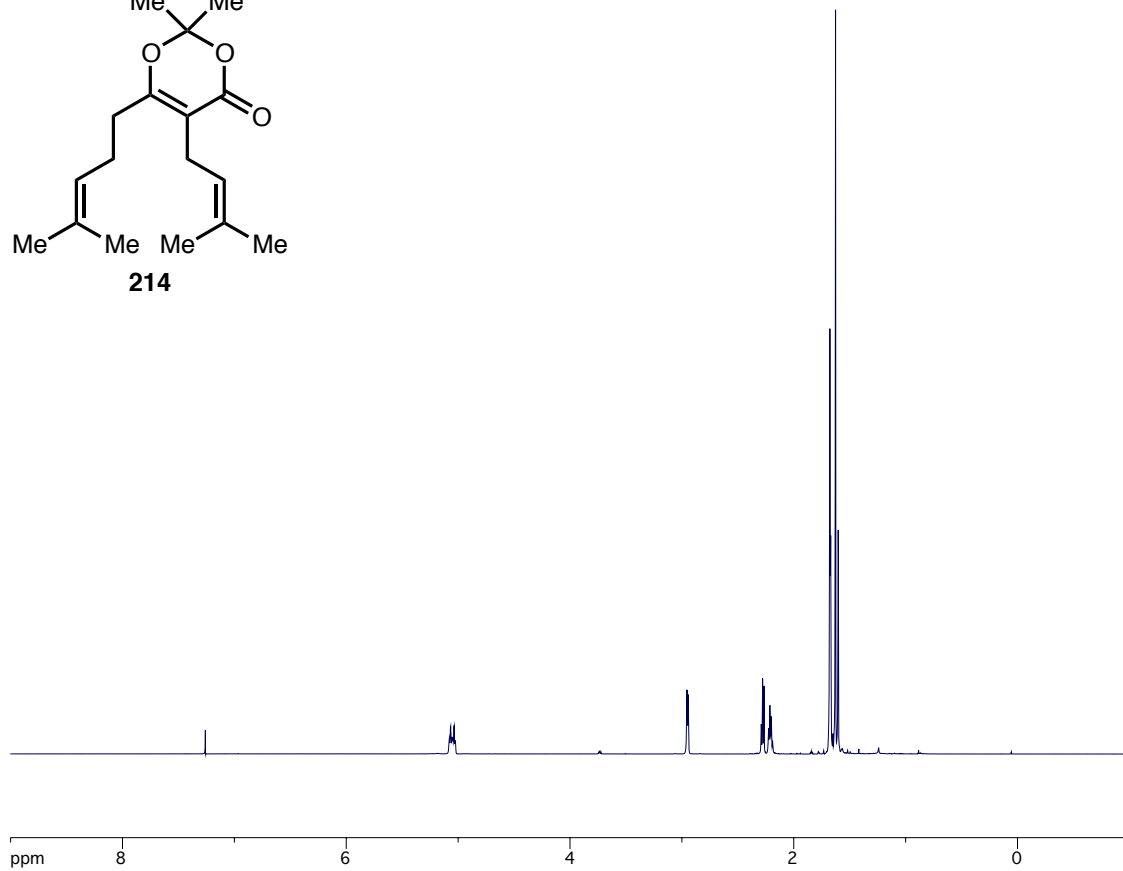
-
- ²²⁶ Díaz-Carballo, D.; Gustmann, S.; Ackikelli, A. H.; Bardenheuer, W.; Buehler, H.; Jastrow, H.; Ergun, S.; Strumberg, D. *Phytomedicine* **2012**, *19*, 1298-1306.
- ²²⁷ Bittrich, V.; Amaral, M. do C. E.; Machado, S. M. F.; Marsaioli, A. J. Z. *Naturforsch.* **2003**, *58c*, 643-648.
- ²²⁸ Henry, G. E.; Raithore, S.; Zhang, Y.; Jayaprakasam, B.; Nair, M. G.; Heber, D.; Seeram, N. P. *J. Nat. Prod.* **2006**, *69*, 1645-1648.
- ²²⁹ Cuesta Rubio, O.; Cuellar, A. C.; Rojas, N.; Velez Castro, H.; Rastrelli, L.; Aquino, R. *J. Nat. Prod.* **1999**, *62*, 1013-1015.
- ²³⁰ Shan, M. D.; Hu, L. H.; Chen, Z. L. *Chinese Chem. Lett.* **2000**, *11*, 701-704.
- ²³¹ Hu, L.-H.; Sim, K.-Y. *Tetrahedron Lett.* **1998**, *39*, 7999-8002.
- ²³² Li, Z.-Q.; Lei, L.; Ma, G.-Y.; Rong, H.; Hu, Z.-H. *Chinese Tradit. Herb. Drugs* **2004**, *35*, 131-134.
- ²³³ Hu, L.-H.; Sim, K.-Y. *Tetrahedron Lett.* **1999**, *40*, 759-762.
- ²³⁴ Hu, L. H.; Sim, K. Y. *Org. Lett.* **1999**, *1*, 879-882.
- ²³⁵ Trusheva, B.; Popova, M.; Naydenski, H.; Tsvetkova, I.; Rodriguez, J. G.; Bankova, V. *Fitoterapia* **2004**, *75*, 683-689.
- ²³⁶ Magadula, J. J.; Kapingu, M. C.; Bezabih, M.; Abegaz, B. M. *Phytochem. Lett.* **2008**, *1*, 215-218.
- ²³⁷ Řezanka, T.; Sigler, K. *Phytochemistry* **2007**, *68*, 1272-1276.
- ²³⁸ Albernaz, L. C.; Deville, A.; Dubost, L.; de Paula, J. E.; Bodo, B.; Grellier, P.; Espindola, L. S.; Mambu, L. *Planta Med.* **2012**, *78*, 459-464.
- ²³⁹ Fukuyama, Y.; Kaneshi, A.; Tani, N.; Kodama, M. *Phytochemistry* **1993**, *33*, 483-485.
- ²⁴⁰ Cao, S.; Low, K.-N.; Glover, R. P.; Crasta, S. C.; Ng, S.; Buss, A. D.; Butler, M. S. *J. Nat. Prod.* **2006**, *69*, 707-709.
- ²⁴¹ Guo, N.; Chen, X.-Q.; Zhao, Q.-S. *Acta Bot. Yunnanica* **2008**, *30*, 515-518.
- ²⁴² Dreyer, D. L. *Phytochemistry* **1974**, *13*, 2883-2884.
- ²⁴³ Talontsi, F. M.; Islam, M. T.; Facey, P.; Douanla-Meli, C.; von Tiedemann, A.; Laatsch, H. *Phytochem. Lett.* **2012**, *5*, 657-664.
- ²⁴⁴ Crichton, E. G.; Waterman, P. G. *Phytochemistry* **1979**, *18*, 1553-1557.
- ²⁴⁵ Waterman, P. G.; Hussain, R. A. *Phytochemistry* **1982**, *21*, 2099-2101.
- ²⁴⁶ Tandon, R. N.; Srivastava, O. P.; Baslas, R. K.; Kumar, P. *Curr. Sci. India* **1980**, *49*, 472-473.
- ²⁴⁷ Botta, B.; Mac-Quhae, M. M.; Delle Monache, G.; Delle Monache, F. *J. Nat. Prod.* **1984**, *47*, 1053-1053.
- ²⁴⁸ Blount, J. F.; Williams, T. H. *Tetrahedron Lett.* **1976**, *17*, 2921-2924.

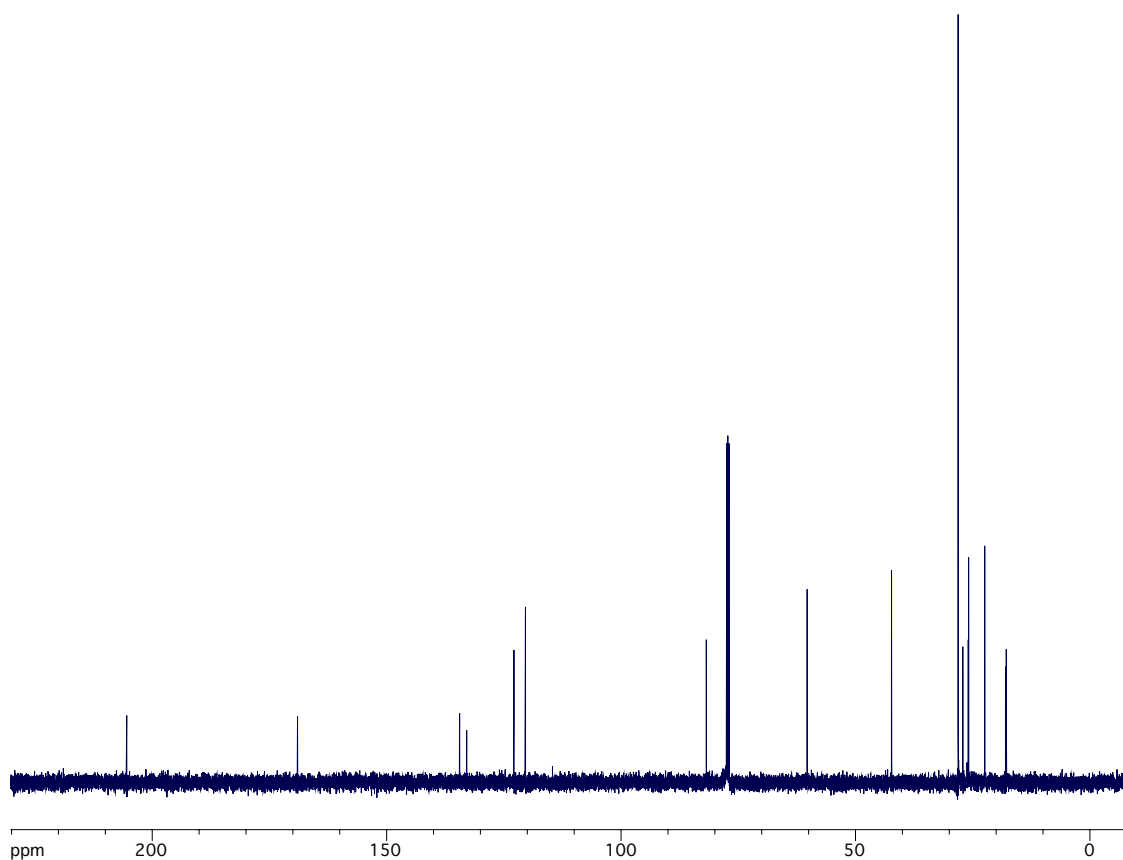
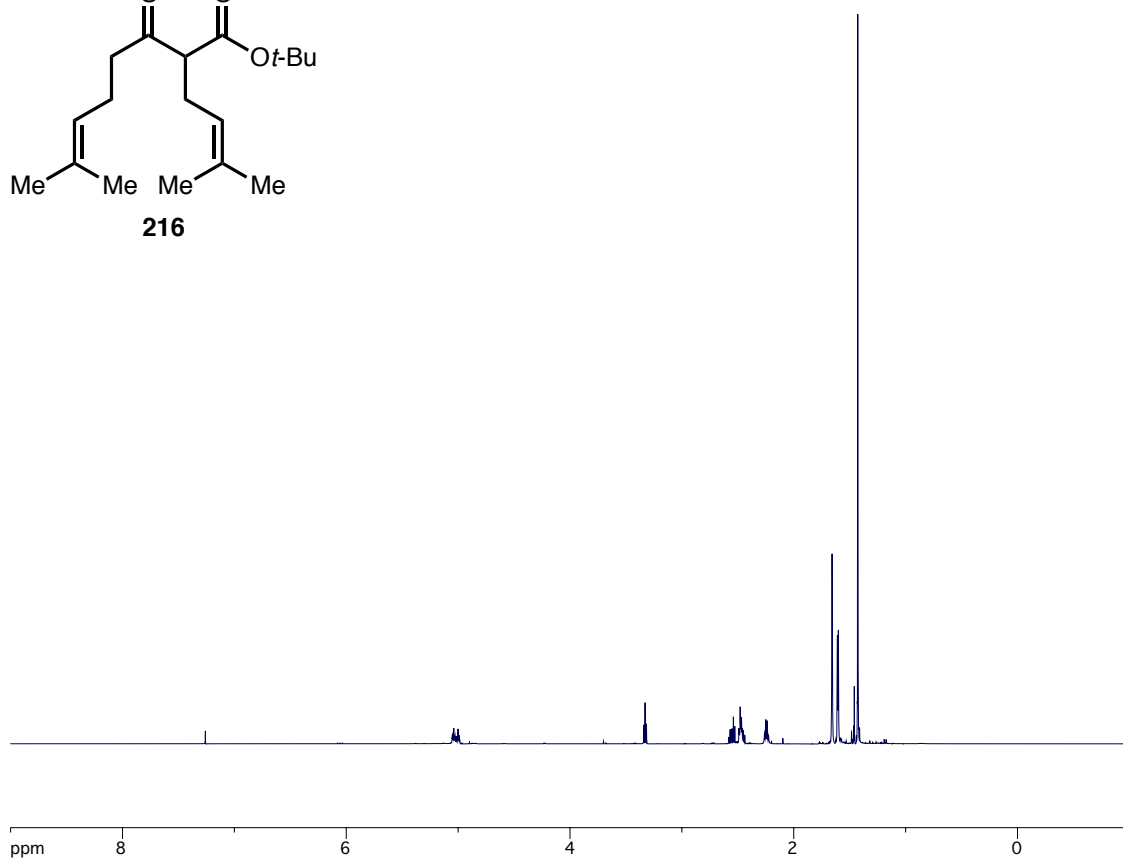
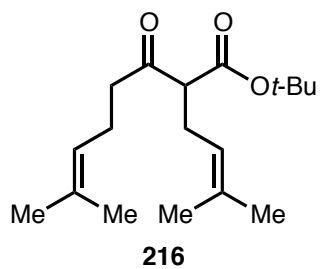
Appendix B
Catalog of Spectra

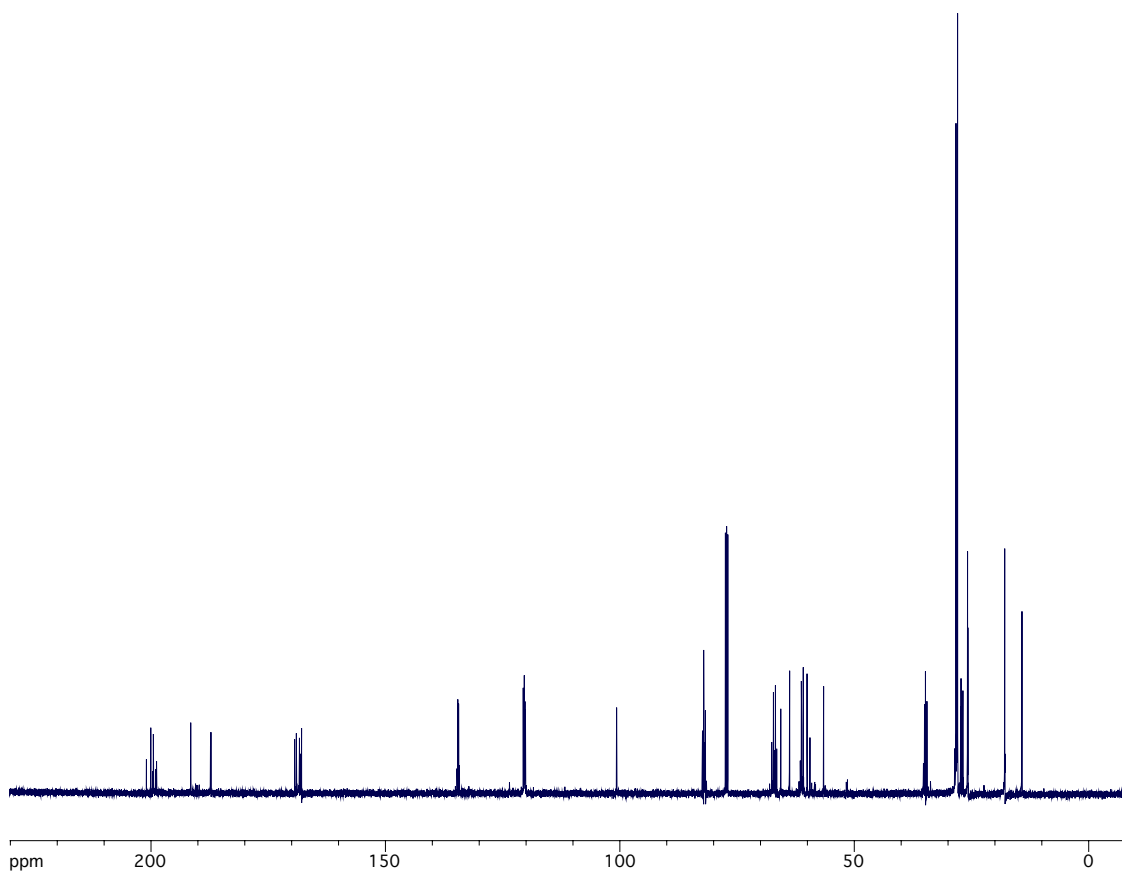
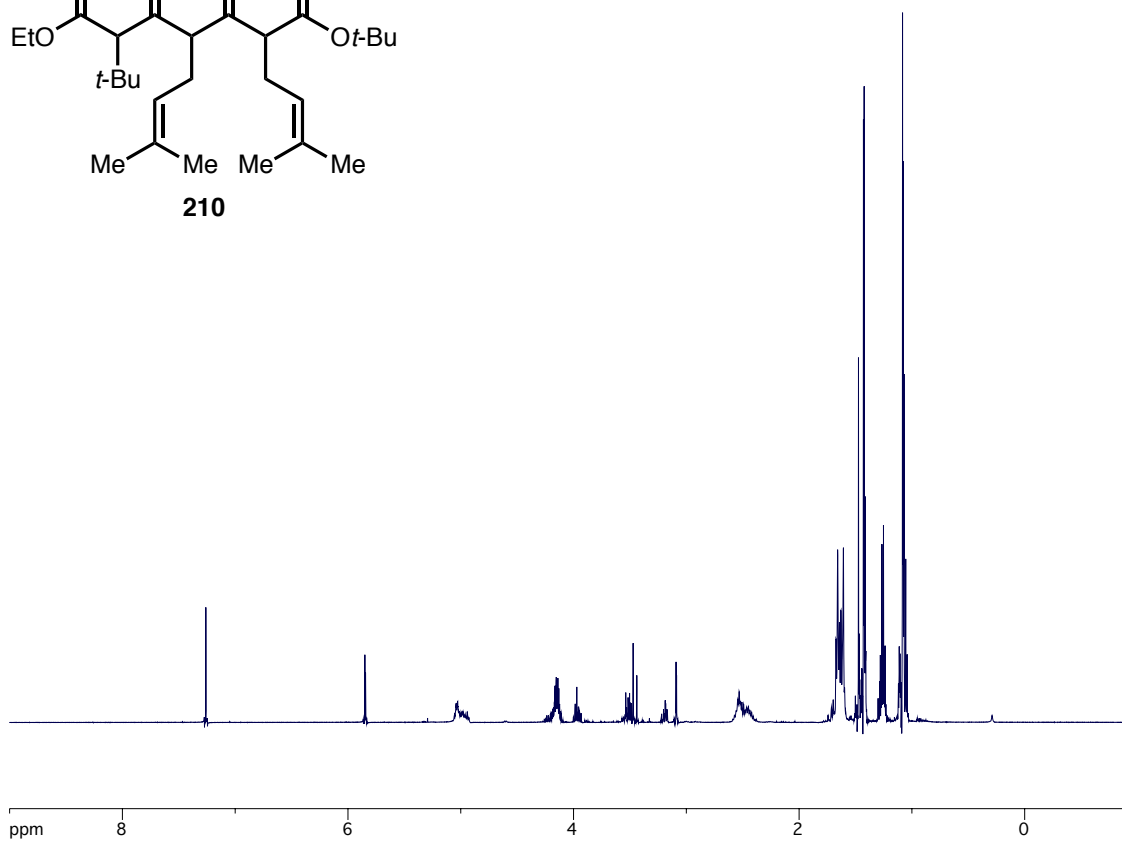
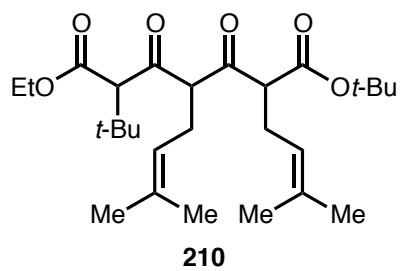


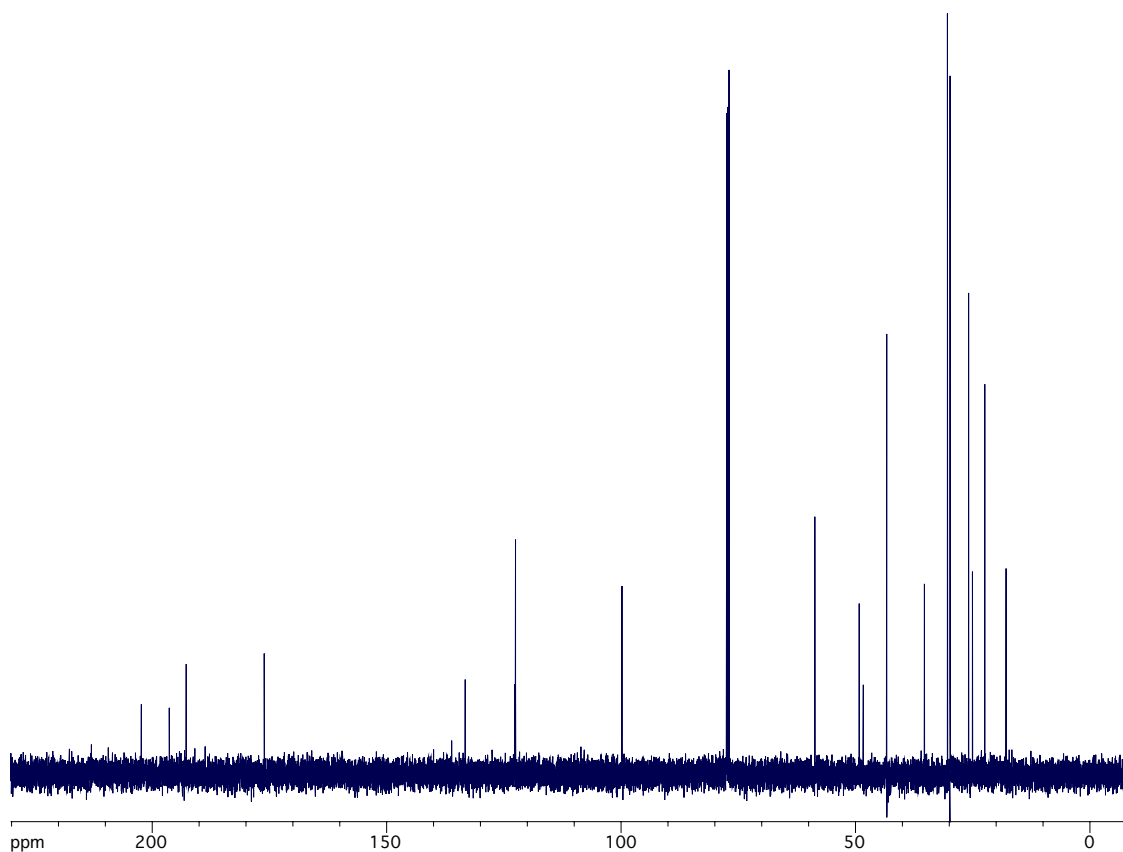
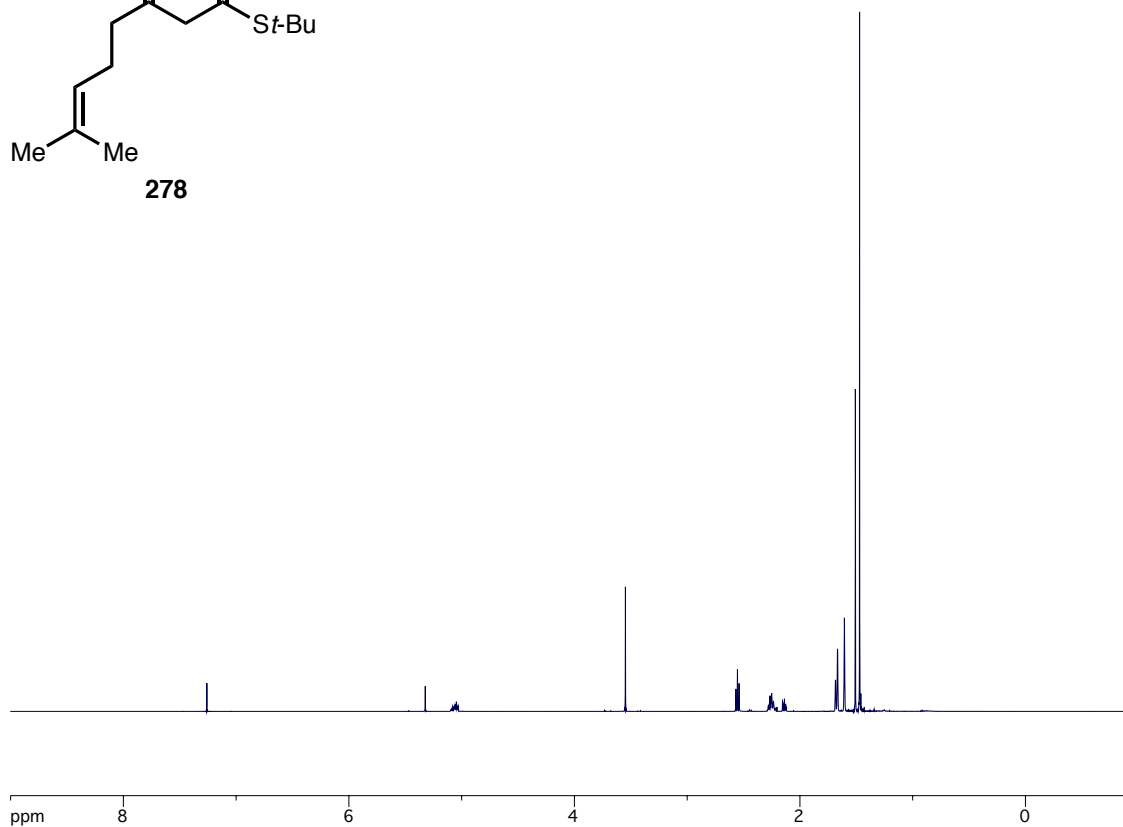
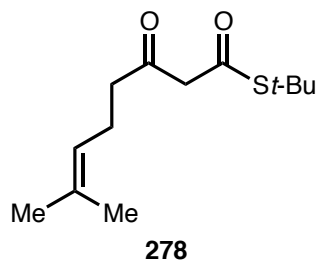


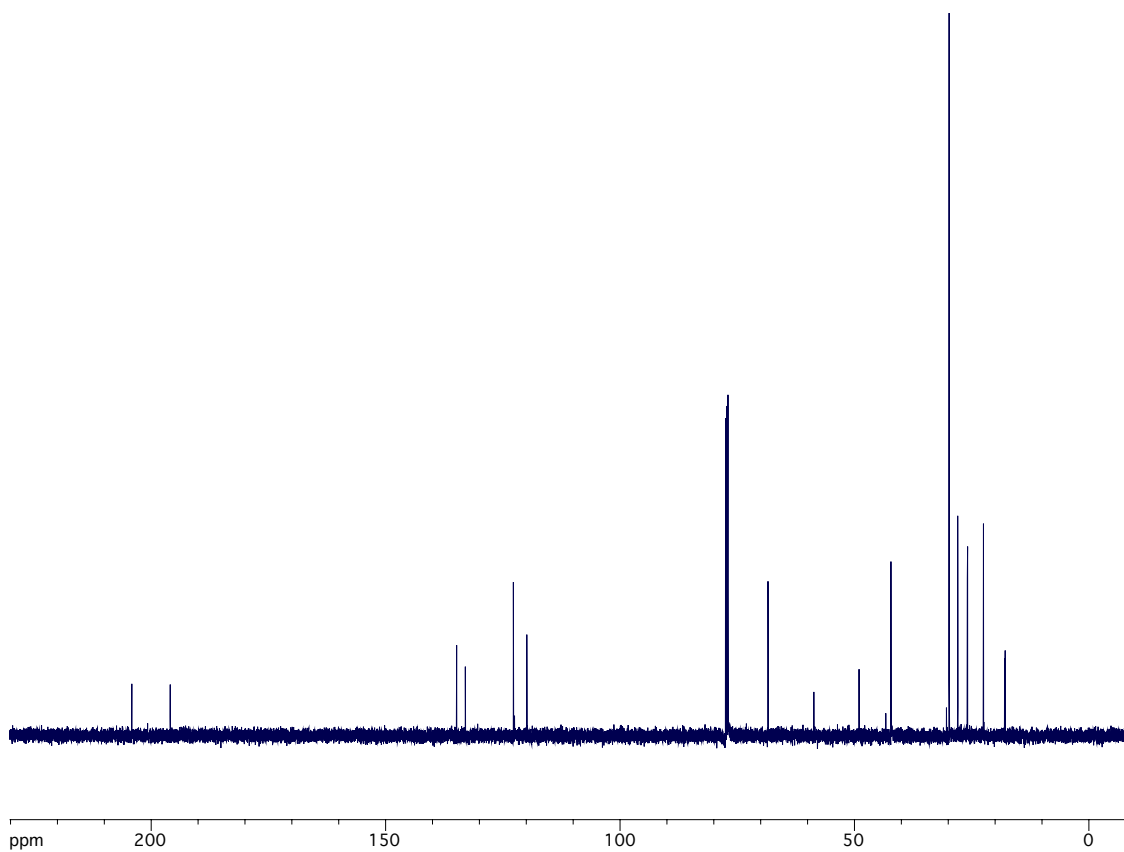
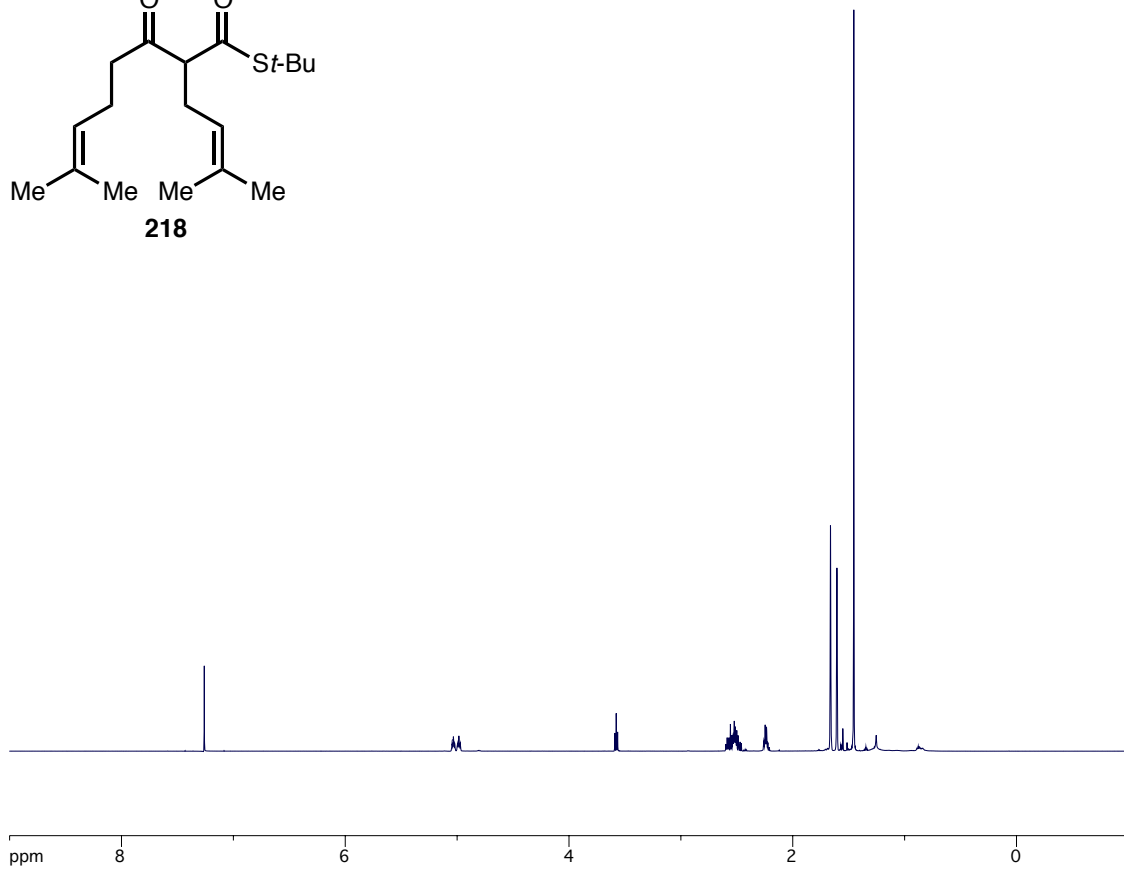
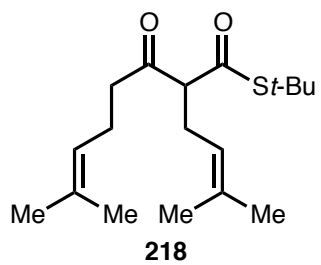
214

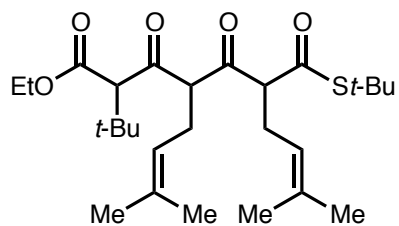




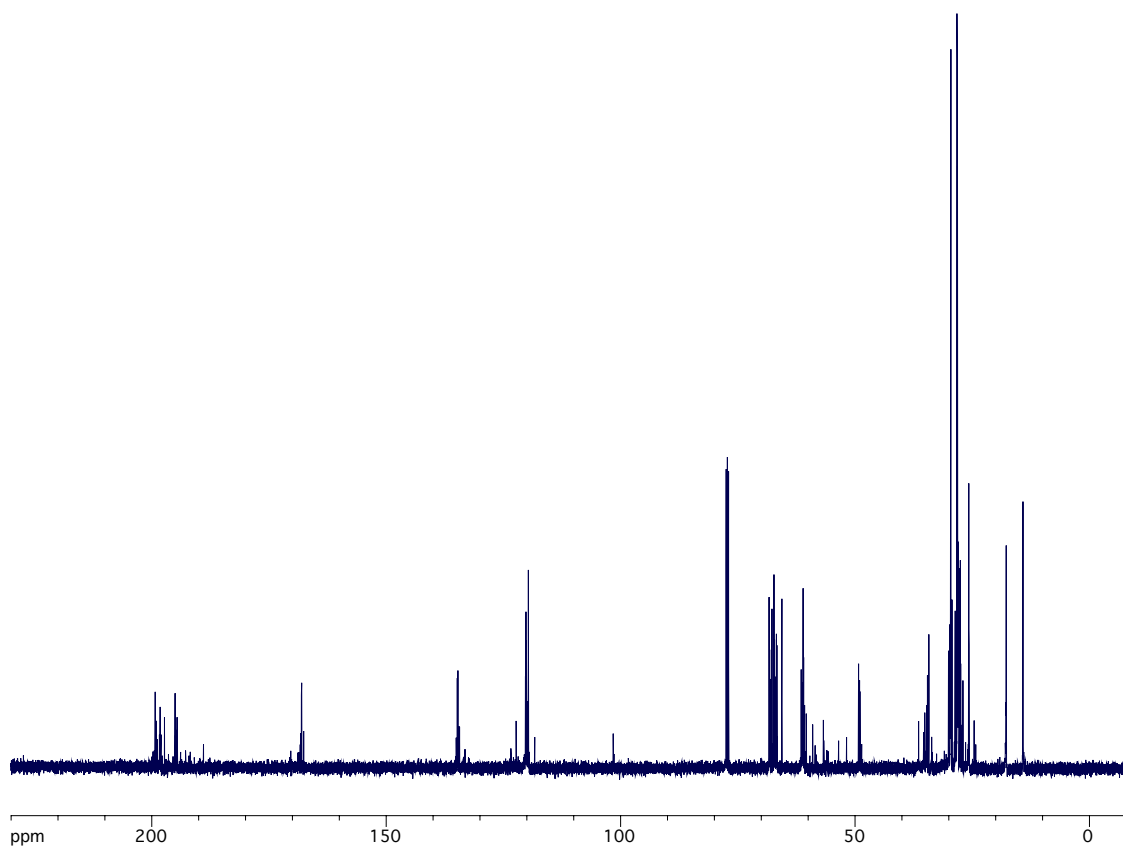
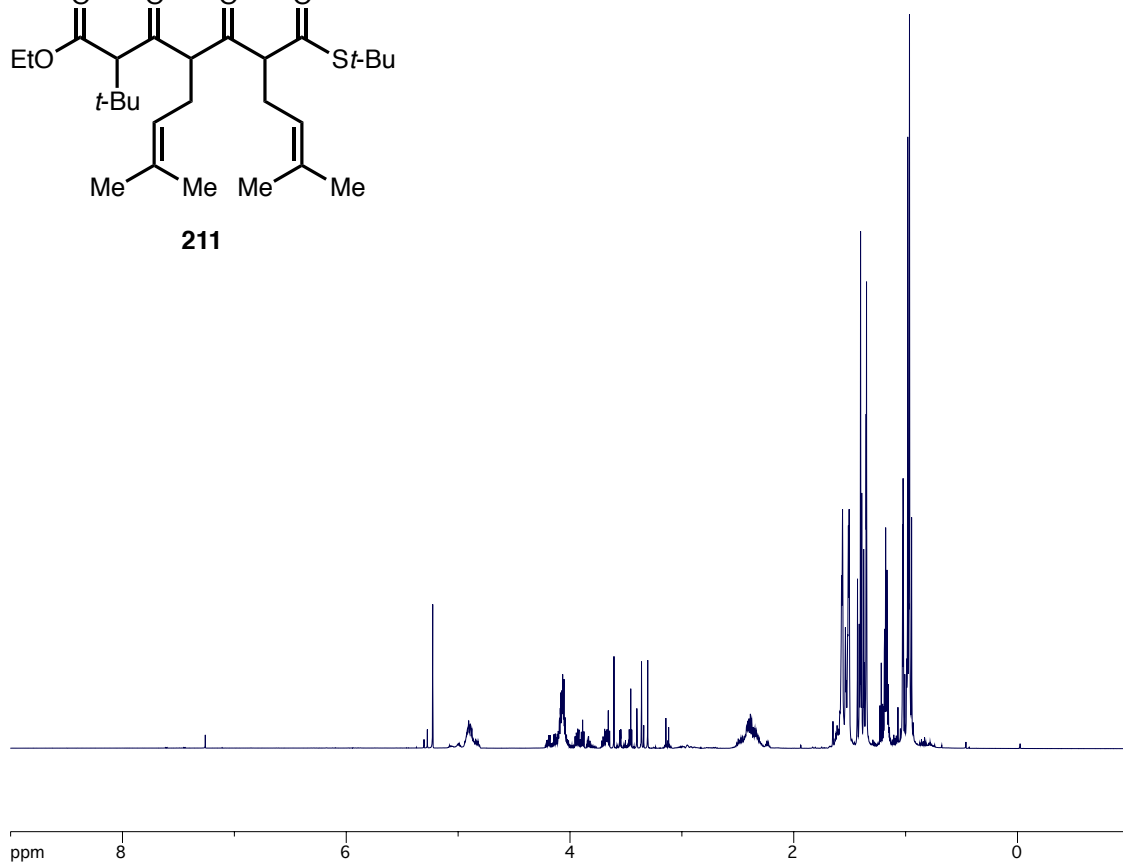


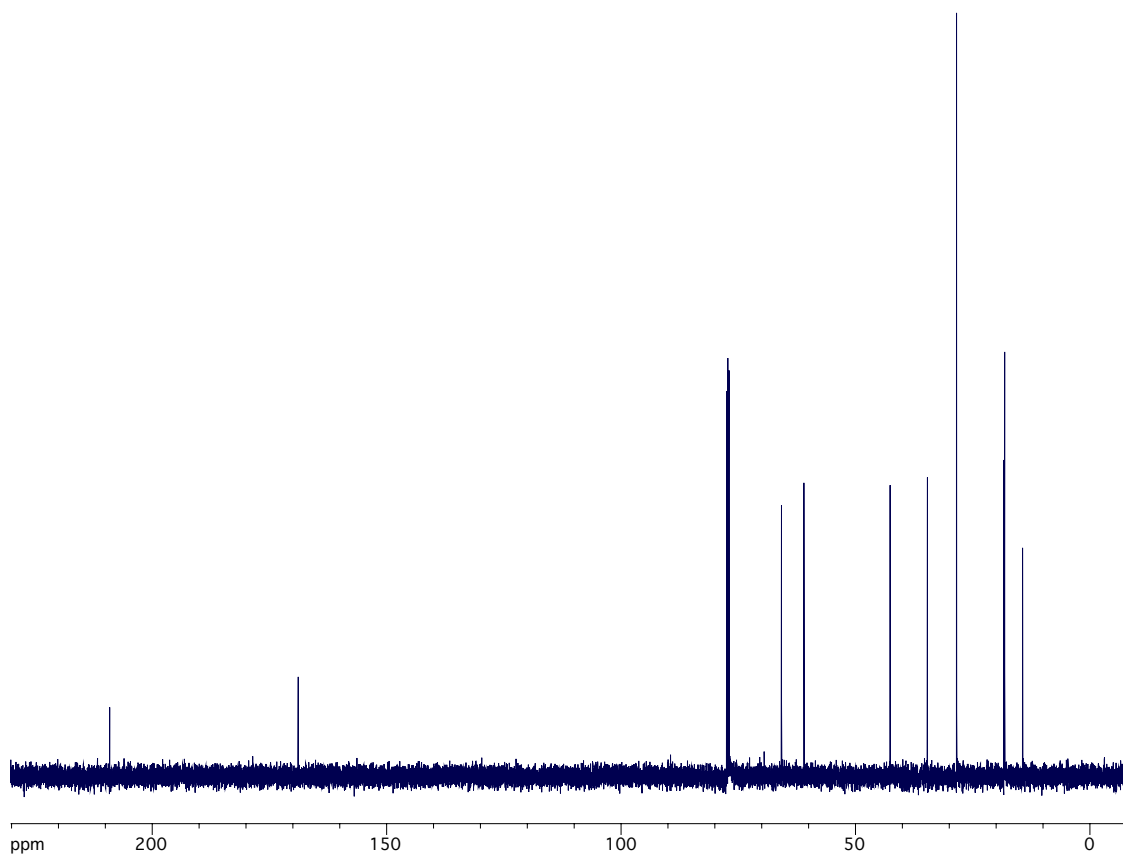
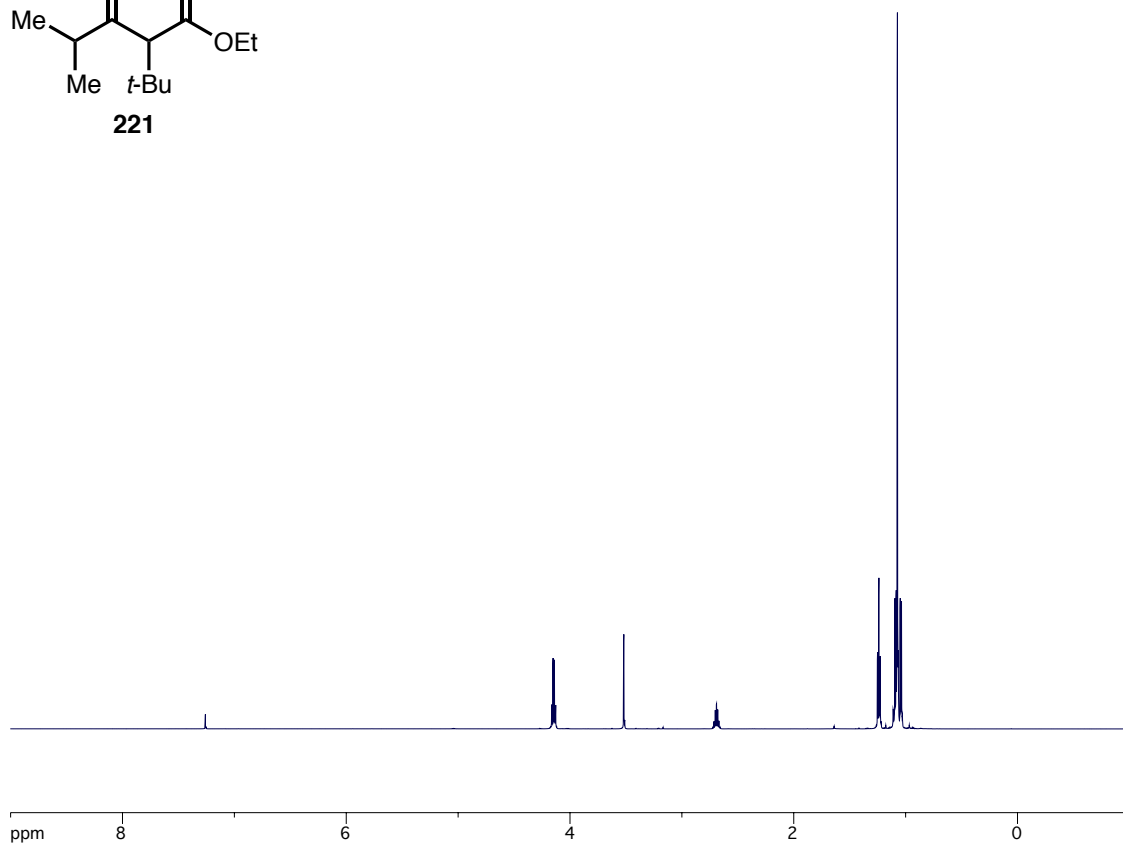
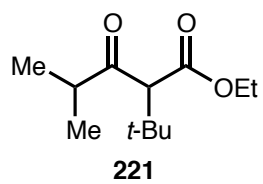


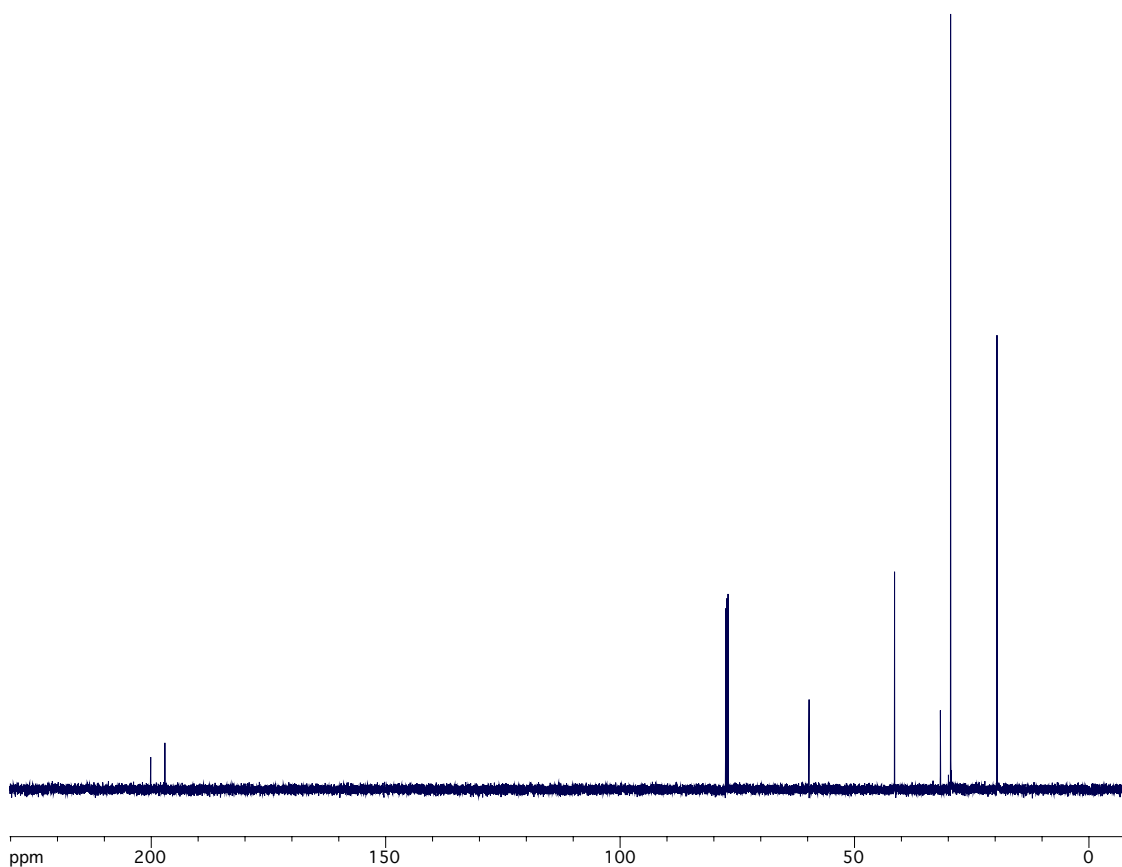
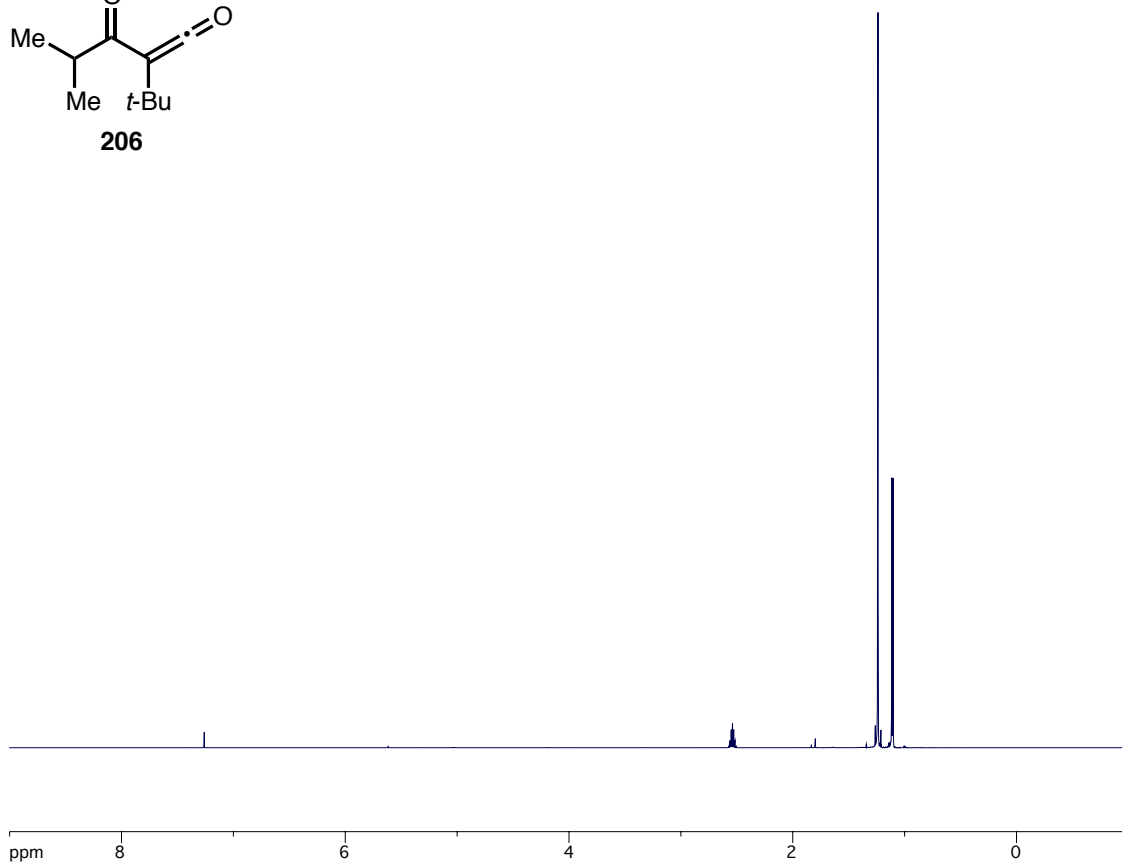
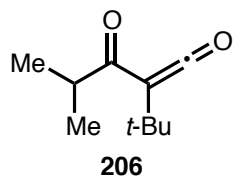


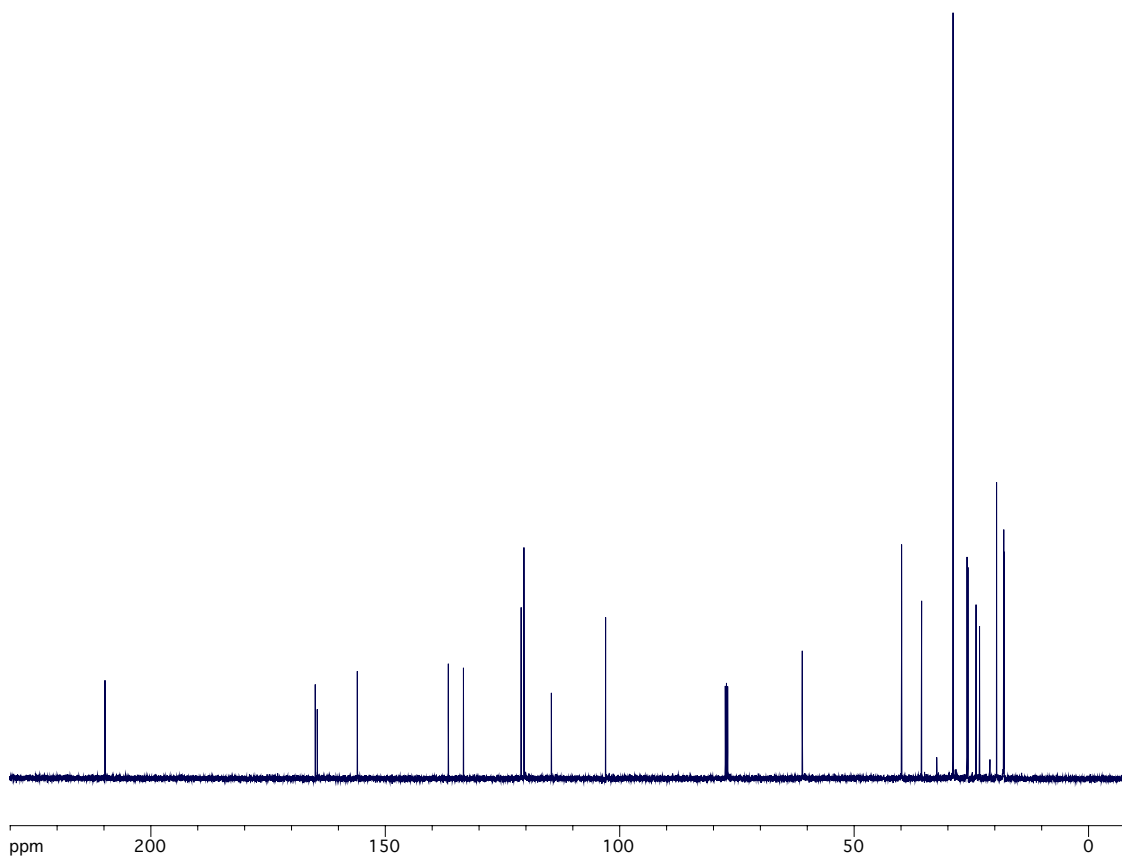
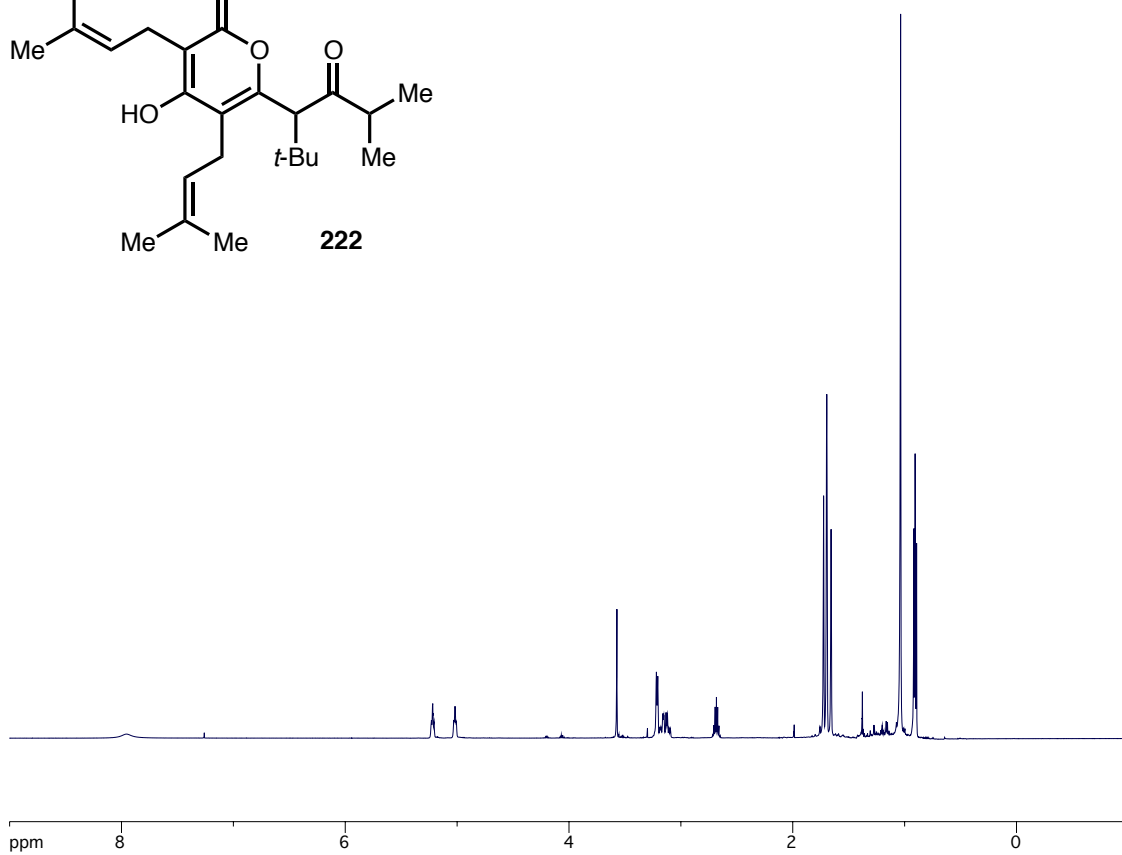
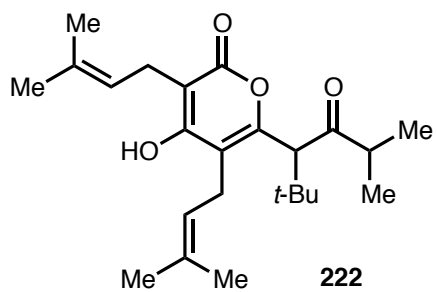


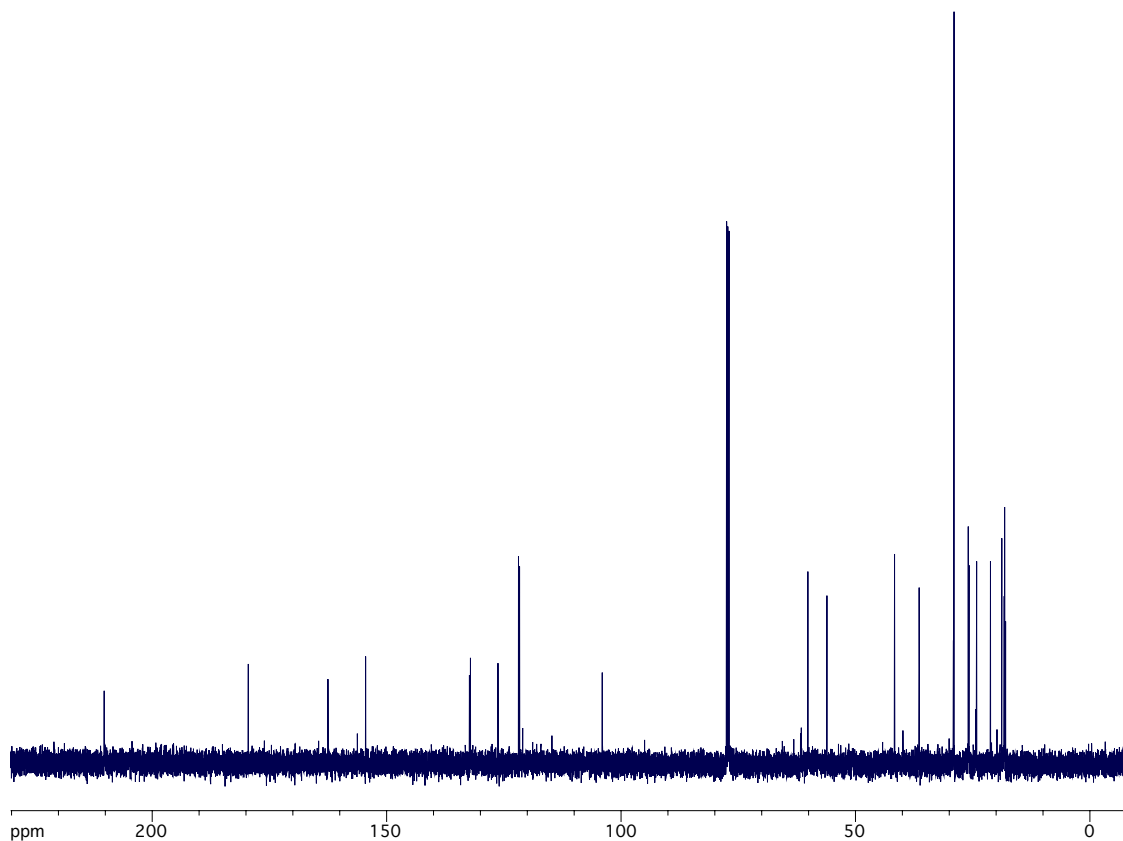
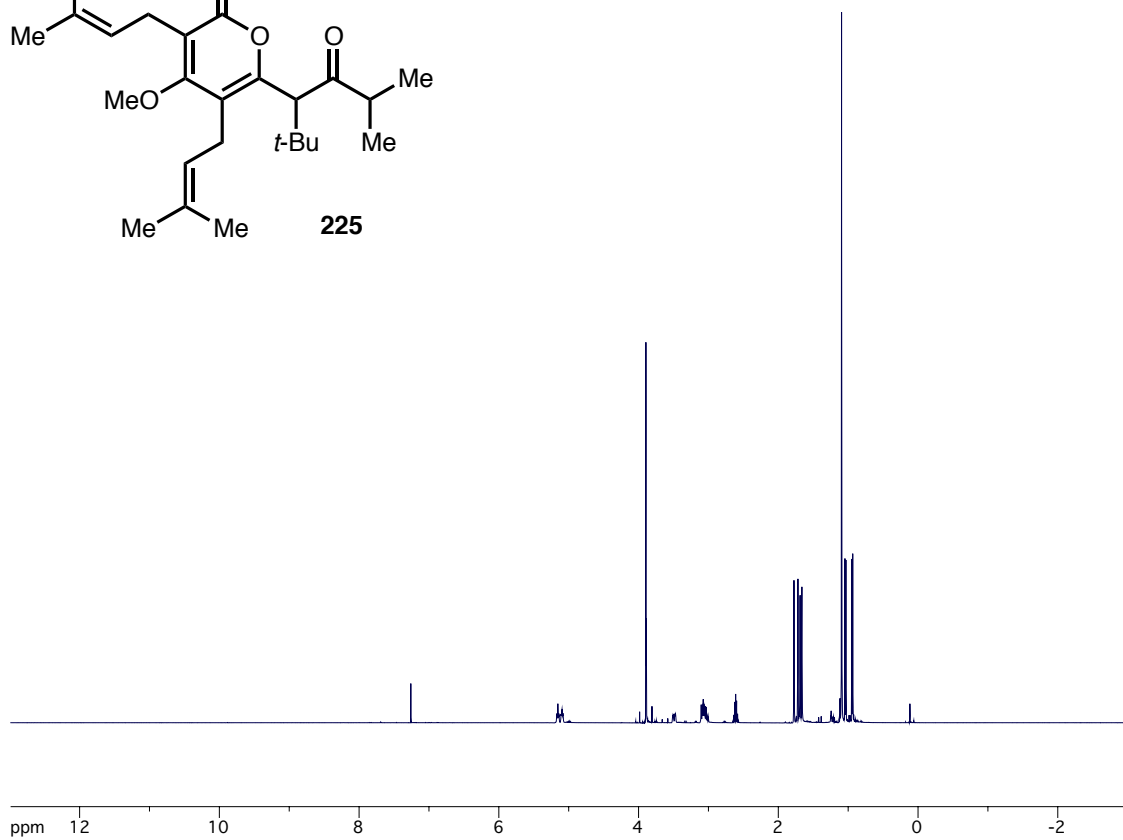
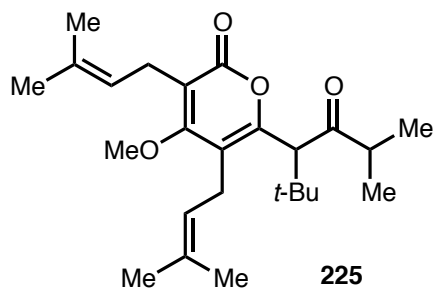
211

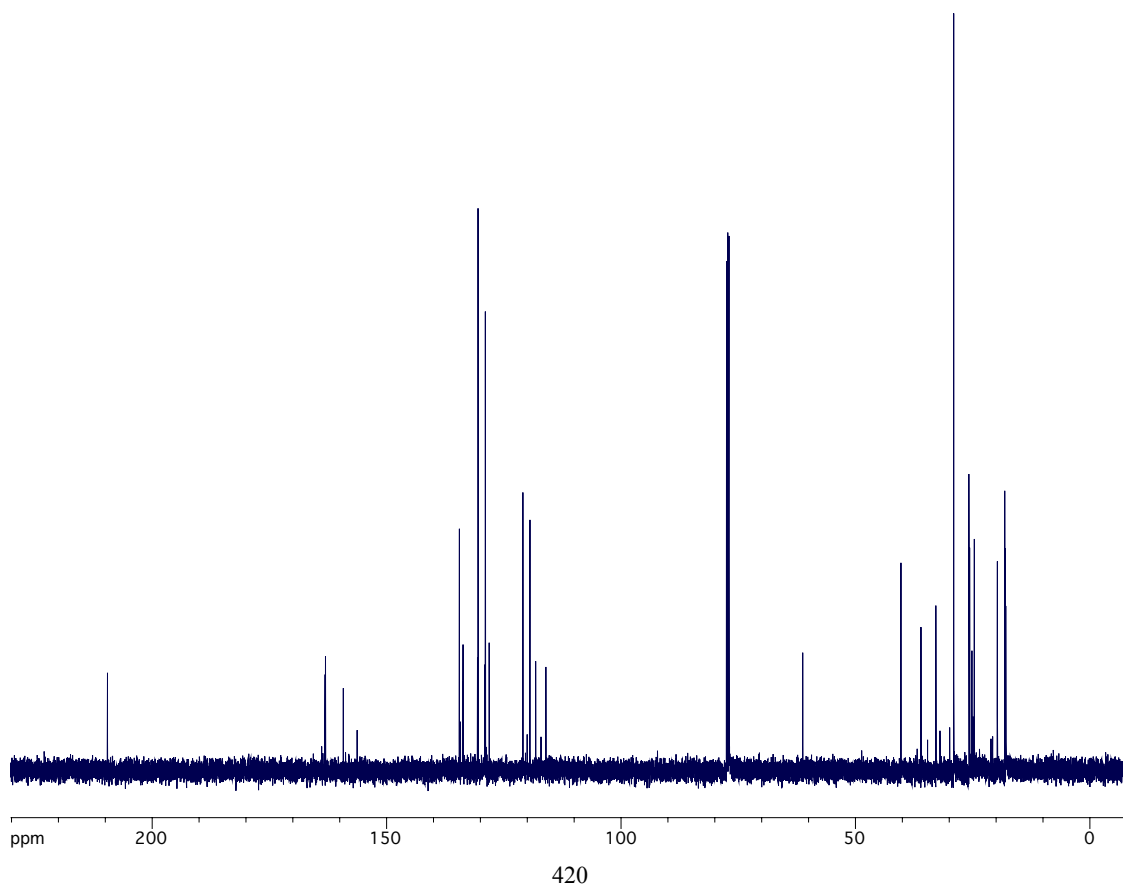
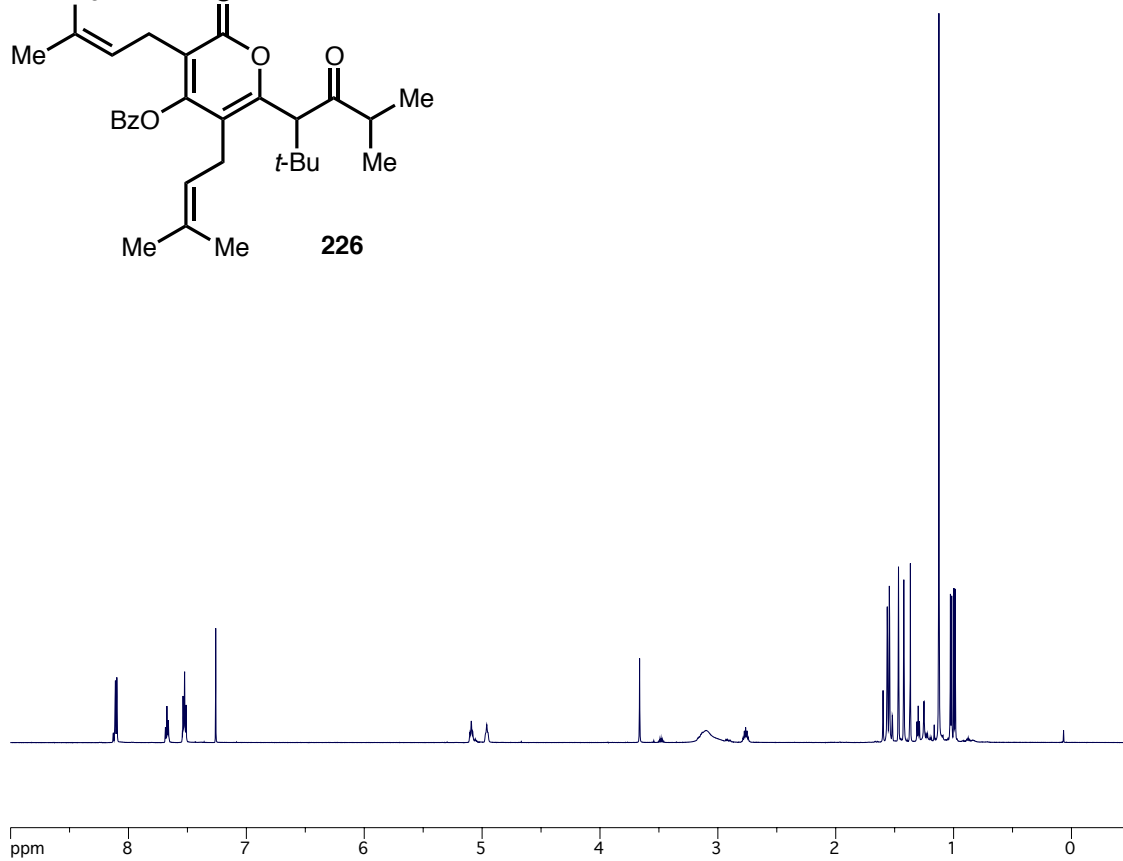
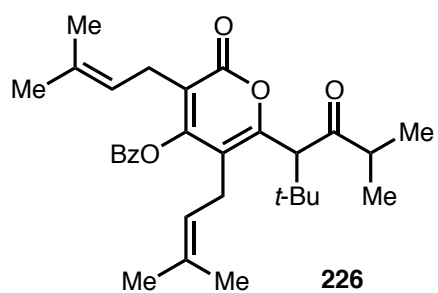


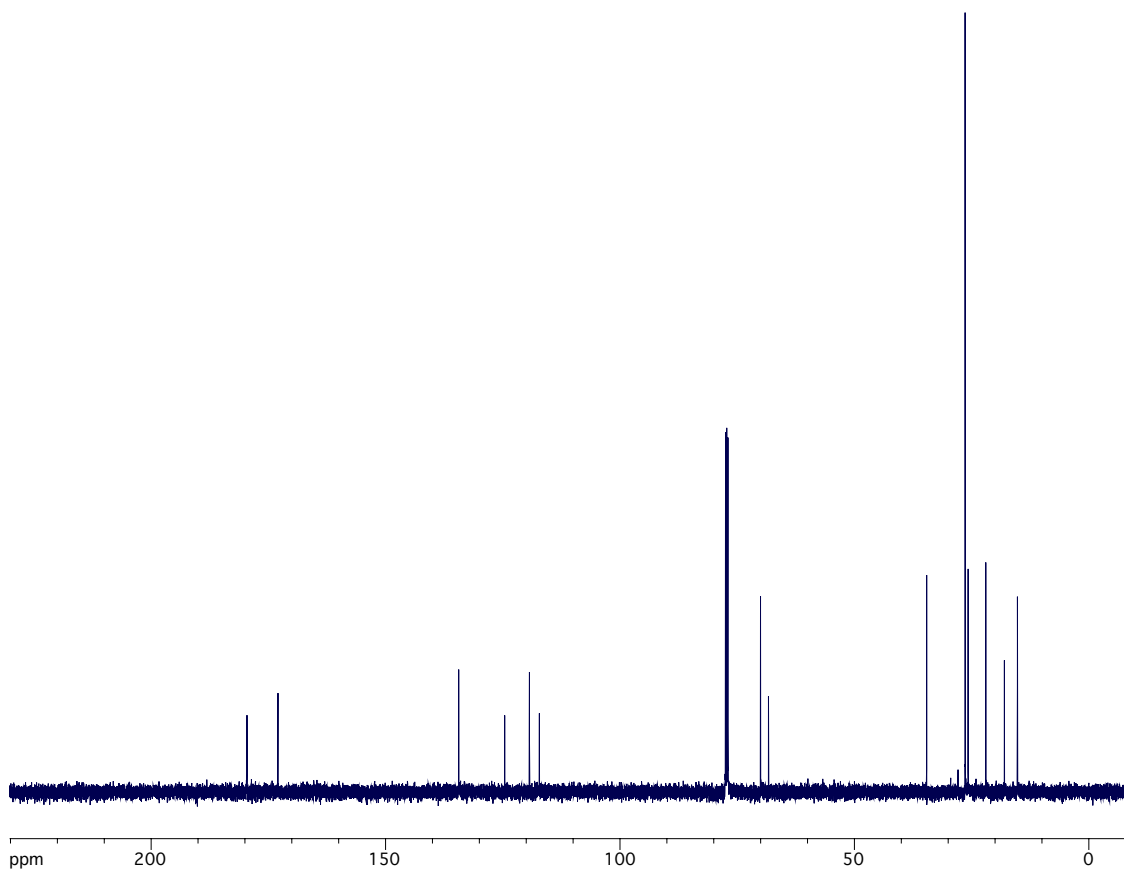
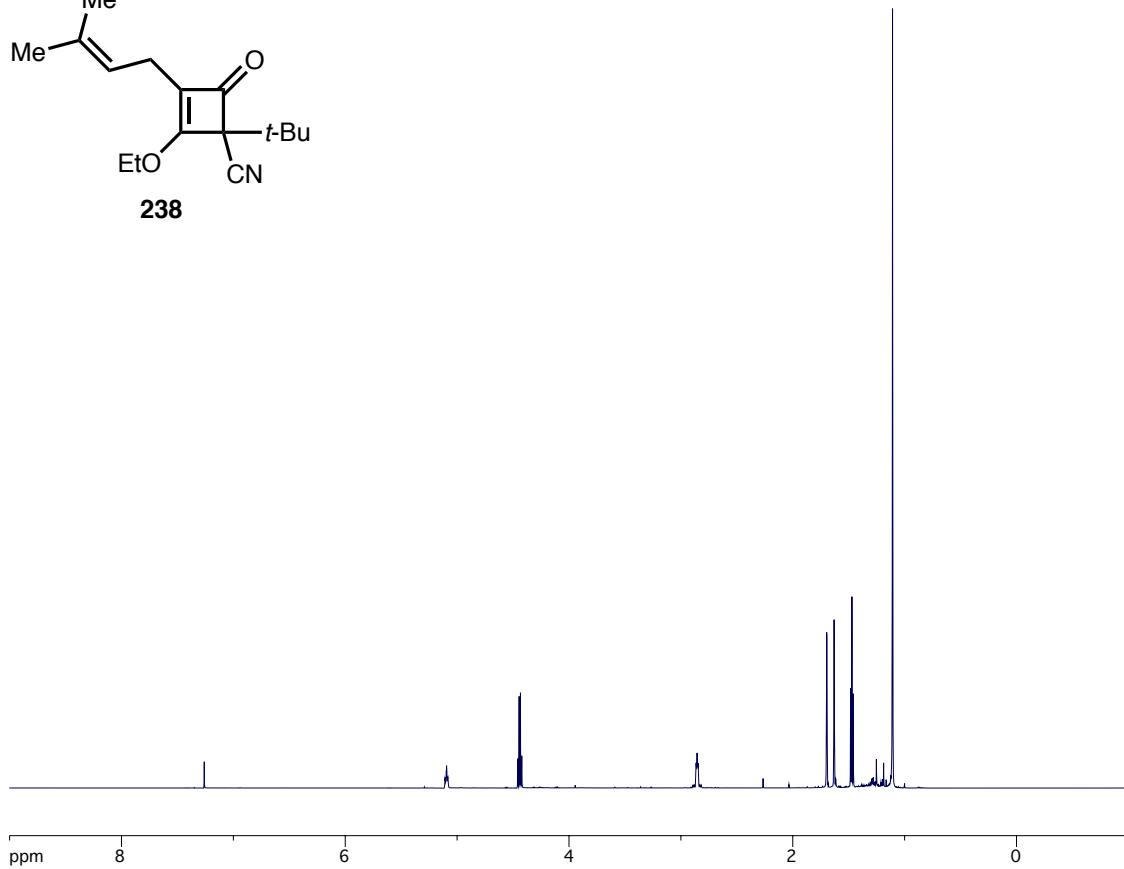
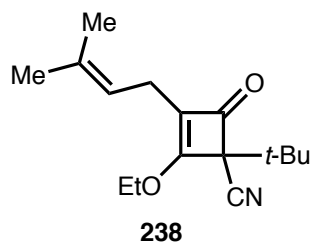


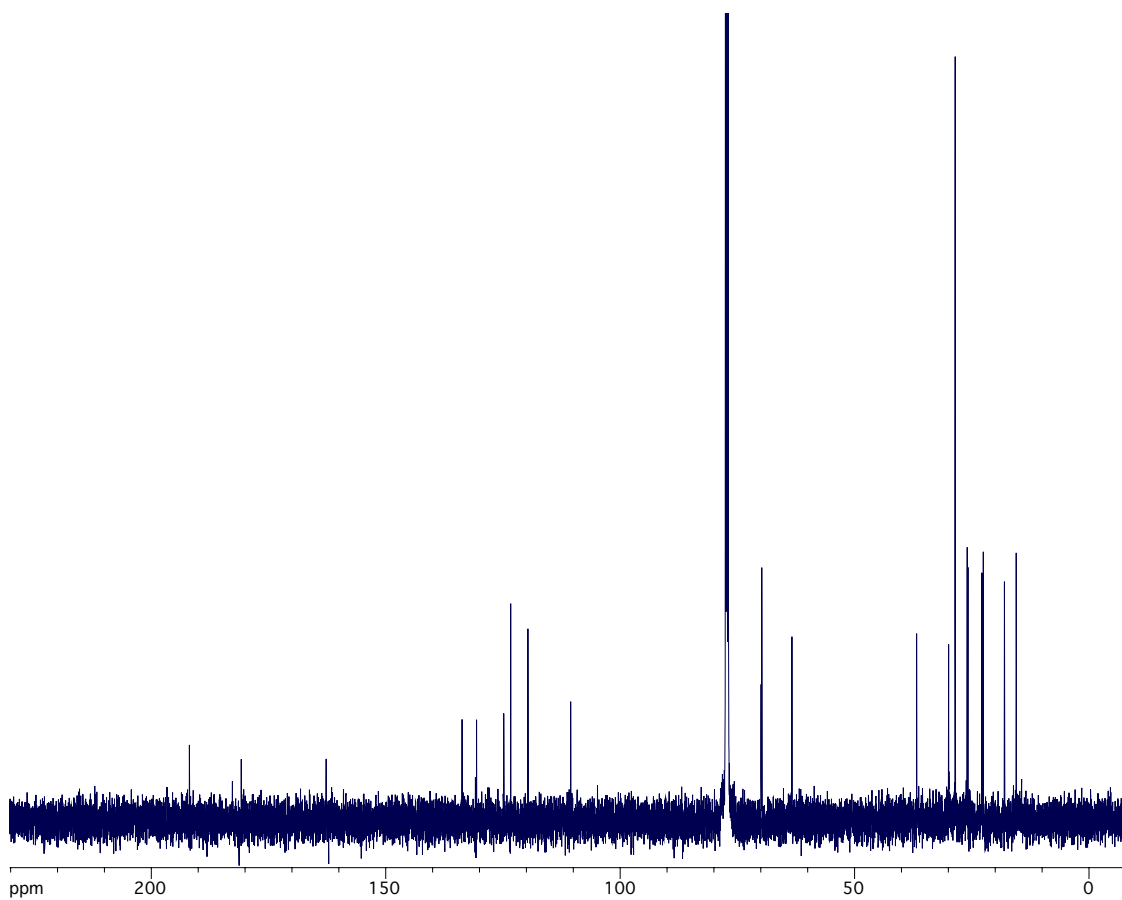
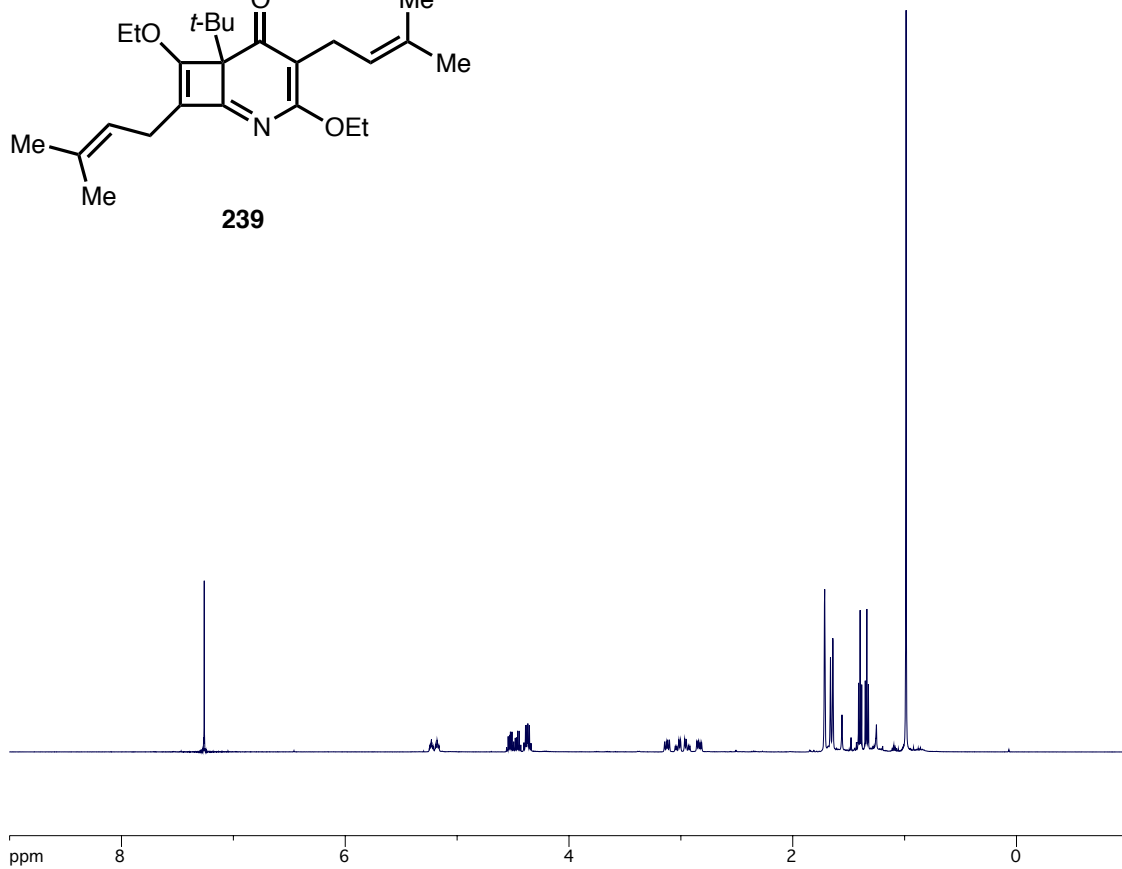
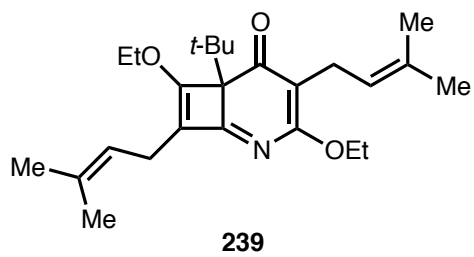


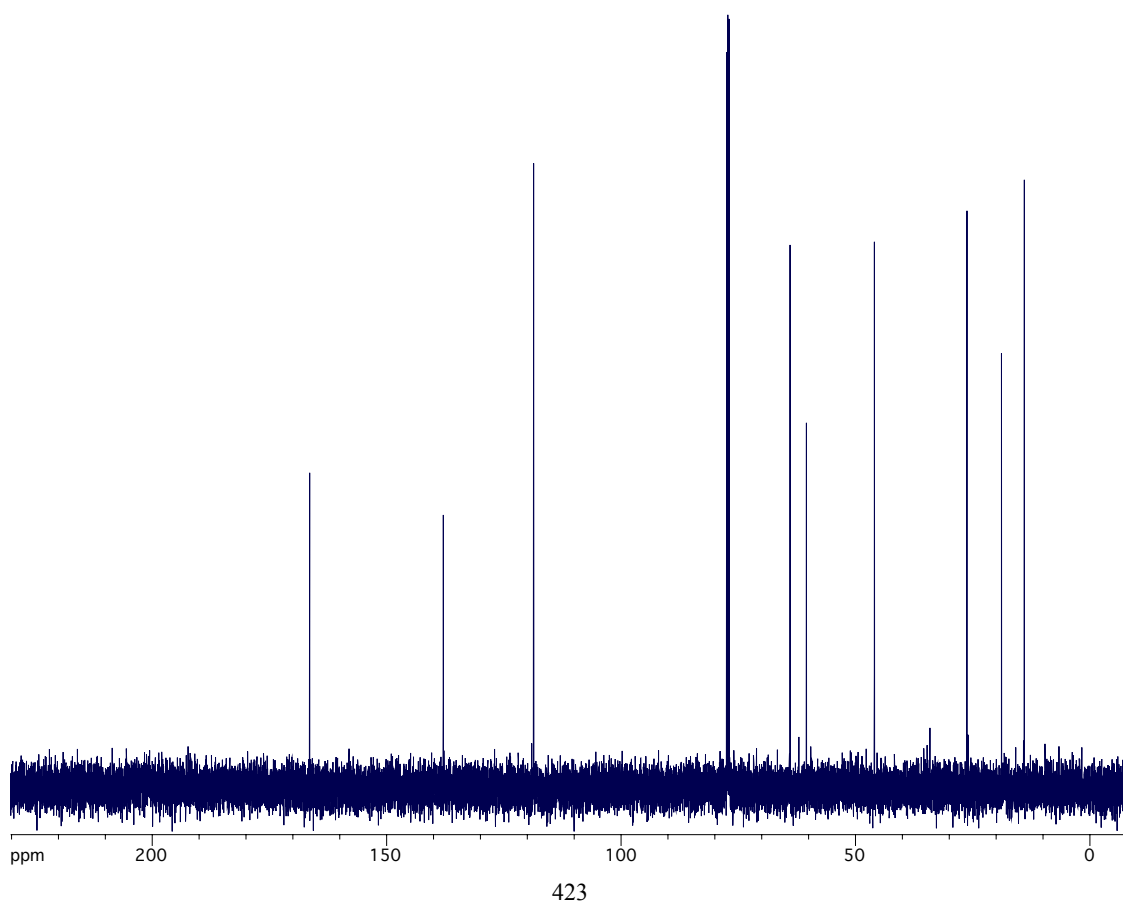
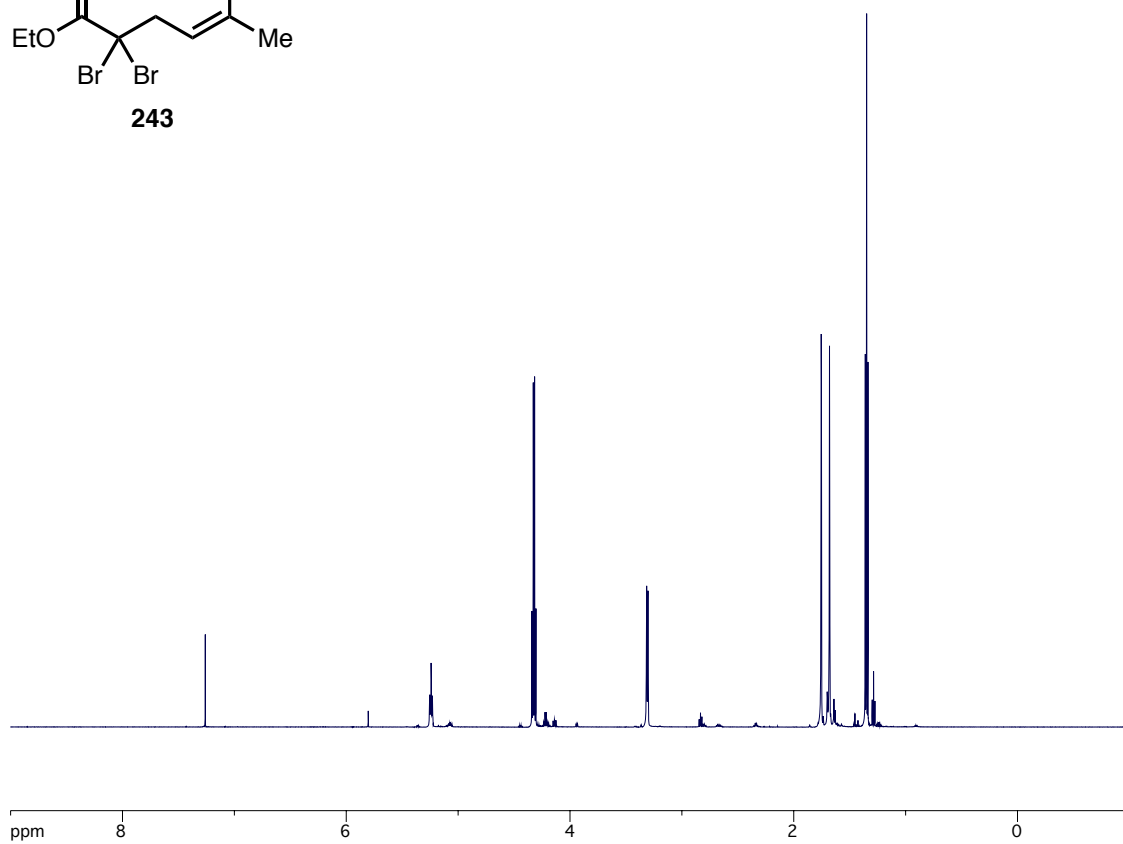
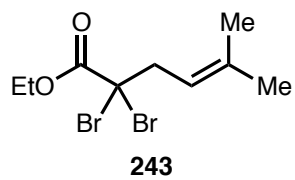


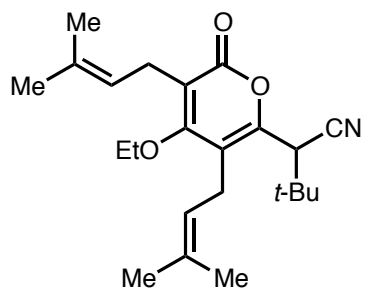




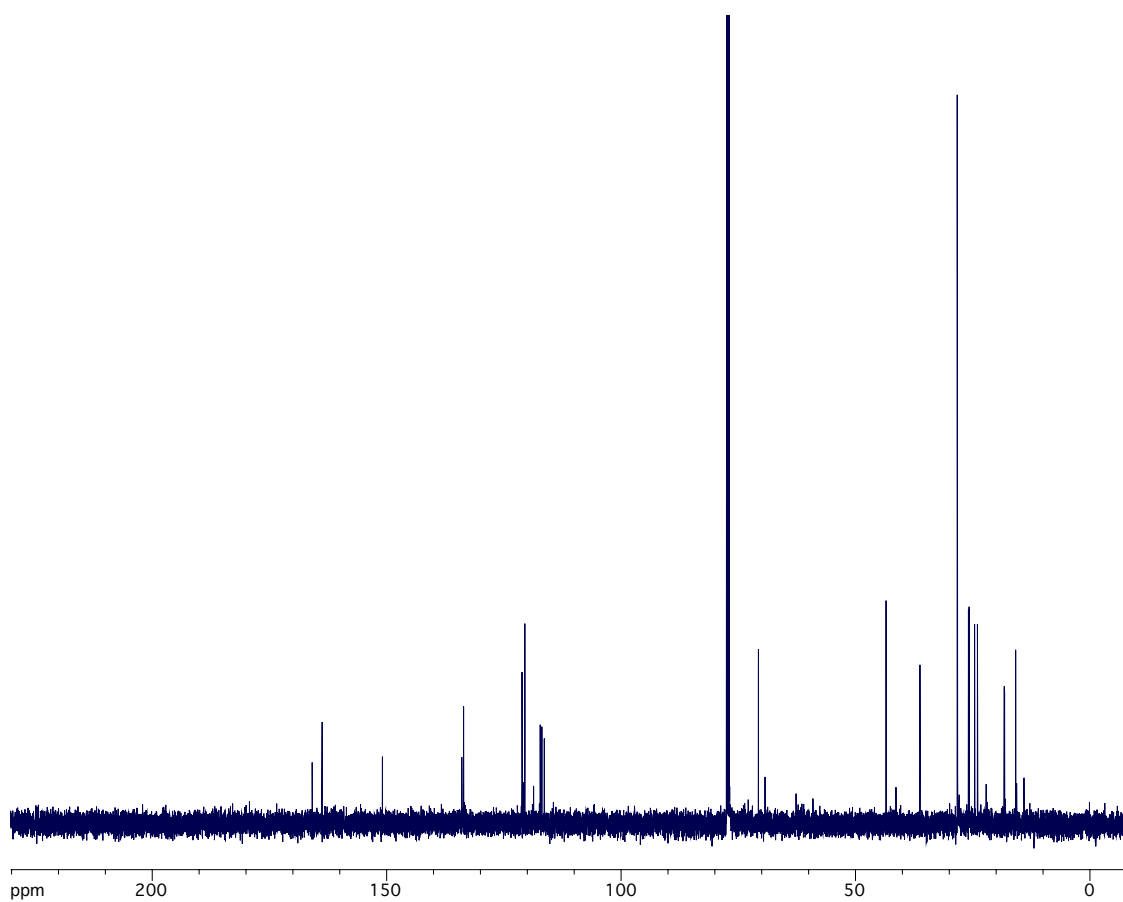
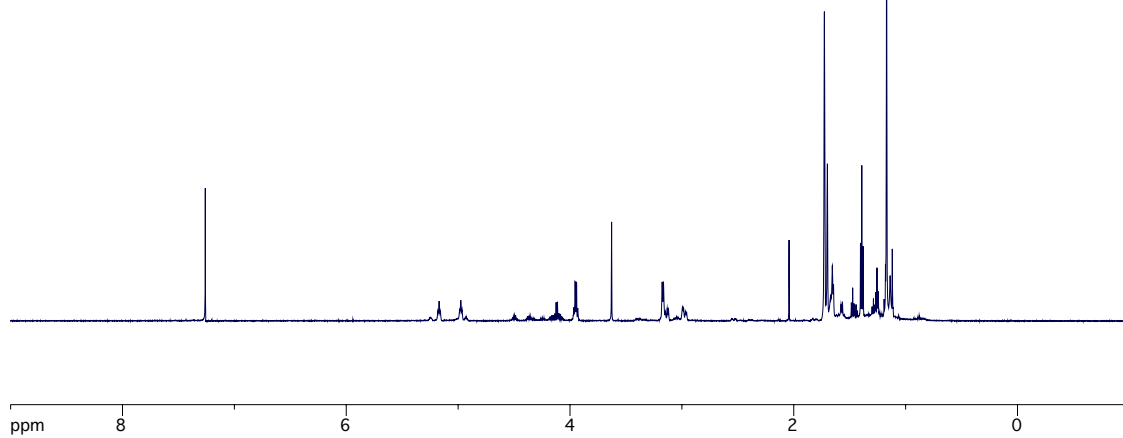


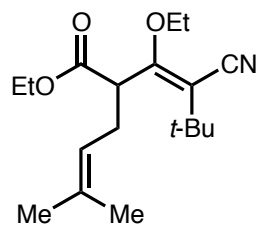




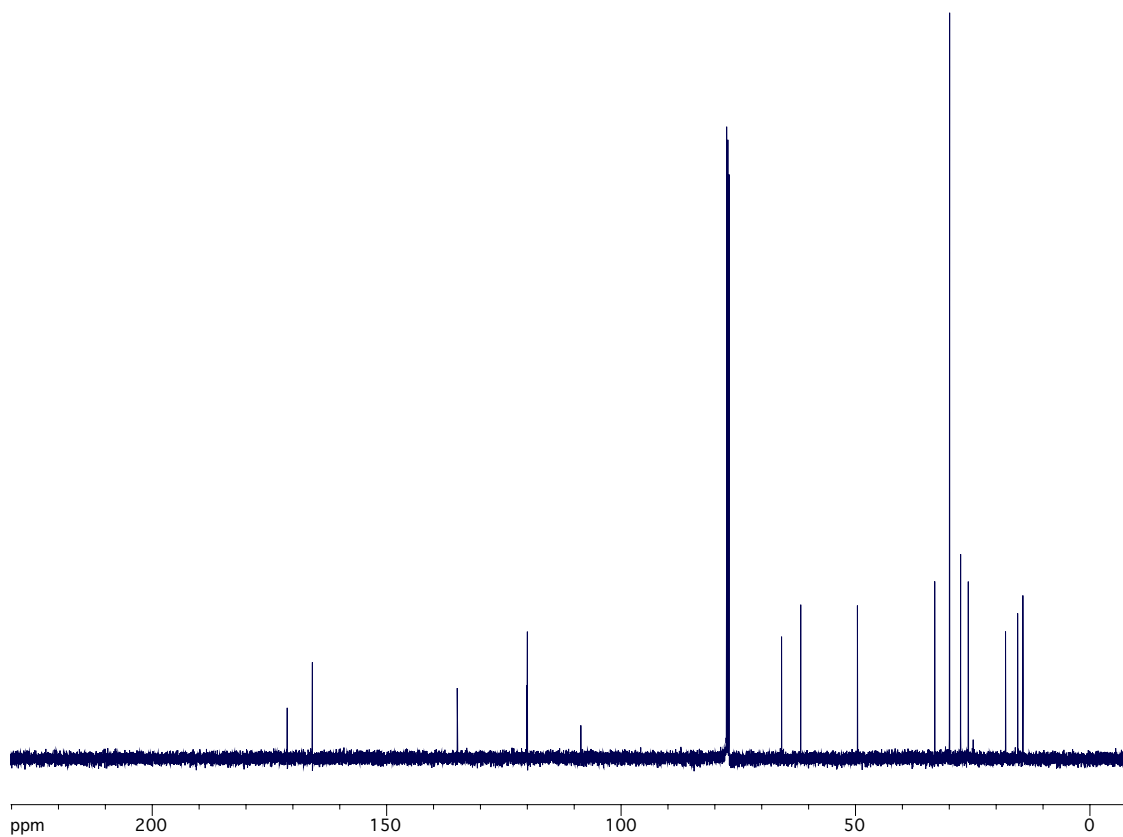
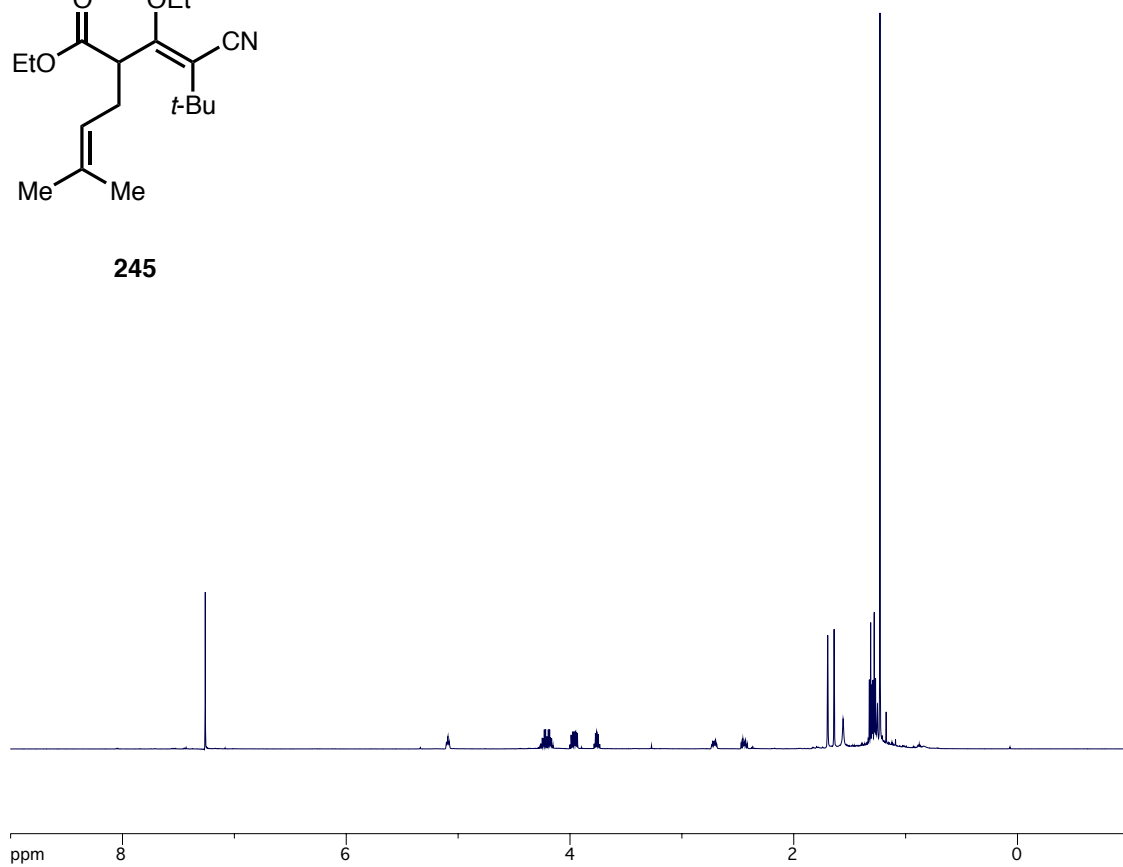


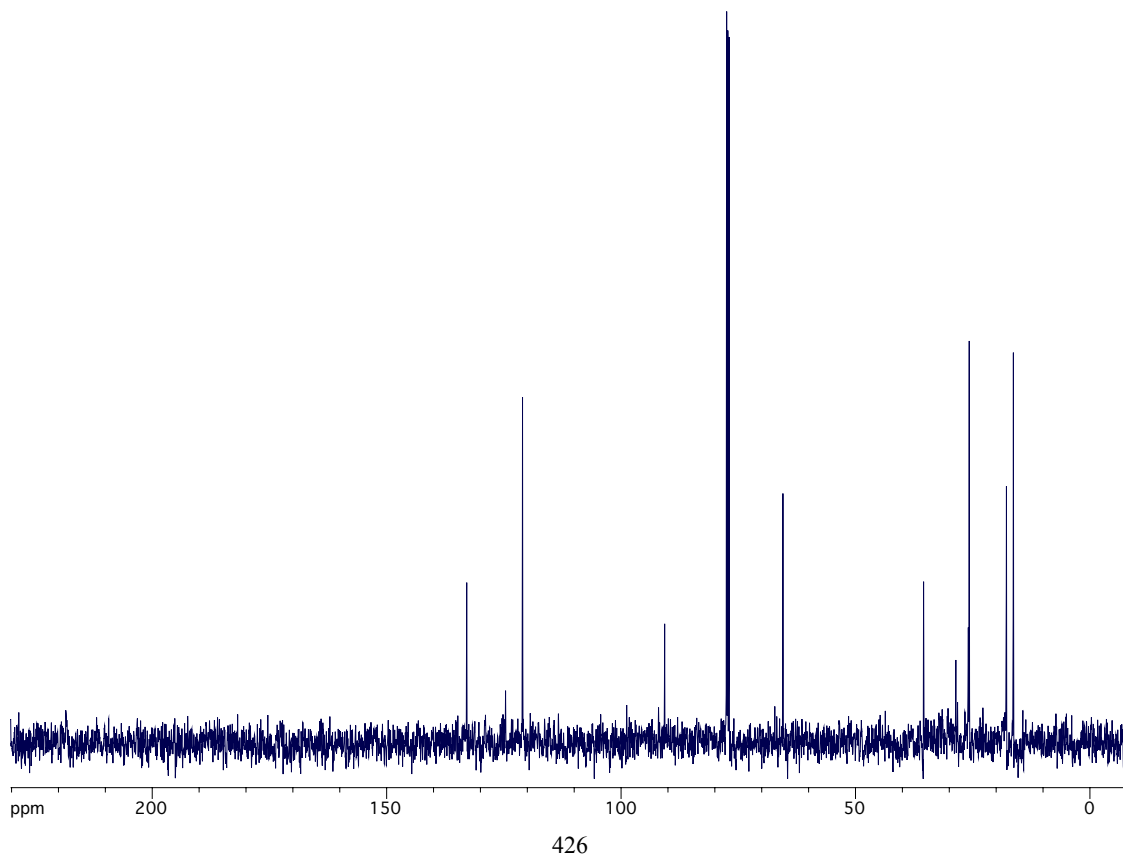
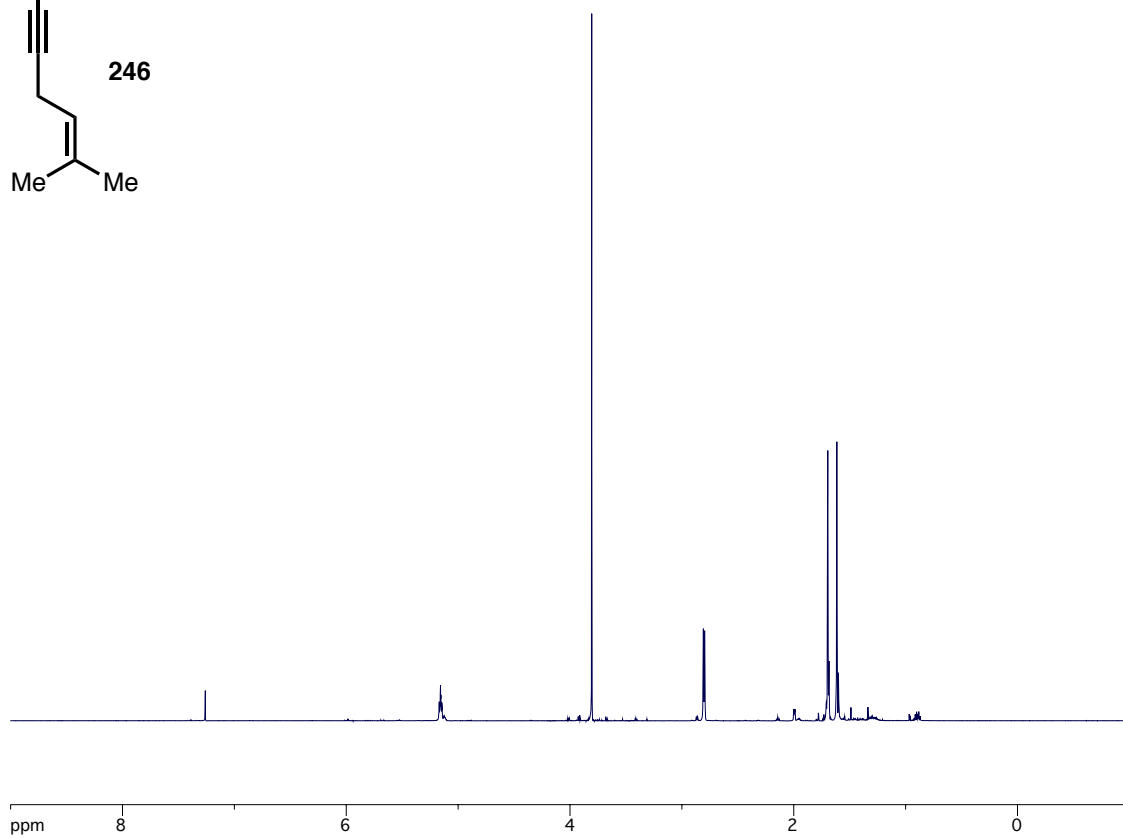
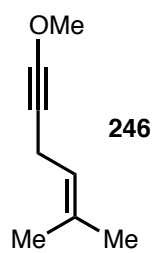
244

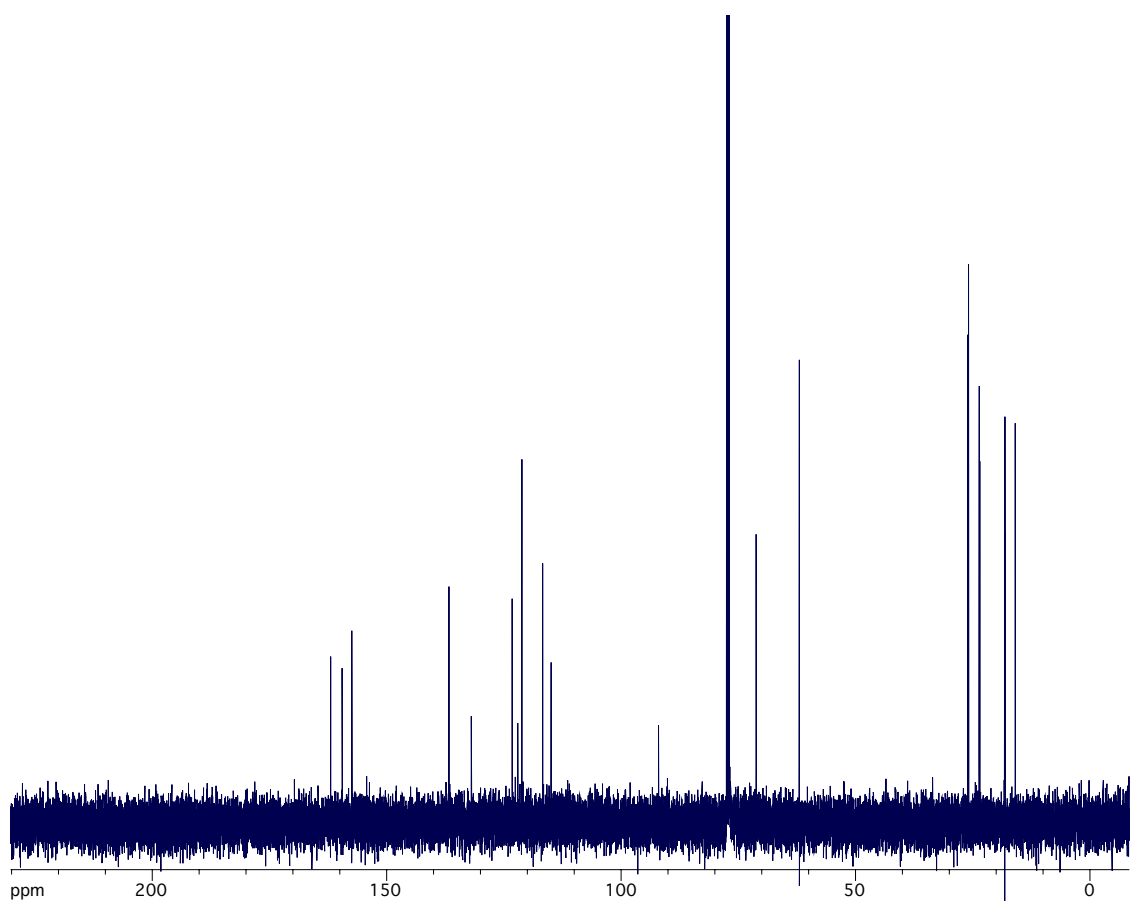
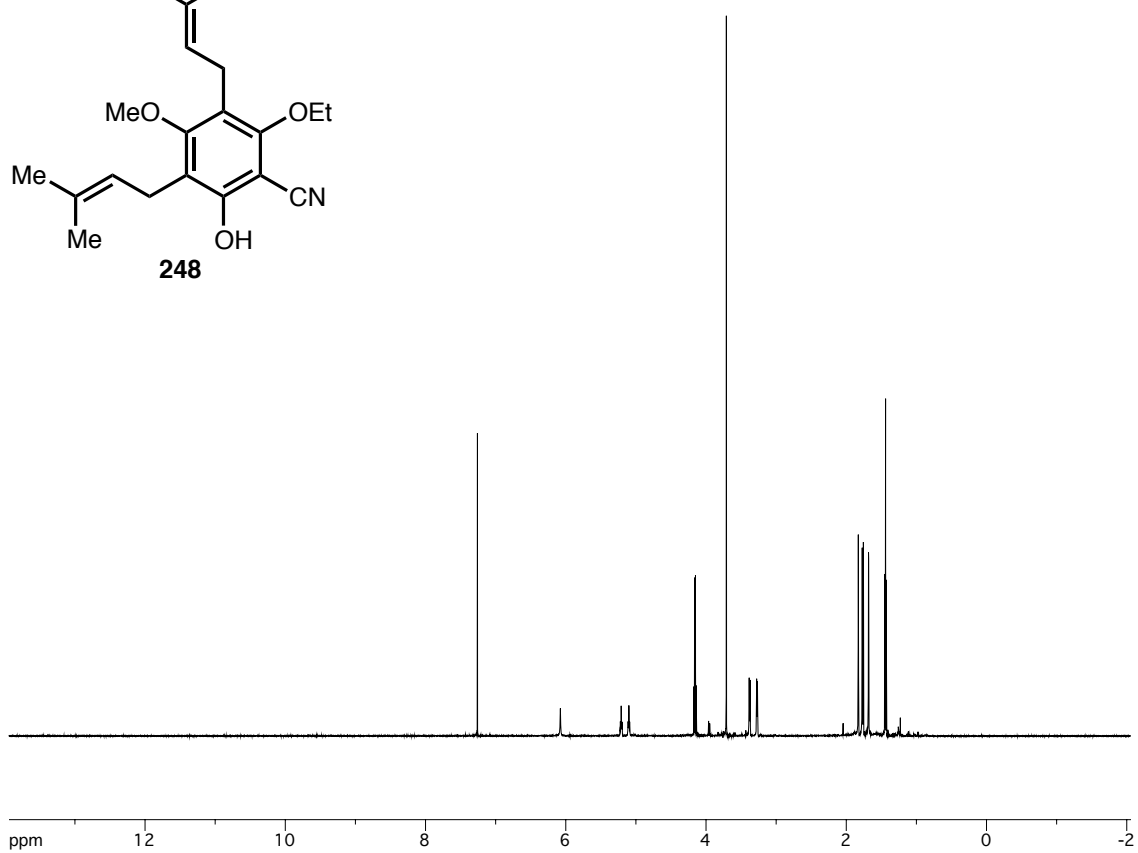
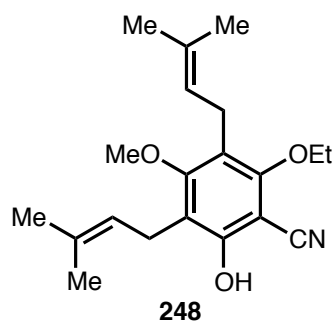


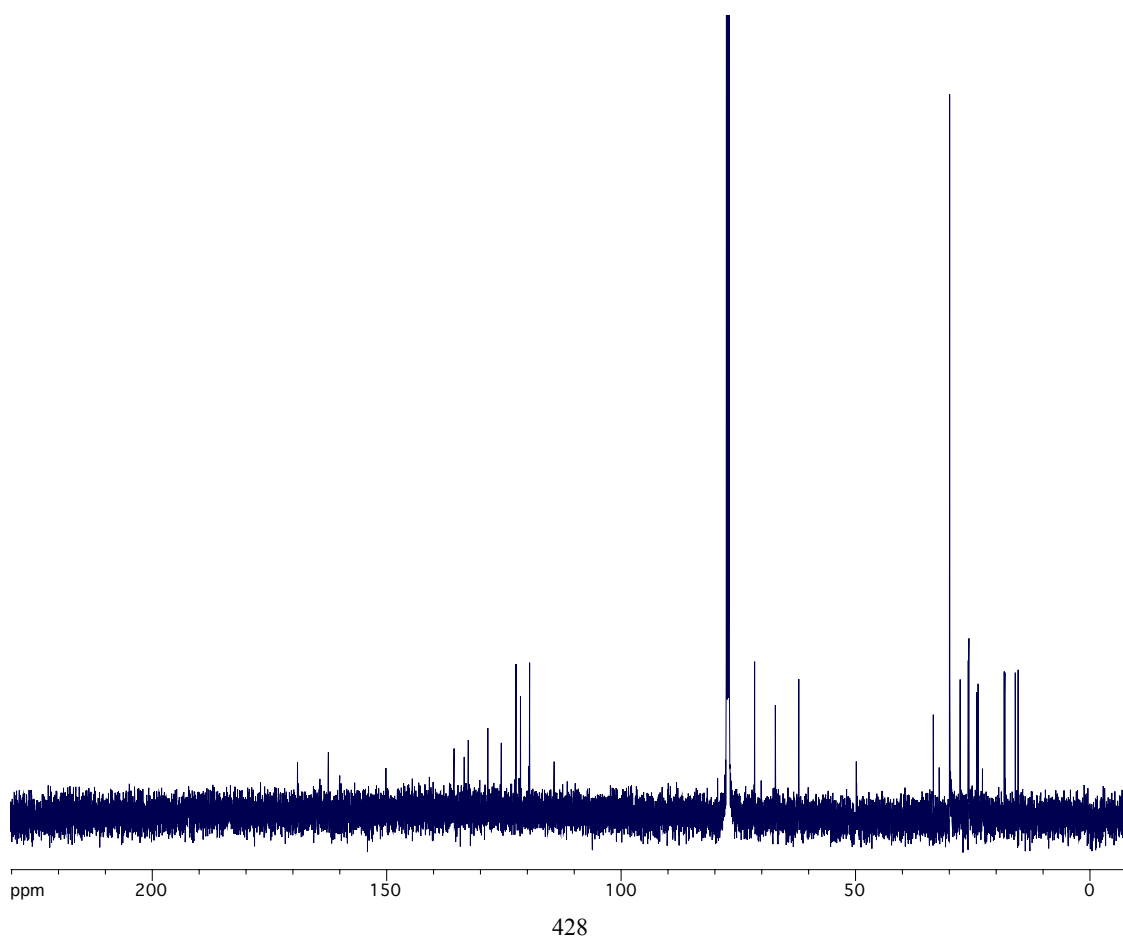
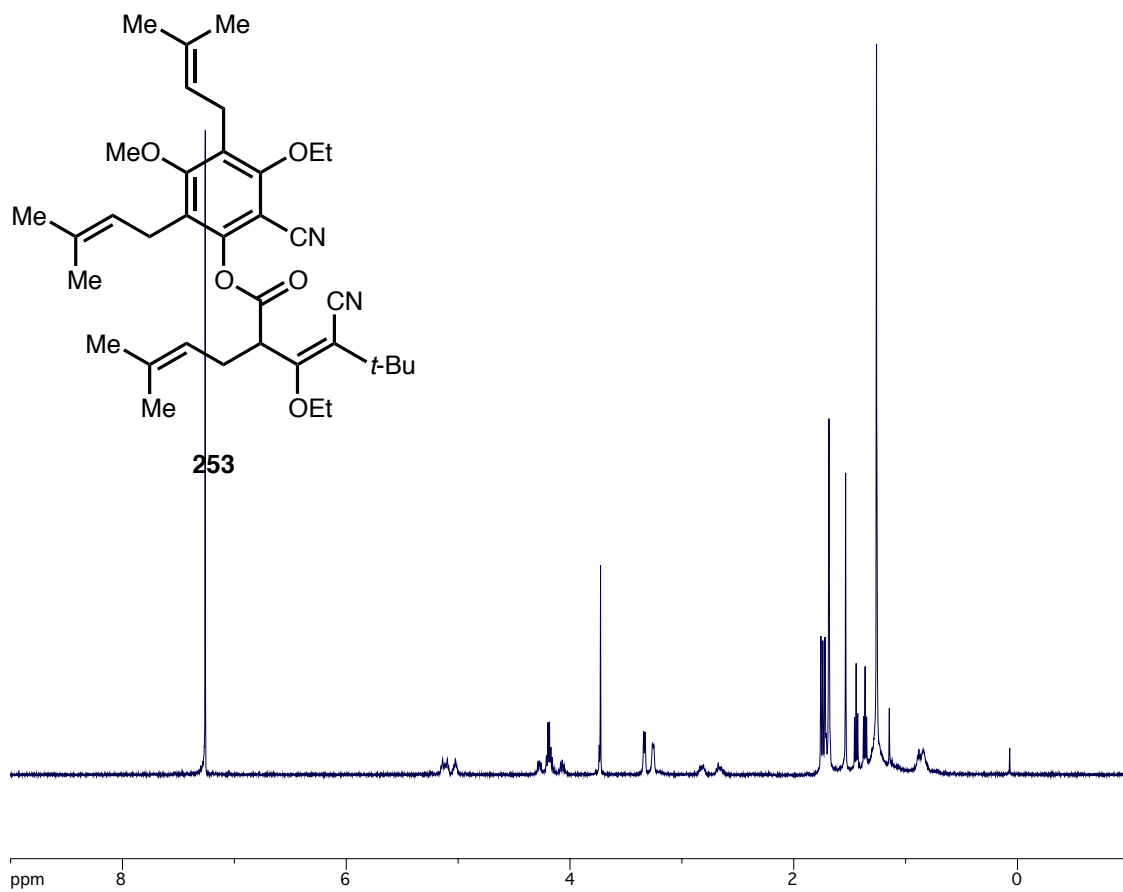


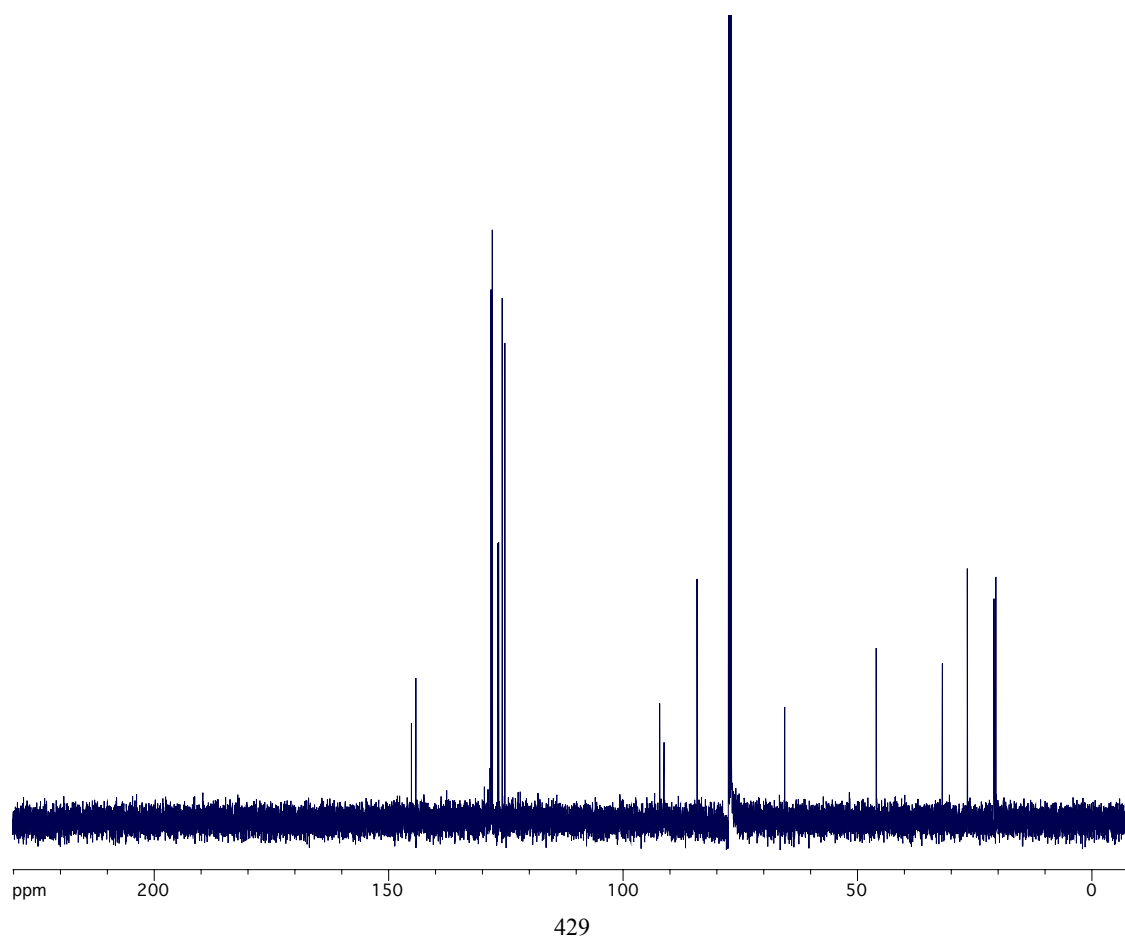
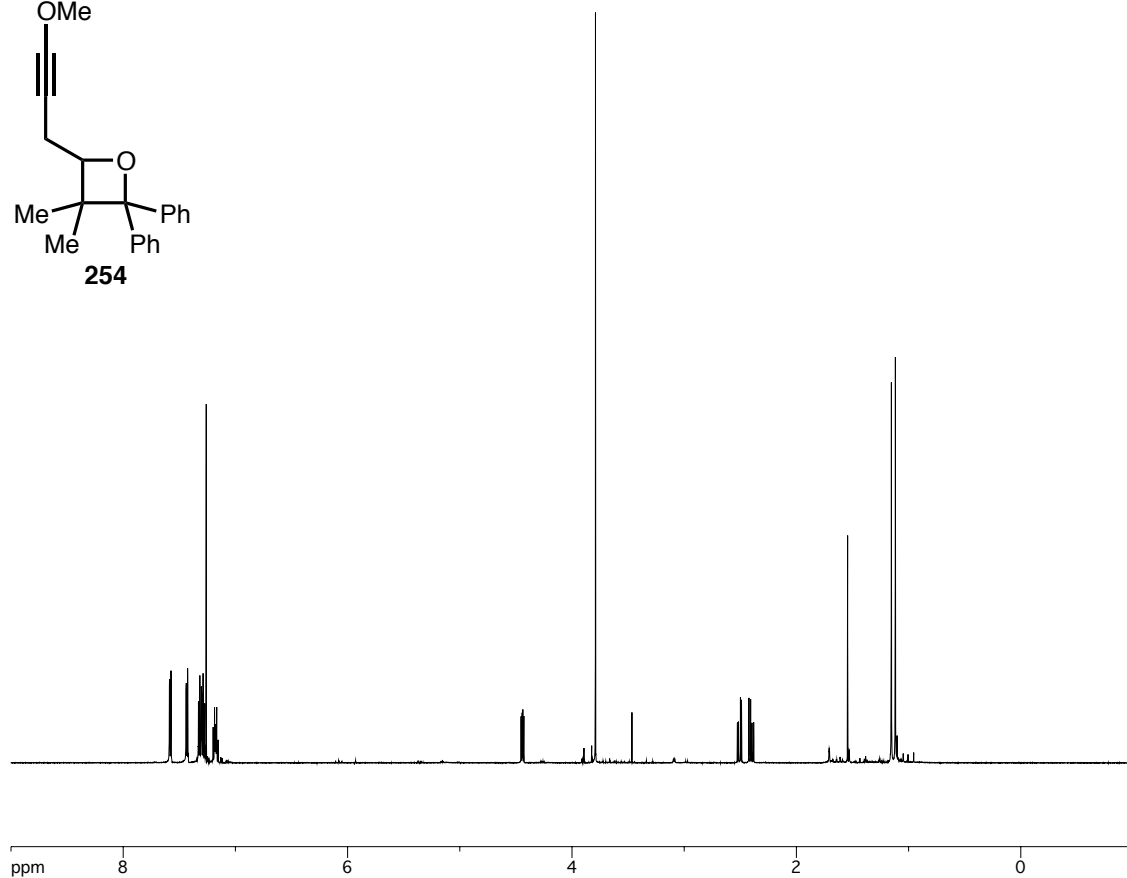
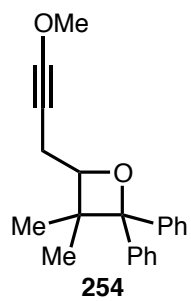
245

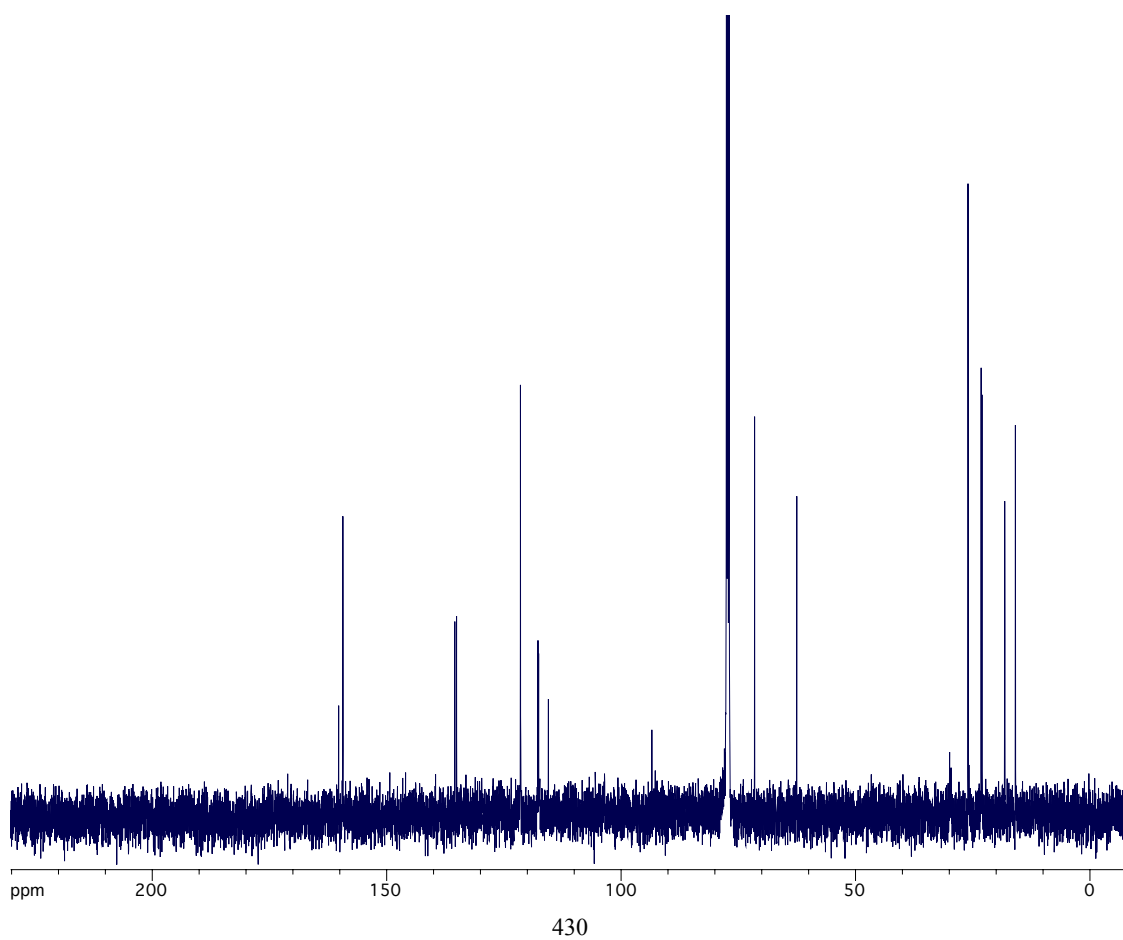
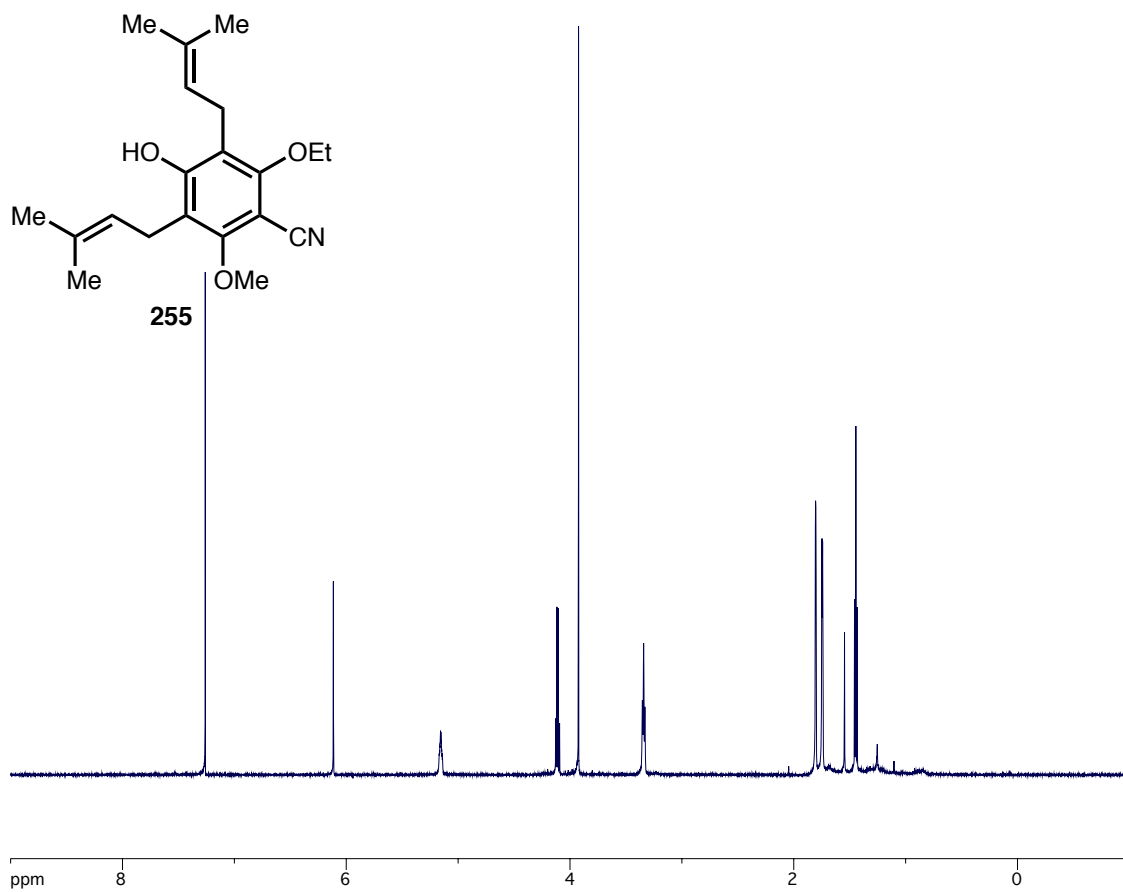


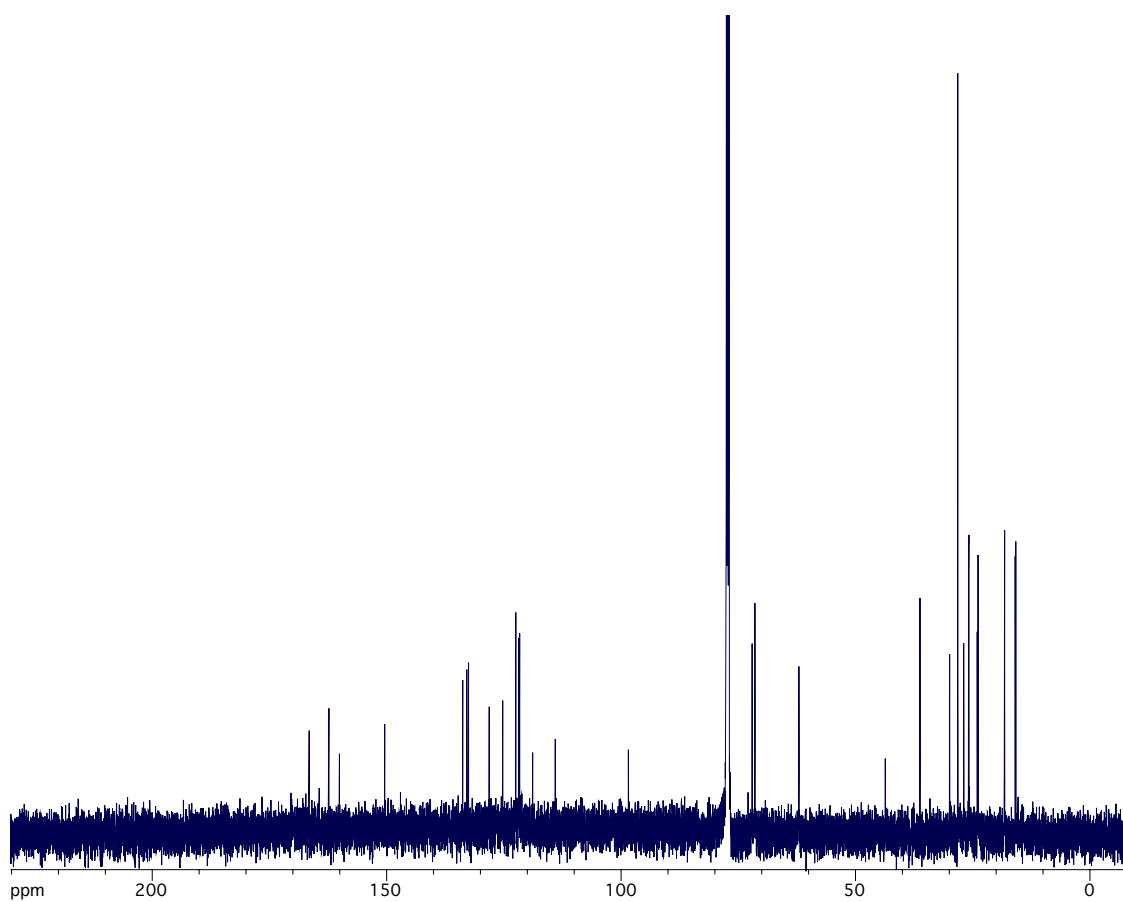


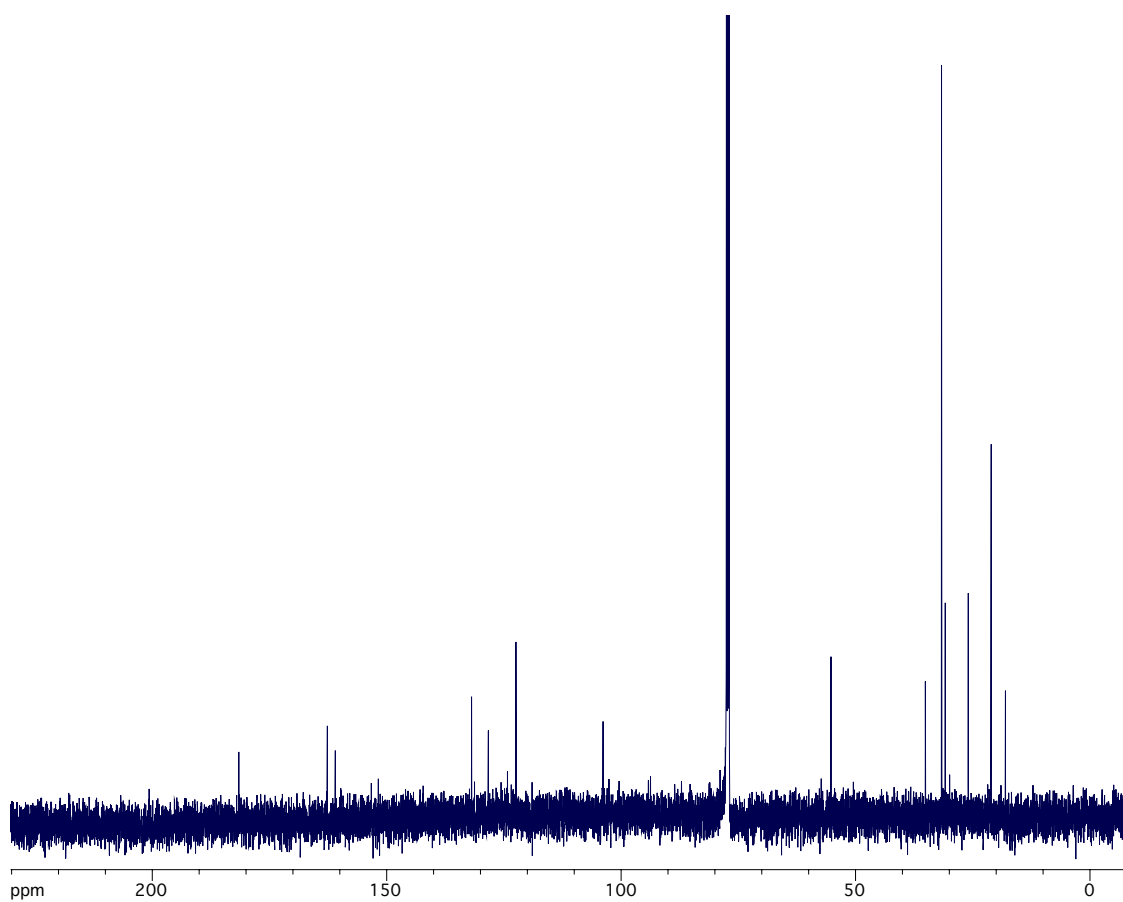
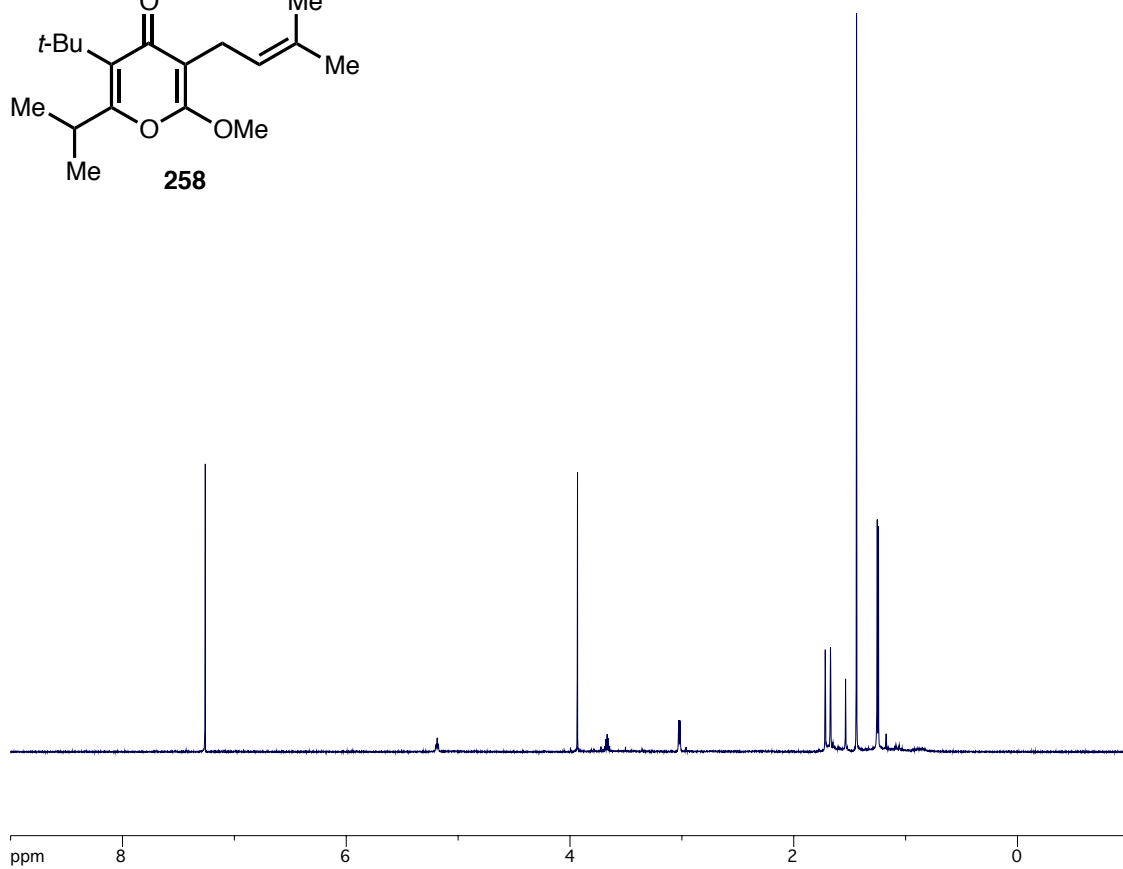
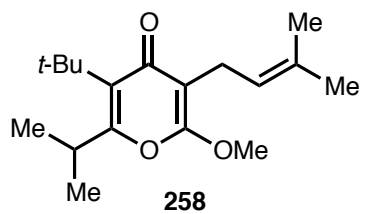


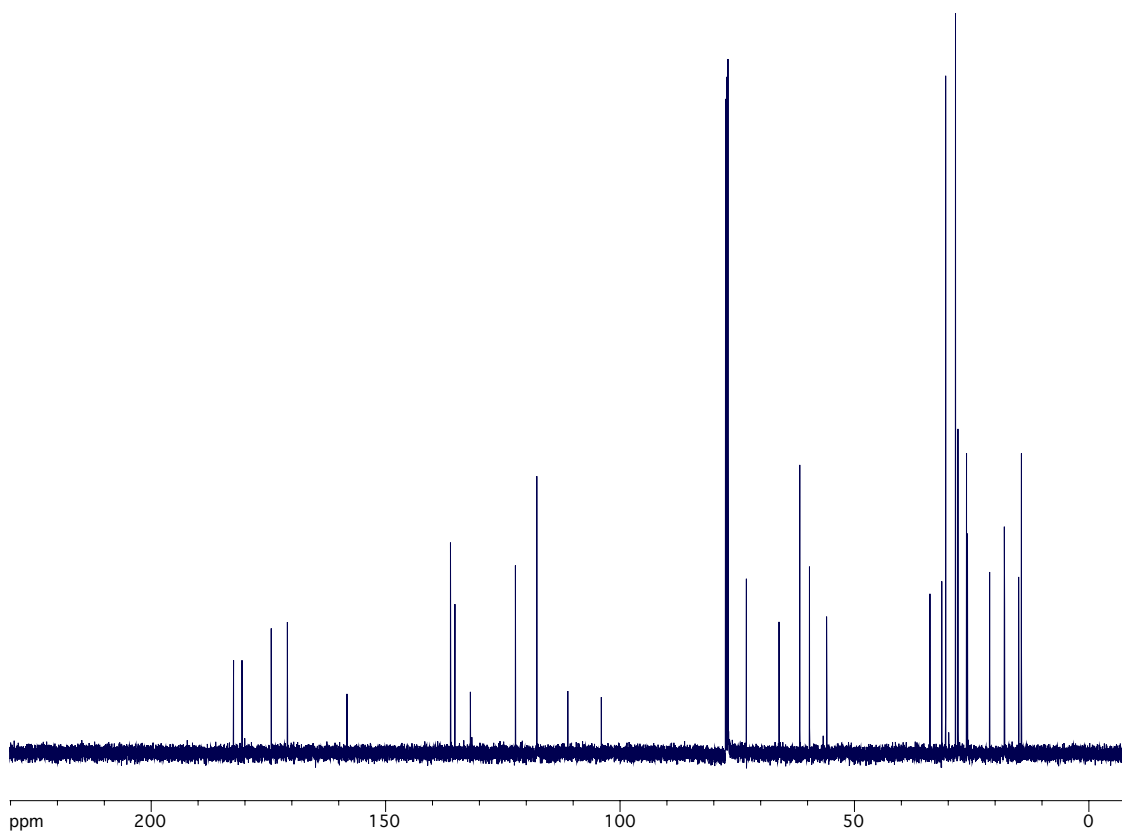
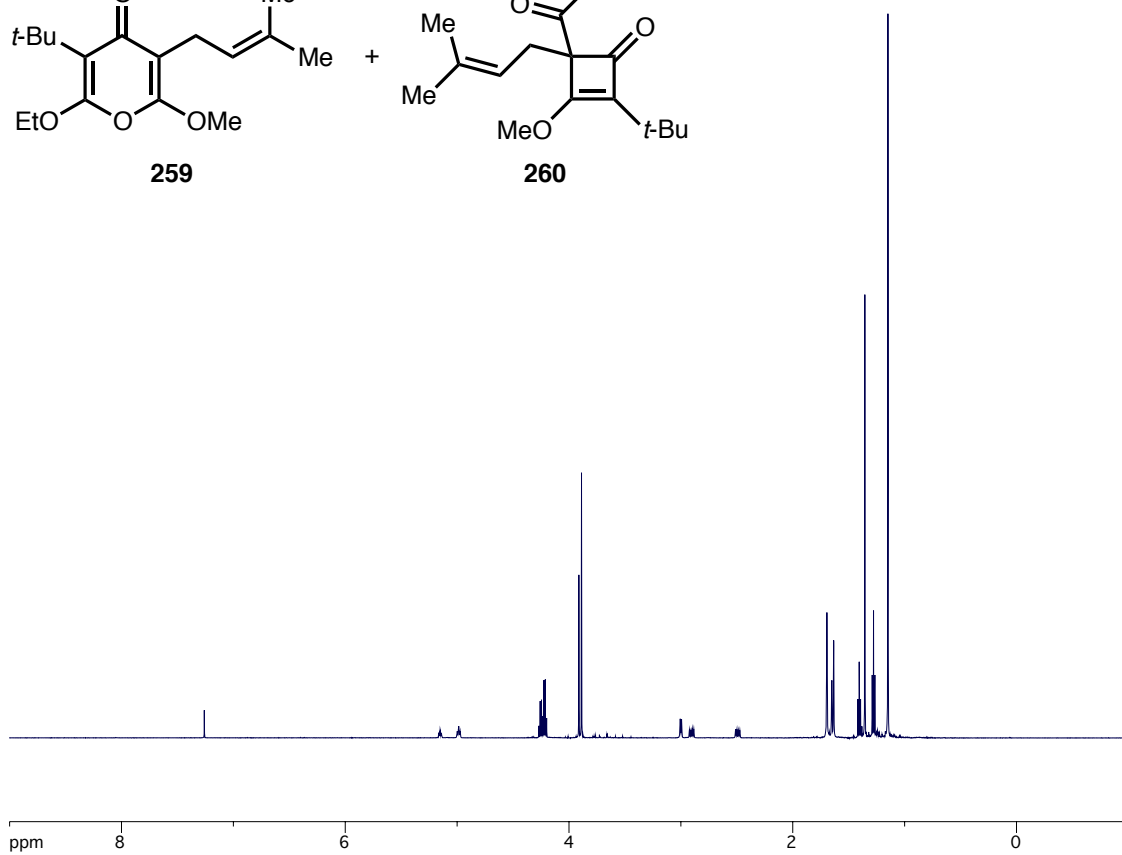
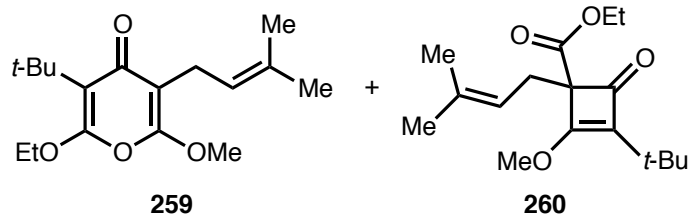


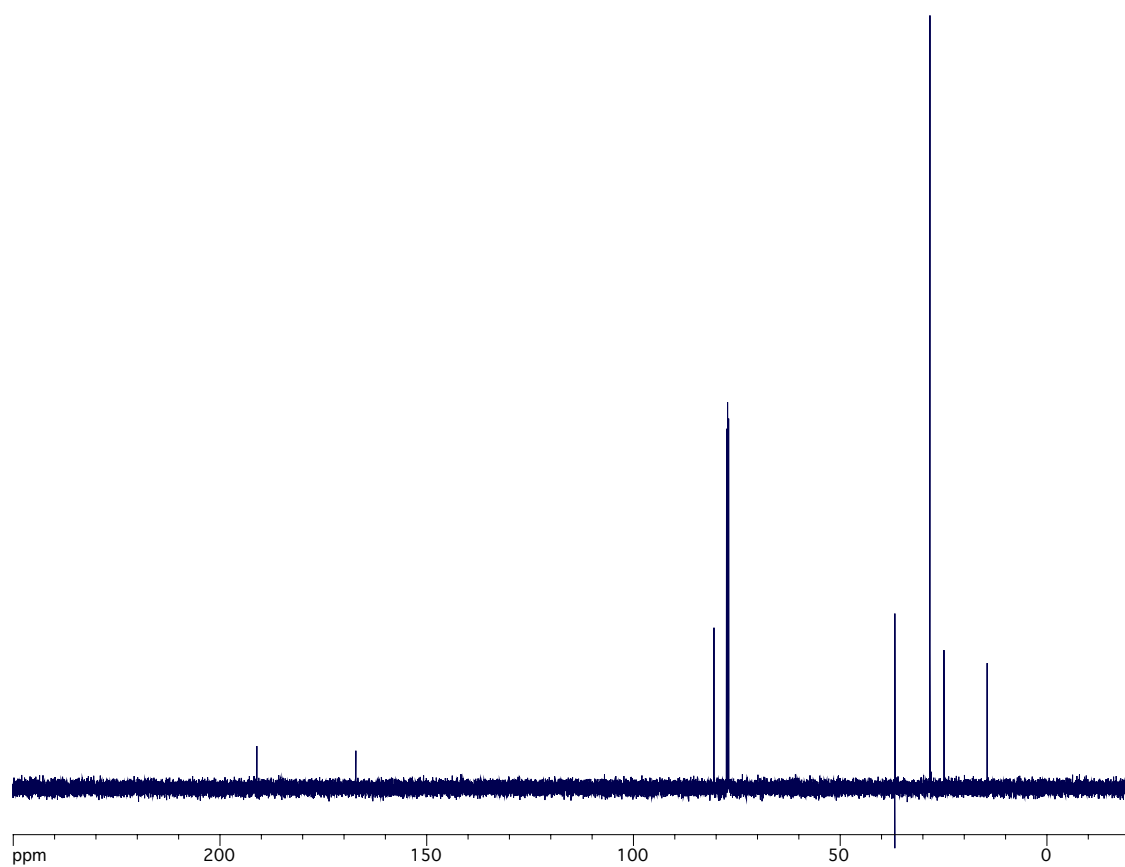
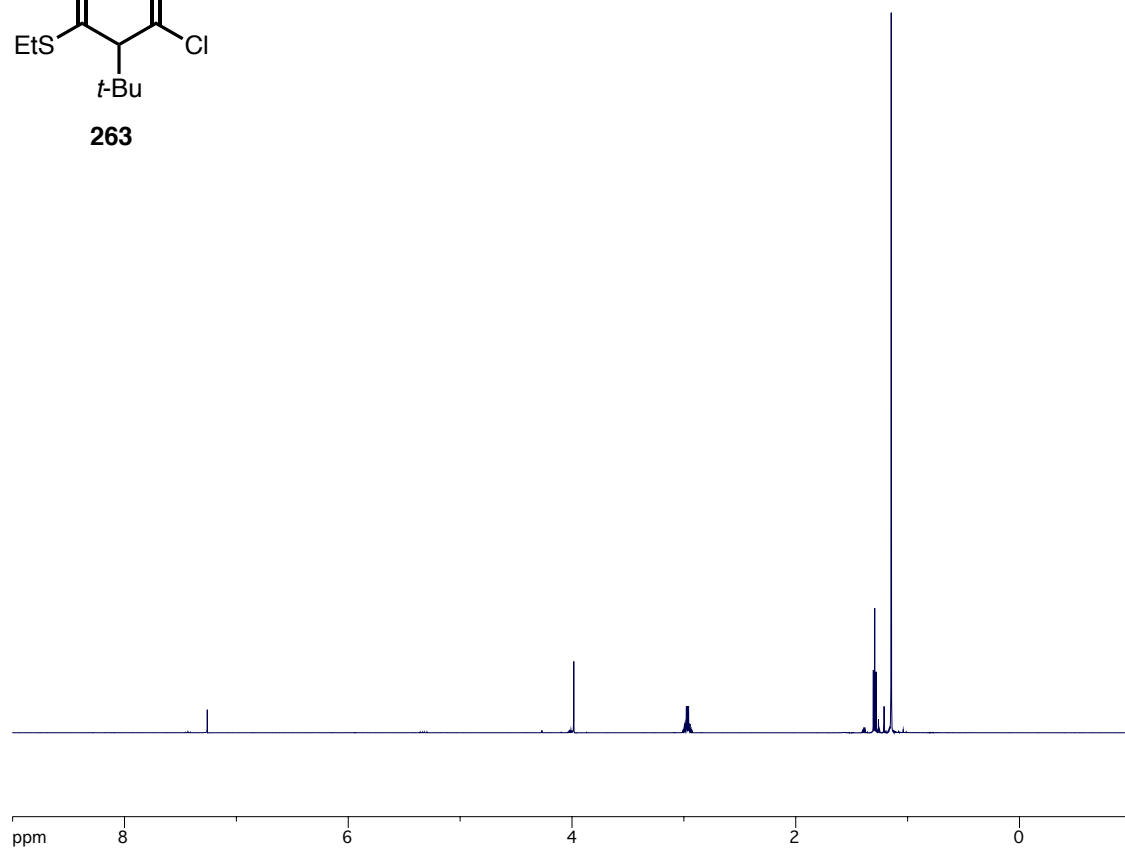
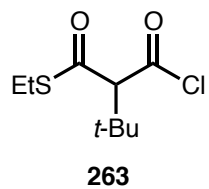


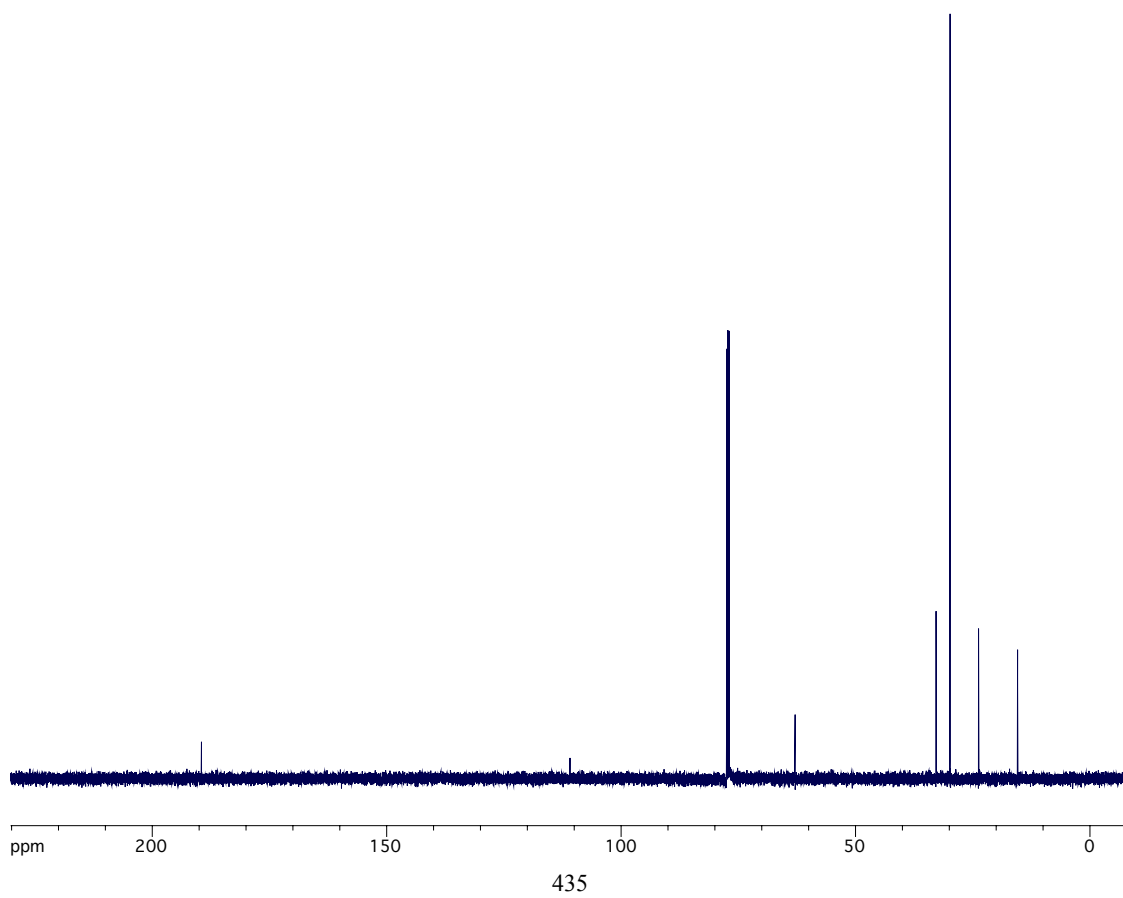
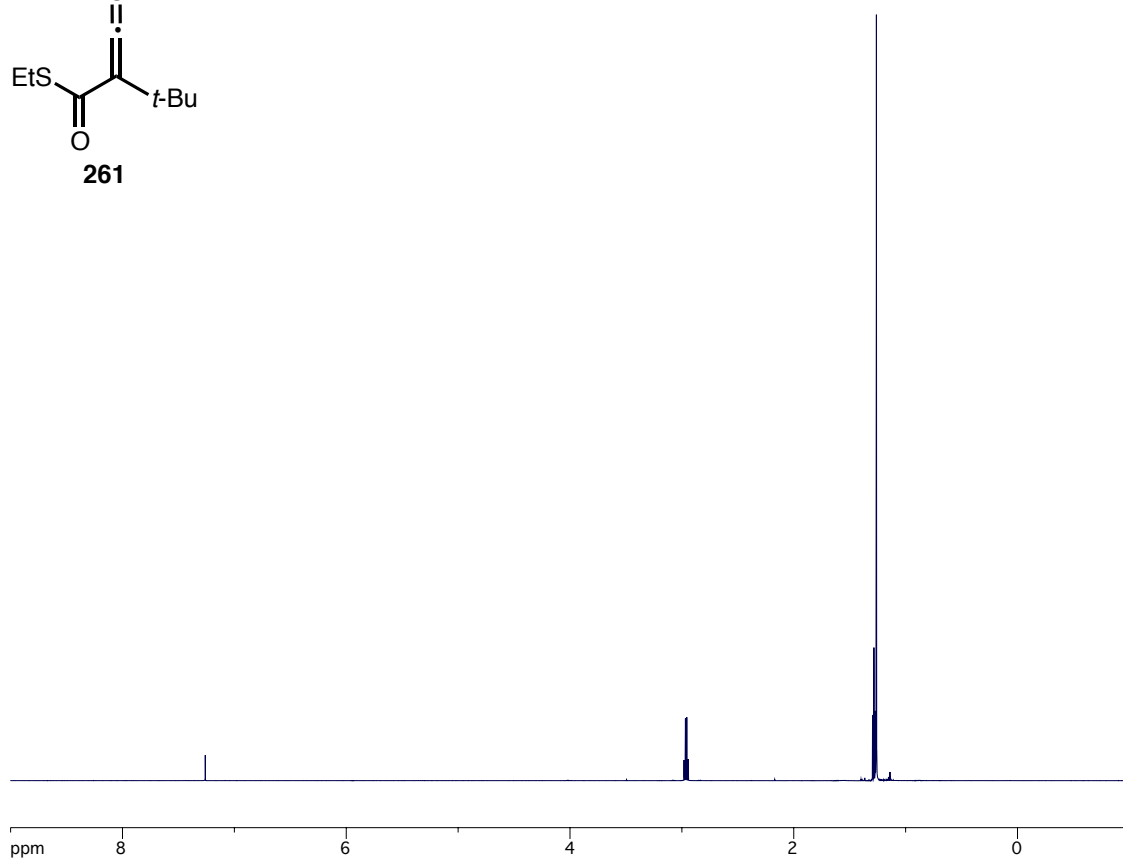
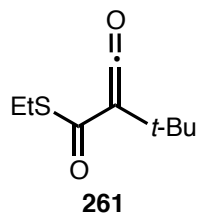


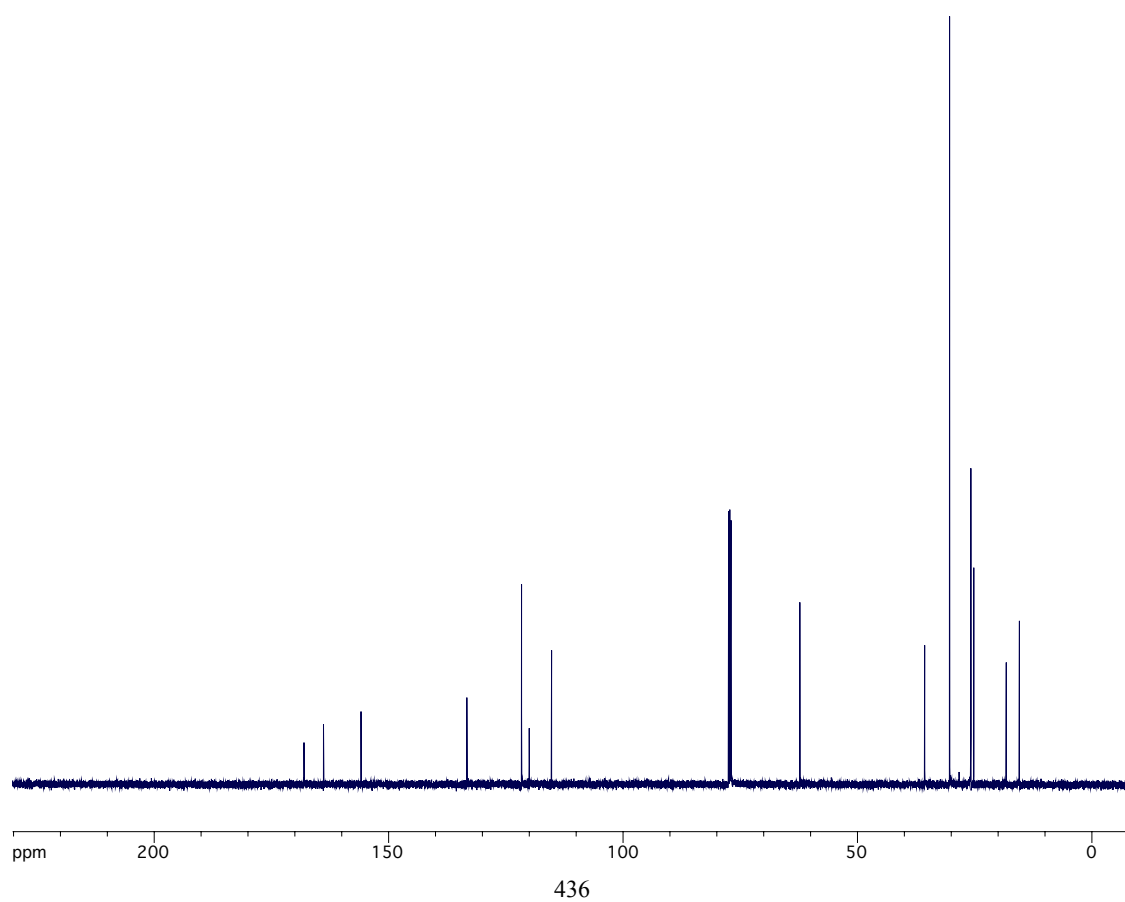
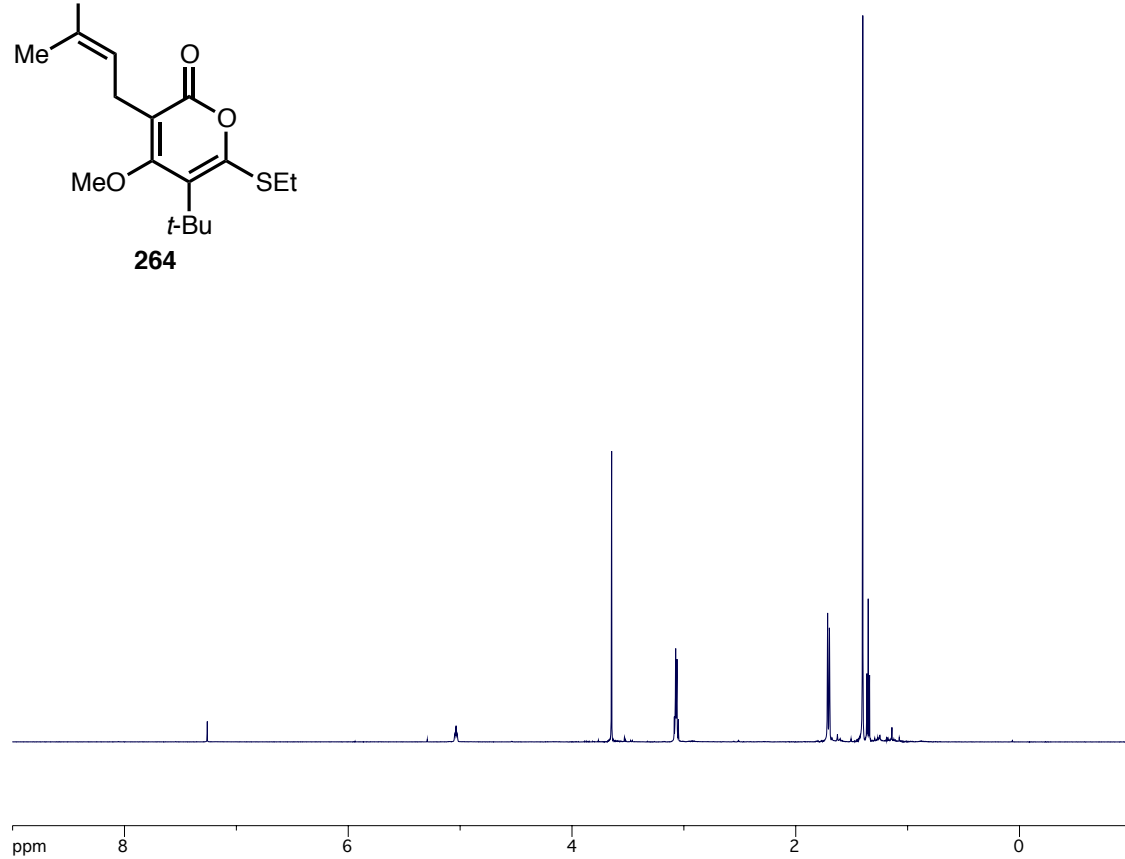
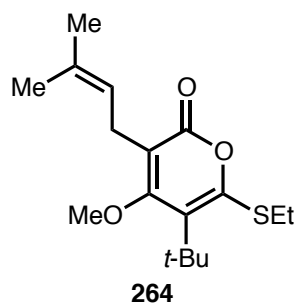


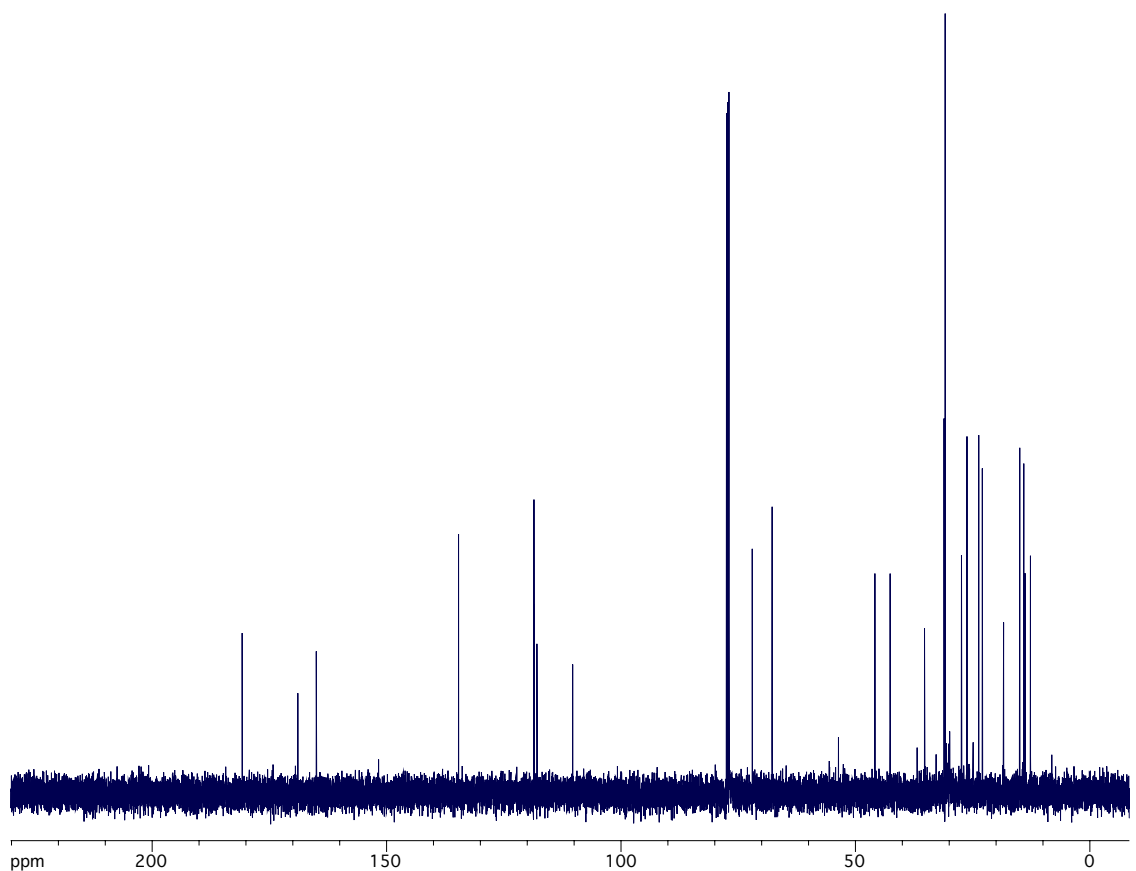
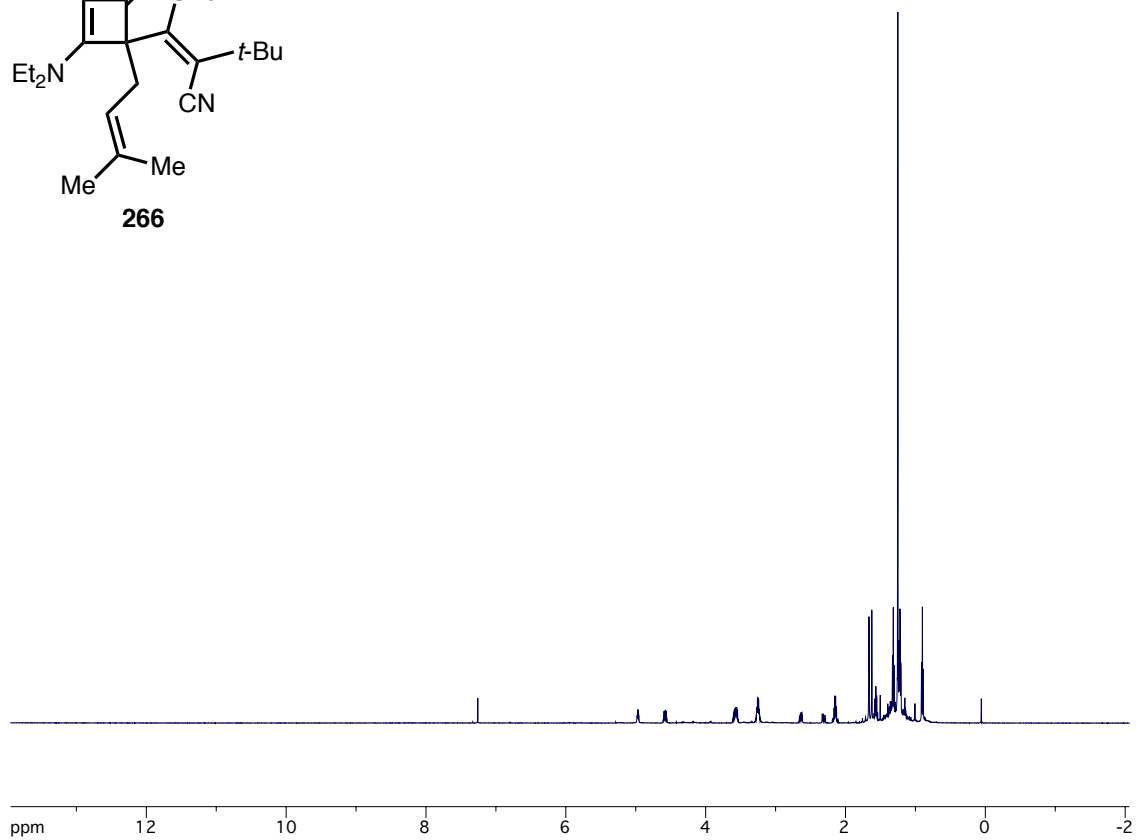
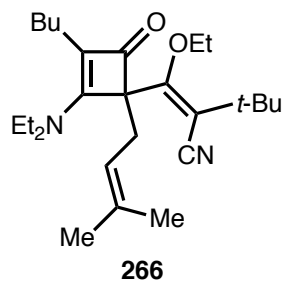


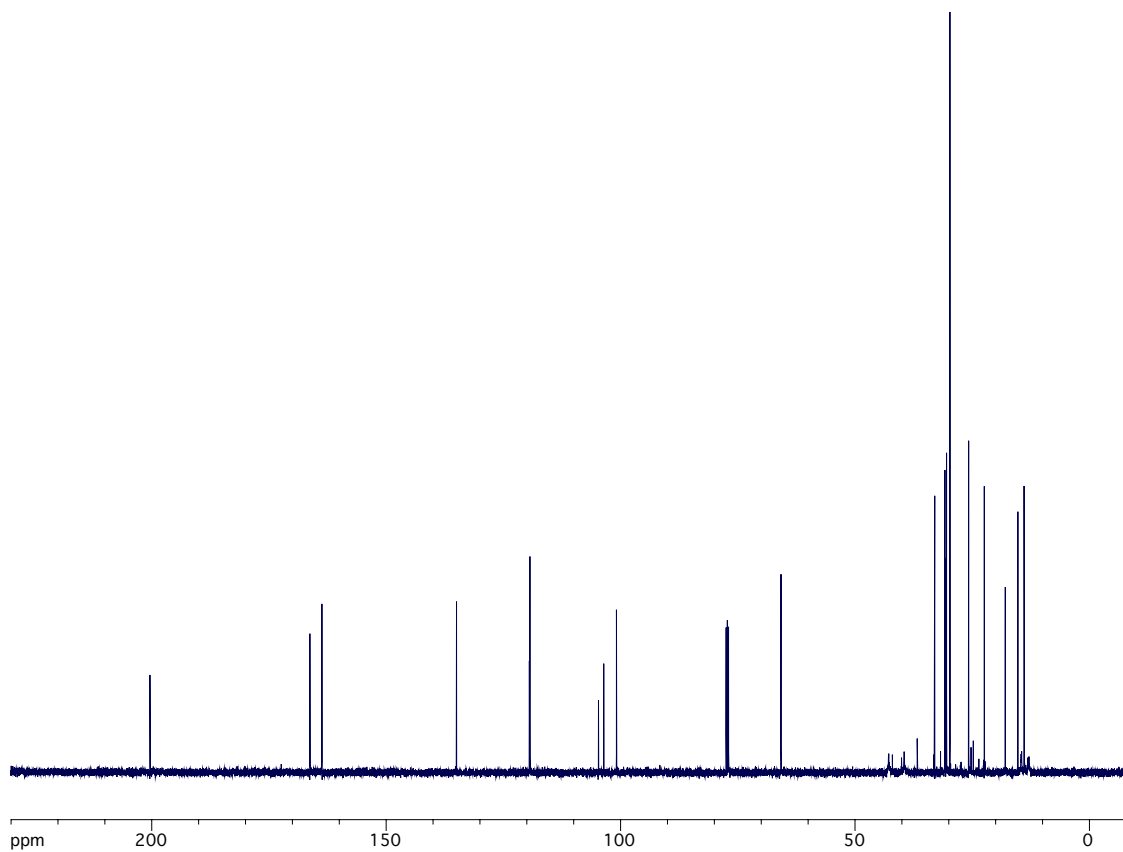
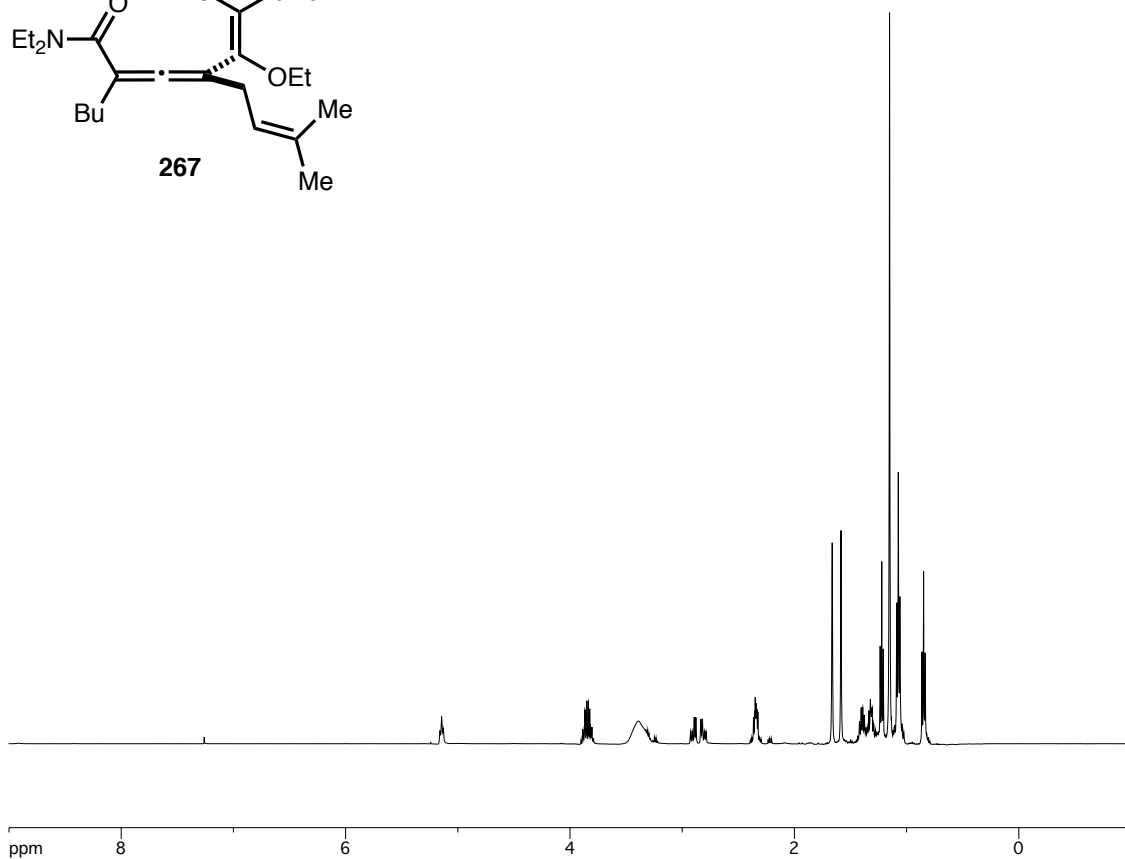


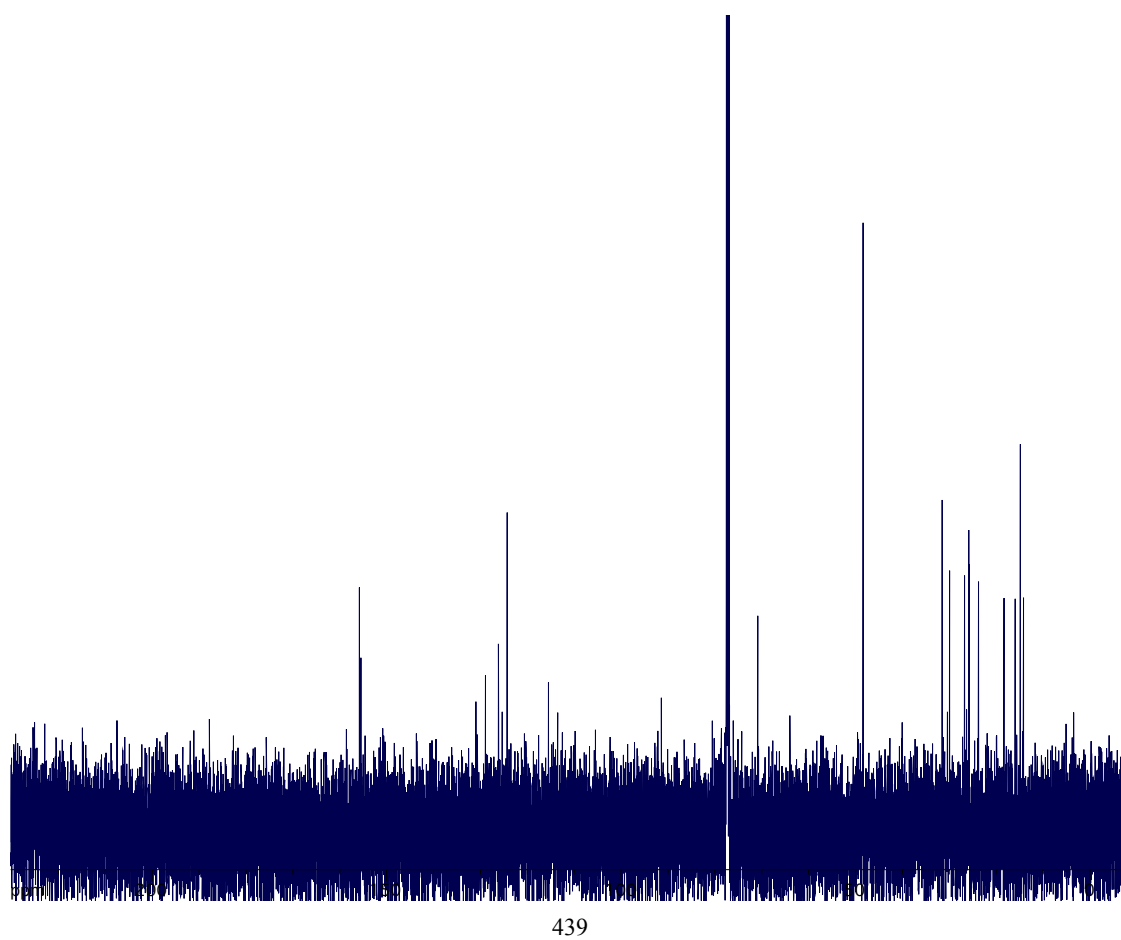
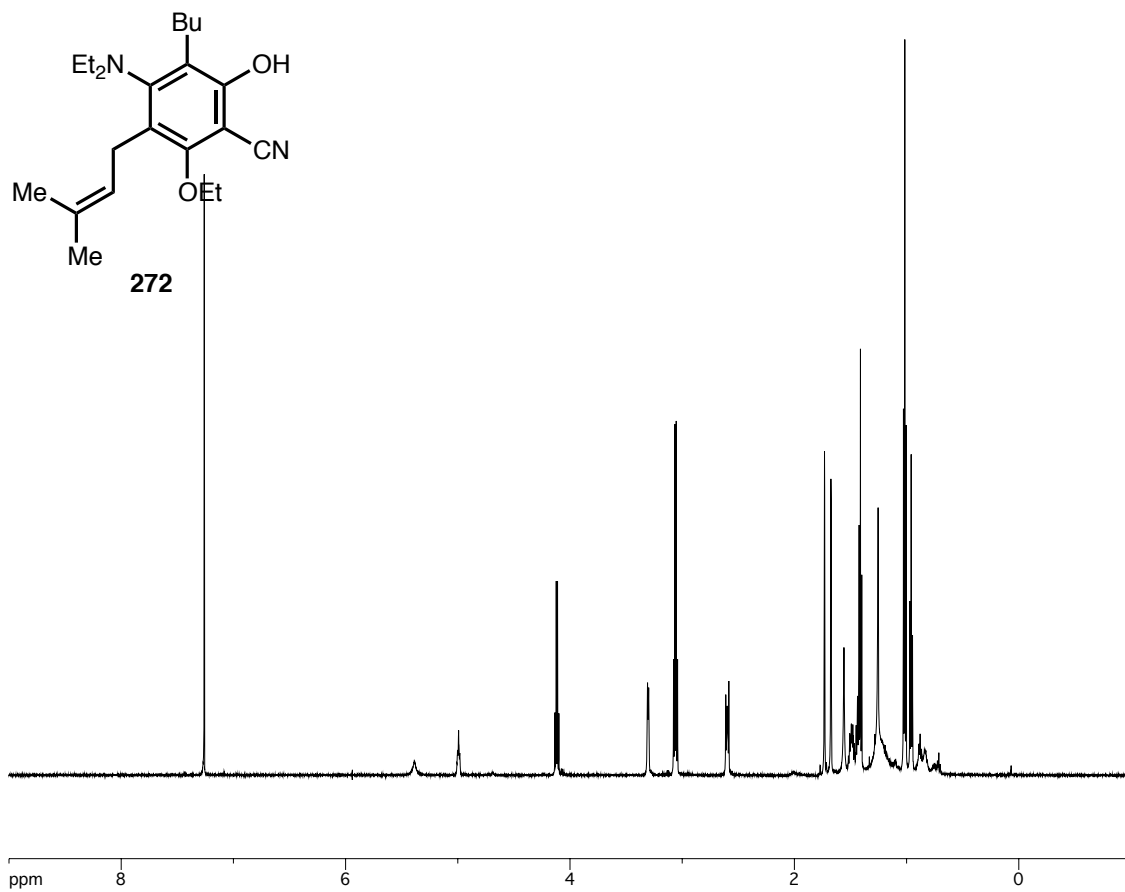


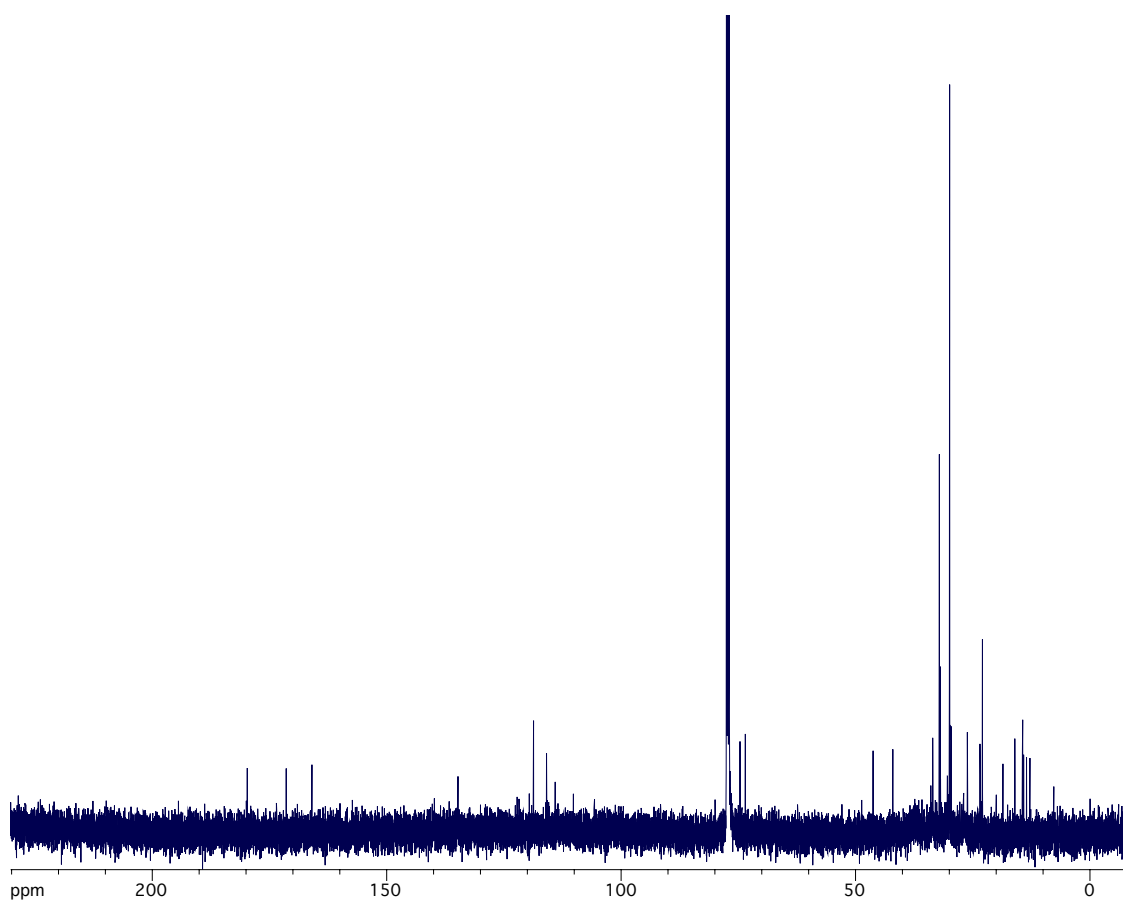
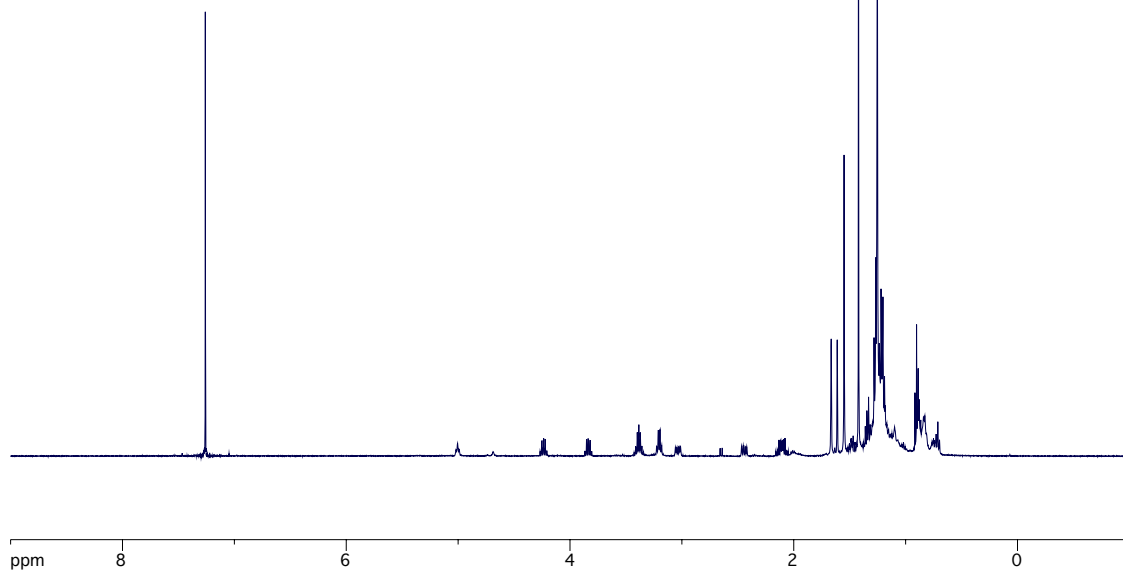
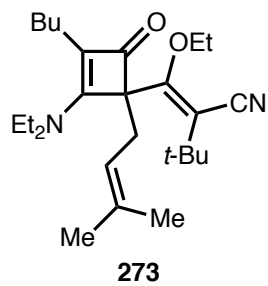


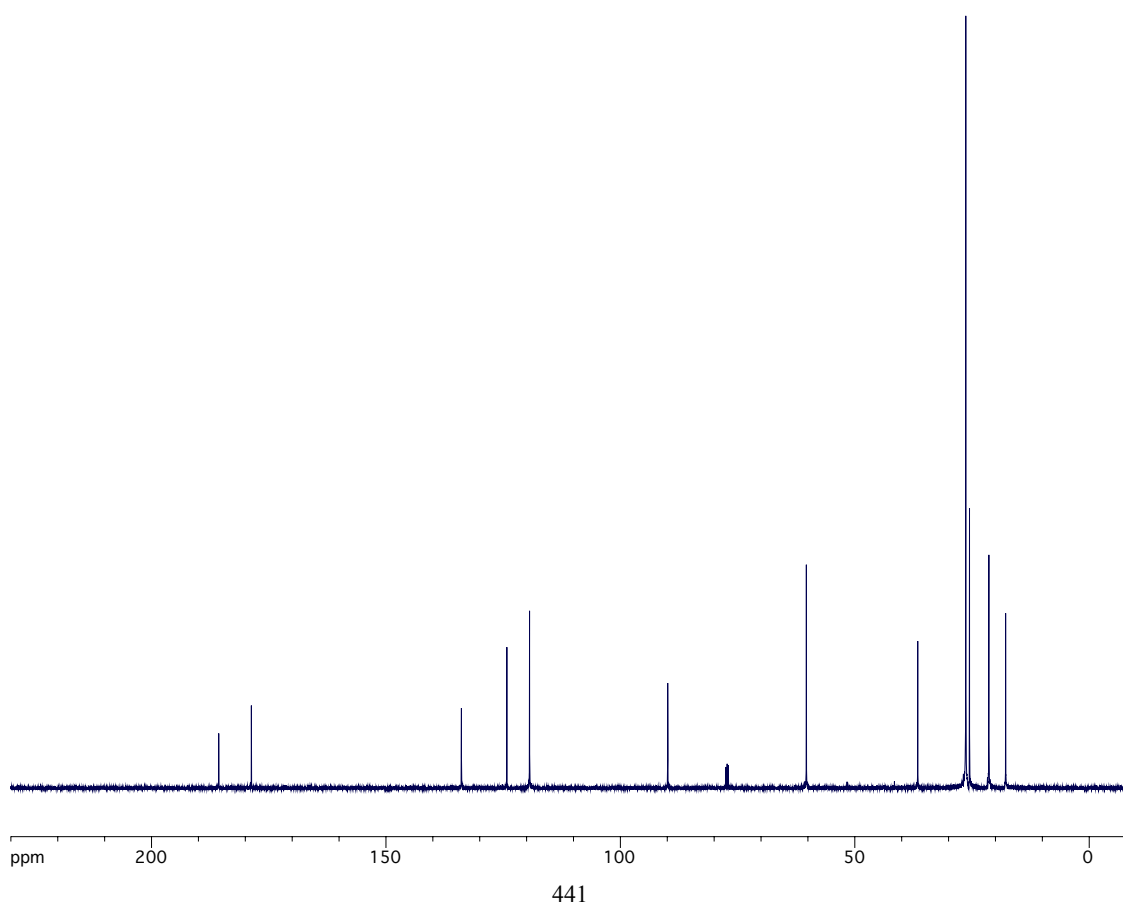
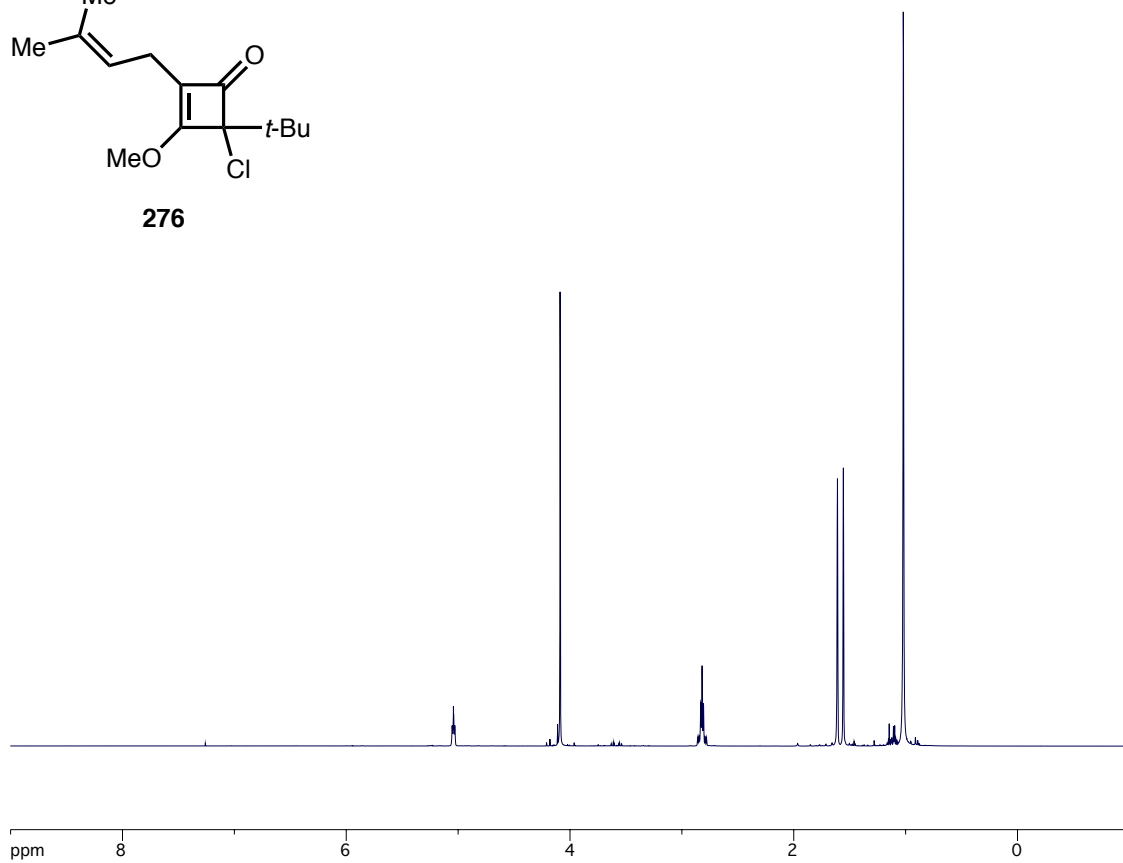
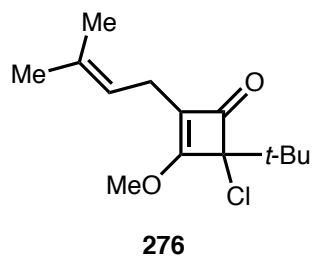


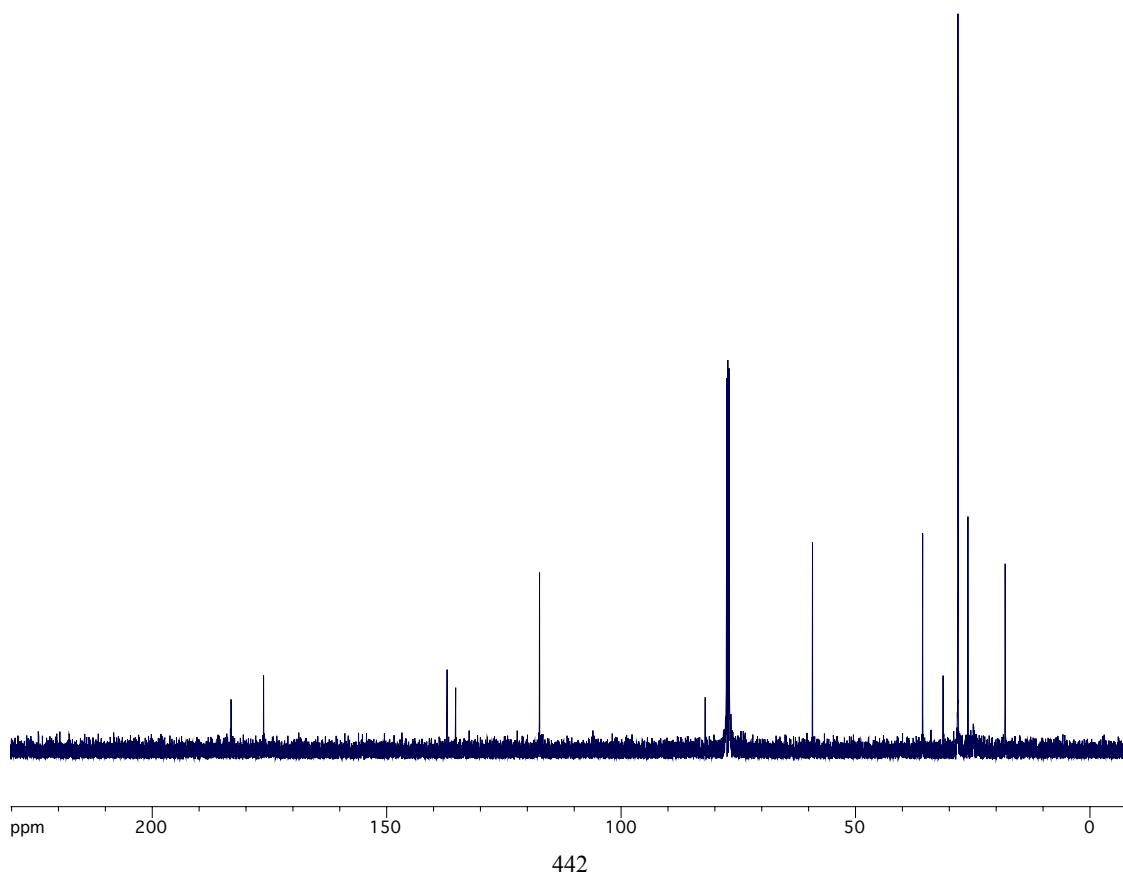
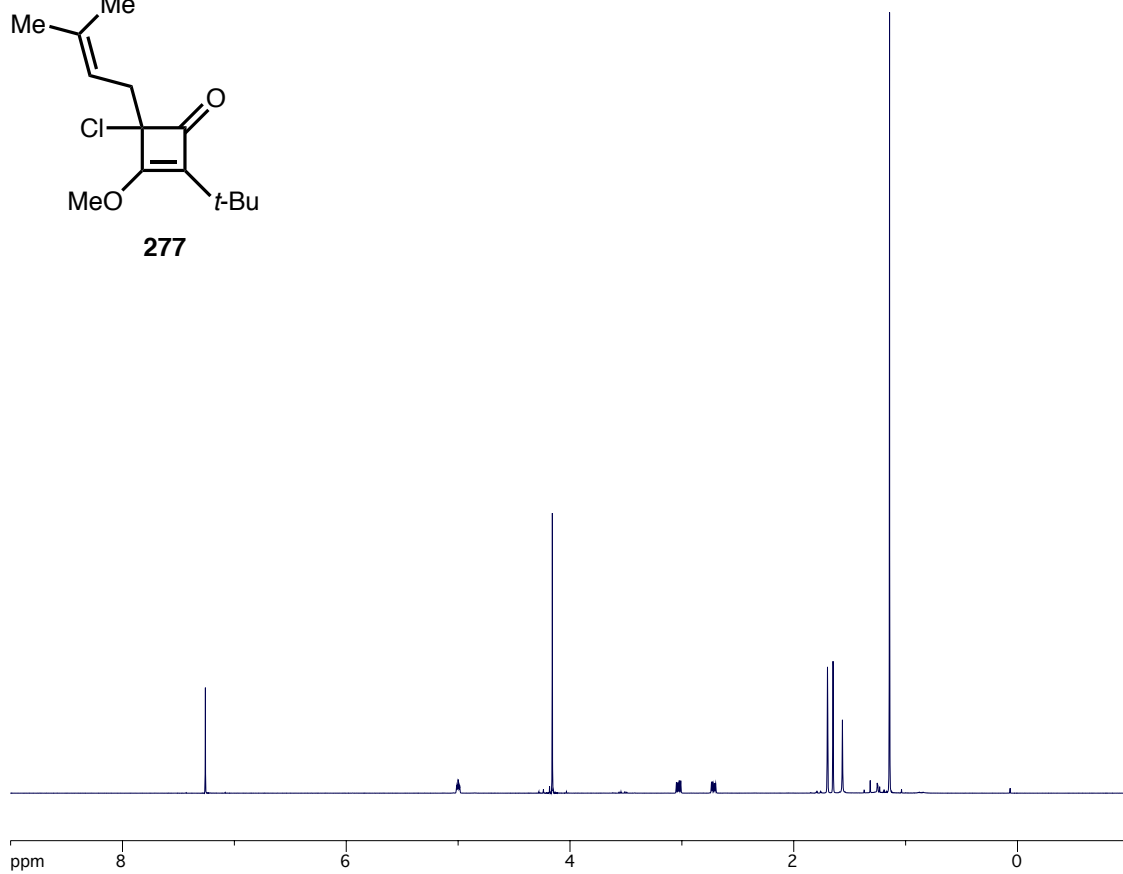
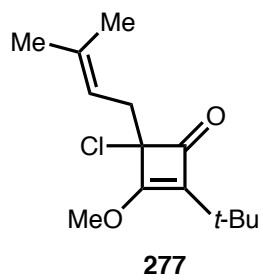


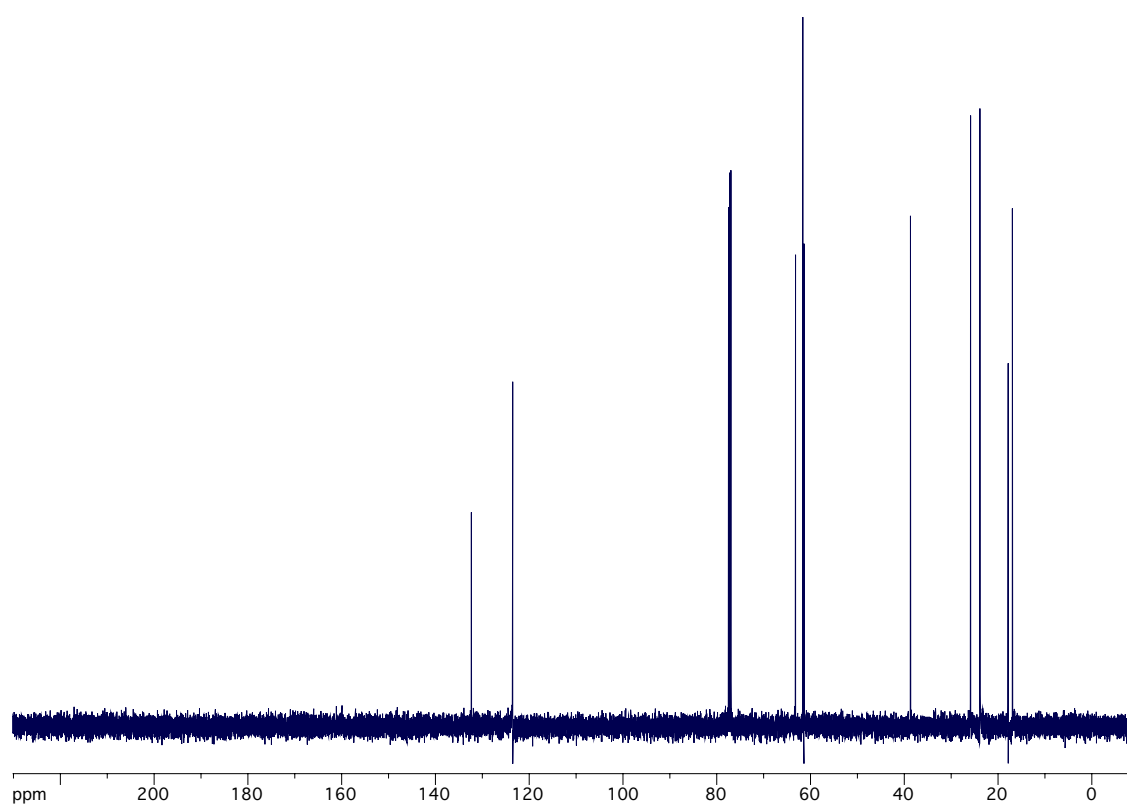
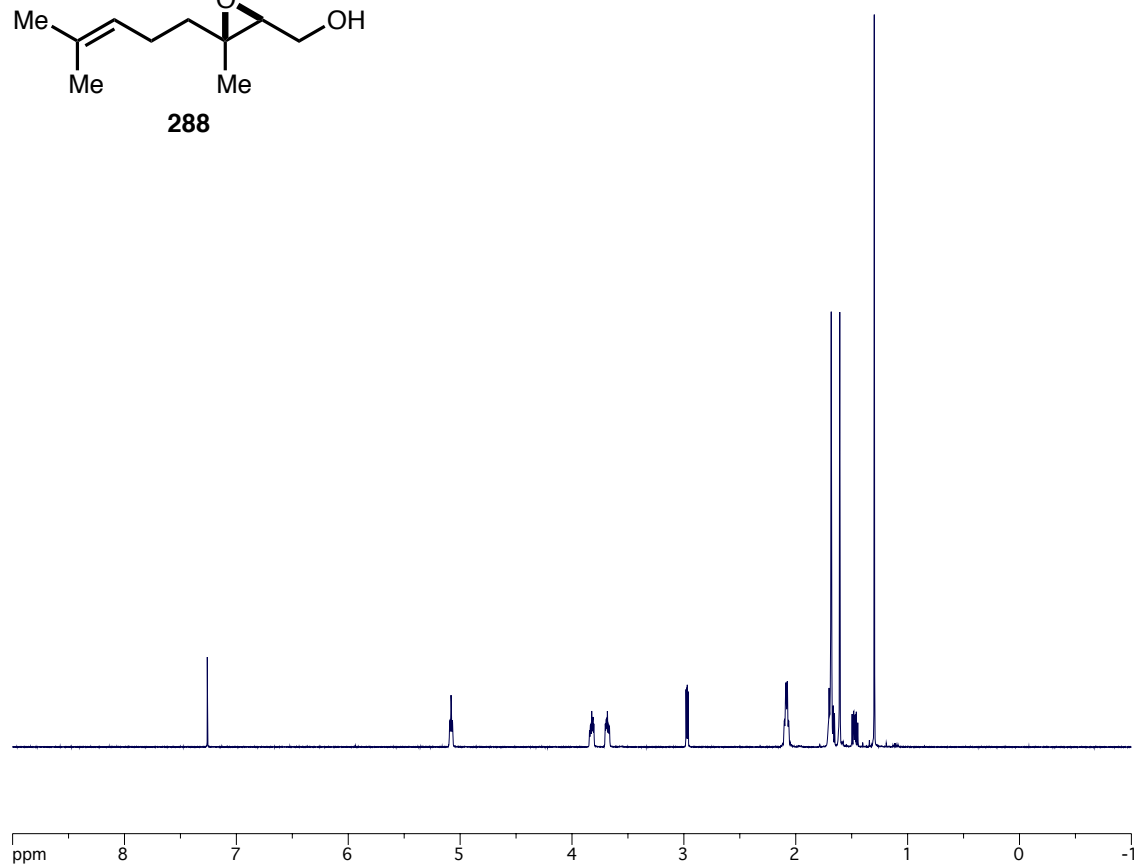
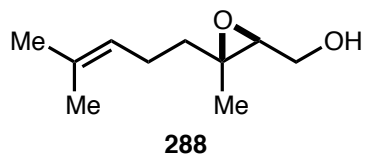


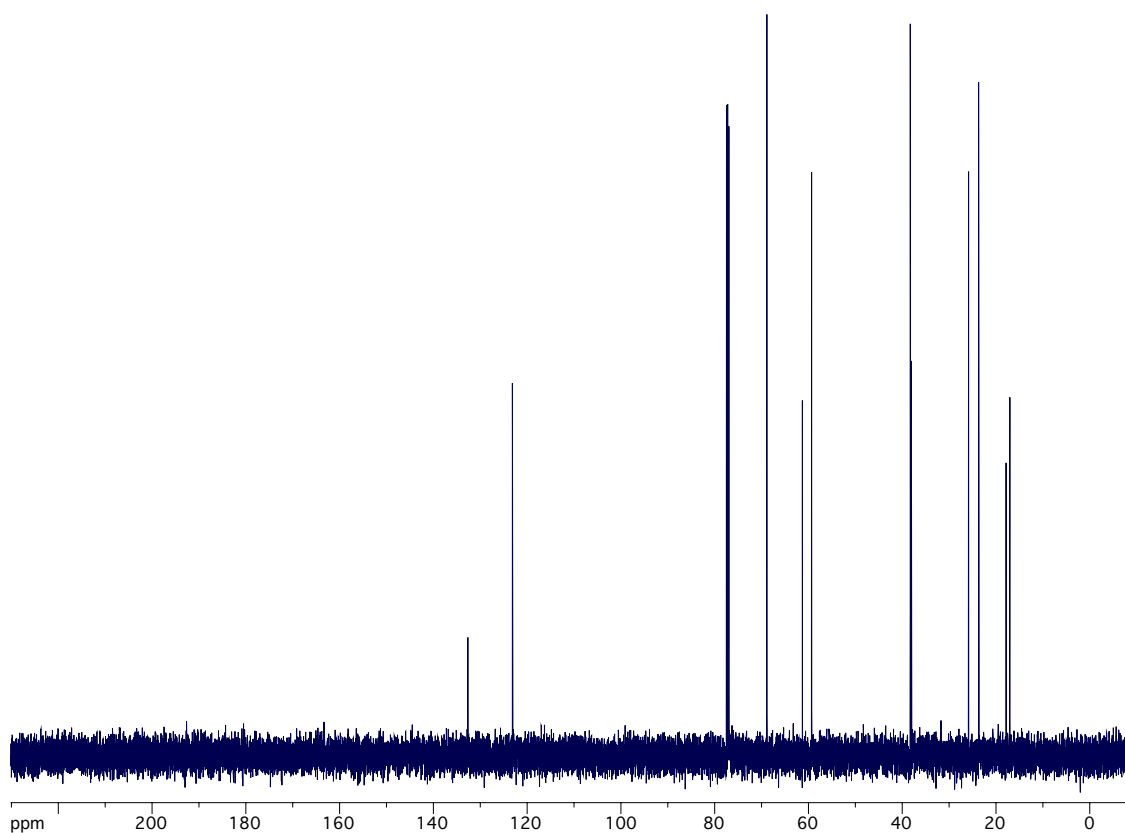
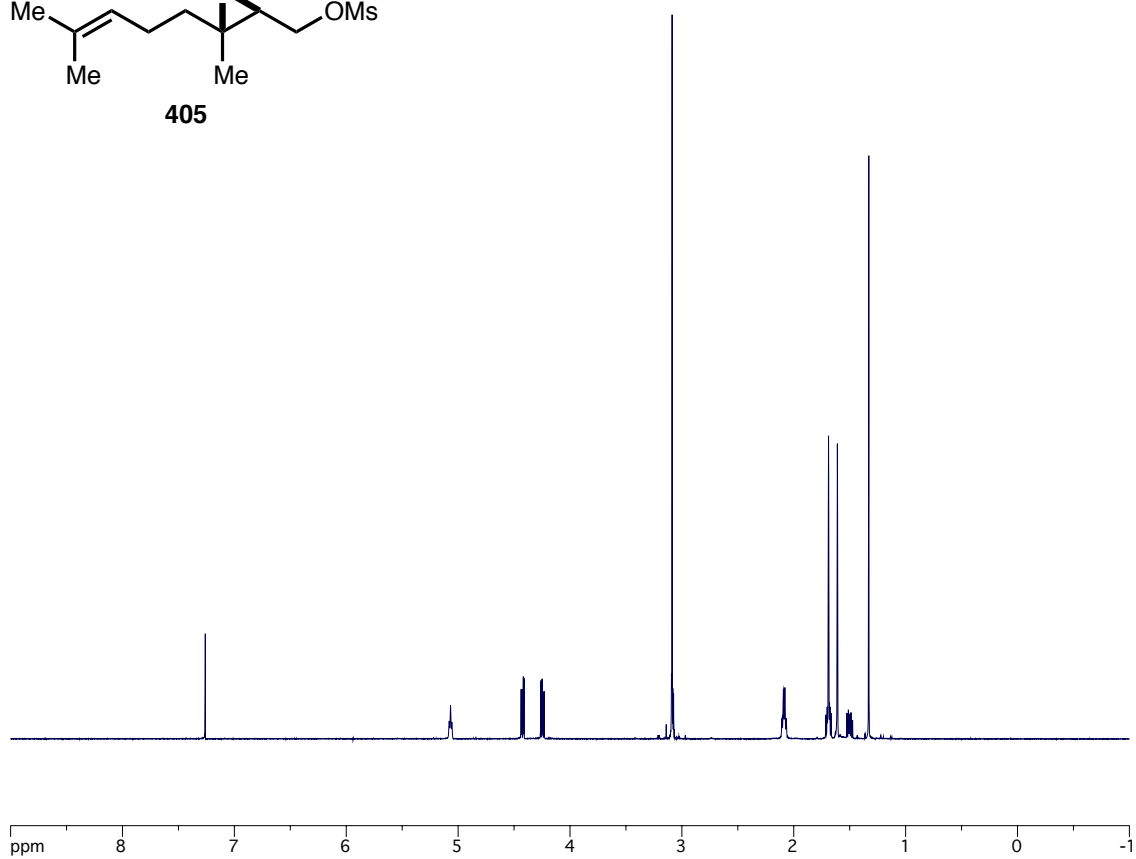
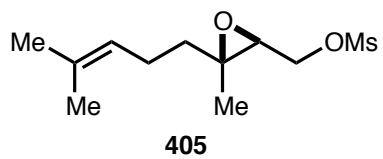


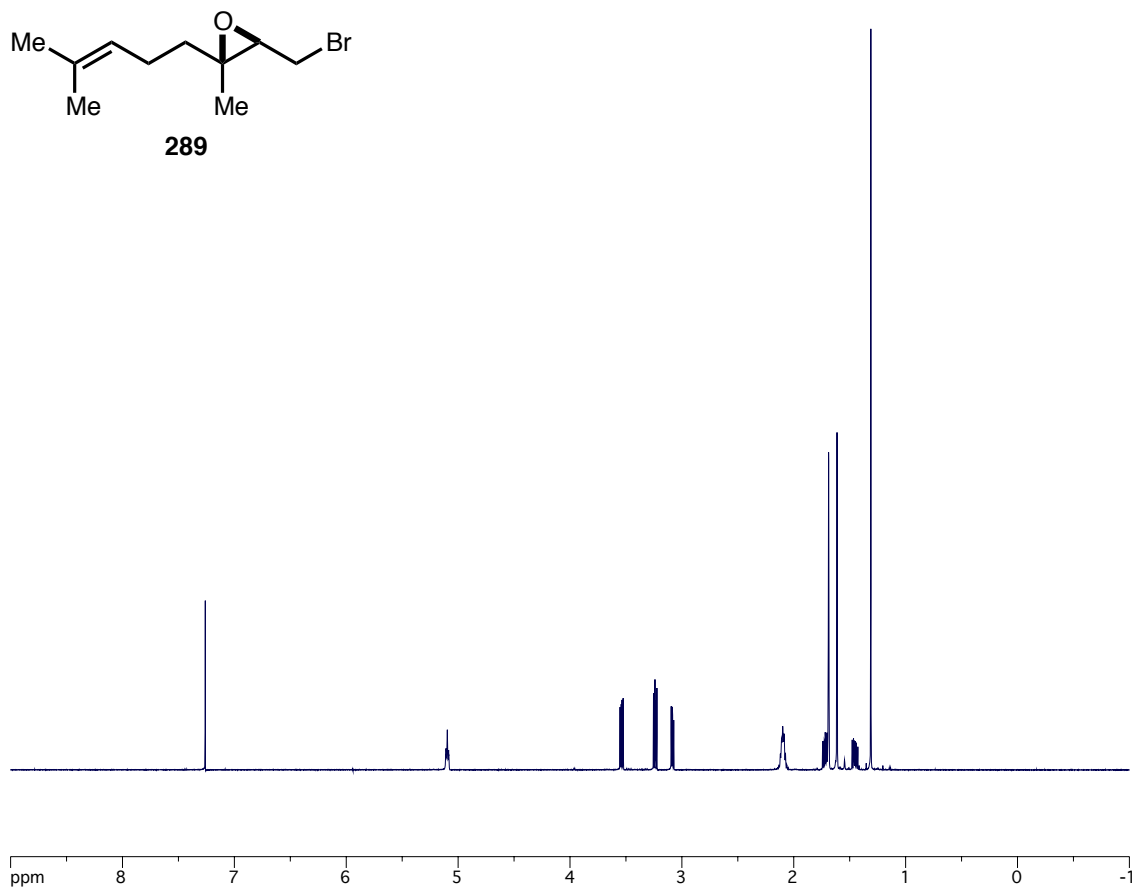


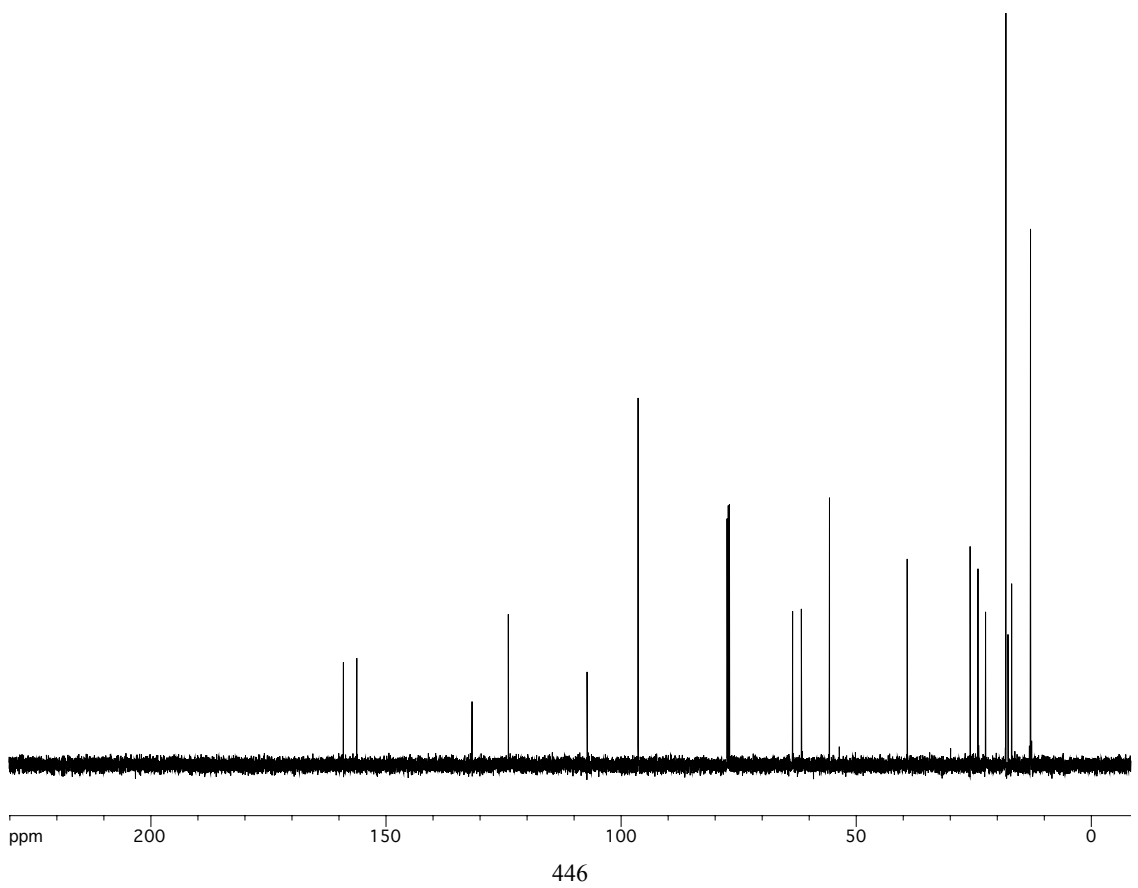
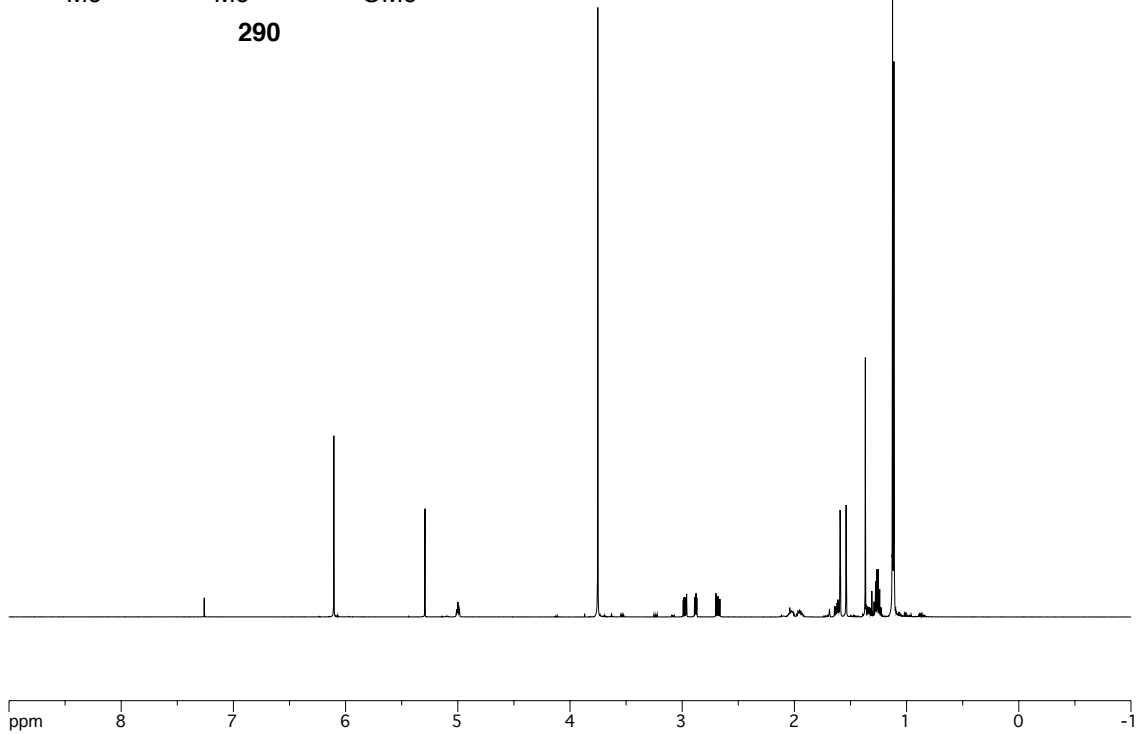
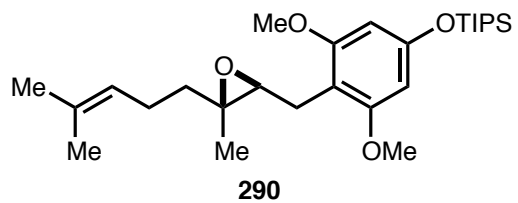


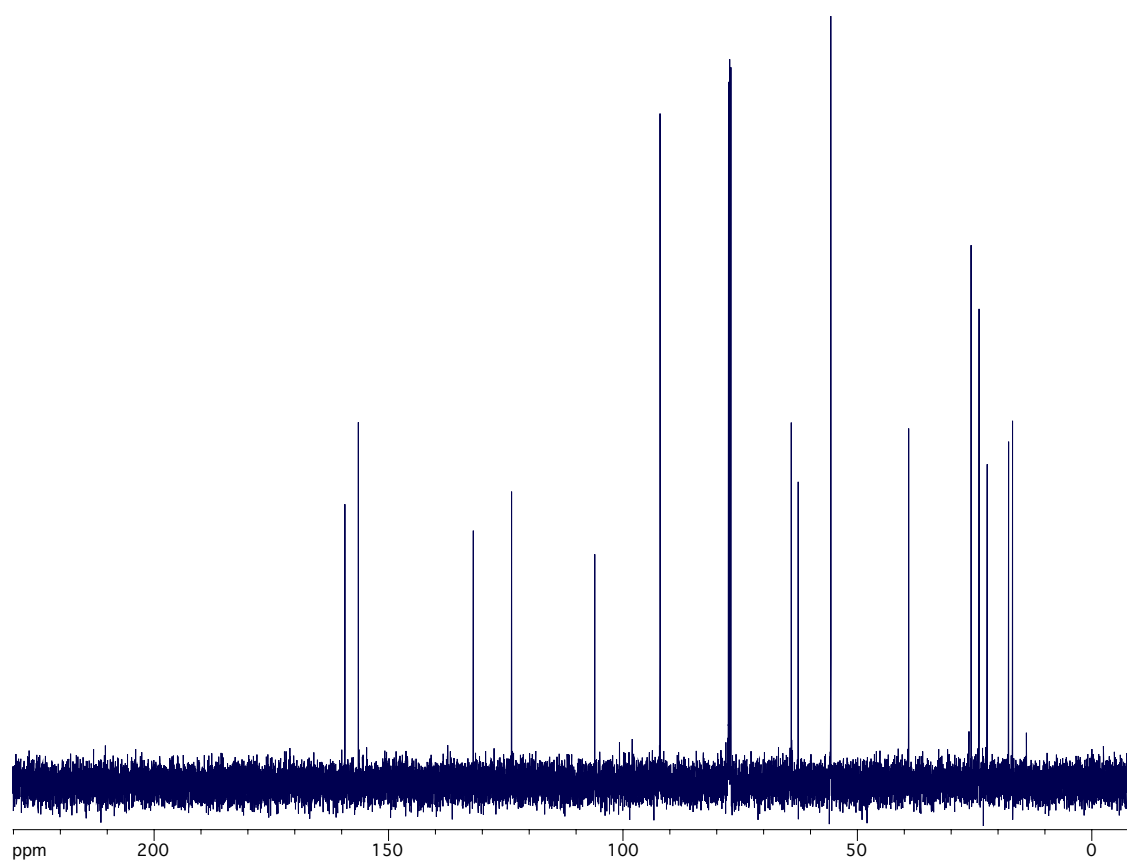
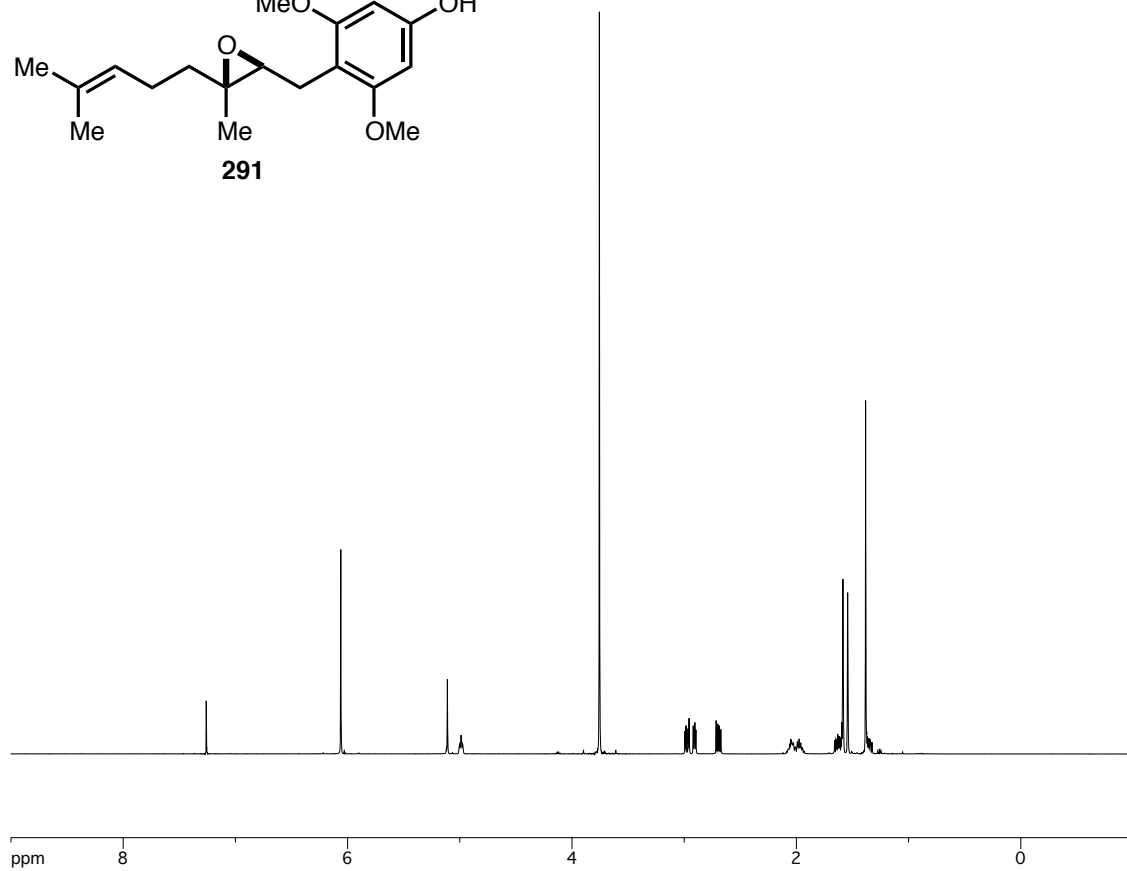
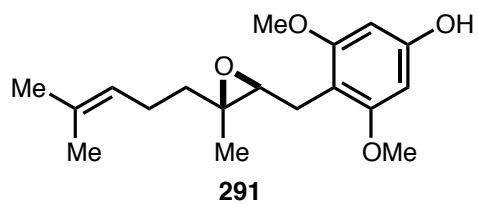


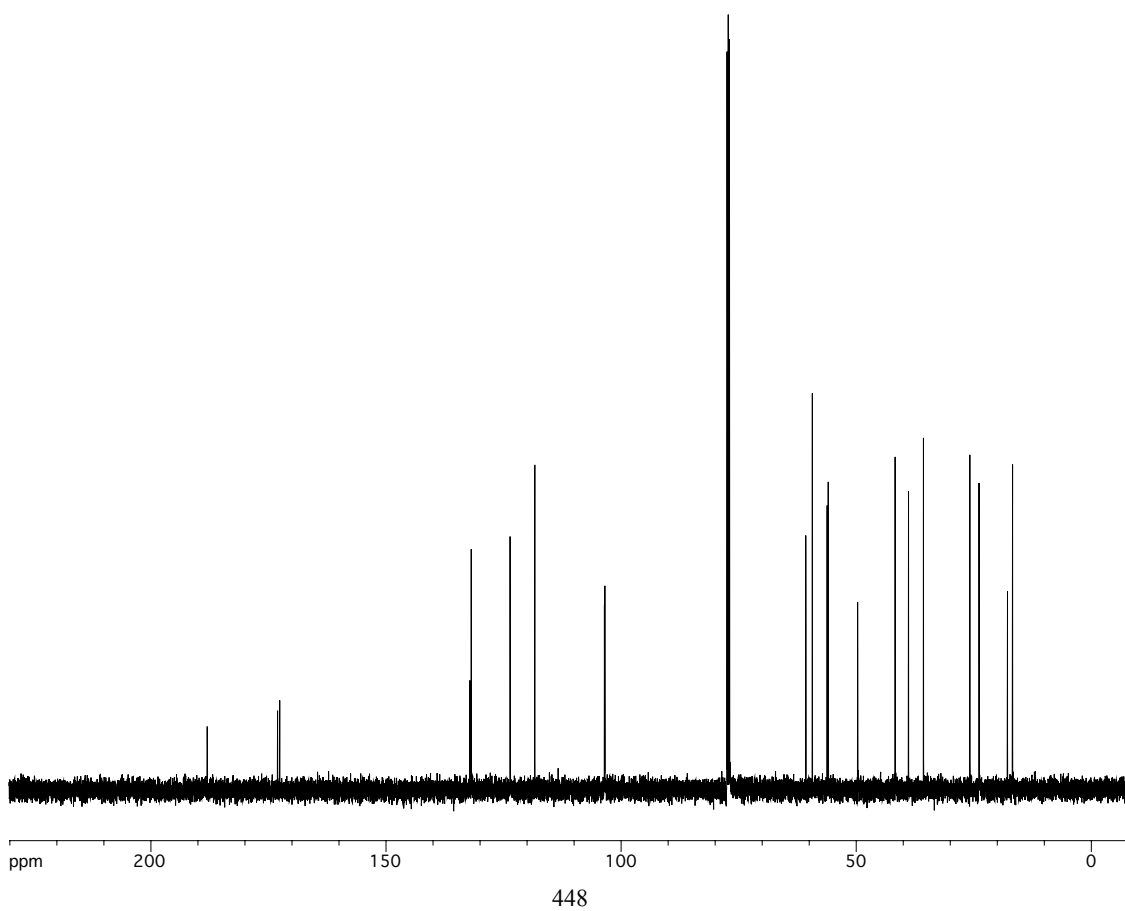
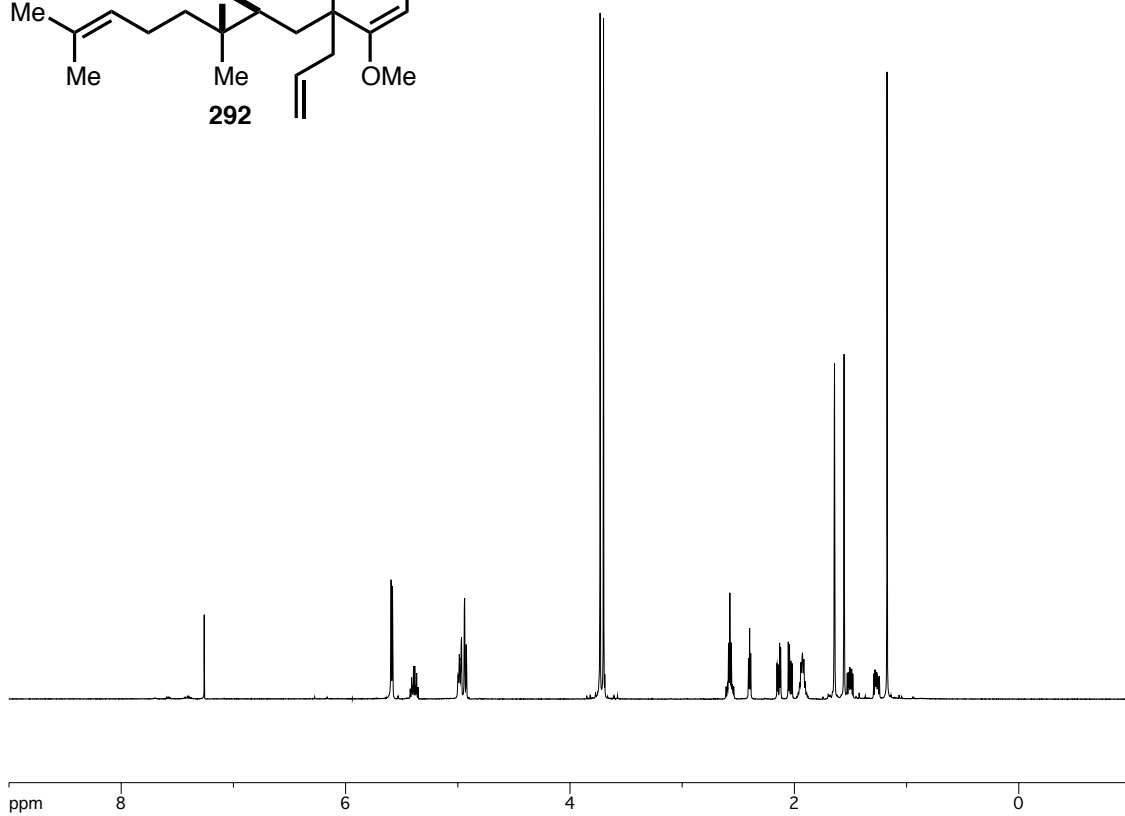
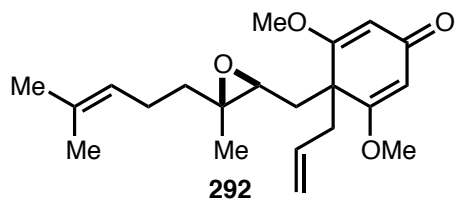


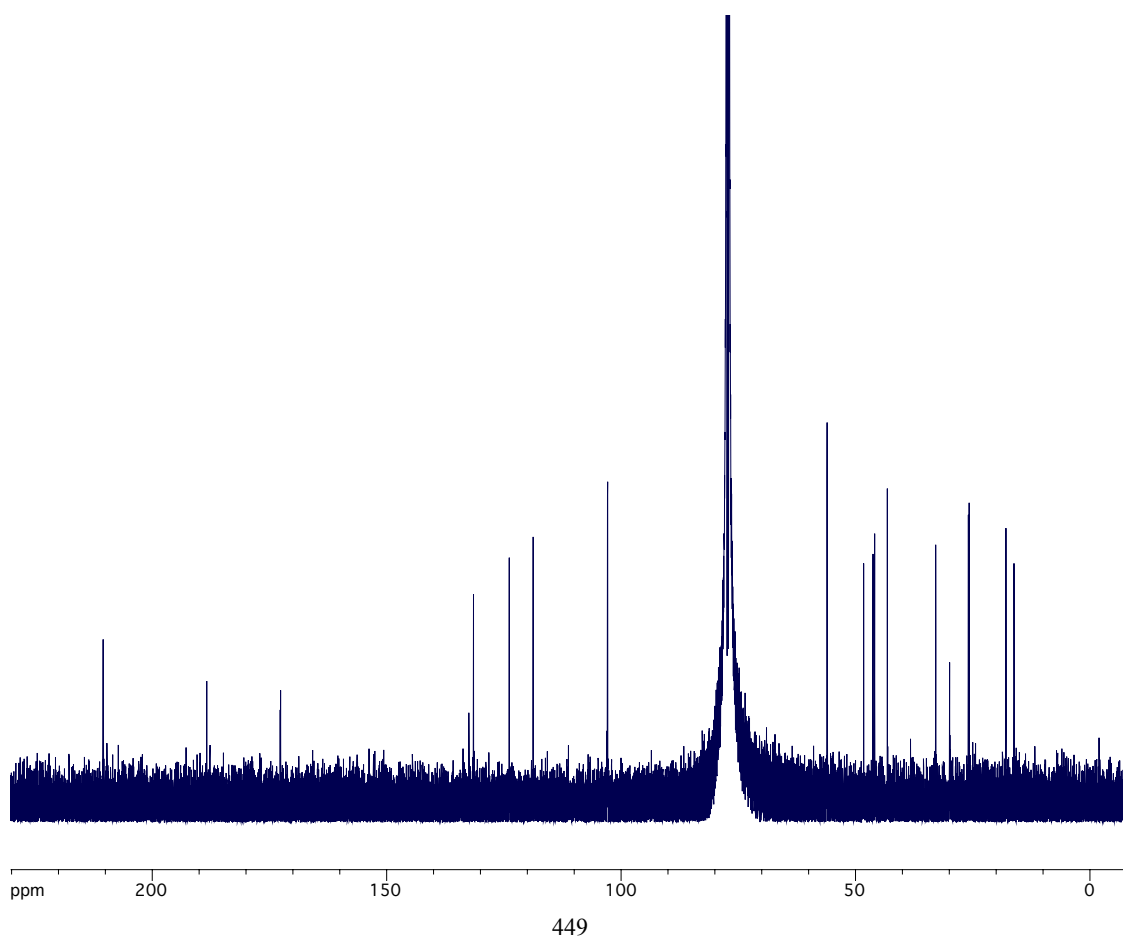
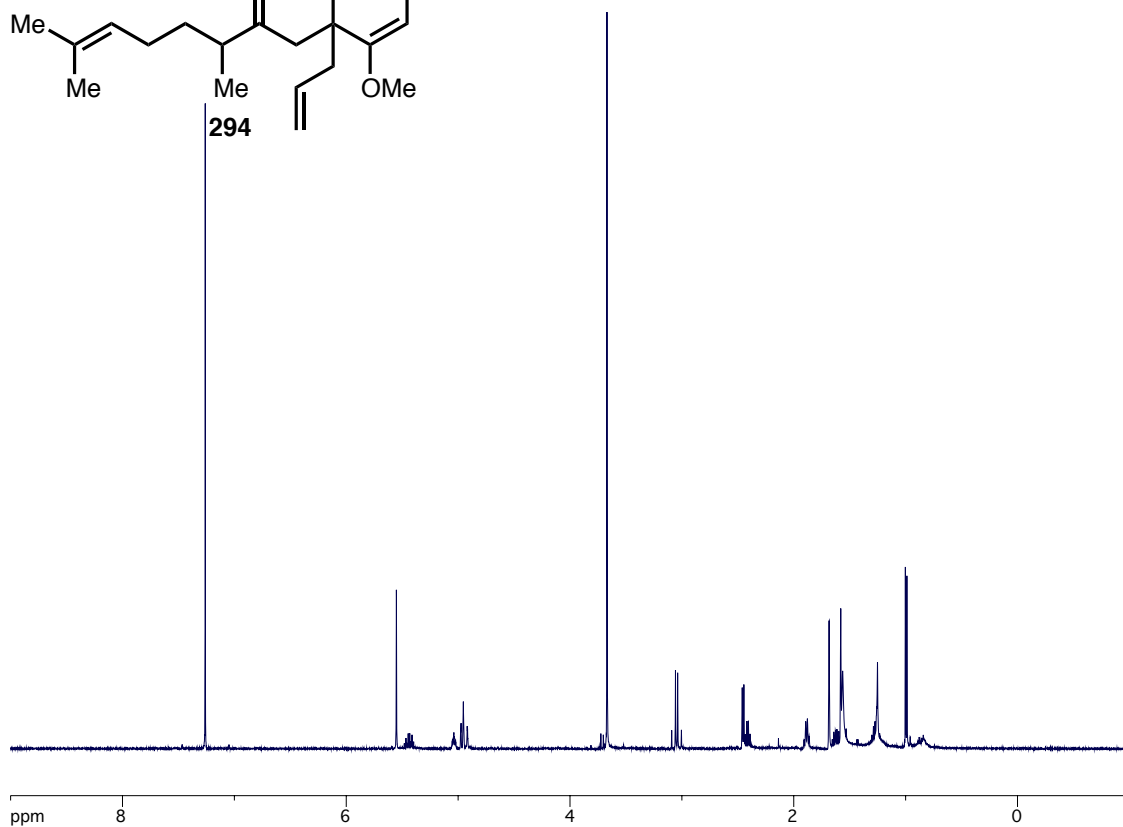
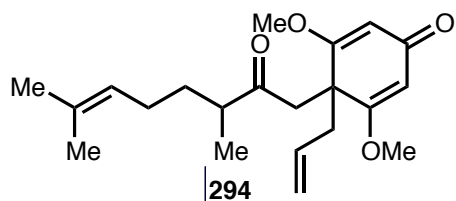


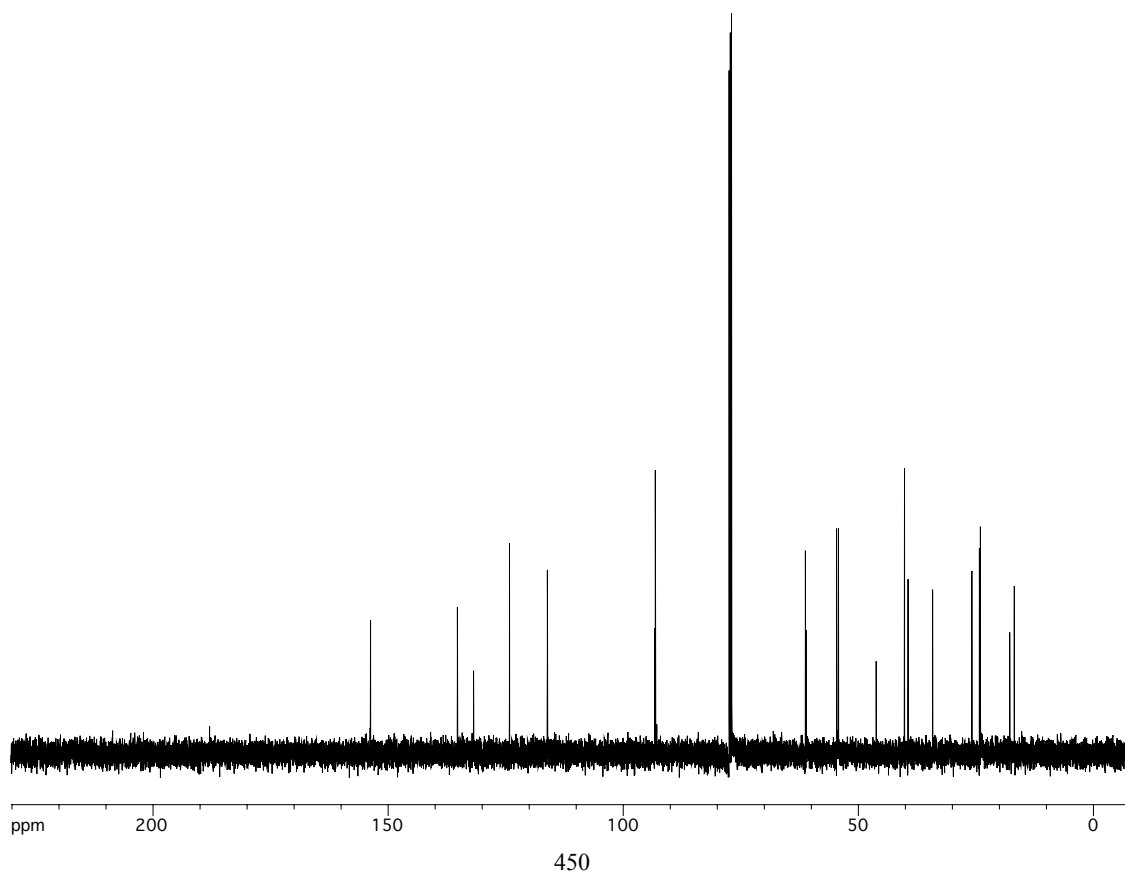
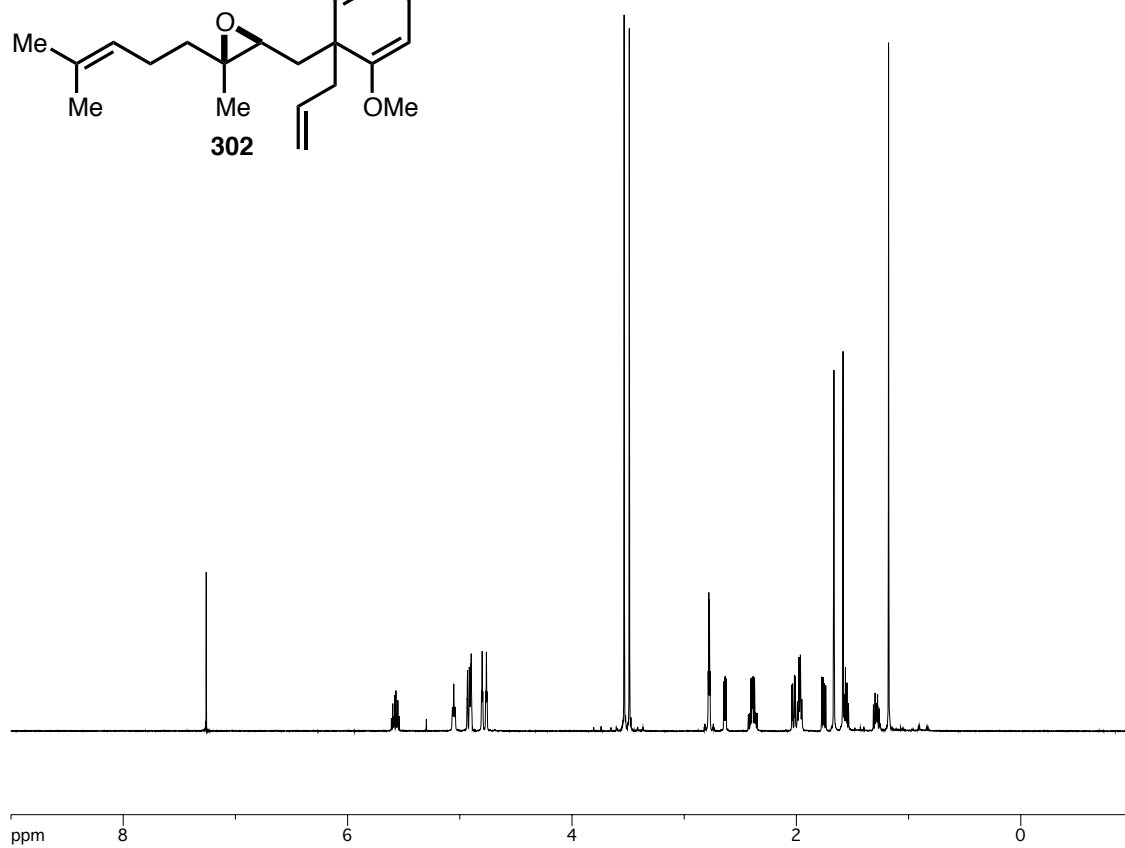
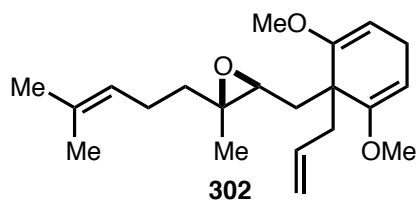


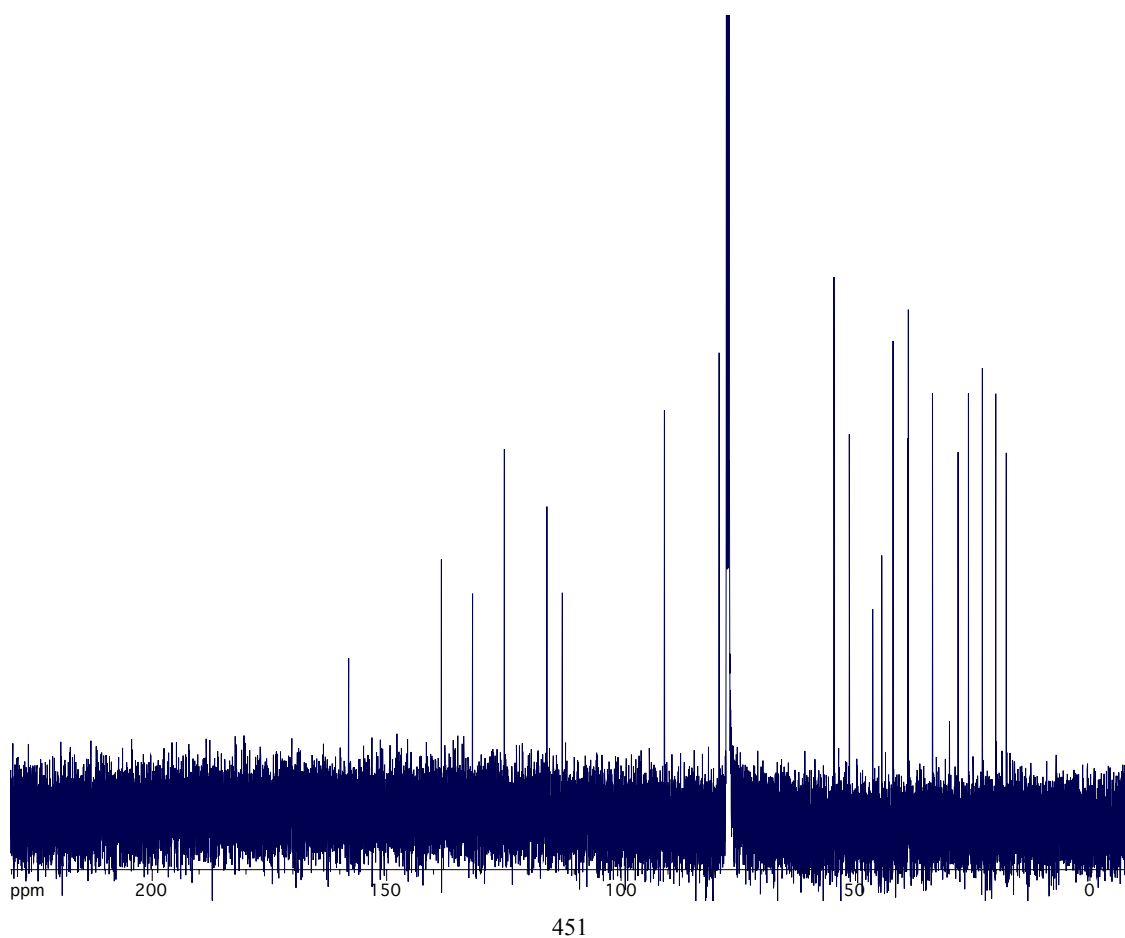
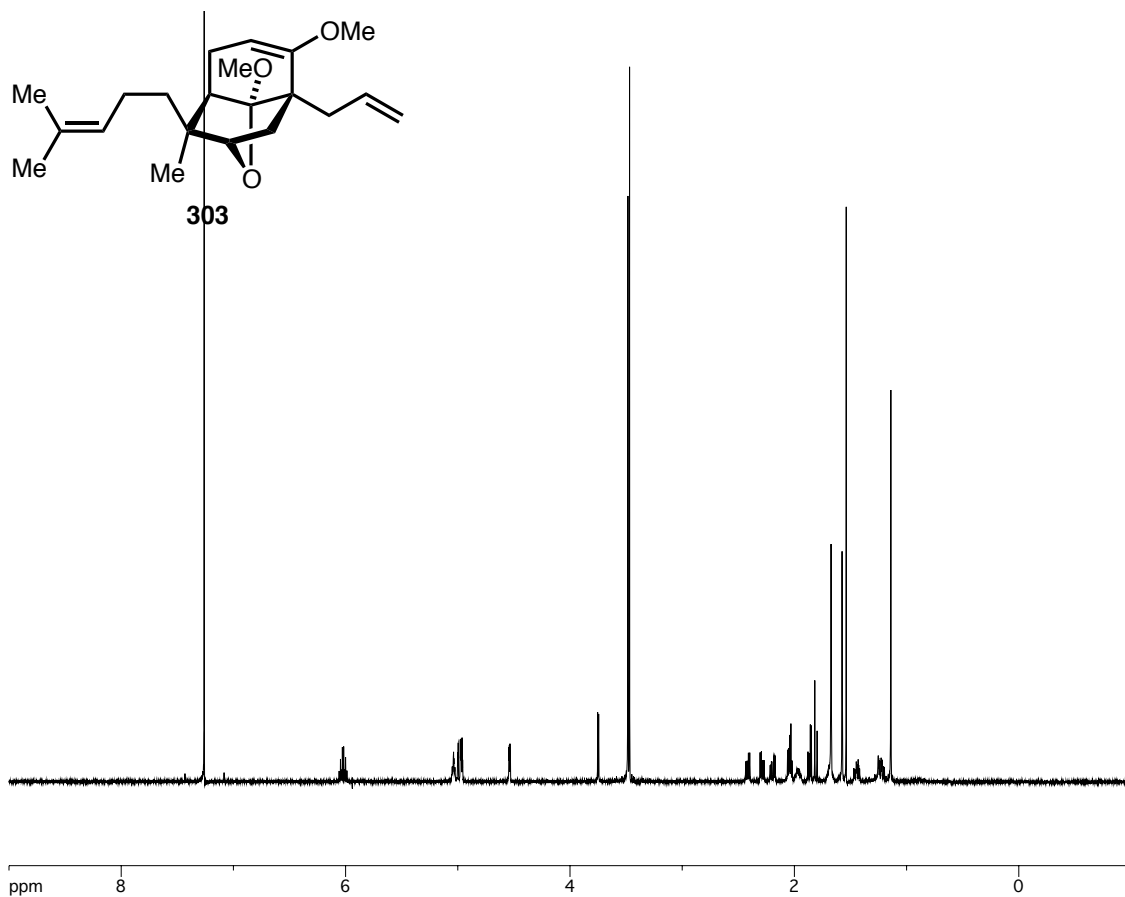


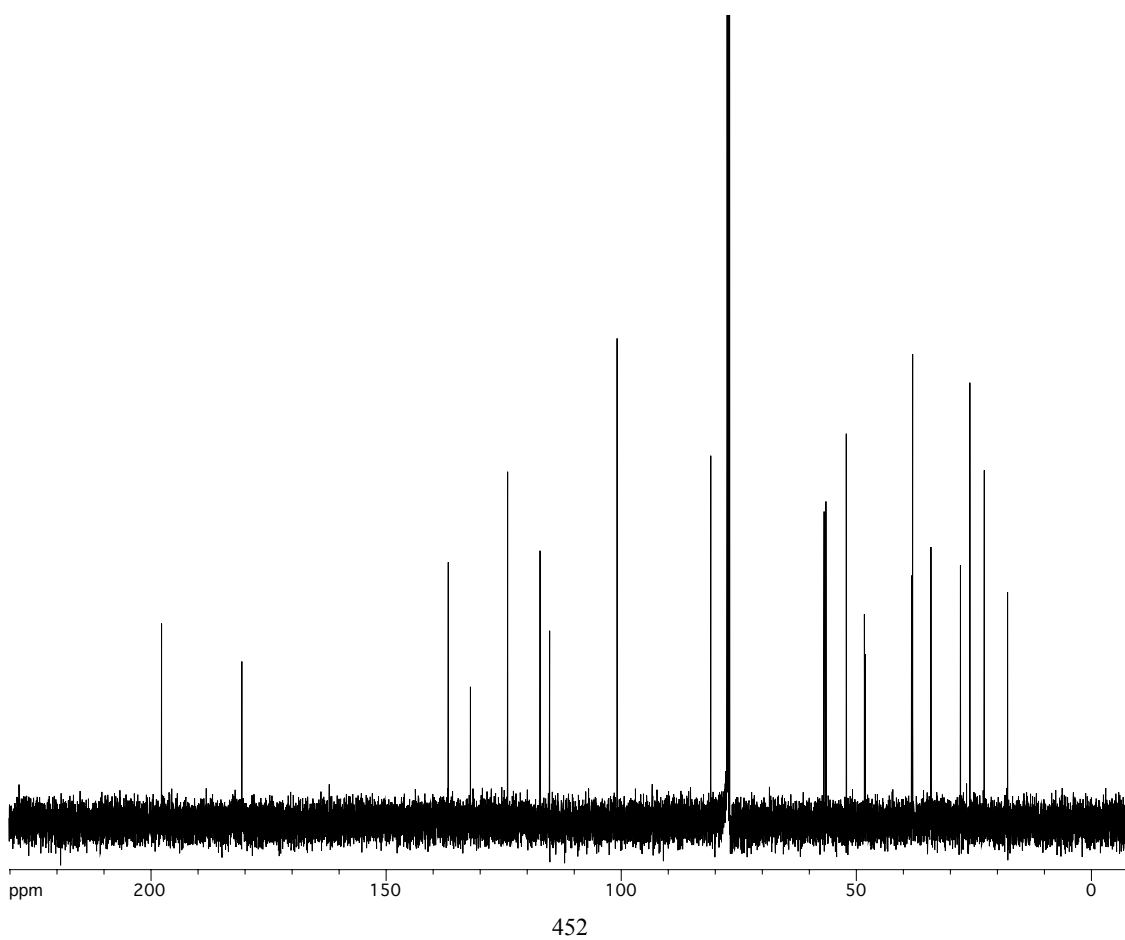
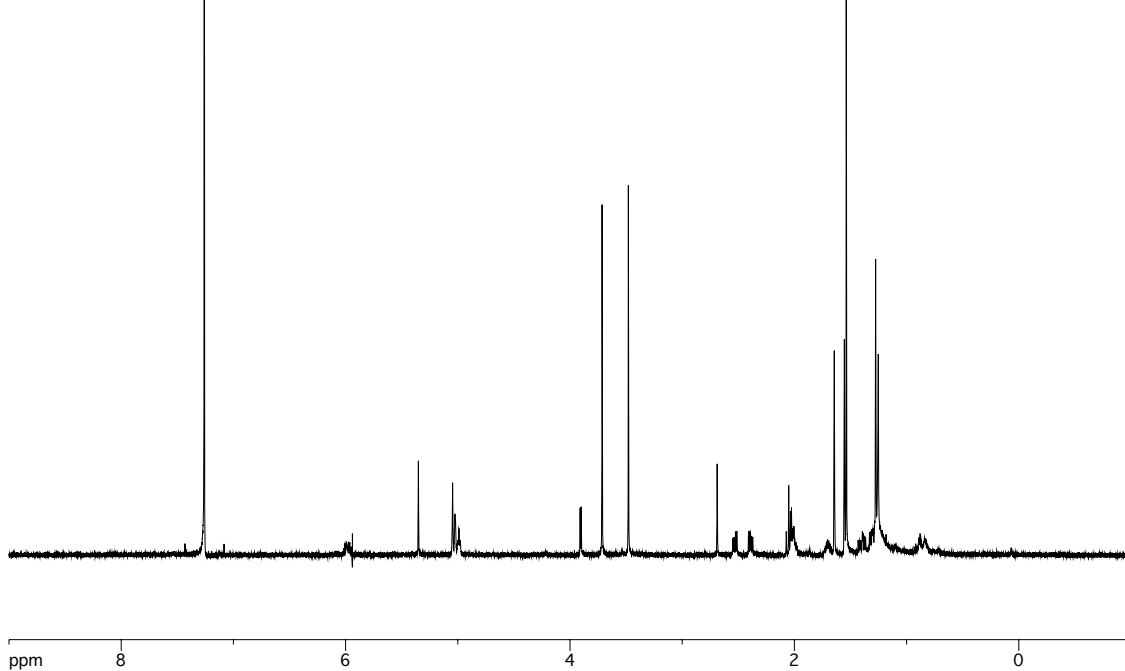
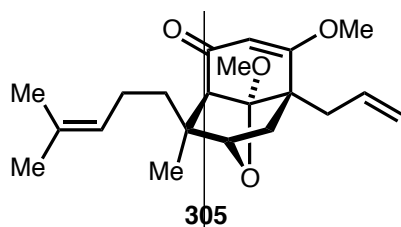


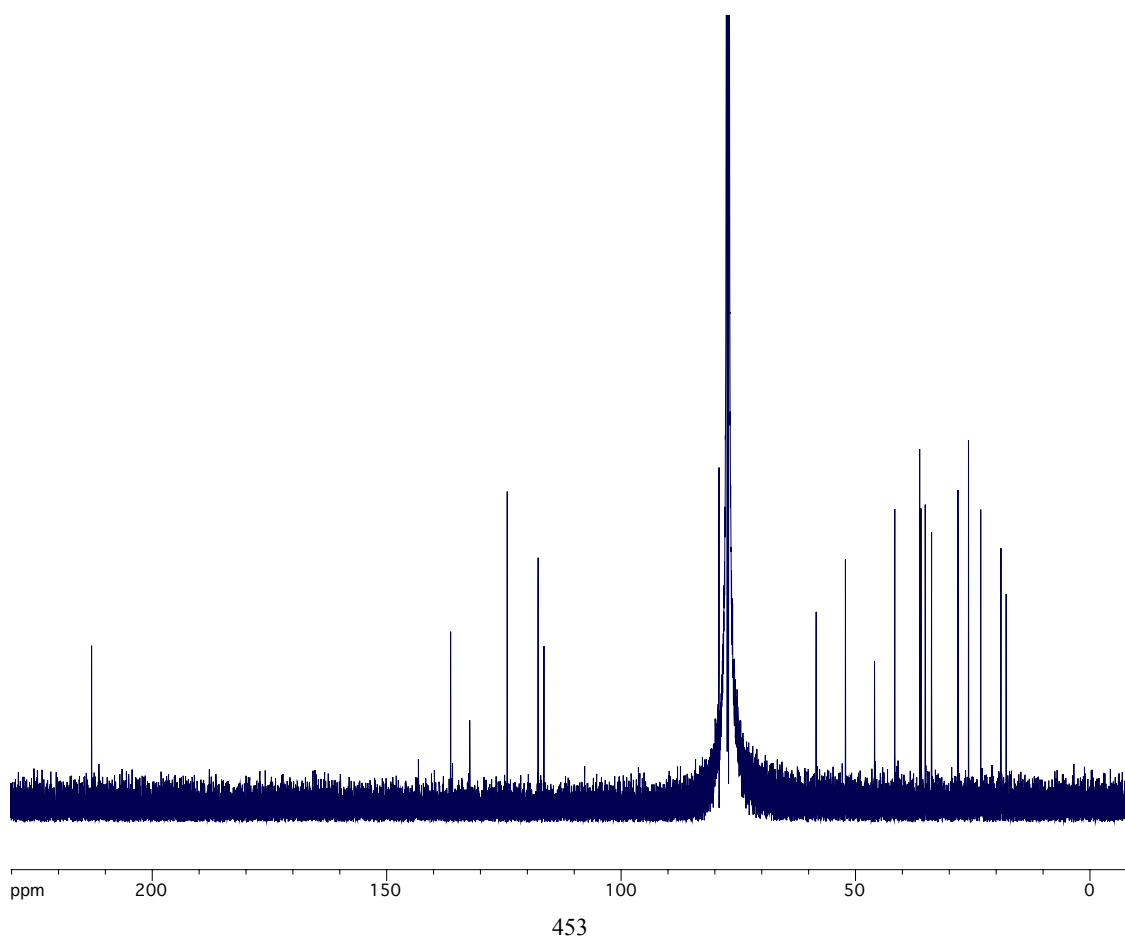
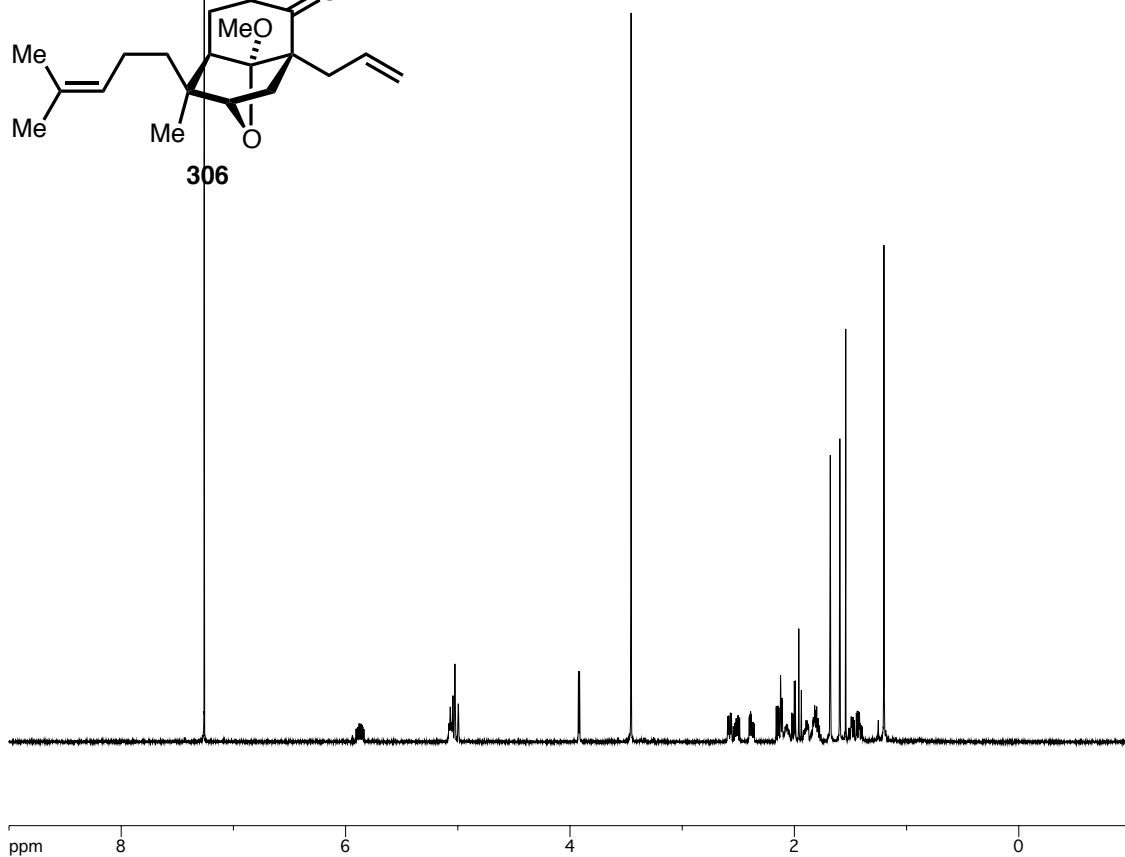
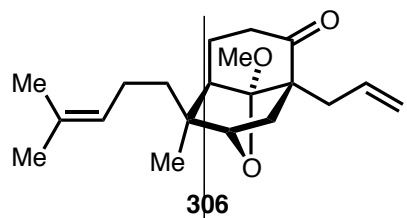


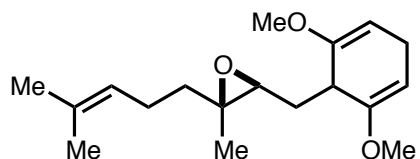




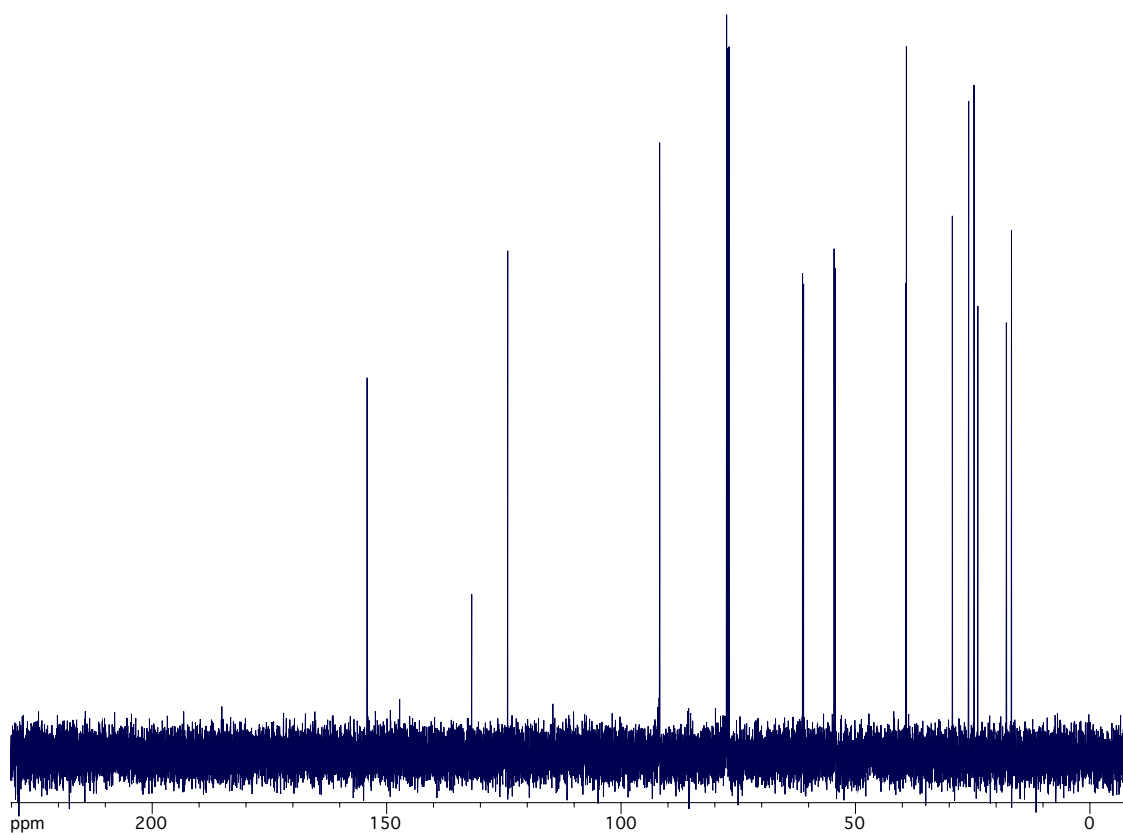
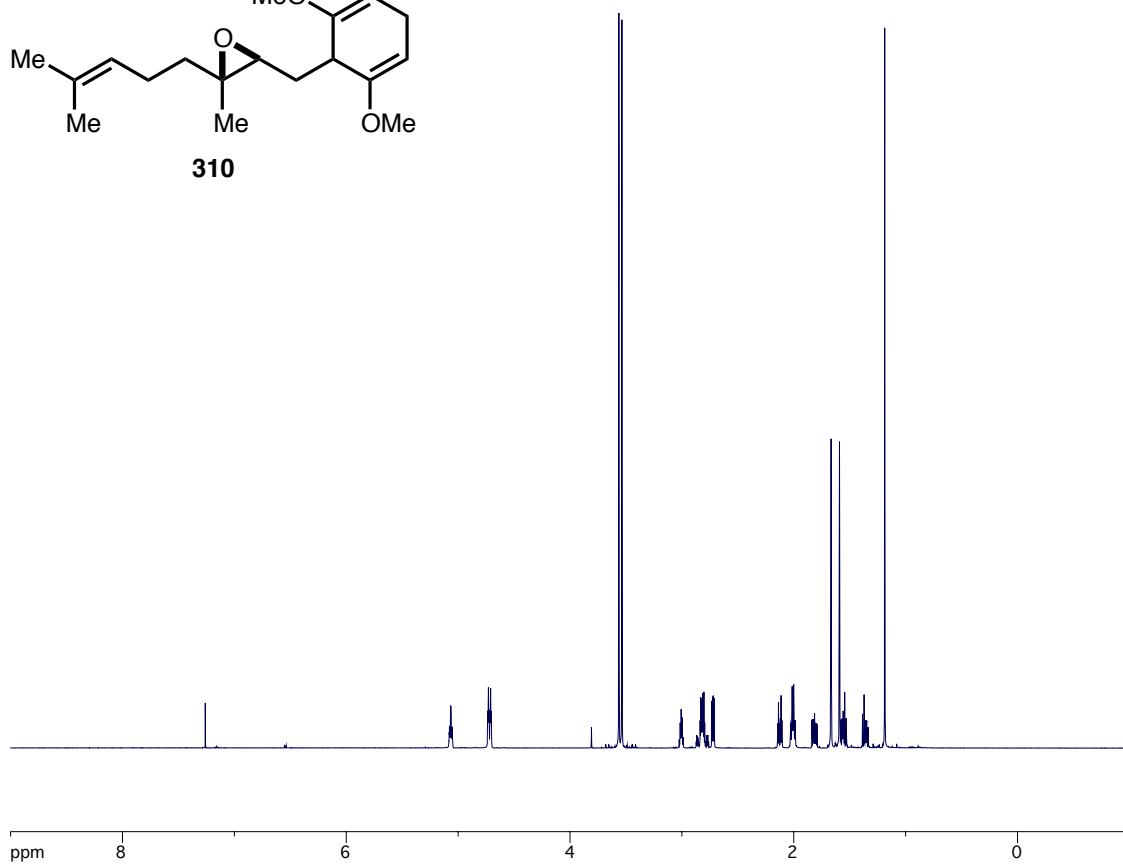


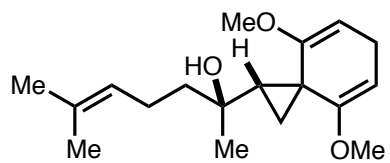




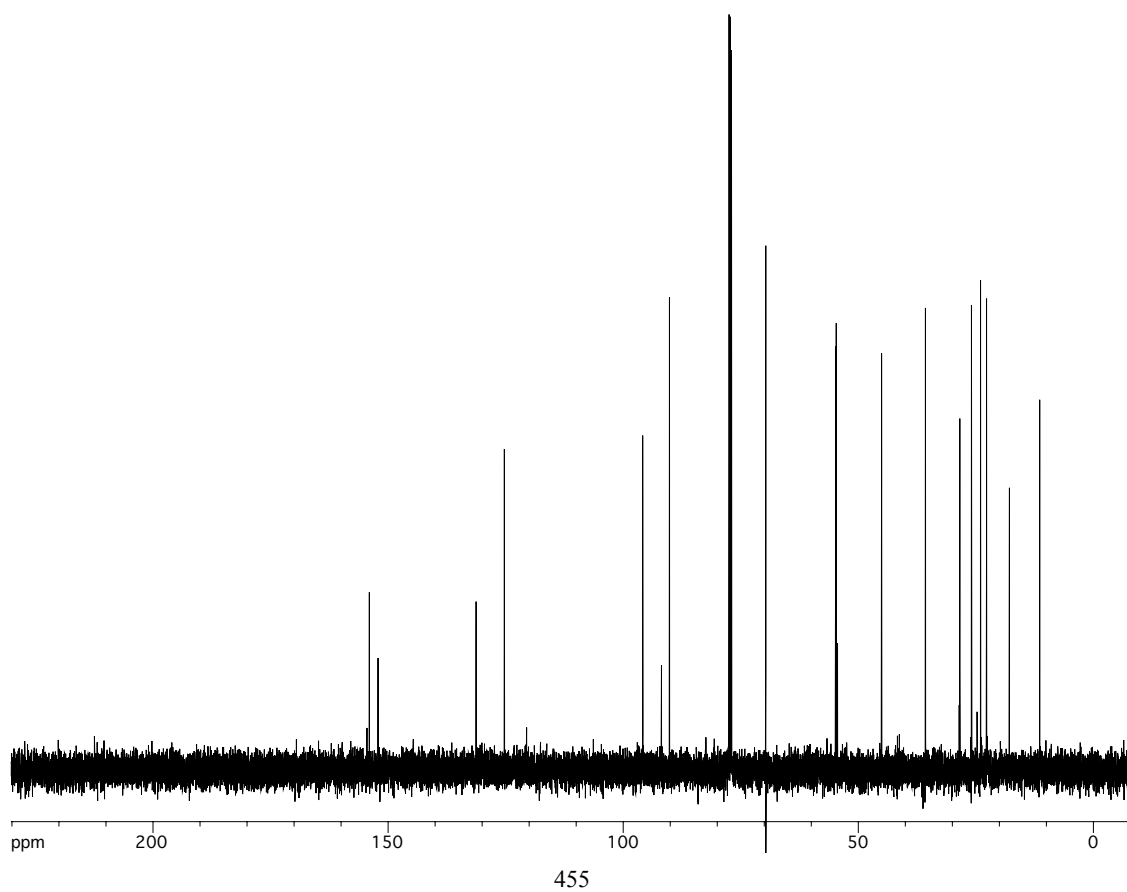
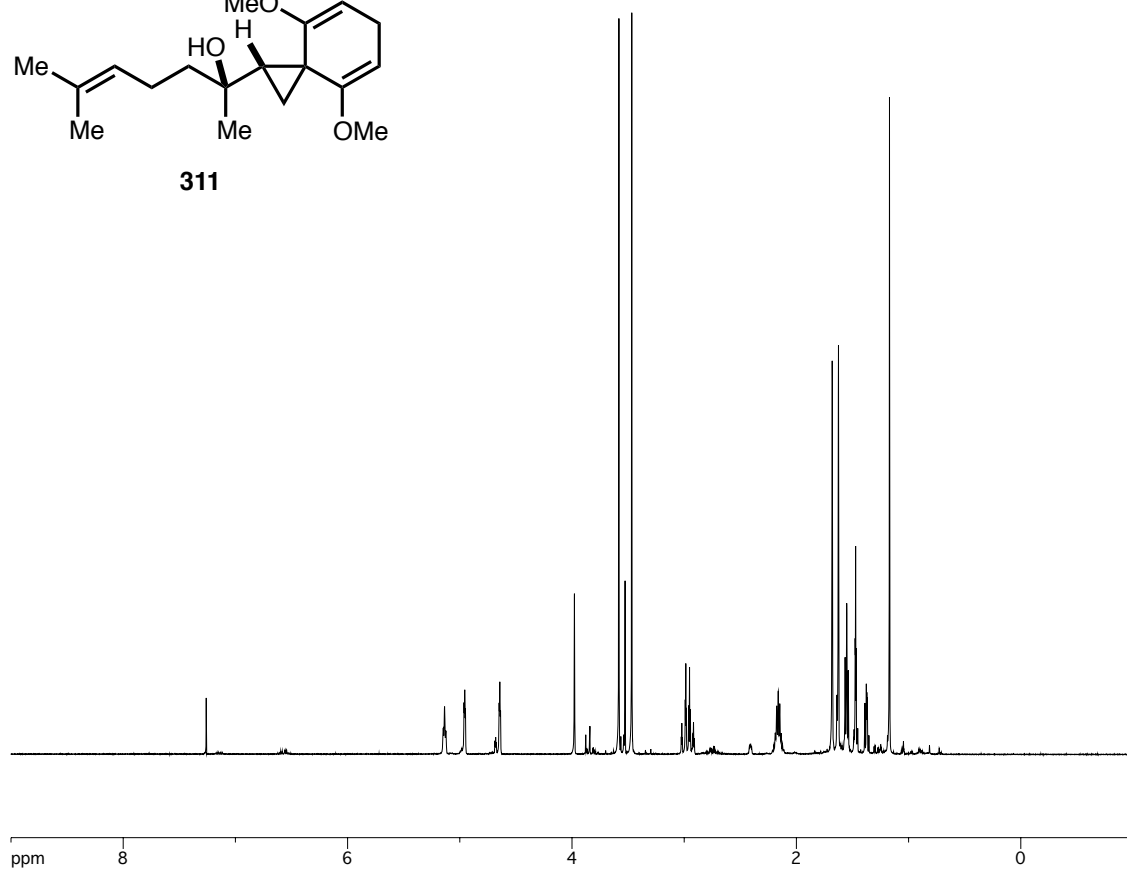


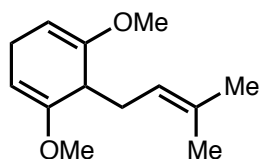
310



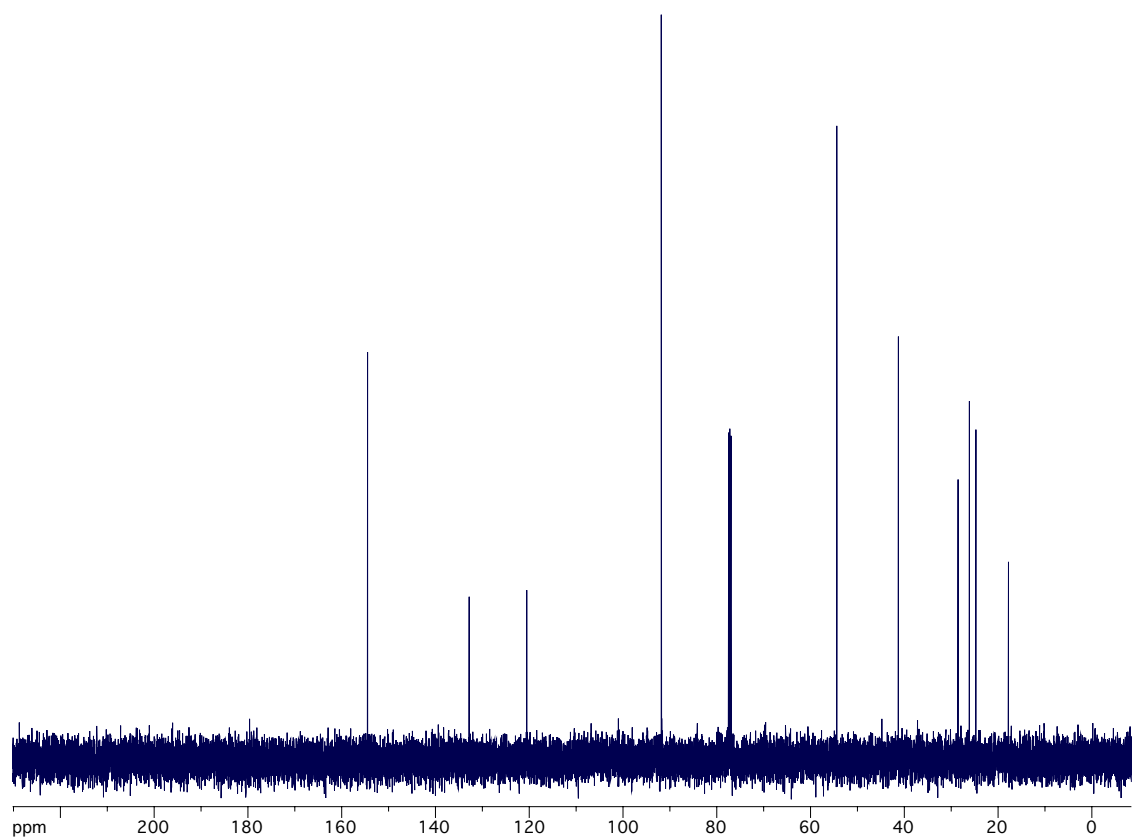
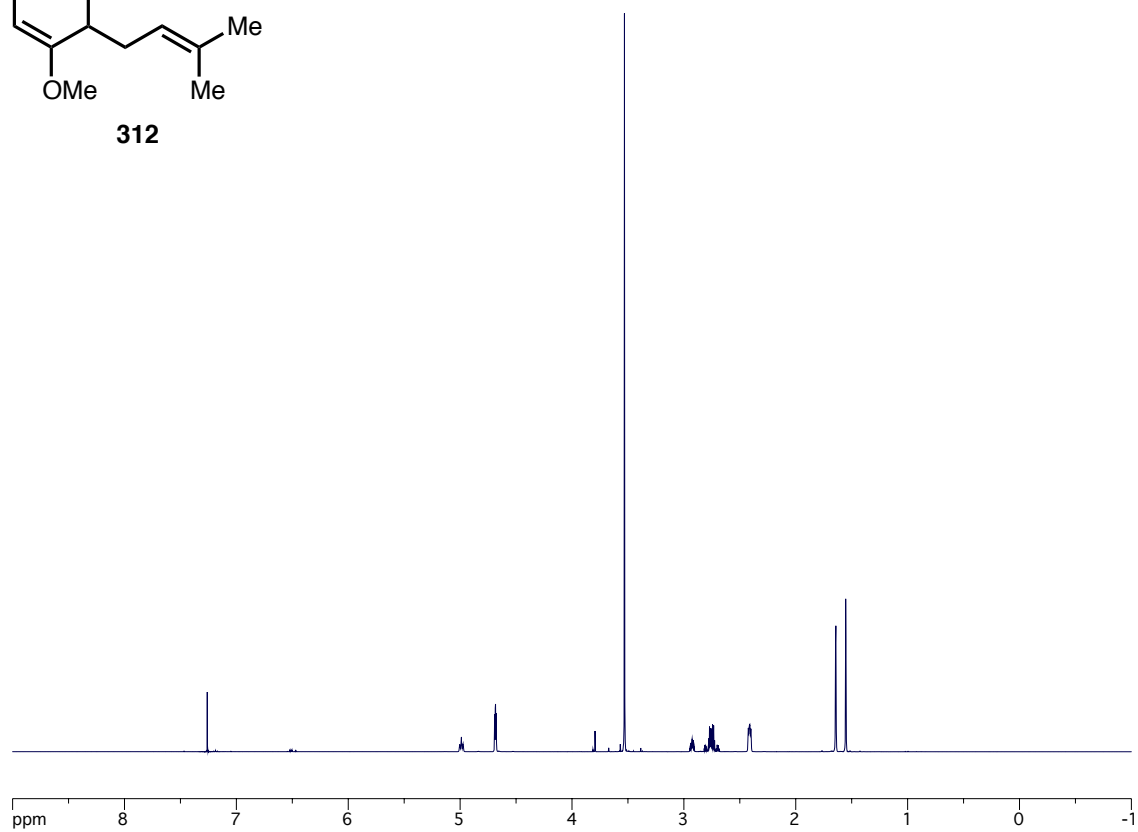


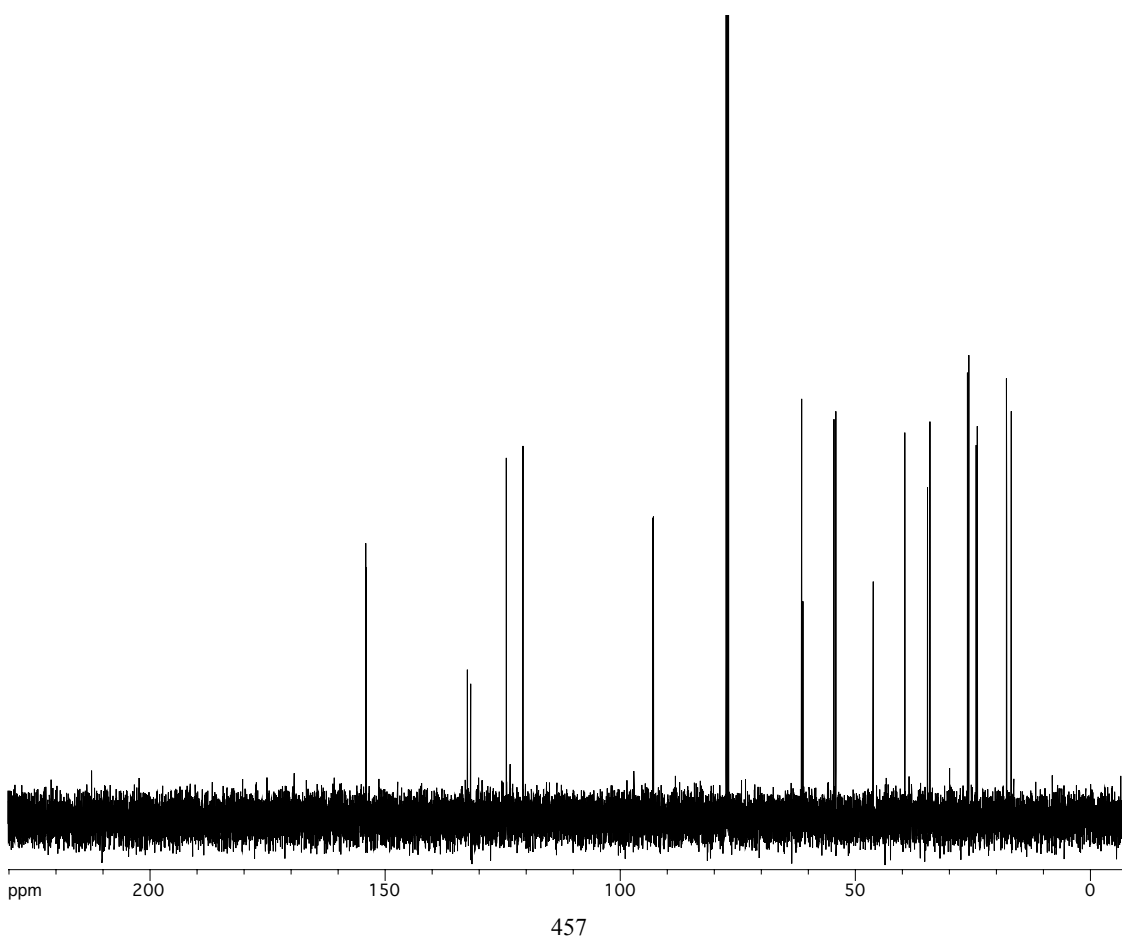
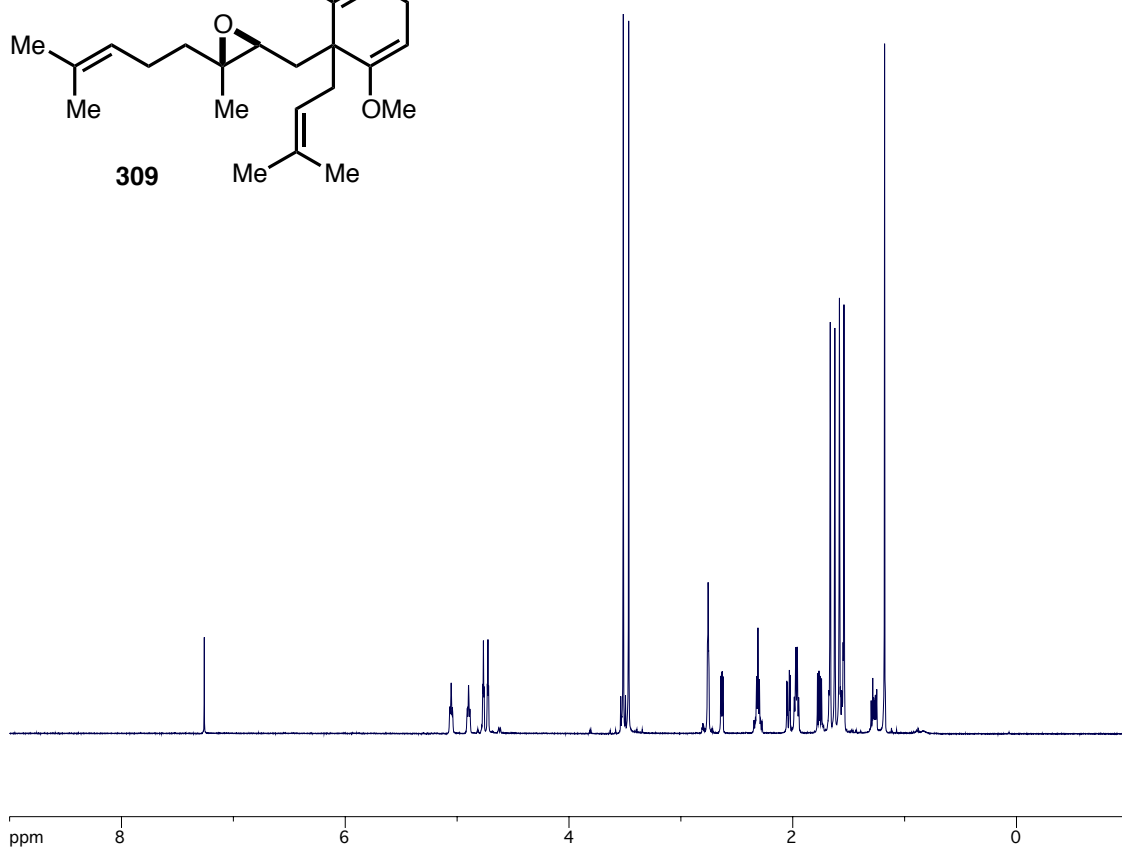
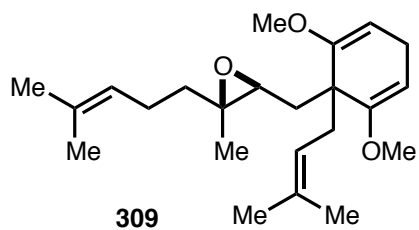
311

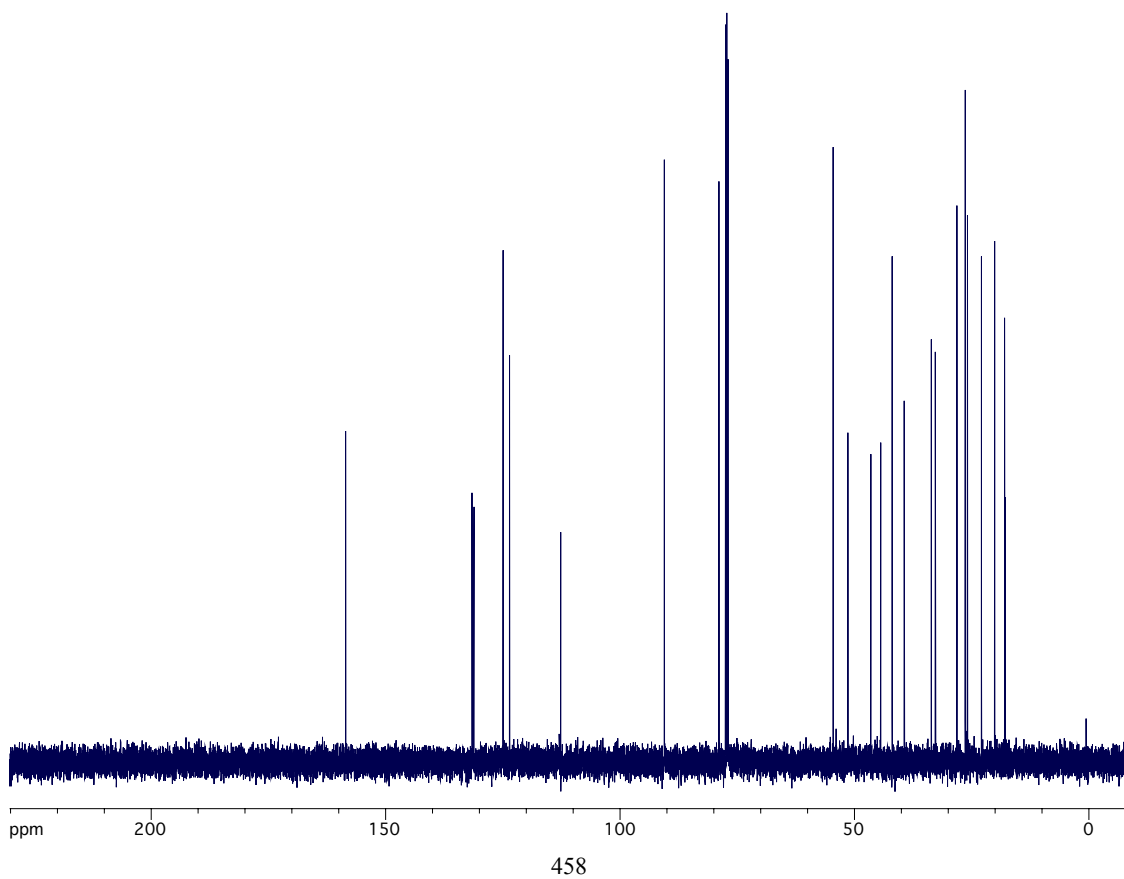
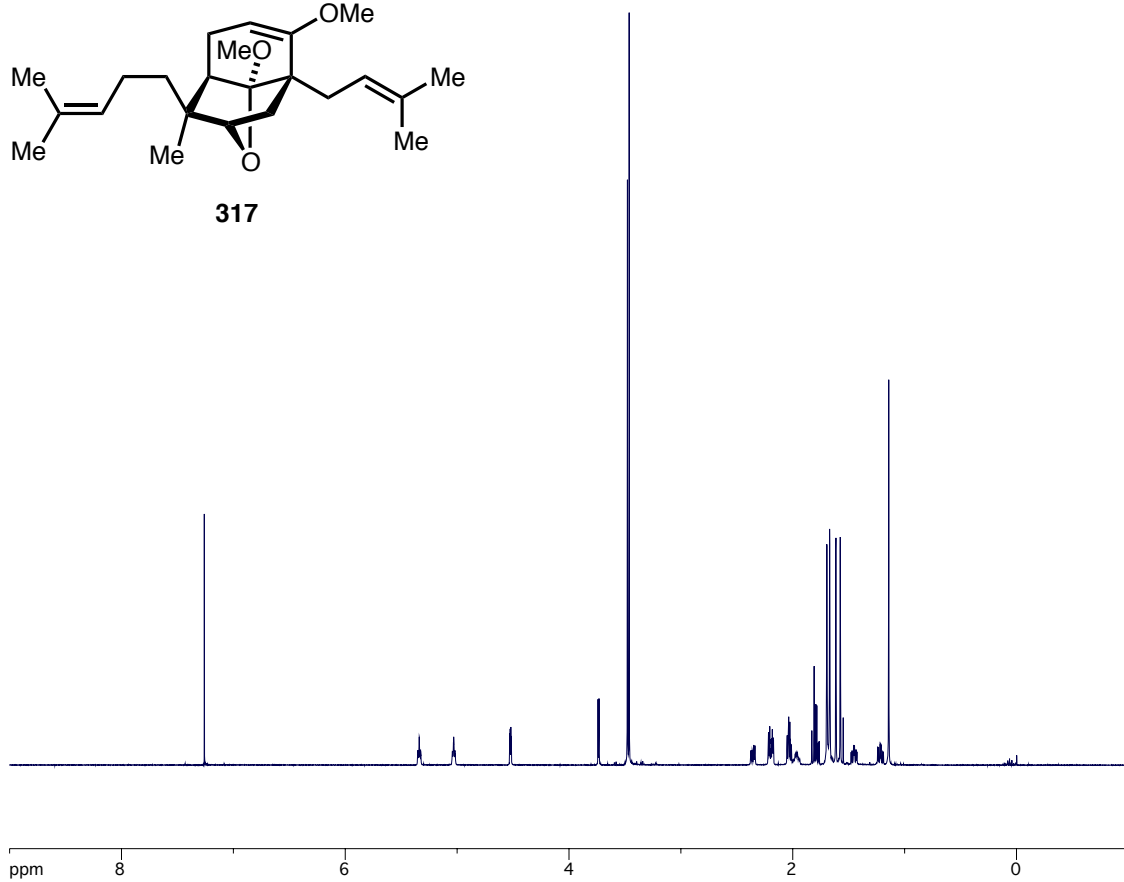
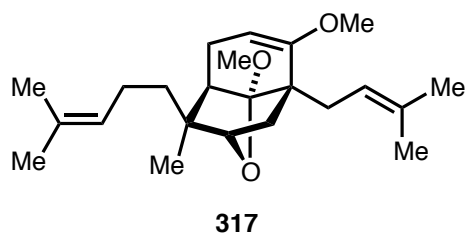


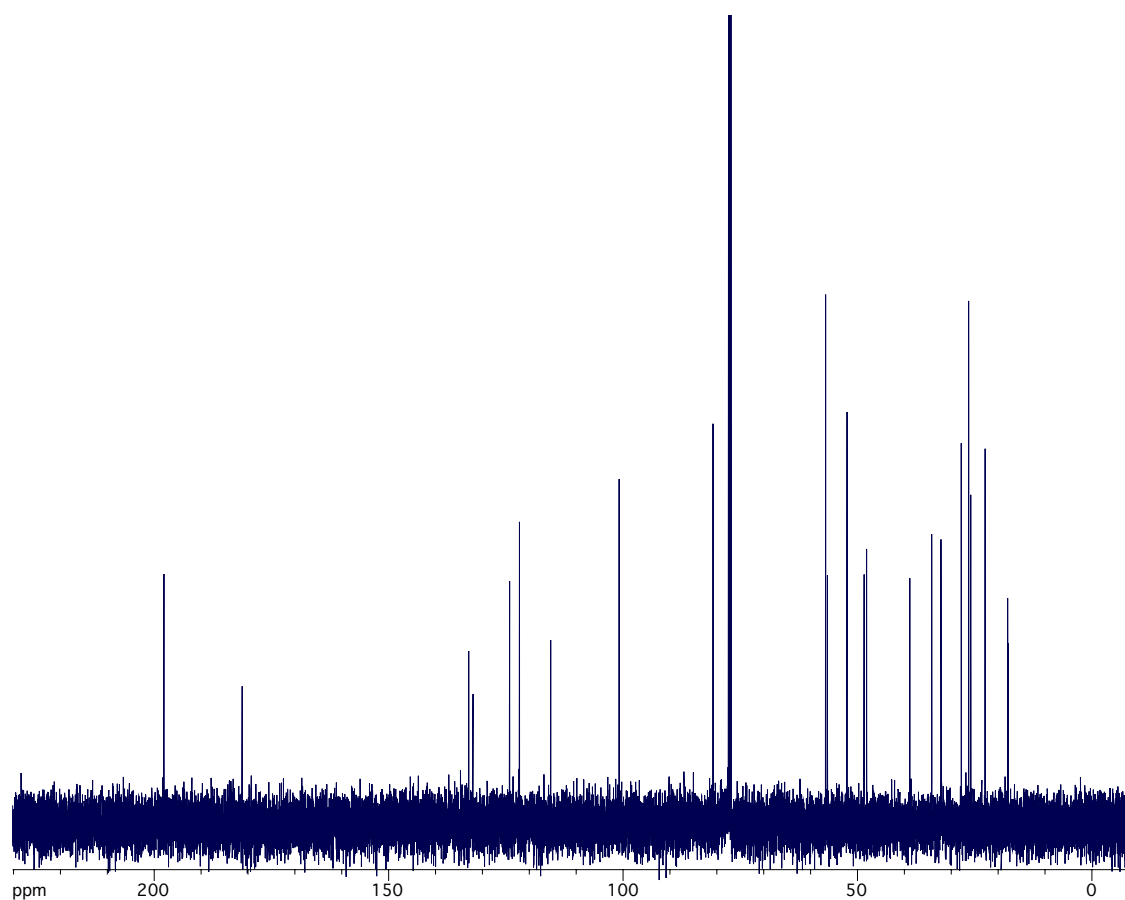
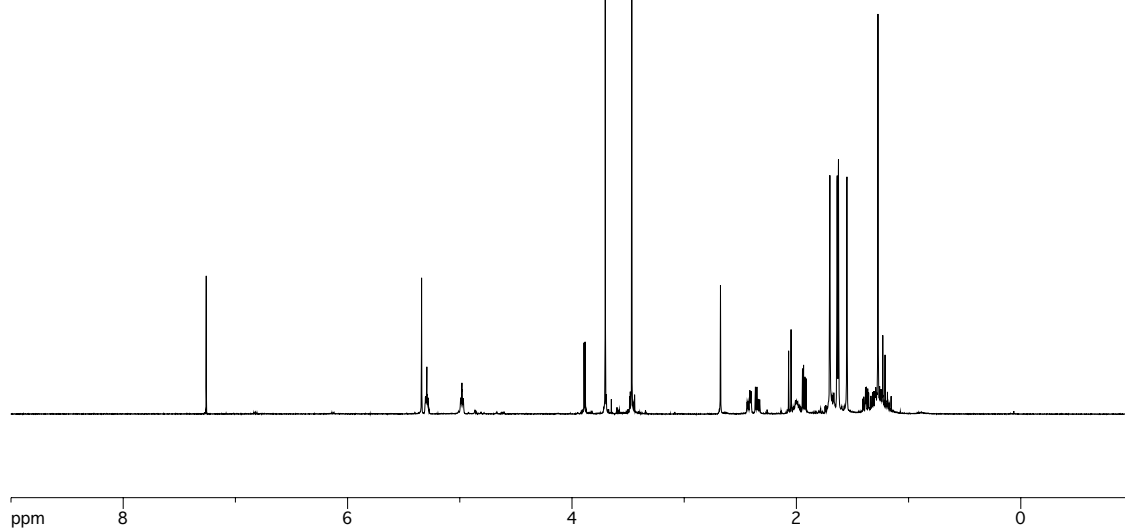
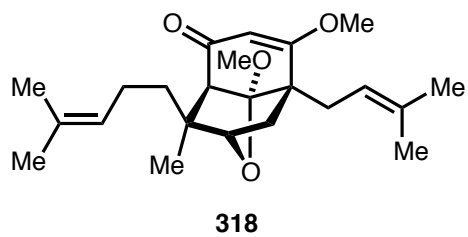


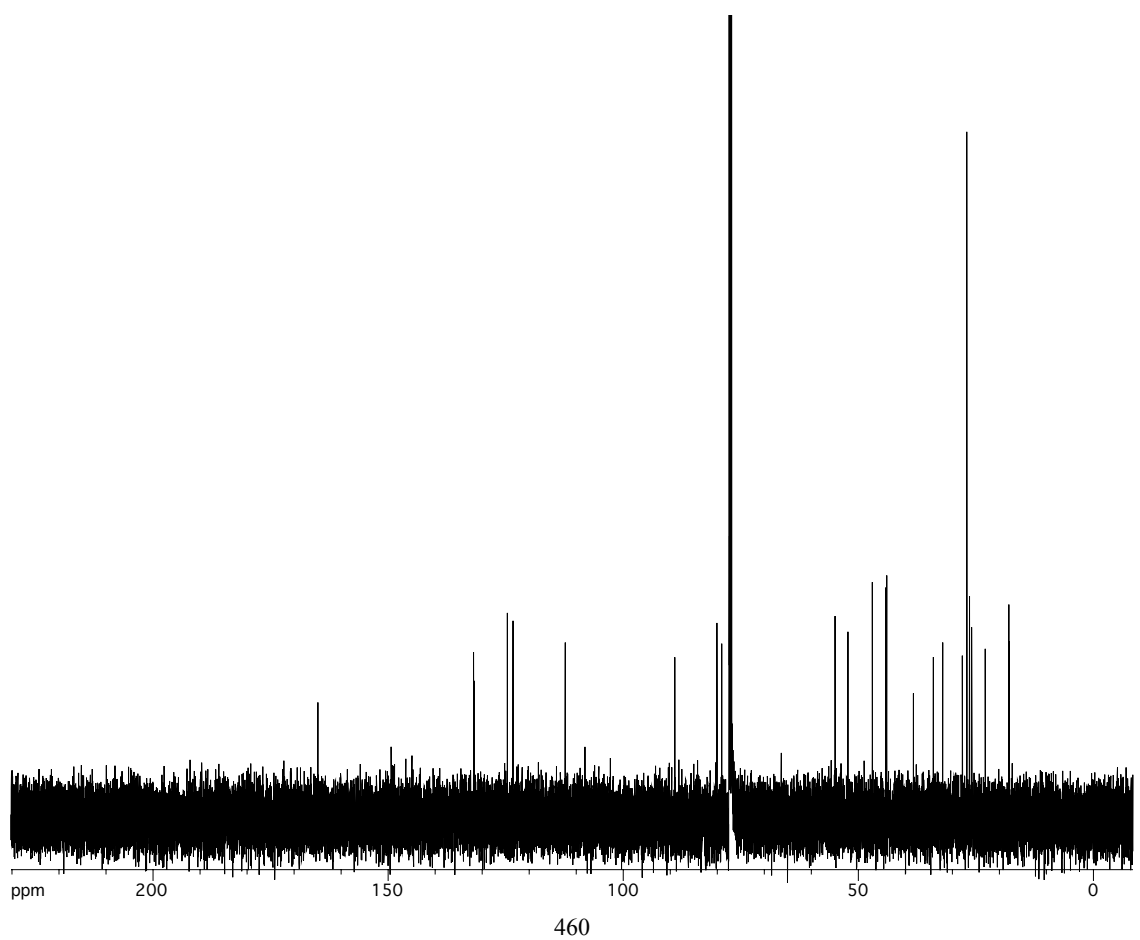
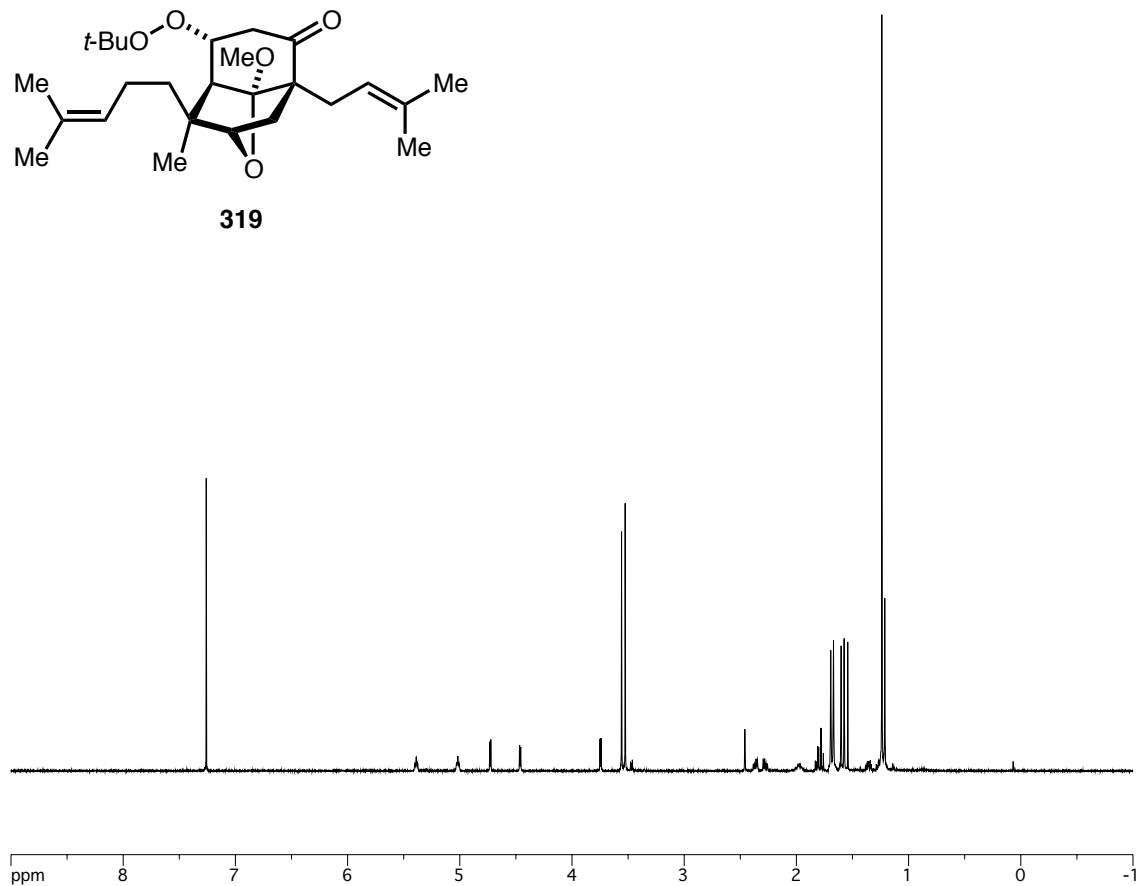
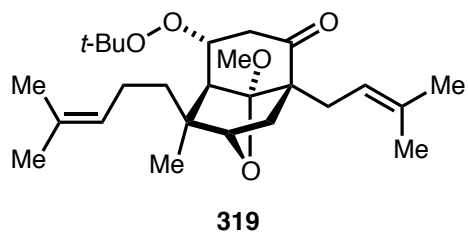
312

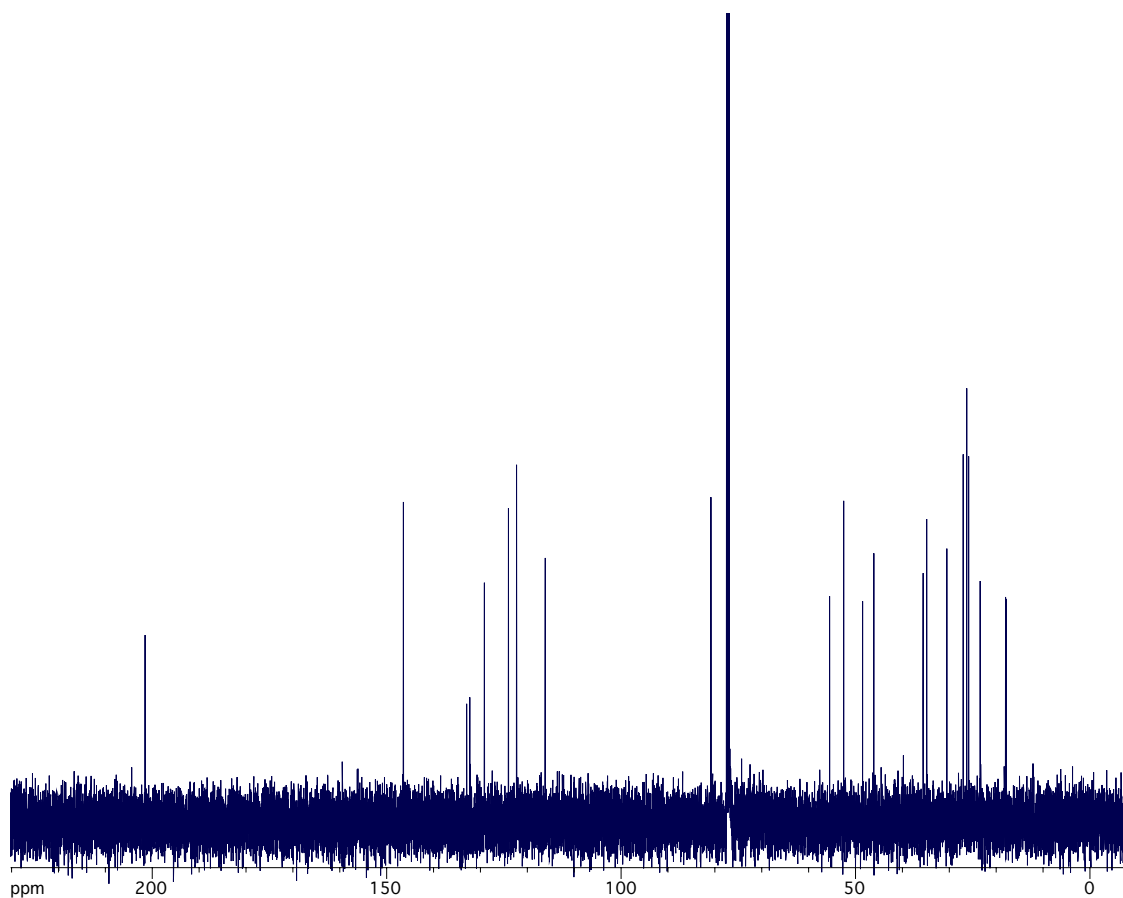
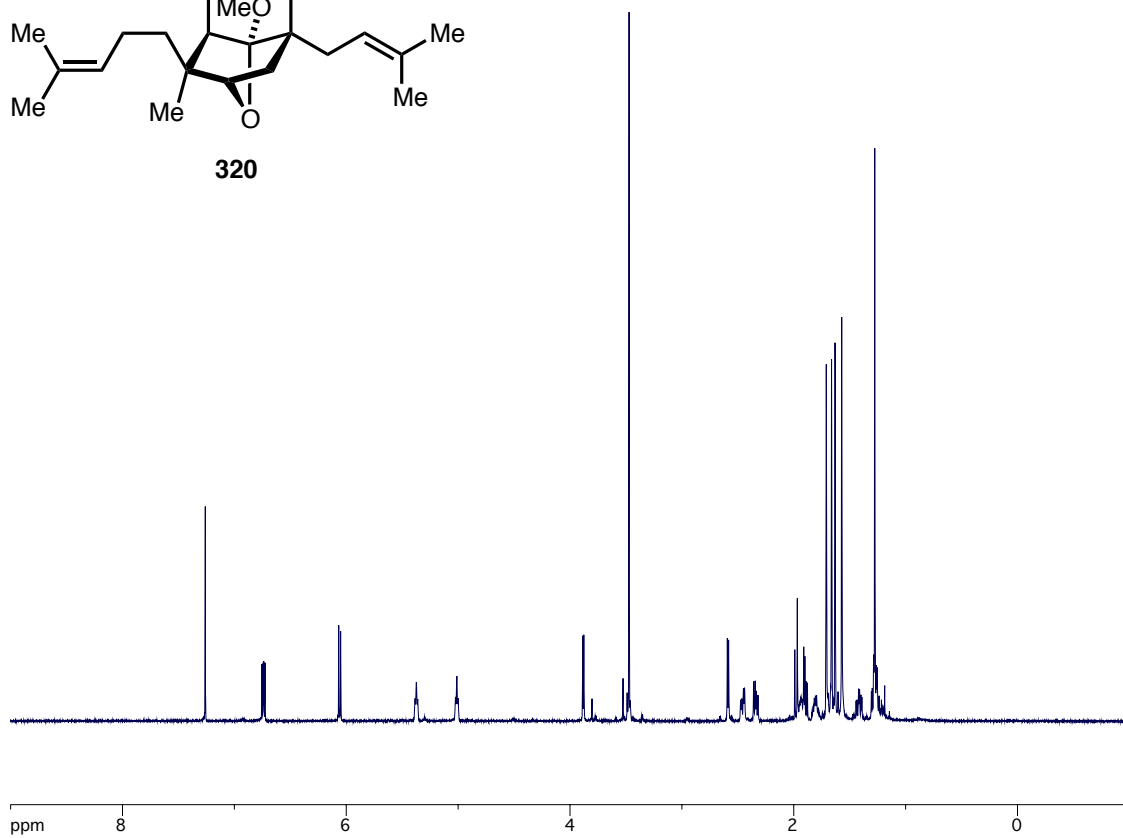
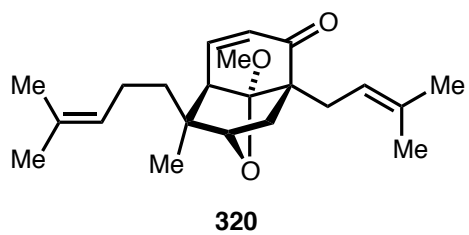


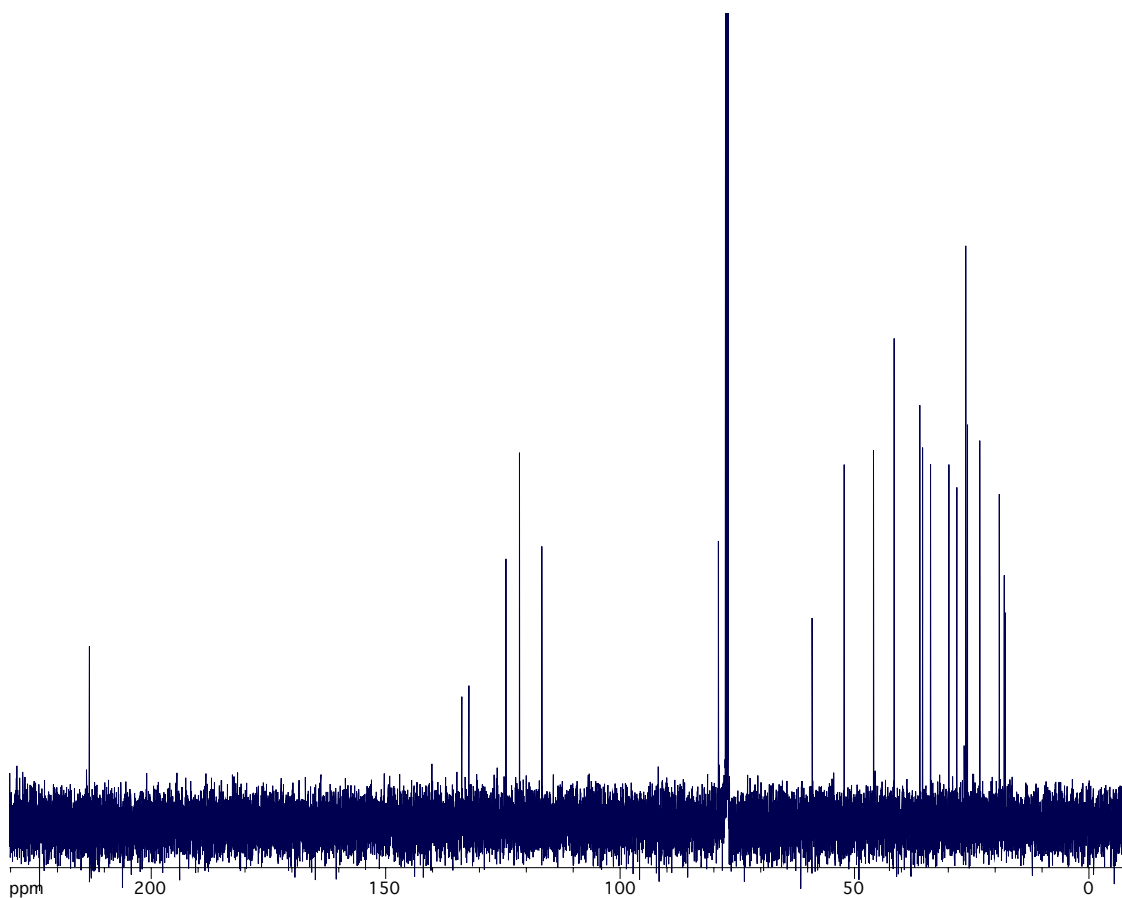
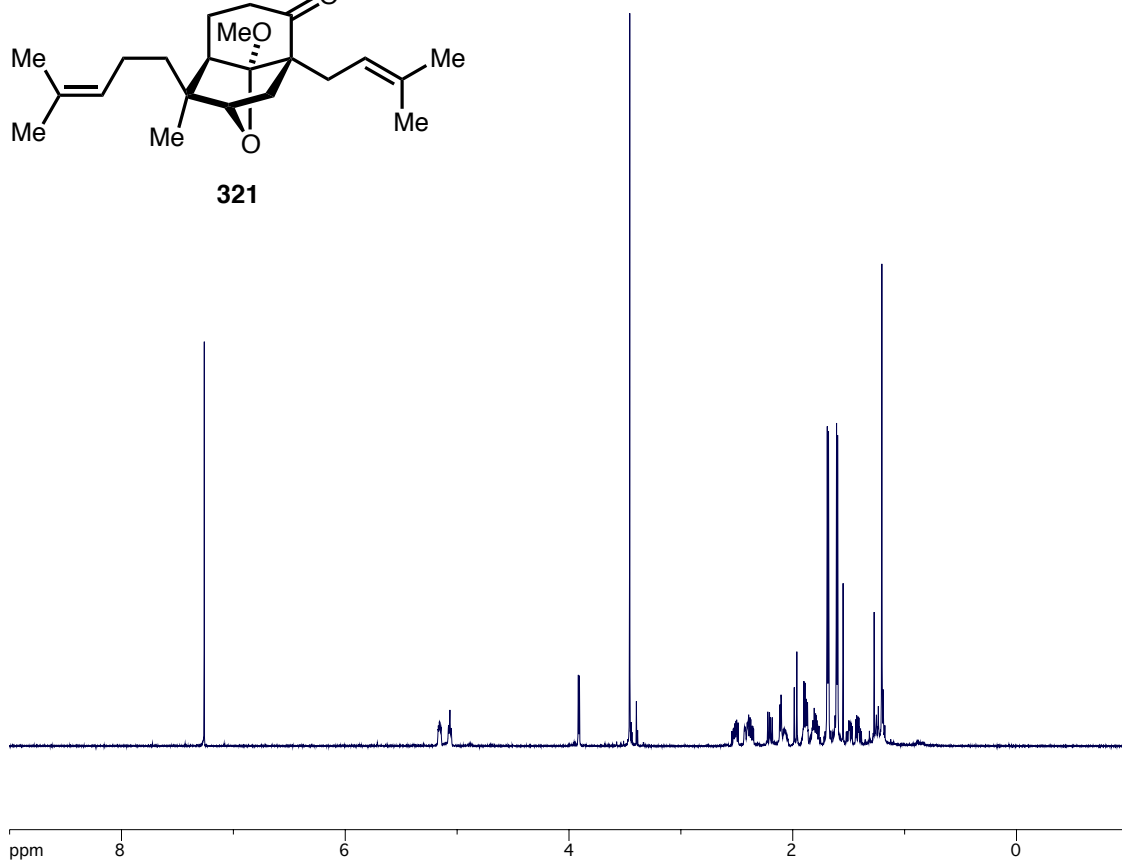
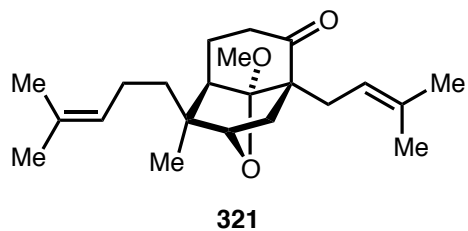


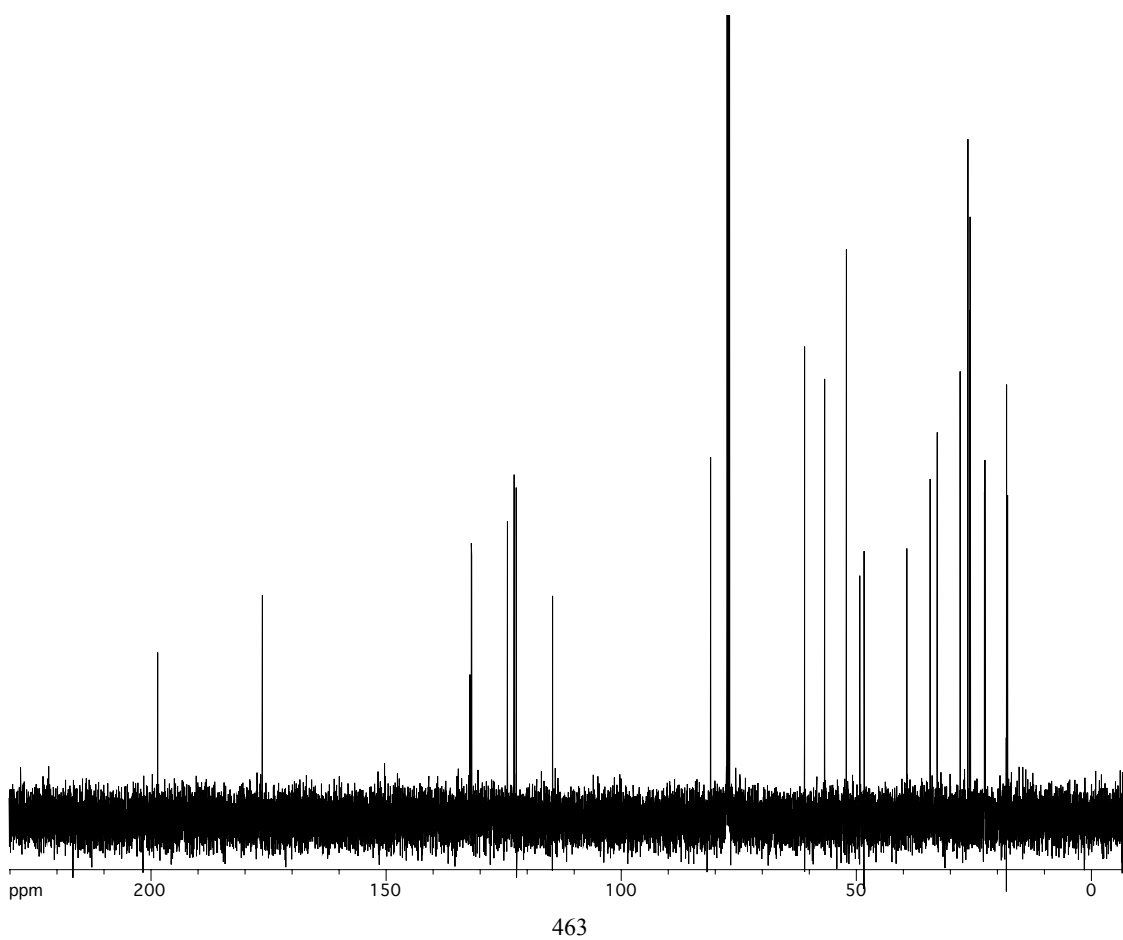
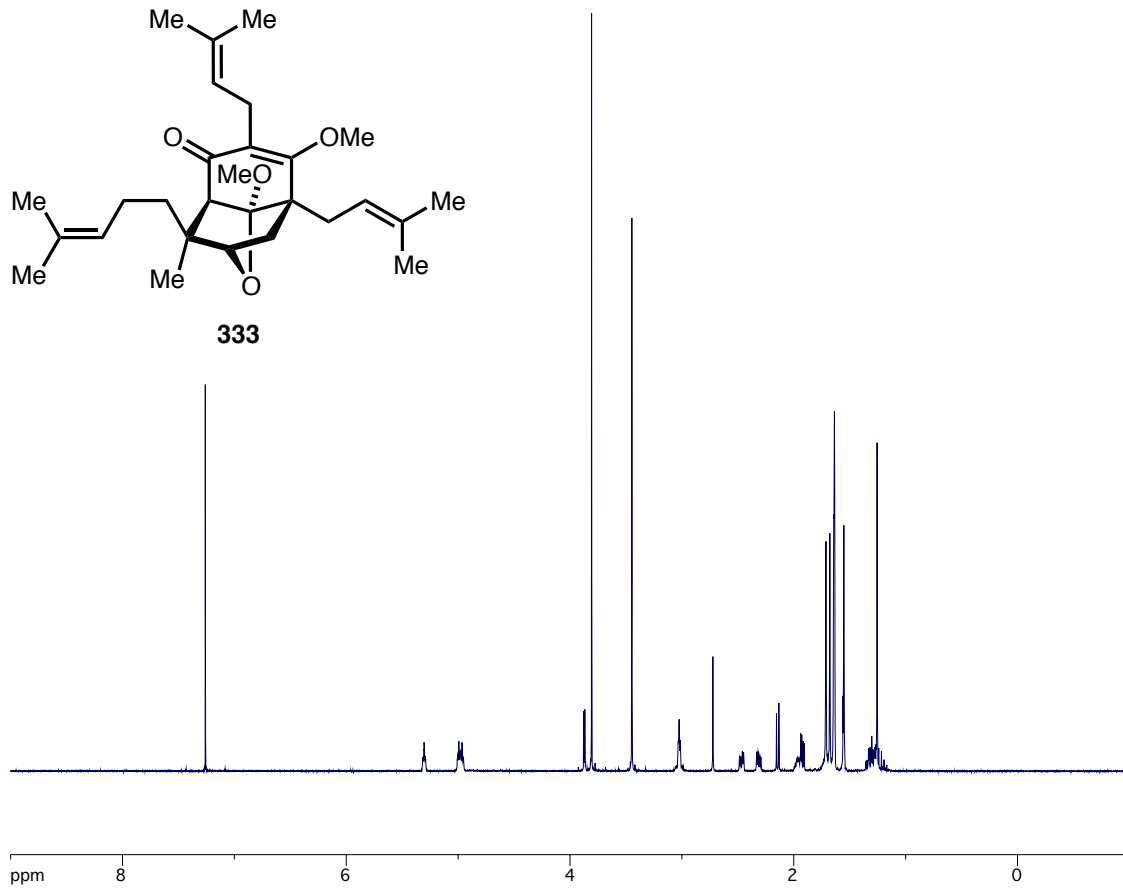
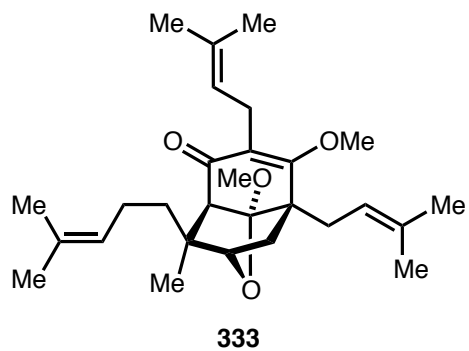


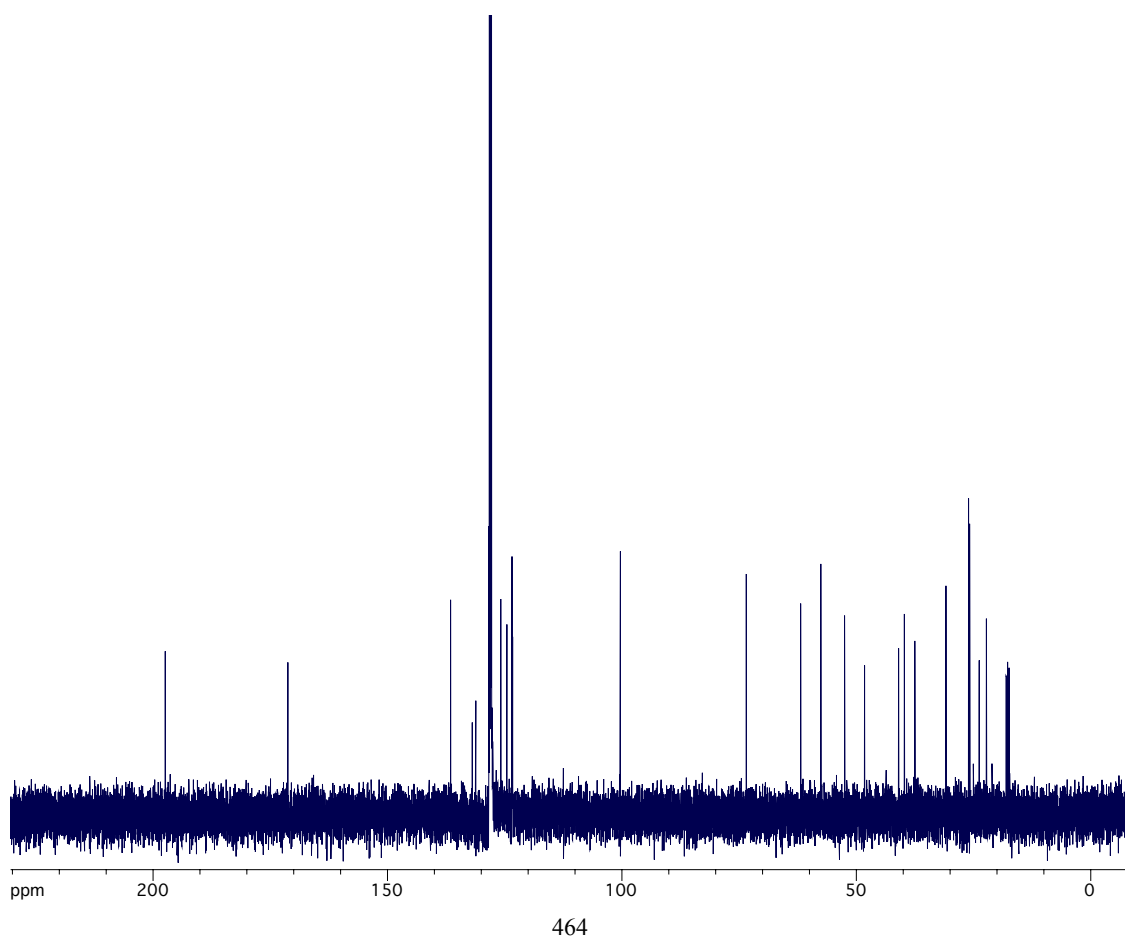
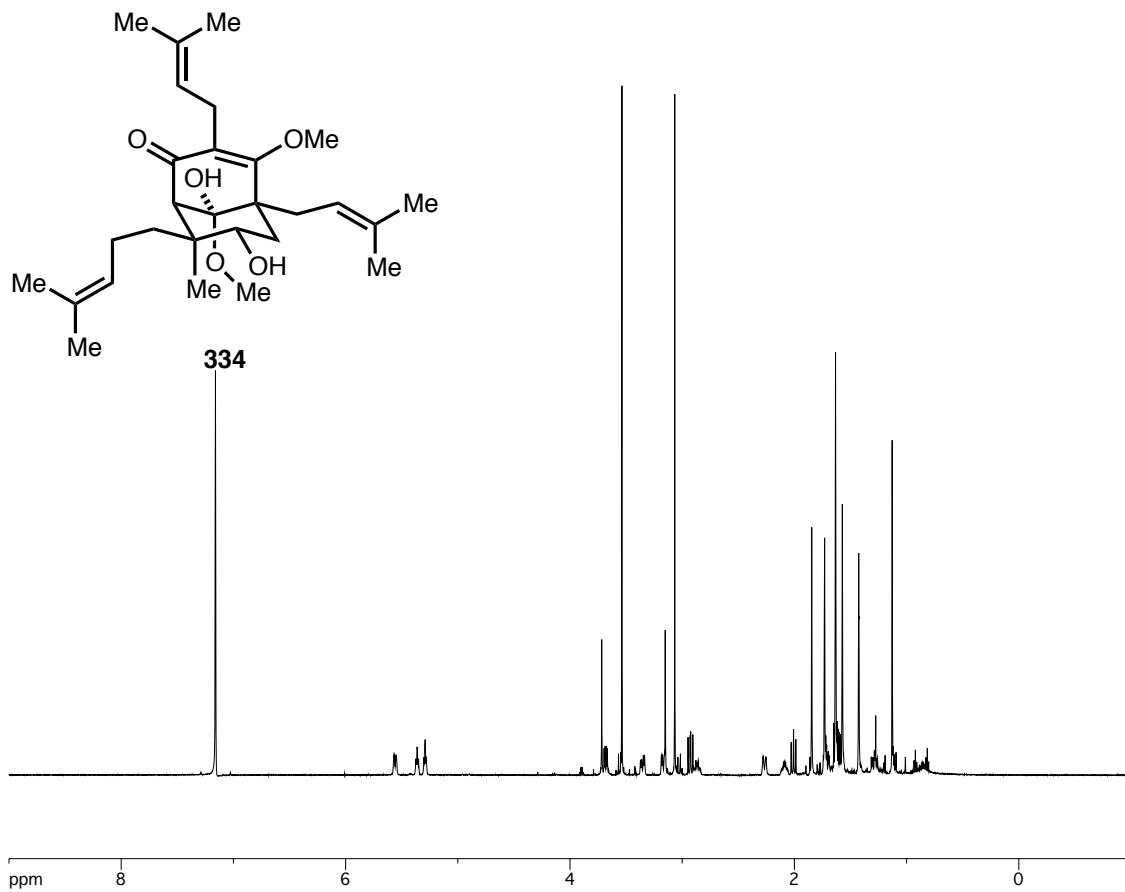


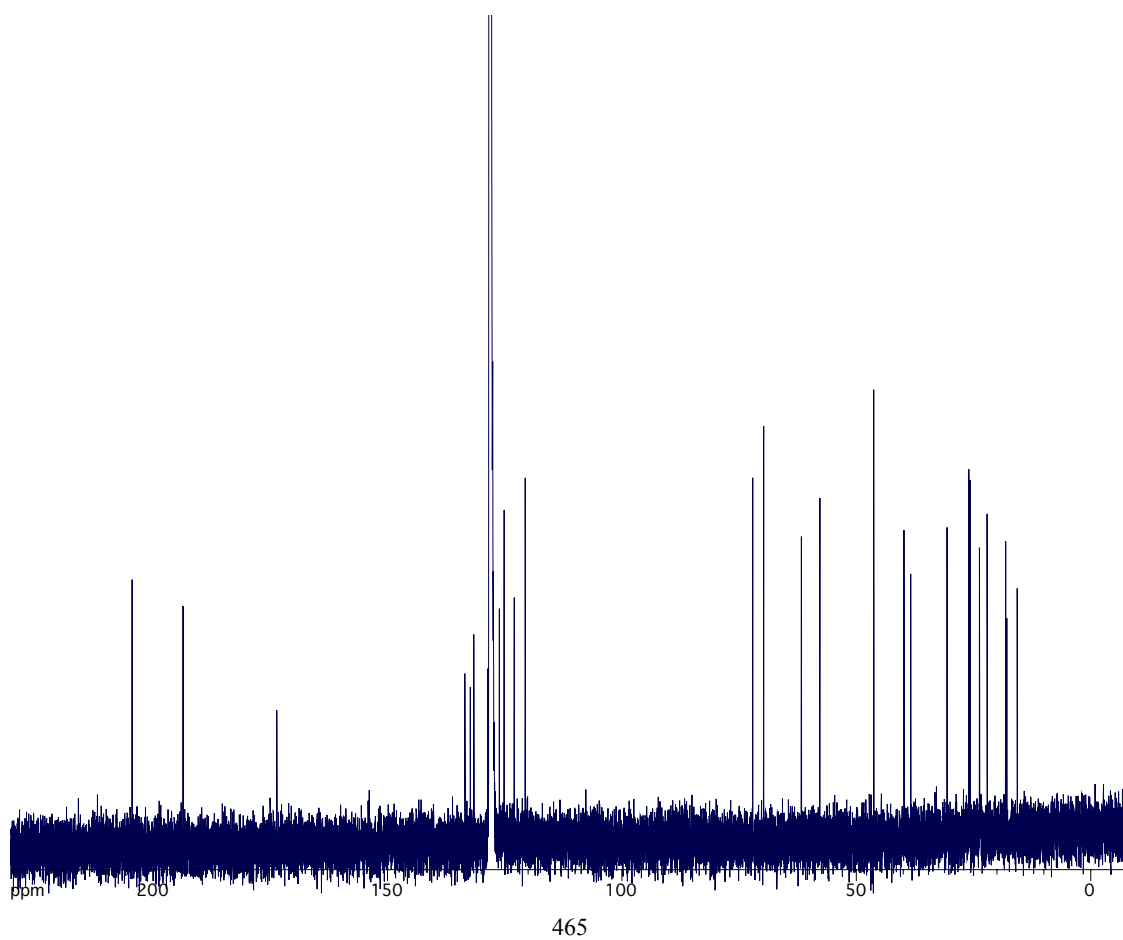
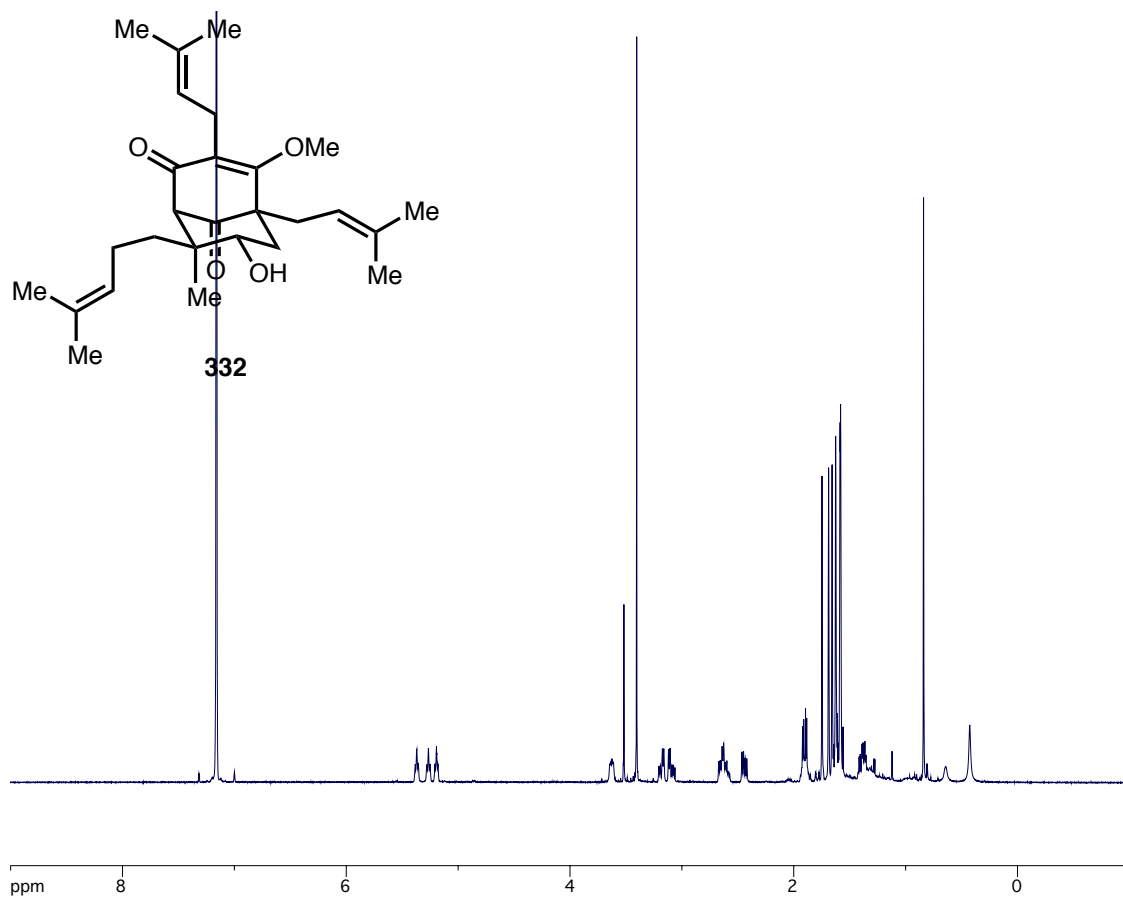


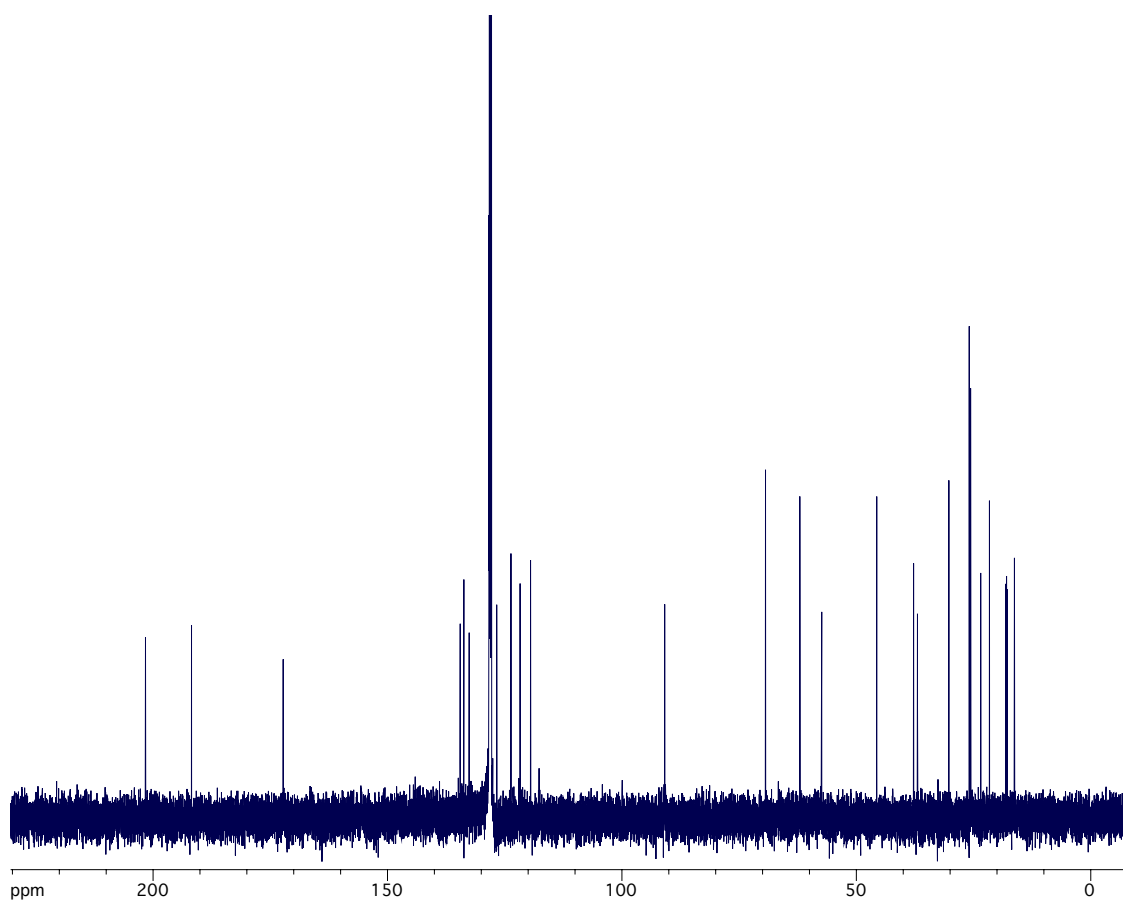
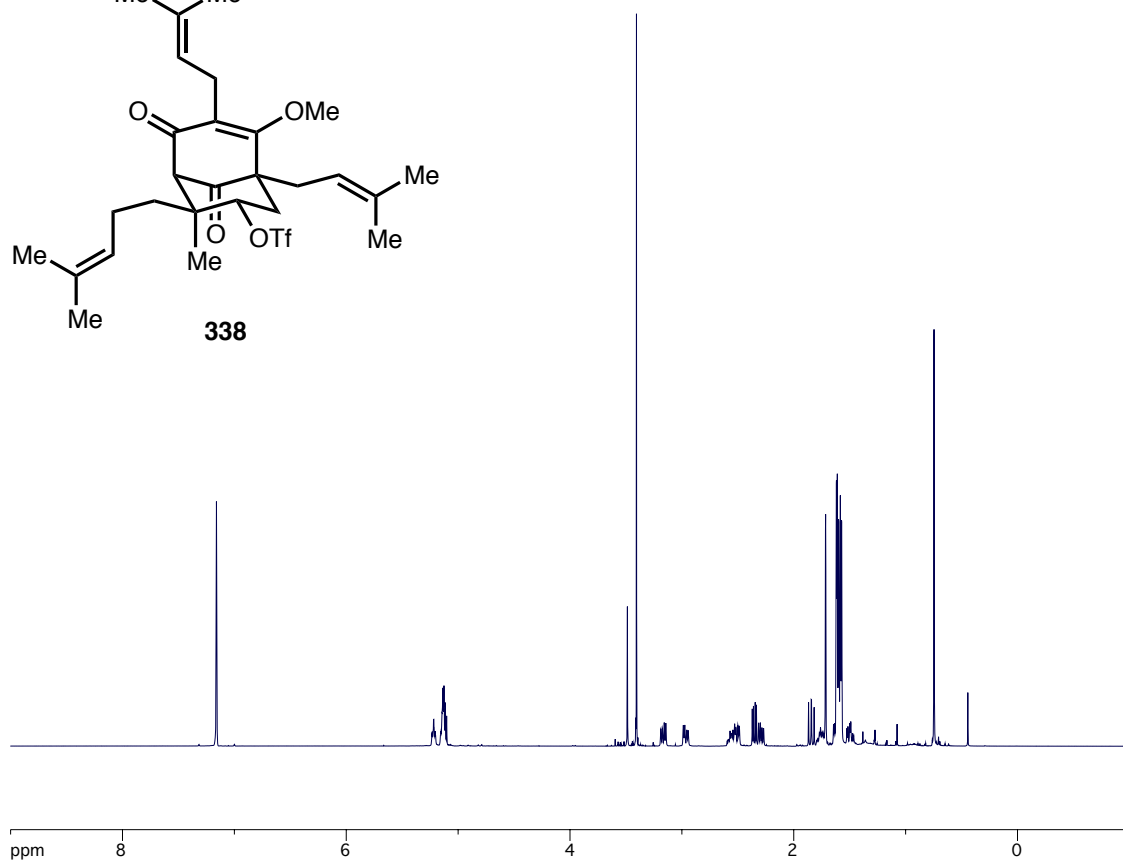
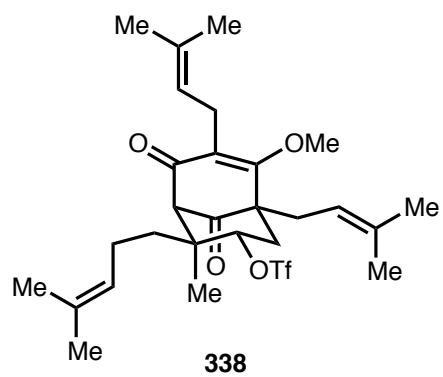


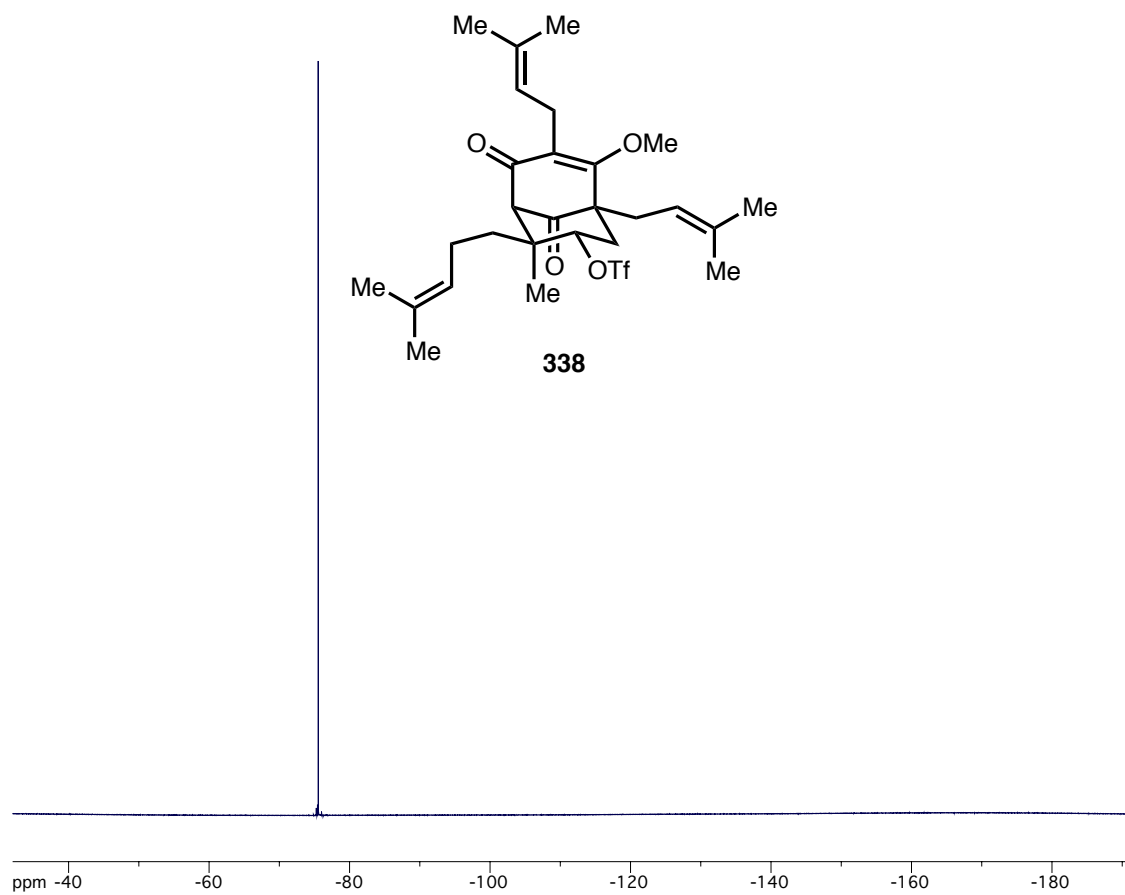


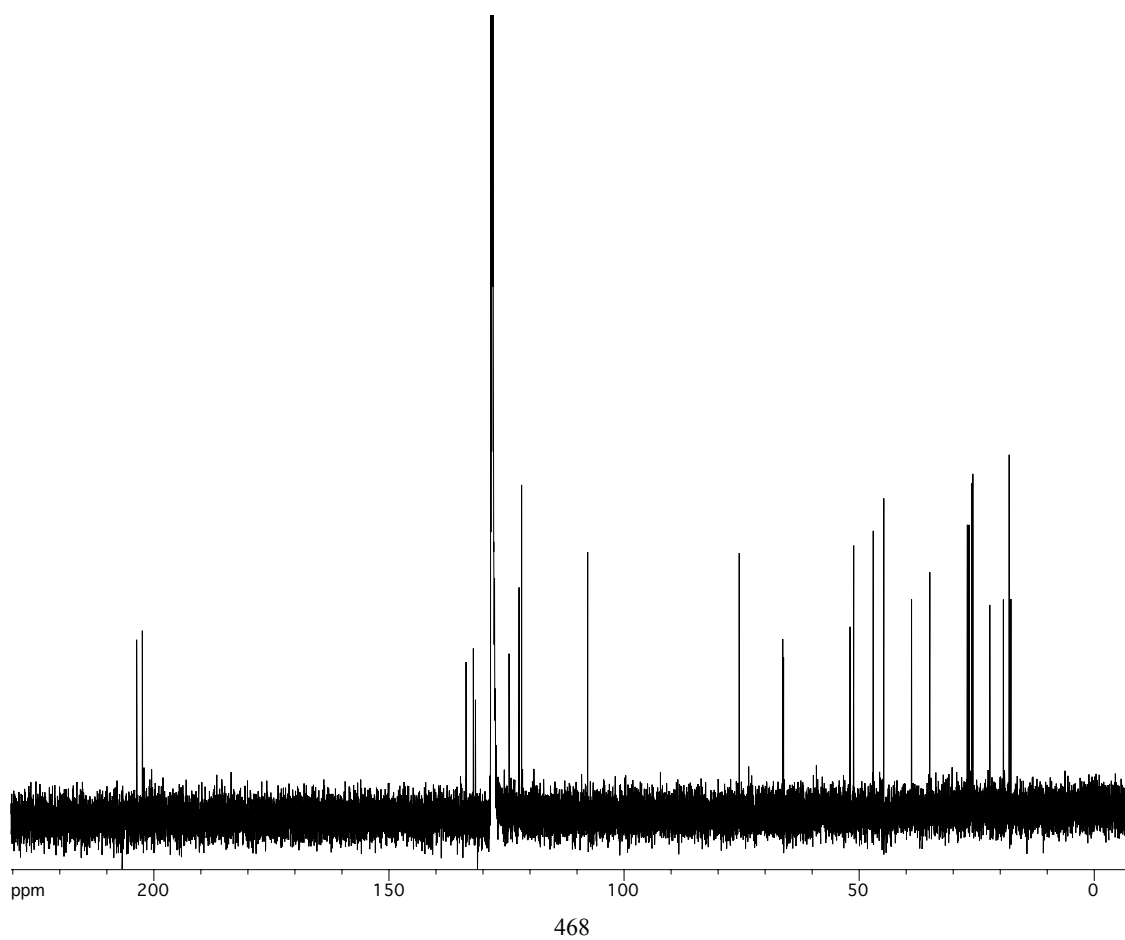
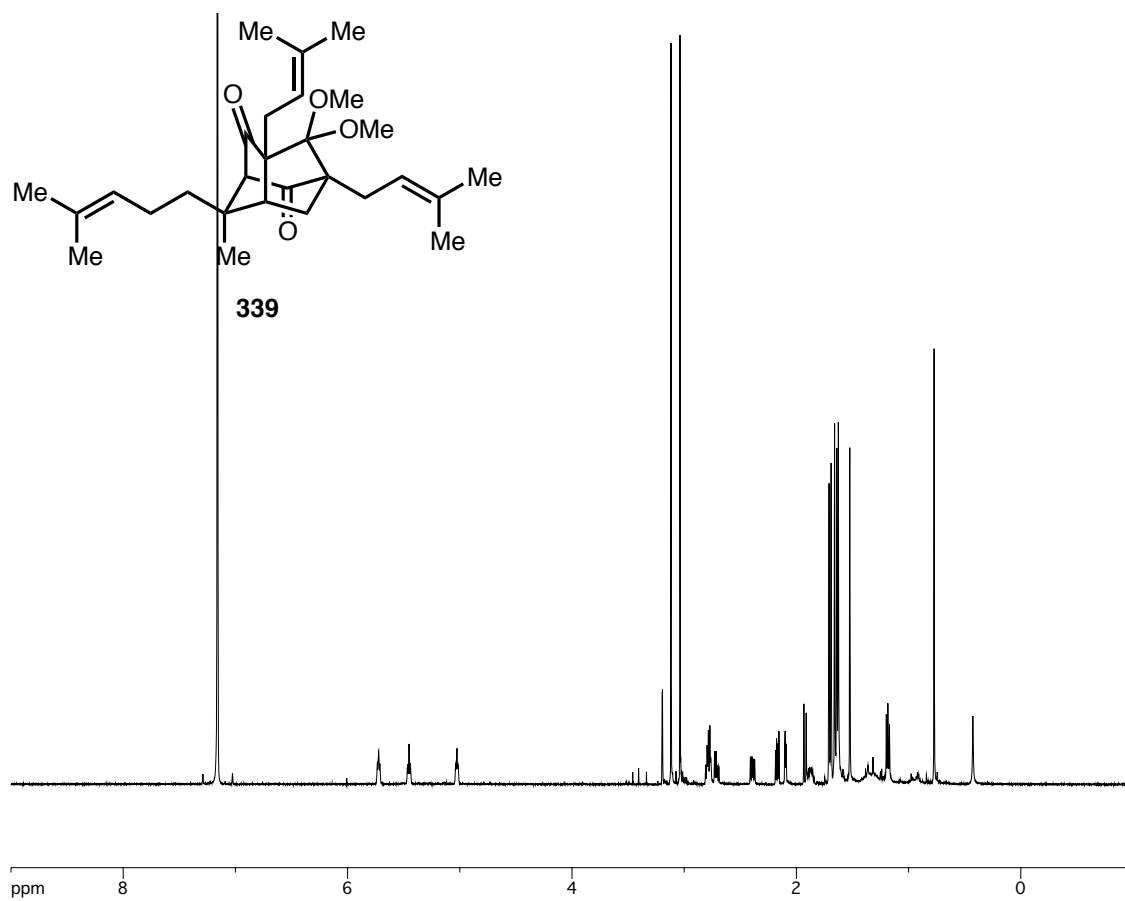


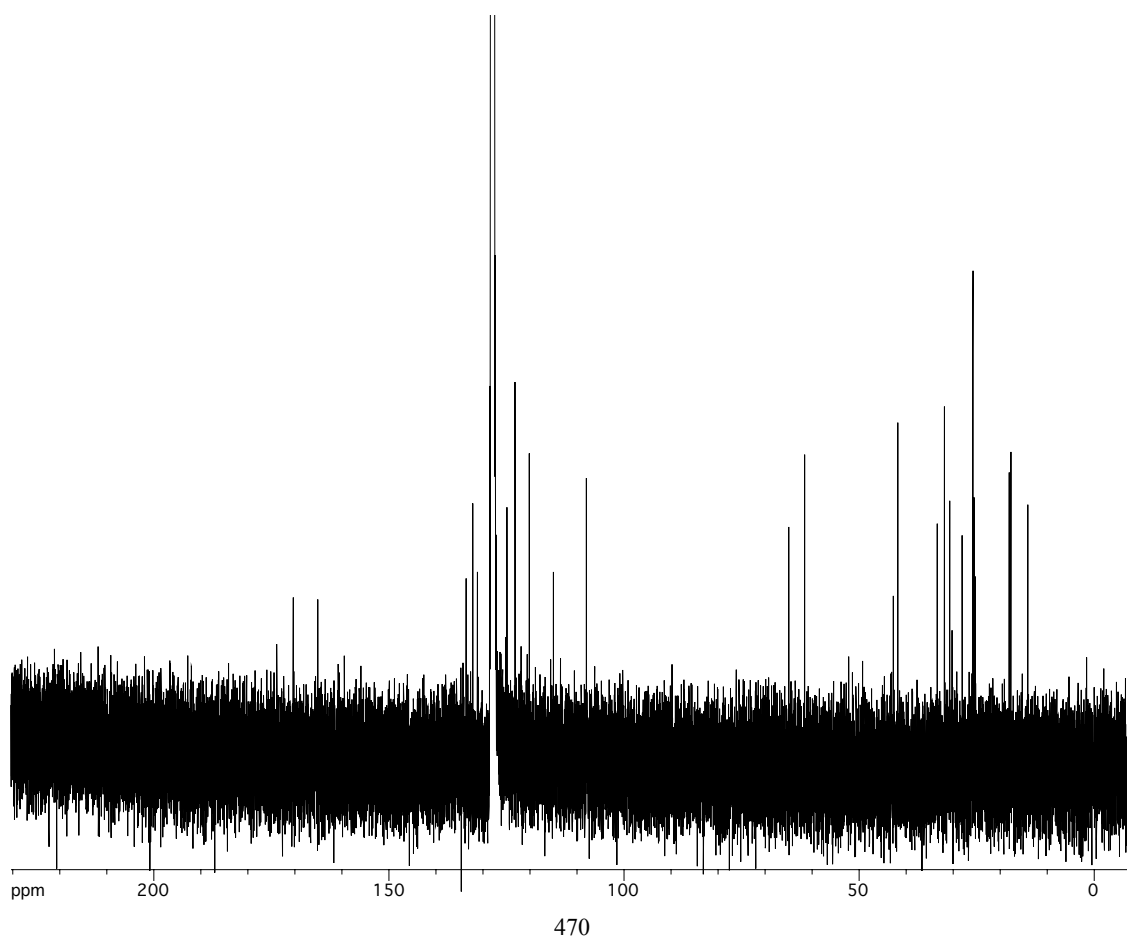
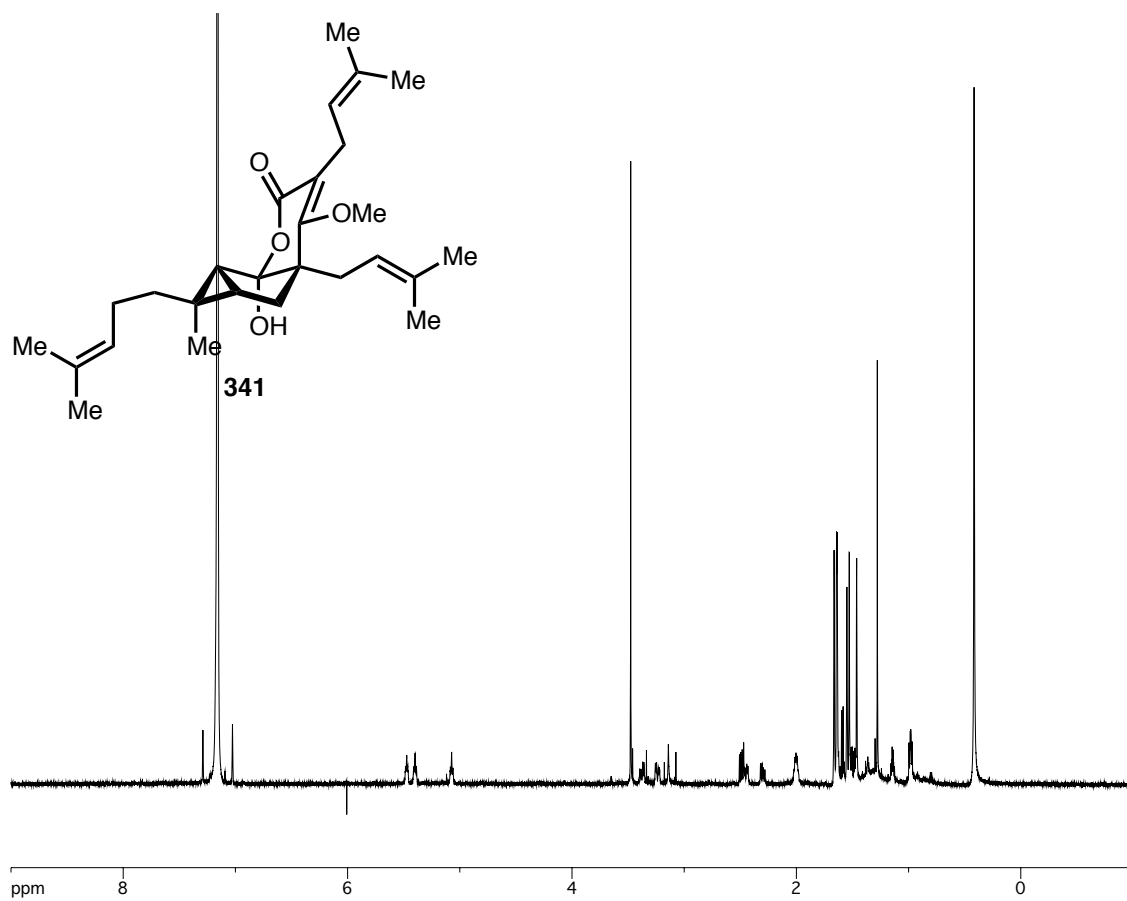


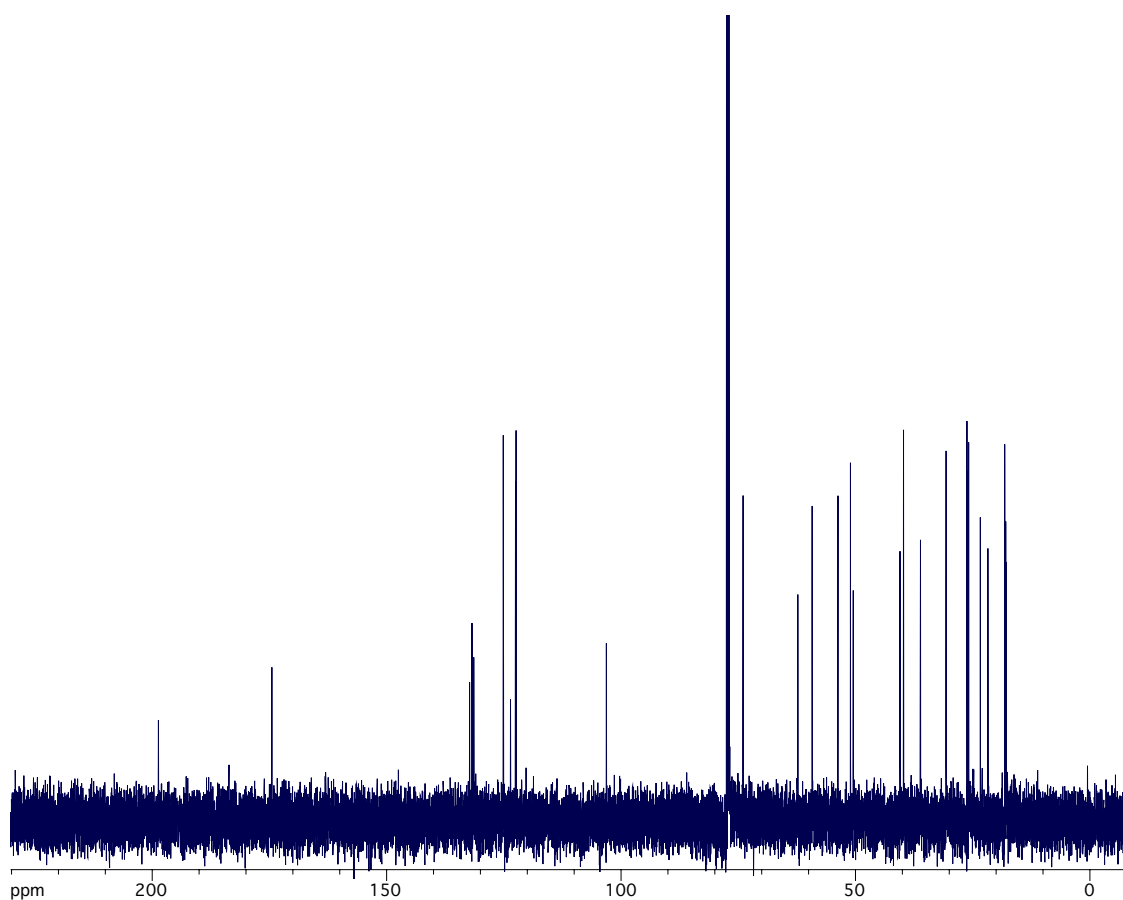
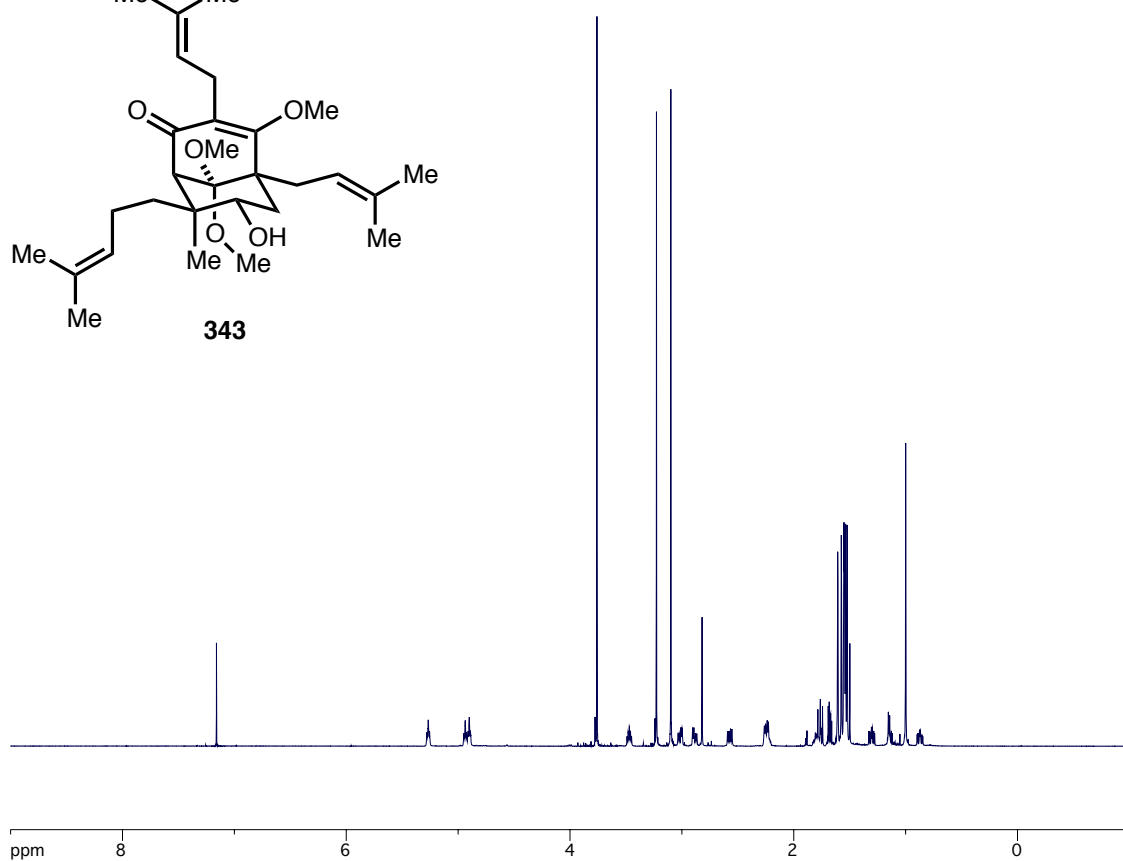
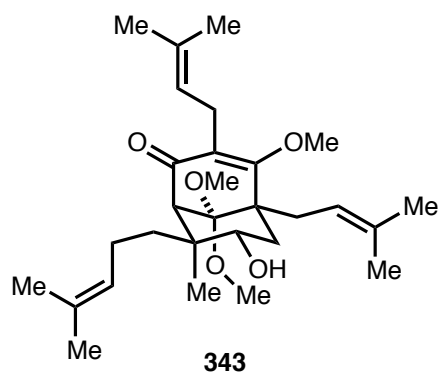


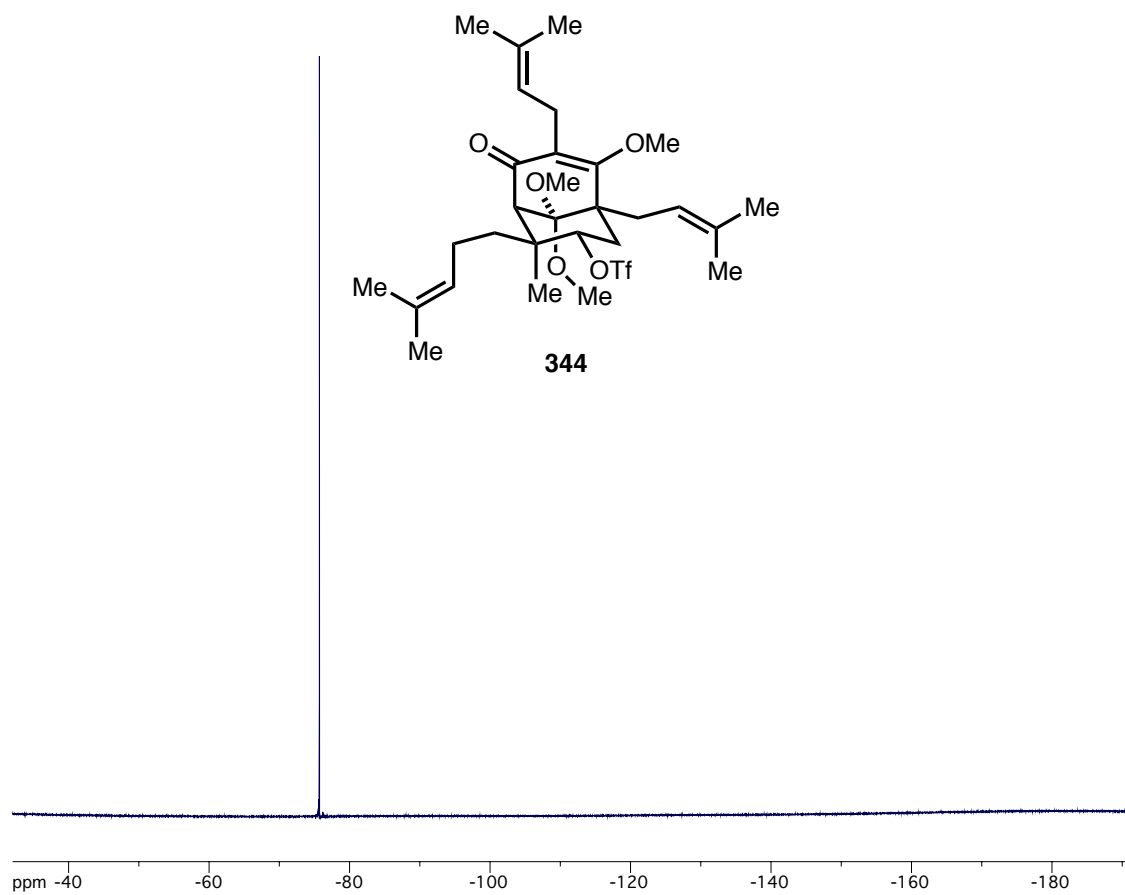


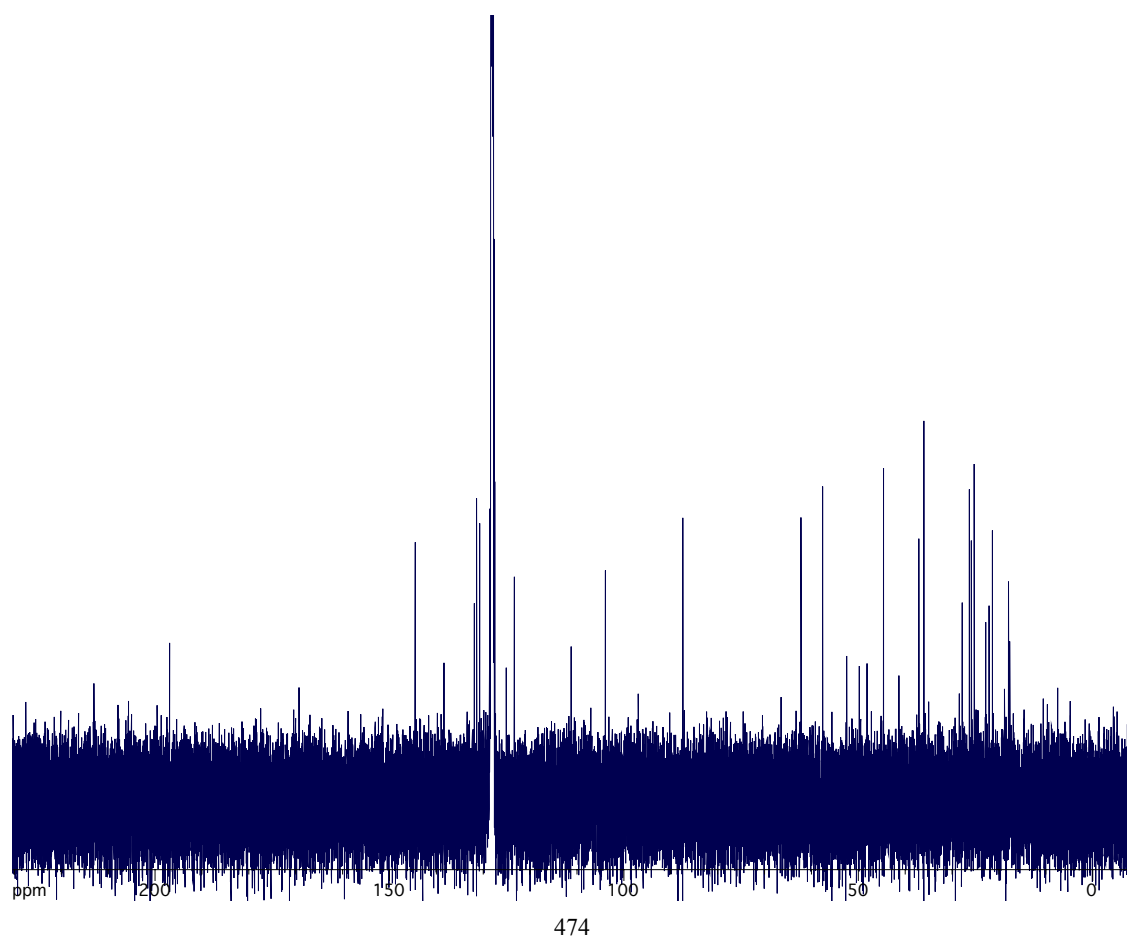
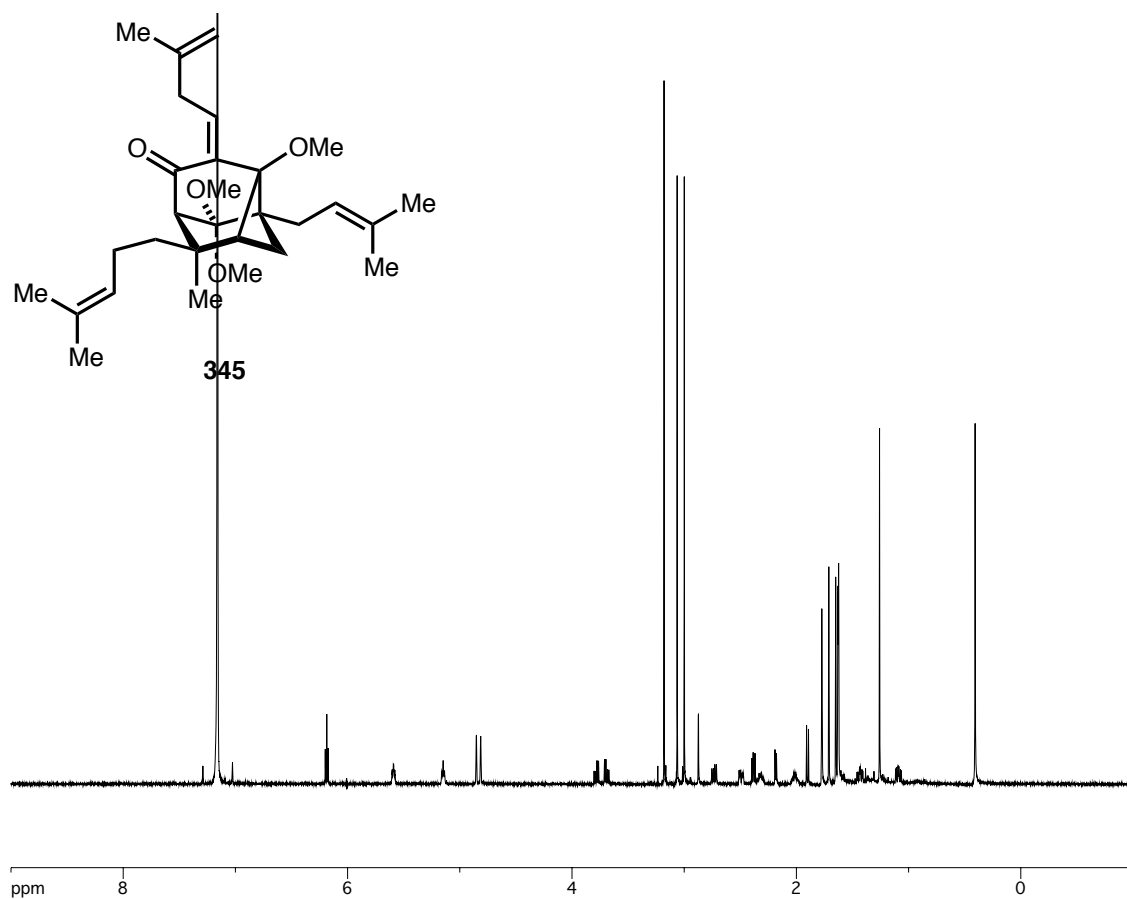


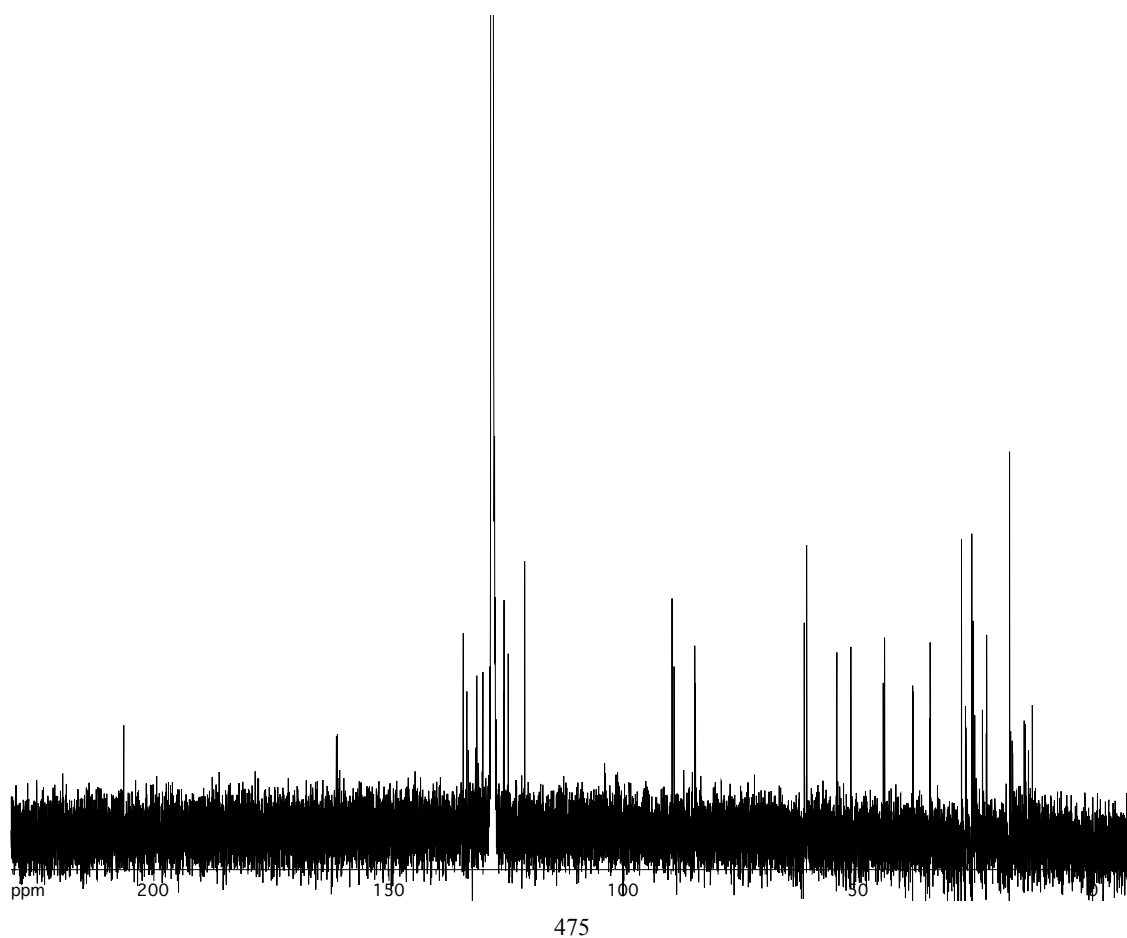
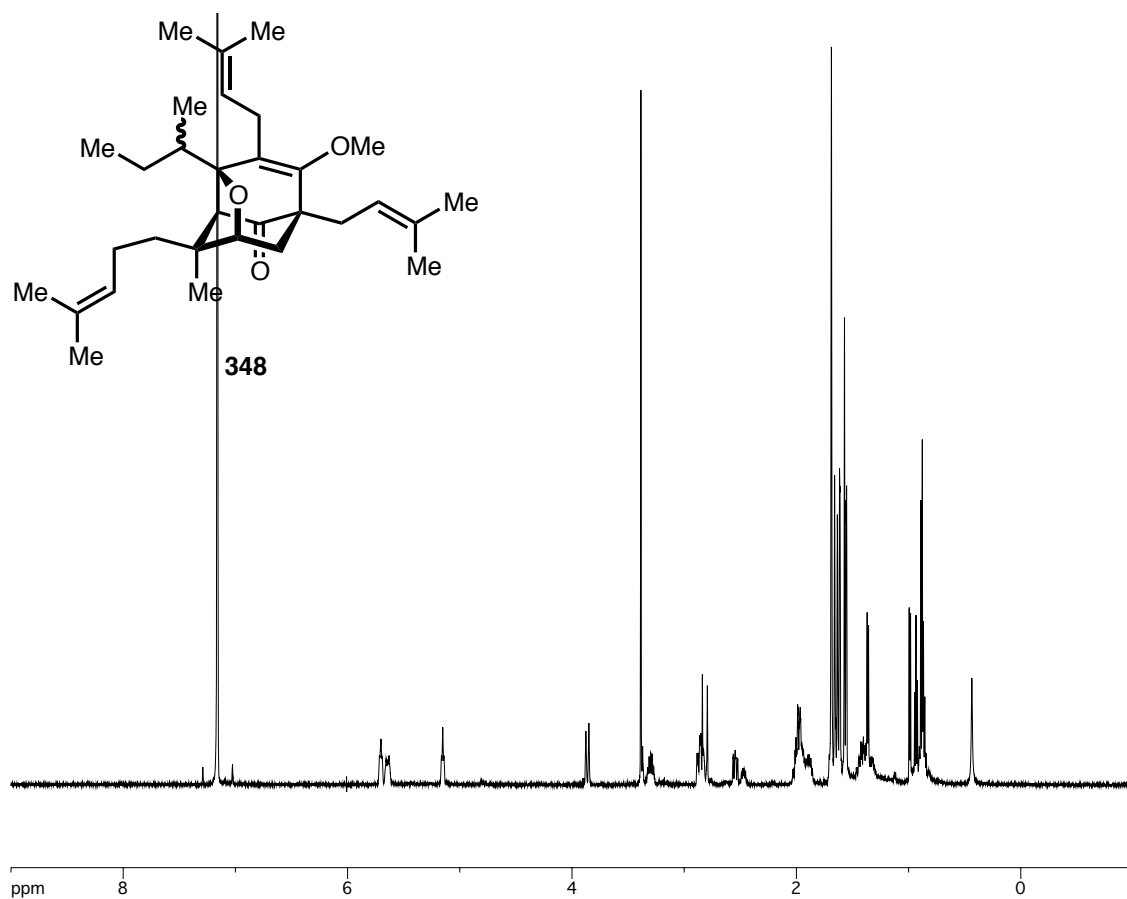


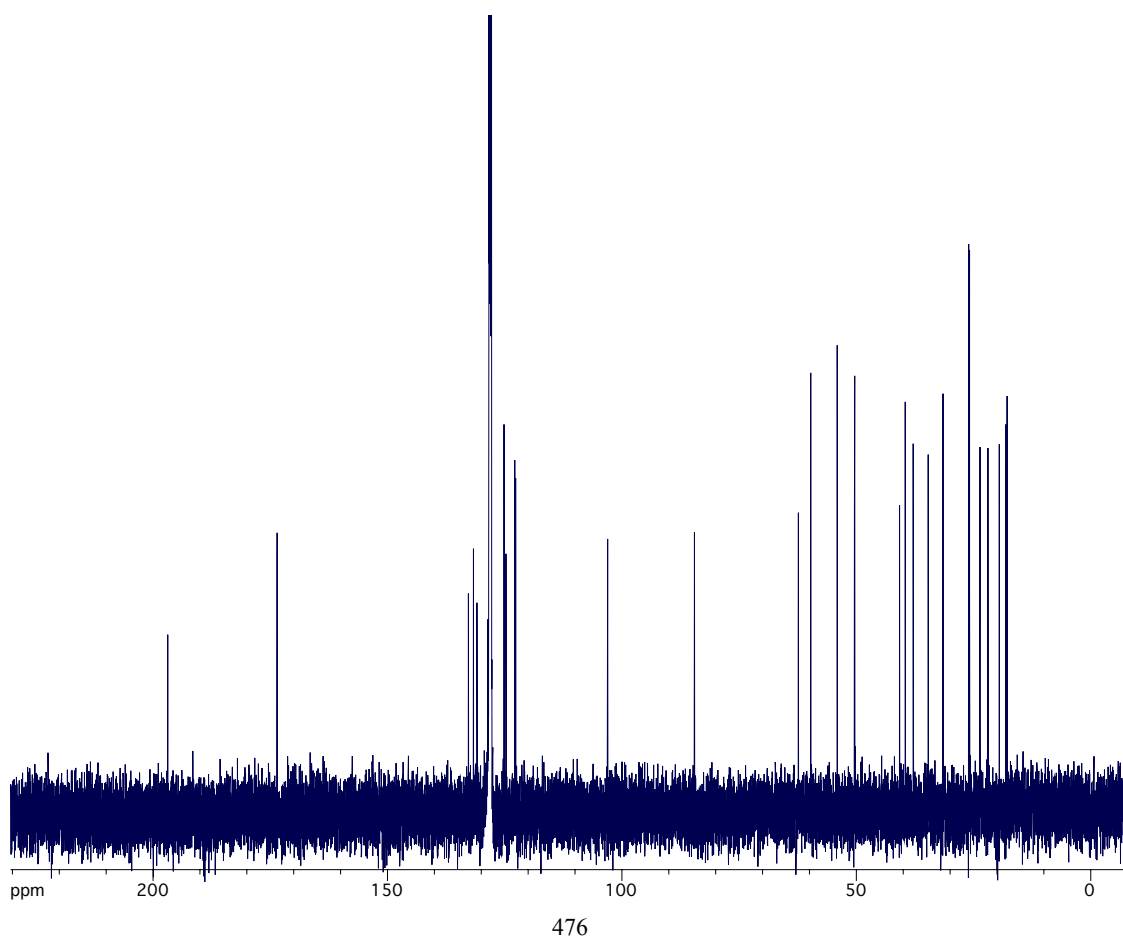
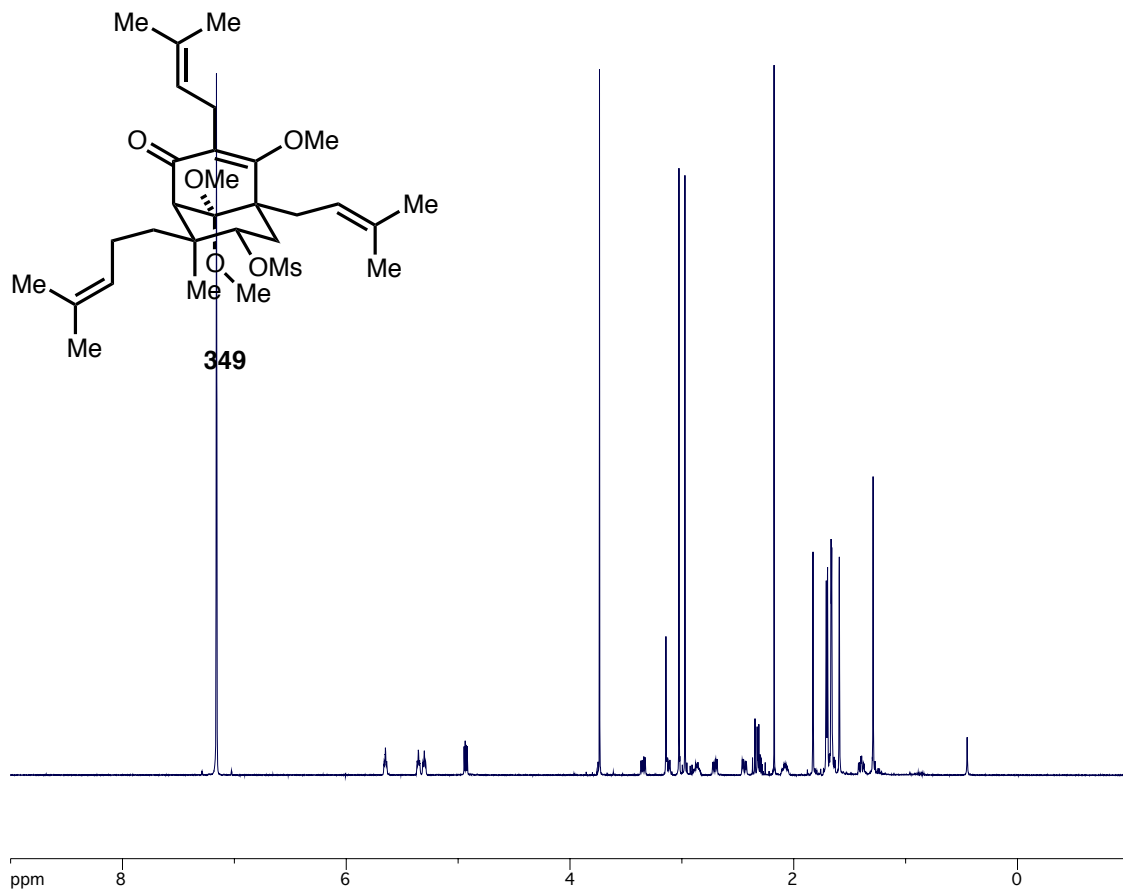


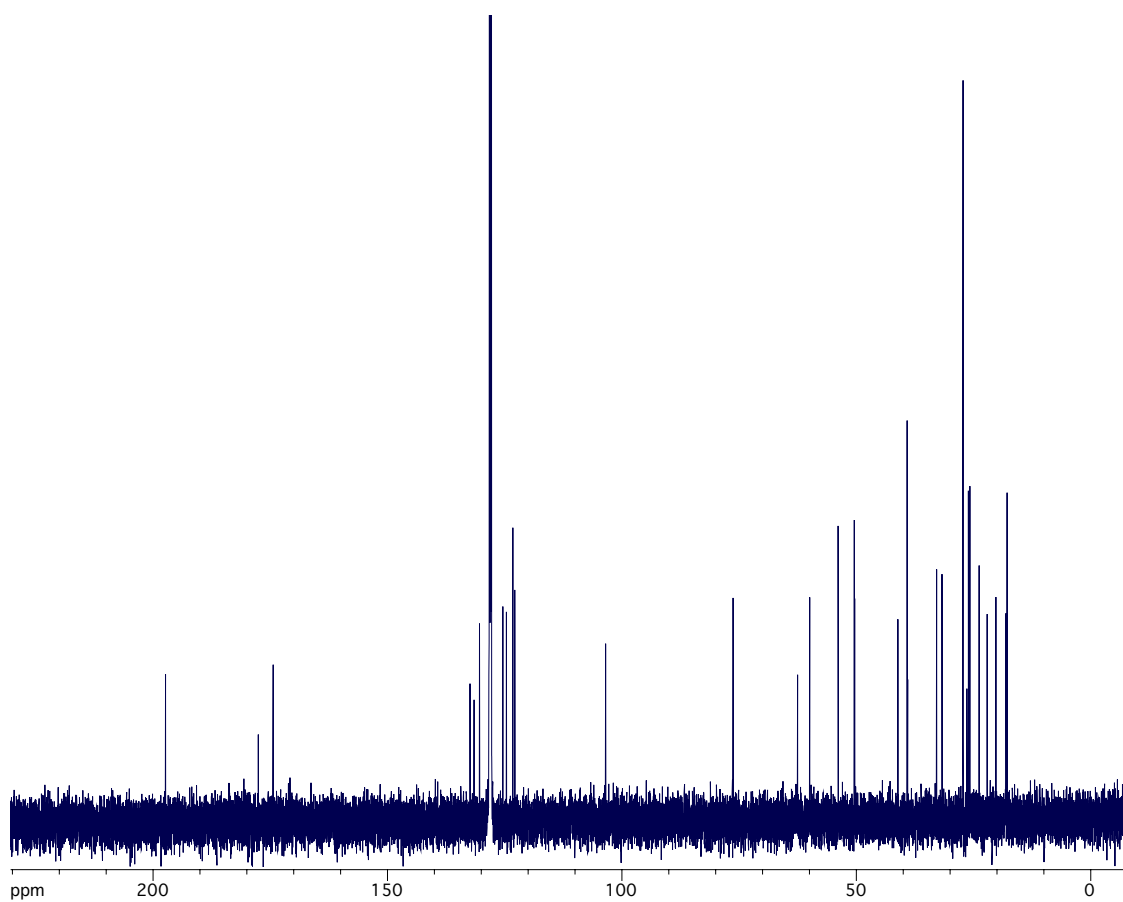
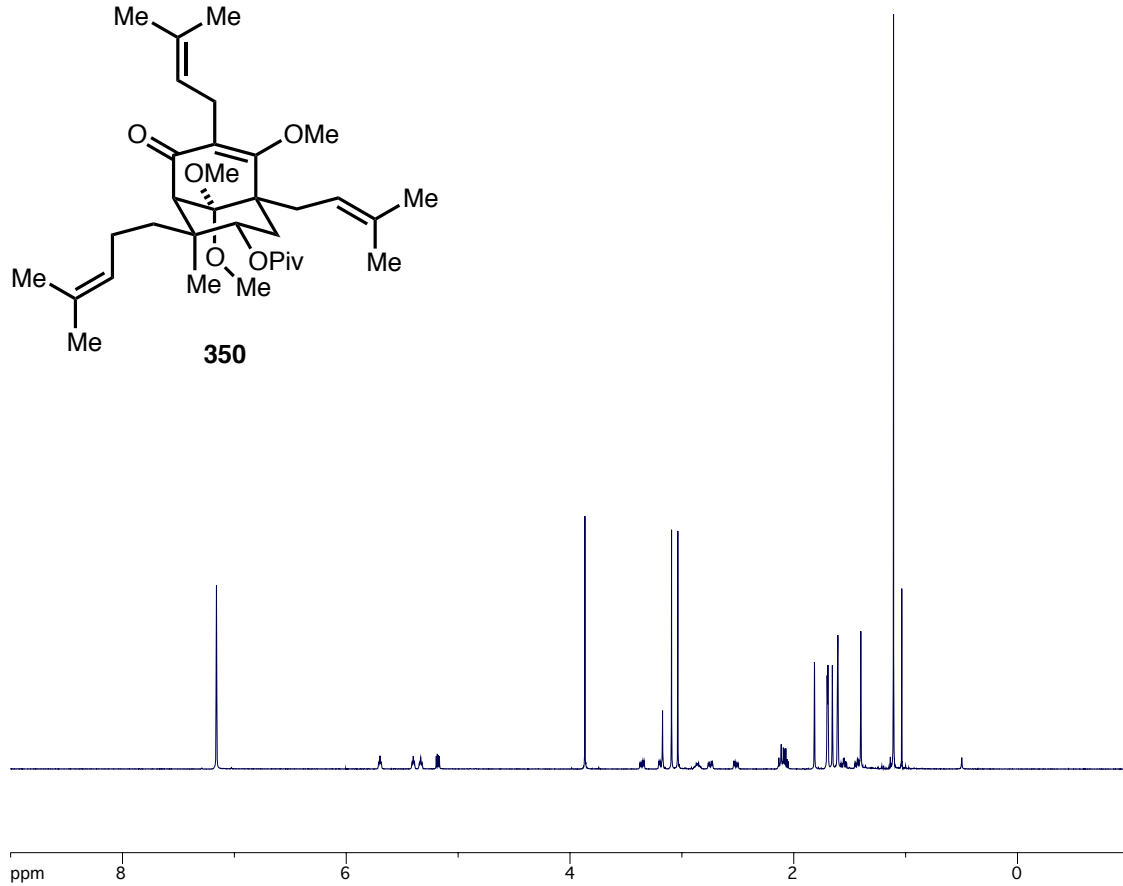
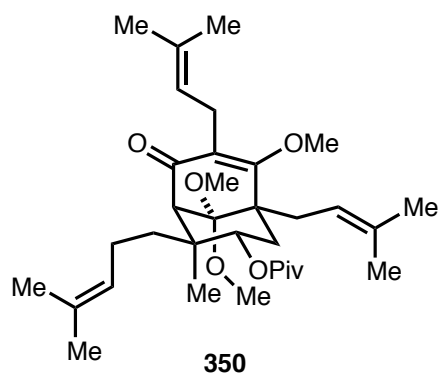


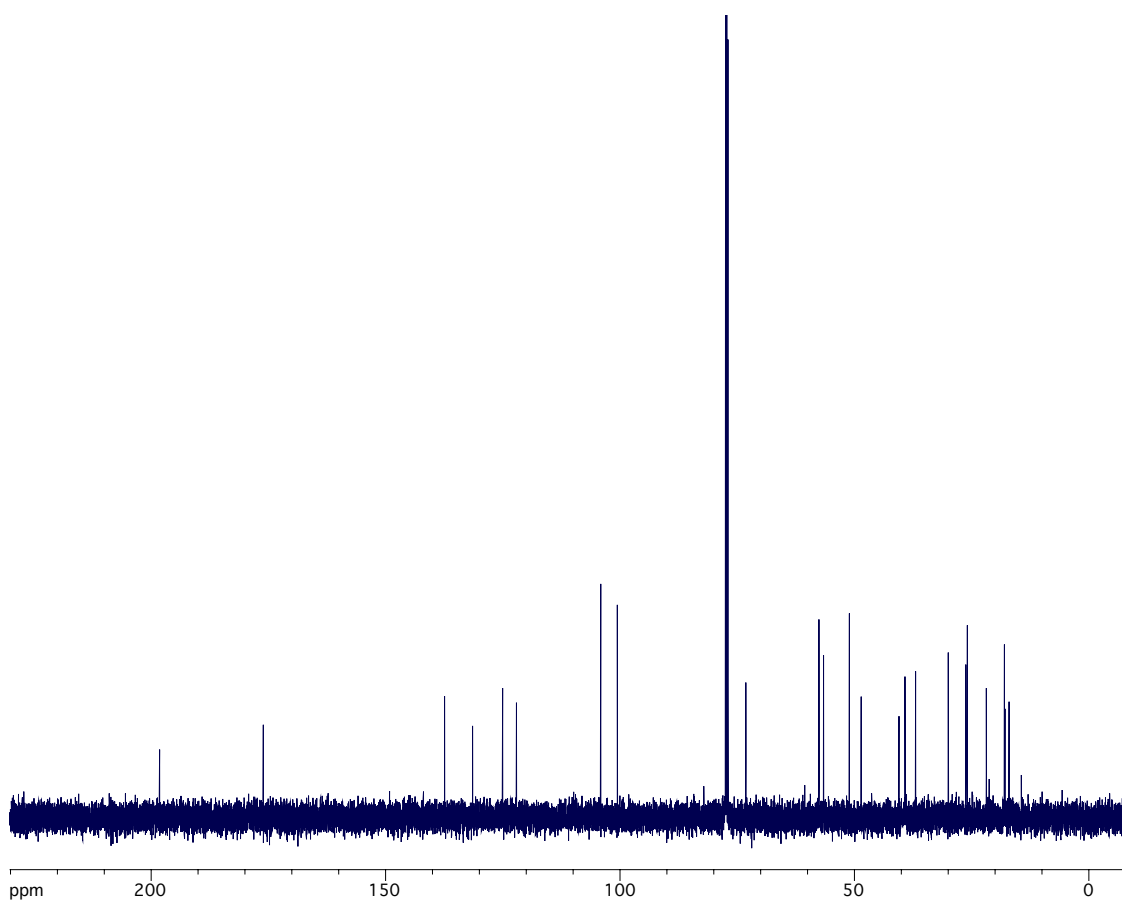
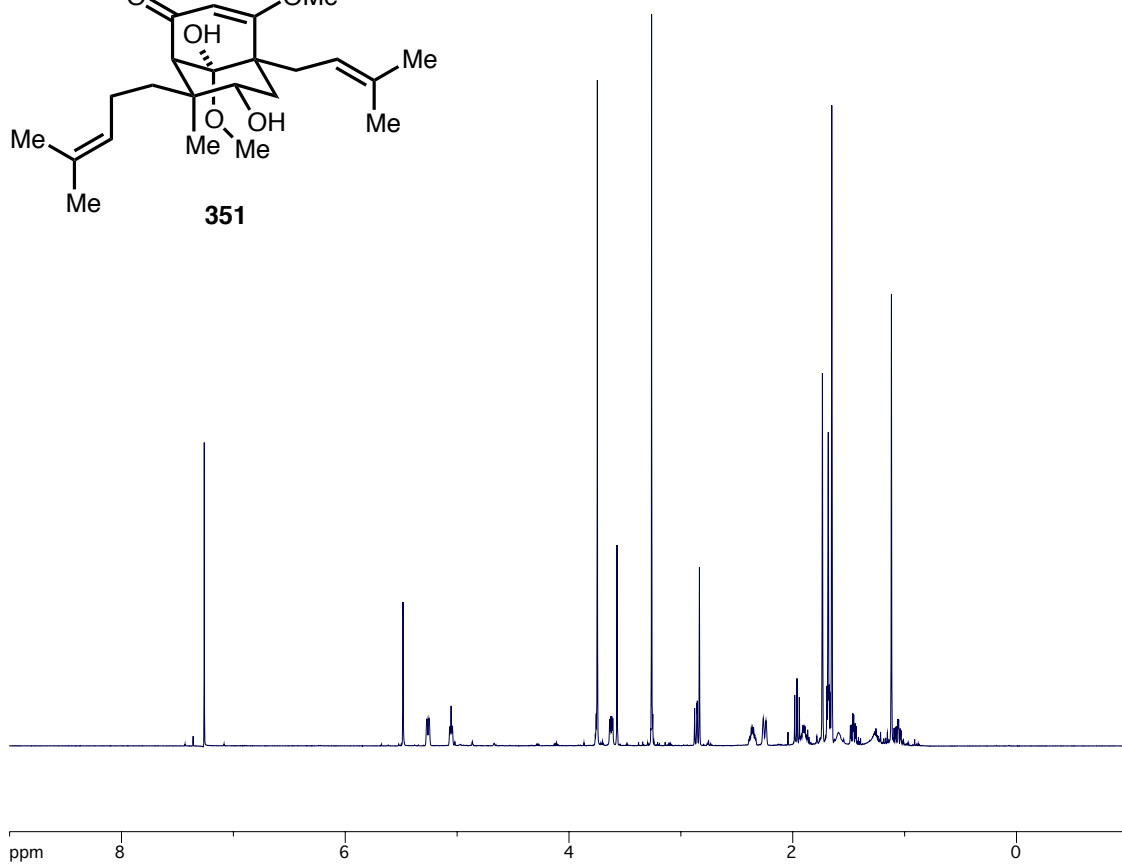
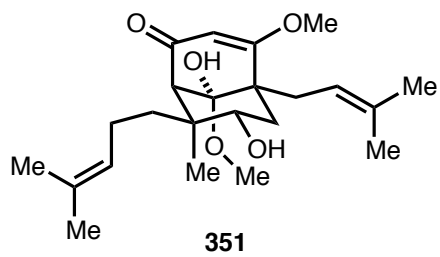


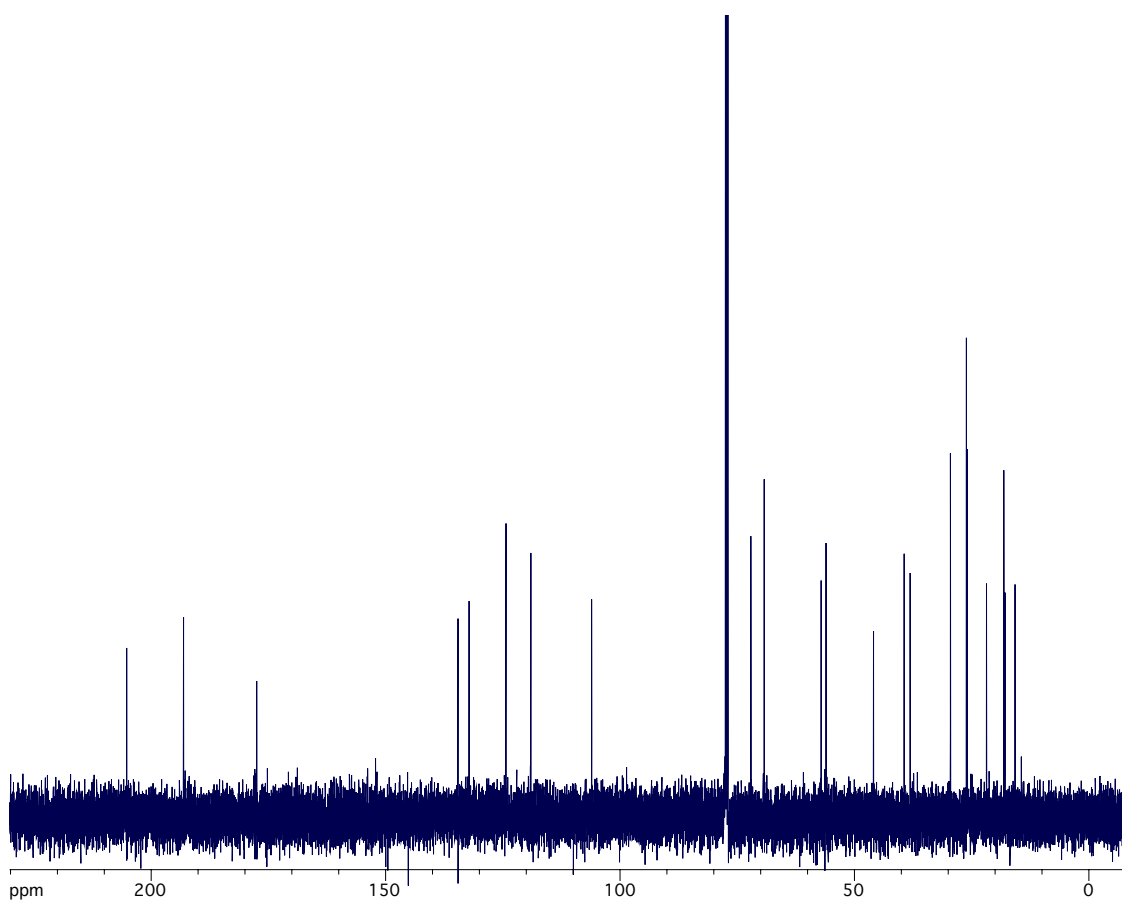
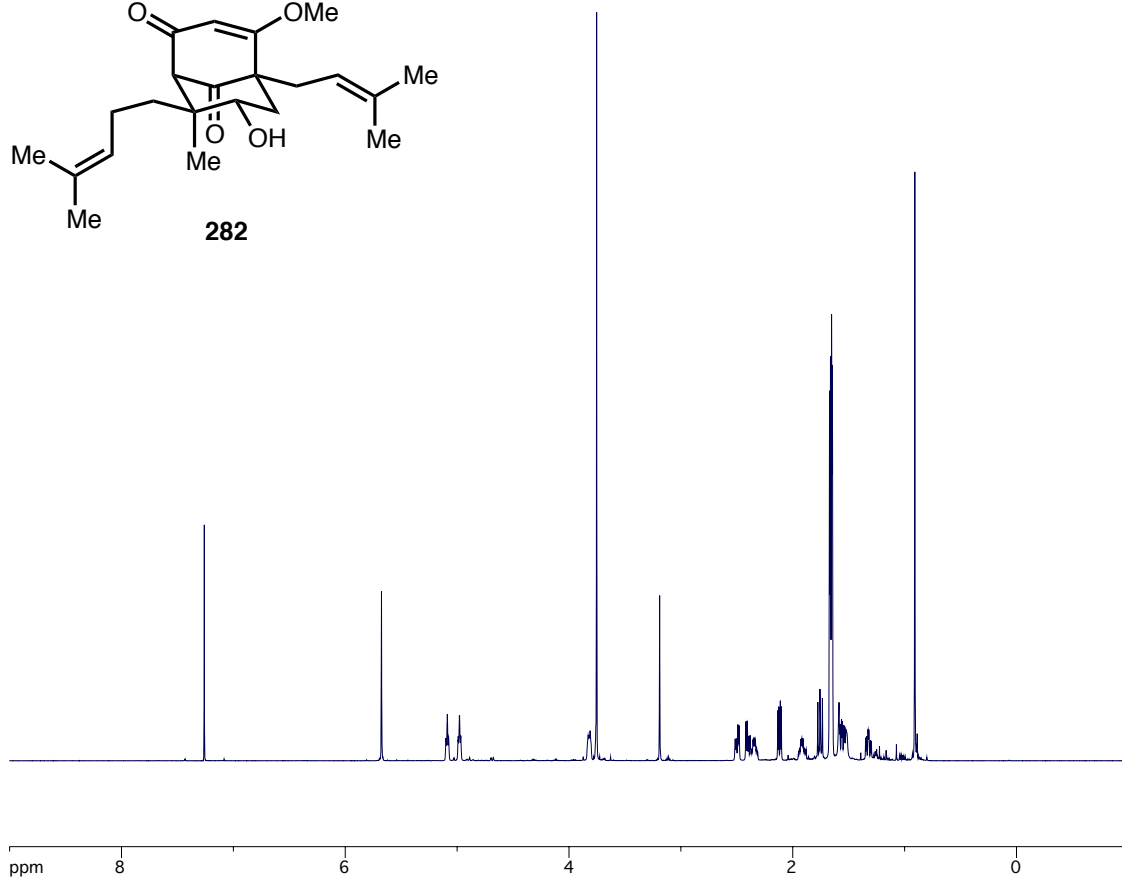
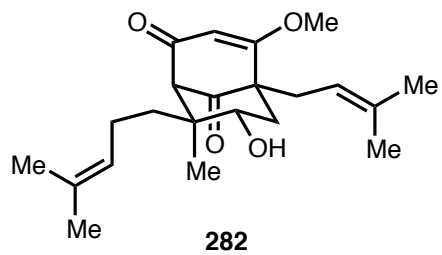


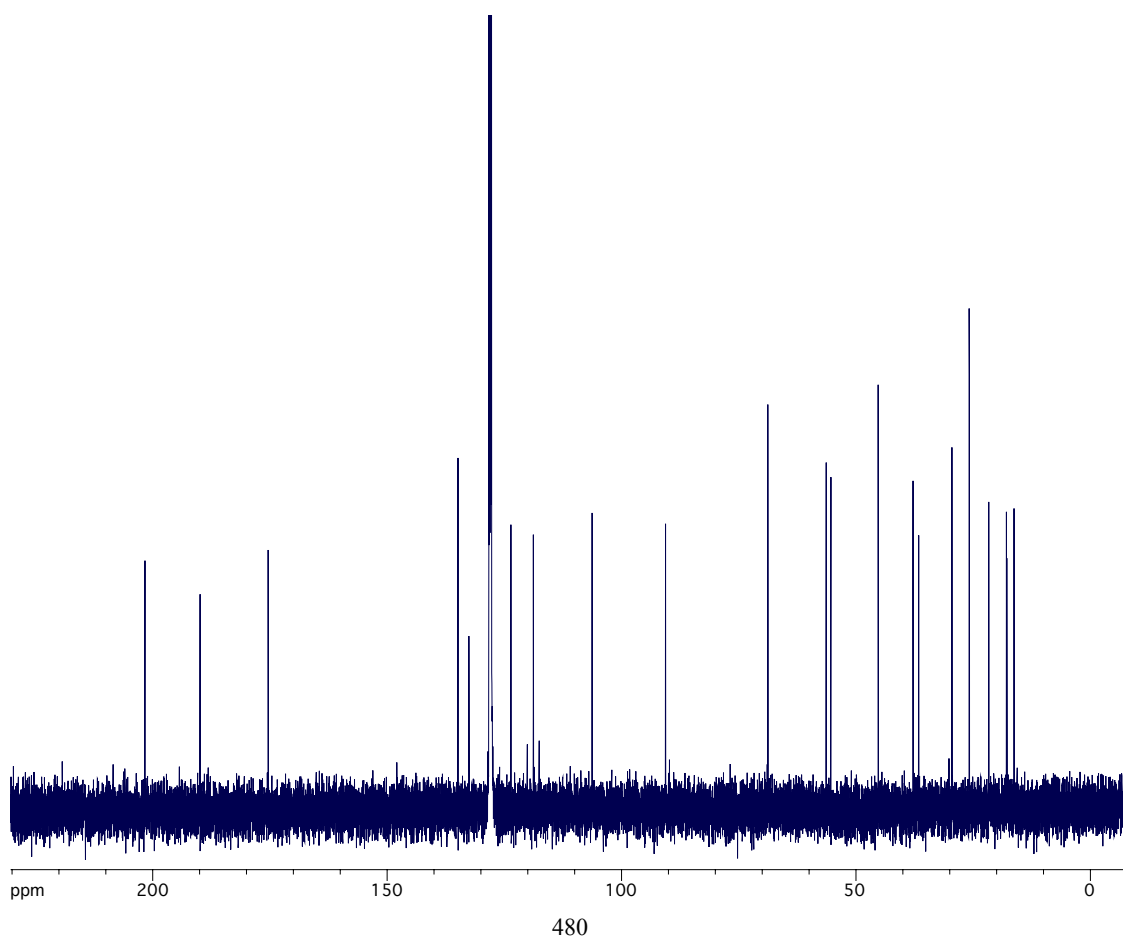
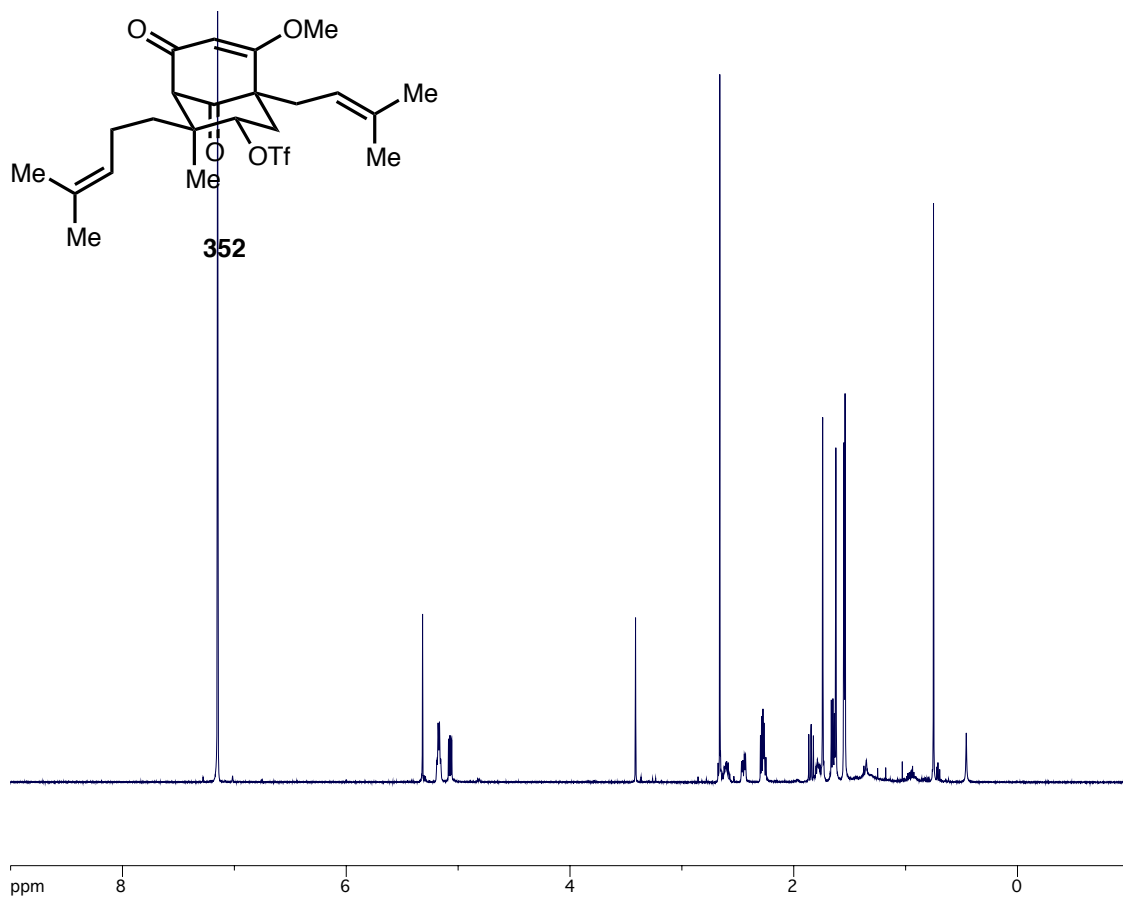


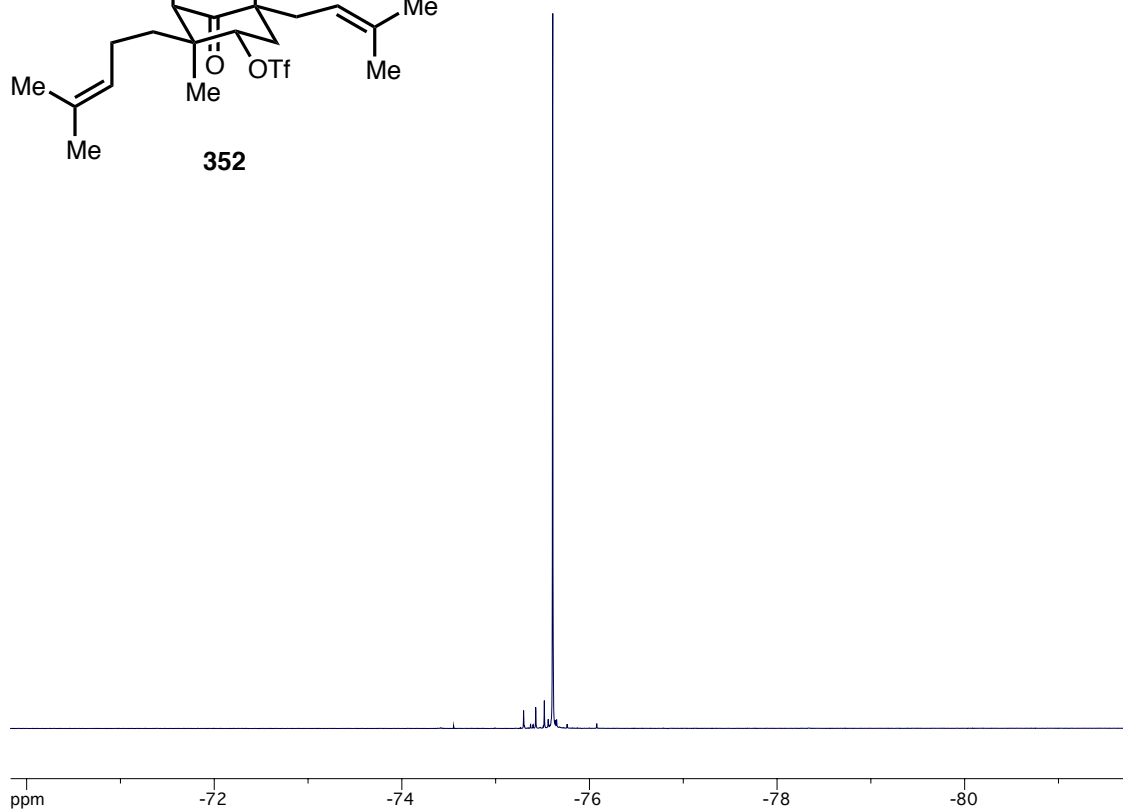
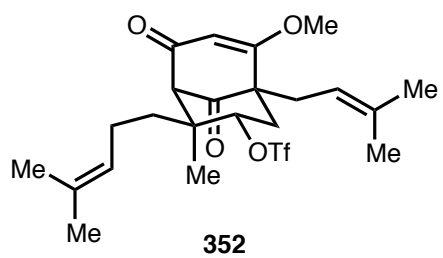


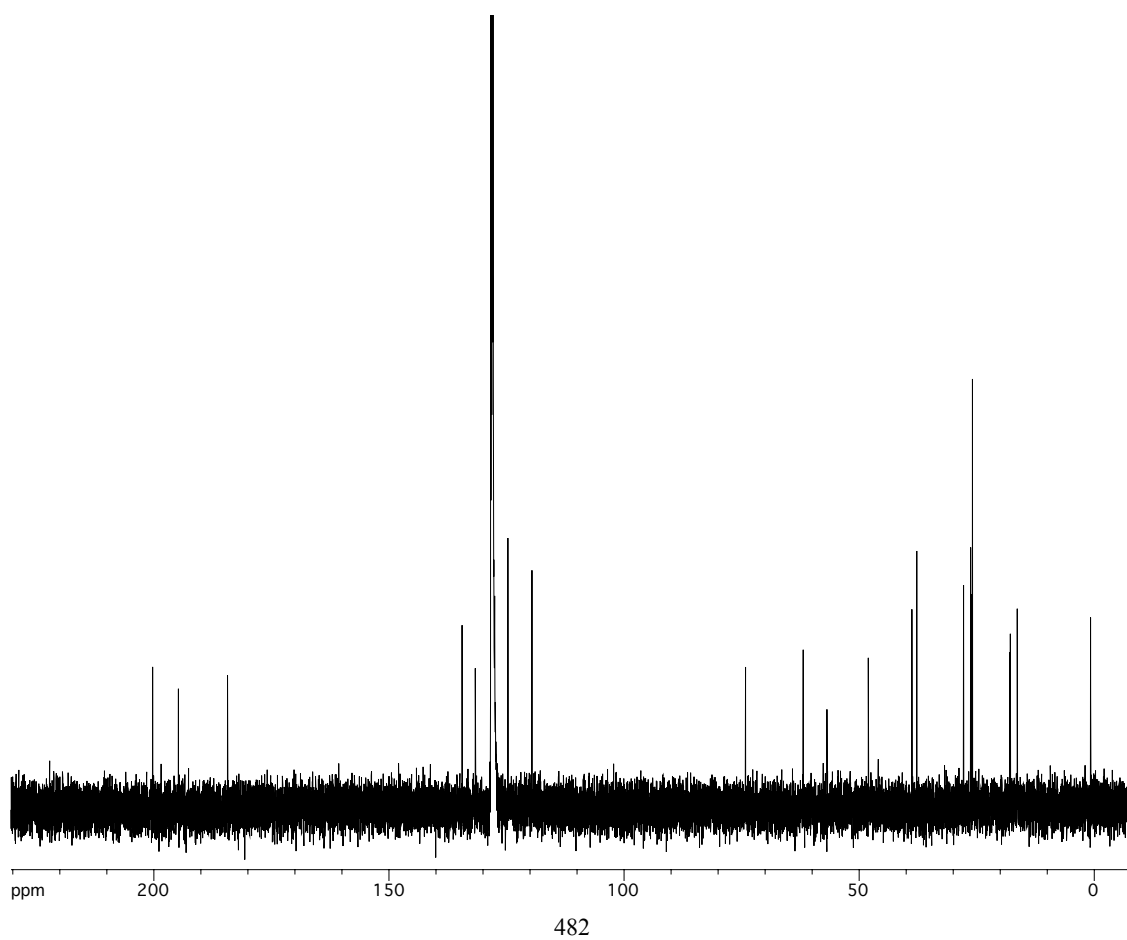
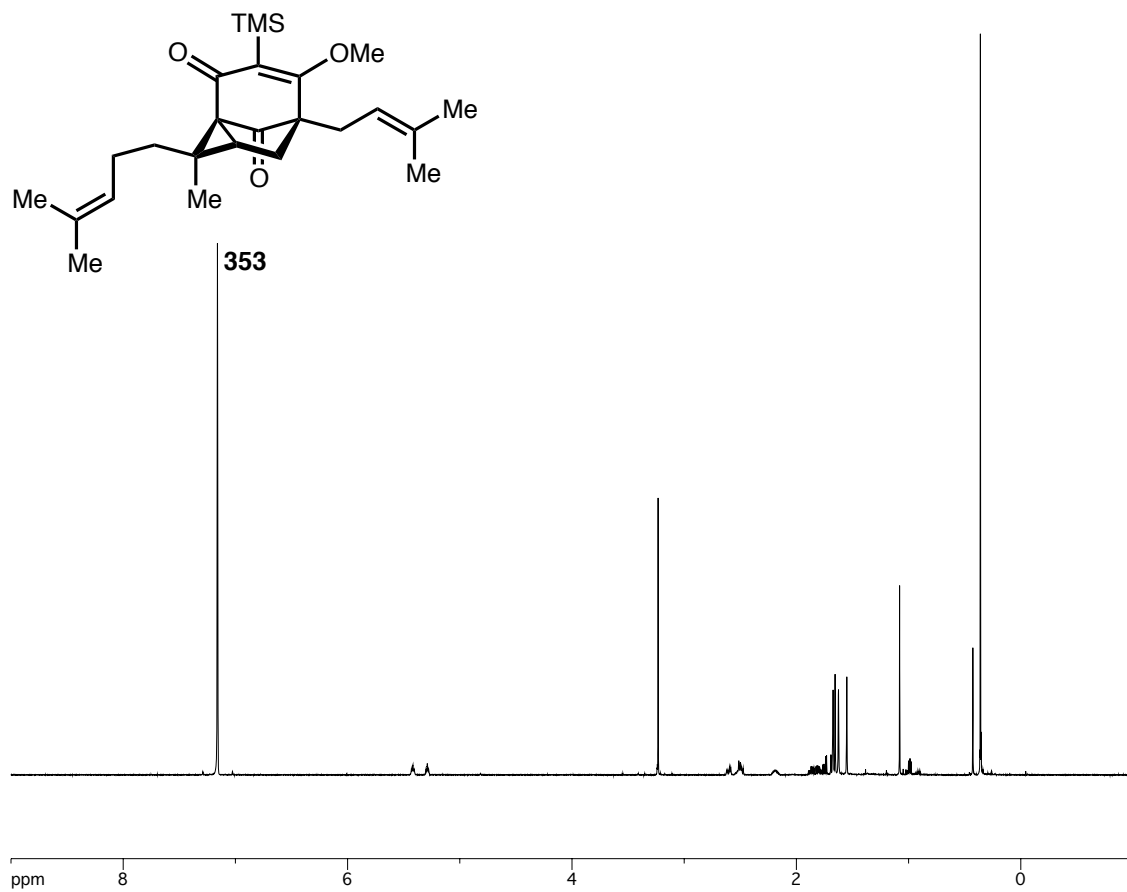


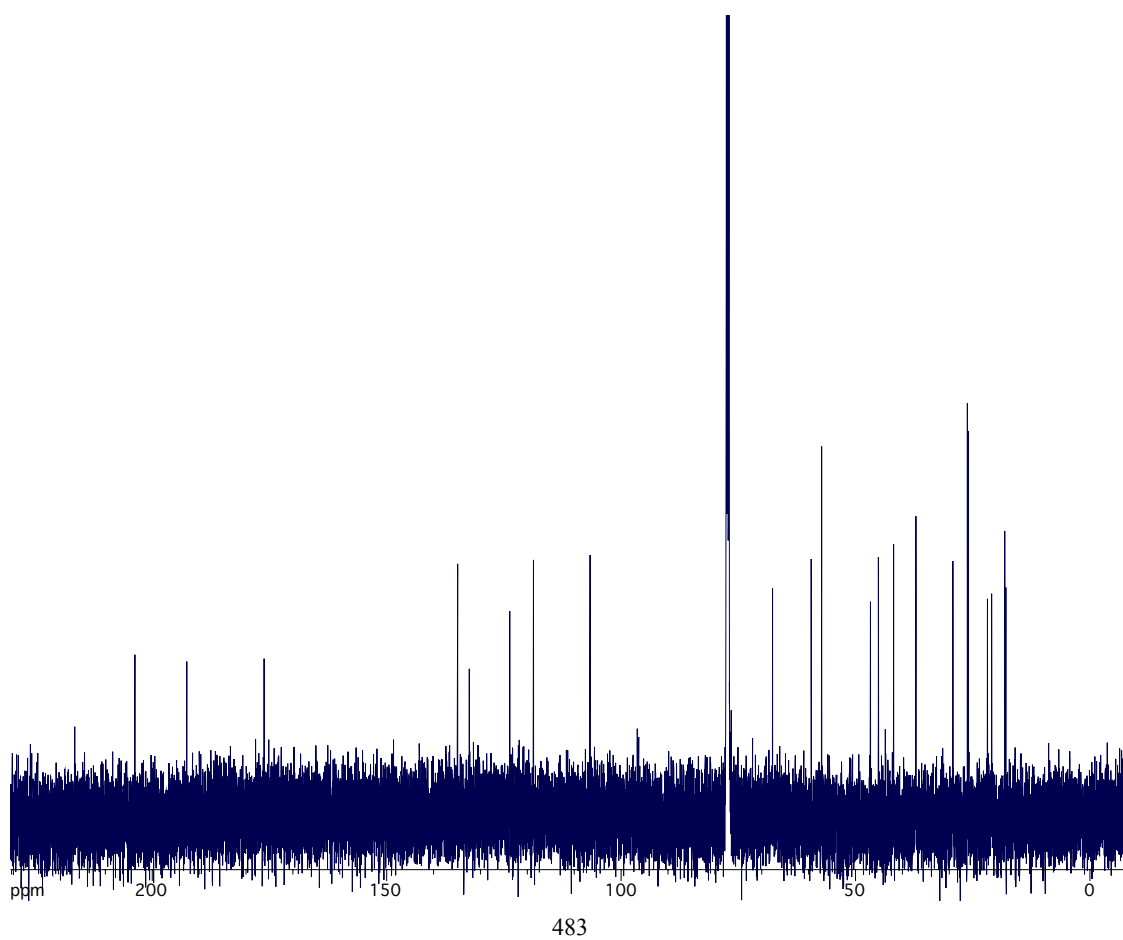
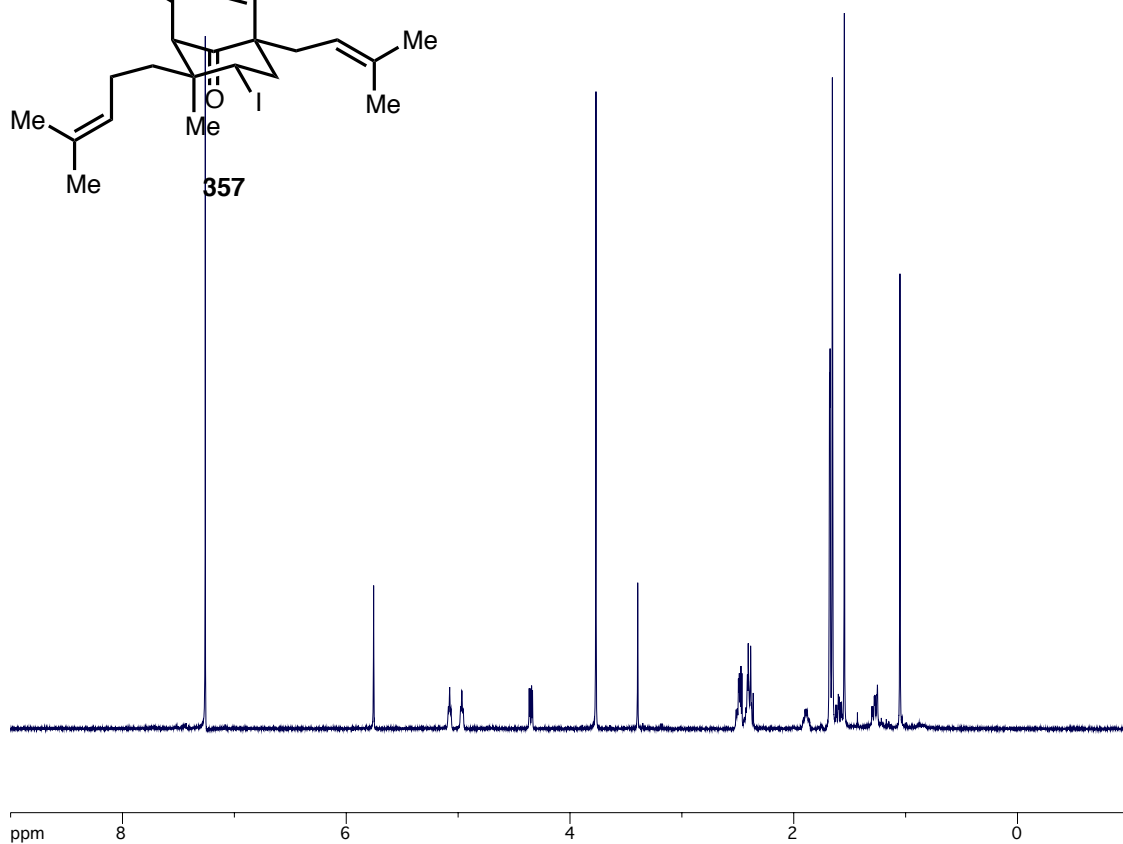


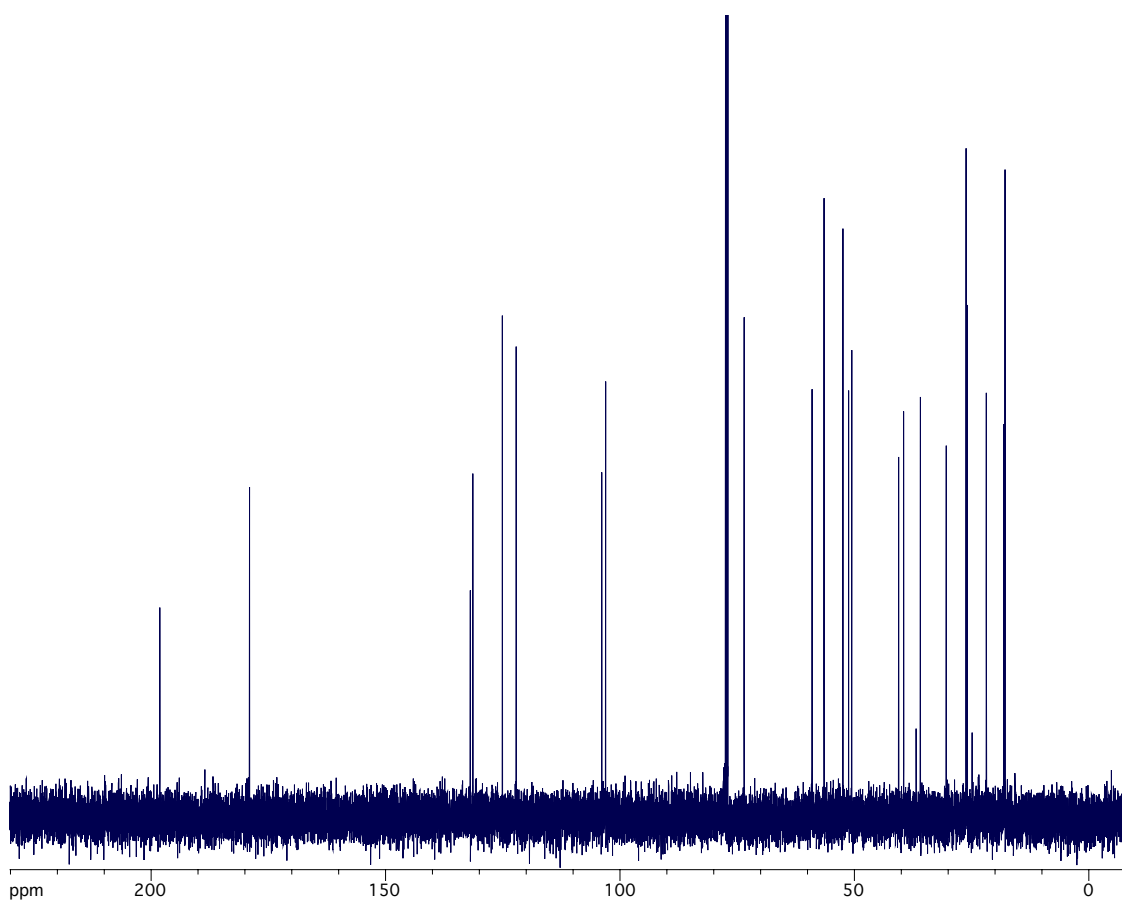
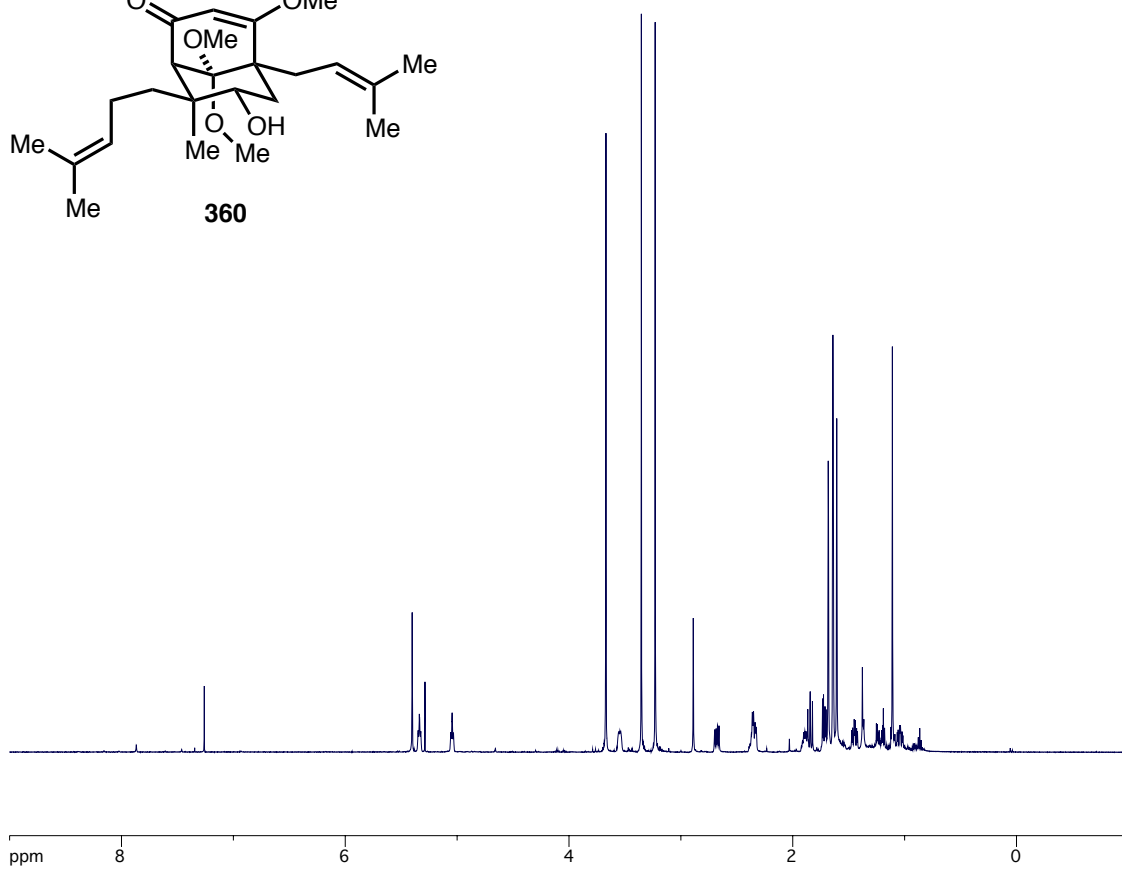
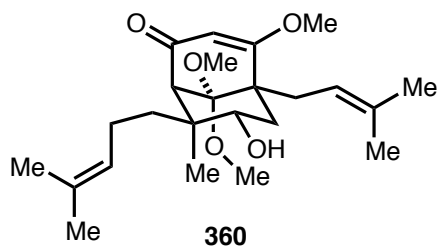


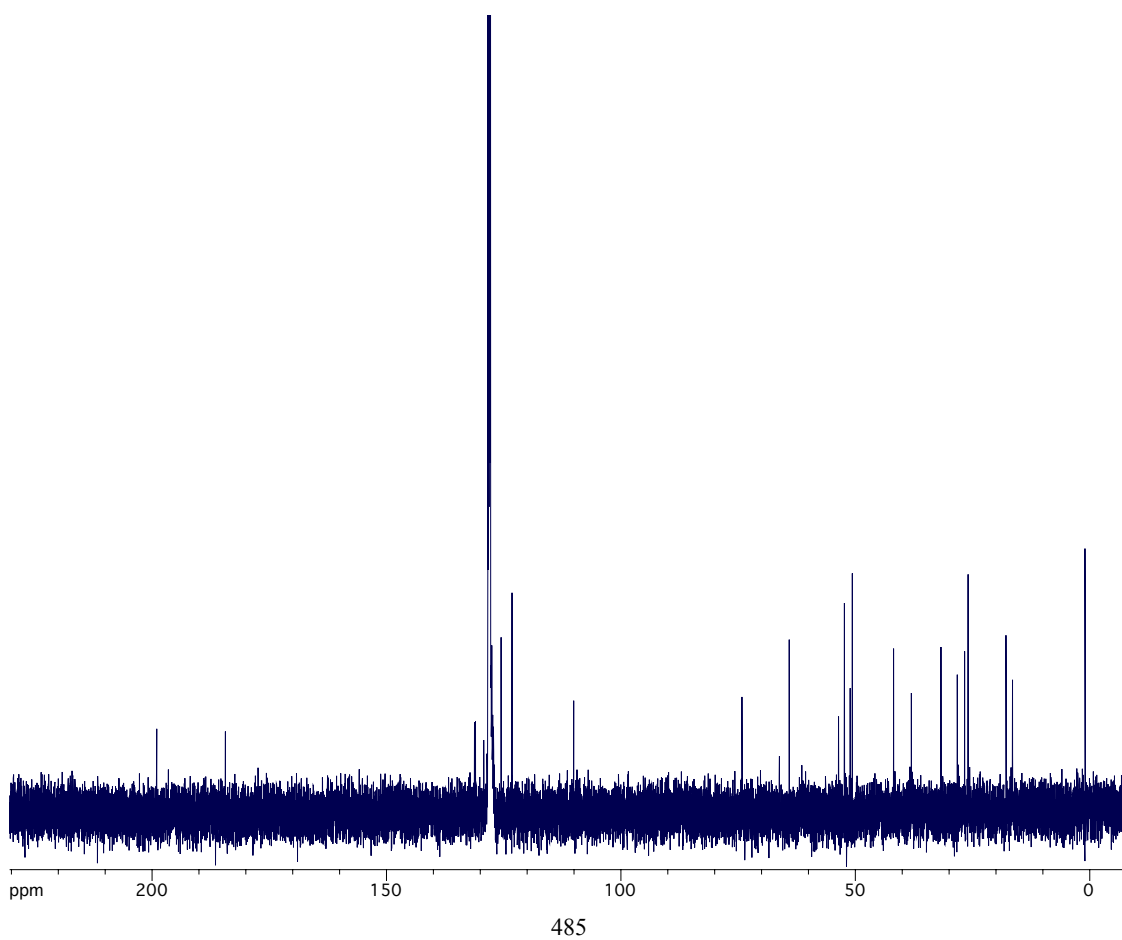
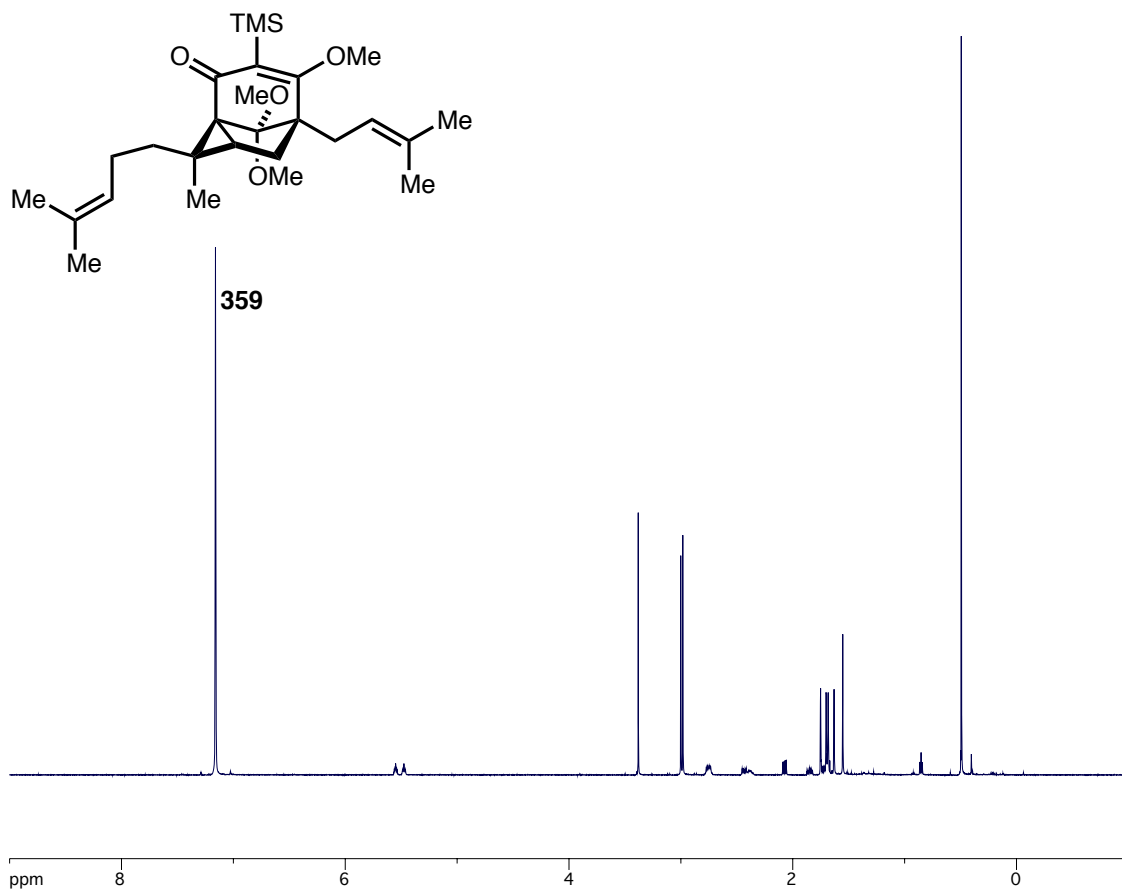


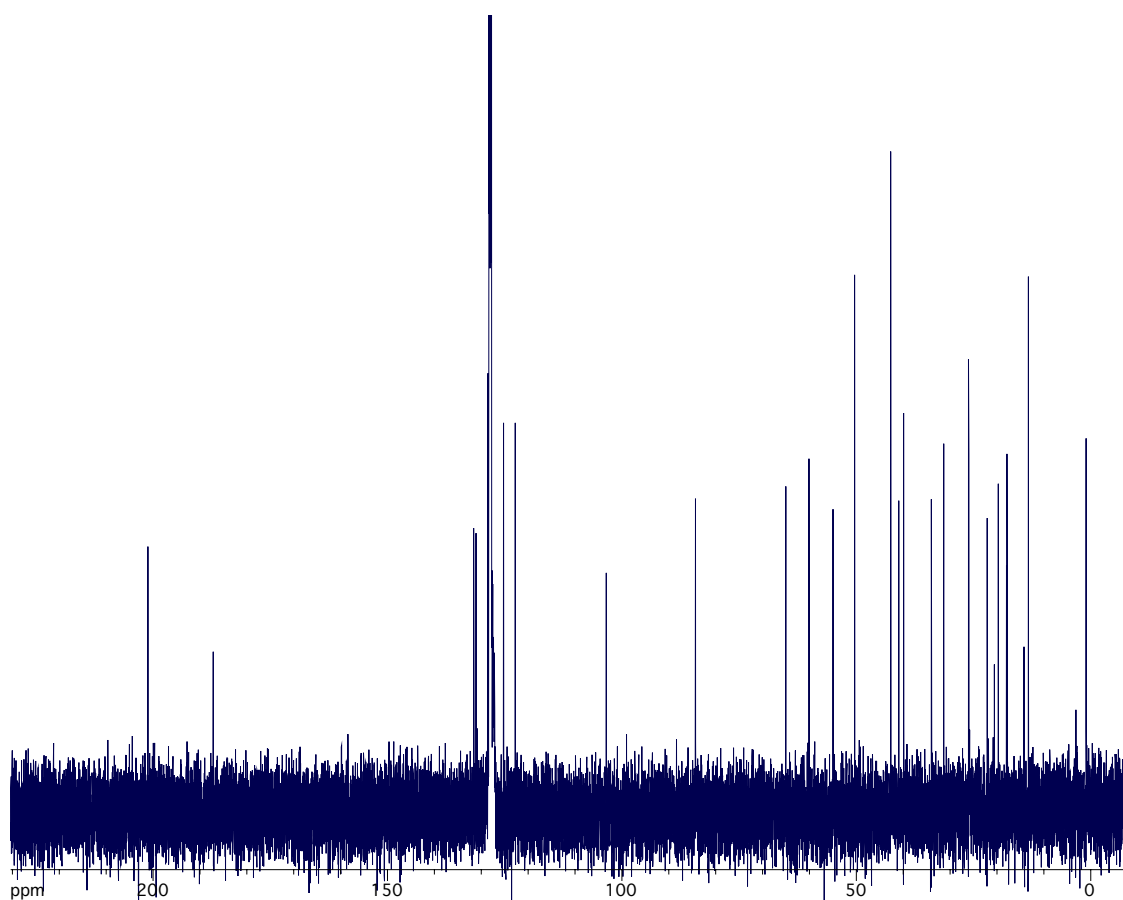
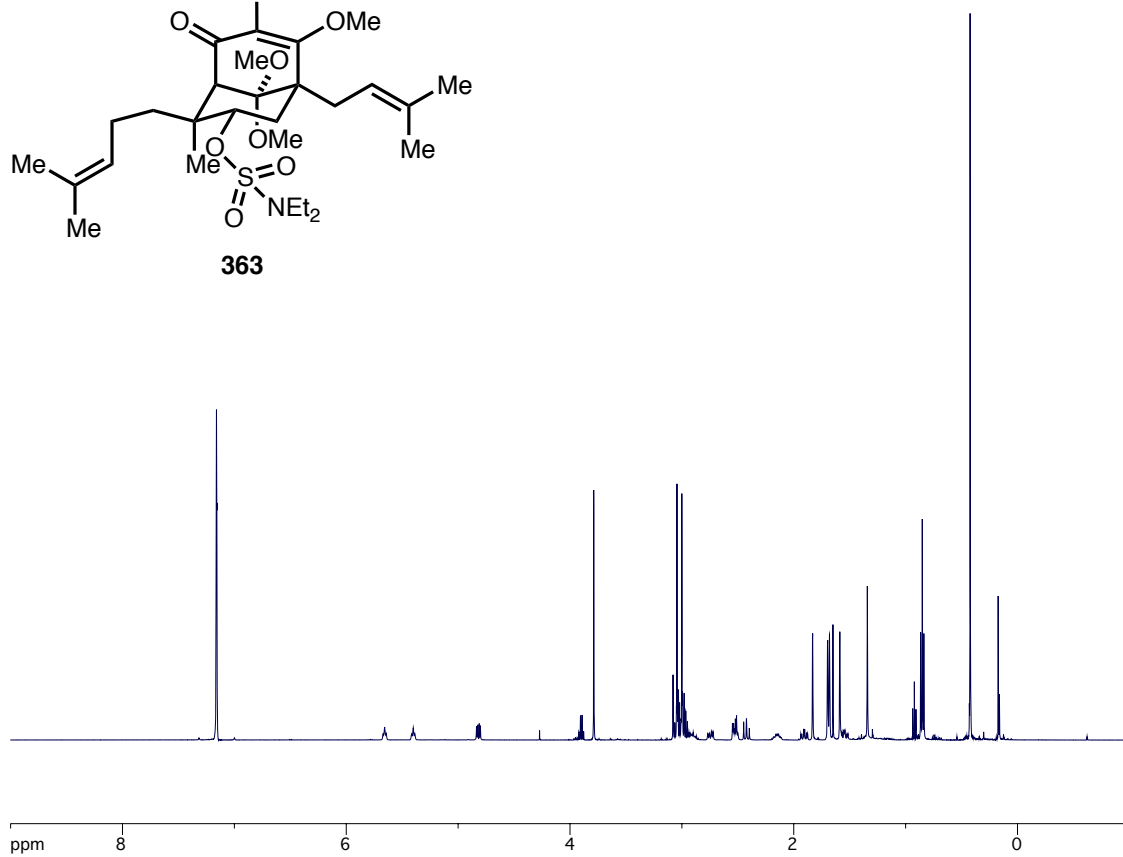
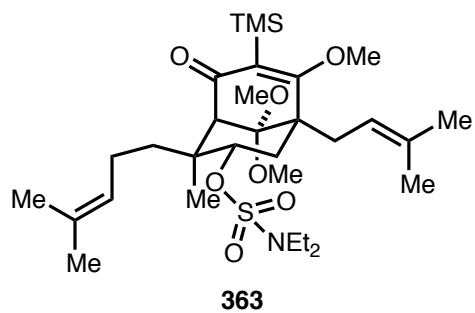


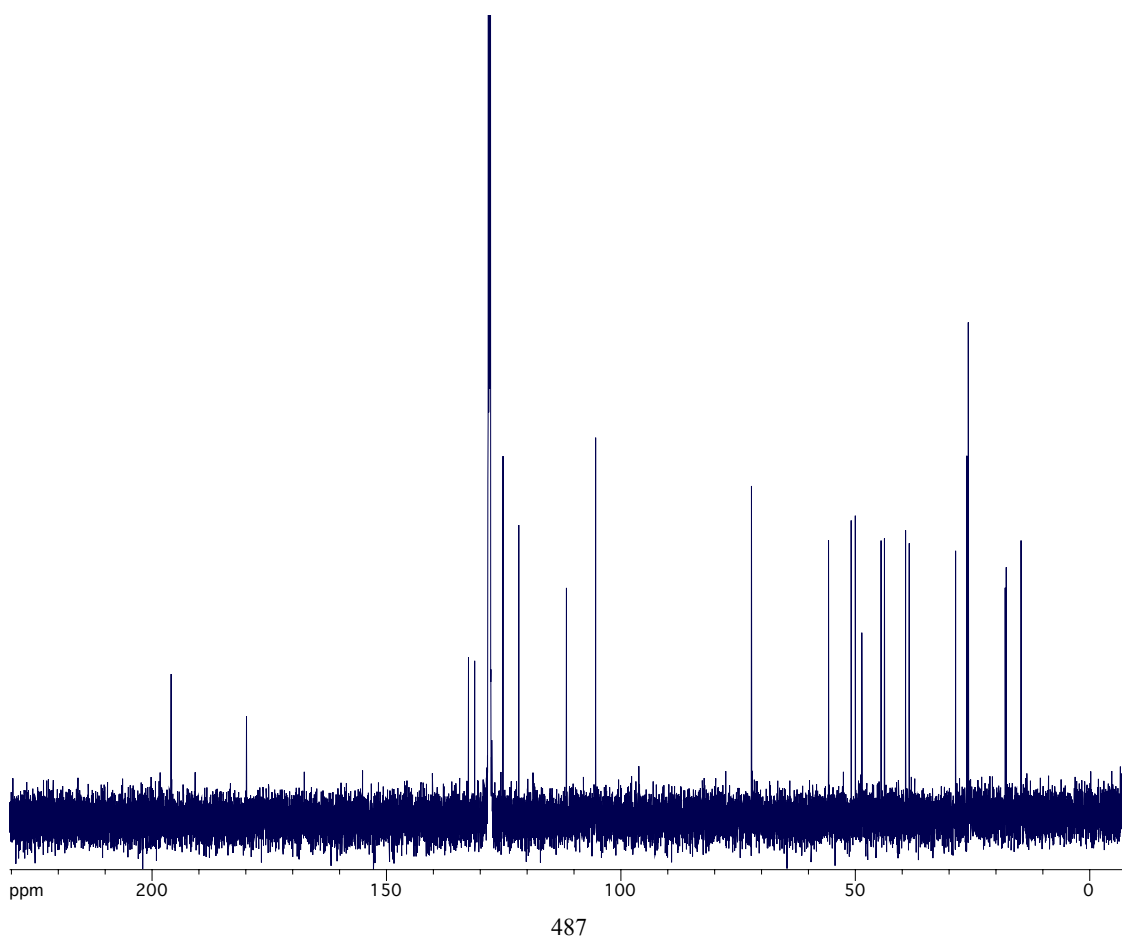
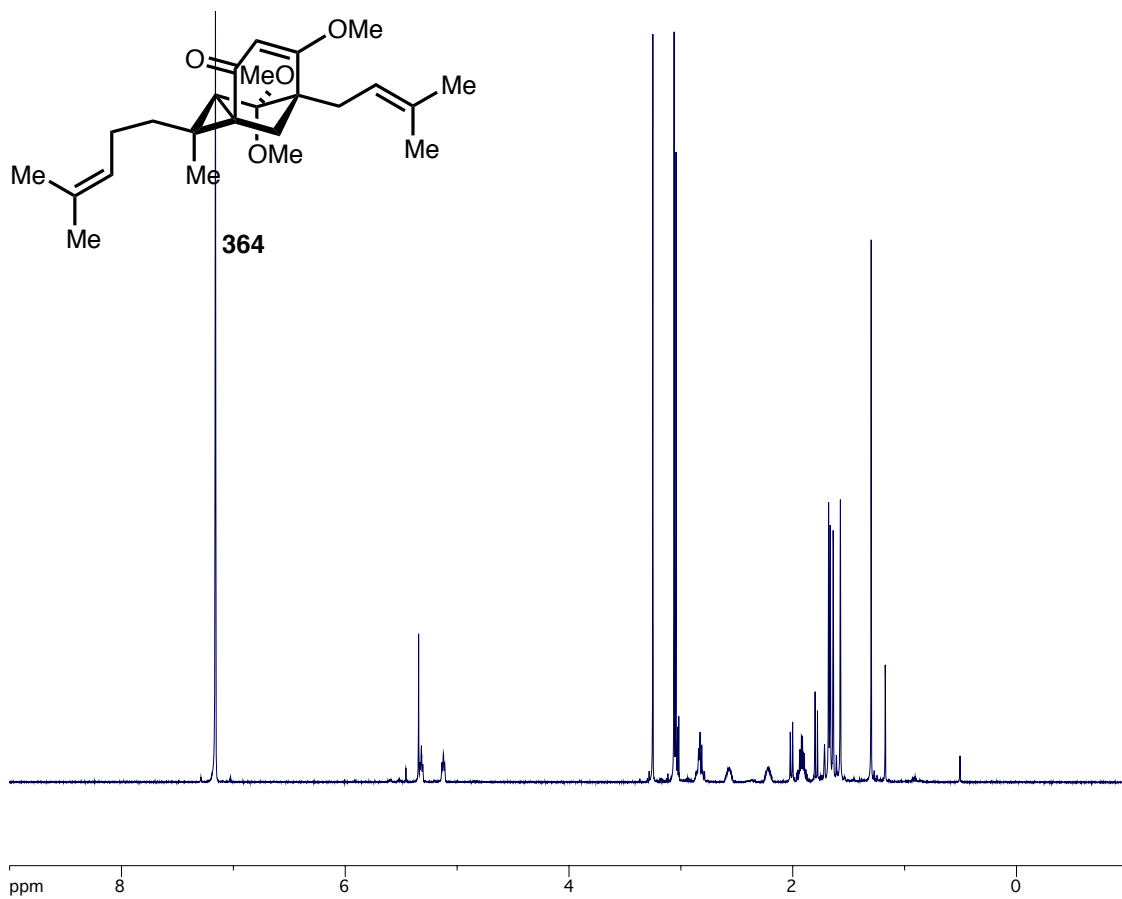


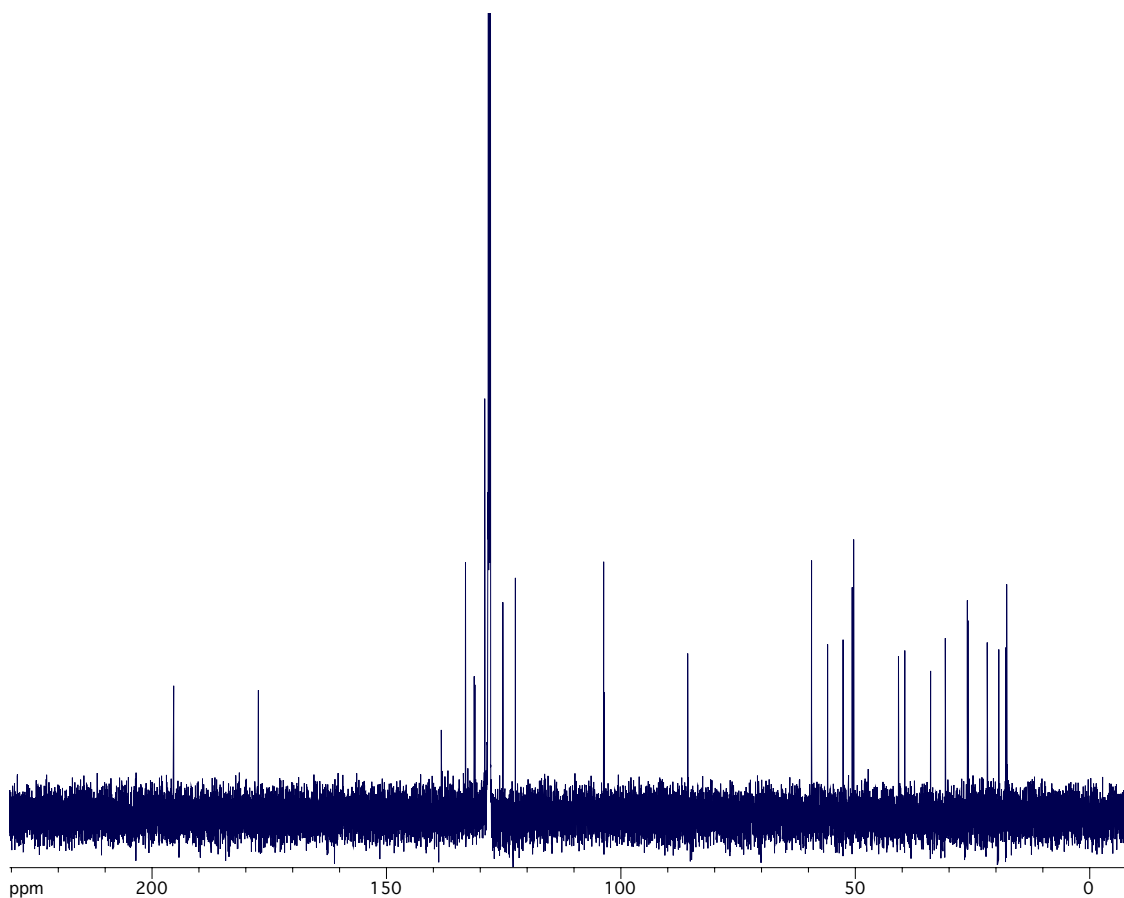
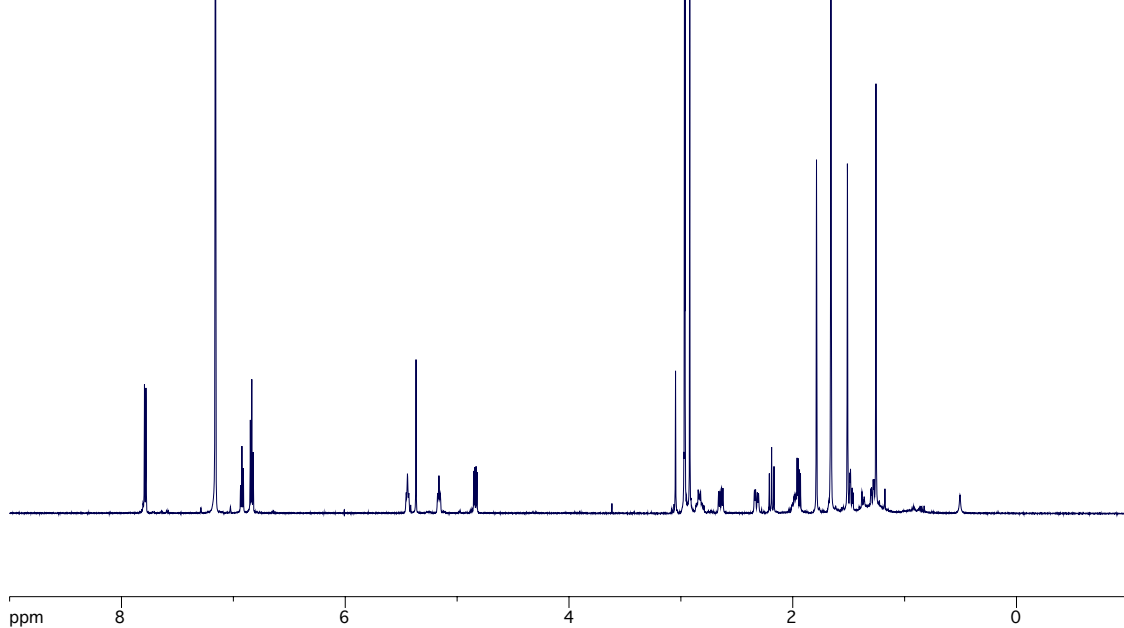
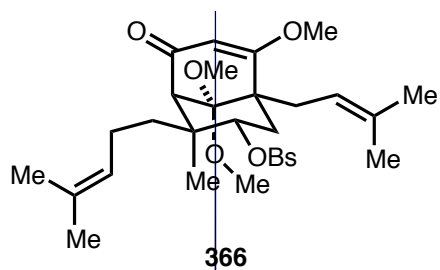


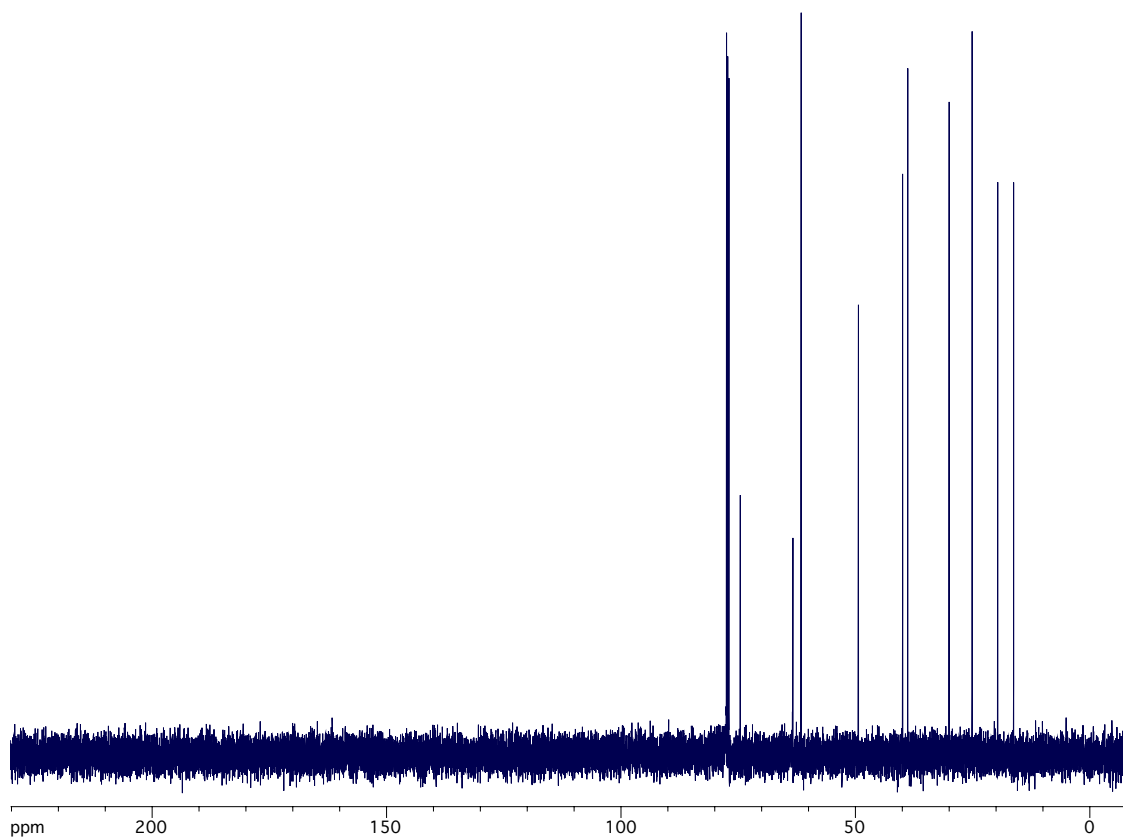
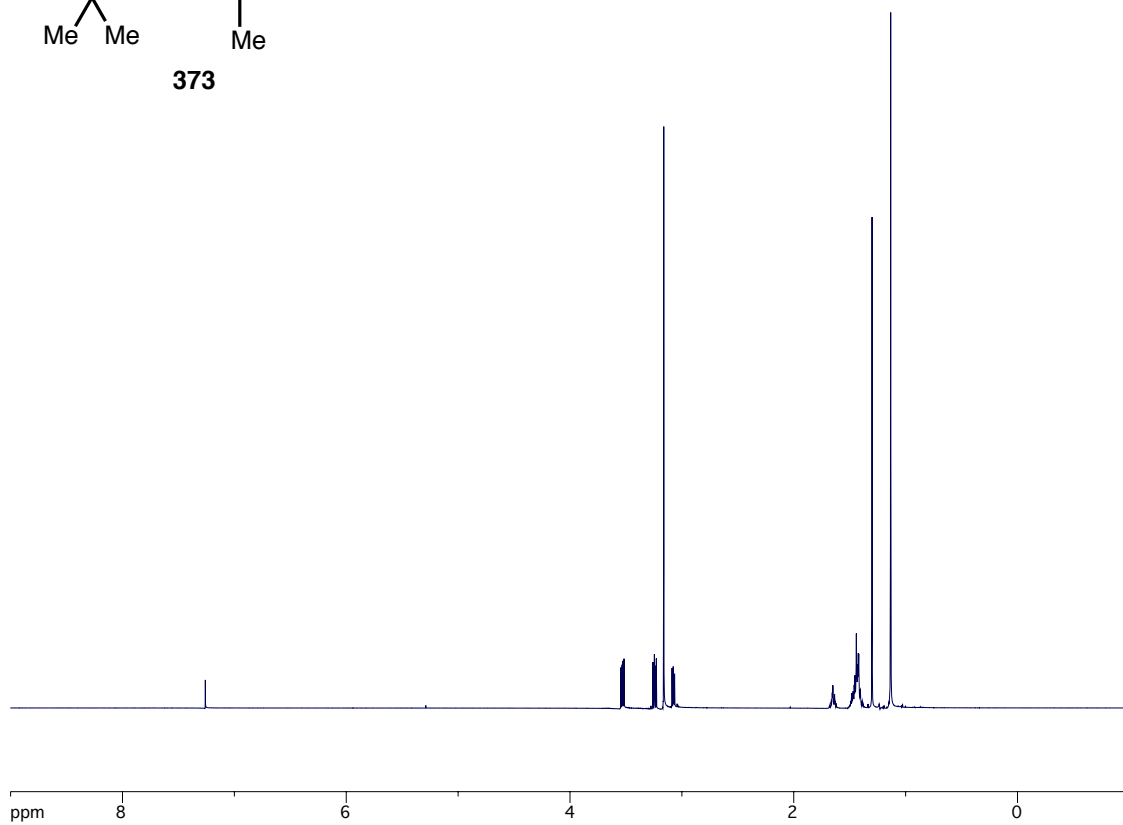
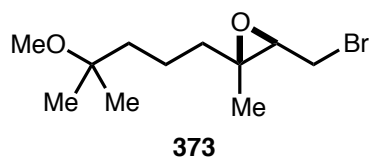


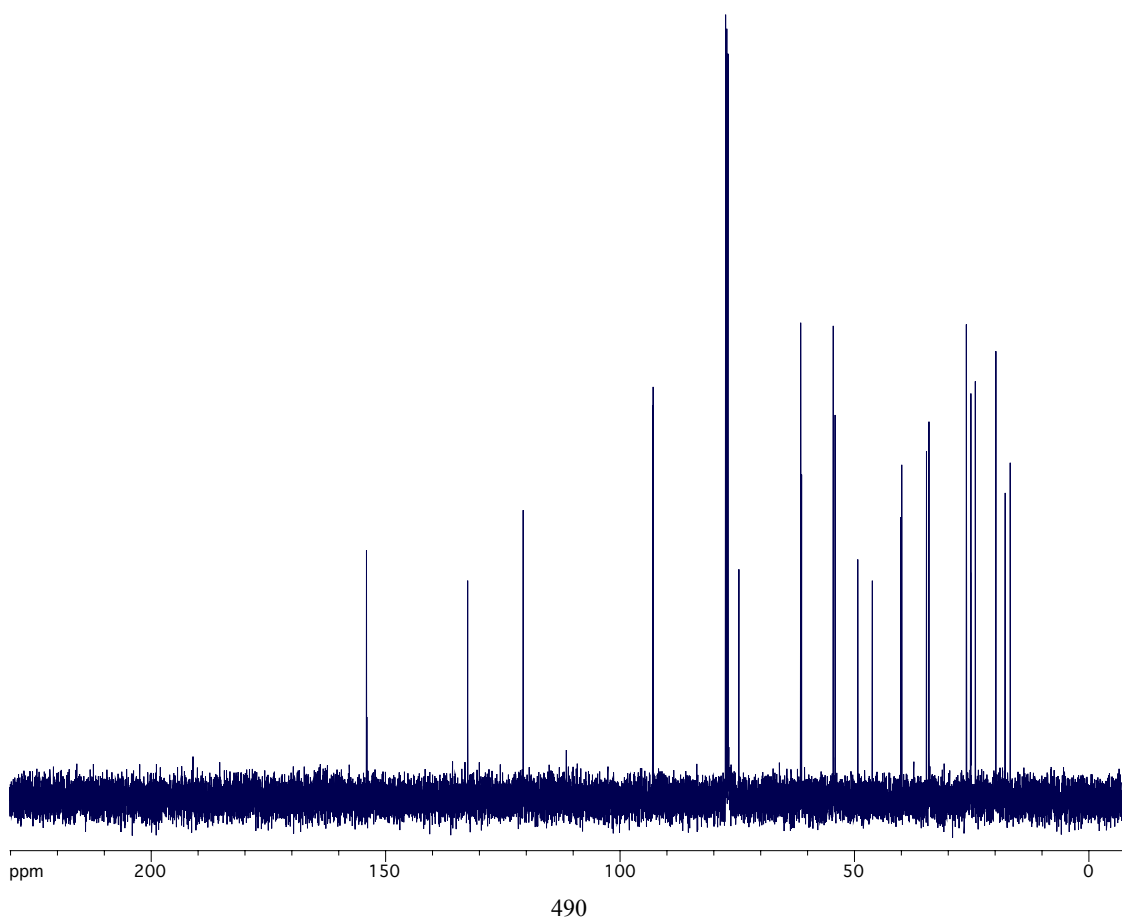
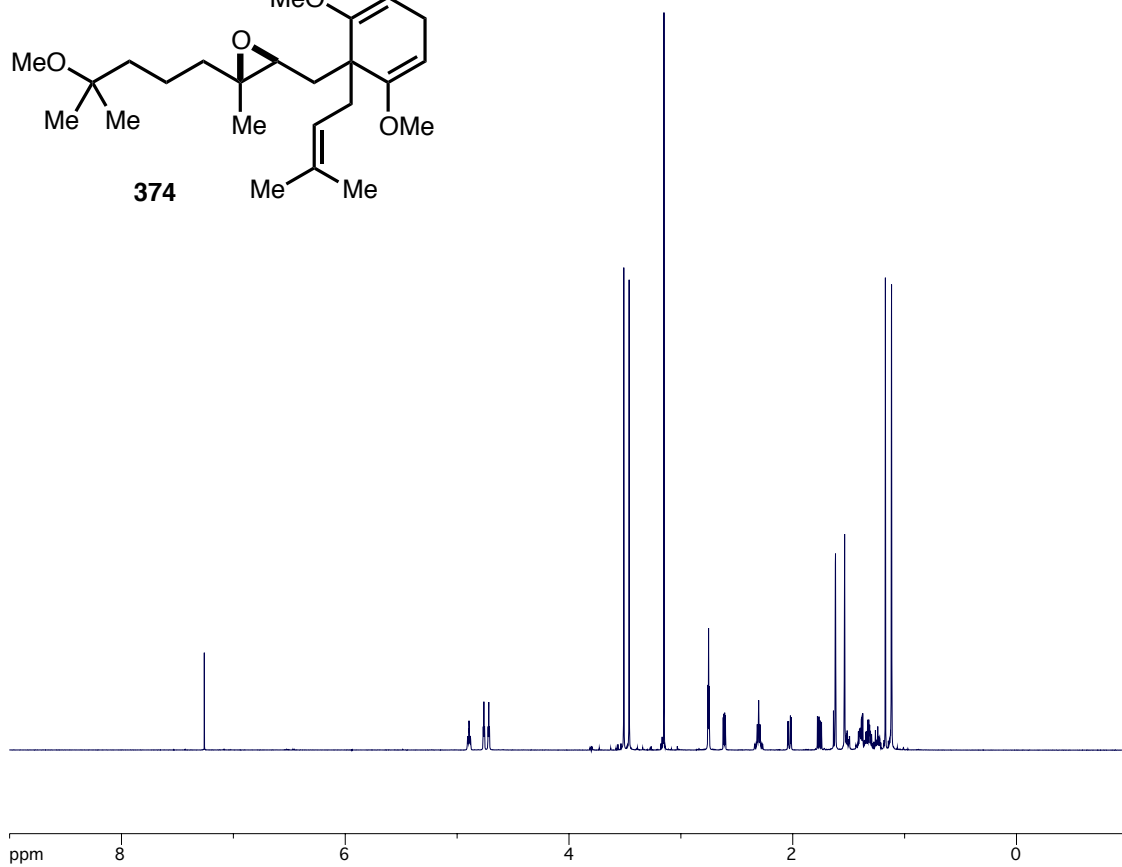
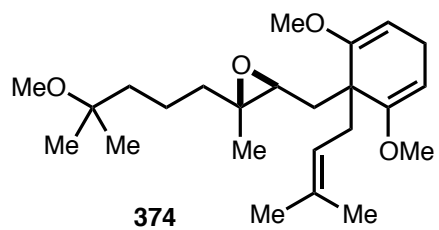


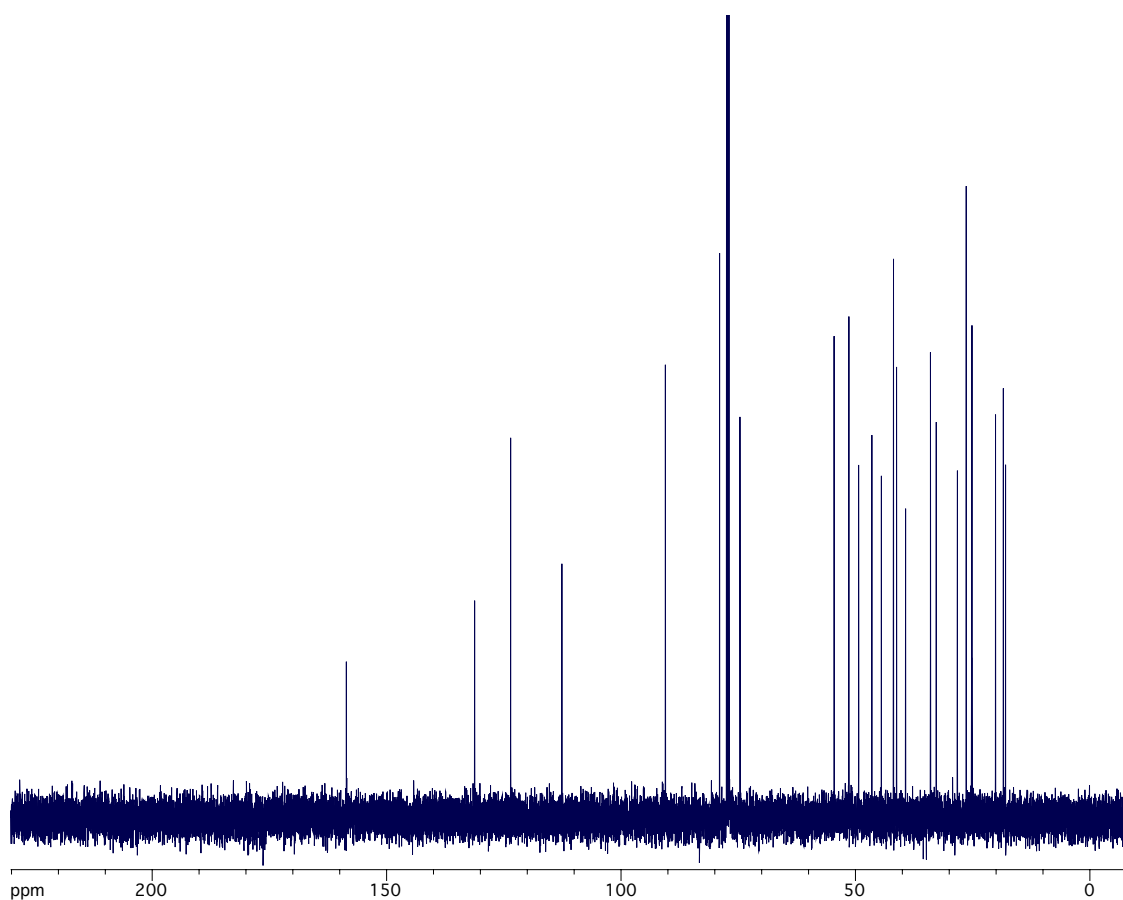
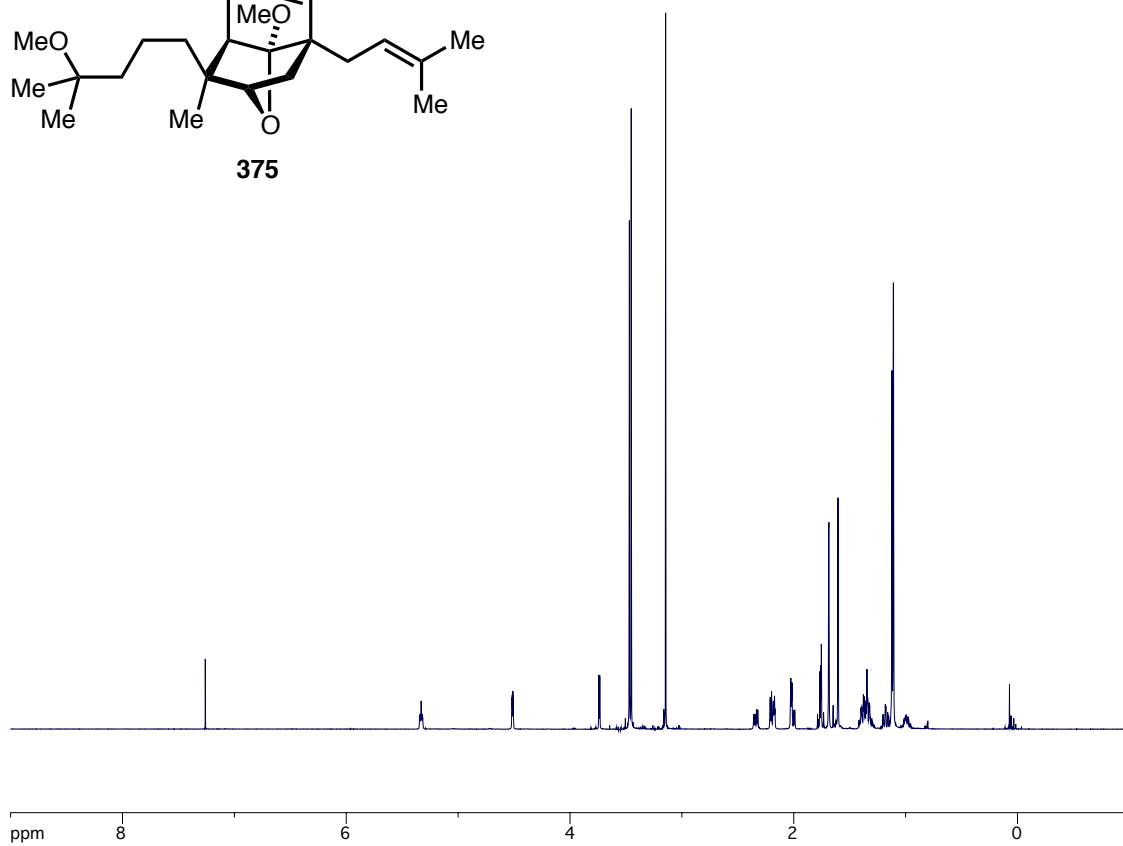
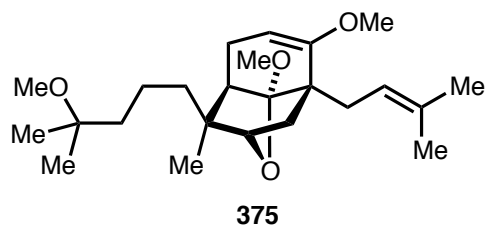


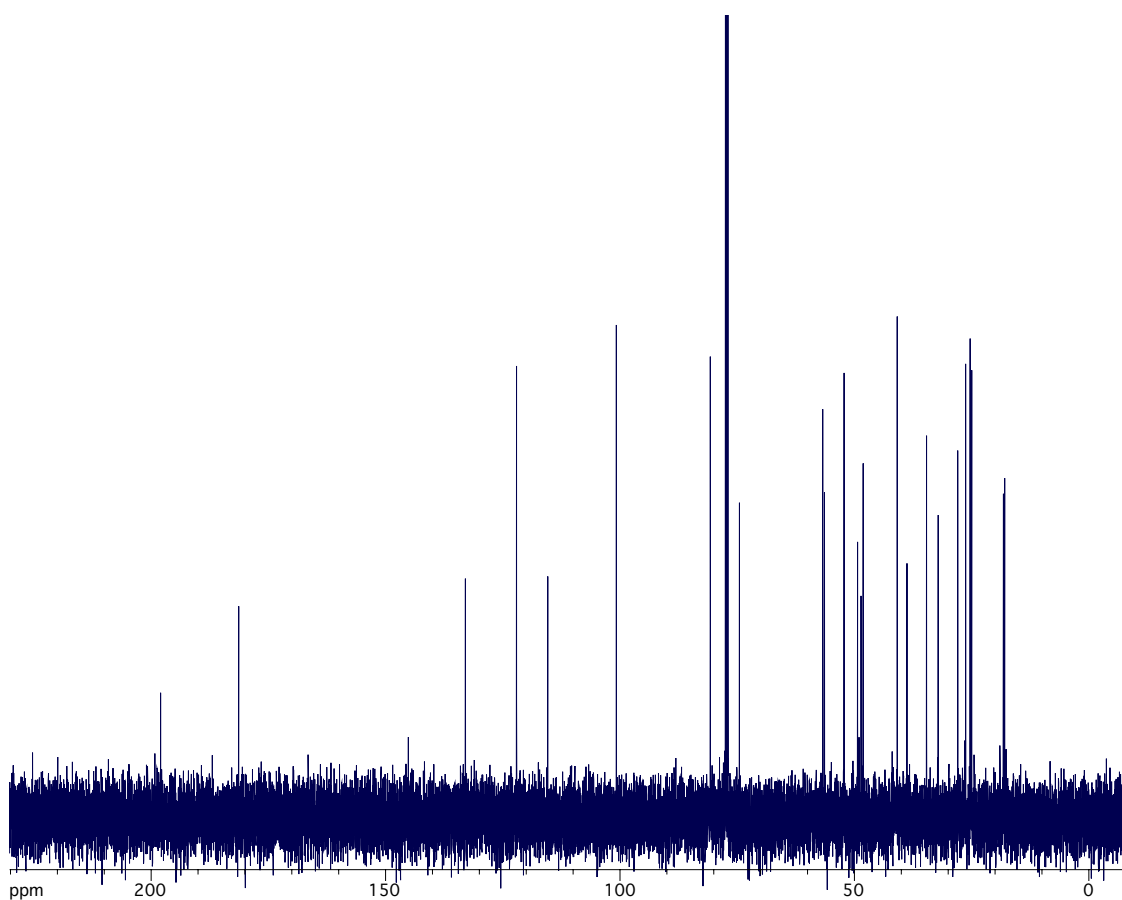
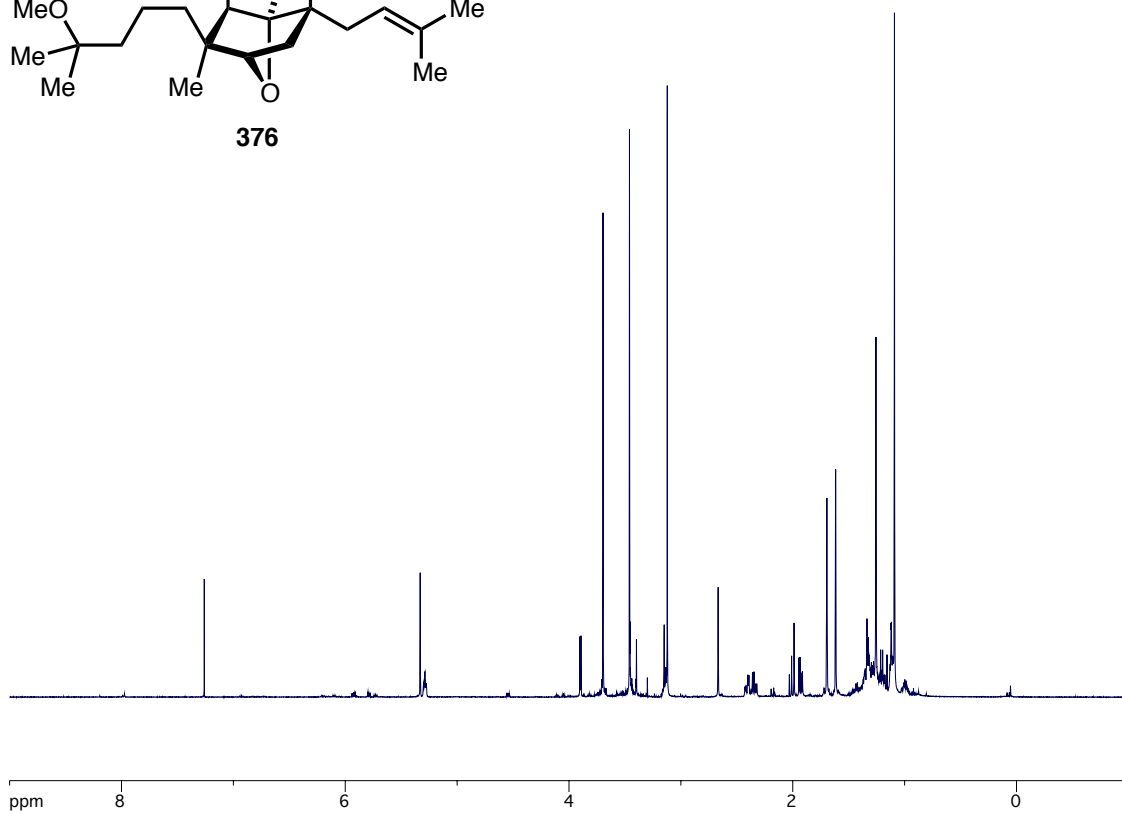
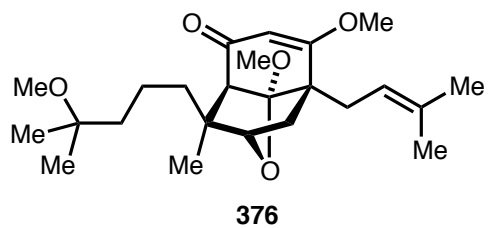


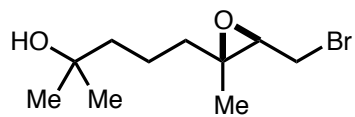




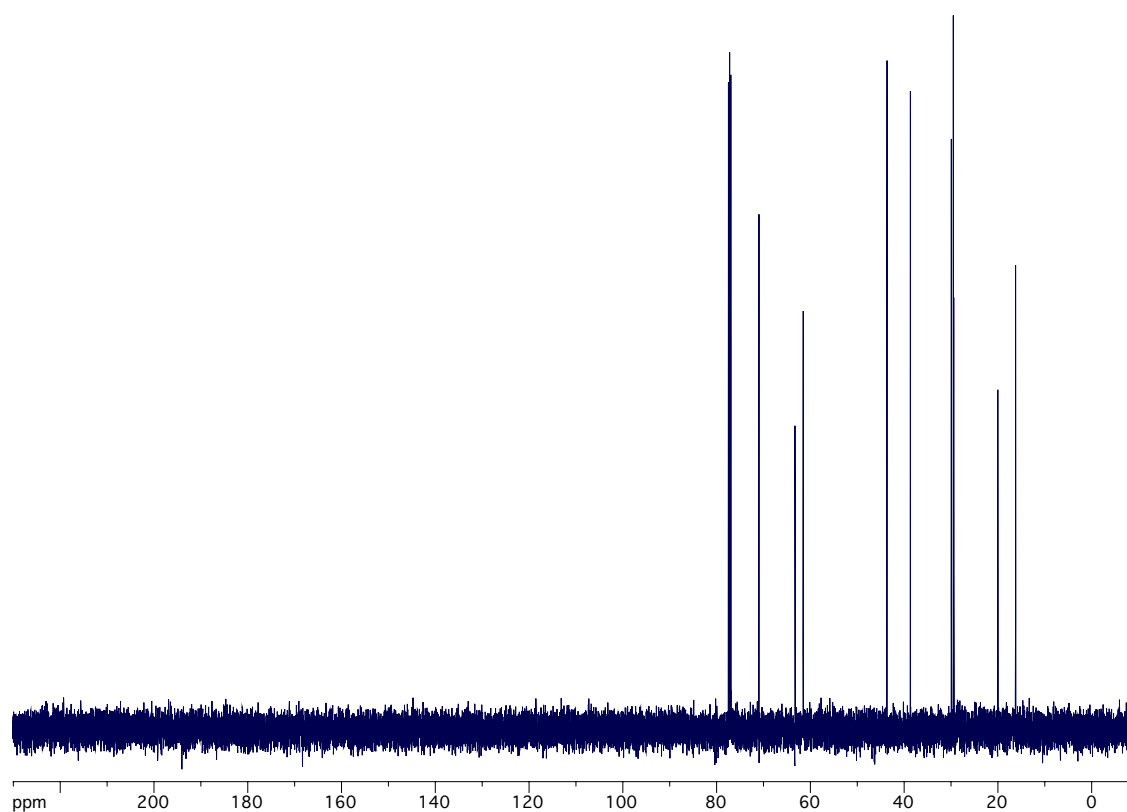
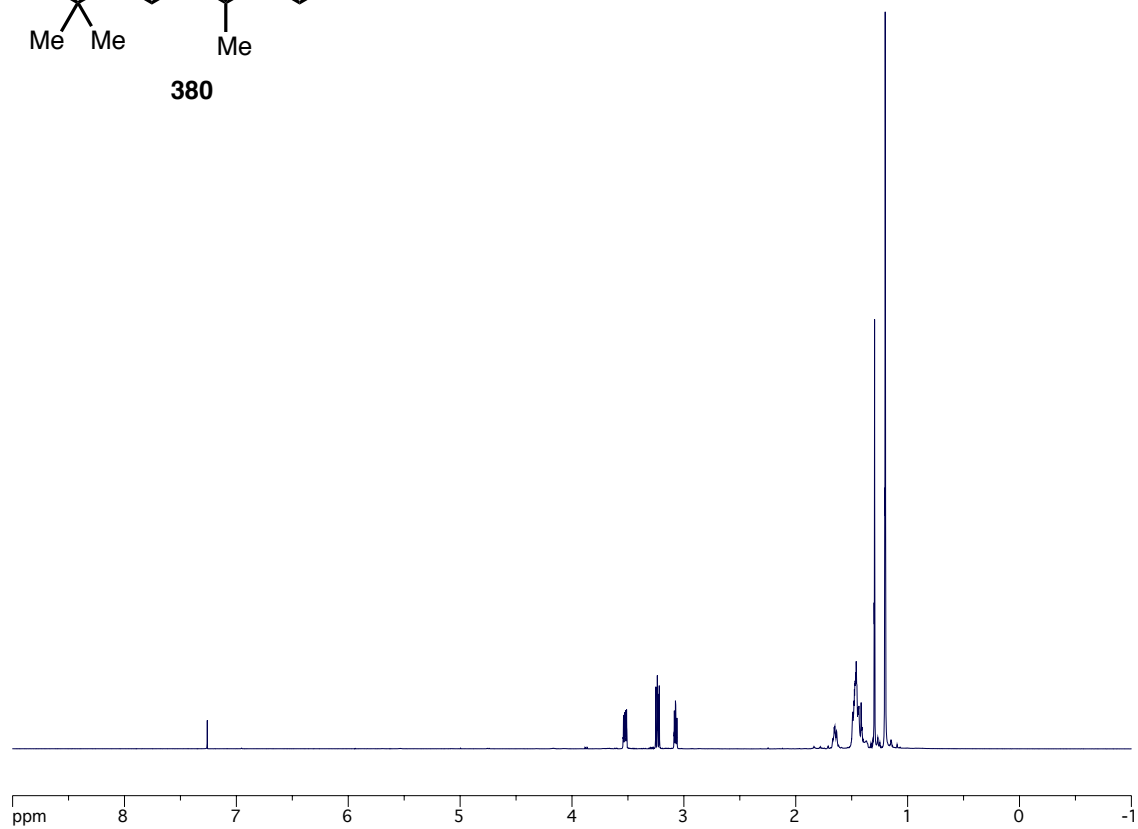


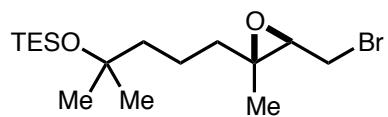




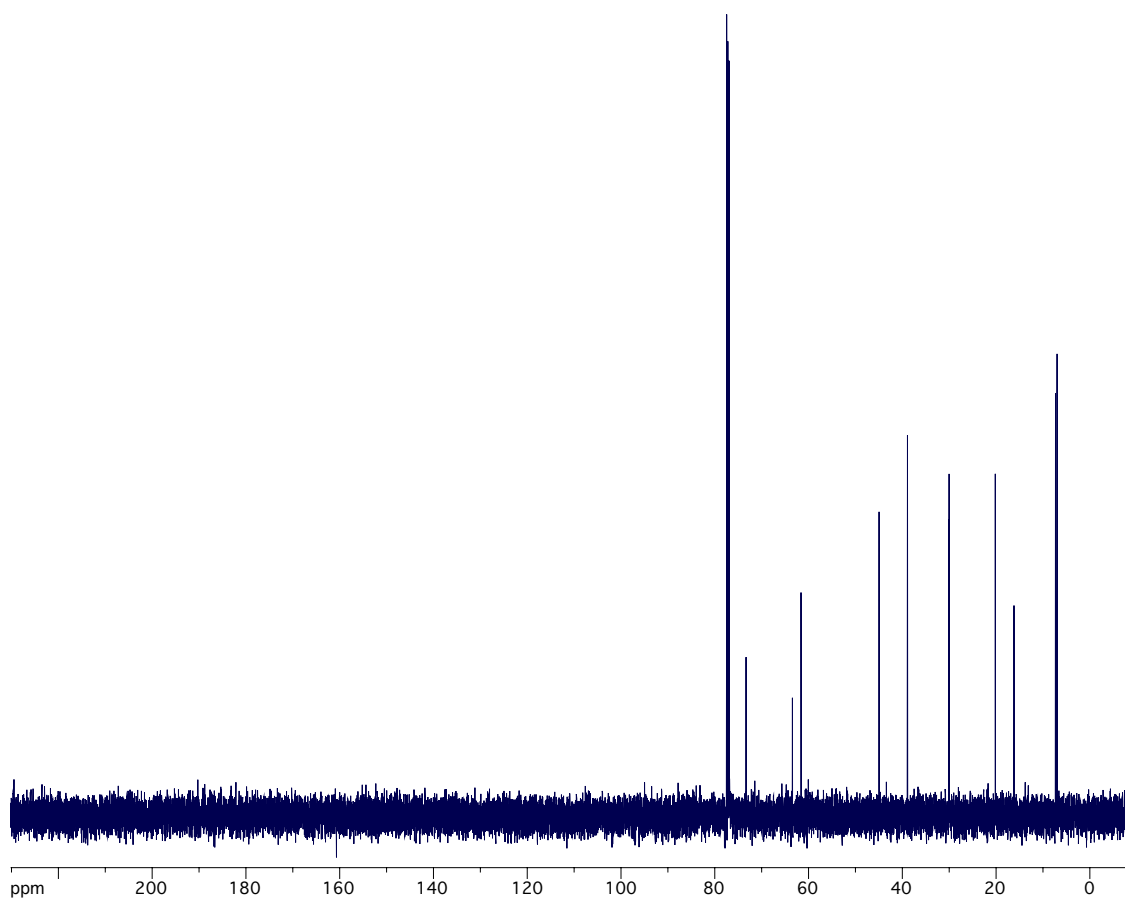
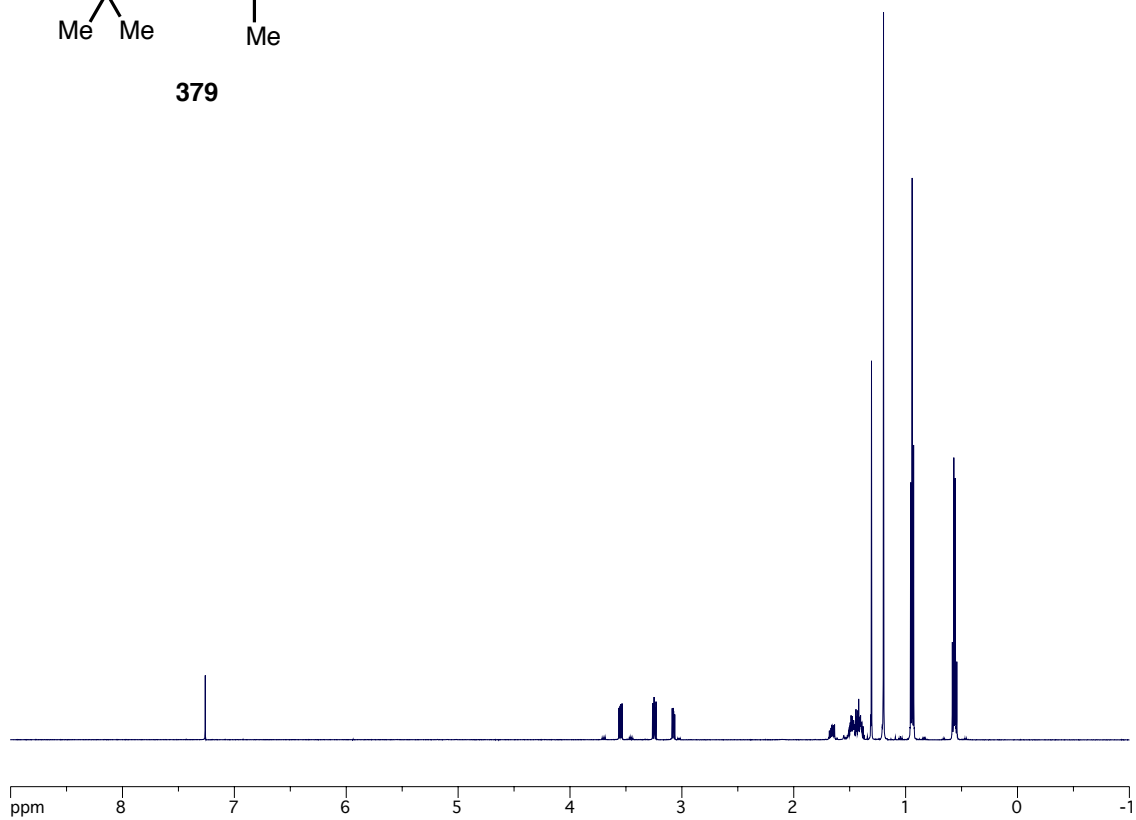


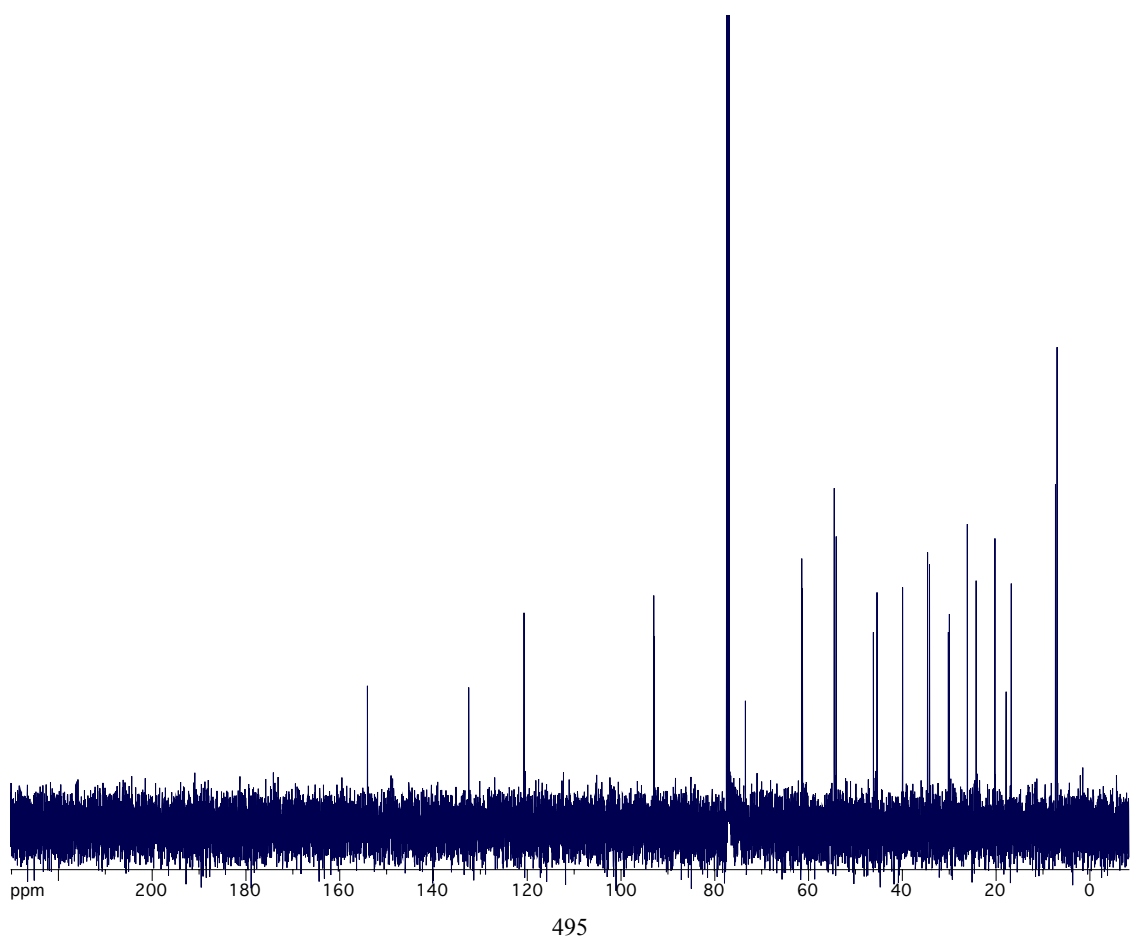
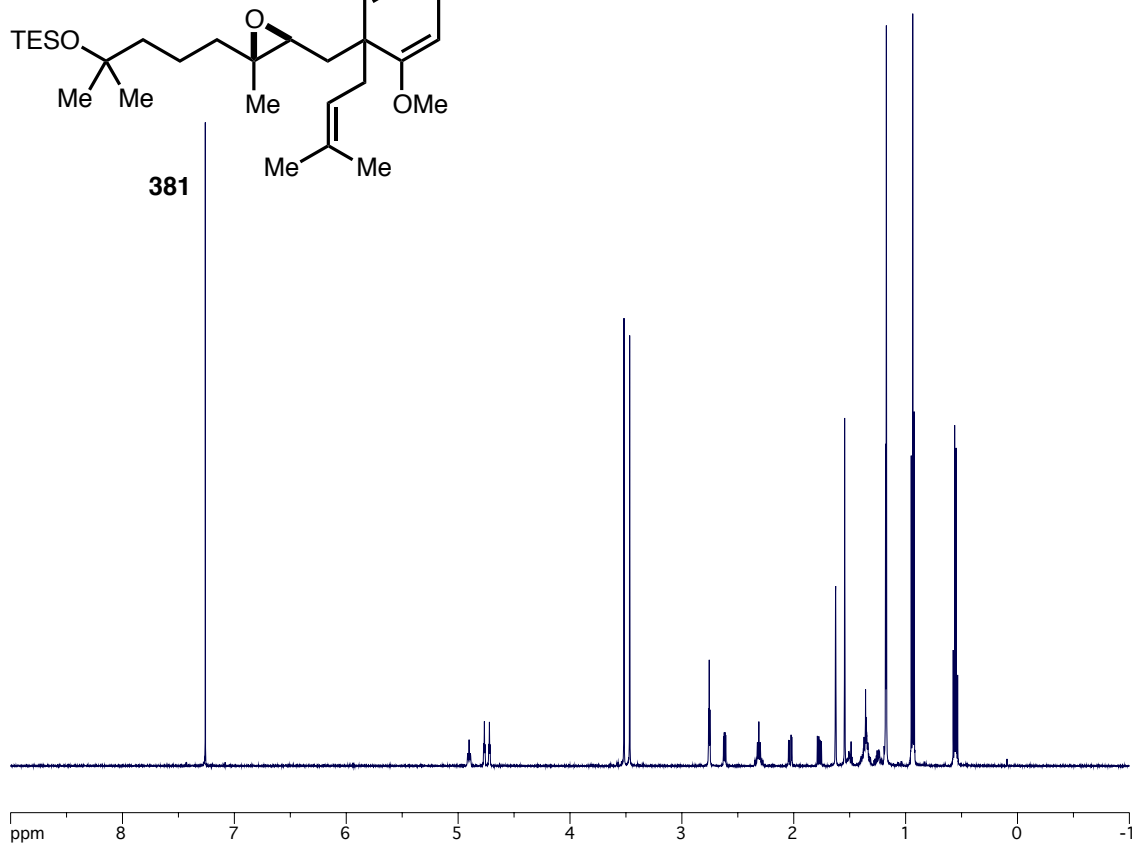
380

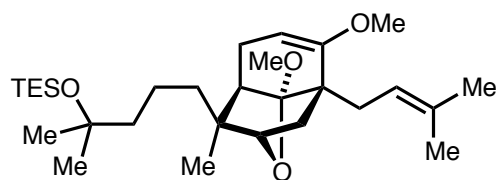




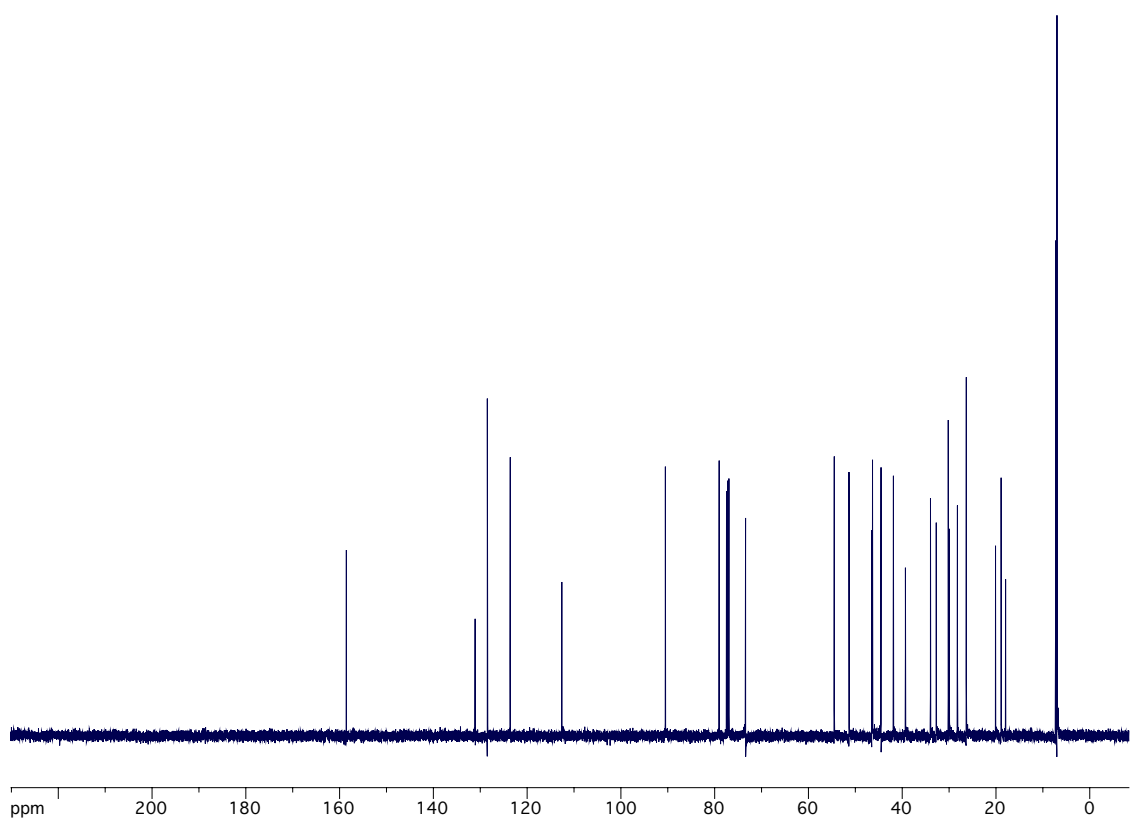
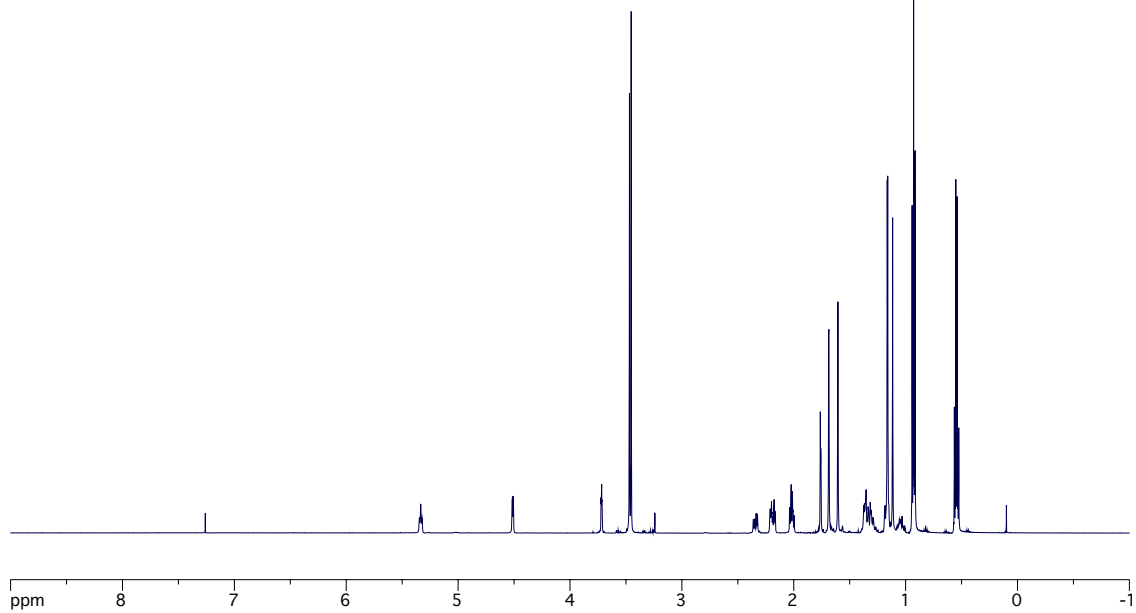
379

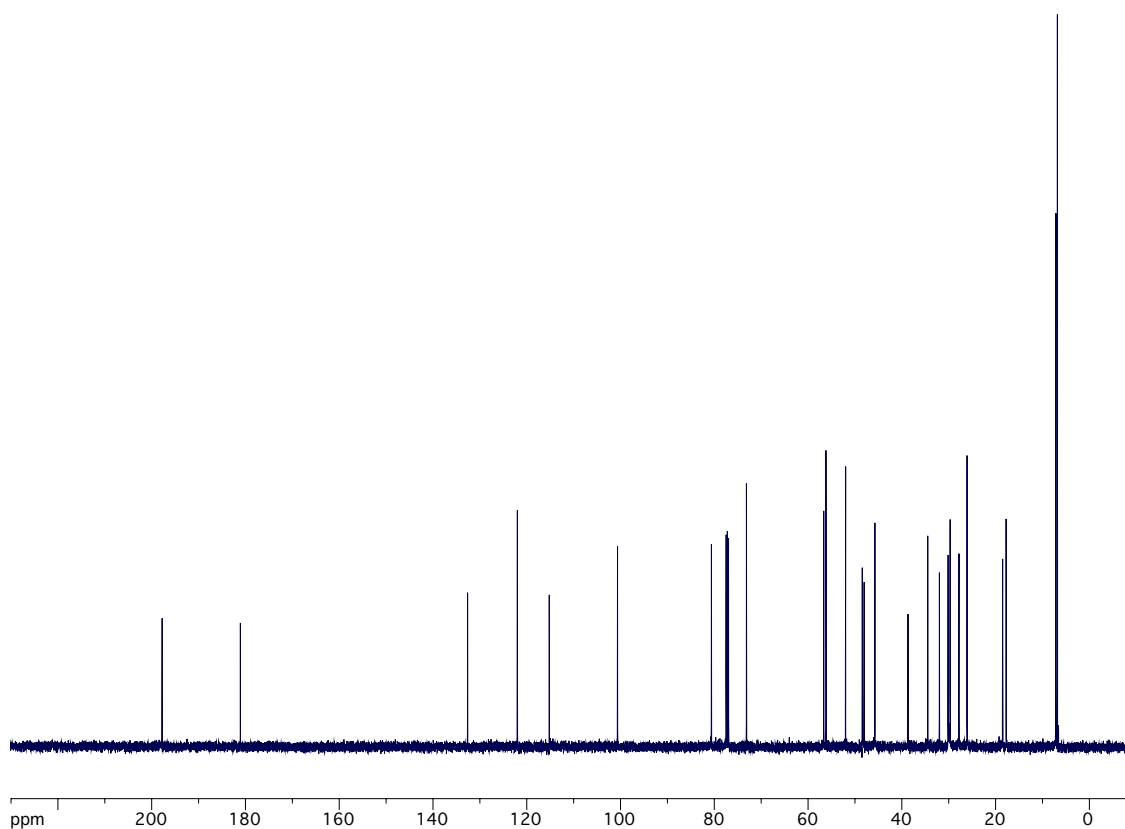
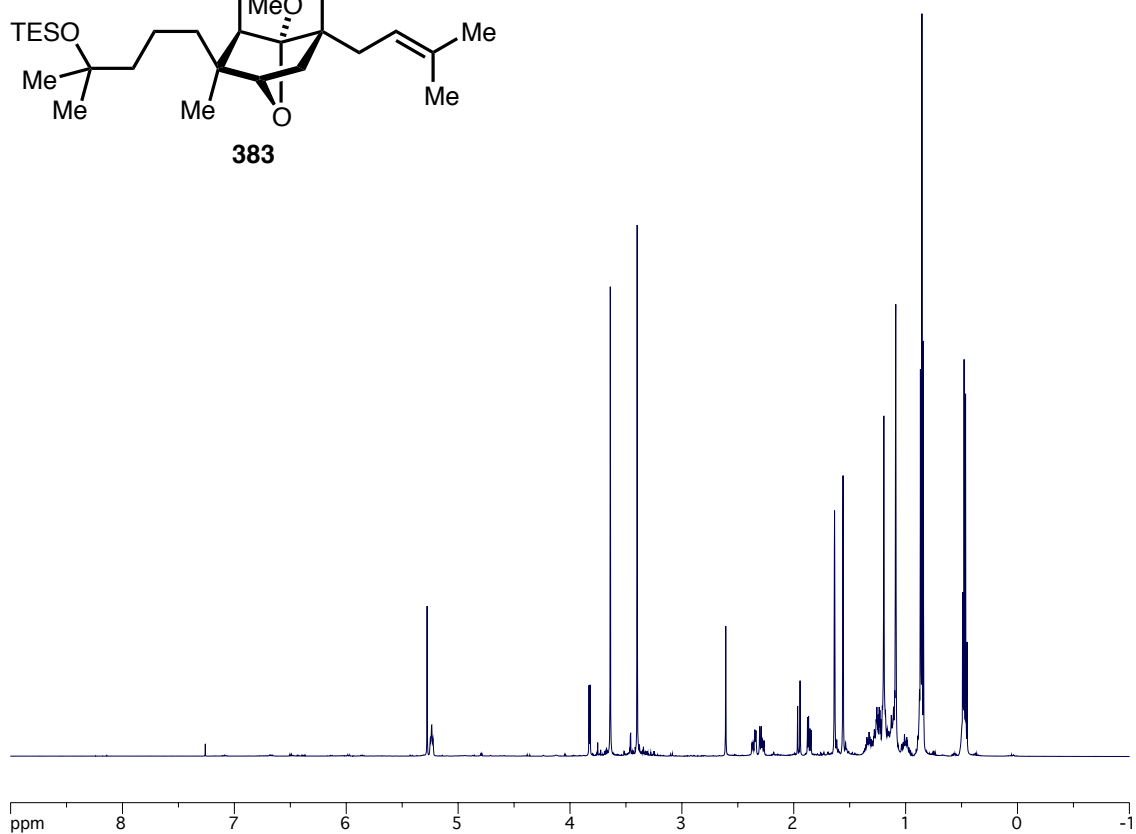
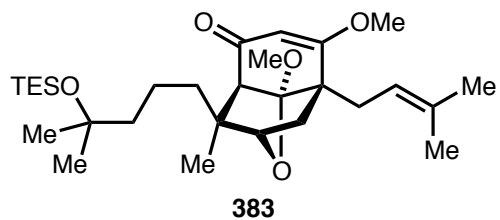


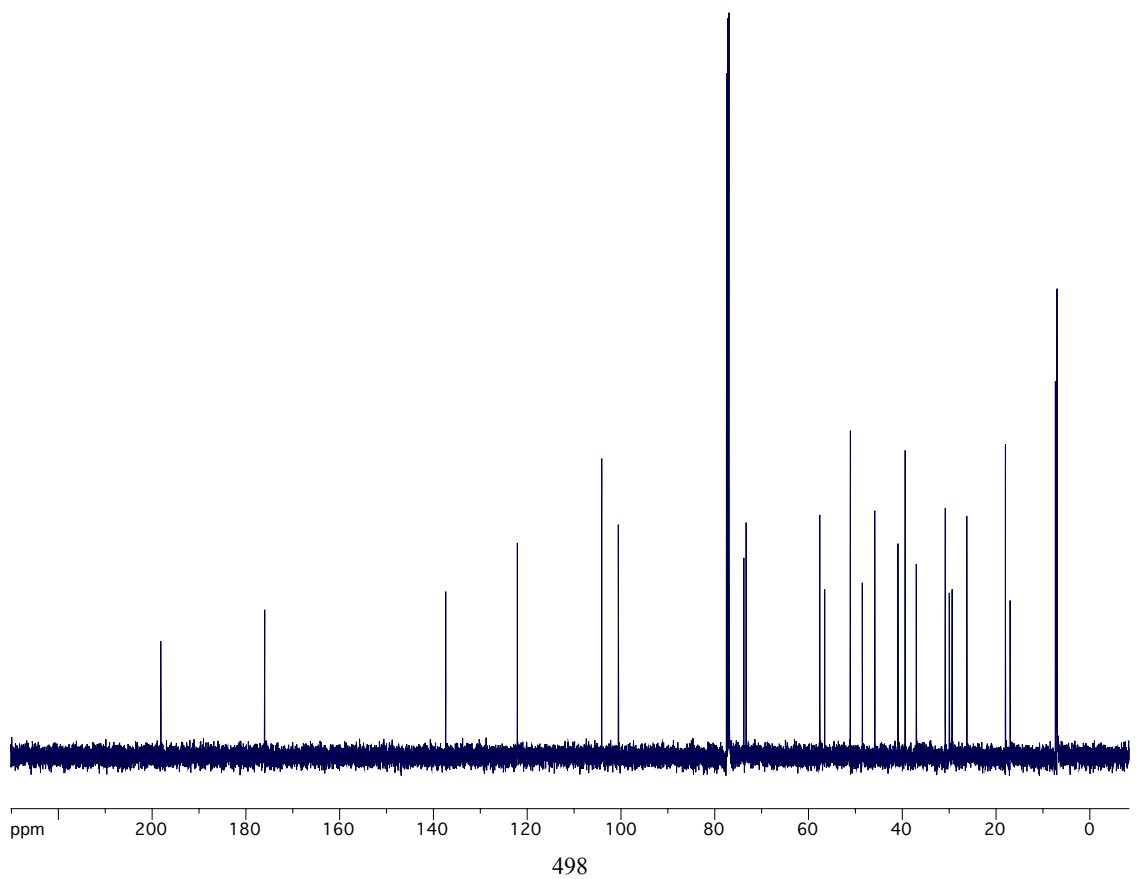
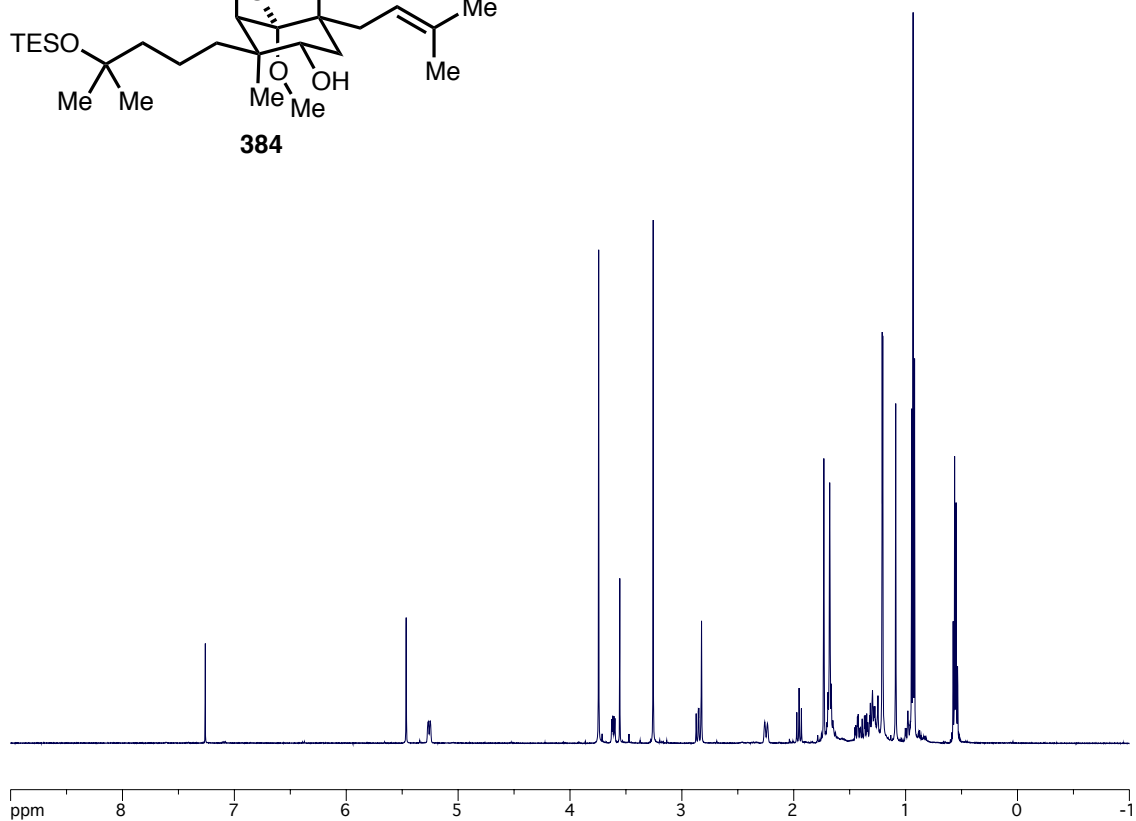
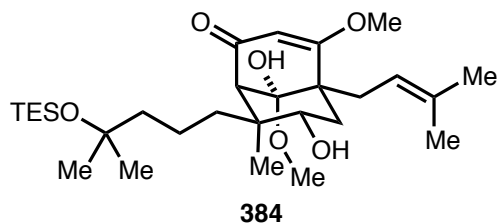


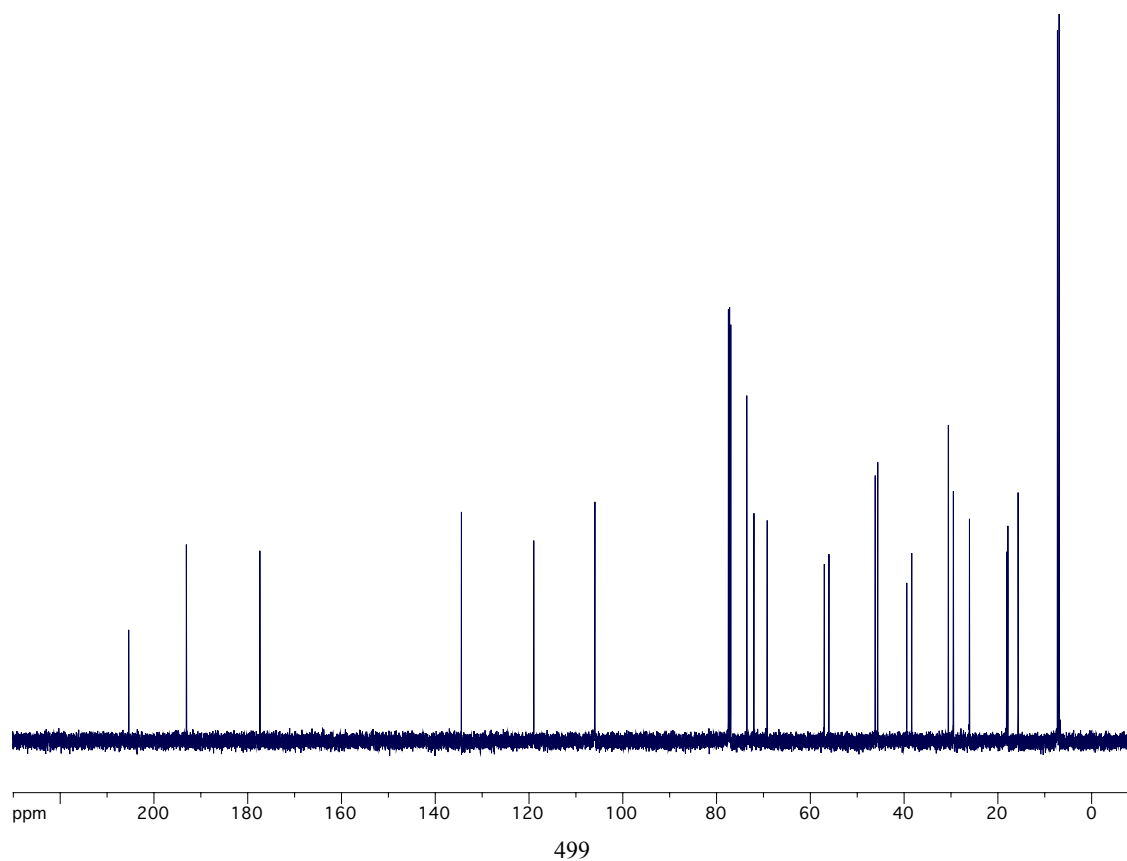
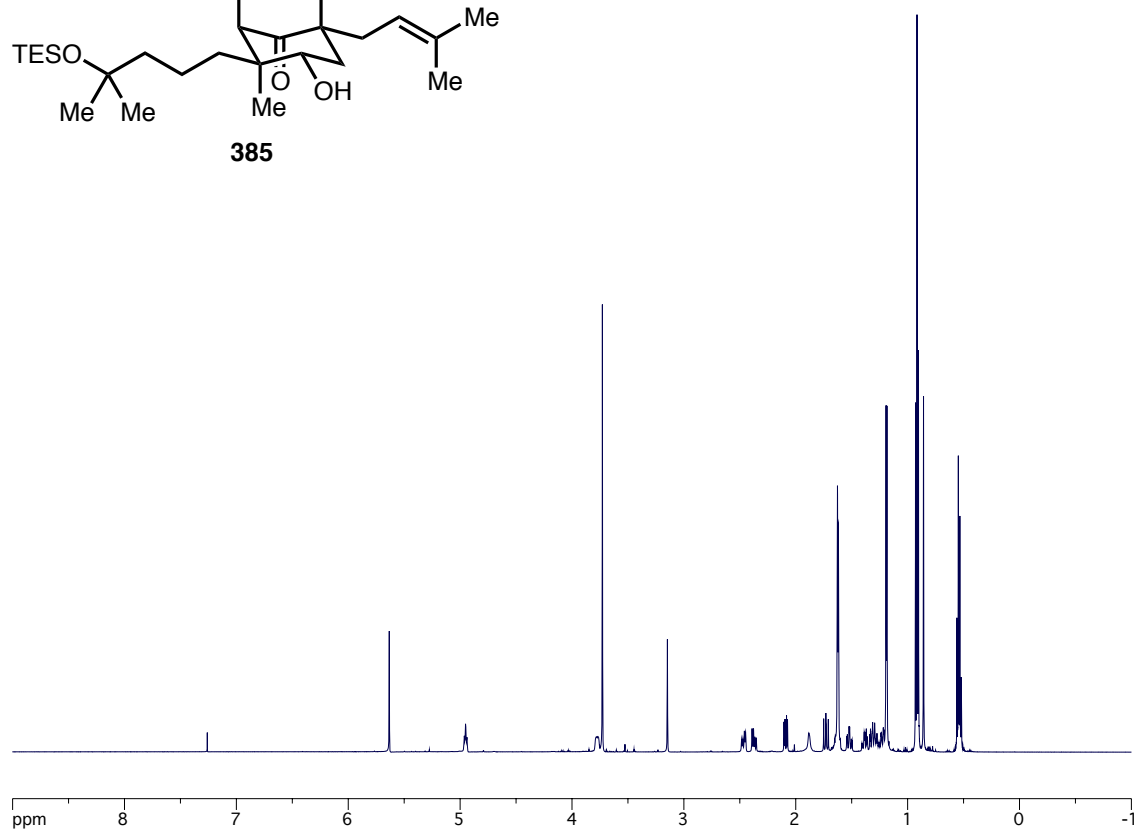
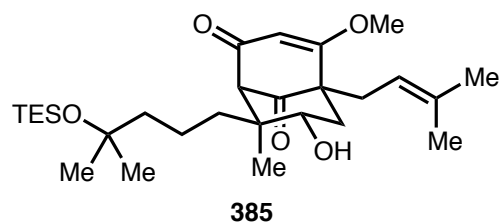


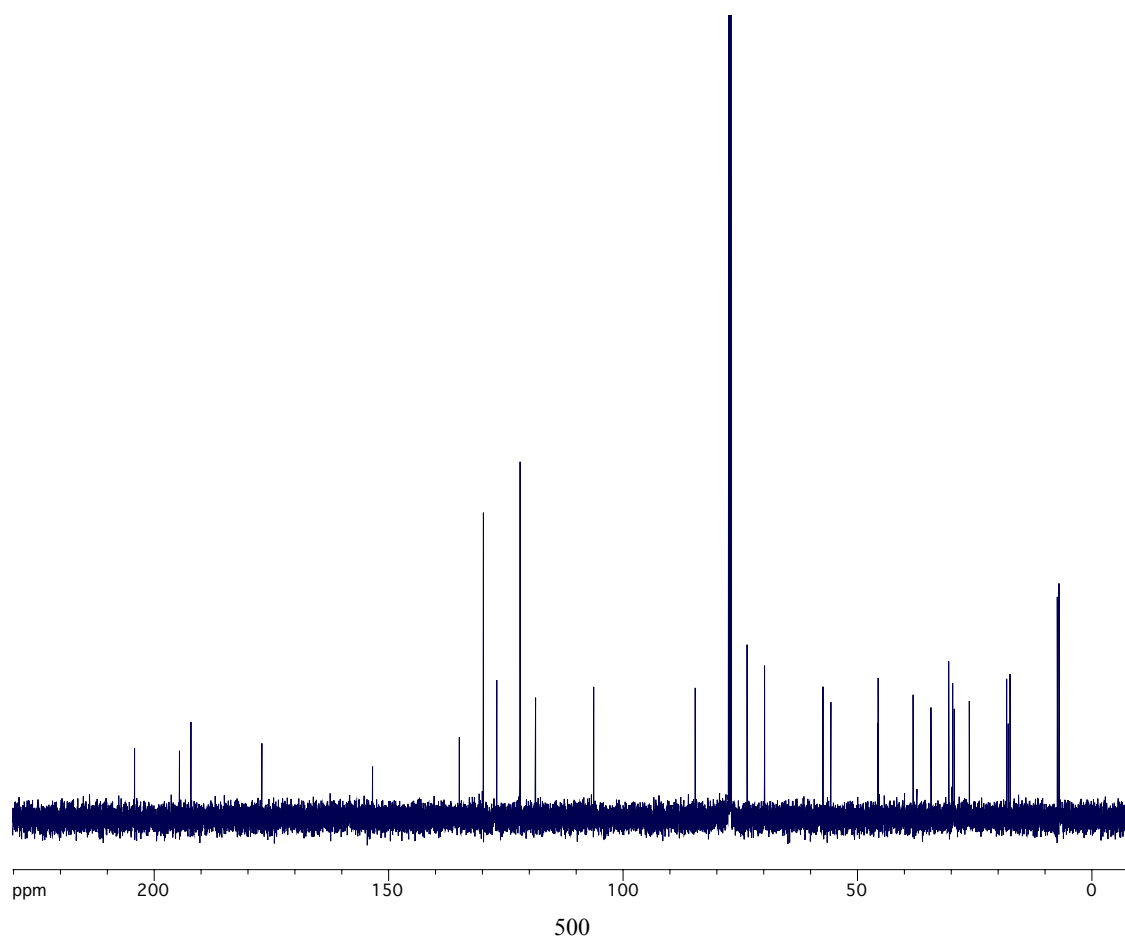
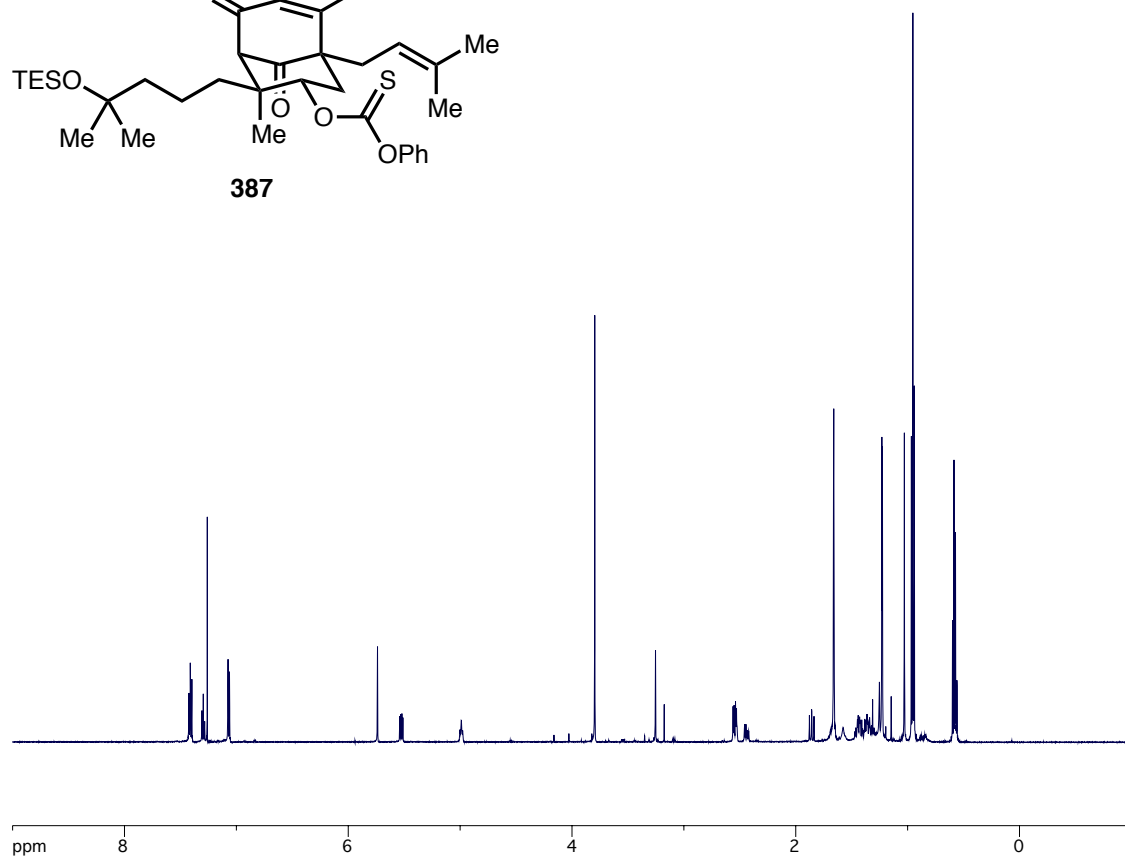
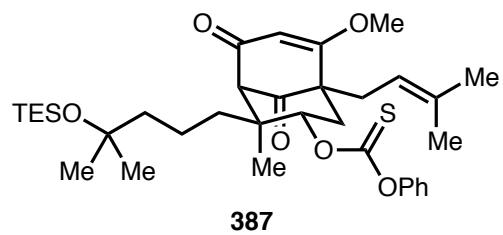
382

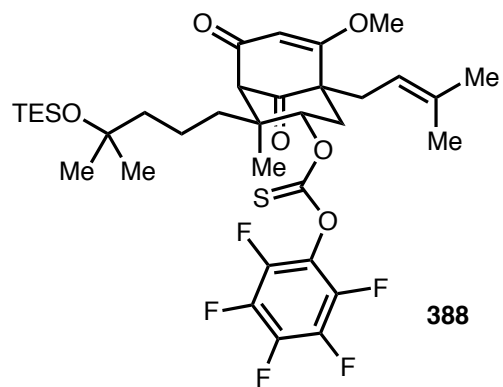




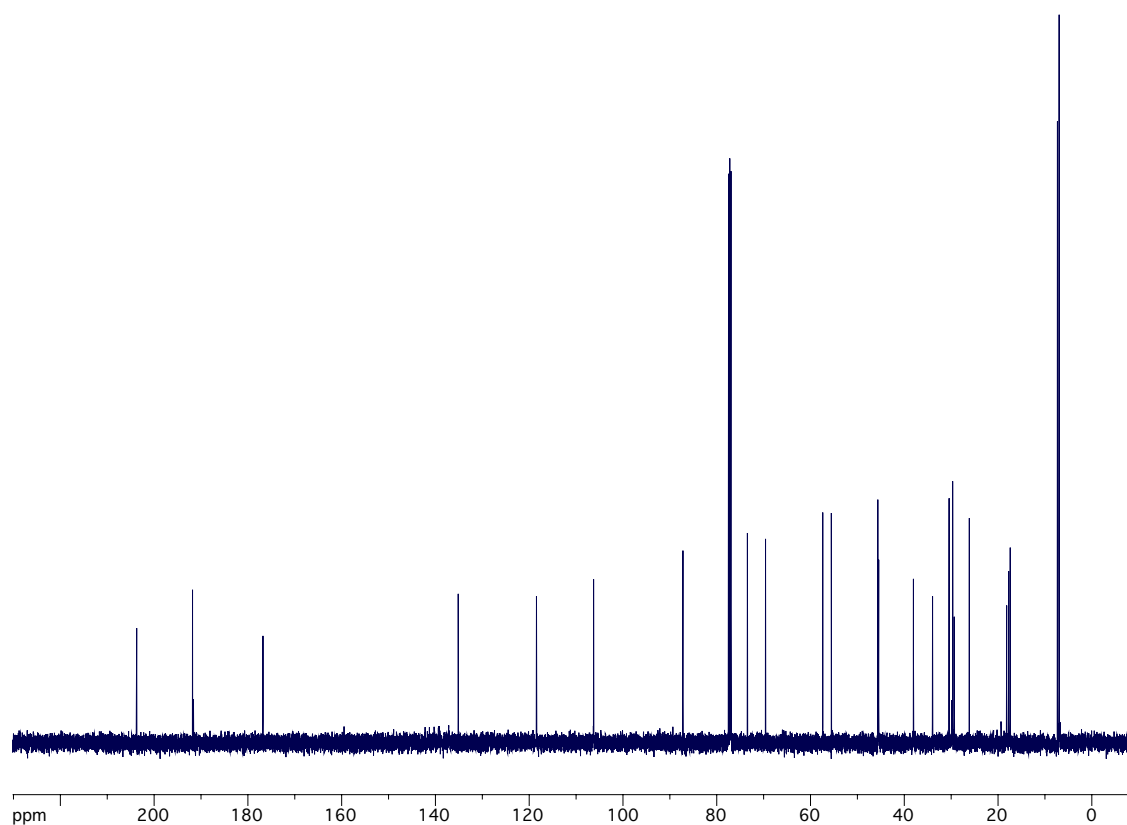
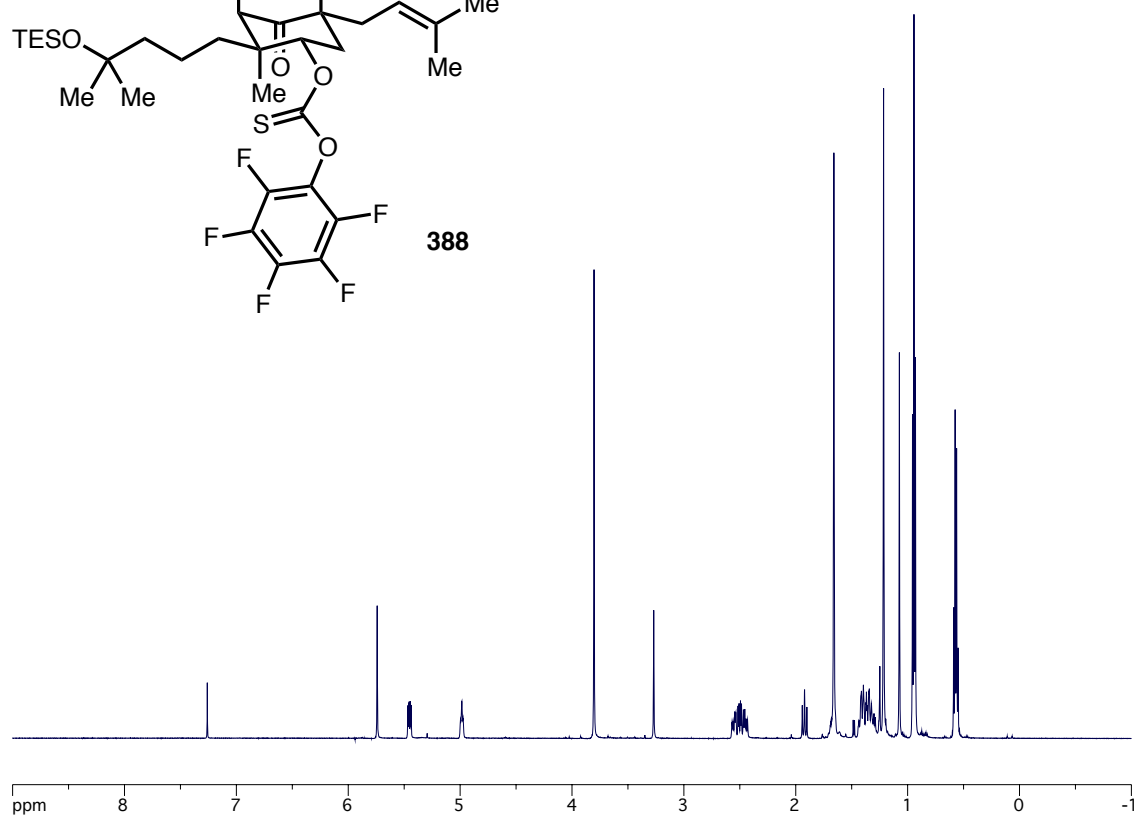


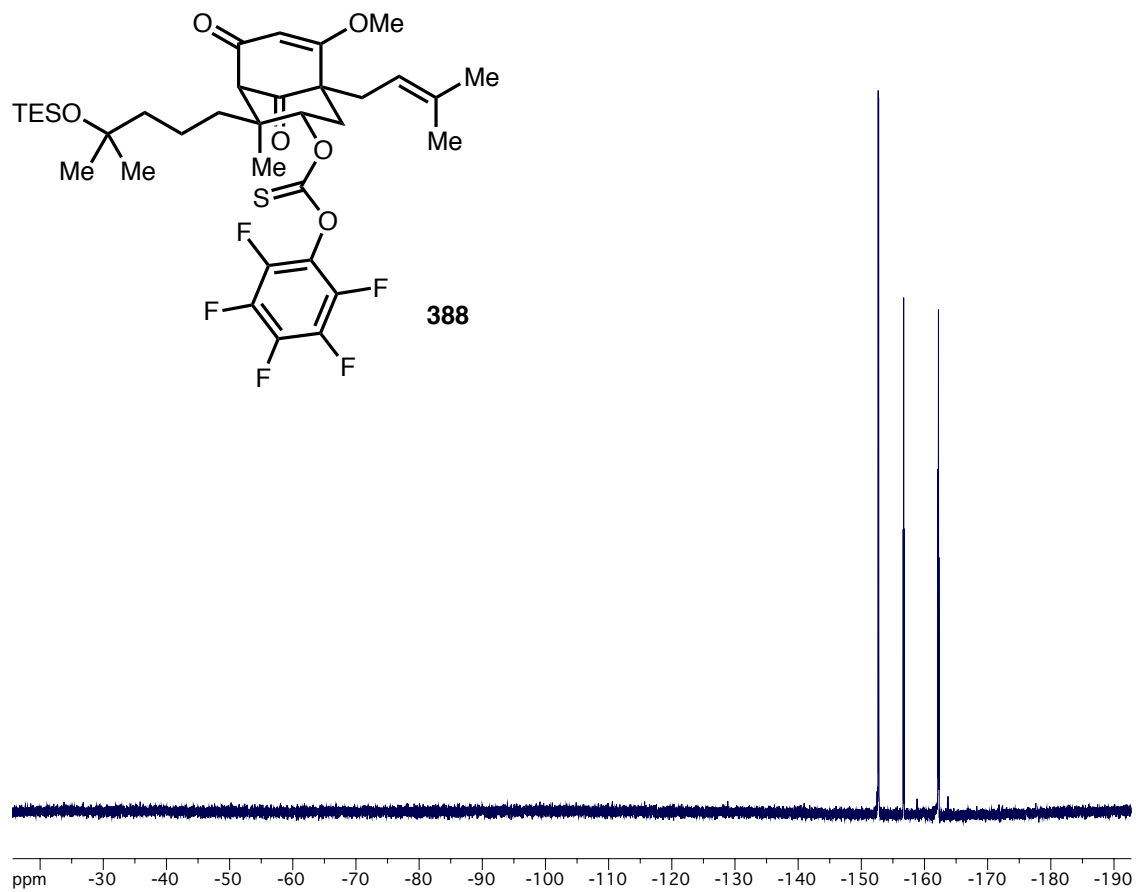


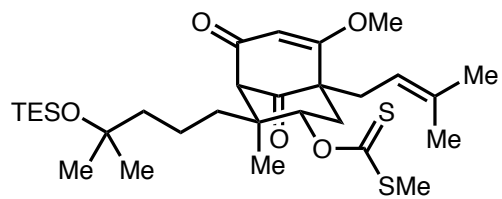




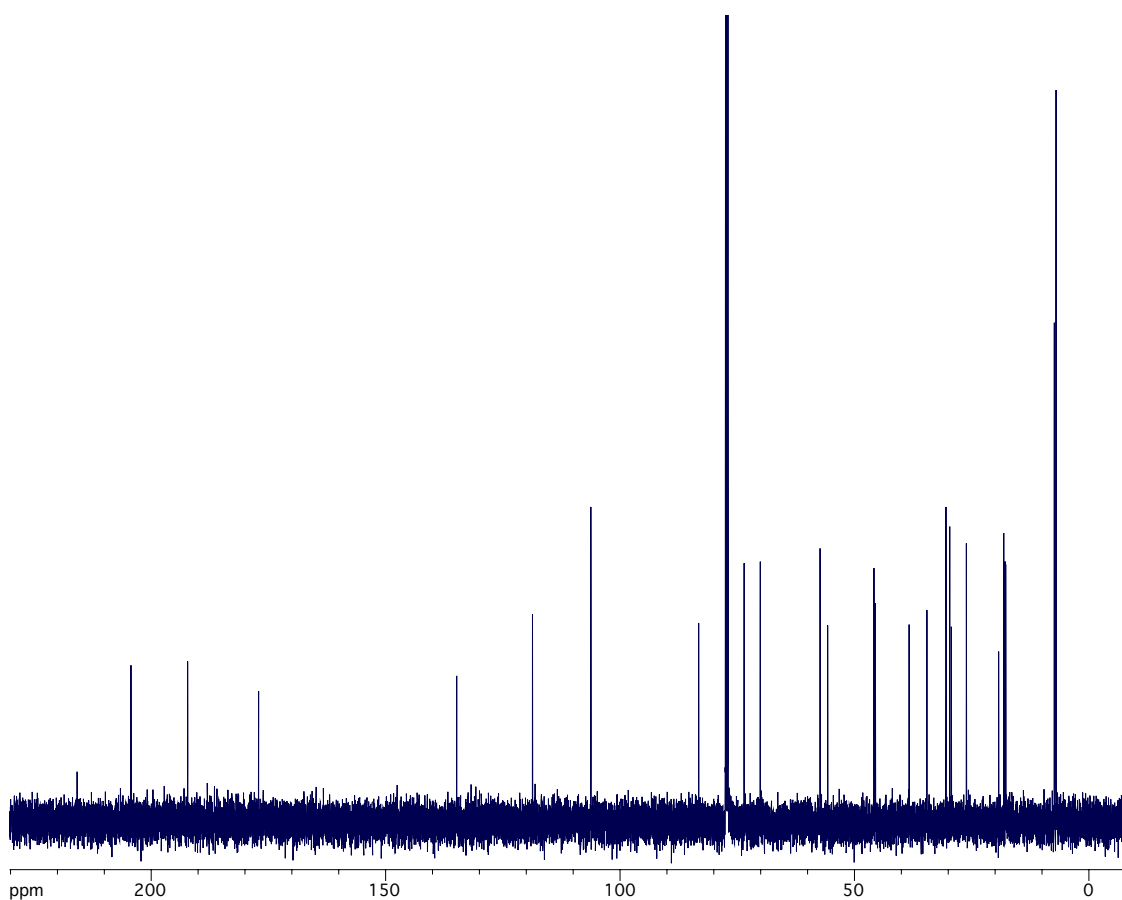
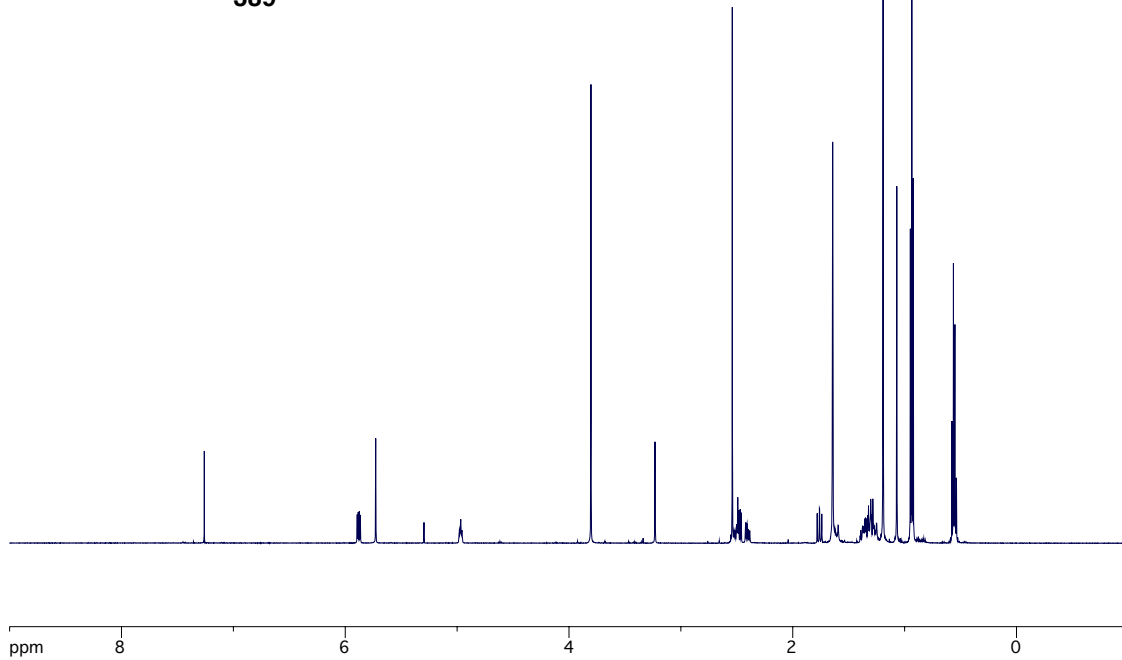
388

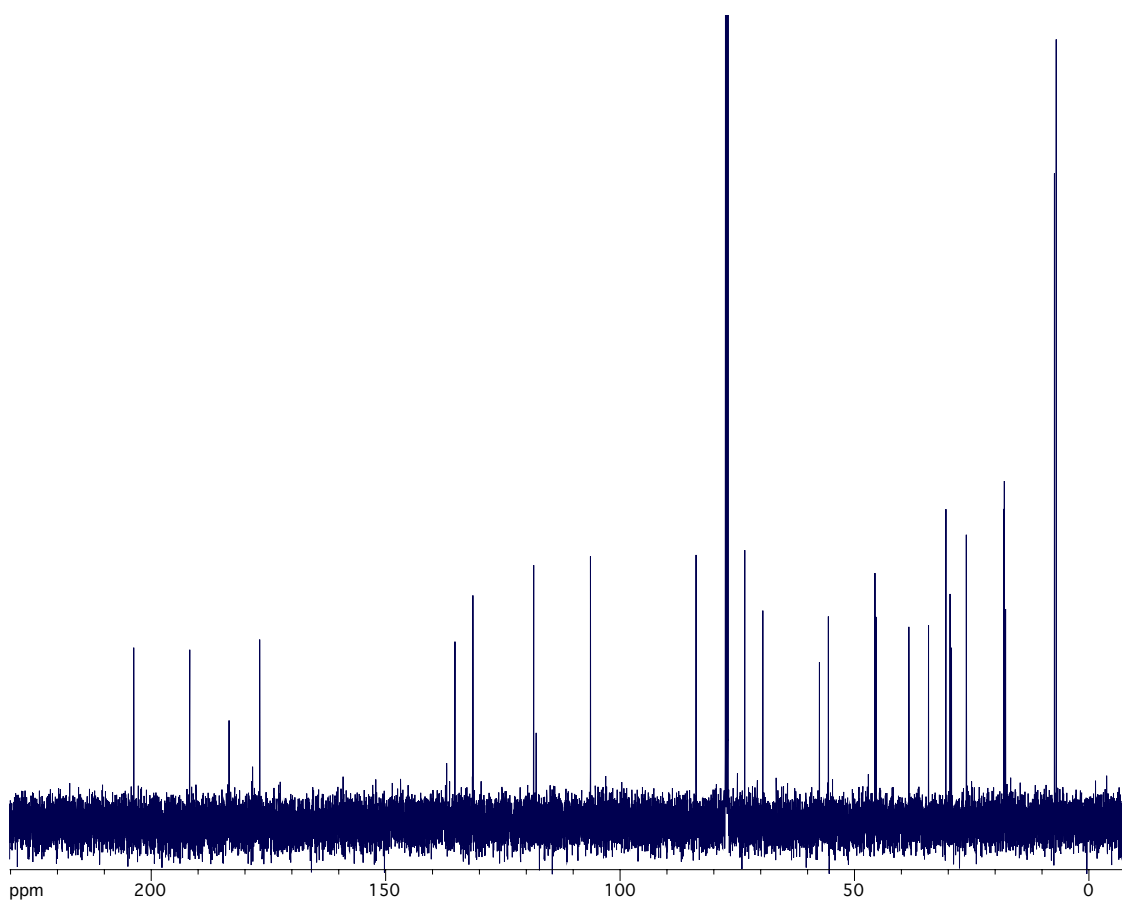
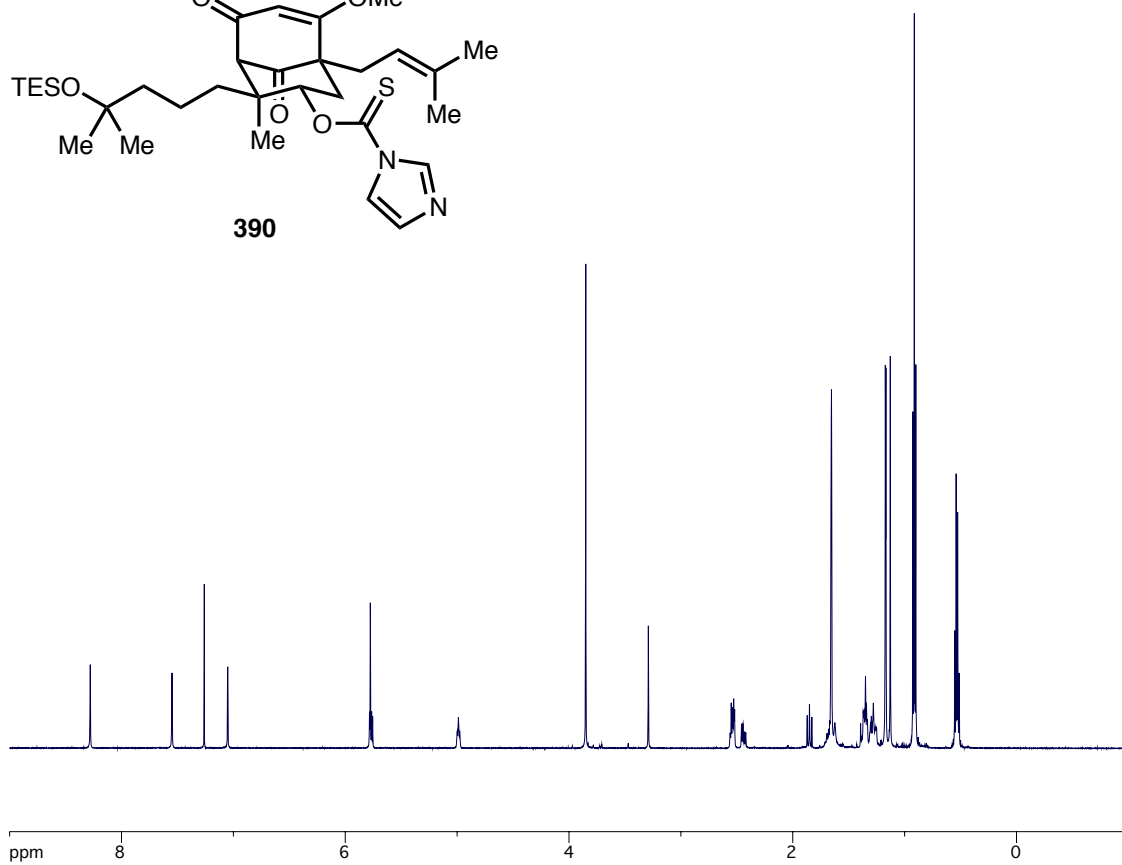
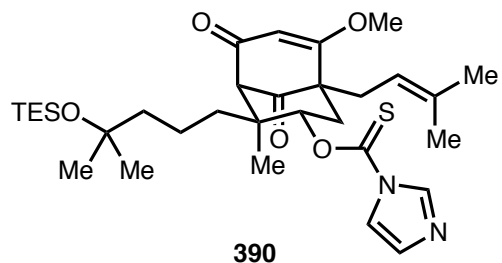


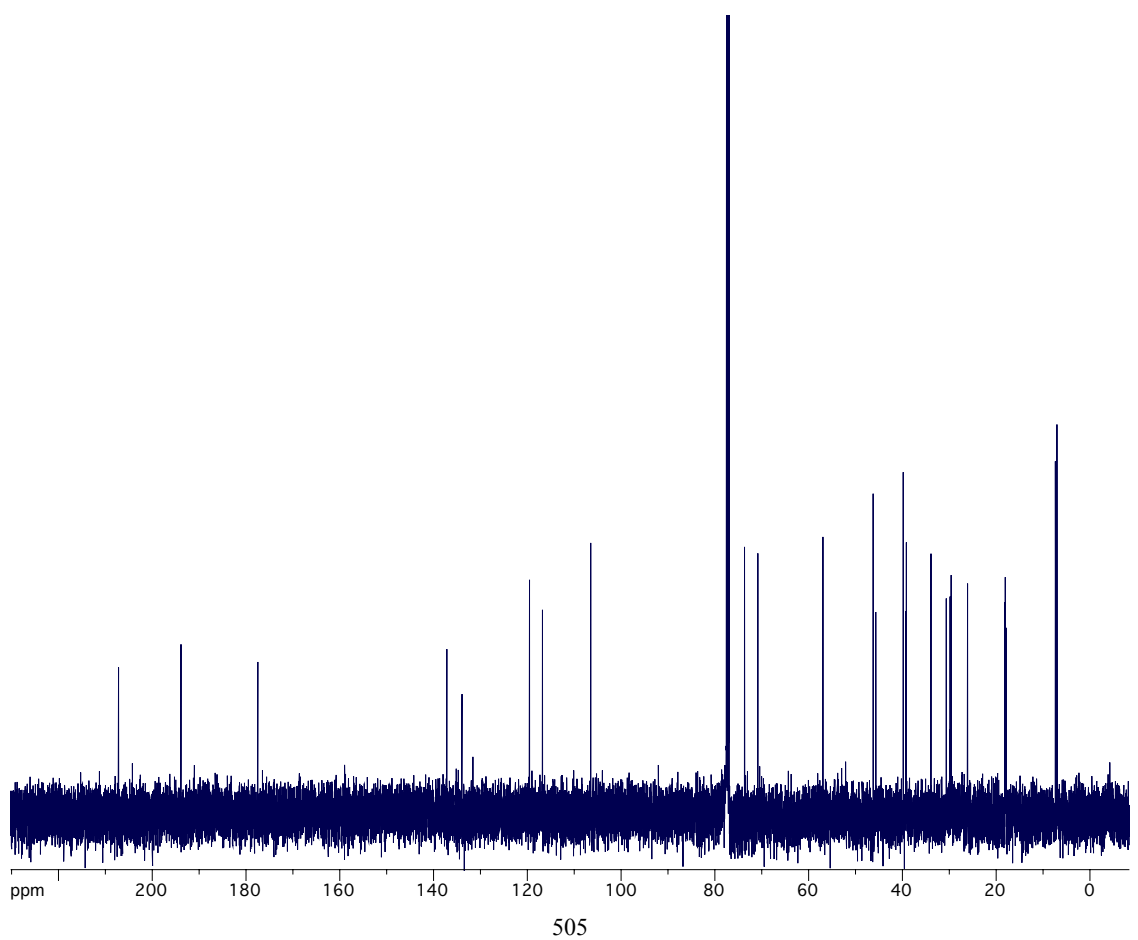
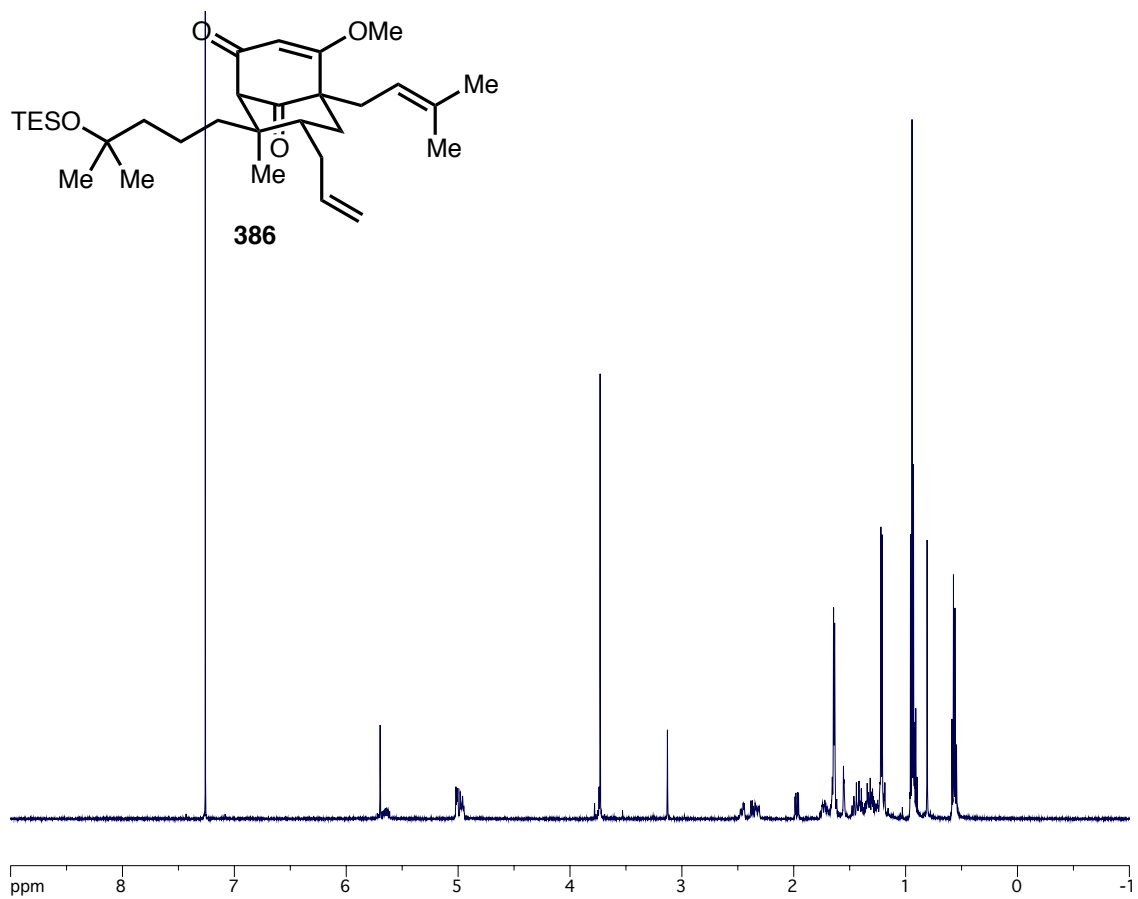


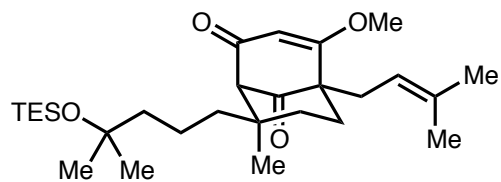


389

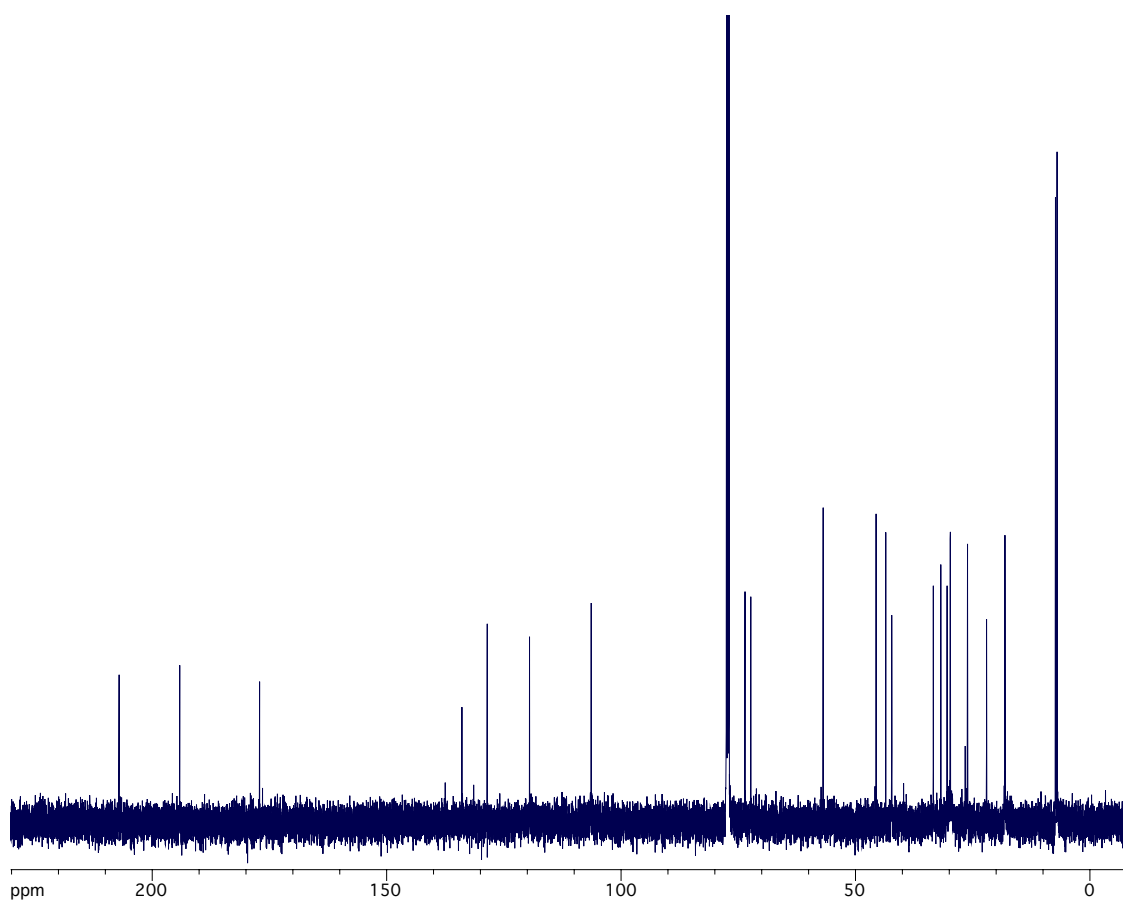
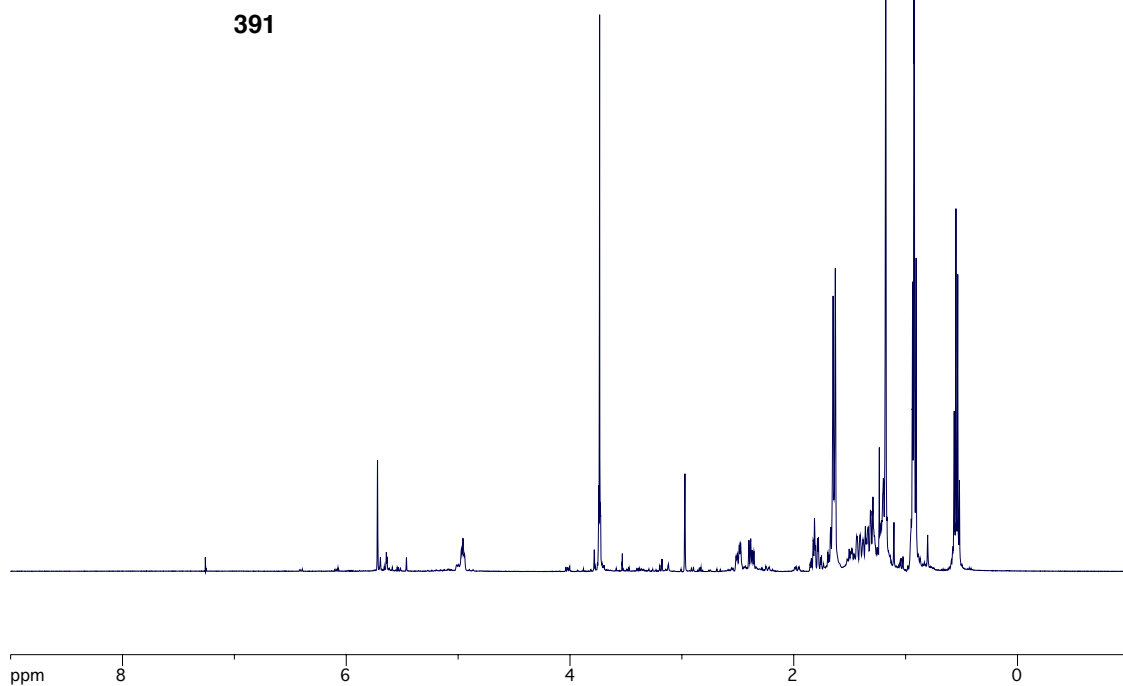


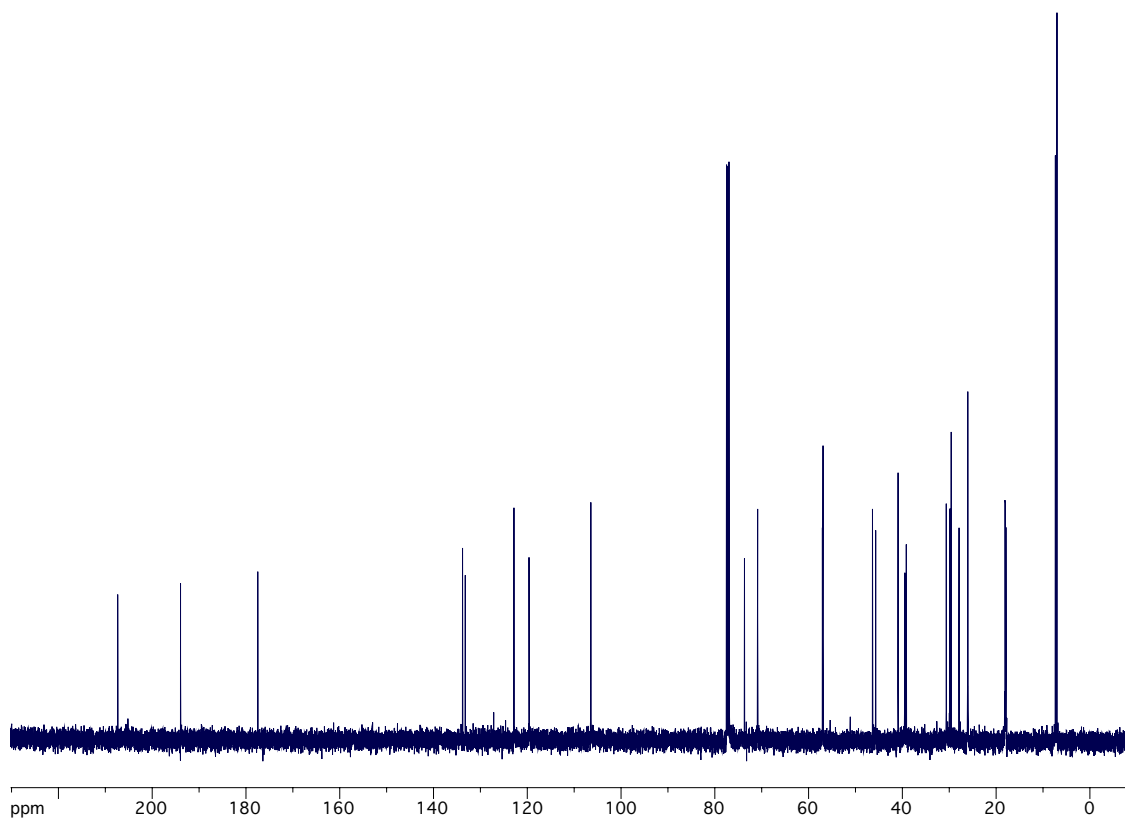
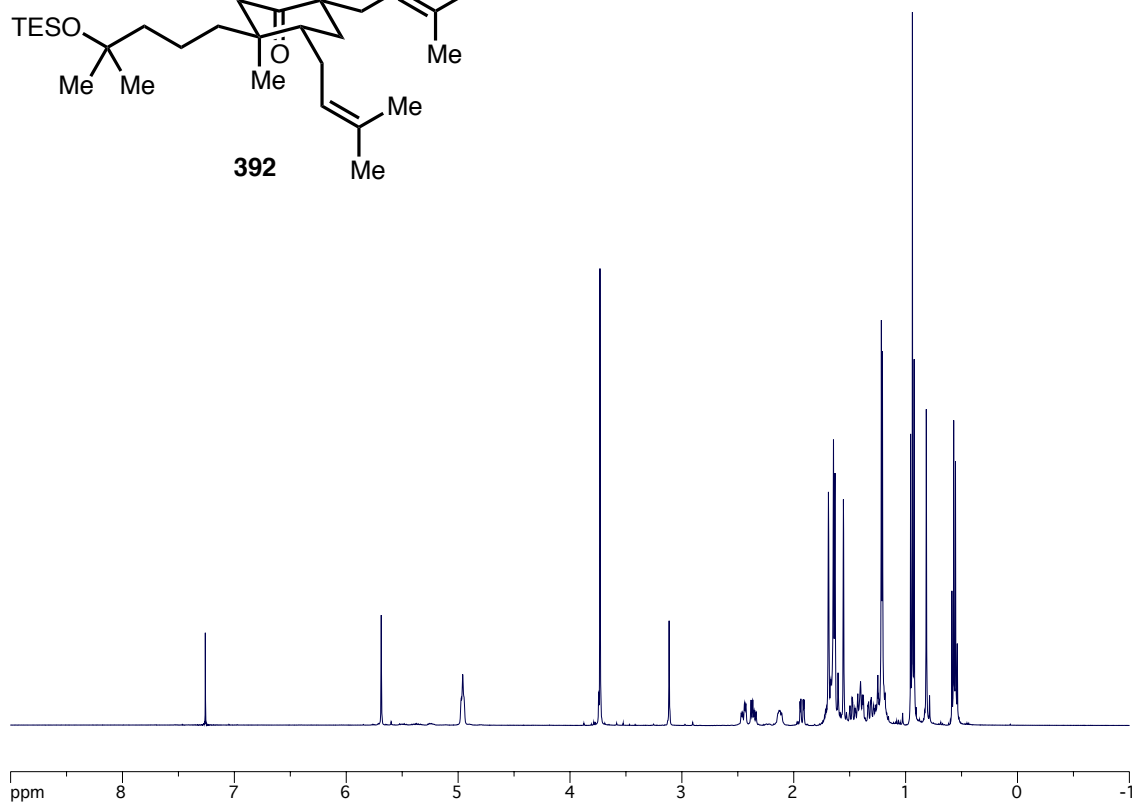
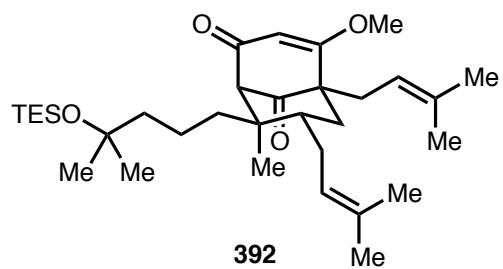


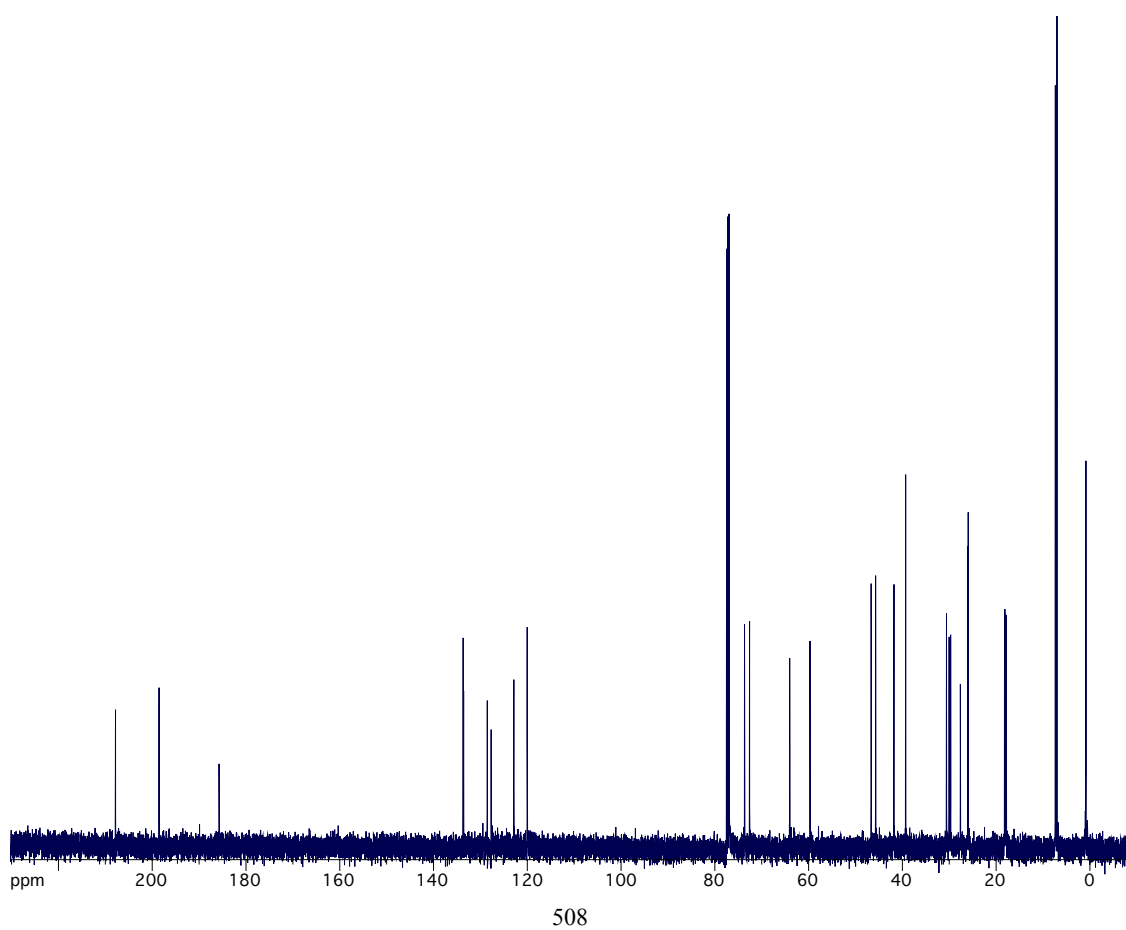
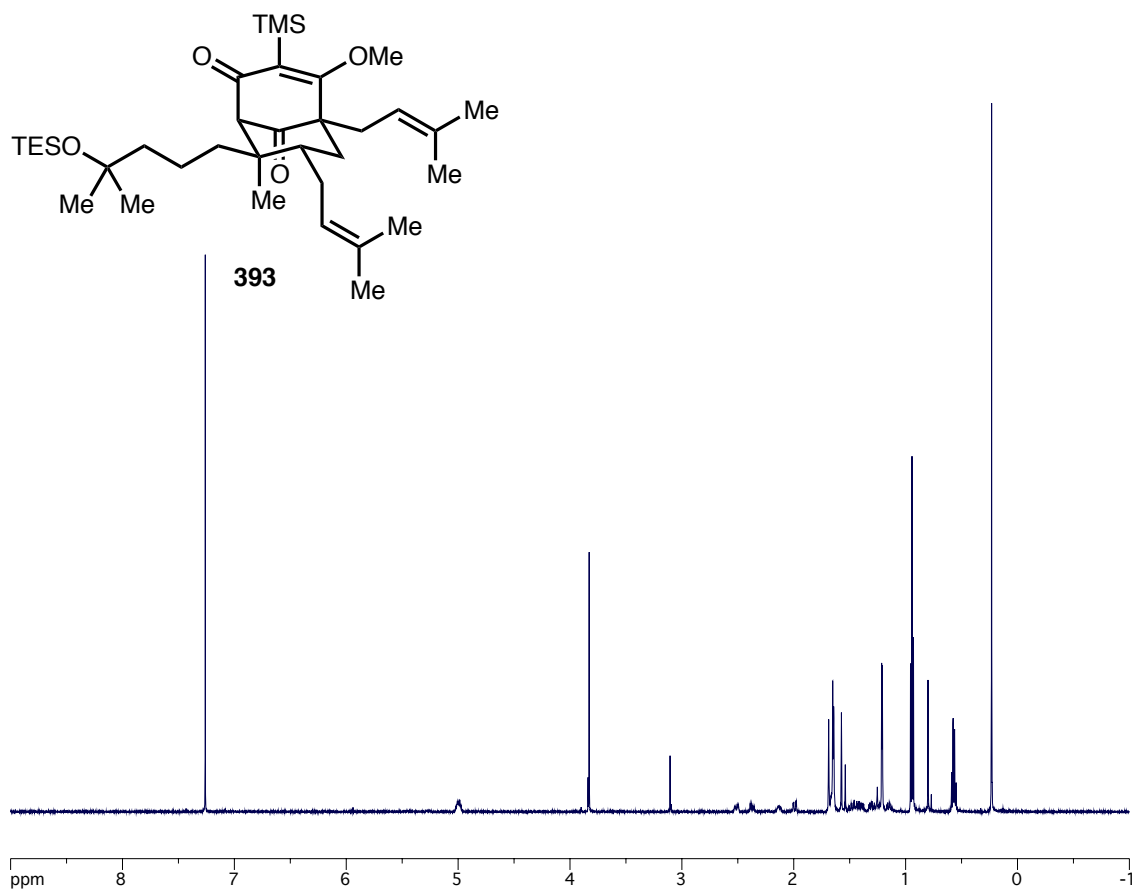


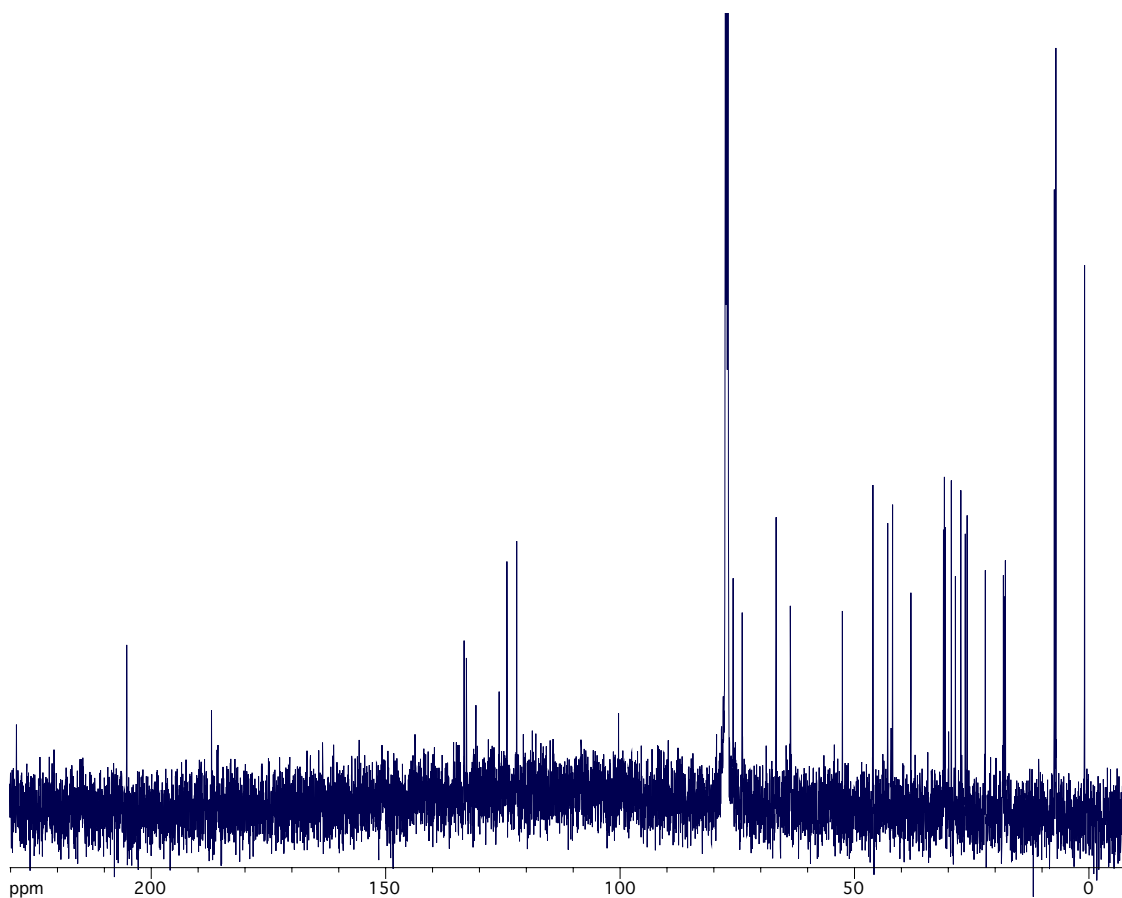
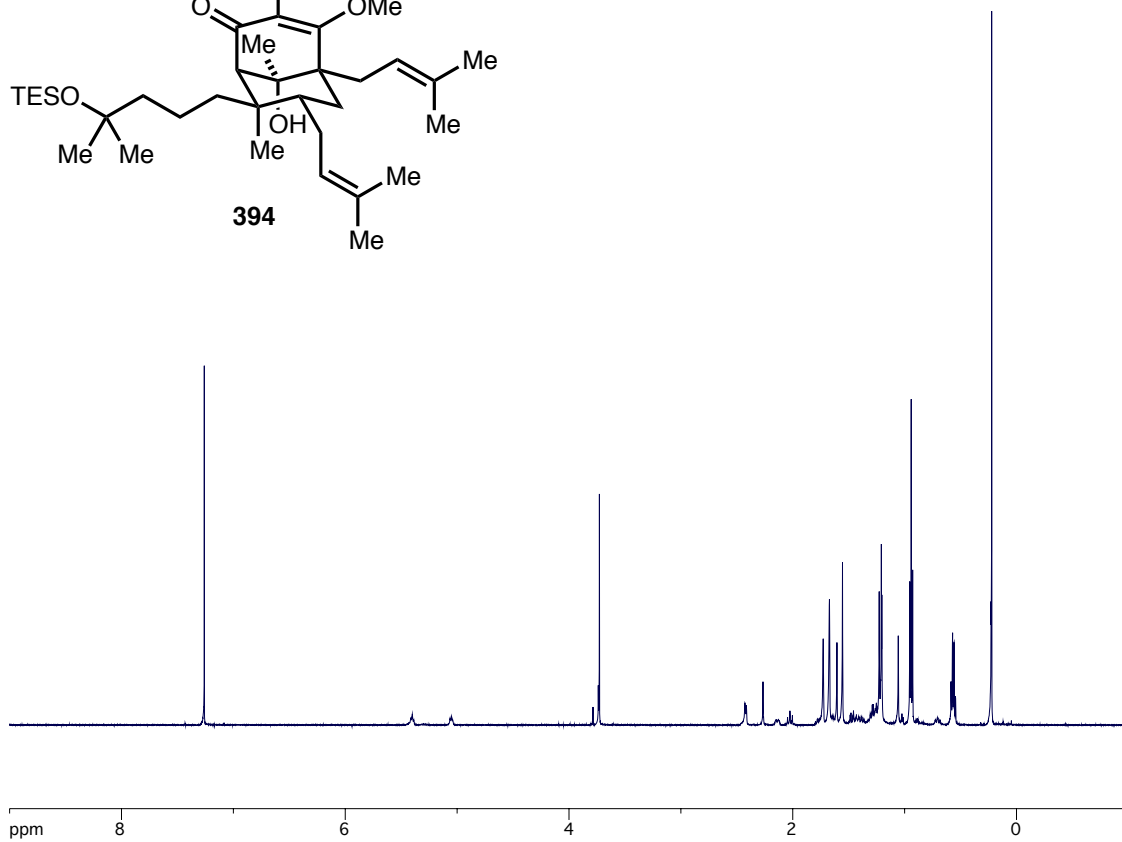
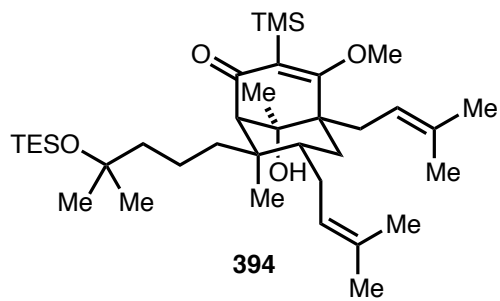


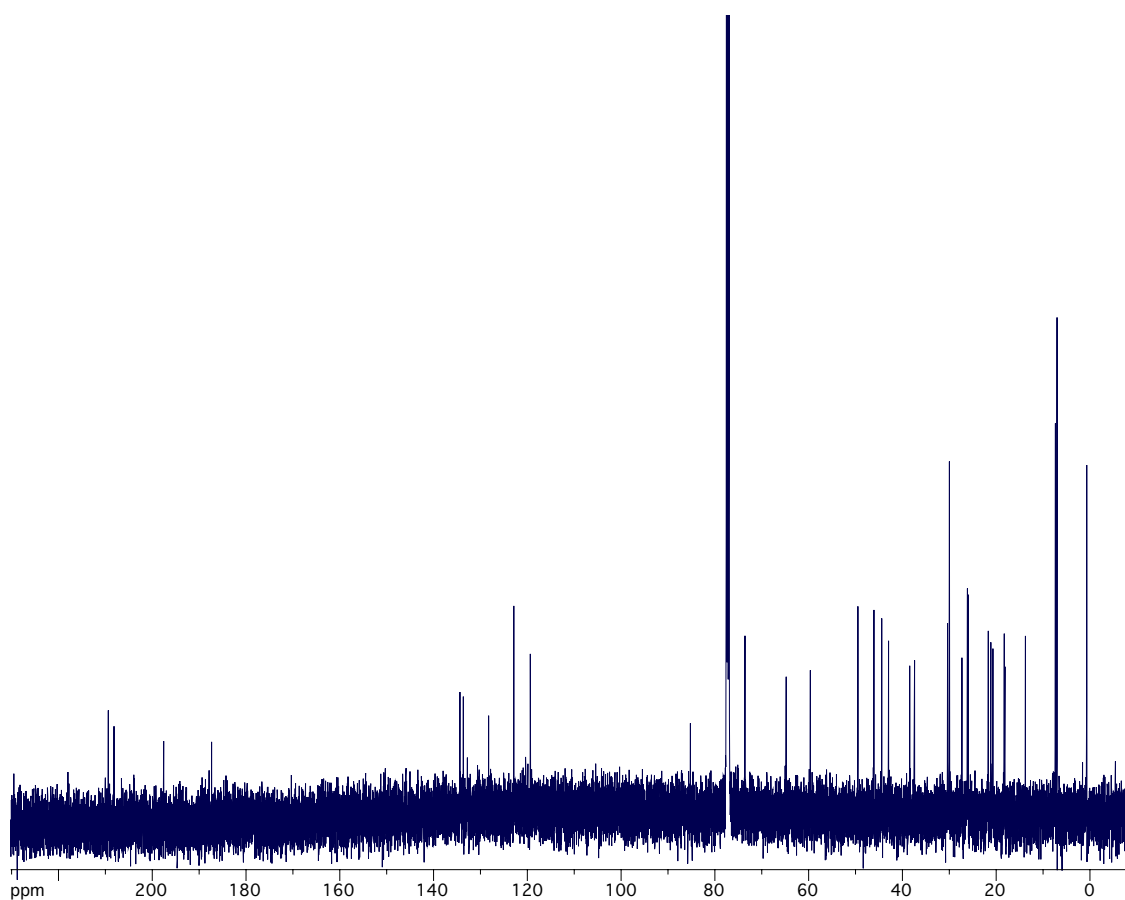
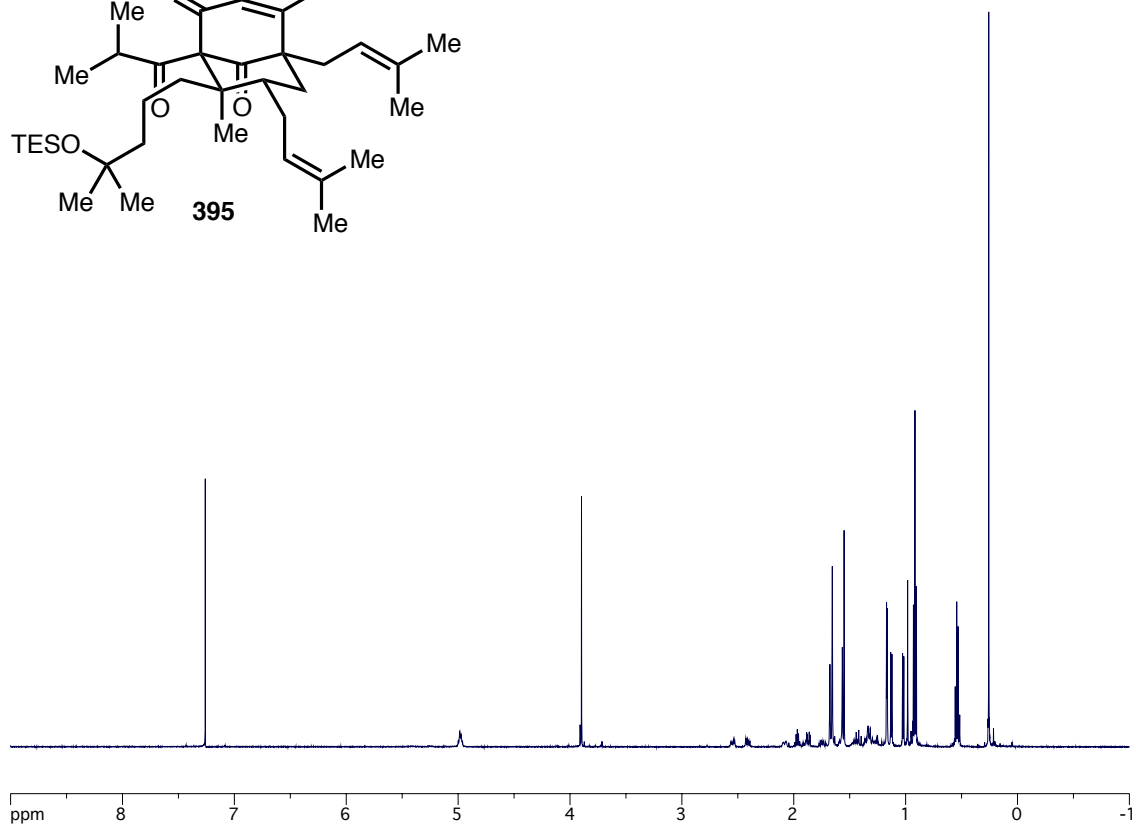
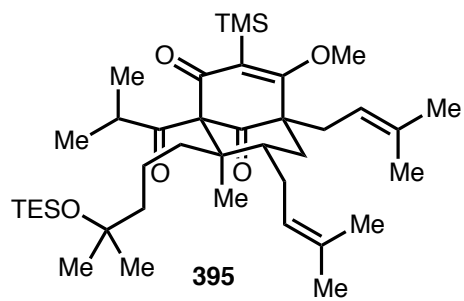
391

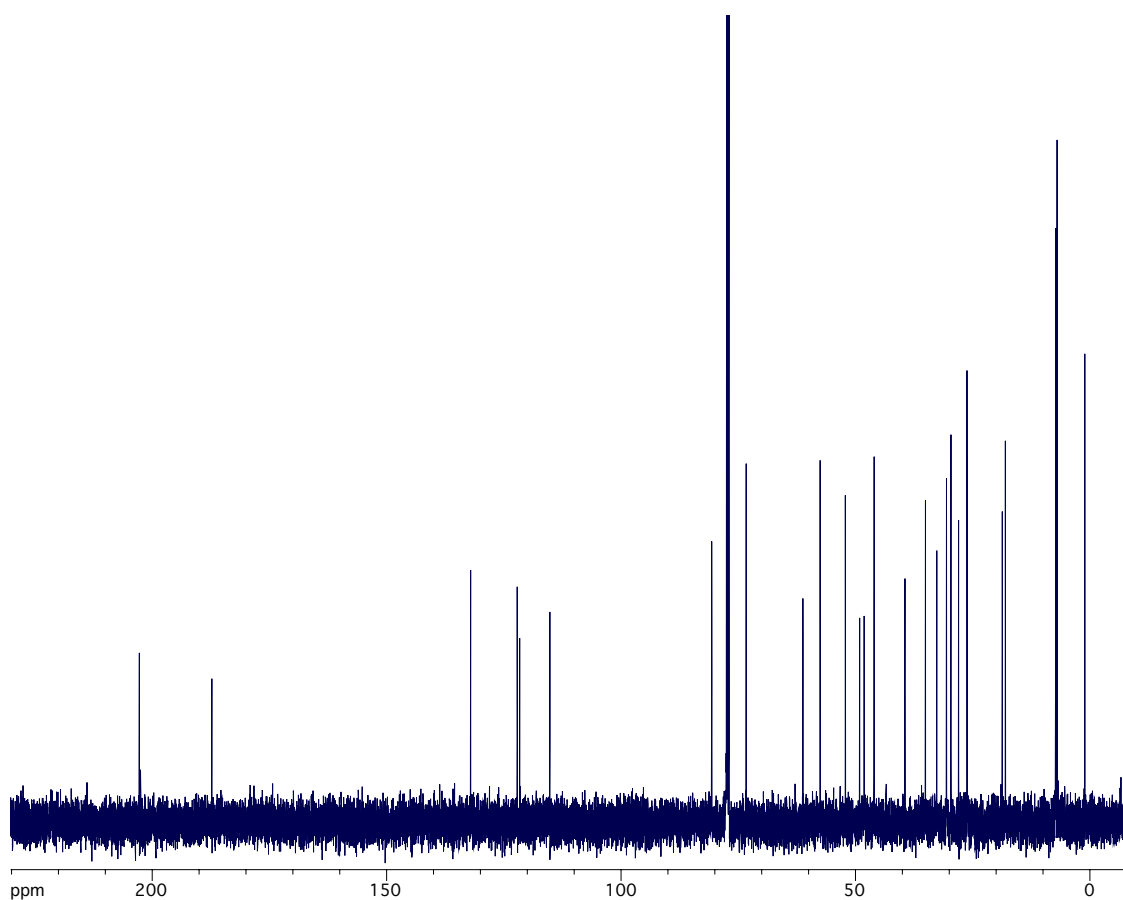
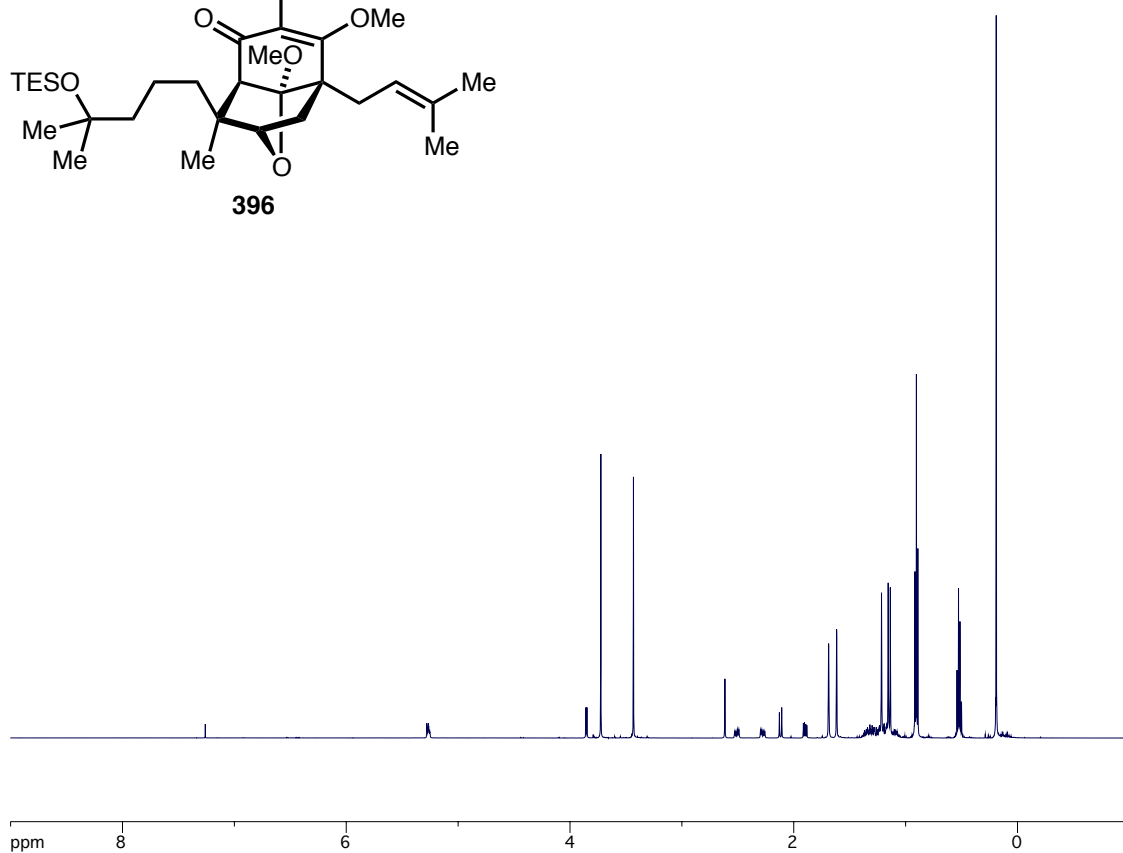
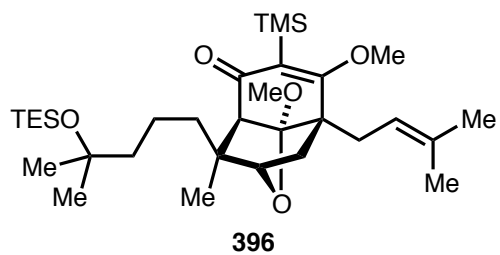


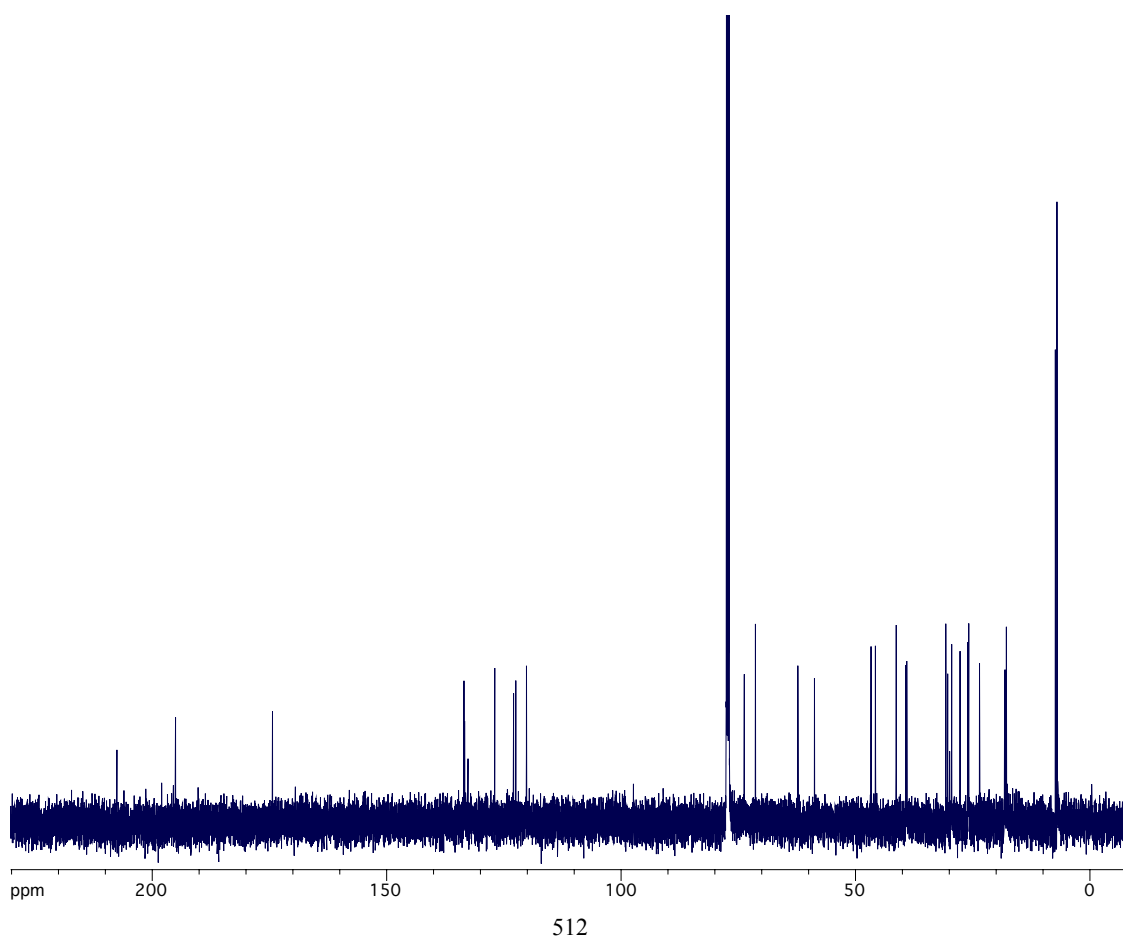
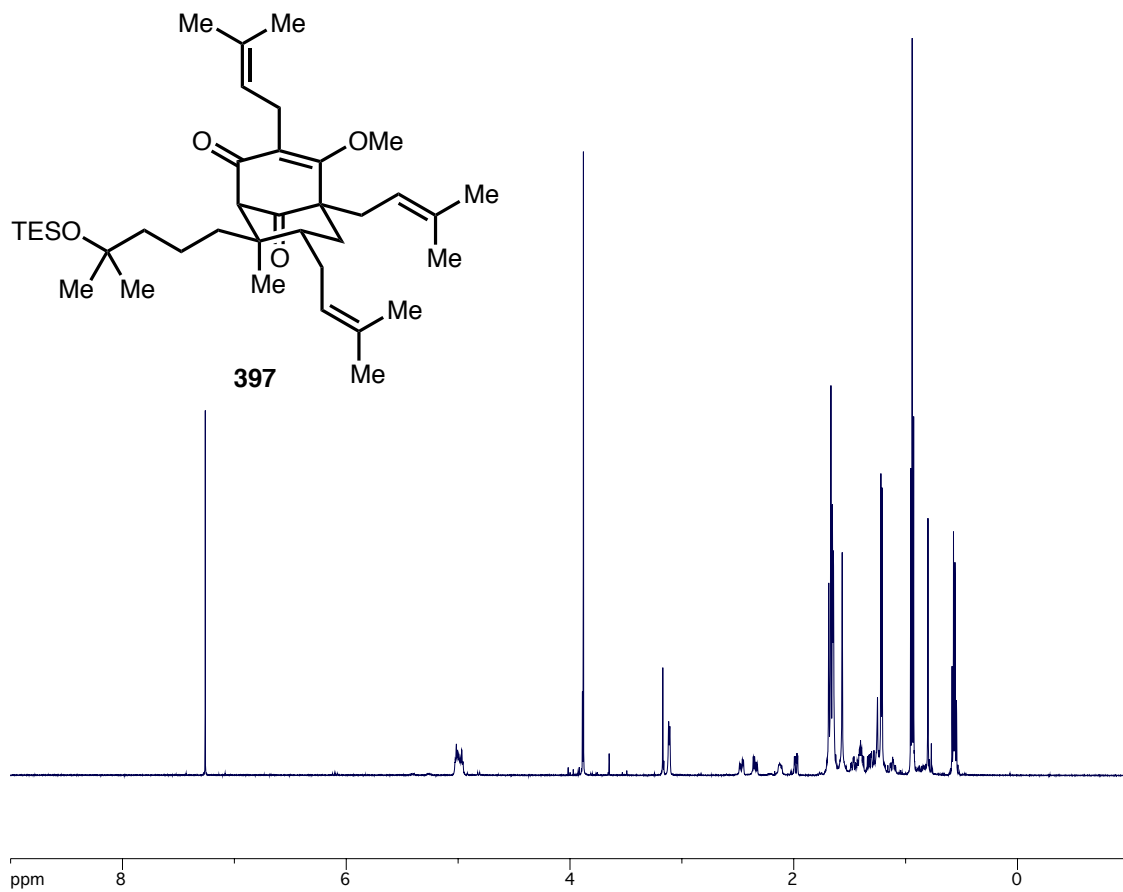


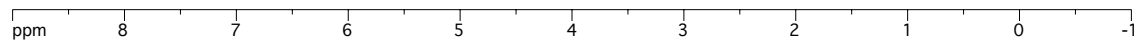


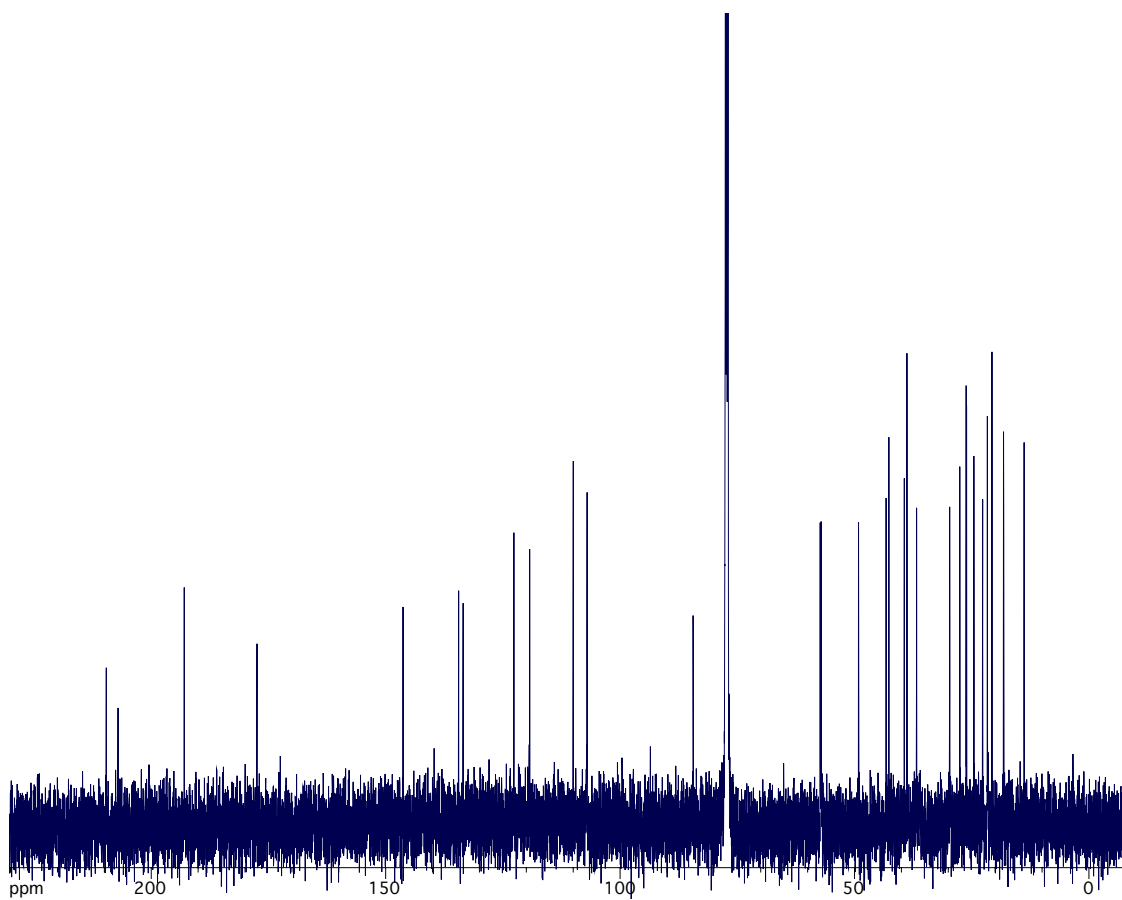
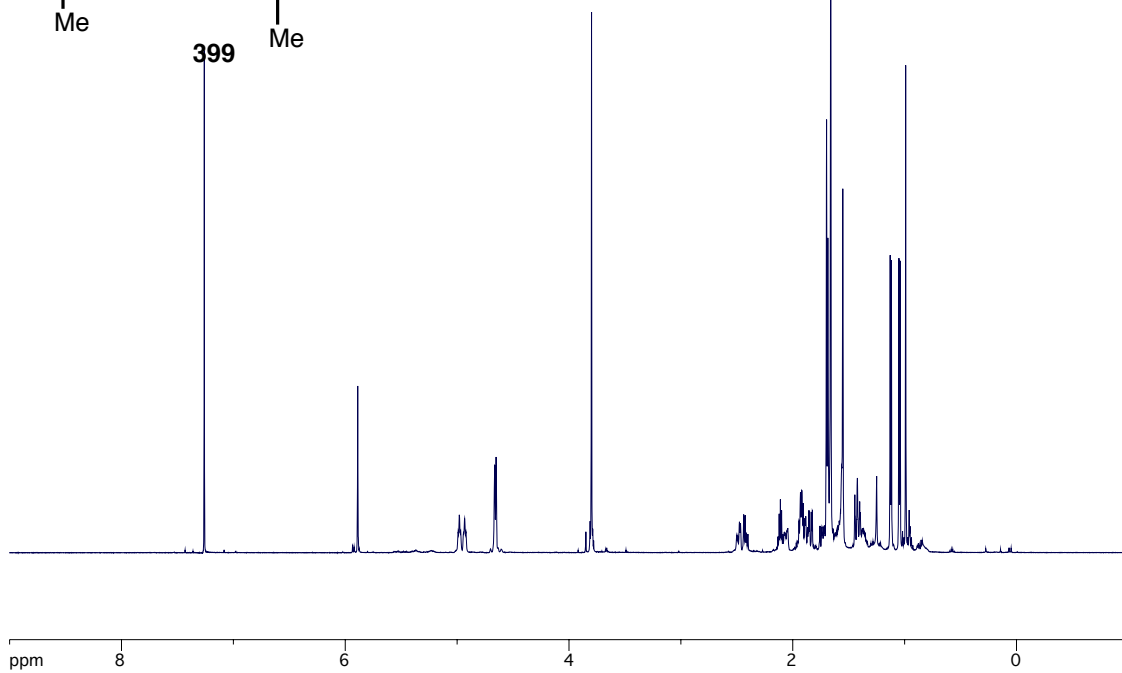
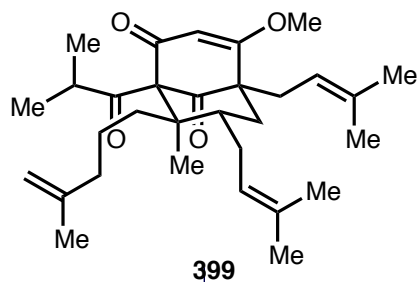


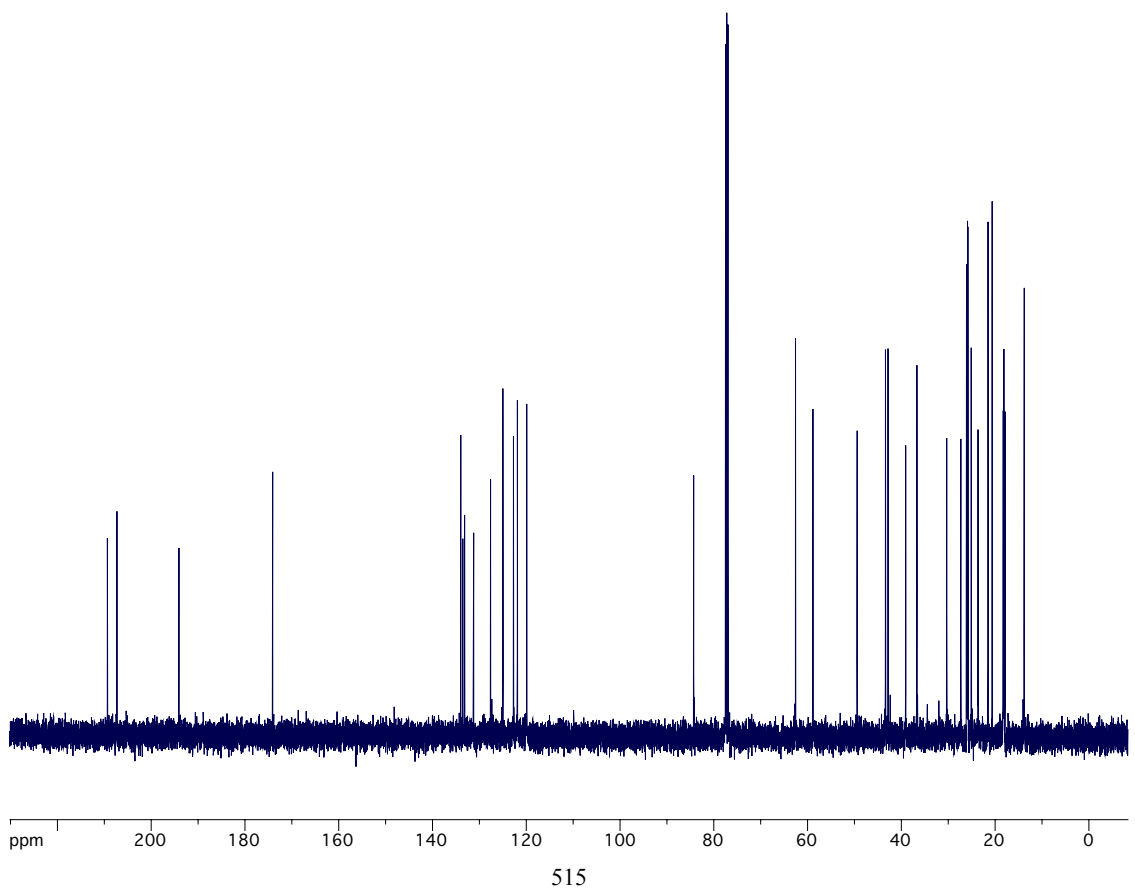
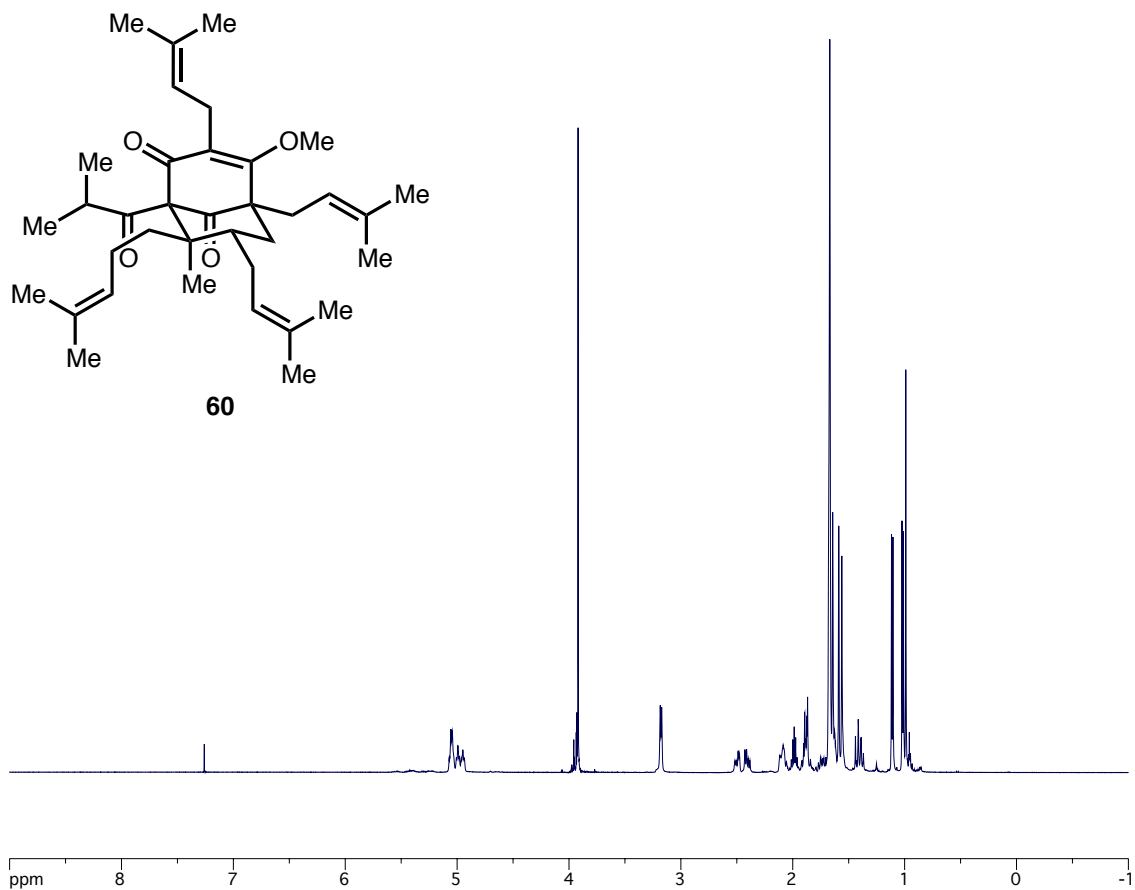


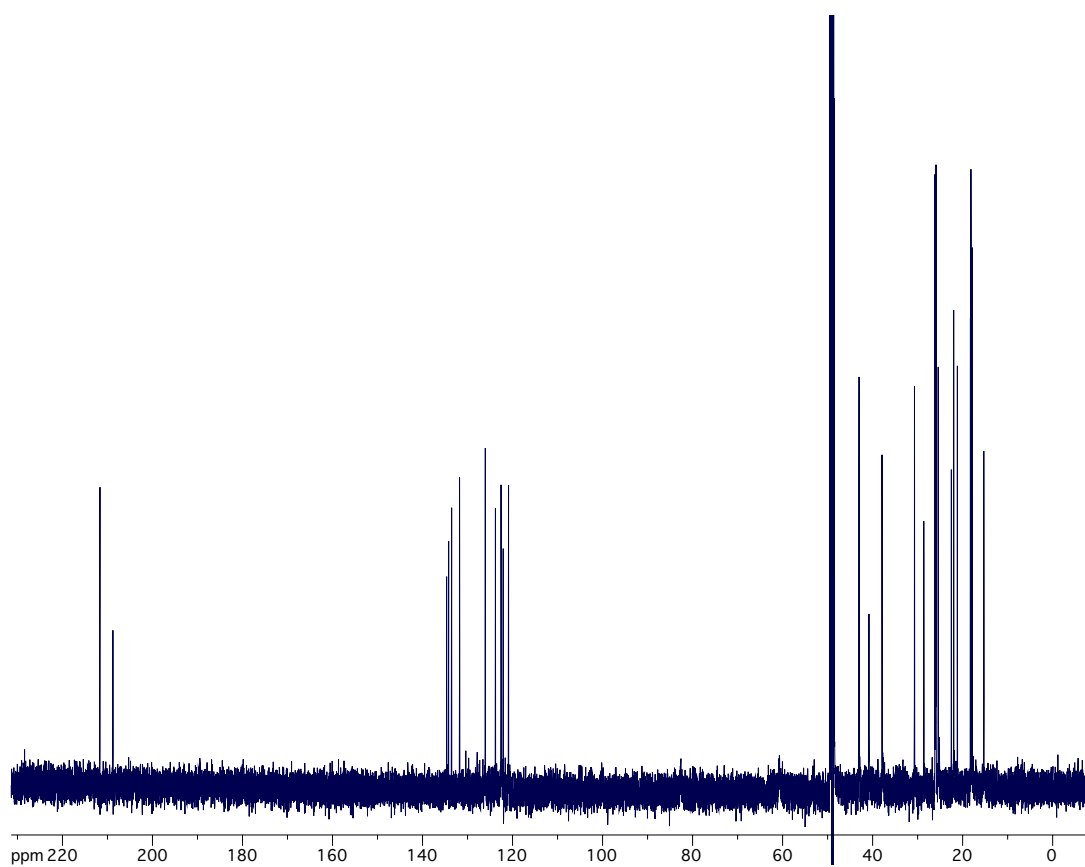
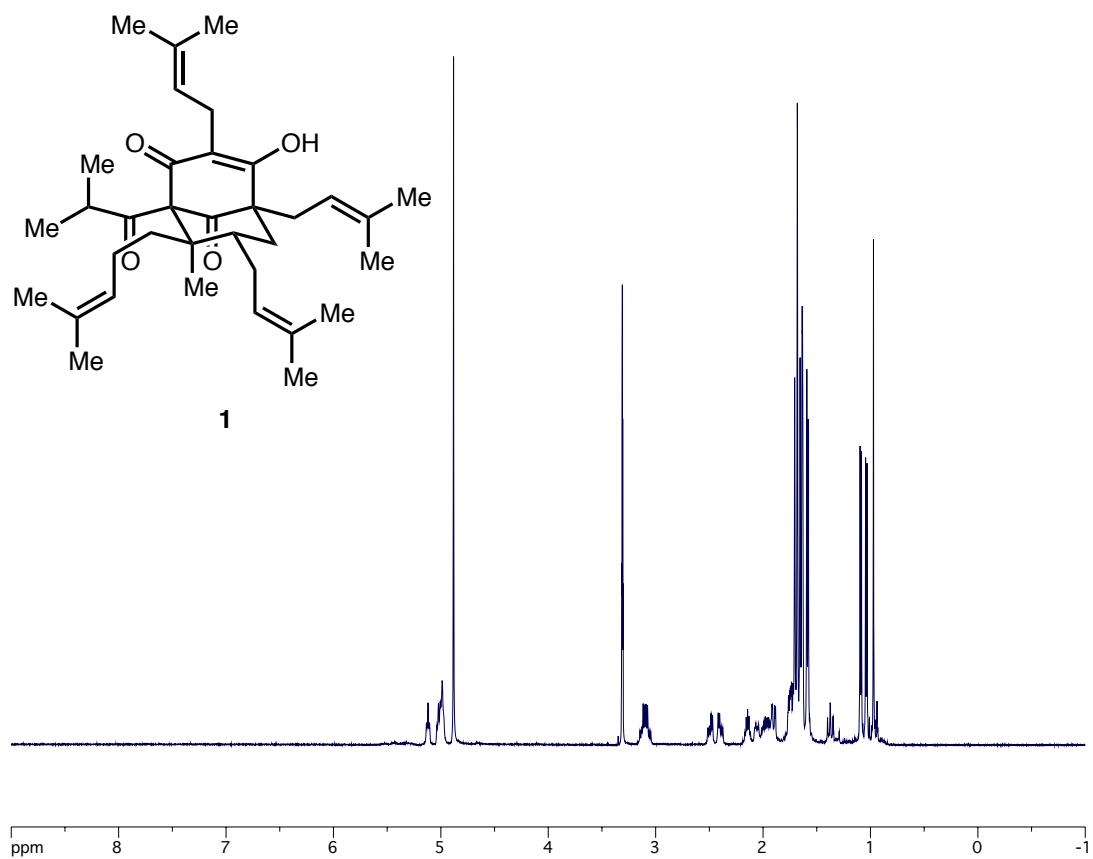


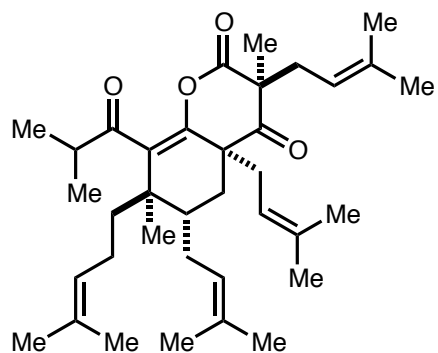




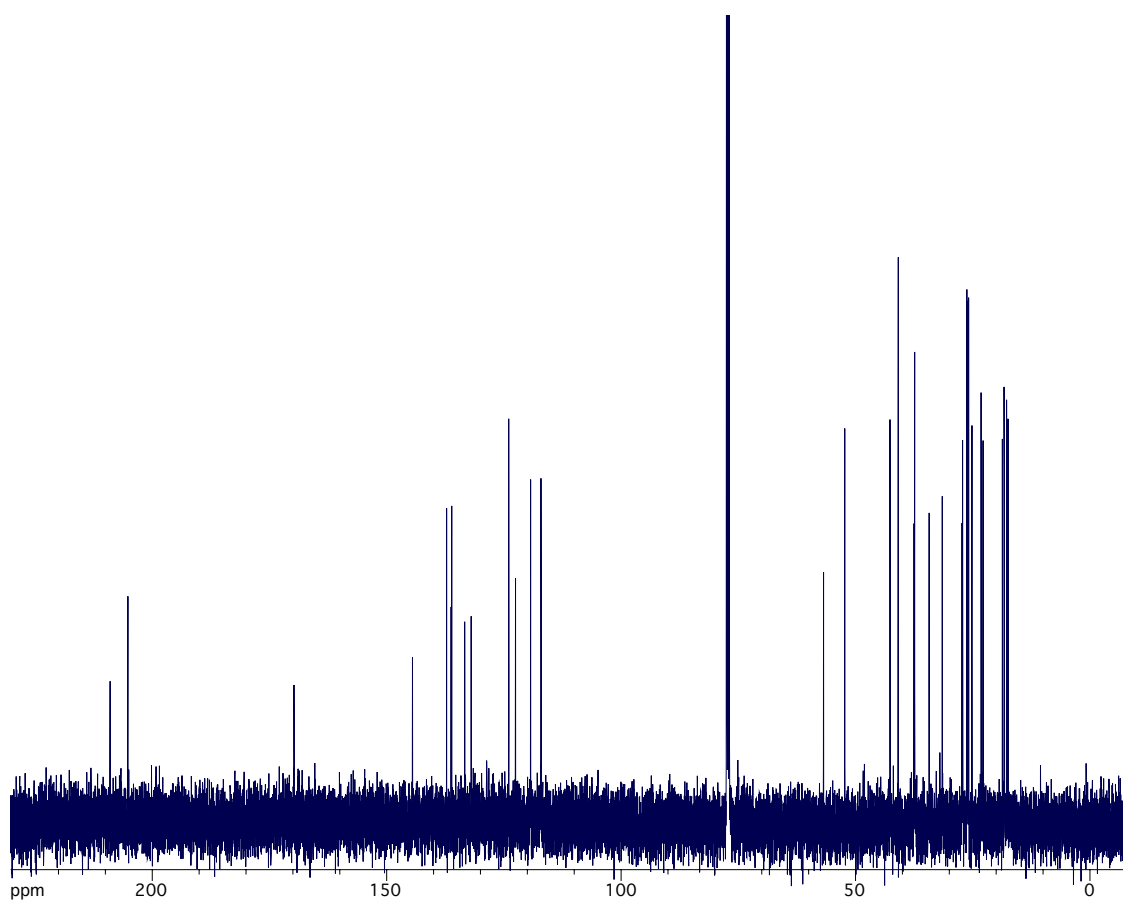
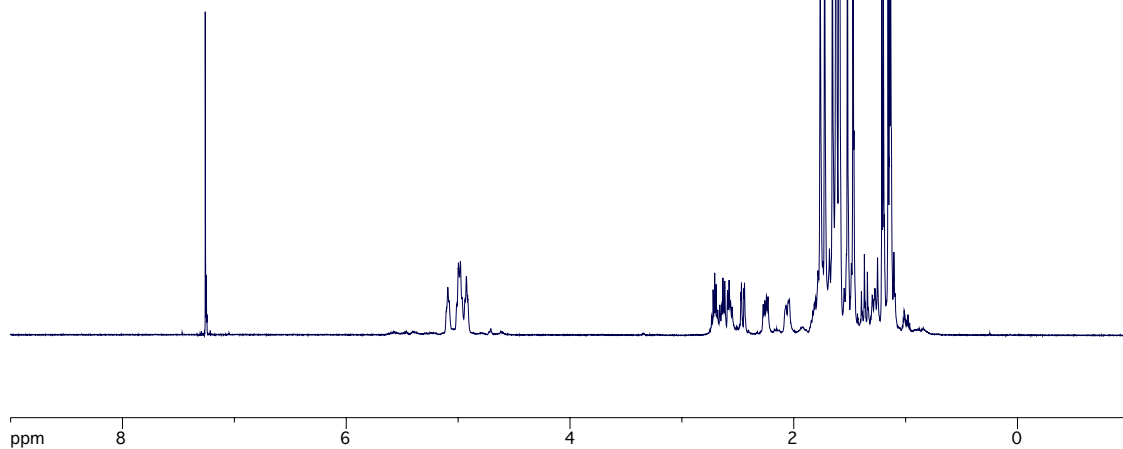


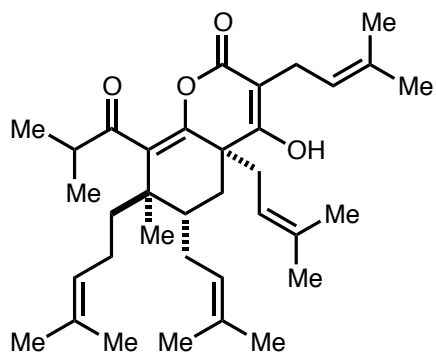






400





401

